

ABSTRACT BOOK

40th Annual MidWinter Meeting

February 11 - 15, 2017



**Baltimore Marriott Waterfront
Baltimore, MD**

ARO OFFICERS FOR 2016-2017

PRESIDENT:	Matthew W. Kelley, PhD (16-17) NIDCD/NIH-Porter Neuroscience Research Center Building 35, Room ID-993, 35 Convent Drive Bethesda, MD 20892 USA
PRESIDENT ELECT:	John P. Carey, MD (16-17) Johns Hopkins School of Medicine Department of Otolaryngology-HNS 601 North Caroline Street, Room 6255 Baltimore, MD 21287-0910 USA
PAST PRESIDENT:	Lawrence R. Lustig, MD (16-17) Columbia University Medical Center Department of Otolaryngology-HNS Harkness Pavillion, Suite 818 180 Fort Washington Avenue New York, NY 10032 USA
SECRETARY/ TREASURER:	Elizabeth S. Olson, PhD (14-17) Columbia University Otolaryngology & HNS 630 West 168th Street New York, NY 10032 USA
EDITOR:	Barbara G. Shinn-Cunningham, PhD (15-18) Boston University Center for Computational Neuroscience & Neural Technology 677 Beacon Street Boston, MA 02215 USA
HISTORIAN:	David J. Lim, MD UCLA Geffen School of Medicine Department of Head & Neck Surgery 1000 Veterans Ave, Rm 31-27 Los Angeles, CA 90024
COUNCIL MEMBERS AT LARGE:	Shi Nae Park, MD, PhD (16-19) Professor, Dept of Otolaryngology – HNS Seoul St. Mary's Hospital The Catholic University of Korea College of Medicine 505 Banpo-dong, Seocho-su Seoul, Korea 137-040
	Sharon G. Kujawa, PhD (14-17) Massachusetts Eye and Ear Infirmary Department of Otology and Laryngology 243 Charles Street Boston, MA 02114 USA
	Jennifer S. Stone, PhD (15-18) Research Associate Professor Department of Otolaryngology VM Bloedel Hearing Research Center CHDD CD 176 Box 357923 University of Washington Seattle, WA 98195 USA
ARO Executive Director:	Haley J. Brust Talley Management Group 19 Mantua Road Mt. Royal, NJ 08061 USA Ph: 1 (856) 423-7222 Ext. 103 Fax 1 (856) 423-0041 Email: hbrust@talley.com headquarters@aro.org

ABSTRACTS OF THE 40TH ANNUAL MIDWINTER MEETING OF THE



Welcome to the 40th Annual ARO Midwinter Meeting, being held for the sixth time at the Marriott Waterfront in Baltimore, Maryland. This year's meeting includes a record 1096 submitted abstracts, 13 symposia and 23 podium sessions. In addition, there will be daily mentoring sessions (*Saturday, Sunday, Monday, 4:00pm -5:00pm and Tuesday, 12:15-1:30 pm*) and workshops aimed at providing new investigators with valuable tools for career success. Credit for the organization of all these activities into a well-coordinated and exciting meeting goes to Ruth Litovsky and the other members of the Program Committee. Their exemplary efforts in this regard cannot be underestimated.

The **Presidential Symposium** (*Saturday 8:00am – 12:15pm*), “Big data from tiny samples; using comprehensive molecular profiling to understand development” will examine new technologies that are rapidly changing the scope of our ability to characterize the state of individual cells. Specific presentations will discuss the use of RNA sequencing, from both single cells and populations of cells, to generate comprehensive mRNA profiles of different development processes and the use of ATAC-Seq and other novel technologies to characterize epigenetic landscapes. Additional talks will discuss advances in the use of Mass Spectrometry to profile protein expression in single cells and examine the use of all these techniques to build a comprehensive understanding of cell and organ development.

Two separate Symposia will honor the lives and contributions of John Niparko (*Tuesday, 10:15 am – 12:15 pm*) and Norman Weinberger (*Monday, 8:00 am-10:00 am*), who both passed away in 2016.

For trainees, spARO will hold a **Town Hall Meeting** on *Saturday, 5:00-6:00 pm* and a **spARO Social** at Heavy Seas Alehouse, 1300 Bank Street, Baltimore also on *Saturday at 8:30 pm*.

At the **ARO Business Meeting** (*Sunday 6:00pm-7:00pm*), we will present an update on the state of the Association, transfer leadership from the 2016 Council to the 2017 Council, including the new President, Dr. John Carey, and hand out prizes – which you can enter to win when you visit the exhibits.

The External Relations Committee has arranged two very exciting events. First, on *Friday evening (7:30 pm-9:30 pm)*, in conjunction with Project Bridge, there will be a **Baltimore Science Café** featuring talks from Drs. Karen Avraham, Dan Polley and Phillip Alvelda. This event will be held at Homeslyce at 3336 North Charles Street in Baltimore. Then, on *Sunday evening at 7:30 pm*, following the Business Meeting, Mr. Vint Cerf, Vice President and Chief Internet Evangelist at Google will present the **ARO Public Lecture** entitled “The Power of Technology to Heal and Enhance”. This presentation will take place in the Harborside Ballroom at the Baltimore Marriott and was arranged in honor of John Niparko.

At the **Awards** ceremony (*Monday 6:00 - 7:30 pm*) and reception (*7:30-8:30 pm*), we will honor individuals that have contributed to auditory research in different ways. These include the **Geraldine Dietz Fox Young Investigator Award**, a special recognition for the important contributions of Drs. Art Popper and Richard Fay as Editors of the long-running and highly successful Springer Handbook of Auditory Research series, and the **ARO Award of Merit** which will be conferred on **Dr. Alan Palmer** for his pioneering research in auditory processing.

Finally, the ever-popular **Hair Ball** (*Tuesday 8:00 pm –12:00am*) returns with live music by the *Rollex Band*. This event began in 2006 as a maverick “Patch-Clampers Ball” instigated by Bill Roberts, Mark Rutherford and Paul Fuchs, but has grown to be one of the most fun traditions of the Midwinter Meeting.

The success of each Midwinter Meeting depends on the hard work and innovative contributions of the many ARO members who serve on different committees, in particular the Program and External Relations Committees, and on the energetic and professional assistance provided by the staff at Talley Management. Without their combined efforts, the Midwinter Meeting could not continue to be the outstanding event that it has become. But because we can always do better, please help us continue to improve by responding to a survey you will be sent after the meeting. We absolutely listen to the likes and dis-likes of the attendees. Also, if you aren't a member of ARO, please consider joining, and if you are already a member, consider becoming a member of one of our committees. This is your best opportunity to play a role in the direction of the Midwinter Meeting and the ARO. Learn more at “About Us” at www.aro.org for options or contact headquarters@aro.org to volunteer.

Best wishes for a productive and enjoyable meeting,

Matthew Kelley
ARO President, 2016-2017

CONFERENCE OBJECTIVES

At the conclusion of the MidWinter Meeting, participants should be better able to:

- Explain current concepts of the function of normal and diseased states of the ear and other head and neck structures
- Recognize current controversies in research questions in auditory neuroscience and otolaryngology
- Describe key research questions and promising areas of research in otolaryngology and auditory neuroscience

REGISTRATION

The 2017 MidWinter Meeting Registration Desk is located in the Grand Ballroom Foyer and will be open and staffed during the following hours:

Friday, February 10	4:00 PM-7:00 PM
Saturday, February 11	7:00 AM-6:00 PM
Sunday, February 12	7:00 AM-6:00 PM
Monday, February 13	7:00 AM-6:00 PM
Tuesday, February 14	7:00 AM-6:00 PM
Wednesday, February 15	7:00 AM-10:00 AM

SPEAKER READY ROOM

The 40th Annual MidWinter Meeting Speaker Ready Room is located in the Falkland Room and will be open and staffed during the following hours:

Friday, February 10	4:00 PM-7:00 PM
Saturday, February 11	7:00 AM-6:00 PM
Sunday, February 12	7:00 AM-6:00 PM
Monday, February 13	7:00 AM-6:00 PM
Tuesday, February 14	7:00 AM-6:00 PM
Wednesday, February 15	7:30 AM-10:00 AM

ADMISSION

Conference name badges are required for admission to all activities related to the 40th Annual MidWinter Meeting, including the Exhibit Hall and social events.

MOBILE APP AND ONLINE WEBSITE

The 40th Annual MidWinter app is available at your app store. Look for ARO2017. For your laptop go to <http://bit.ly/ARO2017> for access to all of the presentations and conference schedule.

MOBILE DEVICES

As a courtesy to the speakers and your fellow attendees, please switch your mobile device(s) to silent while attending the sessions.

RECORDING POLICY

ARO does not permit audio or photographic recording of any research data presented at the meeting.

BREAKS

Complimentary coffee and tea will be available during all morning and afternoon breaks.

ASSISTED LISTENING DEVICES

A limited amount of assisted listening devices are available at the ARO MidWinter Meeting Registration Desk, courtesy of Phonak.

A SPECIAL NOTE FOR THE DISABLED

ARO wishes to take steps that are required to ensure that no individual with a disability is excluded, denied services, segregated or otherwise treated differently than other individuals because of the absence of auxiliary aids and services. If you need any auxiliary aids or services identified in the Americans with Disabilities Act or any assistance please see the ARO staff at the Registration Desk.

2017 ARO MIDWINTER MEETING

PROGRAM COMMITTEE

Ruth Y. Litovsky, PhD, Chair (3/14-2/17)
Carolina Abdala, PhD (3/14-3/17)
Jennifer Bizley, PhD (3/14-2/17)
Rick Friedman, MD, PhD (3/15-2/18)
Erick Gallun, PhD (3/14-2/17)
Ronna Hertzano, MD, PhD (3/15-2/18)
Larry Hoffman, PhD (3/12-2/17)
Ingrid Johnsrude, PhD (3/16-2/19)
Achim Klug, PhD (3/16-2/19)
Hubert Lim, PhD (3/16-2/19)
Jose Antonio Lopez-Escamez (3/16-2/19)
Brian McDermott, PhD (3/15-2/18)
H. Heidi Nakajima, MD, PhD (3/16-2/19)
Christopher Shera, PhD (3/16-2/19)
Barbara Shinn-Cunningham, PhD (3/14-2/17)
Mark Warchol, PhD (3/16-2/19)
Council Liaison: Ruth Y. Litovsky, PhD (3/14-2/17)
spARO Representative: Michelle Valero

Animal Research Committee

Wei Dong, PhD, Chair (3/16-2/17)
Mark Chertoff, PhD (3/16-2/19)
Michael Deans, PhD (3/16-2/19)
Steve Eliades, MD, PhD (3/15-2/18)
James Fallon, PhD (3/14-2/17)
Rudolf Glueckert, PhD (3/14-2/17)
Stéphane Maison, PhD (3/14-2/17)
Hisayuki Ojima, PhD (3/16-2/19)
Sonja Pyott, PhD (3/15-2/18)
Suhred Rajguru, PhD (3/14-2/17)
Catherine Weisz, PhD (3/16-2/19)
Council Liaison: Sharon Kujawa, PhD (3/15-2/17)
spARO Representative: Karolina Charaziak

Award of Merit Committee

Karen P. Steel, PhD, Chair (3/16-2/17)
Catherine E. Carr, PhD (3/14-2/17)
Kathleen Cullen, PhD (3/16-2/19)
Ruth Anne Eatock, (3/16-2/19)
Ana Belen Elgoyhen, PhD (3/15-2/18)
Stefan Heller, PhD (3/14-2/17)
Michael McKenna, MD (3/15-2/18)
John Middlebrooks, PhD (3/14-2/17)
Chris Schreiner, MD, PhD (3/15-2/18)
Edwin Rubel, PhD (3/16-2/19)
Fan-Gang Zeng, PhD (3/16-2/19)
Council Liaison: Past-President Lawrence R. Lustig, MD (3/16-2/17)

Diversity & Minority Affairs Committee

Lina Reiss, PhD, Chair (3/16-2/18)
Evelyn Davis-Venn, PhD (3/15-2/18)
Michael Hoa, MD (3/14-2/17)
Amanda Lauer, PhD (3/16-2/19)
Ivan Lopez, PhD (3/16-2/19)
Mirna Mustapha, PhD (3/14-2/17)
Diana Peterson, PhD (3/14-2/17)
Ramnarayan Ramachandran (3/16-2/19)
Astin Ross, PhD (3/15-2/18)
Suhua Sha, MD (3/16-2/19)
Council Liaison: Shi Nae Park, MD, PhD (3/16-2/19)
spARO Representative: Richard McWalter

External Relations Committee

Dan Lee, MD, Chair (3/15-2/18)
Allison Coffin, PhD (3/16-2/19)
Keith Duncan, PhD (3/15-2/18)
J. Chris Holt, PhD (3/16-2/19)
Hubert Lim, PhD (3/15-2/18)
Yunxia (Yesha) Wang Lundberg, PhD (3/15-2/18)
Stéphane Maison, PhD (3/16-2/19)
Cynthia Morton, PhD (3/14-2/17)
Shinichi Someya, PhD (3/15-2/18)
Joel Synder, PhD (3/16-2/19)
Debara Tucci, MD (3/14-2/17)
Council Liaison: Sharon Kujawa, PhD (3/15-2/17)
spARO Representative: Rebecca Curry

Finance & Investment Committee

Paul Fuchs, PhD, Chair (3/14-2/17)
Thomas Friedman, PhD (3/16-2/19)
Erick Gallun, PhD (3/15-2/18)
Michael Anne Gratton, PhD (3/16-2/19)
Neil Segil, PhD (3/15-2/18)
Christopher Shera, PhD (3/14-2/17)
Ex-officio: Secretary-Treasurer Elizabeth S. Olson, PhD (3/14-2/17)

International Committee

Alan Brichta, PhD: Australia. Chair (3/16-2/18)
W. Robert J. Funnell: Canada (3/16-2/19)
Jonathan Gale: UK (3/16-2/19)
Juichi Ito, MD, PhD: Japan (3/14-2/17)
Hannes Maier, PhD: Germany (3/16-2/19)
ShiNae Park, MD, PhD: Korea (3/15-2/18)
Ulla Pirvola, PhD: Finland (3/16-2/19)
Yilai Shu, MD, PhD: China (3/15-2/18)
Joris Soons, PhD: Belgium (3/15-2/18)
Isabel Varela-Nieto, PhD: Spain (3/16-2/19)
Council Liaison: Jennifer Stone, PhD (3/15-2/17)
spARO Representative: Yew Song Cheng

JARO Editorial Board

Paul B. Manis, PhD, Editor-in-Chief (2011-2017)
Julie A. Bierer, PhD (2015-2018)
Alan M. Brichta, PhD (2015-2018)
Catherine E. Carr, PhD (2016-2019)
Mark A. Eckert, PhD (2013-2017)
Ana Belén Elgoyhen, PhD (2013-2017)
W. Robert J. Funnell, PhD (2013-2017)
Elisabeth Glowatzki, PhD (2015-2018)
Nace L. Golding, PhD (2016-2019)
Michael G. Heinz, PhD (2016-2019)
Ronna Hertzano, MD, PhD (2015-2018)
Richard F. Lewis, MD (2015-2018)
Ruth Y. Litovsky, PhD (2013-2017)
Christian Lorenzi, PhD (2016-2019)
Brigitte Malgrange, PhD (2015-2018)
Colette M. McKay, PhD (2016-2019)
John C. Middlebrooks, PhD (2015-2018)
Adrian Rees, PhD (2015-2018)
Xiaorui Shi, MD, PhD (2013-2017)
George A. Spirou, PhD (2014-2017)
Marcel van der Heijden, PhD (2014-2017)
Joseph P. Walton, PhD (2016-2019)
Robert H. Withnell, PhD (2015-2018)

Long Range Planning Committee

Steven H. Green, PhD, Chair (3/14-2/17)
R. Michael Burger, PhD (3/16-2/19)
Karina Cramer, PhD (3/15-2/18)
Amy Donahue, PhD, NIDCD Rep.
Judy Dubro, PhD (3/15-3/18)
Lisa Goodrich, PhD (3/14-2/17)
Ana Kim, MD (3/15-2/18)
Stephen Lomber, PhD (3/16-2/19)
Tobias Moser, MD (3/14-2/17)
Mark Rutherford, PhD (3/15-2/18)
Council Liaison: President-Elect:
John P. Carey, MD (3/16-2/17)
Chair, International Committee: Alan Brichta, PhD:
Australia (3/16-2/18)
spARO Representative: Anna Diedesch

Membership Committee

Chris J. Sumner, Chair (3/12-2/17)
Deniz Baskent, PhD (3/15-2/18)
Bernd Fritsch, PhD (3/15-2/18)
Sam Gubbels, MD (3/14-2/17)
Colleen Le Prell, PhD (3/14-2/17)
Dan Polley, PhD (3/14-2/17)
William H. Slattery, MD (3/15-2/18)
Council Liaison: Jennifer Stone, PhD (3/15-2/17)

Nominating Committee

Lawrence R. Lustig, MD, Chair (3/16-2/17)
Jeffrey R. Holt, PhD (3/16-2/17)
Sharon Kujawa, PhD (3/16-2/17)
Anil K. Lalwani, MD (3/16-3/17)
Anthony Ricci, PhD (3/16-2/17)

Publications Committee

Hinrich Staecher, MD, PhD, Chair (3/15-2/18)
Maria Chait, PhD (3/14-2/17)
Alan Cheng, MD (3/16-2/19)
Wade Chien, MD (3/16-2/19)
Gestur B. Christianson, PhD (3/15-2/18)
Gregory I. Frolenkov, PhD (3/15-2/18)
Elisabeth Glowatzki, PhD (3/14-2/17)
Kuni H. Iwasa, PhD (3/15-2/18)
Hainan Lang, MD, PhD (3/16-2/19)
Saima Riazuddin, PhD (3/16-2/19)
Isabelle Roux, PhD (3/16-2/19)
JARO Editor: Paul B. Manis, PhD, ex officio
Springer Representative: Gregory Baer, ex officio
Secretary/Treasurer: Elizabeth S. Olson, PhD (3/14-2/17)
Council Liaison: Barbara G. Shinn-Cunningham, PhD
(3/15-2/17)
spARO Representative: David Morris

Travel Awards

Ronna Hertzano, MD PhD, Chair (3/14-2/17)
Karen Banai, PhD (3/15-2/18)
Mike Bowl, PhD (3/14-2/17)
Benjamin Crane, MD, PhD (3/14-2/17)
Elizabeth Driver, PhD (3/14-2/17)
Matt Goupell, PhD (3/14-2/17)
Michael Anne Gratton, PhD, (3/15-2/18)
Hainan Lang, MD, PhD (3/15-2/18)
Tomoko Makishima, MD, PhD (3/15-3/18)
Chandrakala Puligilla, PhD (3/14-2/17)
Regi Santos-Cortez, MD, PhD (3/16-2/19)
Martin Schwander (3/16-2/19)
Robert Withnell, PhD (3/15-2/18)
Norio Yamamoto, MD, PhD (3/15-2/18)
James F. Battey, MD, PhD, NIDCD Dir ex officio
Council Liaison: Shi Nae Park, MD, PhD (3/17-2/21)
spARO Representative: Jeremy Duncan

EXECUTIVE OFFICES ASSOCIATION FOR RESEARCH IN OTOLARYNGOLOGY

19 Mantua Road
Mt. Royal, New Jersey 08061
Phone: (856) 423-0041
Fax: (856) 423-3420
E-Mail: headquarters@aro.org
Meetings E-Mail: meetings@aro.org

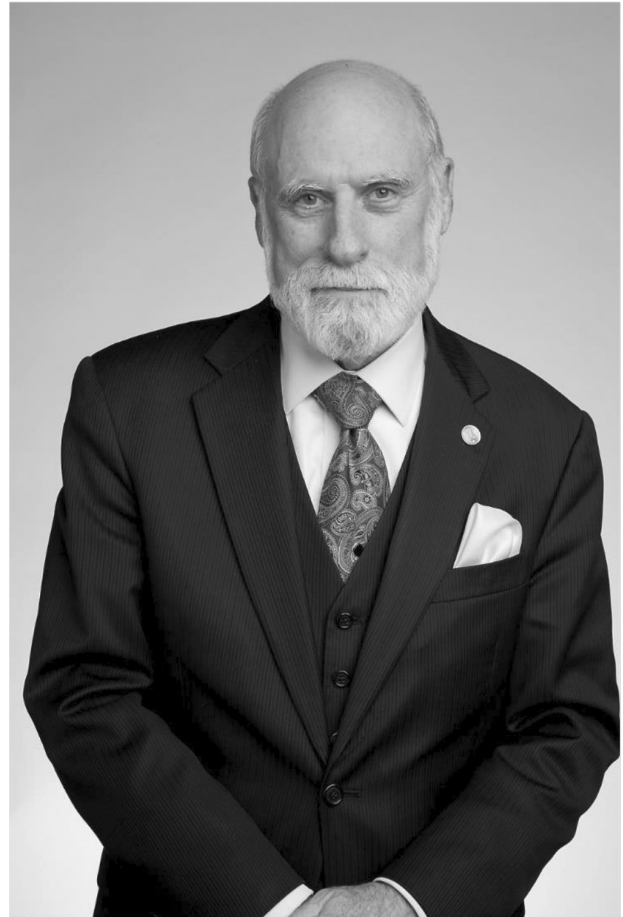
**ARO Public Lecture
Special Guest Presentation
in Honor of Dr. John Niparko**

VINT CERF

**Vice President &
Chief Internet Evangelist**
Google

A “Father of the Internet”

**An authority on global
Internet policy**



Abstract

John Niparko was at the forefront of new hearing technology for those whose hearing deficit could not be cured with simple amplification. The cochlear implant was his solution of choice and my wife, Sigrid, benefited enormously from that technology and John's ministrations. As we look into the 21st Century, we can see new possibilities introduced by better understanding of our neural systems and ways in which we can interface them to electronic devices. This talk will explore these possibilities from the eyes of a layman, not an expert, in neural interfaces.

***The Power of Technology
to Heal and Enhance***

**Sunday,
February 12,
7:30 PM**

**Baltimore Marriott
Waterfront**

Harborside Ballroom

AWARD OF MERIT



2017 Award of Merit Recipient Alan R. Palmer

Award Lecture and Abstract

Exploring Auditory Processing

Alan R. Palmer.

My laboratory has employed a variety of anatomical and physiological methods to elucidate auditory function. In this talk, I will very briefly touch upon a few examples of how we have applied these methodologies at several levels of the auditory system. We have (among others) examined structure/function relationships in the cochlear nucleus, used recordings in the midbrain to support a reassessment of how interaural time differences are extracted and shown selective processing of vocalizations in a ventral processing stream in cortex.

AWARD OF MERIT BIOSKETCH

The 2017 Award of Merit winner Alan Palmer has always defined himself as, 'just a simple biologist'. But in that apparently unassuming guise, he has, over the past forty and more years, made an impressive contribution to our understanding of several fundamental questions in auditory neuroscience.

Indeed, what characterizes Alan's work is the sheer diversity of brain regions he has studied over the course of his career. Starting at the auditory nerve for his PhD studies, he worked progressively upwards to cochlear nucleus, inferior colliculus, superior colliculus, thalamus and cortex - developing techniques as the scientific questions required. A second major facet of Alan's career is his huge influence as a mentor to the many students and postdocs who have worked with him.

Alan was the first from a large working class family to continue in education beyond the age of sixteen. He studied Biological Sciences at the University of Birmingham graduating with first class honours in 1972. As an undergraduate he had developed an interest in vision and his first intention was to gain a PhD in that field. With that goal, he attended an interview at the Department of Communication and Neuroscience at Keele University during which he was persuaded to switch systems and work on the physiology of hearing with Ted Evans. The early 1970s were exciting times in auditory science with an explosion of pioneering measurements on basilar membrane mechanics, hair cell physiology and otoacoustic emissions. Alan's PhD involved cochlear nucleus and auditory nerve recordings where he discovered that in the presence of noise backgrounds the dynamic range of cochlear nerve and cochlear nucleus neurons shifts to keep them within operating range. This work has since been explored and revisited at several levels of the auditory pathway levels.

Following a postdoctoral fellowship with Ted Evans, Alan obtained a staff position at the National Institute for Medical Research in Mill Hill, London – an appointment that gave him carte blanche and to build his own laboratory from scratch. Inspired by the work of Knudsen and Konishi in the owl, and at the encouragement of his Head of Division, Mike Keating, he set up a free-field auditory stimulation system in anechoic space to explore auditory responses in the deep layers of the superior colliculus. He was joined in this work by Andrew King, then a PhD student, and they discovered and reported in *Nature* the now well-established map of auditory space in the mammalian superior colliculus. While at Mill Hill he also got involved in measuring the mechanics of hearing in the frog, a task that included developing with Andrew Pinder a white light method to study vibration in the frog ear, and the first publication of otoacoustic emissions in the frog.

After four hugely productive years at the Mill Hill, Alan was persuaded by Ian Russell and Chris Darwin to apply for one of the Royal Society's new University Research Fellowships to move to the University of Sussex. Only 15 fellowships were available across all areas of science, but Alan was successful with an application to work on the encoding of speech signals in the peripheral auditory system. On arrival at Sussex, Alan was presented with Ian Winter as a PhD student in a *fait accompli*, since Ian had been told he could do a PhD only if Alan obtained the fellowship; fortunately the two of them hit it off! Alan's stay at Sussex was relatively short: a tenured position became available at the MRC Institute of Hearing Research in Nottingham, and such an opportunity could not be dismissed, despite being only two years into his prestigious fellowship. Nevertheless it was a productive period that included a collaboration with Ian Russell demonstrating that the filtering of hair cell membranes is the major limitation to phase-locking in auditory nerve fibres.

Since arriving at the MRC Institute of Hearing Research (IHR) in 1986, Alan has spent the last 30 years as a Program Leader at the Institute, including periods as Deputy and Interim Director. His research has ranged widely, and he often reinvented himself as successful post docs and students continued elsewhere work they had started or developed at Nottingham, amongst others: Adrian Rees on amplitude modulation, David McAlpine on binaural coding, Jasmin Grimsley and David Green on communication sounds. Alan's great generosity as a mentor and colleague means there are many hearing labs across the UK and the rest of the world with a first or second generation connection to Alan. A few of the areas Alan's laboratory has contributed to over the years are worthy of special mention. From the careful characterization of cells in the ventral cochlear nucleus, he and Ian Winter identified a possible source of the wideband inhibition necessary to explain the processing of spectral notches in the dorsal cochlear nucleus. Using juxtacellular labelling, Alan went on to provide direct evidence that these giant multipolar cells provided profuse projections to all other parts of the cochlear nucleus, including commissural connections to the opposite cochlear nucleus. His work

on binaural responses in the inferior colliculus with David McAlpine, Dan Jiang and Trevor Shackleton spurred a major reassessment of the processing of interaural delays, and the neural representation of the binaural masking level difference. More recently his work with Mark Wallace has encompassed the mechanisms of tinnitus and the encoding of animal vocalizations, for which the guinea pig has a rich and varied repertoire.

Most of the data Alan has collected in his career has been hard won from the tip of a microelectrode, but when Mark Haggard, the then Director of IHR, decided that the time was right for the Institute to exploit Nottingham University's expertise in fMRI, Alan played key role in the new imaging group, which amongst other discoveries, developed sparse imaging to overcome the contaminating effect of scanner noise.

Apart from his intellectual contribution, Alan has always been the most practical of scientists, devising often simple, but ingenious, means of solving technical problems. He was thus a natural choice as the manager of Institute's very talented mechanical and electronic engineers. Under Alan's guidance, his team developed a noise cancellation system for fMRI, now taken up commercially, an automated version of the Toy Test, now widely deployed in paediatric audiology clinics, and an otoacoustic emission measurement system using rapid reconstruction of responses to maximum length clicks sequences.

As with his mentoring of colleagues, Alan has always believed that the scientific endeavor depends on a sense of community. He has selflessly given of his time and energy through service on editorial boards, grant awarding bodies, advisory panels and as an examiner. At scientific meetings Alan happily spends hours quizzing PhD students in his incisive manner about their posters, but always leaving them with a deeper understanding of their work and a sense of achievement! Such activities often go unseen, but rank in importance with the extensive list of papers, reviews and other publications that bear his name.

Alan has always been dedicated to his scientific family, throughout his career, but his own family was always his top priority. He and his wife Chris have been together since undergraduate days, and he is immensely proud of his two daughters, his 'girls': Evelyne, a clinician, and Alice, a neuroscience PhD.

In 1997 Alan was appointed to an honorary chair in Auditory Neuroscience at the University of Nottingham, and in 2016 his contribution to hearing was recognized by the award of the William and Christine Hartmann Medal for Auditory Neuroscience from the Acoustical Society of America. He is now emeritus professor at the University of Nottingham. It is a great pleasure to see the many facets of Alan's work celebrated by the 2017 ARO Award of Merit.

ADRIAN REES
IAN WINTER

PRESIDENTIAL CITATION

The ARO will award Presidential Citations to Dr. Arthur Popper, University of Maryland (retired) and Dr. Richard Fay, Loyola University of Chicago (retired) for their contribution to auditory research as founders and Editors of the long-running Springer Handbook of Auditory Research (SHAR) series. Beginning in 1992 with the publication of Volume 1, *The Mammalian Auditory Pathways: Neuroanatomy*, and continuing to the present with the recent publication of Volume 62, *Understanding the Cochlea*, this series has provided comprehensive reviews on virtually all aspects of auditory system biology, from molecular biology to behavior in both vertebrate and invertebrate species. The tireless editorial efforts of Art and Dick provided the driving force behind each of these volumes, resulting in a resource that is unmatched in neuroscience.

Past Presidents

1973-74 David L. Hilding, MD
1974-75 Jack Vernon, PhD
1975-76 Robert A. Butler, PhD
1976-77 David J. Lim, MD
1977-78 Vicente Honrubia, MD
1978-80 F. Owen Black, MD
1980-81 Barbara Bohne, PhD
1981-82 Robert H. Mathog, MD
1982-83 Josef M. Miller, PhD
1983-84 Maxwell Abramson, MD
1984-85 William C. Stebbins, PhD
1985-86 Robert J. Ruben, MD
1986-87 Donald W. Nielsen, PhD
1987-88 George A. Gates, MD
1988-89 William A. Yost, PhD
1989-90 Joseph B. Nadol, Jr., MD
1990-91 Ilsa R. Schwartz, PhD
1991-92 Jeffrey P. Harris, MD, PhD
1992-93 Peter Dallos, PhD
1993-94 Robert A. Dobie, MD
1994-95 Allen F. Ryan, PhD
1995-96 Bruce J. Gantz, MD
1996-97 M. Charles Liberman, PhD
1997-98 Leonard P. Rybak, MD, PhD
1998-99 Edwin W. Rubel, PhD
1999-00 Richard A. Chole, MD, PhD
2000-01 Judy R. Dubno, PhD
2001-02 Richard T. Miyamoto, MD
2002-03 Donata Oertel, PhD
2003-04 Edwin M. Monsell, MD, PhD
2004-05 William E. Brownell, PhD
2005-06 Lloyd B. Minor, MD
2006-07 Robert V. Shannon, PhD
2007-08 P. Ashley Wackym, MD
2008-09 Paul A. Fuchs, PhD
2009-10 Steven Rauch, MD
2011-12 Karen B. Avraham, PhD
2012-13 Debara L. Tucci, MD
2013-14 John C. Middlebrooks, PhD
2014-15 Jay. T Rubinstein
2015-16 Lawrence R. Lustig, MD
2016-17 Matthew W. Kelley, PhD

Award of Merit Recipients

1978 Harold Schuknecht, MD
1979 Merle Lawrence, PhD
1980 Juergen Tonndorf, MD
1981 Catherine Smith, PhD
1982 Hallowell Davis, MD
1983 Ernest Glen Wever, PhD
1984 Teruzo Konishi, MD
1985 Joseph Hawkins, PhD
1986 Raphel Lorente de N6, MD
1987 Jerzy E. Rose, MD
1988 Josef Zwislocki, PhD
1989 4ke Fl6ck, PhD
1990 Robert Kimura, PhD
1991 William D. Neff, PhD
1992 Jan Wers4ll, PhD
1993 David Lim, MD
1994 Peter Dallos, PhD
1995 Kirsten Osen, MD
1996 Ruediger Thalmann, MD & Isolde Thalmann, PhD
1997 Jay Goldberg, PhD
1998 Robert Galambos, MD, PhD
1999 Murray B. Sachs, PhD
2000 David M. Green, PhD
2001 William S. Rhode, PhD
2002 A. James Hudspeth, MD, PhD
2003 David T. Kemp, PhD
2004 Donata Oertel, PhD
2005 Edwin W. Rubel, PhD
2006 Robert Fettiplace, PhD
2007 Eric D. Young, PhD
2008 Brian C. J. Moore, PhD
2009 M. Charles Liberman, PhD
2010 Ian Russell, PhD
2011 Robert V. Shannon, PhD
2012 David P. Corey, PhD
2013 Karen P. Steel, PhD
2014 H. Steven Colburn, PhD
2015 Thomas B. Friedman, PhD
2016 Geoffrey A. Manley, PhD
2017 Alan R. Palmer, PhD

2017 TRAVEL AWARD RECIPIENTS

Alessandro Altoe'	Mario Milazzo
Andrew Ayoob	Jeenu Mittal
Sepand Bafti	Sharlen Moore Corona
Nicole Black	Anna Morgan
Ryan Boerner	Hamid Motallebzadeh
William Bologna	Michael Muniak
Allison Bradley	Amir Nankali
Rogers Brown	James Naples
Alexandria Camino	Yoshie Narui
Franklin Canady	Kenyaria Noble
Giusy Caprara	Bas Olthof
Federico Ceriani	Mary O'Sullivan
Blanca Cervantes	Christopher Pastras
Minghui Chen	Brandon Paul
Zongwei Chen	Sarah Pickett
Laura Coco	Melissa Polonenko
Yuqi Deng	Ulrich Pomper
Lindsay DeVries	Sonal Prasad
James Dewey	Darrin Reed
Yunpeng Dong	Darrin Rice
Maria Duarte	Amanda Rodriguez
Jeremy Duncan	Jason Rudman
Vijayalakshmi Easwar	Mark Rudolf
Nicole Febles	Jessica Sagers
Mary Flaherty	Anshula Samarajeewa
Zahra Ghasemahmad	David Sandlin
Ksenia Gnedeva	Matthew Scarnati
Peter Gottlieb	Sara Schmidt
Laura Hamel	Bahar Shavsavarani
Katherine Hardy	Eliot Shearer
Ryan Harrison	Yilai Shu
Heivet Hernandez Perez	Roosbeh Soleymani
Björn Herrmann	Sarah Sottile
Hui Hong	Rosy Southwell
Marta Iversen	Natalia Stupak
Janani Iyer	Ilmar Tamames
Hsin-I Jen	Pei-Ciao Tang
Lejo Johnson Chacko	Osama Tarabichi
Lashaka Jones	Richard Tilton
Vivek Kanumuri	Tomokatsu Udagawa
Bahar Khalighinejad	Roberto Valdizon
Subong Kim	Jonathon Vargo
Alaa Koleilat	Christopher Ventura
Nadeem Kolia	Anita Wagner
Bonnie Lau	Xiaoyu Wang
Jaewook Lee	Karessa White
Wei Li	Teerawat Wiwatpanit
George Liu	Amanuel Wolde-Kidan
Michael Lohse	Kevin Wong
Steven Losorelli	Calvin Wu
Ngoc-Nhi Luu	Zilong Xie
Sara Miay Kim Madsen	Justin Yao
Salwa Masud	Anusha Yellamsetty
Elizabeth McCullagh	Sijia Zhao

ISSN-0742-3152

The Abstracts of the Association for Research in Otolaryngology is published annually and consists of abstracts presented at the Annual MidWinter Research Meeting. A limited number of copies of this book and previous books of abstracts (1978-2011) are available. Please address your order or inquiry to Association for Research in Otolaryngology Headquarters by calling (856) 423-0041 or emailing headquarters@aro.org.

This book was prepared from abstracts that were entered electronically by the authors. Authors submitted abstracts over the World Wide Web using Cadmium Abstract Management System. Any mistakes in spelling and grammar in the abstracts are the responsibility of the authors. The Program Committee performed the difficult task of reviewing and organizing the abstracts into sessions. The Program Committee; Program Committee Chair, Ruth Litovsky, PhD; and the President, Matthew W. Kelley, PhD constructed the final program. Cadmium and Marathon Printing electronically scheduled the abstracts and prepared Adobe Acrobat pdf files of the Program and Abstract Books. These abstracts and previous years' abstracts are available at www.aro.org.

Citation of these abstracts in publications should be as follows: **Authors, year, title, Assoc. Res. Otolaryngol. Abs.: page number.**

Table of Contents

	Abstract Number	Page No.
Presidential Symposium:		
Big Data from Tiny Samples; Using Comprehensive Molecular Profiling to Understand Development.....	1-7	1-3
Symposium:		
Multisensory Interplay and Plasticity From Cells to Circuits and From Mice to Humans.....	1-5	8-9
Podium:		
Inner Ear: Drug Delivery.....	1-8	3-7
Poster:		
Auditory Nerve I.....	1-11	9-15
Auditory Prosthesis: Speech and More.....	12-21	16-21
Auditory Prosthesis: Surgical and Stimulation.....	23-42	22-33
Brainstem Session I.....	43-53	34-39
Clinical Otolaryngology: Pathology.....	54-62	39-44
Coding of Binaural Cues.....	63-72	44-49
Otoacoustic Emissions.....	73-86	50-56
Development I.....	87-107,766	56-68
Genetics: Illuminating Genetic Architecture for Diagnosis for Hearing Loss.....	108-131	68-82
Hair Cells - Anatomy and Physiology I.....	132-143	82-89
Inner Ear: Damage and Protection I (Poster).....	144-161	89-99
InnerEar: Mechanics & Modeling I.....	162-177	99-107
Middle Ear - Basic Science.....	178-194	107-116
Psychoacoustics: Animal Psychoacoustics.....	195-204	117-122
Regeneration I.....	205-223	122-131
Vestibular: Imbalance, Vertigo and Meniere's.....	224-235	131-138
Podium:		
Speech Perception.....	9-14	138-141
Podium:		
Tinnitus.....	15-21	141-145
Podium:		
Auditory Cortex: Anatomy, Physiology and Function.....	23-30	145-149
NIDCD Workshop #1:		
Applying for NIDCD Training and Career Development Awards.....		149
NIDCD Workshop #2:		
Early Stage Investigators (ESI) and New Investigators (NI).....		149
NIDCD Workshop #3:		
SBIR and STTR Grant Programs for Medical Device.....		150
Symposium:		
How Listeners Discover/Learn And Use Regularities In The Acoustic Environment.....	6-11	150-152
Podium:		
Development I.....	31-38	152-156
Podium:		
Vestibular I: Basic Research.....	39-46	156-161
Podium:		
Inner Ear: Mechanics and Modeling.....	47-54	161-166
Symposium:		
Relating Animal Models to Human Cochlear Implant Use.....	12-15	166-167
Symposium:		
Advances in Genome Editing and its Clinical Applications.....	16-21	167-169
Young Investigator Symposium:		
Neuronal and Non-Neuronal Regulation of Cochlear Wiring and Refinement.....	22-28	169-172

Table of Contents

	Abstract Number	Page No.
Poster:		
Aging: Effects of Age on Hearing.....	236-242	172-176
Auditory Cortex I.....	243-261,934	176-185
Auditory Nerve II.....	262-271	186-191
Auditory Prosthesis: Psychoacoustics.....	272-287,22,92	191-201
Brainstem Session II.....	288-302	201-210
Clinical Otolaryngology: Past, Present, and Future.....	303-314	210-216
Genetics: Deciphering Molecular Mechanisms in Human Hearing.....	315-330	216-224
Hair Cells - Anatomy and Physiology II.....	331-345	224-232
Inner Ear: Damage and Protection II (Poster).....	346-362	232-241
Interactions Between Spatial Acoustic Cues & Non-Spatial Aspects of Perception.....	363-371	241-246
Midbrain: Organization and Coding Properties.....	372-385	246-254
Psychoacoustics: Modulation and Pitch in Tones and Speech: Individuals & Groups.....	386-396	254-260
Sound Localization in Humans and Animals.....	397-408,923	260-266
Speech Perception I.....	409-430	266-278
Thalamus and Primary Auditory Cortex.....	431-440	278-283
Vestibular: VEMPs, SHIMPs, and Other Novel Approaches.....	441-452	284-291
Podium:		
Inner Ear: Damage and Protection I.....	55-62	291-295
Podium:		
Regeneration I.....	63-70	296-300
Symposium:		
Bridging the Gap between Hearing Sciences and Audio Technologies.....	29-32	300-301
Symposium:		
A Tribute to Norman M. Weinberger (1935-2016): A Bridge to the Future of Research on Auditory Cortical Functions.....	33-37	301-302
Symposium:		
Vestibular Influence on Cognitive Function.....	38-42	302-303
Symposium:		
In Vitro Model Technologies for Hearing Regeneration and Ototoxicity Protection.....	43-46	303-305
Podium:		
Hair Cells - Anatomy and Physiology.....	71-78	305-309
Podium:		
Genetics A: Genomics and Gene Regulation.....	79-84	310-313
Young Investigator Symposium:		
Limiting Factors in Cochlear Implants.....	47-54	313-317
Poster:		
Auditory Cortex II.....	453-470	318-327
Auditory Cortex: Human Studies I.....	471-481	327-332
Auditory Nerve III.....	482-494	332-340
Auditory Prosthesis: Animal Models.....	495-507,932	340-348
Brainstem Session III.....	508-521	348-356
Causes and Effects of Tinnitus.....	522-531	356-361
Hair Cells - Anatomy and Physiology III.....	532-550	361-372
Inner Ear: Anatomy & Physiology.....	551-577	372-386
Inner Ear: Damage and Protection III (Poster).....	578-593,933	387-396
Inner Ear: Damage and Protection IV (Poster).....	594-610	396-406
Inner Ear: Mechanics & Modeling II.....	611-624,925	406-413
Plasticity, Learning and Adaptation: Neurophysiology.....	625-637	414-420
Psychoacoustics: Psychoacoustical Models and Methods.....	638-646	421-425
Spatial Hearing in Listeners with Hearing Loss.....	648-657	425-431
Speech Perception II.....	658-668	431-437
Vestibular: Central Circuits.....	669-685,929	437-447

Table of Contents

	Abstract Number	Page No.
Podium:		
Binaural Hearing and Sound Localization.....	85-92	447-451
Podium:		
Genetics B: General.....	93-98	451-455
Podium:		
Inner Ear: Anatomy and Physiology.....	99-105	455-458
Symposium:		
Auditory implants: Improving auditory function from pre-processing to peripheral and central mechanisms (Honoring Bob Shannon).....	55-61	458-461
Symposium:		
To Honor Contributions of Dr. John Niparko.....	62-69	461-464
Podium:		
Auditory Pathways: Brainstem.....	106-113	464-467
Podium:		
Auditory Nerve.....	114-119,22	468-472
Podium:		
Plasticity, Learning and Adaptation to Hearing Impairment.....	120-127	472-476
Podium:		
Inner Ear: Anatomy and Physiology.....	99-105	455-458
Poster:		
Aging: Animals Models and Mechanisms of Aging.....	686-698	477-484
Auditory Cortex: Human Studies II.....	699-708	484-489
Auditory Cortex: Human Studies III.....	709-718	489-494
Auditory Prostheses: Objective Measures.....	719-732,931	495-503
Brainstem Session IV.....	733-746	503-511
Development II.....	747-765,924	511-521
Hair Cells - Anatomy and Physiology IV.....	767-785	522-531
Inner Ear: Damage and Protection V (Poster).....	786-802	532-541
Inner Ear: Drug Delivery.....	803-823	541-554
Midbrain: Auditory and Non-Auditory Modulation and Plasticity.....	824-832	554-559
Middle Ear – Clinical.....	833-848	559-569
Plasticity, Learning and Adaptation: Behavior.....	849-860,928	569-576
Psychoacoustics: Attention, Cognition, and Information.....	861-879	577-586
Regeneration II.....	880-895,927,930	586-596
Tinnitus: Treatments and Mechanisms.....	896-904	596-602
Vestibular: Physiologic Drivers of the Vestibular Periphery.....	905-922	602-612
Podium:		
Auditory Prostheses.....	128-135	612-617
Podium:		
Auditory Cortex: Human Studies.....	136-143	617-622
Podium:		
Inner Ear: Damage and Protection II.....	144-151	622-626
Podium:		
Mechanics of the Middle Ear.....	152-158	626-630
Podium:		
Development II.....	159-166	631-634
Podium:		
Vestibular II: Clinical Research.....	167-174	635-639

Presidential Symposium

PRES SYMP 1

Decoding Neural Transcriptomes and Epigenomes via High-throughput Sequencing

Hongjun Song

Johns Hopkins University

In the dentate gyrus of the hippocampus, adult neurogenesis arises from multiple neural stem cells and is regulated local neuronal circuitry activity. Our previous studies have shown that neuronal activation of dentate granule neurons promotes adult neurogenesis via a pathway involving active DNA demethylation (Ma et al. *Science* 2009). Our laboratory since have focused on the mouse dentate gyrus to generate a blueprint of transcriptome and epigenome of different cell types related to adult neurogenesis via high-throughput sequencing. We have profiled DNA methylation status of dentate granule neurons in vivo upon neuronal activation across the genome with a single-base resolution and found dynamic methylation changes, including both de novo methylation and demethylation (Guo et al. *Nat. Neurosci.* 2011). Recently, we have performed whole-genome bisulfite sequence to generate single-base methylome of dentate granule neurons and identified significant amount of nonCpG methylation in neuronal methylome (Guo et al. *Nat. Neurosci.* 2013). Combined with RNA-seq, our analysis showed that both CpG and nonCpG methylation across the gene anti-correlate with gene expression in neuron, which is in contrast to findings from pluripotent human stem cells in culture. More recently, we have developed single-cell RNA-seq approach to profile individual neural stem cells and different neuronal subtypes that are involved in adult neurogenesis in vivo. These next-generation sequencing techniques provide us tools to obtain a complete molecular signature of cell identify and neuronal activity-induced transcriptional and epigenomic changes.

PRES SYMP 2

The Functional Analysis of Non-coding Variation: A View from the Retina

Joseph Corbo

Washington University School of Medicine

The majority of functional variation in the human genome falls within non-coding regions and is likely to affect the activity of cis-regulatory elements (CREs; i.e., enhancers and promoters).. Consistent with this observation, the majority of hits from genome-wide association studies (GWAS) of complex disease also fall within non-coding regions far from coding sequences and many affect CREs. In this talk, I will discuss our efforts to comprehensively identify the CREs active in the retina.

In addition, I will describe the development of CRE-seq, a novel technique for the massively parallel analysis non-coding variants in vivo. CRE-seq makes it possible to interrogate the effects of thousands of non-coding variants in a single experiment, thus setting the stage for comprehensive 'cis-regulome' analysis (where 'cis-regulome' is defined as all CREs active in a given tissue or a defined disease process). I will present CRE-seq data from retina and brain and discuss its implications for the analysis of genetic variation in both Mendelian and complex disease.

PRES SYMP 3

Mass Spectrometry for Detecting Proteins and Small Molecules

Peter Nemes; Sally A. Moody; Chiara Manzini
George Washington University

Gene products downstream of transcription help paint a dynamic window into the molecular machinery underlying health and disease states. How proteins, their post-translational chemical modifications, and small molecules (called metabolites) are implicated in developmental processes and homeostatic balances is central to a systems cell biology understanding of developmental processes. Mass spectrometry is the analytical technology of choice for measuring the expression of thousands of proteins and small molecules without requiring probes or knowledge of their presence in the specimen under investigation. In this presentation, we will overview metabolomics and proteomics by mass spectrometry and then discuss how we have advanced mass spectrometry sensitivity to the point that we are now able to detect and quantify hundreds–thousands of proteins and hundreds of metabolites in single embryonic cells of the early developing embryo of the South African clawed frog (*Xenopus laevis*). We will also provide vignettes on how we use our single-cell mass spectrometers to uncover previously unknown molecular cell heterogeneity in the 8- and 16-cell embryo, discover molecules that are able to alter the normal tissue fate of embryonic cells, and how we use these results to formulate new hypotheses regarding the functional significance of proteins/metabolites during early embryonic development. Last, we will discuss how these technological developments allow us to study gene translation in small populations of mammalian neurons. Mass spectrometry affords exceptional flexibility in characterizing cellular events downstream of gene transcription, i.e., at the levels of proteins and metabolites, thus opening exciting new research potentials in basic and translational research.

PRES SYMP 4

A Cell Type-Specific Approach Towards Understanding Hair Cell Development and Survival

Ronna Hertzano

Department of Otorhinolaryngology, Department of Anatomy and Neurobiology, and Institute for Genome Sciences, University of Maryland School of Medicine

The inner ear is comprised of a multitude of cell types, which together form the sensory epithelium as well as the non-sensory components of the ear. Understanding the signaling cascades which lead to cell type-specific differentiation and survival is critical for the development of regenerative and preventative treatments for hearing loss. Inner ears from both wild type and mutant mice can be used for this purpose. Cell type-specific expression profiles from wild type tissues can be used to identify the key regulatory transcription factors that determine developmental stage-specific cell fate. The unique cell populations can be obtained using fluorescent activated cell sorting, and the transcriptomes using global gene expression analysis of large cell populations or single cells. Examples of such studies in the ear include the identification of ZEB1 and the RFX transcription factors as necessary for development of the sensory epithelium and hair cell terminal differentiation, respectively. Conversely, cell type-specific analysis of mice with mutations in transcription factors of interest can be used to decipher focused regulatory pathways. Finally, inner ear cell type-specific analysis is not limited to flow-cytometry based approaches. Using Ribotag mice, intact tissue can be used for cell type-specific transcriptome analysis, an approach with great promise towards the understanding of both genetic and acquired hearing loss.

PRES SYMP 5

An Epigenetic and Chromatin Structure Perspective on Development and Regeneration in the Organ of Corti

Neil Segil

Department of Stem Cell Biology and Regenerative Medicine and Caruso Department of Otolaryngology/Head and Neck Surgery

Hair cell regeneration in the auditory epithelium of non-mammalian vertebrates relies on the ability of supporting cells to divide and transdifferentiate into sensory hair cells when the hair cells die. While the mature mammalian organ of Corti does not regenerate, the immature supporting cells surrounding the hair cells in perinatal mice harbor a latent potential for proliferation and transdifferentiation. However, this latent regenerative ability is lost as the organ of Corti matures. We have begun to investigate the molecular mechanisms

underlying this transition from a latent permissive state to a non-permissive state of regeneration potential. The focus of our effort is an analysis of the epigenetic and structural changes in chromatin that accompany this transition, along with those changes observed during embryonic development, specifically with regard to the differentiation of hair cells and supporting cells. These chromatin-based changes are further tied to the transcriptional control networks responsible for differentiation and maintenance of cell fate. In keeping with the theme of this Presidential symposium, I will discuss the application of new techniques that have enabled us to analyze the epigenetic and structural changes in chromatin in the small numbers of cells available from the organ of Corti. Finally, I will discuss the shifting chromatin landscape observed as the inner ear continues to mature postnatally, and which we hypothesize underlies the failure of regeneration in this system.

PRES SYMP 6

The Epigenetic Blueprint of the Inner Ear Sensory Epithelium

Karen B. Avraham

Department of Human Molecular Genetics and Biochemistry, Sackler Faculty of Medicine and Sagol School of Neuroscience, Tel Aviv University

Mechanisms of epigenetic regulation have been studied vigorously, gaining a major boost by coupling traditional molecular biology methods with high-throughput Next Generation Sequencing (NGS). This regulatory level, above the DNA sequence, is controlled by a combination of regulatory non-coding RNAs, dynamic nucleosome occupancy, histone post-translational modifications, and DNA methylation. The mammalian inner ear is a complex morphological structure responsible for hearing and balance, with its development subject to a detailed orchestration of regulation. We predict that epigenetic processes play a major role in governing inner ear cellular differentiation processes and functionality. Despite evidence for the importance of epigenetic regulation for the development of components of the inner ear, the international consortia characterizing epigenomic elements, including ENCODE, have not included the auditory system or cells from the inner ear. The reasons for this omission are surely practical; human inner ear tissue is mostly inaccessible and there are no reliable and sufficiently representative cell lines. Dissection of mouse inner ears is challenging and yields a limited numbers of cells. Recently, however, techniques have been developed that enable a reduction in the starting material. As a result, we are investigating multiple levels of epigenetic regulation of cell circuitry in the mouse inner ear sensory epithelium, including the transcriptome, chromatin structure, histone modification, and

DNA methylation, using advances in high-throughput sequencing coupled with technologies such as ATAC-Seq, ChIP-Seq and MethylC-Seq. Following an integrated analysis to build a hierarchical regulatory scheme of auditory pathways, novel regulatory element governing master regulators of development are being identified, allowing us to gain a better understanding of the regulatory network that leads to a fully functional inner ear organ of Corti. Overall, the breakthroughs enabled by epigenomic analysis may help guide the development of therapeutics for hearing loss, by providing multiple entry points for manipulation of the auditory system.

PRES SYMP 7

Use of Single Cell Gene Expression Data for Reconstruction of Spatial and Temporal Aspects of the Developing, Mature, and Regenerating Inner Ear

Stefan Heller

Department of Otolaryngology – Head & Neck Surgery, Stanford University School of Medicine, Stanford, CA 94305

Flow cytometry and single cell transcriptomics are two technical advances that promise to revolutionize the molecular biological analysis of the inner ear. These technologies allow us to obtain quantitative information of mRNA and other RNA species of individual inner ear cells. The high complexity of data in turn creates challenges for data analysis, visualization and communication of findings. Our laboratory has been applying simple and more advanced bioinformatics strategies to investigate a number of exciting and open questions in our field related to early development, tonotopy, and hair cell regeneration. We implemented spatial reconstruction of the positions of individual cells in the developing inner ear as well as in the functionally mature ear of chickens and mice. Moreover, our work has revealed challenges and strategies with respect to resolve transcriptomic features that are spatially driven from changes in cells' transcriptomes that are temporally driven such as in the developing neuroblast lineage, or to discriminate biologically relevant differences among seemingly homogeneous cells.

In this presentation I will show examples for spatial and temporal reconstruction of the developing mouse inner ear from placode to otocyst, for the developing neuroblast lineage, as well as for reconstruction of the tonotopic map of the organ of Corti in the neonate and young adult. Furthermore, I will introduce a novel bioinformatics algorithm that allows us to reconstruct the time courses of expression of hair bundle transcripts in distinct hair cell subtypes the developing chicken utricle. For the mature chicken utricle I will show reconstruction of the spatial map of supporting and hair cell

types using single cell gene expression data, as well as the identification of transcriptome changes that happen in vestibular hair cells and supporting cells in response to surgical application of a single ototoxic dose of aminoglycoside.

Inner Ear: Drug Delivery

PD 1

Direct Delivery of Antisense Oligonucleotides to the Middle and Inner Ear Improves Hearing and Balance in Usher Mice

Gwenaelle S.G. Geleoc¹; Bifeng Pan²; Christopher M. Tran³; Abhilash Ponnath⁴; Francine M. Jodelka⁵; Hamilton Farris⁶; Frank Rigo⁷; Michelle L. Hastings⁵; Jennifer J. Lentz⁶

¹*Boston Children's Hospital, Harvard Medical School;*

²*Department of Otolaryngology, Boston Children's Hospital, Harvard Medical School;* ³*Department of Otorhinolaryngology, LSUHSC;* ⁴*Neuroscience Center for Excellence, LSUHSC;* ⁵*Department of Cell Biology and Anatomy, Chicago Medical School, Rosalind Franklin University of Medicine and Science, North Chicago, IL, USA;* ⁶*Department of Otorhinolaryngology, Neuroscience Center for Excellence, LSUHSC;* ⁷*Ionis Pharmaceuticals, Carlsbad, CA, USA*

Usher syndrome is a syndromic form of hereditary hearing impairment that includes sensorineural hearing impairment and delayed-onset retinitis pigmentosa (RP). Type 1 Usher syndrome (USH1) is characterized by congenital profound sensorineural hearing impairment and vestibular areflexia, with adolescent-onset RP. Mutations in the USH1C gene account for approximately 6-8% of USH1 cases, however, the USH1C c.216G>A (216A) mutation is responsible for nearly all USH1 cases in the Acadian population in Louisiana, USA and Canada. The 216A mutation creates a cryptic splice site that results in a truncated mRNA and harmonin protein, a protein essential for normal hair cell development and function. Systemic treatment with antisense oligonucleotides targeting the 216A mutation rescues hearing and circling behavior in a mouse model of USH1C containing the c.216G>A mutation. To explore the feasibility of delivering ASOs locally to the ear to treat USH1C, tympanic and round window membrane (RWM) injections of 216A-targeted ASOs were developed in 216AA neonatal mice, and hearing and vestibular function were assessed by auditory-evoked brainstem response (ABR) and circling behavior, respectively. Functional hair cell transduction currents were assessed by evoked stiff-probe deflections of cochlear IHCs. Ush1c gene ex-

pression and splicing was assessed by reverse-transcription PCR analysis of RNA isolated from the inner ear. Normal external ear, tympanic membrane morphology and hearing was observed in 1 month old wild type mice that received trans-tympanic saline or control ASO injections within the first three weeks of life. Although mice younger than 7 days have a particularly underdeveloped middle ear, topical tympanic delivery of ASOs in 216AA mice at postnatal day 4-6 improved Ush1c splicing, partially rescued hearing at low frequency (8 kHz) and significantly reduced circling behavior. P1 injections of 30 microg ASO through the RWM of 216AA mutant mice successfully rescued hearing in the low (5.6 kHz) to mid-frequency (22 kHz) with thresholds as low as 35 dB. Low thresholds were maintained in some but not all mice by 3 months of age. RWM treatment with ASO at P1 also partially rescued cochlear hair cell transduction currents and reduced circling behavior. Correct Ush1c gene transcript splicing, absent from untreated mice, was observed in inner ear tissue after RWM injections. We conclude that local delivery of ASOs to the middle and inner ear in neonatal Ush1c mice can improve hearing and balance, and suggest therapeutic potential of ASOs in Usher syndrome and other hereditary hearing impairments.

PD 2

Fetal Intra-otic Delivery of Antisense Oligonucleotides Restores Hearing and Balance in a Mouse Model of Usher Syndrome Type 1

Lingyan Wang¹; Han Jiang¹; Beth Kempton²; Francine M. Jodelka³; Frank Rigo⁴; Michelle L. Hastings³; Jennifer J. Lentz⁵; John Brigande¹

¹Oregon Hearing Research Center, Oregon Health & Science University; ²Oregon Health & Science University; ³Department of Cell Biology and Anatomy, Chicago Medical School, Rosalind Franklin University of Medicine and Science; ⁴Ionis Pharmaceuticals, Carlsbad, CA, USA; ⁵Department of Otorhinolaryngology, Neuroscience Center for Excellence, LSUHSC

Background

Permanent congenital hearing loss (PCHL) affects 1-3 neonates per 1,000 live births and has a genetic basis in 50% of cases. Novel strategies that correct the causal genetic defect will be required to treat PCHL since regeneration of sensory cells from endogenous, genetically-defective cells cannot be therapeutic. Acadian Usher type 1C patients have a mutation at nucleotide 216 (G>A) in USH1C which encodes the PDZ domain protein harmonin. The mutation introduces a cryptic splice site that is used preferentially producing a deletion in the mRNA, an open reading frame shift, and a truncated protein. The Ush1c216AA mutant mouse

carrying the USH1C mutation is born deaf with vestibular dysfunction and develops vision abnormalities by postnatal day 30 (P30). Neonatal intraperitoneal injection of antisense oligonucleotides (ASO-29) directed against the cryptic splice site mutation increases harmonin protein expression and stereociliary bundle organization, and vestibular function and auditory thresholds are improved. We hypothesize that fetal administration of ASO-29 to the inner ear prior to hair cell formation will facilitate sustained recovery of auditory and vestibular function in the Ush1c mutant mouse.

Methods

200-250 nL of ASO-29 (145 µg/µl) was injected into one otic vesicle per embryo by transuterine microinjection at embryonic day 12.5. Auditory function in ASO-treated mutant and control mice was assessed at P30 by auditory brainstem responses (ABR), distortion product otoacoustic emission testing (DPOAE), and startle responses. Vestibular behavior was evaluated by balance assessments for circling, distance traveled, reaching and swimming. USH1C c.216A splice correction, harmonin immunofluorescence, bundle morphology, and hair cell survival were also quantified.

Results

Average ABR thresholds of 24 ASO-29 treated ears at 8, 16, 24 kHz were 51, 75, and 68 dB SPL and statistically significantly improved compared to untreated mutant thresholds (>85 dB SPL), while no improvement was observed at 32 kHz. A subset of 6/24 treated ears presented average ABR thresholds of 36, 55, 50, and 73 dB SPL and their DPOAE responses were statistically significantly improved. The treated mice exhibited a startle response and failed to demonstrate head bobbing, circling, or reaching abnormalities. Harmonin expression in stereocilia at P30 was restored, bundle ultrastructure was improved, and inner and outer hair cell survival was enhanced.

Conclusion

Fetal, intra-otic delivery of ASO-29 prior to hair cell formation dramatically lowered postnatal auditory thresholds and ameliorated vestibular dysfunction in Ush1c mutant mice. Our data represent the first fetal pharmacotherapeutic intervention to efficaciously treat congenital deafness and vestibular dysfunction.

PD 3

Development Of A Novel Bisphosphonate-7,8-Dihydroxyflavone (DHF) Derivative For Regeneration Of Spiral Ganglion Synapses

David Jung¹; Christine Hamadani¹; Judith S. Kempfle²; Nicholas Koen¹; Kim Nguyen³; Boris Kashemirov³; Charles McKenna³; Albert Edge⁴

¹Harvard Medical School; ²Department of Otolaryngology, Massachusetts Eye and Ear Infirmary, Boston, MA, USA. ³Department of Otolaryngology and Laryngology, Harvard Medical School, Boston, MA, USA. ⁵Department of Otolaryngology, University Tübingen Medical Center, Tübingen, G; ³University of Southern California; ⁴Department of Otolaryngology, Harvard Medical School, Boston, MA, USA, and Eaton-Peabody Laboratory, Massachusetts Eye and Ear Infirmary, Boston, MA, USA

Research background

Improving spiral ganglion neuron (SGN) survival, neurite outgrowth, and synaptogenesis may lead to significant gains for deaf and hearing-impaired patients. There has therefore been intense interest in the use of neurotrophic factors in the cochlea to promote both survival of SGNs and re-wiring of hair cells by surviving SGNs. 7,8-dihydroxyflavone (DHF) is a small molecule that mimics the activity of brain-derived neurotrophic factor (BDNF), which is one of the two primary neurotrophins expressed in the cochlea. Bisphosphonates avidly bind to bone minerals and inhibit osteoclast activity to treat a variety of metabolic bone diseases. We have previously shown that local delivery of bisphosphonate into the mammalian cochlea is non-ototoxic and leads to long-term binding in the modiolus. Our long-term goal, therefore, is to assess the feasibility of exploiting the bone-binding properties of bisphosphonates to anchor DHF and other neurotrophic small molecules within cochlear bone, thereby providing a depot for locally enriched, sustained delivery. As an initial step, we evaluate the activity of a risedronate-DHF hybrid molecule to promote SGN neurite outgrowth and synaptogenesis.

Methods

Risedronate-DHF synthesis: DHF was functionalized by adding a carboxyl group at the para position of its phenyl ring. A DHF-linker intermediate was generated using coupling reagents, and this intermediate was subsequently attached to risedronate, a nitrogen-containing bisphosphonate. Neurite outgrowth and organotypic culture experiments: Dissected SGNs or explants of neonatal cochleae (CBA, p4) were plated. Explants underwent kainic acid treatment, which is thought to model glutamatergic syn-

aptotoxicity. Samples were then treated with risedronate-DHF or control small molecules (400nM). Tissue was fixed for immunohistochemistry using neural and synaptic markers. After imaging with confocal microscopy, neurite outgrowth was measured with ImageJ, and synaptogenesis in explants was evaluated with AMIRA.

Results

The risedronate-DHF hybrid molecule retained ability to stimulate neurite outgrowth in SGN cultures to a degree slightly less than native DHF, while both stimulated neurite outgrowth significantly better than control molecules. Furthermore, in organotypic organ of Corti explant cultures with attached spiral ganglion neurons, risedronate-DHF stimulated synaptic regeneration significantly better than control cultures following kainic acid treatment.

Conclusions

A novel bisphosphonate-DHF hybrid molecule retains neurotrophic properties as measured by neurite outgrowth length and synaptic regeneration in vitro. Future work will assess the functional availability of risedronate-DHF following binding to bone in vitro and in vivo.

Funding

This work was supported by the AAO-HNSF Herbert Silverstein Otolaryngology and Neurotology Research Award.

PD 4

Improved Survival of Spiral Ganglion Neurons Due to the Activation of the p38-mapk Pathway Mediated by Human Platelet Rich Plasma

Athanasia Warnecke¹; Jennifer Schulze¹; Michael Stolle²; Ariane Roemer¹; Thomas Lenarz¹; Martin Dürsinn¹

¹Department of Otolaryngology, Hannover Medical School and DFG Cluster of Excellence Hearing4all;

²Department of Otolaryngology, Hannover Medical School

Platelet-rich plasma (PRP) is an autologous preparation from peripheral blood and contains several growth factors and cytokines involved in tissue repair. Although its neuroprotective and -regenerative properties have been already described, little is known about its effects in the inner ear. We therefore examined the effects of PRP on spiral ganglion neurons (SGN) in vitro.

For all experiments, SGN were isolated from neonatal rats and were cultured in serum-free medium. PRP from human venous blood was added to dissociated spiral ganglion cells. Treatment with PRP (1:10, 1:50) significantly increased the neuronal survival of SGN in dissociated SGN cultures. In addition, PRP promotes neurite

outgrowth when administered in adequate concentrations. Inhibition of the p38-MAPK pathway by SB203580 completely reversed the positive effects of PRP on SGN spiral ganglion neuron survival. The neuroprotective effects of PRP on SGN seem to be also depending on NF- κ B since the increased survival was blocked by the use of Bay11-7082, an irreversible NF- κ B inhibitor.

Overall, PRP improves neuronal survival and neurite outgrowth in SGN in vitro. Preparations from autologous whole blood present an interesting alternative for pharmacological intervention to the inner ear since they contain a balanced and natural composition of trophic factors.

PD 5

Cochlear Purinergic Receptors Contribute to in Vivo Spontaneous Activity in the Developing Auditory System

Travis A. Babola¹; Adam Lombroso²; Alexandra Gribizis²; John Issa¹; Brian Lee¹; Michael Crair²; Dwight Bergles¹

¹Johns Hopkins School of Medicine; ²Yale University

Spontaneous electrical activity is a prevalent feature of the developing nervous system and has been shown to influence the maturation and survival of neurons, as well as refinement of circuits in the brain. In the developing auditory system, bursts of activity originate in the cochlea and propagate through the brainstem and midbrain to the auditory cortex before hearing onset. Although spontaneous activity is initiated in the cochlea, the sequence of events that lead to burst firing of spiral ganglion neurons remains uncertain, in part, because there have been few mechanistic studies performed in vivo. To define the patterns of activity that occur in auditory circuits in vivo and determine the mechanisms responsible, we developed an in vivo method for imaging synchronized neuronal activity in unanesthetized mice before hearing onset. In neonatal prehearing mice, spontaneous activity in the inferior colliculus (IC) was imaged using the genetically encoded calcium indicator, GCaMP6s, expressed in neurons under the SNAP25 promoter. Widefield epifluorescence imaging revealed that periodic large groups of neurons located along the tonotopic axis exhibit spontaneous increases in calcium at this age (P7-9). These events were bilateral, discrete, and spatially restricted. Bilateral cochlear ablation eliminated all activity in the IC, demonstrating that the cochlea is required to generate these events. Unilateral cochlear ablation revealed that although activity from one cochlea is bilaterally represented, there is a strong contralateral bias, consistent with previous in vivo electrophysiological studies of sound evoked activ-

ity after hearing onset. When NBQX, an AMPA receptor antagonist, was applied to the round window membrane of the left ear, activity in the IC mimicked left unilateral cochlear ablation, validating the drug delivery approach. These data indicate that activity in the IC can serve as a proxy of activity in the cochlea, allowing examination of how acute pharmacology and genetic manipulation effect the generation of spontaneous activity in vivo. To test the involvement of the metabotropic ATP receptor P2ry1, which is highly expressed by inner supporting cells in the cochlea, in generating spontaneous activity, a selective P2ry1 antagonist (MRS2500) was applied to the round window membrane. Activity in the IC was dramatically reduced in high frequency zones following acute P2ry1 antagonism, an effect that was mimicked in P2ry1 knockout mice. These studies provide the first in vivo evidence that ATP release within the cochlea promotes burst firing in central auditory circuits.

PD 6

Elucidating the Effects of Sustained Release Steroid-hydrogels on Noise-induced Hearing Loss

Chengjing Zhu¹; Hanna Schöpfer²; Julia Clara Gausterer³; Michael Nieratschker¹; Nodir Saidov¹; Clemens Honeder¹; Franz Gabor³; Christoph Arnoldner¹

¹Department of Otorhinolaryngology, Medical University of Vienna; ²Department of Pathobiology, Institute of Anatomy, Histology and Embryology, University of Veterinary Medicine Vienna; ³Department of Pharmaceutical Technology and Biopharmaceutics, University of Vienna

Glucocorticoids have been widely used for the treatment of inner ear disorders, even though the effectiveness of systemic glucocorticoid application is limited due to low drug concentrations in perilymph and potential concomitant side effects. It has been demonstrated that thermoreversible poloxamer407 hydrogels prolong the delivery of dexamethasone (Dex) to the perilymph and thereby increase drug concentrations in the inner ear. Triamcinolone-acetonide (TAAC), another glucocorticoid, is clinically used in hearing preservation cochlear implantation surgeries. However, the potential otoprotective effects of these two glucocorticoids - applied in poloxamer407-hydrogels - have not been compared in models of noise-induced hearing loss. Therefore, we aimed to directly compare the effects of topical application of Dex- or TAAC-loaded hydrogels on noise-induced hearing threshold shifts.

44 pigmented guinea pigs were exposed to broadband-noise (120dB, 3h). Various hydrogels (6% Dex, 6% TAAC, 30% TAAC and control) were intratympan-

ically applied immediately after noise exposure. Hearing thresholds were recorded by auditory brainstem responses (ABRs) at different points in time. Baseline ABRs were recorded 7 days before the intervention. Additional measurements were performed immediately after noise exposure, immediately after hydrogel injection and at day 1, 3, 7, 14, 21 and 28. After euthanasia, ears were extracted for histological evaluation, which addressed hair cell loss and spiral ganglion cell counts.

All groups showed obvious hearing loss after noise exposure. Hearing threshold shifts at 16 kHz were significantly reduced by the 6% Dex hydrogel at days 1, 3, 7 and 28 and at day 1 in the 6% TAAC group, respectively. No otoprotective effect of the 30% TAAC-hydrogel was found. A preliminary histological analysis showed higher spiral ganglion cell survival in the 6%Dex group. Preliminary data shows a reduced hair cell loss in 6% Dex and 6% TAAC treated animals. Further histological analyses and a final statistical evaluation need be performed to reach a better understanding of the microscopic effects of the glucocorticoid hydrogels.

Our data suggests that sustained topical glucocorticoid delivery exerts otoprotective effects in the setting of noise induced hearing loss and indicates the versatility of drug-loaded hydrogels in the treatment of inner ear disorders.

PD 7

Amniotic Membrane in Cochlear Implantation

Ariane Roemer¹; Mika Sato²; Thomas Lenarz¹; Andrej Kral³; Athanasia Warnecke¹

¹Department of Otolaryngology, Hannover Medical School and DFG Cluster of Excellence Hearing4all;

²Institute of Audioneurotechnology and Department of Experimental Otolaryngology, ENT Clinics, Hannover Medical School, Germany; ³Hannover Medical School, DFG Cluster of Excellence Hearing4all

Why do we need stem cells in cochlear implant surgery? One of the main challenges is poor performance in ambient noise. Immunological processes upon cochlea implantation lead to a fibrotic and osteogenic alteration of the cochlea. To sufficiently activate the neurons, a larger electrical stimulation is needed and a higher threshold is recorded. This in turn leads to higher energy consumption - with more frequent battery changes – and to higher electricity spreading. This spreading leads to an imprecisely electrode-nerve fiber-interaction and thereby to vague speech perception. Due to degeneration of the peripheral process of the auditory nerve, the implant performance is additionally impaired. Amniotic stem cells are known to prevent fibrosis and to exert neuro-

protection by the continuous delivery of growth factors. We therefore hypothesize that amniotic membrane will induce a dendrite growth towards the electrode as well as a reduced scarring during cochlear implantation.

Treating spiral ganglion neurons isolated from neonatal rats with amniotic membrane as well as supernatant derived from culture of amniotic membrane after 48 hours resulted in a significant increase of neuronal survival. This increased survival was highly significant when compared to cultures treated with BDNF. Based on these in vitro finding, animal studies in guinea pigs were performed. After electrode insertion via a cochleostomy, amniotic membrane was used for the coverage of the cochleostomy. In the control group, the cochleostomy was left untreated. All animals were implanted unilaterally and the contralateral side was left untouched and served as control. Auditory brainstem responses as well as radiological imaging were performed after surgery and during recovery time. The termination of the experiment was initiated after 3 weeks after operation. The cochleae treated with amniotic membrane showed an improved healing of the cochleostomy without any adverse effects as confirmed by radiologic or audiologic evaluation.

In summary, amniotic membrane is a promising tool for future biological cochlear electrode implantation. It shows neuroprotective effects as well as advantages in wound healing.

Supported by the Cluster of Excellence “Hearing 4 All”

PD 8

Nanoporous Platinum Coatings on Electrode Surfaces for Local Delivery of Neuroprotective Agents

Jennifer Schulze¹; Kim Kreiskoether²; Dawid Warwas²; Nina Ehlert²; Hans-Christoph Schwarz²; Thomas Lenarz¹; Peter Behrens²; Athanasia Warnecke¹

¹Department of Otolaryngology, Hannover Medical School and DFG Cluster of Excellence Hearing4all;

²Institut für Anorganische Chemie, Leibniz Universität Hannover, Germany and Cluster of Excellence Hearing4all

Overview

The aim of the present study is to improve the function of neural interface electrodes, e.g., cochlear electrode, by enhancing the long-term biointegration and the contact between electrode and nerve fibres. This can be realized by chemical modification of the electrode surface or by integrating a drug delivery system in nanoporous plati-

num coatings. For loading the pores with different drugs, the pore diameter can be adjusted by using different templates. In addition, the impedance can be reduced due to the increased surface of the platinum coatings.

Methods

Nanoporous platinum is deposited electrochemically on metal surfaces using different templates. First, the surfactant Pluronic® F127 is dissolved in aqueous Pt(IV) solution. During the deposition of platinum, Pluronic® F127 is incooperated in the platinum coating and removed subsequently during calcination. Modifications with self assembled monolayers (SAMs) of different thiols are performed to adjust the release behaviour of active agents. Secondly, metal surfaces are coated initially with polystyrene latex beads (PLBs). After template formation, the platinum is deposited electrochemically in the voids of the PLBs layer. Subsequently, the PLBs are dissolved by washing with toluene.

Results

The coatings were characterized by scanning electron microscopy, atomic force microscopy, confocal microscopy, sorption measurements, impedance spectroscopy, and cell culture investigations with NIH3T3 fibroblasts as well as spiral ganglion neurons (SGN) and human bone-derived mesenchymal stem cells (BDMSCs).

Both coating processes lead to coatings containing nanopores with a different size. By using Pluronic® F127 pores with a size of about 10 nm are obtained, applicable for loading with smaller active agents like rolipram. By using PLBs the average pore diameter is increased to 50 nm, corresponding to the size of the beads. These pores can be loaded with larger active agents like the neuroprotective factor BDNF (brain-derived neurotrophic factor) or IGF (Insulin-like growth factor). Depending on the coating thickness, the specific surface area can be increased to 430 cm²·cm⁻². Impedance measurements of the nanoporous platinum coatings show improved impedance in the lower frequency range. Cell culture investigations with NIH3T3 fibroblasts, SGN and BDMSCs indicate a good cell compatibility. Release experiments with rolipram show an adjustable rolipram amount depending on the SAMs.

Conclusion

Nanoporous platinum coatings on electrode surfaces, e.g., cochlear implants, are very promising for biomedical applications by generating a bio-friendly surface and by the delivery of neuroprotective factors. The improved impedance enhances the function of neural electrodes and their long-term stability.

Multisensory Interplay and Plasticity from Cells to Circuits and From Mice to Humans

SYMP 1

Anatomy and Postnatal Development of Multisensory Connections of A1, S1, and V1

Eike Budinger

Leibniz Institute for Neurobiology, Department Systems Physiology

Multisensory integration does not only recruit higher-level association cortex, but also low-level and even primary sensory cortices. I will show that the primary auditory (A1), somatosensory (S1), and visual (V1) cortex of Mongolian gerbils receive convergent inputs from brain structures of non-matched senses. The underlying anatomical pathways include a thalamocortical and a corticocortical system. I will also show that the multisensory connections develop, consolidate, and change within five major phases of the total lifespan of the animals.

SYMP 2

New Insights into Mechanisms Subservicing Cortical Crossmodal Plasticity

M Alex Meredith¹; Stephen G. Lomber²

¹Department of Anatomy and Neurobiology, Virginia Commonwealth University School of Medicine; ²Department of Physiology and Pharmacology, University of Western Ontario

When a major sensory system is lost, the remaining sensory modalities largely take over the vacated neural territories in a process called “crossmodal plasticity.” The mechanisms underlying this phenomenon have long been assumed to involve the expansion of adjacent active areas, the ingrowth of projections from novel sources, and/or the unmasking of existing ‘silent’ inputs. However, our recent experiments indicate that the mechanism of crossmodal plasticity following deafness actually is a more complex process involving a pervasive maintenance of thalamic and cortical connections, of laminar-dependent synaptic alterations related to axonal sprouting and overall cartographic changes that interact and occur on a region-specific basis.

SYMP 3

Crossmodal Reorganization of the Auditory Cortex

Patrick O. Kanold

The University of Maryland

One of the hallmarks of the brain is the ability of its circuits to be sculpted by experience. This is especially evident in primary sensory areas during critical pe-

riods in development but also occurs in adult. There is emerging evidence that primary sensory cortices are functionally influenced by other senses beyond their primary inputs. Such influences are behaviorally unmasked after loss of a sensory modality. Circuit changes within the deprived and spared cortical areas are likely underlying the behavioral adjustments. We investigate the effect of short term visual deprivations on the functional responses, meso-scale organization, and circuitry of the auditory cortex. I will discuss research from our lab in mice that use a variety of methods, including in vivo 2-photon imaging, electrophysiology, and in vitro laser scanning photostimulation to map functional responses and circuits.

We find that short-term (1 week) visual deprivation after the critical period can lead to altered auditory responses and functional organization of the auditory cortex. Here describe these phenomena and analyze the circuits that give rise to them. We find that cross-modal plasticity is due to altered thalamocortical and intracortical circuits within the auditory cortex. This circuit refinement allows for a more reliable processing of auditory stimuli. Together we find that large-scale plasticity in the cerebral cortex does not stop after development but is the product of a complex and dynamically changing cortical circuit and that crossmodal influences are particularly effective in recruiting plasticity after the critical period.

SYMP 4

Extreme Functional Flexibility in Developing Human Cortex

Marina Bedny

Johns Hopkins University

Distinct cortical networks support cognitive functions such as audition, vision and language. How do genes and experience determine this specialization? In this talk I will present evidence that early in development human cortex is pluripotent: capable of assuming a wide range of functions depending on input. We find that in blindness visual cortices are recruited during linguistic and mathematical tasks and show increased connectivity with fronto-parietal networks that support language and numerical cognition. This dramatic plasticity follows a sensitive period and appears in blind children by 4-years-of-age. These findings suggest that human cortex is cognitively pluripotent early in development.

SYMP 5

Visual Regulation of Auditory Cortex Development

Todd Mowery¹; Vibhakar Kotak¹; Dan H. Sanes²

¹NYU; ²New York University

Sensory systems do not emerge synchronously, and become integrated with one another as development progresses. To address how this occurs, we asked whether the onset of visual experience regulates development and plasticity of auditory cortex. Delaying the onset of visual activity halts the development of auditory cortical membrane properties. Furthermore, an auditory cortex critical period, during which synaptic inhibition is vulnerable to hearing deprivation, is also regulated by visual experience. Premature eye opening closes the auditory cortex critical period, while delaying eye opening extends it. Together, these findings suggest that developmental plasticity is a polysensory process.

Auditory Nerve I

PS 1

Different Presynaptic Mechanisms Contribute to the Adaption of Auditory Nerve Responses

Alessandro Altoe¹; Ville Pulkki¹; Sarah Verhulst²

¹Department of Signal Processing and Acoustics, Aalto University; ²Medizinische Physik, Dept. of Medical Physics and Acoustics, Oldenburg University, DE and Waves, Dept. of Information Technology, Ghent University

The responses of auditory nerve fiber (AF) to short tones are well described by the sum of a constant term with two exponentially decaying functions with different time constants. The classical interpretation for this phenomenon is based on the idea that the two exponentially decaying terms reflect the kinetics of depletion and replenishment of multiple pools of neurotransmitters [Westerman and Smith, 1988; Meddis, 1986]. However, this interpretation does not account for the presynaptic adaptation mechanisms that occur prior to the exocytosis of neurotransmitters at the inner hair cell (IHC) ribbon synapse. This study quantifies the contribution of the different presynaptic mechanisms to the adaptation of the AF.

To achieve this, we first developed a biophysical model of the IHC that, in response to ciliary bundle deflection, predicts the amount of Ca²⁺ current flowing through the Cav1.3 channels, a quantity directly related to the exocytosis rate at the synapse. Even though this model shares many similarities with previous approaches, it is substantially different in that (i) it employs the large ionic conductances recently established in mature mamma-

lian IHCs, and (ii), it accounts for the kinetics of both activation and inactivation of the Cav1.3 channels. The model predicts that a significant amount of rapid adaptation is present at the level of the Ca²⁺ current (as a consequence of the activation of the K⁺ channels).

Afterwards, the predicted Ca²⁺ current was employed to predict AF responses through a nanodomain model of Ca²⁺ driven exocytosis, which includes a model of neurotransmitter trafficking at the ribbon synapse. The resulting model predicts AF responses that are in good agreement with animal data. Additionally, the model predicts recovery properties of AF responses (and a number of other features) that match the reference animal data well. This study shows that the interaction of different presynaptic mechanisms can result in realistic AF adaptation properties. Those mechanisms include: the action of the K⁺ outward currents, the inactivation of Cav1.3 channels and the depletion of the available neurotransmitter at the synapse.

Fundings: Supported by DFG PP1608, Aalto ELEC Doctoral School and Academy of Finland.

PS 2

A Phenomenological Model of the Synapse Between the Inner Hair Cell and Auditory Nerve: Implications of Limited Neurotransmitter Release Sites

Ian C. Bruce¹; Yousof Erfani¹; Muhammad S. A. Zilany²

¹McMaster University; ²University of Hail

The auditory-periphery model of Zilany et al. (2009, 2014) introduced fractional Gaussian noise and power-law adaptation into a description of the synapse between the inner hair cell and auditory nerve fiber (ANF) to produce non-Poissonian fluctuations in the spike rate. However, the spike-generation is only driven by a single synaptic release process with instantaneous replenishment, consistent with a large number of release sites. Relative refractoriness is implemented with two time constants of 1 and 12.5 ms, which give an accurate distribution of inter-spike intervals (ISIs), but the statistics of successive ISIs are independent. In contrast, Peterson and colleagues have argued that the synapse may have a limited number of release sites (~4) with relatively long average replenishment times (~16 ms), giving rise to the non-independent successive ISI statistic observed in ANFs (Peterson et al., 2014; Peterson and Heil, 2016). We investigated how the approach of Peterson and colleagues could be incorporated into the synapse and spike-generation model of Zilany and colleagues. We modified the spike-generation description to have four identical parallel synaptic release processes, each with

a quarter of the total desired release rate before refractoriness and a 16-ms average replenishment time, along with a separate mechanism for implementing the refractoriness of the ANF. Because of the inclusion of the 16-ms average replenishment time, only a single, short time constant is needed for the relative refractoriness. Preliminary simulations indicate that this modified model generates physiologically-realistic successive ISI statistics and fluctuations in spike-rate over time, which is important in accurately describing the spiking statistics that set the physiological limits for the neural encoding of sounds.

Peterson AJ, Irvine DRF, Heil P (2014) A model of vesicle-pool depletion and replenishment can account for the interspike interval distributions and non-renewal properties of spontaneous spike trains of auditory-nerve fibers. *J Neurosci* 34:15097-15109.

Peterson AJ, Heil P (2016) A revised model of synaptic release accounts for interspike-interval distributions, spike-count distributions, and non-renewal properties of spontaneous spike trains of auditory-nerve fibers. 39th Annual MidWinter Meeting of the ARO.

Zilany MSA, Bruce IC, Nelson PC & Carney LH (2009) A phenomenological model of the synapse between the inner hair cell and auditory nerve: Long-term adaptation with power-law dynamics. *J Acoust Soc Am* 126:2390–2412.

Zilany MSA, Bruce IC, Carney LH (2014) Updated parameters and expanded simulation options for a model of the auditory periphery. *J Acoust Soc Am* 135:283-286.

Supported by NSERC Discovery Grant 261736.

PS 3

The Biophysical Properties of Morphologically Identified Spiral Ganglion Neurons

Alexander Markowitz; Radha Kalluri
University of Southern California

Previous studies using patch-clamp recordings showed that the cell bodies of spiral ganglion neurons are heterogeneous in their ion channel composition. Such heterogeneity may be an important post-synaptic difference shaping the response of spiral ganglion neurons to stimulus intensity. However, spiking in these bipolar neurons does not originate at the cell body, and whether cell bodies with different ion channel compositions belong to afferents that encode different intensities remains unknown. To bridge this gap in knowledge, we are recording from the cell bodies of rat spiral ganglion neurons in semi-intact preparations where the connections between spiral ganglion neurons and their hair cell partners are preserved. By introducing a labeling dye

through each recording pipette we can simultaneously characterize the ion channel properties of an individual cell body and reconstruct its pattern of connectivity with hair cells. With this approach we are testing if the ion channel properties of spiral ganglion neurons vary by their patterns of connectivity with hair cells.

We have recorded by whole-cell patch-clamp electrophysiology from 48 spiral ganglion neurons in semi-intact cochlear preparations from rats ranging in age from post-natal day (P)1 through P16. We successfully reconstructed connectivity patterns between 22 SGN and their partner hair cells. Whole cell currents grew with age and the number of branches on the peripheral dendrite decreased with age. We classified 10/22 SGN as belonging to modiolar contacting (putative high-intensity coding neurons), 7/22 as pillar contacting (putative low-intensity coding neurons) and 5/22 as type II neurons that contacted many outer hair cells. We did not see significant differences in the types of whole-cell currents found in pillar versus modiolar contacting neurons. Because the age dependent growth of whole-cell currents may have obscured correlations with spatial position we standardizing the data across age. Such preliminary analysis suggests that modiolar facing afferents have on average larger whole-cell outward currents than the population mean and fewer terminal branches. Ongoing work is focused on increasing sample size and on at narrower age ranges to disambiguate the significance of maturation versus spatial position on the biophysics of spiral ganglion neurons.

PS 4

Secondary Degeneration of Spiral Ganglion Neuron After Ototoxic Drug Administration Using Various Delivery Approaches

Jae-Hun Lee¹; Min Young Lee²; Phil-Sang Chung²; Jae Yun Jung³

¹*Beckman Laser Institute Korea, College of Medicine, Dankook University, South Korea;* ²*Department of Otolaryngology-Head & Neck Surgery, College of Medicine, Dankook University, South Korea;* ³*Department of Otolaryngology-Head & Neck Surgery, College of Medicine, Dankook University, South Korea*

Background and Objective

Hair cell in the cochlea can be damaged by various causes such as noise, ototoxic drugs, or genetic problem. This damage progresses to the auditory pathway and can sequentially cause additional destructions in the synapse, neurofilament, and spiral ganglion cell, which is referred as secondary degeneration. Establishing and attenuating the secondary degeneration is important because prognosis of the hearing reha-

bilitation is significantly related to the remnant auditory pathway structures after hair cell loss. Still, there is a debate on this degeneration process, and difference of degeneration was found between drug delivery methods and concentrations. Therefore, in this study, we applied different delivery methods for drug induced ototoxicity and evaluated its consequences of remnant auditory pathways.

Materials and Methods

Thirty-five gerbils were divided into four different groups and 150 mg / ml of Kanamycin was applied by percutaneously, with gel-foam, and RWM injection. ABR was measured after one, four, and twelve weeks after drug administration. Also, outer hair cell (OHC)s and Spiral ganglion neurons (SGN)s were counted to evaluate the secondary degeneration.

Results

The results showed that outer and inner hair cells were damaged in all kanamycin treated group. OHCs in percutaneous and gel-foam group were partially destroyed, whereas, total loss of OHCs was found in RWM injection group. Likewise, in OHC and SGN counting, the degree of damage was the severe in RWM injection group than percutaneous or gel-foam group

Conclusion

We have found that there are severe ototoxic damages and secondary degenerations with RWM injection group and also found that there is a secondary damage even after the local application of ototoxic agent with some delivery medium. This outcome will be especially useful in the purpose of the protection of secondary degeneration using gene therapies or other protective agents.

This study was supported by a grant of the Ministry of Science, ICT and Future Planning grant funded by the Korea government (NRF-2012K1A4A3053142).

PS 5

The Middle Ear Acoustic Reflex as a Biomarker of Auditory Nerve Survival

Mark E. Chertoff; Ashlee Martz; Joey Sakumura; Aryn Kameron; Francisco Diaz
University of Kansas Medical Center

Background

Hearing loss results from damage to the inner ear which can lead to degeneration of auditory nerve fibers. The growing effort to cure hearing loss will require new diagnostic tests that identify the site(s) of damage so that biologic treatments can be targeted to specific location. In this study we develop an animal model of the middle ear acoustic reflex (MEAR) to eventually determine if it

can be used as a biomarker for auditory nerve degeneration. The MEAR is sensitive to alterations in the auditory nerve, thus making it a likely candidate for a clinical test of auditory nerve degeneration.

Methods

The pinna was removed from 18 rats (50-250 grams) and the bulla opened to maintain middle ear pressure. A probe consisting of a high-impedance constant volume velocity 800 Hz source and a microphone was sealed into the ear canal. The output of the probe microphone was amplified, rectified, and output to a digital storage oscilloscope. In the opposite ear, stimuli were delivered through a speaker inserted into the ear canal. Reflex activating signals were 3, 10, and 16 kHz and presented at 50-100 dB SPL. In 5/18 animals the reliability of the reflex was examined by recording sequentially 2 input-output level functions. Sound pressure in the probe ear was recorded for 2 seconds followed by the reflex activating signal in the opposite ear for 6 seconds. This 6 second waveform was fit with a 3-parameter exponential function. One parameter indicated the amplitude of the reflex and the other two parameters estimated the rise and decay time of the reflex.

Results

The average intraclass correlation ranged from 0.34 at low signal levels to 0.97 at moderate-to-high signal levels. The amplitude of the MEAR decreased as a function of signal level and the average threshold was 54, 64, and 76 dB SPL for 3, 10, and 16 kHz respectively. The rise time of the response remained constant at 3 kHz but became longer at 10 and 16 kHz as signal level decreased. There was a small decay in amplitude of the MEAR at 3 kHz and larger decay at 10 and 16 kHz.

Conclusions

An animal model was developed to measure the MEAR. The MEAR was most reliable at moderate-to-high signal levels and showed limited decay at 3 kHz. This frequency may be useful for determining the influence of auditory nerve degeneration.

PS 6

Gender Differences in Noise-induced Cochlear Synaptopathy

Ning Hu¹; Steven H. Green²

¹Biology Department, University of Iowa; ²Department(s) of Biology and Otolaryngology

Background

Noise exposure damages cochlear afferent synapses under inner hair cells, even in the absence of hair cell loss or permanent threshold shift (PTS). This noise-induced cochlear "synaptopathy" (NICS) is detectable

in animal models as reduced synapse number by histological examination and, noninvasively, as reduced auditory brainstem response (ABR) wave I amplitude. Correspondingly, a clinical entity, "hidden hearing loss", has been proposed: hearing impairment – e.g., poor speech comprehension in noise – with normal thresholds. Given the noise environment widely experienced in modern society, hidden hearing loss is potentially a major health issue. Sex hormones have been studied for decades with respect to effects on hearing loss due to noise and aging, but the effects on NICS have not yet been studied.

Methods

12-14 week male and female CBA/CAJ mice were exposed for 2 hr to 100 dB SPL 8-16 kHz octave band noise. ABRs at 8, 16, and 32 kHz were measured prior to noise, on post-noise day 1 (PND1), and on PND14 to obtain, respectively, baseline, temporary threshold shift (TTS), and PTS as well as stimulus-response growth at each timepoint. Threshold and amplitude measures at PND1 and PND14 are normalized to prenoise measures for each mouse. Synapses were counted at 8, 16 and 32 kHz regions in PND14 cochlear wholemounts visualized by confocal microscopy. Postsynaptic densities (PSDs) were labeled with anti-PSD95, ribbons with anti-Ribeye, hair cells with anti-myosin 6/7.

Results

Baseline ABR thresholds and amplitudes are similar in male and female mice. TTS, but no PTS, were confirmed in both genders on PND1 and PND14, respectively. ABR wave I amplitudes and cochlear synapse counts on PND14 are significantly reduced in both genders. However, amplitudes and synapse counts are significantly lower in males than females. Moreover, intersubject variability in measures of ABR amplitudes and synapses differs between females and males. In females, there is a bimodal pattern with ~1/3 showing little amplitude decline and synapse loss, and ~2/3 of females showing changes similar to that of the unimodal pattern of males.

Conclusions

Female mice appear to be less susceptible to NICS. However, there is greater variability in individual susceptibility in female than in male mice. We suggest the following hypotheses to be tested: (1) Female sex hormones are protective against NICS. (2) Variability in susceptibility to NICS in female mice is due to the estrous cycle and consequent fluctuation of circulating female hormones.

PS 7

Changes in Temporal Coding of Frequency Modulation Following Inner Hair-cell Impairment

David R. Axe; Michael G. Heinz
Purdue University

Hearing loss is classically characterized by an increase in the threshold of audibility, measured through a pure-tone audiogram. The sensitivity of this test has been called into question since some who enter an audiology clinic reporting difficulty with auditory tasks (e.g., speech recognition) show normal thresholds. It has been suggested that one possible source for these supra-threshold deficits is from degraded coding brought on by the loss or damage of inner hair cells (IHCs). Recent psychophysical work has suggested that frequency modulated (FM) stimuli are ideal for probing these supra-threshold deficits in temporal coding. Temporal coding of FM stimuli is dependent on robust phase-locking to a rapidly changing carrier frequency. At sufficiently high modulation rates when the auditory system is tasked with encoding cycle to cycle differences, robust coding is dependent on the large amount of redundancy built into the system. Damage to IHCs degrades this redundancy in two ways. First, loss of IHCs reduces the total number of inputs into the brain. The volley theory posits that individual auditory-nerve fibers (ANFs) are not individually capable of encoding all the temporal aspects of a stimulus. In order to overcome this limitation the auditory system relies on the large number of ANFs to fully encode all of the important features. When an IHC is lost, the 10-30 ANFs that synapse onto it lose their input and therefore are no longer able to carry information. The second way in which IHC damage reduces the redundancy of the auditory system is through reduced firing rates in fibers that synapse onto dysfunctional IHCs. Our neurophysiological recordings from ANFs in anesthetized chinchillas treated with carboplatin have demonstrated reduced firing rates and shallower slopes of rate-level functions in these animals with IHC dysfunction. In the present study, the hypothesis that IHC dysfunction disrupts the auditory system's ability to encode FM stimuli is tested. This hypothesis is tested at multiple levels including computational-modeling of individual ANFs and physiological measurements of auditory function, including single-unit recordings from ANFs and evoked frequency following responses (EFRs). Initial results show a strong correlation between reduced firing rate due to IHC dysfunction and reduced salience of FM stimuli features in neural responses. This work was supported by NIH (NIDCD) grant R01-DC009838.

PS 8

Hidden Hearing Loss with Envelope Following Responses (EFR): The Off-frequency Problem

Gerard Encina-Llamas¹; Aravindakshan Parthasarathy²; James M. Harte³; Torsten Dau⁴; Sharon G. Kuja-wa⁵; Barbara Shinn-Cunningham⁶; Bastian Epp⁷

¹*Technical University of Denmark*; ²*Eaton-Peabody Labs, Mass. Eye and Ear; Department of Otolaryngology, Harvard Medical School, Boston, MA*; ³*Interacoustics Research Unit*; ⁴*Hearing Systems group, Department of Electrical Engineering, Technical University of Denmark, 2800 Kgs. Lyngby, Denmark*; ⁵*Harvard Medical School and Eaton-Peabody Labs, Massachusetts Eye and Ear Infirmary, Boston MA*; ⁶*Boston University*; ⁷*Hearing Systems, Technical University of Denmark*

Background

The ability to communicate in challenging situations with high levels of background noise is a fascinating property of the healthy auditory system. Despite normal sensitivity to pure-tones, many listeners complain about having difficulties in such situations. Recent animal studies have shown that noise over-exposure that produces temporary threshold shifts can cause the loss of auditory nerve (AN) fiber synapses. This neuronal degeneration has been termed "hidden hearing loss" or, more accurately, "synaptopathy", since it is not reflected in the traditional pure-tone threshold. The envelope following response (EFR) has been proposed as a potential objective method to assess synaptopathy in humans. In this study, an AN computational model was used to investigate the effects of off-frequency contributions (i.e. away from the characteristic place of the stimulus) and the differential loss of different AN fiber types on EFR level-growth functions. The extent to which background noise can mask these off-frequency contributions was also examined.

Methods

EFRs were measured using a 64-channel EEG system with active electrodes. EFR level-growth functions were recorded in adults for SAM tones with a carrier frequency of 2 kHz. Modulations depths of 25% and 85% were tested at sound pressure levels (SPL) of 40 to 90 dB. Subjects were either normally hearing (NH) or mildly hearing impaired (HI) at frequencies above 2 kHz. A humanized AN model (Zilany et al., 2014) was used to simulate the EFR level-growth functions at the tested modulation depths and levels for several degrees of synaptopathy.

Results

The AN model can account for the general trends obtained from human EFR level-growth functions. The simulations reveal that on- vs off-frequency EFR level-growth functions show completely different shapes. Off-frequency contributions have a large impact in the overall EFR magnitudes. The total EFR responses are strongly dominated by the high-SR fibers, especially at lower intensities. Background noise minimize the effects of off-frequency contributions on the overall EFR.

Conclusions

Off-frequency contributions of high-SR fibers dominate the total model EFR responses, suggesting that the loss of low- and medium-SR fibers has only little impact on measured EFRs. However, the impact of off-frequency high-SR fibers is reduced in broadband noise, placing greater emphasis on low- and medium-SR fiber responses.

Funding

This work was supported by CHeSS at the Technical University of Denmark. This work has been done in collaboration with CompNet at Boston University and the Massachusetts Eye and Ear Infirmary, thanks to an ACN Erasmus Mundus scholarship.

PS 9

Temporal Processing Deficits Due to Noise-induced Synaptopathy Studied Using Envelope Following Responses

Aravindakshan Parthasarathy¹; Gerard Encina-Llomas²; Barbara Shinn-Cunningham³; Sharon G. Kuja-wa⁴

¹Eaton-Peabody Labs, Mass. Eye and Ear; Department of Otolaryngology, Harvard Medical School, Boston, MA; ²Technical University of Denmark; ³Boston University; ⁴Harvard Medical School and Eaton-Peabody Labs, Massachusetts Eye and Ear Infirmary, Boston MA

Introduction

Sound overexposure can result in a loss of synapses between inner hair cells (IHC) and the auditory nerve (AN) fibers. Although not manifested as changes in hearing thresholds, this synaptopathy may affect encoding of temporally complex stimuli, especially in conditions of background noise. Here, population envelope following responses (EFRs) were used to study suprathreshold temporal processing in a rodent model of synaptopathy. By also recreating these responses in a computational model of AN response, contributions of different spontaneous-rate (SR) fiber groups and the influence of off-frequency

neurons to encoding suprathreshold sounds were explored.

Methods

EFRs were obtained from CBA/CaJ mice reared in quiet or after single exposure to a known synaptopathic noise that does not cause permanent hearing threshold elevations. EFR stimuli were tones, sinusoidally amplitude modulated (sAM) at 1024Hz that stimulated either synaptopathic or non-synaptopathic cochlear regions. First, tones were presented in quiet with modulation depths of 25% and 85% and sound levels from 20 to 80dB SPL. In the second experiment, fully modulated sAM tones were presented at a suprathreshold sound level, in varying levels of noise. ABR and DPOAE growth functions also were recorded, and immunostained cochlear whole-mounts were used to quantify hair cells and synapses. Results were compared to model-simulated EFRs with varying degrees of noise-induced synaptopathy. Contributions of off-channel, higher frequency neurons to the EFRs, as well as contributions of low, medium and high SR fibers were explored.

Results

Animals with noise-induced synaptopathy showed reduced EFR and ABR amplitudes, even though ABR and DPOAE thresholds and DPOAE amplitudes were recovered. These synaptopathic animals also showed a decreased dynamic range of noise masking in EFRs, relative to controls. The computational model recreated these responses. Off-frequency contributions of high-SR fibers dominated the modelled EFR amplitudes in quiet; however, these contributions were minimized at supra-threshold levels in the presence of noise masking.

Conclusions

Noise-induced synaptopathy causes deficits in temporal processing, as reflected in the EFR. Modelled results can account for the general trends obtained from the EFRs. Specifically, off-frequency contributions of high-SR fibers dominated the total modelled EFR in quiet. However, high-SR fiber contributions were reduced in broadband noise, consistent with a greater role for low- and medium-SR neurons in the temporal processing of sound signals in noise.

Funding provided by DoD W81XWH-15-1-0103 (SGK); CHeSS, Technical University of Denmark and ACN Erasmus Mundus scholarship (GEL).

PS 10

Antioxidant Treatment Reduces Ribbon Synapse Degeneration After Blast Exposure

Qunfeng Cai; Xiaoping Du; Jianzhong Lu; Donald Ewert; Richard D. Kopke
Hough Ear Institute

Background

We have previously shown that treatment with antioxidants shortly after blast exposure can significantly reduce hair cell loss and spiral ganglion neuron degeneration which lead to permanent hearing loss and tinnitus. Because ribbon synapses play an essential role for auditory system transmits sound carried from the inner ear to the brainstem by the cochlear nerve this study was undertaken to determine how blast and antioxidant treatment affected the ribbon synapse in the cochlea.

Methods

The animals (rats) received a baseline measurement of the auditory brainstem response (ABR) thresholds. Rats were randomly placed in one of three groups: 1) blast-exposed, saline treated; 2) blast exposed, antioxidant treated and 3) no blast, no treatment control group. Animals were exposed to an open-field blast of 14 psi. Animals in the treatment group received either a combination of 2,4-disulfonyl a-phenyl tertiary butyl nitron (HPN-07) with N-acetylcysteine (NAC) or saline beginning one hour after blast exposure and twice on the following two days. At 3 weeks post-blast exposure, the ABR test was repeated and then the animals were sacrificed and cochleas processed for histological analysis. Presynaptic receptor CtBP2(c-terminal binding protein) and postsynaptic receptor GluR2/3 (glutamate receptor 2 and 3) were identified by immunostaining. Images of ribbons were collected at six frequencies (2, 4, 8, 16, 32 and 48 kHz) locations in the cochlea by confocal microscopy. The number of ribbons were quantified using Amira software. Hair cells were also counted from apex to base.

Results

When compared to age matched non-blast exposed rats the number of ribbons expressed in cochlea of blast-exposed, untreated rats decreased at 3 weeks by the following percentages: CtBP2+, 22.01% at 16 kHz, 26.68% at 32 kHz; and GluR2/3+ 27.91% at 16 kHz, 31.62% at 32 kHz. There was no significant decrease in the number of ribbons expressing either biomarker for the HPN-07/NAC treated rats after blast exposure relative to controls. Treatment also contributed to decreased hair cell loss as well as protection of ribbon synapses after blast exposure.

Conclusions

Administration of antioxidants shortly after blast exposure contributes to protection ribbon synapses and hair cells in the cochlea.

Funding

This research was supported by grant AR14-020 from The Oklahoma Center for the Advancement of Science and Technology (OCAST).

PS 11

Impaired Auditory Processing and Altered Synaptic Structure in Mice Lacking the *glua3* Subunit of Ampa Receptors

Sofia Garcia-Hernandez; Maria E. Rubio
University of Pittsburgh

AMPA glutamate receptor complexes with fast kinetics subunits -GluA3 and GluA4- are essential for temporal precision in the auditory system. We evaluated the role of the GluA3 subunit in auditory processing using auditory brainstem responses (ABR), to assess auditory function, and electron microscopy, to evaluate the ultrastructure of the auditory nerve synapse on bushy cells (AN-BC synapse), in wild type mice (WT) and mice lacking GluA3 (GluA3-KO). Since GluA3 subunit localization increases on auditory nerve synapses within the cochlear nucleus in response to transient sound reduction, we investigated the role of GluA3 in experience-dependent changes in auditory processing; we induced transient sound reduction by ear plugging one ear and evaluated ABR threshold recovery for 60 days after ear plug removal in WT and GluA3-KO mice. We found that the deletion of GluA3 leads to impaired auditory signaling that is reflected in decreased ABR peak amplitudes, increased latency of peak 2, premature hearing loss and ultrastructural changes in the AN-BC synapse. Additionally, the lack of GluA3 hampers ABR threshold recovery after transient ear plugging. We conclude that GluA3 is required for normal auditory signaling, normal adaptive plastic changes after transient sound reduction and normal ultrastructure of AN-BC synapses in the cochlear nucleus.

Auditory Prostheses: Speech and More

PS 12

Intelligibility Enhancement of Neutral Speech based on Lombard Effect Modification with Application to Cochlear Implant Users

Jaewook Lee; Hussnain Ali; John H.L. Hansen
Center for Robust Speech System – Cochlear Implant Lab (CRSS-CIL), Department of Electrical Engineering, The University of Texas at Dallas

Background

While most cochlear implant (CI) users are able to achieve high levels of speech comprehension, their performance degrades significantly by environmental noise. To ensure robust speech communication, speakers employ “Lombard effect” within their speech production. The Lombard effect is considered a type of stressed speech introduced in the presence of noise, and has been widely studied for normal hearing listeners. Our previous research (Lee et al., 2015) with CI users also confirmed Lombard perturbation in the speech of post-lingually deafened adult CI individuals in response to environmental noise. It was found that speakers altered their vocal effort, including fundamental frequency, vocal intensity, glottal spectral tilt, and formant characteristics in adverse listening conditions. Motivated by this finding, the present study has focused on developing a Lombard effect based speech enhancement algorithm for CI users. In addition, this study addressed how CI users perceive the algorithmically modified Lombard speech in challenging listening environments.

Methods

In order to develop an effective modification scheme, a previous proposed framework based on Source Generator theory (Hansen, 1994) was employed. This theory presumes that speech under noisy environments can be modified by transformation of the neutral speech parameters. Based on this assumption, we modeled speech parametric variations of neutral and Lombard conditions. The modification areas considered in the proposed algorithm were (1) voice intensity, (2) overall spectral contour, and (3) sentence duration. The models for each of the above parameters were trained with the variations across a number of speakers. The speech dataset used for training was derived from UT-Scope corpus (Ikeno et al., 2007). Modification transformations were then calculated based on differences from neutral speaking conditions. The transformations were finally used to modify the speaking style of input neutral speech to generate Lombard synthetic speech.

Results

Acoustic characteristics for the original and modified speech sentences were analyzed. The proposed modifi-

cation algorithm amplified high-frequency region of input speech signal, where is more robust against noise than low-frequency. The modification of neutral speech also resulted in time-stretched input sentence allowing listeners more chance at hearing speech signal. Subjective listening evaluation was performed with six CI users to demonstrate the effectiveness of the proposed speech modification algorithm.

Conclusion

A new speech modification criterion based on the Lombard speech characteristics was proposed. The results could potentially provide perceptual benefits to CI users in noisy environments.

Fund

Research supported by NIDCD/NIH R01 DC010494-01A

PS 13

Simultaneous Presentation of Visual Information with Auditory Input Simulating Cochlear Implant Processors Reduces Memory in Normal-Hearing Listeners

Jasenia Hartman¹; Sara M. Misurelli²; Alan Kan¹; Jake Bergal³; Ruth Litovsky
¹University of Wisconsin-Madison; ²Waisman Center, University of Wisconsin; ³University of Wisconsin-Madison

For patients who use cochlear implants (CIs), there is variable performance in speech-language outcomes. Part of this variability may be attributed to the limited amount of neurocognitive capacity available to process the degraded auditory signal. Preliminary studies in our lab have shown that children with CIs have poorer performance on object recall tasks compared to their normal-hearing (NH) peers, despite receiving both auditory and visual cues. One hypothesis for the poorer performance observed children who listen with CIs is that degraded auditory signals limit the amount of resources devoted to interpreting visual information. In this study, we systematically investigated the effects of degraded auditory input on memory, especially in the presence of a visual aid.

Twenty-four young NH adults were tested using an adaptive, computerized version of the digit span test. Participants were presented with a list of digits, one at a time, and had to recall lists in either forwards or backwards order as a measure of short-term and working memory, respectively. Auditory stimuli were presented via headphones and corresponding visual stimuli appeared simultaneously on a computer monitor. Digits were presented under five conditions: (1) audio-only, (2) degraded audio-only, (3) visual-only, (4) audio+visual,

and (5) degraded audio+visual. In the degraded audio conditions, stimuli were processed through a 4-channel vocoder ([http:// www. tigerspeech.com/angelsim/angelsim](http://www.tigerspeech.com/angelsim/angelsim)). Individual trials were scored using a mean span metric, which is defined as the list length where the 30% threshold of memory remaining was reached based on an estimation using psychophysical procedures.

Results thus far suggest that performance on the digit span test decreases in conditions with a degraded auditory input, despite the presence of non-degraded corresponding visual input. Consistent with previous findings, listeners had lower mean spans in the degraded audio-only vs. audio-only or visual-only conditions. Furthermore, as expected, mean digit span was highest in the audio+visual condition, suggesting that the ability to store and process information increases when stimuli are presented with both auditory and visual modalities. However, mean span was lower in the degraded audio+visual vs. the unprocessed audio+visual conditions, indicating that a degraded auditory signal interferes with the ability to utilize the visual information. These results suggest that the presence of degraded auditory input might have an impact on some neurocognitive processes, such as memory, which may reduce performance in speech comprehension.

Work supported by NSF-GRFP DGE-1256259, NIH-NID-CD (R01DC003083 to RYL, R03DC015321 to AK) and NIH-NICHD (P30HD03352 to Waisman Center).

PS 14

Binaural Benefits for Speech Recognition in Cochlear Implant Users

Fawen Zhang¹; Lamiaa Abdelrehim²; Chun Liang³; Shawn Stevens¹; Lisa Houston¹; Theresa Hammer¹; Ravi Samy¹

¹University of Cincinnati; ²Univerwsit; ³University of Cincinnati

Bilateral hearing can merge sound information from two ears so that the hearing is better than with one ear alone. This binaural benefit may exist in cochlear implant (CI) users in the following different scenarios: bimodal hearing (one ear wears a CI and the other wears a hearing aid), bilateral CI use (BCI), and CI use with single-sided hearing loss (SSD, one ear wears a CI and the other has normal or near normal hearing). A couple of studies have reported that the hearing symmetry between the two ears in BCI and bimodal users is critical for CI users to derive binaural benefits for speech perception (Firszt et al., 2008; Yoon et al., 2011). Further research on binaural benefits in the aforementioned 3 groups is needed in order to provide evidence-based recommendations

to prospective CI users before and after implantation.

The aim of this study is to quantify the bilateral benefits on speech understanding in the above 3 groups of CI users in the CI center of the University of Cincinnati (UC) using retrospective clinical data. The clinical data of the 3 groups of CI users (bimodal, BCI, and SSD) in the past 5 years from UC were collected. The inclusion criteria are: 1) post-lingually deafened CI users; 2) CI users wearing Cochlear devices; 3) native English speaker; 4) CI users without psychiatric or neurological disorders; 5) users who have used a CI for at least 1 year. The numbers of participants for the above 3 groups are 120 for bimodal, 42 for BCI, and 10 for SSD.

Data obtained from clinical records included: 1) demographic data (e.g., duration of deafness, duration of CI use, the degree of residual hearing, and the interval between the two CI surgeries in an individual, etc.), and 2) speech perception scores (CNC words and AzBio sentences in quiet and noise conditions) with left ear only (L), right ear only (R), and bilateral listening conditions (B). Speech and noise were presented at 0° azimuth in free field at the most comfortable loudness level. The binaural benefit was defined as the difference between bilateral performance and unilateral performance with the better ear (Yoon et al., 2011). The difference in unilateral performance between ears (ear difference) was quantified. The correlations between the amount for binaural benefits and the demographic data as well as the ear difference was examined.

PS 15

Benefits of Cochlear Implantation for Single-sided Deafness for Audiological Measures, Speech Understanding, and Localization: Preliminary Data from the House Clinic-USC-UCLA FDA Trial

John Galvin¹; Qian-jie Fu²; Eric Wilkinson³; Eric Lupo³; Dawna Mills³; Suzannah Hagan³; Monica Padilla⁴; Robert Shannon⁴

¹DGSOM, Department of Head and Neck Surgery, SPAPL; ²SPAPL, Department of Head and Neck Surgery, DGSOM, UCLA; ³House Clinic; ⁴Keck School of Medicine, USC

For patients with single-sided deafness (SSD), a cochlear implant (CI) can restore hearing in the deaf ear and improve spatial perception. The aims of this study were to evaluate the benefit of cochlear implantation in SSD patients' sound awareness, localization, and speech perception in both quiet and noise. Here, we report preliminary data for six SSD patients who have enrolled in this FDA-approved study of cochlear implantation for SSD.

All patients had normal hearing (NH) in one ear and severe-to-profound deafness in the other ear. Audiological thresholds, speech understanding in quiet and in noise, and sound source localization, were evaluated before implantation and six months after the CI was activated. Audiological thresholds were quantified as pure-tone average (PTA) thresholds across 500, 1000, and 2000 Hz. Speech understanding in quiet was measured using CNC words and HINT sentences. Localization was measured in sound field using a 12-speaker array. Sentence recognition thresholds (SRTs), defined as the signal to noise ratio (SNR) needed to produce 50% correct word recognition for HINT sentences in noise, were adaptively measured for three spatial conditions: 1) speech and noise from the center (S0N0), 2) speech from center, noise to the CI ear (S0Nci), and 3) speech from the center, noise to the NH ear (S0Nnh).

Mean pre-surgical PTA thresholds were < 11 dBHL in the NH ear and > 92 dBHL in the ear to be implanted; six months after CI activation, PTA thresholds in the CI ear improved to 35 dBHL. Mean CNC word recognition in the CI ear improved from 0% correct before implantation to 47% correct six months post-activation. Mean HINT sentence recognition in the CI ear improved from 0% correct before implantation to 82% correct six months post-activation. For bilateral localization, the mean RMS error improved from 45° before implantation to 33° six months post-activation. For bilateral speech understanding in noise, mean SRTs improved from -1.0 dB before implantation to -4.3 dB six months post-activation for S0N0, from -7.2 dB before implantation to -7.9 dB six months post-activation for S0Nci, and from 0.2 dB before implantation to -2.9 dB six months post-activation for S0Nnh. These preliminary data suggest that cochlear implantation can substantially improve SSD patients' sound awareness, speech understanding in quiet and in noise, and sound source localization.

PS 16

Effects of Independent and Synchronized Agcs on Localization Ability and Speech Intelligibility in Advanced Bionics Cochlear Implant Users

Chen Chen; Dean Swan; Amy Stein; Leonid Litvak
Advanced Bionics

Background

Automatic Gain Control (AGC) is used in cochlear implant front-end signal processing to better use the neural dynamic range. Traditional AGC (hereinafter referred to as 'Independent AGC'), works independently and applies gain separately on each of the two processors for bilateral CI recipients resulting in a loss of binaural cues, especially interaural-level difference (ILD) cues. This

may contribute to one of the reasons why bilateral CI subjects to date fail to achieve similar binaural benefit to normal hearing listeners with two ears. In our research platform, we synchronized the two AGC (hereinafter referred to as 'Synchronized AGC') via the wireless transmission link so that the same gain is applied to both processors therefore preserving binaural ILD cues. In this study we aimed to examine the effect of independent and synchronized AGC on CI users' spatial hearing performance.

Methods

We evaluated localization capability and speech intelligibility for adult 12 Advanced Bionics cochlear implant users. The subject sat in a chair facing 11 speakers in the front hemifield (-75 degrees to + 75 degrees with 15 degree separation). Speech performance was evaluated with speech and noise being presented spatially separated. Localization capabilities were examined for a variety of stationary and moving sounds. Some subjects were also tested in a unilateral wearing configuration.

Results

There is significant improvement in speech intelligibility for spatially separated speech and noise when using Synchronized AGC compared to Independent AGC, suggesting a greater spatial release from masking. Similar improvement is observed when subjects were tested unilaterally with the speech presented on the side ipsilateral to the processor. There is a significant improvement in localization ability with 'fixed target' configuration, and a much bigger improvement is observed for 'moving target' configuration. Localization improvement is also observed when subjects are tested in a unilateral wearing configuration.

Conclusions

Results show that synchronizing the AGC between the two processors leads to better preservation of binaural cues, and therefore improves localization abilities and speech intelligibility for CI users. Synchronizing the AGC may allow them to hear better in a complex listening environment (such as a cocktail party). Further studies involving chronic experience may be needed to investigate real life benefit of AGC synchronization.

PS 17

Memory Span in Adult Cochlear-Implant Users: Relationships with Age under a Self-Paced Manual Response Format

Tracy Wilkinson; Lauren Wilson; Matthew J.

Goupell; Miranda Cleary

Department of Hearing and Speech Sciences, University of Maryland, College Park

Introduction

Short-term and working memory vary across individuals and lifespan. Studies of memory in cochlear-implant (CI) users usually do not disentangle perceptual influences because these investigations rarely check for correct stimulus identification; instead they assume this by using simple practiced stimuli, like digits. Here we examine whether the accuracy and speed of digit identification are associated with short-term and working memory in adults with CIs as a function of age. We compare an intensive memory span assessment using visual-spatial manual responses with traditional digit-span (reliant on a few speech-based trials).

Methods

We measured forward and backward recall for spoken digits in 25 adults with CIs (M=57 yrs; range 20-82 yrs), 7 older NH adults (ONH; >55 yrs), and 10 younger NH adults (YNH; < 22 yrs). Listeners identified recorded digits one at a time by clicking numerals on-screen and then were cued to recall the list. In a comparison condition, listeners only identified each item. Each list length, 1 through 9, was tested ten times. Span was defined as the length at which a listener correctly recalled the entire list 50% of the time. Backward and forward recall were tested separately. NH listeners completed the tasks also with four levels of signal degradation implemented using a channel vocoder: 4 or 8 channels crossed with 0- or 6-mm simulated tonotopic shift.

Results

CI users rarely misidentified digits, even with items in memory (< 1% errors). NH listeners identified only unprocessed and 8-channel 0-mm-shifted tokens this accurately. Other more degraded vocoder conditions produced more errors. Under conditions of equated accuracy, CI and ONH listeners exhibited slower identification reaction times (RTs) with no load than YNH listeners. CI listeners had longer RTs than similar-aged NH listeners. Memory load increased RTs but obscured group effects. We observed shorter spans with increasing age (forward and backward) for CI and NH groups (although not for traditional span). Longer RTs were associated with shorter spans (controlling for age). Unprocessed vs. 8-channel 0-mm spans did not differ for NH listeners.

Conclusion

For many CI listeners, short-term and working memory for digits can be studied with minimal influence of identification accuracy. CI users exhibit age effects on span and RT. A greater age effect on backward vs. forward recall was not observed, inconsistent with working memory being more susceptible to aging than short-term memory. [Work supported by NIH grant R01-DC014948 and the University of Maryland.]

PS 18

Ear Dominance in Bilateral Cochlear-Implant Listeners

Olga A. Stakhovskaya¹; Joshua G.W. Bernstein²;

Matthew J. Goupell³

¹*Walter Reed National Military Medical Center, Bethesda, MD; Department of Hearing and Speech Sciences,*

University of Maryland, College Park, MD; ²Walter Reed National Military Medical Center, Bethesda, MD;

³*Department of Hearing and Speech Sciences, University of Maryland, College Park*

Introduction

Some bilateral cochlear-implants (BiCI) listeners have interaurally asymmetric speech-understanding scores. Asymmetry could be particularly problematic in dichotic listening tasks if listeners are unable to ignore the input from the dominant ear. In extreme cases, asymmetry could even cause unilateral extinction, where no auditory input perceived in the poorer ear. This study investigated how BiCI listeners perform in dichotic listening tasks and if extinction occurs.

Methods

Two groups of BiCI listeners participated. One group had interaurally symmetric IEEI-sentence identification scores in quiet. The second had $\geq 20\%$ asymmetry. In experiment 1, pairs of rhyming words were presented dichotically. Listeners identified the word they heard in a two-alternative forced-choice task and, in a separate task, reported whether the stimulus were perceived in just the left, just the right, or both ears. In experiment 2, pairs of digits were presented dichotically, and listeners reported all of the digits they heard. Both experiments also included diotic and monaural control conditions.

Results

The symmetric group showed no evidence of a strongly dominant ear and correctly identified the stimulus ear(s) in 90-100% of trials. The asymmetric group demonstrated strong better-ear dominance. In experiment 1, they identified the rhyming words presented to the better ear much more often (up to 82% of trials) than the words presented to the poorer ear (as low as 18%). Further-

more, they perceived no stimulus in the poorer ear in approximately 50% of the dichotic trials. In experiment 2, they correctly identified most of the digits (up to 99%) presented in the better ear, but only about 50% in the poorer ear. The performance difference between ears in the dichotic conditions could not be accounted for by differences in monaural performance.

Discussion

BiCI listeners with asymmetric monaural speech-understanding scores demonstrate better-ear dominance. In dichotic listening tasks, they favor the better ear, have difficulty identifying speech in the poorer ear, and in extreme cases seem to experience perceptual extinction. These results suggest that the two ears encode the signals differently, which might be partially attributable to the different hearing histories in the ears. BiCI listeners with asymmetric hearing and relatively strong better-ear dominance may have reduced spatial-hearing abilities compared to more symmetric listeners. [Supported by NIH grant R01-DC014948 and the University of Maryland. The views expressed in this article are those of the authors and do not reflect the official policy of the Department of Army/Navy/Air Force, Department of Defense, or U.S. Government.]

PS 19

Spectral Resolution in Pediatric Cochlear Implant Users and Normal Hearing Children

Mishaela DiNino; Julie A. Bierer
University of Washington

Prelingually-deafened children who receive cochlear implants (CIs) prior to 3 years of age exhibit more favorable outcomes in speech and language development than children implanted at older ages. However, even with early implantation, speech perception performance remains highly variable among pediatric CI users. Accurate speech identification depends on adequate spectral resolution, the ability to discriminate between the frequency components of complex auditory signals. Individual differences in spectral resolution may thus underlie the wide range of speech perception performance in pediatric CI users. Additionally, spectral resolving capabilities have been found to improve with age in normal hearing (NH) children, but the role of both chronological age and hearing age in spectral resolution of children with CIs had not yet been fully elucidated. The aims of this study were 1) to examine the relationship between spectral resolving capabilities and vowel recognition scores in children, and 2) to determine whether or not a developmental time course contributes to performance on these measures.

Pre- and peri-lingually deafened children with CIs between the ages of 8 and 17 performed the spectral-tem-

porally modulated ripple test (SMRT; an assessment of spectral resolution) and a closed-set test of vowel identification. For bilaterally-implanted children, both CIs were tested separately. A group of 8- to 17 year-old NH children also performed the SMRT and identified vocoded vowels, simulating the reduced spectral resolution of CI hearing, to compare normal auditory development to that with a CI. For children with CIs, SMRT performance and vowel identification scores in noise were significantly positively correlated, consistent with data from post-lingually deafened adults with CIs who performed similar assessments of spectral resolution and speech perception. A significant relationship between these measures was not observed for NH children. In addition, NH children's vocoded vowel identification improved with age and plateaued around age 16, but for children with CIs, neither chronological nor hearing age significantly predicted SMRT or vowel recognition scores in quiet or noise. Several bilaterally-implanted children exhibited better performance on these tests with their later-implanted ear than with their earlier-implanted ear. The results of this study demonstrate that variability within individuals and even between the two CIs in the same individual are stronger predictors of spectral resolution than are chronological or hearing age. Future studies will examine the potential contributions of the electrode-neuron interface to better understand spectral resolution in children with CIs.

PS 20

The Role of Spectral Cues for Spatial Release from Masking

Antje Ihlefeld¹; Ruth Y. Litovsky²

¹*New Jersey Institute of Technology*; ²*Waisman Center, University of Wisconsin*,

Background

Cochlear implant (CI) listeners can understand speech in quiet environments, but often have poor speech intelligibility in noisy environments. Bilateral CIs are intended to improve performance in noise, by providing spatial cues to segregate target speech from maskers. In normally-hearing (NH) listeners, this improvement is quantified as spatial release from masking (SRM). However, SRM is reduced or absent in bilateral CI users. One possibility is that SRM relies on resolving spectral differences between competing sounds, and the spectral cues provided by CIs are insufficiently resolved for SRM to occur. Alternatively, perceived similarity between competing sources may be higher for a lower number of spectral bands, thus increasing SRM. Two prior studies have assessed how spectral resolution affects SRM and disagree on whether SRM increases or decreases with an increased number of stimulat-

ing channels. Using sine-vocoded speech, one study found that the fewer bands are presented, the bigger the SRM (Garadat and Litovsky, *J Acoust Soc*, 2009 126). In contrast, using noise-vocoded speech, another study found the opposite effect, where SRM increased with increasing number of bands (Best et al., *J Acoust Soc Am* 2012 131).

Methods

Three experiments tested NH listeners with noise-vocoded speech that was processed to simulate bilateral CIs. Targets consisted of 25 bisyllabic words, with masking sentences. Speech identification was measured as a function of the target-to-masker ratio (TMR), when the two sounds were either spatially separated or co-located. Sounds were presented via headphones. Experiment 1 measured SRM for 4, 8 and 16-band vocoded speech, simulating current spread with 4 dB/mm attenuation. Experiment 2 assessed SRM for 8-band vocoded speech with either 1, 2 or 4 dB/mm attenuation. Experiment 3 measured SRM for 8-band vocoded speech with 4 dB/mm attenuation and response set sizes of two, four or 25 words.

Results

Performance in Experiment 1 improved with increasing number of spectral bands, by 10 dB for each doubling of the number of bands. Moreover, SRM increased with decreasing number of bands. However, Experiment 2 found that when simulated current spread was widened, SRM decreased. Experiment 3 found a strong effect of set size on overall performance but not on SRM.

Conclusions

Together, results support the conclusion that both the number of bands and the amount of current spread control the effectiveness of spatial cues for SRM.

Acknowledgments

Work supported by NIH-NIDCD (R01 DC003083 to RYL, R03 DC014008 to AI) and NIH-NICHD (P30HD03352 to the Waisman Center).

PS 21

A Neural Timing Code Improves Speech Perception in Vocoder Simulations of Cochlear Implant Sound Coding

Rama Ratnam; Erik C. Johnson; Daniel Lee; Douglas L. Jones; Justin Aronoff
University of Illinois at Urbana-Champaign

Although the timing of auditory nerve action potentials, or spikes, has been well-studied, most cochlear implant coding schemes do not explicitly utilize this information. Our recent work has developed a model of opti-

mal neural spike timing, which predicts a minimum-error neural code given a metabolic energy constraint. This model has successfully predicted the times of experimental spikes from sensory neurons. To initially assess whether such a model could improve speech coding in cochlear implants, we created a vocoder incorporating this neural model. The sound signal in eight channels was encoded as a series of pulses with identical amplitudes. These pulses were timed to mimic encoding with spikes. To reconstruct the sound waveform in a channel, the pulses were low-pass filtered to form an estimate of the signal envelope. The pulses were also filtered to estimate the band-limited, non-sinusoidal carrier, which was modulated by the estimated envelope. This study compares the new spike-time vocoder with a standard noise carrier vocoder to test normal-hearing listeners' speech perception and sound localization abilities. Head-related transfer functions (HRTFs) recorded from a KEMAR were used to create spatial cues. Experiment 1 tested listeners' speech perception for the vocoders using the Hearing in Noise Test (HINT) with diotic presentation of identical waveforms. In Experiment 2, to investigate spatial release from masking and binaural squelch, the HINT was repeated using HRTFs, first with the signal and noise co-located and second with the signal and noise separated by 90 degrees in the azimuth. Finally, in Experiment 3, listeners' localization abilities were tested using a short speech sound processed with HRTFs from 12 possible locations. In the case of both Experiment 1 and Experiment 2 with co-located speech and noise, the normal-hearing listeners demonstrated a significant improvement of 2-3dB in speech perception thresholds using the spike-time vocoder. When speech and noise were spatially separated, the speech perception threshold for the new spike-time vocoder were 8.3 dB lower than the standard vocoder. Finally, the localization experiment showed that the subjects, using the spike-time vocoder, localized stimuli with 3.5 degrees less error than the standard vocoder. These results show it is possible to design a vocoder based on the principles of neural spike timing to improve speech perception and sound localization when compared to a standard vocoder. The precise pulse timing of the spike-time vocoder may help encode important perceptual information, which has possible implications for cochlear implant sound-coding.

Auditory Prostheses: Surgical and Stimulation

PS 23

Micro-mechanical Control of Cochlear Implant Electrode Insertion Decreases Maximum Insertion Forces

Christopher Kaufmann; Marlan R. Hansen
University of Iowa Hospitals and Clinics, Department of Otolaryngology- Head & Neck Surgery

Background

Preservation of residual acoustic hearing provides significant benefits for patients receiving a cochlear implant. Yet, there is wide variability in the percent of patients that retain functional acoustic hearing across patient populations, implant centers, and electrode types. The mechanisms leading to hearing loss after cochlear implantation are poorly understood; intracochlear damage due to electrode insertion represents one likely contributory factor. Understanding the factors that contribute to electrode insertional forces is important to develop better methods of avoiding intracochlear trauma. Here a biomechanical based approach was used to evaluate the hypothesis that slower insertion rates will decrease electrode insertion forces.

Methods

A custom micro-mechanical control system was utilized to perform electrode insertions over 20mm through a round window approach at variable insertion rates (1000, 500, 100 $\mu\text{m}/\text{second}$, $n=3$ each) into both a synthetic cochlea model (Utah, Leon et al., 3D Printer: Stratsys, Polyjet HD, 16 μm layers) and cadaveric cochlea (Human cadaveric temporal bones, Embalmed). The insertion forces were measured using a single axis force transducer (Interface, WMCP-1000G-538) and compared to manual hand-forceps insertions. The synthetic and cadaveric cochleae were secured to the transducer orthogonal to long axis of the cochlea. Saline was injected into the cochlea models to mimic the intracochlear fluid environment.

Results

During manual, by-hand forceps insertion at a timed, average rate of $2018 \pm 424 \mu\text{m}/\text{second}$ and $2845 \pm 295 \mu\text{m}/\text{second}$, the average maximum forces were $144.2 \pm 31.5 \text{ mN}$ and $92.5 \pm 3.4 \text{ mN}$ in cadaver and synthetic cochlea models, respectively. The micro-mechanical insertion control system enabled electrode insertions at substantially slower rates than manual insertion. Control system insertion rates with the corresponding insertion forces in synthetic cochlea are shown in Table 1 and Figure 1. At a constant insertion rate of $100 \mu\text{m}/\text{second}$, the average maximum insertion forces were $20.1 \pm 4.1 \text{ mN}$ and $14.1 \pm 4.6 \text{ mN}$ in cadaver and synthetic cochlea models, respectively. Compared to standard manual by-

hand insertion forces, a $100 \mu\text{m}/\text{second}$ constant insertion rate delivered by a micro-mechanical control system showed a 7x decrease in maximum insertion forces as well as a decrease in insertion force variability.

Conclusions

Electrode insertional forces depend on the speed of insertion. Micro-mechanically controlled insertion rates (micron per second) significantly reduce maximum electrode insertion forces. Controlling and standardizing insertion speed and forces could ultimately enhance preservation of residual cochlear structures and hearing.

PS 24

The Pattern and Degree of Capsular Fibrous Sheath Surrounding Cochlear Electrode Array

Reuven Ishai¹; Barbara S. Herrmann¹; Donald K. Eddington¹; Joseph B. Nadol²; Alicia M Quesnel³

¹*Massachusetts Eye and Ear Infirmary, Harvard Medical School*; ²*Human Otopathology Laboratory, Department of Otolaryngology, Massachusetts Eye and Ear Infirmary and Department of Otolaryngology, Harvard Medical School*; ³*Massachusetts Eye and Ear Infirmary, Harvard Medical School*

Background

Although cochlear implants are considered biocompatible, human temporal bone studies have shown that the development of an inflammatory reaction within the cochlea is common. This is typically manifested by fibrosis adjacent to the electrode array, especially at the cochleostomy site where mechanical trauma often occurs. An observation of a thicker fibrous sheath medial to the electrode array led us to consider whether differences in electrode design and electrical current flow may be contributing factors in the development of the fibrous capsule.

Methods

Temporal bones (TBs) from patients who underwent cochlear implantation with Advanced Bionics Clarion or HiRes90K (Sylmar, CA, USA) and Cochlear Corporation Nucleus (Sydney, Australia) devices were studied. The thickness of the fibrous sheath surrounding the electrode array at lower and upper basal turns of the cochlea was quantified using Image J software at the medial, inferior, and superior aspect of the electrode array. Fracture of the osseous spiral lamina and/or marked displacement of the basilar membrane were evaluated as an indicator of insertional trauma. In addition, post-operative word recognition scores, duration of implantation, and post-operative programming data were studied.

Results

Seven TBs of six patients implanted with Advanced Bionics (AB) devices and five TBs of five patients implanted with Nucleus devices were included. A fibrous capsule was present in all twelve TBs. TBs implanted with AB devices had an asymmetric fibrous sheath, which was significantly thicker at the medial side of the electrode array compared to the inferior or superior sides (paired t-test, $p < 0.01$). TBs implanted with Nucleus devices had no difference in the thickness of the fibrous capsule at medial, lateral, and superior locations (paired t-test, $p > 0.05$). Nine of fourteen (64%) TBs implanted with AB devices had fractures of the osseous spiral lamina and/or marked displacement of the basilar membrane compared to two of ten (20%) TBs implanted with Nucleus devices (Fisher exact test, $p < 0.05$). There was no significant correlation between the thickness of the sheath and the duration of implantation or the word recognition score (Spearman rho, $p = 0.06$, $p = 0.4$ respectively).

Conclusion

A thicker fibrous sheath was found on the medial side of implanted AB electrode arrays. This may be explained by a higher incidence of insertional trauma and also asymmetric current flow.

PS 25

A Novel Proximity Sensor System Using Scanning Electrochemical Microscopy and a Thin Film Electrode for Atraumatic Cochlear Implant Insertion

Hirobumi Watanabe¹; Michael Mirkin²; Anil Lalwani¹; Rodolfo Llinas³

¹Columbia University; ²CUNY Queens college; ³NYU Medical Center

The insertion of cochlear implants into the scala tympani is not still free from traumatic damage of basilar membranes and consequent hearing loss. Precise motion control is essential for the insertion of a cochlear implant which should be ideally done with minimum physical contact between the moving device and the cochlear canal walls or the basilar membrane. Because optical monitoring is not possible, alternative techniques for sub millimeter-scale distance control can be very useful. The first requirement for distance control is distance sensing. And, the second requirement is the ability to detect in all directions.

We developed a novel approach to distance sensing based on the principles of scanning electrochemical microscopy (SECM). Further, the SECM was performed using a thin film MEMS based electrode array. The SECM signal, i.e. the diffusion current to a microelectrode, is very sensitive to the distance between the probe sur-

face and any electrically insulating object present in its proximity. With several amperometric microprobes fabricated on the surface of a cochlear implant, one can monitor the distances between different parts of the moving cochlear implant and the surrounding tissues.

Here, a thin film electrode with 8 gold 50 μm square electrodes was fabricated lithographically. The film was wrapped around a 300 μm diameter polyimide tube such that the 8 electrodes face all directions. The tube was inserted into a plastic scala tympani model filled with artificial perilymph solution using a motorized micro actuator. During the insertion, -700 mV of DC was applied to one of gold electrodes with a Ag/AgCl electrode as a counter electrode and the current was monitored. The insertion was repeated 48 times to test the all 8 electrodes (6 times for each). Here, the same trajectory was repeated for all 48 scans and confirmed using two cameras.

One of the 8 channel showed decrease in the current down to 50 % of the maximum current when the electrode approaches the inner wall of the plastic cochlear model. The other electrodes showed decrease in the current as low as 75 % depending on the distance to the wall but all of them were not close enough to call for the danger of contact. We demonstrated that the SECM with MEMS electrodes as a proximity sensor array for cochlear implantation.

PS 26

Perceptual Differences Between Monopolar and Phantom Electrode Stimulation

Silke Klawitter¹; David M. Landsberger²; Waldo Nogueira¹; Andreas Buechner¹

¹Medical University Hannover, Cluster of Excellence "Hearing4all"; ²New York University School of Medicine

Introduction

Phantom electrode (PE) stimulation is achieved by simultaneously stimulating out-of-phase two adjacent intra-cochlear electrodes with different amplitudes. The resulting electrical field is pushed away from the electrode providing the lower amplitude (i.e. apically) and produces a lower pitch. There is great interest in using PE stimulation in a processing strategy as it can be used to stimulate cochlear regions more apical (and producing lower pitch sensations). However, it is unknown if there are perceptual differences between MP and PE stimulation other than a shift in place pitch. Furthermore, it is unknown if the effect and magnitude of changing from MP to PE stimulation is dependent on electrode location. This study investigates the perceptual changes (including pitch and other sound quality differences) at different electrode positions using MP and PE stimu-

lation using both a multidimensional scaling procedure (MDS) and a traditional scaling procedure.

Methods

10 Advanced Bionics users reported the perceptual distance between 5 single electrode (usually 1, 3, 5, 7, and 9) stimuli in either MP or PE ($\sigma = 0.5$) mode. Subjects were asked to report how perceptually different each pair of stimuli were using any perceived differences except loudness. Each pair was presented 5 times (500 total pairs). Subsequently, each stimulus was presented in isolation and subjects scaled how “high” or how “clear” each sounded. Each stimulus was presented 15 times.

Results & Conclusions

Preliminary results from the MDS task suggest that all stimuli differ along a single perceptual dimension organized by electrode number (e.g. cochlear location). While MP and PE stimulation are both organized by the same dimension, the PE stimuli are generally shifted towards a more apical cochlear location than MP stimulation. This suggests that the only perceptual difference between MP and PE stimulation is place of stimulation and that there are no other sound quality differences. However, the differences between MP and PE are larger towards the base. “High” and “Clear” scaling finds that PE is significantly lower in pitch than MP, but no significant effect of “clearness” was observed. The data are supportive of implementing PE stimulation in a strategy without causing any negative perceptual side-effects.

Support provided by the DFG Cluster of Excellence “Hearing4all” and the NIH/NIDCD (R01 DC012152, PI: Landsberger).

PS 27

Modulation of Electrically Excitable Cells via Visible Light and Gold Nanoparticle Coated Microelectrodes

Parveen Bazard¹; Venkat R. Bhethanabotla²; Joseph P. Walton³; Robert D. Frisina⁴

¹Global Center for Hearing and Speech Research, University of South Florida; ²Department of Chemical & Biomedical Engineering, University of South Florida;

³Communication Sciences and Disorders, University of South Florida, Tampa FL, USA; ⁴Global Center for Hearing and Speech Research, University of South Florida, Tampa, FL, USA

Introduction

Excitation of neural signals is essential to restore partially or completely lost sensorineural functions e.g. restoration of hearing using cochlear implants, and to

study brain functions. Presently, electrical stimulation is the benchmark technique for neural excitation. The main disadvantage with electrical currents is the poor spatial resolution, resulting from the spread of electric fields. For instance, deaf people with cochlear implants are unable to resolve speech optimally, partly due to low spatial resolution. Here, we present a novel method of neural modulation using microelectrodes coated with nanoparticles and green visible light, potentially, achieving better spatial resolution than electrical stimulation. Localized surface plasmonic resonance of gold (Au) nanoparticles is used to stimulate and inhibit action potentials in-vitro.

Methods

Approximately 20 nm size Au nanoparticles were coated onto glass micropipettes via aminosilane linkers to fabricate the microelectrodes. Before electrophysiology experiments, microelectrodes were tested for light-induced temperature jumps in response to a 100 mW, 532 nm green visible laser using an electrochemical cell having three electrodes – microelectrode, platinum electrode and reference electrode (saturated calomel electrode). After initial testing, microelectrodes were used to stimulate SH-SY5Y, human neuroblastoma cells which can be differentiated like neurons, and neonatal cardiomyocytes. The cell stimulation experiments were done using patch clamp techniques. Cells were patched by forming a gigaseal in voltage clamp mode and, subsequently, whole cell configuration was achieved by applying slight negative pressure with a 1 ml syringe.

Results

Scanning electron microscope (SEM) images of microelectrodes confirm the uniform coating of Au nanoparticles on the glass micropipette surface. The photocurrents (100–500 nA) were observed when the microelectrodes were illuminated with the green laser and no photocurrents were observed with uncoated micropipettes. Photocurrents had a linear relationship with the voltage, applied to the electrochemical cell. For cell stimulation experiments, the microelectrode was placed next to the patched cell and the laser was focused on the microelectrode tip with the help of an optical fiber. Action potentials were recorded for 1-5 ms, 100-120 mW laser pulses. For large pulses (>10 ms), a shift in membrane potential was observed. When laser pulses were superimposed on electric current pulses, used to record standard action potentials, a reduction in magnitude, and inhibition of the rate of action potentials was observed.

Conclusion

This technology holds promise as a new mode for neural stimulation with improved spatial and frequency resolution, when compared to current forms of electrical stimulation.

Loudness Coding and Pulse Shapes in Cochlear Implant: Does It Matter for Cortical Neurons?

Victor Adenis¹; Yann Nguyen²; Elisabeth Mamelle³; Pierre Stahl⁴; Dan Gnansia⁴; Jean-Marc Edeline⁵

¹NeuroPSI, Univ Paris-Sud, CNRS, UMR9197 Univ Paris-Saclay, Orsay, France; ²1.Sorbonne Universités, Université Pierre et Marie Curie Paris 6, Inserm, Unité 'Réhabilitation mini-invasive et robotisée de l'audition'; 2.AP-HP, GHU Pitié-Salpêtrière, Service ORL, Otologie, implants auditifs, et chirurgie de la base du crâne; ³INSERM et Université Paris-VI, 75005 Paris, France; ⁴Neurelec/Oticon Medical, Vallauris, France; ⁵UMR9197, CNRS, Univ. Paris-Sud

Improving the coding strategies in cochlear implants (CI) is still the subject of intense investigations: the stimulation mode, the pulse shape and grounding schemes can lead moderate to important effects on the spread of excitation, electrode discriminability and nerve excitability. But little is known on the way such changes act at the level of the auditory cortex. This study aims at comparing, with the help of a new custom 3-D representation, the responses obtained from the auditory cortex to stimulations delivered through a cochlear implant in which several parameters were changed.

Experiments were performed in urethane anesthetized guinea pigs (6-18months old). A map of the primary auditory cortex (AI) was first established by inserting an array of 16 electrodes (2 rows of 8 electrodes separated by 1mm and 350µm within a row) and quantifying the tonotopic gradient in AI based on multiunit recordings. A dedicated electrode-arrays (ø400µm) was then inserted in the cochlea (4 electrodes inserted in the 1st basal turn) and its connector was secured on the skull. The 16-electrode array was placed back in the auditory cortex at the exact same location. A dedicated stimulation platform developed by Neurelec/Oticon was used to generate electrical current delivered by the cochlea-implanted electrode. The eight nerve fibers were then stimulated with 20 levels of pulse amplitudes or 20 levels of pulse duration generating similar charges. We also compared cortical activities obtained with squared, ramped or asymmetric pulse shapes. Those parameters are commonly presented as a way to focus the stimulation whereas pulse amplitude and duration are still debated as a way to convey loudness.

The cortical responses evoked by electrical stimulations were often of shorter duration than the acoustic responses; the firing rate evoked by both the pulse duration and pulse amplitude strategies was usually higher than the

one evoked by pure tones. The patterns of activated cortical sites were heavily correlated with the CI stimulating electrode. Furthermore, little differences in the cortical responses were found when the pulse duration was used rather than the pulse amplitude, suggesting that, at the level of the primary auditory cortex, equivalent cortical activation can be achieved by coding sound loudness with pulse amplitude or with pulse duration. Preliminary data will be presented on potential differences between squared, ramped and asymmetric pulses on cortex activation threshold and strength.

PS 29

A Computational Model of Current Shaping in Single-Channel and Multi-Channel Contexts

Arthi G. Srinivasan¹; Robert Shannon²; David M. Landsberger³

¹House Ear Institute; Boys Town National Research Hospital; ²USC; ³New York University School of Medicine

Novel stimulation modes or manipulations for cochlear implants are often initially evaluated using single-channel psychophysical metrics before being implemented in speech processing strategies. However, single-channel psychophysical metrics (such as electrode or virtual channel discrimination) often poorly correlate with multi-channel metrics (such as multi-channel spectral resolution), or with speech perception. Therefore, novel manipulations may provide promising outcomes in single-channel psychophysical metrics but may not result in clear benefit when implemented in a speech processing strategy. One reason for the lack of correlation may be that single-channel metrics are measured in a localized cochlear region, whereas multi-channel metrics and speech perception cover a much larger cochlear extent.

In a previous study, (Srinivasan et al., 2012) the effects of current focusing on spectral discrimination in single and multiple channel contexts were compared using the same manipulation. Results illustrated that single channel results did not predict multiple channel results. Specifically, we showed that some subjects in some cochlear regions received a benefit with current focusing in a single-channel context but no benefit in a multi-channel context, and conversely, some subjects received little benefit with current focusing in a single-channel context and a large benefit in a multi-channel context.

In this study, we implemented a computational model of the spatial properties of current steered electrical stimulation, with and without current focusing. We used this model to manipulate the variables of distance of the electrodes to neurons and the degree of neural survival

to predict the effects of performance in the experiment provided in Srinivasan et al. (2012). Results suggest that particular properties of the electrode-neuron interface can give rise to discrepancies between single-channel and multi-channel metrics. We show that larger electrode-to-neuron distances may yield a situation where there is little benefit of current focusing in single-channel metrics but a larger benefit in a multi-channel context. Additionally, we show that “dead regions” with little or no neural survival may yield a situation where there is a large benefit from current focusing in a single-channel context but little benefit in a multi-channel context. While the model was originally implemented to explain results of Srinivasan et al. (2012) it can be easily extended to explain the effect of other single channel spectral manipulations on multi-channel outcomes.

PS 30

Perceptual Differences in Single Channel Analog and Pulsatile Stimulation

Natalia Stupak¹; Monica Padilla¹; David M. Landsberger²

¹*NYU School of Medicine*; ²*New York University School of Medicine*

Early cochlear implants often used analog signals to stimulate the cochlea. However, with multi-channel implants, the use of analog stimulation was phased out relatively quickly for a number of reasons including battery life conservation and reducing electric field interactions. In modern implants, temporal information is usually provided by amplitude modulations of a relatively high rate biphasic pulse train (AM) although some strategies directly encode temporal information by adjusting the rate of stimulation (RATE). While the physical differences between analog, AM, and RATE stimulation are clearly defined, the perceptual differences between them (if any) are unknown. In this study, we used a multidimensional scaling task to evaluate the perceptual differences between analog, pulsatile (RATE) and amplitude modulated (AM) signals. In the first experiment, stimuli consisted of equally loud stimulation on electrode 2 of 10 Advanced Bionics users. A total of 9 stimuli were used (100, 200, and 400 Hz presented as either analog, RATE, or AM with a 1600 Hz carrier). Subjects were asked to rate “how different” all pairs of stimuli were from each other using a standard multi-dimensional scaling protocol. After adding 150 Hz to the set of stimuli, subjects were asked to scale how “high” and “clean” each was.

A two-dimensional analysis reveals a dimension corresponding to frequency and a dimension separating analog from AM and RATE. For a given frequency, AM and RATE stimuli were perceived similarly. Higher

rates were consistently ranked as higher pitch. Although there was variability across subjects, analog stimulation was ranked differently than AM and RATE for “clean”.

One potential explanation for the differences between analog and the pulsatile stimuli is that analog stimulation is continuous while pulsatile stimuli have relatively large periods of no stimulation (i.e. the interpulse intervals). A follow-up multi-dimensional scaling experiment was conducted to investigate if reducing the interpulse interval (by increasing the carrier pulse rate) of AM stimulation would produce a quality more similar to analog stimulation. However, preliminary analysis suggests that increasing the AM carrier rate does not produce a sound quality closer to analog.

In summary, results show that analog stimulation is perceived quite differently than either AM or RATE stimulation (which in turn are perceived similarly). However, the explanation for the difference in perceptual quality remains unclear.

PS 31

Frequency Modulated Phase Coding Strategy for Cochlear Implants

Reagan Roberts¹; Christopher Boven²; Chris Heddon¹; Claus-Peter Richter³

¹*Resonance Medical, LLC, Chicago*; ²*Neuroscience Program, University of Illinois at Urbana-Champaign*;

³*Department of Otolaryngology-Head and Neck Surgery, Feinberg School of Medicine, Northwestern University & Resonance Medical, LLC, Chicago*

Background

Despite the success of Cochlear Implants (CIs), their performance declines in challenging listening environments and for music. Contemporary CI coding strategies rely on Continuous Interleaved Sampling to restrict adjacent electrodes from firing at the same time and to reduce interactions at neighboring electrodes. This method reduces the ability of CIs to stimulate frequency channels simultaneously, lowering the number of independent channels, and, consequently, frequency resolution. While this restriction is important in terms of disallowing cross-talk between channels, it also restricts the processor’s ability to provide temporal fine structure to the patient. Both temporal envelope and temporal fine structure are important in recognizing speech, distinguishing speech in noise, and for music appreciation. We have devised a new method of converting sound for cochlear implants called Frequency Modulated Phase Coding (FMPC) that encodes sound by varying pulse rate instead of amplitude; in other words, level changes are encoded by rate changes and pitch by place of the

electrode. FMPC keeps current amplitude levels low so parallel electrode stimulation is possible. Additionally, pulse rate encoding allows for the possibility of recreating temporal fine structure in the pulses applied to the cochlea.

Method

The purpose of this study was to compare speech recognition scores of patients utilizing both their own processing strategies and the novel FMPC method. CI users with two different CI brands were included in the study. The amount of charge delivered to the cochlea for stimulation was also determined.

Results

For FMPC, after a 5-minute adaptation period, one manufacturer's patients saw an average speech recognition score of 44% while the other saw an average score of 65% (compared to the 70% average of traditional coding strategies after 1 month of use). The latter manufacturer's group had 4 out of 7 users score above 80% with FMPC. FMPC potentially saves a significant amount of power over current strategies due to a lower average pulse rate (under 200 Hz per channel compared to >1000 Hz fixed rate per channel in current strategies).

Conclusion

The impact of this research will also have a broader reach, as this novel method can be applied to other neural interfaces, such as spinal cord stimulators and retinal implants.

PS 32

Stimulation Location of Cochlear Infrared Neural Stimulation (INS)

Naofumi Suematsu¹; Claus-Peter Richter²; Hunter Young³; Daniel O'Brien⁴

¹Osaka University; ²Department of Otolaryngology-Head and Neck Surgery, Feinberg School of Medicine, Northwestern University & Resonance Medical, LLC, Chicago; ³Department of Otolaryngology-Head and Neck Surgery, Feinberg School of Medicine, Northwestern University; ⁴Northwestern University

Background

It has been previously shown that infrared neural stimulation (INS) can be used in the cochlea. As a stimulation paradigm for cochlear prosthesis development, INS has a clear advantage over electric stimulation with its spatial selectivity. While there are studies showing that cochlear INS is the result of an optoacoustic wave generated by the heating of the perilymph at the tip of the optical fiber, other studies have shown that infrared radiation must be oriented towards the modiolous to elicit

a response. Further, the INS-generated optoacoustic wave has been measured in the cochlea and was found to be insignificant for the application of an auditory prosthesis in hearing-impaired individuals. If the spiral ganglion cells are directly activated by the INS, the induced neural responses are sensitive to changes of stimulation positions. In this study, we will use a 2x1 fiber optic array to compare differences between adjacent stimulation sites and use imaging and 3-D reconstruction to identify target structures. If INS depolarizes the spiral ganglion neurons or hair cells directly, differences between responses from the optical fibers should be greatest when only one fiber is focused on the target structure. Following the experiment, 3-D reconstruction will allow visualization of exactly what structure the fiber optic is oriented towards.

Methods

Pulsed infrared light was applied via a 2x1 array of optical fibers oriented towards the modiolous through a cochleostomy in the basal turn of normal hearing guinea pigs. Compound action potential (CAP) measurements were recorded from each fiber at a series of irradiation levels through a silver wire electrode at the round window. The fiber bundle was then rotated and measurements were repeated. This process was repeated until the fiber bundle completed a full rotation. At the conclusion of the experiment, the fiber bundle was cemented in place for 3-D imaging.

Results

Preliminary CAPs were used to compare inter-fiber differences between fibers at the same rotation angle. When the fibers were perpendicular to the modiolous (along the transverse plane) there was a smaller difference in response than when the fibers were perpendicular to the modiolous (along the frontal plane). Histological analysis using 3-D reconstructions are pending.

Conclusions

The orientation of the optical fiber towards the target structures is critical for stimulation. Preliminary data suggests that the irradiation must be oriented towards the lamina spiralis ossea, behind which is the spiral ganglion.

Acknowledgements

Funded by NIDCD, R01 DC011855

PS 33

The Effect of Mode of Stimulation on the Performance of Cochlear-implant Listeners on the Stripes and Smrt Tests and on the Identification of Vowels and Spondees

Robert P. Carlyon¹; Alan Archer-Boyd¹; Wendy Parkinson²; Julie A. Bierer²

¹MRC Cognition and Brain Sciences Unit; ²University of Washington

A major aim of cochlear-implant (CI) research is to improve speech performance by developing novel speech-processing algorithms and methods of stimulating the electrode array. The use of speech tests to evaluate these new methods is hampered by the fact that listeners have learnt the relationship between the stimulation provided by their everyday life and speech sounds, leading to the possible under-estimation of the benefits of novel methods. Psychophysical tests may overcome this limitation but, we argue, need to satisfy at least two criteria: (i) the subject needs to perform both spectral and temporal processing to perform the task, and should not be able to do so based on the output of any one channel, (ii) stimuli should contain no recognisable speech segments. The STRIPES (Spectro-Temporal Ripple for Investigating Processor Effectiveness) test fulfils these criteria and is described in our accompanying poster (Archer-Boyd et al, this meeting). Here we determine whether STRIPES fulfils another criterion, which is that it should consistently capture the subject-by-subject differences in the effect of different stimulation methods. This is important because novel methods sometimes improve speech perception in some listeners and degrade it in others. Nine Advanced Bionics users were tested on STRIPES and on another spectro-temporal test (SMRT; Aranoff and Landsberger, 2013), using three 14-channel maps in which stimulation was in monopolar (MP), partial tripolar (pTP), or dynamic tripolar (DT; Bierer et al 2016) mode. Results from the first five subjects indicate that performance correlates across stimulation modes between the STRIPES and SMRT tests, even though there were no consistent overall differences between performance in the different modes. Hence both tests are sufficiently sensitive to reveal individual differences in the effect of stimulation mode. However, there was no across-mode correlation between either test and the vowel-identification-in-noise or spondee-identification scores obtained by Bierer et al (2016) for the same subjects and modes. This may be because either (i) the results of spectro-temporal modulation tests are dominated by perceptual judgements that differ from those important for speech perception, (ii) speech tests are less sensitive than spectro-temporal modulation tests, or (iii) the speech tests, which were obtained after only

a few minutes' practice, were affected by the listeners' familiarity with their clinical maps, and that this was not the case for the spectro-temporal modulation tests.

PS 34

In-vivo Piston Efficiency in Direct Acoustic Cochlear Stimulation

Susan Busch¹; Thomas Lenarz²; Hannes Maier¹

¹Hannover Medical School; ²Department of Otolaryngology, Hannover Medical School and DFG Cluster of Excellence Hearing4all

Introduction

Direct acoustic cochlear stimulation, such as in the Cochlear™ Codacs™ Direct Acoustic Cochlear Implant System, use the motion of a piston prosthesis placed in the oval window via stapedotomy to substitute for stapes footplate motion in natural hearing. The transfer function from piston motion to equivalent stapes footplate motion is therefore an indicator of stimulation efficiency. The study investigates this transfer function and possible contributing factors.

Method

Vibration of the tip of the actuator as a function of driving voltage was measured using laser-Doppler-vibrometry (LDV), both on the bench (data provided by Cochlear), and intraoperatively with the piston inserted into the cochlear fluid, in 53 patients. Clinically, perceived loudness as a function of actuator driving voltage was calculated from bone conduction thresholds and "direct thresholds" (determined by using the implant as a signal source) of 58 patients, and expressed as equivalent sound pressure level (eq. dB SPL) at the tympanic membrane. Combining those two datasets, the displacement of a piston of 0.4 mm diameter required for a loudness sensation equivalent to 94 dB SPL was calculated, and compared to the normal range of stapes movement from Rosowski et al. (2007).

Results

Inserting the piston through the stapedotomy into the cochlear fluid attenuates the motion of the piston between 5.3 dB (at 6 kHz) and 11.3 dB (at 1.5 kHz), compared to bench measurements in air. Piston motion at loudness equivalent to 94 dB SPL exceeded the stapes footplate motion at 94 dB SPL from Rosowski (2007) by 32.0 ± 6.0 dB. The difference between piston movement and stapes footplate motion required for the same loudness perception can be mainly explained by a geometric model which accounts for a piston cross-sectional area that is 25-times smaller than the stapes cross-sectional area. It predicts that the expected piston motion is 28 dB higher than the stapes footplate motion.

Conclusion

The Codacs actuator inserted into the cochlea in-vivo is less efficient than in air on the bench. The difference between observed piston motion and referential stapes footplate motion data can be mainly explained by a geometric model based on relative surface area of piston and stapes footplate.

PS 35

Benefits of Cochlear Implantation for Single-sided Deafness for Tinnitus, Dizziness, and Quality of Life: Preliminary Data from the House Clinic-USC-UCLA FDA Trial

Eric Wilkinson¹; Eric Lupo¹; Dawna Mills¹; Suzannah Hagan¹; Qian-jie Fu²; John Galvin³; Monica Padilla⁴; Robert Shannon⁴

¹House Clinic; ²SPAPL, Department of Head and Neck Surgery, DGSOM, UCLA; ³DGSOM, Department of Head and Neck Suregery, SPAPL; ⁴Keck School of Medicine, USC

For patients with single-sided deafness (SSD), cochlear implants (CIs) have been shown to reduce tinnitus severity and improve quality of life (QoL). A total of 10 patients have been enrolled in this FDA-approved study of for cochlear implantation for SSD. Here, we report preliminary data for 6 patients who have thus far completed the protocol. Tinnitus severity, dizziness severity, and QoL were measured before implantation and six months after CI activation.

All patients had normal hearing (NH) in one ear and severe-to-profound deafness in the other ear. Tinnitus severity was measured using a visual analog scale (VAS) with the CI off or on, and using the Tinnitus Functional Index (TFI). Dizziness severity was measured using the Dizziness Handicap Inventory (DHI). QoL was measured using modified versions of the Glasgow Hearing Aid Benefit Profile (GHABP) and the Spatial, Speech, and Quality (SSQ) questionnaires.

All patients were implanted with Med-EI Flex 28 CIs and used the Sonnet processor for the duration of the trial. No surgical complications were reported. All patients were clinically mapped according to standard guidelines for unilateral CI fitting. Mean tinnitus VAS scores six months post-activation were 4.6/10 with the CI off and 3.0/10 with the CI on. Mean TFI scores were 150/250 before implantation and 97/250 six months post-activation. Mean DHI scores were 21/200 before implantation and 27/200 six months post-activation. Across all listening scenarios in the GHABP, mean difficulty was 3.2/5 before implantation and 2.7/5 six months post-activation;

patients generally found the CI to be helpful (3.1/5) and were moderately satisfied with the CI (3.3/5). For the SSQ, mean scores improved from 45/140 before implantation to 66/140 six months post-activation for speech perception, from 45/170 before implantation to 86/140 six months post-activation for spatial perception, and from 101/190 before implantation to 112/190 six months post-activation for quality perception. These preliminary data suggest that cochlear implantation can reduce SSD patients' tinnitus severity and substantially improve QOL, with no increase in dizziness severity.

PS 36

Effects of Phantom Electrode Stimulation on Vocal Production in Cochlear Implant Users

Meredith T. Caldwell; Charles J. Limb; Patpong Jiradejvong

University of California - San Francisco

Cochlear implant (CI) users often demonstrate deficiencies in perception of low frequency sounds. Partial bipolar stimulation on the two most apical electrodes creates a "Phantom Electrode" that allows CI users to access a broader range of low frequencies. Previous research has established potential sound and music quality benefits of Phantom Electrode Stimulation (PES) in comparison to baseline strategies. Here we examined the degree to which PES impacts vocal production in CI users. Advanced Bionics CI recipients (n=8) aged 18+ with at least one year of implant experience were recruited. We designed a vocal production test battery comprised of five sections: tone repetition, vowel repetition, passage reading, picture description, and automatic modulation. Subjects completed the battery once with their baseline strategy and once with PES, in random order. All vocal production was recorded in a soundbooth. In the tone repetition task, subjects were presented with multiple sets of two-tone intervals and asked to repeat them as accurately as possible. In vowel repetition, subjects repeated a set of vowel sounds in response to a written prompt. The passage reading section required subjects to read a short paragraph out loud. During picture description, subjects described photographs for 30 seconds each. Finally, participants read a series of 36 sentences while their program modulated randomly between the two processing strategies. We extracted frequency for all recorded sound files using Praat software and performed statistical analyses using SPSS Statistics. During the tone repetition test, CI users' responses were significantly more accurate (closer to target frequency) in PES than in baseline, particularly in response to complex tones vs. pure tones. Compared to baseline, mean frequency produced in PES was significantly higher in male subjects (not females) and higher in response to pure tones (not complex). Overall frequency range

was significantly narrower in PES. However, analyses based on tone type revealed that frequency range was significantly broader in PES for pure tones and narrower for complex tones. Gender-specific analyses revealed narrower frequency range in females only. Vowel formant repetition results revealed higher F2 and F3 values in PES in females only. Passage reading and picture description results indicate narrower frequency range in PES vs. baseline. These preliminary results suggest that PES may impact multiple aspects of pitch and voice production. Most importantly, PES may improve accuracy of vocal pitch production. Further research is needed to explore the impact of PES on complex sound perception in CI users.

PS 37

What Is the Optimal Spacing Between Electrodes?

Monica Padilla¹; Natalia Stupak¹; David M. Landsberger²

¹NYU School of Medicine; ²New York University School of Medicine

Background

For a fixed electrode length, increasing the number of sites of stimulation along a cochlear implant array increases the spectral representation but also increases the channel interaction. Presumably there is an optimal spacing between sites of stimulation such that spectral sampling is maximized while channel interaction is minimized. Previous studies in which different numbers of physical electrodes are deactivated have suggested that speech understanding typically plateaus after about 8 channels and that increasing the number of electrodes beyond 8 has little effect on performance. These studies are limited in that disabling electrodes provides gaps along the array where the deactivated electrodes are, but do not fundamentally adjust the spacing between contacts.

Methods

In the present experiment, we implemented CIS-like strategies with between 4 and 18 sites of stimulation in Advanced Bionics users. Sites of stimulation were not necessarily presented at physical electrode locations. Instead, they were presented in virtual channel space so that for a given map, the distance between adjacent sites of stimulation were constant in millimeters across the array and that distance between sites of stimulation varied with the number of sites of stimulation. Using each of these strategies, vowels, consonants, HINT sentences and spectral-temporal resolution (SMRT) were measured.

Results and Discussion

Results suggest that the ideal number of channels (and electrode spacing) varies across subjects and task. The spectral-temporal resolution task (SMRT) typically provides peak performance with 10-12 equally spaced electrodes (1.74mm and 10.5mm stimulation site separations). Peak consonant performance requires more of channels (typically 16 to 18 channels). Peak vowel and HINT sentence performance ranges between 10 and 18 channels. No correlation between number of electrodes needed to perform optimally with the SMRT task and with speech (HINT) was found. Optimal performance for many subjects was higher with a reduced number of channels than with their clinical program. This suggests that spacing between electrodes may be an important factor to reduce channel interaction and produce better performance with cochlear implant devices.

PS 38

Design Parameter for an Optical Cochlear Implant

Claus-Peter Richter

Department of Otolaryngology-Head and Neck Surgery, Feinberg School of Medicine, Northwestern University & Resonance Medical, LLC, Chicago

Photonic stimulation has been proposed for neural stimulation in cochlear implants. Two general approaches have been explored: an optogenetic approach and stimulation with infrared light, also called infrared neural stimulation (INS). Increased spatial selectivity with optical stimulation can result in more independent channels to transfer information to auditory neurons. In order to translate the optical stimulation to a clinically feasible device, several constraints must be addressed.

The power required for optical stimulation is larger than that for electrical stimulation by a factor of about 10 for optogenetics and about 100 for INS. This requires the careful configuration of current source for optical stimulation. Power consumption can be minimized by optimally placing the optical sources or by positioning the light delivery system (LDS) correctly. Distance and orientation of the radiation beam are critical to target the spiral ganglion neurons. Another important aspect in designing the LDS is its size and physical property. The LDS can be an array of miniature light sources, a bundle of optical fibers, or a bundle of waveguides. Likewise, a combined opto-electrical hybrid approach must be considered. Both optogenetics and INS are limited by another crucial factor: pulse repetition rate. While the rate-limiting factor in optogenetics relates to the expression rate of the channels in the membranes of the neurons and by the channel dynamics, for INS it is the heat deposition. With each radiation pulse heat is delivered

to the tissue and can lead to a neat heating with subsequent tissue damage. At present, sustained pulse repetition rates for optical stimulation are typically below 250 pulses per second (pps). It has been argued that with contemporary coding strategies such rates are too slow to encode acoustic information. Therefore, a novel coding strategy must be implemented that accommodates low average pulse repetition rates without sacrificing the performance of contemporary coding strategies.

The poster will list and discuss in detail the design control parameters required for a safe human optical cochlear implant prototype.

Funded with federal funds from the NIDCD, R01 DC011855.

PS 39

Auditory Neural Activity in Congenital Deaf Mice Induced by Infrared Laser Stimulation in Cochlea

Xiaodong Tan¹; Israt Jahan²; Yingyue Xu³; Bernd Fritsch⁴; Jaime Garcia-Anoveros³; Claus-Peter Richter⁵

¹Department of Otolaryngology-Head and Neck Surgery, Feinberg School of Medicine, Northwestern University; ²University of Iowa; ³Northwestern University; ⁴University of Iowa, Dept of Biology.; ⁵Department of Otolaryngology-Head and Neck Surgery, Feinberg School of Medicine, Northwestern University & Resonance Medical, LLC, Chicago

Background

The application of infrared neural stimulation (INS) in novel laser-based cochlear implants (CIs) has been proposed, with the potential benefits of higher spatial resolution and larger number of independent channels. While activation of spiral ganglion neurons (SGNs) by INS has been accomplished in different laboratories, irreconcilable controversies exist regarding whether the stimulation is dominated by laser-induced photoacoustic effects or by direct stimulation of SGNs. In this study, INS was applied to three strains of transgenic mice which are congenitally deaf. Atoh1 conditional knock-out (CKO) mice suffer a major hair cell loss and underdeveloped cochleae. Knock-in with Neurog1 (Neurog1 KI) substituting Atoh1 rescued a large number of hair cells (HCs). VGlut3 knock-out (VGlut3^{-/-}) mice have no synaptic transmission between inner HCs (IHCs) and SGNs.

Methods

Infrared light was delivered with a 200 µm optical fiber to different cochlear turns of these animals, ages of 3-5 months. Irradiation evoked compound action poten-

tials (CAPs) and auditory brainstem responses (ABRs) were recorded. Distortion product otoacoustic emission (DPOAE) was also measured to study cochlear non-linearities, likely originated from the function of outer HCs (OHCs). Immuno-fluorescence histochemistry of whole mount cochleae and synchrotron X-ray micro-computed tomography (µCT) imaging of entire cochleae were performed to verify and evaluate the existence of HCs and SGNs.

Results

1) Although SGNs are largely diminished in Atoh1 CKO but intact in the newborns of Neurog1 KI (P7) and Vglut3^{-/-} mice, none of the three strains has any residual hearing even at high sound levels; 2) INS induced ABR or CAP were measured in the apical to the middle but not in the basal turn of Neurog1 KI (5 out of 6, 5/6) and Vglut3^{-/-} (2/3) mice; 3) µCT imaging revealed a complete loss of HCs and SGNs in the basal turn and a large amount of surviving HCs and SGNs in the apical to middle turn of Neurog1 KI mice cochleae; 4) DPOAE was measured in part of the animals (5/7) with positive INS response (both Neurog1 KI and Vglut3^{-/-} mice), suggesting residual functioning OHCs.

Conclusions

Neural activity induced by INS in congenital deaf mice supports a direct activation of SGNs. Furthermore, functioning HCs in Neurog1 KI mice suggests an unclear causality of their deafness. Studies are still ongoing regarding the physiology of type II neurons in Neurog1 KI and Vglut3^{-/-} mice.

Funding

This work is supported by the NIH, R01-DC011855 to CPR and R03-DC013655 to IJ.

PS 40

Optical Pulse Amplitude Modulation for the Stimulation of the Peripheral Auditory System

Patricia Stahn¹; Hubert H. Lim²; Marius P. Hinsberger¹; Katharina Sorg¹; Michaela Schuermann³; Cathleen Schreiter¹; Benjamin Hoetzer¹; Dietmar Hecker¹; Hans-Jochen Foth³; Achim Langenbacher⁴; Bernhard Schick¹; Gentiana I. Wenzel¹

¹Saarland University Faculty of Medicine, Department of Otorhinolaryngology; ²University of Minnesota, Department of Biomedical Engineering; ³TU Kaiserslautern, Department of Physics; ⁴Saarland University Faculty of Medicine, Experimental Ophthalmology

Introduction

Laser light applied at the tympanic membrane (TM) in-

duces vibrations that activate the hearing system. To develop a useful auditory prosthesis, controlled modulation of different frequency channels of the auditory system is necessary to code complex signals such as speech. Using different light sources within one word is currently not possible and therefore, modulation strategies to code the complete audible spectrum using monochrome laser pulses are needed. To investigate these strategies, we compared our results of in vitro, in vivo and in silico measurements in response to optical and acoustic stimulation.

Methods

We inserted a 365 μm diameter optic fiber into the outer ear canal of explanted guinea pig temporal bones and directed it towards the TM. Using a scanning Laser Doppler Vibrometer (LDV, PSV-500, Polytec GmbH, Waldbronn, Germany), we recorded the vibration velocity of the TM after application of 10 ns laser pulses (532 nm Q-switched, INCA-laser system with acousto-optic modulator, Xiton Photonics, Kaiserslautern) modulated as sinusoids. We calculated the vibration displacement of the TM from the measured velocity data. The modulation frequency (MF) ranged between 0.5 and 16 kHz, the carrier frequency or laser pulse rate (LPR) was 32 kHz or 50 kHz, and maximal energy/pulse was between 0 and 10 dB re $1\mu\text{J}/\text{pulse}$. We compared the ex vivo results with the frequency specific recordings within the central nucleus of the inferior colliculus (ICC) in response to optical stimulation and with the results of a convolution based model with those same optical parameters. We performed the calculations, modeling and signal generation with MATLAB® (R2014a, The MathWorks Inc., Natick, USA).

Results

The spectral data showed a strong fundamental frequency corresponding to the MF between 0.5 and 10 kHz. The second harmonic, as well as the LPR were the dominant additional frequencies in each spectrum. However, by using higher LPR, these distortions tend to be smaller and shifted to higher frequencies with lower chance to be perceived. The LDV signals corresponded with the results observed at the ICC level and validated the modeled data.

Conclusions

The results demonstrate in vivo, in vitro and in silico that pulse amplitude modulation might be the solution to achieve frequency specific activation of the peripheral hearing system with frequencies up to 10 kHz. Studies to further examine the optimal fiber position, energy and modulation strategy for optical stimulation of the peripheral hearing organ and to prove its biocompatibility are in progress.

PS 41

Decrease of the Intracochlear Trauma by the Optimization of the Array Insertion Axis During Cochlear Implantation

Renato Torres¹; Guillaume Kazmitcheff²; Mylene Drouillard¹; Daniele De Seta¹; Jean-Loup Bensimon³; Evelyne Ferrary¹; Olivier Sterkers¹; Yann Nguyen¹

¹*1. Sorbonne Universités, Université Pierre et Marie Curie Paris 6, Inserm, Unité 'Réhabilitation mini-invasive et robotisée de l'audition'; 2. AP-HP, GHU Pitié-Salpêtrière, Service ORL, Otologie, implants auditifs, et chirurgie de la base du crâne; 2. Sorbonne Universités, Université Pierre et Marie Curie Paris 6, Inserm, Unité "Réhabilitation chirurgicale mini-invasive et robotisée de l'audition", Paris, France; 3. Lille Nord-Europe, Université Lille-1, Inria, Team Defrost, Lille, France;*
³*Cabinet de Radiologie, Paris, France*

Research background

The optimization of the electrode array insertion has been associated with a decreased cochlear trauma. Studies showed that the insertion axis of the scala tympani can be determined on the current imaging techniques. However, during surgery the mental representation of this insertion axis was variable among surgeons with around 15° of error (Torres et al. 2015). We assess the relationship between the insertion axis and the intracochlear trauma, in a human temporal bone model.

Methods

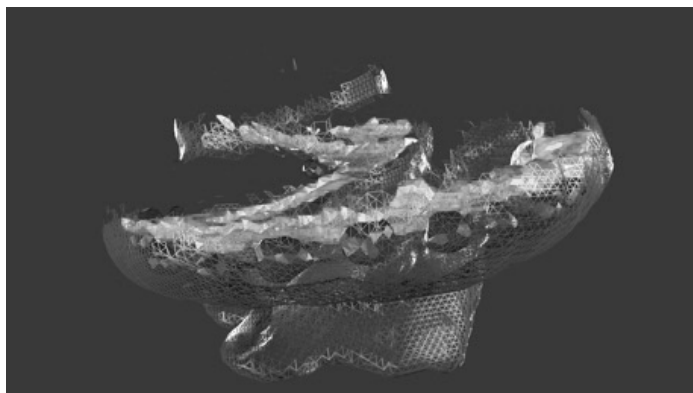
On twelve human temporal bones, a pre-implantation cone beam CT (CBCT) was performed after placement of four fiducial markers (slice interval: 0.125mm). Using Osirix®, the optimal axis was defined considering the inferior extended-round-window cochleostomy site, and the scala tympani center, taking into account the facial nerve position (n=5). The inaccurate axis (n=7) was 15° lower (parallel to the facial nerve position). According to the planned insertion axis, the Digisonic SP EVO® electrode array (Oticon Medical) was loaded in a motorized insertion tool, aligned by a robot prototype (RobOtol, Collin, France) guided by the electromagnetic tracking system FasTrak®, and inserted in a constant speed (0.25 mm/s). A post-implantation CBCT was performed with the same acquisition protocol. A 3D reconstruction was obtained merging the cochlea and the basilar membrane from the pre-operative CBCT and the array from the post-operative CBCT. In order to validate this model, a microscopic analysis of the cochlea was performed to determine the position of each of the 20 electrodes, and the intracochlear trauma associated with the array insertion.

Results

Concerning the position of each electrode, a good reliability was observed between the 3D reconstruction model and the microscopic analysis (Cohen's kappa: 0.67). The use of the inferior extended-round-window cochleostomy was associated with a scala tympani access in all cases. The number of electrodes located in the scala tympani was significantly higher in optimal axis insertions than in inaccurate axis insertions (59% vs. 42%) (Fisher Exact Test $p < 0.05$). Four cases of osseous spiral lamina fracture were observed in the inaccurate axis group (57%).

Conclusion

The 3D reconstruction model is an effective method to identify the position of each electrode of the array in the cochlear scalae. The results of the present study suggest that the optimal insertion axis was associated with a less traumatic insertion than the inaccurate one. Further studies are needed to evaluate the relationship between the electrode position and the hearing of the corresponding frequency.



PS 42

Air- and Bone-Conducted Sources of Feedback with an Active Middle Ear Implant

Renee M. Banakis Hartl¹; James R. Easter²; Mohamed A. Alhussaini¹; Victor Benichoux³; Daniel J. Tollin³; Herman A. Jenkins¹

¹Department of Otolaryngology, University of Colorado School of Medicine; ²Cochlear Boulder, LLC; ³Department of Physiology and Biophysics, University of Colorado School of Medicine

Hypothesis

Active middle ear implants generate both air- and bone-conducted energy that can potentially contribute to the generation of feedback.

Background

Active middle ear implants (AMEI) have been used successfully to treat hearing loss and are particularly useful for patients in whom conventional hearing aids are difficult to fit. Several studies have discussed feedback as a complication in some patients, though the pathway for feedback is not well understood. While reverse propagation of an acoustic signal through the ossicular chain and tympanic membrane can create an air-conducted source of feedback, the implanted position of the device microphone near the mastoid cortex suggests that the bone conduction pathway may be another significant contributor to feedback. Here, we examine the relative contributions of sources of feedback using Laser Doppler vibrometry (LDV) and probe-tube microphone measurements during stimulation with an AMEI.

Methods

Four fresh-frozen hemi-cephalic specimens were prepared with a mastoid antrostomy and atticotomy in order to visualize the posterior incus body. A Carina active middle ear implant actuator (Cochlear Corp.) was coupled to the incus by either of two means: a stereotaxic arm mounted independently of the specimen or a fixation bracket anchored directly to the mastoid cortical bone. The actuator was driven with pure-tone frequencies in $\frac{1}{4}$ octave steps from 500-6000 Hz. Acoustic sound intensity in the ear canal was measured with a probe-tube microphone (GRAS), and bone-conducted vibration was measured using single-axis LDV (Polytec Inc.) from two locations: reflective tape placed on the skin overlying the mastoid, and a titanium implant (Cochlear Ltd.) surgically implanted in the mastoid.

Results

Microphone measurements revealed ear canal pressures of 60-80 dB SPL peaking in the frequency range below 2 kHz. Peak LDV measurements were greatest on the mastoid bone (0.32-0.79 mm/s with the mounting bracket and 0.21-0.36 mm/s with the stereotaxic suspension); peak measurements on the skin ranged from 0.05-0.15 mm/s with the bracket and 0.03-0.13 mm/s with the stereotaxic suspension.

Conclusion

AMEIs produce both air- and bone-conducted signals of adequate strength to be detected by the device microphone and undergo re-amplification. Understanding the relative contribution of these sources may play an important role in the development of specific, targeted mitigation algorithms as well as surgical techniques emphasizing acoustic isolation.

PS 43

Mild Cognitive Impairment Is Characterized by Deficient Hierarchy of Speech Coding Between Auditory Brainstem and Cortex

Gavin M. Bidelman¹; Jill Lowther²; Sunghee Tak³; Claude Alain⁴

¹University of Memphis School of Communication Sciences & Disorders; ²University of Memphis; ³College of Nursing, Seoul National University; ⁴Rotman Research Institute- Baycrest Centre for Geriatric Care

Mild cognitive impairment (MCI) is recognized as a transitional phase in the progression toward more severe forms of dementias and is an early precursor to Alzheimer's disease. Previous neuroimaging studies reveal MCI is associated with aberrant sensory-perceptual processing in cortical brain regions subserving auditory and language function. However, whether the pathophysiology of MCI extends below and prior to engagement of cerebral cortex to negatively impact subcortical speech processing has not been established. Using a novel electrophysiological approach, we recorded both brainstem and cortical speech-evoked brain potentials (ERPs) in hearing-matched listeners who did and did not present with subtle cognitive impairment revealed through behavioral neuropsychological testing. We found that MCI changes the hierarchy of neural coding across various tiers of the auditory brain: declines in neural speech processing were distinct from those of normal aging and emerged as hypersensitivity (larger) brainstem and cortical speech encoding in MCI compared to age-matched controls. Multivariate classification revealed that dual brainstem-cortical speech activity could correctly identify MCI listeners with 80/89% sensitivity/specificity, suggesting application as a biomarker of early cognitive decline. Lastly, among the various classes of ERPs, brainstem responses were a more robust predictor of individuals' MCI severity than cortical activity. Our findings (i) suggest that MCI impacts the neural capture and transfer of speech signals between functional levels of the auditory system and (ii) advance the pathophysiological understanding of cognitive aging by identifying new, subcortical deficits in auditory sensory processing mere milliseconds (< 10 -ms) after sound onset.

PS 44

Comparative Analysis of Spike Threshold Adaptation in Auditory and Vestibular Brain Stem Neural Integrators

Sun Gyeong Rose Lee; Katrina MacLeod
University of Maryland, College Park

Intrinsic firing properties of neurons play a significant role in determining the neural strategies for encoding sensory information. In the chick auditory brain stem, we have found that individual cochlear nucleus neurons employ various input-output functions that range on a spectrum from coincidence detection to broad time scale integration. Furthermore, we found that the variation in intrinsic function correlated with the degree of spike threshold adaptation, suggesting that the dynamic of spike initiation plays an important functional role in these neurons. In the vestibular system, rate coded positional information transmitted by the vestibular afferents is linearly integrated as modulated firing rate outputs by repetitively firing neurons in the medial vestibular nucleus (MVN). We assessed the hypothesis that neurons in MVN achieve linear transformation of sensory information by broad time scale integration and whether such input-output function is related to spike threshold adaptation, similar to the integrator neurons found in the auditory cochlear nucleus. Whole-cell patch-clamp recordings were made from avian medial vestibular nucleus in brainstem slices *in vitro*. To assess intrinsic integration properties, we applied direct, white noise 'fluctuating' current injections into the repetitively firing MVN neurons and measured their firing responses. By systemically varying the mean step amplitude and noise variance, the resulting firing rate-current relation curves resolves repetitively-firing neurons into a range: at one extreme, those that showed the same firing rate regardless of noise fluctuations (integrators); at the opposite extreme, those that showed an increase in firing rate with increased fluctuation amplitudes (coincidence detectors). The quantitative analysis of firing rate curves in MVN clustered the repetitively firing neurons into groups. Most showed no difference in their FI curves with current noise variance, so that firing rate reliably represented the mean current input (integrators); a subset displayed small differences in FI curves with current noise variance (integrator-like). Only a few neurons showed coincidence detector-like properties. To determine the relationship between input-output function and spike threshold adaptation, we compared the sensitivity of voltage threshold with firing rate and mean current amplitude. Integrator MVN neurons exhibited significantly less threshold adaptation compared to other types in MVN, suggesting a relationship between spike threshold adaptation and sensitivity to noisy current fluctuations. These data suggest that one intrinsic property affecting the range of input-output functions of

MVN neurons could be spike threshold adaptation, but other mechanisms, such as afterhyperpolarization, may more strongly modulate spike rate compared to the cochlear nucleus neurons.

PS 45

Frequency-dependent Fine Structure in the Frequency-following Response: The Byproduct of Multiple Generators

Parker Tichko; Erika Skoe

University of Connecticut

The frequency-following response (FFR) is an auditory-evoked response recorded at the scalp that captures the spectrotemporal properties of tonal stimuli. Previous investigations report that the amplitude of the FFR fluctuates as a function of stimulus frequency, a phenomena thought to reflect multiple neural generators phase-locking to the same stimulus with different response latencies. When phase-locked responses are offset by different latencies, constructive and destructive phase interferences emerge, culminating in an attenuation or amplification of the scalp-recorded response in a frequency-specific manner. Borrowing from the literature on the audiogram and otoacoustic emissions (OAEs), we refer to this frequency-specific waxing and waning of the FFR amplitude as fine structure. While prior work was limited by small sets of stimulus frequencies, here, we provide the first systematic investigation of FFR fine structure using a stimulus set that spanned the limits of human pitch perception (90+ frequencies). Consistent with predictions, the magnitude of the FFR response varied systematically as a function of stimulus frequency between 16.35-880 Hz. In our FFR dataset, high points (local maxima) emerged at ~19, 44, 87, 208, and 370 Hz with null points (local minima) emerging ~20, 70, 110, 300, and 500 Hz. To investigate whether these amplitude fluctuations are the result of multiple neural generators with distinct latencies, theoretical FFRs were created to model our FFR dataset. Our modeling revealed that fine structure observed between 16.35-880 Hz can be explained by the phase-interaction patterns created by at least five generators with relative latencies between 0-25 ms. Moreover, our modeling suggests that the longest latency theoretical generator (~25 ms) does not contribute to FFRs above 100 Hz, which is consistent with recent investigations of the anatomical origins of the human FFR that revealed a (longer latency) cortical source for stimulus frequencies around 100 Hz. Collectively, these findings highlight (1) that the FFR is a composite response; (2) that the response at any given frequency can reflect activity from multiple generators; (3) that the fine structure pattern between 16.35-880 Hz is the collective outcome of short- and long-latency generators; (4) that FFR fine structure is epiphenome-

nal in that it reflects how volume-conducted electrical potentials originating from different sources with different latencies interact at scalp locations, not how these different sources actually interact in the brain; and (5) that as a byproduct of these phase-interaction patterns low-amplitude responses will emerge at some frequencies, even when the underlying generators are fully functioning.

PS 46

Changes in Ipsilateral and Contralateral Auditory Brainstem Responses in Preterm Infants During the First Year of Life: The BabyEars Project

Linda J. Hood¹; Beth Prieve²; Mary Edwards¹

¹*Vanderbilt University*; ²*Syracuse University*

Auditory brainstem responses (ABR) show changes in morphology, latency and amplitude well after birth. In particular, responses recorded from contralateral montages show delayed emergence compared to ipsilateral responses (e.g., Coenraad et al., 2011). As part of a longitudinal study of auditory responses in preterm infants (The BabyEars Project), ABR data to date have been collected from preterm infants born at gestational ages from 24-32 weeks. Infants were tested at 33 weeks gestational age (Test 1, n=109 infants), 35 weeks gestational age (Test 2, n=106), 48-52 weeks gestational age (Test 3, n=75) and 62-66 weeks gestational age (Test 4, n=55). ABRs were recorded for click stimuli presented to each ear individually at two intensities (40 and 70 dB nHL) using ipsilateral and contralateral recording montages. Middle-ear and cochlear status were assessed via wideband acoustic absorbance (A) and transient otoacoustic emissions (OAEs). Infants with peaks in A within the 2-4kHz range, present OAEs, and present ABRs for low-intensity (40 dB HL) clicks were included in the current data analysis. Ipsilateral ABRs obtained for clicks at 70 dB nHL were analyzed according to presence of responses, absolute and interpeak latency, and peak-to-peak amplitude. Simultaneously recorded contralateral ABRs were divided into categories of no contralateral response, early latency contralateral response only (in the Waves I-III latency range), and present contralateral response across latencies encompassing the Waves I-V latency range. Ipsilateral ABRs demonstrated expected decreases in latency over the four tests with greater changes for later components. Approximately 10% of infants had no contralateral ABRs on Tests 1 and 2; 55% displayed only early components at Test 1, decreasing to 35% for Test 2. Over 90% of infants demonstrated contralateral responses across the latency range on Tests 3 and 4. Further comparisons examined relationships between ipsilateral response characteristics and emergence of contralateral ABRs. Patterns of ipsilateral and

contralateral ABR latency and morphology changes with age will be presented. The long-term goal of The BabyEars Project is to relate early auditory characteristics to neurodevelopment and speech/language development outcomes. [Supported by NIH-NIDCD R01DC011777]

PS 47

Inter-subject Differences in Amplitude Modulation Encoding Correlate with History of Noise Exposure

Brandon T. Paul; Ian C. Bruce; Sajal Waheed; Larry E. Roberts
McMaster University

Moderate noise exposure has been suggested to permanently damage synapses connecting inner hair cells and auditory nerve fibers while leaving mechanical cochlear function intact. Noise-related synaptic damage appears to be preferential for auditory nerve fibers with low spontaneous rates (LSR fibers) such that suprathreshold encoding is degraded, but threshold responses reliant on high spontaneous rate fibers (HSR fibers) remain relatively unaffected. However there is little evidence linking noise exposure history to suprathreshold encoding deficits in humans with normal audiometric thresholds. In young individuals with normal audiograms, we tested if lifetime noise exposure explained inter-subject differences in two suprathreshold measures: behavioral amplitude modulation detection (AMD) thresholds, and the 86 Hz envelope following response (EFR), an electrophysiological response localizing to the auditory midbrain.

Eleven subjects (3 M, age range 18-19 years, pure-tone thresholds < 25 dB to 16 kHz) have presently participated. Lifetime noise exposure was assessed by questionnaire (Jokitulppo et al., 2006, *Mil. Med.*, 171:112-6). Behavioural detection thresholds for 19 Hz amplitude modulation in a 5 kHz, 75 dB SPL tone were obtained in quiet and in the presence of 1/3 octave narrowband background noise (NBN) at spectrum levels of 25, 40, and 45 dB. EFRs were measured by 32-channel EEG and were evoked by 5 kHz, 75 dB SPL tones that were amplitude modulated at 86 Hz (100% depth). EFRs were also measured in quiet and in the presence of 25, 40, and 45 dB spectrum level NBN. EFR strength was assessed as the phase locking value in each quiet/NBN condition. The effect of background noise on AMD thresholds and EFRs was calculated as the slope of the line fit across the quiet and NBN conditions of each subject.

Preliminary results indicate that subjects with higher lifetime noise exposure had shallower EFR slopes, implying that EFRs of these individuals were less sensitive to changes in increasing background NBN level ($r = 0.61$, $p = 0.04$). Individuals with shallow EFR slopes also tend-

ed to have behavioural AMD thresholds that worsened with increasing NBN level ($r = 0.46$, $p = 0.15$). One interpretation of these results is that individuals with greater noise exposure had more damage to LSR fibers such that phase locking to the AM tone was maximal at low NBN levels and could not decrease further as NBN level increased. As a result, behavioural AM detection at high levels of NBN was degraded. (Supported by NSERC of Canada)

PS 48

Urocortin 3 Signaling in the Auditory Brainstem Decreases the Susceptibility to Age and Noise Induced Hearing Loss

Matthew Fischl¹; James Sinclair¹; Max Bayer¹; Jan Deussing²; Conny Kopp-Scheinplug¹
¹Ludwig-Maximilians University, Munich; ²Max Planck Institute of Psychiatry, Munich

Background

Stress signaling molecules normally associated with the hypothalamic pituitary adrenal axis have been shown to play a role in protection against and recovery from audiogenic stress. Here we look specifically at the stress peptide urocortin 3 (UCN3) and its receptor corticotropin releasing hormone receptor 2 (CRFR2). Our study aims to localize these molecules in the auditory system and gain insight about their role in age and noise induced hearing loss.

Methods

To localize UCN3 in the auditory system we took advantage of a UCN3 Td-Tomato reporter mouse and used various immunohistochemical methods to visualize the expression of UCN3 in the cochlea and auditory brainstem.

Using auditory brainstem response (ABR) recordings, we compare auditory thresholds in UCN3 knockout (UCN3KO) mice against wild type (WT) animals of the same background. We tested thresholds over a range of ages (1-24 months) to calculate rates of aging. We also compared the UCN3KO animals in a noise induced hearing loss protocol where animals were exposed to a single 84 or 94dB noise for 2hr and quantified threshold shifts at several time points (up to two weeks).

Results

We observed immunopositive labeling for UCN3 (UCN3+) in multiple regions of the auditory circuit including the spiral ganglia and cochlear nucleus. UCN3+ terminals were also abundant in the cochlea and in several nuclei of the superior olivary complex. When exposed to noise, the UCN3KOs were more

sensitive (experiencing temporary threshold shifts with 84dB noise) and more susceptible to permanent threshold shifts (significant threshold shifts after 1 week of recovery from the 94dB noise). Even without acoustic overexposure, we found that aging UCN3KO animals tended to lose their hearing more rapidly over the entire mouse audiogram.

Conclusion

Our immunohistochemical data suggest that UCN3 and its receptor CRHR2 show distinct and overlapping expression in multiple areas of the auditory brainstem circuit. The robust staining in auditory neurons and terminals suggests urocortin3 as a new, additional neuromodulator in this system, which rather than being involved in the well-known efferent feedback mechanisms of the MOC and the LOC, may play a novel role in regaining homeostasis after the cessation of audiogenic stress.

PS 49

Modeling the Envelope-Following Response for Mixed Cochlear Gain Loss and Synaptopathy: Towards Improved Hearing Diagnostics

Viacheslav Vasilkov¹; Sarah Verhulst²

¹*Medizinische Physik, Dept. of Medical Physics and Acoustics, Oldenburg University, DE;* ²*Medizinische Physik, Dept. of Medical Physics and Acoustics, Oldenburg University, DE and Waves, Dept. of Information Technology, Ghent University*

Hearing-impaired listeners can have combinations of peripheral hearing deficits yielding reduced sound-discrimination and speech-processing ability. Cochlear gain loss (due to outer-hair-cell deficits) coexisting with synaptopathy (i.e., loss of auditory-nerve synapses at the inner hair cells) could be considered as an example of such a combination that is potentially widespread in humans. Despite the routine audiometric evaluation and increasing focus on auditory evoked responses as a successful approach to reveal synaptopathy, the interplay between these two aspects of hearing loss is still an open question and could play a crucial role in quantifying synaptopathy. In this study we employed a modeling approach to find sensitive envelope-following response (EFR) metrics to isolate synaptopathy in the presence of cochlear gain loss.

The adopted EFR model is a brainstem response model (Verhulst et al, 2012, 2015) that integrates a nonlinear transmission-line representation of cochlear mechanics with a biophysical model of sensorineural transduction (Altoè et al, ARO 2017), and a functional model of the cochlear nucleus and inferior colliculus (Nelson and

Carney, 2004). Frequency-dependent values of gain and width of the modeled cochlear filters were calibrated according to human filter tuning and used to simulate different degrees of gain loss. Cochlear synaptopathy was implemented by reducing the contribution of the different auditory-nerve fiber types.

The simulations show that EFR magnitude and latency can both be affected by cochlear gain loss and synaptopathy. By inducing synaptopathy, the modulated response is (i) decreased (Bharadwaj et al, 2014; Shaheen et al, 2015); and (ii) less delayed, in agreement with the idea that residual high-spontaneous rate fibers have shorter latencies. However, for stimuli at high sound pressure levels (a level-range important for the diagnostics of selective synaptopathy), normal and mild gain loss resulted in an opposite trend for EFR magnitude and delay that compensates the effect caused by synaptopathy. In this context, we suggest a promising role for the first harmonic of the modulation frequency to resolve this contradiction. We examined our model predictions on the basis of recorded amplitude-modulated pure-tone EFR recordings in 20 listeners with mixed hearing pathologies.

A combination of EFR metrics evaluated at the fundamental frequency and harmonics of the stimulus modulator (including EFR magnitude, or magnitude slope as a function of modulation-depth, latency and harmonic strength) is suggested to improve the quantification of synaptopathy in listeners with impaired audiometric thresholds.

Supported by DFG PP1608

PS 50

Relative Brainstem Response Metrics for Isolating Different Aspects of Peripheral Hearing Loss

Markus Garrett¹; Anoop Jagadeesh¹; Sarah Verhulst²

¹*Cluster of Excellence "Hearing4all" and Medizinische Physik, Dept. of Medical Physics and Acoustics, Oldenburg University, DE;* ²*Medizinische Physik, Dept. of Medical Physics and Acoustics, Oldenburg University, DE and Waves, Dept. of Information Technology, Ghent University*

Diagnostic tools such as threshold audiometry are insensitive to cochlear synaptopathy, whereas neurophysiological measures, namely auditory brainstem responses (ABRs) and envelope-following responses (EFRs), have shown a promising link in animal studies. However, the application of ABR/EFR peak measures for diagnostic purposes in humans is aggravated by confounding factors such as head size, gender and noise-floor estimation. Therefore, relative measures of ABR and EFR

metrics, separately or in combination, might be better at disentangling different facets of peripheral hearing loss.

To study the sensitivity of relative ABR/EFR metrics in hearing diagnostics, we measured click-ABRs at different sound intensities and amplitude modulated noise EFRs with different modulation frequencies (120, 40, 5 Hz) and modulation depths (0, -4, -8 dB) in young, normal-hearing listeners with low noise exposure histories (control group). Results were compared to data from hearing-impaired listeners with sloping hearing losses (max. 40 dB HL at 4 kHz).

In the control group we found significant correlations between wave-V amplitudes and 120 Hz EFR magnitudes (SNR) at 100% modulation depth (i.e., at the fundamental frequency as well as the 2nd and 3rd harmonic of the modulator frequency). This suggests that at least a subset of the neurons contributing to the click-ABR, also contribute to the EFR. In agreement with animal physiology observations of cochlear synaptopathy, showing reduced ABR wave growth as a function of increasing intensity and a second independent observation that relates synaptopathy to steeper EFR magnitude-vs.-modulation depth slopes in humans, we found a positive correlation between wave-V amplitude growth and the EFR slope metric. Participants profiting most from an increase in loudness to strengthen the phasic synchrony of the ABRs therefore seem to experience more sustained temporal coding fidelity to decreasing modulation depths. The same relationship was not found in hearing-impaired listeners.

Our results suggest that ABR and EFR measures have partially overlapping neural contributors. However, the hearing-impaired results show a more complex interaction between the ABR/EFR generators as outer-hair-cell loss was shown to impact the relative metrics differently. The use of relative metrics of easily observable neurophysiological correlates of hearing is a promising approach to further shape electrophysiological measures towards a reliable and informative clinical tool.

PS 51

Neurophysiological, Behavioral, and Dosimetric Indices of Noise Exposure in Musicians with Normal Audiometric Thresholds

Erika Skoe; Jennifer Tufts; Christine Hare; Marisa Husereau; Ryan Masi; Sarah Camera
University of Connecticut

Music training has the potential to both strengthen and weaken the auditory system. Recent studies report that musicians have better auditory perception in noise and other acoustically challenging listening conditions, al-

though they are also at an increased risk for noise-induced hearing loss. We currently are undertaking a study that examines the neurophysiological and behavioral indices of noise exposure in college musicians. For seven consecutive days, participants wear a small device, called a dosimeter, that continuously measures environmental sound levels. In this on-going study, we are comparing dosimetry data (LAeqs and noise doses) between musicians and age-matched controls, and examining the degree to which such measures of noise exposure are predictive of hearing thresholds, speech perception in noise (as measured by QuickSIN and Acceptable Noise Level testing), and auditory brainstem response latency and amplitude. The ABR protocol includes suprathreshold click stimuli presented at stimulation rates between 3 and 90 Hz, in addition to a speech stimulus. Preliminary results indicate that college musicians are exposed to considerably higher 24-hour-equivalent sound levels than their non-musician peers, mostly resulting from their participation in music-related activities such as solo practice, rehearsals, and performances. Among the musicians in our current dataset, we are also finding that higher levels of noise exposure are associated with delayed Wave I of the ABR, across both slow and fast stimulation rates. This relationship between noise exposure and Wave I latency emerges even in individuals with clinically normal audiometric thresholds. Moreover, a trend is emerging for individuals with greater noise exposure to have better speech recognition in noise, supporting the possibility that enhanced perceptual abilities in noise observed in previous studies of musicians might be the consequence of increased exposure to high sound levels during music practice and performance. While our question is oriented to musicians, the outcomes of our study may have potential application to the hearing health of any individual at risk for loss of auditory function due to auditory overexposure.

We acknowledge Christopher Briody, Meghan Robitaille, Maggie Small, Michaela Caporaso, and Meghan Brady for their assistance with this project.

PS 53

Multimodal Input Modulates Cartwheel Cell Inhibition of Fusiform Cells in Dorsal Cochlear Nucleus

Calvin Wu; Susan E. Shore
Department of Otolaryngology, Kresge Hearing Research Institute, University of Michigan

Principal output neurons of the dorsal cochlear nucleus (DCN), fusiform cells (FCs), integrate multimodal information from somatosensory, vestibular, and pontine systems, which are relayed by cerebellar-like parallel fibers (PF) of granule cells (Shore and Moore, Hear

Res 1998; Ryugo et al., *Exp Brain Res* 2003). In addition to innervating fusiform cells, PFs also synapse on cartwheel cell (CWC) interneurons that inhibit FCs and other CWCs. How this feed-forward and lateral inhibitory microcircuit in DCN (Roberts and Trussell, *J Neurophysiol* 2010) influences multimodal processing remains unknown. Here, we performed simultaneous CWC and FC recordings in vivo during optogenetic activation of the pontine-cochlear nuclei pathways. We computed spike train cross-correlations to assess inhibitory interactions between CWCs and FCs. As predicted by the spike-timing-dependent plasticity mechanism at the PF-CWC and PF-FC synapses (Tzounopoulos et al., *Nat Neurosci* 2004), bimodal acoustic-pontine nuclei stimulation produced long-term alterations of individual FC and CWC activity. Interestingly, cross-correlation strengths for paired FC-CWC and CWC-CWC were also modified by long-term plasticity, indicating that multimodal input effectively regulates CWC inhibition. These findings suggest that CWCs play an important role in multimodal integration via their influence on FCs, which may be significant in pathologies of hyper-synchrony, such as tinnitus (Wu et al., *J Neurosci* 2016).

Clinical Otolaryngology: Pathology

PS 54

PC-based Evaluation of Mouth Asymmetry in Acute Peripheral Facial Nerve Palsy

Woongsang Sunwoo; Jae Joon Han; Young Ho Kim
Department of otorhinolaryngology, Seoul National University College of Medicine, Seoul National University Boramae Medical Center

Background

The objective evaluation of facial nerve palsy (FNP) is essential for study of the treatment and prognostic assessment of FNP. Existing facial grading systems (FGS) have some issues for betterment. The aim of this study is to investigate the usefulness of this assessment tool with new mensuration of mouth asymmetry in acute peripheral FNP.

Methods

Facial photographs (resting and full mouth smiling) of 58 subjects (10 normal people and 48 acute peripheral FNP patients) were collected. FNP patients diagnosed with Bell's palsy or Ramsey-Hunt syndrome were classified into 3 groups according to the severity (mild, moderate, and severe grade) of mouth asymmetry. Then, 32 photographs (8 in each group, 20 males and 12 females, 16~80 years) were selected randomly and asymmetry of mouth movement in each group analyzed using PC-based FNP grading system (FGS 3.0). PC-

based FNP grading program determined automatically inner area between mouth lips using 8 tracking points. The area was divided at vertical line perpendicular to horizontal line lining both medial canthal points and the ratio (0.0 to 1.0) of two areas was calculated. The comparison of ratios among normal group and FNP groups was performed to evaluate the usefulness of this grading system.

Results

Levene homogeneity variance test regarding randomized sampling used in the present study showed an enough supposition of equal variance ($p=0.102$). Symmetric ratios of normal, mild, moderate, and severe grades were 0.94 ± 0.62 , 0.83 ± 0.12 , 0.67 ± 0.07 , and 0.41 ± 0.16 , respectively ($p < 0.01$, one-way analysis among groups). However, the significant difference between normal and mild FNP grade groups based on Tukey's multiple comparison tests was not found. Cut-off ratios for FNP according to FNP grades (normal vs 3 FNP grades; normal and mild grade vs moderate and severe grade; normal, mild, and moderate grade vs severe grade of FNP) were 84.5%, 67.2%, and 51.4%, respectively. The specificity and sensitivity of each receiver operating characteristic curve was more than 87% and 81%, respectively.

Conclusions

PC-based program assessing mouth asymmetry of FNP may be an appropriate tool to evaluate the severity of FNP. Further reevaluation of FGS is needed for standardized assessment of FNP.

PS 55

Assessment of Vestibulo-cochlear Function in Otic Capsule Sparing Temporal Bone Fracture Patients: Does Preserved Otic Capsule Assure Preserved Vestibulo-cochlear Function?

Hyunju Han¹; Min Young Lee¹; Jae Yun Jung²

¹*Department of Otolaryngology-Head & Neck Surgery, College of Medicine, Dankook University, South Korea;*

²*Department of Otolaryngology-Head & Neck Surgery, College of Medicine, Dankook University, South Korea*

Background/Hypothesis

Head trauma patients complain about various otologic symptoms, with hearing impairment being common following injury. It is reasonable to assume that vestibulo-cochlear dysfunction including dizziness and hearing impairment occur as a sequelae of marked inner ear damage, but not all the patients with these symptoms have abnormal inner ear pathology that can be found in radiologic assessment or physical examination. Traumatic vestibulo-cochlear problems can be consequenc-

es of the extensive damage of otic capsule induced by temporal bone fracture and also relatively minor head trauma like labyrinthine concussion. Furthermore, otic capsule injuries usually lead to the inner ear problem, but it is hard to make an accurate estimate of the amount of inner ear damage in otic capsule sparing temporal bone fracture or minor head trauma patients. Therefore the specific aim of this study is to assess clinical features and classify diverse clinical manifestations of the otic capsule sparing temporal bone fracture.

Methods

Temporal bone fracture patients (n=104) were enrolled during a period of 10 years (2004 - 2014) and their audiometry and vestibular function test were analyzed. Average age of the patients was 40.1 ± 20.1 years (32 females, 108 males).

Results

Hearing loss was observed in 75.8% (n=94) of all patients and included 76.1% (n=86) of the unilateral temporal bone fracture group and 72.7% (n=8) of bilateral temporal bone fracture group. Unilateral hearing loss was found in 55.3% (n=52) but only 2 patients showed contralateral hearing loss. Nineteen patients were diagnosed with benign paroxysmal positional vertigo (BPPV); none was diagnosed in the bilateral temporal bone fracture group. Twenty patients were diagnosed with vestibular hypofunction in the unilateral temporal bone fracture group and two in the bilateral temporal bone fracture group. Most patients (68.4% of those with in BPPV, 80.0% of those with vestibular hypofunction) were more affected on the fracture side. Facial palsy was diagnosed in 31 of all patients, and in 24 (85.7%) patients on the fracture side.

Conclusions

Otic capsule sparing temporal bone fracture patients showed clinical manifestations, such as hearing loss, vestibulopathies, and facial palsy. The temporal bone fracture side showed higher rate of hearing loss, vestibulopathies and facial palsy. The ipsilesional side showed higher rate of conductive hearing loss and the contralateral side showed more frequent incidence of sensorineural hearing loss.

PS 56

Concurrent Use of Cholesterol Lowering Drugs May Reduce the Incidence of Ototoxicity in Cisplatin-treated Patients

Katharine A. Fernandez¹; Paul Allen²; Mark S. Orlando³; Debora Mulford²; Chuan-Ming Li⁴; Aaron Rusheen⁵; Carmen Brewer⁴; Shawn Newlands²; Lisa Cunningham⁴

¹Section of Sensory Cell Biology, National Institute on Deafness and Other Communication Disorders, Bethesda, MD; ²University of Rochester Medical Center; ³Department of Otolaryngology, University of Rochester Medical Center; ⁴National Institute on Deafness and Other Communication Disorders, NIH; ⁵Mayo Medical School

Cisplatin-based chemotherapy is a critical component of the treatment of patients with solid tumors, but cisplatin can also induce significant side effects including ototoxicity. While the mechanisms underlying cisplatin-induced ototoxicity are still under investigation, our previous data indicate that induction of heat shock proteins (HSPs) in the cochlea, specifically heme oxygenase-1 (HO-1, also called HSP32), may inhibit hearing loss and hair cell death in response to stress caused by noise or ototoxic drugs (Baker et al, 2015; Francis et al, 2011). HMG-CoA reductase inhibitors (statins), typically used as cholesterol-lowering drugs, are known to activate HO-1 and decrease reactive oxygen species (ROS). Recent animal studies have shown that pravastatin reduces cochlear injury in noise-exposed mice, while simvastatin protects against aminoglycoside-induced sensory hair cell death in vitro. Here we have explored whether statins provide similar protection against cisplatin-induced ototoxicity in both mice and humans.

To examine the efficacy of statins on minimizing ototoxicity in cisplatin-treated mice, we applied Lovastatin to cisplatin-treated utricles. We've also initiated a retrospective examination of patient data from multiple sources that includes audiometric data collected from time points before, during, and after cisplatin treatment. Changes in hearing are calculated relative to pre-treatment audiograms and the presence of hearing loss are identified according to ASHA, CTCAEv4 and TUNE ototoxicity grading scales.

In mice, lovastatin reduced cisplatin-induced sensory hair cell death in whole-organ cultures of utricles. In our human population, we compared the incidence of hearing loss between subjects taking a statin during chemotherapy and those that did not. Preliminary results suggest a reduced incidence of acquired, cisplatin-induced hearing loss in statin users relative to individuals who were not on a concurrent statin therapy. Patients on statins also showed reduced severity of hearing loss than did non-statin users.

Statins have been in clinical use for decades with few reports of side effects. They have not shown signs of interference with the desired therapeutic effects of platinum-based chemotherapy drugs (Robinson et al, 2013). Concurrent use of statin therapy with cisplatin-based

cancer therapies may offer a low-risk method of protection against ototoxicity.

This work was supported by the NIDCD Division of Intramural Research.

PS 57

Depression is Associated with Chemosensory (Taste/Smell) Alterations in Adults 40+ Years: U.S. National Health and Nutrition Examination Survey (NHANES), 2011–2014

Chuan-Ming Li¹; Howard J. Hoffman¹; Shristi Rawal²; John Hayes³; Valerie Duffy⁴

¹National Institute on Deafness and Other Communication Disorders, NIH; ²Eunice Kennedy Shriver National Institute of Child Health and Human Development, NIH; ³Pennsylvania State University; ⁴University of Connecticut

Background:

Associations between depression and chemosensory function have not been well-studied in nationally-representative population samples.

Objective:

Investigate associations between depression and chemosensory function in U.S. adults.

Methods

Of 7,418 participants aged 40+ years in NHANES 2011–2014, 7,413 self-reported taste and smell function and 6,739 completed a Mental Health–Depression Screener (9-item Patient Health Questionnaire; PHQ-9). Smell function was measured among 3,519 adults with an 8-item odor identification Pocket Smell Test™, which was classified as alteration (anosmia/hyposmia; score < 6) or “normal” function (scores 6–8). Taste function was assessed among 3,112 adults, based on whole-mouth intensities of salty (1 M NaCl) and bitter (1 mM quinine hydrochloride) solutions rated on a generalized labeled magnitude scale (gLMS). Logistic regression was used to estimate odds ratios (ORs) and 95% confidence intervals (CIs) for associations between depression and taste/smell function.

Results

Among U.S. adults 40+ years, 15.0% had “mild” (515) depression. Prevalences of chemosensory alterations among moderately-to-severely depressed adults were: 18.1%, smell problems in the past year; 14.7%, worse ability to smell since age 25; 23.7%, phantosmia; 14.0%, hypersensitivity to odors; 25.4%, taste problems in the past year; 19.2%, worse ability to taste since age 25; 28.8%, persistent (unwanted) taste in mouth in last year;

16.3%, worse ability to taste food flavors since age 25. After adjusting for age, sex, race/ethnicity, education, income, general health status, physical activity, cigarette smoking, alcohol consumption, high blood pressure, heart disease, diabetes, and cancer, moderate-to-severe depression was significantly associated with: smell problems last year (OR=2.69; CI:2.03–3.57), worse ability to smell since age 25 (OR=2.16; CI:1.57–2.98), phantosmia (OR=1.96; CI:1.37–2.80), hypersensitivity to odors (OR=1.84; CI:1.39–2.43), taste problems last year (OR=3.25; CI:1.70–6.22), worse ability to taste since age 25 (OR=2.52; CI:1.66–3.82), dysgeusia or persistent taste in mouth last year (OR=3.38; CI:2.22–5.13), worse ability to taste food flavors since age 25 (OR=1.91; CI:1.17–3.12), and highest 10th percentile for gLMS rated taste intensities of salty and bitter solutions (OR=1.90; CI:1.12–3.21). Depression was not significantly associated with measured smell function, specifically for anosmia/hyposmia versus normal function.

Conclusions

After adjusting for age, sex, lifestyle and health factors, depression was significantly associated with self-reported chemosensory alterations and measured taste function; comparable associations were not observed with measured smell function. Healthcare professionals should be aware of the increased risk of depression among adults with self-reported chemosensory alterations.

PS 58

Intraoperative Changes in Electrocochleography During Superior Semicircular Canal Dehiscence Syndrome Surgery Are Not Attributable to Changes in Intracranial Pressure

Bryan K. Ward; Seth E. Pross; Eva Ritzl; John P. Carey
Johns Hopkins University

Background

Surgical treatment of superior semicircular canal dehiscence syndrome (SCDS) can be performed by middle cranial fossa approach where the temporal lobe dura is retracted in order to approach the canal from above, or the transmastoid approach where the mastoid bone is removed and the canal is approached from its side. Prior to surgery, patients have been observed to have an elevated ratio of summing potential (SP) to action potential (AP) as measured by electrocochleography (ECoChG). Furthermore, changes in this ratio including large elevations in SP commonly occur during surgical intervention by middle cranial fossa approach. We hypothesized that elevations in intracranial pressure due

to extradural temporal lobe retraction could subsequently be transmitted to the inner ear, resulting in endolymphatic hydrops and that these changes would not be noted during the transmastoid approach.

Methods

Patients with SCDS who underwent surgical repair by either transmastoid (n=7) or middle cranial fossa (n=23) approaches were retrospectively reviewed. Simultaneous intraoperative ECoG and auditory brainstem response (ABR) were performed throughout surgery. Intraoperative findings from the two groups were compared.

Results

Changes in SP/AP ratio, SP amplitude and ABR wave I latency were observed in select cases from both groups during surgery, with a large ECoG SP amplitude generating a new wave, identifiable on the ABR and preceding the traditional wave I noted in cases either of transmastoid or middle cranial fossa approach. Prior to plugging the canal median SP/AP ratio was 0.55 and 0.61 for the transmastoid and middle cranial fossa groups respectively and 0.48 and 0.40 after plugging. In 3 cases of transmastoid approach, elevations in the SP/AP ratio were observed just after fenestrating the semi-circular canal.

Conclusions

The findings in some patients during the transmastoid approach of large elevations in summing potential after fenestration of the canal suggests that this phenomenon is not due to increases in intracranial pressure during surgery but likely reflects intralabyrinthine pressure changes, specifically decreases in perilymphatic pressure.

PS 59

Diabetes-Induced Changes in Auditory Function in the T2DN Rats

Alberto A. Arteaga; David S. Sandlin; Shaoxun Wang; Yue Yu; Lan Chen; Jun Huang; William Mustain; Kathleen T. Yee; Douglas E. Vetter; Fan Fan; Richard J. Roman; Wu Zhou; Hong Zhu
University of Mississippi Medical Center

Introduction

Approximately 29.1 million Americans, 9.3% of the population, have diabetes, and more than 90% have Type 2 insulin resistant diabetes (CDC 2014). Although the relationship between diabetes mellitus and hearing impairment has been debated for many years, a recent comprehensive report (Agrawal et al. 2009) indicates that diabetes is a risk factor for hearing loss in US adults. The underlying mechanism, however, has not been

elucidated. In the present study, we examined auditory function of T2DN, a new diabetic rat model that mimics the human Type 2 diabetes mellitus. This normotensive model develops spontaneous diabetes with progressive diabetic nephropathy similar to humans.

Methods

Click or tone burst-evoked auditory brainstem response (ABR) was measured in young (2 months) and aged (18 months) T2DN rats and their age-matched control rats under isoflurane anesthesia as previously described (Zhu et al., 2011, 2014). Clicks, 4kHz, 6kHz and 8 kHz tone burst were delivered via an insert ear phone (ER-3A) at a rate of 21.1 /second. ABR threshold was determined as the lowest intensity at which clicks or tone bursts generated a well-defined and reproducible wave I. Wave I peak-to-peak amplitude was also measured.

Results

As early as 2 months, the T2DN rats showed high blood glucose level (198 mg/dl) compared to the age-matched control rats. Two-way ANOVA analysis revealed significant effects of aging ($P < 0.001$) and diabetes ($P < 0.001$) on suprathreshold Wave I amplitudes, as well as a significant interaction between the two factors ($P < 0.001$), but no significant effects on the ABR threshold. For all the sound parameters tested (clicks, 4kHz, 6kHz and 8 kHz), both young and old T2DN rats, had a significantly greater Wave I amplitude at each sound intensity tested compared to controls. Although an age-related decline in the amplitude of Wave I was observed in both normal and T2DN rats, the decline was more significant in T2DN rats. Preliminary analysis of cresyl violet stained cryostat sections did not reveal significant morphological change to the organ of Corti, spiral ganglion, or lateral wall (stria or spiral ligament).

Conclusions

These preliminary results indicate that auditory function is affected in T2DN rats. Ongoing studies, including an assessment for afferent synaptopathy, will further elucidate the underlying mechanisms.

Supported by NIH R01DC012060 (HZ), R01DC014930 (WZ) R21EY025550 (WZ), R21DC015124 (DEV), R01HL36279 (RJR), R01DK104184 (RJR), P20GM104357 (Core B, C, RJR; Pilot, FF); R21AG050049 (FF).

PS 60

Influence of Prosthesis Positioning After Ossiculoplasty

Mansour Alshamani¹; Alexander Huber²; Ivo Dobrev³; Michail Chatzimichalis⁴; Merlin Schör¹; Christof Roosli³; Jae Hoon Sim³

¹University Hospital Zurich; ²1, Department of Otorhinolaryngology – Head and Neck Surgery, University Hospital Zurich, Zurich, Switzerland; ³Department of ENT, Head and Neck Surgery, University Hospital Zurich, Switzerland; ⁴Dorset County Hospital NHS Foundation Trust

Background

The middle-ear structures can be damaged by various middle-ear pathologies. The damaged middle-ear structures are frequently reconstructed by surgical procedures to rearrange or to replace the impaired middle-ear structures with an implantable prosthesis. Especially, the partial ossicular reconstruction prosthesis (PORP) and total ossicular reconstruction prosthesis (TORP) are used to provide direct connection between the tympanic membrane and the stapes. In such surgeries, it is presumed that the postoperative displacement and angular position change of the prosthesis result in reduced middle-ear sound transmission and thus degraded surgical outcomes in surgeries.

Methods

Effects of possible postoperative position changes of the prosthesis on the middle-ear sound transmission are assessed qualitatively and quantitatively in cadaveric temporal bones. The assessment is done with several types of PORPs and TORPs, which includes new prostheses recently developed to adapt to the postoperative position changes of the prosthesis. With each of the prostheses implanted to the temporal bone, the postoperative prosthesis positioning changes is simulated by controlling position of the prosthesis accurately via 3-axis micro-manipulators. The middle-ear transfer function (METF) at each position change is obtained by measuring the ear-canal pressure using a microphone, and motion of the stapes footplate using a laser Doppler vibrometer (LDV).

Results

The PORPs with flexible ball joint showed relatively small change in the METF for position change of the prosthesis along the short and long axes of the footplate. The PORP with the clip interface showed benefits for the movement of the PORP to the lateral direction. While the TORP with the non-expanded head area showed relatively small change of the METF for position change of the prosthesis along plane parallel to the footplate, the

TORP with the expanded head area showed relatively small change of the METF for position change of the prosthesis to along the medial direction.

Conclusion

The newly-developed prostheses, featuring the flexible ball joint, clip interface, and variable contact area to the tympanic membrane, are presumed to be more adaptive to postoperative changes, thus maintaining their sound transmission functions. The experimental approaches used in this study provide objective ways to predict influence of postoperative prosthesis position change for new prostheses prior to their clinical application.

PS 61

Cryptococcosis in Immunocompetent Patients: Audiologic and Otologic Outcomes

Kelly King¹; Anil Panackal²; Andrea Beri³; Christopher Zalewski¹; Peter Williamson²; Jeff Kim¹; Carmen Brewer⁴

¹NIDCD, NIH; ²NIAID, NIH; ³CC, NIH; ⁴National Institute on Deafness and Other Communication Disorders, NIH

Cryptococcus is a major underlying cause of invasive fungal infections of the central nervous system (CNS), especially in immunocompromised individuals such as solid organ transplant recipients or those with AIDS; however, approximately 20% of individuals with cryptococcal meningoencephalitis (CM) have no known underlying immunodeficiency. While morbidity and mortality can be high, neurologic sequelae such as sensorineural hearing (SNHL) loss may be related to collateral damage from the relatively immunocompetent host immune response rather than pathogen. Ultimately, the risk of insult to and prognosis for the auditory system is poorly understood, with a limited literature largely comprised of case reports. We present audiologic and otologic outcomes in a subset of patients (n=29) recruited through a parent observational study following the course of the disease in previously healthy patients who developed CM. Patients were initially referred to audiology with a bias toward those with auditory symptoms, but referrals were quickly opened to all available patients based on sufficient health status at the time of hospital stay. Comprehensive audiology examinations included middle ear reflex measures, audiometry, otoacoustic emissions, and auditory brainstem response studies, in addition to neurotology assessment. Nearly 80% of our cohort presented with hearing loss in at least one ear, typically of mild to moderate degree. The overwhelming majority (>90%) of patients had SNHL, some with MRI FLAIR enhancement of the cochlea, the retrocochlear auditory nervous system, or both. Available longitudinal data

suggest the course of the disease within the auditory pathway can be dynamic. We explored a variety of clinical, cytokine biomarkers, and microbial markers as risk factors associated with SNHL, including the relationship to yeast burden via the cryptococcal latex agglutination antigen titer. Auditory manifestations of CM in previously healthy adults can be complex, and may be underrecognized or conflated with the presence of cognitive impairment. Our understanding of this infection in patients that appear immunocompetent is nascent; however, these data support the proactive recommendation for auditory assessment in all newly diagnosed CM patients to facilitate intervention and rehabilitation, when necessary.

PS 62

The Hypothesis of k⁺-recycling Impairment Is Not a Primary Deafness Mechanism for cx26 Deficiency Induced Hearing Loss

Hong-Bo Zhao; Yan Zhu; Jin Chen

Dept. of Otolaryngology, University of Kentucky Medical Center

Background

K⁺-recycling is a long-standing hypothesis for deafness mechanism of connexin gap junction deficiency induced hearing loss. It hypothesizes that connexin gap junctional dysfunction may compromise sinking and recycling of expelled K⁺ ions after hair cell and neuron excitation, consequently causing K⁺-accumulation in the extracellular space around hair cells and neurons and K⁺-toxicity; this eventually lead to hair cell and neuron degeneration and hearing loss. Cx26 and Cx30 are two predominant connexin isoforms and co-express in the cochlea. Either Cx26 or Cx30 mutation or deficiency can induce hearing loss. However, so far, there is no evidence demonstrating that Cx26 or Cx30 deficiency impairs K⁺-sinking and recycling in the cochlea, even though this hypothesis has been widely referred as a deafness mechanism for Cx26 or Cx30 deficiency induced hearing loss.

Methods

Cx26 and Cx30 knockout (KO) mice were used. Inner ear gap junctional function, cell degeneration, and hearing function were assessed.

Results

First, we found that inner ear gap junctions in Cx26 KO mice still retain permeability to ions and small molecules, since co-expressed Cx30 exists. Second, Cx26 deficiency induced congenital deafness is prior to hair cell degeneration and is associated with cochlear developmental disorders rather than cell degeneration. Third, hearing remains normal in young Cx26 deficiency-induced late-onset hearing loss mouse model, even Cx26 is already deleted in the cochlea. Fourth, there is

no apparent hair cell and neuron degeneration, even old Cx26 deficiency-induced late-onset hearing loss mice have hearing loss. Fifth, we found that K⁺-sinking, which is the first step for K⁺-recycling, in the cochlea is associated with ATP-purinergic P2X receptor activity rather than connexin channels. Finally, inner ear gap junctions in Cx30 KO mice also retain permeability to ions and small molecules.

Conclusions

K⁺-sinking and recycling in the cochlea is important and required for normal hearing. However, this is not a deafness mechanism for Cx26 or Cx30 deficiency induced hearing loss. Sole Cx26 or Cx30 deficiency also does not eliminate inner ear gap junctional permeability for K⁺-recycling in the cochlea.

Supported by NIH R01 DC 05989 and R56 DC 015019.

Coding of Binaural Cues

PS 63

Coding Of Sound Source Direction In Gecko Auditory Nerve Fibers

Jamie Matthews¹; Jakob Christensen-Dalsgaard²; Catherine Carr³; Daniel A. Butts¹; Catherine E. Carr¹

¹Univ Maryland; ²Department of Biology, University of Southern Denmark; ³University of Maryland College Park

Lizards have coupled ears, and closed field single-unit recordings from auditory nerve in the Tokay gecko showed equal sensitivity to ipsi- and contralateral stimulation, as well as dependence on interaural time and level differences (Christensen-Dalsgaard, Tang and Carr, 2011). To exploit the consequences of coupled ears for directional processing, we investigated responses to directional sound in free field recordings from auditory nerve fibers in the Tokay gecko. We analyzed 152 single unit responses to sound from speakers radially distributed around the gecko, with 0° corresponding to the speaker in front of the gecko. All responses were strongly directional (Figure 1, thick curve). Thus auditory nerve fibers generate strongly lateralized responses, with maximum responses to ipsilateral sound sources around 60-90°. Binaural comparisons should produce strong directionality.

To estimate the accuracy with which a gecko could discriminate between sound sources, we computed the Fisher information (FI) for each neuron in our sample. FI is a measure of the amount of information that neural spike counts provide about a particular stimulus value, such as a single stimulus location, and thus quantifies

the accuracy with which a stimulus is encoded. Practically, high FI this translates to a higher capacity for a neuron to discriminate, for example, two nearby sound sources. For all units, FI was high for regions just contralateral to 0°, and behind the animal (Figure 1, dotted curve). Mid-frequency (1-2 kHz, n=43) and high frequency (above 2 kHz, n=39) location-sensitive neurons discriminate speaker locations with similar acuity, while low-frequency (below 1 kHz, n=70, Figure 1) responses had slightly lower FI.

This analysis suggests that the coupled ear system of the gecko is best at discriminating across the midline, i.e. to lateralize directional stimuli. In contrast, discrimination within the lateral hemifields is not very acute.

PS 64

Intrinsic Electrical Resonances as a Potential Source of Internal Delays in Binaural Neurons

Andrew Brughera¹; David McAlpine²; Jessica J. M. Monaghan²

¹*Boston University*; ²*Macquarie University*

Most physiological studies assume a role for conduction delays in generating neural tuning to interaural time differences (ITDs) in brainstem neurons. Suggested mechanisms include differences in axonal conduction speed from the two ears, and interaural mismatches in the tonotopic innervation of binaural neurons. However, physiological studies have demonstrated that blocking glycinergic inhibitory inputs to an MSO neuron shifts its rate-ITD function such that its most sensitive slope is no longer within the physiological range of ITD, and its best-ITD shifts toward zero. This inhibitory modulation suggests that neuronal mechanisms play a role in determining internal delay in the representation of ITD. Here, we propose a model in which interaural delays in neurons of the medial superior olive (MSO) are generated through bilateral differences in dendritic and somatic membrane properties. We ask whether small spatial gradients in membrane time-constant, membrane potential, or ion-channel densities might contribute to setting the best-ITD via different latencies between ipsilateral and contralateral inputs. While preliminary modeling with bilaterally symmetric resting membrane potentials suggests that physiologically-slow contralateral inhibition produces only slight shifts in best-ITD, the interaction of contralateral inhibition with bilateral differences in membrane properties, as well as the speed of inhibition required to realistically shift the best-ITD, will be investigated.

Building on recent work, we will explore mechanisms of ITD sensitivity in a biophysically-based model of the au-

ditary brainstem. As in (Remme et al. (2014), guinea-pig vocalizations will drive bilateral auditory nerve models (Zilany et al., 2014), which will now drive bilateral ventral cochlear nuclei (VCN) models based on Rothman and Manis (2003). The model VCN neurons then will drive excitatory and inhibitory synaptic inputs to a model MSO neuron (based on Brughera et al., 2013) with realistic membrane impedance properties. In this model the medial nucleus of the trapezoid body (MNTB), which is driven by the VCN via the Calyx of Held, and projects contralaterally-driven inhibition to the MSO, is considered a relay. Within the model MSO neuron, bilateral differences in dendritic and somatic membrane properties will be explored, as to whether reasonably small spatial gradients in membrane time-constant, membrane potential, or ion-channel currents may contribute to setting the best-ITD via different latencies between ipsilateral and contralateral inputs. In addition, the speed of synaptic inhibition required to realistically shift the best-ITD will be further investigated.

PS 65

Response Types in the Superior Olivary Nucleus of the Barn Owl

Anna Kraemer; Catherine Carr
University of Maryland College Park

Inhibition is important for auditory processing. In chickens, the superior olivary nucleus (SO) provides inhibitory feedback to first order nuclei, and has been hypothesized to improve ITD coding (Fukui et al., 2010; Burger et al., 2011; Tabor et al., 2012). Few studies have characterized SO response types in barn owls. Moiseff & Konishi (1983) recorded from response types of the owl SO in vivo, and found the majority of units were only excited by the ipsilateral ear. All units recorded from the SO were ILD insensitive, although the authors noted their search criteria might have increased the percentage of monaural response types (Moiseff & Konishi 1983). The SO is morphologically heterogeneous, however, and projects to multiple targets. Some SO neurons send inhibitory projections to two or more ipsilateral brainstem nuclei, while projections to the contralateral SON may originate from a separate population of neurons (Burger et al., 2005). In addition, some SO neurons project to the inferior colliculus (Takahashi et al., 1988). Given the heterogeneity of SO cell types and projections, it seems likely to contain multiple response types.

In order to examine auditory responses in SO, and to study the effects of descending inhibition provided to the first order auditory nuclei, we recorded in barn owl SO in vivo. Electrolytic lesions confirmed recording locations. We measured tuning curves or response maps, tested for phase locking, and analyzed peristimulus time histo-

grams, latency, regularity and PSTHs in addition to measuring rate-level function responses to noise stimuli. We also analyzed binaural measures of sensitivity to interaural level difference and interaural time difference, to categorize each response type. SO response types analyzed include primary-like, chopper, and onset, which are also found in the nucleus angularis (Koppl & Carr 2003). Other SO single units were broadly tuned and responded more to noise than tones. We conclude that the SO displays similar response types and heterogeneity in response types to nucleus angularis, although more SO units prefer noise stimuli. These broadly tuned responses may serve to regulate the overall firing rate of other auditory brainstem nuclei and/or the contralateral SON.

PS 66

Modeling Age-related Loss of Inhibition and Recovery in the Lateral Superior Olive

Go Ashida¹; Jutta Kretzberg¹; Daniel J. Tollin²

¹Cluster of Excellence "Hearing4all", Department of Neuroscience, Faculty 6, University of Oldenburg;

²Department of Physiology and Biophysics, University of Colorado School of Medicine

Interaural time and level differences (ITD/ILD) are two important binaural acoustical cues for sound localization. Principal neurons in the mammalian lateral superior olive (LSO), which are excited and inhibited by sounds at the ipsilateral and contralateral ears, respectively, change their spike rates according to ILDs. LSO neurons are also sensitive to ITDs of the envelopes of amplitude-modulated sounds. While prior anatomical studies reported age-dependent loss of inhibitory inputs along the entire ascending auditory pathway, electrophysiological recordings have found only relatively small functional changes in the aged LSO. In this study, we used LSO neuron models and examined how age-related loss of inhibitory inputs may affect ILD and ITD coding. More specifically, a nonlinear conductance-based model (presented in ARO midwinter meeting 2015) and a more simplistic coincidence counting model (Ashida et al., 2016, PLoS Comput. Biol.) were used to replicate the computation of LSO. Excitatory inputs from neurons in the anteroventral cochlear nucleus and inhibitory inputs from the medial nucleus of the trapezoid body were modeled as Poisson processes, whose intensity functions were either intensity-dependent (for ILD) or temporally periodic (for ITD). The number of inhibitory fibers in the model was changed to mimic the age-dependent loss of inhibitory inputs. Without the loss of inhibition, output spike rates of the model varied smoothly with ITD and ILD, and replicated empirical tuning properties of LSO. When the number of inhibitory inputs was reduced, two major changes were observed: First, the overall

spike rates were increased due to the lowered inhibitory counts. Second, the modulation depths (defined as the difference between the maximum and minimum spike rates) were decreased, leading to relatively flat tuning curves. In order to simulate the recovery process that compensates the loss of inhibitory fibers (e.g., homeostatic plasticity), we then increased the strength of each inhibitory inputs such that the total amount of inhibitory strengths remained unchanged. By this modification, effects of inhibition loss on simulated spike rates and modulation depths were considerably weakened. These results suggest that activity-dependent plasticity may counteract the age-dependent loss of inhibitory fibers in LSO, which might also explain the observed discrepancy between anatomical and physiological results. Since the two different models yielded quantitatively similar results, we conclude that our findings were not model-specific, but rather represented a general property of ITD and ILD coding in the LSO.

PS 67

Spatial Tuning in the Chicken Midbrain

Roberta Aralla¹; Michael Beckert²; Jose Luis Pena²; Christine Köppl³; Jose Luis. Pena²

¹Carl von Ossietzky University; ²Albert Einstein College of Medicine; ³Cluster of Excellence H4A, Dept. of Neuroscience, Carl von Ossietzky University Oldenburg

Introduction

The representation of auditory space in the inferior colliculus (IC) of the barn owl has become a classic example of a derived sensory map. It is, however, not known whether the principles underlying its formation generalize to other, less specialized animals. We have begun to characterize responses in chicken (*Gallus gallus*) IC, with the ultimate aim of testing for a topographic representation of auditory space and the intermediate steps in its synthesis.

Methods

Spike responses (multi-unit) were recorded from the IC of anesthetized chickens (P21-P59) using glass-insulated tungsten micro-electrodes. We first inserted closed sound systems into both ears to test selectivity for frequency, interaural level (ILD) and time (ITD) differences. Spatial selectivity was then probed at the same recording sites, by noise stimulation in the free field, via a 144-speaker array distributed in azimuth over a range of $\pm 100^\circ$ and of $\pm 80^\circ$ in elevation. Free-field responses were further tested at different levels (5dB, 15dB above threshold), at different frequencies and with a simultaneously-presented second sound.

Results

The analysis of 40 recording sites in 8 chickens revealed spatial receptive fields in 36. All spatially tuned clusters preferred frontal, contralateral or both locations. While selectivity in elevation was not obvious, we identified two classes of spatial selectivity in azimuth: 1) hemispheric fields that extended from the midline to the lateral peripheral limit of the tested range and 2) narrower receptive fields. A majority of clusters with hemispheric spatial tuning displayed broad frequency tuning curves and best frequencies above 1 kHz, while no systematic pattern was found in narrowly-tuned clusters. Additionally, spatial receptive fields were robust to increasing sound level, but were disrupted by ipsilateral concurrent-sound stimulation, suggesting nonlinear bilateral interaction. No dorso-ventral topography was detected.

Discussion

Our study, similar to previous work on chicken, pigeon and bird of prey IC (Coles and Aitkin, 1979, *JCompPhysiol* 134:241-251; Lewald, 1990, *ExpBrainRes* 82:423-436, Calford et al., 1985, *JCompPhysiol* 157:149-160), used free-field stimulation to investigate the spatial tuning in birds other than owls. Our preliminary analysis suggests that chicken IC has a representation of auditory space that differs from barn owl (Singheiser et al., 2012, *FrontNeurCirc* 6:45) by the lack of clear tuning in elevation. However, cells displaying narrow azimuthal selectivity across the frontal hemifield were observed, which may be consistent with a topographic representation of space. Histological analysis is ongoing to assess the presence of a topographic map.

PS 68

Across-frequency Integration in the Barn Owl's Icx Accessed Through an Adaptation Paradigm

Roland Ferger; Lisanne Schulten; Hermann Wagner
Institute of Biology II, RWTH Aachen University

Azimuthal sound localization in the barn owl is mainly based on the interaural time difference (ITD). A realization of the Jeffress-Model allows a cross-correlation like detection of ITDs within narrow frequency bands. Due to its nature, this method results in so called phase ambiguities. To resolve them, information from multiple frequency channels has to be combined. In the barn owl, this happens in the external nucleus of the inferior colliculus (ICX) where a neural map of auditory space is formed.

Extracellular recordings were obtained from neurons in ICX of anesthetized barn owls. Two stimuli (each 100ms duration, 5ms onset/offset ramps) were presented via earphones. The first stimulus covered one of the following bandwidths: (1) Broadband; (2) one octave aligned

to frequency range, the neuron responds to; the (3) middle, (4) lower or (5) upper third of this octave; (6) a combination of 4 and 5. The first stimulus acted as an adapter for the second stimulus that followed after a 6ms silent gap and was always broadband. The broadband stimulus level was chosen to elicit 50% of the saturating response. Levels of band-limited stimuli were adjusted to contain the same energy. By randomly iterating the ITD (equally for both stimuli) we obtained rate-vs.-ITD curves, so called tuning curves, for the first non-adapted band-limited stimulus and the second adapted broadband stimulus. This yielded a total of 12 ITD tuning curves for each neuron.

ITD curves resulting from the first stimulus were analyzed first. Typical broadband ITD tuning curves of neurons in the ICX have a prominent main peak representing the neuron's best ITD and smaller side peaks at a distance equal to the reciprocal of the neuron's best frequency. Octave band stimuli (2) yielded similar tuning curves, but side peaks were less suppressed. With third octave band stimuli (3+4+5), much like with pure tones, all peaks have similar heights and their distance equals the stimulus center frequency. Adapted broadband tuning curves, as evoked by the second stimulus, were dominated by the non-adapted frequency bands concerning peak distance. Adapting with low frequencies, while evoking the weakest response to the first stimulus and no adaptation at the best ITD, was most effective in decreasing side peak suppression.

Frequency specific adaptation can, thus, be used to investigate the mechanisms used to resolve phase ambiguities and the actual contributions of frequency bands to this crucial step in sound localization.

PS 69

Localization of Spatial Positions with Ambiguous Information in Barn Owls

Patrick Schillberg¹; Hermann Wagner²

¹*Institute for biology II RWTH Aachen University*; ²*Institute of Biology II, RWTH Aachen University*

Introduction

The American barn owl (*Tyto furcata pratincola*) has developed an excellent hearing capacity to catch its prey. Sound localization is driven by interaural time difference (ITD), interaural level difference (ILD) and possibly further monaural parameters. These parameters are in turn influenced by the morphology of the ruff and the ear flaps. The influence of these structures on the auditory signals is described by head related transfer functions (HRTF). The main topic of this work is the question whether there are spatial positions specified by the same broadband

ITD and ILD and whether and how the barn owl can discriminate between these ambiguous locations.

Objectives

HRTFs of barn owls were recorded, analyzed and the influence of sound-localization parameters on behavior was investigated. We used advanced technologies to find locations containing the same ITD and the same ILD.

Material & Methods

To record HRTFs, stimuli (sweeps, 500 ms) were presented via a movable speaker at 528 positions varying in azimuth and elevation. Impulse responses (IR) of the stimuli were recorded with small electret microphones 15 mm inside the owls' meatus. After calculation of HRTFs, acoustic stimuli were presented to the owls via earphones. Stimuli were chosen to contain the same broadband ITD and ILD while originating from different locations in space.

Results

Analysis of ITD and ILD values in the HRTF yielded 20 positions with ambiguous information which were tested in behavioral experiments. Preliminary data suggest that it is difficult for the birds to discriminate between such locations.

PS 70

The Gerbil's Lateralization of Bands of Noise with Interaural Time Differences Beyond the Naturally Occurring Range

Sandra Tolnai¹; Rainer Beutelmann¹; Janna Henrike Mrozek¹; Georg M. Klump²

¹Cluster of Excellence "Hearing4all," Animal Physiology and Behavior Group, Department of Neurosciences, School of Medicine and Health Sciences, Carl von Ossietzky University of Oldenburg, Oldenburg, Germany;

²Cluster of Excellence Hearing4all, Animal Physiology and Behaviour Group, Department for Neuroscience, School of Medicine and Health Sciences, University of Oldenburg, D-26111 Oldenburg, Germany

From studies in humans and owls it is known that the perception of narrow-band sounds with interaural time differences (ITD) corresponding to interaural phase differences (IPD) close to half the period length of the centre frequency is ambiguous (Sayers, 1964; Saberi et al., 1998). Also, narrow-band sounds with an ITD that correspond to an IPD of 270° of the centre frequency are lateralized to the side of the sound that is lagging by ITD. That is not the case for sounds with larger bandwidths (Trahiotis & Stern, 1989). The aim of this study was to test if those observations could also be made in an animal model trained to give left/right responses instead

of pinpointing the perceived direction of a sound. We compared those data with data collected with human subjects tested with the same task and corresponding stimuli under identical listening conditions.

Six Mongolian gerbils, trained in a left/right discrimination task, were run under virtual-headphone stimulation: Two loudspeakers presented stimuli to the left and right ear using cross-talk cancellation in order to eliminate the undesired signal paths between the loudspeakers and their respective contralateral ears. The cross-talk cancellation filters were based on head-related transfer functions measured prior to the experiments using a gerbil carcass. This technique allows dichotic stimulation in the free sound field. Human subjects did the same task under virtual-headphone stimulation and actual headphone stimulation. Stimuli were broad band noise bursts and noise bursts of different bandwidth [gerbils: 0, 200, 500, 1000 Hz, humans: 0, 50, 100, 200, 400 Hz, centre frequency: 1250 (gerbils) or 500 (humans) Hz, 60 dB SPL] to which ITD up to $\pm 600 \mu\text{s}$ (gerbils) or $\pm 1500 \mu\text{s}$ (humans) were applied.

We found that gerbils' and humans' left/right responses changed depending on the bandwidth of the sounds and on the ITD applied. Narrow-band sounds with an ITD corresponding to an IPD far below 180° yielded responses corresponding to the sign of the ITD. At an ITD corresponding to an IPD of 270°, responses were in the direction of the sound wave that led with the smaller ITD. For broad-band sounds, responses in both species were more likely to be in the direction of the sound leading by ITD. This is in line with the observations by Trahiotis & Stern (1989).

This study was funded by the DFG (TRR 31 and Cluster of Excellence "Hearing4all").

PS 71

ITD Lateralization without ITDs: Effects of Shifting the Analytic Signal

Tyler Churchill

United States Naval Academy

Psychophysical studies using acoustic signals that are decomposed into an envelope and a temporal fine structure (TFS) carrier have yielded insights into physical cues relevant to physiological processing. In particular, Interaural Time Differences (ITDs) in low-frequency TFS are found to be prominent cues for source lateralization. However, the exact mechanism of ITD processing is not yet settled and warrants further research. The objective of the current study is to help elucidate ITD processing mechanisms by exploring model and psychophysical responses to dichotic, equal-amplitude, distorted-sinu-

soidal stimuli without explicitly-introduced ITDs. Instead, quasi-ITDs are introduced by distorting the waveform TFS shapes.

A common envelope/TFS decomposition technique uses the Hilbert transform of a given waveform to create a harmonic conjugate pair, or analytic signal, which satisfies the Cauchy-Riemann and Laplace equations. The amplitude and phase of the analytic signal then represent the given waveform's envelope and TFS, respectively. Presently, we construct a harmonic conjugate pair explicitly from the quadrature pair of sine and cosine. We then slightly shift the entire unit circle so defined by this analytic signal from its initial origin-centered position. By recalculating θ from the shifted analytic signal using the four-quadrant arctangent function, we next obtain a test signal, $\cos(\theta)$. A second channel is likewise calculated by applying a different shift to the original analytic signal. When presented to listeners dichotically, the resulting stereo waveform can produce lateralized auditory images, depending on the shifts applied to the analytic signal. Listener sensitivity is tested via a two-interval, two alternative, forced-choice exercise in which the analytic signal shifts are reversed between intervals. Several auditory models are also tested to examine agreement with psychophysical data.

Furthermore, by using explicitly-constructed quadrature pair stimuli, we take advantage of a readily-calculable, instantaneous, intra-wave frequency, and explore whether this parameter influences listener or model behavior. This analysis allows us to bypass the time/frequency uncertainty inherent in Fourier-based methods such as the spectrogram, a short-time Fourier transform. Indeed, recent findings elsewhere suggest that traditional time/frequency analyses and thinking of complex waveforms as Fourier series may be insufficient to describe the computations performed by the human brain. A quadrature sampling mechanism based on, e.g., basilar membrane displacement and velocity, may provide sufficient information for corresponding neural calculations.

PS 72

Directionality Through Acoustical Coupling of Eardrums and Lungs in the Green Treefrog, *Hyla cinerea*.

Jakob Christensen- Dalsgaard¹; Norman Lee²; Mark A. Bee²

¹*Department of Biology, University of Southern Denmark;* ²*Department of Ecology, Evolution, and Behavior, University of Minnesota*

For most frogs, vocal communication, and especially the localization of calling conspecific frogs by females,

is fundamentally important. The robust phonotaxis by females has been exploited in behavioral experiments, and treefrogs in the genus *Hyla* are the most thoroughly studied frogs in terms of sound localization and segregation. The underlying mechanism of the directionality is internal acoustical coupling of the eardrums. However, the acoustics of the frog auditory periphery are complicated by the many potential sources for sound input (the two eardrums, the body wall and mouth cavity, among others). The present study is the first attempt to dissect the contributions of the contralateral eardrum and lung to directional hearing.

We used laser vibrometry in six female *H. cinerea* to measure eardrum vibration in response to local sound stimulation of the ipsi- and contralateral eardrums and the contralateral body wall overlaying one of the lungs. We calculated transfer functions as the vibration spectrum divided by the sound spectrum (recorded by a probe microphone close to eardrum or body wall) for ipsilateral, contralateral, and body wall stimulation ($HIL(\omega)$, $HCL(\omega)$, and $HBW(\omega)$, respectively). From these transfer functions, we determined the interaural transmission gain as $TG = HCL(\omega) / HIL(\omega)$, and body wall-ear transmission gain as $TGB = HBW(\omega) / HIL(\omega)$.

The interaural transmission gain function peaks at 1300 and 1800 Hz, where the gain amplitude is -6 dB. Thus, the indirect sound component is reduced by half compared to the direct sound component. However, both of these peaks lie between the spectral peaks emphasized in the mating call (900 and 2700 Hz) and are probably caused by body wall resonance (peak frequency at 1500 Hz). Interaural transmission is reduced at 900 Hz (-10 dB) and is even smaller at 2700 Hz (-15 dB). The interaural transmission gain phase shows a near-linear slope of 0.002rad/Hz, corresponding to a delay of approximately 300 μ s. When the lungs are deflated transmission gain amplitude drops by approximately 10 dB at the peak frequencies.

In conclusion, we have shown prominent interaural transmission that is maximal (with ensuing maximal directionality) at frequencies that are not emphasized in communication signals, but that correspond to the body wall resonance frequency. Thus, the lung resonance may boost the sound transmission from the contralateral ear, but it does not enhance directionality to the mating call in this species. These findings are corroborated by the free-field measurements shown in our other poster.

Otoacoustic Emissions

PS 73

DPOAEs in an *Eleutherodactylus* Assemblage

Ariadna Cobo-Cuan¹; Manfred Kössl²; Emanuel C. Mora¹

¹University of Havana; ²Institute for Cell Biology and Neuroscience, Goethe University

Background

Acoustic communication plays an essential role in the reproductive behavior of anuran amphibians. As in all vertebrates, the sensitivity and frequency selectivity of anuran hearing are benefits accrued from nonlinear mechanical sound processing. As a result of this non-linearity, when stimulated simultaneously with two or more tones, the inner ear produces sounds of still other frequencies, so-called distortion-product otoacoustic emissions (DPOAEs). DPOAEs provide a noninvasive tool for the study of the inner ear mechanics, even in endemic species where physiological studies must be of minimal impact. The genus *Eleutherodactylus* comprises 85% of the Cuban amphibian fauna with a high degree (95%) of endemism on the island. No previous study has evaluated the hearing of Cuban anuran species. Diverse hearing capabilities must be matched with the richness of the acoustical repertoire in this group, thus allowing intraspecific communication in multispecies assemblages.

Methods

Five frog species from a single assemblage, *E. eileenae*, *E. pinarensis*, *E. atkinsi*, *E. planirostris* and *E. limbatus*, were examined for $2f_1-f_2$ and $2f_2-f_1$. Recordings were made with a fixed-frequency ratio $f_2/f_1 = 1.1$. In frequency sweeps, f_2 varied from 0.2 to 10 kHz in 50 Hz steps. The levels of the stimulus tones, $L_1=L_2=55$ dB SPL, were kept constant for all stimulus frequency combinations. We measured input-output (I/O) curves of DPOAEs from two inner ear organs sensitive to airborne sound, the amphibian papilla (AP) and the basilar papilla (BP), and compared their properties. For selected f_2 frequencies, the stimulus level was increased in 2 dB steps from 30 to 84 dB SPL.

Results

Auditory tuning is closely matched to the call frequencies for each species. Species in which the contributions of the AP and BP to the DPOAEs could not be easily distinguished tended to exhibit unimodal DPOAE-audiograms. In *E. limbatus*, one of the smallest known frogs, we found DPOAEs up to 7.5 kHz, which extends the frequency range where this response can be found in amphibians. Unexpectedly, slopes found at low stimulus

levels in DPOAE I/O curves from the BP were ≤ 1 dB/dB, similar to what is found in the curves from the AP of other anurans (Meenderink & van Dijk, 2004).

Conclusions

DPOAEs in *Eleutherodactylus* reflect the diversity of the mechanical responses of the inner ear with clear interspecific variability. These findings set a preliminary stage for future studies to explore potential diversity of strategies nature has discovered to solve anuran communication in complex acoustic environments.

PS 74

The Relationship Between Otoacoustic Emissions and Wideband Acoustic Absorbance in Preterm Infants During the First Year of Life: The Babyyears Project

Beth Prieve¹; Linda J. Hood²; Stefania Arduini¹

¹Syracuse University; ²Vanderbilt University

Transient-evoked otoacoustic emissions (TEOAEs) and wideband acoustic absorbance (A) characteristics change over the first year of life in infants. For term infants, TEOAE levels increase between birth and one month of age, and then decrease over the first year of life in frequency bands from 2000 Hz to 4000 Hz. Wideband acoustic absorbance increases for frequencies less than 2000 Hz, and the relative levels of A change across frequencies between 2000 and 6000 Hz. Although these trends are observed for averaged data, it is uncertain whether responses from individual ears show the same trend, and importantly, whether changes in TEOAEs, indicators of cochlear integrity, are linked with changes in A, measures of the conductive pathway. The few data for preterm infants indicate that TEOAE levels increase from 33 to 41 weeks gestational age. There are no systematic, published A data for newborns born before 33 weeks conceptional age. The goal of this presentation is to (1), describe mean changes in TEOAEs in preterm infants in the first year of life, and (2) determine whether changes in TEOAEs and A measured in individual ears during the first year of life are related. TEOAEs and A were measured longitudinally in preterm infants at 33 weeks and 35 weeks gestational age while they were cared for in the neonatal intensive care unit, and at approximately 50 weeks and 64 weeks gestational age as outpatients. All infants passed newborn hearing screening, and had normal Wave V auditory brainstem response latencies at each visit. Data were included in this analysis for this presentation for newborns who were tested while breathing room air and had $A \geq 0.69$ at any frequency between 1 and 2 kHz. TEOAEs were evoked by tonebursts centered at 2 kHz and 4 kHz. Mean TEOAE levels increased between 33 weeks

(n=52), 35 weeks (n=62) and 50 weeks (n=71) gestational age. There were slight decreases in TEOAE levels evoked by tonebursts of both frequencies between 50 weeks and 64 weeks gestational age (n=54). Eighteen newborns met the inclusion criteria for both ears at all four test ages. Longitudinal analyses of these data suggest that there are greater changes in A than in TEOAE levels across age. This study is part of the BabyEars Project, which relates early auditory characteristics to developmental and language outcomes at 2 years of age. [Supported by NIH-NIDCD R01DC011777]

PS 75

Otoacoustic Emissions Elicited with a Stimulus on the Dura and Air Conduction

Christof Roosli¹; Reto Stump¹; Jae Hoon Sim¹; Rudolf Probst¹; Alexander Huber²; Ivo Dobrev¹

¹Department of ENT, Head and Neck Surgery, University Hospital Zurich, Switzerland; ²1, Department of Otorhinolaryngology – Head and Neck Surgery, University Hospital Zurich, Zurich, Switzerland

Background

Bone conduction (BC) is an alternative to air conduction to stimulate the inner ear. Stimulation for BC can occur directly on the skull bone, on the skin covering the skull bone, or on soft tissue (i.e. eye, dura). All these stimuli can elicit Otoacoustic Emissions (OAE). This study aims to compare OAEs generated by different combination of stimuli in live humans.

Methods

Measurements were performed in five normal hearing subjects undergoing a neurosurgical intervention in general anesthesia with craniotomy. Distortion product OAEs were measured for 0.7, 1, 2, 3, 4 and 6 kHz with a constant ratio of the primary frequencies (f_2/f_1) of 1.22. Sound pressure (L1) was held constant at 65 dB SPL, while L2 was decreased in 10 dB steps from 70 to 30 dB SPL. Distortion product OAEs were generated by f_1 and f_2 as AC tones, by f_1 as AC tone and f_2 by BC tone on the intact skin, and one f_1 as AC tone and f_2 as BC tone on the exposed dura) tone. A modified bone vibrator (Bonebridge; MED-EL, Innsbruck, Austria) was used for BC stimulations and its equivalent perceived SPL was calibrated against a AC tone preoperatively, for stimulation at the temporal region, individually for each patient. DPOAEs were considered present when the level was ≥ 6 dB above the noise floor. Simultaneously, bone vibrations at the front teeth were measured with an accelerometer (Type 4374; Brüel & Kjær, Naerum, Denmark).

Results

It was possible to record DPOAEs for all three stimulation modes. For combined air and dura stimulation, DPOAEs were not present above the noise at frequencies below 1 kHz, but they were well detectable at the other frequencies. Best response was measured with a stimulation level of 60 dB. The acceleration measured on the bone was lower for stimulation on the dura, especially < 3 kHz and > 6 kHz.

Conclusion

Vibratory stimulation on the dura can elicit hearing sensation that differs from bone conduction stimulation.

PS 76

Musicianship Enhances Monaural and Binaural Efferent Gain Control to the Cochlea

Gavin M. Bidelman; Amy Schneider; Victoria Heitzmann; Shaum Bhagat
University of Memphis School of Communication Sciences & Disorders

Human hearing sensitivity is easily compromised with overexposure to excessively loud sounds, leading to permanent hearing damage. Consequently, finding activities and/or experiential factors that distinguish “tender” from “tough” ears (i.e., acoustic vulnerability) would be important for identifying people at higher risk for hearing damage. To regulate sound transmission and protect the inner ear against acoustic trauma, the auditory system modulates gain control to the cochlea via biological feedback of the medial olivocochlear (MOC) efferents, a neuronal pathway linking the lower brainstem and cochlear outer hair cells. We hypothesized that a salient form of auditory experience shown to have pervasive neuroplastic benefits, namely musical training, might act to fortify hearing through tonic engagement of these reflexive pathways. By measuring MOC efferent feedback via otoacoustic emissions (cochlear emitted sounds), we show that both dynamic cochlear gain control both within (monaural) and between (binaural) the ears is enhanced in musically-trained individuals. Across all participants, MOC strength was correlated with the years of listeners’ training suggested that efferent gain control is experience dependent. Our data provide new evidence that intensive listening experience(s) (e.g., musicianship) can strengthen the MOC efferent system and sound regulation to the inner ear bilaterally. Implications for reducing acoustic vulnerability to damaging sounds are discussed.

PS 77

Efferent Effects on Complementary Pre-neural and Neural Distortion Products

Spencer Smith; Kayla Ichiba; David Velenovsky; Barbara Cone
University of Arizona

Distortion product otoacoustic emissions (DPOAEs) and distortion product frequency following responses (DPFFRs) are respectively pre-neural and neural measurements of cochlear nonlinearity. Because cochlear nonlinearity likely arises from outer hair cell electromotility, DPOAEs and DPFFRs may provide complementary measurements of the human medial olivocochlear (MOC) reflex, which modulates outer hair cell function. In this study, we first measured MOC reflex-induced DPOAE inhibition at spectral fine structure peaks in young human adults. The f1 and f2 tone pairs producing the largest DPOAE fine structure peak for each subject was then used to evoke DPFFRs with and without MOC reflex activation to provide a neural measure of efferent inhibition. We observed significant positive relationships between DPOAE fine structure peak inhibition and inhibition of DPFFR components representing neural phase locking to f2 and 2f1-f2 but not f1. These findings support previous reports that the MOC reflex inhibits DPOAE sources differentially. That these effects are maintained and represented in the auditory brainstem demonstrates that the MOC reflex may exert potent "downstream" influence on the subcortical neural representation of sound.

PS 78

Influence of Visual Attention on Suppression of Transiently Evoked Otoacoustic Emissions

Wiktor Jedrzejczak¹; Rafal Milner¹; Krzysztof Kochanek²; Henryk Skarzynski³

¹*Institute of Physiology and Pathology of Hearing;*

²*Department of Experimental Audiology, Institute of Physiology and Pathology of Hearing, Warsaw/Kajetany, Poland;* ³*Oto-Rhino-Laryngology Surgery Clinic, Institute of Physiology and Pathology of Hearing, Warsaw/Kajetany, Poland*

The purpose of the present study was to investigate influence of visual attention on contralateral suppression of transiently evoked OAEs (TEOAEs). Recordings were made in a group of adults with normal hearing. Visual odd-ball procedure was used. The subjects were presented with of two types of visual stimuli: standard and deviant (20% of all stimuli). Each recording session consisted of two parts: active and passive. In active part the subjects task was to count deviant stimuli. In passive

part the subject had to look at the stimuli without counting. During both sessions TEOAEs and evoked potentials were acquired. TEOAEs were recorded using the linear protocol (all stimuli at the same level and polarity); stimulus levels were kept at 65 dB peSPL; and a 60 dB SPL broadband noise was delivered to the contralateral ear as suppressor. Global and half-octave values of TEOAE response levels and suppression were investigated. In case of evoked potentials P1, N1, P2 and P3 waves were analyzed.

PS 79

Correlation Between Otoacoustic Emission and Behavioral Estimates of Contralateral Medial Olivocochlear Efferent Inhibition in Humans

Miriam I. Marrufo-Pérez; Peter T. Johannesen; Al-mudena Eustaquio-Martín; Enrique A. Lopez-Poveda
University of Salamanca

Medial olivocochlear (MOC) efferent effects in human can be assessed only indirectly. The activation of MOC efferents reduces the amplitude of basilar membrane (BM) vibrations for low and moderate level sounds, linearizing BM input/output (I/O) curves. On the other hand, MOC efferents can be activated by contralateral acoustic stimulation (CAS). Based on this, the magnitude of MOC efferent inhibition has typically been assessed by measuring the increase in absolute thresholds or the decrease in otoacoustic emission (OAE) levels caused by CAS. The aim of the present study was to investigate the correlation between those measures. Transient evoked otoacoustic emissions (TEOAEs) at 54 dB pSPL and absolute thresholds at 0.5, 1.5 and 4 kHz were measured for 27 adults. In addition, I/O curves for distortion product otoacoustic emissions and TEOAEs were measured for 17 of the participants at the ear where absolute thresholds were obtained. All measures were obtained in the presence and in the absence of a contralateral broadband noise (10 Hz to 10 kHz) at 60 dB SPL. It was assumed that this noise activated the contralateral MOC reflex without activating the middle-ear muscle reflex. The horizontal shift in the I/O curves, and the differences in absolute thresholds and OAE levels between the control and CAS conditions were taken as indicators of the magnitude of contralateral MOC efferent inhibition. The CAS caused absolute thresholds to increase by 1.5, 2.4, and 2.0 dB at 0.5, 1.5, and 4 kHz, respectively. The increase was comparable across ears and frequencies. For those participants who had TEOAEs, overall TEOAE levels decreased by 0.6 dB and the decrease was larger for the right (1 dB) than for the left ears (0.2 dB). The increase in absolute threshold and the decrease in overall TEOAE level were not correlated. The CAS generally caused OAE I/O curves to shift horizontally but the magnitude of the shift was not correlated with

the increase in absolute threshold. In summary: the effects of the CAS on absolute thresholds, TEOAE levels and OAE I/O curves were broadly consistent with the expected effects MOC efferent activation; these measures, however, cannot be used equivalently to assess the magnitude of contralateral MOC efferent inhibition. [Work supported by the University of Salamanca, Banco Santander, and MINECO (BFU2015-65376-P).]

PS 80

Quantifying the Change in Hearing Due to a Reduction in EP versus OHC Loss Using a Model-based Evaluation of DPOAE I/O Functions in Mice

Robert H. Withnell¹; Kevin K. Ohlemiller²; Mark E. Chertoff³

¹Indiana University; ²Washington University; ³University of Kansas Medical Center

Background

Previous work in humans has shown that a phenomenological model of DPOAE generation can quantify the cochlear mechanical hearing loss in ears with age-related hearing loss from DPOAE I/O functions. In this study, this model was used to quantify the change in hearing that accompanied a reduction in the endocochlear potential (EP) versus OHC loss from DPOAE I/O functions in mice.

Method

Sound pressure measurements were made in the ear canal of mice before and after administration of furosemide or noise exposure. The stimulus consisted of two pure tone stimuli with a stimulus frequency ratio of 1.2. Hearing threshold was quantified by recording the auditory brainstem response. Model-generated DPOAE I/O functions were fit to DPOAE data to quantify the hearing loss. In the model, a feedback parameter controlled gain and a factor in the exponent of the nonlinearity controlled the contribution of the nonlinearity.

Results

DPOAE I/O functions in mice showed a reduction in amplitude without a significant change in slope. This was true for mice with a reduced EP and for mice with OHC loss. The reduction in hearing sensitivity that accompanied the cochlear insult was not well described by the model, the model fit to data showing only a very small change in gain and hearing sensitivity. The model matched the reduction in DPOAE amplitude by a reduction in nonlinearity (OHCs). At high stimulus levels, DPOAEs can be obtained regardless of the value of the EP, commensurate with studies in humans.

Conclusion

The absence of a change in cochlear compression, inferred from the slope of the DPOAE I/O function, subsequent to cochlear insult, is difficult to explain. It is not consistent with DPOAE measurements in other mammalian species. A reduction in nonlinearity, without a reduction in gain, is inconsistent with our understanding of cochlear mechanical amplification.

PS 81

A Taxonomy-Based Approach of Inferring Cochlear Compression from Otoacoustic Emissions

Anusha Yellamsetty¹; Shaum Bhagat²

¹University of Memphis; ²University of Memphis School of Communication Sciences & Disorders

Background

Listeners with normal hearing are capable of detecting minute increments of sound pressure across a wide dynamic range (WDR) of sound levels. A critical process that accommodates listener sensitivity across this WDR is the compression initiated on the basilar membrane (BM). Otoacoustic emission (OAE) input/output (I/O) measures are one of the indirect methods to infer characteristics of cochlear compression in humans. According to current theory, distortion-product OAEs (DPOAE) are classified as primarily distortion source OAEs and stimulus-frequency otoacoustic emissions (SFOAE) are classified as primarily reflection source OAEs. In order to evaluate source contributions to cochlear nonlinearity, compression characteristics were inferred from both DPOAE I/O functions and SFOAE I/O functions in normal-hearing listeners at low and high test frequencies.

Methods

Two models that have been proposed for inferring OAE I/O function compression were utilized. These models consisted of a third-order polynomial regression model and a three-segment linear regression model. Measurements of DPOAE I/O and SFOAE I/O functions were obtained in two groups of normal-hearing listeners. The first group was tested at 750 Hz and 2 kHz, and the second group was tested at 3 kHz, 4 kHz, and 6 kHz. The DPOAE and SFOAE I/O functions were fitted with the two models to derive compression thresholds (CT) and compression slopes (CS).

Results

The results indicated little redundancy between the third-order polynomial model and the three-segment model. There were no statistically significant correlations between DPOAE CT and SFOAE CT at any test frequency within both models. Trends in the data indicated that high test frequencies had lower CT than lower test frequencies. Estimated compression values ob-

tained from CS were higher at higher test frequencies compared with lower test frequencies.

Conclusion

Since there is little redundancy between the models, comparing results across models is not an ideal way to draw conclusions concerning BM compression. The independence of DPOAE and SFOAE CT is indicative of different source origins. Differences in observed inferred compression characteristics, with lower CT and higher values of compression at high test frequencies compared to low test frequencies, is consistent with physiological studies of BM compression in animal models. Efforts at comparing cochlear compression inferred from an OAE taxonomy-based approach with compression inferred from behavioral masking functions will lead to a greater understanding of the cochlear compression mechanisms that accommodate WDR in normal-hearing listeners. Acknowledgements: The authors wish to thank Dr. Enrique Lopez-Poveda for his assistance with the three-segment model.

PS 82

Ageing and Cochlear Nonlinearity as Measured with Distortion OAEs and Loudness Perception

Amanda Ortmann^{1,2}; Yeini C. Guardia¹; Carolina Abdala¹

¹University of Southern California; ²Washington University in St. Louis School of Medicine

The level-dependent growth of DPOAEs provides a rough index of cochlear compression in humans. A recent report from our lab indicates that middle-aged subjects have slightly weakened compressive growth of the DPOAE at high-frequencies (Ortmann & Abdala, 2016); however, the perceptual consequences of these changes are not clear. Ipsilateral DPOAE suppression is another manifestation of cochlear nonlinearity. We applied both of these OAE paradigms, as well as a perceptual measure of loudness growth, to study changes in cochlear nonlinearities in human subjects ranging from 18 to 76 years old. Input/output functions and ipsilateral suppression of the isolated distortion component of the DPOAE were measured from 0.5 to 8 kHz, with primary tones swept upward at 0.5 octave/s using a fixed f_2/f_1 ratio of 1.22. DPOAE compression threshold and a measure of compressive slope were derived from each function. Ipsilateral suppression of the distortion OAE was conducted at suppressor frequencies both above and below f_2 ; suppression threshold and rate of suppression were measured for each suppressor-frequency condition. Finally, categorical loudness judgments were made by all subjects at the same test frequencies.

In middle-aged and older-adult ears, the mean distortion OAE compression threshold was elevated by 8–12 dB compared to young adults. Additionally, the compressive slope (response growth above compression threshold) in older ears was more than double that measured in young-adult ears. Even in a subset of older listeners whose audiometric thresholds were matched to young-adult thresholds, reduced compression (steeper growth of the DPOAE) was noted in the older group. Ipsilateral suppression of the OAE also showed age effects; notably, there was an elevated suppression threshold for suppressors above f_2 in older ears (matched to young-adult ears for audiometric pure tone average). The rate of distortion OAE suppression growth was generally shallower in older subjects as well. Perceptual tests showed steeper growth of loudness for soft-to-medium sounds at high frequencies in older ears; this atypical steepness was associated with distortion OAE compression.

Our results suggest aging-related alterations in two OAE-based measures of cochlear nonlinearity, with the effect becoming stronger with increasing age. Many of these age effects were present even when hearing thresholds between groups were matched to within 5 dB and/or when statistical tests were conducted to partial out the effects of audiometric threshold. Collectively, our findings suggest cochlear nonlinearities weaken with age, producing an observable perceptual consequence.

PS 83

Quick and Objective Tuning Estimation in Humans from SFOAE and TEOAE Measurements

Renata Sisto¹; Arturo Moleti²

¹INAIL Research Department of Occupational and Environmental Medicine, epidemiology and Hygiene;

²University of Rome Tor Vergata, Department of Physics

A new quick and objective technique for tuning estimate in humans is presented based on a time-frequency analysis applied to SFOAE or TEOAE signal. The wavelet technique permits to project the signal on time-frequency two dimensional space. In this space the OAE signal energy occupies an hyperbolic region delimited by a lower and an upper limit spectral delay curve. It is well known that the emission both in the case of SFOAE and TEOAE mainly comes from a linear reflection mechanism due to randomly distributed roughness. The sources must be considered as place-fixed as their position is independent from the stimulus frequency and level. These place-fixed sources are distributed in a relatively wide region extending basally from the tonotopic place. The coherent reflection sources appear in the time-frequency plot as blobs of energy whose position is an in-

dividual characteristic depending on the roughness profile. In addition to the sources situated at the location of maximum activity BM profile, more basal sources can be individuated characterized by a shorter delay. Whilst the position of the backscattering sources remains unchanged as the stimulus level varies, the relative intensity of the blobs of energy varies with the stimulus increasing the importance of the more basally located sources as the stimulus increases or, in other words, the BM tuning decreases. As the more basally located sources tend to become more intense as the excitation profile is broadened the related average spectral delay becomes shorter. In this work, the spectral delay weighted by the wavelet coefficients is proposed as the best parameter for the tuning estimate. The averaging process reduces the spectral fluctuation of the delay associated with the discontinuous distribution of the OAE energy blobs in the time-frequency plane. An empirical relation was found between the average spectral delay and tuning, with the average spectral latency proportional to the square root of tuning. This relation is supported by theoretical considerations based on a simple 1-d transmission line cochlear model. An analytical calculation is also presented in which the scaling symmetry is invoked to simplify the analytical approach. The proposed technique is used to estimate cochlear tuning in human subjects. Our results are compared to those obtained with other techniques based on OAE measurements and behavioral tuning estimates.

PS 84

Swept-tone Stimulus-frequency OAES in Young Adults: Normative Findings and Methodological Considerations

Carolina Abdala; Yeini C. Guardia; Ping Luo; Christopher A. Shera
University of Southern California

Stimulus-frequency otoacoustic emissions (SFOAEs) are reflection-source emissions thought to arise from the backscattering of traveling waves off of mechanical irregularities in the cochlea. In this study, we describe and test a new swept-tone data collection protocol for the recording and measurement of SFOAEs and present normative amplitude and phase data from 30 normal-hearing young adults. SFOAE input-output functions were measured with probe level varying from 20-60 dB SPL (10 dB steps) at frequencies ranging from 1 to 8 kHz. From these input/output functions, we defined the compression knee and quantified SFOAE amplitude growth below and above this threshold. Additionally, we measured SFOAE delay (which has been linked to cochlear tuning) as a function of probe level. As an associated goal, we explored and optimized the various parameters involved in data collection and analysis, including the

number of sweeps, probe-suppressor interactions, and post-processing of the SFOAE with inverse FFT to eliminate multiple internal reflections. Notably, we compare two methods of artifact rejection to enhance data quality, one involving real-time rejection, another including post-hoc processing. One significant improvement increasing the efficiency of data collection considerably is the concurrent presentation of multiple stimulus sweeps, each spanning an octave-wide segment. We conclude from this normative group of young-adult data that optimized measurement of swept-tone SFOAEs produces reliable recordings of response amplitude, phase, and delay.

PS 85

Eartip Modification Greatly Reduces Evanescent Waves

Jonathan Siegel¹; Stephen T. Neely²

¹*Northwestern University*; ²*Boys Town National Research Hospital, Omaha, NE USA*

Introduction

Sounds radiated into the ear canal from a source with a relatively small aperture produce evanescent waves that influence the pressure measured near the source aperture (Keefe and Benade, 1980, JASA; Brass and Locke, 1997, JASA). Because only the plane wave propagates longitudinally along the canal, the pressure measured near the source does not accurately represent the stimulus to the ear.

Methods

The decline in evanescent pressure with distance from the source was measured for an Etymotic Research ER-10X otoacoustic emission probe by advancing a probe tube through the body and central lumen of the replaceable front tube. Sound is emitted through surrounding outer lumens, which all end in the same plane. Pressure at the plane of the probe was also measured using the internal microphone of the ER-10X. In an alternative configuration, the front tube was modified by beveling the most distal ~2 mm of the outer lumens, leaving the central lumen intact. The aperture of the beveled configuration was about twice that of the standard front tube.

Results

The pressure frequency response was measured at longitudinal positions from 0 to 12.7 mm from the end of the probe. Relative to the distant pressure, the pressure measured at the end of the standard front tube increased above 10 kHz to a maximum of ~5 dB at 20 kHz, while the pressure measured 5 mm or more from the source was essentially the same, as expected from theory. In the beveled configuration, the pressure at the end of the front tube remained within 1 dB for all frequencies below 20 kHz. Evidence of evanescent wave reduction was

also observed in both the impulse responses and the spectral magnitudes of pressures measured with the internal microphone. Thévenin calibrations in the beveled configuration showed consistently lower errors in the extraction of source pressure and impedance.

Conclusion

Beveling the standard front tube was intended as a first step toward optimizing the source configuration. The reduction in evanescent waves due to this simple modification was greater than expected. This reduction improves the quality of Thévenin calibrations, which should improve the accuracy of ear-canal impedance measurements. Such improvements could be particularly important for ear canals with larger than average diameter for which evanescent wave contributions to the measured pressure are larger.

Funding

This study was supported by Northwestern University and a grant from NIH/NIDCD.

PS 86

Effects of Ear Canal Acoustics on Sound Calibration and Otoacoustic Emission Measurements

Karolina K. Charaziak¹; Christopher A. Shera²

¹Keck School of Medicine, University of Southern California, Caruso Department of Otolaryngology; ²University of Southern California

Otoacoustic emissions (OAEs) are shaped not only by cochlear mechanisms but also by the acoustics of the residual ear-canal space between the eardrum and recording microphone. For instance, ear-canal standing waves compromise the reproducibility of OAE measurements due to their effects on both the evoking stimulus pressure and the OAE pressure. Proposed remedies to the standing-wave problem include calibrating the stimulus pressure using forward pressure level (FPL) and converting the OAE pressure to emitted pressure level (EPL). FPL represents the sum of all sound waves propagating in the “forward” direction, from the OAE probe towards the eardrum; EPL represents the OAE pressure as it would appear at the eardrum if it were loaded with a reflectionless ear canal. If the Thévenin-equivalent source characteristics of the OAE probe are known, both FPL and EPL can be derived from measurements obtained with the probe sealed near the entrance of the ear canal. Although the assumptions underlying the calculation of FPL and EPL have been tested in uniform tubes, the curvature and/or changing diameter of the ear canal may affect their validity. To explore the accuracy and utility of FPL and EPL in more realistic geometries, we performed measurements in silicon investments of

human ear-canal impressions. A separate OAE probe was sealed at each end of the investment—near the canal entrance and in a place of the eardrum. Analogous measurements were also performed in less complex cavities, including horns and simple tubes of different diameters. Sound pressures were measured at both ends of the investment while the probes were driven, one at a time, with wideband chirp stimuli. Measurements of the probes’ Thévenin-equivalent characteristics were used to derive and compare measurements of FPL and EPL at the two locations (ear-canal entrance and “eardrum”). When the tube diameter matched the diameter of the tubes used for Thévenin-source calibration, both EPL and FPL measured at the canal entrance matched their “eardrum” equivalents within ± 2 dB (up to ~ 16 kHz). Although poorer, the agreement was satisfactory (usually ± 5 dB up to ~ 12 kHz) in the horns, tubes of smaller diameter, and investments. We conjecture that reflections occurring within the residual space (e.g., due to canal curvature) and/or contamination by evanescent waves diminish the accuracy of FPL and EPL in these cavities, especially at higher frequencies. Although imperfect, the combination of FPL calibration and EPL conversion improves the reliability of OAE measurements in real ears.

Development I

PS 87

Generation of Human Embryonic Stem Cell Reporter Lines for Monitoring Otic Progenitor Development in 3D Culture

Emma Longworth-Mills; Jing Nie; Eri Hashino
Indiana University School of Medicine

Our laboratory recently developed a novel 3D culture protocol for generating, from aggregates of mouse or human pluripotent stem cells, inner ear sensory epithelia harboring sensory hair cells, supporting cells, and concurrently arising neurons. This protocol makes use of precisely timed treatments of several signaling molecules to faithfully recapitulate inner ear development in culture, including the differentiation of otic progenitor cells capable of giving rise to sensory hair cells. To monitor derivation and development of otic progenitor cells in 3D culture, a human embryonic stem cell (ESC) reporter line targeting *FBXO2*, a known otic progenitor marker, is being established using CRISPR/Cas9 genome editing technology. Human ESCs are transfected with plasmids encoding a guide RNA (gRNA) and a high fidelity variant of Cas9 (eSpCas9(1.1)). A donor vector with homology arms for *FBXO2* flanking a 2A-tdTomato-PGK-Puro fluorescence/antibiotic cassette is co-transfected. Upon a DNA double-strand break induced by the gRNA and eSpCas9(1.1), the 2A-tdTomato-PGK-Puro cassette

is inserted in-frame immediately downstream of the FBXO2 coding sequence and replace the FBXO2 stop codon. The resultant reporter cells are expected to transcribe tdTomato together with the endogenous FBXO2 as a single mRNA, and during translation the tdTomato protein should be “cleaved off” from FBXO2 due to the self-cleavage activity of the 2A sequence. tdTomato expression should have a pan-cellular localization pattern. Clonal cell lines will be established after puromycin selection, and successful integration of the 2A-tdTomato-PGK-Puro cassette will be confirmed by PCR analysis followed by sequencing of the cloned amplicons. A similar approach will be employed for the generation of a reporter line targeting PAX2, another otic progenitor marker. This PAX2-2A-nGFP reporter line should express GFP localized to the nucleus due to an added nuclear localization signal. Based on our preliminary data with human ESC-derived inner ear organoids, the onset of PAX2 expression precedes FBXO2 expression by 6-10 days. Thus, we expect to observe the first sign of PAX2-2A-nGFP expression in human inner ear organoids earlier than FBXO2-2A-tdTomato. These novel human reporter ESC lines will serve as useful tools for validating, identifying and isolating otic progenitors in our organoid culture model. In addition, various multiplex reporter lines can be generated in the future to allow sequential identification of otic progenitors and sensory hair cells (or neurons) arising in 3D culture. This study was supported by NIH R01DC013294 and F31DC015968.

PS 88

Modeling CHARGE Syndrome with Stem Cell-Derived Inner Ear Organoids

Jing Nie; Eri Hashino
Indiana University School of Medicine

Background

CHARGE syndrome is a congenital multi-organ disorder primarily caused by mutations in the gene encoding CHD7, an ATP-dependent chromatin remodeling protein. The most prevalent clinical feature is malformation of the inner ear structures, resulting in prelingual deafness and vestibular dysfunction. The exact mechanisms how CHD7 mutations lead to inner ear dysfunction is unknown, although Chd7 mutant mice exhibit some of the inner ear phenotypes associated with CHARGE syndrome. We sought to investigate how CHD7 mutations affect inner ear development using a novel stem cell-derived organoid system capable of generating otic precursors that undergo self-guided maturation into vestibular-like sensory epithelium containing functional hair cells and supporting cells.

Methods

We generated monoallelic and biallelic mutant Chd7 mouse embryonic stem cell (ESC) lines via CRISPR/Cas9 genome editing. The resulting mutant ESCs were aggregated and differentiated in vitro towards an inner ear lineages through manipulation of BMP, TGF β , FGF and WNT signaling pathways. To compare expression of potential Chd7 target genes between wild-type (WT) cells and Chd7 mutant cells, we labeled WT ESCs with a tdTomato expression cassette integrated at the Rosa26 locus through CRISPR. By aggregating tdTomato-labeled WT ESCs with unlabeled Chd7 mutant ESCs, we created chimeric inner ear organoids, allowing direct comparison of phenotypes between WT and Chd7 mutant cells in the same samples.

Results

Like WT ESCs, aggregates of Chd7 null ESCs differentiated to derive AP2/Ecad+ non-neural ectoderm and Pax8/Ecad+ otic-epiblastic preplacode on day 6 and 8, respectively, after the start of differentiation. Subsequently, Pax8/Pax2+ otic-like vesicles arose in these cultures at around the same time when otic vesicles arise in aggregates of WT ESCs. However, a striking phenotype manifested itself in the following days in Chd7-null cultures with collapsed Pax8/Pax2+ vesicles. In addition, Pax8/Pax2+ vesicles were devoid of Sox2 expression. At day 20, no inner ear sensory epithelia with Myo7a+ cells were found in Chd7 nulls. Our preliminary data with chimeric organoids also indicate that Chd7 biallelic mutants have smaller otic vesicles than WT populations and have a collapsed morphology, with little or no luminal space.

Conclusions

These results suggest that Chd7 is essential for proper differentiation of otic progenitor cells, but not for nonneural or preplacodal ectodermal cells. In addition, lumen formation and/or maintenance of the otic vesicle appear to be dependent on Chd7. Investigation is currently underway to generate human CHD7 mutant ESC lines with the aim of evaluating species-specific effects of CHD7 inactivation on phenotype manifestation.

PS 89

Isolation and Selective Propagation of Otic Sensory Progenitor Cells from Mouse ES Cells and Embryos via Fbxo2 Reporter Exploitation

Byron Hartman; Robert Böschke; Sawa Keymeulen; Stefan Heller
Department of Otolaryngology – Head & Neck Surgery, Stanford University School of Medicine, Stanford, CA 94305

Otic sensory progenitor cells give rise to the hair cells and supporting cells of auditory and vestibular sensory

epithelial organs. During embryogenesis these progenitors arise from the otic placode and are expanded and maintained within organ primordia until they differentiate to form hair cells and supporting cells of the sensory epithelia. This differentiation is a terminal process in the mature mammalian cochlea, which does not regenerate after damage. Recent developments in embryonic stem (ES) cell guidance allow the generation of otic sensory progenitors and even differentiated organoids within embryoid body-like cell aggregates. This guidance is mediated through experimental application of extrinsic factors and occurs in the context of local microenvironments within heterogeneous cell mixtures. Otic sensory progenitor specification appears to require such a microenvironment but there is evidence suggesting that otic progenitors eventually become fate-committed and are then less dependent on signaling from non-otic cells. We reasoned that if we can purify otic sensory progenitors after they become committed to the otic fate but before they become terminally differentiated we can exert control over their environment and design experiments to understand how they are regulated and maintained. Thus, we aim to apply biological and engineering principles to isolate and propagate both ES cell- and embryo-derived otic sensory progenitors to determine factors and conditions for their expansion and eventual differentiation or assembly into pure sensory epithelia.

The E3 ubiquitin ligase F-box2, encoded by *Fbxo2*, is highly specific to the inner ear and is expressed in the otic sensory lineage throughout the progression from early otic vesicle cells to mature hair cells and supporting cells. Here, we exploit *Fbxo2* reporter and selection markers created by insertion of a multicistronic Venus/HygroR/CreER (VenusHC) cassette to the *Fbxo2* locus with homologous recombination. In mice, the *Fbxo2*-VenusHC reporter is expressed in otic sensory progenitors as well as hair cells and supporting cells during embryogenesis and this expression persists in mature sensory epithelial organs. In ES cell culture, the *Fbxo2*-VenusHC reporter is a robust marker of otic organoid cells, providing an effective means to assess production of these cells in individual experiments and isolate them from heterogeneous cell aggregates. We are currently utilizing flow cytometry and Hygromycin selection to isolate these otic cells from embryonic tissue as well as ES cell aggregates. We are comparing the characteristics and behavior of these cells and testing a variety of conditions for growth, maintenance, and epithelia formation.

PS 90

Mouse Otocyst Cells Transplanted In Vivo Migrate into the Otocystic Cells

Ryosei Minoda¹; Hiroki Takeda¹; Masato Fujioka²; Makoto Hosoya²; Toru Miwa³; Hideyuki Okano⁴; Kaoru Ogawa²

¹Department of Otolaryngology-Head and Neck Surgery, Kumamoto University School of Medicine; ²Department of Otolaryngology-Head and Neck Surgery, Keio University School of Medicine; ³Department of Otolaryngology and Head and Neck Surgery, Kumamoto University; ⁴Department of Physiology, Keio University School of Medicine

Introduction

Mouse otocysts are an attractive experimental target for investigating treatment modalities about inner ear diseases and/or studying inner ear development. Herein, we have demonstrated in vivo cell transplantation into mouse otocysts.

Methods

We utilized WT timed pregnant CD-1 mice at E11.5 as recipients. The timed pregnant mice underwent an injection of one of the three types of cells: m-iPS cells (RIKEN; iPS-MEF-Ng-20D-17); EGFP expressing otocystic cells which are obtained from EGFP expression transgenic mice (C57BL/6-Tg; CAG-EGFP), hereinafter referred to as EGFP-otocystic cells; and, otic progenitor cells derived from human induced pluripotent stem (h-iPS) cells which were then committed to the non-sensory cells, hereinafter referred to as otic progenitor cells. Regarding the EGFP-otocystic cells, the otocysts were extracted from EGFP-mice, subsequently the otocysts were dissociated into single cells. After otocystic injection of these three cells, the treated embryos were evaluated at E13.5, E15.5 or E18.5 utilizing cryosectioning.

Results

The m-iPS cells were detectable in treated ears at E13.5 and E15.5, but not detectable at E18.5. The detected cells were attached to the inner surface of luminal lining cells of the inner ears, but they did not migrate under the surface of the lining epitheliums. The EGFP-otocystic cells were detectable in treated ears at E15.5 and E18.5. The detected cells were in the lumens, on the inner surfaces of the lining epitheliums, in the lining epitheliums or in the subepithelial tissues of the inner ears. The otic progenitor cells were detectable in the treated ears at E15.5 and E18.5. The detected cells were in the lumens, in the lining epitheliums or in the subepithelial tissues of the inner ears.

Conclusions

Our findings in mouse cells suggest that precise time matching of the stage of recipient mice and the stage of donor cells are required. Consistently, after otocystic injection of otic progenitor cells, some of the injected cells were successfully engrafted in the developing inner ears. Further studies of otic progenitor cells using mouse otocystic injection model *in vivo* will provide some clues for developing treatment modalities of congenital hearing loss in humans.

PS 91

Progenitor Proliferation in the Mammalian Otocyst

Jenna Glatzer; Amy Kiernan

University of Rochester Medical Center

Auditory and vestibular disorders result from damage or death of critical inner ear cell types. These provoke permanent hearing impairments or balance difficulties, as mammals lack a biological replacement mechanism for these cell types following damage. The progenitors of these cells begin dividing in the otocyst, an early embryonic structure that undergoes a dramatic increase in size as well as structural changes during development. Knowledge of the molecular mechanisms by which critical cells normally proliferate in this period may be useful for replacement therapies aiming to regenerate these critical cells *in vivo* or *in vitro* after injury. One obstacle to this is the current dearth of information regarding how inner ear progenitors normally proliferate in mammals. In efforts to understand the molecular events surrounding proliferation, we focused on Sox2, a critical gene for inner ear development and additionally for stem cell maintenance. Mice with otic-specific mutations in the Sox2 locus (Sox2Lcc/Lcc mutants) display inner ears with profound sensory defects and gross morphological abnormalities. The extent of these deficits could suggest a failure of early proliferative events in the otocyst; however, a role for SOX2 in otic proliferation has not previously been investigated. In order to test SOX2's role in this process, we conditionally deleted Sox2 using an inducible-Cre mouse line (SOX2-CreER) crossed with a line carrying a floxed Sox2 allele (Sox2^{fl/fl}). Cre was activated by tamoxifen administration at 3mg/40g of body weight at embryonic day (E) 8.5. Samples were collected 48 hours later, at embryonic day (E) 10.5, and processed for cryosectioning, immunohistochemistry, and imaging with AxioVision Software. Proliferating cells were labeled using an antibody to p-Histone H3 (pHH3), a marker of dividing cells. Additionally, an antibody to SOX2 was used to characterize the expression pattern of SOX2 in the E10.5 otocyst. In wildtype controls, SOX2 expression was observed broadly except in the most dorsal portions of the otocyst, and robust proliferation was also observed at this time point. The

overwhelming majority of pHH3+ cells (> 80%) co-localized with SOX2. Notably, SOX2-deficient mutants had about 50% fewer pHH3+ cells and a 40% reduction in otocyst volume. These results point to a novel role for Sox2 in inner ear proliferation. Understanding the role of this gene in proliferation during early embryonic events may yield crucial information for therapies to regenerate critical cell types.

PS 92

Expression of Short Stature Homeobox 2 Transcription Factor During Otic Development

Alejandra Laureano¹; Kathleen Flaherty²; Hatem Saabaawy²; Kelvin Kwan¹

¹*Rutgers University*; ²*The Cancer Institute of New Jersey at Rutgers University*

Introduction

Syndromic hearing loss is highly heterogeneous genetic disorder. The discovery and study of genetic factors that contribute to syndromic hearing loss allows for the advancement of early screening methods, diagnosis and treatment. Studying molecular factors that govern the development of the inner ear will lead to a better understanding of the etiology behind syndromic hearing loss. Using molecular biology and bioinformatics tools, the short stature homeobox 2 gene (SHOX2) was identified as a candidate transcription factor involved in the early process of auditory neuron development. To better understand and recapitulate the role of SHOX2 in human inner ear development zebrafish was chosen as a model organism. Zebrafish, like humans possess both orthologues from the SHOX gene family, SHOX and SHOX2. Whereas mice only have the SHOX2 in their genome.

Results

Zebrafish shox2 has not been previously identified in the inner ear. Utilizing *in situ* hybridization, shox2 transcripts were first detected in the otic placode at 16 hours post fertilization (hpf) during zebrafish development. shox2 is dynamically expressed throughout zebrafish development and continues to be present in otic cell types at 18, 24, 48, and 72 hpf. At these time points, shox2 can also be observed in the cranial ganglia and hindbrain regions. To further assess the importance of shox2 in the developing inner ear, antisense morpholinos were used to reduce expression of shox2 starting from the one cell stage. At 72 hpf, embryos were observed and tested for abnormal behavior. The observed behaviors in shox2 morphants include circling, lack of avoidance behavior and spasms. These behaviors suggested inner ear and neurological deficits. Single fish were acquired after behavioral testing and subjected to qPCR to assess shox2 levels. Embryos with low shox2 levels correlated to ab-

normal behaviors. Similarly, embryos with low levels of *shox2* after morpholino injection showed a trend in the decrease of the hair cell (*atoh1a*) and neuronal (*neurog1*) transcripts.

Discussion

These results provide evidence for the involvement of *shox2* in early otic neurosensory development of hair cells and otic neurons. We propose that *shox2* is essential for determining hair cell and neuronal fate. Generation of a mutant *shox2* using genome editing and employing various reporter lines in zebrafish line will help elucidate the functional role of *shox2* in inner ear development.

PS 93

Early Otocyst Patterning Predicts Mature Planar Polarity Organization

Jeremy Duncan; Michael Deans
University of Utah Medical School

Sensory epithelia of the vestibule and the hair cells that they contain are precisely patterned in order to detect a wide range of stimuli. Detection of motion in specific directions requires precise orientations of stereociliary bundles. Planar cell polarity (PCP) proteins have been shown to be asymmetrically localized in hair cells and supporting cells and coordinate the orientation of stereociliary bundles. While stereociliary bundles within the cochlea and cristae are oriented in the same direction, hair cells of the utricle and saccule are segregated between two distinct populations with oppositely oriented stereociliary bundles separated by a boundary called the line of polarity reversal (LPR). Because PCP protein localization is not altered across the LPR it has been suggested that PCP proteins set up a ground polarity axis and that a second mechanism patterns the LPR. What remains unknown are 1) when the ground polarity axis is established and 2) when the LPR and two domains of opposite stereociliary bundle orientations are specified.

Celsr1 is a core PCP protein that has a polarized distribution in hair cells and supporting cells, and its absence results in misoriented stereociliary bundles. We found that *Celsr1* expression initiates before hair cell differentiation and that the polarized distribution of *Celsr1* protein is established as early as E11.5 in the pro-sensory epithelia, prior to the separation of the pro-sensory domain into distinct vestibular organs. To determine if the early expression of *Celsr1* is correlated with mature stereociliary bundle polarity we took advantage of a mouse mutant (Dreher) where the pro-sensory domain fails to separate. In Dreher mutants the axis of early *Celsr1* polarization seen at E11.5 remains unaltered in the merged gravistatic organ at birth. In order to determine if

the LPR is also established in the pro-sensory epithelia we have taken advantage of Cre lineage tracing using *Emx2cre* which specifically labels hair cells on one side of the LPR. Early in development *Emx2cre* compartmentalizes the pro-sensory epithelia, and at later stages, lineage traced cells are segregated prior to morphological emergence of the LPR. Thus the antecedent of the LPR may be found at this early stage. Altogether these data suggest that early patterning of the pro-sensory epithelia through the polarized distribution of core PCP proteins and transcriptional patterning determines the organization of planar polarity in the mature organ.

PS 94

Dynamic *atoh1* Expression in Prosensory Domain Visualized by 2-color Fluorescence 3D Real-time Imaging

Tomoko Tateya¹; Susumu Sakamoto¹; Fumiyoshi Ishidate²; Itaru Imayoshi¹; Ryoichiro Kageyama¹

¹*Institute for Virus Research, Kyoto University*; ²*World Premier International Research Initiative—Institute for Integrated Cell-Material Sciences (WPI-iCeMS), Kyoto University*

A specialized sensory epithelium of the cochlea of the mammalian inner ear, called the organ of Corti, contains mechanosensory hair cells and supporting cells. During development, the prosensory domain is formed in the floor of the cochlear duct, and then hair cells and supporting cells differentiate from common precursors in the prosensory domain. The activator-type basic helix-loop-helix transcription factor, *Atoh1* is a key player in the hair cell differentiation, and is known to be both necessary and sufficient for hair cell specification and differentiation. Prior to *Atoh1* role in the hair cell specification, it also functions as a proneural gene and is initially expressed in a relatively broad and diffuse stripe of prosensory cells. As development proceeds, *Atoh1* expression becomes restricted to limited number of cells, which eventually give rise to one row of inner hair cells and three rows of outer hair cells. Thus *Atoh1* expression pattern dynamically changes in the prosensory domain during the period of a proneural factor to a commitment factor responsible for hair cell fate decision. This transition period is important because it is the exact process of hair cell specification and organization and occurs in approximately 1-2 days. Given the short transition period, accurate analysis of this process on fixed samples is challenging. To address this problem, we established 2-color fluorescence 3D real-time imaging system using the cochlear explants of the double transgenic mice. We crossed two transgenic lines, *Atoh1*-EGFP, and mCherry reporter mice for the visualization of either *Dll1*, *Hes5* or nuclei. Overnight real-time imaging was performed on

E13.5, E14.5 or E15.5 cochlear explants of the double transgenic mice. The fluorescence intensity and 3D position of individual cells in prosensory domain were detected at each time frame, and some cells were tracked over time. The fluorescence intensity was enough to detect the initial weak Atoh1 expression in cochlear explants, accompanied with a specific trend of changes in fluorescence and migration among the Atoh1-positive cells. We are further analyzing the data to detect dynamic Atoh1 expression and its relation to hair cell and supporting cell specification and differentiation.

PS 95

Expression of Sox2, Sox10 and Gata3 during Spiral Ganglion Development and Maturation in the Mammalian Cochlea

Koji Nishimura¹; Teppei Noda²; Alain Dabdoub³

¹Shiga Medical Center Research Institute, Moriyama, Japan; ²Sunnybrook Research Institute; ³Biological Sciences, Sunnybrook Research Institute, University of Toronto

Introduction

Spiral ganglion neurons (SGNs) are primary auditory neurons that connect cochlear sensory hair cells in the mammalian inner ear to cochlear nucleus neurons in the brainstem. SGNs develop from neuroblasts delaminated from the proneurosensory domain of the otocyst and keep maturing until the onset of hearing after birth. There are two types of SGNs: type I that innervate the inner hair cells (IHCs), and type II that innervate the outer hair cells (OHCs). Glial cells surrounding these neurons originate in the neural crest cells and migrate to the spiral ganglion. Several transcription factors are known to regulate the development and differentiation of SGNs. Here we systemically examined the spatiotemporal expression of three transcription factors: Sox2, Sox10 and GATA3 from early delamination at embryonic day (E) 10 to adulthood.

Materials and Methods

We used three mice lines: Sox2EGFP/+ knock-in mice (Sox2-EGFP), in which the Sox2 open reading frame is replaced by EGFP; Sox10-IRES-Venus mice (kindly donated by Dr. Tsutomu Motohashi, Gifu University); and CD-1 mice (WT). We harvested tissues from E10 to postnatal day (P) 40 for immunohistochemical analyses.

Results

Sox2 and Sox10 are initially expressed in the proneurosensory cells in the otocyst (E10). By E12.5 both Sox2 and Sox10 are downregulated in the developing cochleovestibular neurons; however, Sox2 expression is transiently increased in the neurons around birth and

is downregulated again in mature SGNs. Furthermore, both Sox2 and Sox10 are expressed in neural crest cell-derived migrating glial cells and continue to be expressed in spiral ganglion glial cells through adulthood. GATA3 is initially expressed in all the developing neurons, and then expression is highly maintained only in type II neurons as SGNs mature, demonstrated by co-expression of peripherin and GATA3. We also show that Mafk, a downstream target of GATA3 (Yu et al., 2013), is initially detected in the nuclei of all SGNs, and then is maintained in the nuclei of mature type II SGNs while it is localized in cytoplasm of type I SGNs, suggesting that the GATA3-Mafk transcriptional network, which is involved in synaptogenesis, is maintained in mature type II neurons.

Conclusion

Sox2 and GATA3 play a role not only in development but also in maturation of both type I and type II SGNs.

PS 96

RFX Transcription Factors are Necessary for Hair Cell Terminal Differentiation but not for Survival of Mature Hair Cells

Ronna Hertzano¹; Beatrice Milon²; Zachary Margulies³; Mark McMurray³; Shadan Hadi⁴; Sunayana Mitra³; Gregory I. Frolenkov⁵

¹Department of Otorhinolaryngology, Department of Anatomy and Neurobiology, and Institute for Genome Sciences, University of Maryland School of Medicine, Baltimore, MD USA; ²Department of Otorhinolaryngology, University of Maryland School of Medicine, Baltimore, MD 21201, USA; ³Department of Otorhinolaryngology, School of Medicine, University of Maryland Baltimore; ⁴Department of Physiology, University of Kentucky; ⁵Dept Physiology, University of Kentucky

While several transcription factors for early differentiation of hair cells have been identified such as ATOH1, GFI1 and POU4F3, little is known about factors necessary for late differentiation. We recently identified RFX as a family of transcription factors essential for the survival of the terminally differentiating hair cells in mice. Indeed, embryonic (E16) conditional deletion of both Rfx1 and Rfx3 by a Cre recombinase under the control of Gfi1 promoter (Rfx1flox/flox;Rfx3 flox/flox;Gfi1Cre/+ mice) leads to deafness due to the loss of apparently well-formed outer hair cells (OHC) between P12 and P15. These results suggested that RFX1 and 3 are necessary for 1) terminal differentiation of hair cells and/or 2) survival of hair cells after the onset of hearing. Here we show new data refining the timeframe of the hair cell loss in the Rfx1flox/flox;Rfx3 flox/flox;Gfi1Cre/+ mutants

from P12 to P15 down to P12 to P13, revealing a rapid loss of OHC within 24 hours at the time of onset of hearing. Further, to determine if RFX1 and 3 are needed for hair cell terminal differentiation or for hair cell survival, we crossed *Rfx1flox/flox;Rfx3flox/flox* mice to the inducible *prestin-CreERT2* mice to be able to delete RFX1 and RFX3 at later time points. First, mice were injected with tamoxifen to induce recombination at 3 weeks of age, and their auditory function was measured using auditory brainstem response (ABR) at 4, 5 and 12 weeks. ABR results show that the mutants have similar thresholds when compared to their wildtype littermates. The experiment was then repeated by injecting tamoxifen at P8 and P9 and by measuring hearing thresholds at 4, 8 and 12 weeks. Here again, no differences were detected in the ABR thresholds between the mutants and control mice. Our results with the *Rfx1flox/flox;Rfx3flox/flox;Prestin-CreERT2/+* mice indicate that RFX1 and 3 are primarily involved in the terminal differentiation of hair cells rather than the long term survival of mature hair cells.

PS 97

Role of LIM-only protein LMO7 in Hair Cell and Hearing Function

Tingting Du¹; Shimon Francis²; Jung-Bum Shin¹

¹University of Virginia, Neuroscience Department; ²National Institute on Deafness and Other Communication Disorders

The sensory hair cell harbors two specialized F-actin structures: The mechanosensory hair bundle and the cuticular plate, into which each stereocilium of the hair bundle is inserted. For maximal sensitivity of the hair cell mechanotransduction process, sound-induced vibrations must be translated into stereocilia deflections pivoting at its base. This is only achieved if the insertion points of individual stereocilia, and the entirety of the cuticular plate, are anchored firmly into the hair cell. It is thus expected that defects in cuticular plate integrity will affect hair cell mechanotransduction efficiency and hearing function.

In our studies, we show that in the inner ear, the LIM only protein 7 (LMO7) is highly enriched in hair cells, and localizes to the cuticular plate. To determine the role of LMO7 in hearing, we applied clustered regularly interspaced short palindromic repeat (CRISPR)/Cas9-mediated genome-editing technology to induce targeted mutations into the mouse *Lmo7* gene, resulting in the elimination of LMO7 protein expression. In LMO7 deficient mice, we found normal morphology of hair bundles, but significantly reduced F-actin levels in the cuticular plate. Functional analysis of hearing revealed that LMO7 deficient mice display moderate hearing loss

in high and mid-frequency but severe hearing loss in low-frequency in an age-related fashion. Hearing loss was not caused by loss of hair cells, but was accompanied by loss of hair cell function. Overall, our current results suggest that LMO7 is required for maintaining the integrity of the cuticular plate, and that its deficiency causes age-related hearing loss.

PS 98

Wnt9a Influences Afferent and Efferent Patterning in the Chicken Cochlea

Vidhya Munnamalai¹; Kuhn Hee Song²; Donna M. Fekete³

¹Department of Biological Sciences, Purdue Institute for Integrative Neuroscience; ²Department of Biological Sciences; ³Department of Biological Sciences, Purdue Institute for Integrative Neuroscience, Purdue University Center for Cancer Research

Wnts comprise a major morphogen family that is crucial for embryonic development. Our lab studies whether and how Wnt signaling regulates not only cell proliferation, but also patterning in the cochlea of both mice and birds. The chicken basilar papilla (BP) consists of tall hair cells (THCs) residing on the neural side (named for their proximity to the auditory ganglion) and short hair cells (SHCs) on the abneural side. THCs predominantly receive afferent innervation, while the SHCs predominantly receive efferent innervation. This radial asymmetry is a conserved organizational feature of amniotes.

Wnt9a is expressed in the homogene cell anlage along the neural edge of the BP. To determine whether Wnt9a can regulate radial asymmetries across the cochlea, we induced Wnt9a overexpression (Wnt9a-OE) at a stage of development preceding cell specification and innervation. RCAS virus was first injected into the periotic mesenchyme on embryonic day 2 (E2), followed by injection of RCAS/Wnt9a directly into the otocyst on E3. BPs were harvested on E18 and fixed for histological analyses. Afferent connections were studied by immunolabeling for axons and the presynaptic ribbon foci in hair cells were mapped with a CtBP2 antibody. Efferent connections were traced into the auditory ganglion and BP following implantation of fluorescent NeuroVue® dye filters into the auditory brainstem.

Wnt9a-OE results in an apparent cell fate switch: there is an increase in THCs across the BP with little to no evidence of the SHC phenotype. Afferents spread more evenly across the BP to occupy much or all of its width. In normal ears, CtBP2 puncta are more abundant in THCs compared with SHCs; whereas, consistent with a fate switch in Wnt9a-OE BPs, the number of CtBP2

puncta per HC was greatly increased across the radial axis. The efferent innervation was also abnormal. In controls, efferents enter the cochlea through a narrow and defined region called the habenula perforata. In contrast, Wnt9a-OE leads to a broadening of the entry points for efferents across the BP. Furthermore, efferent neurites appeared to be less exploratory in Wnt9a-OE ears compared to contralateral controls.

These data suggest that Wnts, long known for their ability to enhance proliferation, can also influence patterning. Our studies suggest that in normal ears, the asymmetric source of Wnts on the neural side of the developing BP may be instructive to setting up radial asymmetries across the sensory organ that can subsequently affect afferent and efferent connectivity.

PS 99

Role of Retinoic Acid Signaling in Regional Specification of Vestibular Sensory Organs

Kazuya Ono; Doris Wu

Laboratory of Molecular Biology, National Institute on Deafness and Other Communication Disorders, National Institutes of Health

The vestibular system consists of two macular organs, dedicated to detecting linear acceleration, and three cristae responsible for detecting angular acceleration. Based on morphological criteria, vestibular hair cells (HCs) in each organ are classified into two major cell types: Type I and type II sensory HCs. Pear-shaped Type I HCs are innervated by calyceal nerve endings, whereas bouton type endings contact Type II HCs. The central region of each vestibular sensory organ consists of a high concentration of specialized Type I HCs innervated by pure calyces. These Type I HCs express a gene encoding a calcium-binding protein, oncomodulin, whereas pure calyces are characterized by the expression of another calcium-binding protein calretinin. Despite the postulated importance of the central regions (central zone in cristae and striola in maculae) of the vestibule in mediating vestibular reflexes, functional contribution of this specialized region for maintaining balance has not been demonstrated experimentally. Also, the molecular mechanisms that underlie the formation of this specialized zone during development is unknown.

Retinoic acid (RA) is a derivative of vitamin A that regulates many cellular events including cell differentiation, proliferation, and migration. The availability of RA during embryogenesis is regulated by the tissue-specific expression of RA synthesizing enzymes such as retinaldehyde dehydrogenases (Raldhs), as well as RA degradation enzymes such as Cyp26s. Here we show that regulated RA signaling mediates regionalization of the

vestibular sensory organs. The central region of vestibular organs requires a low level of RA signaling mediated by the expression of one of the RA degradation enzymes, Cyp26b1, whereas the peripheral region of each sensory organ expresses a gene that encodes a RA synthesizing enzyme, Raldh3. The lack of Cyp26b1 resulted in a severe reduction of the central region, based on the loss of oncomodulin-expressing HCs. Consistent with these results, conditional knock out of Cyp26b1 exhibited a loss of pure calyces based on calretinin and calbindin staining. In contrast, in Raldh3 knockouts, in which RA signaling is reduced, an expanded central region was observed. Taken together, our results suggest that regional patterning of the vestibular sensory organs is established by differential RA signaling.

PS 100

Administration of FGF9 In Vivo Rescues Loss of Outer Hair Cells and Supporting Cells Cause by FGF20 Deletion

Sung-Ho Huh¹; David Ornitz²

¹University of Nebraska Medical Center; ²Washington University School of Medicine

Background

The organ of Corti (OC) is a sensory organ that transduces sound vibrations into neuronal signals. The OC contains one row of inner hair cells (IHC) and three rows of outer hair cells (OHCs). In addition, each sensory hair cell is associated with an underlying supporting cell (SC). The mechanisms that regulate the formation of OHCs are significant, since the loss of OHCs is a leading cause of sensorineural deafness and age-related hearing loss. Previously, we have generated Fgf20 knockout mice and found out that mice lacking a functional Fgf20 gene are viable and healthy but are congenitally deaf. Furthermore, we showed that Fgf20 is required for OHCs and Outer SCs (OSCs) differentiation. We also identified that treatment of FGF9, the paralog of FGF20, rescued partially loss of OHCs and OSCs in cultured Fgf20 mutant cochlea.

Methods

To investigate the therapeutic potential of FGF9, we generated FGF9 overexpression mouse model under the control of cre recombinase and doxycycline. FGF9 was induced in vivo from Fgf20 mutant background at the various time point under the FGF20 expressed cells. HCs and SCs were counted with immunostained cochleae. Cochlear length was determined.

Results

Induction of FGF9 between E13.5 to E15.5 completely rescued loss of OHCs and OSCs in addition to cochlear length cause by Fgf20 loss of function. Single injection

of doxycycline at the time of differentiation partially rescued the loss of OHCs and OSCs caused by Fgf20 loss of function.

Conclusions

These data indicate that FGF9 can be substituted by FGF20 during prosensory cells differentiation. These data also suggests that FGF20 is not required for prosensory cell specification.

PS 101

Proliferation and Differentiation of Auditory Hair Cells Is Regulated by the Lin-41 (Trim71)/let-7 axis

Lale Evsen; Angelika Doetzlhofer
Johns Hopkins School of Medicine

Lin-41, as well as its negative regulator let-7 was initially identified in a screen for heterochronic genes in *C. elegans*. Lin-41, an ubiquitin ligase and RNA-binding protein, plays a critical role in stem cell maintenance and proliferation, and negatively controls differentiation events. In contrast, let-7 microRNAs (miRNA) inhibit proliferation. We recently discovered that Lin-41 is highly expressed in progenitors of the neural-sensory lineage in the murine and avian auditory organs. Lin-41 is expressed within the otic vesicle neural-sensory competent domain and later in auditory progenitors, but rapidly declines in expression with increasing hair cell (HC) differentiation in both the murine and avian inner ear, whereas mature let-7 levels increase in expression with increasing HC differentiation, and are maintained post-natally. To address the role of Lin-41 and let-7 miRNAs in auditory sensory development we manipulated their levels in the developing chicken auditory organ using in ovo micro-electroporation together with in ovo cell proliferation assays. We found that over-expression of Lin-41 in the chick auditory organ lead to excess progenitor cell proliferation and an inhibition of HC differentiation. Over-expression of a let-7 sponge, which inhibits the activity of all let-7 miRNAs, resulted in an increase in progenitor proliferation and inhibition of HC differentiation similar to the Lin-41 over-expression phenotype. These findings suggest that Lin-41 is critical for maintaining auditory sensory progenitors in a proliferative and undifferentiated state and let-7 miRNAs function by inhibiting Lin-41 expression/function in the developing auditory organ. Over-expression of let-7b resulted in a decrease in progenitor proliferation; however, surprisingly we did not observe premature HC differentiation, instead we observed an inhibition or delay in Atoh1 transcript expression. This suggests that let-7b negatively regulates Atoh1 mRNA expression and too high let-7b levels delay or halt auditory HC differentiation. In conclusion, the data indicate a fine-tuned balance/gradients of expression levels between Lin-41 and let-7 in regulating proliferation and dif-

ferentiation events within auditory sensory development. Perturbations in this balance lead to an interference of the normal sensory progenitor cell proliferation program and an inhibition of HC differentiation.

PS 102

GSK3 Regulates Hair Cell Fates in the Sensory Epithelium of the Cochlea

Kathryn L. Ellis¹; Takayuki Okano²; Matthew W. Kelley³

¹NIDCD, NIH; ²Department of Otolaryngology, Head and Neck Surgery, Graduate School of Medicine, Kyoto University; ³Laboratory of Cochlear Development, NIDCD, NIH, Bethesda, Maryland, USA

The sensory epithelium of the mammalian cochlea (the organ of Corti, OC) is composed of two types of innervated mechanosensory hair cells – the medial inner hair cells (IHCs) and the lateral outer hair cells (OHCs) and six types of supporting cells. IHCs and OHCs differ structurally and functionally and are separated by a single row of boundary supporting cells. The overall structure comprises an exquisitely patterned mosaic of cells whose proper differentiation and organization is critical for hearing. While many of the molecular mechanisms responsible for specification of the sensory epithelium and the hair cells are well understood, little is known about how an otherwise homogeneous prosensory domain develops into two functionally distinct medial and lateral domains.

Glycogen synthase kinase 3 (GSK3), a serine/threonine protein kinase, has been shown to play an important role in many signaling pathways including Hh, Notch, GPCRs, and most commonly, in canonical Wnt. To determine whether GSK3 plays a role in medio-lateral patterning within the OC, multiple GSK3 antagonists were tested in vitro in cochlear explants. Inhibition of GSK3 leads to a dramatic increase in the size of the medial domain and a proportional decrease in the size of the lateral domain. Lineage tracing reveals that this shift occurs as a result of lateral cells adopting a medial cell fate. This is significantly different from the changes observed in response to activation of canonical Wnt signaling; an increase in the number of overall hair cells. Based on these results, we are working to identify the Wnt-independent roles of GSK3 in cochlear sensory epithelium patterning. We have demonstrated that BMP4, an inducer of the lateral OC domain, and its downstream targets are reduced following GSK3 inhibition and that ectopic BMP4 treatment partially rescues the shift in lateral to medial cell fate. This work will help to elucidate the molecular mechanisms that are necessary for patterning the OC along the medio-lateral axis.

PS 103

Abrogation of Beta Catenin Signaling during Cochlear Development Results in Differentiation Defects in Supporting Cells and Supernumerary Inner Hair Cells

Lina Jansson¹; Jessica Shen¹; Sung-Ho Huh²; Alan Cheng³

¹Stanford University School of Medicine; ²University of Nebraska Medical Center; ³Stanford University, School of Medicine, Department of Otolaryngology

Beta catenin acts as the downstream signal transducer in the canonical Wnt pathway. In the early stages of inner ear development deletion of beta catenin leads to severe defects in otic placode formation. During the late embryonic period, beta-catenin has been implicated in hair cell specification. Here we investigate the effect of deleting beta catenin on hair cell and supporting cell differentiation in the organ of Corti.

We employed the Sox2-CreERT2 transgenic mouse to conditionally delete beta catenin at E13.5 and examined cochlear tissue at E20.5/P0. We detected efficient deletion of the transcript 2 days post injection and found the length of the beta-catenin deficient cochleae to be 10% decreased compared to control. Although knockout and control tissues showed formation of a comparable density of Myosin7a-positive hair cells, they were not organized in the usual distinct four rows. These results were also reproduced in a different model where Fgf20-Cre were used to delete beta catenin.

We found a comparable density of Prox1-expressing pillar and Deiters' cells in knockout and control tissues. However, the supporting cells were similarly disorganized throughout the cochlea. Instead of a single row of p75-NTR-positive pillar cells as normally observed lateral to the IHCs, we instead found ectopic expression of p75NTR in multiple cells surrounding the IHCs in knockout cochlea. In addition, the inner pillar cell marker Lgr6 was absent from the supporting cell area.

Since expression of Fgf8 in IHCs is necessary for the subsequent differentiation of pillar cells we examined the expression of both Fgf8 and its receptor, Fgfr3, in IHCs and supporting cells respectively and found both present in their respective cell types. However, extra-numerary Fgf8-positive IHCs were found in the beta catenin-deleted cochlea at the expense of OHC numbers.

In summary we found that loss of beta catenin during cochlear development does not impair specification and early differentiation of hair cells. Rather it leads to disorganization of medial supporting cells and misexpres-

sion of inner pillar cell markers. Furthermore, there may to be a switch between outer and inner hair cell fate without altering the number of hair cells present.

PS 104

The Roles of Jagged1-mediated Notch Signaling in Supporting Cell Development and Maintenance

Elena Chrysostomou¹; Dean Campbell²; Angelika Doetzlhofer³

¹Johns Hopkins University; ²Johns Hopkins University School of Medicine; ³Johns Hopkins School of Medicine

The cochlear sensory epithelium consists of a precisely organized pattern of hair cells (HCs) and supporting cells (SCs) that arise from a common pool of sensory progenitor cells. Loss of either of these cells results in permanent hearing loss therefore understanding the molecular mechanisms of how these cells differentiate is essential. Notch signaling is well known for its HC-repressive role in lateral inhibition which is mediated by Notch ligands, Delta-like1 and Jagged2, expressed in nascent HCs. We recently described a new instructive role for Notch signaling in SC development. Using genetic gain and loss-of-function strategies we found that Notch signaling is both necessary and sufficient for SC development. Our current aim is to identify the Notch receptors and ligands that mediate these instructive functions and in addition to identify the mechanism(s) involved in SC maintenance. A potential candidate is the Notch ligand Jagged1 (Jag1), which is expressed initially within sensory progenitor cells and continues to be expressed in SCs throughout their lifetime. In order to determine the function of Jag1 in SC development and maintenance we used a recently developed tamoxifen-inducible Sox2-CreER line in conjunction with Jag1 floxed mouse line to delete Jag1 in differentiating SCs. We found that ablation of Jag1 at the onset of SC differentiation (stage E14.5) resulted in a significant reduction of selective SC-specific genes. Amongst these were genes involved in cochlear innervation, suggesting a role for Jag1-mediated Notch signaling in cochlear innervation. Consistent with such role, examination of the Jag1 mutants revealed defects in outer HC innervation, with neuronal fibers turning randomly towards the apex and base. Interestingly, in addition to its potential function in SC-development, Jag1 appears to function in SC maintenance. Disruption of Jag1-mediated Notch signaling in both the differentiating cochlea (stage E14.5) as well as the terminal differentiated cochlea (stage P0/P1) resulted in ectopic inner HCs. In conclusion, our findings indicate that the SC-specific Notch ligand Jag1 plays multiple roles during cochlear differentiation. Our evidence suggests

an instructive role in SC development, but in addition it may be important for SC maintenance. Identification of the precise mechanism(s) that are involved in some of these processes will be essential for identifying potential targets for regeneration.

PS 105

Loss of Notch Signaling in the Inner Ear Prevents the Formation of Vestibular Prosensory Domains and Sensory Organs

Rogers Brown II¹; Martin L. Basch²; Andy Groves¹

¹Baylor College of Medicine; ²Case Western Reserve University School of Medicine

Proper development of the inner ear relies on the use of Notch signaling during neurogenesis, prosensory domain refinement, and hair cell-supporting cell differentiation. Previous studies to analyze the role of Notch in these processes targeted key ligands or receptors in the Notch signaling pathway like Jag1, Jag2, Notch1, and Dll1. These experiments produced a range of distinct phenotypes which suggests that when some of these elements are removed from the ear, other receptors or ligands may be able to compensate in certain situations.

To address this problem, we have tested the effect of a complete loss of Notch signaling in the inner ear by conditionally deleting RBPJ, the transcription co-factor through which the Notch pathway acts. By targeting this bottleneck of the pathway, we aim to abolish all Notch signaling in the inner ear. We deleted RBPJ throughout the inner ear early in development using Pax2-Cre mice. We examined the morphological development of RBPJ conditional knockouts (RBPJ cKO) by performing paint fillings and found that as the semi-circular canal plates grow out, they develop severe truncations. When we examined the vestibular prosensory domains of the cristae and maculae using Sox2 and Jag1 immunostaining, we found that the prosensory domains for both types of organ were greatly reduced as development progressed, although during early otic development no change in expression of either marker was detected in the inner ear. To examine the specific development of the cristae and maculae, we used RNA in situ hybridizations for BMP4 (cristae) and Lfng (maculae). We found that Lfng expression progressively decreased in the developing maculae, and BMP4 expression was either minimal or entirely absent in the developing cristae. The initial maintenance of normal Lfng, Jag1, and Sox2 staining despite RBPJ deletion at an earlier time suggests the Pax2-Cre driven deletion of RBPJ may result in an initial partial loss of function, which could be attributed to the stability of RBPJ protein after genetic deletion.

Our data suggests that the RBPJ cKO represents a loss of Notch signaling in the vestibular system of the inner ear that is very similar to the Jag1 cKO. Both develop a failure of the vestibular prosensory domains to form, although the RBPJ cKO presents a more variable and more severe set of corresponding vestibular truncations and maculae defects.

PS 106

Essential Role of the channel kinase TRPM7 in Cochlear Morphogenesis

Andre Landin-Malt¹; Mandar Kulkarni¹; Michelle Lynskey¹; Bimal Desai²; Xiaowei Lu¹

¹Department of Cell Biology, University of Virginia Health System; ²Department of Pharmacology, University of Virginia Health System

Planar cell polarity (PCP) signaling mediates multiple aspects of cochlear development, including elongation of the cochlear duct and the uniform orientation of V-shaped hair bundles atop sensory hair cells. Recent advances have uncovered multiple pathways for intercellular PCP signaling in the developing cochlea, consisting of the core Frizzled/PCP pathway, the PK7 and the Nectin-mediated signaling pathways. However, how these intercellular PCP signals are integrated to control hair cell PCP is not clearly understood.

To further elucidate mechanisms of PCP signaling during cochlear morphogenesis, we are investigating the function of transient receptor potential-melastatin-like 7 (Trpm7) in mouse inner ear development. Trpm7 is an essential gene, encoding a ubiquitous cation channel with a cytosolic α -kinase domain. In *Xenopus*, TRPM7 functions synergistically with Frizzled/PCP signaling to control convergent extension movements [1]. Furthermore, published RNA-Seq data show that Trpm7 is expressed in the developing cochlea, consistent with a function during cochlear morphogenesis. Using a conditional Trpm7 allele [2] and Foxg1Cre, we have generated inner-ear specific Trpm7 knockout mutant (Trpm7cKO). Analysis of Trpm7cKO cochleae revealed that the cochlear duct was significantly shorter with decreased number of hair cells and disorganized cellular organization, suggesting that Trpm7 is required for cochlear elongation. In contrast to the core PCP mutants, planar polarization of Trpm7cKO hair cells, as indicated by hair bundle orientation and basal body positioning, was largely unaffected. To further understand the cellular patterning defects, we are performing experiments to examine cell proliferation, cell differentiation, cell adhesion and cytoskeletal organization in Trpm7cKO cochleae. We are also interested in determining the specific roles of the ion channel and kinase domains

of TRPM7 in cochlear morphogenesis. Details of our analysis will be presented.

Taken together, our results reveal an essential role of TRPM7 in cochlear morphogenesis.

[1] Wei Liu, Li-Ting Su, Deepak K. Khadka, Courtney Mezzacappa, Yuko Komiya, Akira Sato, Raymond Habas, Loren W. Runnels TRPM7 regulates gastrulation during vertebrate embryogenesis *Dev Biol.* 2011 Feb 15; 350(2): 348–357.

[2] Jie Jin, Long-Jun Wu, Janice Jun Xiping Cheng, Haoning Xu, Nancy C. Andrews, and David E. Clapham The channel kinase, TRPM7, is required for early

PS 107

Stereocilin Paralogs Have Distinct Roles in Zebrafish Inner Ear Development

Kenneth Kramer; Christopher Inserra
Creighton University

In the vertebrate inner ear, sound and movement are transduced into electrical signals by specialized bundles of cilia on the apical surface of sensory hair cells. Each hair bundle is composed of a single Tubulin-filled kinocilium attached to multiple rows of Actin-packed stereocilia. Cilia are linked to each other and to an overlying membrane by a complex of proteins that includes Stereocilin (STRC), a putative GPI-linked protein that is expressed in both stereocilia and kinocilia in mouse auditory and vestibular hair cells. Since loss of STRC in mouse results in defects in the attachments both between neighboring cilia as well as between cilia and the overlying tectorial membrane, we sought to determine if STRC is similarly required in zebrafish inner ear development. Using antibodies that we developed that specifically distinguish the two zebrafish STRC paralogs, we found that STRCa and STRCb are both expressed during hair cell formation but with slightly different expression patterns. STRCb is found on the distal tip of kinocilia when the hair cells first start tethering to the seeding otoliths, while STRCa is found a few hours later in a few punctate locations along the distal half of the kinocilium. Knockdown of *strcb* by injecting antisense morpholinos or eliminating *strcb* in CRISPR/Cas9-generated mutant embryos blocked the ability of kinocilia to tether otoliths to hair cells. In contrast, otolith attachment appeared to be normal in *strca* morphants and mutant embryos. Kinocilia in *strcb* morphant and mutant embryos were normal in length, yet proteins in the unattached otolith were disorganized compared to otoliths in normal and *strca*-deficient zebrafish. We conclude that STRCb is uniquely required for zebrafish otolith attachment and organization.

PS 766

Characterization of the Inner Ear of the Transgenic Doublecortin Mouse Model

Xiaoyi Li¹; Rafal Olszewski¹; Soumya Korrapati²; Michael Hoa³

¹*Division of Intramural Research, NIDCD, NIH, Bethesda, Maryland, USA;* ²*National Institute on Deafness and Other Communication Disorders, National Institutes of Health;* ³*Office of the Clinical Director, Otolaryngology Surgeon-Scientist Program, Auditory Development and Restoration Program, Division of Intramural Research, NIDCD, NIH, Bethesda, Maryland, USA*

Background

The stria vascularis (SV) produces the endocochlear potential which enables proper hair cell functioning in the cochlea. The three dominant types of cells in the SV are marginal cells (MC), intermediate cells (IC), and basal cells (BC). Both MC and IC have irregular digit-like processes projecting from their cytoplasm that interdigitate with each other. Limited cell-type specific gene markers exist for these cells, and the processes of MC and IC are extremely fine, making it difficult to clearly image their structures by conventional imaging methods. We have recently identified a transgenic mouse model (Dcx-DsRed) that selectively labels cell types in the lateral wall that can be used to characterize cell organization during development. Doublecortin (DCX) is a neuronal migration protein which binds and regulates microtubule stability during development. In this study, we sought to characterize the developmental expression of DCX in the SV and use this mouse model to profile proliferation patterns of lateral wall cells at specific time points during development.

Methods

A transgenic Dcx-DsRed mouse model was used. Cochlear lateral walls with SV were harvested and dissected into basal, medial, and apical segments. A developmental survey (P1 – P50) of transgenic and endogenous Dcx was performed. The number of DsRed+ marginal and spindle cells in the SV were quantified using confocal images and ImageJ. EdU (5-ethynyl-2'-deoxyuridine) labeling was performed on cochlear lateral wall from these developmental time points to quantify dividing cells. Cochlear cross sections were immunostained, expanded using expansion microscopy, and imaged on a water immersion confocal microscope.

Results

Developmental expression of Dcx-DsRed parallels endogenous Dcx expression, and is localized to the lateral wall and spiral ganglion neurons. We demonstrate the postnatal developmental time course of doublecortin

expression in the lateral wall from P1 to P50. Early in postnatal development, doublecortin expression is localized to a subpopulation of MC, spindle cells and spiral prominence fibrocytes. Later in development, doublecortin expression progressively becomes restricted to spindle cells and spiral prominence fibrocytes. We characterize the distribution and number of actively dividing cells during development of the lateral wall in the Dcx-DsRed transgenic mouse. Using expansion microscopy, we provide a more detailed view of lateral wall cell types and the interdigitating processes of the marginal and intermediate cells.

Conclusion

The Dcx-DsRed transgenic mouse model is a viable model to investigate lateral wall cell types in the mouse cochlea, and may be useful in characterization of SV cell type development.

Genetics: Illuminating Genetic Architecture for Diagnosis for Hearing Loss

PS 108

Mutation in DMXL2 Cause Dominant Late-Onset Non-Syndromic Hearing Loss and Alter Protein-Protein Interaction with WDR7

Hao Wu¹; Dongye Chen²

¹Department of Otolaryngology Head & Neck Surgery, The Ninth People's Hospital, School of Medicine, Shanghai Jiao Tong University, Shanghai, China; ²1. Department of Otolaryngology Head & Neck Surgery, The Ninth People's Hospital, School of Medicine, Shanghai Jiao Tong University, Shanghai, China

Background

Mutations in DMXL2 have been linked to a syndrome of incomplete puberty, central hypothyroidism, peripheral polyneuropathy, mental retardation, and abnormal glucose regulation, inherited in the recessive mode.

Methods

Linkage analysis and whole-exome sequencing is carried out on the family after a failure to identify mutations in the DFNB / DFNA genes frequently involved. Immunofluorescence analysis determine the expression of DMXL2 in mouse cochlea. The co-immunoprecipitation experiments is conducted to investigate protein interaction changes.

Results

In a dominant family segregated with late-onset, progressive, non-syndromic hearing impairment, linkage analysis revealed a 9.68 Mb candidate region on chromosome 15q21.2 (logarithm of the odds score = 4.03)

that contains DMXL2. Whole-exome sequencing identified a heterozygous p.Arg2417His variant of DMXL2 as the only candidate mutation segregating with the hearing impairment within the family. In perinatal mouse cochlea, we detected a restricted expression of DMXL2 in the hair cells as well as in the spiral ganglion neurons. The co-immunoprecipitation experiments suggested that the p.Arg2417His mutation of DMXL2 interfere Rbc3 α -Rbc3 β binding in vitro.

Conclusions

Our study suggested that the p.Arg2417His mutation of DMXL2 is a probable cause for dominant, non-syndromic hearing impairment. Identification of DMXL2 as a novel synapses gene may shed new light on its specific function in the auditory system.

PS 109

A Novel Susceptibility Locus at 6p21.33 for Bilateral Meniere's Disease Regulates Gene Expression in the TWEAK/Fn14 Pathway

Lidia Frejo¹; Alvaro Gallego-Martinez¹; Teresa Requena¹; Juan Manuel Espinosa-Sanchez¹; Jose Antonio Lopez-Escamez²; Jose A. Lopez-escamez³

¹Otology & Neurotology Group CTS495, Department of Genomic Medicine, GENYO - Centre for Genomics and Oncological Research – Pfizer/University of Granada/ Junta de Andalucía, Granada, Spain; ²Otology & Neurotology Group CTS495 GENYO ²Department of Otolaryngology, Granada University Hospital, ibs. GRANADA, Granada, Spain; ³Center for Genomic and Oncology (GENyO) Pfizer-Universidad de Granada-Junta de Andalucía

Background

Patients with Meniere's disease (MD) have an elevated prevalence of autoimmune diseases suggesting a shared autoimmune background (1). The genotyping of large cohorts of patients with several autoimmune diseases has shown that most of these diseases share susceptibility loci (2). However, no consistent loci or genetic marker have been associated to MD and most of the genetic studies were not replicated in an independent cohort of patients. Our main aim is to define a genetic marker for autoimmune MD.

Methods

A case-control study was performed using a high density genotyping array, containing 195805 single nucleotide polymorphism and 718 small indels, targeting 186 loci previously associated with 12 autoimmune disorders (ImmunoChip, Illumina). After QC, 96899 markers and 1579 samples (681 cases/898 controls) remained for further studies. A susceptibility locus for MD was iden-

tified in the subset of 199 patients with bilateral SNHL. The replication cohort, consisting of 218 patients with bilateral MD and 900 controls, was genotyped by Taqman assays selecting candidate tag-SNP to cover the haploblocks in 6p21.33. We performed a conditional haplotype gene expression assay in peripheral blood mononuclear cells (PBMC) to search for regulatory variants. RNA expression levels were measured using the HumanHT-12 v4 Expression BeadChip (Illumina). Limma R package was used for expression data analysis and normalization and for differential expression analysis. Differentially expressed genes in PBMC (adjusted $P < 0.001$), according to the conditional haplotype, were used to predict involved pathways.

Results

Meta-analysis confirmed a locus associated with bilateral MD (rs9380217; OR= 2.02 (1.59-2.60), ($P = 5.63 \times 10^{-8}$). Gene expression profile of homozygous haplotype-conditioned individuals demonstrates that this region is a trans expression quantitative trait locus (eQTL) for some class II HLA genes in PBMC, showing significant differences in 973 genes ($P < 0.001$). Signaling network analysis predicts several involved pathways, being the TWEAK/Fn14 pathway the top candidate ($P = 3.8 \times 10^{-8}$).

Conclusions

The SNV rs9380217 and rs4947296 could be used as predictors for bilateral SNHL in MD and the results support an immune dysfunction in the carriers of the risk haplotype.

Funding

This study was funded by EU-FEDER Funds for R+D+i by the Grant 2013-1242 from Instituto de Salud Carlos III.

References

1. Gazquez I et al. High Prevalence of Systemic Auto-immune Diseases in Patients with Menière's Disease. *PLoS ONE*. 2011; 6 (10):e26759.
2. Parkes M et al. Genetic insights into common pathways and complex relationships among immune-mediated diseases. *Nat Rev Genet*. 2013 Sep;14(9):661-73.

PS 110

Exome Sequencing Reveals ESRP1 Mutations as a Novel Cause of Bilateral Sensorineural Hearing Loss Associated with Dysplasia of the Lateral Semicircular Canals

Richard K. Tilton¹; Alex Rohacek²; Thomas Bebee²; Sarah E. Noon³; Maninder Kaur³; Jason Mills⁴; Matthew C. Dulik³; Russ Carstens⁵; Douglas Epstein⁵; Ian

D. Krantz⁶; John A. Germiller⁷

¹University of Iowa Hospitals and Clinics; ²University of Pennsylvania; ³The Children's Hospital of Philadelphia; ⁴The University of Pennsylvania; ⁵Perelman School of Medicine, University of Pennsylvania; ⁶The Children's Hospital of Philadelphia and The Perelman School of Medicine at the University of Pennsylvania; ⁷The Children's Hospital of Philadelphia and University of Pennsylvania

Exome sequencing is a single test that screens the exons of nearly all currently known genes and is gaining popularity as a diagnostic tool for children with congenital sensorineural hearing loss. We utilized exome sequencing to discover a novel hearing loss gene. A family of 8 was selected due to large family size, ideal pedigree with autosomal recessive pattern of hearing loss, no identifiable etiology after screening for common genetic causes (including GJB2 mutations), and the presence of a unique inner ear phenotype on imaging. The non-consanguineous parents of European ancestry are healthy with normal hearing and have 2 children affected by congenital profound bilateral sensorineural hearing loss (BLSNHL) and 4 children with normal hearing. There was no other family history of hearing loss. The proband is an 8 year old female with a history of congenital profound BLSNHL treated with unilateral cochlear implant. She has a 14 year old affected brother with congenital severe to profound BLSNHL who has the identical inner ear abnormality as his sister. Temporal bone CT in both affected siblings showed bilateral severe dysplasia limited to the lateral semicircular canal (LSCC), appearing as a heart-shape on axial slices ("valentine vestibule"), with the remainder of the cochleovestibular labyrinth being normal. This family was enrolled under an IRB approved protocol with informed consent at the Children's Hospital of Philadelphia (CHOP). Genomic DNA was extracted from whole blood from all 8 family members using standard procedures. Using exome sequencing, compound heterozygous mutations were identified in a novel candidate hearing loss gene, ESRP1, that segregated in the family, with each parent carrying one of the mutations, the affected carrying both, and none of the unaffected children carrying both mutations. Functional modeling in induced pluripotent stem cells generated from lymphoblastoid cell lines supported pathogenicity of the mutations. A mouse ESRP1 knockout model demonstrated a similar inner ear malformation with dysplasia of the LSCC. An additional cohort of 144 probands without an etiology for their BLSNHL after standard clinical testing was screened for mutations in ESRP1 and in the closely related gene ESRP2. No homozygous or compound heterozygous variants were identified in these genes, leading to the conclusion that although ESRP1 is a can-

didate novel hearing loss gene, it is likely a rare cause of hearing loss.

PS 111

A Novel Missense Mutation of Hyaluronan Synthase 1 Associated with Nonsyndromic Hereditary Progressive Hearing Loss

Sungsu Lee; Dami Kim; Moonyoung Choi; Alphonse Umugire; Hyong-Ho Cho

Dept. of Otolaryngology-Head and Neck Surgery, Chonnam National University Hospital

Introduction

Hereditary hearing loss is getting much interest nowadays due to next-generation sequencing. Hyaluronan synthase(HAS) is a membrane-bound protein that is abundant in epidermis and dermis. HAS1 is known to be expressed especially in fibroblast. In present study, we conducted a whole-exome sequencing(WES) in a familial late-onset hearing loss which revealed to be related to HAS1 gene. We wanted to check the role of HAS1 in the auditory system.

Methods

DNAs were isolated from blood samples of postlingual progressive bilateral moderate-severe hearing loss family. WES was performed from 4 familial members and candidate genes were selected. Confirmatory sanger sequencing(SS) was done from 10 members. Point mutagenesis was done and inserted in a plasmid vector. We transfected it into HEI-OC and HEK293 to see the protein stability. Murine embryonic samples from E10.5-16.5 were collected to see the expression of HAS1, 2, 3. Immunocytochemistry(ICC) was performed with HEI-OC, MS-1, 3T3-L1, B16F10 to see the cellular localization of HAS1.

Results

Through WES and SS, a missense mutation of HAS (p. C361Y) was detected. In silico SIFT, Polyphen2 predicted it to be a functional loss of HAS1. We constructed a vector with point-mutation on the equal site of human HAS1. mRNA or Protein expression were not different between wild type from mutant form. In ICC, mutant form didn't show any localization abnormality. HAS1 was expressed from E10.5 at otic cyst mostly in prosensory region. After late-embryonic period, it was expressed in stria vascularis.

Conclusion

We first report that HAS1 may also be related to auditory function by WES and bioinformatics study. HAS1 is expressed in prosensory region in early period and stria vascularis on late developmental stage suggesting

to play a role on these parts. The precise role of HAS1 in auditory function yet to be established.

PS 112

A New Tool for Translatome Analysis of Zebrafish Hair Cells from Intact Larvae

Maggie Matern¹; Alisha Beir²; Yoko Ogawa¹; Yang Song³; Rani Elkon⁴; Beatrice Milon¹; Katie Kindt²; Ronna Hertzano⁵

¹*Department of Otorhinolaryngology, University of Maryland School of Medicine, Baltimore, MD 21201, USA;* ²*National Institutes on Deafness and other Communication Disorders, NIH;* ³*Institute for Genome Sciences, University of Maryland School of Medicine, Baltimore, Maryland 21201, USA;* ⁴*Department of Human Molecular Genetics and Biochemistry, Sackler School of Medicine, Tel Aviv University, Tel Aviv, Israel;* ⁵*Department of Otorhinolaryngology, Department of Anatomy and Neurobiology, and Institute for Genome Sciences, University of Maryland School of Medicine, Baltimore, MD USA*

Hair cells are the mechanosensitive cells of the inner ear, responsible for detecting changes in sound (auditory) and movement (vestibular) within the environment. Across species, the auditory and vestibular sensory organs are comprised of a variety of cell types, of which hair cells make up only a small percentage. Cell sorting techniques such as fluorescence-activated cell sorting (FACS) have proved to be very informative in studying hair cell-specific changes in gene expression in response to different conditions. However, when using flow cytometry to isolate populations of interest, the tissue dissociation process, loss of lateral inhibition and cell-cell contact, as well as delay from dissection to RNA extraction all result in changes in gene expression.

Here we have developed a transgenic zebrafish model to specifically evaluate the translatome of the inner ear and lateral line hair cells. This model contains a construct consisting of a hemagglutinin (HA) tagged rpl10a gene followed by an IRES-GFP under control of the myo6b promoter (myo6b:rpl10a-HA-IRES-GFP), and results in expression of HA-tagged ribosomes specifically in hair cells. Consequently, intact zebrafish larvae can be flash-frozen, and actively translated mRNA obtained through an immunoprecipitation protocol using an antibody for the HA-tag (similar to the RiboTag mice). We demonstrate that this model can be used to reliably isolate actively translated hair cell mRNA from whole fish extracts by measuring the enrichment of known hair cell expressed transcripts and depletion of non-hair cell expressed transcripts in the immunoprecipitated material

compared with mRNA extracted from whole fish. To extend this analysis, we performed a global hair cell transcriptome analysis by RNAseq, and report the zebrafish hair cell transcriptome as compared to previously published zebrafish hair cell transcriptome datasets. We discuss similarities and differences, reveal top hair cell transcriptome expressed genes, and address the strengths and weaknesses of this model. Overall, we believe that this model will be highly useful for studying changes in zebrafish hair cell-specific gene expression in response to developmental progression, mutations, as well as hair cell damage by noise or ototoxic drug exposure.

PS 113

Single cell RNA-Seq Reveals Gene Expression Heterogeneity Among Mature Auditory Hair Cells

Paul T. Ranum¹; Alexander T. Goodwin²; Diana L. Kolbe²; Abraham M. Sheffield³; Jin-Young Koh²; Alexis Divincenzo²; Huizhan Liu⁴; David Z. Z. He⁴; Richard JH. Smith⁵

¹*Interdisciplinary Graduate Program in Molecular & Cellular Biology, The University of Iowa Graduate College, University of Iowa*; ²*Molecular Otolaryngology and Renal Research Laboratories, Carver College of Medicine, University of Iowa*; ³*Department of Otolaryngology, Head and Neck Surgery, Carver College of Medicine, University of Iowa*; ⁴*Department of Biomedical Sciences, Creighton University School of Medicine*; ⁵*Department of Otolaryngology, Molecular Otolaryngology and Renal Research Laboratories, University of Iowa*

Auditory hair cells are the critical mechanosensory cells at the heart of the auditory system. The presence of healthy hair cells is a prerequisite for hearing function and their absence underlies many forms of deafness. Recent advances in ultra-low input RNA-Sequencing (RNA-Seq) technologies have enabled transcriptome profiling and pathway analysis of auditory hair cells. These experiments can provide novel insight into how hair cells respond to damaging insults and may allow us to identify pathways for drug development to prevent hair cell death.

Here we describe the unpublished results of our work toward the development of a rapid and affordable single cell RNA-Seq workflow for mature mouse auditory hair cells. We have performed this protocol on more than 100 mouse inner and outer auditory hair cells at P15 (the onset of hearing), P35, and P70 timepoints. Our data robustly differentiate inner and outer hair cell types, and demonstrate expected transcriptional heterogeneity between individual cells within groups. By capturing transcriptional information at the single cell level and using

statistical packages including SCDE and PAGODA to assess differential expression between groups we are able to profile gene expression at the level of the individual cell and the population. The resulting datasets contain a wealth of temporal and cell-type specific information about mature auditory hair cells. This approach and the resulting datasets provide a foundation for studies designed to map the molecular pathways of auditory hair cells in disease states with the goal of identifying pathways that can be targeted to preserve hearing function.

PS 114

Characterization of Auditory Phenotype and Cochlear Sensory Epithelium Gene Expression in microRNA-183/96/182 Knockout Mice

Qian Zhang¹; Marsha Pierce¹; Michael Ebeid²; David Z. Z. He³; Haydn M. Prosser⁴; Garrett Soukup¹

¹*Department of Biomedical Sciences, Creighton University School of Medicine*; ²*Developmental Neuroscience, Munroe Meyer Institute, University of Nebraska Medical Center*; ³*Department of Biomedical Sciences, Creighton University School of Medicine, Omaha, NE 68178, USA*; ⁴*Wellcome Trust Sanger Institute*

Background

The microRNA-183/96/182 family is highly conserved and abundantly expressed in sensory cells among diverse species. Mutations that effect function or expression of miR-96 are a hereditary cause of early onset hearing loss in humans. To understand how the miRNAs function in the development and maintenance of auditory hair cells (HCs), we examined the auditory phenotype and profiled gene expression of the cochlear sensory epithelium of miR-183/96/182 knockout (3KO) mice.

Methods

Auditory function was determined by ABR recording. Morphological alterations of HCs and their stereocilia were examined by scanning electron microscopy (SEM), and HC maintenance and innervation were examined by immunofluorescence confocal microscopy. Gene expression profiling of the cochlear sensory epithelium was performed by RNA sequencing.

Results

Neonatal 3KO mice do not survive, limiting postnatal analysis to heterozygous (3HET) and wild type (WT) mice. Analysis of ABR recordings revealed an early onset elevation of hearing thresholds at high frequencies (>22 kHz) in 3HET mice at P90. MyoVIIa staining of HCs in 3HET animals exhibited an early HC loss occurring at the base of the cochlea from P60. MyoVIIa staining of HCs in 3KO mice at P0 demonstrated a marked reduction in HCs with weak staining of MyoVIIa. SEM of

3KO HCs at P0 revealed poorly differentiated HCs with aberrant stereocilia bundles. Tubulin staining of neurons showed that radial fibers extending toward the organ of Corti were fewer and poorly branched in 3KO mice at P0. RNA sequencing of total RNA from cochlear sensory epithelia of 3KO mice identified 163 genes up-regulated by more than 20% compared to WT mice, which include predicted targets of the miRNA family. Changes in expression generally included genes involved in cell morphogenesis and ear development. 164 down-regulated genes were reduced by more than 50% in 3KO cochlear sensory epithelia compared to WT and generally include genes previously shown to be prevalent in HCs of P0 WT mice.

Conclusions

We provide strong evidence of the requirement for miR-183/96/182 in hair cell morphogenesis, viability, maintenance and function. miR-183/96/182 knockout leads to a systemic failure of hair cell development, stereocilia bundle formation, and sensory neuron innervation contributing to early HC loss. The heterozygous animal represents a hypomorphic state that results in early hair cell decline and progressive hearing loss. Transcriptome profiling reveals probable direct miRNA target genes (upregulated) and indirect effects on HC gene expression (downregulated) that underlie the mechanisms of proper hair cell development and maintenance.

PS 115

Spiral Ganglion Morphology and Transcriptome Changes Observed in microRNA-183/96/182 Knockout Mice

Samantha Banks¹; Qian Zhang¹; Marsha Pierce¹; Haydn M. Prosser²; Michael Ebeid³; Garrett Soukup¹
¹*Department of Biomedical Sciences, Creighton University School of Medicine;* ²*Wellcome Trust Sanger Institute;* ³*Developmental Neuroscience, Munroe Meyer Institute, University of Nebraska Medical Center*

The microRNA-183/96/182 gene cluster is highly conserved across species and is critically important in the proper development and function of sensory epithelial cells and sensory neurons in different organs. The cluster is especially important in hearing as demonstrated by an autosomal dominant mutation in miR-96 that leads to progressive high-frequency hearing loss in humans. Both miR-182 knockout (1KO) and miR-183/96 knockout (2KO) mice were previously developed; the latter showing early hearing loss, defects in stereocilia development, hair cell loss and changes in innervation. miR-183/96/182 knockout (3KO) mice were more recently developed and have yet to be fully characterized. Interestingly, the neonatal 3KO animal does not survive, implicating a funda-

mental role for the miRNA family and preventing examination of postnatal homozygous mice. In this study spiral ganglion neurons were examined in P0 3KO, heterozygous (3HET), and wild type (WT) animals, and in P7 3HET and WT animals. NeuroVue lipophilic dye tracing was used to observe the organization of spiral ganglion fibers innervating inner hair cells. At P0, the 3KO cochlea exhibited fewer fiber bundles compared to WT, whereas the 3HET cochlea showed an intermediate phenotype. Spiral ganglion fibers in both P7 WT and 3HET cochleae were more distributed compared to the bundled organization in respective P0 cochleae. Innervation of outer hair cells was examined by immunofluorescent staining of myosinVIIA in hair cells and acetylated-tubulin in nerve fibers. Both P0 3HET and WT cochleae showed proper organization of three rows of outer hair cells with innervation running longitudinally along the rows. The P0 3KO cochlea exhibited disorganization of outer hair cells, and innervation was sparse and likewise disorganized. Although innervation of outer hair cells in 3HET animals appeared decreased at P0, it was similar to WT at P7 suggesting developmental retardation. To examine transcriptome changes, RNA was extracted from spiral ganglion tissue from three P0 mice of each genotype, and RNA sequencing was performed. Although analysis of transcriptome sequencing results is ongoing, many genes were downregulated and upregulated including predicted miR-183 family targets. This study of the miR-183 family in spiral ganglion neuron development might not only reveal important roles in hearing, but may provide understanding of roles in other sensory ganglia and insight into the lethality of the KO phenotype.

PS 116

A Common Mutation in CLDN14 Causes Precipitous, Prelingual Sensorineural Hearing Loss in Multiple Families due to Founder Effect

Justin A. Pater¹; Tammy Benteau²; Anne Griffin²; Cindy Penney²; Susan Stanton³; Sarah Predham²; Bernadine Kielley⁴; Jessica Squires²; Jiayi Zhou²; Quan Li²; Nelly Abdelfatah²; Darren O'Rielly²; Terry-Lynn Young²
¹*Memorial University of Newfoundland, Faculty of Medicine, Discipline of Genetics;* ²*Craig L. Dobbin Genetics Research Centre, Faculty of Medicine, Discipline of Genetics, Memorial University of Newfoundland;* ³*Communication Sciences & Disorders, Western University;* ⁴*Department of Education and Early Childhood Development, Government of Newfoundland and Labrador*

Genetic isolates provide unprecedented opportunities to identify pathogenic mutations and explore the full natural history of clinically heterogeneous phenotypes such as hearing loss. We noticed a unique audiopro-

file, characterized by prelingual and rapid deterioration of hearing thresholds at frequencies >0.5kHz in several adults from unrelated families from the island population of Newfoundland. Targeted serial Sanger sequencing of probands for deafness alleles (n=23) that we previously identified in this founder population was negative. Whole exome sequencing in 4 members of the largest family (R2010) identified a homozygous missense mutation (c.488C>T; p. A163V) in CLDN14, a known autosomal recessive deafness gene (DFNB29). Although not associated with deafness or disease, CLDN14 (p.A163V) has been reported as a variant of uncertain significance. Targeted sequencing of 169 deafness probands identified one homozygote and one heterozygous carrier. Genealogical studies, cascade sequencing and haplotype analysis across 4 unrelated families showed all subjects with the unique audioprofile (n=12) were also homozygous for p.A163V and shared a 1.4 Mb DFNB29-associated haplotype on chromosome 21. Most significantly, sequencing 175 population controls revealed 1% of the population are heterozygous for CLDN14 (p.A163V), consistent with a major founder effect in Newfoundland. The youngest CLDN14 (c.488C>T; p.A163V) homozygote passed newborn screening and had normal hearing thresholds up to 3 years of age, which then deteriorated to a precipitous loss > 1kHz during the first decade. Our study suggests that genetic testing may be necessary to identify at-risk children in time to prevent speech, language and developmental delay.

PS 117

A Homozygous FITM2 Mutation Causes a Dystonia-deafness Syndrome with Motor Regression and Signs of Ichthyosis and Sensory Neuropathy

Hannie Kremer¹; Celia Zazo Seco²; Anna Castells-Nobau³; Seol-hee Joo⁴; Margit Schraders⁵; Monique van der Voet³; Jaap Oostrik²; Erik de Vrieze²; Bart van de Warrenburg⁶; Martin Goepfert⁴; Raheel Qamar⁷; Annette Schenck³; Saima Siddiqi⁸

¹Dept Otorhinolaryngology, Dept Human Genetics, Radboudumc, Nijmegen, The Netherlands; ²Dept Otorhinolaryngology, Radboudumc, Nijmegen, The Netherlands; ³Dept Human Genetics, Radboudumc, Nijmegen, The Netherlands; ⁴Dept Cellular Neurobiology, University of Goettingen, Goettingen, Germany; ⁵Dept. Otorhinolaryngology, Radboudumc, Nijmegen, The Netherlands; ⁶Dept Neurology, Radboudumc, Nijmegen, The Netherlands; ⁷COMSATS Institute of Information Technology, Islamabad, Paksitan; ⁸IBGE, Islamabad, Pakistan

Both syndromic and non-syndromic hereditary hearing impairment can be caused by defects in a large number

of genes (>100). Identification of these genes is important for providing diagnoses and counseling of families and concomitantly provides knowledge on proteins essential for auditory function. Deafness genes that remain to be identified are likely to be involved in a small percentage of cases/families and can be associated with very rare syndromes which is the case in the syndrome presented in this study.

A consanguineous family from Pakistan was ascertained with a novel dystonia-deafness syndrome with motor regression, ichthyosis-like features, and signs of sensory neuropathy. By applying a combined strategy of linkage analysis and whole-exome sequencing in the presented family a homozygous nonsense mutation, c.4G>T (p.Glu2*), in FITM2 was identified. FITM2 and its paralog FITM1 constitute an evolutionary conserved protein family involved in partitioning of triglycerides into cellular lipid droplets. Despite the role of FITM2 in neutral lipid storage and metabolism, no indications for lipodystrophy were observed in the affected individuals. In order to obtain independent support of the involvement of FITM2 in the human pathology, down regulation of the single Fitm ortholog, CG10671, in *Drosophila melanogaster* was pursued by using RNA-interference.

Characteristics of the syndrome were recapitulated in *Drosophila* by progressive locomotor impairment, hearing loss and morphological abnormalities of type IV sensory neurons which is supporting the causative nature of the FITM2 mutation.

PS 118

A Sequential Screening Strategy for Genetic Hearing Loss in a Native South African Population

Jason R. Rudman¹; Rosemary Kabahuma²; Denise Yan³; Bing Zou¹; Xue Liu⁴

¹University of Miami Miller School of Medicine, Department of Otolaryngology; ²Department of Otolaryngology, University of Pretoria; ³Department of Otolaryngology, University of Miami Miller School of Medicine; ⁴Department of Otolaryngology, University of Miami Miller School of Medicine, Miami, FL; Dr. John T. Macdonald Foundation Department of Human Genetics, and John P. Hussman Institute for Human Genomics, University of Miami

Background

Hearing loss is the most common sensorineural disorder worldwide with causative variants in more than 140 genes. While mutations in genes such as GJB2 and GJB6 are highly prevalent as causative mutations in Caucasian, Asian, and Middle Eastern populations with hearing loss, these mutations are rare in persons of Af-

rican descent. The pathologic hearing-loss genes in this population have yet to be determined. There is a need, therefore, to identify the specific deafness-causing mutations in people of African descent. Fortunately, recent developments in high-throughput sequence capture methods and next-generation sequencing (NGS) technologies now allow for rapid screening of all known or suspected deafness-causing genes. We present a sequential screening strategy to diagnose genetic causes of congenital nonsyndromic deafness in a native South African population using next-generation sequencing.

Methods

After ethics board approval and informed consent was obtained, we identified 93 hearing-impaired children (age 5-21 years) from the Limpopo Province in South Africa with no history or physical findings to suggest a clinical syndrome. All were screened for GJB2, GJB6, and mitochondrial (mtDNA) mutations using Sanger sequencing, PCR amplification, and restriction fragment length polymorphism, respectively. If negative for these mutations, the sample underwent screening with the MiamiOtoGenes Panel, a custom capture panel for high-throughput next-generation sequencing of 180 known or candidate deafness genes. Candidate gene sequences are confirmed with Sanger sequencing. Segregation analysis using family members of the affected probands is then performed to confirm suspected inheritance patterns.

Results

All 93 samples were negative for pathologic mutations in GJB2, GJB6, and mtDNA. Next generation sequencing with the MiamiOtoGenes Panel identified several deafness-causing genes in this native sub-Saharan population of Limpopo, South Africa: MITF, OTOGL, SOX10, MARVELD2, and MYO7A. Segregation analysis to confirm inheritance patterns is ongoing at this time.

Conclusion

The mutations responsible for genetic hearing loss in populations of African descent are unique when compared to common causative mutations in other populations. We present deafness-causing genes in a native South African population never before identified in this population. There is a need for ongoing study in patients of African descent. The use of next generation sequencing and population-specific gene panels will aid in identifying rare mutations in a more cost- and time-effective manner.

PS 119

A Large Genome-wide Association Study of Tinnitus

Thomas Hoffmann¹; Neil Risch¹; Lawrence Lustig²

¹Department of Epidemiology and Biostatistics, and Institute for Human Genetics, University of California San Francisco; ²Department of Otolaryngology - Head and Neck Surgery, Columbia University Medical Center

Tinnitus is a complex disease that severely affects the quality of life of those who have it. Research has shown that tinnitus is heritable, but no replicated human locus has yet been found. We conducted a genome-wide association study of tinnitus on 7,483 cases and 95,020 controls in the racially/ethnically diverse Kaiser Permanente Research Program on Genes, Environment, and Health (RPGEH) Genetic Epidemiology Resource on Aging (GERA) cohort (80.8% non-Hispanic white, 8.5% Latino, 7.5% East Asian, and 3.5% African American). These individuals have genome-wide genotype data on over 650,000 SNPs, which have been imputed to millions more from the 1000 Genomes Project, as well as comprehensive electronic health records (EHR) (average 23 years of follow-up), from which we defined tinnitus and other related covariates. We required two ICD-9 codes for the tinnitus phenotype. Using a logistic regression model in each race/ethnicity group, no genome-wide significant loci were found. Larger sample sizes and/or more refined phenotypes will likely be necessary to uncover the genetic architecture of tinnitus.

PS 120

Whole Genome Sequencing (WGS) Reveals Cumulative Variation Effects in Age Related Hearing Loss (ARHL)

Dragana Vuckovic¹; Anna Morgan¹; Marco Brumat¹; Massimiliano Cocca¹; Eulalia Catamo²; Umberto Ambrosetti³; Paolo Gasparini⁴; Giorgia Giroto¹

¹University of Trieste, Trieste, Italy; ²Institute for Maternal and Child Health IRCCS "Burlo Garofolo", Trieste, Italy; ³Univ. Milano U.O.C. Audiologia/Fondazione IRCCS Cà Granda Ospedale Maggiore Policlinico, Milano, Italy; ⁴University of Trieste, Trieste, Italy; Sidra medical research, Doha, Qatar

Background

ARHL is a complex disease characterized by a huge genetic heterogeneity.

In recent years, despite many efforts to define the genetic bases, only few genes were described by GWAS, thus different statistical methods are needed. To increase the genes/variants detection rate here, a huge WGS study

of ARHL cases and controls applying innovative methodologies is described.

Methods

A cohort of 156 cases and controls (Discovery) and another one of 56 subjects (Replication) were used for the analyses. All Italian individuals (aged ≥ 50 y.o.) were selected based on high frequency pure-tone average (PTAH) and classified as Cases (PTAH ≥ 40 dB) and Controls (PTAH ≤ 25 dB). Low-coverage WGS data were generated by Illumina technology and pipelines for calling and quality control were applied. Variations load per gene was compared between Cases and Controls to detect outlier genes. Gene enrichment analysis was performed on outlier genes using PANTHER web-tool and the distribution of coding and non-coding variants was analyzed. Replication was done following the same protocol.

Results

1) Enrichment analysis: two groups of outlier genes were detected: group A characterized by 375 genes more mutated in cases and group B characterized by 371 less mutated in cases. Part of these genes belong to "sensory perception of sound" pathway or other neurological pathways; 2) Variants classification and distribution: the proportion of coding variants was significantly higher in group A genes thus suggesting that these variants might play a significant role in the pathogenicity of the disease; 3) Replication and polygenic effect: after the replication in an independent cohort, only genes confirmed to be extreme outliers and largely affected by damaging variants were taken into consideration. Overall, 14 genes were belonging to the auditory system; five genes (mutated in 29 patients) were already known to be involved in hearing function/loss in human and/or animal models (CACNB2, GRID2, GRIN2B, PRKG1, PTPRQ) while the remaining ones (mutated in 52 patients) were reported as essential for a correct inner ear development in rats and mice. Interestingly, one patient carries an exonic variant at the homozygous state, predicted to be deleterious, in a gene involved in mediating planar polarity of auditory hair cells. Updated results will be presented and discussed.

Conclusions

Here we report the first huge WGS study of ARHL cases and controls identifying new genes/variants possibly involved in ARHL thus shedding the light on the molecular bases of this complex and heterogeneous disorder.

PS 121

Next Generation Sequencing (NGS) and Functional Studies for the Molecular Characterisation of Families and Sporadic Cases Affected by Hereditary Hearing Loss

Giorgia Giroto¹; Anna Morgan¹; Diego Voizzi²; Elisa Rubinato³; Moza Alkowari⁴; Mariateresa Di Stazio³; Ramin Badii⁵; Shruti Bhagat⁶; Khalid Abdulhadi⁷; Umberto Ambrosetti⁸; Martina La Bianca⁹; Paolo Gasparini¹⁰

¹University of Trieste, Trieste, Italy; ²Sidra medical research, Doha, Qatar; ³University of Trieste; ⁴Sidra Medical Research, Doha Qatar; ⁵Hamad Medical Corporation, Doha Qatar; ⁶Hamad Medical Corporation; ⁷Hamad Medical Corporation Doha Qatar; ⁸Univ. Milano U.O.C. Audiologia/Fondazione IRCCS Cà Granda Ospedale Maggiore Policlinico, Milano, Italy; ⁹IRCCS Burlo Garofolo, Trieste, Italy; ¹⁰University of Trieste, Trieste, Italy; Sidra medical research, Doha, Qatar

Hearing Loss (HL) is the most common sensorineural disorder characterised by a huge clinical and genetic heterogeneity. Despite the major role of GJB2, GJB6 and MTRNR1 in the hereditary forms, for more than 60% of cases the molecular diagnosis is not defined and there are huge differences in prevalence among populations. Thus, there is an urgent need to further explore the landscape of causative mutations/genes.

Sixty-two families and 26 sporadic cases were screened for 113 HHL-genes by Targeted Re-Sequencing (TRS) followed, in negative cases, by Whole Exome Sequencing (WES) and by in vitro and in vivo validation of new HHL-candidate genes. Ion Torrent PGM™ (4.356 amplicons ensuring approximately 92,6% coverage of the target region) and Ion Proton™ (293.903 amplicons ensuring approximately >99% coverage of the target region) were used for TRS and WES, respectively. Genomic variants were annotated by ANNOVAR and filtered according to: a) pedigree pattern of inheritance, b) allele frequency data, c) pathogenicity prediction. Functional studies were carried out in vivo using Zebrafish models (expression and generation of K/O-K/I) and by in vitro experiments using expression clones containing either the wild-type cDNA or the mutant one.

TRS allowed us to characterize 30/62 families (48%) and 5/26 (19%) sporadic cases HHL cases.

WES already led to the identification of 3 new genes (BDP1, PSIP1, TBL1Y) and 4 new strong candidates such as LAMC1, PLS1, SPATC1L, ATP2B2. Function-

al preliminary validations include: 1) expression studies of PLS1, LAMC1 and ATP2B2 in Zebrafish larvae revealing a strong gene-expression in the hair cells of the otic vesicle; 2) semi-quantitative RT-PCR of SPATC1L revealing gene expression in whole cochlea of P3, P8, P12 and 2 month-old CD1 mice; 3) in vitro cloning of SPATC1L, ATP2B2 mutations for RNA and protein analysis by RT-PCR and Western-Blot respectively. Other candidates are now under final investigation.

These results illustrate the genetic complexity of HHL and the importance of a combined approach (NGS plus in vivo and in vitro validation studies) in understanding the pathogenesis and in guiding a correct diagnosis in the patients. Updated data will be presented and discussed.

PS 122

Genetic Evaluation of a Large Cohort of Cochlear Implant Recipients: Causes and Consequences

Eliot Shearer¹; Camille Dunn¹; Kevin Booth²; Paul T. Ranum³; Amanda Bierer²; Carolyn Brown⁴; Paul Abbas⁴; Marlan R. Hansen⁵; Bruce Gantz⁴; Richard JH. Smith⁶

¹University of Iowa Hospitals and Clinics; ²University of Iowa Molecular Otolaryngology and Renal Research Labs; ³Interdisciplinary Graduate Program in Molecular & Cellular Biology, The University of Iowa Graduate College, University of Iowa; ⁴University of Iowa; ⁵University of Iowa Hospitals and Clinics, Department of Otolaryngology- Head & Neck Surgery; ⁶Department of Otolaryngology, Molecular Otolaryngology and Renal Research Laboratories, University of Iowa

Background

Cochlear implantation has emerged as an essential treatment modality for patients with sensorineural hearing loss. There is a large set of data showing that cochlear implants improve educational level, decrease health care costs, and improve quality of life; however these same data also indicate a broad range of hearing outcomes for patients with cochlear implants. There are many reasons outcomes with a cochlear implant may vary. Some are environmental and include factors like family support, duration of deafness, and primary mode of communication. Others likely relate to the site of the genetic lesion in the auditory system that caused hearing loss. We hypothesize that we can improve our understanding of cochlear implant outcomes by studying cochlear implant recipients with genetic causes of hearing loss.

Methods

425 patients who received a cochlear implant at the University of Iowa were studied. Genetic evaluation was performed using comprehensive genetic testing of all known deafness genes with targeted genomic enrichment and massively parallel sequencing. Outcomes studied included word and sentence recognition scores in quiet and noise.

Results

A genetic cause of hearing loss was identified in 29% of all cochlear implant patients and varied significantly based on onset of hearing loss and family history of hearing loss. A genetic cause of hearing loss was identified in 48% of pediatric cochlear implant patients. There were causative mutations identified in 35 different deafness genes with mutations in GJB2 being the most common (19%) followed by mutations in Tmprss3 (10%), and mutations in SLC26A4 (9%). Correlational analysis of genetic cause of deafness and word recognition outcomes is ongoing and will be presented.

Conclusions

Given the extreme genetic heterogeneity of hearing loss, a large cohort of patients is essential for uncovering genetic underpinnings of cochlear implant outcomes. Understanding genetic cause of deafness in cochlear implant patients may in the future lead to tailored activation and programming and identify patients at risk for poor performance preoperatively.

PS 123

A Novel NOG Mutation (P170L) Impairs Noggin Secretion and Causes Autosomal Dominant Congenital Conductive Hearing Loss

Yilai Shu¹; Lijuan Wang²; Jun Shen³; Zhengmin Wang¹; Huawei Li⁴; Weiguo Zou⁵; Bing Chen¹; Yilai Shu Shu⁶

¹Department of Otolaryngology-Head and Neck Surgery, Eye and ENT Hospital, Shanghai Medical College, Fudan University, Shanghai, China; ²State Key Laboratory of Cell Biology, Shanghai Institutes for Biological Sciences, Chinese Academy of Sciences, Shanghai, China; ³Brigham and Women's Hospital, Laboratory for Molecular Medicine, Harvard Medical School Center for Hereditary Deafness; ⁴The EENT Hospital of Fudan University; ⁵State Key Laboratory of Cell Biology, Shanghai Institutes for Biological Sciences, Chinese Academy of Sciences, Shanghai, China.; ⁶Eye and Ear, Nose, Throat hospital, Shanghai Medical College, Fudan University

Background

To characterize clinical features and identify the molecular mechanism underlying autosomal dominant congenital progressive conductive hearing loss due to stapes ankylosis.

Methods

We investigated clinical features of a 38-member multi-generational Chinese family with congenital progressive conductive hearing loss. We obtained DNA samples from 22 members including 12 affected and 10 unaffected individuals. We performed whole exome sequencing on the proband to identified candidate variants and studied segregation in remaining family members. We constructed plasmids contain human reference or mutant cDNA, confirmed the sequences, and transfected HEK293T cells to express the protein. We quantified and compared protein expression and secretion in cell lysates and supernatant culture medium between reference and mutant plasmid transfected cells by Western blotting. We also performed stapes surgery on three patients.

Results

Systematic clinical examinations found that all of patients presented progressive conductive hearing loss and hyperopia. Other phenotypes included symphalangism, syndactyly, broad thumbs and toes, tarsal fusions and fused cervical vertebrae various in the patients. The family history conforms to an autosomal dominant inheritance pattern. Genetic analyses identified a novel p.P170L variant in *NOG*, which segregated with hearing loss in all 12 affected members and was not present in unaffected family members. Surgical exploration of three patients revealed fixed and thicken footplate of stapes. The postoperative hearing threshold was improved about 40 dB. In vitro expression of the variant noggin protein in HEK293T cells showed that the p.P170L variant inhibited noggin secretion, thus disrupting the noggin signaling pathway required for normal development.

Conclusion

The phenotypes and family history presented in this large Chinese family are consistent of autosomal dominant stapes ankylosis with hyperopia as well as other skeletal anomalies associated with *NOG* deficiency. We identified a novel *NOG* mutation p.P170Lco-segregating with disease in the family. In vitro functional studies demonstrated that the variant inhibits noggin secretion. Our results indicate that p.P170L causes autosomal dominant congenital progressive conductive hearing loss by disrupting the noggin signaling pathway due to impaired secretion.

PS 124

Genome Wide Association Studies (GWAS), Targeted Re-sequencing (TRS) and Functional Validations for Unravelling Human Complex Traits: The Case of Hearing Function and Age Related Hearing Loss

Anna Morgan¹; Diego Vozzi²; Dragana Vuckovic¹; Martina La Bianca³; Angela D'Eustacchio³; Marco Brumat¹; Umberto Ambrosetti⁴; Paolo Gasparini⁵; Giorgia Giroto¹

¹University of Trieste, Trieste, Italy; ²Sidra medical research, Doha, Qatar; ³IRCCS Burlo Garofolo, Trieste, Italy; ⁴Univ. Milano U.O.C. Audiologia/Fondazione IRCCS Cà Granda Ospedale Maggiore Policlinico, Milano, Italy; ⁵University of Trieste, Trieste, Italy; Sidra medical research, Doha, Qatar

Despite a lot of efforts have been made in identifying new genes involved in the auditory system, the molecular basis of normal hearing function (NHF) and age-related hearing loss (ARHL) is still largely unknown.

To shed the light on the genetics of these complex traits, we developed a multi-step strategy combining GWAS with TRS and functional validation through animal models and in vitro studies.

GWAS on NHF (quantitative trait) and ARHL (qualitative trait) performed on 4150 subjects coming from different European and Asiatic cohorts revealed interesting findings. Two strongly significant loci were identified, one of which (p -value=2.58e-8) includes a gene causing hearing loss in mice and affecting cochlear outer hair cells. Interestingly, this is the first example of a hearing-loss gene involved in modulating the NHF.

To fine-map the impact of these and other findings on ARHL, we developed a custom TRS panel of 46 candidate genes and analysed ~500 patients from our Italian cohorts (both inbred and outbred populations). TRS data were filtered according to quality value, pathogenicity prediction (Polyphen2, MutationTaster, SIFT, LRT) and conservation score (PhyloP). Variants were classified as ultra rare (MAF < 0.001), rare (MAF < 0.01) and common (MAF > 0.01). Fifty-six mutations of interest were identified: 5 frame-shift indels, 2 nonsense, and 49 missense mutations, affecting 22 genes and 128 patients. Interestingly, among them 13 variants are related to eQTL, 5 of them detected in the inferior temporal lobe of the brain. According to the complex genetic structure of ARHL, three scenarios are present: 1) different mutations in the same gene, 2) the same mutation in different patients and 3) different mutations in the same patient.

To validate the pathogenicity of these genes/mutations, functional *in vitro/in vivo* studies are now in progress. As an example, we are testing the role of two interesting mutations identified in SLC44A2 and SLC9A3R1 genes. For both genes *in situ* hybridization in Zebrafish larvae showed a clear expression in the hair cells of the otic vesicle and K/I models are in progress. Moreover, to define the pathogenic mechanisms of these mutations at a molecular level, we are using expression clones containing either the wild-type cDNA or the mutant one for RNA and protein analysis via RT-PCR and Western Blot respectively.

Updated results will be presented and discussed. These results support the usefulness of our approach to detect, prioritize and validate newly NHL and ARHL identified genes.

PS 125

Whole-exome Sequencing Efficiently Detects Mutations in Families with Autosomal Dominant Nonsyndromic Hearing Loss

Zhijie Niu¹; Jie Sun¹; Li Wang²; Denise Yan³; Rahul Mittal³; Xue Liu⁴; Yong Feng⁵

¹China; ²Institute of Medical Genetics, Henan Provincial People's Hospital, People's Hospital of Zhengzhou University, Zhengzhou, China; ³Department of Otolaryngology, University of Miami Miller School of Medicine;

⁴Department of Otolaryngology, University of Miami Miller School of Medicine, Miami, FL; Dr. John T. Macdonald Foundation Department of Human Genetics, and John P. Hussman Institute for Human Genomics, University of Miami, Miami FL; ⁵Department of Otolaryngology, Head and Neck Surgery, Xiangya Hospital of Central South University

Background

Hearing loss (HL) is the most frequent sensory defect in humans and is genetic origin in up to 75% of cases. However, the genetic causes of HL are very heterogeneous. This extreme genetic heterogeneity of deafness has made genetic diagnosis expensive and time consuming using traditional methods. Whole-exome sequencing (WES) has already had an important impact on both research and clinical diagnosis, and provide a more time and cost-efficient strategy in gene discovery for inherited deafness.

Methods

In the present study, we have combined both the Deafness Gene Mutation Detection Array and WES to identify deafness causative variants in 5 multi-generational Chinese families segregating autosomal dominant form of non-syndromic HL (ADNSHL). The array was de-

signed to simultaneously screen 8 most common deafness-causing mutations in Chinese population (GJB2: c.35delG, c.176-191del16bp, c.235delC, c.299-300delA; SLC26A4: IVS7-2A>G, c.2168A>G; mtDNA 12SrRNA: m.1555A>G, m.1494C>T). WES was then used to identify causative variants in mutation-negative cases. Agilent's SureSelect XT Human All Exon v5 (51 Mb) was used for WES.

Results

We ascertained 5 large Chinese families with ADNSHL. In most affected cases, the onset of symmetrical high-frequency sensorineural loss varied from the first to the third decade, followed by a progressive HL in the lower frequencies and continuing to become a moderate-to-severe HL across all frequencies in the later decades of life. Three of the deaf members in one of the families had a history of work related noise exposure. Implication of the common deafness-causing variants in Chinese population has been excluded by array screening. WES in 2 distinct families identifies variants in the ACTG1 and WFS1 genes. In another family, it revealed a single variant (c.512A>G; p.H171R) in ELMOD3, a gene associated with autosomal recessive NSHL. The identified amino acid change, predicted to be pathogenic, alters a highly conserved residue and co-segregates with HL as an autosomal dominant trait. 3D protein structure modeling suggests that this sequence change may impact the functional properties of interaction of the protein. New deafness candidate genes belonging to the cyclic nucleotide phosphodiesterases (PDEs) family and to the human mitochondrial ribosomal proteins (MRPs), have also been identified. Determination of the functional consequences of sequence variants is in process.

Conclusion

WES approach is accelerating the pace of disease-causing gene discovery for genetic hearing loss which also lay the foundation for the genetic diagnosis and the clinical care of deaf persons in the future.

PS 126

A Mutation in a Member of the Cyclic Nucleotide Phosphodiesterase (PDE) Gene Family Causes Autosomal-dominant Nonsyndromic Hearing Loss

Denise Yan¹; Li Wang²; M'hamed Grati¹; Litao Qin²; Tao Li²; Abhiraami Kannan-Sundhari³; Rahul Mittal¹; Prem Chapagain⁴; Yong Feng⁵; Shixiu Liao²; Xuezhong Liu¹

¹Department of Otolaryngology, University of Miami Miller School of Medicine, Miami, FL 33136, USA; ²Institute of Medical Genetics, Henan Provincial People's Hospital, People's Hospital of Zhengzhou University,

Zhengzhou, China; ³University of Miami Miller School of Medicine; ⁴Department of Physics, Florida International University, Miami, Florida; ⁵Department of Otolaryngology, Head and Neck Surgery, Xiangya Hospital of Central South University

Background

While over 70 loci for autosomal dominant non-syndromic hearing loss (ADNSHL) have been reported, the genes for only 36 have been identified. Although the function of many of these genes in the inner ear remains unclear and is compounded by their identification in only one single or a few families, an understanding of the biology of hearing and deafness at the molecular level is slowly emerging.

Methods

In this study, we have used the Deafness Gene Mutation Detection Array, a custom capture genes panel (MiamiOtoGenes) of 180 known genes and the Agilent's SureSelect XT Human All Exon v5 (51 Mb) whole exome sequencing (WES) to identify deafness causative variants in a Chinese family with ADNSHL. The array was designed to simultaneously screen 9 most common deafness-causing mutations in Chinese population (GJB2: c.35delG, c.176del16, c.235delC, c.299-300delAT; GJB3: R180X; SLC26A4: c.IVS7-2A>G, p.H723R; mtDNA 12S rRNA: c.1555A>G, c.1494C>T). For WES method, adapter sequences for the Illumina HiSeq2000 were ligated and the enriched DNA samples from the family were subjected to standard sample preparation for the HiSeq2000 instrument (Illumina).

Results

We ascertained a five-generation Chinese family with ADNSHL. In this family, we have first excluded the implication of known deafness-causing genes by Array and genes panel screening. We then applied WES to identify the causative gene. A simple variants filtering strategy rapidly extracted only 1 heterozygous variant shared by the 2 affected siblings subjected to WES. This missense variant is located in a mammalian cyclic nucleotide phosphodiesterase (PDE) gene and was absent in 220 ethnically matched controls. Its co-segregation with the phenotype in the family was confirmed via Sanger sequencing. Our structural models strongly suggest that the mutation will likely destabilize the helix-helix interactions and affect the cyclic nucleotide binding selectivity. By whole-mount immunofluorescence on postnatal day 9 rat cochlea, we show its expression in outer (OHC) and inner (IHC) hair cells right underneath the cuticular plate in presumably the lysosomal compartment. In vitro and in vivo models studies using innovative approaches to determine the functional consequences of the mutation is undergoing.

Conclusion

We present this member of the PDE family as a causative gene for ADNSHL. Our studies suggest that the mutation in this gene may disrupt the pH homeostasis of cellular organelles and affect the role of the protein in membrane trafficking and phagocytosis. We will present the functional studies on this new class of deafness gene.

PS 127

Cost Effectiveness of Screening Strategies for Identifying Deafness-causative Mutations in an Ethnically Diverse Nonsyndromic Deafness Cohort from South Florida

Opeoluwa Fawole¹; Denise Yan²; Haiqiong Shang¹; Rahul Mittal²; Susan H. Blanton³; Xue Liu³

¹Department of Otolaryngology, University of Miami Miller School of Medicine, Miami, FL; ²Department of Otolaryngology, University of Miami Miller School of Medicine; ³Department of Otolaryngology, University of Miami Miller School of Medicine, Miami, FL; Dr. John T. Macdonald Foundation Department of Human Genetics, and John P. Hussman Institute for Human Genomics, University of Miami, Miami FL

Background

Genetic causes of hearing impairment are very heterogeneous. Over 145 loci with mutations in 90 genes have been identified for nonsyndromic hereditary deafness. The extraordinary genetic heterogeneity of hearing loss has been a great challenge for molecular testing. Technological advances now allow for the identification of mutations in heterogeneous diseases such as deafness.

Methods

The dataset consists of 75 probands with nonsyndromic hearing loss (NSDHL) from South Florida. It is an ethnically diverse cohort. All individuals were screened with the CapitalBioMiamiOtoArray, which detects variants in five genes that are common in most Caucasian populations. They are GJB2 (c.35delG, p.W24C, p.L90P, c.167delT); GJB6 c.309kb deletion; SLC26A4 (p.L236P, p.T416P); and mtDNA m.1555A>G and m.7444G>A. Individuals not captured with the array were then screened with a custom capture panel (MiamiOtoGenes, MOG), which screens for 180 deafness genes using the Agilent's SureSelect Target Enrichment (Agilent, Santa Clara, CA) system.

Results

22 of the 75 (29%) probands were positive for the array. When only pathogenic and likely pathogenic variants from the MOG panel were taken into account, the underlying genetic cause was identified in 9 of the remain-

ing 53 probands, providing an etiologic diagnostic rate of 17% in the cohort. The genes in these families include MYO7A, MYO15A, SLC26A4, USH2A, MYO6, TRIOB, POU4F3, TMC1. The cost of screening of 9 mutations in 5 genes using the array is approximately US\$30 per subject. The MiamiOTOgenes panel allows screening of 180 known genes for both syndromic and NSHL, is estimated to cost \$212-305 per panel for research grade.

Conclusion

The cost of screening first with the array followed by the MOG panel is approximately \$16,325 (assuming \$275 for MOG) and a final diagnostic rate of 31/75 (41.3%). If all samples had been subjected to the MOG panel, the cost would have been \$20,625; therefore, the two step screening saved over \$4,000. These savings would of course vary greatly depending on the frequency of the five array variants in the population studied.

PS 128

Identifying Novel Deafness Genes For Hearing Loss Using Sequential Screening Strategies

Abhiraami Kannan-Sundhari¹; Denise Yan²; Bing Zou³; Rahul Mittal²; M'hamed Grati²; Steven Lang⁴; Saber Masmoudi⁴; Mohan Kameswaran⁵; Mansoor Salehi⁶; Sudhamaheswari Sivaramakannan⁵; Xue Liu⁷
¹University of Miami Miller School of Medicine; ²Department of Otolaryngology, University of Miami Miller School of Medicine; ³University of Miami Miller School of Medicine, Department of Otolaryngology; ⁴University of Miami; ⁵MERF; ⁶Isfahan University of Medical Sciences; ⁷Department of Otolaryngology, University of Miami Miller School of Medicine, Miami, FL; Dr. John T. Macdonald Foundation Department of Human Genetics, and John P. Hussman Institute for Human Genomics, University of Miami, Miami FL

Abstract

Hearing loss (HL) is a relatively common, monogenic disorder among the human population with profound congenital HL presenting itself at the rate of one in 1000 births. However, at least 50% of prelingual HL seems to be of genetic origin with only HL as a phenotype, with approximately 80% being autosomal recessive and the rest autosomal dominant, X-linked and mitochondrial. To date, causative variants associated with nonsyndromic HL are approximately 140 loci, making it one of the most genetically heterogeneous traits.

Methods

This study utilized a Gene-Chip specific to each ethnic cohort to search for known mutations associated with population and families negative for them were sent

for custom capture Miami Otogene panel. This target and sequence method covers an array of 180 known HL-causing genes with a target size of 1.158 Mb comprising 3494 regions. The sequence data were analyzed to filter variants based on read depth, minor allele frequency (MAF) and pathogenicity prediction. Segregation analysis was performed on family members whenever available and Sanger sequencing was done to confirm the mutation. Families that were negative in the panel qualified for Whole Exome Sequencing (WES).

Results

This study was done on patient samples from India, Tunisia, Iran and South Florida. The genetic cause of HL based on pathogenic and likely pathogenic variants provided an estimate of 26% in Indian, 26% in Tunisian, 90% in Iranian and 17% in South Floridian families. WES results for potential candidate genes in families that were negative for variants in known genes include TSPAN2, CDC73, SLC25A4, LIN54, NOV, LRP1, HES1, WDR12, SLC12A2, SLC10C1, LAMC1, SCCPDH amongst 9 South Floridian, PLEKHA2 and PLOD2 in 1 Indian, LR-TOMT and CIB2 amongst 16 Tunisian and LHFPL5 and TJP2 amongst 6 Iranian families.

Conclusions

This study has utilized Next Generation Sequencing strategies for variant detection in a multi-ethnic cohort and resulted in the identification of sequence variants in 26 known genes including 11 novel mutations. Some multiplex families were categorized as uncertain due to the presence of at least one variant with unknown significance. Further computational and functional analysis will be performed to validate the impact of the mutation and their role in deafness.

PS 129

Novel Neuro-audiological Findings and Further Evidence for C10orf2 Involvement in Perrault Syndrome

Monika Oldak¹; Dominika Ozieblo¹; Agnieszka Polak¹; Iwona Stepniak¹; Michal Lazniewski²; Urszula Lechowicz¹; Krzysztof Kochanek³; Mariusz Furmanek⁴; Grazyna Tacikowska⁵; Dariusz Plewczynski²; Tomasz Wolak⁴; Rafal Ploski⁶; Henryk Skarzynski⁷

¹Department of Genetics, Institute of Physiology and Pathology of Hearing, Warsaw, Poland; ²Laboratory of Functional and Structural Genomics, Centre of New Technologies, University of Warsaw, Warsaw, Poland; ³Department of Experimental Audiology, Institute of Physiology and Pathology of Hearing, Warsaw/Kajetany, Poland; ⁴Bioimaging Research Center, Institute of Physiology and Pathology of Hearing, Warsaw/Kajetany, Poland; ⁵Department of Otoneurology, Institute of

Physiology and Pathology of Hearing, Warsaw, Poland;
⁶*Department of Medical Genetics, Medical University of Warsaw, Warsaw, Poland;*
⁷*Oto-Rhino-Laryngology Surgery Clinic, Institute of Physiology and Pathology of Hearing, Warsaw/Kajetany, Poland*

Hearing loss and ovarian dysfunction are key features of Perrault syndrome (PRLTS). Progressive neurodegeneration occurs occasionally in some patients. Mutations in one of five different genes HSD17B4, HARS2, LARS2, CLPP or C10orf2 cause the autosomal recessive disorder but they are found only in about two thirds of patients. The aim of the study was to identify pathogenic variants in two siblings with a clinical picture resembling a severe, neurological type of PRLTS. With whole exome sequencing we found two rare biallelic mutations in C10orf2 that segregated with the disease. One c.1196A>G (p.Asn399Ser) recurred for the first time in a patient with PRLTS and the second one c.1802G>A (p.Arg601Gln) was novel for the disorder. Neuroimaging studies showed diminished cervical enlargement of the spinal cord and for the first time in PRLTS partial atrophy of the vestibulocochlear nerves and decreased grey and increased white matter volumes of the cerebellum. Comprehensive audiological assessment revealed that not only auditory neuropathy but also partial cochlear dysfunction underlies hearing impairment. Our study unveils novel features on the phenotypic landscape of PRLTS and provides further evidence that the newly identified for PRLTS C10orf2 gene is involved in its pathogenesis.

PS 130

The SLC26A4 p.Leu236Val Variant is a Frequent Cause of Hearing Impairment in Filipino Cochlear Implantees

Regie Lyn P. Santos-Cortez¹; Ma. Rina T. Reyes-Quintos²; Talitha Karisse L. Yarza²; Celina Ann M. Tobias-Grasso³; Anushree Acharya⁴; Suzanne M. Leal⁴; Eva Maria Cutiongco-de la Paz⁵; Charlotte M. Chiong²

¹*University of Colorado School of Medicine;* ²*Philippine National Ear Institute and Newborn Hearing Screening Reference Center, University of the Philippines Manila-National Institutes of Health;* ³*MED-EL;* ⁴*Center for Statistical Genetics, Department of Molecular and Human Genetics, Baylor College of Medicine;* ⁵*University of the Philippines Manila*

Cochlear implantation is now a standard rehabilitation option for congenital hearing impairment worldwide. In lower income countries like the Philippines where health insurance is limited in scope, the cost burden for cochlear implantation is largely carried by the patient.

The study of risk factors such as genetic variants that may help predict cochlear implant outcomes is therefore highly beneficial. DNA samples from 29 GJB2-negative Filipino cochlear implantees were Sanger-sequenced for the coding exons of the SLC26A4 gene. Four cochlear implantees were homozygous for the SLC26A4 c.706C>G (p.Leu236Val) variant, thus the prevalence of this variant among cochlear implantees was 13.8%. The minor allele frequency of the p.Leu236Val variant in Filipino controls is 0.001 and in ExAC Latino alleles is 0.0003. This variant is predicted to be pathogenic based on bioinformatic prediction and a previously reported mutation p.Leu236Pro at the same variant site. All four SLC26A4-positive cochlear implantees were also homozygous for SLC26A4 c.200C>G (p.Thr67Ser) which is predicted benign and is probably a polymorphism that is in linkage disequilibrium with p.Leu236Val. Exome sequencing of the DNA samples from the four SLC26A4-positive cochlear implantees did not reveal additional variants that are potentially pathogenic. Of the four SLC26A4-positive implantees, one had bilateral Mondini dysplasia, one had bilaterally enlarged vestibular aqueducts, and two had normal CT findings. When comparing the four SLC26A4-positive implantees against 25 SLC26A4-negative implantees, there were no significant differences in age at implantation, duration of implant use, occurrence of temporal bone abnormalities, audiometric thresholds pre- and post-implantation, and PEACH scores. On the other hand, implantees with temporal bone abnormalities (n=11) had better median audiometric thresholds compared to those with normal CT findings prior to implantation (p=0.02) but not post-implantation, suggesting that cochlear implantation was equally effective in both groups. In summary, the SLC26A4 c.706C>G (p.Leu236Val) variant is a frequent cause of congenital hearing impairment in Filipinos, but does not confer any difference in audiological profiles compared to non-variant-carriers before or after cochlear implantation.

PS 131

Exome Sequencing Reveals Multiple Genes That May Contribute to Progressive Adult-onset Hearing Loss

Karen P. Steel¹; Morag A. Lewis²; Lisa S. Nolan³; Barbara Cadge³; Lois J. Matthews⁴; Bradley A. Schulte⁴; Judy R. Dubno⁴; Sally Dawson³

¹*King's College London; Wellcome Trust Sanger Institute;* ²*King's College London; Wellcome Trust Sanger Institute;* ³*University College London;* ⁴*Medical University of South Carolina*

Adult-onset progressive hearing loss is one of the most common sensory deficits in the population, and it has a

strong genetic component. However, although over 100 genes underlying human deafness have been identified, most of these are involved in childhood deafness, and the vast majority of genes involved in progressive hearing loss remain unknown. To discover genes underlying progressive hearing loss, we sequenced the exomes of thirty people with well-characterised adult-onset hearing loss. Twenty of these had family histories of hearing loss, ten with a dominant pattern of inheritance and ten with a recessive pattern. The remaining ten were older adults with no known family history. After sequencing, variants were detected and filtered based on sequence quality, frequency in the population, and predicted severity of impact on protein function. We examined the results for evidence of very rare variants each with predicted large effects that could potentially explain the phenotype of individuals. In parallel we looked for common variants that were found in multiple hearing-impaired people that might each have a smaller additive impact on hearing. We firstly analysed genes known to be involved in deafness in the mouse or in humans (n=357 genes), then analysed all genes (n=20,000). Both approaches yielded interesting candidate genes for further study, including genes not previously associated with human deafness such as NEDD4 and RBPJ that are mutated in multiple individuals. Seven people were found to have mutations of PAX2, a gene not previously linked to non-syndromic hearing loss. A notable finding was that each of the 30 people sequenced carried predicted pathogenic mutations in at least ten genes known to be associated with deafness, which has implications for diagnostic sequencing. Furthermore, when we analysed a large public dataset of people unselected for hearing ability, 2334 of the 2504 individuals in the group carried at least one predicted pathogenic mutation in a known dominant human deafness gene, suggesting these mutations are extremely common. Our results illustrate the complexity of the genetic contribution to hearing loss and the caution required in interpreting sequence data, and offer candidate genes for focussed studies to elucidate their involvement in hearing.

Funding: NIH/NIDCD P50 000422; the Wellcome Trust (100669 and 098051); the MRC; NIH/NCATS UL1 TR000062 and UL1 TR001450; Research into Ageing (Ref 223); Teresa Rosenbaum Golden Charitable Trust; Telethon Foundation (GGP09037); the Haigh Fellowship in age related deafness, Deafness Research UK.

Hair Cells - Anatomy and Physiology I

PS 132

Molecular and Cellular Mechanisms of Hair Cell Aging

Richard Hallworth¹; David Z. Z. He²; Huizhan Liu²; Lei Chen¹; Kirk Beisel¹

¹Creighton University; ²Department of Biomedical Sciences, Creighton University School of Medicine

Background

Age-related hearing loss (ARHL), the most prevalent form of hearing loss in humans, is most commonly caused by degenerative changes (or biological aging) and death of the cochlear inner and outer hair cells (IHCs, OHCs). Despite the fact that ARHL has been extensively studied using various mouse models, the causes of hair cell aging are still largely unknown. Methods: 1,500 IHCs and 1,500 OHCs from two age groups (1 and 26 months old) of CBA mice were collected using the suction pipette technique. RNA-seq was used to analyze their transcriptomes. We analyzed the genes that are known to be related to hair cell specializations, metabolism, cell cycle control, and transcription factors.

Results and Conclusions

Most genes that are related to hair cell unique functions are significantly down-regulated. In OHCs, *Tmc1* expression is reduced 5 fold, *Kcnq4* 6 fold, *Chrna9* 45 fold, *Chrna10* 22 fold. Astonishingly, *Slc26a5* (prestin) is reduced 284 fold. Hair cell markers, *Myo6* and *Myo7a* are reduced by half. Interestingly, some genes showed significant up-regulation. These include those for actin, spectrin, and (afferent) synaptic transmission-related genes. For example, *Actb* expression is increased about 100 fold. *Otof* is increased 5 fold, and *Slc7a14* and *Slc17a8* are up-regulated 12 to 15 fold. The increased expression of afferent synaptic-related genes in OHCs suggests an altered pattern of innervation in aging hair cells. Although we observed a significant up-regulation of actin and spectrin, which are an important part of stereocilia bundle and cytoskeleton, axial stiffness of OHCs is significantly reduced. Since prestin is down-regulated 284 fold, it is not surprising to see a significant reduction in OHC stiffness. Similar to OHCs, we also observed an increased expression of actin- and spectrin-related genes. However, most other genes are significantly down-regulated. Our study shows, for the first time, the cellular and molecular changes associated with biological aging of hair cells.

PS 133

Deafness in a Tricellulin knockout mouse results from deficiencies of the reticular lamina barrier function

Saima Riazuddin¹; Jochen Weigle¹; Xiaohong Deng¹; Gowri Sarangdhar²; Matthew Starost³; Thomas B. Friedman⁴; Andrew Forge⁵; Zubair Ahmed⁶

¹Laboratory of Molecular Genetics, Department of Otorhinolaryngology Head & Neck Surgery, School of Medicine, University of Maryland; ²Cincinnati Children's Hospital Research Foundation, University of Cincinnati;

³Division of Veterinary Resources, National Institutes of Health; ⁴Section on Human Genetics, Laboratory of Molecular Genetics, National Institute on Deafness and Other Communication Disorders, National Institutes of Health; ⁵Centre for Auditory Research, University College London, London, UK.; ⁶Department of Otorhinolaryngology Head & Neck Surgery, School of Medicine University of Maryland

Background

Mutations in TRIC, which encodes a tricellular tight junction protein, are known to cause prelingual hearing loss (DFNB49) in humans. Previously, we reported a mouse model of DFNB49 that carries a premature translation stop codon of Tric, p.R497* that results in rapidly progressive hearing loss and hair cell degeneration. However, to understand inner ear cell type specific function of tricellulin, we develop a conditional knockout allele of Tric.

Methods

The first coding exon of Tric was floxed to generate conditional knockout allele (TricKO/KO). Hair cells (TricKO/hKO) and supporting cells (TricsKO/sKO) specific mutants of tricellulin were generated using the cell type specific Cre mice. Inner ear function in all three alleles was determined by ABR and DPOAE. The cochlear and vestibular sensory epithelia were examined by immunofluorescence. The effects of the mutation on the ultrastructure of the tight junctions in the cochlear epithelia were determined by freeze fracture microscopy.

Results

Mice homozygous for the germline TricKO/KO mutation displayed early onset rapidly progressing hearing loss and were completely deaf by 3 weeks of age. Progression of hearing loss coincided with OHC degeneration, followed by loss of inner hair cells. The mutation appeared to affect the ultrastructural organization of the tricellular tight junctions in the organ of Corti, marginal cell layer of the stria vascularis and the vestibular epithelia. Consistent with our previously reported knockin

allele (Gowri et al., 2013), the hair cell loss in the mutant mice was rescued in vivo on lowering the endocochlear potential by deleting Pou3F4 function that is necessary for stria vascularis function. Similar to TricKO/KO mice, the hair cell specific knockout (TrichKO/hKO) mouse also has progressive hearing loss and are completely deaf by 4 weeks of age. In contrast, the supporting cells knockout mice (TricsKO/sKO) have early onset mild hearing loss and residual hearing was maintained even at 5 weeks of age. Currently, comprehensive phenotypic screening in TricKO/KO is in progress and we expect to present the result of these studies at the meeting.

Conclusion

Loss of tricellulin leads to organ of Corti degeneration largely due to a defective paracellular barrier function of the reticular lamina. Our data also support the conclusion that loss of tricellulin to its possible barrier function within the stria vascularis does not significantly contribute to the hearing loss of Tric mutant mice.

PS 134

Connexin-mediated Signalling in Non-sensory Cells is Crucial for the Development of Sensory Inner Hair Cells in the Mouse Cochlea

Federico Ceriani¹; Stuart L. Johnson¹; Oliver Houston¹; Roman Polishchuk²; Giulia Crispino³; Veronica Zorzi⁴; Fabio Mammano⁴; Walter Marcotti¹

¹University of Sheffield; ²Telethon Institute of Genetics and Medicine; ³Istituto Veneto di Medicina Molecolare, Italy; ⁴CNR Institute of Cell Biology and Neurobiology

Background

In mammals, the sense of hearing relies on mechano-electrical transduction performed by the primary sensory receptor inner hair cells (IHCs) and the outer hair cells (OHCs). These sensory hair cells are embedded in a matrix of epithelial non-sensory cells which are interconnected by gap junction channels, creating an extensive functional syncytium in the cochlear sensory epithelium (Kikuchi et al 1995 Anat Embryol 191:101). Gap junction channels in the mammalian cochlea are primarily formed by connexin 26 (Cx26) and connexin 30 (Cx30) and mutations of the genes encoding for Cx26 (Gjb2) and Cx30 (Gjb6) are associated with the most common form of prelingual congenital hearing impairment in humans (DFNB1). ATP-induced signalling from connexin extrajunctional hemichannels (Anselmi et al 2008 PNAS 105:18770) has also been proposed to induce Ca²⁺-induced action potential (AP) activity in sensory IHCs both directly (Tritsch et al 2007 Nature 450:50) and indirectly (Wang et al 2015 Cell 163:1348), although a more modulatory role for ATP on the IHC firing has also been shown (Johnson et al 2011 Nat Neurosci 14:711). Despite the

involvement of Cx26 and Cx30 in cochlear function and hearing, their exact role and the relative functional contribution of the two connexins to mammalian cochlear physiology during pre-hearing stages of development is still unclear.

Method

Whole-cell patch-clamp recordings and confocal imaging were performed from IHCs of Cx30 (-/-), Cx30 Δ/Δ and Cx26Sox10Cre mice and their littermate controls. IHCs were studied in acutely dissected cochleae from postnatal day 3 (P3) to P25, where the day of birth is P0. Recordings were performed at near-physiological conditions (body temperature, 1.3 mM extracellular Ca²⁺; 1 mM intracellular EGTA). Animal work was performed following UK and Italian animal regulation procedures.

Results

We show that release of ATP from the non-sensory cells of the immature mouse cochlea is not required for the generation of APs in IHCs. Although immature IHCs from connexin knockout mice show spontaneous AP activity, their frequency is modulated by ATP-dependent Ca²⁺ signalling. Moreover, we demonstrate that connexins are crucial for the functional maturation of the mouse cochlea.

Conclusions

These results show that APs are an intrinsic characteristic of immature IHCs. Moreover, IHCs from connexin knockouts remain stuck at pre-hearing stages of development, and as such are unable to process sound information

Supported by grants from The Wellcome Trust to WM & Fondazione Telethon GGP13114 to FM. SLJ is a Royal Society URF.

PS 135

Inhibition of Mitochondrial Division Protects Neuro-mast Hair Cells Against Cisplatin Toxicity

Jonathon W. Vargo¹; Steven Walker²; Suhasini Gopal¹; Aditi R. Deshmukh¹; Brian M. McDermott²; Kumar N. Alagramam²; Ruben Stepanyan²

¹University Hospitals Cleveland Medical Center, Case Western Reserve University; ²Department of Otolaryngology - HNS, Case Western Reserve University

Cisplatin and other related platinum antineoplastic drugs are commonly used in the treatment of a variety of cancers in both adults and children. The platinum drugs act on cancerous cells by forming nuclear DNA adducts, which may initiate signaling leading to cell cycle arrest or apoptosis. However, use of these drugs comes with

a host of undesirable effects, including ototoxicity, which affects most patients treated. Cisplatin's effects on the cochlea are multifaceted, culminating in irreversible damage to the hair cells starting in the basal turn's outer hair cells. Auditory hair cells do not proliferate in mammals, therefore cisplatin-induced toxicity to hair cells may also include other mechanisms of damage. It was reported that cisplatin may induce mitochondrial DNA damage in non-cancerous cells. Therefore, protecting mitochondria may alleviate cisplatin-induced damage to normal cells. In addition, an important consideration is to find a protection method that does not affect the anti-tumor actions of the platinum-based drugs. Here we tested the protective effect of Mdivi-1, which was identified as a regulator of apoptosis and mitochondrial fission and fusion. Moreover, it has been reported that Mdivi-1 increases the apoptosis of cells that are resistant to cisplatin in both in vitro and in vivo studies. We conducted experiments using the Tübingen strain of zebrafish of either sex, cdh23 mutant, and transgenic zebrafish stably expressing GFP in the hair cells (pvalb3b::GFP). Larvae at 5 – 6 days post fertilization, were placed in varying concentrations of cisplatin (50 – 200 μ M) and/or Mdivi-1 (3 – 10 μ M) for 16 hours. Then, the larvae were transferred for observation. To evaluate hair cell viability, the number of hair bundles were counted in approximately 10 neuromasts per fish. To assess hair cell function, we used the FM1-43 uptake assay and recordings of neuromast microphonic potentials. Here we tested whether Mdivi-1 can protect neuromast hair cells against cisplatin induced toxicity. Our results demonstrated that Mdivi-1 protected hair cells of lateral line neuromasts against 50 μ M of cisplatin. In addition, our data show that functional mechanotransduction strongly potentiate cisplatin-induced hair cell toxicity. Mitochondria might buffer larger amounts of calcium entering through functional hair cell mechanotransduction channels causing hair cells to become more vulnerable to toxic insult. Together, our data suggests that protection of mitochondria may increase viability of hair cells to cisplatin-induced toxicity.

PS 136

Reinforcement of Junctional P120-catenin Is Cor-related with the Absence of Hair Cell Regeneration in Postnatal Mammalian Cochlear

Wenwei Luo¹; Ning Cong¹; Xiaoyu Yang²; Dong-Dong Ren³; Juanmei Yang³; Fanglu Chi³; Dongdong Ren⁴

¹Department of Research Center, Eye, Ear, Nose and Throat Hospital, Fudan University, Shanghai, China;

²Department of Research Center, Eye, Ear, Nose and Throat Hospital, Fudan University, Shanghai 200031,

P.R. China; ³Department of Otolaryngology and Skull Base Surgery, Eye, Ear, Nose and Throat Hospital; Fudan

Background

Sensory hair cell losses lead to severe hearing and balance deficits in mammals and nonmammals, but supporting cells (SCs) in the ears of non-mammals can divide and give rise to hair cells to recover from sensory impairments that are irreversible for mammals. It remains unknown what prevents hair cell regeneration from occurring in mammals. Studies have shown that thick F-actin bands in maturing mammals may have an important role in limiting hair cell regeneration. Investigations in the mammalian balance epithelia showed that postnatal accumulation of junctional E-Cadherin is inversely linked to the capacity for supporting cells to convert into hair cells. This study aims to explore whether the junctional cadherins is correlated with the absence of hair cell regeneration in mammalian cochlears.

Methods

Cochlear sensory epithelium from postnatal day0 (P0), day3 (P3) and day7 (P7) mice were dissected and immunolabeled with Ecadherin and P120-catenin(P120). The level of cadherins was detected by western blot. We then cultured cochlears in the presence of DAPT from day 0 to day 4 in vitro (DIV4). DMSO treatment was served as control. Myo7a+ cells and Prox1+ cells were counted separately on the apex, midapex, midbase, and base turn. We observed the level of cadherins between two groups from P0, P3, P7 mice by immunostaining, western blot and qRT-PCR. DAPT treatment of P0 cochlears were fixed at DIV2, DIV4 and DIV6 separately to explore the effect of longer DAPT treatments.

Results

Cadherins expression increased at the SC-SC and SC-HC junctions from P0 and P7. After 4 days of continuous DAPT treatment, a large number of Myo7a+ cells were observed in the sensory region with depletion of P120 and Prox1+ cells occurred specifically in a gradient from apex to base. Longer DAPT treatment led to significantly expanded depletion area of P120 with more Myo7a+ cells produced and less Prox1+ cells resided. However, the SCs in the base turn retained P120 and failed to convert into HCs even after long DAPT treatments. P120 deletion and the capacity for the differentiated SCs converting into HCs declined with age and ceased by P7. Though endocytosis was apparently occurred in the sensory region of DAPT-treated cochlears, the levels of Ecadherin remained unchanged compared with DMSO treatment.

Conclusion

Together, temporal and spatial differences in postnatal mammalian SC-to-HC phenotypic conversion capacity are

linked to the junctions of P120, which might account for the limits to hair cell regeneration in mammals.

PS 137

A Zebrafish Model for Studies of Hearing Loss and Brain Injury Induced by Blast Wave

Jiping Wang¹; Zheng Yan²; Jian Wang³; Yaqin Wu⁴; Haibo Shi¹; Shankai Yin¹; Hai B. Shi⁵

¹Department of Otorhinolaryngology-Head & Neck Surgery Affiliated Sixth People's Hospital, Shanghai Jiao Tong University; ²Shanghai Marine Electronic Equipment Research Institute; ³School of Human Communication Disorders, FHP, Dalhousie University; ⁴Department of Otorhinolaryngology Head & Neck Surgery, The Sixth People's Hospital Affiliated to Shanghai Jiaotong University; ⁵The Sixth People's Hospital Affiliated to Shanghai Jiaotong University

Blast wave exposure can cause significant hearing loss and brain injury. Mammals are commonly used as the animal models. Zebrafish (*Danio rerio*) has the potential to regenerate the injured organs and tissues but never been reported for regeneration research after blast injury. In this study, an underwater blast wave generator has been made and zebrafish was subjected to blast wave exposure. The peak sound pressures produced by this generator were up to 224 dB SPL (160 kPa) 25 cm away from the machine that were qualitatively similar to those made by muzzle blasts or explosions. The hearing sensitivity of zebrafish was examined by analysing the auditory evoked potentials (AEPs) from 1-35 days post blast wave exposure. Cell apoptosis and proliferation in the hair cells (HCs) of the inner ear including saccule, lagena and utricle and brain tissue were investigated. Significant difference in AEP thresholds was observed across the four groups. The AEP thresholds demonstrated both blast induced hearing loss and recovery improvement of hearing sensitivity during the observed time. Apoptosis test showed that TMR positive HCs in the saccule, lagena and utricle were in a dose-dependent manner as compared with that of control group. TMR positive cells in brain sections also demonstrated significant difference between blast wave-treated and untreated groups. Interestingly, the number of PCNA+ HCs in inner ear recovered to a normal level in 3 weeks, whereas PCNA+ cell number in brain took about 5 weeks to get close to control level. These results revealed that this zebrafish model demonstrated hearing loss and brain injury and cell regeneration after blast injury in inner ear and brain tissues. Together, this zebrafish model can be a reliable animal model for blast injury and regeneration research of HCs and brain.

Attenuation of Noise Induced Hearing Loss by Near-Infrared-Light Pre-Treatment

Ira Strübing¹; Moritz Gröschel¹; Dan Jiang²; Patrick Boyle³; Arne Ernst¹; Dietmar Basta¹

¹Department of Otolaryngology at Unfallkrankenhaus Berlin, University of Berlin, Germany; ²Department of Otolaryngology, Guy's and St Thomas' NHS Foundation Trust, London, UK; ³Advanced Bionics European Research Center, Hanover, Germany

Noise induced hearing loss (NIHL) is accompanied by a reduction of cochlear hair cells and spiral ganglion neurons. Different approaches are applied to prevent noise induced apoptosis / necrosis and physical intervention is one technique currently under investigation. Specific wavelengths within the near-infrared light (NIR)-spectrum are known to influence cytochrome-c-oxidase activity which leads in turn to a decrease of apoptotic mechanisms. It has been shown recently that NIR can decrease the cochlear hair cell loss significantly if applied daily after a noise exposure. However, it is unclear until now if a single NIR-treatment just before a noise exposure could induce similar protective effects. Therefore, the present study aimed at investigating the effect of a single NIR-pre-treatment to prevent or limit NIHL.

The cochleae of adult NMRI-mice were pre-treated with NIR-light for 5; 10; 20; 30; 40 or 50 minutes via the external ear canal. All animals were noised exposed immediately after the pre-treatment by broad band noise (5 – 20 kHz) for 30 minutes at 115 dB SPL. Frequency specific ABR-recordings for determination of auditory threshold shift were carried out before all treatments and two weeks after the noise exposure. Spiral ganglion cell densities and cochlear hair cell loss were determined. One group was noise exposed only and served as control.

Two weeks after noise exposure, ABR threshold shifts of NIR-treated animals were significantly lower ($p < 0.05$) at three frequencies in the 5-minute pre-treatment group and for the entire frequency range in all other treatment groups compared to controls. Our results suggest that a single NIR pre-treatment induces a very effective protection of cochlear structures, whereby 10 minutes seem to emerge as optimal dosage for our experimental setup.

This study was supported by Advanced Bionics GmbH, Hanover, Germany.

RNA Interference Prevents Autosomal Dominant Hearing Loss

Seiji B. Shibata¹; Richard JH. Smith¹; Paul T. Ranum²; Alexander T. Goodwin³; Goodman Shawn⁴; Paul Abbas⁴; Jeffrey R. Holt⁵; Hideaki Moteki⁶; Bifeng Pan⁷

¹Department of Otolaryngology, Molecular Otolaryngology and Renal Research Laboratories, University of Iowa; ²Interdisciplinary Graduate Program in Molecular & Cellular Biology, The University of Iowa Graduate College, University of Iowa; ³Molecular Otolaryngology and Renal Research Laboratories, Carver College of Medicine, University of Iowa; ⁴University of Iowa; ⁵Department of Otolaryngology, F.M. Kirby Neurobiology Center, Boston Children's Hospital, Harvard Medical School; ⁶Shinshu University School of Medicine; ⁷Department of Otolaryngology, Boston Children's Hospital, Harvard Medical School

Background

Hearing impairment is the most common sensory deficit. It is often caused by the expression of an allele carrying a single dominant missense mutation. Herein we show that hearing loss can be prevented for up to 35 weeks in the Beethoven (Bth) mouse, a murine model of non-syndromic human deafness caused by a dominant gain-of-function mutation in transmembrane channel-like 1 (Tmc1), with a single intracochlear injection of an artificial microRNA carried in a viral vector.

Methods

RNAi oligonucleotides were designed and cloned, potency of knockdown was tested in vitro, candidate sequences were packaged into rAAV2/9. The rAAV2/9-RNAi constructs were injected into the inner ear of Bth mice via the round window membrane at P0-2, hearing thresholds were subsequently assessed by ABRs and DPOAEs over 35 weeks. In vivo RNAi knockdown was assessed with qPCR using allele-specific primers 4 weeks post-injection. The number of surviving hair cells was quantified in all treated mice and compared to the contralateral side and control vector injected ears.

Results

Three of 15 RNAi oligonucleotide sequences decreased expression of the Bth allele in vitro by >80% as quantitated by qPCR. In vivo RNAi knockdown was confirmed by allele-specific qPCR, which showed reduced expression of Tmc1M412K in treated as compared to untreated contralateral ears. In the best performing mice, hearing thresholds were significantly improved in ears injected with rAAV2/9-RNAi as compared to both contralateral non-injected ears and rAAV2/9 scramble-sequence-in-

jected Bth mice for the entire study (35 weeks). Inner hair cell survival was also significantly greater in treated ears.

Conclusions

Allele-specific RNAi gene therapy in Bth mice significantly attenuates the progression of Tmc1M412K-induced sensorineural hearing loss. This outcome is noteworthy as the first study to demonstrate the feasibility of long-term suppression of an endogenous deafness-causing allele to prevent progressive hearing loss.

PS 140

The Intersection of Hair Cell Mechanotransduction, Mitochondrial Metabolism, and Ototoxic Vulnerability in Lateral Line Hair Cells

Sarah Pickett¹; Robert Esterberg²; Tor Linbo¹; Joy Y. Sebe³; David W. Raible⁴

¹University of Washington; ²Novartis; ³University of Washington, Seattle; ⁴University of Washington, Seattle

Mitochondria are key players in hair cell damage and hearing loss. Mitochondrial calcium uptake and oxidation are important aspects of hair cell damage and death induced by aminoglycoside antibiotic exposure. Mutations in several genes required for mitochondrial function are also known to cause hearing loss. In order to determine the cellular consequences of such mitochondrial mutations, a more thorough understanding of how mitochondria function within hair cells and respond to normal energetic demands is required. To this end, this study examines the intersection of mitochondrial activity, hair cell activity, and vulnerability to damage in hair cells of the zebrafish lateral line system. We expressed genetically encoded indicators in hair cells to visualize mitochondrial oxidation, biogenesis, and ATP metabolism. We initially characterized these indicators during normal hair cell development, observing a substantial increase in mitochondrial biogenesis and mitochondrial oxidation as hair cells mature. Within mature neuromasts, we observed variability in mitochondrial oxidation levels across hair cells. To test whether mitochondrial biogenesis and oxidation corresponded with potential increased metabolic need as cells become functionally active, we measured these indicators in mechanotransduction mutants. Mitochondrial biogenesis is unchanged in these mutants, suggesting that it is an independent, developmentally regulated process. Conversely, mitochondrial oxidation was decreased in mechanotransduction mutants relative to wildtype siblings. Given the increased mitochondrial oxidation incurred by mechanotransduction activity and the variability observed in mature neuromasts, we sought to determine whether relative oxidation level is an informative predictor of hair cell

vulnerability to aminoglycoside antibiotic exposure. After treatment with neomycin, hair cells with higher baseline mitochondrial oxidation were indeed more susceptible to damage than those with lower baseline oxidation in the same neuromast. Future studies will examine mitochondrial and hair cell activity in mutants for mitochondrial deafness genes.

PS 141

Roles of USH1 Proteins and PDZ Domain-containing Ush Proteins in the USH2 Complex Integrity in Cochlear Hair Cells

Jun Yang¹; Junhuang Zou¹; Qian Chen¹; Ali Al-mishaa²; Pranave Dinesh. Mathur¹; Tihua Zheng¹; Cong Tian³; Qing Y. Zheng³

¹University of Utah; ²Department of Communication Sciences and Disorders, University of Utah; ³Case Western Reserve University

Usher syndrome (USH) is the most common cause of inherited deaf-blindness, manifested as USH1, USH2 and USH3 clinical types. The protein products of USH2 causative and modifier genes, USH2A, ADGRV1, WHRN and PDZD7, interact to assemble a multiprotein complex at the ankle link region of the mechanosensitive stereociliary bundle in hair cells. Defects in this complex cause stereociliary bundle disorganization and hearing loss. The four USH2 proteins also interact in vitro with USH1 proteins including myosin VIIa, USH1G (SANS), CIB2 and harmonin. However, it is unclear whether the interactions between USH1 and USH2 proteins occur in vivo and whether USH1 proteins play a role in USH2 complex assembly in hair cells. In this study, we identified a novel interaction between myosin VIIa and PDZD7 by FLAG pull-down assay. We further investigated the role of the above-mentioned four USH1 proteins in cochlear USH2 complex assembly using USH1 mutant mice. We showed that only myosin VIIa is indispensable for USH2 complex assembly at ankle links, indicating the potential transport and/or anchoring role of myosin VIIa for USH2 proteins in hair cells. However, myosin VIIa is not required for USH2 complex assembly in photoreceptors. We further showed that, while PDZ protein harmonin is not involved, its paralogous USH2 proteins, PDZD7 and whirlin, function synergistically in USH2 complex assembly in cochlear hair cells. In summary, our studies provide novel insight into the functional relationship between USH1 and USH2 proteins in the cochlea and retina as well as the disease mechanisms underlying USH1 and USH2.

NanoSPD 2.0: Improved Nanoscale Pulldowns for Studying Protein-Protein Interactions in Live Cells

Jonathan E. Bird¹; Melanie Barzik¹; Thomas B. Friedman²

¹NIDCD/NIH; ²Section on Human Genetics, Laboratory of Molecular Genetics, National Institute on Deafness and Other Communication Disorders, National Institutes of Health, Bethesda, MD, USA.

Many molecules mutated in hereditary hearing loss assemble into macromolecular complexes that are critical for hair cell and stereocilia function. Identification of the molecules within these assemblies and how they interact is a proven approach in sensory biology to understand the molecular basis of deafness. We recently introduced the nanoscale pulldown (NanoSPD) as a microscopy based assay to detect molecular interactions within live cells [1]. In a NanoSPD assay, EGFP-tagged myosin 10 (MYO10) is cloned in frame with a C-terminal 'bait' protein, with the resulting chimera trafficking along actin filaments to the tips of cellular filopodia. Quantitative microscopy is used to measure the relative intensity of fluorescently-tagged prey(s) that are co-transported and infer the presence of an interaction. Unlike traditional co-IP and pulldown assays that require specific antibodies to capture proteins on an extracellular affinity support, and subsequently for detection by western blotting, NanoSPD assays are performed within the native cytoplasm and the assay is directly examined using confocal microscopy in situ.

Here, we present a significantly revised NanoSPD assay that eliminates cloning of chimeric EGFP-MYO10-bait expression vectors. Instead, we couple MYO10 non-covalently to EGFP-bait molecules using a nanobody that selectively binds EGFP with nanomolar affinity [2]. We show that the MYO10-nanobody can capture and transport EGFP-bait along filopodia, in tandem with bound mCherry-prey. Critically, the MYO10-nanobody does not transport mCherry-prey in isolation, confirming that filopodia targeting of prey requires a specific bait interaction. To further streamline the assay, we engineered a clonal HeLa(NanoSPD) cell line that stably expresses the MYO10-nanobody. In conclusion, NanoSPD 2.0 assays can now be performed by transfecting HeLa(NanoSPD) cells with EGFP-tagged bait and mCherry/RFP-tagged prey proteins. The wide availability of EGFP and mCherry/RFP-tagged proteins from plasmid repositories will allow most protein-protein interactions to be assayed by NanoSPD with no cloning required.

Acknowledgements: This work is funded by the intramural program of the NIDCD to T.B.F. All plasmid (Addgene) and cell line (ATCC) reagents are being deposited

for easy access to the research community.

References:

- [1] Bird & Barzik et al., (2016). Harnessing Molecular Motors for Nanoscale Pulldown in Live Cells. *bioRxiv* doi:10.1101/053744
 [2] Rothbauer et al., (2006). Targeting and tracing antigens in live cells with fluorescent nanobodies. *Nature Methods* doi:10.1038/nmeth953

PS 143

Gad2-IRES-Cre Mediated GCaMP5G-tdTomato Expression in the Mouse Inner Ear

Holly A. Holman¹; Ali Almishaal²; Richard D. Rabbitt¹

¹University of Utah; ²Department of Communication Sciences and Disorders, University of Utah

Introduction

To examine calcium signaling in the inner ear we crossed two established transgenic mouse strains, Gad2-IRES-Cre and GCaMP5G-IRES-tdTomato, generating a new [Ca²⁺] reporter, Gad2-Cre::GCaMP5G-tdTomato. Gad2-IRES-Cre knock-in mouse strain contains Cre-recombinase inserted into the 3'-untranslated region of the Gad2 gene and when crossed with GCaMP5G-IRES-tdTomato expresses GCaMP5G-tdTomato in cells expressing Cre-recombinase. Here we describe expression of GCaMP5G-tdTomato in outer hair cells, inner hair cells, cytoskeletal structures, and neurons in cochlea spanning different ages in Gad2-Cre::GCaMP5G-tdTomato mice. Studies included immunolabeling with MYO7A, GAD2, efferent and afferent specific antibodies and cytoskeletal dyes performed on fixed vestibular tissues revealing GCaMP5G-tdTomato expression in hair cells and neurons of cristae and utricles. Auditory brainstem responses (ABRs) and distortion product otoacoustic emissions (DPOAEs) tests suggest that Gad2-Cre::GCaMP5G-tdTomato mice have normal hearing throughout their lifespan.

Methods

Gad2-IRES-Cre (Gad2tm2(cre)Zjh) mouse strain was previously generated using C57BL6/S129 hybrid embryonic stem cells [1]. The calcium indicator strain, GCaMP5GPolr2atm1(CAG-GCaMP5g,-tdTomato)Tvrtd [2], was previously designed with a cassette containing GCaMP5G and tdTomato under control of the CAG CMV-IE enhancer/chicken beta actin/rabbit beta-globin hybrid promoter. This GCaMP5G-tdTomato expression cassette was inserted into the intergenic region downstream of the endogenous Polr2a gene. Expression of Cre-recombinase from the Gad2-IRES-Cre mouse removes the floxed STOP cassette resulting in both GCaMP5G and tdTomato expression in Cre-expressing cells. ABR thresholds were determined as the lowest in-

tensity at which the response was clearly discernible. DPOAEs were measured using digitally generated stimuli of two primary tones f_1 and f_2 ($f_2/f_1 = 1.2$) with $f_2 = f_1 - 10$ dB. Primary tones (f_1) were stepped from 30 to 80 dB SPL in 10 dB increments and swept from 8 to 32 kHz in $1/2$ octave steps.

Results

Gad2-Cre::GCaMP5G-tdTomato transgenic mice express GCaMP5G-tdTomato in hair cells and neurons of the cochlea and vestibular system. Whole mount tissue preparations reveal GCaMP5G expression within the tips of stereocilia, and GCaMP5G-tdTomato expression at the apex of hair cells in cochlea, cristae and utricles, as well as in both bouton and calyceal synaptic terminals. $[Ca^{2+}]$ transients recorded in stereocilia, hair cells, and terminals are reported in a companion presentation [3].

Conclusion

The Gad2-Cre::GCaMP5G-tdTomato transgenic mouse strain introduced here provides a new tool to examine $[Ca^{2+}]$ signaling in both the auditory and vestibular hair cells and neurons over a wide age range.

Funding

NIDCD R01 DC006685

[1] Taniguchi et al. (2011) *Neuron* 71(6): 995-1013

[2] Gee et al. (2014) *Neuron* 83(5): 1058-1072

[3] Holman et al. (2017) ARO

Inner Ear: Damage & Protection I

PS 144

Effects of Cochlear Synaptopathy on the Middle-Ear Muscle Reflex in Unanesthetized Mice

Michelle D. Valero; M. Charles Liberman
Massachusetts Eye and Ear Infirmary, Harvard Medical School

Cochlear synaptopathy is an important problem in aging, noise damage, ototoxicity, and possibly other types of acquired sensorineural hearing loss. Because behavioral thresholds are insensitive to the pathology until ~90% of the cochlear nerve fibers are lost, new approaches are needed to diagnose this condition in humans. The subset of cochlear nerve fibers with high thresholds and low spontaneous rates (SRs) are the most vulnerable to many types of damage, and they may be particularly important drivers of the middle-ear muscle reflex (MEMR). Because one role of the MEMR is to protect the inner ear from noise damage, loss of low-SR fibers could lead to a vicious cycle wherein the ear becomes progressively more damaged by subsequent trauma. Because ther-

apeutic interventions may be possible, an early diagnostic tool would be of great value.

To cleanly separate the MEMR from the medial olivocochlear reflex (MOCR), we used a mutant mouse strain that is functionally de-efferented due to the absence of the alpha-9 nicotinic acetylcholine receptor expressed on outer hair cells. We first titrated the exposure level required to induce temporary threshold shifts, as measured by auditory brainstem responses (ABRs) and distortion-product otoacoustic emissions (DPOAEs), and permanent cochlear synaptopathy. The optimal exposure level was 4-dB lower than that required for CBA/CaJ mice (93.5 vs. 97.5 dB SPL), but there was no difference between knockout (KO) and wild-type (WT) mice of the same strain.

We compared contralaterally evoked MEMRs in unanesthetized, head-fixed a9-KO vs. a9-WT mice, with synaptopathy ranging from 0-50% in the basal half of the cochlea, as confirmed by cochlear histopathology. Reflex threshold was strongly correlated with the percentage of synapses lost. When the reflex elicitor spanned the synaptopathic region (22.6-45.2 kHz passband), the threshold was elevated by up to ~16 dB in synaptopathic mice, but there was no difference in reflex threshold when the elicitor spanned the non-synaptopathic region (5.6-11.3 kHz passband). This internal control indicated that reflex threshold elevation was caused by a reduced input from the afferent limb of the circuit, rather than a central deficit or reduced motor output to the stapedius muscle. The data confirm our prior report on anesthetized mice and further highlight the potential utility of the MEMR in the early detection of cochlear synaptopathy.

PS 145

Chronic Cigarette Smoke Exposure Results In Spiral Ganglion Neuron Losses And Fibrosis In C57/BL6J Mice

Stephen Paquette; Ryan Dawes; Isaac Sundar; Irfan Rahman; Edward Brown; Patricia White
University of Rochester

Cigarette smoking strongly correlates with high-frequency hearing loss, yet very little is known about the reason for the typically observed loss of function. This is especially true for industrial and military settings where damaging levels of noise exposure may occur. In this study we investigate the effects of chronic application of cigarette smoke (CS) on the sensory lamina and spiral ganglia of mid-range and high-frequency regions of the cochlea. We determine that there is an abrogation of apoptotic response in exposed inner hair cells. This is interestingly paired with an observation of neuron losses of both peripherin and non-peripherin expressing spiral

ganglion neurons. Second-harmonic and two-photon imaging show spiral ganglion neurons experience an increased metabolic load in exposed animals. Additionally, regions of neuron losses are back-filled with fibrotic collagen in cigarette smoke exposed cochlea. Invasive fibrotic signatures are not seen in the unexposed condition. To further investigate the causative relationship between increased levels of intracellular metabolic markers and regions of cell losses in the spiral ganglion of CS exposed mice, we explored the effects of nicotine exposure on efferent terminals synapses. The efferent regulatory projections from lateral olivocochlear (LOC) and medial olivocochlear (MOC) small and shell neurons were examined for volume changes in terminal plexuses. Efferent terminal arborization changes were also characterized to explore the role of nicotinic acetylcholine receptor down-regulation as it relates to increased susceptibility to noise-damage in CS exposed animals.

PS 146

Hartley Guinea Pigs Supplied by Different Breeders Exhibit Different Responses to High Decibel Noise

Donna S. Whitlon¹; Hunter Young¹; Claus-Peter Richter²

¹Department of Otolaryngology-Head and Neck Surgery, Feinberg School of Medicine, Northwestern University; ²Department of Otolaryngology-Head and Neck Surgery, Feinberg School of Medicine, Northwestern University & Resonance Medical, LLC, Chicago

Background

Determining the appropriate animal model for noise induced hearing loss (NIHL) experiments is not straightforward. Studies using inbred lines usually show low inter-animal variability, but they can also narrow the general applicability of the findings and can miss physiology that might otherwise have been obvious on a different genetic background. Genetic background is therefore often a key element in scientific reporting of inbred mouse experiments. On the other hand, outbred stocks are generally not so well understood or described. Unlike inbred strains, an outbred stock is bred to maintain maximum heterozygosity and have been standard in NIHL studies. However, but most reports do not fully describe the source, the stock, the breeding parameters, the diet or other factors that may unintentionally influence the hearing responses to noise of breeding stocks, regardless of the source of their original breeding pairs.

Using the outbred Hartley guinea pig for NIHL studies, we, as have others, observed high variability in individual threshold changes after high decibel noise exposure. In going over the data, we realized that we had evaluat-

ed as one group, Hartley guinea pigs from two different breeders. We then separated out the data from animals acquired from different breeders to determine whether any of the variability came from intermingling two different Hartley guinea pig stocks.

Methods

Adult guinea pigs were exposed to octave band noise (4-8 kHz, 120dB SPL, 4 hours). We analyzed ABR threshold shifts in adult Hartley guinea pigs from two different breeders before and 28 days after the noise insult.

Results

As expected high decibel noise sensitivity varied even among guinea pigs within each stock. However the representation of the different ABR threshold shifts in the population differed between stocks. Overall, the population of guinea pigs supplied by Breeder 1 (median threshold change 35dB, N=15) appeared to be more sensitive to hearing damage than those derived from Breeder 2 (median threshold change 10dB, N=12).

Conclusions

These studies are important to take into account when carrying out NIHL experiments on outbred stocks. Studies using only one stock may be inadequate. If we had used only Breeder 2 we might have concluded that our noise paradigm had little effect on guinea pig hearing. Had we carried out the study only in animals from Breeder 1, we might have overlooked the possibility that some guinea pigs can show a significant resistance to noise.

Supported by ONR Grants #N000141210173 and #N00014152130

PS 147

IGF-1 and the APAF-1 Inhibitor LPT99 Promote Survival of HEI-OC1 Auditory Cells

Blanca Cervantes¹; Lourdes Rodriguez-de la Rosa²; Isabel Sanchez-Perez³; Marta Torrecilla-Parra⁴; Carmen Herrero⁵; Isabel Varela-Nieto¹

¹Instituto de Investigaciones Biomedicas 'Alberto Sols' CSIC-UAM, Madrid, Spain; Centro de Investigacion Biomedica en Red de Enfermedades Raras, Madrid, Spain.; ²Instituto de Investigaciones Biomedicas 'Alberto Sols' CSIC-UAM, Madrid, Spain; Centro de Investigacion Biomedica en Red de Enfermedades Raras, Madrid, Spain; IdiPAZ, Instituto de Investigacion Hospital Universitario La Paz, Madrid, Spain.; ³Instituto de Investigaciones Biomedicas 'Alberto Sols' CSIC-UAM, Madrid, Spain; Dpto. Bioquimica. Fac. Medicina UAM, Madrid, Spain.; ⁴Instituto de Investigaciones Biomed-

The House Ear Institute-Organ of Corti 1 (HEI-OC1) is a mouse auditory cell line that shows sensitivity to ototoxic drugs, including aminoglycoside antibiotics and anti-neoplastic agents. Therefore, HEI-OC1 cells are widely used to test otoprotective drugs and to understand their mechanisms of action. Cisplatin is a chemotherapeutic agent that causes sensorineural hearing loss secondary to apoptosis of mammalian sensory hair cells. We have studied the pro-survival actions of the well-known anti-apoptotic insulin-like growth factor-1 (IGF-1) and of LPT99, a novel synthetic inhibitor of APAF-1, in HEI-OC1 cells. To do so, we have used two triggers of apoptosis: serum deprivation and treatment with cisplatin. Viability and growth rate of HEI-OC1 cells were determined using a crystal violet based staining method. Activation of caspase-3 was measured by immunocytochemistry as a read-out of apoptosis. Long-IGF-1 (10-100 nM) significantly protected from apoptosis induced by serum deprivation ($P < 0.05$) by activating the classical signaling mechanisms. On the other hand, cisplatin (0-5 $\mu\text{g}/\text{ml}$) caused a dose-dependent decrease in cell viability that was reduced by treatment with 1 μM LPT99. The IC50 of cells treated with cisplatin shifted from and IC50 of $4.47 \pm 1.94 \mu\text{g}/\text{ml}$ to $10.51 \pm 3 \mu\text{g}/\text{ml}$ in the presence of LPT99. Therefore, treated cells tolerated higher doses of cisplatin. In addition, immunofluorescence studies showed that the activation of caspase-3 after cisplatin treatment was reduced in the presence of LPT99. These data taken together show that the survival of HEI-OC1 is promoted by blockade of the intrinsic apoptotic pathway by classic trophic factors and by novel synthetic inhibitors of APAF-1. BC holds a Marie Curie fellowship from FP7-PEOPLE-2013-IAPP-TARGEAR

PS 148

Protective Effect of Juzen-taiho-to Against Cisplatin Ototoxicity.

Tadao Okayasu; Tadashi Nishimura; Akinori Yamashita; Tadashi Kitahara

Department of Otolaryngology-Head and Neck Surgery, Nara Medical University

Background

Cisplatin is one of the most commonly used chemotherapeutic agents in the treatment of malignant tumors. However, Ototoxicity associated with the administration of cisplatin is one of the major problems. Juzen-taiho-to is a representative traditional herbal formulations in Kampo medicine (Japanese traditional herbal medicines). Previous study reported that Juzen-taiho-to ameliorates cisplatin-induced nephrotoxicity. However,

no animal experimental study has been conducted to access the effect of Juzen-taiho-to on cisplatin-induced ototoxicity. In the present study, we examined the effects of Juzen-taiho-to on the cisplatin ototoxicity in guinea pigs

Method

Male Hartley guinea pigs (n=28) were assigned to 2 groups: control group (n=14), JT group (n=14). The control group received water (1.5 ml) by oral injection once daily from the days 1 to 12. The JT group received JT water (1.5 ml) which contains the 1.7 g/kg of JT-48 once daily on days 1 to 12. On the day 4, 30 minutes after the orally administration of JT, a single injection of cisplatin (8 mg/kg, i.p.) was administrated i.p. ABR measurements were performed in all guinea pigs on 7 to 3 days before the day 1 (baseline) and from the day 15 to 20 (post-administration). After the ABR measurement, guinea pigs of the control group (n=6: total 12 cochleae) and the JT groups (n=6: total 12 cochleae) were fixed by intracardiac perfusion. Both temporal bones were removed. The number of OHCs was counted in each individual transection of both the right and left cochleae. All experimental protocols were approved by the Animal Care and Use Committee of Nara Medical University.

Results

The threshold shifts for control group were significantly larger than those for JT group. The remaining OHCs of JT group is significantly more those of control group. The remaining OHCs of the apical turn were significantly more than that of middle and basal turn.

Conclusion

This study demonstrates that JT reduces the cisplatin-induced ototoxicity in the guinea pig model. Therefore, JT is expected to be useful as protective drug for cisplatin-induced ototoxicity.

Funding: This study was supported by Investigation Research Grant for Yamato-Kampo medical pharmacy.

PS 149

Extracellular Vesicles Derived from Human Vestibular Schwannomas Associated with Poor Hearing Damage Cochlear Cells

Takeshi Fujita¹; Vitor Soares²; Nadia Atai³; Sonam Dilwali²; Sarada Sivaraman⁴; Lukas D. Landegger⁵; Fred Hochberg⁶; Carlos Oliveira⁷; Xandra Breakefield⁴; Konstantina M. Stankovic⁵

¹Massachusetts Eye and Ear, Kindai University Faculty of Medicine; ²Massachusetts Eye and Ear; ³University of Amsterdam; ⁴Department of Neurology and Radiol-

ogy, Massachusetts General Hospital and Program in Neuroscience; ⁵Eaton Peabody Laboratories, Department of Otolaryngology, Massachusetts Eye and Ear, Harvard Medical School; ⁶Department of Neurosurgery, University of California at San Diego; ⁷Health Science Program and Department of Otolaryngology, University of Brasilia

Background

Vestibular schwannoma (VS) is a tumor of the vestibular nerve that transmits balance information from the inner ear to the brain. Sensorineural hearing loss occurs in 95% of patients with these tumors, but the cause of this loss is not well understood. We posit a role of VS-secreted extracellular vesicles (EVs) as a major contributing factor in cochlear nerve damage.

Methods

Using differential centrifugation, we isolated EVs from VS cell line HEI-193 and primary cultured human VS cells from patients with good hearing or poor hearing. The EVs were characterized using a Nanosight device and transmission electron microscopy and by extracting their RNA content. The EVs' effects on cultured murine spiral ganglion cells and organotypic cochlear cultures were studied using a transwell dual-culture system and by direct labeling of EVs with PKH-67 dye. EV-induced changes in cochlear cells were quantified using confocal immunohistochemistry. Transfection of VS cells with a green fluorescent protein-containing plasmid was confirmed with reverse transcription PCR.

Results

Human VS cells, from patients with poor hearing, produced EVs that could damage both cultured murine cochlear sensory cells and neurons. In contrast, EVs derived from VS cells from patients with good hearing did not damage the cultured cochlear cells.

Conclusions

Our findings strongly motivate future work to identify the EV-derived cargo mediating cochlear damage, as this could provide insight into much needed prognostic and therapeutic targets for prevention and treatment of hearing loss due to VSs and potentially other causes. Understanding mechanisms of hearing loss due to VS, such as by VS-secreted EVs, can expedite the path to pharmacotherapies against this common, debilitating symptom of VS for which approved nonsurgical therapies do not exist.

PS 150

Investigation of Low-Sound-Level Auditory Processing Deficits

Warren M H. Bakay; Christopher Plack; Michael Stone
Manchester Centre for Audiology and Deafness (Man-CAD), University of Manchester

Introduction

The audiogram is recognized as being an insensitive measure for quantifying hearing damage, since there may be changes in hearing even when audiometric thresholds are within the "normal" range. Early detection of these sub-clinical changes in humans has attracted increasing attention. Sub-clinical hearing loss due to noise exposure, with no change in absolute threshold, has previously been demonstrated in different forms. One form, Hidden Hearing Loss (HHL) has been observed in animals (Kujawa & Liberman, 2009), and changes in electrophysiological measures in humans (Schaeffe & McAlpine, 2011), this latter report being consistent with the animal work. These changes only appear at medium to high sound levels (Furman et al., 2013; Hesse & Bakay et al., 2016). Another form of sub-clinical loss, appearing only at low sound levels has been reported in humans either without any change (Stone, Moore, & Greenish, 2008), or with small but sub-clinical changes (Vinay & Moore, 2010) in absolute threshold. This does not fit with the suspected mechanism of HHL: cochlear synaptopathy of high threshold fibres. People so far identified with this low-level hearing deficit have a history of exposure to high-level noises, such as from recreational noise (clubbing, live music events, motorsport, shooting). People with traditional hearing losses have a compressed hearing range, and this sub-clinical impairment at low sound levels should occupy a larger portion of their reduced range. Goal. To quantify these low-sound-level deficits and determine their correlation to sound exposure history, if there are any related electrophysiological changes, and whether they affect the ability of the subject in speech comprehension.

Methods

Subjects were recruited as first time candidates for hearing aid fitting, with no previous experience wearing hearing aids and mild to moderate hearing losses (20-70dB). They were then screened in to different noise exposure groups using a slightly modified version of the HSE Noise Exposure and Rating questionnaire. Three different experiments were run. Firstly, click Auditory Brainstem Response and Frequency Following Response measures, using tip-trodes to maximize wave I amplitudes. Secondly, speech intelligibility testing using filtered speech segments with reduced temporal fine structure information in the frequency range associated

with noise induced hearing loss (2-5kHz). Finally, psychoacoustic stimuli were presented through a simulated hearing aid to determine the smallest change detectable in the temporal fine structure.

Acknowledgements

This research was supported by grant MR/M023486/1 from the Medical Research Council (MRC) and was sponsored by the University of Manchester.

PS 151

Inhibition of Mitochondrial Calcium Uniporter Attenuates Noise-induced Hearing Loss

Su-Hua Sha; Xianren Wang; Haishan Long; Kayla Hill
Medical University of South Carolina

Background

Mitochondria play a key role in the balance of cytosolic and organelle calcium homeostasis. This action is mediated in part by the selective calcium channel, mitochondrial calcium uniporter (MCU). Here, we tested the hypothesis using adult CBA/J mice that noise exposure resulted in mitochondrial calcium overload in sensory hair cells via stimulation of MCU, accelerating calcium uptake and leading to noise-induced permanent hearing loss.

Methods

Male CBA/J mice at 12 weeks of age were exposed to an octave band noise (OBN) with a frequency spectrum from 8 to 16 kHz for 2 h at 103 dB sound pressure level (SPL) to induce permanent threshold shifts (PTS) with loss of inner hair cell synaptic ribbons and outer hair cells only or 108 dB SPL to induce more severe PTS with loss of both types of sensory hair cells assessed 2 weeks after the exposure. Auditory thresholds were measured by auditory brainstem response (ABR). Outer hair cell loss was quantified from surface preparations labeled with myosin VII and then stained with DAB. Cochlear surface preparations, cryosections, silencing techniques, and specific inhibitors were utilized to elucidate detailed molecular and cellular mechanisms responsible for noise-induced losses of hair cells and synaptic ribbons and NIHL.

Results

Our results revealed that levels of MCU expression increased in cochlear cells, including sensory hair cells, spiral ganglion cells, marginal cells, and fibrocytes. Inhibition of MCU via MCU siRNA silencing or administration of the specific MCU inhibitor Ru360 attenuated noise-induced loss of sensory hair cells and synaptic ribbons, and subsequent noise-induced hearing loss (NIHL). This protection was afforded, at least in part, through reduced cleavage of caspases 8 and 9.

Conclusions

These results indicate that noise exposure leads to loss of hair cells and synaptic ribbons by mitochondrial calcium overload via stimulation of MCU. Targeting MCU may provide a novel route to prevent NIHL and noise-induced cochlear synaptopathy.

Acknowledgements

The research project described was supported by the grant R01 DC009222 from the National Institute on Deafness and Other Communication Disorders, National Institutes of Health.

PS 152

Roles of Thioredoxin 2 in the Maintenance of Thioredoxin Antioxidant Defense and Cellular Survival in Mouse Cochlea

Mi-Jung Kim¹; Chul Han¹; Hyo-Jin Park¹; Karessa White²; Dalian Ding³; Richard Salvi⁴; Shinichi Someya¹
¹*University of Florida, Department of Aging and Geriatric Research*; ²*University of Florida, Department of Aging and Geriatric Research*; *Department of Speech, Language, and Hearing Science*; ³*State University of New York at Buffalo*; ⁴*Center for Hearing & Deafness, Department of Communicative Disorders and Science, State University of New York at Buffalo*

Backgrounds

The mitochondrial thioredoxin (TXN2) system is one of the major antioxidant defense systems in mitochondria. There are three major players in the TXN2 system: thioredoxin 2 (Txn2), thioredoxin reductase 2 (Txnrd2), and peroxiredoxin 3 (Prdx3). In mitochondria, NADPH-dependent Txnrd2 catalyzes the reduction of oxidized Txn2 (oxiTxn2) to regenerate reduced Txn2 (redTxn2). Subsequently, redTxn2 catalyzes the reduction of oxidized Prdx3 (oxiPrdx3) to regenerate reduced Prdx3 (redPrdx3) which plays a role in the removal of hydrogen peroxide (H₂O₂) in cells. The overall goal of this project is to investigate the roles of Txn2 in maintaining thioredoxin and glutathione antioxidant defenses and cellular survival in the cochlea of CBA/CaJ mice.

Methods

To investigate the roles of Txn2 in auditory function, we performed auditory brainstem response (ABR) tests to measure ABR thresholds, wave I amplitudes, and wave I latencies in young Txn2 wild-type (Txn2+/+) and Txn2 heterozygous knockout (Txn2+/-) mice that have been backcrossed onto the CBA/CaJ mouse strain for 4 generations. To confirm these physiological test results, we performed histological analyses, including cochleograms, spiral ganglion neuron counting, and stria vascularis thickness measurements in the cochlea from young

Txn2^{+/+} and Txn2^{+/-} mice. To investigate the roles of Txn2 in maintaining thioredoxin and glutathione antioxidant defenses in the cochlea, we measured thioredoxin and glutathione antioxidant defense parameters in the nuclei, mitochondria, and cytosol of the cochlea from young Txn2^{+/+} and Txn2^{+/-} mice. To investigate if Txn2 knockdown increases oxidative stress-induced cell death, we performed oxidative stress tests followed by cell viability tests in the mouse auditory cell line HEI-OC1 (House Ear Institute-Organ of Corti 1) transfected with scrambled siRNA (si-Con) and siRNA targeted to mouse Txn2 (si-Txn2).

Results

There were no significant differences in ABR thresholds between young Txn2^{+/+} and Txn2^{+/-} mice at 8, 16, 32, or 48 kHz. There were no significant differences in the numbers of inner hair cells and outer hair cells between young Txn2^{+/+} and Txn2^{+/-} mice. There were no significant differences in mitochondrial thioredoxin reductase activity in the cochlea between young Txn2^{+/+} and Txn2^{+/-} mice. Txn2 knockdown did not affect cell viability under oxidative stress conditions in the HEI-OC1 cell line.

Conclusions

These results suggest that Txn2 is not essential for the maintenance of the thioredoxin antioxidant defense and cellular survival in the cochlea of CBA/CaJ mice.

Funding

Supported by NIH/NIDCD grants R01 DC012552 (S.S.), R01 DC014437 (S.S.) and R03 DC011840 (S.S.).

PS 153

An Insufficient Therapeutic Window for Protection against Ototoxicity by Histone Deacetylase Inhibitors in Vivo

Su-Hua Sha¹; Chao-Hui Yang²; Zhiqi Liu¹; Deana Dong¹; Jochen Schacht²; Dev Arya³

¹Medical University of South Carolina; ²University of Michigan Medical School; ³Clemson University

Background

Epigenetic modification of histones is an important form of chromatin regulation controlling cell responses, including the transcription of genes related to stress response and cell fate. Previous studies have reported that modification of histones alters aminoglycoside- and noise-induced hair cell death and hearing loss. In this study, we investigated histone deacetylase (HDAC) inhibitors as protectants against aminoglycoside-induced

ototoxicity in mouse explants and in vivo using both guinea pigs and CBA/J mice to provide information for future translational research.

Methods

Postnatal-day-3 (p3) explants from CBA/J mouse pups, adult CBA/J mice at 5 weeks of age, and pigmented guinea pigs at a body weight of 200–250 g were used to test if treatment with HDAC inhibitors could attenuate aminoglycoside-induced hair cell loss and hearing loss. Immunolabeling for acetyl-histone H3 (Lys9) (H3K9ac) and acetyl-histone H4 (Lys8) (H4K8ac) was used on explants to assess post-translational modifications of histones in sensory hair cells. Three FDA approved HDAC inhibitors (vorinostat/SAHA, belinostat, and panobinostat) were evaluated in their ability to prevent gentamicin-induced hair cell loss in explants. One of the HDAC inhibitors, SAHA, was further utilized to assess its potential protective effects by measurement of auditory thresholds with auditory brainstem response (ABRs) using both guinea pigs and mice in vivo. Sensory hair cells were quantified from surface preparations.

Results

The three HDAC inhibitors showed protective effects against gentamicin-induced hair cell loss in explants. One of the HDAC inhibitors, SAHA, was further assessed by immunohistochemistry, showing that treatment with SAHA reversed gentamicin-diminished H3K9ac and H4K8ac in OHC nuclei in the basal region of explants. However, treatment with SAHA showed attenuation of neither gentamicin-induced hearing loss and hair cell loss in guinea pigs nor kanamycin-induced hearing loss and hair cell loss in mice in these chronic ototoxic models in vivo. Increasing SAHA doses to treat guinea pigs resulted in thrombocytopenia. Conclusions: These findings suggest that treatment with the HDAC inhibitor SAHA attenuates aminoglycoside-induced ototoxicity in an acute, but not in a chronic model. This implies that the therapeutic window of SAHA against ototoxicity is too narrow in vivo and that testing compounds against aminoglycoside-induced ototoxicity in an acute model alone is insufficient for clinical application.

Acknowledgements

The research project described was supported by grant R42GM097917 from the National Institute on General Medicine Sciences, National Institutes of Health.

PS 154

Noise-induced Hearing Loss in TrpV1 Knockout Mice

Hongzhe Li¹; Alisa Hetrick²; Brandon Yeoh²

¹Research Service, VA Loma Linda Healthcare system; ²Department of Otolaryngology - Head and Neck

Introduction

Several transient receptor potential (TRP) channels including TRPV1 are located in the cochlea. The gating mechanisms of these channels are associated with cellular stress, inflammation, and cytoplasmic uptake of aminoglycoside antibiotics. TrpV1 mutant mice demonstrate extended life span compared to wildtype mice, and maintain a youthful metabolic profile. Interestingly, although these mice present normal hearing sensitivity as young adults, we recently found accelerating age-related hearing loss in the mutant. Here, we assessed the deterioration and partial recovery of hearing sensitivity after noise exposure in TrpV1 mutant mice, and compared with their littermate controls.

Methods

TrpV1 mutant mice (B6.129X1-Trpv1tm1Jul/J, stock #3770) were crossed with C57Bl/6 (JAX stock #0664) to generate F1 offspring, and then backcrossed with the initial TrpV1 mutant mice to generate experimental animals. Animals were housed in a Specific Pathogen Free-modified room, without sound treatment of ambient noise. Auditory brainstem responses to a broad frequency range, from 4 to 32 kHz, were measured at multiple age points. Temporary threshold shifts were introduced by exposing the animal to sustained broad-band noise at 85 dB with closed-field sound delivery and ketamine/xylazine anesthesia.

Results and Conclusion

TRPV1 is not required for normal development of cochlear function, as suggested by typical hearing sensitivity in juvenile TrpV1 mutant mice. Mice with a B6 background typically begin exhibiting age-related hearing loss around 12 weeks of age. This early onset of hearing loss is expedited in mice with genetically disrupted TRPV1 expression. In addition, TrpV1 mutant mice exhibited marginally increased susceptibility to acoustic overstimulation. Similar to TrpV1 mice, at 2 months of age, there was no significant difference in ABR thresholds between TrpV4 mutant mice and wild type controls, but thresholds elevated in TrpV4 mutants at 6 months of age compared to controls. This suggests TRP channels are involved in progressive hearing loss. Further research is required to determine the otoprotective role of TRPV1 channel and homologues, in maintaining auditory sensitivity as mice age. As TRPV1 becoming functionally indispensable in aged mice, it is worth to investigate whether TrpV1 channels facilitate additional drug trafficking and elevate the risk of drug-induced ototoxicity.

Funded by W81XWH1410006 to HL.

PS 155

Calcium and Integrin Binding Protein 2 (CIB2) Haploinsufficiency Causes Increased Susceptibility to Noise-Induced Hearing Loss

Mary J. Freeman¹; Arnaud P.J. Giese²; A. Catalina Velez-Ortega³; Zubair Ahmed²; Gregory I. Frolenkov⁴

¹*Department of Physiology, College of Medicine, University of Kentucky, Lexington, KY, 40536-0298, USA;*

²*Department of Otorhinolaryngology Head & Neck Surgery, School of Medicine University of Maryland, Baltimore, MD, 21201, USA;* ³*Department of Physiology, University of Kentucky, Lexington, KY, USA;* ⁴*Dept Physiology, University of Kentucky*

Calcium and integrin binding protein 2 (CIB2) is localized to the mechanosensory stereocilia of inner ear hair cells and is essential for hearing. Mutations in CIB2 underlie Usher syndrome type I and non-syndromic deafness in humans (Riazuddin et al. 2012). We have recently generated a knock-in mouse model that carries a p.F91S mutation in Cib2, recapitulating a deafness-associated point mutation in humans (see accompanying presentation by Giese et al. ARO 2017). While homozygous Cib2 mutant mice are deaf, the heterozygotes seem to have normal hearing thresholds. However, the p.F91S mutation is located in an EF-hand domain of the CIB2 protein and may influence calcium binding. Having in mind that acoustic stimulation leads to a large calcium influx into inner ear hair cells, the decreased amount of wild type CIB2 may increase the susceptibility of these cells to acoustic trauma in heterozygous Cib2 mutant mice. Therefore, in this study, we used auditory brainstem responses to measure the hearing thresholds of heterozygous Cib2 mutant mice and their wild type littermates before and after exposure to damaging noise (wide band 100 dB SPL for 30 minutes). We found that hearing thresholds of the heterozygotes do not recover to the same extent as those of wild type mice following noise exposure. These results suggest that the heterozygous Cib2 mutant mice are, in fact, more susceptible to noise-induced hearing loss than their wild type littermates. We conclude that CIB2 haploinsufficiency may represent a risk for noise-induced or age-related hearing loss in humans.

Supported by NIDCD/NIH (R01DC012564 to Z.M.A. and R01DC014658 to G.I.F.)

Effect of Pyridoxamine on the Hearing Function in the Mouse Model of Metabolic Syndrome

Kazuma Sugahara¹; Junko Tsuda²; Takeshi Hori³; Yoshinobu Hirose¹; Makoto Hashimoto¹; Hiroshi Yamashita¹

¹Department of Otolaryngology, Yamaguchi University Graduate School of Medicine; ²Yamaguchi University Graduate School of Medicine; ³Yamaguchi University Graduate School of Medicine,

Introduction

The metabolic syndrome is characterized by obesity concomitant with other metabolic abnormalities such as hypertriglyceridemia, hyperlipidemia, elevated blood pressure and diabetes. It is known that the prevalence of hearing loss is high in the patients with diabetes. TSOD (Tsumura-Suzuki-Obese-Diabetes) male mouse presented metabolic abnormality such as obesity and hyperlipidemia, high blood pressure, diabetes with aging. In the last meeting, we reported that the mice showed the age-related hearing loss related with the angiostenosis in the inner ear. In the present study, we evaluated the effect of pyridoxamine on the age-related hearing loss in TSOD mice.

Materials and Methods

TSOD male mice used in study were derived from the Tsumura Research Institute. Animals were divided into two groups (control group, pyridoxamine group). Pyridoxamine was administrated in the water (2 mg/ml) in pyridoxamine group. We evaluated the ABR thresholds, the weight and blood glucose level. In addition, the histological examination was performed in the end of experiments.

Results

There were no difference between 2 group in the 6 months aged TSOD mice. The elevation of ABR thresholds were observed in 6 month aged TSOD mice. in each group. However, the thresholds of 12 months aged were more in control groups than in pyridoxamine group.

Conclusion

The result suggested that pyridoxamine could prevent the hearing loss in the animal model of metabolic syndrome.

Potential of Excitotoxicity in Spiral Ganglion Neurons (SGNs) by cpt-cAMP

Sriram Hemachandran¹; Steven H. Green²

¹The University of Iowa; ²Department(s) of Biology and Otolaryngology

Introduction

Noise exposure destroys cochlear afferent synapses between inner hair cells (IHCs) and spiral ganglion neurons (SGNs) even in the absence of hair cell loss or permanent threshold shift. This cochlear "synaptopathy" is a result of excess release of the neurotransmitter glutamate from IHCs and consequent glutamate excitotoxicity, which is mediated by Ca²⁺ entry via Ca²⁺-permeable glutamate receptors. SGNs are innervated by lateral olivocochlear efferents that modulate the activity of SGNs via multiple neurotransmitters. One such neurotransmitter is the neuropeptide CGRP. The CGRP receptor signals intracellularly via the second messenger cyclic AMP (cAMP). CGRP and cell membrane-permeable cAMP analogs (e.g., cpt-cAMP) exacerbate excitotoxic damage to synapses. Here we investigate the mechanism focusing on Ca²⁺ channels recruited by cAMP signaling to increase Ca²⁺ influx during excitotoxic trauma.

Methods

Cochlear explant cultures from postnatal day 5 rat pups were prepared as described by Wang et.al, 2011. These cultures maintain intact a portion of the organ of Corti, associated SGNs, and synaptic connections. Synaptopathy is caused by addition of the glutamate agonist kainic acid (KA). In these experiments, a low concentration (0.01 mM) of KA was used that, by itself, causes minimal synaptopathy. The explants were co-treated with KA and CGRP (10 nM) or cpt-cAMP (1 mM) for 2 hr, the cultures then fixed and labeled. Synapse counts were compared among experimental conditions and controls. Labeling anti-Ribeye (presynaptic ribbons), anti-PSD95 (postsynaptic densities) and anti-Myosin 6/7 (IHCs). Co-localization of a ribbon and a postsynaptic density was defined as a 'synapse'. Calcium imaging was performed on dissociated SGNs using the Ca²⁺ reporter Oregon Green BAPTA1. The SGNs were pretreated with cpt-cAMP for 15 min and the Ca²⁺ fluorescence measured after KA treatment and compared to controls not treated with cpt-cAMP or KA.

Results and conclusions

(1) A 0.01 mM KA by itself does not cause significant synapse loss, but, co-treatment with CGRP or cpt-cAMP results in significant loss of synapses. (2) The percentage of cells showing elevated cytosolic Ca²⁺ in response to KA exposure significantly increased when

the SGNs were pretreated with cpt-cAMP. This suggests that exacerbation of KA excitotoxicity by cpt-cAMP is due to increased Ca²⁺ entry. (3) Increased Ca²⁺ entry in cpt-cAMP-pretreated cells appears to be via a novel route, not via KA-activated Ca²⁺-permeable glutamate receptors. Nevertheless, Ca²⁺ entry via these different routes appears to be additive in causing synaptopathy.

PS 158

Viral-mediated Ntf3 Over-expression in the Normal Cochlea Disrupts Neuronal Patterns and Hearing

Min Young Lee¹; **Yehoash Raphael**²; Takaomi Kurioka³; Megan Nelson³; Diane Prieskorn³; Donald L. Swiderski⁴; Yohei Takada³; Lisa A. Beyer⁴

¹*Department of Otolaryngology-Head & Neck Surgery, College of Medicine, Dankook University, South Korea;* ²*Department of Otolaryngology - Head and Neck Surgery, University of Michigan;* ³*Department of Otolaryngology-Head and Neck Surgery, Kresge Hearing Research Institute, University of Michigan, Ann Arbor, Michigan, USA;* ⁴*Kresge Hearing Research Institute, Department of Otolaryngology, University of Michigan*

Background and Objectives

Synaptopathy in the cochlea occurs when the connection between inner hair cells and the auditory nerve is disrupted, leading to impaired hearing and eventually to nerve degeneration. Acoustic trauma and ototoxic insults are the main causes of synaptopathy in the cochlea. Experiments using transgenic mice have shown that over-expression of NT-3 induced in supporting cells after noise exposure repairs noise-induced synaptopathy. To harness this therapeutic concept for clinical use, it would be necessary to activate the neurotrophin receptor on auditory neurons by other means, such as gene therapy, while minimizing off-target effects. To address the latter issue, the impact of viral-mediated NT-3 over-expression on the pattern of innervation and hearing thresholds in the normal guinea pig cochlea was assessed.

Materials and Methods

Adult guinea pigs were confirmed to have normal hearing using ABRs measured at 8, 16 and 32 kHz, and then divided into 4 groups based on material injected into their perilymph: normal saline (NS), Adenovirus.Empty, Adenovirus.Ntf3 and AAV.Ntf3 (an adeno-associated virus vector). In guinea pigs, injection of Adenovirus into perilymph leads to transduction of mesothelial cells lining the scala tympani. AAV transduces mesothelial cells and also cells of the auditory epithelium. ABR thresholds were measured again at 1 and 3 weeks post-injections. Histologic evaluation of hair cells, nerve endings

and synaptic puncta were performed at the 3 week time point.

Results

ABR threshold shifts were observed in Adenovirus.Ntf3 and AAV.Ntf3 inoculated groups but not in the two control groups, NS and Adenovirus.Empty. Adenovirus.Ntf3 group showed earlier hearing loss than AAV.Ntf3 group. At 3 weeks, Adenovirus.Ntf3 induced a larger threshold shift than AAV. Histology revealed that animals with NT-3 over-expression caused disorganization of peripheral nerve endings in the auditory epithelium as well as loss of auditory nerve fibers in the outer hair cell area. Additionally, disruption of synaptic connections between inner hair cell and peripheral nerve endings were found in both neurotrophin over-expressing groups.

Conclusions

The data suggest that elevation of NT-3 levels in the perilymph can disrupt innervation and degrade hearing. The practical implication is that an alternative delivery method is needed for treating synaptopathy; one that will facilitate a localized over-expression in the area of the inner hair cell.

Supported by the Hearing Restoration Project (HRP-HHF), and NIH/NIDCD grants R01-DC010412, R01-DC007634, R01-DC009410 and P30-DC05188.

PS 159

The Role of Peroxiredoxin I in Cisplatin-induced Ototoxicity

Quang Le¹; Keiji Tabuchi²; Eiji Warabi³; Akira Hara⁴

¹*Graduate School of Comprehensive Human Sciences, University of Tsukuba, Japan;* ²*Department of Otolaryngology, Faculty of Medicine, University of Tsukuba, Japan;* ³*Institute of Community Medicine, Graduate School of Comprehensive Human Sciences, University of Tsukuba;* ⁴*Department of Otolaryngology, Faculty of Medicine, University of Tsukuba*

Peroxiredoxin (Prx) is a new family of antioxidative proteins. Prx I is ubiquitously expressed in various tissues and is important in the defense of tissues from increases in reactive oxygen species (ROS). The present study was designed to examine the expression of Prx subtypes in the mouse cochlea and to show the possible involvement of Prx I in protecting the cochlea against cisplatin ototoxicity. Postnatal-day-3-to-5 wildtype mice and Prx I-deficient mice were used. Prx expression in the cochlea was assessed by real-time PCR assay. Prx I protein expression was examined by immunofluorescence staining. Cochlear explants were exposed to 2, 5, and 10- μ M cisplatin for 48 hours, and the cochlear

hair cell losses of the wildtype and Prx I-deficient mice were compared. In addition, the histologic features of the cochlear lateral wall were examined after cisplatin incubation. mRNAs of all Prx subtypes were expressed in the mouse cochlea. Prx I was one of the abundant subtypes and was upregulated after 48-hour exposure to 5- μ M cisplatin. Immunofluorescence staining showed the ubiquitous expression of Prx I in the cochlea. No difference in cochlear hair cell loss induced by cisplatin was found between the wild-type mice and the Prx I-deficient mice. However, spiral ligament fibrocytes of Prx I-deficient mice were significantly sensitive to cisplatin at 20- μ M or lower. Prx I is important for the protection of at least the spiral ligament fibrocytes of the cochlear lateral wall in cisplatin ototoxicity.

PS 160

Intra-tympanic Administration of Pioglitazone, a Peroxisome Proliferator-Activated Receptor Gamma Agonist, Protects from Noise-Induced Hearing Loss

Fabiola Paciello¹; Matthew B. Wright²; Alexander Bausch²; Rolando Rolesi³; Gaetano Paludetti³; Anna Rita Fetoni³

¹*Institute of Otolaryngology, Catholic University School of Medicine*; ²*Strekin AG*; ³*Catholic University School of Medicine*

Disabling hearing loss affects more than 278 million people worldwide. Multiple causes lead to development of this condition, including exposure to noise, ototoxic chemicals, and aging. Mechanisms involving inflammatory signaling, oxidative stress, and metabolic dysfunction lead to auditory hair cell death.

Pioglitazone, used for the medical treatment of diabetes, is an agonist of the peroxisome proliferator-activated receptor- γ which regulates the expression of genes controlling glucose and lipid metabolism. PPAR- γ has emerged as a potential target in other indications involving inflammation, oxidative stress, and cellular dysfunction. We developed a formulation of pioglitazone (1.2% w/v) for intra-tympanic administration and evaluated its effectiveness in a model of noise-induced hearing loss.

Acute acoustic trauma was induced either in guinea pigs or rats by exposure to a continuous pure tone of 10 kHz. Anesthetized animals were placed in a sound-proof room in a fixation cradle and exposed for 60 min at 120 dB SPL, presented to both ears in free field via loudspeakers. To assess the effects of pioglitazone, animals were treated with a single intra-tympanic injection of pioglitazone or placebo at various times before and

after the exposure to noise. Hearing function was evaluated by measuring auditory brainstem responses (ABR) at multiple time points. Morphological and immunohistochemical assessments were performed to evaluate effects on cochlear oxidative imbalance induced by noise exposure.

Five independent studies demonstrated that pioglitazone reduces noise-induced hearing loss. The greatest efficacy was observed in rats receiving pioglitazone immediately (1 hr) after noise exposure where thresholds were significantly improved by approximately 20 dB immediately after noise, and returned to normal pre-noise levels by 3 weeks. Significant, although lesser protection, was observed when pioglitazone was administered 48 hrs after noise exposure, as confirmed also by morphological and immunohistochemical data.

These data suggest that intra-tympanic pioglitazone may be an effective treatment for hearing loss.

PS 161

AAV-Mediated Neurotrophin Gene Therapy Promotes Survival of Cochlear Spiral Ganglion Neurons in Neonatally Deafened Cats

Patricia A. Leake¹; Stephen J. Rebscher¹; Chantale Dore¹; Lawrence R. Lustig²; Bas Blits³; Omar Akil¹

¹*Department of Otolaryngology-HNS, University of California, San Francisco, CA, USA*; ²*Columbia University Medical Center*; ³*UniQure*

The efficacy of cochlear implants (CI) depends partly upon survival of the cochlear spiral ganglion (SG) neurons, which degenerate progressively following deafness. In early-deafened cats, electrical stimulation from a CI partly prevents SG degeneration, and intracochlear infusion of brain-derived neurotrophic factor (BDNF) via an osmotic pump further improves neural survival. However, high concentrations of BDNF also elicit disorganized, ectopic sprouting of radial nerve fibers, which could be detrimental to optimum CI function due to loss of precise tonotopicity. Further, use of osmotic pumps is problematic for clinical application. The current study explores the potential for using adeno-associated viral vectors (AAV) to elicit targeted neurotrophic factor expression in the cochlea of normal and deafened cats.

Kittens were deafened prior to hearing onset by systemic injections of neomycin sulfate. ABRs showed profound hearing loss by 16-18 days postnatal. At ~4 weeks of age, AAV2-GFP (green fluorescent protein), AAV5-GFP, AAV2-BDNF, or AAV5-GDNF (glial-derived neurotrophic factor) was injected (10ul) through the round window into the left scala tympani. Animals were studied ~4 weeks

later for GFP immunocytochemistry; after AAV-neurotrophic factor injections, animals were studied at 14 or 24 weeks post-injection to evaluate SG survival.

Following AAV2-GFP injections, immunohistochemistry showed strong expression of the GFP reporter gene in inner (IHCs), outer hair cells (OHCs), inner pillar cells, and some SG neurons. AAV5-GFP elicited robust transduction of IHCs and some SG neurons, but few OHCs and supporting cells expressed GFP. Data from deafened cats examined 14 or 24 weeks after AAV2-BDNF injections showed significant neurotrophic effects, with higher SG densities and improved radial nerve fiber survival vs. contralateral. Importantly, no ectopic sprouting of radial nerve fibers was observed. Similar neurotrophic effects on SG survival were elicited by AAV5-GDNF (14 wks), but disorganized, ectopic fiber sprouting into scala tympani also occurred in all ears injected with AAV5-GDNF.

In conclusion, AAV-GFP (both serotypes) elicits GFP expression in IHCs and SG neurons; AAV2-GFP additionally transduced OHCs and some inner pillar cells. A single injection of AAV2-BDNF elicits sufficient expression of BDNF in the deafened cat cochlea over ~3 months to promote improved SG neuron and radial nerve fiber survival. Similar neurotrophic effects were observed with AAV5-GDNF in deafened cats, but potentially deleterious ectopic radial nerve fiber sprouting also occurred.

The authors thank K. Bankiewicz and uniQure biopharma B.V. for donating the AAV vectors for these studies. Research supported by NIDCD Grant R01DC013067, the Epstein Fund, and uniQure biopharma B.V.

Inner Ear: Mechanics & Modeling I

PS 162

Sound-Induced Vibrations within the Guinea Pig Cochlear Apex

John S. Oghalai¹; Alberto Recio-Spinoso²

¹Department of Otolaryngology - Head & Neck Surgery, Stanford University; ²Universidad de Castilla-La Mancha

While most of human speech information is contained within frequencies < 4 kHz, only a few mechanical measurements have been made in cochlear regions responsive to such low frequencies. Furthermore, the data that do exist are difficult to interpret given the technical difficulties in performing the experiments and/or the artifacts that result from opening the otic capsule bone to visualize the organ of Corti. Here, we overcame historical technical limitations and non-invasively measured

sound-induced vibrations within the apex of the guinea pig cochlea using volumetric optical coherence tomography vibrometry (VOCTV). We found that vibrations within apical cochlear regions, with neural tuning tuned to frequencies < 2 kHz, demonstrate low-pass filter characteristics. There was evidence of a low-level of broad-band cochlear amplification that did not sharpen frequency selectivity. We compared the vibratory responses we measured to previously-measured single-unit auditory nerve tuning curves in the same frequency range, and found that mechanical responses do not match neural responses. These data suggest that, for low frequency cochlear regions, inner hair cells not only transduce vibrations of the organ of Corti but also alter the frequency response to sharpen frequency tuning.

Supported by NIH-NIDCD DC014450, DC013774, and DC010363.

PS 163

Hair Bundles in the Inner Ear Optimize Their Fluid-dynamic Drag Through Shape and Arrangement

Tobias Reichenbach¹; Amanuel Wolde Kidan²; Nikola Ciganovic¹

¹Imperial College London; ²Freie Universitat Berlin

Background

Hair bundles in the mammalian cochlea come in two distinct shapes: hair bundles of inner hair cells exhibit a linear shape, whereas those of outer hair cells are shaped as a V. The biophysical rationale behind these different morphologies, however, remains unknown. Inner and outer hair cells have different functions in the inner ear: outer hair cells provide mechanical amplification of weak sound stimuli, whereas inner hair cells forward the evoked electrical signal to the brain. Whether, and if so, how these different functions may be supported by the different shapes of the hair bundles is poorly understood.

Methods

We analyzed the fluid-dynamic drag of rows of hair bundles that we considered as V-shaped with different opening angles. We computed their drag using both an analytical approximation based on lubrication theory and computational fluid dynamics simulations. For the latter we employed the open-source CFD-code OpenFOAM.

Results

Our analytical approximation shows that the drag is minimized for a row of bundles in which the opening angle is approximately 100 degrees. This matches the opening angle of hair bundles of outer hair cells. A dense row of planar hair bundles as encountered for inner hair cells,

however, maximizes its resistance to fluid motion. We confirmed these findings through computational fluid-dynamics simulations that also show that the minimization of the drag at an angle of 100 degrees arises from an intriguing interplay of pressure and friction drag. Moreover, our analytical as well as numerical results evidence that these different optimization strategies rely on the regular and close arrangement of hair bundles in rows.

Discussion

Our results show that inner and outer hair optimize their fluid-dynamic drag in different ways. Hair bundles of the inner hair cells maximize their resistance to fluid which aids their stimulation by fluid flow. Hair bundles of the outer hair cells, however, minimize fluid dynamic drag. This can facilitate the efficient flow of fluid around them which may serve to increase stimulation of the inner hair cells. The distinct optimization strategies thus accord with the different functions of the two types of hair cells.

PS 164

Active-Process Enhancement of Reticular Lamina Motion and Auditory Nerve Responses

John J. Guinan¹; Hui Nam²

¹Mass. Eye and Ear Infirmary; Harvard Medical School;

²Eaton-Peabody Lab, Mass. Eye and Ear Infirmary

Objective

Recent cochlear mechanical measurements from two labs show that active processes increase the motion response of the reticular lamina (RL) at frequencies more than an octave below the local best frequency (BF) for BFs above 5 kHz. A possible correlate is that in high (>5 kHz) characteristic frequency (CF) auditory-nerve (AN) fibers, responses to frequencies 1-3 octaves below CF ("tail" frequencies) can be inhibited by stimulation of medial olivocochlear (MOC) efferents. Thus, active processes enhance the sensitivity of tail-frequency RL and AN responses. Perhaps related is that apical low-CF AN fibers have tuning-curve (TC) "side-lobe" response areas at frequencies above and below the TC-tip region and, like high-CF tails, these are MOC inhibited. We enquired whether tail and side-lobe responses are enhanced by the same active mechanisms as CF cochlear amplification.

Methods

If the enhancements of responses to CF tones, tail-frequency tones, and TC-side-lobe tones are all due to prestin motility controlled by outer-hair-cell (OHC) transmembrane voltage, they should depend on OHC stereocilia position in the same way. To test this, we cyclically changed the OHC-stereocilia mechano-electric-transduction (MET) operating point with low-frequency "bias"

tones (BTs) and increased the BT level until one BT phase caused OHC MET saturation that suppressed the gain of OHC active processes. While measuring cat AN-fiber responses, 50 Hz BT level series, 70-120 dB SPL, were run alone and with tones at CF, or a 2.5 kHz tail frequency, or a side-lobe frequency. BT-tone-alone responses were used to exclude BT levels that produced AN responses that might obscure BT suppression. Data were analyzed to show the BT phase that suppressed the tone responses at the lowest sound level.

Results

AN responses to tones at CF, at 2.5 kHz tail frequencies and at side-lobe frequencies were suppressed at the same BT phase in almost all cases.

Conclusion

The data are consistent with cochlear amplification of low-level CF responses, enhancement of tail-frequency AN responses and enhancement of low-CF side-lobe responses all being due to the same OHC-stereocilia MET-dependent active process. In both the cochlear base and in low-frequency apical regions, OHC active processes influence AN responses at frequencies outside of the cochlear-amplified TC-tip region. Although not proven, the data suggest that actively-enhanced, below-BF RL motion leads to enhanced AN excitation. This may be by traditional RL-TM shear and/or by changing the RL-TM gap. More work is needed to understand the relationship between RL motion and IHC-stereocilia drive.

PS 165

Radial and Transverse Vibrations of the Organ of Corti

Jessica Huhnke; Jonathan Becker; Jong-Hoon Nam
University of Rochester, Rochester, NY

The organ of Corti is sandwiched between two matrices reinforced with collagen fibers—the tectorial and basilar membranes. The basilar membrane underlies the mechanical tonotopy of the cochlea—the gradient of mechanical stiffness along the cochlear coil. Compared to the clear role of the basilar membrane, how the tectorial membrane contributes to tuning and amplification is under active investigation. For example, whether the tectorial membrane can be considered a 'second' resonator remains unclear.

Cochleas were harvested from young gerbil (15-21 days old). The middle turn was isolated and bone above and below the organ of Corti for a segment of the turn removed allowing an apical perspective, and then affixed to a micro-chamber. The micro-chamber system has two ports for fluid circulation and two ports for pressure ap-

plication and release (analogous to oval and round windows in the cochlea). It also has a slit on which the tissue is attached. Gold-coated micro-beads were spread on the tectorial and basilar membrane surfaces. As acoustic pressures were delivered, the displacements of the beads were measured along the transverse and radial directions using a laser velocity meter and a dual-phodiode sensor. The measurement data were compared with computer model simulations of the organ of Corti.

At the measurement location (5~9 mm from the basal end), the vibration amplitudes were greater at the tectorial membrane than at the basilar membrane. Within our measurement precision, there was no difference between the best responding frequencies of the tectorial and basilar membranes. Neither could we resolve the differences between the best responding frequencies of the tectorial membrane in the transverse and the radial directions. Computer model analyses showed similar trends. Our observations, albeit preliminary, are in line with the view that the sub-structures of the organ of Corti vibrate coherently when there is no active feedback from the outer hair cells.

[Supported by NIH NIDCD R01 DC014685]

PS 166

Computational Study on Different Vibration Patterns of the Organ of Corti

Wenxiao Zhou; Talat Jabeen; Jong-Hoon Nam
University of Rochester, Rochester, NY

The organ of Corti complex (OCC) is highly organized with structurally significant matrices such as the tectorial and basilar membranes and cells such as the pillar cells, Deiters cells and outer hair cells. Recent progresses in experiments provide more details on OCC mechanics. Those new observations may unveil the operating mechanisms of the OCC. For example, the fine structures in the OCC vibrate out of phase under certain conditions. The consequences of complex vibration patterns are not fully appreciated yet. We present our computational effort on different vibration modes of the OCC.

A recent cochlear model (Liu, Gracewski, Nam, 2015) was modified to incorporate nonlinear mechano-transduction. The assumption of anti-symmetric pressure distribution across the cochlear partition was relaxed. The model solves three physical domains simultaneously—solid, fluid and hair cell electro-mechanics. The cochlear partition was represented by a 3-D finite element model with detailed organ of Corti structures. The fluid domain was discretized with the finite difference scheme. Known physiological properties were incorporated to represent the hair cell mechano-transduction and electro-motility.

Using the computer model, a mechanical and an electrical impulse were simulated. The vibration patterns of the OCC were distinctly different depending on the stimulating methods and on the outer hair cell's mechanical feedback. When there is no outer hair cell feedback, the OCC fine structures vibrate in phase upon a mechanical impulse. With the outer hair cell feedback, initial response is similar to the passive case, but after first couple of oscillatory cycles, the top and bottom surfaces of the OCC vibrate out of phase, similar to the response to an electrical impulse. Although the traveling waves along the top and bottom surfaces of the OCC are differentiated by their phases and amplitudes, we did not observe a difference in vibrating frequencies between the two surfaces. Our model simulations show that the outer hair cell's mechanical feedback modulates the OCC vibration patterns.

[Supported by NIH NIDCD R01 DC014685]

PS 167

An Efficient Fluid-Structure Representation of the Arched Gerbil Basilar Membrane

Hongyi Xia¹; Charles Steele¹; Sunil Puria²

¹*Stanford University*; ²*Massachusetts Eye and Ear, Harvard Medical School*

Background

The gerbil basilar-membrane (BM) differs from other mammalian BMs in that the lower layer of the pectinate zone (PZ) is an arch so that between the two BM layers there is a large gap filled with a gel-like substance. The role of this arch has been unknown but can be elucidated by models. In a typical simple beam model (SBM) the BM upper and lower collagen-fiber layers are represented as a single layer in both the PZ and the arcuate zone (AZ). In our new arch-beam model (ABM), the upper collagen layer is flat while the lower layer forms an arch in the PZ and they combine to form the flat portion of the BM in the AZ. We tested the computational efficiency of three different fluid representations using the SBM. We used the most efficient approach for testing a model with the ABM representation for the gerbil BM.

Methods

In a 3D cochlear box model the BM fiber layers were modeled as a shell imbedded in an upper viscous-fluid chamber. The BM stiffness along the length of the cochlea was a function of BM width, upper and lower fiber layer thickness and volume fraction. The three SBM fluid-viscosity modeling approaches tested were: (1) Thermo-acoustics - full Navier-Stokes, (2) Narrow-acoustics - approximations of Navier-Stokes, and (3) Two-layer Thermo-Pressure (TLTP) - a thin thermo-acoustic lay-

er on top of the BM. In the SBM, the BM was a shell with varying thickness and orthotropic material properties with the AZ and PZ combined. For the ABM the BM arch in the PZ was a parametric curve and the gel was a solid with a low Young's modulus. With tones of various frequencies applied at the stapes we computed the BM velocity versus BM length.

Results

All three SBM models produced cochlear frequency-position maps consistent with Greenwood's cochlear map. The TLTP model was 5 times faster than the other two models. The ABM with the Thermo-Pressure model produced a similar tonotopic mapping and amplitude as did the SBM. In this model AZ flexing dominates the BM response, suggesting that the arch acts as a nearly rigid link.

Conclusions

All four models produce similar traveling waves and cochlear maps. The TLTP model is computationally the fastest. In the ABM, the arch is effectively rigid so its properties have little influence and AZ thickness, width and collagen volume fraction determine BM mechanics.

PS 168

Mechanical Distortion in the Apex of the Mouse Cochlea

James B. Dewey¹; Brian E. Applegate²; John S. Oghalai¹

¹Department of Otolaryngology - Head & Neck Surgery, Stanford University; ²Department of Biomedical Engineering, Texas A&M University

The mechanics of the mammalian cochlea are highly nonlinear, as evidenced by distortions measured directly on the basilar membrane, or in the ear canal as distortion product otoacoustic emissions (DPOAEs). The predominant concept is that nonlinearities in outer hair cell (OHC) stereociliary mechanotransduction introduce distortions in the OHC receptor potential that are then amplified by active forces produced by the OHC soma and/or stereocilia. However, this view is complicated by observations of DPOAE responses to high-level stimuli postmortem, as well as in mice without OHC somatic motility. The nonlinear mechanisms giving rise to distortions are therefore still not precisely understood. To further examine the origins of cochlear distortion, we used volumetric optical coherence tomography vibrometry (VOCTV) to measure harmonic distortion in tone-evoked vibrations from the apical turn of the intact mouse cochlea. To determine how distortion depends on active and passive mechanics, as well as specific structural and functional properties of the organ of Corti, measurements were made in

live and dead wildtype (CBA/CaJ) mice and in several mouse strains with targeted genetic mutations. In live wildtype mice, harmonic distortions were measurable on the basilar membrane, reticular lamina, and tectorial membrane down to low stimulus levels for near-characteristic frequency tones, with higher level tones eliciting harmonics over a broader range of stimulus frequencies. Postmortem, harmonic distortions disappeared for low stimulus levels, consistent with a dependence of these distortions on OHC transduction and active processes. However, at higher stimulus levels, distortions persisted after death. At these stimulus levels, harmonic distortions in live and dead mice were largest near the frequency of the peak postmortem response, and were similar in magnitude near this frequency. Harmonic distortions were similar in mice with targeted mutations that altered organ of Corti biomechanics, and the frequency response resembled those of dead, wildtype mice. Data from mutant mice suggest that the generation of distortion at high stimulus levels does not require OHC somatic motility or normal mechanotransduction. Such distortions could arise via nonlinearities in the passive mechanics of the stereocilia or the sensory epithelium as a whole. Nonlinearities in the passive mechanics of the organ of Corti may also contribute to the generation of distortion at lower stimulus levels in cochleae where the active, OHC-mediated amplification process is intact.

Supported by NIH-NIDCD DC014450, DC013774, and DC010363.

PS 169

On the Dynamics of Mechanical Suppression in the Mammalian Cochlea

Nigel Cooper; Marcel van der Heijden
Erasmus MC

Dynamic aspects of mechanical suppression were studied by recording basilar membrane (BM) vibrations evoked by multi-tone stimuli in the 11-19 kHz region of healthy gerbil cochleae. A lightly amplitude modulated tone served as a "probe" stimulus, evoking low-level (~1 nm) vibrations near the characteristic frequency (CF) of the BM site under study. Two other tones formed a beating "suppressor" complex that was centered well below the site's CF (typically at CF/2.5 or CF/3.5). The frequencies of the suppressor's two components were varied to produce a range of suppressor beat rates, and the components' amplitudes were carefully balanced to produce near perfect periodic cancellations, visible as sharp notches in the envelope of the BM's response to the suppressor. Suppression of the probe-evoked BM responses was observed to vary dynamically with the instantaneous level (i.e. the envelope) of the suppressor complex: maximum suppression occurred just after the

peaks of the suppressor's envelope, and minimal suppression occurred just after the notches. Dynamic suppression was strong at low beat rates (e.g. 20-160 Hz) but weakened at high rates (e.g. > 1 kHz). This weakening occurred because the probe responses failed to recover fully from previous periods of suppression within the more limited time frame of the faster beat cycles. We suggest that this occurs because the instantaneous gain at each site on the basilar membrane is low-pass filtered by a gain control system (see ref. 1). Suppression of the probe responses was also delayed with respect to the envelope of the suppressor complex: the delay was dependent on the beat rate, typically falling from 300-400 microseconds at the lowest beat rates (10-40 Hz) to ~100-200 microseconds above 100 Hz. These delays exceed those associated with simply changing the gain of the CF probe responses (which typically amounted to ~50 microseconds; see ref. 1). We suggest that the excess delay associated with suppression reflects a combination of two phenomena: (i) suppression is produced at a more basal location on the basilar membrane than our point of observation, and (ii) near CF (probe) energy takes longer to travel to the site of observation than below CF (suppressor) energy does. [1] Cooper, N. P., & van der Heijden, M. (2016). *Advances in Experimental Medicine and Biology*, 894, 267-273

PS 170

Modeling Suppression, Gain, and Age-Related Effects Using an Auditory-Nerve Model

Erica L. Hegland; Elizabeth A. Strickland; Michael G. Heinz
Purdue University

Background

With increasing age, speech perception in noise becomes more difficult, even for those with auditory thresholds within the normal range. This may be due in part to decreased cochlear nonlinearity, which could occur due to reductions in the endocochlear potential. Two-tone suppression is understood to be a sensitive measure of cochlear nonlinearity. Previous psychoacoustic and physiological studies have supported the idea that suppression may decrease with age. In addition, previous physiological studies have suggested that suppression may decrease with elicitation of the medial olivocochlear reflex (MOCR), an efferent reflex that decreases cochlear gain in a time- and level-dependent manner. In the present study, the interaction between suppression and the MOCR was investigated using a well-established computational model of the peripheral auditory system. The effect of age was modeled by systematically varying the model variables controlling gain for both the inner hair cells (CIHC) and outer hair cells (COHC) and by varying the total strength of the MOCR. Suppression

amounts were compared between the various conditions for suppressors both above and below the signal frequency. Suppression in the model was compared with psychoacoustic results from younger and older adults.

Methods

Suppression and gain reduction were investigated using a model of the auditory periphery [Zilany, Bruce, & Carney, 2014, *JASA* 135:283-286]. Results from this model were compared to a version of the same model that includes a gain-reducing feedback loop modeling MOCR effects. Auditory nerve spikes were generated by the model and analyzed. Thresholds for high (HSR), medium (MSR), and low (LSR) spontaneous rate fibers were determined by finding the level at which the rate reached 0.1 in normalized rate-level functions. Suppression for a 2-kHz, 10-ms signal at 20 dB SL was measured following the methods used in a related psychoacoustic experiment. Suppression was measured in a forward-masking paradigm with a 1.2-kHz suppressor (low-side suppression) and a 2.4-kHz suppressor (high-side suppression).

Results/Conclusions

The spike output of the model was analyzed using rate-level functions and detectability measures (d'). The patterns and interpretations of the results were compared between the various suppression conditions. The psychoacoustic results suggested that suppression tended to decrease with age. Suppression decreased in conditions long enough to elicit the MOCR, but only for the younger participants. In the model results, suppression decreased when total gain decreased, whether from elicitation of the MOCR or manipulation of the hair cell gain parameters.

[Research supported by NIH(NIDCD) F31-DC014359 and R01-DC0008327]

PS 171

Traveling and Fast Waves: Propagation of Distortion Products in the Cochlear Fluid Using a Computational Model

Thomas Bowling¹; Charlise E. Lemons¹; Julien Meaud²

¹*G.W.W. School of Mechanical Engineering, Georgia Institute of Technology*; ²*G.W.W. School of Mechanical Engineering and Petit Institute for Bioengineering and Bioscience, Georgia Institute of Technology*

In response to stimulation by two primary tones (f_1 and f_2), the cochlea generates distortion products (DPs) that propagate through the middle ear. Two hypotheses have been proposed for the propagation of DPs from their generation site to the middle ear: as a fast compressional

wave through the cochlear fluid or as a slow wave along the basilar membrane. In this work, a physiologically based computational model of the gerbil ear based on a nonlinear two-duct three-dimensional cochlear model is used to examine these hypotheses. Simulations of the intracochlear fluid pressure at the DP frequency are first used to provide information about how DPs propagate. Results show that while the fluid pressure is highly localized and three dimensional close to the best places at the primary and DP frequencies, the pressure is much more uniform at more basal locations. These results are generally consistent with previously reported in vivo measurements of the fluid pressure in response to a two tone stimulus. Furthermore, the spatial variations of the fluid pressure are to a large extent qualitatively similar to the variations that are observed in response to a pure tone. This suggests that the cochlea operates similarly when driven by an acoustic stimulus in the ear canal and when driven by intracochlear sources and that energy primarily propagates as a slow wave both in the case of a pure tone stimulus and of DP propagation. Computation of the energy flux at the DP frequency is used to further analyze how DPs propagate.

PS 172

Sensitivity of the Basilar Membrane and Reticular Lamina Motion to Organ of Corti Cytoarchitecture Parameters

Hamid Motallebzadeh; Sunil Puria
Massachusetts Eye and Ear, Harvard Medical School

Background

The functions of many cochlear anatomical features are poorly understood. The “Y”-shaped structures between basilar membrane (BM) and reticular lamina (RL) formed by the basally-tilted, force-generating outer hair cells (OHC), the apically-tilted phalangeal processes (PhP) and vertical Deiter-cell (DC) body, has been hypothesized to be an essential building block for cochlear amplification (Yoon et al., 2011). In this study we altered organ of Corti (OoC) characteristics systematically to study the sensitivity of cochlear amplification to morphology. We wondered what happens to BM and RL motions and cochlear amplification if the locations of the OHCs and PhPs were swapped or if PhP length was changed by altering the number (N) of OHCs that one PhP spans. We also did a sensitivity analysis of the dependence of cochlear amplification on the material properties of these elements.

Methods

A finite-element model of the mouse cochlea was developed, taking into account 3-D fluid-structure interactions and the spatial arrangement of Y-shaped elements of single OHC row. Active amplification was modeled by

introducing OHC axial force proportional to the pressure difference across the BM. The model was validated by comparing its results with previously reported BM and RL motion responses, for both passive and active cases, at the cochlear apex (Lee et al., 2015) and base (Ren et al., 2016).

Results

The normal-morphology model produced a 40 dB BM-response gain (re stapes velocity) for low-level sounds (~10 dB SPL) in the apical region. In the basal region, the gain was 32 dB for ~20 dB SPL tones. In the active model, RL motion was always higher than BM motion (up to 15 dB at BF and 20 dB below BF). The model with OHCs and PhPs swapped in position not only generated significantly lower gains (especially for low frequencies), but also resulted in broader response peaks. With no PhPs, the OHC-DC structures are anchored only at their ends and buckling occurred with active OHC contractions resulting in unstable BM responses, lower gains and broader response peaks. Changing PhP lengths from N=1 to N=4 increased BM gain and shifted the best frequency (BF) toward the base. Above N=4, the gain decreased substantially and the BF shifted further toward the base.

Conclusions

These results demonstrate the high efficiency of the natural OoC cytoarchitecture and imply that the particular form of the Y-shaped OHC-Deiter-cell combination is important for cochlear amplification. (Supported by NIH grant R01 DC 07910)

PS 173

Prediction of the Audiogram for the Humpback Whale (*Megaptera novaeangliae*)

Aleks Zosuls¹; Darlene Ketten²; Andrew Tubelli³

¹*Boston University*; ²*Otology and Laryngology, Harvard Medical School, Boston, MA, United States*; ³*Department of Biomedical Engineering, Boston University, Boston, Massachusetts, United States*

As one of the larger marine species, Humpback Whales are among the marine species that are potentially impacted by low frequency anthropogenic sounds in the oceans. Knowledge about their typical hearing range is important for risk assessments from any human sound sources deployed in their critical habitats and for determining optimal sound sources for auditory brainstem response measurements that are planned for testing hearing in live stranded whales.

MicroCT, Ultra high resolution CT, dissection, and histology were employed to calculate the inner ear frequency

maps based on anatomical features of the inner ears of this species (n=5), including basilar membrane thicknesses, widths, lengths, cochlear turns, radii of curvature, cochlear turn radii, and axial heights. The predicted average total functional frequency range for the humpback cochlea is 18 Hz to 24 kHz.

In tandem with the anatomical measurements, direct measurements of frequency response and stiffness measurements of the middle ear components were coupled with the anatomical measures of the ossicular chain and associated soft tissues in the middle ear for input to a finite element model (FEM) to obtain the middle ear transfer function. The anatomical measures for the FEM inputs were obtained from 3D reconstructions of ultra-high resolution CT scans. The frequency response was measured at the stapes footplate in response to stimulation of the glove finger (the dense, hypertrophied, everted tympanic membrane of baleen whales) and separately of the tympanic bulla to test membrane vs bone conduction inputs.

The FEM models predicted a best frequency range (-40 dB of peak) of 20 Hz to 3 kHz for stimulation of the glove finger and 200 Hz to 9 kHz for stimulation of the tympanic bone. The direct measurement of frequency response from stimulation of the glove finger (n=1) yielded a frequency range of 10 Hz to 8 kHz.

PS 174

Somatic Electromotility is Sufficient to Explain the Nonlinearity Seen in the Chan-Hudspeth Experiment

Amir Nankali; Aritra Sasmal; Karl Grosh
University of Michigan

Somatic Electromotility is Sufficient to Explain the Nonlinearity Seen in the Chan-Hudspeth Experiment

The input sounds to the mammalian ear produce waves that travel inside the cochlea from base to apex. The traveling waves stimulate microstructure of the organ of Corti (OoC) sited in the center of the cochlea. The OoC displacements are boosted by a distinct nonlinear amplification process that enables sound processing in a broad frequency and intensity ranges. An important question of the biophysics of the cochlea is the active mechanism underlying the cochlear nonlinear amplifier. Two active processes are hypothesized as the main source of the cochlear nonlinear amplification: the outer hair cell (OHC) electromotility and hair bundle (HB) motility. Using the active excised cochlear segment experiment devised by Chan & Hudspeth [1,2] as a model problem, we develop a computational model for studying contribution of the active processes on the cochlear nonlinear response.

We have shown that there exists traveling wave for this small segment of the cochlea; however, its effect on the cochlear mechanics in this preparation is not significant. This finding enables the local dynamics of the OoC in an active, but isolated, cochlear segment to be represented by a lower-order model. An analytical nonlinear model of the experiment is developed by reducing the macroscopic fluid dynamics of the configuration to a loading added mass on the OoC.

It is shown that the OHC somatic electromotility is sufficient to predict the nonlinearities observed in the Chan-Hudspeth experiments. Replacement of the K⁺ rich endolymph by channel-impermeant NMDG in the experiment was shown to reduce the microphonic response by 57% and increase the power-law dependency of the compressive nonlinearity from 0.74 to 0.85 (1 being linear). When we simulate the same conditions (allowing only Ca²⁺ ions to pass through the mechano-electric transducer (MET) channel) the model predicts a 56% reduction in cochlear microphonic and power-law changes from 0.75 to 0.86. This shows that the OHC somatic electromotility could be the sole source of the changes in the Chan-Hudspeth experiments under NDMG replacement of K⁺.

This work was supported by NIH grants DC-004084 and T32DC-00011.

[1] Chan, D. K., and A. J. Hudspeth, 2005. "Ca²⁺ current driven nonlinear amplification by the mammalian cochlea in vitro". *Nature Neuroscience* 149–155.

[2] Chan, D. K., and A. J. Hudspeth, 2005. "Mechanical Responses of the Organ of Corti to Acoustic and Electrical Stimulation In Vitro". *Biophysical Journal* 89:4382–4395.

PS 175

A Computational Model to Quantify Hair Cell and Neural Contributions to the Ongoing Part of ECochG Signals Using Tones

Tatyana E. Fontenot; Christopher K. Giardina; Andrew K. Pappa; William C. Scott; Kevin D. Brown; Harold C. Pillsbury; Douglas C. Fitzpatrick
University of North Carolina Department of Otolaryngology-Head and Neck Surgery

Background

Electrocochleography (ECochG), has emerged as a potentially clinically valuable technique for predicting post-operative outcomes in cochlear implant (CI) recipients, among other uses. Current analysis is limited by an inability to quantify hair cell and neural contributions to low frequencies where they are mixed in the ongoing part of the signal.

Methods

Using analytical and statistical equations, we developed a computational model to separate the cochlear microphonic (CM) and auditory nerve neurophonic (ANN) which represent the hair cell and neural components of the ongoing response, respectively. The CM was modeled using a sinusoid with parameters of rectification and saturation. The ANN was modeled as a convolution of a unit potential and cycle histogram, including a parameter for spread of excitation (SOE) using a generalized extreme value curve, with SOE defining the width of the curve. The model was tested with responses from the round window to 500 Hz tones (30-90 dB SPL) from gerbils before and after application of the neurotoxin kainic acid (KA), and in human CI subjects, also from the round window to 500 Hz tones (107 dB SPL) at the time of surgery. The ECoHG waveforms were the input to the model, which performed adaptive fitting of the above parameters to yield phases and root-mean-square (RMS) of amplitudes for the CM and ANN.

Results

In gerbils and humans the modeled waveforms and their FFTs matched the original responses with R^2 typically exceeding 0.95.

In gerbils, the RMS magnitudes of the CM and ANN increased with intensity with a steeper increase for the CM, resulting in a ANN/CM ratio that's twice as large at low compared to high intensities. After application of KA, the CM was unchanged but the ANN was drastically reduced, although not typically eliminated, indicating incomplete removal of neural activity. In humans, the ANN as a proportion of the CM was highly variable, ranging from nearly none to actually being larger than the CM. Cases with cochlear nerve deficiency showed extremely small levels of ANN.

Conclusions

The computational model provides a means for quantitative estimates of the amount of hair cell and neural activity present in the ongoing response to tones. Based on its ability to capture changes in the relative strength of neural contribution due to KA in gerbils, it can be inferred that relatively small ANNs measured in CI recipients may indicate a lesion of the neural components of the peripheral auditory system.

PS 176

Super Resolution Model of Sub-Synaptic Cistern and Efferent Synaptic Currents in Outer Hair Cells

Bhaskar G. Chennuri¹; Joseph L. Greenstein¹; Paul A. Fuchs²; Raimond Winslow¹

¹*Institute for Computational Medicine, Department of Biomedical Engineering, Johns Hopkins University;*

²*Johns Hopkins University School of Medicine*

Overview

Outer hair cells (OHCs) are one of the two types of sensory hair cells in cochlea of inner ear. OHCs form a c-synapse, characterized by the presence of a sub-synaptic cistern (SScistern) apposing postsynaptic membrane (14 nm separation) with efferent fibers. The role of SScistern in synaptic transmission is poorly understood. SScistern encapsulates a nano-domain called sub-synaptic cleft (SScleft) of high impedance for Ca^{2+} ions which enter through highly Ca^{2+} -permeable 92103 nicotinic acetylcholine receptor (nAChR) ion channels on OHC membrane. Elevated $[Ca^{2+}]_{SScleft}$ (order of ~ 10 s of mM) increases open probability of small conductance Ca^{2+} -activated K^+ (SK2) channels co-localized with nAChRs. SK2 openings result in a hyperpolarizing K^+ current which underlies inhibitory postsynaptic current (IPSC) in OHCs. Two phenotypes of IPSCs occur in OHCs: (1) A short duration (200 ms) IPSC1 is thought to be mediated by nAChR and SK2 channels, and (2) a long duration (2 s) IPSC2 is thought to be shaped by postsynaptic nAChRs, SK2s, and L-type Ca^{2+} channels, and possibly by Ca^{2+} release through RyR1 channels on the SScistern. Our hypotheses, SScistern plays (1) a very limited role in IPSC1, and (2) major role in IPSC2.

Methods

Similar restricted nano-domains are found in cardiac myocytes (dyads) and are essential for Ca^{2+} -induced Ca^{2+} release (CICR). We adopted the cardiac Super Resolution Spark (SRS) model previously developed in our lab to model Ca^{2+} signaling in the OHC SScistern. We modeled SScistern as a 1 μ m x 1 μ m x 14 nm domain with 3 nAChRs and 39 SK2s on the OHC membrane. Each nAChR is modeled as a 2 state channel which closes exponentially with decay = 8 ms. SK2s are modeled as 6 state channels with 4 closed and 2 open states. The nAChRs are distributed uniformly with 13 SK2s/nAChR in the domain.

Results

We established an interaction distance of 100 nm ($(I_{SK2}(100 \text{ nm})/I_{SK2}(0 \text{ nm})) = \exp(-1)$), between a nAChR and a SK2 channel. Within this 100 nm radius SK2 binding sites are fully saturated by Ca^{2+} ions from

nearby nAChRs. An IPSC1 can be reproduced solely by nAChR-mediated Ca²⁺ influx.

Conclusions

Experimental evidence suggests that nAChR and SK2 channels are co-localized, and in chicken embryonic OHCs nAChRs may be physically tethered to SK2s. Our model produced similar results with an interaction distance of 100 nm. Therefore, the cistern might play little to no role in shaping IPSC1 in the tonotopic organization of cochlea.

PS 177

Optical Coherence Tomography (OCT) Measurements of In Vivo Organ of Corti Vibration Within the Gerbil Cochlear Apex

Wei Dong¹; John S. Oghalai²; Anping Xia³; Sunil Puria⁴

¹VA Loma Linda Healthcare System; ²Department of Otolaryngology - Head & Neck Surgery, Stanford University; ³Stanford University; ⁴Massachusetts Eye and Ear, Harvard Medical School

Background

Most of the reported literature on organ of Corti vibration patterns has come from high frequency basal regions. There is mounting evidence that cochlear mechanics in the base is different than in the low frequency apical regions. However, this region of the cochlea has been difficult to record from because of the surrounding bony otic capsule. In order to study how low-frequency sounds (< 4 kHz) are transduced, we measured sound-induced vibrations of the organ of Corti within apical turns 2 and 3 of the gerbil cochlea using volumetric optical coherence tomography vibrometry (VOCTV), imaging non-invasively through the otic capsule bone in vivo.

Methods

The gerbil was deeply anesthetized. The left pinna was removed and the bulla was opened to expose the cochlea. A calibrated sound system was coupled to the ear canal and controlled by custom software. Pure tone stimuli were swept in frequency from 0.1-4.5 kHz and the intensity ranged from 10-80 dB SPL. Cochlear conditions before and after the vibratory measurements were verified by click-evoked auditory brainstem responses. The experiments were approved by the Institutional Animal Care and Use Committee of Stanford University.

Results

Vibratory recordings with the best signal-to-noise ratio came from the region of the outer hair cells. Responses from nine animals provided several consistent findings. In turn 3, the most apical turn, there was little frequen-

cy selectivity and the displacement-versus-frequency curves had low-pass filter characteristics with a corner frequency of ~0.8 kHz. The vibratory magnitude demonstrated compression at all frequencies as the stimulus intensity was increased, with a gain of 20-40 dB. In turn 2, band-pass filter responses were noted with characteristic frequencies (CFs) ~2.5 kHz. The gain at the CF was ~60 dB. In addition, there was 30-40 dB of gain in the responses at frequencies far below CF. In both turns, the nonlinear gains were physiologically vulnerable and disappeared post mortem.

Conclusions

In contrast to previously published data measured at basal cochlear locations, these data indicate that there is substantial compressive amplification far below the BF region in the gerbil cochlear apex.

Supported by NIH-NIDCD DC011506 (Dong), DC07910 (Puria), DC014450, DC013774, and DC010363 (Oghalai)

Middle Ear -- Basic Science

PS 178

Effects of Tympanic-membrane Perforation on Middle-ear Transmission in the Gerbil

Wei Dong; Glenna Stomackin
VA Loma Linda Healthcare System

Perforations of the tympanic-membrane (TM) alter its structural and mechanical properties resulting in a deterioration of sound transmission, which presents itself as a conductive hearing loss (CHL). For a reasonably-sized perforation, the resulting CHL is mainly due to the loss of the pressure difference across the TM between the outer ear-canal space and the middle-ear cavity. However, the influence of TM perforations on ossicular motion and the output of the middle ear, i.e., pressure at the stapes in scala vestibuli (SV), has not been systematically investigated.

This study in gerbils systematically explored middle-ear transmission under several TM-perforation conditions. The care and use of animals were approved by the Institutional Animal Care and Use Committee (IACUC) of our VA facility. Single or two equilevel (L1=L2) primary tones at f1 and f2, with a fixed f2/f1 ratio, were generated and responses acquired using Tucker-Davis Technologies (TDT) System III, MATLAB and the TDT visual-design studio. Pressure responses at the TM near the umbo (PTM) and in the SV near the stapes (PSV), along with the velocity of the umbo (Vumbo), were simultaneously measured using a Sokolich ultrasound probe-tube microphone, a micro-pressure sensor, and a laser Doppler

vibrometer following mechanically-induced TM perforations ranging from miniscule to its complete removal leaving only the ossicular chain intact. Middle-ear transmission under these conditions was illustrated by the variation of PTM, Vumbo, and PSV.

Our results suggested that increasing the size of TM perforations led to a reduction in middle-ear pressure gain (i.e., the pressure difference between PSV and PTM), which appeared to be mainly due to the change in the effective/initial drive to the umbo. With perforation sizes up to a quarter of the TM, middle-ear transmission along the ossicular chain varied little, however, further enlarged perforations appeared to dramatically reduce sound transmission through the ossicular chain. Two-tone evoked distortion product otoacoustic emissions (DPOAEs) were measurable with TM perforations greater than a quarter of the TM, but varied according to the resulting changes in the middle-ear pressure gain, which reduced more significantly over low- and high-frequency regions.

Since TM perforations in humans are usually caused by either trauma or infection, with infection being the most common cause, our results contribute towards providing insight to understanding middle-ear transmission under pathological conditions, as well as promoting the application of DPOAEs in the evaluation and diagnosis of deficits in middle-ear transmission.

PS 179

Measurement of Surface Motion of Human Tympanic Membrane after Blast Exposure

Shangyuan Jiang; Xuelin Wang; Don U. Nakmali; Rong Gan
University of Oklahoma

Introduction

The tympanic membrane (TM) damage caused by blast overpressure waves is one of the injuries faced by military personnel in the battlefield. Although the variation of the mechanical properties of TM induced by blast waves has been measured in our laboratory, the impact of these changes on the membrane surface motion is not well demonstrated. In this paper, we report the recent study on measurement of the human TM surface motion before and after blast exposure by using the scanning laser Doppler vibrometry (SLDV). A finite element (FE) model of the human TM was also built for investigating the blast-induced TM surface motion change in relation to the structural damage in the membrane.

Methods

Three fresh human temporal bones were used in this study. The TM surface motion was recorded by the

SLDV (Polytec) under the chirp stimuli of 80 dB SPL in the frequency range of 0.5-10 kHz before and after blast exposure. The blast test was conducted inside the high-intensity sound chamber with a compressed nitrogen-driven blast apparatus. The measured TM displacements over entire surface after blast exposure were compared with that of normal tissues at the tested frequencies. A FE model of human TM with multiple fibrous layers was created and the blast-induced tissue damage was simulated by removing the fibers or adjusting the mechanical properties of the fibers or membrane matrix. The model-derived TM surface motion was compared with the experimental results to explain the manner of how the membrane microstructural change affects its surface motion.

Results

The maximum value of the displacement on the TM surface increased after the blast exposure at the frequencies of 3-4 kHz (Fig. 1). The vibration patterns showed some difference before and after the blast exposure at the frequencies between 1 kHz and 8 kHz. The FE modeling analysis suggested that the blast overpressure may alter the TM surface motion by partially breaking the fibers or redistribution of the membrane structure.

Conclusions

Blast overpressure imposes the TM surface motion change in membrane displacement at frequencies of 3-4 kHz as measured by SLDV. The damaged TM fibrous structure caused by blast waves may be responsible to the measurement results as predicted by the FE model of the human TM.

Acknowledgements: This work was supported by DOD W81XWH-14-1-0228 and NIH R01DC011585.

PS 180

Shift of Middle Ear Muscle Reflex and Auditory Brainstem Response Thresholds after High Intensity Sound Exposure in Chinchillas

Zachary Yokell; Don U. Nakmali; Rong Gan
University of Oklahoma

Background

High intensity sounds such as those encountered in industry can cause substantial shifts in hearing level over time. The stapedius activates in the middle ear muscle reflex (MEMR) to damp the motion of the stapes in response to high intensity sound, but the threshold of activation of the MEMR can shift upward with hearing damage. Auditory brainstem response (ABR) measurement is a common method for estimating hearing levels in animals. Chinchillas are popular models for hearing studies due to the similarity between their hearing range

and that of humans. While certain aspects of noise-induced damage have been studied in chinchillas, there are no published data regarding electromyography (EMG) analysis of the MEMR before and after noise exposure. This study reports a comparison of the shifts in MEMR activation threshold and ABR in chinchillas when exposed to damaging levels of noise.

Methods

Healthy adult chinchillas were used in this study. The stapedius muscle was surgically exposed in one ear, and a bipolar electrode was inserted into it while another electrode was inserted into the animal's leg as a ground. Data was acquired using TDT System 3 and BioSig software. The MEMR threshold was determined through EMG and both EMG and ABR were measured before noise exposure. Each animal was then placed in a sound isolation chamber and subjected to 130 dB noise for either one or two hours, after which stapedius EMG and ABR were tested again.

Results

Results were obtained using both EMG and ABR over a range of frequencies as shown in Fig. 1. On average, EMG thresholds were elevated 53 dB with noise for both one hour and two hour exposures. The average ABR threshold shift was 64 dB with one hour of exposure and 75 dB with two hours of exposure.

Conclusions

ABR and EMG thresholds were significantly elevated after both one and two hour exposures. The difference in threshold shifts between MEMR and ABR suggests that different parts of the ear are damaged asymmetrically by exposure to high intensity sound.

(Supported by DOD W81XWH-14-1-0228 and NIH R01DC011585)

PS 181

A Comparison of X-ray Microtomography Images of the Middle Ear of Three Mammalian Species

Eileen Y. Brister¹; Claus-Peter Richter²; Xiaodong Tan³; Carmen Soriano⁴; Robert H. Withnell¹

¹Indiana University; ²Department of Otolaryngology-Head and Neck Surgery, Feinberg School of Medicine, Northwestern University & Resonance Medical, LLC, Chicago; ³Department of Otolaryngology-Head and Neck Surgery, Feinberg School of Medicine, Northwestern University; ⁴Argonne National Laboratory

Background

Non-invasive studies of the structure and function of the middle ear typically involve magnetic resonance im-

aging (MRI) or using dedicated commercial x-ray systems. Such studies contribute valuable data regarding the mechanics of the middle ear. One limitation of these systems is insufficient contrast of soft tissues. Imaging using synchrotron x-rays provides visualization of both soft and hard tissues, allowing for non-invasive imaging of the complete system.

Method

Tissue samples were scanned at beamline 2-BM, at the Advanced Photon Source (APS), Argonne National Laboratory (Argonne, IL, USA). Middle ears in three mammalian species: mouse, guinea pig, and cat were imaged using coherent synchrotron x-rays with a photon energy of 22 kiloelectron volts (keV). These three species have contrasting middle ears, the micro-type ear (mouse), fused malleus-incus (guinea pig), and freely mobile type (cat).

Results

This study was confined to static imaging of the structures of the middle ear. Of particular interest was the supporting middle ear ligaments, the relationship between the size of the malleus versus the incus, and the structure of the stapes. X-ray microtomography images of the middle ear of the three species were compared and contrasted.

Conclusion

Differences in the structure of the middle ear of the three species studied support the varied upper limits of hearing, although the fused malleus-incus complex in the guinea pig negates a synovial joint-enabled pivoting motion. The weight of the ossicles appears to be supported by the ligaments that attach to the malleus and incus. Reconstructed images of x-ray microtomography provide valuable data for modeling middle ear function. Future studies will examine the motion of the ossicles.

[This research used resources of the Advanced Photon Source, a U.S. Department of Energy (DOE) Office of Science User Facility operated for the DOE Office of Science by Argonne National Laboratory under Contract No. DE-AC02-06CH11357.]

PS 182

In Vivo Experimental Study of Gerbil Eardrum Vibrations Under Static Pressures

Orhun Kose¹; W. Robert J. Funnell²; Sam J. Daniel³

¹BioMedical Engineering, McGill University, Canada;

²Departments of BioMedical Engineering and Otolaryngology, Head & Neck Surgery; ³Depts. Pediatric Surgery and Otolaryngology - H&NS, McGill University, Canada

Measurements of eardrum vibrations provide essential data for finite-element models of the middle ear. Mongolian gerbils are utilized in middle-ear research for their easily accessible eardrum, the availability of prior research data, and their low cost of maintenance. We previously reported preliminary measurements of the effects of static pressurization on the vibrations of post mortem gerbil eardrums. Here we present the results of similar experiments done in vivo. A single-point laser Doppler vibrometer is used to measure the vibration of the eardrum using glass-coated beads. Vibration measurements are normalized with respect to the sound pressure level near the eardrum, and presented over the range of 0.2 to 11 kHz. Vibration measurements were done at several points on the manubrium, the pars tensa and the pars flaccida under static pressures. The vibration response is flat at low frequencies, rises up to a resonance peak, then decreases and becomes complex for frequencies higher than the "break-up" frequency. The eardrum vibration magnitudes decrease as the static pressure is increased and the break-up frequency shifts to higher frequencies. The presence of hysteresis and the repeatability of the measurements between cycles are explored. Study of the effects of static pressurization on the gerbil eardrum will provide data that can be used to validate numerical gerbil middle-ear models. Those models will help guide the development of human models, which in turn will provide insight into clinical tympanometry.

PS 183

Finite-Element Modelling Of Tympanic-Membrane Vibrations Under Pressurization

Sahar Choukir¹; W. Robert J. Funnell²

¹Dept. BioMedical Engineering, McGill University,

Canada; ²Departments of BioMedical Engineering and Otolaryngology, Head & Neck Surgery

Early detection of hearing loss accompanied by appropriate early intervention is important in order to avoid problems associated with delayed language development, and its impact on daily communication, educational achievement, psychosocial development and later employment opportunities. High false-positive rates are associated with current newborn hearing screening methods, and are attributed to transient conditions in the external and middle ear in the first 48 hours post partum. Tympanometry (acoustical input admittance measurement in the presence of a range of quasi-static pressures) is a promising tool for evaluating the status of the middle ear in newborns. Tympanometry involves large deformations and non-linear responses; viscoelastic (time-dependent) effects; and complex dynamic responses. The tympanic membrane contributes to the

overall response more than other middle-ear components do. Previous finite-element models of the tympanic membrane, however, have been either dynamic non-linear or static linear. The goal of this study is to combine these two features in a dynamic non-linear viscoelastic model based on experimental data reported in the literature. The constitutive equation of this model is a convolution integral, composed of a first-order Ogden hyperelastic model and an exponential time-dependent Prony series with three time constants. Material properties are taken from previous measurements and estimates. The tympanic membrane is assumed to be homogeneous and nearly incompressible. The loading conditions, combining high quasi-static pressures with low-amplitude sound pressures, correspond to those involved in tympanometry, in which a large sweeping ear-canal pressure (e.g., -300 to +200 daPa) is applied in less than 10 s. We report admittance measurements as well as stored-energy and lost-energy results in the frequency domain. The model was verified by comparing results from different finite-element solvers. The simulation results can be validated by comparison with measured data from experimental animals and from human newborns and adults. Our numerical models of the dynamic non-linear viscoelastic tympanic membrane will provide quantitative insight into the mechanics of the middle ear and establish a groundwork for the clinical application and interpretation of admittance measurements in newborns where the response to tympanometry is not well understood.

PS 184

Finite-element Modelling of the Human Eardrum Based on X-ray Micro Computed Tomography and Doppler Optical Coherence Tomography in the Same Ear

Xuan Wang¹; Dan MacDougall²; Josh Farrell²; W. Robert J. Funnell³; Robert Adamson⁴; Manohar Bance⁵

¹Department of BioMedical Engineering, McGill University; ²School of Biomedical Engineering, Dalhousie

University; ³Departments of BioMedical Engineering

and Otolaryngology, Head & Neck Surgery; ⁴School of Biomedical Engineering, Electrical and Computer

Engineering Department, Dalhousie University; ⁵De-

partment of Surgery, School of Biomedical Engineering, Dalhousie University

The eardrum plays a critical role in transferring sound into vibrations in the inner ear. The vibration patterns of the eardrum, particularly at high frequencies, have been broadly investigated but are still not well understood. Computational modelling of the eardrum and middle ear offers a pathway toward better understanding of the me-

chanical function of these structures, but the tuning and validation of such models require accurate anatomical and mechanical experimental data. Such data usually come from populations of ears and little is known about how differences in individual middle-ear geometry and material properties affect eardrum function.

Recent advances in Doppler optical coherence tomography (OCT) of the middle ear have demonstrated its ability to simultaneously capture anatomical image data and Doppler-mode vibration data of the ear in response to sound. In the present study, we obtain brightness-mode (B-mode) OCT images of a human temporal bone for which simultaneous Doppler-mode OCT images were collected. For the same ear we also collect 3D X-ray micro computed tomography (microCT) images. The microCT data provide a higher spatial uniformity of resolution than OCT and are free from shadowing and multiple scattering artifacts which are present in the OCT B-mode data. The microCT images are manually segmented to create a finite-element model for the eardrum. The Doppler OCT images, masked by the B-mode OCT images to reduce noise, are also segmented and the resulting 3D model is transformed to Cartesian coordinates and aligned with the microCT-based model. The simulated vibration patterns are compared with the measured Doppler-mode OCT velocity data to validate the finite-element model. This method of combining anatomical and vibration data from the same ear can be used to generate a set of finite-element models for a range of human ears, in order to advance our clinical understanding of the effects of natural variations in eardrum shapes, of eardrum pathologies, and of various surgical reconstruction techniques.

PS 185

Finite Element Modelling of Cartilage Tympanoplasty and Ossicular Chain Replacement by an Artificial Prosthesis

Thanos Bibas¹; Nikos Ellinas²; Panagiotis Katrakas²; Nikolaos Tachos³; Antonis Sakellarios³; Dimitris Fotiadis³; Dimitris Koutsouris²

¹National and Kapodistrian University of Athens;

²National Technical University of Athens; ³University of Ioannina

Introduction

In cases of poor hearing where the ossicular chain is not intact, it is considered necessary to replace it (or a part of it) with an artificial prosthesis. In the current project we have created a three dimensional Finite Element Model (FEM) to study the full replacement of the ossicular chain by a Total Ossicular Replacement Prosthesis (TORP) and simulate its behavior in different cases of tympanoplasty.

Methods

Our FE model is designed as a simplified version of our previously created detailed model that was constructed using microCT imaging data, while keeping the size of its components, the properties of the materials and the angle between the tympanic membrane and the stapes footplate (Spiridon I et al, 2015). The middle ear cavity was added to the model as well as a TORP in the place of the ossicular chain. The material used for the prosthesis was CP Titanium Medical Grade 2 (ASTM F67). We studied the effect of combining the use of a TORP in different cartilage tympanoplasty techniques and the effect on stapes footplate displacement. Four clinical scenarios were simulated: a) full TM replacement with cartilage of 1mm thickness, b) full TM replacement with cartilage of 0.5mm thickness, c) full TM replacement with strips of cartilage (palisade technique) and d) use of only a small piece of cartilage on top of the prosthesis head. (Figure 1). The input chosen was acoustic pressure of 90 SPL magnitude perpendicular to the tympanic membrane or the cartilage and the output was the frequency response of the displacement of the stapes footplate. In order to fully simulate the function of the middle ear, the cochlear fluid was represented as a Kelvin-Voigt element at the external surface of the stapes footplate with a damping coefficient of $5.4 \cdot 10^{-2} \text{ N}\cdot\text{s/m}$. Responses were obtained in the frequency range of 100-8100 Hz. The output frequency response is shown at Figure 2. Results: The best results were obtained when the cartilage was only covering the head of the prosthesis (almost equal to normal TM). The palisade techniques showed better results than the total TM replacement with a 0.5 mm cartilage. It was also confirmed that using a 0.5mm cartilage gives superior results than the 1mm one.

PS 186

Multiphysics Finite Element Model of a Balanced Armature Transducer used in a Contact Hearing Device

Morteza Khaleghi¹; Sunil Puria²

¹Earlens Corporation; ²Massachusetts Eye and Ear, Harvard Medical School

Background

The Earlens Contact Hearing Device (CHD) is a custom-made hearing aid that provides wide-bandwidth (0.1-10 kHz) amplification of sounds. An accurate mathematical model of the CHD is essential for a better understanding of design parameters and optimizations. The goal of this work is to report on development and validation of a Finite Element (FE) model of a Balanced Armature Transducer (BAT) coupled to a model of a human middle ear that simulates the drive mechanics.

Methods

A multiphysics FE model of the balanced-armature-based CHD system is developed. Electrical, magnetic, acoustic, and solid mechanics fields are coupled to simulate the system from electrical input to the stapes output of the middle ear. Results from the isolated BAT FE model are verified with measurements of the armature's velocity and electrical impedance, over a frequency range of 0.1 to 10 kHz. In addition, the FE results are compared with a 1D lumped-element two-port model of the isolated BAT (Kim and Allen, 2013). The BAT model is then assembled with two bias springs, chassis, and umbo and sulcus platforms to realize a complete model of the CHD. This is then coupled to a previously validated FE model of a human middle ear (O'Connor et al., 2016).

Results

Consistent with the experimental measurements, the isolated BAT's FE model exhibits the first natural frequency of the armature's velocity around 3,800 Hz. This frequency is determined by both the primary stiffness of the armature and from a negative stiffness introduced by magnetization of the BAT (i.e., the DC magnetic field from the two permanent magnets located inside the BAT). The FE results of the armature's velocity and the electrical impedance are in good agreement with the corresponding experimental measurements. The stapes velocity predicted by the model resulting from a constant-current-driven CHD correlates well with experimental measurements made in human temporal bone measurements (Puria et al., 2016).

Summary

A multiphysics FE model consistent with both electrical input and stapes output of the CHD system was developed and validated. This paves the path towards the numerical investigation and improvement of the CHD design parameters including the number of turns and wire gauge diameter of the BAT coil, geometrical (the thickness and its geometry) and material (density and elastic modulus) properties of the armature, and the magnetic properties of the armature and casing that houses the BAT.

PS 187

The Vibration Conduction Effectiveness of Active Middle-ear Implant: A Comparative Research Between LP, Bell and Clip FMT-coupler

Tao Chen¹; Liujie Ren¹; Dongming Yin¹; Jia Li¹; Lin Yang²; Peidong Dai¹; Tianyu Zhang¹

¹EENT Hospital of Fudan University; ²EENT Hospital of Fudan University

Background

The active middle ear implant Vibrant Soundbridge provides a variety of coupling modalities of the floating mass transducer (FMT) to various structures of the ossicular chain. The aim of this study was to (1) determine the efficacy of different stapes FMT coupling modalities, such as stapes Clip FMT-coupler and Bell FMT-coupler (2) identify best coupling method for aural atresia case which is feasible to install FMT on incus and stapes.

Methods

An extended antrotomy and a posterior tympanotomy were performed in 8 fresh human temporal bones. As a control for normal middle-ear function, the tympanic membrane was stimulated acoustically (94 dB SPL) and the vibration of the stapes footplate was measured by laser Doppler vibrometry (LDV). FMT-induced (35 mV rms per spectral line) vibration responses of the stapes footplate were measured for the long process incus coupler (MED-EL, LP FMT-coupler). Then the incus was removed, we applied the FMT onto the Clip and Bell coupler (MED-EL Clip and Bell FMT-coupler) and then the device was installed onto the stapes head consecutively. The same voltage was used in all FMT-induced LDV measurements.

Results

In general, our preliminary data indicates improvement on sound transmission of Clip and Bell coupler compared to the LP coupler. For both the Clip and Bell couplers, the average velocity amplitude of the stapes footplate was about 15 dB higher than the LP coupler between 1-6 kHz; only a drop of ~10dB occurred at around 0.5 kHz. Quantitatively, there is no significant difference between the Bell and Clip coupler. However, if the top of FMT contacted with the handle of malleus, the velocity amplitude in temporal-bone preparations showed decreased amplitudes at 2-5 kHz. After removing the malleus, LDV measurements were repeated with FMT stimulation and the velocity amplitude regained to the mean level of other Clip coupling.

Conclusion

In conclusion, attachment of the FMT to the stapes head with the Clip and Bell coupler leads to generally good mechanical and functional coupling in temporal-bone experiments. The conforming Clip and Bell coupler provides an alternative and effective way to stimulate the stapes. And the top of FMT connect with the handle of malleus will affect the vibration conduction efficiency.

Acknowledgments

We like to thank Hamidreza Mojallal and Samuel Blanc for their generous support. This work was funded by National Natural Science Foundation of China (NSFC, No.81570934) and Shanghai Committee of Sci-

ence and Technology, China (No. 13DZ1940902 and 13DZ1940903).

PS 188

Validating a Method to Characterize the Efficiency of Implantable Middle Ear Hearing Devices in Cadaver Ears by Intracochlear Pressure

Martin Grossöhmichen¹; Susan Busch¹; Bernd Waldmann²; Thomas Lenarz³; Hannes Maier¹

¹Hannover Medical School; ²Cochlear Ltd.; ³Department of Otolaryngology, Hannover Medical School and DFG Cluster of Excellence Hearing4all

Background

The standard method to characterize the output level of an implantable middle ear hearing device (IMEHD) in preclinical cadaver studies is measurement of stapes footplate (SFP) vibration by laser Doppler vibrometry (LDV) according to ASTM F2504-05. This method is limited to IMEHD stimulations of the intact and mobile ossicles. A potential alternative method to characterize IMEHD efficiency is the measurement of the intracochlear pressure difference (ICPD). The goal of this study was to validate this assumption by comparing IMEHD actuator output levels calculated from ICPD measured in cadaver to outputs levels determined by SFP vibration and to clinical data.

Methods

Experiments were performed in human cadaveric temporal bones (TBs) compliant to the modified acceptance criteria (Rosowski et al., 2007) of ASTM F2504-05. First, the eardrum was stimulated acoustically. Second, the incus body was stimulated mechanically by an IMEHD actuator (Cochlear™ MET® Middle Ear Implant System.), coupled at a controlled static preload force. In both stimulation modes, SFP vibrations were measured using LDV (Polytec) and intracochlear pressures in scala tympani (ST) and scala vestibuli (SV) were measured using FISO FOP-M260 pressure sensors (Grossöhmichen et al., 2016). The ICPD was calculated as a vector difference between ST and SV pressure. The equivalent sound pressure levels (eq SPL) generated by the actuator stimulation were calculated both based on SFP vibration and based on ICPD. Clinical measurements were performed on 24 recipients of a MET system (Otolitics or Cochlear). Bone conduction thresholds and “direct thresholds” were measured with the fitting software using the sound processor as a signal generator, and were converted to actuator driving voltage.

Results

The mean MET output level measured in cadaveric TBs by ICPD was 100 to 120 eq dB SPL_FF @1V_RMS and

flat across frequencies. The output levels calculated from SFP vibration (ASTM) were the same. The output levels in cadaver TBs were similar to clinical results within 10-15 dB, showing a similar frequency dependency.

Conclusion

In incus stimulation IMEHD actuator output levels calculated from ICPD were similar to output levels based on SFP vibration (ASTM) and to clinical data. Based on our results, ICPD can be used as a measure to predict clinical performance of IMEHDs in cadaver studies.

PS 189

Mechanical Instabilities of the Incudostapedial Joint

Majid Soleimani¹; W. Robert J. Funnell²; Willem F. Decraemer³

¹Department of BioMedical Engineering, McGill University, QC, Canada; ²Departments of BioMedical Engineering and Otolaryngology, Head & Neck Surgery; ³Department of Biomedical Physics, University of Antwerp, Belgium

Although the joints between the ossicles significantly affect sound transmission through the middle ear, the mechanical behaviour of these joints has remained poorly understood. This has resulted in either oversimplified or inaccurate assumptions in the models of these joints. We have previously presented finite-element (FE) models of the incudostapedial joint (ISJ) that were based on histological serial sections and X-ray microCT, and realistic estimates for material-property parameters with or without the presence of the synovial fluid (SF) in the joint, and we made preliminary comparisons with experimental tension and compression measurements. We later presented an analytical model of the ISJ with a simplified geometry using the theory of large deformations of elastic membranes to model the joint capsule. We proposed that the ISJ mechanical behaviour may be influenced by the mechanical instabilities of the joint capsule that were observed when increasing the SF volume while fixing the cartilage surfaces. In this work, we extend our analytical model by maintaining a constant SF volume while moving the cartilage surfaces. We show that the capsule becomes unstable in certain parts of a tension-compression test, which can result in a jump in the corresponding force-displacement curve. Our FE models confirm the existence of this unstable region. This suggests that the strong non-linearity observed in experimental tension-compression tests of the ISJ may be due at least in part to a jump driven by capsule mechanical instabilities, while the apparent asymmetry may be due in part to an uncertainty in determining the zero-load condition.

Predictions and Measurements of Reverse Middle-ear Transmission in Chinchilla

Michael E. Ravicz¹; Peter N. Bowers²; John J. Rowski³

¹*Eaton-Peabody Laboratory, Mass. Eye & Ear Infirmary; Dept. of Otolaryngology and Laryngology, Harvard Medical School;* ²*Speech and Hearing Bioscience and Technology program, Harvard and M.I.T.; Eaton-Peabody Laboratories, Massachusetts Eye and Ear;* ³*Eaton-Peabody Laboratory, Mass. Eye & Ear Infirmary; Department of Otolaryngology and Laryngology, Harvard Medical School; Speech and Hearing Bioscience and Technology program, Harvard and M.I.T.*

Introduction

The properties of the middle ear when driven from the cochlea (“in reverse”) are important for evaluating otoacoustic emissions and also provide insight into middle-ear function with normal (“forward”) sound transmission. We and others have provided some descriptions of normal forward middle-ear function in chinchilla, a species commonly used for auditory research, especially for noise hazard and damage studies. From these measurements, two-port transmission-matrix models of chinchilla middle-ear function have been formulated (see e.g., ARO 2012 #126). The transmission-matrix model is particularly useful for predicting middle-ear function under conditions different from those in which data to construct the model were measured. Though the data that go into these models appear similar, the models have substantially different predictions of the middle-ear load with forward stimulation (the cochlear input admittance or impedance) as well as middle-ear behavior when driven in reverse (e.g., the load the middle ear presents to the cochlea, and the effect of ear-canal modifications on that load). We can now test the models with measurements of ME function in reverse.

Methods

Umbo and stapes velocity and sound pressures in the ear canal and the cochlear vestibule were measured in chinchillas while the ear was stimulated with ear-canal sound or a mechanical actuator applied to the round window.

Results and Discussion

We compare two measures of middle-ear function in the forward and reverse directions: The “lever ratio” between umbo and stapes motion, and the admittances at the border between the middle and inner ear: the cochlear input admittance Y_c , the load seen by the ME with normal sound transmission, and the reverse middle-ear input admittance Y_{mer} , the load the ME exerts on the

cochlea for reverse transmission such as otoacoustic emissions. Variations in the “lever ratio” provide insight into flexibility and lost motion in the middle ear. From these admittances we compute a Power Utilization Ratio that describes power absorption and reflection at the boundary between the middle and inner ear.

Supported by NIDCD R01 DC00194

PS 191

Third Window Effects on Stapes and Round Window Membrane Velocities at Infrasound

Stefan Raufer¹; Salwa F Masud²; Hideko H. Nakajima³

¹*The Harvard Speech and Hearing Bioscience and Technology Program;* ²*Harvard Medical School;* ³*Dept. of Otolaryngology, Harvard Medical School & Massachusetts Eye & Ear, Boston, MA USA*

Background

In this work we present stapes and round window (RW) membrane velocities below the common measured low-frequency limit of 100 Hz, down to 1 Hz; a territory that has not been explored and that offers interesting insights into hearing mechanics. Beyond the characterization of low frequency transfer functions in normal ears, we made perturbations (third-window lesions) in the otic capsule to study effects on inner ear impedances at low frequencies.

Methods

Five fresh human temporal bones were prepared to study stapes and round window membrane velocities at frequencies between 1–2000 Hz. An extended facial recess approach was used to access the middle ear cavity; we exposed the epitympanic area to access the superior semicircular canal. A modified headphone speaker delivered sound; ear canal pressures were measured with a Bruel and Kjaer infrasound microphone; Laser-Doppler vibrometry was used to measure velocities.

Results

Whereas middle ear transfer functions are highly variable across ears at frequencies above 500 Hz, we observe little variability in the response characteristics of low-frequency stapes and round-window membrane velocities. Below about 300 Hz, they decrease with a slope of 20 dB/decade. In this frequency range, stapes and RW move in opposite directions (½-cycle difference). With a third-window lesion (in this case through the opening of the superior semicircular canal), the ½-cycle relationship breaks down, mainly because of the decrease in RW velocities below 300 Hz. Interestingly, even normal “intact” ears show deviation from the ½-cycle relationship at frequencies below 20-50 Hz.

Experimental results are presented along with a model to discuss impedance variations of the inner ear at low frequencies and to explain the mechanisms responsible for the observed results.

Conclusions

Middle ear transfer functions below 300 Hz vary little among ears. Third window leaks in the inner ear result in considerable alterations of RW velocities, while stapes movements remain relatively stable for frequencies below 300 Hz. Studying RW velocities is a simple mean to study the effects of a dehiscence in the otic capsule. An extension of the frequency range towards lower frequencies (1-20 Hz) is desired to capture the variability of individual data in dehiscent bones, as well as identifying small leaks in normal bones.

PS 192

Intracochlear Sound Pressure Measurements in Human and Sheep Temporal Bones

Alexander Huber¹; Flurin Pfiffner²; Lukas Prochazka³; Patrizia Sulser²; Dominik Péus²; Adrian Dalbert²; Francesca Paris⁴; Joris Walraevens⁴; Jae Hoon Sim²; Ivo Dobrev²; Christof Roosli²

¹Department of Otorhinolaryngology – Head and Neck Surgery, University Hospital Zurich, Zurich, Switzerland; ²Department of ENT, Head and Neck Surgery, University Hospital Zurich, Switzerland; ³Institute of Fluid dynamics, Swiss Federal Institute of Technology (ETHZ), 8092 Zurich, Switzerland and Streamwise GmbH, 8005 Zürich, Switzerland; ⁴Cochlear Technology Centre Belgium, Mechelen, Belgium

Background

Intracochlear sound pressure (ICSP) measurements are constrained by the small dimensions of the human inner ear and the requirements imposed by the liquid medium. The aim of this project is, (1) to design and fabricate a robust intracochlear acoustic receiver (ICAR) for repeated use with a simple data acquisition system that provides the required high sensitivity, (2) to compare ICSP measurements in human and sheep temporal bones in order to determine the usefulness of sheep as an experimental model for implantable hearing devices.

Methods

The presented ICAR consists of a MEMS condenser microphone (MEMS CMIC) and a sensing head. The sensing head includes a passive protective diaphragm (PD) sealing the MEMS CMIC against the liquid medium enabling insertion into the inner ear. The electro-mechanical function of the components of the ICAR were simulated by a lumped element model (LEM) and compared

to the experimentally validated performance of fabricated ICARs. The new sensors were applied for ICSP measurements in the scala tympani and scala vestibuli, each normalized to the measured acoustic sound pressure level in the ear canal.

Results

Good agreement was achieved between the LEM and the measurements with different sizes of the PD. The ICSP measurements in a human cadaver temporal bone yielded data in agreement with the literature. The ICSP measurements in the scala vestibuli of sheep temporal bones showed a maximum gain of 24 dB, relative to the ear canal pressure.

Conclusion

A novel ICAR concept, based on MEMS condenser microphone, for evaluation of the biomechanical hearing process by quantification of ICSP is presented. Our results confirm that the presented new ICAR sensor is a promising technology for measuring ICSP in human and sheep temporal bones in the audible frequency range. A comparison between experimental results in sheep and reference data in human showed similar cochlear function. We conclude that sheep is an appropriate large animal model for the research and development of implantable hearing devices in humans. In addition, the sensor concept has potential as an acoustic receiver in totally implantable cochlear implants.

PS 193

The Skull Vibration Properties Under Unilateral Bone Conduction Stimulation: An Experimental Research Based on Scanning LDV Measurements

Liujie Ren¹; Jia Li¹; Tao Chen¹; Dongming Yin¹; Lin Yang²; Peidong Dai¹; Tianyu Zhang¹

¹EENT Hospital of Fudan University; ²EENT Hospital of Fudan University

Objective

In order to get an overview of the sound transmitting properties during BC, This study measures the vibration of the surface of skull bone during BC stimulation. Based on the measurements, the transcranial attenuation and skull vibration pattern under different frequencies are investigated.

Methods

Two fresh and intact cadaver heads were engaged in the measurements. The heads were stably placed on a soft basement. A B71 BC vibrator was anchored to the temporal bone on the mastoid, powered by the built-in signal generator of PSV-500 scanning laser Doppler vibrometer (LDV). Two types of signals were given: (1)

sweep signal (3V,5V,7V) ranging from 0.1k to 10k Hz; (2) Single frequency signals between 0.25k and 6k Hz. Vibrations of four areas of each head were measured by the scanning LDV, including the ipsilateral side, the contralateral side, top of the head and the forehead. The transfer functions of the average velocity between the four areas are calculated to estimate the transcranial attenuation. Then the measured displacement and phase of the areas are mapped to an entire 3D skull model and the vibration patterns of the skull at various frequencies are discussed.

Results and Discussions

The average velocity increases linearly with the input voltage (3V,5V,7V) of the vibrator. The velocity of the four areas peaks at about 500 Hz, mainly owing to the strong response of B71. Also a velocity peak at 2.5-3kHz can be observed, which may be caused by the resonance of the cadaver head. The transfer functions of the different areas were calculated to estimate the transcranial attenuation. The attenuation was quite low below 2kHz, while it became significantly higher between 2kHz to 5kHz. This means low frequency vibrations are easier to affect the contralateral side of the skull, while high frequency vibrations tends to affect a limited region near the vibrator. According to the vibration pattern results, rigid body motion dominates at low frequencies. Vibration patterns becomes complicated above 2kHz, where out-of-plane wave appears and propagates at the skull surface, with the speed of around 400-500 m/s. These experimental results are in good agreement with previous findings.

Acknowledgements

This study is funded by National Natural Science Foundation of China (NSFC, No.81570934) and Shanghai Committee of Science and Technology, China (No. 13DZ1940902 and 13DZ1940903). We also thank Polytec China Ltd. and engineers Chao Fang and Jian Yin for their technical support.

PS 194

Quantifying the Effects of Inner- and External-ear Bone-conduction Mechanisms in Chinchilla

Peter N. Bowers¹; Michael E. Ravicz²; John J. Rosowski³

¹Speech and Hearing Bioscience and Technology program, Harvard and M.I.T.; Eaton-Peabody Laboratories, Massachusetts Eye and Ear; ²Eaton-Peabody Laboratory, Mass. Eye & Ear Infirmary; Dept. of Otolaryngology, Harvard Medical School;

³Eaton-Peabody Laboratory, Mass. Eye & Ear Infirmary; Department of Otolaryngology, Harvard Medical School; Speech and Hearing Bioscience and Technology program, Harvard and M.I.T.

Introduction

Bone conduction (BC), the transmission of sound to the inner ear by way of skull vibration, is important clinically, as it is used to diagnose and treat chronic and congenital middle-ear disease. The relative contributions of the mechanisms which bone conduction comprises are not fully understood. Here we address two BC mechanisms: The contributions of inner ear BC mechanisms to BC hearing are examined with intracochlear sound pressure measurements made in the normal and modified auditory system. The external-ear component of BC hearing is estimated using existing impedance and pressure measurements in the ear canal.

Methods

To explore inner-ear mechanisms, sound pressures within the vestibule and scala tympani were measured simultaneously in chinchillas a) after the incudostapedial joint (ISJ) was interrupted and b) when the oval and round windows were occluded. ISJ interruption isolates the inner-ear BC source from the external- and middle-ear sources, while occlusion of both cochlear windows reduces the effects of fluid inertia during BC stimulation. The differential “fast-wave” pressure across the basilar membrane at the basal end of the cochlea was computed from the pressure measurements. The velocities of the petrous bone and stapes footplate were also measured to quantify the degree of occlusion.

External-ear mechanisms were explored with existing bone conduction data in chinchilla—middle-ear input impedance (Ravicz and Rosowski, 2012) and ear canal sound pressure at the TM in the occluded and unoccluded ear (Chhan, 2015)—and an analytically-derived reverse input impedance of the external-ear canal. We estimate a volume velocity source representative of the combined external-ear mechanisms of BC hearing.

Results and Conclusions

Intracochlear sound pressure measurements suggest that reduction of the cochlea fluid-inertia contributions to BC by occlusion of both cochlear windows does not result in decreased bone-conduction stimulus to the inner ear. Instead, the results suggest that the effects of cochlear compression and/or sound pressure transmission via “third window” pathways increase due to an increase in impedance at the windows. Estimates of the contribution of the ear-canal BC source are in agreement with experimental data (Chhan et al., 2016), showing that when the ear is occluded, the ear-canal source is a significant contributor to BC hearing at mid-frequencies (1–3 kHz). These data are important components of a model for bone-conduction hearing in chinchilla.

Psychoacoustics: Animal Psychoacoustics

PS 195

Local Tuning in a Tropical Amphibian Along an Altitudinal Gradient

Peter M. Narins¹; Sebastiaan W.F. Meenderink²; Patricia M. Quiñones¹

¹University of California Los Angeles; ²Dept. of Physics and Astronomy

Introduction

Both the size of males of Puerto Rican Coqui frogs (*Eleutherodactylus coqui*) and the spectral and temporal parameters of their advertisement calls vary systematically with height above sea level from 30-1000 m in eastern Puerto Rico. At low altitudes, small males produce rapid, high-pitched calls, whereas at high altitudes, larger males emit slower, lower-pitched calls. Moreover, the spectral content of the calls has been shown to be closely correlated with the inner ear sensitivity along the same altitudinal gradient. Here we investigated the vocal response behavior of frogs to playbacks of a wide range of synthetic call note frequencies to determine the range of altitudes over which a male would engage in acoustic territorial defense.

Methods

A microphone and loudspeaker fixed to an extendible boom mounted on a tripod were placed within 1 m of an isolated calling male Coqui in his natural habitat. Fifty low-level "Co-Qui" calls with parameters corresponding to the altitude of the male under test were broadcast to an individual male Coqui and the number of his one-note, synchronized "Co"-note calls was recorded and used as a response metric. The stimulus level was then increased in discrete steps of 3 dB until a threshold response level was reached, defined as a call level that evoked 20 one-note calls in response to 50 stimuli. The playback level was adjusted to be 3 dB above threshold for each male tested. Next, a series of 50 synthetic calls corresponding to those from different elevations separated by at least 100 m was played back to the male and the number of one-note responses again noted.

Results & Discussion

In general, males inhabiting a given altitude produce the most vigorous vocal responses to playbacks of conspecific calls containing similar spectral peaks to their own. Playbacks of call notes with higher or lower frequencies (corresponding to habitats lower or higher above sea level) to a male Coqui result in a reduced vocal response from this male. This is particularly evident for males inhabiting the extremes of the altitudinal range. For the mid-elevation males, despite the relatively small sample size, males also show a tendency to produce the most

robust responses to calls from their own altitude. These results support the hypothesis that Coqui frogs are behaviorally and neurophysiologically "tuned" to communicate best with frogs from their own local population.

Funding

Work supported by UCLA Academic Senate Grant 3501 to PMN.

PS 196

Pure Tone Audiometry and Audiograms in Rats

Naoki Wake¹; Kotaro Ishizu¹; Tomoyo I. Shiramatsu²; Ryohei Kanzaki²; Hirokazu Takahashi²

¹Department of Mechano-Informatics Graduate School of Information Science and Technology, The University of Tokyo; ²Research Center for Advanced Science and Technology, The University of Tokyo

Background

Pure tone audiometry and audiograms have been commonly used in a diagnosis of human hearing, but not in animal studies. Auditory brainstem response (ABR) has been routinely used as an electrophysiological index of normal hearing in animals, yet such an objective audiometry is not able to measure the actual hearing threshold due to its low S/N ratio. Here, we have developed an operant behavioral test for rodents to perform pure tone audiometry and obtain audiograms.

Methods

Head-fixed rats were trained to pull a lever spout according to tone presentations. A lightweight ABS head attachment was attached to a rat skull with tiny anchor screws under isoflurane anesthesia. After several days for recovery from the surgery, the animals were deprived of drinking water in the home cage, and a drop of water was given as a reward in daily behavioral tasks. On the first-day, the head of animal was fixed to the training apparatus (O'hara Co. Ltd., TaskForcer) in a dark sound-proof room. Animals were then trained to stay quietly and pull a spout-level with their forelimb to obtain a drop of water (10 μ l). On the second day or later, lever-pulling was rewarded only during cue tones with a duration of 1 s, intensity of 60 dB SPL, and varied frequencies (4, 8, 16, and 32 kHz). Cues were presented after the lever was released for 1 to 3 seconds. A light was provided as a negative feedback when the lever was not released except for a drinking period of 2 seconds after each water supply. Once this initial task was completed, tones with varied intensity levels of 60, 50, 40, 30 dB, and 0 dB (silent) were presented and the lever-pulling behavior was quantified. After the behavioral training, ABR was also measured at the same head position.

Results & Conclusion

The latencies of the pulling response was quantified with respect to the cue onset. When the tone intensity was high, the response latency exhibited a consistent peak around 300 ms. As the intensity decreased, the peak disappeared. This behavioral index was consistent with ABR, but the behavioral thresholds were slightly lower than ABR thresholds. Thus, our results indicate that pure tone audiometry in rodents is feasible.

PS 197

Poorer Hearing-in-noise Despite Full Recovery of Thresholds in Rats; Functional Evidence of “Hidden Hearing Loss”?

Edward Lobarinas¹; Christopher Spankovich²; Samantha Morril³; Colleen Le Prell¹

¹The University of Texas at Dallas, School of Behavioral and Brain Sciences; ²University of Mississippi Medical Center, Department of Otolaryngology and Communicative Sciences; ³University of Florida, Department of Speech, Language, and Hearing Sciences

Noise exposures that produce robust temporary threshold shift (TTS) can reduce auditory brainstem response (ABR) wave-I amplitude. This has been labeled “hidden hearing loss” as any functional deficits are “hidden” behind the normal, recovered, thresholds. The functional deficits associated with this loss are unknown, but have been speculated to include compromised hearing-in-noise performance as well as tinnitus and hyperacusis. In the present experiments we assessed hearing in noise at various signal to noise ratios (SNR) in rats before and after noise exposure. Following 109 dB SPL octave band noise (8-16 kHz, 2h) exposure, 5 out of 6 animals showed reduced ABR wave-I amplitudes at 16 and 24 kHz, despite complete recovery of thresholds at 2 weeks post exposure. In these animals, we found frequency specific hearing in noise deficits at 20 dB SNR for 16 kHz; 20 dB SNR was empirically determined to be the most difficult condition in which rats reliably detected the signal in noise prior to noise exposure. These results suggest a correlation between reduced wave-I amplitude and poorer hearing in noise at lower SNR levels after noise exposures that produced TTS>30 dB at 24 hours post exposure. However, this type of acoustic injury (TTS exceeding 30 dB 24 hours post noise) would not typically be observed in humans after recreational noise exposure or as a consequence of typical occupational noise. Thus, insight into damage risk criteria and potential functional deficits are urgently needed in rodent models and in humans.

PS 198

Comparison of Psychometric and Neurometric Amplitude-Modulation Detection Thresholds in Normal-Hearing Chinchillas

Amanda C. Maulden; Michael K. Walls; Mark Sayles; Michael G. Heinz
Purdue University

Background

Slow fluctuations in amplitude are important for speech perception in quiet and noisy backgrounds. The effects of sensorineural hearing loss on modulation coding have been hypothesized to have implications for listening in real-world environments, both in cases of permanent threshold shift due to hair-cell dysfunction and in cases of temporary threshold shift where permanent, but “hidden,” cochlear synaptopathy occurs. Animal studies correlating neural with behavioral modulation-detection thresholds have suggested a close correspondence between the two metrics in birds, but not in mammals. In addition, avian thresholds appear to match more closely with human thresholds than data from other mammals. Here, we examine the correspondence between neural and behavioral thresholds in chinchillas.

Methods

Behavioral amplitude-modulation (AM) detection thresholds were determined for 10 chinchillas using the method of constant stimuli. Animals were trained to discriminate a sinusoidal AM (SAM) tone (4-kHz carrier) from a pure tone. Stimuli were embedded in a notched-noise masker to prevent off-frequency listening. Successfully trained animals were tested at a range of AM depths (3-dB steps between -30 and 0-dB), for a range of modulation frequencies. In a separate group of animals, responses were recorded under barbiturate anesthesia from a population of single units in the auditory nerve and ventral cochlear nucleus. Spike times were collected in response to SAM tones (characteristic-frequency-tone carrier, range of modulation frequencies and depths), and analyzed in terms of synchronization to the modulation frequency. Within a signal-detection-theoretic framework, both psychometric and neurometric AM-detection thresholds were computed as a function of modulation frequency.

Results

Behavioral thresholds were consistent across individual animals, typically in the range -25 to -15 dB. The most-sensitive single-unit neurometric temporal AM-detection thresholds were similar to whole-animal behavioral performance at a range of modulation frequencies.

Conclusions

The low behavioral AM-detection thresholds found here

contrast with previous work on other mammalian species (e.g., rabbits, gerbils). Our data are more in line with AM-detection thresholds found in avian species (e.g., budgerigars) and in humans. The establishment of a mammalian model with corresponding neural and behavioral modulation thresholds will allow us to examine the effects of cochlear synaptopathy on behavioral and neural assays of temporal processing following “hidden hearing loss.”

Funding

Supported by NIH (NIDCD) R01-DC009838 (MGH) and an Action on Hearing Loss Fulbright scholarship (MS).

PS 199

Discrimination of Schroeder-phase Stimuli in the Mongolian Gerbil by Temporal Fine Structure and Envelope Cues

Henning Oetjen; Georg M. Klump

Cluster of Excellence Hearing4all, Animal Physiology and Behaviour Group, Department for Neuroscience, School of Medicine and Health Sciences, University of Oldenburg, D-26111 Oldenburg, Germany

Background

Schroeder-phase stimuli provide both temporal fine structure (TFS) and envelope cues, and a behavioral discrimination experiment can reveal the role of these cues in perception. Discrimination of Schroeder-phase stimuli has been studied in humans and birds (e.g., Leek et al., 2001; Drennan et al., 2008). However, there are no behavioral studies of mammals that can serve as a model for human processing of such stimuli. Here we investigate the behavioral sensitivity of gerbils discriminating Schroeder-Phase stimuli in two experiments, one providing both the envelope and TFS cues and one providing mainly TFS cues.

Methods

Young (< 12 month) Mongolian gerbils were trained in an operant repeated background Go/No-Go paradigm with food rewards. Hit rate and false alarm rate were measured to estimate the discriminability. Schroeder-phase stimuli are harmonic tone complexes with a phase relation of $\phi_n = (c \cdot \pi n(n+1))/N$ between harmonics (n = harmonic number, N total number of harmonics, c is a scalar value being related to the duty cycle). Fundamental frequencies of 50, 100, 200, 400Hz were used and the overall level was 60 dB SPL. Stimulus duration was 0.4 s. In experiment A target stimuli with c ranging from -1 to +1 (step size 0.25) had to be discriminated from background stimuli with c -values of -1, 0 or 1, respectively. To solve this task the gerbils could either use TFS or the envelope cues. In experiment B only Schroeder-phase

stimuli with positive and negative c -values had to be discriminated that only provided TFS cues. Both complexes with positive and negative c -values served as the background.

Results and Conclusions

Current data of 3 animals showed a highly significant decrement of the hit rate with increasing fundamental frequency in both experiments (mixed model ANOVA). In experiment A the hit rate for all three backgrounds was significantly related to the difference in c -values of target and background indicating that the duty cycle of the envelope plays a role for the discrimination. The comparison of opposite c -values in experiment B revealed a significant effect of the absolute value of c and the sign of c of the background with higher hit rates being observed with negative sign. Significant interactions between the fundamental frequency, the absolute value of c and the sign of the background could be observed. How the representation of the acoustic cues in the cochlea and the auditory pathway affects the discriminability is subject to further studies.

PS 200

Discrimination of Ultrasonic Jump Calls and their Corresponding Distortion Products by Mice

Lisa M. Strand¹; Anastasiya Kobrina¹; Elena J. Mahrt²; Christine V. Portfors²; Micheal L. Dent³

¹University at Buffalo, SUNY; ²Washington State

University Vancouver; ³University at Buffalo, the State University of New York

Mice produce ultrasonic vocalizations (USVs) that are presumed to be their primary vocal communication signals. This communication method is incongruent with the spatial representation of the mouse's auditory system, however. There is an underrepresentation of neurons in the inferior colliculus (IC), in particular, responsive to the ultrasonic frequencies in USVs. USVs that contain frequency jumps may create distortion products (DPs) in the cochlea. These DPs are much lower in frequency than the calls themselves and are hypothesized to be important for vocalization encoding in the IC. We used a go/no-go task to establish the ability of the CBA/CaJ mouse to discriminate the difference between a jump call and its own emulated distortion product. The mouse is asked to discriminate a distortion product target from its jump call background. We then rely on the mouse's hit rate of the distortion product target to see if they are able to discriminate between the sounds. The task is also done in reverse with a distortion product as the background and its corresponding jump call as a target. The results of this experiment demonstrate that mice are able to discriminate the distortion prod-

uct background from a jump call target. However, they are unable to reliably discriminate the jump call background from a distortion product target. These results provide further evidence that mice may use distortion products to encode high frequency jump calls. This is a functional mechanism that can explain how neurons in low frequency tonotopic regions of the IC can encode high frequency vocalizations. Combining the behavioral data from our awake, behaving mice with physiological results paints a more complete picture of the processing of the acoustic signals used for communication by mice. This work was supported by NIH DC-012302 to MLD.

PS 201

Discrimination of Natural from Synthetic Ultrasonic Vocalizations by Laboratory Mice

Anastasiya Kobrina¹; Laurel A. Screven²; Elena J. Mahrt³; Christine V. Portfors³; Micheal L. Dent²

¹University at Buffalo, SUNY; ²University at Buffalo, the State University of New York; ³Washington State University Vancouver

Mice produce spectrotemporally complex ultrasonic vocalizations (USVs) which are thought to be important for social interactions, such as maternal behavior, mate attraction, and courtship. Previous research has established that mice are capable of detecting and discriminating natural, synthetic, and altered USVs using physiological and behavioral methodologies. The current research examined whether mice are capable of discriminating between natural USVs and their synthetic renditions. Discrimination performance was tested in six adult mice using operant conditioning procedures with positive reinforcement. Mice were trained to nose poke to one hole during a repeating natural or synthetic USV, which would begin a trial. Subjects were required to poke to a second hole when they discriminated a change in the repeating background. The stimuli that the mice discriminated between were natural and synthetic versions of the same USVs, as well as other USVs. Mice were able to discriminate between some natural USVs and their synthetic renditions but not others. Overall, discrimination performance across all of the natural and synthetic USVs was correlated with spectrotemporal similarity, where calls that were dissimilar were more easily discriminated than calls that were similar. Duration, bandwidth, and peak frequency all affected discrimination performance as well. Finally, male and female mice used different spectrotemporal signal features for USV discrimination. These results add to our understanding of the ways USVs may be used for acoustic communication in mice. This work was supported by NIDCD grant R01-DC012302 to MLD.

PS 202

Inferring Sound Feature-dimension Interactions from Sound Categorization in the Behaving Mouse

Livia de Hoz¹; Chi Chen²

¹Max Planck Institute of Experimental Medizin; ²Max Planck Institute of Experimental Medizin and International Max Planck Research School for Neurosciences

Sounds, like stimuli in other modalities, can vary along several dimensions. Where visual stimuli might vary in colour or shape, auditory stimuli will vary in frequency, duration, or rate of change. Little is known about the way these dimensions are processed during auditory perception and the extent to which they are treated independently when identifying a sound. In this series of behavioural experiments we used spontaneous categorization, the ability to bundle different stimuli together based on a common property, as a way to infer the sound dimension hierarchy underlying auditory perception in mice.

We used frequency-modulated (FM) sweeps that differed in two out of four dimensions (frequency range, duration, rate of change, and direction). Mice were trained to discriminate between two sounds differing in two dimensions. One sound could be an upward FM with low frequency range while the other would be a downward FM with high frequency range. One of the two sounds, the 'safe' sound, was associated with water availability. The other, the 'conditioned' sound, was associated with an air-puff if the mice tried to drink during its presentation. Once the mice were discriminating well between the two sounds, we tested their response to novel sounds that resembled the 'safe' sound in one dimension and the 'conditioned' in the other. Mice were C57BL/6J adult female mice. They lived in an Audiobox (TSE) which consists of a home-cage connected by a long corridor to a specialized sound-attenuated corner and where they were continuously and individually monitored via an implanted subcutaneous transponder. Food was available ad libitum in the home-cage and water was available in the corner. Visits to the corner were accompanied by the presentation of auditory stimuli.

Mice tended to either avoid or approach the novel sounds, reflecting whether they perceived them as similar to the 'conditioned' or the 'safe' sound respectively. We found that when frequency range was one of the dimensions used, categorization occurred mainly across this dimension. Frequency may, thus, be high up in the hierarchy of acoustic features. Generalization could, however, also happen in both dimensions, for example when using duration and direction. Actively teaching animals to categorize along the non-preferred dimension was possible but seemed to be limited to the trained fre-

quency ranges. Thus, the dimensions used were generally perceived independently as reflected in categorizations that were along one but not the other of the two dimensions used.

PS 203

The Discrimination of Ultrasonic Vocalizations by Socially Experienced and Socially Isolated Mice

Laurel A. Screven; Micheal L. Dent

University at Buffalo, the State University of New York

Mice produce ultrasonic vocalizations (USVs) that differ in multiple spectrotemporal parameters, including frequency, duration, and intensity. Mice emit USVs in social situations, and despite their widespread use as a model for human communication, not much is known about how mice use their vocalizations for communication. Previous attempts to determine if mice are able to discriminate between their vocalizations found that mice rely on spectrotemporal similarity to discriminate different vocalizations, where decreased spectrotemporal similarity led to increased discrimination (Neilans et al., 2014). That study used only chronically socially isolated mice, so it is possible that this relationship is more complex when using animals that have previous social experience. We expected that socially experienced animals would perform better on a vocalization discrimination task than animals that had been chronically socially isolated. Determining if mice are able to discriminate between vocalizations is a critical step in discovering if mice are using their vocalizations for communication, and if socialization is a necessary component for normal USV perception. In the current experiment, female mice were trained and tested using operant conditioning procedures and positive reinforcement to discriminate between natural female USVs of three different spectrotemporal categories: chevron, complex, and upsweep. Discrimination performance was measured for all combinations of USVs, with each USV serving as both a background and target stimulus. The animals were required to respond when they heard a change in the repeating background. Mice perform better on the call discrimination task when they have social experience with other females than when they have been socially isolated since weaning. Additionally, socially experienced animals are better able to discriminate between calls when the USV that serves as the background is from a familiar female than an unfamiliar female. These results indicate that socialization is a critical component to normal USV perception. Female mice that have been chronically socially isolated show deficits in vocalization discrimination compared to socially housed animals, indicating that previous experience with hearing USVs is a necessary component to understanding vocalizations and potentially for using them for communication. So-

cialization should therefore be taken into consideration when testing mice on vocalization perception. This work was supported by NIH DC012302.

PS 204

Assessing Salicylate-Induced Hyperacusis in Rats Using an Operant Behavioral Reaction Time Procedure

Kelly Radziwon¹; David Holfoth²; Julia Lindner²; Zoe Kaier-Green²; Rachael Bowler²; Maxwell Urban²; Richard Salvi¹

¹*Center for Hearing & Deafness, Department of Communicative Disorders and Science, State University of New York at Buffalo;* ²*Center for Hearing and Deafness, SUNY at Buffalo*

The use of auditory reaction time is a reliable measure of loudness perception in both animals and humans with reaction times (RT) decreasing with increasing stimulus intensity. Since abnormal loudness perception is a common feature of hyperacusis, a potentially debilitating auditory disorder in which moderate-intensity sounds are perceived as painfully loud, we used RT measures to assess rats for salicylate-induced hyperacusis. Our previous research using an operant conditioning RT procedure found that high-dose sodium salicylate induced hyperacusis-like behavior, i.e., faster than normal RTs to moderate and high level sounds, when rats were tested with broadband noise stimuli. However, it was not clear from that study if salicylate induces hyperacusis-like behavior in a dose- or frequency-dependent manner. Therefore, the goal of the current study was to: (1) Using noise bursts, determine how RT-intensity functions were altered by different doses of salicylate (i.e., which doses of salicylate induced hyperacusis and over what intensity range does hyperacusis occur?), and (2) Using tone bursts, determine if salicylate induces hyperacusis-like behavior across the entire frequency spectrum or only at certain frequencies (i.e., hyperacusis spectral profile). Seven Sprague-Dawley rats were trained to detect noise and tone bursts (1-42 kHz bandwidth, 4, 8, 16, and 20 kHz; 300 ms duration; 5 ms cosine rise/fall times) using a go/no-go operant conditioning procedure. RTs were taken from the onset of the noise/tone burst to the time the rat made a response. After baseline RT-intensity functions were collected, the rats were tested once per week with either a single injection of salicylate, at varying doses (50, 100, 150, 200, 250, and 300 mg/kg for the noise burst task; 200 and 250 mg/kg for the tone burst task), dissolved in saline (50 mg/mL), or an equivalent volume of saline (control). The injections were always administered 2 hours prior to testing.

We found that salicylate causes a reduction in RTs in a

dose-dependent manner and across a range of stimulus frequencies, suggesting that both the RT paradigm and the salicylate model are useful tools in the broader study of hyperacusis. Furthermore, our behavioral results appear highly correlated with the enhanced sound-evoked responses in the inferior colliculus and auditory cortex seen by previous researchers following salicylate treatment and noise exposure pointing to a common central mechanism in the generation of hyperacusis. Ultimately, the use of the salicylate model of hyperacusis provides the necessary groundwork for future studies of noise-induced hyperacusis and loudness recruitment.

Regeneration I

PS 205

In Vitro Hair Cell Regeneration Induced by Manipulating Notch Signaling Pathway in Adult Mouse Utricle

Huawei Li¹; Wenyan Li¹; Shan Zeng¹; Wenli Ni¹; Zheng-Yi Chen²

¹The EENT Hospital of Fudan University; ²Department of Otolaryngology, Harvard Medical School and Eaton-Peabody Laboratory Massachusetts Eye and Ear Infirmary

In mammals, the loss of hair cells leads to permanent hearing loss and vestibular dysfunction. Regeneration of hair cells, especially in mature inner ear, is an essential route that could lead to restoration of hearing and vestibular function. Notch signaling has been shown to be important for the determination of prosensory domains and the development of hair cell and supporting cell through lateral induction and lateral inhibition. In the current study, we showed that the hair cell could be regenerated through transient and bidirectional manipulation of Notch signaling in damaged adult utricle sensory epithelium. The utricles from tetracycline-controlled rtTa/tet-NICD transgenic mice were used for the explant culture, and the hair cell damage was induced by the exposure to neomycin. In explanted utricles, the up-regulation of Notch signaling was achieved through the supplement of doxycycline in the culture medium, with the medium subsequently replaced by addition of DAPT for the down-regulation of Notch signaling. The EdU was used for tracing the synthesis of DNA, served as a marker for proliferation. We observed the EdU+/Sox2+ supporting cells after the up-regulation of NICD in the cultured utricles, which mainly appeared in the striolar region. After the down-regulation of Notch signaling, some proliferated supporting cells could differentiate into hair cells, leading to an increase in the hair cell number. Phalloidin labeling identified immature stereocilia in the newly generated hair cells. We demonstrate that the mitotic regen-

eration of utricular hair cells in adult could be achieved through manipulating one single pathway. The transient and bidirectional manipulation of Notch signaling could overcome the restriction on proliferation of supporting cells in the adult utricles, and further regulate the cell fate of the proliferating cells.

PS 206

Fate-mapping Identifies Supporting Cell Subtypes Capable of Spontaneously Regenerating Cochlear Hair Cells

Melissa McGovern¹; Brandon C. Cox²

¹Department of Pharmacology, Southern Illinois University School of Medicine; ²Department of Pharmacology & Department of Surgery Southern Illinois University School of Medicine

The mammalian organ of Corti contains distinct subtypes of supporting cells (SCs) that surround and aide sensory hair cells (HCs). Little is known about the differences among subtypes and their plasticity. Recently, our lab has identified pillar cells (PCs), Deiters' cells (DCs), and Hensen cells (HeCs) as potential sources of spontaneous HC regeneration in the neonatal mouse cochlea. Specifically, our preliminary data showed that PCs and DCs downregulate the Notch effector Hes5, a direct inhibitor of HC fate, during the window of spontaneous HC regeneration observed in the neonatal mouse cochlea. No changes in Hes5 expression was observed in other SC subtypes. Importantly, some PCs/DCs downregulated the cell cycle inhibitor p27Kip1 after HC damage occurred suggesting these cells retain mitotic potential. Additionally, we observed a decrease in the number of Sox2+ HeCs after HC damage suggesting HeCs may also play a role in regeneration. To investigate which SC subtypes can act as the source for spontaneously regenerated HCs, we have fate-mapped three distinct groups of SC subtypes. Using the Pou4f3DTR/+ mouse to induce HC damage at postnatal day (P)1 and stimulate the spontaneous HC regeneration process, we fate-mapped SC subtypes using three CreER lines paired with the ROSA26tdTomato reporter. To target PCs and DCs, Prox1-CreERT2 was used; for inner phalangeal and border cells, Plp-CreERT2 was used; and to investigate cells of the greater epithelial ridge as well as Hensen cells, GLAST-CreERTM was used. For all three groups, tamoxifen was administered at P0 to induce tdTomato expression in SCs prior to HC damage induced at P1. Preliminary data confirm our hypothesis and suggest that PCs and DCs are capable of spontaneously regenerating HCs in the neonatal mouse cochlea. Further studies will investigate the ability of each group to regenerate HCs via mitotic regeneration vs direct transdifferentiation by incorporating a mitotic tracer in the study. Identifi-

fying the SC subtypes capable of spontaneously regenerating HCs will aid future research by identifying which SCs are plastic and therefore narrowing potential therapeutic targets to initiate regeneration in adult animals.

Funding: Supported by the Office of Naval Research (N00014-13-1-0569) and (N00014-15-1-2866), the Office of the Assistant Secretary of Defense for Health Affairs (W81XWH-15-1-0475), and NIDCD (R01DC014441-01A1).

PS 207

Evaluating the Mechanisms of Regeneration in Response to Different Amounts of Hair Cell Damage in the Neonatal Mouse Cochlea

Michelle R. Randle¹; Brandon C. Cox²

¹Department of Pharmacology, Southern Illinois University School of Medicine; ²Department of Pharmacology & Department of Surgery Southern Illinois University School of Medicine

Background

When 70-80% of hair cells (HCs) are killed, the neonatal mouse cochlea has the capacity to spontaneously regenerate them via direct transdifferentiation and mitotic regeneration (Cox et al., 2015 Development). Previous studies have shown that regeneration of pancreatic beta cells occurs by different mechanisms depending on the amount of cell loss (Nir et al., 2007 J Clin Invest; Thorel et al., 2010 Nature). Therefore, we have damaged different amounts of cochlear HCs and investigated the mechanisms of regeneration. Based on previous studies in chicken, we hypothesize that the amount of direct transdifferentiation will be proportional to the level of HC damage and the amount of mitotic regeneration will remain constant regardless of HC damage amount. To determine tamoxifen (TM) doses needed to target different amounts of HCs, Atoh1-CreERTM::CAG-eGFP mice were injected with TM to express eGFP specifically in cochlear HCs. The TM dose was adjusted to target ~70%, ~50%, ~20%, or ~10% of HCs. We determined that 3mg/40g TM given at P0 and P1 targets ~70% of HCs (Dose 1); 1.5mg/40g TM given at P0 targets ~50% (Dose 2); 0.25mg/40g TM given at P0 targets ~20% (Dose 3); and 0.1mg/40g TM given at P0 targets ~10% (Dose 4). The four doses were used in a similar mouse model, Atoh1-CreERTM::ROSA26DTA, to ablate different amounts of HCs through forced expression of diphtheria toxin fragment A (DTA). After TM injection(s), BrdU was injected twice a day (~6hrs apart) between P3-P6 to detect HCs formed by mitotic regeneration. Cochlea were analyzed at P7 (~24hrs after the final BrdU injection). There was no difference in number of BrdU+ HCs or BrdU+ SCs between Doses 1-3; however, no BrdU+

HCs and a small number of BrdU+ SCs were observed with Dose 4. We are currently developing a model to measure direct transdifferentiation by fate-mapping supporting cells (SCs) using the Tet-On system. Preliminary data indicate HC regeneration occurs when at least 20% of HCs are ablated. However, further analysis is required to determine if direct transdifferentiation can occur when less than 20% of HCs are killed. In addition, the amount of mitotic regeneration did not change when 70-20% of HCs were killed. This suggests a threshold of HC damage is required to initiate mitotic regeneration in the murine cochlea.

Funding

Supported by the Office of the Assistant Secretary of Defense for Health Affairs (W81XWH-15-1-0475), NIDCD (R01DC014441-01A1), and the Office of Naval Research (N00014-13-1-0569 and N00014-15-1-2866).

PS 208

Electrophysiology of Regenerated Hair Cells in the Adult Mouse Utricle

Antonia Gonzalez-Garrido¹; Jennifer S Stone²; Ruth Anne Eatock¹

¹University of Chicago; ²University of Washington

Hair cells are lost from vestibular epithelia through disease, drugs, and aging, and the loss can lead to severe balance dysfunction. There is great interest, therefore, in the ability of mammalian vestibular epithelia to regenerate after damage. In a mouse model of regeneration in which hair cells are killed by diphtheria toxin, some new hair cells are made, and anatomical evidence from the utricle suggests that the regenerated hair cells are type II (Golub et al., J Neurosci 32:15093, 2012). With time, many of the regenerated cells, like a large fraction of normal mature mouse utricular type II hair cells (Pujol et al., J Comp Neurol 522:3141, 2014), express striking basolateral processes that contact not just afferents but also supporting cells and even hair cells. We are using the whole-cell patch clamp method to record electrophysiological properties of regenerating hair cells in semi-intact acutely excised preparations of the mouse utricle. We ask whether hair cells that emerge via in vivo spontaneous regeneration following extensive damage acquire mature electrophysiological properties over time.

To stimulate hair cell regeneration, we treated Pou4f3+/DTR mice with diphtheria toxin, which kills the majority of utricular hair cells, affecting type II cells more than type I cells (Golub et al., *ibid.*). We recorded from regenerating hair cells, recognized by their small hair bundles, between 14 and 140 days post-treatment. Small trans-

duction currents could be measured from the small hair bundles. All resembled type II or immature hair cells in the expression of delayed rectifier K channels that activate positive to resting potential, and all lacked the type I-specific low-voltage activated conductance, g_{KL}, and afferent calyceal terminals (Rüsch et al., *J Neurosci* 18: 7487, 1998). Many regenerated hair cells (20/53) had voltage-gated Na⁺ (Na_V) conductances, consistent with an immature state (Wooltorton et al., *J Neurophysiol* 97: 1684, 2007). Such channels may facilitate neurotransmission by enhancing rapid depolarizations and activation of calcium channels, (Masetto et al., *J Neurophysiol* 90: 1266, 2003). Many of the regenerated hair cells (23/53) bore basolateral extensions, which appear to be a mature feature in control mice (Pujol et al., *ibid.*).

Despite a long recovery window (up to 140 days), regenerated hair cells retain several immature properties and are reduced significantly in number (Golub et al., *ibid.*), suggesting that in mammalian vestibular epithelia there are barriers to full recovery of function following widespread hair cell death.

Funding

NIDCD R21DC013358, JSS and RAE
NIDCD R01DC012347, RAE

PS 209

Differential Gene Expression in the Striolar vs. Extrastriolar Regions of the Chick Utricle

Mark Warchol¹; Rose Veile²; Anastasia Filia³; Michael Lovett³

¹*Dept of Otolaryngology, Washington University School of Medicine, St Louis MO;* ²*Washington University School of Medicine;* ³*Imperial College London*

Background

The vestibular maculae possess a specialized region – known as the striola – which exhibits a number of morphological and functional specializations. Little is known about the molecular signals that specify cell phenotype in the striola. We have used RNA-Seq to characterize regional differences in gene expression in the chick utricle.

Methods

The striola of the avian utricle is located near the lateral edge of the sensory epithelium and can be reliably separated from the larger extrastriolar region. Iridectomy scissors were used to isolate the striolar and extrastriolar portions of utricles from ~P14 chicks. These fragments were then treated in thermolysin and the sensory epithelia were removed from the underlying stromal tissues. RNA-Seq studies were conducted on both freshly

harvested utricles and on utricles that were placed in organotypic culture, treated for 24 hr in 1 mM streptomycin, and allowed to recover for 0–48 hr. Other cultures were maintained for seven days and used to quantify hair cell regeneration. RNA-Seq raw data were aligned against the *gga3* genome using Tophat 2 and quantification was measured using Cufflinks. An ANOVA test was performed to identify differentially expressed genes.

Results

In untreated utricles, 328 genes were differentially expressed (>|1.8|-fold & FDR < 0.1) in the striola, when compared with the extrastriola. Among the largest relative expression differences were genes for *Tectb* and *Dlx5* (both higher in the striola). Members of the BMP, WNT, FGF, TNF α and CXCL12/CXCR4 signaling pathways were enhanced in the striola, as were multiple genes encoding ion channels. Expression of the transduction channel candidate *Tmc2* was ~10-fold greater in the striola vs. extrastriola. Eleven transcription factors were differentially expressed, of which nine were more highly expressed in the striola. Ototoxic injury resulted in numerous regionalized changes in gene expression. We used organotypic cultures to assess whether identified pathways were involved in hair cell regeneration. Streptomycin-treated utricles were maintained for seven days with small molecule inhibitors of candidate signaling pathways. Inhibition of WNT reduced hair cell recovery throughout the chick utricle. In contrast, inhibition of FGF and IGF signaling pathways led to region-specific changes in regeneration.

Conclusions

Results reveal a discrete set of testable differences between the striola and extrastriola at the level of gene expression. Many genes enhanced in the striola are likely to be specific for type I hair cells. Results also identify new candidate pathways that may have regionally specific roles in hair cell regeneration.

PS 210

Proliferative Regeneration After Ablation of Lgr5-positive Cochlear Supporting Cells

Tomokatsu Udagawa¹; Patrick J. Atkinson²; Alan Cheng³

¹*Stanford University School of Medicine;* ²*Department of Otolaryngology-HNS, Stanford University;* ³*Stanford University, School of Medicine, Department of Otolaryngology*

Background

The cochlea requires supporting cells for hair cell maintenance and survival. Previous studies have demonstrated that the neonatal mouse cochlea exhibits the ca-

capacity to regenerate lost cochlear supporting cells. The greater epithelial ridge is hypothesized to harbor cells contributing to regeneration via a non-mitotic mechanism. Here we have characterized a novel supporting cell ablation model with the goal of identifying the source of regenerating cells. A subset of supporting cells expresses *Lgr5* in the neonatal (inner phalangeal cells, inner pillar cells, and the third row of Deiters' cells) and adult mouse cochlea (the third row of Deiters' cells). Using *Lgr5*DTR-EGFP/+ mice where the human diphtheria toxin receptor (DTR) is driven by the *Lgr5* promoter, we have ablated supporting cells in a spatiotemporal specific manner.

Methods

*Lgr5*DTR-EGFP/+ mice were injected with diphtheria toxin (DT) at P1 to selectively ablate *Lgr5*-positive supporting cells. Cochleae were harvested for histological analysis at P4, P7, P14 and, P21. Immunostaining was performed for various markers for supporting cells and hair cells. To assess proliferation, mice were injected with EdU. DPOAE and ABR thresholds were measured at P21.

Results

In *Lgr5*DTR-EGFP/+ mice treated with DT, there was a significant loss of Sox2+ inner phalangeal cells, pillar cells and, Deiters' cells when examined at P4. EdU and Sox2 double positive cells were found within the inner phalangeal cells, pillar cells and Deiters' cells regions. At P7, P14, and, P21, the number of inner phalangeal cells was restored and EdU-labeled cells are found in the inner phalangeal cell area. Furthermore, EdU-labeled cells are found to express the inner phalangeal cell marker, *Glast*. Inner hair cell number did not significantly change over time. By contrast, Sox2+ pillar cells and Deiters' cells progressively degenerated with a delayed loss of outer hair cells. At P21, auditory brainstem response and DPOAE thresholds of *Lgr5*-DTR treated mice were significantly elevated relative to control animals.

Conclusions

Selective ablation of *Lgr5*-positive cochlear supporting cells causes irreversible loss of Deiters', pillar and outer hair cells. Loss of inner phalangeal cells results in spontaneous mitotic regeneration of these supporting cells and preservation of inner hair cells.

Funding

California Initiative in Regenerative Medicine RN3-06529; NIH/NIDCD RO1DC013910; Akiko Yamazaki and Jerry Yang Faculty Scholarship, Department of Defense MR130316.

PS 211

Identification of Downstream Targets of Beta-Catenin in the Newborn Mouse Cochlea

Danielle R. Lenz¹; Alain Dabdoub²; Albert Edge¹

¹*Department of Otolaryngology, Harvard Medical School, Boston, MA, USA, and Eaton-Peabody Laboratory, Massachusetts Eye and Ear Infirmary, Boston, MA, USA;* ²*Biological Sciences, Sunnybrook Research Institute, University of Toronto*

Beta-catenin upregulates *Atoh1* and can generate supernumerary hair cells during development. Its absence inhibits hair cell differentiation and it is therefore essential for hair cell development and regeneration. While hair cells do not spontaneously regenerate in the mature cochlea, stabilization of beta-catenin during a short period after birth results in proliferation of supporting cells in the pillar cell region and subsequent differentiation of a subset of the cells into hair cells. This phenomenon was observed at P1 but not at P4. Stabilization of beta-catenin was induced by tamoxifen in-vivo in supporting cells using *Sox2-Cre-ER;beta-catenin-flox(exon3)* mice at either P1 or P4 for 72h. The inner ears were subsequently dissected out and the sensory epithelium was separated from the neurons and mesenchyme and collected from individual mice according to their genotype. RNA-Seq was performed on three treated and non-treated samples from each time-point using Illumina NextSeq500 Single-End 75bp (SE75).

Stabilization of beta-catenin at P1 resulted in a substantial change in gene expression that included significant upregulation of 216 genes and downregulation of 218 genes. Subsequent analysis of pathways revealed significant enrichment for both canonical and non-canonical Wnt-signaling, as well as Notch-signaling, Ras and GTPase transduction pathways, stem cell differentiation and inner ear development. In contrast, only 136 genes were differentially expressed as a result of beta-catenin stabilization at P4. The list included 8 Wnt-associated genes, but was not significantly enriched for any specific pathway. Altogether, stabilization of beta-catenin at P1 resulted in a more substantial change in gene expression compared to P4. As expected, the sensory epithelium of the inner ear appears more sensitive to manipulation that might lead to regeneration at earlier time-points. Further analysis of the subset of genes presented here can shed light on various downstream targets of beta-catenin during early hair-cell maturation and potential regeneration as part of Wnt-signaling.

PS 212

In Vivo Induction of Atoh1 and Pou4f3 for Auditory Inner Hair Cell Regeneration

Laura D. Hamel¹; Jian Zuo²

¹St. Jude Children's Research Hospital; ²Dept. of Developmental Neurobiology, St. Jude Children's Research Hospital, Memphis, TN, USA

Hearing loss is one of the most common health impairments in the United States. Many things contribute to hearing loss including aging, illness, acoustic trauma, genetic predisposition and ototoxicity from a multitude of drugs. Unlike non-mammalian vertebrates, mammals are unable to regenerate damaged auditory hair cells (HCs) which results in permanent hearing loss. In the auditory field, ectopic expression of the transcription factor Atoh1 has been used to convert neonatal mammalian supporting cells (SCs) into hair cell like-cells that express many endogenous hair cell markers. In the chicken, damage to auditory hair cells results in an up-regulation of Atoh1 in SCs but less than 60% of the Atoh1-positive SCs become new HCs. However, Atoh1-mediated conversion rates in mice are much lower and result in HCs of limited maturity. Recently, it was shown that targeting the SCs surrounding the inner hair cells (IHCs), the inner phalangeal (IPh) and inner border (IB) cells, results in a greater conversion rate than that of targeting the SCs surrounding the outer hair cells (OHCs). Interestingly, Atoh1-mediated conversion results in a low level of expression of an additional transcription factor, Pou4f3. We hypothesized that increased expression of Pou4f3 may increase the rate of SC conversion. To determine whether ectopic expression of Atoh1 combined with Pou4f3 increased the rate of SC conversion, we generated a mouse model that conditionally expresses Atoh1 and Pou4f3 in the adult mouse IPh and IB cells. We will analyze *Glast*/CreERT2; Atoh1-HA; Pou4f3-mCherry mice induced with tamoxifen at postnatal day 28 (P28) and analyzed at P42 (3 weeks post-induction). These mice will be analyzed for hearing thresholds by audio-brain response (ABR) studies, and further analyzed by scanning electron microscopy (SEM) and immunofluorescence.

PS 213

Isl1 and Atoh1 Synergistically Mediate Cochlear Hair Cell Transdifferentiation

Fei Zheng¹; Zoe Kellard²; Tetsuji Yamashita¹; Jian Zuo¹

¹Dept. of Developmental Neurobiology, St. Jude Children's Research Hospital, Memphis, TN, USA; ²Dept. of Developmental Neurobiology, St. Jude Children's Research Hospital, Memphis, TN, USA; ²University of Bath, Bath, Somerset, UK.

Cochlear hair cell (HC) regeneration is one of the most promising therapeutic strategies for hearing loss. Although adult mammalian cochleae cannot spontaneously regenerate HCs, recent studies from other mammalian tissues including heart, pancreas and central nerve system, indicate that combined transcription factors can directly convert mature somatic cells to other cell types (transdifferentiation). Our lab and others have demonstrated that by ectopically expressing Atoh1 (a bHLH transcriptional factor), cochlear supporting cells (SCs) are phenotypically converted to hair cells. However, the conversion is not efficient - only about 6-20% of Atoh1-overexpressing SCs were reprogrammed to the HC fate. Recently, we investigated the transcriptome of endogenous supporting cells (SCs), outer hair cells (OHCs), and Atoh1-converted hair cells (cHCs) in adult murine cochlea by RNA-seq and single-cell qPCR, and identified 52 transcription factors that are differentially expressed. *Isl1*, which is enriched in OHCs but low in SCs and cHCs, is known to regulate the expression of 6 other transcription factors that also exhibit the expression pattern similar to *Isl1* among SCs, cHCs, and OHCs. Overexpressing *Isl1* in greater epithelial ridge cells in cochlear explants failed to convert these cells to HCs. However, together with Atoh1, *Isl1* significantly increased the transdifferentiation efficiency by nearly two-fold. Moreover, we generated a mouse model to conditionally overexpress *Isl1* in supporting cells in vivo. With this model, we aim to validate *Isl1* function in both neonatal and adult murine cochleae. These studies thus validate novel transcription factors in HC transdifferentiation. This work was supported, in part, by the National Institutes of Health [grant nos. 1 R01 DC015444-01 (to J.Z.), 2R01DC006471 (to J.Z.), 1R01DC015010-01A1 (to J.Z.), 1R21DC013879-01 (to J.Z.), and P30CA21765 (to St. Jude)], Office of Naval Research [grant nos. N000140911014, N000141210191, N000141210775, and N000141612315 (to J.Z.)] and ALSAC.

PS 214

Anatomical Observations of Sensorineural Degeneration and Regeneration After Destruction of Hair Cells in Adult Mouse Utricles

Jennifer Stone¹; Remy Pujol²; Lindsay Schlobohm³; Connor Finkbeiner⁴; Antonia Gonzalez-Garrido⁵; Ruth Anne Eatock⁵

¹University of Washington, Seattle, WA; ²INSERM Unit 1052, University of Montpellier, Montpellier, France;

³Speech and Hearing Sciences, University of Washington, Seattle; ⁴Otolaryngology Department, University of Washington, Seattle, WA; ⁵University of Chicago

Vestibular hair cells die as a result of genetic deficiency

cies, ototoxic drugs, and aging, and this loss can cause severe balance dysfunction. Our group studies the natural ability of mature mammals to regenerate hair cells after damage using Pou4f3+/DTR mice, in which administration of diphtheria toxin (DT) causes near-complete hair cell loss (Golub et al., J Neurosci 32:15093, 2012). Approximately 20% of hair cells regenerate, and all are type II. Here, we address whether regenerated type II hair cells acquire mature anatomical properties over time.

We injected adult wildtype or Pou4f3+/DTR mice (CBA/CaJ or C57Bl/6J background) with DT. We used light microscopy, transmission electron microscopy (TEM), and confocal microscopy to study utricular maculae from 7 to 170 days post-DT. Wildtypes served as age-matched negative controls. At 7 days, degenerating type I and II hair cells were evident. TEM revealed retraction of calyces from type I hair cells and supporting cell processes encircling damaged neurites and hair cells. At 14 days, few hair cells remained. Large clumps of neurites filled with mitochondria were observed, indicative of degenerating calyces and large afferent fibers. At 28 days and later, healthy-appearing neural elements re-emerged. Regenerated type II hair cells increased in number over time and acquired cell-specific features in a manner paralleling normal development. Some cells appeared to be supporting cells transitioning into hair cells: they had a basal nucleus, like supporting cells, and cytoplasm resembling hair cells (numerous polyribosomes but no granules typical of supporting cells). Additional cells were clearly immature hair cells: they had cytoplasm with multiple polyribosomes and nuclei located halfway between the basal lamina and lumen, but they lacked defined cuticular plates or stereocilia. Such cells were contacted by re-growing boutons that were immature (small and multivesiculated), and the cells had ribbon precursors in the cytoplasm, characteristic of developing ribbon synapses. Mature-appearing type II hair cells were seen at 42 days and later. These cells had nuclei closer to the lumen, well defined stereocilia, basolateral processes, and well formed ribbon synapses opposed to afferent boutons with post-synaptic densities. Many TEM observations were confirmed using immunolabeling and confocal microscopy. Further, at 170 days, regenerated hair cells were properly oriented toward the line of polarity reversal, and we noted no loss of vestibular ganglion neurons. Somewhat surprisingly, we noted that transitioning cells and immature-appearing hair cells were seen at all survival times, suggesting new hair cells are added over a long period.

PS 215

Characterization of the Transcriptomes of Lgr5+ Hair Cell Progenitors and Lgr5- Supporting Cells in the Mouse Cochlea

Renjie Chai¹; Cheng Cheng²; Luo Guo³; Haibo Shi⁴; Shasha Zhang¹; Chengwen Zhu⁵; Yan Chen³; Mingliang Tang¹; Xia Gao⁶; Xiaoli Zhang⁵; Huawei Li⁷

¹MOE Key Laboratory of Developmental Genes and Human Disease, State Key Laboratory of Bioelectronics, Institute of Life Sciences, Southeast University, Nanjing 210096, China.; ²St. Jude Children's Research Hospital; ³Department of Otorhinolaryngology, Hearing Research Institute, Affiliated Eye and ENT Hospital of Fudan University, Shanghai; ⁴Department of Otorhinolaryngology-Head & Neck Surgery Affiliated Sixth People's Hospital, Shanghai Jiao Tong University, 600 Yishan Road, Shanghai 200233, P.R.China.; ⁵Department of Otolaryngology, the Affiliated Drum Tower Hospital of Nanjing University Medical School; ⁶Department of Otolaryngology, Nanjing Drum Tower Hospital, The Affiliated Hospital of Nanjing University Medical School, Nanjing 210008, China.; ⁷The EENT Hospital of Fudan University

Cochlear supporting cells (SCs) have been shown to be a promising resource for hair cell (HC) regeneration in the neonatal mouse cochlea, and Lgr5+ progenitors are able to regenerate more HCs than Lgr5- SCs. It is important to understand the mechanism promoting the proliferation and HC regeneration of these progenitors. Here, first we isolated Lgr5+ and Lgr5- SCs from Lgr5-EGFP-CreERT2/Sox2-CreERT2/Rosa26-tdTomato mice via flow cytometry. As expected, we found that Lgr5+ progenitors had significantly higher proliferation and HC regeneration ability than Lgr5- SCs. Next, we performed RNA-seq to determine the gene expression profiles of Lgr5+ and Lgr5- SCs. We analyzed the genes enriched and differentially expressed in Lgr5+ and Lgr5- SCs, and found 12 cell cycle genes, 9 transcription factors, and 28 cell signaling pathway genes that were uniquely expressed in one population. Last, we made a protein-protein interaction network to further analyze the role of differentially expressed genes. In conclusion, we present a set of genes that might regulate the proliferation and HC regeneration ability of Lgr5+ progenitors, and might serve as potential new therapeutic targets for HC regeneration.

PS 216

Transcriptional Targeting of Adult Mammalian Cochlear Supporting Cells

Michael Hoa¹; Rafal Olszewski²; Alvin DeTorres²; Xiaoyi Li²; Kevin Isgrig²; Wade W. Chien³; Ivan Lopez⁴; Fred Linthicum⁴; Robert Morell⁵; Matthew W. Kelley⁶

¹Office of the Clinical Director, Otolaryngology Surgeon-Scientist Program, Auditory Development and Restoration Program, Division of Intramural Research, NIDCD, NIH, Bethesda, Maryland, USA; ²Division of Intramural Research, NIDCD, NIH, Bethesda, Maryland, USA; ³Office of the Clinical Director, Otolaryngology Surgeon-Scientist Program, Inner Ear Gene Therapy Program, Division of Intramural Research, NIDCD, NIH, Bethesda, Maryland, USA; ⁴UCLA School of Medicine; ⁵Genomics and Computational Biology Core, NIDCD, NIH, Bethesda, Maryland, USA; ⁶Laboratory of Cochlear Development, NIDCD, NIH, Bethesda, Maryland, USA

Introduction

Restoration of hearing through regeneration of lost hair cells within the adult organ of Corti will most likely require the transdifferentiation of existing supporting cells into hair cells. While previous studies have demonstrated that immature (perinatal, juvenile) supporting cells can serve as progenitors for new hair cells, adult cochlear supporting cells have lost this capacity. To circumvent this limitation, current strategies to target cochlear supporting cells combine strong but non-specific expression constructs with viral transfer. The non-specific nature of these constructs has the potential to drive ectopic gene expression in non-relevant cell types leading to deleterious effects. Previous work from our laboratory used single-cell mRNA-Seq (scRNA-Seq) to generate transcriptional profiles of adult cochlear supporting cells. One potential outcome of this work is the identification of genes that are active in adult supporting cells and therefore might be used to target gene therapy specifically to those cells. Previous work in other organ systems (nervous system, retina) has demonstrated the utility of cell type-specific promoters.

Methods

Previously constructed scRNA-Seq libraries from FACS-purified adult cochlear supporting cells captured as single cells on the Fluidigm C1 microfluidics platform were analyzed. Our analyses focused on genes ubiquitously expressed in adult cochlear supporting cells. Adult supporting cell-specific genes were identified and validated in both adult mouse organ of Corti and human temporal bone specimens with fluorescent immunohistochemistry. These promoter regions of these validated

genes were cloned into reporter constructs and tested for expression specifically in mouse adult cochlear supporting cells both in vitro and in vivo.

Results

We confirm cell type-specific expression in adult cochlear supporting in both adult mouse and human inner ear specimens by fluorescent immunohistochemistry. We demonstrate the feasibility of targeted expression in adult cochlear supporting cells utilizing promoter elements from this set of validated supporting cell-specific genes. We compare our results to currently available non-specific methods of gene delivery.

Conclusions

Adult supporting cell-specific gene promoters can be utilized to target gene expression to adult cochlear supporting cells. Our data point to the utility and relevance of adult cochlear transcriptional profiles towards attempts at targeting supporting cells for hair cell regeneration.

PS 217

Understanding the Mechanism of Atoh1 Function by Profiling Atoh1-induced Hair Cells

Hsin-I Jen; Andy Groves
Baylor College of Medicine

Atoh1 is a bHLH transcription factor that is necessary and sufficient for hair cell formation. Ectopic overexpression of Atoh1 in the neonatal cochlea and adult utricle can cause supporting cells to trans-differentiate into hair cell-like cells. These Atoh1-induced cells are partially functional, but do not appear to express all hair cell markers. To understand the identity of Atoh1-induced hair cells, we studied their transcriptome with RNA-seq. We infected adult utricle supporting cells with an adenovirus that expresses Atoh1 and TdTomato (Adx-TdTomato-Atoh1) or a control (Adx-TdTomato) virus. We verified that our virus specifically infects supporting cells, and that in neonatal cochlea and adult utricles, Adx-TdTomato-Atoh1 infected supporting cells trans-differentiate and express myosin VIIa. In the utricle, more than 80% of infected supporting cells become myosin VIIa positive within 10 days after Adx-TdTomato-Atoh1 infection. We isolated and performed RNA-seq on these adenovirus-infected cells and identified hair cell genes that are up regulated in these Adx-TdTomato-Atoh1 infected cells.

Current evidence suggests that Atoh1 alone cannot induce hair cell trans-differentiation in adult cochlear supporting cells. Thus, we hypothesize that chromatin accessibility of hair cell genes is required for Atoh1 to activate gene expression in neonatal cochlear and adult utricle supporting cells. To address this question, we

also compared ATAC-seq profiles of supporting cells, hair cells and Atoh1-induced hair cell-like cells.

PS 218

Coordinated Wnt/ β -catenin Activation and Inhibition of Hes1-Mediated Notch Signaling Induces Synergistic Increases in Cochlear Hair Cell Numbers

Richard D. Kopke; Matthew B. West; Xiaoping Du; Wei Li; Ibrahima Youm; Jianzhong Lu; Weihua Cheng; Qunfeng Cai
Hough Ear Institute

Background

The sensory epithelium of the inner ear is composed of a complex mosaic of auditory hair cells (HCs) and supporting cells (SCs). Although HC loss in mammals is irreversible, recent studies have demonstrated that a subpopulation of postnatal SCs retain stem cell-like properties that imbue them with the phenotypic plasticity to transdifferentiate into new HCs in response to genetic or pharmacologic manipulation. The observation that these responsive SCs are competent for canonical (β -catenin-dependent) Wnt pathway signaling suggests that it may be possible to potentiate the HC regenerative response induced by pharmacogenetic manipulation of the Notch pathway, using Hes1 siRNA (siHes1) nanoparticle (NP) technology, by priming the sensory epithelium of the OC with agents that amplify Wnt/ β -catenin signaling throughout the SC population.

Methods

Postnatal murine cochleae were exposed to the ototoxic aminoglycoside, neomycin, in vitro and then cultured under conditions in which Wnt pathway activation and inhibition of Hes1 signaling were alternately manipulated. This was carried out by pharmacologic inhibition of glycogen synthase kinase 3β , which promotes activation of Wnt/ β -catenin signaling, and pharmacogenetic inhibition of Hes1, using siHes1 biomolecules, delivered by either a transfection reagent or poly(lactide-co-glycolide acid) (PLGA) NPs. A combination of molecular and immunohistological examinations were then employed to discern the degree and manner in which these manipulations impacted phenotypic plasticity and HC transdifferentiation.

Results

Pharmacologic inhibition of GSK3 β was sufficient to induce Wnt/ β -catenin signaling and a mitotic response among SCs in cultured OCs. Combined inhibition of GSK3 β and siRNA-mediated knockdown of the Notch effector protein, Hes1, led to synergistic increases in HC numbers following ototoxic neomycin exposure. From our comparative analyses, we found that staged inhibi-

tion of GSK3 β followed by Hes1 knockdown resulted in the most robust increases in HC numbers, consistent with a priming effect induced by Wnt pathway activation.

Conclusions

The observation that staged inhibition of GSK3 α/β and Hes1 can lead to synergistic increases in HC numbers in ototoxin-damaged murine cochlea provides an important insight into the development of therapeutic strategies for regenerating lost mammalian auditory sensory epithelia. As substantial loss of SCs through siHes1-mediated transdifferentiation may limit the long-term viability of regenerated HCs or adversely affect auditory function, the ability of Wnt pathway activation to either potentiate the regenerative efficiency of siHes1 NPs or mitotically repopulate SCs may enhance the long-term therapeutic efficacy of this approach.

This research was supported by grant AR15-005 from The Oklahoma Center for the Advancement of Science and Technology.

PS 219

tnks1bp1 Is Required for Proper Hair Cell Development and Regeneration in the Zebrafish Lateral Line

Luis R. Colón-Cruz¹; Gaurav Varshney²; Aranza Torrado¹; Shawn Burgess³; Martine Behra¹

¹*University of Puerto Rico - Medical Sciences Campus;*

²*National Human Genome Research Institute/NIH;*

³*National Human Genome Research Institute, NIH, Bethesda, MD*

Higher vertebrates lack the capacity to regenerate mechanosensory hair cells (HCs) of the inner ear which are required for hearing and balance. By contrast, fish and amphibians can regenerate HCs in their inner ears but also in an evolutionary linked sensory organ, called the lateral line (LL). This superficial organ informs fish on movements in the surrounding waters through stereotypically distributed sensory patches called neuromasts (Ns). Each N is composed of centrally located HCs and surrounding supporting cells (SCs) which contain progenitor cells that will divide to replace and regenerate lost HCs. We have previously shown that tankyrase 1 binding protein1 (tnks1bp1) is expressed specifically in all SCs of the LL. This poorly characterized gene is postulated to interact with tankyrase (tnks), a better described gene which has been implicated in several important biological mechanisms, but more relevant to our interest in maintenance of telomeres' length during successive divisions of stem cell populations. We hypothesized that if tnks1bp1 is involved in such a fundamental mechanism as maintenance of stemness of a pool of progenitors, a loss of function of this gene in SC would

have a dramatic effect on proper development and/or regeneration of HCs. To test this, we generated mutant alleles using the CRISPR/Cas9 system. We targeted *tnks1bp1* in two exonic regions and co-injected the two gRNAs with synthetic mRNA Cas9 in a double transgenic background Tg(*tnks1bp1:EGFP*) x Tg(*atoha1:TOM*), which allowed us to directly visualize defective development of the LL and altered HC regeneration using *in vivo* techniques. We have raised potential founders to sexual maturity and inbred them. The offspring (F1) have been genotyped for confirmation of insertion/deletions (INDELS) close to the PAM site. Three different alleles have been identified: *tnks1bp1+2nt*, *tnks1bp1+8nt*, and *tnks1bp1+17nt*. Visual inspection of the LL in offspring of those identified carriers was performed from 3 to 6 day post fertilization (dpf). Numerous aberrant features were observed in ¼ of the larvae including faulty migration and early HCs differentiation. Those preliminary results suggest that *tnks1bp1* is crucial for proper development of the LL. Future work will assess the effect on HC regeneration and aim at establishing the link to telomere length maintenance. This will expand our understanding of HC regeneration and bring us closer to translational solutions addressing HC loss and its devastating consequences on human hearing.

PS 220

Break-down of Hair Cell Regeneration Process in Zebrafish Neuromast

Liu Dong; Yuting Wu; Xiaoxiao Mi; Hong Guo; Dong Liu

School of Life Sciences, Peking University

Zebrafish posterior lateral line (pLL) neuromast regenerates its lost hair cells (HCs) readily. Our recent work indicated that direct conversion of supporting cells (SCs) to HCs happens first as a quick response to neuromast damage, followed by HC regeneration via mitosis of SCs, suggesting that pLL HC regeneration is perhaps not a simply recurring process of HC development. The signaling and cellular basis of the regeneration remains to be fully understood.

In present study, using transgenic fish labeling HCs or SCs or over-expressing genes, live imaging and chemical blockage, we have determined that newly divided SCs prior to HC damage are competent to direct conversion cues mediated by Notch/Wnt signaling during cisplatin treatment; whereas some SCs newly at S phase of cell cycle continue cell division to give rise to HCs (mitotic regeneration) after cisplatin removal. By analyzing a viable homozygous mutant, *sim1b*, that develops pLL normally but fails to restore its lost HCs upon cisplatin insult, we have found that the mutant defect is apoptosis- and Wnt- dependent and its mitotic regeneration

is mainly blocked. The regeneration defect can be rescued by temporarily supplying *Sim1b* or Wnt/ β -catenin, indicating a relationship between Wnt signaling pathway and *Sim1b*. Interestingly, in rescued *sim1b* mutant neuromasts, directly converted HCs are dominant but normally, mitotically regenerated HCs prevail in wild-type regenerating neuromasts.

Our study indicates: 1) Cell cycle states of proliferating SCs prior to HC damage determine how these SCs contribute to nascent HCs; 2) A state of low Notch and high Wnt activity determines direct conversion mode of HC regeneration; and 3) *Sim1b* is crucial for HC regeneration triggered by apoptosis through regulating Wnt signaling pathway but it is not essential for normal neuromast HC development.

(National Basic Research Program of China--973 Program 2012CB944503; National Science Foundation of China-- 31571496)

PS 222

Assessment of *Atf5a* Contribution to Hair Cell Regeneration in the Zebrafish Lateral Line

Roberto E. Rodriguez¹; Gaurav Varshney²; Shawn Burgess²; Martine Behra³

¹*University of Puerto Rico, Medical Sciences Campus;*

²*National Human Genome Research Institute/NIH;*

³*University of Puerto Rico - Medical Sciences Campus*

Hair cells (HCs) are the mechanoreceptors that are found deeply buried within the inner ear of all vertebrates, and their loss is the leading cause of deafness in humans. Mammals are unable to regenerate this sensory tissue, however lower vertebrates such as birds, amphibians and fish have the capacity to regenerate HCs after injury. We use the zebrafish animal model, which also has an evolutionarily linked superficial mechanosensory system called the lateral line (LL) which is composed of stereotypically distributed neuro-sensory patches referred to as the neuromasts (Ns). In these patches centrally located HCs are surrounded by supporting cells (SCs) from which a sub-population has been shown to be HC progenitors. In order to characterize further the SCs, in earlier work our laboratory interrogated by micro-array FAC sorted GFP positive cells from the Tg(*tnks1bp1:GFP*) larvae. This transgenic larvae expresses green fluorescent protein (GFP) exclusively in SCs from the LL but also from the nasal placodes. We found enriched expression of an EST that we have now mapped to the Activating transcription factor 5a (*Atf5a*) gene. In mouse *Atf5a* is expressed exclusively in olfactory sensory neurons (OSNs) which when destroyed are regenerated in mammals. *Atf5a* KO mice were completely lacking

OSNs, therefore implying that this gene is important for differentiation, survival and possibly regeneration of OSNs. In addition, microarrays performed in regenerating avian inner ear sensory tissue showed strong up-regulation of *atf5a*, suggesting a role for this gene in HC regeneration of auditory tissues. Thus, we decided to investigate further the role of *atf5a* in zebrafish and postulated that it was relevant for olfactory and auditory sensory tissue development and/or regeneration. To this end, we have targeted *atf5a* using the CRISPR-Cas9 genome editing tool. We have already isolated at least one loss of function allele and are pursuing our genotyping efforts. We will analyze the off-spring of the recovered stable mutant lines. We will (1) establish where this gene is expressed and (2) interrogate if it affects development of OSNs in nasal placodes and/or HCs in the LL and (3) if it has a role in their regeneration. Preliminary results of the mutant characterization will be presented along with genotyping results. *Atf5a* is a good candidate gene for explaining the differential regeneration capacity in vertebrates and a better understanding of its role will help us make progress toward restoring it in mammals and in humans.

PS 223

Single Cell RNA-Seq Expression Profiling of Homeostatic and Regenerating Zebrafish Support and Hair Cells

Nina Koenecke; Kate Hall; Allison Peak; Anoja Perera; Jungeun Park; Tatjana Piotrowski
Stowers Institute for Medical Research

Neuromasts are mechanosensory organs located along the bodies of zebrafish that detect water motion via centrally positioned hair cells. Zebrafish hair cells resemble human inner ear hair cells, but in contrast to humans, continuously regenerate throughout the life of the animal. Thus, the zebrafish lateral line is a powerful model to elucidate the signaling interactions between cells that underlie hair cell regeneration. In regenerating species, such as zebrafish and chicken, support cells proliferate after hair cell death to give rise to new hair cells. Therefore, our studies aim to identify genes that are up- or downregulated in support cells. We have determined the order of signaling pathways modulation after hair cell death using temporal transcriptome analyses of bulk neuromast cells (Jiang et al., PNAS 2014). However, gene expression of candidate genes and time-lapse analyses revealed that at least 4 functionally distinct types of support cells support cell types exist: 1) mantle cells, 2) dividing, amplifying support cells, 3) dividing, differentiating support cells and 4) quiescent support cells (Romero-Carvajal et al., Dev Cell 2015). All these cells need to communicate with each other to ensure the persistent ability to regenerate a functional sensory or-

gan. Importantly, we have discovered unexpected heterogeneity within these four support cell types, which is masked in bulk support cell RNA-Seq analyses. To study how individual support cells integrate signals during homeostasis and regeneration we require the higher resolution of single cell approaches. We successfully established a single cell RNA-Seq protocol for FACS isolated GFP-labeled zebrafish neuromast cells. To validate the single cell RNA-Seq results we classified cells in a pilot experiment into potential mantle cells, hair cells and support cells based on candidate genes. Clustering using all differentially expressed genes confirmed the initial cell type classifications demonstrating that the single cell RNA-Seq analysis is sensitive and of high quality. In addition, we were able to identify new differentially expressed neuromast genes among these cell types. We are currently performing single cell expression analyses of hundreds of homeostatic and regenerating neuromast cells to distinguish support cells on different trajectories, temporally order them along those trajectories, and identify new regulatory factors controlling hair cell differentiation. The results of this study will be informative for the future interpretation and design of pathway manipulations in the mouse to induce regeneration, as well as for in vitro protocols to induce hair cells from iPS or ES cells.

Vestibular: Imbalance, Vertigo and Meniere's

PS 224

Oculomotor, Vestibular, and Reaction Time Testing Abnormalities in College Athletes After Sports Related Concussions

Mikhaylo Szczupak¹; James K. Buskirk¹; Michael H. Berger¹; Eric Barbarite¹; Patel Kunal¹; Alexander Kiderman²; Jonathan Gans³; Kimball John¹; Nathan Schoen¹; Adam Kravitz¹; Kaitlin McIntyre¹; Constanza Pelusso¹; Carey D. Balaban⁴; Michael E. Hoffer⁵

¹*Department of Otolaryngology University of Miami*;

²*Neuro Kinetics, Inc.*; ³*Neuro kinetics, Inc.*; ⁴*University of Pittsburgh*; ⁵*Department of Otolaryngology and Neurological Surgery, University of Miami*

Background

Mild traumatic brain injury (mTBI), known as concussion, is a heterogeneous condition with a diverse clinical presentation known to affect athletes of all levels. Accurate diagnosis and prognosis of mTBI remain critical issues. Currently, many diagnostic criteria rely on subjective factors (history and physical exam) as well as patient self-report. Our group has been examining a set of neurosensory sequelae that can be objectively tested using oculomotor, vestibular, and reaction time (OVRT) tests.

Methods

A portable, virtual reality driven goggle device (iPortal PAS, Neuro Kinetics, Inc. Pittsburgh, PA) was utilized for baseline and post injury/post season testing. Post injury testing was performed immediately after mTBI, 1 week after mTBI, 1 month after mTBI and 3 months after mTBI. This population included 172 University of Miami NCAA and club sport athletes from 15 different teams during the 2015-2016 athletic. Six athletes with new onset mTBI were compared to two control groups, a gender control group (107 male athletes or 65 female athletes) and an identical team/athletic level control group (values vary by team).

Results

Abnormalities were described as test performance values falling below the control group's fifth percentile in performance. Using this definition, OVRT performance abnormalities in at least one of the following parameters, among several others, was seen for all mTBI athletes: smooth pursuit vertical 0.10 Hz velocity gain saccade percentage (3/6), predictive saccade mean overall latency (4/6), antisaccade overall prosaccadic error percentage (4/6) and subjective visual vertical mean overall error (4/6). In all mTBI subjects there was a decreased total number of OVRT abnormalities seen from immediate post injury testing to 3 month post injury testing.

Conclusions

These OVRT deficiencies can be accurately measured and characterized using a portable eye-tracking platform. Describing pathological dysfunction in the unique population of college athletes with mTBI will be a valuable tool in the progression of mTBI management in athletics. OVRT data can be used as a marker in return to play decision making for high level athletes.

PS 225

Oculomotor, Vestibular, and Reaction Time Testing Patterns in College Athletes

James K. Buskirk¹; Mikhaylo Szczupak¹; Eric Barbarite¹; Michael H. Berger¹; Patel Kunal¹; Alexander Kiderman²; Jonathan Gans³; Kimball John¹; Nathan Schoen¹; Adam Kravitz¹; Kaitlin McIntyre¹; Constanza Pelusso¹; Carey D. Balaban⁴; Michael E. Hoffer⁵

¹Department of Otolaryngology University of Miami;

²Neuro Kinetics, Inc.; ³Neuro kinetics, Inc.; ⁴University of Pittsburgh; ⁵Department of Otolaryngology and Neurological Surgery, University of Miami

Background

Mild traumatic brain injury (mTBI), known as concussion, is a heterogeneous condition with a diverse clin-

ical presentation known to affect athletes of all levels. Accurate diagnosis and prognosis of mTBI remain critical issues. An ideal testing system would be portable, operable by individuals without an advanced medical degree, and provide objective data in a repeatable manner. We have previously reported on the development of a portable device that measures oculomotor, vestibular, and reaction time (OVRT) performance as a measure of mTBI. In order to utilize this device to make point of injury decisions, accurate normative values that reflect the population from which an injured individual is drawn will provide the best diagnostic accuracy. In this work we describe the baseline characteristics of a population of college athletes.

Methods

A portable, virtual reality driven goggle device (iPortal PAS, Neuro Kinetics, Inc. Pittsburgh, PA) was utilized for baseline and post season testing. Baseline testing was performed on over 200 University of Miami NCAA and club sport athletes from 15 different teams during the 2015-2017 athletic seasons. Post season testing (within 10 months of baseline) was performed on 55 athletes who did not suffer mTBI. This testing was performed at their respective athletic facilities. Analysis of the outcomes of each of the OVRT tests was compiled for the group as a whole as well as specified subgroups divided by gender and type of sport.

Results

Normal population values were described for a variety of the OVRT tests performed. These values included horizontal and vertical smooth pursuit velocity gain, saccadic tracking measures, antisaccadic and prosaccadic error percentage, subjective visual vertical, subjective horizontal vertical, and vergance analysis. Characteristics of these normal patterns can be utilized to determine which tests are best for both point of injury diagnosis and well as prognostic and return to play decision making. Gender, sports specific and athletic level (NCCA vs. club sport) differences were described. A correlation between completion of an athletic season and improvement in all reaction time parameters was demonstrated while the same pattern was not found for all oculomotor parameters.

Conclusions

OVRT characteristics of college athletes can be utilized to perform point of injury measurements of these individuals after mTBI. Baseline testing data to describe population normal values is a critical step to more widespread use of this portable technology.

Clinical Imaging of the Vestibular Aqueduct for Meniere's Disease

Andreas H. Eckhard¹; Ngoc-Nhi Luu²; Samuel R. Barber³; Arianne Monge Naldi¹; Judith S. Kempfle⁴; Hugh D. Curtin⁵; Steven D. Rauch⁶; Alexander Huber¹; Joe C. Adams²

¹1, Department of Otorhinolaryngology – Head and Neck Surgery, University Hospital Zurich, Zurich, Switzerland; ²2, Department of Otolaryngology, Massachusetts Eye and Ear Infirmary, Boston, MA, USA. ³3, Department of Otolaryngology, Harvard Medical School, Boston, MA, USA; ³2, Department of Otolaryngology, Massachusetts Eye and Ear Infirmary, Boston, MA, USA; ⁴2, Department of Otolaryngology, Massachusetts Eye and Ear Infirmary, Boston, MA, USA. ³3, Department of Otolaryngology, Harvard Medical School, Boston, MA, USA. ⁵5, Department of Otolaryngology, University Tübingen Medical Center, Tübingen, G; ⁵2, Department of Otolaryngology, Massachusetts Eye and Ear Infirmary, Boston, MA, USA. ³3, Department of Otolaryngology, Harvard Medical School, Boston, MA, USA. ⁴4, Department of Radiology, Harvard Medical School and Massachusetts Eye and Ear; ⁶6 Harvard Medical School, Mass Eye and Ear

Background

Meniere's disease (MD) is a syndromic disorder of the inner ear that poses a significant diagnostic challenge. The accepted diagnostic criteria for MD are rather non-specific and overlap considerably with other vertigo-associated diseases. The existence of etio-pathologically and clinically distinct "subgroups" of MD patients has been proposed but, to date, has not been demonstrated. Herein we report radiographic criteria that define a clinically distinct subgroup of MD patients based on the morphology of their vestibular aqueduct (VA). Preliminary results suggest that this morphologic variant is correlated with specific clinical features of the disorder.

Methods

Retrospective study: 1) Radiographic analysis of CT (cone beam/conventional) and MRI (3T) temporal bone scans from MD patients (n=35) and healthy adults (controls; no history of vertigo and otologic disease, n=11) were used to determine the angle of the proximal VA merging into the vestibule (a), and the angle of the distal VA merging into the posterior cranial fossa (b). 2) chart review of clinical history of MD patients in regards to course of the disease.

Results

Among the control cases (n = 11) the values for both angles showed only little interindividual variation (a = 22.8° +/- 8.7°, b = 104.5° +/- 12.3°). However, in MD patients (n = 35), two groups of patients were distinguished based on significant different values for b (b (VA angled) = 94.7° +/- 11.9°, b (VA straight) = 148.2° +/- 7.6°, p < 0.001). Overall, in approximately 70 % of the investigated MD cases angled VAs were identified, while in 30 % of the cases VAs with a straight morphology were found. In case histories of MD patients we note that those with the morphologic variant tend clinically to have bilateral morphologic changes, onset of active Meniere symptoms at a younger age and bilateral disease.

Conclusions

In summary, we have used CT radiographic criteria to define morphologically distinct subgroups of MD patients. A preliminary retrospective analysis of clinical history in these patients suggests that these patients can also be distinguished clinically. Future studies will show whether these two subgroups of MD patients in fact exhibit significantly different phenotypic traits in the course of their disease.

PS 227

M. Menière's re- What Is the Price to Pay If Endolymphatic Sac Exposure or Drainage Is of No Benefit?

Ioana Tereza Herisanu¹; Martin Westhofen²; Ioana Tereza. Herisanu¹

¹ENT University Clinic Aachen; ²ENT University Clinic Aachen

Introduction

We evaluated over the years different operative methods regarding M. Menière patients with vertigo with or without residual hearing. In functional deaf patients, we concluded that after resolving the vertigo, a cochlear implant is of benefit for the hearing rehabilitation. (ARO 2015) In patients with residual hearing we opted for endolymphatic sac exposure (ARO 2016), the drainage could be an option. In patients with no response to the endolymphatic sac operation, the next operative step could be a labyrinthectomy or a neurotomy. We present a third solution: the cochleo-sacculotomy with simultaneous cochlear implantation.

Material and Method

We did a retrospective study on 18 patients with M. Menière implanted between 2013 and 2016 in our cochlear implant program. After Schuknecht, with a 3 mm hook, through the round window membrane the lamina spiralis ossea is being perforated, establishing a permanent shunt between the ductus endolymphaticus and

the ductus perilymphaticus. The hook should reach the middle of the stapes footplate, which opens the hydroptic sacculus in the vestibulum as well.

Results

From 18 patients, all with high doses of Betahistin as conservative medication for M. Menière, seven had undergone an endolymphatic sac drainage-operation in advance. All patients had repetitive typical M. Menière attacks with severe hearing loss between 70-100 dB, with no benefit from hearing aid. Directly after the operation, 12 patients had acute vertigo. In 9 from 18 patients the compensation occurred within three months. Four patients still had M. Menière attacks. In one we performed a revision surgery with Gentamycin application through a horizontal semicircular canal fistula. The other ones refused surgery. Six patients still complained about ongoing dizziness after 3 months, four of them heaving also a vestibular affection of the contralateral ear. All patients were deaf on the operated ear, but all of them profited from the cochlear implant, reaching a mean speech understanding in quiet of 63% monosyllables at dB opt with the implant alone.

Conclusion

The cochleo-sacculotomy with simultaneous cochlear implantation is an option for patients still heaving M. Menière attacks after conservative therapy or even sacculus exposure or drainage. With this therapy is in most of the cases the attack-form of the disease eliminated. The cochlear implant is the solution for hearing rehabilitation, these being good candidates with short rehabilitation needs. One should consider though the vestibular function of the opposite side, the compensation mechanisms and possibilities in every patient.

PS 228

Furosemide Loading VEMP for Meniere's Disease - Confirming Rupture of Membranous Labyrinth Theory -

Toru Seo¹; Takeshi Fujita²; Katsumi Doi¹

¹Kindai University; ²Massachusetts Eye and Ear, Kindai University Faculty of Medicine

Background

We previously reported that the p13-n23 peak-to-peak amplitude in vestibular evoked myogenic potential (VEMP) increased after furosemide administration in the patients with Meniere's disease (Furosemide loading VEMP: F-VEMP). The recording procedures of VEMP have been developed since then. The first is tone-burst stimulation were used to record VEMP instead of click sound. The second is to neglect variability of muscular tonus, amplitude were evaluated after normalization by integrated EMG. We adjusted

the examination to apply up-to-date clinical setting. We also studied the factors which affected the results. Subjects and methods: Subjects were 25 cases with unilateral Meniere's disease who underwent F-VEMP. The peak-to-peak amplitudes of VEMP were recorded before (AB) and after (AA) 20mg of furosemide administration. The improved ratio (IR) was calculated by the following formula: $IR = 100 \times (AA-AB)/AB$. Tone burst sound stimuli of 105 dB SPL and 500Hz were delivered on an ipsilateral ear. The normalized amplitude was obtained from the raw amplitudes divided by the integral EMG value during 20msec before sound stimuli. According to the prior study, we defined the results as positive when $IR > 22\%$.

Results

The positive ratio was 63% on the affected ear of Meniere's disease, and 24% on the intact ear. The ratio was independent on their age, stage and duration of the disease. The ratio of the cases within 2 weeks after the attack was lower than those over 2 weeks after the attack.

Discussion

Our result seems irrational. Furosemide increases the amplitude of VEMP by the diuretic effect for saccular hydrops on Meniere's disease. Schuknecht suggested that the contamination of perilymph with endolymph by rupture of membranous labyrinth result in the attack of Meniere's disease. Within a short period time after the attack, the rupture should still be existed thus the furosemide could not affect decreasing endolymph in the saccule. After the ruptured membrane repairs, the endolymph accumulate and the reformed hydrops should be decreased by the furosemide. Our interesting result supports the Shuknecht's rupture of membranous labyrinth theory.

PS 229

One Year Follow-up of Treatment of the Mal de Debarquement Syndrome (MdDS) in 91 Cases

Sergei B. Yakushin¹; Bernard Cohen¹; Catherine Cho²; Mingjia Dai¹

¹Icahn School of Medicine at Mount Sinai; ²NYU Langone Medical Center

We conducted a follow-up of 149 patients with the Mal de Debarquement Syndrome (MdDS) who were treated over a year ago. MdDS can be induced by passive motion (classic), generally on water, or can occur spontaneously. The treatment was based on the postulate that MdDS is a result of maladaptation of the vestibulo-ocular reflex (VOR) (Dai et al, *Frontiers in Neurology*, 2014; 5:124). Follow-up forms were completed by 91 (61%) of the 149 patients. Within this group, 78 patients (86%)

had the classic form and 13 (14%) had the spontaneous form of MdDS. The severity of symptoms was measured subjectively on a 10-point scale by comparing their symptoms at the end of treatment to those they experienced at the beginning of treatment. We define the initial success of treatment by a reduction in symptom severity by at least 50%. Immediately after treatment, 65 classic cases (83%) and 7 spontaneous cases (54%) reported a reduction in severity of more than 50%. Some patients who showed immediate improvement after treatment had their symptoms return to the pretreatment levels shortly after returning home. One year later, 34 of the 78 classic cases (44%) and 6 of the 13 spontaneous cases (46%) reported a reduction in severity of $\geq 50\%$ compared to pretreatment levels. Of these patients, 14 classic cases (18%) and 1 spontaneous case (8%) were completely asymptomatic after one year. As yet, the failure of the other 58 patients to respond to the follow-up form is unknown. Thus, the MdDS treatment was successful for $\approx 44\%$ of the patients who responded to the calls for follow-up. Further investigation into the outcome of patients who failed to answer is necessary to determine the overall success rate of the MdDs therapy. Development of an at-home treatment may improve the success rate and increase the long term benefits for patients with MdDS.

PS 230

Treatment of Mal de Debarquement Syndrome (MdDS) in 271 Cases

Mingjia Dai¹; Catherine Cho²; Bernard Cohen¹; Sergei B. Yakushin¹

¹Icahn School of Medicine at Mount Sinai; ²NYU Langone Medical Center

Mal de Debarquement Syndrome (MdDS) is a sensation of constant rocking that follows a motion event (classic case) or occurs without a motion (spontaneous case). We proposed that MdDS was a result of maladaptation of vestibulo-ocular reflex (VOR) and could be treated by readaptation of the VOR by visual-vestibular interaction (Dai et al, 2014). During treatment, we examined patient's history, rock frequency and direction, body drifting, and nystagmus. They were then treated according to the findings for 4-5 days. The treatment was considered to be successful if the severity on a 10-pt scale was reduced by better than 50%. Since 2014 we have treated 271 MdDS patients (Female: 84%; Age: 49 ± 14 year (18 – 87 year); Classic: 83%; Spontaneous: 17%) with an average history 3.0 ± 4.5 years (2 weeks to 41 years). They showed a rocking frequency 0.26 ± 0.19 Hz and a sway frequency 0.32 ± 0.21 Hz, measured by static posturography and tilt sensors. Most patients were diagnosed with visits to more than 5 MDs and

26% of them were on-line self-diagnosed that was finally confirmed by a MD. MdDS symptoms increased in 14% cases when they had one drink of alcohol. Visual and noise intolerance were significantly increased in 42% and 25% cases respectively. A large portion of patients developed motion intolerance, headache/pressure, ear fullness/tinnitus, nausea, lethargy and woozy feeling. Anxiety and depression were reported by 68% and 55% cases, respectively. Treatment was successful in 75% classic and 47% spontaneous cases immediately after the completion of treatment. There were 15% patients reported symptoms free after the treatment. This study shows that MdDS severely affects all ages of people in a long run and that until now the readaptation of the VOR is effective on treating MdDS.

PS 231

What Happens with the Spontaneous Nystagmus During Sleep in Patients with Acute Vestibular Neuritis?

Angela Wenzel¹; Boris A Stuck²; Karl Hörmann¹; Roland Hülse¹

¹University Hospital Mannheim, Department of Otorhinolaryngology Head and Neck Surgery; ²University Hospital Essen, Department of Otorhinolaryngology Head and Neck Surgery

Background

It is known that a spontaneous nystagmus in patients with acute vestibular neuritis can be suppressed by anesthetic or other medication. Less is known whether or how a spontaneous nystagmus alters during the different stages of sleep. Therefore, the aim of the present study was to analyze the spontaneous nystagmus during sleep in patients with acute vestibular neuritis.

Methods

15 patients with vestibular neuritis and a spontaneous horizontal-beating nystagmus were included in this prospective monocentric study. According to the standards of the American Academy of Sleep Medicine (AASM) a cardio-respiratory polysomnography was performed in all patients and electronystagmography was conducted simultaneously. The frequency and amplitude of nystagmus were analyzed during the different phases of sleep and compared to baseline characteristics during waking state.

Results

All patients ($n=15$) showed a mid-frequency horizontal-beating nystagmus with 1.5-4.0 beats/ second when the patients were awake and alpha and beta-waves were present in electroencephalography. When alpha-

and beta activity started to slow down, the amplitude of nystagmus significantly diminished, with no change in frequency. Both frequency and amplitude of nystagmus continuously vanished the closer the patient came towards sleep stage N1. Approximately one minute before sleep stage N1 was attained, the nystagmus was absent in all patients. Accordingly, in sleep phases N2 and N3 no nystagmic eye movements were seen in electronystagmography. If an arousal occurred during sleep phases N1, N2 or N3, the nystagmus immediately recovered for the time of the arousal and disappeared again, when the patient fell asleep.

Conclusions

We could demonstrate that even before sleep phase N1 is attained, the spontaneous nystagmus in patients with acute vestibular neuritis is completely suppressed. We presume that central vestibular structures have influence on this deprivation, additionally also supranuclear structures are involved. Further studies are needed to evaluate if this deprivation of nystagmus during sleep is specific to peripheral vestibular disorders.

PS 232

Derealization and Depersonalization in Adults Suffering from Vertigo

Alexis Bozorg Grayeli¹; Michel Toupet²; Christian Van Nechel³; Sylvie Heuschen⁴; Charlotte Hautefort⁵; Ulla Duquesne⁶; Anne Cassoulet²

¹Otolaryngology Dept., Dijon University Hospital and Le2i, CNRS UMR-6306, Dijon, France; ²Centre d'Explorations Otoneurologiques, Paris, France; ³Clinique des vertiges, and CHU Brugmann, Brussels, Belgium; ⁴Centre d'Explorations Fonctionnelles Otoneurologiques, Paris, France; ⁵Service d'ORL, CHU Lariboisière, AP-HP, Paris, France; ⁶Clinique des Vertiges, Brussels, Belgium

Introduction

The aim of this study was to investigate the relation between chronic vertigo, personality disorders, anxiety and depression.

Materials and Methods

321 patients followed-up in a tertiary referral center for chronic dizziness (> 3 months) were included in this prospective study. The population included 215 females and 106 males. The mean age was 58 ± 17.4 years (range: 13-90). All patients underwent clinical examination, caloric tests, eye saccade and pursuit analysis, and subjective visual vertical test. Three auto questionnaires were administered: Hospital Anxiety and Depression scale (HAD, Zigmond & Snaith, 1983), derealiza-

tion and depersonalization inventory (Cox and Swinson, 2002), and questions concerning dizziness in every-day life situations (dish-washing, sport, crossing the street, moving crowd, stairs, screens, acceleration, forward tilt, large empty spaces). In the latter, dizziness was scored from 0 (easy) to 11 (total eviction). Vestibular hypersensitivity was defined as a score of every-day life dizziness > 35/99. Patients were categorized based on clinical and instrumental work-up as follows: Benign Positional Paroxysmal Vertigo (44%), stress (11%), Ménière's disease (10%), migraine (9%), undetermined cause (5%), normal work-up (5%), otolithic disorder (3%), unilateral vestibular weakness (3%), bilateral vestibular weakness (1%), central disorder (3%), miscellaneous (6%).

Results

Patients with a history of migraine (n=111) expressed higher dizziness scores in every-day life situations ($p < 0.05$, ANOVA) and had higher anxiety scores also (9.4 ± 4.72 , n=60 versus 7.6 ± 4.17 , n=103, $p < 0.01$, unpaired t test). Patients with vestibular hypersensitivity had higher depression scores than those with a dizziness score below 35 (6.3 ± 3.77 , n=38 versus 4.4 ± 3.57 , n=113 respectively, $p < 0.01$). Derealization and depersonalization inventory also showed higher scores in patients with a history migraine (6.1 ± 6.40 , n=110 versus 4.0 ± 4.41 , n=210, $p < 0.001$) and in those with vestibular hypersensitivity (6.3 ± 6.35 , n=71 versus 4.3 ± 4.88 , n=271, $p < 0.01$). This score appeared to be related to the vertigo since it was higher during vertigo spells than during the basal dizziness level (9.6 ± 6.67 , n=312 versus 4.7 ± 5.57 , n=320, $p < 0.0001$, paired t-test).

Conclusions

Anxiety, depression and dereality are often associated to the vertigo and appear to be more pronounced in patients with migraine or vestibular hypersensitivity. The impact of vertigo on patient's psychological status appears significant and depends on the background.

PS 233

Evaluation of Emotional Distress in Patients with Dizziness using Hospital Anxiety and Depression Scale

Eun Jin Son; Kyoung Jin Roh; Seong Ah Hong; Sun Geum Kim; Ji Hyung Kim
Yonsei University College of Medicine

Psychological comorbidities are more common in patients with dizziness. Common disorders such as anxiety and depression often complicate the patients' ability to cope with dizziness. The Hospital Anxiety and Depression Scale (HADS) is a widely used self-report instrument used to screen for anxiety and depression in medical outpatient settings. The purpose of this study was to in-

investigate the emotional distress using HADS and compare the results with subjective severity of dizziness using the Dizziness Handicap Inventory (DHI) in patients presenting with dizziness. A retrospective review of patients presenting with dizziness was performed. The HADS and DHI were administered to 275 patients. We investigated the correlation between subjective dizziness handicap and emotional distress using total and subscale scores. The results revealed moderate correlation between the DHI-total scores and HADS-total scores ($r=0.49$). By comparing the subscales of DHI with HADS scores, DHI-E showed higher correlation with HADS (total, Anxiety- and Depression-subscores) than did DHI-F or DHI-P. Our findings suggest that the HADS could be used in conjunction with DHI as a tool to inquire into emotional distress caused by anxiety and depression, which are common psychological conditions in patients with dizziness.

PS 234

Updated Norms for Epidemiologic Screening Tests of the Vestibular System

Helen Cohen¹; Jasmine Stitz²; Ajitkumar Mulavara³; Brian Peters³; Chris Miller³; Haleh Sangi-Haghpeykar⁴; Susan Williams⁵; Jacob Bloomberg⁶

¹Dept of Otolaryngology, Baylor College of Medicine;

²University of Applied Sciences/ Upper Austria; ³KBR Wyle; ⁴Dept of Obstetrics and Gynecology, Baylor College of Medicine; ⁵Dept of Medicine, Baylor College of Medicine; ⁶NASA/ Johnson Space Center

Based on our previous work and on the many screening tests of vestibular system function in the literature we have developed a battery of vestibulo-spinal and vestibulo-ocular tests that may be useful for screening vestibular function. The ultimate goal is to use the battery for epidemiologic studies of the United States population. The battery will also be useful in primary care clinics, nursing homes and other health facilities that do not have access to complex diagnostic testing, and for screening astronauts at remote landing sites after missions to the International Space Station, the Moon or to Mars. The composition of the final test battery is yet to be determined. We present updated norms and statistics on sensitivity and specificity for the tests used in the current battery, including tandem walking, standing balance, dynamic visual acuity, and video head impulse tests.

Supported by NIH grant 2R01DC009031 (HSC), a grant from the National Space Biomedical Research Institute through NASA NCC 9-58 (APM, JJB) and a fellowship from the Austria Marshall Plan Foundation (JS).

PS 235

SENS-111, a New H4R Antagonist, Concentration Dependently Reduces Vertigo Sensation in Healthy Volunteers (HV)

Pierre Attali¹; Frederic Venail²; Eric Wersinger¹; Roberto Gomeni³

¹Sensorion; ²CHU Montpellier, France; ³Pharmacometrika

SENS-111 was reported to reduce vestibular dysfunction in non-clinical models of peripheral vestibular lesions. We have conducted a clinical trial to evaluate overall safety, pharmacokinetic profile and effects of SENS-111 on nystagmus and vertigo induced by a caloric test in HV.

Five cohorts of 12 HV were given either a capsule of SENS-111 (9 subjects/cohort) or placebo (3 subjects/cohort) orally once daily for 4 days (50, 100, 150 mg/d) or 7 days (200 and 250 mg/d) according to a randomized, double-blind, dose-escalating design. Safety was evaluated every day. Pharmacokinetic parameters were determined on the first (D1) and last day (D4 or D7) of treatment and plasma concentrations were measured every day before dosing. Nystagmus and vertigo symptoms induced by a modified caloric test were evaluated at 3 baseline recordings before treatment and then daily (2h post dosing), using videonystagmography, questionnaires (latency, duration of appearance/disappearance of vertigo), Visual Analog Scale (intensity) and European Evaluation Vertigo Scale. A population PK analysis was conducted on all data collected in the study. Two descriptive PK/PD analyses were conducted on the change from baseline values considering SENS-111 exposure and a model based approach was developed to account for the individual trajectories of the response.

Overall 21 mild or moderate TEAEs were reported (placebo: 36 %, SENS-111: 16%), with no serious or severe adverse events. Pharmacokinetics were linear with dose until 200 mg/d and then slightly over-proportional. Steady state was reached at D6. At baseline, nystagmus and vertigo endpoints displayed a large inter-individual variability (17 to 44%). Therefore, no significant difference between placebo and SENS-111 could be detected. However, despite this variability, SENS-111 was shown to significantly ($p < .05$) improve vertigo (latency of appearance, latency of disappearance, duration, intensity sensation), and motion illusion endpoints at doses from 100 to 200 mg as compared to baseline. Positive correlations were seen with either C_{max} or AUC until 200 mg. The latency of vertigo appearance significantly increased with exposure at concentrations below 500 ng/mL while it decreased with concentrations above 500 ng/mL. Consistently, the duration of vertigo and the

latency of vertigo disappearance decreased with the increase of exposure at concentrations below 500 ng/mL.

SENS-111 is well tolerated and improved vertigo symptoms in a concentration dependent manner up to 500 ng/mL where the effects are maximal. These data support the rationale for the choice of doses to be evaluated in patients suffering of acute vertigo symptoms from peripheral vestibular diseases.

Speech Perception

PD 9

Phase-synchronized Responses to Speech in the Guinea Pig Inferior Colliculus Extends past 3000 Hz

Travis White-Schwoch¹; Trent Nicol¹; Daniel Abrams²; Catherine Warrier¹; Nina Kraus¹

¹Northwestern University; ²Stanford University

Phase-locking in the inferior colliculus (IC) has been studied extensively using pure tones and click trains, and it is widely accepted that IC neurons are unable to phase-lock to temporal features greater than 1000 Hz. Less is known about how IC neurons handle speech sounds, which are often differentiated by features > 1000 Hz. Here, we tested the hypothesis that synchronized activity in the IC extends to frequencies above 1000 Hz, thereby contributing to the coding of speech sound identity.

Single-electrode recordings were made from the central nucleus of IC in anesthetized guinea pigs. The stimuli were six synthesized speech sounds that varied parametrically in spectrotemporal structure: [da], [ba], [ga], [ta], [du] and [a]. Across-trial phase synchrony of multiunit responses to each stimulus was evaluated. Consistent with our hypothesis, phases of responses corresponding to the fundamental frequency (100 Hz) and first and second formants (occurring around 700 and 1200 Hz in our stimuli) were strongly synchronized. Importantly, a small, but reliable, amount of phase-synchronized extracellular activity corresponding to the third and fourth formants of our stimuli was also observed (occurring up to 3300 Hz).

To understand the mechanisms driving these response characteristics, spikes from single units in our recordings were identified and their phase-locking properties were computed using vector strength (the extent to which action potentials temporally align with the phase of the stimulus). Phase-synchronized spiking aligned with the fundamental frequency and first and second formants, which can contribute to vowel identification. This suggests that the output of IC neurons conveys sufficient

information to identify vowels. In contrast, single units did not phase-lock to the third or fourth formants, which provide important redundant cues and can contribute to consonant identity.

Thus, phase-synchronized responses to frequency cues > 3000 Hz are evident in multiunit IC responses, but not in single unit output. This hints at a mechanism where, in a coordinated population code processes information beyond the phase-locking limit of single neurons.

Supported by NIH R01 HD069414 and the Knowles Hearing Center.

PD 10

Signs of Post-Stimulus Auditory Processing in Pupillary Responses

Matthew Winn

University Of Washington

Pupil dilation has long been used to measure effort or general cognitive arousal in a variety of tasks. Traditionally, the main outcome measure is peak pupil dilation or the mean pupil dilation within some target window. In this presentation, we explore how another feature, the time course of the growth and decay of pupil dilation, can lend further insight into post-stimulus auditory processing.

A series of pupillometry experiments presented listeners with sentence-length stimuli that included various challenges such as spectral degradation, unpredictable sentence content, concurrent memory tasks, or the need to reflect on what was heard to produce a new response. Conditions included situations in which the challenge was in the form of signal degradation (impacting sensory encoding), inability to predict sentence content (linguistic predictive processing), the need for post-stimulus lexical restoration, or post-stimulus auditory processing that could interfere with such restoration. Stimuli included IEEE sentences and R-SPiN (including low- and high-context) sentences.

Conventional measures of peak and mean pupillary responses generally confirmed original hypotheses, but some effects were observed at specific time landmarks that specifically indicated effects of stimulus condition or linguistic content during or after the target sentence. For spectrally degraded sentences, there were signs of reduced effort following sentences that were repeated correctly, and sustained elevated effort for incorrectly perceived sentences, suggesting continued processing well after the stimulus. There was clear reduction

of effort after high-context sentences regardless of intelligibility, suggesting quicker release from processing load when the signal was predictable. Participants with hearing loss (including cochlear implant users) generally showed sustained elevated pupil size, especially in the presence of post-stimulus distractor sounds, consistent with sustained post-stimulus processing. The introduction of post-stimulus sound (including digit sequences or unintelligible noise) interfered with post-stimulus reduction of pupil size, suggesting interference with linguistic resolution, or “retrieval interference”.

These results suggest that the timing of the pupil response decay can be interpreted as a signature of post-stimulus auditory processing, which can be elusive in traditional tests of intelligibility. This can be a useful measure in situations where listeners make linguistic judgments or other complicated decisions about stimuli, or where integration of multiple auditory signals results in a single behavioral response. Evidence of interference with pupil reduction after a stimulus suggests that continuous speech in normal conversation could potentially interfere with complete processing of recent sentences.

PD 11

Prevalence and Assessment of Functional Hearing Deficits in Blast Exposed Individuals with Normal to Near-normal Hearing Thresholds

Ken W. Grant¹; Lynn Bielski²; Douglas S. Brungart³; Andrew Fallon⁴; Hector Galloza²; LeeAnn Horvat²; Melissa Kokx-Ryan²; Geneviève Krackau⁵; Lina Kubli⁶; General Lee²; Sandeep Phatak²; Carole Roth-Abramson⁵; Olga A. Stakhovskaya⁷; Kenneth W. Grant²

¹Walter Reed National Military Medical Center, Bethesda, MD; ²Walter Reed National Military Medical Center;

³National Military Audiology and Speech Pathology Center, Walter Reed National Military Medical Center, 4954 North Palmer Road, Bethesda, MD 20889-5630;

⁴WHASC.BAMC - San Antonio; ⁵NMC - San Diego;

⁶Department of Veterans Affairs; ⁷Walter Reed National Military Medical Center, Bethesda, MD; Department of Hearing and Speech Sciences, University of Maryland, College Park, MD

It is well established that listeners with normal-hearing thresholds can have difficulty understanding speech in complex noisy backgrounds. This is especially true for military personnel who have been exposed to sub-concussive, high-intensity blast(s). Whether or not this problem is a manifestation of a “hidden” hearing loss undetected by standard clinical measures, or a central or cognitive processing deficit is unknown. To better understand this problem and to devise a strategy for de-

veloping effective rehabilitation practices, a two-phase multisite study was conducted to estimate the prevalence of functional hearing problems in a military population with normal to near-normal hearing thresholds and normal OAEs, and develop an assessment protocol to determine the probable causes of these functional hearing deficits. Over 3000 participants were in the study. Each participant provided subjective responses to a modified version of the Speech, Spatial, and Qualities of Hearing questionnaire (SSQ) and four brief listening tests evaluating binaural hearing and speech recognition. Results showed that blast exposure increases the likelihood of performing poorly (> 2 standard deviations from the mean of a non blast-exposed, normal-hearing threshold control group) on the SSQ or on binaural and speech processing tasks by as much as a factor of five. In Phase II we examined some of the potential causes of this problem using a battery of tests that probe peripheral, central, and cognitive processes. Two groups of subjects were evaluated. One group had normal-hearing thresholds (≤ 20 dB HL from 250-8000 Hz), no blast exposure, normal SSQ, and normal scores on Phase I measures. The second group was blast exposed, had normal to near-normal hearing thresholds, and performed abnormally compared to our Phase I controls. The battery included roughly 20 tests using auditory and visual stimuli to determine if the effects of blast exposure were limited to auditory processing or could be more generally attributed to cognitive processing deficits. Electrophysiological tests were also used to determine the integrity of neural signals propagating to higher brain centers. By examining peripheral, central, and cognitive function, we aim to develop a strategy to separate hidden hearing loss from other processing deficits caused by blast exposure.

[The views expressed in this article are those of the authors and do not reflect the official policy of the Department of Army/Navy/Air Force, Department of Defense, or U.S. Government.]

PD 12

Improvement in Speech Intelligibility for Familiar Voices is Robust to Manipulations of Fundamental Frequency and Vocal Tract Length

Emma Holmes; Ysabel Domingo; Ingrid S. Johnsrude
University of Western Ontario

When multiple talkers speak simultaneously, a listener finds speech more intelligible if the target talker is someone familiar, such as a friend or spouse. However, the voice characteristics that underlie this improvement in intelligibility are currently unknown. We investigated whether simulated changes to fundamental frequency (F0) or vocal tract length (VTL) reduced (1) the ability to

recognise familiar voices, and (2) the speech intelligibility benefit gained from a familiar compared to unfamiliar target talker.

We recruited pairs of participants who had known each other for at least 6 months and who spoke regularly. Participants recorded sentences from the BUG corpus (Kidd et al., 2008), which follow the structure: "Name verb number adjective noun". Sentences were processed (using Praat) to simulate changes in F0 or VTL. In Experiment 1, we first measured each participant's 90% threshold for detecting manipulations to F0 and VTL. Next, participants completed an explicit recognition task, in which they had to detect sentences that were spoken by their familiar partner, and a speech intelligibility task, in which participants heard two sentences spoken simultaneously by different talkers and had to identify words from the sentence that began with a target name. Each task used three voice manipulation conditions: (1) the original F0 and VTL were preserved, (2) F0 was manipulated to the participant's F0 discrimination threshold, and (3) VTL was manipulated to the participant's VTL discrimination threshold.

Although participants could reliably detect differences in F0 and VTL, participants still (1) recognised their familiar partner and (2) found familiar target talkers more intelligible than novel talkers; these two effects were similar for sentences with manipulated F0 and VTL as sentences with the original F0 and VTL. Experiment 2 used larger modifications (five times the median threshold from Experiment 1), corresponding to changes of 40.25% and 26.75% of the original voice F0 and VTL respectively. We also introduced a condition in which both cues were manipulated in combination. Preliminary results indicate that participants discriminate all three manipulations with close to 100% accuracy. All three manipulations degraded the ability to recognise the familiar voice, but none affected the speech intelligibility benefit gained from the familiar voice.

Overall, these preliminary results show that the speech intelligibility benefit gained from familiar voices is robust to large differences in simulated F0 and VTL. The results also suggest that familiar voices do not need to be explicitly recognised to be more intelligible than unfamiliar voices.

PD 13

How Amplitude Envelope and Spectral Resolution Interact with Word Predictability to Facilitate Speech Intelligibility

Bahar S. Shahsavarani¹; Thomas Carrell²; Ashok Samal³

¹*Department of Communication Disorders, University of Nebraska-Lincoln; Boys Town National Research Hospital;* ²*Department of Communication Disorders, University of Nebraska-Lincoln;* ³*Department of Computer Science and Engineering, University of Nebraska-Lincoln*

Normal-hearing children and some children with cochlear implants have demonstrated different patterns of benefit from contextual information in speech perception (Conway et al., 2014). Previous research has discussed the role of non-acoustic factors such as linguistic and cognitive capabilities in this aforementioned discrepancy (Conway et al., 2014; Eisenberg et al., 2002). However, the interaction of acoustic properties such as spectral or temporal information with context effects has been mostly neglected. We found earlier that the benefit from context was enhanced by increasing frequency information from four bands to eight bands in a study of normal-hearing listeners presented with spectrally-degraded speech in noise (Shahsavarani et al., 2015, 170th Meeting of the Acoustical Society of America, Jacksonville). The goal of the present study was to investigate more precisely how temporal and spectral information interact with word predictability to benefit speech perception. A secondary goal was to examine whether better intelligibility was sufficient to prompt the context facilitation. Noise-vocoded speech signals were used as the basis of all stimuli and were processed to examine three levels of frequency quality (four, six, and eight channels), two levels of amplitude envelope resolution (8 and 16 Hz), and two levels of word predictability (low and high). All participants were normal-hearing native speakers of American English. The major finding was that the interaction of the spectral and amplitude envelope information affected the benefit from context. In 4- and 6-band speech, increasing envelope information did not change the intelligibility of low-predictability words. Albeit, the intelligibility of the high-predictability words was significantly improved. This implies that amplitude envelope enhancement helped listeners benefit from predictability to a greater extent. On the contrary, in 8-band speech, increasing envelope information improved intelligibility of low-predictability words, but was not beneficial in the use of context. This intimates that the enrichment of the amplitude information did not aid listeners to take advantage of context facilitation. Consequently, no significant correlation was observed be-

tween the intelligibility improvement and context benefit. Taken together, the results suggest that when frequency resolution is poor, temporal information has a substantial effect on the usefulness of contextual cues. We propose that the ability of cochlear-implant users to encode amplitude envelope information may affect their benefit from contextual cues. This may be especially effective for individuals with poor frequency representation in their auditory nerves (equivalent to four or six frequency channels).

PD 14

The Effect of Acoustic Cue Weighting Strategy on Listening Effort in Acoustic Simulations of Cochlear Implants: A Pupillometry Study

Yue Zhang

University College London

This study examined the relation between cognitive effort and intelligibility of cochlear implant acoustic simulations at different levels of perceptual difficulty, and whether listeners' acoustic cue-weighting strategies affected the behavioral gain from any increase in cognitive effort. Normal hearing listeners were first tested with 8-band 4-mm frequency-shifted noise-vocoded sentences in quiet in order to determine their maximum performance level. Following that, adaptive procedures were used to determine two Speech Reception Thresholds (SRTs) for sentences in speech-shaped noise (also frequency-shifted and noise-vocoded). These were the speech-to-noise ratios (SNRs) required for each listener to obtain 40% and 80% of their performance in quiet. They were then tested with sentences fixed at these two SNR levels and both their percentage correct and cognitive load (measured by pupil mean dilation, peak dilation and peak latency) were recorded. Listeners' weighting strategies on duration and spectral cues were measured with a tense and lax vowel categorization task in quiet, with stimuli processed in the same way.

When perceptual difficulty was high (SRT for 40% correct), higher listening effort was associated with better behavioral performance, but this effect was smaller compared to the perceptually easy condition (SRT for 80% correct). In addition, there was a significant interaction between individual acoustic cue-weighting strategy and pupil response on behavioral performance, suggesting that the acoustic cue-weighting pattern explained a significant amount of variance in the relation between listening effort and sentence recognition. Further trend analysis showed a significant linear trend for cue-weighting pattern in its interaction with pupil response: for individuals with more weighting on the duration cue, higher listening effort was associated with a lower level of performance; while for individuals weighting more on the

spectral cue, higher listening effort was associated with a higher level of performance. This experiment indicated a dynamic relationship between changes in cognitive load and behavioral performance, with the behavioral gain from cognitive effort depending upon individual differences in cue-weighting strategy and levels of perceptual load.

Tinnitus

PD 15

In-Vivo Histological Assessment for Receptor-Mediated Transport of Custom Designed Nanoparticles Across the Brain Barriers into Brain Regions Associated with Tinnitus

Angela Dixon¹; Avril Genene Holt²; Magnus

Bergkvist³; Mirabela Hali¹; Aaron K. Apawu⁴; Antonela Muca⁵; Andre Kuhl⁵; Stephanie Curley³; James Cas-tracane³; Anthony Cacace¹

¹Wayne State University; ²Wayne State University School of Medicine/ JD Dingell VAMC; ³SUNY Poly-technic Institute, College of Nanoscale Science and Engineering; ⁴Wayne State University Medical School; ⁵Wayne State University School of Medicine

Particular auditory brain regions, such as the cochlear nucleus (CN) and inferior colliculus (IC), display noise-induced changes in spontaneous neural activity that can evolve into tinnitus. The design of theranostic nanoparticles (NPs) that localize to these regions would be a giant step forward in the diagnosis and treatment of this condition. The ability to transport drug-loaded NPs across the blood-brain-barrier (BBB) that is impenetrable to many neurotoxins and drugs, presents a fundamental challenge. We have investigated the facilitation of transporting BBB-targeted NPs into the brain.

Three constructs with various biological properties were created: MS2-AP2-FAM (MAF) is a MS2 viral capsid ($\Phi = 30$ nm), conjugated to angiopep2 (AP2) ligand, with a fluorescein (FAM) fluorolabel; MS2-BDP (MB) contains only the capsid linked to a Bodipy (BDP) fluorolabel; and AP2-FAM (AF) is AP2 ligand conjugated to FAM. Low-density lipoprotein receptor-related protein 1 (LRP1) is produced in endothelial and ependymal cells that form blood vessels and line ventricles of the brain, respectively. Since the AP2 peptide (19 amino acids) binds to LRP1, NPs conjugated to AP2 should transport across these barriers.

The constructs were either injected into the fourth ventricle or carotid artery. After 1 hour, brains were removed, and 40 μ m coronal cryostat sections were col-

lected. Regions spanning the rostro-caudal extent of the IC and rostral portion of the CN were analyzed. In each region, 4-6 fields at specific dorso-ventral and medio-lateral coordinates were delineated and assessed to determine the fraction of brain parenchyma covered by nanoparticles, relative to the distance from the ventricle or blood vessel.

While both delivery methods resulted in the presence of each construct within brain, the MB construct was present at a dramatically lower level when compared to AF and MAF constructs. The pattern of distribution for AF and MB constructs was biased ventrally. The MAF construct did not display such a bias in distribution. Both the AF and MB constructs showed a gradient, with the area of NP coverage decreasing laterally from rostral to caudal (AF = 1.26-0.24%; MB = 1.8-0.22%). As observed in dorso-ventral regions, the pattern of MAF construct distribution was also not readily correlated with medio-lateral coordinates.

The more diverse (dorso-ventral, medio-lateral), coordinate-independent distribution of MAF constructs suggests higher transport efficacy (possibly via active transport mechanisms). Lower penetration and more passive migration is implied for AF and MB constructs. Together these results suggest that AP2 facilitates NP transcytosis across brain barriers.

PD 16

Manipulation of the Amygdalo-Auditory Cortex Circuit Influences the Perception of Tinnitus in Rats.

Diana Coomes. Peterson

High Point University

The current study examined whether deactivation of the amygdalo-auditory cortex circuit impacts tinnitus behavior in rats. The perception of tinnitus is caused by cortical neuronal firing in the absence of an auditory stimulus. Amygdalar projections to cortex influence cortical firing based on the significance of incoming auditory stimuli. Because the tinnitus precept is not significant, we hypothesize that amygdalar circuits may be responsible for dampening these signals.

Methods

To identify whether amygdalo-auditory cortex circuits influence tinnitus perception, we injected an optogenetic inhibitory vector construct (AAV-CaMKIIa-eNpHR3.0-EYFP) into the amygdala and implanted a fiber-optic ferrule into auditory cortex. After surgery, animals were allowed to recover for 2-3 weeks to allow the optogenetic vector construct to be transported throughout the neurons and initiate the creation of light-sensitive chloride channels. These channels functionally deactivate affected neurons

by keeping them in a hyperpolarize state. Such deactivation only occurs when the channels are activated by light.

To induce tinnitus, animals were presented with a 120 dB broadband noise located 10 cm from the cranium for one hour while under surgical anesthesia. Animals were tested for tinnitus with acoustic startle gap protocols before surgery (control), 1 day after surgery (so show tinnitus induction), and then immediately prior, during, and after light deactivation of the amygdalo-cortical circuit.

Results

Examination of the tissue indicated that the vector construct was transported both anterogradely and retrogradely throughout the brain. Within auditory cortex, a plethora of labeled axons and boutons were observed in both primary and secondary regions of cortex. Only a few labeled neurons were observed. These results indicate that the injections successfully labeled amygdalar neurons that project to auditory cortex.

Tinnitus induction was successful in all animals. It was observed throughout the duration of the experiment in control conditions. When the fiber optic light was turned on (deactivating the amygdalo-cortical circuit), acoustic startle responses reverted to the non-tinnitus state. This reversion was sustained only for the duration of the time in which the light was turned on. Immediately after laser cessation, acoustic startle results returned to levels indicating tinnitus. These results were repeated numerous times with each animal.

Conclusion

Deactivation of the direct amygdalo-auditory cortex circuit can eliminate tinnitus behavior in rats. However, because tinnitus perception returned after the pathway was released from deactivation, it is likely that other circuits are responsible for the initiation of prolonged tinnitus activity.

PD 17

Tinnitus Correlates with Upregulation of Glutamatergic Synapses in the Cochlear Nucleus Marginal Areas

Chris Chung¹; Amarins Heeringa¹; David T. Martel¹; Calvin Wu²; Susan E. Shore¹

¹*Department of Otolaryngology, Kresge Hearing Research Institute, University of Michigan;* ²*University of Michigan*

Somatic tinnitus is a common form of tinnitus in which patients can modulate their tinnitus with somatic maneuvers of the head and neck. Animal studies have shown that cross-modal auditory-somatosensory plasticity in

the cochlear nucleus (CN) is altered following noise-induced tinnitus (Koehler and Shore, *J Neurosci*, 2013). Furthermore, somatosensory projections to the CN are increased following cochlear damage (Zeng et al., *J Neurosci*, 2009). Therefore, we hypothesize that tinnitus is associated with an upregulation of projections from the somatosensory system to the cochlear nucleus. In the CN, projections of the somatosensory system mostly colabel with vesicular glutamate transporter (VGLUT)2 and sometimes with VGLUT1 (Zhou et al., *J Comp Neurol*, 2007). Furthermore, somatosensory neurons project primarily to marginal areas of the CN, including the small cell cap (SCC), the fusiform cell layer of the dorsal CN (DCN2), and the granule cell domain (GCD), but also to the magnocellular regions of the ventral CN (VCN). To test our hypothesis, we studied the expression of VGLUT1 and VGLUT2 in the different areas of the CN in noise-exposed animals with tinnitus and without tinnitus.

Guinea pigs were noise-exposed unilaterally and behaviorally tested for tinnitus in a gap-prepulse inhibition acoustic startle paradigm. Following transcardial perfusion, brains were isolated, sectioned, and immunohistochemically stained with antibodies against VGLUT1 and VGLUT2. Each area of both CNs was photographed (40X-63X) and puncta density was determined using automated thresholding and puncta counting (ImageJ).

Preliminary results show increases in VGLUT2 puncta density in the ipsilateral GCD and anteroventral CN (AVCN) in tinnitus animals, but not in no-tinnitus animals. Furthermore, VGLUT1 puncta density was increased in ipsilateral DCN2 and the deep layer of the DCN (DCN3) in tinnitus animals, but not in no-tinnitus animals.

Changes in VGLUTs in the CN are much more subtle after noise-exposure than after cochlear ablation. The increase of VGLUT2 puncta density in the GCD and the AVCN suggest a small upregulation of somatosensory projections to the CN with noise-induced tinnitus. The increases in VGLUT1 puncta density in DCN2 and DCN3 are unlikely a result of upregulation of auditory nerve innervation following tinnitus; however, it is likely that VGLUT1-associated somatosensory projections are upregulated following tinnitus-inducing noise exposure. In summary, our results suggest that tinnitus is associated with a maladaptive upregulation of somatosensory projections to the marginal areas of the CN.

Supported by NIH R01-DC004825 (SES) and NIH P30-DC05188

PD 18

Blast-induced Neural Activity and Immunocytochemical Changes in the Auditory Brain Structures of Rats with Tinnitus

Xiuyuan Liang¹; Hao Luo²; Bin Liu²; Edward Pace³; Ruishuang Geng⁴; Lin Chen⁵; Jinsheng Zhang⁶

¹Wayne State University, School of Medicine; ²School of Medicine, Wayne State University; ³Department of Otolaryngology, Wayne State University School of Medicine; ⁴University Hospitals Cleveland Medical Center, Case Western Reserve University; ⁵University of Science and Technology of China; ⁶Wayne State University School of Medicine

Tinnitus is an auditory phantom sensation (ringing of the ears) experienced in the absence of an external acoustic stimulus is present. Bomb explosions are very common in modern war zones and may cause traumatic brain injury (TBI) and accompanying tinnitus. In the current research, we investigated neural activity and immunocytochemical changes in the dorsal cochlear nucleus (DCN), inferior colliculus (IC), and auditory cortex (AC) of rats with blast-induced tinnitus. GAP detection and PPI behavioral tests were used to assess behavioral evidence of tinnitus and hearing status before and after blast exposure. Auditory brainstem response (ABR) was also performed to assess hearing thresholds. Electrophysiologically, we measured changes in spontaneous firing rate (SFRs) and bursting activity in the left DCN, right IC and right AC following blast exposure with the right ears plug-protected. Immunostaining was performed to determine inflammatory changes in these structures. Our results showed that blast exposure induced significant evidence of tinnitus at all frequencies and elevation of ABR thresholds. We also found elevated spontaneous firing rate and bursting rate in post-blast rats compared to post-sham blast control group. The immunostaining results showed changes of GFAP, IBA-1 and IL-18 in post-blast group compared to control group. In conclusion, the evidence of enhanced spontaneous firing rate and bursting activity, and immunocytochemical changes associated with behavioral results of tinnitus indicate that blast has far effects on neural coding of auditory processing in the auditory related brain regions.

PD 19

Neural Correlates of Tinnitus in the Guinea Pig Ventral Cochlear Nucleus

David T. Martel; Amarins Heeringa; Susan E. Shore
*Department of Otolaryngology, Kresge Hearing Research Institute, University of Michigan***Introduction**

Tinnitus, the phantom perception of sound, is correlated with increased neural activity throughout the central auditory system. To date, most studies showing neural correlates of tinnitus in the cochlear nucleus (CN), the first nucleus in the auditory pathway, have focused on plastic changes to fusiform cells of the dorsal cochlear nucleus (DCN). We have shown that tonotopically-restricted increased spontaneous firing rate (SFR) and cross-unit spontaneous synchrony in fusiform cells correlate with behavioral measures of tinnitus (Wu et al., *J Neurosci* 2016). However, this picture is incomplete because humans with tinnitus show enhanced later waves of the auditory brainstem response (ABR) (Schaeffe and McAlpine, *J Neurosci* 2011; Gu et al., *J Neurophys* 2012), which are generated by bushy cells and not fusiform cells. This suggests that bushy cells of the ventral cochlear nucleus (VCN) also play a role in tinnitus. Here we examined the role of the bushy cell pathway in tinnitus generation by recording ABRs and neural activity from bushy cells in animals with behaviorally-verified tinnitus.

Methods

Guinea pigs were exposed to unilateral narrow band noise (1/2 octave, centered at 7 kHz, 97 dB SPL) for two hours to induce temporary threshold shifts. Tinnitus was assessed using gap/prepulse-inhibition of acoustic startle (GPIAS; Turner et al., *Behav Neurosci* 2006), and quantified using distribution differences between pre- and post-exposure GPIAS values. Once chronic tinnitus was established ($p < 0.05$; Student's t-test; 8 weeks after noise-exposure), the animals were anesthetized with ketamine/xylazine, ABRs measured, and 16-channel probes were stereotaxically inserted into the VCN. Individual ABR wave amplitudes were manually identified and normalized by the corresponding wave I amplitude. Spontaneous and tone-evoked activity was recorded from bushy cells in the VCN, which were identified by their location in CN and PSTH pattern (Winter and Palmer, *J Acoust Soc Am* 1990).

Results

Animals with tinnitus demonstrated greater relative suprathreshold ABR wave II-V amplitudes than animals without tinnitus. Furthermore, bushy cells in animals with tinnitus showed increased spontaneous firing rates.

Conclusions

Our results demonstrate that, in addition to DCN fusiform cells, VCN bushy cells potentially play an important role in noise-induced tinnitus pathology. By characterizing the mechanisms of tinnitus in VCN bushy cells, the ABR could potentially be developed into an objective diagnostic test for tinnitus in animals as well as in humans. Future studies are necessary to reconcile tinnitus-related activity in DCN and VCN.

Funding

R01-DC004825 (SES)
T32-DC00011 (DTM)

PD 20

Hyperacusis and Tinnitus Development over Age and the Influence of Noise Exposure in the Rat Behavioral Model

Dorit Möhrle; Kun Ni; Dan Bing; Ksenya Varakina; Ulrike Zimmermann; Marlies Knipper; Lukas Rüttiger
University of Tübingen, Department of Otolaryngology, Tübingen Hearing Research Centre (THRC), Molecular Physiology of Hearing

Hyperacusis and Tinnitus both often occur in conjunction with a loss of hearing sensitivity, but neither hearing threshold loss nor cochlear hair cell loss is essential to develop either condition [1]. In the present study we explore how the reduced sensory function of the cochlea and changes of central activity patterns in the ascending auditory pathway through noise-induced or age-related hearing loss (NIHL or ARHL) is involved in the development of Tinnitus or Hyperacusis. To investigate the effects of ARHL and NIHL on loudness perception (Hyperacusis) and Tinnitus, an animal model based on operant conditioning was applied in young, middle-aged and old rats [2]. Changes in hearing threshold, supra-threshold auditory processing at sensation level, and outer hair cell function were measured by auditory brainstem response (ABR) and distortion product otoacoustic emission (DPOAE). Immunohistochemistry was performed on cochlear sections to analyze the hair cell molecular phenotype. Behavioral measurements of Hyperacusis and Tinnitus, before and after auditory overstimulation, were correlated to changes in peripheral and central hearing function and to morphological specifications of cochlear and brain molecular phenotypes. The results suggest that the development of Tinnitus and/or Hyperacusis involves a distinct failure to adapt the central responsiveness and an insufficient compensation of the reduced cochlear output after auditory overstimulation.

This study was supported by grants from the Deutsche Forschungsgemeinschaft (FOR 2060 project FE 438/5-

1, DFG-Kni-316-4-1, KN316/12-1, and RU713/5-1), Action on Hearing Loss (RNID Grant 54), and the Hahn Stiftung (Index AG).

[1] Dauman R., Bouscau-Faure F. (2005) "Assessment and amelioration of hyperacusis in tinnitus patients." *Acta Otolaryngol.* 125(5):503-9.

[2] Rüttiger, L., et al. (2003). "A behavioral paradigm to judge acute sodium salicylate-induced sound experience in rats: a new approach for an animal model on tinnitus." *Hear. Res.* 180(1-2): 39-50.

PD 21

Hyperexcitability of Inferior Colliculus Neurons Caused by Age-related Hearing Loss

Wei Sun¹; Binbin Xiong¹; Senthilvelan Manohar²; Guang-Di Chen²; Richard Salvi²

¹University at Buffalo, The State University of New York; ²Center for Hearing & Deafness, Department of Communicative Disorders and Science, State University of New York at Buffalo

Object

There is a high incidence of chronic tinnitus and hyperacusis in the elderly population with age-related hearing loss. However, the physiological changes in the central auditory system associated with age-related tinnitus and hyperacusis is poorly understood.

Methods

To identify the age-related neurophysiological changes occurring in the inferior colliculus (IC) of C57BL/6J mice with early onset age-related hearing loss, we recorded the sound driven activity and the spontaneous firing rates of IC neurons with 16 channel electrodes in 2, 6 and 12 month old mice.

Results

The averaged threshold of IC neurons increased from 22.2 ± 0.82 dB ($n = 81$) in 2 month old mice to 37.6 ± 0.73 dB ($n = 66$) in 6 month old mice and 59.2 ± 1.97 dB ($n = 60$) in the 12 month old group. The averaged characteristic frequency (CF) of IC neurons shifted from 10.9 ± 6 kHz ($n = 81$) in the 2 month old group to 9.9 ± 2 kHz ($n = 66$) in the 6 month old group, and 8.0 ± 1 kHz ($n = 60$) in the 12 month group. In the 6 month group, there was no response of IC neurons with CFs higher than 16 kHz. These data indicate a tonotopic map change associated with the onset of aging related hearing loss. Interestingly, the spontaneous firing rates and sound evoked activity of IC neurons increased significantly in the 6 month old group compared to the 2 month old group. The increased spontaneous activity, similar to that found in noise-induced hearing loss

model, may be a neural correlate of tinnitus associated with age-related hearing loss whereas the increase in sound-evoked activity may be related to hyperacusis. These neurophysiological changes may be caused by reduced central inhibition. Spontaneous and sound evoked activity in the 12 month old group was less than in the 6 month old group, but still greater than the 2 month old group; the decreases between 6 and 12 months may be related to the increased of age-related hearing loss.

Conclusion

Our results suggest that the excitability changes in the IC induced by age-related hearing loss may be a physiological evidence of tinnitus/hyperacusis particularly at level of moderate hearing loss. These functional changes may be related to tinnitus and hyperacusis seen in aging population.

Auditory Cortex: Anatomy, Physiology & Function

PD 23

Noise-Induced Hyperacusis/Recruitment in Rats and the Underlying Hyperactivity in the Central Auditory Areas

Guang-Di Chen; Kelly Radziwon; Benjamin D. Auerbach; Richard Salvi
Center for Hearing & Deafness, Department of Communicative Disorders and Science, State University of New York at Buffalo

Besides elevating threshold, sensorineural hearing loss dramatically alters loudness growth, often leading to loudness recruitment. However, in some cases, individuals develop hyperacusis, a condition in which suprathreshold sounds are perceived as much louder than normal at moderate to high intensities. The neural mechanisms underlying loudness recruitment and hyperacusis are poorly understood, but there is growing awareness that these disorders may arise from aberrant neural activity within the central auditory pathway. To address this issue, we obtained behavioral loudness growth functions in rats by measuring reaction time-intensity (RT-I) functions before and after inducing a high-frequency hearing loss. Afterwards, we measured sound-evoked neural responses in the auditory cortex (AC) and lateral amygdala (LA).

The rats were continuously exposed to a narrowband noise (16-20 kHz) at 105 dB SPL for 7 weeks. Behavioral RT-I functions to tone bursts and audiograms were measured pre- and post-exposure. We used 16-channel microelectrodes to record multi-unit spikes discharge and local field potentials from the AC and LA. Afterwards, we measured the neural output of the cochlea

by recording the compound action potential (CAP). The cochleae were harvested for hair cell counting.

At frequencies within the noise band, RTs were slower than normal at low intensities, but at 90 dB SPL, RTs were normal, indicative of loudness recruitment. In contrast, neural input/output functions in the high-frequency regions of the AC never reached control values (i.e., hypoactive). Interestingly, the neural input/output functions in the LA caught up to control levels consistent with the behavioral measures of loudness. Importantly, the low-frequency RT-I functions showed evidence of hyperacusis, i.e., faster than normal RTs at moderate to high intensities. Consistent with the behavioral measures of hyperacusis, the neural I/O functions in both the AC and LA were much larger than normal in the noise-exposed rats (i.e., hyperactive).

Prolonged exposure to high-frequency noise induced behavioral evidence of loudness recruitment in the region of high-frequency hearing loss and hyperacusis in the low frequency regions where hearing thresholds were normal. The hyperacusis-like behavior at the low frequencies was associated with neural hyperactivity in both the AC and LA at high intensities. In contrast, loudness recruitment-like behavior at the high frequencies was associated neural hypoactivity in the AC, but normalized neural responses in the LA at high intensities. These results suggest that both the AC and LA may play a role in loudness perception. Research supported by grants from NIH (R01DC014693, R01DC014452 and F32DC015160).

PD 24

Sequence Context Influences Behavioral Recognition of and Neural Responses to Familiar Courtship Song in Zebra Finches

Jeffrey Knowles¹; Michael S. Brainard²

¹UCSF Department of Neuroscience; ²UCSF Departments of Physiology and Psychiatry

Many natural communication sounds are composed of sequences of acoustic features, yet it remains unclear how brains aggregate information from these sequences to identify acoustic objects. We asked whether sequential context contributes to behavioral recognition and cortical representation of zebra finch courtship songs, natural communication sounds that have sequential structure resembling that of human speech. We trained female zebra finches to recognize a target motif from a set of distractor motifs, while limiting which sequence elements the birds could use to distinguish the stimuli. We found that when birds were operantly trained to recognize target motifs based on particular information bearing syllables (IBS), behavioral responses depended

on both IBS and non-informative prefix sequences. We then asked whether neurons in the auditory forebrain of trained birds displayed an enhanced representation of IBS compared to non-information bearing syllables (NIBS) and novel syllables (NS). We further compared neural responses to known motifs (KM) and novel motifs (NM) to test the importance of sequence context on the representation of IBS. We found that neurons in the thalamocortical recipient area L2 displayed facilitated responses to IBS compared to NIBS and to KM compared to NM. However, in higher regions including CM, neurons displayed enhanced representation of KM but not IBS presented in isolation. Motif responses in L2 were well predicted by a linear sum of syllable (LSS) responses, whereas motif responses in higher stations were poorly predicted by a LSS model. Many neurons in secondary regions displayed striking context sensitivity in their responses to decompositions of the target motif. Neural responses to manipulated target motifs correlated more strongly with behavioral responses in secondary stations than in the primary area L2. These experiments suggest that the representation of information bearing features is modulated by the sequential context of non-informative elements of communication sounds and neural sensitivity to sequential context seems to emerge between primary and secondary regions in the auditory forebrain.

PD 25

L5 Corticocollicular and L6 Corticothalamic Neurons Support a Parallel and Complementary Analysis of Auditory Stimulus Features

Ross S. Williamson¹; Graham Voysey²; Daniel B. Polley³

¹Eaton Peabody Laboratories, Massachusetts Eye and Ear Infirmary; ²Boston University; ³Eaton-Peabody Laboratories, Massachusetts Eye and Ear Infirmary

Introduction

Neurons in layers (L) 5 and 6 of the auditory cortex (ACtx) give rise to a massive subcortical projection that innervates all levels of the central auditory pathway as well as non-auditory areas including the amygdala, striatum, and basal ganglia. L5 and L6 neurons feature distinct morphology, connection patterns, intrinsic membrane properties and synaptic properties, yet little is known about how these differences relate to sensory selectivity in vivo. Here, we focused on two distinct ACtx L5 and L6 projection neurons; L5 corticocollicular neurons (L5CCol), and L6 corticothalamic neurons (L6CT).

Methods

We developed a dual-channel antidromic optogenetic “phototagging” strategy to isolate single L5CCol and

L6CT units from extracellular recordings in awake, head-fixed mice. We injected two adeno-associated viral constructs (AAV) into ACtx of Ntsr1-Cre transgenic mice, in which cre recombinase is expressed only in L6CT neurons. One cre-dependent AAV encoded Chrimson (a red-shifted channelrhodopsin) and a second non-specific AAV encoded hChR2. One optic fiber was then implanted near the surface of the inferior colliculus and a second near the medial geniculate body. By evoking antidromic spikes from L5CCol neurons with blue light and L6CT neurons with red light, we could simultaneously isolate and characterize both types of projection neurons with a single multi-channel recording probe in ACtx.

Results

L5CCol neurons exhibited shorter response latencies and broader frequency tuning than L6CT neurons. Linear spectrotemporal receptive field (STRF) fits were able to explain a higher percentage of response variance in L5CCol neurons, indicating a higher degree of linearity in their responses when compared to L6CT units. Finally, we used a closed-loop evolutionary stimulus optimization strategy to identify the best stimulus for L5CCol and L6CT neurons across a 4-dimensional stimulus manifold. The evolutionary search strategy manipulated the modulation frequency, level, spectral bandwidth, and center frequency of noise tokens in real time based on spike feedback to identify an optimal stimulus. We found that L5CCol neurons featured a lower multi-dimensional sparseness index, indicating a reduced stimulus selectivity and a broader response distribution than L6CT neurons.

Conclusions

These findings suggest a functional dichotomy in the form of stimulus-related modulation imposed by L5 and L6 neurons to subcortical targets. Future work will entail recording from these projection neurons during task engagement to establish how these functional differences are adaptively used in service of goal-directed behavior.

PD 26

Neural Correlates of Multisensory Behavior in the Auditory Cortex

Fernando R. Nodal¹; Amy Hammond-Kenny¹; Victoria M. Bajo¹; Andrew J. King²

¹Oxford University; ²University of Oxford

Our perception of everyday events relies on the integration of information from different sensory modalities. The multisensory processing required for such integration has been observed even at the level of early sensory cortices. However, most of the studies have been performed under anesthesia, and therefore the behavioural

relevance of the cross-modal interactions observed remains to be determined. Here, we explore the multisensory nature of the ferret auditory cortex by recording local field potentials (LFPs) and neuronal spiking activity while animals perform an auditory-visual localization task, thereby enabling correlation of neural and behavioural changes. Initially, ferrets were trained by positive operant conditioning to localize unisensory (auditory or visual) and spatiotemporally coincident auditory-visual stimuli presented from one of seven locations spanning the frontal hemifield. During the localization task, we recorded the initial head orienting response and the subsequent choice of which target location to approach in order to receive a reward.

Head orienting responses to auditory-visual stimuli were more accurate and faster than those made to visual but not auditory targets, suggesting that these movements were guided principally by sound alone. In contrast, approach-to-target localization responses were more accurate and faster to auditory-visual stimuli throughout the frontal hemifield than to either visual or auditory stimuli alone. Race model inequality analysis of head orienting reaction times and approach-to-target response times indicates that different processes, probability summation and neural integration, respectively, are likely to be responsible for the effects observed on these two measures of localization behaviour.

Once behavioural abilities were established, neural activity was recorded from the auditory cortex during task performance via bilaterally implanted electrode arrays. Stimulus evoked changes in LFP amplitude and simultaneously recorded spiking activity were observed that varied with the characteristics of the stimulus and the location of the recording electrodes. A total of 509 single units that exhibited excitatory responses to auditory and/or visual stimulation were identified and confirmed, by histological analysis, to reside within the ectosylvian gyrus, where auditory cortex is located. Of these units, 16% (81/509) produced responses that were enhanced or suppressed by visual stimulation. The largest modulation of neural responses occurred at 34 dB SPL, near most unit thresholds, whereas multisensory behavioural gains peaked at 20 dB SPL and declined steadily with increasing stimulus intensity. Our results also show a correlation between neural activity and behavioural outcome. Correct approach-to-target responses were significantly correlated with lower spontaneous firing rates and higher evoked firing rates.

PD 27

Cortical Mechanisms of Perceptual Learning

Melissa L. Caras; Derek Wang; Dan H. Sanes
New York University

Auditory perceptual learning is defined as a long-term improvement in the detection or discrimination of acoustic stimuli. One hypothesis is that sound encoding in core auditory cortex is necessary for learning to occur. To test this idea directly, we both recorded and manipulated auditory cortical activity while Mongolian gerbils (*Meriones unguiculatus*) trained on an aversive Go-Nogo amplitude modulation (AM) detection task. To establish a quantitative relationship between auditory cortical activity and perceptual learning, we implanted chronic microelectrode arrays into left auditory cortex of a group of naïve animals. We wirelessly recorded single and multi-unit activity as animals trained on the AM detection task described above. Neurometric sensitivity was tracked across days and directly compared to psychometric performance. As performance improved, we observed a significant correlation between simultaneously recorded neural and behavioral thresholds within individual animals. However, when recordings were made from animals while they were disengaged from the task, we found that neural thresholds remained relatively constant across days and were not correlated with behavioral performance. To determine whether auditory cortex activity is necessary for behavioral improvement, we used a low dose of muscimol to reversibly attenuate auditory cortical activity bilaterally in a separate group of naïve animals during perceptual training. Muscimol infusions impaired behavioral improvement while still permitting animals to generate psychometric functions. This finding suggested that either muscimol infusion prevented learning from occurring, or prevented its expression. To distinguish between these possibilities, we subjected the same animals to additional training sessions during which saline was infused into auditory cortex. Training paired with saline infusions improved detection thresholds. Together, these findings indicate that reducing auditory cortical activity during training prevents perceptual learning. Collectively, our results suggest that auditory training leads to behaviorally-gated enhancements of cortical sensitivity that ultimately support perceptual learning.

PD 28

Single-neuron Correlates of Auditory Spatial Attention in Auditory and Prefrontal Cortex

Corrie Camalier; Anna Leigh Brown; Jessica Jacobs; Mortimer Mishkin; Bruno Averbeck
Laboratory of Neuropsychology, National Institute of Mental Health/NIH

Auditory spatial attention describes our effortless ability to listen to sound from one location while suppressing distracting sounds from other locations. This is critical for everyday interactions, especially the “cocktail party problem”. Studies from humans have suggested that two key areas implicated in this ability are auditory cortex and prefrontal cortex, but a more detailed understanding of how sound is spatially filtered has been hampered by the lack of a robust animal model, particularly one that shares key similarities with humans.

To address this, we have developed a novel spatial auditory selective attention task for macaques (n=4), based closely on human directed listening paradigms. In this task, a macaque monkey is cued to a particular side and must report the presence of a difficult-to-detect auditory target (embedded in noise) only if it appears on the cued side. If it appears on the uncued side, he must ignore it. In this way, we are able to compare attention effects under identical auditory conditions.

We collected single neuron data from prefrontal cortex (caudal principal sulcus; n = 449) and caudal auditory cortex (A1/CM/CL/TPT; n = 477) in two monkeys during this task. In both areas, attention deployed to contralateral space significantly affected baseline firing rates in about 20% of the responsive neurons and also significantly affected 20-40% of responses to the masking noise, but direction of effects was mixed, possibly reflecting the mixed spatial tuning properties of these areas.

PD 29

Characteristics of Bottom-up Auditory Attention in the Brain

Emine Merve Kaya; Mounya Elhilali; Merve Kaya
Johns Hopkins University

In recent years, there has been increasing interest in understanding mechanisms of bottom-up auditory attention. The field has been particularly biased towards psychoacoustical investigation of what makes certain sound elements salient and correlate such stimulus-specific attributes to behavioral responses from subjects. A limiting factor of such studies is the difficulty of separating a true exogenous account of auditory salience from conscious top-down decision making processes that occur when

subjects perform behavioral experiments. One way to address this shortcoming is to explore neural responses to unattended signals while stimulus characteristics are being manipulated.

Here, we employ EEG recordings to present an unbiased account of bottom-up auditory attention across the cortex. Auditory stimuli interspersed with rare salient sound segments are delivered to the ears of subjects attending to a silent movie. Despite the complexity of using naturalistic sounds as stimuli, we demonstrate attentional gain in a variety of spectro-temporal metrics. Further, we characterize the neural mechanisms as a filter acting on the incoming sound and illustrate the adaptations that occur when exposed to salient sounds of varying acoustic features, such as pitch, loudness and timbre. We find that the bottom-up attentional modulations occur most prominently in the delta (1-3Hz) and theta (3-8Hz) bands, where inter-trial phase coherence is strongest. Importantly, we note a strong interaction between features of the salient sound across the investigated metrics, with the implication that bottom-up feature processing is not executed in parallel across feature maps, but is interdependent. This observation is in line with previous work demonstrating feature interactions from behavioral data. With the methodology used here, we not only corroborate prior psychoacoustical results, we extend our understanding of how the brain processes auditory attention and saliency with information directly obtained from neural activity.

PD 30

Robustness to Real-world Background Noise Increases Between Primary and Non-primary Human Auditory Cortex

Alexander J. E. Kell; Josh H. McDermott
MIT

In everyday listening, the sounds from sources we seek to understand are often embedded in background noise. This noise alters the pattern of spikes in the auditory nerve, often to a profound degree. In order to recognize sources of interest, the brain must to some extent be robust to the effects of these background noises. To study the neural basis of listening in real-world background noise, we measured fMRI responses in human auditory cortex to a diverse set of thirty natural sounds, presented in quiet as well as embedded in thirty different everyday background noise textures (e.g., a bustling coffee shop, crickets chirping, heavy rain hitting pavement). We quantified the extent to which neural responses were robust to background noise by correlating each voxel's response to the natural sounds in isolation with its response to those same natural sounds mixed with background noise. Responses in core regions (TE

1.1 and 1.0) were substantially affected by background noise. However, voxel noise-robustness increased with distance from these primary areas: nearby non-primary areas were slightly more robust, while more distal areas were hardly affected by the background noises. Mean responses in primary and non-primary regions were both only slightly lower in the presence of background noise, indicating that this effect was not due to the background noises differentially suppressing responses in primary areas. Our results provide a neural correlate of the noise robustness of real-world listening, and offer evidence of a hierarchical organization in human auditory cortex.

NIDCD Workshops

Melissa Stick¹; **Bracie Watson**¹; **Katherine Shim**¹;
Roger Miller¹; **Shiguang Yang**¹; **Vasant Dasika**²;
Cherish Guisto²; Amy Donahue¹; Alberto Rivera-Rentos¹

¹NIDCD, NIH, Bethesda, Maryland, USA; ²FDA

Workshop #1: Applying for NIDCD Training and Career Development Awards

This workshop will include an overview of research training and career development opportunities appropriate for graduate students, postdoctoral fellows and new clinician investigators. The presentation will include essential information on the submission and review of individual NRSA fellowship awards (F30, F31 & F32), as well as selected mentored career development (K-) awards. Drs. Alberto Rivera-Rentas and Melissa Stick will lead the discussion and provide updates on these funding mechanisms.

Workshop #2: Early Stage Investigators (ESI) and New Investigators (NI)

This workshop will provide information for junior scientists seeking to obtain their first research project grant. The goal is to answer questions and clarify the application, review, and award process for the NIDCD Early Career Research (ECR) R21 Award and the NIDCD R01 award with respect to ESIs and NIs. This workshop is intended for both postdoctoral trainees ready to transition to independence and individuals who have recently transitioned to independence, e.g. accepted a new faculty position in the early stages of establishing an independent research program. The presentation will include an overview of the NIDCD Early Career Research (ECR) R21 Award and provide information to facilitate the most expeditious route to funding for R01s. Drs. Bracie Watson and Katherine Shim will lead the discussion.

Workshop #3: SBIR and STTR Grant Programs for Medical Device Development

This workshop will provide an overview of these unique grants, which have funds set aside for awards to small businesses based in the U.S.A. Postdocs considering a new career path or a brief foray into commercialization are especially encouraged to attend. NIDCD staff Drs. Roger Miller and Shiguang Yang will share insights on this unique grant program and Drs. Vasant Dasika and Cherish Giusto from the ENT branch of the FDA will be available to answer questions about regulatory process for medical device development. Brief presentations will go over the crucial elements of successful applications, but substantial time will be allowed to answer questions raised by attendees.

Patterns In Sound Sequences - How Listeners Discover/Learn And Use Regularities In The Acoustic Environment

SYMP 6

Rapid Learning Updates the Mapping of Input to Auditory Objects According to Short-term Input Statistics

Lori Holt

Carnegie Mellon University

Multiple acoustic dimensions contribute to natural sounds' identities, but some dimensions are more diagnostic than others. Listeners are sensitive to these patterns. For example, in speech categorization, listeners give greater 'perceptual weight' to the acoustic dimensions most diagnostic of phonetic category identity. But, sensitivity to long-term input statistics can be deleterious in the short-term when local signal statistics deviate from the norm. Such is the case in speech recognition when listeners encounter foreign-accented speech. I will present a series of studies demonstrating that listeners rapidly adjust perceptual weights according to the short-term regularities of the acoustic environment, without destroying sensitivity to long-term regularities. Our results indicate that the auditory system tracks correlations among acoustic dimensions across sequences of sounds. Moreover, in response to correlations that deviate from the norm the system rapidly adjusts the effectiveness of dimensions in signaling objects while leaving the perceptual representation of the dimension intact. I will describe the results in the context of an error-driven supervised learning model and present fMRI evidence consistent with cerebellar involvement in generating an error signal to drive rapid updating of the mapping from acoustic input to auditory objects.

SYMP 7

Figure-ground Analysis Based on the Sequential Grouping of Spectral Patterns

Timothy D. Griffiths¹; Maria Chait²; Inyong Choi³; Pradeep Dheerendra⁴; Phillip E. Gander⁵; Sukhbinder Kumar⁶; Sundeep Teki⁷

¹Newcastle University; ²Ear Institute, University College London, UK; ³Department of Communication Sciences and Disorders, University of Iowa; ⁴Institute of Neuroscience, Newcastle University; ⁵Human Brain Research Laboratory, The University of Iowa; ⁶Institute of Neuroscience; ⁷DPAG, University of Oxford

This work addresses generic mechanisms for recognition of auditory targets in noisy backgrounds using stochastic stimuli. The work specifies a general system relevant to speech-in-noise perception. Deficits in speech-in-noise perception are a ubiquitous symptom of cochlear and central disorder.

Non-invasive human MEG and fMRI work specifies a system involving auditory cortex and intraparietal sulcus. Invasive human local field potentials in auditory cortex demonstrate high-frequency oscillatory activity corresponding to figure emergence. Macaque fMRI is starting to define a model system that allows systematic neural characterisation.

This paradigm allows an intermediate level of assessment between the pure tone audiogram and speech being piloted in clinical studies.

SYMP 8

Rapid Implicit Learning of Sound Schema for the Cocktail Party Problem

Kevin Woods¹; Josh H. McDermott²

¹Department of Brain and Cognitive Sciences, MIT;

²MIT

Auditory scene analysis is believed to rely on regularities of natural sound sources, but little is known about how such regularities are acquired. We explored whether listeners internalize source "schemas" – the abstract structure shared by different occurrences of the same type of sound source – during cocktail-party listening. We measured the ability of listeners to track one of two concurrent sources as they evolved stochastically in three features (pitch and the first two formants). On a subset of trials, the tracked source's trajectory through this space took a similar shape, each time transposed and time-dilated to avoid exact repetition. Rapid improvements in performance were seen over the first ~15 presentations of this

trajectory shape, indicative of learning. We were able to observe this rapid effect by crowdsourcing data from a large number of subjects online. Learning appeared to be implicit, in that participants were equally likely to report hearing recurring trajectory shapes in the distractor voice when they only occurred in the target. When the distractor voice did in fact contain similar sources, tracking performance was unaffected, indicating that only attended sources could be learned. The results identify a mechanism for internalizing abstract source regularities on the scale of seconds, facilitating accurate perceptual organization of sound sources similar to those attended in the past.

SYMP 9

Hearing Statistical Regularities in Irregular Patterns: Perceptual and Computational Insights

Mounya Elhilali; Ben Skerritt-Davis
Johns Hopkins University

The brain's ability to extract statistical regularities from sound is an important tool in auditory scene analysis, necessary for object recognition, structural learning (in speech or music), texture perception, and novel event detection. Traditionally, the study of statistical structure of sound patterns has focused on first-order regularities; particularly mean and variance measures. In this work, we explore perceptual and computational principles underlying how the brain collects complex patterns in sound sequences, and how it uses them to detect changes in statistical structure, even in inherently random processes such as the fractal melodies that lack absolute predictability.

SYMP 10

Do Acoustic Patterns Capture Attention?

Maria Chait¹; Rosy Chait²

¹*Ear Institute, University College London, UK*; ²*UCL*

In this series of behavioural and electroencephalography (EEG) experiments we investigate the extent to which repeating patterns of sounds capture attention. Work in the visual domain has revealed attentional capture by statistically predictable stimuli, consistent with predictive coding accounts which suggest that attention is drawn to sensory regularities. Here, stimuli comprised rapid sequences of tone pips, arranged in regular (REG) or random (RAND) patterns. EEG data demonstrate that the brain rapidly recognises predictable patterns manifested as a rapid increase in responses to REG relative to RAND sequences. This increase is reminiscent of the increase in gain on neural responses to attended stimuli often seen in the neuroimaging literature, and thus consistent with the hypothesis that predictable sequences

draw attention. To study potential attentional capture by auditory regularities, we used REG and RAND sequences in two different behavioural tasks designed to reveal effects of attentional capture by regularity. Overall, the pattern of results suggests that regularity does not capture attention.

SYMP 11

Neural Oscillations Support Perception in Temporally Regular Acoustic Environments

Björn Herrmann

University of Western Ontario

Environmental stimuli are often characterized by some degree of temporal regularity. Empirical observations indicate that a listener's auditory system utilizes such regularities to guide perception in acoustic environments, for example, by generating temporal expectations (i.e., anticipating when an event will occur) and structuring attention in time. However, how utilization of temporal regularities is implemented behaviorally and neurally remains uncertain.

Oscillator models established in cognitive behavioral research propose that attention is not stable over time but instead waxes and wanes (i.e., oscillates) at an intrinsic or natural idling frequency (i.e., an internal periodicity). These internal, attentional fluctuations can become synchronized with (coupled to) external rhythmic stimulation in temporally regular contexts. Synchronization of the internal periodicity with an external rhythm is hypothesized to provide a temporal reference frame on the basis of which temporal expectations are generated and attention to sounds is structured in time. Using a mathematical oscillator model in combination with psychophysical data from younger and older human listeners, I will show that the probability of detecting a near-threshold acoustic change in a temporally variable sequence depends on the timing of this change relative to the fluctuations of a synchronized oscillatory process.

Low-frequency neural oscillations might provide a biological implementation of internal periodicity and thus a biological substrate for attending in time. Animal electrophysiology suggests that neural oscillations reflect rhythmic fluctuations between high-excitability and low-excitability phases/states of neural populations. Neural oscillations can become synchronized with an external stimulus rhythm such that the high-excitability phase aligns with attended or high-energy portions of sound inputs. Synchronization may then provide the means by which sounds that coincide with the environment's regular temporal structure (and thus with the high-excitability phase) are optimally processed. Consistent with this prediction, I will show for younger and older adults that

the probability of detecting a near-threshold acoustic change depends on the phase of synchronized neural oscillatory activity. The data further indicate that neural synchronization to slow stimulation rates and modulation of change-detection by low-frequency neural oscillatory activity remains intact in older listeners. Aging, however, appears to affect neural oscillatory activity in frequency bands that are not directly related to a stimulus rhythm.

In sum, by referring to animal electrophysiology, oscillator models of temporal attending, and human neural oscillations and psychophysics, I will discuss how temporal regularity in acoustic environments shapes perception via complex neural oscillatory dynamics in different neural frequency bands.

Development 1

PD 31

An Atlas of Cell-Type-Specific Transcriptomes in the Newborn Mouse Cochlea

Joseph C. Burns¹; Adam Palermo¹; Michael C. Kelly²; Matthew W. Kelley³

¹*Decibel Therapeutics*; ²*Laboratory of Cochlear Development, NIDCD, NIH*; ³*Laboratory of Cochlear Development, NIDCD, NIH, Bethesda, Maryland, USA*

Single-cell transcriptional profiling has emerged as a powerful, unbiased tool for dissecting cellular heterogeneity at the molecular level. qPCR of single cells from the developing inner ear has been used to characterize gene expression patterns critical for lineage specification, differentiation, and subtype identity. RNA-Seq of single cells from the sensory regions of the newborn mouse cochlea and utricle has demonstrated the feasibility of extending these studies to the whole transcriptome level, allowing for more comprehensive identification of genes and pathways. Collecting sufficient numbers of single cells in a cost- and time-efficient manner has been a critical limitation to these techniques, but recent adaptations in droplet microfluidics have improved the throughput 100-fold. Given the relatively small size of the mouse inner ear, this improvement in throughput theoretically permits organ-wide profiling of all the cell types in the cochlea in a single experiment. To test this, we separated the entire cochlear portion of the newborn mouse inner ear, dissociated the tissue, and captured single-cell transcriptomes for RNA-Seq using a droplet microfluidics platform from 10X Genomics. From an input of ~16,000 cells, we captured 4,251 single cells. The capture process took 5 min, demonstrating that tissue dissociation is the only substantial time constraint with this system. Unbiased clustering revealed 23 distinct clusters of cells. Based on expression of known marker

genes, 15 of the 23 clusters were identified and included hair cells, supporting cells, neurons, glia, cells of the stria vascularis, interdental cells, and non-sensory epithelial cells of the inner and outer sulcus. Cells within the remaining clusters are likely fibrocytes, mesenchymal cells, immune cells, osteolineage cells, and mesothelial cells; however, their exact localization and identity remains to be determined. At least one cluster of cells could not be ascribed to any known cell type in the cochlea at this stage. The numbers of cells in each cluster were within expected ratios. Differential expression analysis revealed 5,821 genes driving the differences between the 23 cell types, many of which have not previously been localized within the inner ear. This dataset reveals that single-cell RNA-Seq technology has advanced sufficiently that all the major cell types in the cochlea can be profiled in a single experiment. Future applications include comprehensive resolution of cellular fate commitment during development and organ-wide, cell-type-specific responses to insults in adults.

PD 32

A Comprehensive Map of Mammalian Auditory Sensory Cell Development Generated Using High-Throughput Transcriptional Profiling

Michael C. Kelly¹; Joseph C. Burns²; Adam Palermo²; Joseph C. Mays³; Kathryn L. Ellis⁴; Robert Morell⁵; Matthew W. Kelley⁶

¹*Laboratory of Cochlear Development, NIDCD, NIH*; ²*Decibel Therapeutics*; ³*Laboratory of Cochlear Development, NIDCD, Bethesda, Maryland, USA*; ⁴*NIDCD, NIH*; ⁵*Genomics and Computational Biology Core, NIDCD, NIH, Bethesda, Maryland, USA*; ⁶*Laboratory of Cochlear Development, NIDCD, NIH, Bethesda, Maryland, USA*

The exquisite structural and functional architecture of the mammalian organ of Corti is generated through a highly coordinated developmental program that involves cell-type specific gene expression. This program is composed of the dynamic and heterogeneous transcriptional states of diverse cells types within the developing organ of Corti. A characterization of these various states could provide powerful insight into the genes involved in the development of the mammalian auditory end organ. This information has been relatively inaccessible due to technical limitations, but recent advancements in single cell RNA-Seq (scRNA-Seq) techniques have now made analysis on this scale possible.

Through a combination of high-throughput droplet-based and cell-per-well scRNA-Seq approaches, we have built an extensive high-resolution gene expression database

of the cells of the organ of Corti and their surrounding epithelial cells from multiple embryonic and early post-natal timepoints. The complete array of hair cells, supporting cells, and surrounding non-sensory cell types are uniquely identified using known marker genes, and additional genes that show cell-type specific expression are revealed. Moreover, the large number of independent observations of each cell type's transcriptional state over development allow a computational reconstruction of transitions representing cellular differentiation. We use these reconstructed models to identify potential transcriptional cascades that may direct cell fate decisions and changes in plasticity with the organ of Corti. By building branched relationship trees based on transcriptional similarities of cell types representing specific cell types at multiple stages of differentiation, we can also infer lineage relationships and anticipate restrictions. These lineage relationships are supported by preliminary genetic clonal lineage tracing studies, and candidate transcriptional regulators involved in cell fate decisions and differentiation can be evaluated by gain and loss of function studies.

These results further our understanding of the genetic pathways involved in organ of Corti development and patterning, provide a basis of comparison for potential aberrant states in mutant and disease models, and may help identify sets of transcriptional regulators that can direct the differentiation of unique cell types. This work also suggests a pattern of developmental lineage restrictions that provide important developmental context for cell type conversion strategies such as those proposed for auditory hair cell regeneration.

PD 33

Generation of Three-Eared Chickens Reveal Afferent Pathfinding Properties of Central Projections

Karen Elliott-Thompson; Bernd Fritzsch
University of Iowa, Dept of Biology.

Background

The inner ear makes stereotyped connections between the periphery and the CNS, though little is known about how these inner ear neurons find their vestibular and auditory target nuclei within the hindbrain. During development, inner ear afferents of the auditory and vestibular neurons project directly into the correct nuclei before the second order neurons become postmitotic, suggesting some attraction of these nuclei primordia for ingrowing ear afferents. Central projections thus behave like peripheral fibers who project to the organ of Corti area lacking hair cells (Pan et al., 2011). Grafting an additional ear in frogs results in transplanted and native ear projections overlapping to the vestibular nucleus, suggesting that ear afferents use molecular cues to

find the vestibular column. Work on salamanders and zebrafish suggests that central projections of the various cranial nerves follow a medial-lateral spatiotemporal pattern in the hindbrain based on the timing of entry. Our previously transplanted frog ears could have used such spatiotemporal cues. To test whether the ear is guided molecularly or spatiotemporally, we transplanted an additional ear rostral to the native ear in the chicken, which has a larger hindbrain and a more pronounced auditory system than frogs, at various time points, including at approximately the time neurons in the native ear are delaminating. This creates a delay in entry of ear afferents into the hindbrain from the transplanted ear relative to the native ear.

Methods

Otic vesicles were transplanted at various stages (HH 15-19) adjacent to the native ear in chicken embryos in an eggless culture system. Axonal projections were labeled using tracing of the native and transplanted ears. Results: Vestibular axons from the transplanted ear enter the hindbrain after axons from the native ears, as observed by dye labeling. Vestibular axons from the rostrally transplanted ears enter the hindbrain either with the trigeminal nerve and reroute from the trigeminal tract into the vestibular nucleus or enter as a separate entity and project immediately into the vestibular nucleus. In addition, labeling of auditory fibers in the transplanted ear resulted in a distinct projection lateral to the vestibular nucleus, indicating segregation of auditory and vestibular fibers.

Conclusion

These results suggest that inner ear afferents are molecularly targeted to project to their respective nuclei in the hindbrain regardless of entry point or timing. We are currently transplanting mouse ears to chickens to test for molecular conservation across species with respect to axon guidance.

PD 34

Lineage Analysis of Sonic Hedgehog Expressing Cells in the Developing Mouse Spiral Ganglion

Lok Sum Wong; Doris Wu

Laboratory of Molecular Biology, National Institute on Deafness and Other Communication Disorders, National Institutes of Health

Background

It has long been established that hair cell precursors at the apex of the organ of Corti (oC) begin to exit from cell cycle at E11.5 but remain undifferentiated until E17.5, whereas their counterparts at the base undergo differentiation promptly after terminal division starting at E13.5. The delay in hair cell differentiation at the

apex is attributed to a subpopulation of Sonic Hedgehog (Shh)-expressing spiral ganglion neurons (SGNs) in proximity to the cochlear apex during cochlear duct formation. Since this base-to-apex order of hair cell differentiation is thought to pre-stage tonotopic organization of the oC, understanding the regulation and nature of these Shh-positive SGNs is important. Here, we lineage traced Shh-expressing cells during cochlear development to determine whether Shh expression represents a restricted population of SGNs that migrates to the apex or it represents a particular stage of SGN development.

Methods

Tamoxifen-inducible ShhCreER transgenic mice were bred to Cre-reporter strains (RosaYFP or RosatdTomato). We then compared Shh lineage cells in the spiral ganglion of ShhCreER;RosaYFP or ShhCreER;RosatdTomato ears, in which Cre was activated at different times during cochlear development.

Results

When tamoxifen was administered at E14.5, labeled neurons were found at the cochlear apex at E17.5, comparable to the known location of Shh transcripts. However, earlier induction of tamoxifen at E10.5 showed that majority of the SGNs at E17.5 was fluorescently labeled from base to mid-apex. The position of these lineage-labeled cells along the cochlear duct at E17.5 suggested that Shh-expressing cells at E10.5 gave rise to neurons at the base and mid regions, whereas they stopped expressing Shh by E14.5 and only apical SGNs were Shh-positive at this stage. Together, these results reveal that SGNs only express Shh transiently. Extrapolating the birth dating data by R.J. Ruben (1967) showing that neuronal precursors exit from cell cycle in a base-to-apex direction starting at E12 to our lineage results, we hypothesize that Shh is only expressed transiently in dividing or nascent neurons.

Conclusion

Our lineage results suggest that Shh expression in the developing spiral ganglion represents a stage of neuronal development that all SGNs undergo rather than a sub-population of neurons with a restricted fate. We are currently investigating the relationship between timing of Shh expression and cell cycle progression in SGNs and the functional significance of this transitory Shh expression.

PD 35

Activation of Wnt Signaling Through the Neonatal Stages Induces Support Cell Proliferation and Promotes Hair Cell Induction in Response to Notch Inhibition

Anshula Samarajeewa¹; Lihong Xie²; Dara O'Connor²; Joanna Mulvaney²; Alain Dabdoub²

¹Department of Laboratory Medicine & Pathobiology, University of Toronto; ²Biological Sciences, Sunnybrook Research Institute, University of Toronto

Background

Support cells (SC) of the neonatal mouse cochlea can transdifferentiate into hair cells (HC) when Notch signaling is inhibited. This transdifferentiation can occur up to postnatal day (P) 3 and comes at the cost of SC loss. Since the canonical Wnt pathway plays a role in proliferation and HC differentiation during cochlear development, it is a potential target for preserving SC numbers and regenerating HCs. The key effector of canonical Wnt signaling is stabilized β -catenin. Here, we investigated whether stabilization of β -catenin in vitro can promote proliferation prior to HC induction in the post-mitotic cochlea in order to preserve SC numbers and induce HCs.

Methods

We exogenously activated Wnt in cochlear explants at embryonic day (E) 13, P0 and P5 and quantified the response in terms of proliferation and HC induction after six days in vitro. Next, we used western blots to quantify β -catenin in cochleae transiently exposed to a Wnt activator at the same three stages – E13 when Wnt signaling is active, P0 when endogenous Wnt signaling is diminished and exogenous Wnt activation leads to proliferation, and P5 when endogenous Wnt is absent and exogenous Wnt has no effect. Finally, we treated P0 explant cultures for five days with Wnt activator or control media before inhibiting Notch signaling on P5 to investigate whether transdifferentiation of SCs to HCs occurs.

Results

Wnt activation promoted progenitor cell proliferation and an increase in HCs in E13 cochleae. Wnt activation at P0 promoted proliferation of SCs; however, this effect was no longer observed by P5. Quantification by western blots revealed an increase in active β -catenin and a significant increase in total β -catenin following Wnt activation in all three stages, indicating that although Wnt signaling was active in these cells, Wnt target genes were no longer responsive by P5.

When Wnt signaling was exogenously activated from P0, followed by Notch inhibition on P5, we observed SC proliferation and subsequent transdifferentiation of

a subset of these cells into HCs. In contrast, P0 cultures maintained in control media prior to Notch inhibition at P5 demonstrated a lack of proliferation or production of new HCs.

Conclusions

Although the cochlea loses its responsiveness to Wnt activation as it matures, β -catenin can be stabilized in both embryonic and neonatal stages. Activation of Wnt signaling through neonatal stages can induce proliferation of SCs, and can promote subsequent generation of HCs in response to Notch inhibition.

PD 36

Regional Differences in the Requirement of G-protein in Hair Bundle Establishment

Tao Jiang; Doris Wu

Laboratory of Molecular Biology, National Institute on Deafness and Other Communication Disorders, National Institutes of Health

Sensory hair cells of the inner ear relay sound and head positional information to the brain by converting mechanical stimuli in the form of vibrations to neurotransmitter release. Deflection of the hair bundle on the apical surface of a hair cell towards its kinocilium opens mechanical-electrical transduction channels (MET) and causes the cell to depolarize and increase neurotransmitter release. Deflection of hair bundle towards the opposite direction causes hyperpolarization. Thus, the asymmetric location of hair bundle on the cell surface determines the directional sensitivity of the hair cell.

The establishment of hair bundle polarity pattern within a sensory organ requires collaborations between inter- and intra-cellular polarity signals. The well-established core planar cell polarity (PCP) proteins such as Van Gogh, Frizzled and Dishevelled, are required to coordinate hair bundle alignment among neighboring hair cells. On the other hand, the spindle orientation complex, Par/LGN/Insc/Gai, establishes the hair bundle location within cochlear hair cells by moving the kinocilium to its location at the cell periphery where the hair bundle is subsequently constructed.

To investigate whether Gai complex is also required for establishing intracellular polarity in vestibular hair cells, we perturbed Gai signaling using pertussis toxin (Ptx). Similar to previous results of the cochlea, ectopic expression of Ptx in vestibular hair cells showed reduced Gai accumulation across the sensory epithelia. However, regional differences in bundle orientation were observed. Hair cells within the medial region of the utricle as well as outer region of the saccule exhibit normal polarity despite the reduced Gai expression. By contrast,

the lateral region of the utricle and inner region of the saccule showed hair bundle reversal or mis-orientation. Furthermore, Ptx has no effect in changing hair bundle polarity in the cristae. Notably, regions where hair bundle orientation were affected by Ptx normally express the transcription factor Emx2. Taken together, the regional differences in the requirement of Gai complex may be related to the expression of Emx2, which controls hair bundle polarity. Further investigations on mechanisms other than Gai that are likely to be more important for kinocilium positioning in hair cells outside of the Emx2 domain are needed.

PD 37

Fate-mapping and Timed Deletions of SOX2 During Inner Ear Development Reveals Its Dynamic Regulation of Non-sensory and Sensory Specification in the Mammalian Inner Ear

Aleta Steevens; Amy Kiernan

University of Rochester Medical Center

The transcription factor SOX2 is critical for inner ear sensory development, and has been suggested to be an early sensory marker. Previous expression studies have demonstrated that it is expressed in the early otocyst, and eventually becomes specific to the sensory regions as they differentiate. However, it is not known if SOX2 specifically marks all sensory progenitors throughout development, nor when it is required for proper sensory development. To gain insight into these questions, SOX2 was simultaneously fate-mapped and deleted throughout early otocyst stages, by crossing Sox2-CreERT2 mice with Rosa26CAGtdTomato/Sox2+/*fl* mice and inducing Cre recombination at either, E8.5, E10.5, or E12.5. Cre was activated with either 3mg/40g of body weight or 1.5 mg/40g of body weight. Embryos were harvested when ears were more mature, at E18.5, for analysis. In the cochlea, the fate-mapping results show that early (E8.5-E10.5) SOX2 expression is reported mainly in non-sensory cells. Importantly, SOX2 is not reported extensively in the organ of Corti, in all cochlear turns, until E12.5. In the vestibule Sox2 was reported in scattered cells in both non-sensory and sensory cells at E8.5 and E10.5. However, by E12.5 SOX2 reported expression is specific to the sensory regions. Deleting Sox2 at early times (E8.5-E10.5) induces both non-sensory and sensory defects in both the cochlea and vestibule. Specifically, deleting SOX2 at E8.5 results in a severely truncated cochlea duct and agenesis of the vestibule, except for a small portion of the saccule and posterior crista. With the E10.5 SOX2 deletion, the non-sensory defects in the cochlea are less severe; the vestibule forms, albeit all organs are smaller and misshapen, and the lateral crista is frequently absent. At E12.5 deletion of SOX2 leads to a near complete loss of the organ of

Corti, while the non-sensory portions of the cochlea form fairly normally. Interestingly, despite specific expression in the vestibular sensory regions, deletion of SOX2 at this time shows no overt effects. In conclusion we show that SOX2 does not mark all the sensory progenitors from the earliest developmental time points and the morphological defects seen in the timed deletion experiments suggest that early SOX2 may play a role in both sensory and non-sensory development. Together these results show that the requirements of SOX2 for different cell populations change over time in the developing inner ear.

PD 38

SOX11 and CHD7 Act in a Common Gene Regulatory Network to Promote Inner Ear Development

Donna M. Martin¹; Ethan D. Sperry²; Ronus Hojjati³; Donald L. Swiderski⁴; Guoqiang Wan⁵; W. Michael King⁶; Gabriel Corfas⁵; Yehoash Raphael⁶

¹*Department of Pediatrics and Communicable Diseases, University of Michigan;* ²*Medical Scientist Training Program, Department of Human Genetics, University of Michigan;* ³*College of Literature, Science, and the Arts, University of Michigan;* ⁴*Kresge Hearing Research Institute, Department of Otolaryngology, University of Michigan;* ⁵*Kresge Hearing Research Institute, The University of Michigan;* ⁶*Department of Otolaryngology - Head and Neck Surgery, University of Michigan*

Background

Development of the inner ear depends on accurate spatiotemporal control of gene expression via transcriptional networks in the cell nucleus. SoxC transcription factors are a class of proteins that are emerging as critical mediators of inner ear morphogenesis. In humans, heterozygous mutations in SOX11 cause Coffin-Siris (CS) syndrome, which presents with craniofacial and neurologic malformations and, in some cases, hearing loss. In central nervous system neural stem cells, Sox11 expression is regulated by CHD7, an ATP-dependent chromatin remodeling protein mutated in CHARGE syndrome. As in CS, individuals with CHARGE syndrome exhibit complex craniofacial anomalies and sensory impairments, including inner ear malformations. Here, we sought to explore potential common molecular genetic pathways of SOX11 and CHD7 during inner ear development.

Methods

We performed inner ear paintfilling, qRT-PCR, and histologic analyses of Sox11 and Chd7 mutant embryos. Functional studies were conducted to identify auditory and vestibular deficits in Sox11 and Chd7 mutant mice.

Results

Lateral and posterior canal abnormalities were detected in 46% (12 of 26) of Sox11^{+/-} and 100% (12 of 12) of Sox11^{-/-} E14.5 ears. E12.5 Sox11^{-/-} embryos showed a failure of lateral canal fusion plate formation, consistent with the Chd7Gt/+ inner ear phenotype. Sox11^{+/-} mice exhibited mild high-frequency hearing loss by ABR testing and reduced P1 latencies by vestibular sensory evoked potential testing. QRT-PCR on microdissected E10.5 and E12.5 Sox11^{-/-} ears showed misregulation of several genes critical for inner ear morphogenesis, including Bmp2, Bmp4, Chd7, Lrig3, Ntn1, Otx1, Otx2, and Shh. In situ hybridization demonstrated spatiotemporal mislocalization of Bmp4 and Otx1 in E10.5 Sox11^{-/-} embryos. Localization of the canal fusion plate markers Ntn1 and Laminin were unchanged in E12.5 Sox11^{-/-} ears. QRT-PCR on microdissected E10.5 and E12.5 Chd7Gt/+ and Chd7Gt/Gt ears showed dosage-dependent reductions in Sox11 mRNA, consistent with restricted or absent SOX11 immunofluorescence in Chd7Gt/+ and Chd7Gt/Gt inner ears, respectively. Chd7Gt/+;Sox11^{+/-} mice exhibited malformed semicircular canal structures similar to those observed in Chd7Gt/+ mice, suggesting lack of epistasis.

Conclusions

We conclude that loss of murine Chd7 or Sox11 results in a similar pattern of semicircular canal malformations and spatiotemporal misregulation of genes critical for inner ear development. Notably, Sox11 acts downstream of CHD7, suggesting they may have common therapeutic targets. These studies help clarify the molecular and genetic relationships between SOX and CHD proteins in inner ear development, and provide insights about potential pathogenic mechanisms involved in CS and CHARGE syndromes.

Vestibular I: Basic Research

PD 39

Heterogeneity of Utricular Hair Cell Synapse Architectures Across Spatial Scales

Larry Hoffman¹; Ivan Lopez²; Lacey Nelson¹; Katerina Oikonomou¹; Mark Terasaki³; Felix Schweizer⁴

¹*Department of Head & Neck Surgery;* ²*UCLA School of Medicine;* ³*Department of Cell Biology;* ⁴*Department of Neurobiology*

We have recently applied an integrated approach to investigations of synapse architectures in hair cells of the mouse utricle to glean insight into how they may be modified by exposure to altered conditions of ambient static loading. We have investigated the architectural heterogeneity exhibited by synaptic ribbons using con-

ical transmission electron tomography (CT) and field emission scanning electron microscopy (FESEM). Additionally, immunohistochemistry (IHC) has been employed to elucidate synapse distributions across the topography of the utricular epithelium. These data are summarized in this presentation to provide a broad perspective of synaptic heterogeneity across spatial scales spanning 4-5 orders of magnitude (i.e. nanometers to hundreds of microns) and how they may contribute to information transmission in afferent circuits. Young adult C57Bl/6 mice were deeply anesthetized and decapitated, temporal bones rapidly infused with fixative and utricles were harvested. Postfixation processing procedures (e.g. sectioning, staining, and/or immunolabeling) depended upon the analytical method for which the specimen was destined. Following resin embedding, CT specimens were sectioned at 150 nm and placed on mesh grids. FESEM specimens were sectioned at 50nm and serially collected onto kapton tape. Immunolabeling was conducted on intact utricles or 15µm cryosections, immunostained with antibodies to C-terminal binding protein 2 (CtBP2, targeting synaptic ribbons), glutamate receptor subunit 2 (targeting AMPA receptors), calretinin (targeting striolar calyces), and beta-3-tubulin (targeting all calyces). Synaptic ribbons exhibited spheroid or plate-like morphologies, which appeared as singly or closely situated pairs (simple) or as clusters (complex). Simple ribbons exhibited lengths or diameters ranging 300 – 500nm, though a few very large simple ribbons were found that extended almost 1µm into the hair cell interior. When in clusters, plate-like ribbons often appeared with a secondary density sandwiched between the ribbon and vesicles. Even for relatively large clusters, serial FESEM images revealed that close apposition between a ribbon and the active zone was very limited, and most ribbons did not make contact with the presynaptic membrane. Synaptic vesicles were manually segmented from the CT reconstructions, and exhibited estimated diameters between 28 – 42nm. They appeared densely packed around individual ribbons; when organized in clusters a single row of vesicles was interlaced between adjacent ribbons. IHC and confocal microscopy revealed both large and small CtBP2-immunolabeled puncta, which likely correlated with clustered and simple architectures. Ongoing investigations are dedicated to resolving how this synaptic heterogeneity converges upon afferent dendrites and contributes to the heterogeneity in discharge.

PD 40

Synaptopathy; A Potential Mechanism for Age-related Vestibular Dysfunction in Mice

Gabriel Corfas¹; Guoqiang Wan¹; Lingchao Ji¹; Thomas Schrepfer²; Guo-Peng Wang¹

¹Kresge Hearing Research Institute, The University of Michigan; ²University of Michigan

Dizziness, vertigo and imbalance are among the most common complaints in patients over 75 years of age, and fall-related injuries are the sixth leading cause of death in the elderly, with an estimated 20% mortality rate. Histopathological studies of postmortem human inner ears suggest that degeneration of vestibular end organs and neurons is a major cause of the functional decline. However, the specific impact of aging on the structure of vestibular sensory epithelia, the time course of such age-related changes and their impact on vestibular function remain to be determined. To gain insights into these questions, we examined the function and structure of the vestibular end organ in aging mice.

Auditory and vestibular function in FVB/N mice was tested at different ages (2, 5, 9, 18 and 24 months) including auditory brainstem responses (ABRs); distortion product otoacoustic emissions (DPOAEs) and vestibular evoked potential (VsEPs). Following the physiological recordings, inner ear tissues were harvested and subjected to histological analysis. Utricular sensory epithelia were analyzed by immunostaining/confocal microscopy; vestibular ganglion neurons (VGN) were analyzed by plastic sections. Parameters measured included VGN density; size of utricular macula; hair cell density; density of type I hair cells; density of calyx terminals and ribbon synapses in both striolar and extrastriolar regions.

ABR and DPOAE thresholds did not show significant elevation until 18 months, but the ABR peak 1 (P1) amplitudes were clear reduced by 5 months, suggestive of cochlear synaptopathy. In contrast, vestibular thresholds, P1 amplitudes and latencies showed alterations only at 24 months, suggesting that, similar to humans, age-related vestibular dysfunction has a later onset than age-related hearing loss. Histological analysis showed that at 24 months of age most aspects of utricular sensory epithelium morphology remain unchanged, including macular size, hair cell density, type I hair cell density. However, ribbon synapse and calyceal synaptic terminals are significantly reduced in extrastriolar but not in striolar regions. Importantly, we observed no change in the number of VGNs.

Our findings suggest that loss of calyceal synapses at the utricular extrastriolar region may be a key periph-

eral contributor to age-related vestibular dysfunction. Together with the early-onset synaptopathy previously observed in aging cochlea, our study indicates that synaptic degeneration in the inner ear may be one of the earliest and possibly major contributors to both age-related hearing loss and vestibular impairment.

Supported by NIDCD Grant R01DC004820

PD 41

Cholinergic Synaptic Transmission in Vestibular Hair Cells of Ageing C57BL/6 Mice

Lauren A. Poppi¹; Mark J. Bigland¹; Robert J. Callister¹; Paivi M. Jordan²; Joseph C. Holt²; Rebecca Lim¹; Alan M. Brichta¹; Douglas W. Smith¹

¹University of Newcastle, Australia; ²University of Rochester

Introduction

The decline of cholinergic networks has long been associated with ageing, and is not confined to memory and cognitive pathways of the forebrain. Acetylcholine influences a number of crucial peripheral functions including cardiovascular rate, smooth muscle contraction, gastrointestinal motility, and gland secretion – all known to change with age. However, it is not known if peripheral vestibular function is affected by potential age-related changes associated with the cholinergic efferent innervation. We used our semi-intact preparation of the mouse vestibular organs to determine if there were any functional changes in postsynaptic efferent actions on type II vestibular hair cells of juvenile (3 weeks), adult (6 months), and aged (~28 months) C57BL/6 mice. We also compared the number and size of cholinergic terminals in whole cristae across the three age groups using immunofluorescence and confocal microscopy. In addition, we examined the expression of cholinergic receptor subunit mRNA in whole homogenized cristae of C57BL/6 mice at the same time points.

Methods

Using patch clamp recordings, we measured the responses of type II hair cells to application of 300µM acetylcholine (ACh) in cristae of mice from the three age groups. ACh was applied briefly (100ms) using a secondary pipette coupled with a picospritzer. Cholinergic responses were recorded at membrane potentials of -44 mV, -64 mV and -94 mV to determine the contribution of various ionic currents at different holding voltages. Antagonists against nicotinic acetylcholine receptors containing alpha9 subunit (strychnine; 1µM) and small conductance calcium-activated potassium channels, SK, (apamin; 0.1µM) were used to characterize channel activation in response to ACh. Isolated whole cristae from

the inner ears of mice from the three age groups were homogenized, and using RT-PCR, the expression levels of acetylcholine receptor mRNA in were compared.

Results

Current responses show the peak amplitude and duration of cholinergic responses were significantly reduced in the aged cohort compared to juvenile mice. This was attributed to a decrease in both alpha9 nicotinic receptor subunit and SK channel conductances. Similarly, there was a large (~50%) concomitant decrease in alpha9 nicotinic receptor subunit mRNA in the cristae of aged mice compared to juvenile mice.

Conclusions

Age-related effects on the vestibular peripheral function include changes associated with the peripheral cholinergic efferent system. Our data show significant decreases in both the expression and activity of alpha9 subunit nicotinic receptors with increasing age.

PD 42

Identification of Na⁺ Current Components in Vestibular Calyx Afferent Terminals

Frances L. Meredith¹; Annika Divakar²; Katherine J. Rennie²

¹University of Colorado School of Medicine; ²UC Denver School of Medicine

Background

Voltage-dependent Na⁺ channels drive the initiation and propagation of action potentials in excitable cells. Although large Na⁺ currents (I_{Na}) are present in spontaneously firing vestibular afferents, underlying contributions of Nav subunits (Nav1.1-1.9) are unknown. Na⁺ currents were recently described in cell bodies isolated from rat vestibular ganglia and exhibited differing sensitivities to the blocker tetrodotoxin (TTX) (TTX-sensitive, -insensitive or -resistant) (Liu et al. 2016). Vestibular ganglion neurons terminate as calyx endings on type I vestibular hair cells or bouton endings on type II hair cells and can form calyx-only, bouton-only or dimorphic fibers. Nav1.6 (TTX-sensitive) immunoreactivity was detected at the heminode of dimorphic afferents, whereas Nav1.5 (TTX-insensitive) immunoreactivity was localized to the inner face of calyces, predominately in central zone (CZ) (Lysakowski et al. 2011; Wooltorton et al. 2007). We investigated the expression of I_{Na} and underlying subunits in peripheral zone (PZ) and CZ vestibular calyces.

Methods

I_{Na} was recorded from calyx terminals in slices of gerbil cristae (100-110 µm) using whole cell patch clamp.

The patch pipette solution contained Cs⁺ to isolate INa. Pharmacological blockers of Nav subunits were applied to PZ and CZ cells. Immunohistochemistry was performed on crista slices to probe expression of Nav subunits in afferent terminals.

Results

TTX (200–500 nM) completely blocked INa in PZ (n=6) and CZ (n=3) calyces at postnatal days (P)21-29. However, at P9 a small INa remained in 200 nM TTX suggesting that TTX-insensitive INa is more prevalent at early postnatal ages. We also confirmed the presence of a TTX-insensitive current in P6-P9 hair cells: 200 nM TTX blocked an average of 72% of peak INa (n=3). At 50 nM, TTX completely blocked INa in 2 out of 4 calyces, whereas a residual TTX-insensitive current was present in 2 PZ calyces. Jingzhaotoxin III, a selective blocker of Nav1.5 channels, reduced INa in 2 of 6 calyces. Immunostaining for Nav1.5 subunits was seen in a small subset of CZ and PZ calyx terminals at P21. 4,9-Anhydrotetrodotoxin (100 nM), a selective blocker of Nav1.6 channels, reduced INa by ~ 59% in 3 PZ calyces. The blocked current showed relatively fast inactivation kinetics, but also showed a persistent component.

Conclusions

There was no evidence for TTX-resistant INa in calyces by the fourth postnatal week. Nav1.6 channels may contribute to TTX-sensitive INa in mature PZ dimorphic afferents, whereas TTX-insensitive Nav1.5-mediated currents may be present in a minority of calyx afferents.

PD 43

Understanding the Role of Hyperpolarization-activated Cationic Currents on the Firing Patterns of Rat Vestibular Ganglion Neurons

Christopher Ventura¹; Radha Kalluri²

¹University of Southern California, Otolaryngology;

²University of Southern California

The *in vivo* firing patterns of vestibular afferents are remarkably diverse in the regularity of their spike timing. Such differences may influence the encoding of vestibular sensory information but the mechanisms underlying these differences remain poorly understood. Our previous studies on vestibular ganglion neurons (VGN) suggested that spike-timing regularity is shaped by intrinsic differences in the density of low-voltage gated potassium currents (IKL). VGN with large (IKL) responded to simulated synaptic currents with irregularly-timed firing patterns. Those with less IKL produced more regularly-timed firing patterns but not with the extreme regularity that is observed *in vivo*. Several recent studies suggested that extreme regularity relies on the action

of hyperpolarization-activated cationic currents (IH; famous for pace-making in the heart). If this is true then we hypothesized that the IH current may have been inactive in our previous studies because its reliance on second messenger systems makes it highly susceptible to experimental conditions. Here we tested if the *in vitro* firing patterns of VGN can be regularized when IH activation is enhanced by increasing the intracellular concentration of cAMP (a known enhancer of IH).

We recorded using whole-cell patch clamp methods from dissociated and briefly cultured rat vestibular ganglion neurons (VGN; post-natal day (P)8 thru P18). Recording pipettes contained either 10 or 100 μ M cAMP. Results were compared against our previous data set where recordings were made by perforated-patch methods where cAMP is not explicitly controlled. After injecting 16 VGN with currents that mimicked the random timing of synaptic input we quantified the regularity of firing patterns by the coefficient of variation (CV; lower more regular). A broad range of spike trains were evoked (CVs ranged from 0.5 to 1.05). When compared across similar spike rates, the most regular firing patterns observed here (CV 0.5) were considerably more irregular than seen in the previous *in vitro* study (CV 0.2) or observed *in vivo* (CV 0.01). These preliminary results suggest that enhancing IH by increasing cAMP levels does not regularize spike timing. Ongoing experiments and modeling will test if further increasing cAMP levels or speeding up ion channel kinetics by recording closer to body temperature (up from 25°C to 37°C) will uncover extreme regularity.

PD 44

Use of Imperceptible Levels of Random Galvanic Vestibular Stimulation to Improve Otolith Function and Sway

Jorge Serrador¹; Michael C. Schubert²; Scott Wood³

¹Rutgers biomedical health sciences; ²Johns Hopkins University; ³Azusa Pacific University

Loss of neural function is a common problem with aging and disease. We have previously found that aging is associated with loss of vestibular function, specifically otolith-ocular function, which is also associated with increased sway. Enhancing the remaining neural function could greatly improve quality of life. A novel paradigm that has been shown to enhance neural function is the use of imperceptible levels of electrical noise applied at the sensory receptor. Our hypothesis was that applying this random electrical signal to the vestibular nerve would improve vestibular function and balance control.

To test this we screened a group of 76 veterans, to find 29 that had reduced levels of otolith function (defined as

ocular torsion gain less than 0.12 during +/- 20 degree sinusoidal roll tilt). We then had these veterans stand on a force plate for four 30 second periods with eyes open on fixed support, eyes closed on fixed support, eyes open on foam block, eyes closed on form block. For each condition, two trials were conducted with imperceptible levels of random electrical stimulation to their ear lobes, and two trials were sham trials. Application of electrical stimulation was randomly determined and the subject and experimenter were blind to the stimulation level. Stimulation levels were set as a percentage of threshold that caused sway.

Application of random electrical stimulation resulted in a significant reduction in mediolateral sway in the eyes open on foam block trial (Sham - 0.474±0.169 vs. Stim - 0.3289±0.169, $P < 0.001$). In contrast there was no effect on sway during any of the other trials. These results demonstrate that imperceptible levels of random electrical stimulation can produce a significant reduction in sway (~31%). The finding that the improvement in sway only occurred during eyes open on the foam surface was surprising since we have previously found that sway improved during eyes closed conditions in civilians.

The improvement in sway on an unstable surface with visual input suggests that the improvement in vestibular function associated with the random electrical stimulation is improving the sensory integration of vestibular and visual information when proprioceptive information is unstable. We are currently testing to see if this improvement in static sway translates to improvement in gait. We are also developing a portable version of the stimulator that could allow imperceptible levels of electrical noise to be used as a treatment for veterans with balance loss. Supported by CDMRP grants W81XWH-14-1-0598, W81XWH-14-2-0012.

PD 45

Direction Specific Bayesian Integration of Visual and Inertial Stimuli for Heading Perception

Nadeem R. Kolia¹; Benjamin T. Crane²

¹University of Rochester Medical Center; ²University of Rochester

Background

Heading perception is determined from a combination of visual and inertial cues, but how these cues are integrated over a range of headings when the reliability of the stimulus is direction dependent is unknown. The Bayesian integration theory proposes that multi-modal perception is derived from a weighted average of sensory signals in proportion to the signal's relative reliability. Thus heading perception from combined visual-inertial stimuli should be predictable from the responses to iso-

lated visual and inertial stimuli.

Methods

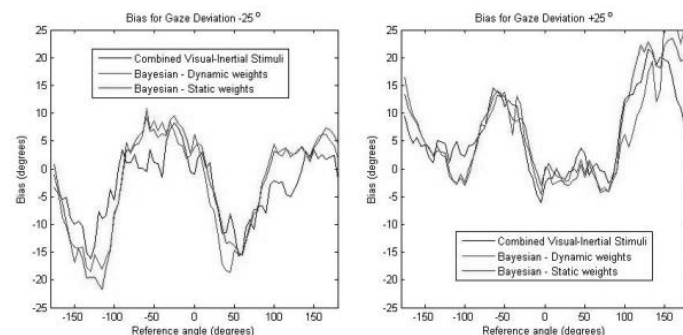
Heading estimation in response to motion stimuli was measured in nine human subjects. Stimuli of 16cm of motion were presented over a 360° range of motion at 5° intervals. Visual, inertial, and combined visual-inertial stimuli were presented in separate trials with a ±25° gaze deviation. Eye motion tracking confirmed subjects maintained gaze deviation. Visual stimuli coherence was reduced to 70% to degrade visual performance. Subjects rotated a dial in the direction of perceived motion. A psychometric function was fit for each reference heading by considering all responses within 90° of the reference angle, and the point of subjective equality from the psychometric function interpreted as the bias for that reference heading. Bayesian integration of the visual and inertial performance data was used to model performance from the combined stimuli trials. Paired t-tests were used to compare biases.

Results

Gaze deviation resulted in a bias in visual heading perception but not inertial heading perception. Across all subjects, the mean bias for visual stimuli for +25° and -25° gaze deviation was 11.1±12.8° and -7.6±12.9° ($p < 0.001$) respectively. For combined stimuli the bias was 7.1±6.4° and -3.3±5.5° ($p < 0.001$) respectively. For inertial stimuli alone the bias was 0.4±6.7° and 0.9±6.7° ($p=0.389$), respectively. For left gaze deviation the Bayesian Integration model predicted actual bias with a root mean squared error (RMSE) of 4.5°. For right gaze deviation the model predicted actual bias with a RMSE of 5.0°. For both right and left gaze deviation, biases predicted from the Bayesian model were not statistically different from the observed biases ($p=0.054$ and $p=0.090$ for left and right gaze deviation respectively).

Conclusion

Gaze deviation causes shifts in perceived heading estimation for visual, but not inertial, stimuli. Heading estimation from combined visual and inertial stimuli can be modeled from responses to individual visual and inertial stimuli in proportion to the signals relative reliability, suggesting that Bayesian integration is valid for heading perception.



Funding

NIDCD R01 DC013580; NIDCD K23 DC011298

PD 46

Vestibular Perception and Gait Coordination

Yoav Gimmon¹; Jennifer Millar¹; Elizabeth Liu²; Rebecca Pak¹; Michael C. Schubert¹

¹Johns Hopkins University; ²Johns Hopkins University School of Medicine

Background

Healthy human gait is symmetric and exhibits anti-phased left-right stepping, ensuring an inter-limb coordination to maximize postural control and energy efficiency. This coordination is generated by neuronal inter-connections between central pattern generators in the spinal cord that are governed by cortical areas. Mal-function of central vestibular processing areas generates vestibular symptoms in the absence of an identifiable peripheral vestibular system lesion. For example, patients with vestibular migraine have a false perception of their body orientation in space. Walking in the dark enforces a coordinated afference primarily from the vestibular and somatosensory systems. This task, coupled with patients that have abnormal central vestibular processing information (vestibular migraine) or abnormal peripheral vestibular function (vestibular hypo-function or BPPV) enables a platform to tease out the relative sensory contribution and their integrated output responsible for this common task. We hypothesized that patients with aberrant peripheral vestibular function would demonstrate unique spatiotemporal gait characteristics, and have impaired accuracy and consistency of gait coordination compared with those patients with abnormal central vestibular processing and healthy controls.

Methods

One hundred and eighteen subjects were recruited. Peripheral vestibular function (n=61) was determined based on ocular and cervical vestibular evoked myogenic potential testing, video head impulse testing, and clinical examination. Patients with abnormal central vestibular processing (n=22) had normal vestibular function testing. Subjects were instructed to walk at a comfortable pace during three visual conditions; eyes open, eyes open and closed intermittently, and eyes closed. Subjects walked twice in each condition on a 6.7 meter GAITRite system. Spatio-temporal gait characteristics and variability (rhythmicity) for each subject were measured. Accuracy and consistency of gait coordination was calculated from step and stride times (known as phase coordination index, PCI), and asymmetry.

Results

Both patient groups showed a similar spatiotemporal gait pattern, which was significantly different than the pattern of the healthy controls. However, only the central vestibular patient group had an abnormal PCI. There were no significant interactions between the groups and walking conditions.

Conclusions

Our data suggest: 1) Patients with abnormal perception despite a healthy peripheral vestibular end organ have impaired bilateral coordination of gait. This suggests vestibular processing affects the neuronal circuits controlling gait coordination. 2) The lack of interaction between groups and walking conditions suggests that humans react similarly to changes in visual conditions as long as somatosensation is preserved.

Inner Ear: Mechanics & Modeling

PD 47

Modeling Longitudinal Propagation of Radial and Longitudinal Motion on Isolated Tectorial Membrane Segments

Charlsie E. Lemons¹; Jonathan B. Sellon²; Dennis M. Freeman³; Julien Meaud⁴

¹Georgia Institute of Technology; ²Harvard-MIT Division of Health Sciences and Technology and Research Laboratory of Electronics, Massachusetts Institute of Technology; ³Harvard-MIT Division of Health Sciences and Technology; Research Laboratory of Electronics, Massachusetts Institute of Technology; and Department of Electrical Engineering and Computer Science, Massachusetts Institute of Technology; ⁴G.W.W. School of Mechanical Engineering and Petit Institute for Bioengineering and Bioscience, Georgia Institute of Technology

In recent years, examination of cochlear physiology in genetically modified mice has demonstrated that the mutation of genes affecting tectorial membrane (TM) proteins causes changes in key characteristics of cochlear function: thus, it is clear that the tectorial membrane plays an important role in hearing mechanics. Knowledge of the mechanical properties of the TM is critical in order to develop theories about the role of the TM in cochlear function. Several groups have measured wave propagation on isolated TMs to estimate the mechanical properties of the TM at acoustic frequencies. However, these previous studies assume longitudinally propagating shear waves on the TM. While shear theory is valid for a semi-infinite isotropic medium, the isolated TMs used in these experiments have finite dimensions

and curvature; furthermore, due to presence of radially oriented fibers in the TM, the TM is strongly anisotropic. The objectives of this study are (1) to determine the effects of the finite dimensions, curvature and anisotropy on wave propagation on isolated TMs and (2) to implement an inverse modeling methodology to determine accurate estimations of the anisotropic material properties of the TMs of wild-type and mutant (*Tectb*^{-/-} and *Tecta*^{Y1870/C+}) mice. Optical images of isolated TMs in response to radial excitations were used to determine the amplitude and phase of the motion at acoustic frequencies. Interestingly, in addition to the longitudinally propagating radial motion that has been reported in previous studies, motion in the longitudinal direction is also observed. Shear wave theory, used in previous investigations, cannot account for this longitudinal motion. Hence, finite element models with an anisotropic, viscoelastic constitutive model are developed. These models take into account the curvature and finite dimensions of the TM. Parametric studies are first used to investigate how the dimensions, curvature and anisotropy affect wave propagation on isolated TMs; the amplitude and phase of the longitudinal and radial motions from numerical simulations are compared. An inverse methodology is then used to determine the effective properties of the TM. Preliminary results indicate that (1) the finite dimensions, curvature and anisotropy all significantly affect wave propagation and (2) the TM is significantly stiffer than what was found in previous wave propagation studies.

PD 48

What's Up With the Calcium Concentration in Endolymph and the Tectorial Membrane?

Clark Elliott Strimbu¹; Anders Fridberger²; Clark E. Strimbu³

¹Linköping University (Currently: Columbia University Medical Center); ²Linköping University, Linköping, Sweden; ³Columbia University Medical Center

Many *in vitro* experiments show that calcium ions regulate the open probability of the mechanoelectrical transduction (MET) channels in hair cells. Yet, it remains questionable whether this occurs *in vivo*, since the effect is considerably reduced at low extracellular calcium concentrations similar to those likely to prevail *in vivo*.

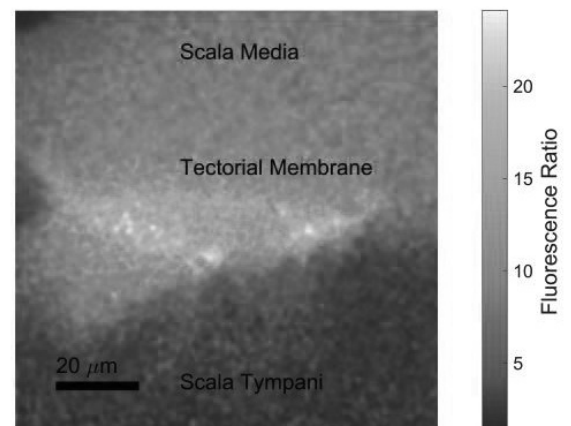
We used the low affinity version (*K_d* in endolymph ≈10.7 micromolar) of the ratiometric dye Asante Calcium Red and fluorescence confocal microscopy to measure the extracellular calcium concentration in the apical region of the guinea pig cochlea. Conventional electrophysiological techniques were used to measure the cochlear microphonic potential in response to acoustic stimulation

on each preparation. Our results show that the calcium concentration in the tectorial membrane (TM) is significantly higher than in the bulk endolymph, corroborating a long-held hypothesis that the TM acts a calcium sink. Furthermore, we observe calcium hot spots –regions of saturating fluorescence -- along the underside of the membrane near the outer hair cell bundles and also near Henson's stripe close to the inner hair cell bundle. This suggests that the local calcium concentration near the hair bundles exceeds approximately 100 micromolar. Results from fluorescence correlation spectroscopy with the calcium fluorophore Oregon Green BAPTA corroborate that the local calcium concentration is higher in the TM.

To investigate a possible role for calcium in temporary threshold shifts, we combined calcium imaging with brief (10 min.) acoustic overstimulation. Following loud sound exposure, both the fluorescence ratio in the TM and the cochlear microphonic potential drop dramatically with the recovery of the the two signals showing strong correlation. In another set of experiments, we injected the calcium chelator EGTA into scala media resulting in a temporary decrease in the local calcium concentration. Both the fluorescence signal in the TM and the microphonic potential decreased following the EGTA injection and both showed recovery on the same time scale. These results suggest that extracellular calcium can act as a partial control parameter for temporary threshold shifts.

Our results suggest that inner and outer hair cell bundles experience a local calcium concentration that is significantly higher than the bulk endolymphatic concentration (≈25 micromolar) that has been measured with microelectrodes. This finding has implications for the operating point of the hair bundles *in vivo* and contributions to cochlear amplification from the hair-bundle amplifier.

This work was supported by the Swedish Research Council and the Wenner-Gren foundation through a postdoctoral scholarship to CES.



Round Window Dynamics: Modelling the Influence of Cochlear Implantation and Direct Excitation

Stephen Elliott; Guangjian Ni
ISVR University of Southampton UK

The dynamic behaviour of the round window is important to the mechanical function of the cochlea. In this paper a 3D finite element model of the round window with fluid on one side is used to investigate two separate phenomena: the effect on residual acoustic hearing of the stiffening of the round window after cochlear implantation, and the acoustic efficiency of directly driving the round window.

The stiffening of the round window due to the presence of a cochlear implant is estimated from the finite element model by assuming that it is clamped around a cochlea implant passing through it, which is immobile. The acoustic stiffness of the round window is found to be increased by about a factor of 100. A lumped element model is then used to predict the effect of this on the acoustic excitation of the cochlea by the stapes. It is found that an increase of round window stiffness by a factor of 100 reduces the acoustic excitation of the cochlea by about 20 dB below 1 kHz. This is similar to the average value for the reduction of sensitivity in residual acoustic hearing after cochlear implantation measured in a number of centres internationally.

The second use of the finite element model is to study the effect of direct round window stimulation. Of particular interest is to compare the effects of two direct stimulation strategies: using a relatively large inertial electromagnetic actuator, such as the Vibrant Soundbridge, or with a small separate magnet on the round window, driven by an external coil. The finite element model of the round window is modified to account for the change in its dynamics as a result of attaching either of these actuators, and the responses in one such case, together with the response including the cochlear implant described above, is shown in the supplementary material. The effect of the inertial actuator is considerably greater than that of the floating magnet, since it is larger, although the attached magnet was assumed to be at the smaller end of those that have been used in experimental studies. The cochlear excitation due to these two types of actuator is then modelled using a lumped parameter circuit that is similar to that used above. The results indicate that the inertial actuator is less effective than the moving magnet device below its natural frequency, although the results are more similar above this frequency.

Time Sequence of Reticular Lamina and Basilar Membrane Vibrations in Sensitive Gerbil Cochleae

Tianying Ren; Wenxuan He
Oregon Health & Science University

Background

Normal sensitivity of mammalian hearing depends on an active process inside the cochlea, which uses the outer hair cell-generated force to boost sound-induced basilar membrane vibrations. Although the time relationship between the cellular force and the basilar membrane vibration determines how the cochlear active process works, the time sequence of acoustically induced reticular lamina and basilar membrane vibrations remains contentious.

Methods

Young Mongolian gerbils with normal hearing were used in this study. After the cochlea was surgically exposed, the cochlear partition at the basal turn was visualized through the round window. Magnitude and phase of basilar membrane and reticular lamina vibrations were measured using a custom-built heterodyne low-coherence interferometer as a function of frequency at different sound levels. The malleus vibration was also measured for estimating transfer functions of basilar membrane and reticular lamina vibrations. The latency difference was derived from the slope of the linear regression line of the phase difference between the reticular lamina and basilar membrane vibration as a function of frequency.

Results

The latency of the outer hair cell-driven reticular lamina vibration was greater than that of the basilar membrane vibration. The phase relationship between the reticular lamina and basilar membrane vibration varied with frequency. While the reticular lamina and basilar membrane vibrated in approximately opposite directions at low frequencies, they moved in synchrony with each other near the best frequency. The latency difference was absent postmortem.

Conclusion

Outer hair cell-driven reticular lamina vibration occurs after, not before the basilar membrane vibration as previously reported. Due to the latency difference, the reticular lamina vibration interacts with the basilar membrane vibration not only in the transverse direction but also in the longitudinal direction through the cochlear fluid, resulting in a maximum vibration at the apical ends of outer hair cells at the best frequency location.

Funding

Supported by NIH-NIDCD grant R01 DC004554.

PD 51

Two Effects Increase the Vibration Energy of Active Auditory Systems

Daibhid O Maoileidigh; A J Hudspeth
The Rockefeller University

The auditory systems of all vertebrates likely possess an active process that enhances their responsiveness to sound. This process boosts the sound-induced vibrations of auditory organs such that the amplitude of motion can be ten thousand-fold greater in living animals than after death. Owing to the complexity of auditory mechanics, several aspects of the active process remain a matter of controversy. It is unclear whether the active process adds energy to the vibration of auditory organs or whether an active organ simply extracts more energy from the sound input. In addition, the conditions for which energy gain occurs are unknown. In principle, an active process could raise or reduce an auditory organ's response to sound input.

To understand the active process, we employ a simplified description based on the known physiology of hair cells and fundamental physical principles. The description, which is designed to capture features common to all active auditory systems, relies only on assumptions for which there is widely accepted experimental evidence. The process is inherently nonlinear owing to the gating of the hair cells' mechanotransduction channels. Activity arises from electrochemical energy sources within the hearing organ, such as the electrical and Ca²⁺ gradients across the membranes of hair cells. We study energy flow through this system in response to stimuli of varying amplitudes and frequencies. The effects of activity are assessed by comparing the system's responsiveness in the presence of the energy sources with that in their absence.

We find that the active process can simultaneously augment the energy of input-induced vibrations and enable the system to extract more energy from the stimulus. The energy gain diminishes as the stimulus amplitude grows or as the stimulus frequency deviates from an optimal value. Energy gain depends upon the system's parameter values. We describe the conditions under which energy gain is possible and the circumstances for which the active process decreases the system's responsiveness to external stimulation.

We conclude that the active process can amplify vibration amplitudes within hearing organs by two distinct means: the process adds energy to stimulus-induced displacements and increases the energy withdrawn from the input. It is possible for an active process to lower a system's responsiveness to stimulation, but we argue

that this is unlikely in auditory systems. Despite their differences, the auditory amplifiers of all vertebrates rely on common physical principles that endow their ears with exquisite sensitivity to weak sounds.

PD 52

The Spatial Profile of Basilar Membrane Vibration

Marcel van der Heijden; Nigel Cooper
Erasmus MC

The spatial profile of basilar membrane (BM) vibration was studied by recording the response to multi-tone stimuli in the 16-30-kHz region of gerbil cochleae. We recorded BM motion at multiple adjacent BM locations in each cochlea, enabling us to determine both the radial and longitudinal variations. Radial phase variations were generally small. The radial magnitude profile resembled a triangular shape with the maximum displacement occurring near the feet of the outer pillar cells, where the arcuate and pectinate zones (AZ & PZ) of the BM meet. The radial motion pattern thus resembled that of an asymmetric pair of saloon doors, the AZ being shorter than the PZ. This radial vibration pattern confirms previous findings in guinea pig and gerbil [1] and contradicts previous claims of bi-modal response profiles [2]. The longitudinal phase variations of the vibrations enabled us to study the wavelength and phase velocity of the traveling waves, and in particular their variation with frequency, sound pressure level (SPL) and longitudinal position. Waves near the characteristic frequency (CF) had wavelengths of ~400 μm , confirming previous reports in gerbil [3,4]. Phase velocity rose sharply with decreasing frequency, reflecting the strong dispersion of cochlear waves. The phase velocity of near-CF waves systematically increased with SPL. Below-CF waves, however, showed the opposite SPL dependence: their phase velocity dropped with increasing SPL. The reversal of the SPL effect occurred at ~0.5 octave below CF; at this frequency phase velocity was largely SPL independent. Waves of all frequencies became shorter as they traveled toward the apex, as expected from the longitudinal gradient of BM compliance. Low-SPL, near-CF waves showed an almost asymptotic behavior, their wavelength saturating at a minimum value of ~250 μm in the region immediately apical to their characteristic place.

1. Cooper NP (1999) Radial variation in the vibrations of the cochlear partition. In *Recent Developments in Auditory Mechanics*, Wada et al, Eds. World Scientific, Singapore, pp. 109–115.
2. Russell IJ, Nilsen KE (1997) The location of the cochlear amplifier: spatial representation of a single tone on the guinea pig basilar membrane. *Proc. Natl. Acad. Sci. USA*, 94, 2660-2664.
3. Ren T (2002) Longitudinal pattern of basilar mem-

brane vibration in the sensitive cochlea. *Proc Natl Acad Sci USA* 99:17101–17106

4. Van der Heijden M, Versteegh CPC (2015) Energy flux in the cochlea: Evidence against power amplification of the traveling wave. *J. Assoc. Res. Otolaryngol.* 16: 581-597.

PD 53

Relative Contributions of Oscillatory Shear and Fluid Motions at the Inner Hair Cell Bundle in a Cross Section Model of the Cochlea

Nima Maftoon¹; John J. Guinan²; Sunil Puria³

¹*Massachusetts Eye and Ear Infirmary, Harvard Medical School*; ²*Mass. Eye and Ear Infirmary; Harvard Medical School*; ³*Massachusetts Eye and Ear, Harvard Medical School*

Despite many years of investigation into cochlear mechanics, the mechanisms that drive the inner hair cell (IHC) stereocilia remain to be characterized. IHC stimulation is hypothesized to consist of multiple inputs including the classic ter-Kuile shear motion between the reticular lamina (RL) and tectorial membrane (TM) as well as oscillatory fluid motion in the sub-tectorial space (STS). The mix of these mechanisms is thought to change from base to apex. This study explores the relative contributions from these mechanisms using a vibroacoustic finite-element-model representation of an organ of Corti cross section. We explore the sensitivity of these mechanisms to changes in material properties and anatomy.

A 3D model of a cross section of the organ of Corti including the BM, RL, TM, inner sulcus and the fluid in the STS and above the TM is formulated based on the anatomical measurements of Edge et al., (*Hear. Res.* 1998; 124: 1–16) from the gerbil apical turn. The spiral limbus is assumed to be rigid. Each of the IHC and OHC bundles is represented by a single stereocilium with equivalent bundle stiffness. Linearized continuity and Navier-Stokes equations coupled with linear-elastic equations discretized with tetrahedral elements are solved in the frequency domain. We varied material properties including the stiffness and mass of the tectorial membrane, the stiffness of the organ of Corti and cilia as well as the viscosity of the endolymph. Anatomical variations include changes in the angle of the RL and TM relative to the BM.

Dynamic changes in the sub-tectorial gap dimensions are evaluated, and their relationship to the STS fluid flow in the radial and longitudinal directions are reported. The contributions of the relative radial motion between the TM and RL (shear) to the motion of the inner stereocilia is investigated and compared to transverse TM and RL

motions and the resulting oscillatory fluid flow stimulation of the IHC stereocilia. These will be calculated with variations in material properties and anatomy to show the sensitivity to each parameter.

PD 54

Active Control of Organ of Corti Amplification by Hair Bundles

Aritra Sasmal; Amir Nankali; Karl Grosh
University of Michigan

The mammalian ear owes its remarkable transduction properties to active processes in the cochlea. Although it is well accepted that the active processes are integral to the hearing apparatus, the actual process of amplification in the mammalian cochlea is still debated. The current consensus is that the amplification of the traveling wave is due to two processes acting individually or in combination: membrane electromotility of the outer hair cell (OHC) and the hair bundle (HB) motility. Prestin based OHC activity persists whenever there is a current flux through the OHC and is required for amplification of organ of Corti (OoC) motion. The HB activity filters the mechano-electrical transduction (MET) current flux and holds the potential to add energy on a cycle-by-cycle basis through the action of an adaptation motor.

In this study, we incorporated both the OHC somatic motility as well as the HB active process in a dynamical cross-sectional model of the cochlea. The coupled non-linear active process in the OoC was simulated and we studied the regimes in which they are individually relevant and their interplay.

We found that although HB motility alone is not sufficient for amplification, there are two separate mechanisms through which the HB activity affects the OoC amplification. The first mechanism requires the HB active process to operate near a Hopf point of the system. The HB activity injects power by tuning its adaptation apparatus to harness the electrochemical potential across the MET channels. At low frequencies, the drastic loss of MET current sensitivity due to the HB adaptation can reduce the amplification by the somatic motility, reducing net OoC amplification, making this mechanism ineffective at the apex. We find a second mechanism involving antiphase displacement of the HB adaptation motor with respect to the HB that can boost the dynamic sensitivity. Although in this mode the HB does not directly add energy to the system, it increases the MET current to improve the OHC somatic drive which results in higher net amplification of the OoC. This mode of amplification is linearly stable and occurs only at low frequencies making this mode ideally suited for the apex of the cochlea. In this article, we delineate these two mechanisms by

which HB motility interacts with the somatic motility and discuss the differences in their mode of operation. Further, we explore the coupled effect of these active processes on the non-linear response of the OoC.

Relating Animal Models to Human Cochlear Implant Use

SYMP 12

Developmental Plasticity in Paediatric Cochlear Implant Users

Karen A. Gordon

The University of Toronto, The Hospital for Sick Children

To achieve optimal outcomes of paediatric cochlear implantation, we need to understand the extent of deafness-related changes in individual children and limitations of present devices for hearing development. Data from animal models and cohorts of children are consistent, showing that rudimentary auditory pathways form despite deafness in early life but remain immature. Delays and abnormalities in auditory development are related to aetiology and duration of both bilateral and unilateral hearing loss. Advances in human neuroimaging provide insights into how children using cochlear implants process sounds and compensate for their hearing loss.

SYMP 13

Physiological Changes That Occur with Cochlear Implant Training in Rats

Julia King¹; Ina Shehu²; Mario A. Svirsky³; Robert C. Froemke⁴

¹*Skirball Institute of Biomolecular Medicine, Neuroscience Institute, Department of Otolaryngology, Department of Neuroscience and Physiology, and Medical Scientist Training Program, New York University School of Medicine;* ²*Skirball Institute of Biomolecular Medicine and Department of Otolaryngology, New York University School of Medicine;* ³*Department of Otolaryngology, New York University School of Medicine;* ⁴*Skirball Institute of Biomolecular Medicine, Neuroscience Institute, Department of Otolaryngology, and Department of Neuroscience and Physiology, New York University School of Medicine*

Recent methodological advances enable a new study of the changes to neural circuits that occur with cochlear implant use in rodents. Here we will describe a behaviorally-validated and physiologically-calibrated system for multi-channel cochlear implant use in trained rats. The novel surgical approach allows for one full turn of in-

tracochlear electrode array. We will discuss the changes that occur with implant use and differences between 'high-performing' and 'low-performing' animals.

Female Sprague-Dawley rats are trained on a self-initiated frequency detection task. Once animals have learned the task ($d' > 1.7$), they are bilaterally deafened and unilaterally implanted with an 8-channel array. Following surgical recovery and objective sound processor programming, the animals are tested on the frequency detection task using CI stimulation as their exclusive input. They then receive further targeted training to improve their behavioral performance. Day 1 initial performance is variable ($n=4$; $d'=0.13 \pm 0.08$) but overall relatively poor; while learning trajectory and peak performance differ across animals, all animals improve significantly after a few weeks compared to their initial performance ($n=4$; $d'=1.32 \pm 0.26$, $p < 0.01$).

In order to explore the neural correlates of these phenomena, we are using chronic micro-electrocorticography (μ ECoG) in CI animals throughout the behavioral testing and learning period with the CI. In collaboration with the Viventi lab, the Froemke lab has developed a μ ECoG system for recording from auditory cortex in awake, freely moving animals (Insanally et al., 2016). The 60-contact arrays can record stable tonotopic maps over a period of weeks to months. In naïve animals acutely implanted with both a CI and a μ ECoG array, stimulation of any of the intracochlear electrodes results in evoked cortical responses. Though there is poor discriminability between responses to nearby electrodes, there is segregation of responses to stimulation of the deepest and the shallowest intracochlear electrodes. Upon acute μ ECoG array implantation in a trained CI animal, we observed clear cortical responses to the target electrode as well as weaker, separate responses to the non-target electrodes. We are expanding this setup to include chronic cortical recordings within the behavior boxes during CI learning and performance. Based on our preliminary findings, we expect that representations of CI channels will be overlapping in the initial post-implantation phase, correlating with relatively poor initial performance, and that the CI channel representations will become more defined with training and experience, correlating to improved behavioral performance with the CI.

SYMP 14

The Importance of Neural Health for Cochlear Implant Performance

Bryan E. Pfingst¹; Kara Schwartz-Leyzac¹; Ning Zhou²; Deborah Colesa¹; Aaron P. Hughes¹; Donald L. Swiderski¹; Yehoash Raphael³; Teresa A. Zwolan¹
¹University of Michigan; ²East Carolina University; ³Department of Otolaryngology - Head and Neck Surgery, University of Michigan

A basic premise of much of the animal research on cochlear implants is that if we can improve the biology of the implanted cochlea, we can improve the performance of the patient. However, this premise is controversial given that human temporal-bone studies often fail to show a significant correlation between postmortem histology and speech recognition measured when the subjects were alive.

In order to develop and test models for improving health of the implanted cochlea, we must conduct coordinated animal and human research. The steps include 1) identifying ways of improving the biology of the impaired cochlea that are safe and effective for human use; (2) determining the functional benefits of these biological manipulations; and (3) demonstrating that those functional changes are important for speech recognition with cochlear implants.

For step 1, we are examining hearing-preservation procedures and the effects of neurotrophin gene therapy (NGT) to preserve, restore or improve biological conditions in the implanted cochlea. The NGT procedure results in long-term preservation of many spiral ganglion neurons (SGNs) in the deaf ear and also sprouting of non-myelinated peripheral neurites.

For step 2, we are examining the relationship between stable biological conditions in the cochlea and psychophysical and electrophysiological measures of implant function. To achieve a large range of biological conditions in guinea pigs we use a variety of treatment procedures including placing cochlear implants into a hearing ear; deafening the ear with neomycin prior to implantation; and deafening the ear followed by NGT treatment and implantation. Effects of these manipulations of cochlear biology are detectable by the functional measures. Good psychophysical temporal integration and multipulse integration are more likely to be achieved in animals with excellent cochlear health including high SGN densities, surviving hair cells, and ensemble spontaneous activity. Slopes of electrically-evoked compound action potential (ECAP) amplitude-growth functions (AGFs) and the effects of stimulus interphase gap (IPG) on these func-

tions reflect SGN densities over a broad range.

For Step 3, we have used these functional measures in humans, employing within-subject designs to reduce effects of cognitive and other across-subject variables that are known to affect speech recognition. Both psychophysical and electrophysiological measures that are related to cochlear biology can predict ear differences in speech recognition in subjects with bilateral implants, confirming their potential for identifying conditions that are important for implant function.

Work supported by NIDCD R01 DC010786, R56 DC010786 and P30 DC005188, and a MED-EL contract.

SYMP 15

Selective Neuronal Activation by Cochlear Implant Stimulation in Auditory Cortex of Awake Marmosets

Xiaoqin Wang

Department of Biomedical Engineering, The Johns Hopkins University, Baltimore, MD, USA

How CI devices engage the brain at the single neuron level has remained largely unknown, in particular in the primate brain. By comparing neuronal responses to acoustic and CI stimulation in marmoset monkeys unilaterally implanted with a CI electrode array, we discovered that CI stimulation was surprisingly ineffective at activating most neurons in auditory cortex, particularly in the hemisphere ipsilateral to the cochlear implant. Further analyses revealed that the CI-nonresponsive neurons were narrowly tuned to frequency and sound level when probed with acoustic stimuli; such neurons likely play a role in perceptual behaviors requiring fine frequency and level discrimination, tasks that CI users find especially challenging. These findings suggest potential deficits in central auditory processing of CI stimulation, and provide important insights into factors responsible for poor CI user performance in a wide range of perceptual tasks.

Advances in Genome Editing and its Clinical Applications

SYMP 16

Defining, Optimizing, and Altering the Specificities of CRISPR-Cas Nucleases

J. Keith Joung

Massachusetts General Hospital and Harvard Medical School

CRISPR-Cas nucleases are widely used for research and are being advanced for use as therapeutics for gene-based diseases. In this talk, I will provide a brief

introduction to genome editing technology using CRISPR-Cas nucleases. I will then discuss work from my group to define, improve, and change the genome-wide specificities of these nucleases in human cells. Our work has developed unbiased methods to define nuclease genome-wide specificities, CRISPR-Cas variants that exhibit few, if any, detectable off-target effects, and engineered reagents that greatly expand the targeting range of this platform. Taken together, these results provide insights and reagents important for the ultimate clinical translation of these nucleases.

SYMP 17

Nucleic Acid Delivery Systems for Rna Therapy and Gene Editing

Daniel Anderson

Massachusetts Institute of Technology

High throughput, combinatorial approaches have revolutionized small molecule drug discovery. Here we describe our work on high throughput methods for developing and characterizing RNA delivery and gene editing systems. Libraries of degradable polymers and lipid-like materials have been synthesized, formulated and screened for their ability to delivery RNA, both in vitro and in vivo. A number of delivery formulations have been developed with in vivo efficacy, and show potential therapeutic application for the treatment of genetic disease, viral infection, and cancer.

SYMP 18

Targeted Gene Activation Using Engineered Nucleases

Pablo Perez-Pinera

Department of Bioengineering. University of Illinois at Urbana-Champaign

During the past decade, the genomic revolution has fundamentally transformed biomedical research through advances in DNA sequencing that have facilitated the analysis of the genomes of many organisms. In parallel with these breakthroughs, gene editing has recently emerged as a technology for precise modification of genomes as well as for targeted regulation of gene expression within a natural chromosomal context. However, despite our ability to induce targeted double strand breaks in DNA in vivo, integration of heterologous DNA at those sites remains challenging. Our laboratory has developed methods for rapid and efficient sequence-specific recombination of DNA within complex genomes. We also demonstrated that these procedures can be adapted to precisely manipulate endogenous gene expression. Importantly, since this multiplexable platform bypasses native promoters, it achieves unprecedented

levels of gene activation. These techniques can be used to create cell lines for modeling human diseases such as cancer, to study transcriptional regulation or even to perform functional genetic screenings.

SYMP 19

The Novel CRISPR Tools and the Latest Trends in Genome Editing

C. B. (Guru) Gurumurthy

Munroe Meyer Institute for Genetics and Rehabilitation

Because of its simplicity and high efficiency, the CRISPR system has emerged as a very popular tool for genome editing. The CRISPR tool can be used for developing genetically engineered animal models and cell lines rapidly, very efficiently and easily. The tool is also used in multiple other ways including transcriptional regulation, epigenetic genome modification, genome-wide screening assays and developing therapeutic strategies for many human genetic diseases including hearing loss. The field moves with an unprecedented speed and new tools are being added to the toolbox constantly. Here I present i) how CRISPR system has brought paradigm shifts in animal genome editing during the recent couple years, ii) present novel tools such as a) Easi-(efficient additions with ssDNA inserts) CRISPR and b) CRISPR-fisrt;PITT-next, the new tools that have improved insertion of large DNA molecules at Cas9 cut sites and b) GONAD (Genome editing via Oviductal Nucleic Acids Delivery), a method that can bypass all the three major steps of animal transgenesis including microinjection. The presentation will also include latest trends in genome editing field with a particular emphasis on hearing research.

SYMP 20

Genetic Correction of iPSCs from Deaf Patients with MYO7A and MYO15A Mutations Results in Morphologic and Functional Recovery of the Derived Hair Cell-like Cells

Jin-Fu Wang

Institute of Cell and Development, Zhejiang University

Mutation correction in the pluripotent stem cells (iPSCs) induced from somatic cells of genetic hearing loss (HL) patients holds a promise as potential treatment. The mutation-corrected iPSCs could provide a rich source of cells for transplantation. I will present our work on correcting compound heterozygous MYO7A and MYO15A mutations in the iPSCs generated from deaf patients by CRISPR/Cas9-mediated genome editing. The corrected iPSCs (CP-iPSCs) retained cell pluripotency, and induced to differentiate into hair cell-like cells with stereocilia-like structure and electrophysiological charac-

teristics of normal hair cells. iPSC combined with CRISPR may facilitate the development of gene therapy for genetic HL.

SYMP 21

Application of CRISPR Technology as Treatment for Genetic Hearing Loss

Zheng-Yi Chen¹; Yong Tao²; Xue Gao³; Veronica Lamas²; Bifeng Pan⁴; Mingqian Huang²; Yujuan Hu²; Ariel Yeh³; Pu Dai⁵; Weijia Kong⁶; Shiming Yang⁷; Jeffrey R. Holt⁸; David Liu³

¹Department of Otolaryngology, Harvard Medical School and Eaton-Peabody Laboratory Massachusetts Eye and Ear Infirmary; ²Department of Otolaryngology, Harvard Medical School, Massachusetts Eye & Ear Infirmary; ³Department of Chemistry and Chemical Biology, Harvard University; ⁴Department of Otolaryngology, Boston Children's Hospital, Harvard Medical School; ⁵Department of Otolaryngology-Head and Neck Surgery, Chinese PLA General Hospital; ⁶Department of Otolaryngology, Union Hospital of Tongji Medical College, Tongji Medical College; ⁷Department of Otolaryngology-Head and Neck Surgery, Chinese PLA General Hospital; ⁸Department of Otolaryngology, F.M. Kirby Neurobiology Center, Boston Children's Hospital, Harvard Medical School

Mutations in a large number of genes are associated with genetic hearing loss in human for which there is no treatment. AAV-mediated gene therapy, anti-sense oligos and RNAi have been used to treat genetic hearing loss in animal models. For each technology clear limitations exist that need to be overcome for them to be clinically relevant. Rapid progress in CRISPR/Cas9-mediated genome editing technology has opened a new avenue to develop novel treatment for genetic hearing loss. Genome editing has the potential to permanently correct mutations, by disruption or repair of mutations, with the lasting effect on hearing recovery. To use genome editing to treat genetic hearing loss it is essential to establish the approach is suitable for inner ear delivery that can minimize the risk such as off-target effect with demonstrated efficacy.

We aim to achieve the goal by developing direct delivery of protein and nucleic acid complex into the mammalian inner ear. We will present the data to show application of CRISPR/Cas9-mediated genome editing to target a dominant mutation in *Tmc1* gene in a mouse model with progressive hearing loss, Beethoven (Bth). We designed a series gRNAs to target the Bth mutation and performed in vitro assay to select the most specific

gRNAs for in vivo study. Cas9 protein and gRNAs complexed with lipid formulation were injected into neonatal Bth mouse inner ear. Subsequent study showed significant hearing recovery across most frequencies. By high-throughput sequencing we demonstrated genome editing effects by the presence of indels at the mutation site in the injected inner ear only. We further showed the hearing rescue effect is gRNA specific. Genome editing resulted in survival of auditory hair cells and improved startle reflex. Finally we detected very low off-target rate, a strong indication that protein-gRNA mediated genome editing could be ideal to treat genetic hearing loss. Combined with our previous work on hearing rescue in the *Pmca2* genetic hearing loss mouse model, we have demonstrated our approach can target dominant mutations of hair cell origin, establishing a new treatment paradigm for dominant genetic hearing loss.

Young Investigator Symposium: Neuronal and Non-neuronal Regulation of Cochlear Wiring and Refinement

SYMP 22

Microglia: Dynamic Sensors of Neural Activity and Regulators of Brain Plasticity

Dorothy Schafer

University of Massachusetts Medical School

The entire body is mapped on to the CNS in the form of synaptic connections. Early in development these synaptic maps initially form in approximately the right location within the CNS. Sensory experience (hearing, touch, vision, etc.) then regulates the refinement of this connectivity into highly precise maps of the body. For over 50 years we have known that sensory experience and neural activity regulate this activity-dependent synaptic refinement, but the underlying cellular and molecular mechanisms have remained to be fully deciphered. We made the initial, unexpected discovery that microglia, the resident CNS immune cells, regulate activity-dependent refinement in the developing visual system by engulfing less active synaptic connections. We are now exploring how this mechanism may be applied to refinement of developing cortical maps. Using the mouse barrel cortex, a robust and highly plastic system for studying experience-dependent refinement of brain maps, we have identified new roles for microglia at developing neural circuits. Our new data demonstrate that microglia are regulating the connectivity within the developing barrel cortex by engulfing a subset of synapses. Furthermore, synaptic engulfment by microglia is regulated by changes in sensory experience and increase by 3-fold following sensory deprivation. We are now exploring novel mechanisms regulating microglia-dependent synaptic refinement. Answers have implications for

understanding how developing neural circuits refine to uncovering etiologies of devastating neurological disorders such as autism and schizophrenia with underlying defects in sensory perception, synaptic connectivity, and glial cell reactivity.

SYMP 23

Interactions Between Spiral Ganglion Neurons and Glia Influence Intrinsic Neuronal Programs During Early Targeting

Noah Druckenbrod¹; Lisa V. Goodrich²

¹Harvard Medical School; ²Department of Neurobiology, Harvard Medical School

Description

The mature cochlea contains all the necessary components to transmit sound information to the brain. This feat requires the precise arrangement of hair cells (HCs) and spiral ganglion neurons (SGNs). This arrangement requires that SGN neurites first extend radially, then group into ordered radial bundles, and target synaptic partners. These stereotypical features are important for normal hearing and many animal models of deafness exhibit disorganized neuronal terminals and bundles. This suggests a crucial, yet delicate step to normal organization occurs during the initial emergence of SGN neurites. Because SGN projections also become disorganized following age or noise-induced hearing loss, finding the molecular and cellular controls of SGN patterning may support therapeutic strategies to re-routing SGN fibers. What signals guide these morphological and targeting decisions through the three-dimensional, multicellular terrain of the cochlea? Most studies have focused on the roles of classically described guidance cues, which act over long distances to attract or repel axons. While many of these classic molecules are sufficient to promote survival or guidance *in vitro*, no molecular or cellular cues are known to control early outgrowth and bundling of SGNs. Less is known about the role of short-range contact-dependent signaling between SGNs or with neural crest-derived glial cells (NCGCs). This is due in part to the obstacles towards gathering high-resolution, time-lapsed information on the spatial relationships between SGNs and NCGCs *in situ*. Using mouse genetics, an organotypic imaging platform, pharmacology, and 3D-morphometry, we have identified novel characteristics of early SGN outgrowth and ganglia organization. These experiments have also provided live imaging of SGN-NCGC interaction for the first time in the cochlea. We show that as neurites first emerge from the ganglion and move through the cochlear mesenchyme, they undergo a rapid transition from exploratory to highly directed behavior. We have identified cellular mechanisms for these different growth phases that implicate

ganglia heterogeneity, pioneering SGN projections and SGN-NCGC interaction. We explore how these mechanisms are affected in animal models of deafness and explore the contribution of the neuregulin-signaling pathway. Taken together, our preliminary data expand upon evidence from recent studies and support the hypothesis that contact-dependent signaling between SGNs and NCG are required for normal development of inner ear neural architecture and hearing.

SYMP 24

Sorting Afferents and Efferents in the Organ of Corti: The Role of Inner Hair Cells and Neurotrophins

Bernd Fritzschn¹; Israt Jahan²; Jennifer Kersigo³

¹University of Iowa, Dept of Biology.; ²University of Iowa; ³University of Iowa, Department of Biology

Two types of cochlear hair cells (IHCs, OHCs) are differentially innervated by two types of afferents (type I +II) and efferents (LOC, MOC). The majority of afferents (~95%) innervate the IHCs, and the majority of efferents (LOC, ~65%) innervate only type I afferents near IHCs. All afferents and efferents nearly simultaneously reach through the habenula perforate, the area around IHCs in mice (around E16.5), and sort out the adult distribution over the next 7 days. Neither the mechanisms nor the function of type II or MOC growth has been experimentally resolved. Descriptive analysis has revealed some details of afferent and efferent fiber progression. However, testable hypotheses largely revolve around neurotrophins for guidance. Some past and more contemporary research suggest type II afferent growth to OHCs is reduced in BDNF mutant mice and can be enhanced *in vitro* with BDNF treatment. However, BDNF is expressed in ALL hair cells and the high affinity receptor, TrkB, is co-expressed with TrkC in ALL spiral ganglion neurons. Neither receptor nor ligand show a differential expression in OHCs and SGNs, respectively, needed for a differential effect of BDNF via TrkB on type II neurons. It appears more likely that observations of a differential effect of BDNF reflect a quantitative effect. In line with this re-interpretation are more sophisticated manipulations showing that misexpression of BDNF under *Ntf3* control leads to exaggerated afferent growth to OHCs, including redirection of vestibular afferents to the cochlea. More importantly, entirely eliminating the second ear specific neurotrophin, *Ntf3*, leads to equal loss of fiber growth to OHCs and a profound longitudinal loss of SGNs (base loses all SGNs).

To reveal the mostly hypothetical role of IHCs, and neurotrophins expressed in IHCs, requires eliminating either these cells or the neurotrophins expressed therein. . We will present preliminary data on conditional deletion of

some or all IHCs in various mutants and how this affects afferent growth to OHCs. We will show that peripherin positive, presumed type II afferents can be found near IHCs and peripherin negative fibers near OHCs adding to the controversy of peripherin mutation on OHC innervation. We will also report how targeted deletion of one or both neurotrophins in all or only IHCs affects the innervation pattern of afferents and efferents. Combined, our data indicate that type I afferent interaction with IHCs defines the outcome of all other innervation of the organ of Corti.

SYMP 25

Plasticity at Hair Cell Synapses During Establishment of Afferent Innervation

Johanna Montgomery

The University of Auckland

During the development of the cochlea, new synaptic contacts are formed onto both inner and outer hair cells (IHC and OHC), followed by a period of synapse elimination and neurite retraction to establish afferent type I synapses solely onto IHC. Our data show that postsynaptic proteins play distinct functions in the cochlea during afferent synapse formation and elimination. Moreover, attenuation of sound stimulation induces plasticity in the molecular make-up of IHC glutamatergic synapses. Together these data show significant postsynaptic regulation of the plasticity of afferent innervation in the cochlea.

SYMP 26

Semaphorin Signaling Controls Selective Hair Cell Innervation by Spiral Ganglion Neurons

Thomas M. Coate¹; Homero Cantu¹; Nathalie Spita²

¹*Department of Biology, Georgetown University*; ²*Johns Hopkins University*

The development of hearing function depends on precise connectivity between spiral ganglion neurons (SGNs) and hair cells in the cochlea, but the molecular mechanisms involved in this process are poorly understood. The most conspicuous subdivision of SGNs is the type I SGNs that connect with inner hair cells (IHCs) and the type II SGNs that connect with outer hair cells (OHCs). In addition, there is a somewhat "bimodal" distribution of type I SGNs: thick fibers with high spontaneous discharge rates have been shown to innervate the pillar cell side of IHCs, whereas thin fibers with low spontaneous discharge rates have been shown to innervate the modiolar side of IHCs. Using genetic sparse labeling, time-lapse imaging and detailed morphometric analyses, we have begun to map different populations of type I and type II SGNs over several points in development. Secreted Semaphorins (Sema3s) are a well-known class

of axon-guidance ligands that bind to Neuropilin (Nrp) and Plexin (Plxn) co-receptors complexes to play various roles in nervous system formation and plasticity. Previously, we showed that Sema3F/Nrp2 interactions restrict type I SGN projections to IHCs and that loss of either of these factors increases the number of SGNs that innervate OHCs. In more recent analyses of individually-labeled type I SGNs, we found that their innervation patterns are surprisingly dynamic: at early stages (E17.5, P0, and P2), the average diameter of fibers contacting the modiolar side of the IHC is significantly lower than the diameter of fibers contacting the pillar side of the IHC, but by P8 these differences are not apparent. In the P8 cochlea, both thin and thick fibers innervate each side of the IHC with an equivalent distribution. Using genetic, in vitro, and imaging approaches, we are attempting now to identify factors that may determine how type I SGNs innervate IHCs. In particular, Sema3a is expressed by distinct populations of cells in the organ of Corti while Nrp1 appears to be expressed by SGNs. Results from preliminary experiments suggest a potential role of Sema3A and its receptor Nrp1 in the synaptic organization of type I SGNs.

SYMP 27

An Inducible *Trek1* Mouse Model and the Role of Spontaneous Activity in the Developing Auditory Organ

Yukako Asai¹; Gwenaelle S.G. Geleoc²; Jeffrey R. Holt³

¹*Boston Children's Hospital*; ²*Boston Children's Hospital, Harvard Medical School*; ³*Department of Otolaryngology, F.M. Kirby Neurobiology Center, Boston Children's Hospital, Harvard Medical School*

Cochlear inner hair cells have spontaneous electrical activity prior to the onset of hearing, which has been hypothesized to contribute to maturation of the auditory organ. To investigate this hypothesis, we generated a novel transgenic mouse model in which inner hair cell spontaneous activity is suppressed by expression of TREK1 potassium channels. We used a novel inducible and regulatable hair cell specific promoter derived from the lac operator/repressor (lacO/lacI) system. In the lac regulatory system, gene expression is regulated by binding of a suppressor protein, LacI, to lac operator sequences inserted in promoter regions that flank the transcriptional start site. The regulation is reversible, as addition or removal of the inducer, Isopropyl β -D-1-thiogalactopyranoside (IPTG), in the drinking water, respectively turns on or off gene expression at any point during the animal's life. We engineered a human Myosin7a promoter, whose activity in the inner ear is restricted to hair cells. The Myosin7a promoter was modified to include

two lac operator sequences rendering it inducible, yet preserving its activity in hair cells as assessed by GFP expression via adenoviral vector transfection. Using the modified Myosin7a (Myo7a*) promoter, we generated a transgenic mouse that express TREK1 K⁺ channels in hair cells. We found that IPTG induction drove expression of TREK1 potassium currents and “clamped” the hair cell resting potential near EK⁺, which effectively silenced the cells. To assay for behavioral consequences of TREK1 expression we measured acoustic startle responses. Administration of IPTG for 3 days completely abolished startle responses in TREK1 mice. These results indicate induced expression of TREK1 effectively silenced hair cell electrical activity. This novel mouse model will be used to investigate the role of hair cell activity during inner ear development. Further work will be presented that discusses hair cell and spiral ganglion neuron survival, innervation pattern and synaptogenesis in the novel TREK1 mice.

Conclusions

1) The Myo7a* promoter maintains hair cell specific activity and can be turned on by addition of IPTG in drinking water. 2) The Myo7a* promoter drives TREK1 expression in hair cells of transgenic mice and successfully silences electrical activity. The inducible hair cell-specific Myo7a* promoter and the TREK1 mouse model developed for this study will likely be valuable for future work aimed at regulating gene expression and manipulating hair cell activity in vivo.

SYMP 28

Activity-dependent Refinement of Spiral Ganglion Neuron Dendritic Terminals in the Developing Cochlea

YingXin Zhang-Hooks

Karl Kandler Lab, Auditory Research Group, University of Pittsburgh

Spontaneous activity in developing sensory systems is thought to play common roles in promoting the maturation of neural circuits to orderly represent sensory space. In the developing auditory system before hearing onset, inner hair cells (IHCs) periodically release glutamate to excite spiral ganglion neurons (SGNs) resulting in bursts of action potentials. Our studies indicate that when glutamate signaling between IHCs and SGNs in the developing cochlea is perturbed, SGN dendrites fail to undergo refinement, suggesting that the sound-independent spontaneous activity plays an important role in establishing the exquisite unitary connections between IHCs and SGNs.

Aging: Effects of Age on Hearing

PS 236

Effect of Informational Content of Noise on Neural Speech Representations, with and Without Peripheral Hearing Loss

Alessandro Presacco¹; Katlyn Bostic²; Jonathan Z. Simon³; Samira Anderson⁴

¹University of California, Irvine; ²University of Maryland;

³University of Maryland, College Park; ⁴Department of Hearing and Speech Sciences, University of Maryland, College Park

Introduction

The ability to understand speech is significantly degraded by aging, particularly in noisy environments. Several behavioral studies and our most recent work have shown that older adults gain significant benefit in focusing on and understanding speech if the background is spoken by a talker in a language that is not comprehensible to them (i.e. a foreign language). An important variable to consider when investigating central auditory deficits is the influence of age-related peripheral hearing loss. In order to better understand how much hearing sensitivity affects the neural representation of speech in noise, we tested three groups of participants: clinically normal hearing younger adults (YNH), clinically normal hearing older adults (ONH) and clinically hearing impaired older adults (OHI). We used neuroimaging techniques (electroencephalography (EEG) and magnetoencephalography (MEG)) to measure the midbrain and the cortical response, respectively.

Methods

Participants comprised 17 NHY (18–27 years old), 15 NHO (61–73 years old) and 11 HIO (62 – 78 years old). Midbrain activity was assessed by recording frequency following responses (FFR) to a 170-ms /da/ speech syllable presented with and without competing speech, and cortical activity was assessed by recording MEG responses while listeners attended to one of two simultaneously presented speech streams. Responses were recorded in quiet and in the presence of competing speech signals at different signal-to-noise ratio levels (+3, 0, -3 and -6 dB). The competing speech signal was either meaningful (narrated story in English) or meaningless (narrated story in Dutch).

Results

In the midbrain, the NHY's speech envelope was more robust to noise than that of both NHO and HIO. No significant differences were observed between NHO and HIO. Effect of noise type (meaningless vs. meaningful) was consistently observed across all the noise conditions only in NHY and only in the transition region. In the

cortex, an exaggerated response (over-representation) was found in both NHO and HIO. No significant differences were found between NHO and HIO. Only older adults' responses were affected by background type, such that reconstruction fidelity of the target speech envelope improved in the presence of Dutch vs. English background narrations in both NHO and HIO.

Conclusions

The fact that results did not differ between older adults with and without peripheral hearing loss suggests an underlying age-related deficit in central auditory processing.

PS 237

Age Effects in Duration Discrimination for Leading and Trailing Components of 2-tone Stimulus Sequences

Sandra Gordon-Salant; Peter Fitzgibbons
Department of Hearing and Speech Sciences, University of Maryland, College Park

Background

Perceived stress or accent within speech or non-speech sound sequences can be influenced by increasing the duration of one or more sequence components. Earlier experiments with tonal sequences have shown that the presence of a stressed component can diminish listener temporal sensitivity (Hirsh et al., 1990), particularly for older listeners (Fitzgibbons & Gordon-Salant, 2010). The present experiment uses simple 2-tone sequences as targets to examine the influence of leading and lagging component stress on duration discrimination performance of younger and older listeners. The target sequences are tested in isolation, and when embedded within longer context tonal patterns.

Methods

The target sequences had an overall duration of 500 ms, and consisted of leading and trailing 250-ms tone segments of 880 Hz and 1100 Hz. In separate conditions, a duration DL was measured for increments in the duration of the stressed 1100 Hz segment, in leading or lagging position, using an adaptive forced-choice procedure. The duration DLs were also measured for the same targets embedded within an early or late position of a longer context sequence featuring tone-burst frequencies above and below those of the target sequence. The context sequences also featured uniform or variable timing characteristics. Listeners included one group of younger normal-hearing adults, and two groups of older adults with and without hearing loss (N = 15/group). All stimuli were presented monaurally via insert earphone at 85 dB SPL.

Results

The duration DLs of the two older listener groups were equivalent, indicating a minimal influence of hearing loss on discrimination. Discrimination performance of the younger listeners was substantially better than that of the older listeners. Younger listeners also produced smaller DLs for the target sequences with leading-component stress compared to final-component stress; older listeners performed similarly for leading and trailing component stress. For most listeners, discrimination performance was equivalent for isolated and embedded targets, with timing characteristics of the context sequences having little influence on the measured DLs.

Conclusions

Older listeners show clear deficits in sensitivity to duration cues for leading and lagging components of simple 2-tone stimulus sequences. This age-related deficit was similar in magnitude for the stimuli tested in isolation and embedded at different locations within longer context tone sequences featuring different timing characteristics. The results aid our understanding of aging and sequential processing, and the specific age-related difficulties in processing stress within multi-component stimulus sequences.

Research Supported by NIH Grant #AG09191

PS 238

Temporal Processing Deficits in Age-related Cochlear Synaptopathy

Aravindakshan Parthasarathy¹; Eve Y. Smith²; Sharon G. Kujawa³

¹*Eaton-Peabody Labs, Mass. Eye and Ear; Department of Otolaryngology, Harvard Medical School, Boston, MA;* ²*Massachusetts Eye and Ear Infirmary;* ³*Harvard Medical School and Eaton-Peabody Labs, Massachusetts Eye and Ear Infirmary, Boston MA*

Introduction

Middle aged and older adults with normal hearing thresholds often exhibit decreased ability to process complex sounds in challenging listening conditions, an outcome suggested to reflect changes in brainstem or central processing. Our work in a mouse model of normal auditory aging has provided evidence of peripheral changes that also may contribute to such declines. We have identified an age-progressive loss of synapses between cochlear inner hair cells (IHCs) and auditory nerve fibers that precedes threshold sensitivity and hair cell loss. Functional consequences of this disconnected communication remain poorly understood, but may include altered temporal coding of sound, particularly in noise. Here we explored the relationship between this age-related

cochlear synaptopathy and changes in temporal processing, using population envelope following responses (EFRs). By manipulating the stimulus parameters, different generators were emphasized, and changes in temporal processing along the auditory pathway with age were studied.

Methods

Distortion product otoacoustic emissions (DPOAEs), auditory brainstem responses (ABR wave 1) and EFRs were measured from CBA/CaJ mice in an age-graded series. Cochleae from these animals were immunostained for markers of pre-synaptic ribbons (CtBP2), post-synaptic glutamate receptors (GluA2), hair cell bodies (MyosinVIIa) and neuron specific β -tubulins (TuJ1).

Results

Outer hair cell (OHC)-based DPOAEs showed minimal changes in thresholds and amplitudes up to 64 weeks of age, followed by gradual declines for older animals which correlated well with OHC loss. Neural-based ABR wave 1 thresholds followed a similar pattern of decline. However, ABR amplitude declines began at young ages, progressed throughout the entire lifespan and were tightly correlated with the progressive loss of synapses. EFRs elicited to an AM frequency that isolated responses from the auditory nerve (1024Hz) showed similar, age-progressive amplitude declines which were correlated with synapse losses, even when compensated for elevated hearing thresholds. Aged animals were also more affected by reduced envelope cues and exhibited decreased dynamic range of masking in noise. However, EFRs to an AM frequency that emphasized cortical generators (32Hz) showed smaller declines with age, suggesting the presence of compensatory mechanisms at higher levels of the auditory pathway.

Conclusions

These results suggest that age-related synaptopathy alters complex sound encoding in the peripheral auditory pathway. These deficits are exacerbated by reduced envelope cues or the addition of noise. Responses evoked from more central generators suggest the presence of some compensatory mechanisms with age.

Funding by DoD (W81XWH-15-1-0103)

PS 239

Temporal Processing as a Function of Pulse Rate and Age: Behavior and Electrophysiology

Casey Gaskins; Erin Walter; Sandra Gordon-Salant; Samira Anderson; Matthew J. Goupell
Department of Hearing and Speech Sciences, University of Maryland, College Park

Introduction

Rate limitations of the auditory system affect a listener's ability to process rapid temporal information. Younger normal-hearing (NH) listeners' ability to encode temporal information in bandlimited acoustical pulse trains decreases as pulse rates increase beyond a few hundred pulses per second (pps). Previous studies have yet to investigate whether or not these effects occur in older NH listeners. As one ages, temporal processing deficits occur. Thus, we hypothesized that age-related temporal processing deficits would decrease temporal rate discrimination abilities in older compared to younger NH listeners, particularly as rate is increased, and that this could be reflected both in behavioral and electrophysiological measurements.

Methods

Six younger (22.2 ± 3.5 yrs) and twelve older (69.9 ± 3.0 yrs) NH listeners participated. Listeners were presented with 80-, 200-, and 400-pps pulse trains, behaviorally, in addition to 20- and 40-pps pulse train conditions in order to measure optimal cortical responses during electrophysiological procedures. All stimuli were presented monaurally. Behavioral performance was measured while listeners performed a forced-choice task. In order to eliminate the use of overall level to perform the task, the pulse trains were presented at 75 dB-A and roved in level over a 20-dB range. Electrophysiological performance was measured using the auditory steady-state response (ASSR) to assess neural energy at different rates at a fixed level of 75 dB-A.

Results

Behavioral testing demonstrated that older listeners were worse at the rate discrimination task compared to the younger listeners. The difference between groups in rate discrimination performance increased as pulse rate increased. These results support the main hypothesis that age-related temporal processing deficits occur as pulse rate is increased. In the electrophysiological ASSR recordings, spectral energy between groups was equivalent at the lower rates, but the younger listeners had higher spectral energy compared to older listeners for the 200- and 400-pps conditions. The ASSR results are consistent with behavioral findings showing greater age-related decrements in performance at higher rates, suggesting that older NH listeners may be experiencing

temporal processing deficits at central levels of the auditory system.

Conclusions

Results demonstrate that age-related differences in rate discrimination occur as rapid rate changes limit one's ability to encode short duration timing cues. Current findings have implications for understanding the peripheral vs central mechanisms related to age-induced temporal deficits and neural encoding. [Work supported, in part, by the University of Maryland.]

PS 240

Rate Discrimination and Sentence Recognition in Young and Elderly Normal Hearing Adults Using Vocoded Speech

Lendra M Friesen¹; Gongqiang Yu²; Lendra M. Friesen³

¹University of Connecticut; ²University of Connecticut Health Center; ³University of Connecticut

In cochlear implant listeners, rate discrimination up to 300 Hz has been linked to good speech understanding. However, this has not been tested in elderly adults with cochlear implants. Temporal envelope processing, critical for speech perception under spectral degradation, may decline in many older patients. As a first step, we are studying the relationship between sentence recognition and rate discrimination in normal hearing young and elderly adults using stimuli that have been processed using CI-type processing (vocoded) in quiet and in different levels of noise. Listeners' psychophysical sensitivity to the temporal envelope cue will be measured using broadband noise amplitude-modulated by periodic signals. We hypothesize that older listeners will show poorer performance than younger listeners in the speech recognition task and that an interaction will be observed between age, vocoding and SNR. In addition, we expect that age-related declines in temporal-envelope sensitivity will be observed. We hypothesize that temporal-envelope sensitivity will predict listeners' performance in the speech recognition task under conditions of vocoding and background noise.

To date, we have tested 8 normal hearing young adults (20-29 years) and 8 elderly adults (> 65 years of age) with normal hearing thresholds up until 1000 Hz. We also tested sentence recognition in quiet and in several different noise conditions for both the vocoded and unvocoded stimuli. As we decreased the SNR, sentence scores decreased for both vocoded and unvocoded stimuli for both groups of listeners. The elderly listeners performed more poorly than younger listeners in all conditions. These results, together with results of on-

going psychophysical measures of temporal envelope coding, will be presented. Findings will have implications for age-related changes in the perception of speech in noise by older normally hearing listeners and cochlear implant users.

PS 241

On the Value of Brief Sound Audiometry as a Diagnostic Tool for Cochlear Synaptopathy

Enrique A. Lopez-Poveda¹; Peter T. Johannesen¹; Byanka C. Buzo¹; Filip Rønne²; Niels H. Pontoppidan²; James M. Harte³

¹University of Salamanca; ²Eriksholm Research Center; ³Interacoustics Research Unit

Cochlear synaptopathy (or the loss of primary auditory synapses) is thought to be caused by noise exposure and/or aging and remains a subclinical condition. Based on a model, it has been suggested that synaptopathy leads to a relatively larger increase in detection thresholds for short than for long duration sounds [Marmel et al., 2015, *Front. Aging Neurosci.* 7:63]. Conversely, cochlear mechanical loss would tend to lead to larger threshold increases for long versus short duration sounds. The present study investigates the use of brief-sound audiometry for the diagnosis of synaptopathy. On the assumption that for listeners with normal audiograms synaptopathy is correlated with age and noise exposure, we hypothesized that the threshold difference between short and long durations sounds increases with increasing age and noise exposure. To test this hypothesis, absolute thresholds for stimulus durations from 2 to 500 ms were measured for 24 listeners with normal audiograms (thresholds < 15 dB HL) and ages from 24 to 68 years. Stimuli included wideband noises (0.1-10 kHz) and pure tones with frequencies of 0.5, 1.5, 4.0, 8.0, and 12.0 kHz. Self-reported life-span exposure to loud sounds was assessed using a questionnaire. As expected, thresholds were higher for the shorter than for the longer stimuli. In contrast to the hypothesis, however, the threshold difference between the short and the long duration sounds decreased with increasing age and noise exposure. The threshold difference also decreased with increasing the long-sound thresholds. Altogether, the pattern of results was more consistent with the effects of cochlear mechanical loss on thresholds than with synaptopathy, something surprising given that participants had normal audiograms. We conclude that either the modeled effects of synaptopathy on threshold-duration functions are nonexistent or washed out by the effects of subclinical (< 15 dB HL) mechanical losses, or that synaptopathy is less frequent than is thought to be. [Work supported by the Oticon Foundation.]

PS 242

An Oral Modulator of Voltage-gated Potassium Channels (AUT00063) for the Management of Age-related Hearing Loss: Results from the CLARITY-1 Trail

Victoria A. Sanchez¹; Robert D. Frisina²; Theresa H. Chisolm¹; Celia Riffel³; Sornaraja Thasma⁴; John Hutchison⁴; Charles H. Large⁴

¹*Auditory Rehabilitation & Clinical Trials Laboratory, University of South Florida, Tampa, FL, USA; Global Center for Hearing & Speech Research, University of South Florida; Dept. Communication Sciences & Disorders, University of South Florida;* ²*Global Center for Hearing and Speech Research, University of South Florida, Tampa, FL, USA;* ³*Auditory Rehabilitation & Clinical Trials Laboratory, University of South Florida, Tampa, FL, USA; Dept. Communication Sciences & Disorders, University of South Florida;* ⁴*Autifony Therapeutics Ltd., London, UK*

During ARO 2016, as part of the symposium on “Translating Science to Medicine: An Update of Phase 2 Clinical Trials in Specific Otologic Indications”, we introduced the CLARITY-1 trial (Clinicaltrials.gov ID#: NCT02345031). The CLARITY-1 trial concluded in June of 2016, and was a randomized double-blind, placebo-controlled, parallel group study examining the effects of AUT00063 on measures of hearing performance among older adults (50-89 yr) with age-related hearing loss.

AUT00063 is a novel small molecule that positively modulates Kv3 channel function. Kv3 potassium channels are expressed at all levels of the auditory system, and allow neurons to fire rapidly and with precise timing, such as in circuits involved in decoding speech. Evidence from animal models indicates Kv3 channels are important for salient auditory function, decline with age in the auditory brainstem, and AUT00063 may improve neural synchrony and auditory temporal processing. Furthermore, during pre-clinical studies and first-in human studies, AUT00063 showed great promise as a safe and potential therapy for hearing loss.

During the CLARITY-1 trial, twelve sites across the USA enrolled 78 subjects. Active and placebo treatment groups were balanced for age, sex and baseline characteristics, including baseline scores for the primary outcome measure evaluating speech recognition in noise through the Quick Speech-in-Noise Test (QuickSIN). Efficacy of AUT00063 (600 mg administered once daily) was assessed as a comparison between treatment group performance on the QuickSIN from baseline to Day 28. Both treatment groups showed improvement on the QuickSIN at Day 28 compared to baseline; however,

the difference between treatments was not statistically significant ($p=0.0638$). Additionally, none of the secondary measures showed a significant difference, hence supporting the primary analysis. Secondary measures included a time-compressed sentence recognition test, speech-in-noise test with varying spatial cues, psychoacoustic measure of temporal resolution, test of auditory working memory, and questionnaires assessing self-perceived hearing abilities. Although the planned measures failed to show improvement, AUT00063 was safe and well tolerated by the subjects. The safety profile was benign with dizziness and somnolence reported more frequently for the AUT00063 group; and, comparatively, adverse events occurred in 63% of subjects taking AUT00063 and 60% taking placebo. The safety profile is commendable; and, furthermore, the trial data were of high quality, with excellent compliance and retention, thus, delivering a conclusive outcome. Results of the trial as well as the logistical lessons learned while completing the first-in kind phase 2a clinical trial for age-related hearing loss will be presented.

Auditory Cortex I

PS 243

Pitch Deviance Detection of Lexical Tones Along the Auditory Hierarchy

Qin Gong; Xiaolin Li
Tsinghua University

Both pitch level and pitch contour are important dimensions of lexical tones for a tonal language. A number of event-related potential (ERP) studies have been conducted to investigate the sub-process in pitch perception at an early pre-attentive stage with the mismatch negativity (MMN), which is elicited within 100 to 250ms of deviance occurrence. Recently, a lot of evidence shows that some deviance detections have been observed in different components of the middle latency response (MLR), which suggests the regularity-based comparison process occurs earlier and can be reflected in subcortical structures along the auditory pathway. In the current study, we aimed to investigate the change detection in an early time course of pitch level and pitch contour in humans by measuring the deviance-related MLR and the MMN during oddball paradigms. A synthesized vowel /a/ was used in oddball blocks: (i) flat tone /a/ (136Hz) as deviants vs. flat tone /a/ (122Hz) as standards; (ii) rising tone /a/ (122Hz rising to 136Hz) as deviants vs. flat tone /a/ (122Hz) as standards. We found that: 1) For both flat tone deviants and rising tone deviants, the Na and Pa components of MLR showed larger amplitude and smaller latency comparing with the standard stimuli in a stimulation block. However, the rising tone deviants induced a smaller and later Na than

the flat tone deviants. No significant differences were reported with respect to Pa component between the two deviants. 2) For the MMN responses, the rising tone deviants also elicited a significant later MMN, while the amplitude is larger than the flat tone deviants. In conclusion, both MMN and Na component of MLR suggest the auditory system requires more complicated processing for the analysis of rising tones. In addition, the opposite amplitude variation between the two deviants of the Na component and MMN indicate that deviant stimuli with different pitch changing patterns induce different responses along the auditory hierarchy. The later enhancement of the rising tone deviants reflected by MMN possibly suggest the later occurrence of categorical discrimination.

PS 244

Neural Responses to Behaviorally Relevant Syllable Sequences in the Ferret Auditory Cortex

Daniel Duque¹; Shihab Shamma²; Jonathan Fritz¹

¹) *Neural System laboratory, Institute for System Research, University of Maryland*; ²) *Neural System laboratory, Institute for System Research, 2) Electrical and Computer Engineering Department, University of Maryland*

Speech communication relies not only on the ability to segregate and recognize individual phonemic elements in ongoing speech, but also in understanding that ordered sequences of such discrete elements are combined to form objects and that the specific order of the individual elements matter. The creation of these auditory objects, known as words, is essential for language since once a sound-to-meaning association is generated, such “word memories” may be stored in associative cortices and retrieved when an acoustic memory template is matched by a sound input. Encouraged by a previous study (Mesgarani et al., 2008), demonstrating that neuronal responses in ferret primary auditory cortex are sufficiently diverse to encode and discriminate all English phoneme classes, and recent behavioral studies on phoneme sequence discrimination in ferrets (Bizley et al., 2015) we initiated a behavioral study to investigate whether ferrets can form specific memories for particular phoneme sequences (Duque et al., 2016). Three ferrets were trained on a conditioned avoidance GO/NO-GO task to lick a spout for water upon presentation of distractor “words” (e.g. ABX) but to refrain from licking the spout after a target “word” (e.g. ABC) was presented, in order to avoid a mild shock. All “words” were composed of a sequence of three synthetic consonant-vowel phonemes. One of the ferrets was also trained to respond selectively to the target word, only if spoken in a female

voice (even in the presence of ongoing background male voice distractors). Once the animals learned the discrimination tasks, a head-post was implanted to enable neurophysiological recording in primary auditory cortex (A1) and higher order auditory cortical areas while the animals were performing the behavioral tasks. Preliminary population neurophysiological data indicate that A1 neurons have a consistent response that closely matches the spectrotemporal properties and amplitude envelope of the waveform of the words, while some responses in higher order areas of the auditory cortex reveal a larger difference between target and distractor “words” based on associated behavioral meaning, rather than acoustic differences. The current study provides evidence that individual neurons can encode specific, ordered phoneme sequences and will help us understand the neural basis for the representation of complex sound sequences in auditory cortex.

PS 245

Modulation of Vocal Production by Auditory Cortical Activity

Steven Eliades¹; Joji Tsunada²

¹*Department of Otorhinolaryngology - Head and Neck Surgery, University of Pennsylvania Perelman School of Medicine*; ²*Department of Otorhinolaryngology - Head and Neck Surgery, University of Pennsylvania Perelman School of Medicine*

Human speech is a sensory-motor process requiring constant self-monitoring to ensure accurate communication. Such monitoring of auditory feedback allows for rapid adjustment of vocal production in order to compensate for perceived changes in output. The underlying neural mechanisms of this vocal self-monitoring and feedback control remain largely unknown. Previous work has demonstrated suppressed neural firing in the auditory cortex that is sensitive to altered feedback during vocal production, however the function of this activity is unknown. We investigated the contribution of auditory cortical activity during feedback-dependant vocal control using marmoset monkeys. We combined real-time frequency-shifted feedback, chronic neural recordings, and electrical microstimulation of auditory cortex and found that auditory cortex neural activity correlates with changes in vocal feedback as well as subsequent feedback-induced compensatory changes in produced vocal acoustics. We further demonstrate that electrical stimulation of auditory cortex can induce novel changes in vocal production. This effects is more prominent in belt regions of auditory cortex, consistent with known anatomical connections between frontal and temporal lobes. These results suggest a causal role for auditory cortex activity in self-monitoring during vocal produc-

tion and resulting feedback-dependent vocal control. This work was supported by NIH/NIDCD Grant K08-DC014299.

PS 246

Transformation in Neuronal Responses to Vocal Sounds between the Core and Parabelt Regions

Yoshinao Kajikawa¹; Deborah Ross¹; Troy Hackett²; Charles Schroeder³

¹Nathan Kline Institute; ²Vanderbilt University; ³Columbia University

Several cortical regions, from the primary auditory cortex (A1) to the prefrontal cortex (PFC), respond to vocal sounds. The parabelt region is one of regions located between A1 and PFC. It is often considered to prefer complex sounds like vocalization to simple sounds like tones. However, the parabelt region has been not been explored well yet. Thus, it is unknown how the parabelt region responds to vocal sounds. We trained 3 macaque monkeys to perform the audiovisual oddball tasks using vocal sounds/movies of 9 exemplar vocalizations as stimuli. Animals were implanted with recording chambers targeting bilateral core, right core and left parabelt, or only left parabelt regions. Multi-channels array electrodes were used to record the multiunit activity in the core and parabelt areas during tasks. We averaged the granular layer MUA responses to vocal sounds across trials for a 300 ms period starting from -40 ms relative to the onset of sounds. Mean MUA responses were analyzed using principal component (PC) analyses, treating the temporal patterns of MUA responses as observations and response magnitudes at selected time points as the observed variables.

Several patterns of response occurred in both the core and parabelt regions. PC1, accounting for the most response variability, was linked to a sustained change in the MUA magnitude following response onset. PC1 scores did not differ significantly between the core and parabelt regions, suggesting that a sustained response component occurred in both regions. However, median PC1 scores in the core and parabelt were negative and positive, respectively, reflecting sustained MUA suppression in the core and MUA elevation in the parabelt during the analyzed period. PC2 had an onset peak, similar to the PC1, followed by a rebound in the other direction. PC2 scores for the core were positive, and those for the parabelt was negative. Overall our results indicate that: 1) while sustained MUA responses could occur similarly in the core and parabelt regions, directions of MUA change differ. 2) the dynamics of onset, rebound and late responses differ between 2 regions. These findings are consistent with significant

response transformations occurring between core and parabelt processing stages.

PS 247

Social Vocal Interactions by Marmoset Monkeys in Naturalistic Social Contexts

Joji Tsunada¹; Steven Eliades²

¹Department of Otorhinolaryngology - Head and Neck Surgery, University of Pennsylvania Perelman School of Medicine; ²Department of Otorhinolaryngology - Head and Neck Surgery, University of Pennsylvania Perelman School of Medicine

Vocal communication plays a key role in maintaining group cohesion and social bonds. Successful vocal communication, however, requires coordination of vocal interactions with group members according to the social context. The marmoset monkey (*Callithrix jacchus*), a vocal New World primate species, exhibits many human-like social vocal behaviors. Although experiments in isolated laboratory conditions have reported rule-based antiphonal vocal interactions between pairs of marmosets, interactive vocal communication in more complex social environments remains largely unstudied. In this study, we examined how marmosets coordinate their vocal interactions in complex, naturalistic social contexts. We recorded vocalizations from an entire group of marmosets housed in a colony environment (N = 12 marmosets, total recording time 50 hours under two different colony configurations) and tracked their vocal interactions in order to determine which animals or groups responded to other's vocalizations and in what order. The pattern and frequency of vocal interactions was quantified using Markov chain analysis, focusing particularly on the marmoset twitter call which has a presumed role in social communication. We found that twitter call production is non-random, but rather produced as part of interactive vocal exchanges. Interestingly, we also found that, in vocal exchanges, co-housed family group members produce twitter calls no more often than individual animals, implying the role of twitter calls as an inter-group communicative signal. We also found that individual animals exhibited preferences about which animals they interacted with and that these preferences were broadly maintained even when exchanges involved different types of vocalizations. These results are the first quantitative measurements of marmoset vocal interaction in the social environment of a marmoset colony and demonstrate social rules used in social vocal communication. These findings will have important implications for future studies of vocal communication, and can potentially be combined with neurophysiological studies to demonstrate the neural basis of interactive social behaviors.

PS 248**Neural Encoding for Robust Representation of Noisy Vocalizations in Primary Auditory Cortex**

Luke A. Shaheen; Stephen V. David
Oregon Health and Science University

The mammalian auditory system is remarkably adept at processing relevant sounds despite competing background noise. Determining the mechanisms responsible for noise robustness in normal hearing individuals is crucial for understanding why hearing in noise is impaired with both age and hearing loss. Neurons along the ascending auditory system demonstrate increasing invariance to additive noise: neural responses in primary auditory cortex (A1) to vocalizations are less affected by additive noise than the responses of auditory nerve fibers. Decoding analysis of A1 activity evoked by noisy sounds suggest that mechanisms responsible for noise invariance include adaptation to sound statistics, synaptic depression, and gain normalization (Mesgarani et al. 2014; Rabinowitz et al. 2013).

Although computational models for robust encoding have been proposed, the effects of noise on the encoding of natural sounds by single units has not been tested experimentally. We fit spectro-temporal encoding models directly to the activity of A1 neurons in awake ferrets recorded during presentation of conspecific vocalizations both with and without additive broadband white noise. This allowed identification of features of the neural response profile affected by the addition of noise. Sound encoding was characterized using a classic linear-nonlinear model: a cochlear filterbank followed by a linear spectro-temporal filter and static output nonlinearity. A crucial step for achieving adequate statistical power to fit models to the noise data was to factorize and parameterize the linear filter (Thorson et al. 2015). Models were evaluated by the correlation between the time-varying neural response and model prediction. Performance was significantly improved when model parameters were fit separately for quiet and noise data over those fit to both simultaneously, indicating nonlinear adaptation to the noisy condition that was not captured by the linear-nonlinear model. This improvement was not reproduced when parameters allowed to vary between the two conditions were constrained to the spectral filter but was almost completely reproduced by allowing only the temporal filter or the output nonlinearity to vary. Across neurons, changes to the temporal filter between conditions were not systematic in our preliminary analysis. However, in models where only the output nonlinearity varied, responses were selectively enhanced in the noisy condition for stimuli that evoked strong responses and slightly suppressed for stimuli that drove the neurons more weakly. These results suggest

that A1 neurons narrow their spectro-temporal tuning to selectively enhance responses to preferred sound features in the presence of additive noise.

PS 249**Auditory Cortical Representation of Harmonic Vocalizations**

Nina So; Sarah M. Woolley
Columbia University

The ability to detect and recognize vocal sounds is critical for social communication. Auditory systems that process social vocalizations must robustly encode acoustic features that distinguish vocalizations from other sounds. An acoustic hallmark of speech and other animal vocalizations is harmonicity. Harmonic sounds contain energy at integer multiples of a fundamental frequency and evoke the perception of pitch. Zebra finches (*Taeniopygia guttata*) are songbirds that communicate using songs composed of syllables that range from high to low harmonicity, making them ideal animals for studying how the brain extracts social information from harmonic communication sounds. We tested the hypothesis that specific populations of auditory cortex (AC) neurons encode harmonicity in vocal sounds by identifying zebra finch AC neurons that respond selectively to highly harmonic song syllables. In primary AC, the intermediate region (L2) receives input from the thalamus, and sends information to superficial (L1/CM) and deep output (L3) regions. Using multichannel polytrodes, we recorded the electrophysiological responses of single AC neurons to song syllables spanning the natural range of harmonicity from awake, restrained zebra finches. Results show that the responses of L2 neurons are not correlated with harmonicity. In contrast, the responses of deep output region (L3) neurons are correlated with harmonicity; higher firing rates to syllables with high harmonicity evoke higher firing rates than do syllables with low harmonicity. To quantify the distinct contributions of acoustic frequency tuning and harmonicity to each neuron's selectivity for harmonic syllables, we recorded responses to pure tones of frequencies spanning the zebra finch hearing range from L2 and L3 neurons. We computed tone receptive fields for each neuron and measured the degree to which a syllable's frequency content mapped onto a neuron's tone receptive field (RF). We then used tone RFs and harmonicity to predict each neuron's firing rate to each of the song syllables. Responses were better predicted by tone tuning in L2 neurons than in L3 neurons. In contrast, responses were better predicted by harmonicity in L3 neurons compared to L2 neurons. Findings suggest that neural selectivity for the harmonic structure of communication vocalizations emerges between the input and deep output regions of primary auditory cortex. This research is funded by NIH R01DC009810 and

the Croucher Scholarship for Doctoral Study.

PS 250

Relative Saliency of Spectral and Temporal Features in Auditory Long-term Memory in the Ferrets

Pingbo Yin¹; Jonathan Fritz¹; Shihab Shamma²

¹) Neural System laboratory, Institute for System Research, University of Maryland, College Park, Maryland, USA; ²) Neural System laboratory, Institute for System Research, 2) Electrical and Computer Engineering Department, University of Maryland, College Park, Maryland, USA

Background

Most natural acoustic stimuli are complex sounds that have spatial as well multiple spectrotemporal feature dimensions such as intensity, pitch contour, timbre, amplitude and frequency modulation rates, and bandwidth. All of these features are represented in neuronal responses in auditory cortex and some are mapped. However, the relative saliency of these features, alone or in combination, in auditory object recognition and memory, remains unresolved. The present study explores the representation of dual independent sound features in auditory long-term memory (LTM).

Methods

Two groups of ferret were trained on Go vs Nogo, 3-zone classification tasks. The sound stimuli differed primarily along the spectral and temporal dimensions. In Group-1, two ferrets were trained to: (i) classify tones based on their frequency (Tone-task), and subsequently learned to (ii) classify white noise based on its amplitude modulation rate (AM-task). In Group-2, two different ferrets were trained to classify tones based on correlated combinations of their frequency and AM rate modulation (AM-Tone task). Both groups of ferrets learned their tasks and were able to generalize performance to novel stimuli along the trained spectral (tone frequency) or temporal (AM rate) dimensions. Insights into stimulus representations in memory were gained when the animals were tested with a diverse set of novel probes that mixed features from the two dimensions.

Results

Animals exhibited a complex pattern of responses to the probes reflecting primarily the probes' spectral similarity with the training stimuli, and secondarily the temporal features of the stimuli: (1) the animals weighted the spectral dimension cues relatively highly compared to the AM rate (a form of primacy of frequency over AM rate); but (2) that both the spectral and the temporal dimensions (among others such as bandwidth) were attended to and exploited to perform the tasks; and (3) that, as a simple

rule, the more that a probe stimulus deviated from training stimuli, the greater was the decrease in the animal's ability to retrieve its meaning correctly.

Conclusion

Ferrets can be trained on an auditory LTM task to classify sounds over different ranges along spectral or temporal dimensions. The diverse behavioral decisions to different probes could be well accounted for by a nearest-neighbor classifier model that relied on a multiscale spectrotemporal cortical representation of the training and probe sounds.

PS 251

Rate Coding of High Frequency Amplitude Modulations During Behavior

Justin Yao; Dan H. Sanes

New York University

Background

The fluctuating temporal structure of amplitude modulated (AM) sounds provides important cues for communication signals, as well as the perceptual qualities of rhythm, flutter, roughness, and pitch. Here, we examined cortical encoding across a broad range of modulation rates, as adult Mongolian gerbils (*Meriones unguiculatus*) performed an AM detection task.

Methods

Freely-moving animals were tested on an appetitive Go-Nogo AM detection task while recordings were obtained telemetrically from a 16-channel array implanted in auditory cortex. "Go" stimuli consisted of amplitude-modulated signals (broadband noise carrier, AM rates: 4-1024 Hz, modulation depths $\leq 100\%$). The noise carrier was frozen, such that the same noise carrier was used for all animals across all sessions. The "Nogo" stimulus consisted of unmodulated (0% modulation) broadband noise. Correct responses on "Go" trials ("Hits") were rewarded with water, and incorrect responses on "Nogo" trials were scored as false alarms ("FAs"). Task performance was quantified by a sensitivity metric, $d' = z(\text{proportion of Hits}) - z(\text{proportion of FAs})$.

Results

Animals were capable of detecting AM rates up to 512 Hz ($d' \geq 1$). Performance for AM rates at or above 512 Hz varied amongst animals. To determine whether animals were using an average level cue, we varied AM and unmodulated noise tokens across a 12 dB range. Performance was tolerant across level suggesting the animals relied on a temporal cue, rather than an average level cue. To determine a plausible auditory cortical encoding mechanism that could account for these behavioral results, we quantified neural sensitivity using both spike

rate metrics. A neural template-matching classifier revealed that sensitivity to fast AM rates were sufficiently encoded by spike rate. AM detection sensitivity thresholds (-20 log m re: 100% modulation depth) were also measured as a function of AM rate (4-512 Hz). Temporal modulation transfer functions (TMTFs) displayed greater sensitivity for AM frequencies below 32 Hz, with a threshold shift of 2-3 dB per octave.

Conclusion

Gerbils are capable of detecting AM noise at fast modulation rates. A neural template matching classifier analysis revealed that neurometric sensitivity to fast AM rates is sufficiently encoded by spike rate. Behavioral and neural sensitivity will be measured in gerbils reared with conductive hearing loss to examine potential sensory deficits that involve temporal processing.

Word Limit: 327/400

Funding: T32 MH019524 and R01 DC014656

PS 252

2-Photon Ca²⁺ Imaging of Neuronal Population Activity in the Auditory Cortex of Awake Behaving Mice

Nikolas A. Francis¹; Daniel E. Winkowski²; Zac Bowen¹; Patrick O. Kanold¹

¹The University of Maryland; ²University of Maryland

Spatiotemporal patterns of ongoing cortical activity (i.e., avalanches) are described by a power-law that indicates a stable neural network that is believed to optimize information encoding across neural populations. Neural responses to sound in auditory cortex are modulated by auditory task performance, but it remains unclear how task performance affects neuronal avalanches. Here, we investigate neuronal avalanches during a pure-tone detection task using in vivo 2-photon Ca²⁺ imaging of GCaMP6s in auditory cortex layer (L) 2/3 of four head-fixed mice. The mice were trained to lick a waterspout upon detection of a 1 s, 75 dB SPL, 15 kHz pure-tone. Preliminary results indicate that ~67% of neurons in a field of view were responsive to tones. During task performance, neurons in L2/3 clustered into two populations with either enhanced or suppressed responses to the target tone. Furthermore, the magnitude of neural responses was greater during correct than incorrect behavioral responses to target tones. Further analysis of the dataset will investigate the relationship between task performance, individual neuronal responses to target tones, and avalanches that arise in close temporal proximity to the target tone. Our study will provide insight into how task-related information is distributed across the spatiotemporal patterns of activity in L2/3 neuronal populations.

PS 253

In Vivo Neural Activity in the Orbitofrontal and Auditory Cortices of Mice

Jason Middleton¹; Spencer Brown¹; Diana Hobbs²

¹LSU Health Sciences Center; ²University of New Orleans

Anatomical and functional neural circuitry forms the basis for cortical representations of the sensory world. This circuit architecture needs to be both plastic and adaptable to allow for the cognitive flexibility animals need to survive in complex and dynamic sensory environments. In the auditory system, neural responses to tone frequency exhibit plasticity when acoustic stimuli arrive concurrently with synaptic inputs from modulatory brain centers. This results in a functional reorganization of the auditory tonotopy, i.e. the ordered distribution of frequency specific responses across the surface of the auditory cortex. "Top-down" pathways are responsible for attention, extracting contextual information, cross-modal sensory integration and signaling other internal brain states. The prefrontal cortex (PFC) has a role in many of these higher cognitive functions. We are interested in how a particular PFC sub region, the orbitofrontal cortex (OFC) is involved in mediating plastic changes in the auditory cortex. The OFC plays a critical role in evaluating reward outcomes, signaling aversive stimuli and regulating emotional behavior. It has established anatomical connections with the primary auditory cortex (A1) and can modulate auditory cortical responses. In order to understand how the OFC influences functional circuitry and signal processing in the auditory cortex we performed in vivo multielectrode array recordings simultaneously in the auditory cortex and the OFC. We calculated cross correlations of activity in these two areas to quantify functional coupling. Additionally, we optogenetically activated OFC neurons and measured the resultant LFP responses in auditory cortex. We found that the functional properties of inputs from OFC to auditory cortex were dependent on the rostro-caudal position of the auditory cortex recording. The characterization of this pathway is an important first step in understanding the mechanisms underlying OFC dependent modulation of auditory processing.

PS 254

Understanding Circuit Mechanisms of Modality-Specific Attention

Jennifer Bizley; Stephen Town; Jonatan Nordmark; Jenny Bizley
University College London

The brain is bombarded by sensory information. Making sense of it requires the brain to process competing sensory signals according to current behavioural needs. The ability to selectively assign and update value to sensory information requires cognitive flexibility: an ability which is supported by the prefrontal cortex. Understanding how attention – to stimuli within and across sensory modalities- allows listeners to select target signals within noise could have implications for the development of hearing aids and for rehabilitation strategies for hearing-impaired listeners. Ferrets are an established model in auditory research. Single-unit activity in ferret frontal cortex has previously been shown to be selective for the attended sensory modality during a selective-attention task (Fritz et al., 2010). Here we develop a new audio-visual behavioural task probing the neural mechanisms underlying cognitive flexibility in the auditory system.

We trained five ferrets to switch between auditory and visual stimuli in three-choice localisation task. Animals were initially trained to localize either light flashes or noise bursts in return for water-reward. Animals were then presented with simultaneous but spatially separated visual and auditory stimuli for which only one modality was rewarded. Rewarded modality was indicated by interleaving blocks of unisensory and multisensory trials, and so that animals were required to direct attention based on trial history. Across several training sessions animals switched between modalities, thus demonstrating successful task reversal learning.

We implanted two animals with microelectrode arrays in anterior sigmoid gyrus (frontal cortex) and in auditory cortex. Using data from one animal, we have so far found unisensory stimuli modulate spiking in frontal cortex (Visual stimuli: 20.1 % (93/462) unit sessions; Auditory: 16.5 % (42/255) unit sessions; $p < 0.05$, paired Student's T-test) and auditory cortex (Visual: 16.5 % (79/478) unit sessions; Auditory 35.8 % (96/268) unit sessions; $p < 0.05$, paired Student's T-test). We are currently how activity is shaped by the attentional condition and characterizing functional connectivity during attend-auditory versus attend-visual conditions.

Funding

This work was funded by grants from the Wellcome Trust / Royal Society (WT098418MA) and Human Frontiers Science Foundation (RGY0068).

PS 255

Decoding Auditory Spatial Attention Using EEG

Yan Gai; Yue Dong; Kaan Raif
Saint Louis University

Although our human body frequently receives mixed sensory inputs from multiple spatial locations, the brain is able to focus on a specific source or point in space. Selective attention can significantly improve perceived signal-to-noise ratios by suppressing undesired sensory inputs from other sources, such as the cocktail-party scenario. Covert attention refers to attentional shifts without corresponding movements of head or gaze. Decoding covert spatial attention based on brain signals is an important topic in brain-computer interface (BCI) for paralyzed patients. Here we recorded Electroencephalography (EEG) using a 32-channel system in healthy human subjects while they were performing simple behavioral tasks. Virtual-space sounds were created by filtering the sound with head-related transfer functions before being delivered to the subjects via headphone. A phase-tagging technique was used for decoding auditory attention to concurrent virtual-space sound. Briefly, noise or speech carriers were amplitude modulated; the modulation phase differed for each sound token. The subject was instructed to pay attention to the sound that agreed with the location of a visual target on a computer. Recorded EEG signals were classified based on the magnitude and phase of the component at the modulation frequency after Fourier Transform. The algorithm was found to be effective in decoding spatial attention and can have wide applications in various BCI systems.

PS 256

Capturing Single-Unit and Non-Invasive Phenomena in an Extensive Computational Model of Auditory Cortex

Patrick J. C. May

MRC Institute of Hearing Research, University of Nottingham, UK

The auditory cortex (AC) is characterized by a structure where feedforward activation progresses from a relatively few core fields to multiple surrounding belt and parabelt fields. It also shows adaptation and forward masking effects which have a lifetime of several seconds. These features are captured in a computational model which diverges from other modelling efforts by including as much of the auditory cortex as possible at the cost of keeping the local dynamics as simple as possible. The intuition behind this has been that many phenomena of auditory neuroscience emerge from large-scale interactions in the auditory system. The computational unit of the model is the cortical microcolumn comprising a set

of interacting excitatory (pyramidal) and inhibitory (interneuron) cell populations, each described by a mean firing rate and leaky-integrator dynamics. The columns are organized into multiple fields with a core-belt-parabelt structure mimicking that of the primate AC, resulting in multiple streams of feedforward and feedback activation. The model explains a wide range of single/multi-unit phenomena: forward masking, stimulus-specific adaptation, two-tone facilitation, and selective responding to complex sounds such as tone sequences and speech. Non-invasive phenomena explained by the model include the adaptation of the N1 response (the most prominent wave of cortical auditory evoked potential) and the dependence of the N1 on stimulus statistics (the so-called mismatch response or MMN). All of the above phenomena require the contribution of short-term synaptic depression of the excitatory synapses. Also, the serial structure of AC supports selective responding by the columns to complex sounds. The current approach could serve as the basis for developing a comprehensive model of central auditory processing and of central problems in hearing.

PS 257

Synaptically Released Zinc Tunes Auditory Cortical Responses and Auditory Processing

Charles Anderson¹; Shanshan Xiong¹; Thanos Tzounopoulos²

¹University of Pittsburgh; ²Department of Otolaryngology and Neurobiology, University of Pittsburgh

Fine-tuning of sensory processing affects behavior advantageously, but the underlying mechanisms remain unknown. Changes in zinc metabolism are associated with major neurological disorders characterized by deficits in the fine-tuning of sensory processing, such as schizophrenia and autism. Although synaptically released zinc is concentrated within synaptic vesicles in many excitatory synapses in the brain, including in more than 50% of excitatory presynaptic terminals in the neocortex, and inhibits excitatory neurotransmission, little is known about the role of zinc on sensory-evoked responses and sensory processing. Here we show that synaptic zinc is a modulator of auditory-evoked responses and its absence leads to major auditory processing deficits.

To investigate the effects of synaptic zinc on sensory processing, we used two-photon in vivo calcium imaging of GCaMP6 expressing neurons in the primary auditory cortex (A1) of unanesthetized mice. By employing specific high-affinity zinc chelators, as well as ZnT3 knock out (KO) mice lacking synaptic zinc, we find that synaptic zinc shapes cortical responses to sound frequency

and intensity, two major parameters of auditory stimuli. Synaptic zinc signaling reduces the amplitude of sound-evoked responses and sharpens the frequency tuning of layer 2/3 (L2/3) A1 neurons in response to auditory stimuli of 70 dB or louder.

Given the opposite effects of zinc on the gain of sound intensity and frequency tuning, we assessed frequency discrimination acuity and sound level encoding in mice with disrupted synaptic zinc signaling, either genetically in ZnT3 KO mice or locally with infusion of zinc chelators into A1. Disruptions in synaptic zinc signaling caused significant deficits in frequency discrimination acuity of mice. Moreover, ZnT3 KO mice display startle responses to sounds at lower sound intensities compared to wildtype mice. Therefore, in the absence of synaptic zinc mice are tuned very differently to the external auditory world: they startle to sounds that are not threatening and they exhibit significantly reduced ability in detecting behaviorally meaningful changes in the auditory environment.

Because these deficits in the fine-tuning of sensory processing are crucial for the accurate processing of the sensory world and because similar deficits are associated with schizophrenia and autism, our results provide novel mechanistic insights into the crucial role of zinc in normal and pathological neural processing.

Supported by NIDCD, R01 DC007905 to TT

PS 258

Synaptic Zinc Sharpens the Receptive Fields of Primary Auditory Cortical Neurons via Control of NMDA Receptor-mediated Activation of Parvalbumin-containing Interneurons

Manoj Kumar; Thanos Tzounopoulos
Department of Otolaryngology and Neurobiology, University of Pittsburgh

Vesicular (synaptic) zinc inhibits AMPA and extra-synaptic NMDA receptors validating its role zinc as an activity-dependent neuromodulator. Recent studies in our lab, using in vivo transcranial and 2-photon calcium imaging of GCaMP6 expressing neurons in the primary auditory cortex (A1) of awake mice, showed that synaptic zinc shapes sound-evoked response properties in a stimulus-dependent manner. Namely, synaptic zinc inhibits sound-evoked responses and restricts the bandwidth of L2/3 neuron tonal receptive fields to sounds louder than 70 dB. To determine the role of zinc-mediated inhibition AMPA and NMDA receptor in this modulatory effect, we studied the effect of zinc chelation on sound-evoked responses of A1 neurons in presence and absence of NMDA receptors antagonist APV, and AMPA receptor

antagonist NBQX. Injection of NBQX and APV abolished the tone evoked responses. Chelation of synaptic zinc with ZX1 increased the tone-evoked responses of A1 neurons to sounds louder than 70 dB. However, in the presence of APV, zinc chelation showed reduced potentiation effects at 70 dB. Surprisingly, in the presence of APV the potentiation effect of zinc chelation was now revealed at lower sound intensities (>50dB instead of >70dB) suggesting that zinc-mediated NMDA receptor signaling shapes auditory receptive field and mediate synaptic zinc inhibition effects.

Because injection of APV alone increased the tone-evoked responses of A1, we hypothesized that the increase in sound-evoked responses with APV is the result of disinhibition caused by blocking of parvalbumin-containing (PV) interneurons, which express NMDA receptors and form strong inhibitory synapses onto the somatic and perisomatic region of principal neurons. To test this hypothesis, we used PV-cre mice expressing GCaMP6 selectively in PV interneurons. Supporting our hypothesis, application of APV decreased the tone-evoked responses of PV interneurons whereas chelation of zinc increased the tone-evoked responses significantly. Our findings suggest that synaptic zinc shapes sound-evoked A1 responses through modulation of NMDA receptors expressed in PV. Supported by NIDCD, R-01 DC007905 award to TT

PS 259

Surface Grids Enable Multiunit Activity Recording from the Guinea Pig Auditory Cortex

Wiebke Konerding¹; Ulrich Frioriep²; Florian Evertz²; Andrej Krai³; Peter Baumhoff¹

¹Hannover Medical School; ²Blackrock Microsystems Europe GmbH; ³Hannover Medical School, DFG Cluster of Excellence Hearing4All

Recording from auditory cortex at the resolution of action potentials is critical for detailed understanding of spatio-temporal activation patterns. However, spiking activity is commonly only assessable using penetrating probes, which have the disadvantage that the brain tissue is damaged during sampling of the cortex. This is especially disadvantageous for chronic recordings in behaving animals. Subdural surface grids used in electrocorticograms permit simultaneous recording of multiple sites over a large area of the cortex without penetrating the brain tissue. However, distance to the neuronal tissue and high impedances (~ 1 MOhm) limit recordings to local field potentials (LFP).

To overcome this we employ newly developed minimally invasive surface grids with low impedances. These cov-

er the auditory cortex of the guinea pig for simultaneous recording of LFP and multi-unit activity (MUA). The grids are based on a thin parylene C substrate (20 µm thickness) to achieve high flexibility and to enable intimate contact at the electrode-tissue interface. The latter consists of 16 AU contacts (100 µm in diameter) with impedances around 200 kOhm (measured at 1 kHz). Defined holes in the grids enable simultaneous insertion of penetrating multi-electrode arrays (16 contacts). We recorded activity in the auditory cortex from guinea pigs (isoflurane anaesthetized) in response to different acoustic stimuli under closed field condition: pure tones, white noise and click trains.

The surface grid recordings display, after respective filtering, also a signal closely related to MUA. They had unitary appearance and a short duration of < 1 ms. We show similarities between surface and penetrating electrodes by comparing shape and distribution of spiking activity. The surface MUA appeared around the time of synchronous spiking activity recorded with the penetrating electrode and was mainly stimulus-related. The MUA activity on the surface grid was distinct from LFP responses both in timing and morphology. The results confirm the potential of thin-film surface grid technology for chronic multi-site recordings of LFPs and signals related to action potentials, paving the way for minimally invasive cortical recordings at high density.

This work was supported by the German Federal Ministry of Education and Research (Project FlowTrode, FKZ 13GW0050B) and Deutsche Forschungsgemeinschaft (Cluster of Excellence Hearing4All).

PS 260

Hierarchical Computation in Human Auditory Cortex Revealed by Deep Neural Networks

Alexander J. E. Kell¹; Daniel L. K. Yamins²; Sam V. Norman-Haignere¹; Josh H. McDermott¹

¹MIT; ²MIT, Stanford

Sensory processing is thought to unfold hierarchically, but there is little evidence of hierarchy in human auditory cortex. Recently, deep neural networks (DNNs) have been shown to replicate well-established hierarchical aspects of the primate ventral visual stream (e.g., Yamins, Hong et al. 2014). We use DNNs in an analogous fashion to explore potential hierarchical organization in human auditory cortex. We trained a DNN to recognize words and musical genres. The resulting model performed each task as well as humans and exhibited similar error patterns. When used to predict cortical fMRI responses to natural sounds, the DNN performed substantially better than a standard spectrotemporal fil-

ter model (Chi, Ru, Shamma, 2005) despite not having been optimized for neural predictivity. When individual layers of the DNN were used to predict voxel responses, early layers predicted responses in primary areas well, while non-primary areas were best predicted by later DNN layers, providing an objective measure of an increase in computational complexity between primary and non-primary auditory cortex. Our results suggest a computational hierarchy in human auditory cortex and illustrate that DNNs are a useful tool to understand sensory systems beyond the ventral visual stream where they were developed.

PS 261

Temporal Sound Processing in the Auditory Cortex Depends on Both Myelin Integrity and Oligodendrocyte-dependent Metabolic Support

Sharlen Moore¹; Wiebke Möbius¹; Iva Tzvetanova¹; Klaus-Armin Nave¹; Livia de Hoz²

¹Department of Neurogenetics, Max Planck Institute of Experimental Medicine, Göttingen, Germany; ²Max Planck Institute of Experimental Medizin

Our understanding of the roles that myelin and oligodendrocytes (OLs) play in information processing in the brain has widened in the past years. The static view of myelin as an insulator is changing. For example, the capability of OLs to transport glycolytic end-products directly to the axon confers them an important metabolic support role, which might be essential during periods of high frequency firing. With the aim to dissect the partially independent roles of myelin and OLs in supporting the reliable firing of axons, we studied sound processing in the auditory cortex in mice with either different degrees of dysmyelination, or an OL-specific metabolic impairment.

We performed in vivo multiunit recordings in the auditory cortex of anesthetized mice, using sounds protocols that aimed to test both spectral and temporal auditory processing. To test temporal acuity, we used a gap-in-noise detection protocol. This protocol was paralleled by comparable behavioral tests, in order to understand the relationship between the neuronal responses and perception.

We used four mouse models with either 1) complete (shiverer *-/-* mice) and 2) partial (MPB-hypomorph *-/-* mice) dysmyelination, 3) cortical-specific dysmyelination (Emx1-cre::MBPfl/fl) and 4) OL-specific inducible glycolytic dysfunction (Plp1-CreERT2::Hif1 α fl/fl). As expected, we found that dysmyelination caused a major increase in response latencies, whose magnitude was correlated with the extent of dysmyelination.

In addition, complete dysmyelination caused hyperexcitable responses, which might have been caused by the mislocalization of Na²⁺ and K⁺ channels in naked axons. Both complete dysmyelination and OL-metabolic dysfunction caused neuronal-population fatigue and temporal acuity deficits, which could not be explained simply by a delay in conduction velocity. Strikingly, all aspects specific to spectral processing were normal. Likewise, partial dysmyelination caused an increase in the behavioral gap detection threshold, a common measure of temporal acuity, in the absence of a frequency discrimination deficit.

In summary, we found that both, complete dysmyelination and OL-specific metabolic dysfunction without dysmyelination, generated deficits in auditory temporal processing while leaving spectral processing intact. This suggests that specifically temporal-detection mechanisms require axons that are not only fast and reliable, but also metabolically stable. These characteristics are given by the structure of myelin and the OLs metabolic capacities, respectively.

PS 934

A High-frequency Tonotopic Reversal in Marmoset Parabelt Auditory Cortex

Darik W. Gamble¹; Xiaoqin Wang²

¹Johns Hopkins University; ²Department of Biomedical Engineering, The Johns Hopkins University, Baltimore, MD, USA

The current working model of primate auditory cortex comprises the hierarchical arrangement of a series of functionally distinct information processing stages: a primary 'core' region, a secondary 'belt' region, and a tertiary 'parabelt' region. Combined anatomical, physiological, and imaging experiments in monkeys have subdivided core and belt into multiple tonotopic subfields (Kaas & Hackett 2000). Human fMRI investigations have attempted to find homologues of the primate core fields A1 and R by looking for a low-frequency tonotopic reversal near Heschl's gyrus (HG), the histologically-identified site of human primary auditory cortex. While many studies have found such a reversal, a long-standing contradiction exists between results supporting an auditory cortex oriented parallel to HG, and others perpendicular to HG (Baumann, Petkov & Griffiths 2013; Moerel, de Martino & Formisano 2014). Using a single neuron mapping technique in awake and behaving marmosets, we have identified a previously unrecognized high frequency tonotopic reversal in putative parabelt auditory cortex, immediately lateral to the previously known low frequency reversal in lateral belt. Such a spatial arrangement of high and low frequency

regions in adjacent fields could conceivably be mistaken for a single field with a tonotopic axis perpendicular to the true cortical configuration. Thus this high frequency region may explain the mutually contradictory patterns of results observed in human imaging studies. Neurons in this high frequency region exhibit long response latencies, strong selectivity for acoustic parameters, such as bandwidth, intensity, temporal modulation, and spatial location, as well as response modulation by behavioral engagement.

Auditory Nerve II

PS 262

eCAP Recordings in Chronically Implanted Guinea Pigs: Effects of Deafening, Electrical Stimulation, and Anaesthesia

Dyan Ramekers; Sjaak F.L. Klis; Huib Versnel
University Medical Center Utrecht

Background

The electrically evoked compound action potential (eCAP) is thought to contain a wealth of subject-specific information that could be used to the benefit of individual cochlear implant (CI) users. However, in practice the eCAP is only minimally exploited for such purposes. A possible reason for this discrepancy between theory and practice is that many aspects of the eCAP – such as its shape or its exact origin – are still poorly understood. By recording eCAPs in guinea pigs longitudinally and under controlled laboratory conditions, we have attempted to relate specific eCAP characteristics to changes in cochlear conditions.

Methods

Normal-hearing guinea pigs were implanted with an intracochlear electrode array. Four weeks after implantation the animals were deafened by co-administration of kanamycin and furosemide. Using a MED-EL PULSAR cochlear implant, awake eCAP recordings were performed at least weekly during the entire 7-11 weeks of implantation. In addition, eCAPs were recorded under anaesthesia at three time points. In each session eCAPs were recorded in response to single biphasic current pulses of which the current level, phase duration and inter-phase gap were systematically varied (Ramekers et al. [2014] *J Assoc Res Otolaryngol* 15).

Results

Gradual changes in eCAPs over time after implantation involved increases in maximum amplitude and slope, and a decrease in threshold. Acute effects of both electrode insertion and anaesthesia were substantially longer latencies than in awake conditions. After deafening the amplitude and slope progressively decreased;

remarkably, a transient decrease in threshold was observed, which was restored to normal levels typically within a week. The eCAP latency followed a similar pattern immediately after deafening, and fluctuated over the course of weeks following deafening. Gradual changes of the eCAP morphology over time were observed after implantation in the normal-hearing situation, and to a lesser extent after deafening, and these changes mainly concerned the longer-latency (~0.5-1.5 ms) P2-N2-P3 complex.

Conclusion

We conclude that performing eCAP recordings in awake guinea pigs is feasible, even with current levels needed to evoke saturation-level eCAPs. The stability of eCAP recordings over time allows for a close examination of subtle changes in neural responsiveness to CI stimulation following multiple manipulations.

PS 263

Individual Differences in Suprathreshold Hearing and Relationship to Cochlear Synaptopathy

Hari Bharadwaj¹; Barbara Shinn-Cunningham²
¹*Purdue University*; ²*Boston University*

Threshold audiometry is the foundation upon which current clinical hearing evaluations are based. Yet, many individuals with normal hearing thresholds have difficulty communicating in noisy settings. Over the last few years, we have documented that even among listeners with normal thresholds and no hearing complaints, large individual differences exist in the ability to perceive subtle temporal features of clearly audible sounds, and to selectively process target speech in the presence of competing sounds (Ruggles et al., *Proc Natl Acad Sci USA*, 2011; *Curr Biol*, 2012; Bharadwaj et al., *J Neurosci*, 2015). Furthermore, we find that these suprathreshold differences in individual perceptual sensitivity correlate with physiological measures of suprathreshold auditory processing from the brainstem and auditory nerve (Bharadwaj et al., *J Neurosci* 2015). These measures, based on brainstem envelope-following responses, auditory brainstem responses, and the middle-ear muscle reflex, show that perceptually-relevant physiological differences among individuals may be present very early along the auditory pathway.

Recent animal studies of acoustic overexposure and aging have robustly demonstrated that the afferent synapses and nerve terminals innervating the cochlea are especially vulnerable to damage (Kujawa and Liberman, *Hear Res* 2015). These studies also show that even a significant loss of cochlear synapses (“synaptopathy”) does not lead to changes in thresholds. Such synaptopathy, if also present in humans, can account for the large

individual differences that we observe, and explain, in part, the hearing difficulties in some human listeners despite normal thresholds (Bharadwaj et al., *Front Syst Neurosci*, 2014; Plack et al., *Trends Hear*, 2014). However, the hypothesis that synaptopathy is a significant contributor to suprathreshold hearing variation in humans is (as of this writing) yet to be directly tested. Here, we summarize and update the human evidence that is indirectly in support of this notion, discuss the several challenges that remain with this interpretation, and identify areas for future experiments. Finally, we compile results from many of our previous unpublished experiments (using otoacoustic-emission and electrophysiological measurements) to review both the promising, and the challenging aspects of translating synaptopathy markers from small laboratory animals to humans.

PS 264

Analysis of the Genomic Response to Auditory Nerve Injury in an Adult Mouse Model

Ryan Boerner¹; Mary Bridges²; Yazhi Xing²; Jeremy Barth³; Judy R. Dubno⁴; Hainan Lang²

¹*Department of Otolaryngology, Head and Neck Surgery - Medical University of South Carolina*; ²*Department of Pathology and Laboratory Medicine - Medical University of South Carolina*; ³*Department of Regenerative Medicine and Cell Biology - Medical University of South Carolina*; ⁴*Medical University of South Carolina*

Background

Without external intervention, the loss of spiral ganglion neurons secondary to aging, genetic mutations, or cochlear injury is irreversible, and ultimately leads to sensorineural hearing loss. A subset of glial cells in the adult animal auditory nerve has been previously demonstrated to express characteristics of neural stem/progenitor cells following acute injury. MicroRNAs (miRNAs) modulate as much as 60% of the mammalian genome and are important regulators of cellular proliferation. We hypothesize that miRNAs serve regulatory roles directing the molecular mechanisms that coordinate the transition of mature glial cells to a regenerative state in the acutely injured auditory nerve.

Methods

Using a well-established surgical approach, adult mice were subjected to round window application of ouabain, a cardiac glycoside that selectively degenerates type I spiral ganglion neurons. Auditory brainstem responses were recorded on post-operative day three (POD3) to assess changes in auditory function. Microarray analyses were conducted on auditory nerve preparations from POD3 ouabain-treated mice targeting differentially expressed miRNAs and mRNAs. RNAs differentially ex-

pressed between ouabain-treated mice and non-treated controls were analyzed using Ingenuity Pathway Analysis (IPA) software to identify mRNA targets, highest-ranking canonical pathways, and predicted interaction networks. Quantitative RT-PCR and in situ hybridization studies were performed on miRNA candidates with significant fold changes and predicted involvement with neurogenesis pathways to validate downregulation and localization within Rosenthal's canal.

Results

Ouabain exposure resulted in differential expression of 175 miRNAs at POD3. Filtering for significance and fold change resulted in 22 miRNAs targeting 294 experimentally observed mRNAs. Of the 22 miRNAs identified, miR-124 targeted 129 of the observed mRNAs and miR-34a targeted 14 of the observed mRNAs. Cellular development and cellular growth and proliferation ranked among the most significant functions of miR-34a and miR-124. Further analysis revealed a 35-gene network pertaining to nervous system development and function. Significant downregulation of miR-34a and miR-124 on POD3 following acute injury with ouabain was validated using qRT-PCR. In situ hybridization localized miR-34a and miR-124 to glial and neuronal cells within Rosenthal's canal. Decreased signal strength was also observed in the treated specimens.

Conclusion

Numerous miRNAs and their putative mRNA targets are differentially expressed following acute auditory nerve injury with ouabain. These molecules are linked to cellular development and proliferation. Further validation with gain/loss of function assays will continue to illuminate how these miRNAs constitute the genomic response following acute auditory nerve injury.

PS 265

P7C3 Protects Rat Spiral Ganglion Neurons After Deafening

Muhammad T. Rahman¹; Bo Peng¹; Catherine J. Kane¹; Benjamin M. Gansemer¹; Steven H. Green²

¹*Department of Biology, The University of Iowa, IA-52242*; ²*Department(s) of Biology and Otolaryngology*

Background

Spiral ganglion neurons (SGNs) receive their sole input from hair cells, the auditory sensory cells and gradually die after destruction of hair cells with aminoglycosides (Alam et al. *J Comp Neurol*, 2007). P7C3, an aminopropyl carbazole has been shown to exert proneurogenic and neuroprotective roles in animal models of neurodegenerative disorders including Parkinson's disease (De Jesús-Cortés et al. *PNAS*, 2012) and Amyotrophic Lat-

eral Scerois (Tesla et al. PNAS, 2012) by activating the rate-limiting enzyme (NAMPT) in the NAD salvage pathway (Wang et al. Cell, 2014). We assessed the ability of an active analog of P7C3, P7C3A20, to protect SGNs after deafening.

Methods

Sprague Dawley rats were injected intraperitoneally with kanamycin daily postnatal day 8 (P8)-P16 to destroy hair cells. Rats showing auditory brainstem response below 95 dB SPL were excluded from the experiment. From P22-P70, rats were injected daily intraperitoneally with P7C3A20, 20 mg/kg in vehicle (DMSO/corn oil) or, as a control, vehicle only. Rats were euthanized at P70 and cochleae fixed, cryosectioned parallel to the mid-modiolar plane, labeled with myosin 6/7 antibodies to detect hair cells, and with NeuN and NF200 antibodies to detect, respectively, SGN nuclei and somata/axons. Only near-midmodiolar sections were used for analysis. Deafening was confirmed by absence of hair cells. Quantitation was done using the FIJI ImageJ package with some macros written in the lab. The outline of Rosenthal canal for each turn in the midmodiolar plane was manually traced for calculation of cross-sectional area. NeuN-labeled images were processed in ImageJ for automated counting of SGNs and calculation of SGN density in each turn.

Results

Kanamycin injection resulted in profound deafness, confirmed by loss of outer and inner hair cells and absence of ABR. By P70, SGN density was significantly reduced in the basal region of the cochleae of deafened control vehicle-injected rats relative to hearing control animals. SGN loss at P70 in apical region of the cochleae was not significant. SGN in the basal region of the cochleae was significantly ($P < 0.05$) reduced in deafened rats injected with P7C3. We conclude that P7C3 appears to be protective against SGN death after aminoglycoside deafening. This further suggests that dysregulation of NAD⁺ metabolism plays a role in the death of SGNs after deafening.

PS 266

Deciphering Spiral Ganglion Neurons Heterogeneity by Single-neuron Transcriptome Profiling

Gopal Pramanik¹; Mirna Mustapha¹; Joerg Waldhaus²; Stefan Heller³

¹Stanford; ²Stanford, OHNS Department; ³Department of Otolaryngology – Head & Neck Surgery, Stanford University School of Medicine, Stanford, CA 94305

In the mammalian cochlea, two major types of auditory neurons exist: Type I spiral ganglion neurons (SGNIs)

are myelinated and carry all the auditory information from organ of Corti inner hair cells to the auditory brainstem. More than 90% of all auditory neurons are SGNIs. In sharp contrast, the remaining 10% unmyelinated type II SGNs (SGNIIs) innervate outer hair cells. In addition to the difference between the two types of neurons, SGNIs are themselves morphologically and physiologically diverse; they consist of low and high threshold subtypes. Moreover, they differ in their susceptibility to noise insult. These differences between types and subtypes are likely driven by distinct gene expression profiles. Studies that define the molecular profiles of these different types and subtypes of neurons have been hampered by the inability to isolate pure populations of this group of neurons. We used a transgenic mouse with the unique feature of fluorescently labeled SGN I and SGN II and single cell gene expression profiling to distinguish between type I and type II SGNs. Moreover, to distinguish different SGN I subtypes that we hypothesize correlate with low and high threshold phenotype, we employed quantitative single cell RT-PCR for a preselected group of 192 candidate genes aimed to specifically distinguish among types and subtypes of SGNs. These studies will contribute to elucidate significant questions in the field such as molecular profiles that define the different types of SGNs (SGNI and SGNII) as well as different SGN I subtypes.

PS 267

Using Thresholds in Noise to Identify Hidden Hearing Loss in Humans

Daniel M. Rasetshwane¹; Courtney L. Ridley²; Judy G. Kopun¹; Stephen T. Neely³; Michael P. Gorga¹

¹Boys Town National Research Hospital; ²Boys Town National Research Hospital & University of Florida;

³Boys Town National Research Hospital, Omaha, NE USA

Background

Recent animal studies suggest that noise-induced synaptopathy may underlie hidden hearing loss (HHL). Noise exposure preferentially damages low spontaneous rate auditory nerve fibers, which are involved in the processing of moderate-to-high level sounds and are more resistant to masking by background noise. Therefore, the effect of synaptopathy may be more evident in suprathreshold measures of auditory function, especially in the presence of background noise. The purpose of this study was to develop a statistical model for estimating HHL in humans using thresholds in noise as the outcome variable and experimental measures that reflect the integrity of sites along the auditory pathway as predictor variables. Our working definition of HHL is that it is the portion of the variability in the thresholds in

noise that is not dependent on thresholds in quiet, but is evident in other measures of suprathreshold function.

Methods

Study participants included 13 adults with normal hearing (≤ 15 dB HL) and 20 adults with sensorineural hearing loss (> 20 dB HL at 4 kHz). Experimental measures were (1) distortion-product otoacoustic emissions, (2) auditory brainstem response (ABR), (3) electrocochleographic action potential (AP) and summing potential (SP), and (4) categorical loudness scaling (CLS). All measurements were made at two frequencies (1 and 4 kHz). ABR and ECochG measurements were made at 80 and 100 dB SPL, while wider ranges of levels were tested during DPOAE and CLS measurements. The residual of the correlation of thresholds in noise with thresholds in quiet was calculated using correlational analysis and served as our estimate of HHL.

Results

HHL was correlated with SP/AP ratio ($r^2=0.34$, $p=0.01$) and SP ($r^2=0.18$, $p=0.02$) at 1 kHz and 100 peSPL, and with gender ($r^2=0.14$, $p=0.04$) at 4 kHz. In a second model utilizing the ratio of the variables at 4 kHz to variables at 1 kHz, HHL was correlated with ABR Wave-I amplitude ($r^2=0.25$, $p=0.01$) and Wave-V amplitude ($r^2=0.30$, $p < 0.05$) at 100 dB peSPL. Predictions of HHL using the first model accounted for 44% and 39% of the variance in the measured HHL at 1 and 4 kHz, respectively.

Conclusions

SP/AP ratio, SP, and ABR Waves I and V were the most significant indicators of HHL. The model predictions support our approach as being predictive of HHL. The results are consistent with suggestions that IHC and auditory-nerve pathology may underlie suprathreshold auditory performance.

Funding: This study was funded by NIH NIDCD.

PS 268

Reliability of Wave I of the Auditory Brainstem Response and Relation to Noise Exposure

Christopher Plack¹; Wenhe Tu¹; Hannah Guest¹; Gareth Prendergast¹; Karolina Kluk²

¹Manchester Centre for Audiology and Deafness (Man-CAD), University of Manchester; ²Manchester Centre for Audiology and Deafness, University of Manchester, Manchester Academic Health Science Centre, UK.

Background

In rodent models noise exposure can cause destruction of the synapses between inner hair cells and auditory nerve fibers (cochlear synaptopathy) without affecting

threshold sensitivity. There is currently intense interest in developing diagnostic tests for synaptopathy in humans. The amplitude of wave I of the auditory brainstem response (ABR) is a measure of auditory nerve function and is related to synaptopathy in the rodent models, suggesting that this measure could be a useful non-invasive index of synaptopathy in humans. Although it is regularly reported that wave I in humans is weak and highly variable, potentially limiting its diagnostic utility, it has not been clear whether this variability is random, or due to stable physiological differences between individuals.

Methods

ABRs were measured to 110 dB peSPL clicks presented to 30 audiometrically normal young female participants, divided equally into low noise exposure and high noise exposure groups using a questionnaire-based estimate of lifetime exposure. ABRs were recorded from both mastoid and tiptrode (ear canal) electrodes, with a reference on the high forehead. Recordings were made on two separate days to estimate repeatability.

Results

Although wave I measured using the tiptrode had a higher amplitude than the mastoid response, the coefficient of variation (ratio of standard deviation to mean) was similar for the two montages, implying similar reliability. Surprisingly, the intraclass correlation coefficient across the two sessions was high for both montages, having a value of about 0.83. Consistent with recent results from our laboratory, there was no significant relation between ABR amplitude and noise exposure history.

Conclusions

Variability in wave I of the ABR to high-level clicks most likely results mainly from stable physiological differences between individuals rather than procedural or random variability. If the sources of individual variability unrelated to auditory nerve function can be quantified or reduced, for example by using a differential measure within an individual, wave I may turn out to be a reliable measure of auditory nerve function in humans.

Funding

Supported by the Medical Research Council UK (MR/L003589/1) and by Action on Hearing Loss.

PS 269

Computational Model Predictions of Level-Dependent Changes for Concurrent Vowel Identification

Harshavardhan Settibhaktini; Ananthakrishna Chintanpalli; Anantha Krishna Chintanpalli
BITS Pilani, India

Background

Younger adults with normal hearing have a remarkable ability to segregate two or more simultaneous speeches when presented at varying levels. Difference in fundamental frequency (F0) is an important cue for segregating multiple speeches. Concurrent vowel identification is often studied to understand the effect of F0 difference that helps identify two simultaneously presented vowels. Younger adults with normal hearing showed an improvement in identification score as the vowel level was increased from low-to medium and then decline was observed at higher levels. Similar pattern was noticed for F0 benefit (i.e., difference in identification scores with and without F0 difference). Previously, computational modeling has suggested that the level-dependent changes in phase locking of auditory-nerve (AN) fibers to formants and F0s of vowel pairs may have sufficient information to predict the scores across levels (Chintanpalli et al, JARO, 2014). Now, the current study here attempts to predict the level-dependent scores of concurrent vowels for different and same F0 conditions using the model of AN responses and F0 based segregation algorithm.

Methods

The vowel pairs were formed using the five different vowels that were used in previous studies. The individual vowel ranged from 25 to 85 dB SPL and the vowel pairs either had same (100 Hz) or different F0s (100 and 126 Hz). A physiologically based computational model was employed by cascading the auditory-nerve model (Zilany et al, JASA, 2014) with an F0-based segregation algorithm (Meddis and Hewitt, JASA, 1992). This type of modeling framework has also been used in previous studies to capture the effect of F0 difference in vowel identification for a given level. The present work here further applies this model to study if it can predict the level-dependent changes in identification scores across various levels.

Results

The computational model, based on the segregation of the temporal cues of AN fibers, can almost explain the level-dependent changes in identification scores of both vowels with and without F0 difference. The F0 benefit pattern is observed to be consistent, as it was in the behavioral study.

Conclusions

The results from the computational modeling suggest that the phase locking of AN fibers to vowel's formants and F0s may contain sufficient information for segregating and identifying the concurrent vowel scores across various levels and F0 difference conditions.

Work supported by OPERA and RI Grants.

PS 270

Modelling Polarity and Pulse Shape Effects on the Physiology of Spiral Ganglion Neuron Under Electro-stimulation

Matthieu Recugnat¹; Jaime Undurraga²; David McAlpine¹

¹Macquarie University; ²MacQuarie University

The efficacy of electrical stimulation in cochlear implantation (CI) depends critically on the electrode-neuron interface. Factors such as electrode-neuron distance, spread of excitation along the cochlea, and the status of the auditory nerve fibres determine the number of effective independent neural channels representing sounds as neural spikes. Current research in the field focuses on improving that interface; biologically through increased 'bio-mimicking' of electrical stimulation strategies, pharmacologically with neuro-trophic or -protective drug coatings applied to the electrode array, or through parallel advances in signal processing. This study focuses on polarity and pulse shape effects on the auditory nerve by means of a physiologically inspired model of a single Spiral Ganglion Neuron (SGN) using Finite Element Methods. This model aims to investigate the effect of electrical stimulation in a realistic SGN model in order to evaluate stimulation strategies and determine the efficacy of other proposed improvements in CI devices.

The model incorporates relevant physiological characteristics that generate action potential and result in refractoriness, facilitation, accommodation and spike-rate adaptation. The model also allows for parameterization of ionic channels dynamics and position as well as geometry characterization.

Specifically, we study the effects of polarity and pulse shape on the firing pattern of a single SGN undergoing several degrees of degeneration – from partial (decrease of peripheral myelination) to total peripheral degeneration. Results are compared with published data from animal and computational models.

PS 271

In Silico Examination of Hidden Hearing Loss

Jerome Bourien¹; Katharine A. Fernandez²; Jean-Luc Puel¹; Sharon G. Kujawa³

¹*Institute for Neurosciences of Montpellier-Inserm U1051; University of Montpellier, France;* ²*Section of Sensory Cell Biology, National Institute on Deafness and Other Communication Disorders, Bethesda, MD;* ³*Harvard Medical School and Eaton-Peabody Labs, Massachusetts Eye and Ear Infirmary, Boston MA*

Background

In experimental and clinical settings, sound-evoked compound action potentials (CAPs) of the auditory nerve can be used to detect a cochlear neuropathy - a loss of auditory nerve fibers (ANFs) or their function. In the case of noise- and age-related 'hidden hearing loss', ANF fibers with low spontaneous rates of firing have been implicated as early targets. The contribution of ANF subtypes to the CAP waveform is, however, difficult to directly address because the CAP reflects an ensemble of fibers spiking in synchrony.

Methods

In this study, we developed a computational model of the mouse cochlea to examine the relationship between ANF spiking (neurogram) and the CAP waveform. The model considers the main biophysical properties of the mouse cochlea, including the place frequency map, the number of ANFs per inner hair cell (IHC) all along the tonotopic axis, and the proportion of low-, medium- and high-spontaneous rate fibers per IHC.

Results

This in silico model allows us to simulate different scenarios of neuropathy (including noise exposure, aging or aging after noise exposure) that are difficult to probe in vivo.

Conclusion

In complement to experimental studies, the systematic use of in silico models will provide a better understanding of the neuronal disorders underlying the cochlear neuropathy phenotype with a normal audiogram (hidden hearing loss).

Supported by Office of Naval Research Grant N00014-16-1-2867

Auditory Protheses: Psychoacoustics

PS 272

Spectral Resolution and Auditory Language Growth in Prelingually-deaf Infants with Cochlear Implants

David Horn¹; Meg Meredith²; Susan Norton³; JongHo Won⁴; Jay Rubinstein⁵; Lynne Werner⁶

¹*Department of Otolaryngology - University of Washington;* ²*Seattle Children's Hospital;* ³*Department of Otolaryngology Head and Neck Surgery University of Washington;* ⁴*Virginia Merrill Bloedel Hearing Research Center University of Washington;* ⁵*University of Washington;* ⁶*Department of Speech and Hearing Sciences University of Washington*

Background

Spectral resolution matures during infancy in normal-hearing (NH) children and is mature by at least school-age in prelingually-deaf cochlear implant (CI) users. Spectral resolution through the clinical CI processor is correlated with speech perception in postlingually-deaf adults and is a non-linguistic marker of CI candidacy and clinical device efficacy. The present study investigated whether spectral resolution is correlated with growth rate of auditory language development measured from pre-implant to 1-2 years post-activation in prelingually-deaf infants with CIs.

Methods

Listeners were participants in an ongoing, longitudinal study of auditory resolution in prelingually-deaf CI recipients implanted prior to 24 months of age. Spectral resolution was measured using the spectral ripple discrimination (SRD) task. Listeners were presented with spectrally-modulated noises and responded when spectral envelope peaks were inverted. The highest "density" of spectral modulation for which the listener achieved 80% correct was measured at two spectral modulation depths in counterbalanced order using a single-interval observer-based psychoacoustic procedure. Stimuli were presented in soundfield at 65dBA in a double-walled sound booth and listeners used their best or first CI and preferred device settings. Infants ranged from 11 to 26 months of age at testing. When possible, infants were tested twice at 3 and 6 months post-activation; otherwise they were tested at 6 to 13 months post-activation. The best SRD performance at each ripple depth was used in the statistical analyses. Auditory language development was measured before implantation and at 1 year intervals post-implantation using the Preschool Language Scales-5th edition (PLS-5). Individual PLS scores for expressive and receptive language were used to calculate a linear slope for each listener to signify the rate of language growth.

Results

For 8 infants to date with at least one post-activation PLS score, 10dB SRD was significantly and positively correlated with slope: better SRD was associated with better language receptive and expressive language growth. The 20dB correlations did not reach statistical significance.

Conclusions

Preliminary results suggest that spectral resolution is related to later spoken-language development. Testing of a larger group of children is necessary to verify the current preliminary findings. Spectral resolution may provide a useful measure of clinical device efficacy and outcome prognosis in this population.

Supported by NIDCD R01DC00396, P30DC04661, K23DC013055K23, AOS Clinician Scientist Award, Seattle Childrens Foundation Surgical Pioneers Research Fund, & gift from the estate of Verne J. Wilkens and Motors West.

PS 273

The Effect of Demyelination on Encoding of Amplitude-Modulated Pulse Trains

Arthi G. Srinivasan¹; Mohsen Hozan²; Monita Chatterjee³

¹House Ear Institute; Boys Town National Research Hospital; ²University of Nebraska-Lincoln; Boys Town National Research Hospital; ³Boys Town National Research Hospital

Cochlear implants utilize amplitude modulation of pulse trains to encode fluctuations in incoming sound signals. Consequently, it is crucial that the envelope of the pulse train accurately convey the envelope of the sound signal. It is known that demyelination of an axon can reduce the conduction velocity of propagated action potentials. However, it is unknown what effect different degrees of demyelination of the spiral ganglion axons have on the encoding of amplitude-modulated pulse trains.

Hozan and Chatterjee (2015) implemented a MATLAB/Simulink model of a spiral ganglion neuron incorporating Hodgkin-Huxley dynamics with varying degrees of myelination. They showed that for relatively low carrier rates (i.e., less than 1000 Hz), spike propagation in response to a constant amplitude pulse train is robust even for substantial degrees of demyelination, but that at higher carrier rates, demyelination causes substantial failure of spike propagation relative to the fully-myelinated condition. In this study, we used this model to investigate the effects of demyelination on encoding of amplitude-modulated pulse trains.

Preliminary results indicate that accurate encoding of the envelope of an amplitude-modulated pulse train fails at a lower carrier rate when the degree of demyelination is increased. In particular, the results indicate that, for a single spiral ganglion neuron, the spike propagation delay caused by demyelination causes spike failure at the last central node of the spiral ganglion axon at lower carrier rates compared to the fully-myelinated condition, which causes the spike train to no longer track the carrier rate of the pulse train. Additionally, the results indicate that when multiple spiral ganglion neurons are simulated each at varying distances from a stimulating electrode, a compound action potential indicating neural activity over the group of neurons accurately encodes the envelope of the amplitude-modulated pulse train at low carrier rates (e.g., 400 Hz) even with substantial demyelination. However, at higher carrier rates (e.g., greater than 800 Hz), while the envelope of the pulse train appears to be well encoded in the compound action potential in the fully-myelinated condition, encoding breaks down with increasing demyelination.

PS 274

Validation and Development of the Stripes Test as a Measure of Spectro-temporal Processing in Cochlear-implant Listeners

Alan Archer-Boyd¹; Rosy Southwell²; John M. Deeks¹; Richard Turner³; Robert P. Carlyon¹

¹MRC Cognition and Brain Sciences Unit; ²University College London; ³University of Cambridge

A number of methods, e.g. novel speech-processing algorithms, for improving performance by cochlear implant (CI) users have been proposed. However, it has not always proved possible to demonstrate the benefits of these approaches. This may be due to the absence of a genuine benefit, or test limitations. Listeners have learnt the relationship between their regular speech processing strategy and speech segments, making it difficult to know if a new strategy is effective on the basis of a speech test, which could result in an underestimation of the benefits of a new method. This obstacle can be overcome by using psychophysical tests; however these typically require either spectral or temporal processing, but not both.

The STRIPES (Spectro-Temporal Ripple for Investigating Processor Effectiveness) test requires, like speech, both spectral and temporal processing to perform well. It is robust to learning effects and contains no recognisable phonemes, overcoming the problems associated with learned speech segments.

The test requires listeners to discriminate between stim-

uli comprising of temporally overlapping exponential sine sweeps (the “stripes”) whose frequencies increase or decrease over time. The task is to detect which of three consecutive stimuli contains stripes of the opposite direction to the other two. The starting time is varied in successive presentations and the onsets and offsets are masked with noise, requiring the listener to use the global, multi-channel perception of the stripe direction, not simply cues from a single spectro-temporal segment. The task difficulty is increased by increasing the sweep density (number of sweeps present at the same time). As sweep density increases, the gaps between the sweeps are reduced and the stripe direction becomes more difficult to determine.

Results from six Advanced Bionics CI users show good performance with a 12-channel map using logarithmically spaced filters and poorer performance with a 12-channel map using wider, overlapping logarithmically spaced filters, modelling the effect of increased current spread in the cochlea. All listeners were able to perform the discrimination task, producing both convincing psychometric functions, and convergent thresholds using an adaptive staircase method.

The results of a single-interval discrimination task using the same stimuli will also be presented, and pilot results using STRIPES in speech-like noise. We conclude that the current STRIPES test can provide fast, reliable verification and optimization of new speech-processing and fitting algorithms for CIs. A companion poster (Carlyon et al; this meeting) uses STRIPES to explore the effect of stimulation mode on spectro-temporal processing.

PS 275

The Relationship Between Amplitude Modulation Detection and Spatial Selectivity of Neural Excitation in Cochlear Implant Users

Ning Zhou; Lixue Dong; Matthew Cadmus
East Carolina University

Introduction

Previous research suggests that cochlear implant users' speech recognition performance is related to their ability to detect amplitude modulation. Better amplitude modulation detection thresholds (MDTs) measured in the middle array or averaged along the tonotopic axis predict better speech recognition. Within subjects, speech recognition is also better using just the stimulation sites measured with good MDTs compared to using the whole electrode array. The current study tested the hypothesis that MDT, which is thought to be a temporal acuity measure, depends on spatial selectivity of neural excitation.

Methods

A group of Cochlear Nucleus implant users participated in the study. Within each subject, two stimulation sites estimated with broad and narrow neural excitation were selected. Spatial selectivity of neural excitation at these sites were quantified by measuring a psychophysical forward-masked tuning curve (PTC) in monopolar stimulation (MP 1+2). These stimulation sites were further assessed for modulation detection in monopolar and bipolar stimulation at 250 and 1000 pulses per second (pps). Stimuli were loudness balanced to 50% dynamic range of the monopolar 250-pps stimulus at the broad tuning site. MDTs were measured twice at the loudness-balanced levels. The test was repeated two more times with roving levels to remove any loudness cues that might contribute to MDT.

Results

Results showed that MDTs tended to be better for stimulation sites measured with sharper PTCs, better in bipolar stimulation, and at lower stimulation rates. Preliminary data from a small subgroup of subjects indicated that PTC became sharper as stimulation rate decreased, which suggested that improved MDT at lower rates may be attributed to narrower neural excitation. There were interactions between the examined variables. Using bipolar or low-rate stimulation improved MDT at sites with broad tuning, but MDTs were found comparable across conditions at the sharp tuning sites. As stimulation rate and mode varied, the stimulus dynamic range and the absolute current level at which modulation detection was measured also varied. Our results indicated that MDT was not related to these factors.

Conclusions

These results suggest that modulation detection is dependent on spatial selectivity of neural excitation, with more focused neural excitation yielding better modulation detection. These data also suggest that the improvement of speech recognition achieved by deactivating stimulation sites with poor MDTs reported previously could be a result of improving channel independence.

PS 276

The Relationship Between Multipulse Integration and Psychometric Function for Detection in Human Cochlear Implant Users

Lixue Dong; Ning Zhou
East Carolina University

Introduction

Multipulse integration (MPI) is a function that relates the psychophysical detection threshold to pulse rate for a fixed-duration pulse train. Our previous study has shown that steeper MPI was associated with broader spread

of neural excitation at a high stimulation rate. The aim of the current study was to test an alternative hypothesis that MPI is also related to loudness growth at the stimulation sites. If the slope of neural excitation versus current level function is steep, to maintain threshold, the amount of current reduction needed to compensate for an increase in stimulation rate would be small. Therefore, we hypothesized that steep neural excitation growth would predict shallow MPI.

Methods

A group of Cochlear Nucleus device users participated in the study. For each subject, MPI was measured across the electrode array by obtaining detection thresholds at 160 and 640 pulses per second (pps) in both monopolar (MP 1+2) and bipolar (BP0) modes. In each ear, two stimulation sites were further assessed for neural excitation growth by obtaining psychometric functions (d' versus current level) for detection for the two stimuli in both stimulation modes (2 rates \times 2 sites \times 2 modes). The slopes of the psychometric functions for detection were quantified by fitting log d' versus dB current level.

Results

Results showed that the MPI slopes were significantly shallower in bipolar mode than in monopolar mode, but no significant differences were found in the psychometric functions between the two modes. Slopes of the psychometric functions were not correlated with the absolute current levels. Interestingly, slopes of the psychometric functions did not predict the slopes of MPI in monopolar mode but significantly predicted those in bipolar mode, with steeper neural excitation growth predicting shallower MPI. Finally, a linear regression model showed that monopolar MPI slopes averaged across the stimulation sites negatively correlated with the subjects' speech recognition performance (steeper MPI predicting worse performance), but the bipolar MPI slopes positively correlated with the speech performance (steeper MPI predicting better performance).

Conclusions

These results demonstrated that MPI is not correlated to neural excitation growth in monopolar stimulation, which supported the earlier finding that MPI is related to the number of excitable neurons in the current field. However, as current field narrows such as in bipolar stimulation, MPI is dependent on the steepness of neural excitation growth. Jointly the monopolar and bipolar MPI slopes significantly predict implant users' speech recognition performance.

PS 277

Electrical Cues Underlying Acoustic Spectral Tilt Detection in Listeners With Cochlear Implants

Adam Bosen; Monita Chatterjee
Boys Town National Research Hospital

For listeners with cochlear implants, gross spectral shape (i.e. spectral tilt and spectral modulation) is a cue associated with speech recognition. However, to date the majority of studies on spectral shape discrimination in these listeners have used acoustic stimulation over a wide (multi-channel) frequency range, which makes it difficult to identify the precise electrical cues that listeners are using to discriminate different spectral shapes. The goal of this project is to develop a direct stimulation task that provides the necessary cues for spectral shape discrimination, to identify the specific electrical cues that determine spectral shape sensitivity in listeners with cochlear implants.

Postlingually deafened listeners with cochlear implants completed a three alternative forced choice task, in which two intervals contained two electrodes were stimulated with interleaved pulse trains that were "flat", i.e. equal in loudness (the standard), and one interval contained the same electrodes but "tilted", i.e. stimulated at an unequal loudness (the target). Stimulated electrodes were either adjacent or separated by two electrodes. In one version of the experiment the distribution of current levels between the standard and targets was equal, to eliminate the possibility of using within-channel cues to perform the task, and in a second version of the experiment the overall loudness of the standards was balanced to the targets, to eliminate the possibility of using overall loudness cues to perform the task. Results of these experiments will be compared to acoustic spectral modulation detection thresholds at multiple spectral densities, to determine the extent to which these tasks are related.

Preliminary subjective reports indicate that subjects perceive the manipulation of cross-electrode loudness difference as a change in stimulus pitch, which they can use to pick out the tilted target. Detection thresholds for tilted targets are asymmetric with respect to whether the stimulation is louder on the basal or apical electrode, with smaller detection thresholds for basal-louder stimuli than for apical-louder targets. Additionally, detection thresholds are variable across individuals. Results of this task are expected to predict listener ability to detect acoustic spectral modulation and perceive differences in speech spectra.

PS 278

Estimation of Intracochlear Place-of-Stimulation with Pitch Matching and Interaural-Time-Difference Discrimination for Cochlear-Implant Listeners with Single-Sided Deafness.

Olga A. Stakhovskaya¹; Gerald I. Schuchman²; Matthew J. Goupell³; Joshua G.W. Bernstein²

¹Walter Reed National Military Medical Center, Bethesda, MD; Department of Hearing and Speech Sciences, University of Maryland, College Park, MD; ²Walter Reed National Military Medical Center, Bethesda, MD;

³Department of Hearing and Speech Sciences, University of Maryland, College Park

Introduction

For individuals with single-sided deafness (SSD), a cochlear implant (CI) can provide some spatial-hearing benefits, including improved sound-source localization, and the ability to benefit from head shadow and binaural squelch for improved speech perception in noise. Because binaural processing requires matched intracochlear place-of-stimulation, interaural mismatch caused by standard CI frequency-to-electrode allocation may be particularly detrimental to SSD-CI listeners. As a step toward reducing interaural mismatch, this study compared two psychoacoustic methods for estimating the interaural place-of-stimulation for SSD-CI listeners: pitch matching and interaural-time-difference (ITD) discrimination.

Methods

ITD discrimination was measured by presenting 500-ms bursts of 100-pulses-per-second (pps) electrical pulse trains to a single CI electrode and bandlimited pulse trains with variable carrier frequencies to the acoustic ear. Listeners discriminated between two "reference" intervals (four bursts each with constant ITD) and a "moving" interval (four bursts with variable ITD). Interaural pitch matching was measured by presenting 25-pps acoustic pulse trains (or pure tones) with variable carrier frequencies to the acoustic ear and 25- (or 900-pps) pulse trains to a single CI electrode. Listeners judged whether the pitch of the acoustic stimulus was higher or lower than the pitch of the electric stimulus. Two acoustic-stimulus frequency ranges were used for each electrode to control for non-sensory biases.

Results

Preliminary results are reported for 7 SSD-CI listeners, with 2-5 electrodes tested for each participant. For most of the SSD-CI listeners and electrodes tested, the function describing the relationship between ITD-discrimination performance and carrier frequency had a maximum where listeners achieved 70-100% performance. On av-

erage, this peak occurred 0.41 octaves above the standard CI frequency allocation (range: -0.8–1.15 octaves). The pitch-matching data showed a substantial effect of the acoustic-stimulus frequency range, suggesting a non-sensory bias (i.e., monaural assessment of pitch) rather than an interaural pitch comparison.

Discussion

The repeated observation of frequency-range effects for the pitch-matching estimates in our SSD-CI users may preclude determining the intracochlear place-of-stimulation using pitch-matching tasks. ITD discrimination was a more promising method of estimating intracochlear place-of-stimulation, yielding performance peaks that for most listeners and electrodes were consistent with the expected upward frequency shift relative to a standard CI frequency-to-electrode allocation. [The views expressed in this article are those of the authors and do not reflect the official policy of the Department of Army/Navy/Air Force, Department of Defense, or U.S. Government.]

PS 279

Effect of Age on Gap Detection Thresholds in Cochlear-Implant Users

Maureen Shader; Matthew J. Goupell

Department of Hearing and Speech Sciences, University of Maryland, College Park

Cochlear implants (CIs) are considered a safe and effective treatment for severe hearing loss in adults of all ages. However, older CI users may not perform as well as younger users on measures of speech understanding. One possible reason for poorer performance in older CI users is the presence of age-related deficits in auditory temporal processing ability. Age-related auditory temporal processing deficits are well-documented in normal-hearing and hearing-impaired listeners, but have not yet been established for CI users. The ability to accurately encode temporal cues is particularly important for this population as CIs convey speech information using primarily temporal cues because spectral information is greatly reduced. The purpose of this study was to investigate auditory temporal processing using gap detection in older CI users to identify age-related deficits.

Gap detection thresholds (GDTs) were measured in older (>65 yrs) and younger (< 45 yrs) CI users using single-electrode direct stimulation. Stimuli were 300-ms constant-amplitude pulse trains presented at stimulation rates of 100, 500, 1000, or 4000 pulses per second (pps). GDTs were measured at five electrode locations in each participant. In order to isolate age-related changes in temporal processing ability from issues of neural survival, electrically evoked compound action potential

(ECAP) amplitude growth functions were also measured at the same five electrode locations.

Preliminary data show that GDTs for younger participants ranged from 2.4-15.5 ms with an average GDT of 5.8 ms. GDTs for older participants ranged from 0.7-42.6 ms with an average GDT of 7.3 ms. GDTs decreased with increasing stimulation rate. Some participants showed large differences in GDTs across electrodes and across ears; these within-participant differences seemed related to neural survival because steeper ECAP slopes were associated with better gap detection performance.

These preliminary results suggest that auditory temporal processing ability, as measured by GDTs, declines with increasing age in CI users. Duration of deafness is likely a confounding factor because poor neural survival, as inferred by shallower ECAP amplitude growth functions, also negatively affects GDTs. Results of this study not only initiate the establishment of age-related temporal processing deficits for CI users, but may also be useful in the implementation of age-specific programming strategies in order to maximize CI performance. [Work supported by NIH grant R01-DC014948 and the University of Maryland.]

PS 280

Multi-Source Localization in Binaural Electric Hearing

Matthew J. Goupell¹; Regina M. Baumgärtel²; Adelia Witt¹

¹Department of Hearing and Speech Sciences, University of Maryland, College Park; ²1 Medizinische Physik, Forschungszentrum Neurosensorik, and Cluster of Excellence "Hearing4All", Carl-von-Ossietzky Universität Oldenburg, Germany.

Normal-hearing (NH) listeners are able to precisely localize single sound sources by processing interaural differences in level and time. They can also localize multiple sound sources simultaneously in complex acoustic environments in a seemingly effortless manner. Additionally, the ability to localize and separate several sound sources yields a benefit regarding speech intelligibility in noise. The interaural differences exploited by NH listeners are only transmitted to a limited extent in current cochlear-implant (CI) systems. While interaural level differences and envelope interaural time differences are available yet potentially distorted, fine-structure interaural time differences are not made available at all. Despite these limitations, bilateral CI users using such clinical devices have been shown to be able to localize single sound sources; however, it is unclear how well bilateral CI users localize multiple simultaneous sound sources

with distorted and diminished interaural cues. Therefore, the current study investigated the ability of bilateral CI listeners to localize multiple concurrent sound sources.

Listeners were presented with up to three simultaneous presentations of different IEEE sentences produced by the same speaker at the same level. Sound sources were either collocated or separated in space. The spatial information was provided using virtual acoustics in an anechoic environment and presented to the listeners via open-backed headphones. Listeners were asked to indicate how many sound sources they perceived and where these sources were located with respect to the head. Measurements were conducted in bilateral CI listeners wearing their clinical devices as well as NH listeners presented vocoded signals.

The ability of bilateral CI listeners to separate and localize several sound sources will be discussed on average as well as individually and will be compared to NH listeners' performance. Data from nine CI listeners showed that they were on average able to identify one-source conditions 96% of the time. Two-source conditions were correctly identified 71% of the time. Three-source conditions were correctly identified 27% of the time and were mostly mistaken for two-source conditions. Additionally, the localization accuracy decreased as the number of sources increased. Finally, some listeners demonstrated idiosyncratic localization patterns where one ear dominated and biased the overall sound perception. These results suggest that while bilateral CIs provide reasonably good sound localization, they are much less effective in complex auditory environments and steps should be taken to improve the cues that facilitate sound source separation. [Work supported by NIH grant R01-DC014948 and the University of Maryland.]

PS 281

The Effects of Level on the Upper Limit of Temporal Pitch Perceived by Cochlear Implant Users

François Guérit; John M. Deeks; Robert P. Carlyon
MRC Cognition and Brain Sciences Unit

Cochlear implant (CI) listeners typically perceive an increase in pitch with an increase in pulse train rate, but only up to an "upper limit", around 300 pps, that varies across electrodes and listeners. The limit is thought to originate from a coding limitation at or prior to the inferior colliculus. Here we investigate the effect of level on this upper limit and on rate discrimination thresholds at a low rate, in 9 CI listeners (4 Advanced Bionics, 4 Cochlear and 1 Medel). Stimuli were 400 ms long pulse trains, presented in monopolar mode on a single electrode in the mid or apical region. The upper limit of temporal pitch was measured with a pitch ranking procedure us-

ing eight rates spaced logarithmically between 120 and 981 pps. The obtained ranking function was fit with a broken stick function, with the upper limit defined as the rate at the intersection of the two sticks. Rate discrimination thresholds were measured adaptively, with the signal and standard rates logarithmically centred on 120 pps. For each subject, the levels at 60, 80 and 100% of the dynamic range (DR) for a 90 pps pulse train were obtained. These served as the reference for a procedure in which 4 rates (90, 162, 399 and 981 pps) were successively loudness matched to each other. Loudness-rate functions were interpolated from this procedure and used for both pitch ranking and rate discrimination tasks. Tests were conducted in blocks consisting of two runs of rate discrimination and one run of pitch ranking. To compensate for any training effect, two blocks were obtained at each level, in a counterbalanced order. Preliminary results (7 out of 9 subjects), showed there was a mean level change of 1.3 dB per 20 % of the dynamic range. Some subjects showed marked increases of the upper limit with level, and at least one showed the opposite trend, but there was no overall effect of level either for the upper limit of for low-rate discrimination. For each task there were strong correlations between the two blocks, both in terms of overall performance and in the effect of level, but the tasks did not correlate with each other - suggesting that low-rate discrimination and the upper limit are limited by different mechanisms. These preliminary results also indicate that level does not have a consistent effect on temporal pitch perception of CI users.

PS 282

The Effect of Compression on Contralateral Unmasking in Vocoder Simulations of Cochlear Implants for Single-sided Deafness

Jessica M. Wess¹; Joshua G.W. Bernstein²

¹University of Maryland and Walter Reed National Military Medical Center; ²Walter Reed National Military Medical Center, Bethesda, MD

Background

For listeners with single-sided deafness (SSD), a cochlear implant (CI) can facilitate the perceptual separation of spatially separated concurrent talkers to better hear the target talker of interest. This squelch effect is contingent on integration of binaural cues. SSD-CI listeners likely rely on interaural level differences (ILD) to facilitate binaural hearing since interaural time-difference cues are poorly encoded by CIs. However, differences in loudness growth between the acoustic and CI ears could disrupt ILD cues. This study presented vocoder simulations

of SSD-CI listening to normal-hearing (NH) listeners to investigate how amplitude compression or expansion would affect squelch in a multi-talker speech task.

Methods

Head-related transfer functions (HRTFs) were used to simulate free-field listening. For the left (simulated-acoustic) ear, signals were processed using a pinna HRTF. For the right (simulated-CI) ear, signals were processed using a behind-the-ear (BTE) microphone HRTF, then with an eight channel noise-vocoder (100-10,000 Hz). Listeners identified target speech presented from the acoustic-ear side (-60°) with two same-gender interferers presented from the front (0°) or from the vocoder-ear side (+60°). Instantaneous compression or expansion was applied independently to the envelope in each vocoder channel before the envelope was applied to the noise carrier. Four compression ratios were tested: 0.25, 0.5, 1 (no compression) and 2 (expansion). Speech-identification performance for Coordinate-Response Measure sentences was evaluated over a range of target-to-masker ratios (TMRs) in both monaural (acoustic ear only) and bilateral configurations.

Results

Preliminary results showed a negative effect of compression on squelch, with bilateral performance decreasing to monaural levels. For a subset of listeners, expansion increased squelch beyond that provided by an uncompressed signal.

Discussion

In this virtual cocktail party, single-sided vocoder listeners were able to take advantage of large differences in ILD between the target and interfering speech to perceptually separate the concurrent voices. The decrease in performance with vocoder compression likely reflected a reduction in the effective ILDs and therefore the target-masker ILD difference. Conversely, amplitude expansion would tend to increase the difference between target and masker ILDs, facilitating speech understanding. Although technological constraints exist, these results suggest that spatial hearing for SSD-CI listeners might be optimized by adjusting the CI loudness-growth function.

[Supported by a grant from the Defense Medical Research and Development Program. The views expressed in this article are those of the authors and do not reflect the official policy of the Department of Army/Navy/Air Force, Department of Defense, or U.S. Government.]

PS 283

Binaural Pitch Fusion in Children with Hearing Aids and Cochlear Implants

Lina Reiss; Curtis Hartling; Bess Glickman; Jennifer Fowler; Gemaine Stark; Yonghee Oh
Oregon Health & Science University

Background

Recent studies indicate that many hearing-impaired adults who use hearing aids and/or cochlear implants have broad binaural pitch fusion, such that sounds with large pitch differences are fused across the two ears and lead to binaural averaging of spectral information (Reiss et al., JARO 2014) and interference in speech perception (Reiss et al., JARO 2016). The goal of this study was to determine whether children with hearing aids and/or cochlear implants also experience broad binaural pitch fusion, how they compare to adults, and how different device combinations influence pitch fusion.

Methods

Binaural pitch fusion was measured longitudinally in four groups of children starting between 6-9 years old, with: 1) normal-hearing (N=25); 2) bilateral hearing aids (N=9); 3) bimodal cochlear implant and hearing aid (N=7); and 4) bilateral cochlear implants (N=12). Stimuli used were tones or electrodes, depending on listening modality. Fusion ranges were measured by simultaneous, dichotic presentation of reference and comparison stimuli in opposite ears, and varying the comparison stimulus to find the range that fused with the reference stimulus. Pitch matching was also conducted to measure mismatches in pitch between the ears.

Results

Children in all groups except the bimodal group had broader fusion, i.e. fused sounds with greater differences in pitch across ears, compared to their equivalent adult cohorts. Across groups, normal-hearing and bimodal children had sharper fusion than hearing aid children. The bilateral cochlear implant group was highly variable, with some children fusing all electrode pairs across ears, and others exhibiting no fusion between any electrode pairs.

Conclusions

The findings suggest that fusion is still developing at this age even in normal-hearing children, and that hearing device combination may influence the development of fusion in hearing-impaired children. In children with cochlear implants, the duration of experience with one or two implants may also influence fusion. As in adults, broad fusion may explain the variability of binaural benefits for speech perception in quiet and noise in children. The results of the long-term longitudinal study will in-

dicating how fusion changes during development in children, and the clinical implications of these group differences for hearing device selection and rehabilitation.

Funding: Supported by NIH-NIDCD grant R01 DC013307.

PS 284

Perception of Musical Consonance and Dissonance by Cochlear Implant Users

Adam T. Schwalje¹; Lex J. Gomez²; Inyong Choi³

¹*University of Iowa Hospitals and Clinics*; ²*University of Iowa Interdisciplinary Graduate Program in Neuroscience*; ³*Department of Communication Sciences and Disorders, University of Iowa*

Background

Music perception in the cochlear implant (CI) patient is a frequently studied area. One approach to this work has been to separately investigate CI users' abilities to perceive the individual elements which comprise music. Elements which have been studied in this way include timbre, pitch, timing, melodic contour, voice number, and more recently dissonance. In music, the terms consonance and dissonance refer to the result when two or more tones are played simultaneously. Consonance sounds open and resolved while dissonance sounds harsh and needs resolution. In one study on dissonance, CI users' ratings of pleasingness of a musical example were not affected by increasingly dissonant chordal accompaniments, though they were affected for normal hearing listeners (Coldwell, 2016). The isolated perceptual task of differentiating between consonance and dissonance has not yet been examined.

Methods

Adult normal hearing listeners and CI users with more than three months experience participated in the study. There were no restrictions on mode of amplification for the CI users. Musical stimuli were created in Max 7 using antialiased sawtooth waves. Just intonation was used for consonant intervals, and equal temperament tuning was used for dissonant intervals. The stimuli were presented using a custom Matlab script. Participants completed a questionnaire on musical training and a brief introduction to the concepts of consonance and dissonance. The first set of stimuli involved repeated presentations of major seventh (dissonant) and octave (consonant) intervals above A#4 (466.16 Hz) and G#5 (830.61 Hz). Participants were asked to press one for consonance and two for dissonance. The second set of stimuli involved repeated presentations of two consonant (perfect fifth and octave) or dissonant (augmented fourth and major seventh) intervals followed by a third

target interval, which was either consonant or dissonant (octave or major seventh). Participants were asked to press one if the target was a similar type to the preceding intervals, and two if the target was a different type than the preceding intervals. Statistical analysis was performed using Matlab.

Results

CI users scored near or below chance levels in assigning the labels “consonance” or “dissonance” to a given interval.

Conclusions

Consonance and dissonance are essential elements of musical structure and carry musical meaning. CI users exhibit a deficit in perception of consonance and dissonance. Further research is necessary to determine the extent to which this deficit affects music appreciation, and whether perceptual training is possible in this area.

PS 285

Interactions Between Pitch and Timbre Perception in Normal-hearing Listeners and Cochlear Implant Users

Xin Luo

Arizona State University

Introduction

Pitch and timbre are two important dimensions of auditory perception. Fundamental frequency (F0) is the primary acoustic correlate of pitch perception, while several other acoustic features contribute to timbre perception. For example, the timbre of a sound is sharper when the spectral slope is higher with more emphasis on high frequencies. Although F0 variations have been shown to affect sharpness perception, little is known about the effects of spectral slope variations on pitch perception. This study tested the interactions between pitch and sharpness perception in normal-hearing (NH) listeners and cochlear implant (CI) users.

Methods

Pitch- and sharpness-ranking thresholds were first measured using a two-alternative, forced-choice task with a two-down/one-up adaptive procedure. In each pitch-ranking trial, two harmonic complex tones had the same spectral slope of -8 dB/octave but different F0s centered on 200 Hz. In each sharpness-ranking trial, the two stimuli had the same F0 of 200 Hz but different spectral slopes centered on -8 dB/octave. The intensity level of each stimulus was roved around 65 dBA to minimize the loudness cues associated with F0 and spectral slope changes. A method of constant stimuli was then used to test the interactions between pitch and sharpness perception. In each trial, the two stimuli var-

ied in both F0 and spectral slope by the same multiple (0.5-4) of individual thresholds measured above. Half of the trials had congruent F0 and spectral slope changes (both increased or both decreased), while the other half had incongruent F0 and spectral slope changes (one increased while the other decreased). The same stimuli were used for both pitch and sharpness ranking.

Results

CI users had significantly poorer pitch- and sharpness-ranking thresholds than NH listeners. NH listeners' pitch-ranking sensitivity significantly increased when the F0 changes increased and when there were congruent rather than incongruent spectral slope changes. NH listeners' sharpness-ranking sensitivity also significantly increased with more spectral slope changes and in congruent rather than incongruent trials. For CI users, the pattern of pitch-ranking results was similar to that in NH listeners. However, sharpness-ranking sensitivity with CIs was not significantly affected by the congruence between F0 and spectral slope changes.

Conclusions

This study was the first to show a deficit in sharpness (spectral slope) perception with CIs. Pitch and sharpness perception had symmetric interactions in NH listeners, while the interactions were one-directional in CI users. Congruent spectral slope changes enhanced CI users' pitch-ranking sensitivity than incongruent spectral slope changes.

PS 286

ITD-based Benefits with a Temporally Sparse Sound Coding Strategy for Cochlear Implants

Zachary M. Smith; Naomi B.H. Croghan

Research & Technology Labs, Cochlear Limited

Listening in complex acoustic environments remains a challenge for recipients of cochlear implants. While bilateral implantation generally improves hearing performance with the addition of a second ear, evidence suggests that much of the benefit can be attributed to monaural effects and little usage of interaural time differences (ITDs). A temporally sparse coding strategy, FAST, was developed with the aims of 1) delivering more salient ITD cues and 2) increasing power efficiency. Here we report binaural hearing results in two bilateral cochlear implant subjects who have chronic listening experience with the FAST coding strategy over multiple years. While previous results from acute experiments demonstrated significantly improved ITD sensitivity with FAST over conventional coding strategies, this study aims to measure any functional utility of ITD for various complex listening tasks. Results show significant levels of unmasking in a competing talker task based on real-

istic ITD cues and demonstrate the role of ITD in spatial perception for these listeners.

PS 287

Contralateral Efferent Suppression of Human Hearing Sensitivity in Single-sided Deaf Cochlear Implant Users

Waldo Nogueira¹; Enrique A. Lopez-Poveda²; Andreas Buechner¹; Benjamin Krueger¹

¹Medical University Hannover, Cluster of Excellence "Hearing4all"; ²University of Salamanca

Introduction

Cochlear implants (CIs) are being implanted in people with unilateral hearing loss because they can improve speech intelligibility and sound source localization. Though designed to restore the afferent auditory stimulation, the CI possibly restores some efferent effects. The present study aimed at investigating this possibility. Specifically, we investigated the potential suppressing effect of CI electrical stimulation on the normal-hearing ear via activation of the contralateral medial olivocochlear (MOC) efferents.

Methods

Five Advanced Bionics unilateral CI users with less than 30 dB hearing loss up to 4 kHz in their acoustic ear participated in the study. Absolute thresholds for their acoustic ears were measured for pure tones of 500 and 4000 Hz with durations of 10 and 200 ms in the presence and in the absence of contralateral broadband electrical stimulation delivered with the CI. The electrical stimulus consisted of pulse trains (symmetric biphasic pulses with phase duration 36 μ s) on all 16 electrodes sequentially stimulated at a rate of 416 pps. Its duration was 500 ms and its intensity was set to have loudness equal to the loudness of a broadband noise at a level of 50 or 60 dB SPL in the acoustic ear, the level typically used to activate the contralateral MOC reflex in normal-hearing listeners without activating their middle-ear muscle reflex. Thresholds were measured using a three-interval, three-alternative, forced-choice procedure with a two-down, one-up adaptive rule to estimate the level for 71% correct in the psychometric function. The difference in thresholds between the conditions with and without contralateral electrical stimulation was regarded as an estimation of the inhibitory effect of the contralateral MOC reflex evoked by the CI.

Results

As expected, thresholds measured without the contralateral electrical stimulus decreased with increasing tone duration, and the rate of decrease was faster at 500 than at 4000 Hz. The contralateral electrical stimu-

lation increased thresholds by 0.59 and 0.61 dB at 500 and 4000 Hz, respectively. This increase appears smaller than previously reported for normal hearing listeners. These preliminary results support the notion that for single-sided deaf CI users, the CI modulates hearing in the normal, acoustic ear via activation of the contralateral MOCR. Further research is required to fully characterize such modulations.

This work was supported by the DFG Cluster of Excellence EXC 1077/1 "Hearing4all".

PS 22

Development of First Health-Related Quality of Life Instruments for Children with CIs and Their Parents

Alexandra Quittner¹; Ivette Cejas²; Michael Hoffman¹

¹University of Miami; ²University of Miami Miller School of Medicine, Department of Otolaryngology

Background

Severe to profound hearing loss is associated with measurable deficits in health-related quality of life (HRQoL), reflecting the cascading effects of deafness on multiple domains of functioning (e.g., social functioning). Results are presented on the creation of the first cochlear implant- (CI) specific HRQoL instruments for deaf children, ages 6 to 12, and their parents. Importantly, items are presented to these young children in a pictorial format with audiotaped recordings of the items and response options.

Methods

Instrument development followed procedures outlined in the FDA Guidance on Patient-Reported Outcomes (2009). Phase I included a systematic literature review to generate a conceptual framework; this was used to guide focus group interviews with key stakeholders (e.g., audiologists, physicians), followed by open-ended interviews with children and their parents. In Phase II, stakeholders (n = 40), children with CIs and their parents (n = 24 dyads) were interviewed at two CI Clinics (University of Miami, Children's Hospital of Philadelphia). Data were uploaded into NVivo and coded using FDA guidelines. The process included: 1) agreement on initial codes, 2) independent coding of each transcript and calculation of interrater agreement, and 3) review of content by investigators to ensure comprehensiveness. Saturation of content was calculated by assessing the frequency with which each item was mentioned by children and parents, and the point at which no new content was elicited. Next, draft instruments were created. In Phase III, we conducted cognitive interviews with a new group of 24 parent-child dyads to test the clarity, comprehensiveness and use of the rating scales. All items for children with CIs ages 6-12 years were administered

in a multi-modal format, using pictures, audiotaped recordings of the items and response options.

Results

Themes from the interviews included: parental acceptance, device management, language skills, academic difficulties, emotional and social functioning. Saturation of content with both children and parents was achieved after coding 10-12 interviews. The child self-report measure has 8 domains: Noisy Environments, Academic Functioning, Child Acceptance, Oral Communication, Social Functioning, Fatigue, Emotional Functioning, and Device Management. The parent-proxy version includes 55 items assessing the domains listed above, plus Behavior Problems and a Parenting Stress module.

Conclusions

This is the first study to develop HRQoL measures specific to school-age children with CIs and their parents. Future directions include a national psychometric validation of these measures. CI-specific instruments will enable us to track long-term outcomes, identify key targets for intervention, and analyze cost-effectiveness.

PS 926

Ordinal and Rational Pitch Perception with a Cochlear Implant: Through The Processor and on a Single Electrode

David M. Landsberger¹; Ann E. Todd²; Natalia Stupak³; Griet Mertens⁴; Paul Van de Heyning⁵

¹New York University School of Medicine; ²New York University; ³NYU School of Medicine; ⁴Antwerp University Hospital + University of Antwerp; ⁵University of Antwerp

Music perception and enjoyment through a cochlear implant is generally poor. One of many issues with delivering pitch through a cochlear implant is that processing strategies are designed to be “ordinal” in pitch (i.e. higher frequencies will be perceived as higher in pitch than lower frequencies) but not “rational” (i.e. a doubling of a frequency is not perceived as an octave increase in pitch.) Without rational pitch, melodies, chords, and harmonic structures are all distorted. In one set of experiments, ordinal and rational pitch were measured for cochlear implant users through their clinical processors in order to evaluate the pitch distortions present with clinical implementation. Ordinal pitch was measured using pure tones with the Melodic Contour Identification task (Galvin et al., 2007 Ear and Hearing) demonstrating that, provided the semitone difference between notes was large enough, subjects were able to perceive ordinal pitch. Rational pitch was measured by playing the song “Happy Birthday” using

pure tones. The spacing between the notes was uniformly either expanded or compressed across trials such that a semitone in the melody would be represented by more or less than a semitone in pure-tone frequency space. Cochlear implant users were either not sensitive to changes in semitone spacing or preferred a distorted semitone spacing, suggesting rational pitch is not correctly represented through the processor. Normal-hearing control subjects demonstrated excellent ordinal and rational pitch through the same protocol. A second experiment was designed to evaluate if temporal coding on a single electrode provided rational pitch. In this experiment, the “Happy Birthday” rational pitch experiment was reproduced using a research interface to provide stimulation on single electrodes where the rate of amplitude modulations (AM) was adjusted to represent frequency. The experiment was repeated on many different electrodes. Subjects were mostly not sensitive to changes in semitone distortions in AM rates suggesting that temporal pitch alone does not provide rational pitch. Either AM is insufficient to generate rational pitch or the relationship between AM rate and pitch has a non-linear distortion. In summary, rational pitch is not available to cochlear implant users clinically and temporal coding of a frequency alone does not address this limitation. Further work needs to be done to provide rational pitch to a cochlear implant user.

Brainstem Session II

PS 288

Test-retest Reliability Across Brainstem and Cortical Classes of the Auditory Evoked Potentials

Gavin M. Bidelman; Monique Pousson; Calli Dugas; Amy Fehrenbach
University of Memphis School of Communication Sciences & Disorders

Event-related brain potentials (ERPs) have proven useful in the objective evaluation of sound encoding at multiple tiers of auditory processing. The utility of ERPs for use in clinical assessment and empirical research relies critically on the precision and test-retest repeatability of the measure. Neuroelectric potentials are recordable at different stages of the auditory pathway (brainstem, cortex). We aimed to determine how these different classes of neural responses directly compare in terms of their internal consistency and test-retest reliability. We recorded auditory brainstem responses (ABR), brainstem frequency-following responses (FFR), and cortical (P1-N1-P2) auditory evoked potentials elicited by speech sounds within the same set of listeners. We reassessed responses within each of four different test sessions over a period of one month, allowing us to detect possible changes in latency/amplitude characteris-

tics with finer detail than in previous studies. Our findings show that brainstem and cortical amplitude/latency measures are remarkably stable; with the exception of slight prolongation of the P1 wave, we found no significant variation in any response measure. Moreover, intraclass correlation analysis revealed that the speech-evoked FFR amplitude and latency measures achieved superior repeatability (ICCavg = 0.89) among the more widely used obligatory brainstem (ABR; ICCavg=0.62) and cortical (P1-N1-P2; ICCavg=0.45) auditory evoked potentials. We infer (i) the repeatability of auditory neural responses decreases with ascending level along the auditory neuroaxis (cortex < brainstem) and (ii) speech-FFRs might provide a more stable measure of auditory function than the conventional (click-evoked) ABR.

PS 289

Diverse Neurophonic Responses Implicate Both Excitation and Inhibition in a Model of the Medial Superior Olive

Joshua Goldwyn¹; Myles Mc Laughlin²; Eric Verschooten²; Philip X. Joris²; John Rinzel³

¹Ohio State University; ²University of Leuven; ³New York University

Background

Patterns of auditory brainstem field potential responses to monaural sound stimuli can resemble, strikingly, extracellular voltage (Ve) patterns generated by current dipoles (Biedenbach and Freeman 1964, Mc Laughlin et al 2010). A long-standing view is that medial superior olive (MSO) neurons generate these field potentials (the “auditory neurophonic”). Dendrite-targeting excitation to MSO neurons is a “current sink” and the net outward current flow through the soma and opposite dendrite is the “current source” that completes the dipole. We have observed, however, that spatial patterns of Ve appear more “monopole-like” in response to low frequency tones (< 1000 Hz) and transition to “dipole-like” patterns in response to higher frequency tones. We show, using model-assisted data analysis, that the combination of dendrite-targeting excitation and soma-targeting inhibition in MSO can account for diverse Ve patterns observed in vivo.

Methods

We previously recorded neurophonic responses to monaural pure tones in anesthetized cats (Mc Laughlin 2010). Here, we construct an idealized model of MSO neurons to simulate these Ve responses. We assume the neurophonic is generated by a homogeneous subpopulation of MSO neurons and describe all neurons by the equation for current flow in a passive cable (Rall 1977). The combination of off-center (“dendrite-target-

ing”) input and centered (“soma-targeting”) input drive bipolar MSO model neurons. Crucially, we can infer the time courses of these input currents so that simulated Ve patterns match experimentally measured Ve patterns.

Results

We accurately reproduce diverse neurophonic responses to contralateral and ipsilateral pure tones ranging from 600 Hz to 1800 Hz in five MSOs (see Figure). In the process of fitting simulated Ve to data, we obtain time courses of inputs to the model. We find that dendrite-targeting inputs are negative-valued (inward current) and soma-targeting inputs are typically positive-valued (outward current). Consequently, we plausibly identify these inputs as excitation and inhibition, respectively. Additional observations support this interpretation: putative excitation exhibits a “best frequency”, putative inhibition attenuates at high frequency, and putative inhibition precedes excitation (cf. Roberts 2013).

Conclusion

MSO neurons perform a critical role in sound localization and binaural hearing. By solving an inverse problem to uncover (putative) synaptic inputs from neurophonic responses we provide a new perspective on in vivo MSO physiology. Moreover, our model makes testable predictions: pharmacological block of synaptic inhibition should render neurophonic responses “dipole-like” and pharmacological block of synaptic excitation should render neurophonic responses “monopole-like.”

PS 290

Audiograms Measured in Mice with the Amplitude-Modulated Frequency Following Response (AMFR) Are Superior to Those Using Tone ABRs.

Alice Burghard; Kevin Reid; Shigeyuki Kuwada; Douglas Oliver
UConn Health, Dept of Neuroscience

Mice, especially genetically modified strains, are a powerful tool to study the mechanisms underlying hearing disabilities. An initial and essential step is to establish frequency-specific hearing thresholds (audiograms) and any age-related changes in the chosen mouse strain. So, considerable effort has been directed towards using electrical audiometry (e.g., auditory brainstem response, ABR, to tone pips) or behavioral techniques. Behavioral audiograms are the gold standard but are very labor intensive. Hence, the quest to develop sensitive electrical techniques.

We have tested 4 mice strains at different ages using the AMFR with narrow-band carriers (1/3 octave) centered on frequencies ranging from 2-40 kHz. The shape of the modulation envelope was a sine raised to exponent 8

and the modulation frequency was 42.9 Hz. The AMFR produced lower thresholds than the tone ABR. We tested VGAT-ChR2 (H134R)-EYFP (VGAT) mice which expresses channelrhodopsin-2 (ChR2) in GABAergic and glycinergic cells, allowing an in vivo identification of these neurons. The problem with this strain is that it is on a C57BL/6 background, a strain known for its early onset of age-related high frequency hearing loss. The B6.CAST-Cdh23Ahl+/Kjn (B6.CAST) mice were bred specifically to avoid this phenotype. We therefore aimed to create a hybrid of these two strains which expresses ChR2 without a high frequency hearing loss phenotype. Additionally, we tested CBA/J mice as the hearing of this strain has been tested extensively in the past. The animals were anesthetized and the speaker was placed 10 cm above the animal's head.

The hearing threshold in 5-8 week-old CBA/J and hybrids mice was lower with the AMFR methods than that to tone ABR thresholds reported in the literature. Both 6 month-old hybrid mice and 1 year-old pure-bred B6.CAST and VGAT mice showed a relatively normal audiogram, albeit with an elevated hearing threshold but not a clear high-frequency hearing-loss phenotype.

Thus, the AMFR is a very useful tool to phenotype the hearing of transgenic and normal mouse strains with complete audiograms over the life-span. AMFR produces thresholds closer to the behavioral threshold than those from ABR recordings, and AMFR is useful at younger ages than those required for behavioral testing.

Supported by NIH R21DC013822, NSMRL IPA N66596-15, and Health Center Research Advisory Committee

PS 291

Auditory Brainstem Response Derived from Continuous Natural Speech

Ross K. Maddox¹; Adrian KC. Lee²

¹University of Rochester; ²University of Washington

The auditory brainstem response (ABR) is a measurable scalp potential that allows researchers and clinicians to examine function in the early parts of the auditory pathway. Because the brainstem and midbrain are quite deep compared to cortical sources, and the nuclei themselves are quite small, it is impossible to use the scalp field patterns to accurately localize brainstem and midbrain activity to a given generator. However, what the response lacks in spatial information it makes up for in the temporal domain: the distinct waves that make it up (designated as waves I-V, with I, III, and V being the most prominent) have been linked with specific structures through careful comparative work. Because these

responses come at short latencies, the stimuli used to evoke them must be similarly short, leading to a rather restricted stimulus set—typically periodic trains of clicks or brief tone pips. This fact leads to a limited set of experimental options, particularly if one wishes to investigate how these areas respond to natural stimuli or how cognitive processes like selective attention may impact their function.

Here we propose a solution the problem of necessarily-short stimuli: present long, complex stimuli and use system identification to derive a stereotyped response with similar properties to the standard click-evoked ABR. Specifically, we present longform speech (taken from audiobooks) in minute-long intervals and recorded the responses. We then used deconvolution to solve for the set of weights across lag (i.e., the impulse response) that best relate the input (acoustic stimulus, rectified) to the output (recorded scalp potential). Such approaches have been used with great success for late cortical responses by turning the input speech into a “slow” (band-limited) envelope. Here, by rectifying the input stimulus instead of using the envelope, we preserve the detailed temporal information necessary for deriving the ABR.

The grand average derived response (based on N = 23) has largely the same morphology as the click-evoked ABR, with two main differences. First, the individual waves of the speech-derived ABR are somewhat smeared in time. Second, the speech-derived response is shifted earlier in time compared to the standard ABR. This is likely because the response is stronger at the onset of an acoustic wave rather than its peak. Despite these issues we believe this new method represents a significant step forward for studying subcortical auditory structures while subjects are engaged in a realistic behavioral paradigm listening to natural stimuli.

PS 292

Complex Auditory-brainstem Response to the Fundamental Frequency of Continuous Natural Speech

Antonio Forte; Octave Etard; Tobias Reichenbach
Imperial College London

Background

Speech elicits a complex response of the auditory brainstem which reflects, for instance, the fundamental frequency of the speech signal. This speech-evoked brainstem response is typically measured through averaging the neural response to hundred- or thousand-fold repetition of a short speech stimulus such as a single syllable or word. Due to neural adaptation, however, such a large number of repetition makes it difficult to assess the potential modulation of the auditory brainstem response

by higher cognitive processes. Recently we have shown that the brainstem response reflects the fundamental frequency of a continuous, nonrepetitive monotone speech signal in which the fundamental frequency is constant. Natural speech, however, has a fundamental frequency that varies in time which compounds a readout of the brainstem's response.

Methods

We sought to develop a method to quantify the response of the auditory brainstem to continuous natural speech. We employed empirical mode decomposition (EMD) of speech stimuli of several minutes in duration to identify an empirical mode that corresponds to the fundamental frequency of the speech signal; we refer to this mode as the 'fundamental mode' of the speech stimulus. EMD can indeed extract non-linear, irregular oscillations and has recently been used to determine the time-varying pitch of speech. We then recorded the brainstem response to the natural non-repetitive speech stimuli in several volunteers. We correlated the computed fundamental mode of the speech signal to the measured brainstem response.

Results

We found a statistically-significant peak in the correlation of the brainstem response to the fundamental mode of the speech signal. The peak occurred at a latency of around 8 ms, in agreement with previously measured latencies in the auditory brainstem. The peak could be detected from recordings of only one minute in duration.

Conclusions

We have developed the computational methodology to detect the response of the auditory brainstem to the fundamental frequency of natural non-repetitive speech. The brainstem's response exhibits a characteristic latency and shows that the brainstem responds to the pitch structure of the speech stimulus. Brainstem responses can already be obtained from one minute of recording, which makes the method clinically applicable. Because the method does not require repetition of the speech signal it may be useful to investigate the role of the brainstem in speech processing, such as speech comprehension and attention to speech.

PS 293

Psychophysical and Electrophysiological Measures of Temporal Fine Structure Processing in Normal-hearing Listeners

Aravindakshan Parthasarathy¹; Jonathon Whitton²; Kenneth Hancock³; Daniel B. Polley²

¹Eaton-Peabody Labs, Mass. Eye and Ear; Department of Otolaryngology, Harvard Medical School, Boston, MA; ²Eaton-Peabody Laboratories, Massachusetts Eye and Ear Infirmary; ³Eaton-Peabody Labs, Mass. Eye and Ear

Introduction

Encoding of stimulus temporal fine structure (TFS) cues is vital for hearing in noise, where envelope cues are distorted. TFS processing can be estimated from the threshold for detecting frequency modulation (FM) in low frequency tones that offer no amplitude modulation cues. It is generally assumed that FM detection thresholds using this stimulus paradigm depend on the accuracy of temporal coding in the early stages of central auditory processing yet objective physiological measures have yet to be described. Here, we provide a direct link between the perception of temporal cues and TFS coding at early stages of auditory processing through parallel behavioral and electrophysiological measures in individual subjects.

Methods

We measured behavioral detection thresholds to FM from young adult subjects with normal hearing thresholds at two carrier frequencies, 0.5 and 1kHz, which were frequency modulated at a low rate (2Hz). ABRs were obtained and their wave-1 amplitude measured to account for changes in hearing due to neural or synaptic deficits at the level of the auditory nerve. We then characterized electrophysiological encoding of TFS in the same subjects by measuring synchronization in the frequency following response (FFR) to a 500Hz tone with FM ranging from 0Hz to 20Hz. By simultaneously recording from multiple channels and different electrode-montages, we were able to emphasize different generators along the auditory pathway, and explore the contributions of each to TFS coding.

Results

Mean behavioral detection thresholds for the FM deviation was 0.66% (3.3 + 1Hz) at 0.5kHz and 0.64% (6.5 + 1.5Hz) at 1kHz. ABR wave-1 amplitudes did not explain a significant fraction of the variance in the FM behavioral detection thresholds. The FFR measured in these listeners exhibited robust phase-locking to the FM stimuli. The neural phase-locking component of the FM stimulus near threshold (5Hz FM) was a strong indicator of be-

behavioral performance in the FM detection task, explaining ~65% of the variance.

Conclusions

These results suggest that brainstem measures of FM phase-locking serve as a useful biological marker of TFS processing, and may identify a neural predictor for suprathreshold hearing impairments associated with aging or hearing loss. Changes in these responses can also be studied to explore the neural bases for perceptual changes following auditory training.

PS 294

Comparison of Time Course of Frequency Following Response and Otoacoustic Emission Following Short-duration Acoustic Exposure

Sho Otsuka¹; Minoru Tsuzaki²; Satomi Tanaka²; Shigeto Furukawa³

¹NTT Communication Science Laboratories, NTT Corporation; ²Kyoto City University of Arts; ³NTT Communication Science Labs

Background

Recent animal studies have revealed that even exposure to non-traumatic sound can induce the neuronal degeneration of auditory nerve fibers, thereby causing temporal processing deficits. However, there is limited evidence that acoustic exposure degrades temporal coding in humans. To answer this question, we tested violin players during regular practice, where the left ear was exposed to intense violin sounds in the 90-100 dB range, which are sufficient to induce temporary hearing loss. We investigated whether acoustic exposure during a short period of instrument practice affects both the cochlear mechanical function and neuronal temporal coding, which we evaluated via otoacoustic emissions (OAEs) and frequency following responses (FFRs), respectively.

Methods

Seven audiometrically normal students and graduates whose major is/was the violin participated in the experiment. FFRs were recorded with transposed stimuli, which were generated by multiplying a half-wave rectified 100-Hz pure tone with a 4-kHz pure tone. The duration of the stimuli was 270 ms, including 10-ms rise/fall times. The stimuli were presented at 80 dB SPL. OAEs were recorded with clicks, which were presented at a rate of 50/s, and the amplitude around 4 kHz was evaluated. Clicks were presented at 60 dB peak-equivalent SPL. A measurement block was composed of two transposed stimuli (original and inverted) and eight clicks. This block was repeated alternately to the right and left ears 2000 times (approximately 60 min) before and af-

ter a one-hour practice session. The temporal change in the FFR and OAE amplitudes during the measurement periods was monitored.

Results

For the left ears, the OAE amplitude decreased significantly immediately after the end of the violin practice and then returned to the pre-practice level within 10 min. In contrast, no significant FFR decrease was observed right after the practice session, but the FFR amplitude gradually decreased as time proceeded and reached its minimum value (on average 6 dB lower than before the practice session) approximately 15 min later and then recovered within 10 min.

Conclusion

This study observed that FFR and OAE amplitudes decreased temporarily after acoustic exposure. The difference in the time course between FFR and OAE suggests that the changes in FFR do not merely reflect the deterioration of the cochlear mechanical function, and thus implies that acoustic exposure can affect neuronal processes that underlie temporal coding.

PS 295

An Auditory Brainstem Response to Complex Sounds with Cochlear Delay Compensation

Takashi Morimoto¹; Gaku Yabushita¹; Yoh-ichi Fujisaka¹; Yasuhide Okamoto²

¹RION Co., Ltd.; ²Keio University Hospital

Subjective measurement methods, regarding speech intelligibility test for diagnosis of hearing loss or temporal resolution, have been utilized to assess an auditory senses in clinical site. In subjective measurement, a lack of concentration or a difficulty to understand experimental task may cause some undesired result, although measurement time become short in order to reduce the task efforts of subjects by several proposed simplified methods. It seems that to develop objective measurement method is one of solutions in order to avoid the above issues. Auditory brainstem response to complex sounds (cABR), which represents temporal characteristics of complex sound stimuli, attracted people's attention as an objective method to measure temporal auditory sense, e.g., detection ability of temporal modulation and speech intelligibility in background noises. However, the magnitude of recorded neural activation, i.e., amplitude of cABRs, in each subjects are different since there are individual differences in amplitude of cABR and it depends on awakening state, the arrangement place of electrodes, etc. In addition, measurement environments may also cause some issues as artifact. Therefore, it spends many time-consuming in the measurement be-

cause it is required many recorded responses to improve a signal-to-noise ratio (SNR) of the averaging response. In normal ABR measurement, it is well known that a stimulus which are designed to compensate the cochlear delay (compensated stimulus) can be evoked more clear and large response than traditional click stimulus (normal stimulus). We conducted the comparative experiment to verify that the effect of the cochlear delay is observed also in cABR. For 12 normal hearings, the responses of both synthesis syllable /da/ and sinusoidal amplitude modulated noises show that there were significant differences between the cABRs with the normal and compensated stimuli. Hence, it is more easy to recognize the response characteristic in compensated case compared with the normal one. Therefore, the number of averaging, which is required to satisfy a certain SNR of cABR with compensated stimuli, was reduced to about half that of the normal one. Hence, it is more easy to recognize the response characteristic in compensated case compared with the normal one. Therefore, the number of averaging, which is required to satisfy a certain SNR of cABR with compensated stimuli, was reduced to about half that of the normal one. From our result, to apply cABR using compensated stimuli leads to establishment of objective measurement which is extracted of many auditory characteristics.

PS 296

Differences in the Upper Frequency Limit of the Human Frequency Following Response Suggest Different Neural Generator Sites

Chandan Suresh; Ananthanarayan Krishnan
Purdue University

The scalp recorded human frequency following response (FFR) reflects sustained phase-locked neural activity in an ensemble of neurons along the auditory pathway in the brainstem. While it is commonly accepted that the longer latency (6-7 ms) FFR recorded using vertical electrode configuration reflects activity from the inferior colliculus structures, FFRs with shorter latency (2-4ms), reflecting activity from more caudal structures can be recorded using a horizontal electrode montage. It is also known that the upper frequency limit for neural phase-locking decrease as we ascend the auditory neuraxis. Given this, comparison of the FFRs recorded using vertical and horizontal recoding configurations will allow us to characterize both the level of the generator site and the upper frequency limit of neural phase locking. To this end we recorded FFRs in response to tone bursts varying in frequency from 200-3200 Hz (200 Hz steps) from a total of fourteen normal hearing subjects using both vertical (High forehead-to-C7; High forehead-to-ipsi mastoids, and High-Forehead to Tip-

trode) and horizontal (Tiptrode-to-contralateral mastoid; mastoid-to-contralateral Tiptrode) recording configurations. In addition, we compared several other vertical and horizontal electrode combinations in an attempt to isolate neural from receptor potentials. Spectral analyses revealed that the vertically derived FFRs, presumably reflecting activity from more rostral generators, were discernible for stimulus frequencies up to 1600 Hz, although percentage detectability was down to 40% at 1400 and 1600 Hz. For the horizontal derivation, responses were discernible for stimulus frequencies up to 3200 Hz at nearly 100% detectability. As expected, for both derivations response magnitudes were higher at low frequencies and decreased dramatically for frequencies above about 400 Hz. Estimation of response latency showed relatively shorter latencies for the horizontally derived responses compared to the vertically derived responses. The robust nature of the horizontally derived responses even at frequencies above 1600 Hz, and their relative invariant latency suggests that these responses contain both neurogenic and receptor (cochlear microphonic) components. Taken together these results suggest that caudal generators of FFR does indeed have an extended upper frequency limit for neural phase locking compared to the FFRs from more rostral generating sites.

PS 297

Speech-ABR: Influence of Stimulus Duration, Background, and Consonant in Normal-hearing Adults

Ghada BinKhamis¹; Agnès Léger²; Martin O'Driscoll³;
Karolina Kluk²

¹*Manchester Centre for Audiology and Deafness, University of Manchester, Manchester Academic Health Science Centre, UK, King Fahad Medical City, Riyadh, Saudi Arabia;* ²*Manchester Centre for Audiology and Deafness, University of Manchester, Manchester Academic Health Science Centre, UK.;* ³*Manchester Centre for Audiology and Deafness, University of Manchester, Manchester Academic Health Science Centre, UK and Manchester Auditory Implant Centre, Central Manchester University Hospitals NHS Foundation Trust, Manchester, United Kingdom*

The speech-ABR is an auditory brainstem response to short consonant-vowel stimuli. The speech-ABR has been used in research for the past decade to assess brainstem encoding of speech, discrimination between short consonant-vowel stimuli, and speech intelligibility in noise. Different stimulus durations were used in the literature, including shorter stimuli (e.g. 40ms) that contain onset and transition periods with no sustained vowel period, and longer stimuli (e.g. 170ms) that contain onset,

transition, and sustained vowel periods, with a preference towards longer durations to assess discrimination and speech intelligibility in noise.

The reason behind this preference and the differences in speech-ABRs to shorter versus longer stimuli has not been addressed in the literature. Shorter stimuli would be advantageous over longer stimuli as they would require shorter recording sessions and hence would encourage the use of the speech-ABR as a clinical audiological measure. On the other hand, the advantage of longer stimuli may be that they contain a sustained vowel period that is not present in the shorter stimuli, and would hence result in longer frequency following responses that contain more components. This study aimed at evaluating the effect of stimulus duration, background noise, and type of consonant-vowel stimuli. Three stimulus durations (40ms, 50ms, 170ms), two backgrounds (quiet and noise), and three consonants ([ba], [da] and [ga] stimuli) were used.

Preliminary results from normal-hearing adults suggest that consonant-vowel stimuli of different durations elicit speech-ABRs of different latencies but similar amplitudes. The addition of background noise to every consonant-vowel stimuli results in longer latencies and smaller amplitudes of speech-ABRs. At odds with current literature, type of consonant-vowel stimuli does not have an effect on latencies of the speech-ABRs.

These preliminary results suggest that, in normal-hearing adults: 1) shorter stimuli may be used for speech-ABR, provided that stimulus specific normative data are established; 2) the effect of noise background on speech processing can be assessed using speech-ABR; 3) the speech-ABR may not be a useful tool in assessing consonant discrimination.

PS 298

Novel MRI Techniques for Examining Structure and Function of the Central Auditory Pathway

Rebecca Dewey¹; Susan Francis²; Deborah Hall³; Christopher Plack⁴

¹*School of Physics and Astronomy, University of Nottingham. NIHR Nottingham Hearing Biomedical Research Unit.*; ²*School of Physics and Astronomy, University of Nottingham*; ³*NIHR Nottingham Hearing Biomedical Research Unit*; ⁴*Manchester Centre for Audiology and Deafness (ManCAD), University of Manchester*

A current focus of auditory neuroscience concerns the physiological mechanisms that may underlie hidden hearing loss. Animal studies indicate that even short

duration noise exposure and 'low level' noise exposure are sufficient to cause permanent damage to certain hair-cell synapses for high threshold auditory nerve fibres. To date these findings have been shown in several mammalian species, the next important question is whether these patterns of deficit associated with a hidden hearing loss can also be detected in humans. The overall aim of our MRC-funded programme is to understand the damage to the human auditory system that results from cumulative lifetime noise exposure, focusing on exploring behavioural and neuroimaging techniques for detecting and diagnosing hidden hearing loss. Objectives of the neuroimaging work are to determine:

- which neuroimaging measures in the human central auditory system are associated with hidden hearing loss, and
- whether these measures are also associated with tinnitus or hyperacusis.

Here, we report structural and functional magnetic resonance imaging (MRI) data collected on a Philips Ingenia 3.0 T MR scanner (Philips Medical Systems, The Netherlands) with a 32-element head coil.

Subcortical structures within the central auditory pathway cannot easily be localised visually, and so their identification is often estimated using standardised atlases. Here, by combining structural scans from multiple MR pulse sequences with different contrasts, we show that we can improve the confidence in identifying the cochlear nucleus, auditory thalamus and other relevant nuclei involved in auditory processing. Image analysis was performed using SPM12 and software toolboxes coded in Matlab.

Detection of sound-evoked activation was optimised by comparing different functional MRI (fMRI) scan parameters: continuous versus sparse acquisition, cardiac gating (synchronising the timing of each image acquisition to the same point in the cardiac cycle), and active noise cancellation using the OptoACTIVE Optical MRI Communication System (Optoacoustics Ltd., Israel) system. In each condition, broadband noise was presented for 24-seconds followed by a 64-second rest period. Functional MRI data were motion corrected and smoothed using a Gaussian kernel of FWHM 3 mm. Statistical analyses were performed using a general linear model including motion parameters as covariates of no interest. Here, we present findings from this optimisation procedure.

This work is supported by Medical Research Council (MRC) reference MR/L003589/1 awarded to the University of Manchester.

The Auditory Brainstem Response in Unanesthetized Mice

Katrina M. Schrode¹; Takashi Kodama²; Richard J. Sima¹; Sascha du Lac²; Amanda M. Lauer¹

¹*Johns Hopkins School of Medicine*; ²*Johns Hopkins University School of Medicine*

Introduction

The auditory brainstem response (ABR) has become a standard tool for assessing auditory sensitivity and function in clinical research with humans and preclinical research with animals. However, an important consideration is that while the ABR is typically recorded in conscious humans, animals are almost always anesthetized during the ABR recording. This difference means that the ABR recorded in animals is not subject to all of the same factors that are present during recordings in humans. To address this issue, we developed a technique for recording ABRs from unanesthetized, head-fixed mice. We assert that by recording the ABR in unanesthetized animals, we can better approximate the conditions under which the ABR is recorded in humans, thus making these recordings potentially more translatable to clinical research and screening in patients. Furthermore, the unanesthetized ABR could be a useful assay for investigating the effects of neural processes that are affected by wakefulness on auditory function, for example by integrating recordings with optogenetic techniques.

Methods

Mice were implanted with a headplate and electrodes for ABR recording. Bone screws were fastened into the skull. We attached metal wires to the screws to serve as the electrodes and positioned a small plate over the screws. The apparatus was secured with dental cement. For recording, the subject was placed a cylindrical treadmill, and the head was held stationary by screwing the headplate to a suspended post. We adjusted the position of the post as necessary to ensure the subject could move comfortably.

Results

ABRs recorded in unanesthetized mice appeared normal and had a high signal-to-noise ratio. As in the ABR of anesthetized mice, five peaks could be identified in the ABR of unanesthetized mice. The signal to noise ratio was not significantly affected by small movements of the animal, including walking or running. However, the shape of the waveform was strongly dependent on the particular placement of electrodes, with some configurations resulting in much larger waveforms, and others resulting in poorer signal-to-noise ratios.

Conclusions

The ABR recorded in unanesthetized mice is similar to that recorded in anesthetized animals. The unanesthetized ABR will be useful as an early step in approximating clinical conditions in preclinical research, and as an assay to investigate how auditory function is affected by factors that are diminished by anesthesia, such as attention and olivocochlear stimulation.

PS 300

Synaptically Released Zinc Provides Homeostatic Regulation of AMPAR-mediated Neurotransmission During Trains of Synaptic Activity

Bopanna Kalappa¹; Thanos Tzounopoulos²

¹*Department of Otolaryngology, University of Pittsburgh*; ²*Department of Otolaryngology and Neurobiology, University of Pittsburgh*

Since the surprising discovery that zinc is concentrated within synaptic vesicles in many excitatory synapses in the brain, including in more than 50% of excitatory presynaptic terminals in neocortical areas, numerous investigators have studied the possible roles of this metal during neurotransmission. Nonetheless, due to the paucity of zinc-selective tools optimized for neurobiological studies, the physiological roles of zinc during synaptic transmission remained elusive until recently. Our recent studies in the dorsal cochlear nucleus (DCN), used novel tools for chelating and tracking zinc in central synapses and established zinc as an inhibitory neuromodulator in excitatory synapses. In response to a single presynaptic action potential, synaptic zinc is released and inhibits postsynaptic glutamate AMPA receptors (AMPA). Moreover, during repetitive synaptic stimulation, zinc inhibits extrasynaptic glutamate NMDA receptors (NMDARs) and is necessary for activation of endocannabinoid signaling and glutamate release inhibition. However, the dynamics of the different forms of zinc-mediated inhibition and how do they interact among themselves and with glutamate neurotransmission to shape ongoing excitatory glutamatergic signaling remain unknown.

To answer these questions, we recorded AMPAR EPSCs from cartwheel cells, inhibitory interneurons of the DCN, during repetitive stimulation of zinc-rich parallel fibers. At low stimulation frequencies (5 Hz and 20 Hz, 20 pulses) and low probability of release (Pr), chelation of zinc using ZX1, a fast zinc chelator, resulted in AMPAR EPSC amplitudes that were higher than control conditions throughout the train. At higher stimulation frequency (50 Hz, 20 pulses) and/or higher Pr, AMPAR EPSC amplitudes following ZX1 application were higher than control initially, but, surprisingly, were lower than con-

tol conditions later in the train. All zinc-mediated effects were absent in ZnT3 knockout mice, which lack vesicular (synaptic) zinc. Based on these results we propose that synaptic release of zinc shapes excitatory synaptic strength in a frequency- and activity level-dependent manner. Namely, during low probability of release (Pr) and low-frequency stimulation zinc inhibits AMPAR EPSCs; however, during higher Pr and prolonged presynaptic stimulation zinc enhances steady-state responses. We therefore, propose that synaptically released zinc acts as a homeostatic regulator opposing, and in fact balancing the effects of glutamatergic neurotransmission throughout trains of synaptic activity. Our findings on the dynamics of zinc-mediated modulation add zinc as a new key player of short-term plasticity in excitatory synapses.

This work was supported by R01-DC007905 (TT) and 2T32DC011499-06 (BK)

PS 301

Rapid Tissue Dynamics During the Formation of the Calyx of Held

Dakota Jackson¹; John Heddleston²; Shilajeet Ray³; Michael Morehead³; Stansilav Pidhorskyi³; Paul S. Holcomb¹; Samuel Young⁴; Teng-Leong Chew²; Thomas Deerinck⁵; Mark Ellisman⁶; George Spirou¹

¹*Sensory Neuroscience Research Center and Centers for Neuroscience, WVU School of Medicine;* ²*Janelia Research Campus;* ³*West Virginia University;* ⁴*Max Planck Florida Institute for Neuroscience;* ⁵*National Center for Microscopy and Imaging Research, University of California, San Diego;* ⁶*National Center for Microscopy and Imaging Research, University of California at San Diego, San Diego, CA, USA*

The calyx of Held (CH) innervation the medial nucleus of the trapezoid body (MNTB) exhibits hallmark features of competition and pruning to sculpt neural circuit organization. Previously, using serial block-face scanning electron microscopy (SBEM) on tissue collected from littermate mice at 24-48 hour intervals during the first postnatal week, we found that most cells resolve from multiple small competing inputs to a single large calyceal terminal between postnatal (P) days 2 and 4. During these ages the average growth rate of calyces, measured as apposed surface area with the MNTB cell soma, exceeded 200 μm^2 per day. The 24-hour time points likely underestimate the actual growth rate, however. We have since taken advantage of fast light microscopy to increase temporal resolution in live tissue imaging experiments. Transgenic mice were used to fluorescently label globular bushy cells (GBCs) within

the ventral cochlear nucleus (VCN), including their axons that give rise to the CH innervating the MNTB. In a subset of experiments a viral vector driven with the PUNISHER cassette was delivered into the MNTB of newborn mice to differentially label postsynaptic targets within 48 hours. Brainstem slices between 300 μm and 600 μm that contained the VCN and MNTB were collected daily between P0-14. Whilst being imaged, tissue was actively perfused with warm, oxygenated aCSF to sustain viability over long imaging sessions of 1-3 hours. Volumetric time-series were imported into syGlass, a custom software package designed in-house, that allows users to analyze data in an immersive virtual reality (IVR) system. Points were manually placed along the leading tip of key structures to allow the growth trajectory, displacement, velocity and acceleration of growth cones to be quantified at each age. For example, growth cones at P3 had a relatively high average velocity of $367 \pm 17 \mu\text{m/hr}$. These average velocities tended then to drop at older ages, $252 \pm 47 \mu\text{m/hr}$ at P4, and $104 \pm 9 \mu\text{m/hr}$ by P5. Moreover, we previously observed long spicules extending from the edges of CHs and from the soma of MNTB cells in our EM volumes. It was thought these structures represented static features of the two cellular compartments. Live imaging, however, has revealed these too are dynamic and exhibit interesting interaction between pre- and postsynaptic spiculation. These data are effective in monitoring the navigation patterns of assembling neural circuits and more accurately reflect the dynamic nature of growth and retraction that may otherwise be missed without sufficient temporal resolution.

PS 302

Lack of BDNF Impairs Fast Synaptic Transmission in the Auditory Nervous System

Jun Hee Kim; Jie Xu; Miae Jang
University of Texas Health Science Center, San Antonio

Brain-derived neurotrophic protein (BDNF) has been shown to regulate synaptic structure and function, activity-dependent plasticity, and neuronal survival and growth at excitatory synapses in the central nervous system. Recent studies suggest that BDNF plays an important role in vesicular neurotransmitter release and fast synaptic transmission. We investigated the role of endogenous BDNF in fast and reliable neurotransmission in the calyx of Held synapse and its physiological relevance in the auditory brainstem. Using the pre- and postsynaptic whole-cell recordings, we found that reduction of endogenous BDNF decreased spontaneous and evoked vesicular glutamate release from the calyx terminal in heterozygous BDNF (bdnf^{+/-}) mice. This result was caused by the reduction in the readily releasable pool (RRP) size without changes in presynaptic Ca²⁺

influx and release probability. A smaller RRP at the pre-synaptic terminal resulted in a much higher incidence of postsynaptic action potential failures in response to high frequency stimulation in *bdnf+/-* mice. Consequently, this impairment in fast synaptic transmission severely altered *in vivo* auditory function. In the auditory brain response (ABR) test, *bdnf+/-* mice displayed decrease in the amplitude of ABR waves and increase in the central conduction time. Our results suggest that BDNF signaling is crucial for large and fast-transmitting synapses in the auditory pathway.

Clinical Otolaryngology & Pathology: Past, Present, and Future

PS 303

Otology at the Academy of Gondishapur East and West 200 – 600 CE

Robert Ruben

Albert Einstein College of Medicine/ Momtefiroo Medical Center

During the period 200 to 600 CE, at a time when little progress in medicine was being made in Greco-Roman western Europe, southern Persia was home to preservation and dissemination of medical knowledge. Medical information that had been developed earlier in the East -- India -- and the West was studied, preserved, taught and developed through the establishment of the Academy of Gondishapur in southern Persia during the third century CE. This Academy was, in so far as known, the first ever teaching hospital. Medicine from the known world, East and West, was incorporated into the curriculum and texts. The translations of these documents have been analyzed for the diagnosis and care of otological diseases and disorders and are systematically summarized. Amongst the many interesting findings is a heretofore unappreciated description detailed in the *Shruta Samhita* of the use of a pedicle cheek flap for the reconstruction of the pinna. This technique is not mentioned by either Paré or Tagliacozzi.

PS 304

Readability of Spanish Language Patient-Reported Outcome Measures

Laura Coco¹; **Nicole Marrone¹**; **Sonia Colina¹**; **Samuel Atcherson²**

¹*University of Arizona*; ²*University of Arkansas at Little Rock*

The purpose of this report was to examine the readability level of the Spanish versions of several patient-reported outcome measures and include a readability

analysis of two translation approaches. Patient-reported outcome measures are important tools in the field of audiology and otolaryngology used to measure the effects of interventions. If administered to an individual with a literacy level unmatched to the level of the text, the data collected could be unreliable and compromise quality of care metrics. Previous studies have shown that widely used outcome measures in English are beyond the 5th/6th grade reading level suggested for the average population (Aleigay et al 2008; Atcherson et al 2011, Greywoode et al 2009; Kelly 1996; Kelly & Kahn 1991; Kelly-Campbell et al. 2012; Nair & Cienkowski 2010). When translated to Spanish, the readability of the text may be altered. Therefore, the current study's primary aim was to calculate the readability level of several audiology and otolaryngology measurements that have been translated to Spanish. Recently, Colina et al. (2016) demonstrated an alternative to the traditional translation approach used in audiology, in which an interdisciplinary team makes decisions based on the cultural and linguistic needs of the population being tested. This functional approach may reduce linguistic difficulty if required by the needs of the population tested, and could therefore impact the instrument's readability. Therefore, a secondary aim of this study was to compare the readability levels of translated measures created using two methodologies (functional vs. traditional). Readability levels were calculated using the FRY graph adapted for Spanish, as well as the Fernandez-Huerta and the Spaulding formulas. Results showed readability scores were beyond the recommended level for the general public for the traditional versions. Overall, the functional versions yielded lower readability levels than the traditional versions. In many cases, the functional versions were within the recommended reading level for the general public. Our results suggest improved readability scores using the functional approach to translation. Future analysis of the suitability of outcome measures should move beyond readability and include an evaluation of the individual's comprehension of the written text.

PS 305

Diffusion Tensor Imaging in Candidates for the Auditory Brainstem Implant

Vivek V. Kanumuri¹; Julian Klug²; Elliott Kozin³; Aaron Remenschneider⁴; Samuel R. Barber⁵; Mary Cunnane²; Chris Brown²; Daniel J. Lee⁶

¹Massachusetts Eye and Ear Infirmary/Harvard Medical School; ²Massachusetts Eye and Ear Infirmary; ³Massachusetts Eye and Ear Infirmary; ⁴University of Massachusetts / Massachusetts Eye and Ear Infirmary; ⁵2, Department of Otolaryngology, Massachusetts Eye and Ear Infirmary, Boston, MA, USA; ⁶Harvard Medical School

Magnetic resonance imaging (MRI) is routinely performed to determine candidacy for the auditory brainstem implant (ABI) by highlighting cochlear nerve morphology, access to the cochlear nucleus (target of ABI electrode) and any associated tumor pathology. Diffusion tensor imaging (DTI) is a novel technique that complements conventional MRI by determining the organization of white matter in the central nervous system. Recent studies suggest a role for DTI in a) determining the integrity of auditory neural microstructure and b) predicting cochlear implant outcomes in patients with peripheral deafness. However, imaging of the central auditory pathways can be difficult to interpret in ABI candidates who often have macroscopic auditory nerve or brain anomalies, cerebellopontine angle tumors, or distortion from their metallic implants. Our goal was to examine the feasibility of utilizing DTI measures of fractional anisotropy (FA) and mean diffusivity (MD). In a cohort of eight ABI candidates, preoperative and/or postoperative (i.e. after ABI surgery) diffusion weighted imaging (DWI) data were processed retrospectively and measures were made for 5 regions of interest (ROIs): trapezoid body, superior olivary complex, inferior colliculus, auditory radiation and white matter of Heschl's gyrus. Data for all selected ROIs on the implanted side of the auditory pathway could be collected from 75% (n=6) of the patients. Both FA and MD measures could be performed even in patients with significant anatomic distortion. One subject had DTI measures before and after surgery. MD levels were found to be on average 13% lower in ROIs near the site of ABI placement and 5% higher along downstream auditory pathways. Our data suggest that DTI is sensitive enough to detect an increase in fiber density of the central auditory tracts that may correlate with electrical stimulation of the cochlear nucleus and hearing outcomes. DTI is a feasible approach for the assessment of neural microstructure in ABI candidates. Supported by the Bertarelli Foundation

PS 306

Correlation Between Word Recognition Score and Intracochlear New Bone and Fibrous Tissue After Cochlear Implantation in the Human

Takefumi Kamakura¹; Joseph B. Nadol²

¹Human Otopathology laboratory, Department of Otolaryngology, Massachusetts Eye and Ear Infirmary and Department of Otolaryngology, Harvard Medical School; ²Human Otopathology Laboratory, Department of Otolaryngology, Massachusetts Eye and Ear Infirmary and Department of Otolaryngology, Harvard Medical School

Background

Cochlear implantation is an effective, established procedure for patients with profound deafness. Although implant electrodes have been considered as biocompatible prostheses, surgical insertion of the electrode induces various changes within the cochlea. Immediate changes include insertional trauma to the cochlea. Delayed changes include a tissue response consisting of inflammation, fibrosis and neo-osteogenesis induced by trauma and an immunologic reaction to a foreign body. Objectives: The goal of this study was to evaluate the effect of these delayed changes on the word recognition scores achieved post-operatively.

Methods

Seventeen temporal bones from patients who in life had undergone cochlear implantation were prepared for light microscopy. We digitally calculated the volume of fibrous tissue and new bone within the cochlea using Amira® three-dimensional reconstruction software and assessed the correlations of various clinical and histologic factors.

Results

The postoperative CNC word score was positively correlated with total spiral ganglion cell count. Fibrous tissue and new bone were found within the cochlea of all seventeen specimens. The postoperative CNC word score was negatively correlated with the % volume of new bone within the scala tympani, scala media/vestibuli and the cochlea, but not with the % volume of fibrous tissue. The % volume of new bone in the scala media/vestibuli was positively correlated with the degree of intracochlear insertional trauma, especially trauma to the basilar membrane.

Conclusions

Our results revealed that the % volume of new bone as well as residual total spiral ganglion cell count are important factors influencing post-implant hearing performance. New bone formation may be reduced by limiting

insertional trauma and increasing the biocompatibility of the electrodes.

PS 307

Accuracy and Observer Variability in Estimation of Cochlear Duct Length using Clinical Computed Tomography

John E. Iyaniwura¹; Mai Elfarnawany¹; Sadegh Riya-hi-Alam¹; Hanif M. Ladak¹; Sumit K. Agrawal²

¹Western University; ²London Health Sciences Centre

Background

With cochlear implant surgery, it is important that the surgeon has an accurate estimate of the cochlear duct length (CDL) in order to select and implant an electrode of the most appropriate length. The CDL can be estimated from clinical computed tomography (CT) images using a single measurement, the A-value, which is the distance from the middle of the round window to the furthest point on the basal turn passing through the apex. These clinical CT images can be viewed in a standard view or a multiplanar reconstructed (MPR) view. The MPR view is produced from the reconstruction of the image in an oblique plane, which allows for better visualization of the basal turn.

Objective

This study aims to assess the accuracy, as well as the inter- and intra-observer variability of A-value measurements, made in standard and MPR views, in order to compare the clinical performance of both. Methods: Clinical CT and micro-CT images of a set of 20 cadaveric cochleae were acquired. The clinical CT images were presented to four specialists to measure A-values from each image using both views (standard and MPR). Each observer then repeated these measurements, with a minimum of 2 weeks between measurement sessions. A-value measurements, from high-resolution micro-CT images, were used as a reference to evaluate the accuracy of the observers' clinical CT measurements and t-tests were used to examine for significant differences. Intra- and inter-observer variability was evaluated using the intra-class correlation (ICC) statistical test.

Results

The absolute mean percentage difference for the standard and MPR views from micro-CT were $14.53 \pm 5.4\%$ ($p < 0.05$) and $9.48 \pm 4.3\%$ ($p < 0.05$) respectively. ICC values for inter-observer variability were 0.63 and 0.57 for the standard and MPR views, respectively. For intra-observer variability, the lowest ICC values were 0.52 for the standard view and 0.41 for the MPR view.

Conclusions

These results indicate the use of MPR view to make A-value measurements improves the accuracy of measurements. Furthermore, it supports the need to develop an automated method for measuring, in order to reduce observer variability, consequently improving the applicability of the A-value measurement in clinical practice.

Keywords

A-value, cochlear duct length, cochlear implant, inter-observer, intra-observer, computed tomography, multiplanar reconstruction

PS 308

Audiometric Correlates of Primary Auditory Neuropathy: A Temporal Bone Study

Jessica E. Sagers¹; Lukas D. Landegger¹; Joseph B. Nadol²; Konstantina M. Stankovic¹

¹Eaton Peabody Laboratories, Department of Otolaryngology, Massachusetts Eye and Ear, Harvard Medical School; ²Human Otopathology Laboratory, Department of Otolaryngology, Massachusetts Eye and Ear Infirmary and Department of Otolaryngology, Harvard Medical School

Previous work in our laboratory shows that the principal diagnostic tool of the clinical hearing research community, the audiogram, is not capable of indicating cell-type specific damage to the inner ear. Here, we compare medical and histopathological data from deceased human patients with age-appropriate hearing with data from primary auditory neuropathy patients, in whom cochlear hair cells are intact but spiral ganglion neurons are missing. We present a linear mixed model to correlate the degree of primary neuronal loss with audiometric thresholds and speech discrimination scores. Analysis of 51 ears from 34 patients shows that for each ten percent increase in neuronal loss, average thresholds across all patients at each audiometric test frequency increase by 2.85 dB. There is a weak correlation between increased neuronal loss and increased speech discrimination scores. Histopathological study of the human inner ear continues to emphasize the need for non- or minimally invasive clinical tools capable of establishing cellular-level diagnoses.

PS 309**Using A Large Biomedical Database, AudGenDB, to Assess Tympanometric Values in Normal and Down Syndrome Pediatric Patients****E Bryan Crenshaw***Children's Hospital of Philadelphia*

To overcome the obstacles of acquiring clinical research data, a biomedical-computing infrastructure that collects information from several clinical data sources and integrates them into a central relational database has been developed, which is called the Audiological and Genetic Database (AudGenDB). To further enhance the utility of this database, an intuitive, powerful web-based user interface that can build complex queries of data across datasets from several clinical disciplines has been developed (<http://audgendb.chop.edu>). AudGenDB currently contains anonymized data from over 105,000 patients, including 4.4 million diagnoses, ~203,000 audiograms, and ~123,000 tympanograms. The advantage of using databases of this size is that they provide the ability to evaluate normative values with high statistical significance, and to compare these to rare population of patients. To demonstrate the power of using the AudGenDB database to this end, we have evaluated the tympanometric values of normative population and compared them to those values in Down Syndrome (DS) patients, an uncommon condition occurring in about 0.15% of births in the US. After limited our analyses to patients with normal hearing and no measure of tympanic membrane pathology or otitis media, we evaluated 6,320 tympanograms from 1,573 patients, and derived values for normative (90%) range. Additionally, due to the large number of tympanograms that were evaluated were able to assess temporal changes in these values from patients aged, < 1 years old to 18 yo. A detailed description of the temporal changes in these normative data will be discussed in the presentation. Subsequently, we compared the means and distributions of these data to DS patients. They had reduced external canal volumes, lower median static admittance values, and a broader peak pressure distribution. These data demonstrate the power of using a large biomedical database to characterize the hearing health of both normal patients and those with conditions that occur with low incidence in the population.

PS 310**Characterization of Activity Along the Auditory Pathway in Rats Using Positron Emission Tomography (PET)****Simone Kurt**¹; Martin Mamach²; Jens P. Bankstahl²; Ross L. Tobias²; Wilke Florian²; Lili Geworski²; Frank M. Bengel²; Georg Berding²¹*Saarland University*; ²*Hannover Medical School*

In patients, studies with auditory activation using PET (positron emission tomography) are established for the assessment of the central auditory pathway and its function. Voxel based statistical analysis is the gold standard for these studies in humans. We inversely translated this approach for studies in rats as an in vivo method to examine the central auditory pathway. Imaging with a dedicated small animal PET/CT system (Inveon, Siemens) was performed in Sprague Dawley rats using radiotracers reflecting either glucose metabolism (F-18-fluorodeoxyglucose, FDG) or GABAA receptor binding (F-18-Flumazenil, FMZ). Metabolic activity was studied in awake, calmed rats placed into a motion restriction tube within a sound attenuating box with three different auditory conditions: (i) 55 dB laboratory background noise (BG), (ii) 65 dB continuous white noise (WN) and (ii) 95 dB pulsed rippled noise (RN). GABAA receptor binding potentials were calculated based on image-derived input functions using cerebellum and pons as reference. Activation and binding potentials were assessed in normal hearing and bilateral cochlea ablated (ab.) rats in the nucleus cochlearis (NC), the inferior colliculus (IC), the mediate geniculate body (MGB) and the auditory cortex (AC).

During sound stimulation compared to reference conditions (BG, WN) an increased activity was measured in the NC, IC, MGB and AC in normal hearing rats. Compared to cochlea ablated animals normal hearing animals showed additionally activation in the olivary complex and the lateral lemniscus. FMZ revealed a high specific uptake in the brain, especially in auditory regions. Image derived time activity curves allowed to assess regional GABAA receptor binding potentials with reasonable inter-subject variation. Our data demonstrate in small animals the ability of: (i) FDG PET to detect activations throughout the auditory pathway with spatial differentiation of all important substructures and (ii) FMZ PET to quantify inhibitory GABAergic neurotransmission in auditory brain regions. Therefore PET appears to be a promising research tool for evaluating hearing disorders in animal models in vivo.

A Preliminary Protocol for Replacing Word-recognition in Quiet with Speech-in-noise Testing in the Audiologic Test Battery

Matthew Fitzgerald¹; Amanda Burke¹; Daniel Krass¹; Honey Gholami¹; Jannine Larky¹; Sarah Levy¹; Grace Nance²; Devon Palumbo³; Austin Swanson¹; Goutham Telukuntla¹; Steven Losorelli¹

¹Stanford University; ²Louisville University; ³University of Texas Dallas

Word-recognition in quiet has been a staple of the audiologic test battery for over 60 years, and has played a number of roles in assessing audiologic outcomes. However, there is increasing awareness that word-recognition in quiet has little relationship with the real-world communication abilities of the patient. For example, the primary complaint of most individuals with hearing loss is difficulty hearing in background noise, yet this ability has no relationship with word-recognition scores in quiet. Similarly, word recognition in quiet is incapable of assessing other subtle auditory deficits which may be associated with noise exposure, increasing age, or auditory processing disorders.

To address these issues, we are devising a new clinical protocol in which speech-in-noise testing, rather than word-recognition in quiet, is the default speech test in the audiologic test battery. In addition to our basic audiometric testing, we have added two additional features: a) monaural and binaural speech-in-noise testing via the QuickSIN, and b) the SSQ12 (Speech Spatial Questionnaire 12). We presently have data on over 1200 adults, which we have used to determine whether we could predict instances in which word-recognition in quiet is likely to be suboptimal, and therefore have diagnostic significance. We identified 'suboptimal' as a value that differed significantly from 100% correct according to the 95% confidence interval for a monosyllabic word list. To date our data suggest the following:

1. Once the signal is audible, most patients have excellent word-recognition scores in quiet.
2. There is no relationship between word-recognition in quiet and speech understanding in background noise. A number of individuals had QuickSIN values that suggest a difficulty in understanding speech in background noise, despite having excellent word-recognition in quiet, and in some cases having normal hearing thresholds.
3. Most instances in which word-recognition in quiet is excellent can be predicted with a combination of audiometric thresholds and QuickSIN values. This suggests that clinical criteria can be created to determine when word-recognition in quiet is likely to have diagnostic sig-

nificance, and should be conducted.

Taken together, these results provide a framework by which speech-in-noise testing can become the default speech test in the audiologic battery, with guidelines as to when word-recognition in quiet is likely to be diagnostically relevant. Making this subtle, but fundamental shift in the audiologic test battery is likely to have both research and clinical implications, allowing for better diagnosis and management of individuals with hearing loss.

PS 312

The Development of Machine Learning Audiometry

Dennis L. Barbour; Xinyu D. Song
Washington University in St. Louis

The pure-tone audiogram is a perceptual test of hearing threshold as a function of sound frequency and is considered a clinical practice standard for aiding in the diagnosis of hearing loss. The principles of modern audiometry have their roots in classical psychometric theory, which drives most current perceptual testing of any sort. Recently, new forms of inference have emerged from the machine learning field that have been successfully applied to diverse areas such as computerized speech recognition, face detection, shopping recommendations and autonomous vehicle control, but have been slow to permeate psychometrics. Exploiting the power of machine learning, we have devised a novel audiogram estimation procedure that provides all the same information as conventional audiometry, yet can be customized on the fly to achieve other useful clinical goals. New capabilities made possible by machine learning audiometry include reduced testing time, continuous-frequency audiometry (as opposed to octave resolution), audiometric fine structure estimation, enhanced detection of erroneous/misleading subject responses, explicit comparisons to past test results, confidence estimates of clinical diagnoses, and more. The ability to extract so much additional information from the same tone detection task opens up numerous possibilities for improved diagnoses and patient outcomes without substantively changing clinical practice. This presentation will document recent progress in the development of machine learning audiometry and outline its value in clinical practice.

Global Need for Cochlear Implantation: Vast Unmet Need to Address Deafness Globally

Mehmet I. Sahin¹; Konstantina M. Stankovic²

¹*Eaton-Peabody Laboratories and Department of Otolaryngology, Massachusetts Eye and Ear Infirmary;*

²*Eaton Peabody Laboratories, Department of Otolaryngology, Massachusetts Eye and Ear, Harvard Medical School*

Hearing loss (HL) is the most common sensory deficit in the world. The World Health Organization (WHO) reports that more than 5% of the world's population has disabling HL. The most common type of HL is sensorineural hearing loss (SNHL). Therapies for SNHL are limited to assistive devices, including hearing aids, and cochlear implants (CIs). Although novel regenerative therapies are being developed they are years from being in routine clinical use. Therefore, we must leverage the existing technologies.

CIs, which facilitate functional hearing in people with severe to profound SNHL, are the most successful neural prostheses; however, only a small fraction of candidates utilize this technology. Importantly, the number of CI candidates in the world has not been previously calculated. We estimate this number here using data from the WHO, US Census Bureau, World Bank, and existing literature.

Today's world population comprises 7.35 billion people and the average birth rate is 18.9/1000; thus, around 139 million newborns augment the population yearly. Considering the lowest reported incidence of HL (2/1000), we estimate that at least 278,000 newborns need medical support for HL every year, of these newborns, 150,000 are candidates for CI annually. Twenty five percent of today's world population is children younger than 15 years old. Given that 0.2% of children experience profound HL, 3.6 million children are potentially candidates for CI globally. Eleven million adults suffer from severe HL all around the world, and half of these individuals are deaf.

Our analyses indicate that CI technology could immediately benefit large numbers of people across the world. However, at present only a small fraction of this medical need is being met.

The most significant barriers to global CI distribution and implementation are financial. The majority of CI candidates live in low- and middle-income countries; most of these candidates cannot afford CIs with their annual incomes. The ratio of gross domestic product per capita to CI cost ranges from 0.5-3 in high and upper middle-in-

come countries, but is only 0.1 or lower in lower middle-income countries.

Additional complications involve cultural factors, and general-professional awareness. Inadequate infrastructure affects most of the world, and is closely related to economics.

The key factor that, if improved, would facilitate more widespread access to CI technology is global pricing. Besides this, technological improvements such as telesurgery and telementoring could help address some aspects of the problem.

PS 314

The Audiological and Genetic Database Project: A Large Biomedical Informatics Platform for Hearing Research

E Bryan Crenshaw¹; Jeff Pennington²; Byron Ruth²; Jeff Miller²; Aaron Masino²; Joy Peterson²; John A. Germiller³; Ian D. Krantz⁴; Tamar Gomes⁵; Derek Stiles⁵; Juliana Manganello⁵; Margaret Kenna⁵; Linda J. Hood⁶

¹*Children's Hospital of Philadelphia;* ²*The Children's Hospital of Philadelphia;* ³*The Children's Hospital of Philadelphia and University of Pennsylvania;* ⁴*The Children's Hospital of Philadelphia and The Perelman School of Medicine at the University of Pennsylvania;* ⁵*Boston Children's Hospital;* ⁶*Vanderbilt University*

Recent developments in research and clinical practice have improved detection of childhood hearing impairment, the ability to ameliorate its impact on social and cognitive development of children, and the understanding of the genetic basis for hearing impairment. Newborn screening programs detect hearing loss at an early age, and the advantages of early detection and intervention are well documented. Hearing aids and cochlear implants are profoundly important for speech and language development and rehabilitation, and appropriate assessments of these outcomes are crucial for developing evidence-based guidelines for use and quantification of benefit. Genetic analyses hold the promise of improved early detection and diagnosis, prediction of outcomes of therapies, and development of new therapies to reverse hearing impairment. These technologies are already widely used in the clinical setting, potentially providing a plethora of data that could serve to further improve diagnosis and describe the outcomes of therapy. However, most of these data are recorded in disparate written records, clinical systems, or database formats that are incompatible and, if in different institutions, often unknown to each other, and therefore difficult to

compare or to use effectively in large-scale studies. To overcome these difficulties, the AudGenDB project extracts, transforms, and loads data from these disjointed, incompatible information sources into a single relational database, and subsequently provides a powerful, web-based user interface (UI) for querying these data. Here, we will discuss the latest developments that expand the range and complexity of data within the database. The long term goal of AudGenDB is to build a national network for the exchange of patient-oriented data to facilitate research in pediatric hearing health. [Supported by NIH-NIDCD R24 DC012207.]

Genetics: Deciphering Molecular Mechanisms in Human Hearing

PS 315

Subtypes of Type I Spiral Ganglion Neurons Uncovered by Single-cell RNA-seq

Brikha R. Shrestha; Chester Chia; Lisa V. Goodrich
Department of Neurobiology, Harvard Medical School

Faithful transmission of sound information from the inner ear to the brain is dependent on spiral ganglion neurons (SGNs), the primary sensory neurons of the auditory pathway. Functional and anatomical investigations have revealed intriguing details about their heterogeneity, which has in turn informed models of intensity coding at the periphery and selective SGN vulnerability to damage. Yet the molecular underpinnings of SGN heterogeneity remains largely a mystery. Here we sought to gain insight into the molecular basis of SGN heterogeneity by conducting an unbiased and comprehensive single-cell RNA-seq analysis of SGNs from posthearing mice. cDNA libraries of ~200 individual SGNs were sequenced at an average read depth of 4 million/cell using the Illumina NextSeq platform. Following unsupervised clustering methods, we derived a classification that revealed at least three Type I SGN subtypes with distinct gene expression profiles, indicating notable local molecular heterogeneity across the tonotopic axis of the cochlea. Genes that define SGN subtypes were found to span multiple functional categories, from canonical sensory ganglia-enriched transcription factors to genes involved in ion transport and calcium homeostasis. These subtypes emerge over postnatal development with progressively restricted expression of marker genes, as revealed by immunostaining of cochlear sections. Our findings establish a useful framework for further inquiries into the developmental emergence and functional relevance of SGN heterogeneity as well as the molecular basis of SGN vulnerabilities in hidden and age-related hearing loss.

PS 316

Manipulation of Claudin 9 Gene Expression and Its Effects on Early-Onset Hearing loss in Mice.

Braulio Peguero¹; Jin Li²; Carol A. Robbins²; Linda C. Robinson²; Bruce L. Tempel³

¹*University of Washington Department of Otolaryngology Head/Neck Surgery*; ²*University of Washington*;

³*Department of Otolaryngology Head/Neck Surgery*

Mice with age-related hearing loss (AHL) are used as genetic and physiological models of presbycusis. More than 18 AHL loci have been identified in mice; however, we know very little of their gene identity, only 4 genes have been localized to date. The inbred mouse 129S6/SvEvTac (129S6) was shown to be noise resistant (NR) to acoustic trauma and have early-onset AHL. Our laboratory previously reported of a locus for noise resistance (nr1) on Chromosome (Chr) 17 of the 129S6 mouse. The same region was also shown to be associated with early-onset, high frequency hearing loss (nphl) that contributes to AHL. Our objectives for this study are two fold. To understand the relationship between the nphl and the nr1 phenotypes which reside in the same genomic region. To investigate the hypothesis that differences in Claudin 9 (Cldn9) expression contribute to the hearing phenotypes observed in the 129S6 mouse.

Using selective breeding approaches, we transferred short segments of proximal Chr 17 derived from 129S6 to the good hearing CBA/CaJ (CBA) mouse. Mice were exposed for 2 hours to a 103dB SPL noise band and we measured hearing sensitivity using auditory brainstem responses (ABRs) and distortion product otoacoustic emissions (DPOAE). Our results support evidence that nphl and nr1 share the same genomic loci within a 7.6 Mb region of Chr 17. To investigate the role of Cldn9 expression in hearing, we created a knock-in mouse with a tetracycline-dependent transcriptional transactivation system upstream of Cldn9. We regulated the genetic expression of Cldn9 by introducing Doxycycline in the water of the mice. A 1.0 mg/ml dose of doxycycline completely knocks out expression of Cldn9 effectively causing hearing loss in 1-month old mice. The overexpression of the Cldn9 gene also caused hearing loss. We are investigating how the genetic regulation of Cldn9 could determine changes in hearing loss and noise sensitivity. Our findings will help improve our understanding of the genetics and physiological mechanisms associated with AHL and NR and identify the causal genes for 129S6 hearing phenotypes.

PS 317

Cell Fate Commitment, a Potential Role for NuRD and PRC2 in the Mammalian Inner Ear

Wanda S. Layman¹; Dan Williams¹; Malerie McDowell¹; Jie Fang¹; Bryan Kuo²; Jian Zuo³

¹St. Jude Children's Research Hospital; ²University of Tennessee Health Science Center; ³Dept. of Developmental Neurobiology, St. Jude Children's Research Hospital, Memphis, TN, USA

Cellular reprogramming offers tremendous potential for therapeutics, disease studies, and developmental processes. However, direct reprogramming through ectopic expression of defined transcription factors is a slow and inefficient process with most cells failing to reprogram. In the auditory field, ectopic expression of Atoh1 has been used to convert mammalian supporting cells into cells that express many endogenous hair cell markers. In vivo studies of hair cell regeneration found that induction of ectopic Atoh1 in supporting cells during the first postnatal week, leads to the formation of hair cell-like cells. However, induction of Atoh1 at later postnatal ages (P8-P14) showed a dramatic decrease in supporting cell conversion, and by P30, induction of Atoh1 alone no longer leads to the formation of hair cell-like cells. These data suggest that cochlear supporting cells lose their cellular plasticity and capacity for cellular reprogramming during inner ear development. The loss of reprogramming potential in the inner ear has remained a central unresolved question in the auditory field. Cellular reprogramming studies in other systems have shown that the epigenetic memory of the donor cell can greatly impact its ability to be reprogrammed. To address whether similar epigenetic mechanisms also limit the ability of supporting cells to become hair cells, we focused on understanding the role of repressive histone modifying complexes such as the nucleosome remodeling and deacetylation (NuRD) complex and polycomb repressive complex 2 (PRC2). NuRD and PRC2 are highly conserved and required for gene silencing during multiple developmental processes. Using the cre-lox system at late embryonic and neonatal time points, we found that conditional loss of PRC2 or the NuRD enzymatic subunit Lsd1 causes no obvious phenotypic defect in organ of Corti development. However, loss of these factors does cause alterations in the expression of key developmental signaling pathways such as the Notch pathway. Since Notch regulation has been implicated as a factor limiting inner ear reprogramming, we generated mice that have Cre-mediated ectopic Atoh1 expression combined with loss of PRC2 or Lsd1. Interestingly, loss of either of these factors combined with ectopic Atoh1 expression results in a dramatic increase in reprogramming potential that includes a large increase in reprogramming efficiency

and, for the first time, terminal differentiation of some reprogrammed cells. Altogether these data suggest that PRC2 and NuRD negatively regulate genes that are vital for maintaining cellular plasticity but are not required for terminal differentiation of cells in the organ of Corti.

PS 318

Transcription of The Highly Specific Otic Gene Fbxo2 is Regulated by Proximal and Distal Cis Elements

Byron Hartman; Stefan Heller

Department of Otolaryngology – Head & Neck Surgery, Stanford University School of Medicine, Stanford, CA 94305

Fbxo2 is one of the most abundant and specific genes in the mammalian inner ear. It encodes the ubiquitin ligase F-box2, which is essential for cochlear homeostasis and hair cell survival. We generated knock-in reporter mice to define expression of Fbxo2, which is present throughout the early otic vesicle and then becomes concentrated in the floor of the developing cochlear duct. In the neonatal cochlea, Fbxo2 is expressed throughout the organ of Corti as well as the lesser epithelial ridge. Ultimately, in the adult, Fbxo2 is expressed strongly in auditory hair cells and supporting cells, is exceptionally high in Boettcher and Claudius cells, and is found at lower levels in some cells of the lateral wall and spiral ganglia as well as a subset of vestibular hair cells.

Here we aim to decipher how the robust and specific expression of Fbxo2 is regulated and identify cis-elements for directing future gene therapies specifically to the inner ear. Phylogenetic comparison of Fbxo2 across vertebrate species reveals several conserved noncoding regions, including a ~2kb promoter and nine highly evolutionarily conserved regions (ECRs) downstream. Several potential binding sites were identified in silico, including sites for Pax2/5/8, Gata3, and Sox10. Conservation and clustering of binding sites within the promoter and ECRs suggests combinatorial transcription factor binding. We hypothesized that Fbxo2 is regulated through multiple cis-regulatory modules located within the promoter and ECRs.

Thus, we produced a reporter mouse (Fbxo2*tdTomato) with a transgene that mimics the native 100kb Fbxo2 locus while condensing it to about 10kb by excluding non-conserved regions and replacing the Fbxo2 coding region with tdTomato. All nine of the ECRs were individually positioned similar to their native orientation and loxP and FRT sites were strategically included to allow subsequent excision of ECRs in two groups. The proximal ECRs 1-5 can be removed with Cre recombination while the distal ECRs 6-9 can be removed with Flip re-

combination. Crossing to the Fbxo2-H2BVenus enables direct comparison of the Fbxo2*tdTomato expression pattern with that of nuclear Venus driven by the native locus. The full-length transgene determines whether all of the conserved elements are sufficient to confer the normal pattern of Fbxo2 expression, while Cre/Flip excision tests for necessity within the ECR clusters. We find that the fully intact Fbxo2*tdTomato reporter accurately recapitulates the major features of Fbxo2 expression and that downstream ECRs contain elements that enhance expression in otic cells and repress expression in off-target cells.

PS 320

The Edison Mouse Mutant in the Nischarin Gene Causes Chronic Otitis Media

Steve D.M. Brown¹; Michael Crompton²; Hilda Tateosian²; Tom Purnell²; Hayley E. Tyrer²; Andrew Parker²; Greg Ball²; Rachel E. Hardisty-Hughes²; Richard Gale²; Debbie Williams²; Charlotte H. Dean³; Michelle M. Simon¹; Ann-Marie Mallon²; Sara Wells⁴; Michael T. Cheeseman⁵; Mahmood Bhutta⁶; Martin J. Burton⁷

¹MRC Harwell Institute, Mammalian Genetics Unit, Harwell Oxford, OX11 0RD, UK; ²MRC Harwell Institute, Mammalian Genetics Unit, Harwell Oxford, UK; ³Leukocyte Biology, National Heart and Lung Institute, Imperial College London, UK; ⁴MRC Harwell Institute, Mary Lyon Centre, Harwell Oxford, OX11 0RD, UK; ⁵The Roslin Institute and Royal (Dick) School of Veterinary Studies, University of Edinburgh, UK; ⁶Ear Institute, University College London, UK; ⁷Nuffield Department of Surgical Sciences, University of Oxford, UK

Background

Otitis media (OM) is characterised by inflammation of the middle ear (ME) and is a common cause of conductive hearing impairment that places a substantial social, medical and economic burden on healthcare systems globally. Otitis media with effusion (OME) is the commonest cause of hearing impairment in children and the commonest reason for surgery in children. Evidence from studies of the human population suggests that there is a significant genetic component predisposing to the development of chronic OME (COME), however the underlying genes conferring susceptibility are largely unknown. Nevertheless, a number of mouse models of COME have been identified and are illuminating the genes and pathways involved and elaborating the molecular pathological mechanisms. Mouse models of COME, such as Junbo, Jeff and Tgif mutants, have uncovered the role of Transforming growth factor beta (TGF- β) signalling in OM and its interplay with hypoxia

which is a feature of the inflamed microenvironment in COME, reflecting the cross-talk between TGF- β and HIF-1 α signalling pathways (see Cheeseman et al. 2011, PLoS Genet. 7, e1002336; Tatessoian et al. 2013, Hum. Mol. Genet. 22, 2553).

Results

Using N-ethyl-N-nitrosourea mutagenesis we identified a recessive mouse mutant, edison, that spontaneously develops a conductive hearing loss at 21 days as measured by ABR. Histological analysis showed the hearing loss was due to COME, characterised by middle ear cavities filled with a cellular exudate and lined with a thickened mucoperiosteum. Additionally, edison mice display craniofacial and lung abnormalities. The causal mutation was identified as a missense change in a relatively unknown gene, Nisch (Nischarin). NISCH interacts directly with a number of proteins, one of which is ITGA5 which is thought to have a role in modulating VEGF-induced angiogenesis and vascularization. We identified a significant genetic interaction between Nisch and Itga5 that impacts upon development of COME. Mice heterozygous for Itga5-null and homozygous for edison mutations display a significantly increased penetrance and severity of COME. Analysis of interacting partners and downstream pathways implicates PAK1, LIMK1 and RAC1 in the development of COME and further affirms the importance of TGF- β signalling pathways in the development of COME.

Conclusions

The edison mouse highlights a new candidate gene for susceptibility to COME and provides further insight into the genetic pathways and molecular processes involved.

PS 321

Use of Proteomic Imaging Coupled with Gene Expression Analysis to Identify Biomolecules Responsive to Cochlear Injury

Kenyarria Noble¹; Yazhi Xing²; LaShardai Brown³; Mary Bridges²; Michelle Reyzer⁴; Jeremy Barth⁵; Kevin Schey⁶; Edward Krug⁵; Hainan Lang²

¹Department of Pathology and Laboratory Medicine, Medical University of South Carolina; ²Department of Pathology and Laboratory Medicine - Medical University of South Carolina; ³Department of Pathology and Laboratory Medicine - Medical University of South Carolina; ⁴Tissue Core, Mass Spectrometry Research Center - Vanderbilt University; ⁵Department of Regenerative Medicine and Cell Biology - Medical University of South Carolina; ⁶Mass Spectrometry Research Center - Vanderbilt University

Background

Exposure to noise or ototoxic-drugs often results in degeneration of cells in the sensory epithelium and auditory nerve, but the molecular mechanisms underlying cochlear cell loss remain unclear. Global transcriptomic analysis with gene arrays can determine molecular changes in the cochlea after noise- or drug-induced insults, but does not provide precise spatial localization or specify changes in protein levels. Coupling gene arrays with matrix-assisted laser desorption/ionization-time of flight mass spectrometry (MALDI-TOF MS) imaging offers high resolution spatial signatures of the molecular responses to cellular alterations. Thus, the purpose of this study is to identify and characterize regulatory proteins in the cochlea responsive to noise or ototoxic-drug exposure using this complementary proteogenomics approach.

Methods

Young adult CBA/CAJ mice were subjected to octave-band noise at 106 or 112 dB SPL for two hours. Auditory brainstem responses (ABR) were recorded immediately (< 1 hr), and 1-14days post-noise exposure. Microarray analysis was performed on mRNAs of the cochlear lateral wall (LW) and auditory nerve (AN). mRNA expression array data for 1-day post-noise exposure were compared to data previously collected from cochlear tissues after ouabain exposure. dChip software identified differentially expressed mRNAs meeting the criteria of a) increase in expression and b) statistically significant difference ($p < 0.05$). MALDI imaging was conducted on cochlear sections prepared from both noise- and ouabain-exposed mice and putative identifications for observed m/z ratios were compiled using established proteomic databases.

Results

Gene expression results indicate that 394 genes are significantly upregulated in response to injury in both models. MALDI imaging of cochlear sections revealed 14 proteins exhibiting spatially distinct patterns that localized to various cochlear regions including LW and AN in both ouabain- and noise-exposed ears. Convergent analysis of the mRNA and protein data yielded 15 candidates, including molecules related to chemotaxis, apoptosis and protein processing. Select candidates will be examined further using immunohistochemistry and qRT-PCR assays.

Conclusion

The combined analysis of proteomic candidates with gene array data provides a new strategy to acquire functionally active gene products responsive to cochlear injury. The tissue preparation protocol preserves cochlear structures facilitating analysis of warehoused tissue specimens, therefore representing an approach that can

be applied for investigation of human tissue samples.

Funding: Supported, in part, by NIH R01 DC007506, NIH P50 DC000422, NIH P30 GM103342, NIH P20 GM103499, NIH P41 GM103391, and NIH R25 GM072643

PS 322

Two New CreER Alleles with Expression in the Inner Ear of Neonatal and Juvenile Mice

Yuanzhao L. Darcy¹; Brandon C. Cox²

¹*Southern Illinois University, School of Medicine, Department of Pharmacology*; ²*Department of Pharmacology & Department of Surgery Southern Illinois University School of Medicine*

Background

The Cre/loxP system is used to conditionally delete genes or to express a fluorescent protein for fate-mapping studies. More than 30 Cre/CreER lines have been described in the cochlea. However, most lines target multiple supporting cell (SC) subtypes and there have been no reports of Cre/CreER lines expressed in Claudius cells (CCs). For the utricle, few CreER lines have been described. Therefore, studying the expression pattern of new CreER lines in inner ear could provide new tools for the field. Here, two CreER mouse lines (Id2CreERT2 and Sox9-CreERT2) were characterized for the first time in neonatal and juvenile cochlea and utricle.

Methods

Each CreER line was bred with ROSA26tdTomato reporter mouse line. For neonatal studies, tamoxifen (3mg/40g, IP) was given at postnatal day (P) 0 and temporal bones were collected at P6. For juvenile studies, tamoxifen (3mg/40g, IP) was given at P12 and temporal bones were collected at P18. Samples were analyzed by immunostaining and confocal microscopy. To test for Cre leakiness, we examined mice untreated with tamoxifen, which expressed both CreER and tdTomato.

Results

In the neonatal cochlea, the Id2CreERT2 line showed tdTomato expression in all SC subtypes, but at varying levels: CCs >90%, Hensen cells (HeCs) 70%-80%, Deiters' cells (DCs) ~70%, pillar cells (PCs) ~65%, inner phalangeal/border cells (IPhCs/BCs) ~40%, and cells of the greater epithelial ridge (GER) ~60%. 20% of hair cells (HCs) in the apical turn expressed tdTomato which decreased to ~1% in middle and base. In the juvenile cochlea, tdTomato expression was mosaic in HeCs, DCs, and PCs (< 10%), but continued to label the majority of CCs (>80%). In the neonatal utricle, tdTomato expres-

sion was mosaic in SCs (< 10%), with most labeled cells in the striola. Less than 10 HCs were labeled. In the neonatal cochlea, the Sox9-CreERT2 line showed tdTomato expression in >70% of all SC subtypes except for CCs. Expression of tdTomato in HCs decreased in a gradient from apex (~90%) to base (~5%). Studies are underway in the utricle.

Conclusion

To the best of our knowledge, the Id2CreERT2 allele is the first to show expression in CCs, and its mosaic labeling of SCs in the utricle contrasts with the robust labeling of SCs in the cochlea. Sox9-CreERT2 is expressed in all SC subtypes except for CCs

Funding: Supported by Office of the Assistant Secretary of Defense for Health Affairs (W81XWH-15-1-0475), NIDCD (R01DC014441-01A1), and the Office of Naval Research (N00014-15-1-2866).

PS 323

Hearing Preservation in Kcne1^{-/-} mice Achieved by Postnatal Injection of AAV2/1-CB7-Kcne1

Cuiyun Cai; Xi Lin; Jianjun Wang; Wenwen Wang
Emory University School of Medicine

Background

Kcne1 (also named as Isk or minK) is an accessory subunit of the potassium channel Kcnq1. Their coassembly in forming a functional potassium (KV) channel is required for normal hearing functions. These proteins are expressed exclusively in the marginal cells of the cochlear stria vascularis and dark cells in the vestibular crista ampullaris. KV channel is essential for maintaining high potassium concentration and the endocochlear potential (EP) in the endolymph, which is essential for high-sensitivity mechano-transduction of cochlear hair cells. Kcne1 null mutation results in profound hearing loss and balance impairments. The mouse phenotypes are similar to Kcnq1 null representing the human Jervell and Lange-Nielsen syndrome. Currently no mechanism-based therapy is available. It is unclear whether a virally-mediated gene replacement therapy approach expressing a channel accessory unit itself is sufficient to preserve the hearing in the mutant mice, and this was tested in this study.

Methods

Wild type (WT) and Kcne1^{-/-} mice were injected with AAV1-CB7-Kcne1 (1 μ l, 5.0 \times 10¹² genome copies/ml) between postnatal day 0 (P0) and P2 in the endolymphatic space. Only one side of the cochlea was injected and the other side was used as a self-control. Immunolabeling, histological examinations and auditory functional tests were performed to evaluate the treatment effect.

Results

Cochlear sections showed that the cochleae in adult Kcne1^{-/-} mice exhibited a number of abnormal cochlear morphologies (e.g., degeneration of hair cells and the organ of Corti, collapsed Reissner's membrane), which were corrected in the treated cochleae. Auditory brainstem responses (ABRs) showed that injections of AAV1-CB7-Kcne1 into the endolymph didn't damage the normal hearing of WT mice, and there was significant hearing preservation for injected Kcne1^{-/-} mice. Compared to non-injected side the hearing improvement ranged from 20dB to complete correction of the deafness phenotype between 4-32 kHz. This treatment effect was stable for at least 6 months.

Conclusion

Hearing loss and morphology abnormalities in Kcne1^{-/-} mice were prevented by Kcne1 gene replacement therapy in the immature cochlea. This was the first demonstration that expression of a channel accessory subunit is sufficient to correct deafness phenotype by the gene therapy approach. Further studies are needed to test how virally-mediated Kcne1 interacts with the native Kcnq1 in the Kcne1^{-/-} mice to achieve the long-term (>6 months) treatment effects.

PS 324

Functional Characterization of Pendrin and Its Disease-Associated Mutants

Kazuaki Homma; Samuel K. Rosenberg; Satoe Takahashi
Northwestern University

Pendrin is the member of the solute carrier 26 gene family (SLC26A4), and its anion transport function is essential for normal hearing. Over 300 disease-associated mutations have been found in the coding region of the pendrin gene in human patients, but the great majority of these mutations remain uncharacterized. It is imperative to elucidate the functional consequences of these mutations experimentally to determine their pathogenic effects. Such effort will also help define the pathological mechanisms of the mutations, which is important for the subsequent development of potential clinical solutions against each of them. In order to characterize a large number of pendrin mutants with sufficient statistical power, ensemble assays are preferable to individual cell-based assays (e.g., cell imaging-based assays, whole-cell recordings, etc.). Transient transfections of cell lines with plasmids encoding mutant proteins of interest have been frequently used for functional characterization of mutants. However, significant heterogeneity in transient protein expression levels within the transfected cell population may mask small changes in pendrin functions that may account for various disease

phenotypes. In order to cope with such difficulties, we generated human stable cell lines and yeast strains that express human pendrin and its mutants in a drug (doxycycline or β -estradiol)-inducible manner. The function of the pendrin proteins in these expression systems was examined by measuring iodide/chloride antiport activity using the halide-sensitive fluorescent protein, mVenus H148Q/I152L, and by measuring bicarbonate/chloride antiport activity using the pH-sensitive fluorescent probe, SNARF. We expect that functional characterization of pendrin mutants in these drug-inducible protein expression systems will greatly facilitate efforts to better grasp the relationship between functions of pendrin mutants and disease phenotypes. This work deepens our understanding of the physiological roles of pendrin and the pathological mechanisms of many mutations found in the pendrin gene in human patients.

Funding

Work supported by NIDCD (DC014553).

PS 325

Large-pore Channels in Hearing and Noise-Induced Hearing Loss

Julia M. Abitbol; John J. Kelly; Kevin Barr; Dale W. Laird; Brian L. Allman
University of Western Ontario

Connexin (Cx) and Pannexin (Panx) large-pore channels allow the passage of small molecules and ions through the plasma membrane and are expressed in the cochlea. Cxs form the two gap junction networks in the cochlea; the epithelial and connective tissue networks that facilitate cochlear homeostasis. The most prevalent Cxs in the cochlea, Cx26 and Cx30, are essential in the auditory system as loss of either leads to deafness. Another Cx family member, Cx43, has also been reported in the cochlea, although its localization and function remains controversial. Panxs have been more recently studied in regards to the auditory system where all three Panx isoforms (Panx1, -2, -3), were shown to be expressed in the cochlea. Previous studies have reported that mice lacking Panx1 in specific regions of the cochlea have severe hearing loss. However, our group recently discovered that global ablation of Panx1 or Panx3 does not lead to hearing deficits. In addition, global ablation of Panx3 led to decreased susceptibility to noise-induced hearing loss. To further investigate the role of large-pore channels in hearing, we have obtained a Cx43 mutant mice with ~50% Cx43 function, (Cx43I130T/+) that mimics the human disease, oculodendodigital dysplasia (ODDD), in order to determine if these mice harbour hearing deficits. Furthermore, we have generated a novel Panx1Panx3 double knock-out mouse (Panx1-/-Panx3-/-) to determine if loss of both

Panxs together leads to hearing loss, or if these Panx channels are redundant in the process of hearing. To assess hearing sensitivity in our Cx43 mutant and Panx knock-out mice, auditory brainstem responses (ABRs) to click and tonal (4-24 kHz) stimuli were recorded in 2-3 month-old male mice. Preliminary results suggest that Cx43I130T/+ mice do not exhibit severe hearing loss at 2-3 months of age; however, we observed elevated hearing thresholds to the high-frequency tones in two of the six mutant mice tested. Ongoing experiments will determine if Cx43I130T/+ mice are more susceptible to noise-induced hearing loss than wildtype mice. Furthermore, we will determine if Cx43 is involved in age-related hearing loss by assessing ABRs in 6 month-old Cx43I130T/+ mice. Consistent with our previous findings in single Panx knock-out mice, Panx1-/-Panx3-/- mice did not exhibit baseline hearing impairment. Moreover, Panx1-/-Panx3-/- mice were more resistant to noise exposure than wildtype mice, similar to Panx3-/- mice. We are currently investigating possible mechanisms involved in Panx3-related hearing preservation. Supported by the CIHR to DWL and BLA.

PS 326

Virally-expressed connexin26 (but Not connexin30) at Postnatal Stages Significantly Preserved Hearing in a Mouse Model of Human connexin30 Null Deafness

Wenwen Wang; Xi Lin; Jianjun Wang; Qi Li; Cuiyun Cai
Emory University School of Medicine

Background

Mutations in GJB2 (coding for connexin 26 (Cx26)) and GJB6 (coding for Cx30) are the most common causes of human nonsyndromic hereditary deafness. Currently no mechanism-based therapy is available. Cx26 and Cx30 coassemble to form the major type of gap junctions (GJs) in the cochlea. In this study, we used a modified adeno-associated viral vector (AAV1) to drive the expression of either Cx30 or Cx26 in the scala media of Cx30 null mice, and tested the effect of different gene therapy protocols.

Methods

AAV1-CB7-Gjb2 or AAV1-CB7-Gjb6 vector (~1.0 μ L, titer of 1.0-1.5x10¹³ viral particle/mL) was injected into one side of the scala media of Cx30 null mice between P0 to P2. The non-injected contralateral side was used as a control. Treatment effects were evaluated by examining: (1) Cx expression levels by Western blot and immunolabeling assays; (2) Cochlear morphological changes; (3) The endocochlear potential (EP) and auditory brainstem responses (ABRs).

Results

Immunostaining showed the extensive puncta of Gjb2 or Gjb6 in the cell membrane of the Claudius, Outer Sulcus and Hensen's cells. Strong ectopic expressions in the cytoplasm of marginal cells and spindle-shaped cells were observed and such expressions didn't seem to affect the hearing sensitivity of wild type mice. The total expression of Gjb2 or Gjb6 after viral inoculations was significantly increased as shown by western blots. The ABR thresholds of the ears injected with AAV1-CB7-Gjb2 were significantly lower than the control ears when recorded at the age of one month (n=50). The EP of injected ears was restored to +80 mV, while the EP of control ears was near 0mV. The threshold improvements between the two ears were in the range of 30-40 dB between 4-32 kHz (tone burst tests). We also observed a progressive decline of the hearing improvements when tests were done at two and three months. In contrast, we never found any significant functional hearing restoration (n=43) when AAV1-CB7-Gjb6 was injected into the scala media of Cx30 null mice.

Conclusion

Virally-mediated expression of Cx26, but not Cx30, into the scala media of Cx30 null mice significantly preserved the hearing sensitivity of Cx30 null mice, although the effect declined with time. Our results challenge the gene therapy dogma that focuses on the replacement of the mutated gene, and suggest the importance to study the gene-gene interactions as the basis for mechanism-based therapy.

PS 327

Characterization of CEACAM16 Mutants Discovered in DFNA4B Patients

Yingjie Zhou; Samuel K. Rosenberg; Satoe Takahashi; Jing Zheng
Northwestern University

The tectorial membrane (TM), an essential component of the organ of Corti required for normal hearing, is composed of radially-oriented collagen fibers and a striated-sheet matrix consisting of several secreted proteins including α -tectorin (TECTA), β -tectorin (TECTB), and carcinoembryonic antigen-related cell adhesion molecule 16 (CEACAM16). Defects in CEACAM16 are known to cause non-syndromic autosomal dominant hearing loss (DFNA4B). Our previous work showed that CEACAM16 binds to both α - and β -tectorin. Although CEACAM16 mRNA and protein are expressed well into adulthood, no new tectorin proteins appear to be synthesized after weaning, implying that CEACAM16 may serve to stabilize and maintain the tectorin-based matrix. Since the detailed molecular mechanism underlying these interactions is unclear, we studied the interactions

between CEACAM16 and α -tectorin in more detail using a heterologous expression system. CEACAM16 belongs to the CEACAM family, a group of immunoglobulin (Ig)-related glycoproteins with diverse functions. CEACAM proteins are generally composed of one N-terminal Ig variable (IgV)-like domain (N domain), followed by a variable number of two different types of Ig constant (IgC)-like domains (named A and B) (Beauchemin and Arabzadeh 2013). Unlike other CEACAM family members, CEACAM16 has two N domains at its N- and C-termini, N1 and N2, respectively. The N domain is generally involved in protein-protein interactions. Three missense mutations have been found in human patients: T140P (Chen et al, 1995), which is in between the N1 and A domains and is a predicted N-glycosylation site; G169R (Wang et al., 2015), which is in the A domain; and L365R (Hofrichter et al., 2015), which is in the N2 domain. We created plasmids carrying mouse Ceacam16 with the matched human mutations (G169R and L365R), and tested their interactions with α -tectorin using co-immunoprecipitation assays alongside that previously characterized for the mouse T142P mutant (Zheng et al., 2011). Neither G169R nor L365R affected binding to α -tectorin as previously shown for mouse T142P (Zheng et al., 2011). Consistent with this observation, binding assays using Ceacam16 fragments carrying different domains suggested that the N1 domain of CEACAM16 is likely involved in binding to α -tectorin. Interestingly, our data also indicated that T140P and L365R do not have secretion issues, while the G169R mutation showed reduced secretion and increased protein aggregation. In order to elucidate the pathogenicity of these mutations, further investigation is underway to determine whether the N2 domain is also involved in interaction with α -tectorin and/or other proteins. (Work supported by NIDCD grants DC011813).

PS 328

Analysis of the Immune Cell Population of the Neonatal Mouse Inner Ear

Maggie Matern¹; Xiaoyu Zhang¹; Beatrice Milon¹;
Ronna Hertzano²

¹Department of Otorhinolaryngology, University of Maryland School of Medicine, Baltimore, MD 21201, USA; ²Department of Otorhinolaryngology, Department of Anatomy and Neurobiology, and Institute for Genome Sciences, University of Maryland School of Medicine, Baltimore, MD USA

In the past, the inner ear was thought to be an immune-privileged organ, lacking resident immune cells due to the existence of the blood-labyrinth barrier. However, recent studies have indicated an important role for immune system responses upon damage to the inner

ear by noise or ototoxic drug exposure. This response is mediated by two populations of resident macrophages; the first being cochlear macrophages present in the spiral ligament, and second being perivascular macrophage-like melanocytes present in the stria vascularis. As an incidental finding to a recent investigation into the recombination pattern of the Gfi1-Cre mouse model by crossing to the robust reporter line Ai14, we have observed that in addition to hair cells, Gfi1-Cre induces recombination in an even greater number of non-hair cells throughout the inner ear of newborn mice. Using fluorescence-activated cell sorting (FACS), we identify this population of Cre expressing non-hair cells within the cochlea of 4 day old mice, to be positive for the broad immune cell marker CD45. These results are not entirely surprising, as GFI1 is a transcription factor primarily characterized for its importance in the development of hematopoietic cell lineages, in addition to being required for proper inner ear hair cell development and function. Next, using age matched wildtype mice, we further characterize this population of CD45 positive immune cells within the cochlea to consist mainly of CD11b+Gr1-monocytes/macrophages, but also small numbers of CD11b+Gr1+ granulocytes, CD3+ T cells, CD3-DX5+ NK cells, and B220+ B cells. These results indicate that a large population of immune cells is present already in the neonatal mouse inner ear. In addition, while these results demonstrate that Gfi1-Cre does not result in hair cell-specific recombination as was previously described, it leads to the possibility of this model also being used to study the role of resident macrophages in the inner ear (such as for observing inner ear immune cell activity in response to noise or ototoxic drug induced damage).

PS 329

Dominant Deafness Mutations of ATP-purinergic rReceptors P2X2 are Loss-of-function Variants and Co-expression of Wild-type P2X2 Can Restore Their Function

Yan Zhu; Hong-Bo Zhao; Ning Yu

Dept. of Otolaryngology, University of Kentucky Medical Center

Background

ATP-purinergic signaling has a critical role in hearing. Recently, it has been found that purinergic ATP receptor P2X2 mutations (V60L and G353R) can induce nonsyndromic hearing loss (DFNA41). These deafness mutations are dominant mutations, i.e., the mutations are heterozygous to cause deafness. P2X receptor is a trimer, composed of three isoforms. This means that these mutants may have dominant-negative effect on either wild-type (WT) P2X2 or other partner(s). In this study, we tested whether the dominant deafness P2X2

mutants are dominant-negative to WT P2X2 and whether co-expression of WT P2X2 can restore their function.

Methods

P2X2 WT, V60L and G353R mutants were cloned and co-transfected into HEK 293 cells. ATP-evoked responses were recorded by patch clamp. Channel-gating activity and the effect of mutant(s) on partner(s) were also analyzed by computer modeling.

Results

Both P2X2 V60L and G353R mutants targeted to plasma membrane but had no response to ATP stimulation. After co-transfection with WT P2X2 receptors, the ATP-evoked inward current was visible, dependent on the co-transfection ratio of WT and mutant. Computer modeling analysis showed that both mutations can form heterotypic channels with WT P2X2 isoform and that both mutations have no dominant-negative effect on WT P2X2 isoforms.

Conclusions

P2X2 V60L and G353R dominant deafness mutants are loss-of-function variants and have no dominant negative effect on WT P2X2 isoforms. Co-expression of WT P2X2 can restore the channel function.

Supported by NIH R56 DC 015019. Ning Yu was supported by Major State Basic Research Development Program of China (No. 2014CB943002) and National Natural Science Foundation of China (No. 81470700).

PS 330

Kelch-like 18 (Klhl18) Deficiency Leads to an Inner Hair Cell Auditory Neuropathy in Mice

Neil J. Ingham¹; Morag A. Lewis²; Selina Pearson³; Julia L. Crunden⁴; Karen P. Steel⁵; Sohinder Rekhi⁶; Jacqueline White⁶

¹King's College London, Guy's Campus, London SE1 1UL, UK; ²King's College London; Wellcome Trust Sanger Institute; ³Wellcome Trust Sanger Institute; ⁴King's College London; ⁵King's College London; Wellcome Trust Sanger Institute; ⁶N/A

We have investigated 2 mutant alleles of Klhl18 (Kelch-like 18) which demonstrated a hearing impairment affecting the lower frequency ranges of the mouse hearing spectrum. One allele was a conditional-ready targeted mutation, Klhl18. The second was a spontaneous mutation (Klhl18) which was present in multiple lines carrying other targeted mutations. Mice carrying the low frequency impairment phenotype were isolated and the mutation was determined to be a missense (V55F; Valine to

Phenylalanine substitution) point mutation (9:110455454 C>A) of Kihl18, predicted to have a damaging effect on protein structure (SIFT & PolyPhen2). In a complementation study, we found that mice that were compound heterozygotes for both the Kihl18 and Kihl18 alleles also expressed the low frequency hearing impairment phenotype, supporting evidence that the spontaneous Kihl18 mutation does indeed cause the auditory phenotype.

Kihl18 homozygous mutants had normal tympanic membranes and middle ears. No abnormalities were noted in the middle ear ossicles or their structural arrangement. Gross structure of the inner ear was found to be normal in glycerol-cleared samples. Mid-modiolar sections showed that the overall structure of the cochlea and organ of Corti was normal in Kihl18 mutant mice.

Kihl18 homozygote mutant mice aged 3 weeks old had normal threshold sensitivity as measured by both auditory brainstem responses (ABR) and distortion product otoacoustic emissions (DPOAE). ABR measurements demonstrated a progressive hearing loss predominantly in the lower frequency ranges, from 4 to 14 weeks old. However, DPOAE measurements were comparable in mutant and control mice at 6 weeks old.

We have imaged immunolabelled organs of Corti from 6 week old mice using confocal microscopy. Neurofilament labelling indicated normal innervation patterns in Kihl18 mutant mice and no swelling of neurons. CtBP2-labelling of hair cell ribbon synapses indicated no obvious differences in the numbers of ribbons present at different cochlear regions in Kihl18 mutant mice compared to controls.

Scanning electron microscopy of the organ of Corti at 6 weeks old indicated that outer hair cells appeared normal in Kihl18 mutant mice. However, the hair bundles of inner hair cells were abnormal and stereocilia appeared elongated and tapered in width in Kihl18 mutant mice. The degree of defect worsened from the base to the apex of the organ of Corti, complementing the pattern of hearing impairment seen from ABR recordings.

These observations suggest that the progressive low frequency hearing impairment in Kihl18 mutant mice is an auditory neuropathy primarily affecting the inner hair cells.

Hair Cells - Anatomy and Physiology II

PS 331

Manipulation of phosphoinositol-4,5-bisphosphate Membrane Levels Effects Met-channel Pore Properties of Inner Hair Cells

Anthony J. Ricci; Thomas Effertz; Lars Becker
Stanford University, School of Medicine, Department of Otolaryngology

Hearing requires specialized sensory cells, hair cells, to translate mechanical stimuli into electro/chemical responses. This translation happens in the hair cell sensory organelle, the hair bundle. A mature hair bundle consists of three rows of actin filled stereocilia arranged in a staircase pattern. Deflections toward the tallest row of stereocilia generate a force that is relayed to mechano-electrical transduction (MET) channels, residing at the tops of 2nd and 3rd row stereocilia, resulting in their opening. How exactly the mechanical deflection of the hair bundle gates the MET-channels remains unknown. One can imagine that a chain of protein/protein interactions relay forces but also that the cell membrane can modulate or directly serve as a force bearing element.

Previous data showed compartmentalization of the lipid membrane along the shaft of stereocilia, suggesting its biological relevance for hair cell function (Zhao et al. 2012). We found that phosphoinositol-4,5-bisphosphate (PIP2) is concentrated at stereocilia tips, bringing it close to the presumed location of the MET-channels in mammalian hair cells. Furthermore, artificial modulation of free PIP2 levels in the cell membrane effects MET-currents. We used, among others, phenylarsine-oxide to block the enzymatic replenishment of PIP2, leading to an almost complete loss of PIP2 labeling after about 15 minutes (as previously described: Hirono et al. 2004), demonstrating a high rate of turnover of PIP2. We found a reduction of peak MET-current, an increase of resting open probability, and a loss of fast adaptation in rat inner hair cells. Here we show that the reduction of MET-current after PAO treatment is due to a reduction of single channel conductance. We also identified a change in the reversal potential and a reduction in the calcium block of the MET channel. Intracellular application of an excess amount of PIP2 was sufficient to protect against the effects of PAO, indicating that the observed effects are directly PIP2 related. Together these data suggest that PIP2 may influence channel pore geometry. How changes in pore properties controls fast adaptation remains to be determined.

PS 332

The Mechanoelectrical Transducer Current is Required to Maintain the Expression of the Mature Phenotype in Inner Hair Cells

Laura Corns¹; Terri Roberts²; Kishani Ranatunga²; Corné J. Kros²; Walter Marcotti¹

¹University of Sheffield; ²University of Sussex

Background

For inner hair cells (IHCs) to be functionally mature they must undergo a coordinated change in ion channel expression. From the onset of hearing at postnatal day 12, the inward rectifying potassium current, that is prominent in immature IHCs, is gradually downregulated and the large, fast Ca²⁺-activated K⁺ current, IK,f, and the hyperpolarisation-activated K⁺ current, IK,n, emerge (Marcotti 2012 *Exp Physiol* 97:438). The mechanism that triggers these changes is currently unknown. Numerous models of deafness, including those caused by faulty stereociliary proteins, fail to undergo this maturational change. We hypothesise that the presence of the mechanoelectrical transducer (MET) current in IHCs is necessary for the expression of the mature configuration of ion channels.

Methods

We investigated how the removal of myosin VIIa, an important stereociliary protein, affected the expression of IK,f and IK,n. We used both Myo7a6J/6J mice, which have greatly reduced levels of myosin VIIa, and Myo7a-fl/fl X Myo15-cre⁺/- mice (gift from C. Petit), which allows the specific knockdown of Myo7a in hair cells from ~P3 onwards (Caberlotto et al. 2011 *PNAS* 104:5825). We performed whole cell patch clamp recordings from IHCs and OHCs in acute organ of Corti dissections from these mice. MET function was assessed by applying sinusoidal stimuli via a fluid jet, whilst recording in voltage clamp. Basolateral function was assessed in both current and voltage clamp.

Results

OHCs from Myo7a6J/6J mice showed MET currents only during unphysiologically large stimulation and they have properties that resemble the anomalous MET current (Kros et al 2002 *Nat Neurosci* 13:45; Marcotti et al 2014 *J Neurosci* 34:5505). OHCs from Myo7a-fl/flMyo15-cre⁺/- mice have normal MET currents in the first postnatal week, although their size rapidly declines from P8 and are substantially reduced by P10. In IHCs of Myo7a-6J/6J mice, IK,f and IK,n conductances are not present at P20, while in cells from the Myo7a-fl/flMyo15-cre⁺/- mice we found that both currents are present at P20. By P30, however, the IHCs of Myo7a-fl/flMyo15-cre⁺/- mice lose both IK,f and IK,n conductances.

Conclusion

Our preliminary findings suggest that a functional MET current is necessary to initiate the expression of channels that underly the IK,f and IK,n. Moreover, it indicates that MET is required to maintain the mature configuration of ion channels in adult IHCs. Discovering the link between MET and the expression of these channels could be fundamental in the attempt to produce functionally mature IHCs.

Funding

The Wellcome Trust & MRC

PS 333

Oncomodulin, an EF-hand Calcium Buffer, Alters the Time Course of Calcium Transients in Cochlear Outer Hair Cells

Dwayne D. Simmons¹; Federico Ceriani²; Aenea Hendry²; Walter Marcotti²

¹Baylor University; ²University of Sheffield

Oncomodulin (Ocm), a member of the parvalbumin family, is found almost exclusively in outer hair cells (OHCs) of the cochlea. Although several EF-hand calcium buffers are expressed in immature OHCs, Ocm is preferentially expressed in mature OHCs. Targeted deletion of Ocm in mice gives rise to progressive cochlear dysfunction. We hypothesized that Ocm mutant OHCs have altered calcium signaling that leads to hearing loss. In mice with a targeted deletion of Ocm, we investigated the time-course of induced calcium transients in OHCs.

We used a conditional Cre-lox knockout line driven by the β -actin promoter (Ocm) expressed at embryonic day 1. Cochleae were dissected from Ocm mutant and littermate wild-type mice, grown on collagen-coated coverslips for 24 hours, and loaded with 10 μ M Fluo-4 AM, de-esterified, and transferred to a chamber mounted on the stage of a multiphoton system. The change in calcium concentration was probed by the fractional change in fluorescence ($\Delta f/f_0$) signal. To depolarize OHCs, consecutive pulses of 40 mM KCl were perfused onto 3rd row cells.

The onset of Ocm expression in the mouse inner ear occurs around postnatal day (P) 2. At P0, OHCs from both mutant and wild-type cochleae had indistinguishable times to peak response after KCl-induced depolarization. The time constant (τ) was 12.3 ± 6.1 s (mean \pm sd) in wild-type and 8.9 ± 3.8 s in mutant OHCs. The response times to the second KCl stimulus were nearly identical to the first, although they exhibited reduced amplitudes. The KCl-induced calcium responses at P3 had a significantly longer for both wild-type and Ocm mutant OHCs

than at P0. Ocm mutant OHCs at P3 responded with a τ of 57 ± 15 s (stimulus 1) and 60 ± 15 s (stimulus 2). Wild-type OHCs at P3 had an even longer τ (122 ± 35 s, stimulus 1 and 99 ± 27 s, stimulus 2). There was no difference shown in the recovery between Ocm mutant and wild-type control at either P0 or P3. The faster from Ocm mutants compared to wild-type controls at P3 suggest that Ocm acts as a fast onset buffer in OHCs. As such, it would be expected to lower the amplitude of a calcium signal, restricting it temporally and spatially.

The absence of Ocm shortens the rising phase of calcium signals. Faster rise times could lead to higher levels of calcium and eventually lead to increased vulnerability, accelerated hair cell damage and threshold elevation as seen in young adult Ocm mutant mice.

PS 334

TMC2 Modifies Permeation Properties of the Mechano-Electrical Transducer Channel in Mouse Outer Hair Cells

Corné J. Kros¹; Walter Marcotti²; Laura Corns²
¹University of Sussex; ²University of Sheffield

Background

The ability of cochlear hair cells to convert mechanical stimuli into receptor potentials relies on the mechano-electrical transducer (MET) channels in their stereociliary bundles. Despite the channel's importance, its full molecular identity is still unknown. There is strong evidence implying that transmembrane channel-like protein 1 (TMC1) is the pore forming subunit of the mature MET channel (Pan et al 2013 *Neuron* 79:504; Corns et al 2016 *J Neurosci* 36:336), yet its expression is delayed compared to the onset of mechanotransduction. Instead the expression of TMC2 coincides with this onset, suggesting that it could be the initial pore forming subunit of the MET channel. Therefore, we have used the *Tmc2* KO mouse to provide further evidence for a direct role of TMC2 in MET in mouse outer hair cells (OHCs).

Methods

OHCs from *Tmc2* KO mice were studied in acutely dissected organs of Corti using whole-cell patch clamp recordings. MET currents were elicited by mechanical steps or saturating 50 Hz sinusoids using a piezoelectric fluid jet placed close to the hair bundles. All experiments were performed in accordance with UK Home Office regulations.

Results

We found that TMC2 confers a higher Ca^{2+} permeability and conductance to the MET channel at P3-P4, compared to MET channels in which TMC2 is not present. Moreover, we discovered that the permeant MET chan-

nel blocker dihydrostreptomycin (DHS), an aminoglycoside antibiotic, had a higher affinity for MET channels lacking TMC2, when applied from either the extracellular or intracellular sides, with the difference in affinity being most pronounced during intracellular application. Fitting the results for extracellular DHS with a two-barrier-one-binding site model of the MET channel (Marcotti et al 2005 *J Physiol* 567:505; Van Netten & Kros 2007 *Curr Top Membr* 59:375) showed that the binding site for DHS in the pore was stronger in the absence of TMC2 (8.04 kT for *Tmc2*^{+/+} versus 9.63 kT for *Tmc2*^{-/-} OHCs, $p < 0.01$). Although TMC2 modifies pore properties of the MET channel during a crucial stage of development, the MET current and basolateral membrane properties of *Tmc2*^{-/-} OHCs appeared to develop normally.

Conclusions

Although the functional significance of TMC2 expression in immature OHCs remains unknown, our results show that TMC2 is part of the MET channel complex and contributes to its permeation pore during the first postnatal week.

Funding

Wellcome Trust & MRC

PS 335

Role of Myosin Motors in Cochlear Hair Cell Mechanotransduction

Giusy A. Caprara¹; Anthony W. Peng²

¹University of Colorado Anschutz Medical Campus;

²Department of Physiology and Biophysics, University of Colorado School of Medicine, Aurora, CO 80045

Hair cells of the inner ear are mechanosensors that transduce mechanical forces arising from sound waves and head movement to provide our senses of hearing and balance. Sound deflects the hair bundle, a cross-linked cluster of stereocilia on the apical surface of a hair cell, and causes the opening of mechanically sensitive ion channels to start the mechanotransduction (MET) process. The MET complex is built around the tip-link, an extracellular filament that connects the top of the shorter stereocilia with the side of the next taller row. A variety of unconventional myosins are present within the MET complex, but, in mammalian, their precise role is unclear. The classic model of MET adaptation proposes a direct link between Ca^{2+} influx through MET channels and the movement of myosin motors to release tension and close the channel. Recent evidence shows that in mammalian species, MET channels and myosin motors have a different localization (Beurg, M. et al. 2009, Grati, M. et al. 2011, Waguespack, J. et al. 2007) and Ca^{2+} is not directly involved in fast adaptation in the mam-

malian auditory system (Peng, A. et al. 2013). Also new characterizations of mechanically activated currents in mammalian hair cells indicate that the role of myosin motors in mammalian auditory system need to be revisited (Marcotti et al 2014). Using rat auditory hair cells and a new high-speed imaging techniques, I investigated the role of myosins in the mammalian MET process by interfering with myosin's ATPase cycle. The ATPase activity of myosin is coupled to the binding and release of actin. The data obtained by using ATPase blockers in the intracellular solution are consistent with a role of myosin motors in the modulation of tip-link tension and gating of MET channels.

PS 336

Systemic Fluorescent Gentamicin Enters Neonatal Mouse Hair Cells Predominantly Through Mechanoelectrical Transduction Channels

Ayane Makabe¹; Yoshiyuki Kawashima²; Ayako Maruyama¹; Kiyoto Kurima²; Andrew Griffith²; Takeshi Tsutsumi¹

¹Tokyo Medical and Dental University; ²NIDCD/NIH

Background

Systemically administered aminoglycoside antibiotics (AGs) enter inner ear hair cells (HCs) and trigger apoptosis. In vivo mechanisms by which AGs enter HCs remain poorly understood. Aminoglycosides could enter mouse HCs by endocytosis or through channels such as mechanoelectrical transduction (MET) channels, P2X channels, or transient receptor potential (TRP) channels. Transmembrane channel-like 1 (TMC1) and TMC2 are essential for MET and are components of the stereocilia MET channel complex. HCs from neonatal Tmc1-, Tmc2- deficient (Tmc1 Δ ;Tmc2 Δ) mice appear to have intact hair bundles and tip links but lack functional MET. We use Tmc mutant mice to show that AGs enter HCs in vivo predominantly through MET channels.

Methods

The study was approved by the Institutional Animal Care and Use Committee of Tokyo Medical and Dental University (No. 0170300A). We employed gentamicin-conjugated Texas Red (GTTR) and Tmc1- and Tmc2- mutant mice: Tmc1 Δ , Tmc2 Δ , and Tmc1-mCherry line 3. In Tmc1-mCherry line 3, the transgene derived from bacterial artificial chromosomes (BACs) encoding mouse genomic Tmc1, in which the native stop codons were replaced with cDNA encoding mCherry, was integrated on the X chromosome, resulting in mosaic expression of TMC1-mCherry in HCs of female heterozygous mice. GTTR or PBS was subcutaneously injected in Tmc1 Δ ;Tmc2 Δ mice and wild-type mice at postnatal day 0 (P0), P2, P4 or P6, and the mice were euthanized 3 hours lat-

er. Cochlear epithelia were dissected out, and HCs were immunolabeled with anti-Myosin VI antibodies. Fluorescence intensity of GTTR in HCs was quantified. Next, GTTR was subcutaneously injected in Tmc1-mCherry line 3 mice on Tmc1 Δ ;Tmc2 Δ background at P4. Three hours later, the mice were sacrificed, and the isolated cochleae were exposed to 5 μ M FM1-43FX for 10 seconds. Cochlear epithelia were dissected out, and HCs and stereocilia were immunolabeled by anti-Myosin VI and phalloidin, respectively.

Results

In wild-type mice, GTTR fluorescent intensity gradually increased along with the development of HCs. In Tmc1 Δ ;Tmc2 Δ mice, the intensity was mostly stable from P0 through P6. Subtracting the intensity in Tmc1 Δ ;Tmc2 Δ mice from that in wild-type mice, the rise of GTTR intensity coincided with the spatiotemporal onset of MET. In Tmc1-mCherry line 3 cochleae, almost every HC appears to have intact hair bundles, whereas only HCs that showed significant uptake of GTTR took up FM1-43FX.

Conclusion

These results provide evidence that AGs enter hair cells in vivo predominantly through MET channels.

PS 337

Modulation of BK Currents in Chick Hair Cells by Protein Kinases

Dhasakumar Navaratnam¹; Jun ping Bai²; Joseph Santos-Sacchi³

¹Yale School of medicine, Department of Neurology and of Neuroscience; ²Yale University; ³Yale Medical School, Surgery, Cellular and Molecular Physiology, and Neuroscience

Large conductance potassium channels (BK) in hair cells of nonmammalian vertebrates plays a critical role in electrical tuning, a mechanism of frequency selectivity. Hair cells in auditory epithelium are arranged tonotopically have an intrinsic oscillation in membrane potential that changes as a function of tonotopic location. The oscillation in membrane potential is brought about by an inward Ca²⁺ current and an outward BK current. BK-channels consist of an alpha subunit (Slo) and a variable number of ancillary subunits. BKchannels consist of an alpha subunit (Slo) and a variable number of ancillary subunits. The interaction of these channels with protein kinase A (PKA) and protein kinase C (PKC) are well studied in other tissues, but little is known of the effects of these kinases on BK channels in hair cells. Differential effects have been noted on BK channel kinetics with the sequential phosphorylation by PKC, PKA and PKG.

Moreover, these effects vary with specific splice variants at the C terminus and the inclusion of the strex exon. In an attempt to understand the role of protein kinases in various BK activities, we explore the effects of PKA and PKC on BK channels in chick hair cell using the patch clamp technique.

Results

In low and mid frequency hair cells, where the strex exon is expressed, H-89, a PKA inhibitor, reduced BK currents after 10 minutes of perfusion. H-89 also decreased the average activation time constants. Notably however, it increased the average deactivation time constants at different voltages; deactivation time constants have been demonstrated to be the best surrogate marker of BK kinetics along the tonotopic axis. Forskolin, a PKA activator, has no effects on BK currents when recorded with 0 micromolar intracellular Ca²⁺, but increased BK currents with 100 micromolar intracellular Ca²⁺. The role of PKC on the PKA effects on BK currents was also determined.

Conclusion

The increase in BK currents in response to PKA suggests that the presence of the STREX exon is complicated by ancillary subunits or that C terminal variants that have PKC phosphorylation sites are variably expressed and affect the response of the channel to PKA. Our data with the PKA inhibitor also suggests that there is constitutive PKA activation in low to mid frequency hair cells.

PS 338

A Non-toxic Dose of Cobalt Chloride Blocks Hair Cells of the Zebrafish Lateral Line

James Liao¹; William Stewart²; Jacob Johansen³

¹University of Florida, Whitney Lab for Marine Bioscience; ²Eastern Florida State College; ³University of Texas Marine Science Institute

Experiments on the flow-sensitive lateral line system of fishes have provided important insights into the function and sensory transduction of vertebrate hair cells. A common experimental approach has been to pharmacologically block lateral line hair cells and measure how behavior changes. Cobalt chloride (CoCl₂) blocks the lateral line by inhibiting calcium movement through the membrane channels of hair cells, but high concentrations can be toxic, making it unclear whether changes in behavior are due to a blocked lateral line or poor health. Here, we identify a non-toxic treatment of cobalt that completely disables lateral line hair cells. We exposed 5-day post fertilization zebrafish larvae to CoCl₂ concentrations ranging from 1-20 mM for 15 minutes and measured 1) the spiking rate of the afferent neurons

contacting hair cells and 2) the larvae's health and long-term survival. Our results show that a 15-minute exposure to 5 mM CoCl₂ abolishes both spontaneous and evoked afferent firing and leads to over 85% survivability after 5 days. Weaker treatments of CoCl₂ did not eliminate afferent activity, and stronger treatments caused close to 50% mortality. Our work provides a guideline for future investigations in the zebrafish model system where blocking hair cells is desired.

PS 339

Transcriptional Regulatory Mechanism of Atoh1 on the Inner Ear Development

Hyong-Ho Cho; Dami Kim; Moonyoung Choi; Alphonse Umugire; Sungsu Lee

Dept. of Otolaryngology-Head and Neck Surgery, Chonnam National University Hospital

Introduction

Inner ear hair cell development is regulated by multiple genes and signal pathways. Among them, the transcription factor Atoh1 is both necessary and sufficient for the differentiation of hair cells, and is strongly upregulated during hair-cell regeneration. To identify genes involved in hair cell development and function, we performed RNA-sequencing profiling of forced induction of Atoh1 in mouse embryonic stem cells.

Methods

Atoh1 was cloned into pMSCV-IRES-GFP vector. This vector contained a TRE, forced-expression of Atoh1 by tetracycline. After transfecting into A172 murine embryonic stem cell(mESC), stable cell line was established by neomycin selection. We used both 2D culture(monolayered, 2days spontaneous differentiation followed by 2days tetracycline) and 3D culture(3 days embryoid body followed by 2 days doxycycline) methods. We collected protein sample to confirm the over-expression of Atoh1. Immunocytochemistry(ICC) was performed to see the sensorineural differentiation with Sox2, Myosin 7a. RNA samples were collected to check several known downstream molecules of Atoh1 like Pou4f3, Gfi1. We finally performed RNA-sequencing to see the overall transcriptome regulation of Atoh1.

Results

iAtoh1-mESC was successfully generated with robust Atoh1 expression by tetracycline. Pou4f3, Gfi1, NeuroD1, Jag1 were upregulated by Atoh1 induction. By ICC, Sox2 and Myosin7a expression were seen on the surface of the embryoid body suggesting differentiation toward sensorineural lineage. RNA-sequencing identified 76 up-regulating inner ear related transcripts and 34 down-regulating inner ear related transcripts in Atoh1 over-expressed mESC. Up-regulated transcripts are

Notch signaling, Cochlear and inner ear development related gene. Down-regulated transcripts are Wnt- & BMP signaling and Mesoderm formation related gene.

Conclusion

Expression of hair cell related genes (Pou4f3, Gfi1, NeuroD1 and Jag1) are increased by Atoh1 gene induction in two different condition. In RNA-sequencing analysis, Notch signaling, Cochlear and inner ear development related gene was up-regulated by Atoh1 overexpression. On the contrary, Wnt- & BMP signaling and Mesoderm formation related gene were down regulated by Atoh1 overexpression. We are extending our study to see the functional role of several down-stream targets of Atoh1.

PS 340

Different Distribution and Contribution of Ion Channels Along the Tonotopic Turns of the Rat Cochlea

Gi Jung Im¹; Eunyong Yi²; Se Hee Lee¹; Sung Ho Lee¹; Sung Won Chae¹; Hak Hyun Jung¹

¹Department of Otolaryngology-Head and Neck Surgery, Korea University College of Medicine; ²College of Pharmacy and Natural Medicine Research Institute, Mokpo National University

Background

The Cochlea is tonotopically mapped, and sensitive to specific frequencies of the sound. High frequency sounds stimulate the basal turn of the cochlea, whereas low frequency sounds stimulate the apex. Various ion channels are distributed through the hair cells of cochlea, and tonotopic distribution of ion channels may be different. The aim of this study was to investigate the tonotopic distribution/contribution of ion channels in rat cochlea using both whole-cell patch-clamp recordings and molecular works.

Methods

Electrophysiology and molecular experiments were performed using organs of Corti dissected from the cochlea of rat postnatal days 8-11. Three tonotopic regions of the organ of Corti were examined: the apex, middle, and base. The electrophysiological responses of ACh were recorded in the inner hair cells of three regions. Multiple ion channels were analyzed in three regions using RT-PCR: ACh receptor 9 & 10, BK channel, SK channel, Ryanodine receptor 1-2-3, SERCA pump.

Results

The patch-clamp recordings showed that the efferent response of inner hair cells was different along the tonotopic turns of the cochlea, and ACh response of basal region was stronger than apex. In the basal turn of cochlea, real time PCR detected more distribution of ACh

receptor, BK channel, Ryanodine receptor, and SERCA pump. It seems that the distribution of SK channel was the most in middle turn of cochlea.

Conclusion

This is a challenging study for investigation of the tonotopic distribution of ion channels in the three regions of rat cochlea. Both efferent response using path-clamp and the distribution of ion channels using RT-PCR were different along the tonotopic turns of cochlea. Different distribution and contribution of ion channels can play a role in tonotopical detection of sound in the cochlea, and may influence the frequency specific discrimination of sound. It also may be related to different sensitivity against both ototoxic drugs and noise damages.

Funding

This work was supported by a National Research Foundation of Korea grant funded by the Korean Government Ministry of Education, Science and Technology Research Promotion Fund (R1429733). These funding sources only provided financial support and played no specific scientific role in this study.

PS 341

Mechanical Load on Multi-state Models of Outer Hair Cells

Kuni H. Iwasa

NIH

Background

While the basic mechanoelectric effect of prestin (SLC26A5), the motile element in the lateral wall of outer hair cells, can be described by two-state models, its dependence on intracellular anion concentration, interaction with salicylate, and relaxation with respect to voltage changes calls for multi-state models. Those multi-state models so far proposed are capable of predicting the behavior of prestin (and the mechanoelectric coupling of outer hair cells determined by prestin) only under load-free condition. Since the role of outer hair cells for the cochlear amplifier can be performed only under mechanical load, describing the behavior of prestin under mechanical load is important for its function. The present paper is an attempt of introducing the effect of mechanical load into those multi-state models.

Methods

The model proposed by Song and Santos-Sacchi(1) has four states. Of transitions between those four states, of which transitions between two of them involve mechano-electrical coupling. Here, it is assumed that the transitions between these two states are determined not by the protein's intrinsic transition rates but by electric driv

ing force and mechanical load, analogous to an earlier attempt for a two-state model(2).

Results

- While this extension does not change the behavior of the model under load-free conditions, analytical expressions are obtained for length changes and the membrane capacitance for small periodic voltage changes on top of steady state conditions.

- The extension leads to equations that describe the load dependence of electrical displacement (including the membrane capacitance) and mechanical displacement of prestin contains a term, which is the same as in two-state models.

- The effect of turgor pressure and that of force applied to the axial direction can be distinguished by considering their effect on prestin in a membrane model rather than on pure one-dimensional model.

Conclusions

The four-state model proposed by Song and Santos-Sacchi leads to relatively simple expressions incorporating mechanical load. A similar extension can be made on their later model with a greater number of states(3). The three state model proposed by Homma and Dallos(4) is more complex to introduce the effect of mechanical load because transitions between all three states involve electromechanical coupling.

References

- (1) L.Song and J.Santos-Sacchi, PNAS (2013)110,3883-3888
- (2) K.H.Iwasa, arXiv.org/pdf/1601.11643.pdf
- (3) J.Santos-Sacchi and L.Song, Biophys J (2014)107,126-133
- (4) M.Homma and P.Dallos, J Biol Chem (2011)286,2297-2307

PS 342

Prestin is Required for Normal Efferent Innervation of Outer Hair Cells

Satoe Takahashi; Aisha Ahmad; Mary Ann Cheatham; Jing Zheng
Northwestern University

Background

Outer hair cells (OHC) are required for high sensitivity and sharp frequency selectivity, the hallmarks of mammalian hearing. Prestin, an OHC-specific molecular motor, powers somatic electromotility and is required for cochlear amplification. Modulation of OHC motor action is also associated with the medial olivocochlear (MOC) efferents. Acetylcholine (ACh) released from MOC pre-

synaptic termini activates $\alpha 9/\alpha 10$ nicotinic ACh receptors (nAChR) that are coupled to potassium channels, SK2 and BK. The resulting hyperpolarization is thought to reduce cochlear gain. This efferent feedback system is thought to improve signal selection in noisy environments, and to protect against noise-induced trauma and aged-related hearing loss. As prestin mediates OHC function, we sought to investigate whether prestin itself contributes to the establishment and/or maintenance of efferent innervation.

Methods

We examined cochlear samples from prestin wild-type (WT), knockout (KO), and mutant knockin (499-KI) mice that carry non-functional prestin. OHCs and their innervation at three different ages (P5, P12, and adult) were investigated using immunofluorescence. Antibodies against NF200, Tubb3, synaptophysin, VACHT, CtBP2, prestin, and PMCA2 were used to label OHCs and components of the MOC-feedback system. Images were captured using the Nikon A1R+ laser scanning confocal microscopy system, and analyzed with Imaris 8.

Results

OHC-associated nerve fibers (both afferents and efferents) were indistinguishable between prestin-WT, KO and 499KI cochleae at all ages. Synaptophysin staining of adult cochleae revealed that MOC terminals are often in singlets in prestin-KO as compared to multiple clusters in WT and 499KI, a phenotype reminiscent of knockout mouse models for $\alpha 9$, $\alpha 10$, and BK. Although the innervation densities appeared similar among WT, KO, and 499KI, MOC terminals in prestin-KOs were not constrained to the basal end of the OHCs as in WT and 499KI. This trend was evident as early as P12. The number of synapses vesicles in the supporting cell region also increased in 499-KI compared to WT and KO.

Conclusion

Although the development of afferent and efferent innervation to OHCs seems independent of the presence or function of prestin, prestin is required for normal morphology of the MOC terminals. Non-functional prestin (499-KI) also appears to alter connections between MOC and type II afferent fibers and/or supporting cells. These results indicate that prestin plays a role in the structural maturation of efferent-OHC synapses, and may influence the integration of local microcircuits.

Funding

Work supported by NIDCD grant DC000089, American Hearing Research Foundation, and the Knowles Hearing Center.

PS 343

Prestin: Investigation of the Central Cavity by Cysteine Accessibility Scanning

Julia Hartmann¹; Dmitry Gorbunov¹; Florian Nies²;
Dominik Oliver¹

¹Philipps University Marburg; ²Ph

Mammalian prestin (SLC26A5) functions as an area motor contracting or expanding in response to changes in membrane potential, a process termed electromotility. These ultrafast conformational changes require interaction with intracellular anions and are tightly coupled with substantial transmembraneous charge movements that can be measured as a non-linear capacitance (NLC) [1].

We established and experimentally validated a structural model of prestin, characterized by a 14 transmembrane domain topology [2]. Geertsma et al. solved the crystallographic structure of a prokaryotic SLC26 homolog (SLC26Dg) directly confirming our model [3]. This structure and experimental structures of more distantly related transporters suggest that transport in SLC26 is mediated by tilting of a core domain against a gate domain resulting in alternate access of the central binding site to extra- and intracellular sides. Together with transmembrane domain 3 (TMD3), the discontinuous helix of TMD10 is part of the binding site. It is accessible from the intracellular side in non-transporting mammalian prestin but from both intra- and extracellular sides in transport-capable orthologues [2]. These findings comply with the idea that electromotility of mammalian prestin evolved from the operation mode utilized by related transporters.

We examined accessibility of cysteines introduced into TMD3 of rat prestin to membrane impermeable methanethiosulfonate reagents. NLC of prestin heterologously expressed in CHO cells was used as a functional read-out. We found that the N-terminal end of the helix predicted to contribute to the binding site is accessible from the intracellular side, whereas its C-terminal part is accessible from the extracellular side. These results support the recent structural model of prestin and related SLC26 transporters, in which TMDs 3 and 10 form partial transmembrane helices that are oriented antiparallel and cradle the central binding site.

Furthermore, a mutation (V139C) predicted at the inner end of the TMD3 helix was highly sensitive to mechanical membrane tension: when fluid flow was applied to the cell, NLC of this mutant strongly increased. According to the recent experimental structures of related transporters, this region may form a pivot-point around which the core domain rotates to allow for alternating access transport. Altered mechanical sensitivity of prestin

in V139C is consistent with the idea that such pivoting movement of core versus gate domain is also underlying voltage-dependent charge movement and consequently electromotile activity of prestin.

[1] Ashmore J, *Physiol. Rev* 2008, 88(1):173-210

[2] Gorbunov D et al., *Nat Commun*, 2014;5:3622

[3] Geertsma ER et al., *Nat Struct Mol Biol.*, 2015;22(10):803-8

PS 344

Evidence of Subunit Cooperativity in Prestin

Richard Hallworth

Creighton University

Prestin is a membrane-bound motor molecule that drives a unique form of cellular motility found only in the outer hair cell of the mammalian cochlea. It is well-established that prestin is a homo-tetramer, however, prestin sub-units have been thought to function independently. Prestin coupled to eGFP was expressed in cultured human embryonic kidney cells. The electrical signature of prestin function, non-linear capacitance (NLC), was measured under voltage clamp. Prestin NLC is characterized by two parameters: V_{half} , the membrane potential at maximum NLC, and z , the charge transfer accompanying prestin's conformation change. Two mutations of prestin were studied, D154A and D342Q, which change V_{half} in opposite directions while leaving z unaffected. If prestin subunits function independently, co-expression of D154N and D342Q should yield cells with NLC resembling the linear sum of the two mutant NLCs. However, we observed that prestin NLC in co-expressing cells had an intermediate value of V_{half} and a reduced value of z . Further, the NLC function was best fit by a three-step model. This result strongly suggests that prestin monomers influence the protein's physiological properties in a cooperative manner. Funding: INBRE NIH P20GM103427 (NIGMS) and the Phillip E. Heflin Auditory Research Fund.

Limiting the Extent of Cochlear Amplification: Role of Prestin's Leakage Conductance

Dhasakumar Navaratnam¹; Jun-Ping Bai²; Lei Song³;
Joseph Santos-Sacchi⁴

¹*Yale School of medicine, Department of Neurology and of Neuroscience;* ²*Yale Medical School, Neurology;* ³*Ear Institute, Shanghai No. 9 Hospital, Shanghai Jiao Tong University Medical School;* ⁴*Yale Medical School, Surgery, Cellular and Molecular Physiology, and Neuroscience*

Prestin is an evolved anion transporter family (SLC26) member that underlies outer hair cell (OHC) electromotility (eM). The signature electrical characteristic of voltage-driven prestin activity (eM) is a nonlinear capacitance (NLC), which reports on movements of its voltage-sensor during conformational changes. Prestin's transport pathway is deduced from the crystal structure of its homologue SCL26Dg and by homology modelling with UraA. We find that prestin possesses a leakage conductance, similar to other membrane residing transporters (e.g., EAAT), that is robustly revealed using the highly permeant SCN⁻ anion. It is distinct from the transport pathway as revealed by single site mutations that lie remote to the transport pathway. The leakage conductance, which shows similar characteristics to that of the OHC lateral membrane conductance GmetL, is membrane tension sensitive, and thus able to alter intracellular Cl⁻ levels during mechanical activity of the OHC. In turn, intracellular Cl⁻ is known to modify voltage-driven, prestin-based OHC mechanical activity. Our observations set the stage for a potential feedback mechanism controlling the OHCs' influence on hearing.

In order to test the effects of this leakage conductance on hearing, we created knock-in mice using CRISPR; single point mutations were introduced that blocked the leakage conductance but spared NLC. Preliminary ABR measures of homozygotes show an abnormally rapid rise in Wave 1 amplitude with increases in sound intensity. We find this "recruitment-like" response in two animals, thus tested. We speculate that the leakage conductance is important for limiting supra-threshold responsiveness of OHCs, thereby reducing cochlear amplification at high sound levels.

(Supported by NIDCD DC00273 and NIDCD DC008130)

MEGF10: A Mediator of Supporting Cell Phagocytic Activity

Shimon Francis¹; Lisa Cunningham²

¹*National Institute on Deafness and Other Communication Disorders;* ²*National Institute on Deafness and Other Communication Disorders, NIH*

Background

We and others have shown that supporting cells (SCs) phagocytose dead/dying hair cells (HCs), and SCs also form epithelial scars that preserve the integrity of the epithelial barrier (Monzack et al, 2015). The signals and mechanisms that mediate SC recognition and subsequent engulfment of dead HCs are largely unknown. Megf10 is the mammalian ortholog of Ced-1 (*C. elegans*) and Draper (*D. melanogaster*), where it mediates synaptic pruning, phagocytosis of apoptotic cells, and clearance of dead neurons, respectively. We have investigated the role of MEGF10 as a receptor that mediates SC identification of dead/dying HCs for engulfment.

Methods

We analyzed MEGF10 expression in explants of the adult mouse utricle by immunofluorescence. We also investigated whether MEGF10 is required for SC phagocytic activity, using an established *ex vivo* model system in which tdTomato fluorescence in HCs indicates viability, and loss of tdTomato indicates HC death (*Atoh1-Cre x Rosa26-tdTomato*, Monzack et al, 2015). We utilized two inhibitors of MEGF10 signaling to examine whether it is required for SC phagocytosis of dead/dying HCs.

Results

MEGF10 expression was enriched in SCs relative to HCs. Inhibition of MEGF10 signaling resulted in significant accumulation of dead HCs (HC corpses) in the sensory epithelium, suggesting that MEGF10 inhibition reduced the phagocytic activity of SCs.

Conclusions

MEGF10 is enriched in inner ear SCs. In addition MEGF10 signaling is required for efficient SC clearance of dead HCs. We conclude that MEGF10 functions in the SC phagocytic response to dead/dying HCs. We are currently examining the role of MEGF10 as a mediator of SC phagocytic activity using MEGF10 KO mice.

This work was supported by the NIDCD Division of Intramural Research.

PS 347

Cell-type Specific Transcriptional and Translational Responses to Heat Shock in Mouse Utricle

Lindsey May¹; Matthew Ryals¹; Beatrice Milon²; Erich Boger¹; Ronna Hertzano³; Robert Morell⁴; Lisa Cunningham¹

¹National Institute on Deafness and Other Communication Disorders, NIH; ²Department of Otorhinolaryngology, University of Maryland School of Medicine, Baltimore, MD 21201, USA; ³Department of Otorhinolaryngology, Department of Anatomy and Neurobiology, and Institute for Genome Sciences, University of Maryland School of Medicine, Baltimore, MD USA; ⁴Genomics and Computational Biology Core, NIDCD, NIH, Bethesda, Maryland, USA

Background

We showed previously that supporting cells act as mediators of hair cell survival by secreting HSP70 (May et al. 2013, JCI). Our data indicate that heat shock induces HSP70 in supporting cells but not in hair cells, indicating that these two cell types respond differently to stress. This project is aimed at elucidating the differential responses of hair cells and supporting cells to a protective heat stress.

Method

We are using two RNA sequencing approaches to examine cell-type-specific stress responses. One approach is single cell RNA sequencing (Burns et al. 2015, Nature Communications). The second approach utilizes the RiboTag pulldown method (Sanz et al. 2009, PNAS). This method utilizes a transgenic mouse carrying a Cre-activated RPL22 ribosomal protein (RiboTag) tagged with hemagglutinin (HA). We employed Gfi1-Cre to activate expression of RPL22-HA in hair cells only. This method allows us to collect the transcripts that are being actively translated in hair cells (translatome) by immunoprecipitating the HA-tagged ribosomes. These hair cell-expressed transcripts are then examined by RNA sequencing.

Results

The efficiency of RiboTag-mediated pull-down of hair cell-specific transcripts was examined using qRT-PCR. TaqMan probes were designed for hair cell-specific genes (Gfi1, Myosin 7a), supporting cell-specific genes (Slc1a3, Hes1), and non-sensory cell-specific genes (Lmx1a, Gata2). An 8-fold enrichment of hair cell markers was seen in the immunoprecipitated RNA over the RNA in the supernatant and input. These data indicate that the RiboTag method resulted in efficient isolation of hair cell-specific transcripts from control and heat-shocked utricles.

Conclusions

Using the RiboTag pulldown method, we have collected transcripts that are actively translated in control and heat shocked hair cells. The RNA sequencing of these transcripts is underway and will allow us to report the hair cell-specific translatome that is activated by protective heat shock.

This work was supported by the NIDCD Division of Intramural Research.

PS 348

Stiffness and Diameter of the Electrode Array Influenced the Post Implantation Hearing in Guinea Pigs

Mylene Drouillard¹; Renato Torres¹; Elisabeth Mammelle²; Daniele De Seta¹; Olivier Sterkers¹; Evelyne Ferrary¹; Yann Nguyen¹; Mylène Drouillard³

¹Sorbonne Universités, Université Pierre et Marie Curie Paris 6, Inserm, Unité 'Réhabilitation mini-invasive et robotisée de l'audition'; ²AP-HP, GHU Pitié-Salpêtrière, Service ORL, Otologie, implants auditifs, et chirurgie de la base du crâne; ³INSERM et Université Paris-VI, 75005 Paris, France; ³1. Sorbonne Universités, Université Pierre et Marie Curie Paris 6, Inserm, Unité "Réhabilitation chirurgicale mini-invasive et robotisée de l'audition", Paris, France 2. AP-HP, GHU Pitié-Salpêtrière, Service ORL, Otologie, implants auditifs et chirurgie de la base du crâne, Paris, France

Introduction

During cochlear implantation, electrode array insertion has to be controlled to avoid translocation and less traumatic as possible in order to preserve residual hearing. The aim of our study was to evaluate the physical parameters of the array (external diameter and stiffness) on residual hearing and cochlear structures during insertion.

Materials and Methods

Three electrode arrays prototypes (Oticon medical) with different stiffness or external diameter were implanted; via a mechatronic inserter carried on a robotic arm, to normal hearing Harley albinos male guinea pigs. The prototype 0.4 had a 0.4 mm external diameter and an arbitrary axial stiffness set to 1. The prototype 0,4R had 0.4 mm diameter and a 6.8 calculated stiffness. The prototype 0.3 had a 0.3 mm diameter and a 0.8 calculated stiffness. Each electrode array was respectively implanted in 7, 7, 6 animals. Insertion forces were recorded during the electrode array insertion. The hearing was recorded by ABR in pre-operative, at day 7 and day 30. A histological study was realized on 12 cochleae harvested at day 30.

Results

At day 7, guinea pigs implanted with 0.4R electrode array had significantly poorer hearing results than those implanted with 0.3 (26 +/- 17.7, 44 +/- 23.4, 33 +/- 20.5 dB, 7 vs 5 +/- 8.7, 10 +/- 11.6, 12 +/- 11.5 dB, 6, mean +/- ESM, n, respectively at 8, 16 and 24 kHz, $p < 0.01$) and than those implanted with 0.4 (44 +/- 23.4 dB, 7, vs 28 +/- 21.7 dB, 7 at 16 kHz, $p < 0.05$). Hearing at Day 7 and day 30 were not significantly different between ($p > 0.05$). Insertion force maximal peak was higher with 0.4R than with 0.3 (56 +/- 23.8 mN, 7 vs 26 +/- 8.7 mN, 6). Nevertheless, no correlation between hearing loss and insertion forces could be evidenced. Macroscopic observation of the cochleae evidenced that incorrectly positioned electrode array or fibrosis were associated to a hearing loss > 40 dB (16 kHz).

Conclusion

Thinner or less stiff electrode arrays should allow to be less traumatic and to decrease the hearing loss/to preserve low frequencies residual hearing. An optimal position in the scala tympani and fibrosis prevention have also to be sought.

PS 349

Transcriptional Analysis of Heat-Shocked Mouse Utricle: Aligning Transcriptome to Drug Response

Matthew Ryals¹; Lindsey May¹; Katie Spielbauer¹; Michael C. Kelly²; Joseph C. Burns³; Erich Boger¹; Matthew W. Kelley⁴; Ronna Hertzano⁵; Robert Morell⁶; Lisa Cunningham¹

¹National Institute on Deafness and Other Communication Disorders, NIH; ²Laboratory of Cochlear Development, NIDCD, Bethesda, Maryland, USA; ³Decibel Therapeutics; ⁴Laboratory of Cochlear Development, NIDCD, NIH, Bethesda, Maryland, USA; ⁵Department of Otorhinolaryngology, Department of Anatomy and Neurobiology, and Institute for Genome Sciences, University of Maryland School of Medicine, Baltimore, MD USA; ⁶Genomics and Computational Biology Core, NIDCD, NIH, Bethesda, Maryland, USA

Many instances of drug-induced hearing loss are caused by two major classes of ototoxic agents: aminoglycosides and cisplatin. Our lab has shown that heat shock can protect cultured utricles against aminoglycoside-induced hair cell death, and that heat shock results in increased expression of heat shock proteins (HSPs). Here we have used RNA-Seq in order to characterize the full transcriptional response to heat shock beyond the canonical HSP family.

Gene expression was analyzed at the whole tissue and single cell levels within the utricle epithelium. A subset of the differentially-expressed transcripts identified by RNA-Seq was validated using RT-qPCR. Actively-translated mRNA species from hair cell -specific populations were isolated via affinity-tagged ribosomal (Ribotag) immunoprecipitation. Enrichment for hair cell-derived transcripts was validated from these samples using RT-qPCR. Using the Library of Integrated Cellular Signatures (LINCS), a list of compounds (perturbagens) that induce gene expression profiles that are similar to the utricle heat shock response was determined. Ability of selected perturbagens to elicit heat shock like transcriptional changes was evaluated by RT-qPCR, and perturbagen capacity for otoprotection against aminoglycoside exposure was determined.

A profile of differentially-expressed transcripts, or signature, in the heat-shocked utricle was determined from whole-tissue RNA-Seq data. This signature contained transcripts from multiple gene families including those regulating proteostasis, stress signaling, and protein folding. Single cell RNA-Seq transcriptome data clearly delineated hair cells versus supporting cells within the epithelium, and a different expression profile was observed for heat shocked cells versus control cells. Ribotag immunoprecipitation of hair cell transcripts elucidated the actively-translated mRNA species within the hair cells following heat shock. A search of LINCS perturbagens with similar signatures identified several compounds including HSP90 inhibitors and proteasome inhibitors. Expression profiling of utricles exposed to selected perturbagens indicate that these compounds can induce a 'heat shock-like' expression within the utricle. Preliminary in vitro testing of selected perturbagens suggests that some may offer protection against aminoglycoside ototoxicity.

A medium-throughput screen of perturbagens for otoprotective capacity may reveal additional compounds capable of mediating a heat-shock conditioned protective effect against ototoxicity. Analysis of cell-specific gene differences identified in the single-cell and Ribotag experiments will further hone the matching of perturbagen gene expression profiles and reveal cell-type specific responses to stress within the sensory epithelium of the inner ear. This work was supported by the NIDCD Division of Intramural Research.

PS 350

Hair Cell Regeneration and Innervation in the Severely Traumatized Mouse Vestibular Sensory Epithelium

Guo-Peng Wang¹; Yehoash Raphael²; Lisa A. Beyer³; Hiu Tung Wong³; Donald L. Swiderski³

¹Kresge Hearing Research Institute, The University of Michigan; ²Department of Otolaryngology - Head and Neck Surgery, University of Michigan; ³Kresge Hearing Research Institute, Department of Otolaryngology, University of Michigan

Background

The damaged vestibular sensory epithelium of mammals has a limited capacity for spontaneous hair cell regeneration, which largely depends on the transdifferentiation of surviving supporting cells. This regeneration occurs when differentiated supporting cells change phenotype. However, changes that occur in supporting cells after a severe lesion and the impact of such lesions on the regenerative capacity are not well understood. Here we evaluate the histology of the utricular vestibular epithelium after a severe ototoxic insult, the pattern of hair cell regeneration and the changes in innervation that ensue.

Methods

A high dose of streptomycin (400 µg) was injected into the mouse posterior semicircular canal to induce a severe lesion in the utricle. The mice were sacrificed at 1 or 3 months after surgery, and the utricles prepared for histology with emphasis on hair cells, supporting cells, nerve terminals and neuron soma density in the superior vestibular ganglion, using immunofluorescence, scanning electron microscopy and plastic sections.

Results

Streptomycin induced severe pathological changes including loss of utricular hair cells and formation of a flat epithelium lacking distinctive features of differentiated cells characteristic of this sensory organ. The capacity for spontaneous hair cell regeneration in the flat utricular epithelium was dramatically diminished compared to the non-flattened state. Some flat cells were negative for hair cell and supporting cell markers. Nerve fibers and the vestibular ganglion neurons declined in numbers.

Conclusions

The mouse utricular epithelium turns into a flat epithelium after a severe lesion, with dramatic reduction of the capacity for spontaneous hair cell regeneration. However, degeneration of neural components is slower than that of hair cells. The survival of neurons in the flat epithelium is important for designing treatments to restore

balance, such as hair cell regeneration, stem cell therapy or vestibular prosthesis.

PS 351

Mechanisms Involved in Loss of Residual Hearing in Implanted Cochlea, Exposed to Noise

Adrien A. Eshraghi¹; Amit Wolfowitz¹; Noah Shaikh¹; Carolyn Garnham¹; Peter Ashman¹; Kadri Ila¹; Esperanza Bas²; Christopher O'toole¹; Jeenu Mittal¹

¹University of Miami; ²University of Miami-Miller School of Medicine

Background

Electrode insertion trauma (EIT) can cause damage to different structures of the inner ear resulting in loss of residual hearing. Even with soft surgical techniques where there is none or minimal macroscopic damage (grade 0,1or 2), we can still observe generation of molecular events that may initiate programmed cell death via various mechanisms like oxidative stress, release of pro-inflammatory cytokines, and activation of the caspase pathway which can result in apoptosis within the damaged tissues of the cochlea, leading to loss of residual hearing. The objective is to study the effect of noise trauma (NT) in implanted cochlea and the mechanisms affecting hearing in cochlear implanted animals exposed to NT.

Methods

Guinea pig model of EIT is used and divided in 3 groups. Group 1: EIT with/without dexamethasone eluting electrode, and exposed to NT on day7. ABR was performed to analyze the threshold shift 1 and 30 days post NT. Group 2: cochlea were harvested to analyze the expression of apoptosis and fibrosis genes (before and after NT) at different time intervals. Group 3: cochlea were harvested to test the oxidative stress enzymes (before and after NT) at different time intervals.

Results

Group 1: The threshold shift was significantly greater in the NT controls compared to EIT+NT in day 1 and 30 post NT. No significant difference in threshold shift was noted between +/- Dex eluting electrodes in either time frames or frequency. Group 2: pro-apoptotic (TNF- α , TNF- α R1a) and pro-fibrotic (TGF- β) genes were markedly upregulated in the animal exposed to EIT and to EIT+NT but to lesser extent in the later. TNF- α R1b genes are markedly downregulated in EIT+NT animal. Group 3: SOD and catalase are increased following EIT before exposure to NT.

Conclusion

Dex releasing electrode revealed to have otoprotective properties against initial EIT and a later noise exposure. Significantly smaller threshold shift in ABR along with a markedly decreased expression of pro-apoptotic and pro-fibrotic genes in animals exposed to NT post EIT, shed light on possible endogenous antioxidative and antiapoptotic protective mechanism against NT in implanted ears.

Funding: MED-EL Corporation, and HERA Foundation to Dr. AA Eshraghi

PS 352

Stress Sensitizes Lateral Line Hair Cells to Aminoglycoside Damage

Tamasen Hayward¹; Alex Young²; Sterling Gray¹; Erica Crespi³; Allison B. Coffin⁴

¹Washington State University Vancouver; ²Arizona College of Osteopathic Medicine; ³Washington State University Pullman; ⁴Washington State University, Vancouver

Aminoglycoside antibiotics have potent antibacterial properties, but cause hearing loss in up to 25% of patients. These drugs are commonly administered in stressful environments such as neonatal intensive care units, yet the interaction of stress and hearing loss has not been explored. In this study, we investigated the effect of the glucocorticoid stress hormone, cortisol, on hair cells in the zebrafish lateral line as a first step in understanding how physiological stressors modulate hair cell survival. The lateral line is a system of hair cells stereotypically located along the exterior of fish that is used to detect local changes in fluid dynamics for behaviors such as predator avoidance and prey detection. Using this system, we tested the hypothesis that elevated cortisol levels can modulate hair cell sensitivity to aminoglycosides. We found that either exogenous cortisol or the synthetic cortisol, hydrocortisone, sensitized hair cells to aminoglycoside damage. Additional experiments indicated that cortisol sensitization is partially dependent on glucocorticoid signaling and genomic mechanisms. We will use RNA-seq to investigate further downstream signaling targets of cortisol sensitization. Additional studies will be used to determine how endogenous stressors, such as kinetic stress or fish fear pheromones, and the resultant changes in cortisol levels modulate hair cell sensitivity to aminoglycoside antibiotics. Our work demonstrates that stress may contribute to drug-induced hearing loss, advising therapeutic intervention to reduce stressors and the potential for hearing loss in this patient population.

PS 353

Berbamine Derivatives Mitigate Ototoxic Hair Cell Damage in the Zebrafish Lateral Line

Alexandria Camino¹; Robert Boney¹; Bruce Blough²; Allison B. Coffin¹

¹Washington State University, Vancouver; ²Research Triangle Institute

Aminoglycoside-induced hearing loss affects 20% of the patients requiring these life-sustaining antibiotics. Although aminoglycosides are efficacious in treating bacterial infections in life threatening diseases such as cystic fibrosis and sepsis, they often result in the adverse side effect of hair cell damage. To date, there are no FDA-approved drugs that prevent damage from aminoglycosides. Our goal is to develop a drug that prevents aminoglycoside-induced hearing loss, using a natural product as the chemical scaffold. A previous study by our lab identified four natural compounds that share a modified quinolone scaffold and strongly protect zebrafish lateral line hair cells by attenuating aminoglycoside uptake, likely via partial block of the mechanotransduction channel. The present study builds on previous work, investigating analogs of our berbamine compounds to determine the core protective structure and the specific molecular targets that are responsible for protection. Recent findings suggest that co-treatment of our analogs with aminoglycosides or cisplatin robustly protect hair cells from ototoxic damage at higher potencies than the parent compounds. Analogues containing a phenyl functional group were found to be particularly efficacious, implying that those structures might play a crucial role in protection. Additional washout experiments further suggest that berbamine analogs may be modulating protection of hair cells via multiple mechanisms. Future studies will continue exploration of the quinolone-ring derivative chemical structure to refine the functional groups for lead optimization as an otoprotectant for aminoglycoside and cisplatin toxicity. This work demonstrates that we have promising lead compounds for further development to meet the therapeutic goal of devising a protective hearing loss drug candidate.

SR-3306, a Small Molecule c-Jun N-terminal Kinase (JNK) Inhibitor, Prevents Hair Cell Death in an Experimental Model of Cochlear Implantation

Esperanza Bas¹; Philip LoGrasso²; Christine Dinh¹; Thomas R Van De Water¹

¹University of Miami-Miller School of Medicine; ²The Scripps Research Institute, OPKO Health

Cell damage induced by pro-inflammatory cytokines and/or reactive oxygen species can trigger the activation on the JNK pathway, also known as the stress-activated protein kinase (SAPK) pathway. In the inner ear, JNK activation is associated with hair cell (HC) and neuronal death. JNK inhibitors have been shown to protect against different traumas to the inner ear, including noise (Coleman et al. 2007; Wang et al. 2007), acute labyrinthitis (Barkdull et al. 2007), cochlear implant electrode insertion (Eshraghi et al. 2013) and aminoglycoside ototoxicity (Pirvola et al. 2000; Wang et al. 2003), and have recently shown efficacy in Phasell clinical studies for acute sensorineural hearing loss (Suckfuell et al. 2014).

SR-3306 is a highly selective and orally bioavailable JNK inhibitor that has shown efficacy in models of Parkinson's disease (Chambers et al. 2011; Crocker et al. 2011). In this preliminary study we investigated: 1) the ototoxic profile of SR-3306 in vitro and in vivo, both locally and oral administration and 2) the otoprotective effects of SR-3306 in an in vitro model of electrode induced insertion trauma (EIT).

In vitro studies: organ of Corti were dissected from 3 days old Sprague Dawley rats and distributed into six groups: Control; SR-3306-only; EIT, EIT+SR-3306 0.25uM; EIT+SR-3306 0.5uM; and EIT+SR-3306 1uM. The EIT procedure is described in the literature[11]. The cultures were incubated for 48h, then fixed and stained with anti-phospho-c-Jun, phalloidin (HC bundles) and DAPI. In vivo studies: 3 months of age Norway Brown rats were assigned to either the transtympanic (TT) or oral gavage studies and further distributed between control and treatment groups. The dosage regimen for the TT study comprised of bilateral injections of SR-3306 (3.6uM)/vehicle, twice, 1 week apart. Oral gavages of SR-3306 (15mg/kg)/vehicle were administered daily for 2 weeks. Hearing tests were performed before treatment and on a weekly basis up to 12 weeks, then the rats were euthanized and histological analyses were conducted on the dissected cochleae.

SR-3306 was found safe for the inner ear, both in vitro and in vivo. Furthermore, SR-3306 significantly and in a dose dependent manner prevented HC loss and JNK activation, measured as levels of p-c-Jun in an in vitro model of EIT.

The oral bioavailability and the positive preliminary results in the inner ear, make of SR-3306 a promising molecule for preventing hair cell associated to the activation of JNK following an insult to the cochlea, e.g. cochlear implantation and sensorineural hearing loss.

PS 355

The Cochlear Histopathology of Mice Exposed to High Levels of Sound

Niliksha Gunewardene¹; Takahisa Watabe¹; Albert Edge²

¹Department of Otolaryngology, Harvard Medical School, Boston, Massachusetts 02115, and Eaton-Peabody Laboratory, Massachusetts Eye and Ear Infirmary, Boston, Massachusetts 02114; ²Department of Otolaryngology, Harvard Medical School, Boston, MA, USA, and Eaton-Peabody Laboratory, Massachusetts Eye and Ear Infirmary, Boston, MA, USA

Substantial evidence suggests that acute exposure to high levels of sound causes permanent threshold shifts (PTS) and loss of outer hair cells (OHCs). Here, we characterize the cochlear histopathology of mice exposed to a 1-octave band of noise (8-16 kHz) at either 116 (n=6), 118 (n=6), or 120 (n=6) dB SPL for 2 hours at 4 weeks old. Given that several transgenic mouse models are of a mixed strain background, we also compared the pathology of mixed-strain vs. pure C57BL/6J mice. Twenty-four hours and 1-week post-noise exposure, cochlear function was tested by auditory brainstem responses (ABRs) and distortion product acoustic emissions (DPOAEs), and cochlear whole mounts were examined histologically at 1-week post-exposure. At all three noise levels, ABR and DPOAE thresholds did not recover within 1 week, verifying PTS. Following the 116 dB SPL exposure, apical OHCs were preserved, and the OHCs were partially lost in the middle and basal cochlear regions. Conversely, following 118 and 120 dB SPL exposures, no OHCs remained in middle and basal turns, and damage extended to the apical turn, where there was partial OHC preservation. The inner hair cells remained intact in each exposure. Notably, a loss of supporting cells was observed in animals exposed to 120 dB SPL noise, particularly in the middle and basal regions. Synaptopathy and retraction of auditory nerve fibers accompanied the OHC loss. Importantly, the cochlear histopathology of mixed and C57BL/6J mice were comparable following 118 and 120 dB SPL exposures, but there was more variability in the mixed strain (relative to C57BL/6J mice) when exposed to 116 dB SPL noise. Specifically, at least partial OHC preservation was observed throughout the cochlea, and thresholds were measurable in some animals, suggesting that the

threshold shift could be due to stereocilia damage. Collectively, our findings indicate that an acute exposure to 118 dB SPL noise in pre-pubescent mice consistently induces OHC loss and synaptopathy, in the middle and basal regions, and preserves supporting cells in both mouse strains. These observations directly inform regeneration studies which require reliable noise-induced hearing loss animal models.

PS 356

Reversible p53 Inhibition Prevents Cisplatin Ototoxicity Without Blocking Chemotherapeutic Efficacy

Nesrine BENKAFADAR¹; Julien Menardo²; Jérôme Bourien²; Régis Nouvian²; Florence François²; Jean-Luc Puel³; Jing Wang²

¹UMR 1051-INSERM, University of Montpellier; ²UMR 1051, INSERM, University of Montpellier; ³Institute for Neurosciences of Montpellier-Inserm U1051; University of Montpellier, France

Research background

Cisplatin (CDDP) is a widely used chemotherapy drug, but with significant ototoxic side effects. To date, the mechanism of CDDP-induced ototoxicity remains unclear, and hearing preservation strategies without impacting chemotherapeutic efficacy of CDDP in patients is lacking.

Methods

Here, we examined the molecular pathway of CDDP ototoxicity from the cellular to the whole system. In addition, to identify a protective strategy that would be suitable for clinical use, we evaluated the efficiency of hearing protection with systemic and local administration of a reversible inhibitor of p53 in CDDP intoxicated adult mice. Finally, to check whether the systemic administration of p53 inhibitor would interfere with the anticancer effects of CDDP, we used two xenograft models of triple-negative human breast cancer with either wt or mutant p53 status.

Results

We found activation of the ATM-Chk2-p53 pathway to be a major determinant of CDDP ototoxicity. However, prevention of CDDP-induced ototoxicity is hampered by opposite effects of ATM activation upon sensory hair cells: promoting both outer hair cell death and inner hair cell survival. Encouragingly, however, genetic or pharmacological ablation of p53 substantially attenuated cochlear cell apoptosis, thus preserving hearing. Importantly, systemic administration of a p53 inhibitor in mice bearing patient-derived triple negative breast cancer protected auditory function, without compromising the anti-tumor

efficacy of CDDP, and even sensitizes TP53 mutant tumors to CDDP.

Conclusion

Altogether, these findings highlight a novel and effective strategy for hearing protection in CDDP-based chemotherapy.

PS 357

Quercetin Protects Against Hair Cell Loss in the Zebrafish Lateral Line and Guinea Pig Cochlea

Yoshinobu Hirose¹; Kazuma Sugahara¹; Yousuke Takemoto²; Makoto Hashimoto¹; Hiroshi Yamashita¹

¹Department of Otolaryngology, Yamaguchi University Graduate School of Medicine; ²Department of Otolaryngology, Yamaguchi University Graduate School of Medicine, Ube, Yamaguchi, Japan

Quercetin is one of the famous supplement that is circulated in Japan. We confirmed whether quercetin could protect hair cells against neomycin and noise exposure in zebrafish and guinea pigs.

Dose-Response Testing in zebrafish

The zebrafish were administered quercetin one hour before neomycin exposure. Dose-response curves were generated to evaluate the protective effect on hair cells. Quercetin protects hair cells against neomycin. Quercetin was examined to see higher dose of neomycin exposure. Zebrafish were exposed to the 100 μ M of quercetin for 1 hour prior to concentrations of 100, 200 and 400 μ M of neomycin exposure. Also quercetin protects hair cells against higher dose of neomycin.

ROS Detection with H2DCFDA in zebrafish

We examined the generation of reactive oxygen species using 2',7'-dichlorofluorescein (H2DCFDA). Larvae were left untreated or treated with 100 μ M quercetin for 1 hour, incubated for 5 minutes with 10 μ M H2DCFDA (prepared in embryo medium) and were washed in fresh embryo medium. Three minutes after neomycin exposure, the neomycin group showed increased staining, decreased for four to five minutes. However, the quercetin group showed little staining. These results suggest that administration of quercetin can limit the generation of oxidation products generated in response to free radicals.

Uptake study of Texas red-conjugated gentamicin (GTR) in zebrafish

Zebrafish were pretreated with quercetin (100 μ M \times 15 min), then treated with 50 μ M GTR for 3 minutes with the protective drug still present. The SO2 neuromast was then examined with fluorescence microscopy. Uptake

study of Texas red-conjugated gentamicin showed that quercetin protected hair cells not by blocking neomycin uptake.

Noise Exposure in guinea pigs

The identified drugs were also investigated to determine whether they protect the cochlea against noise-induced hearing loss in guinea pigs. The drugs were administered via the intraperitoneal route in the guinea pigs 3 days before and 4 days after noise exposure. Seven days after noise exposure (130-dB sound pressure level for 3 hours), the auditory brainstem response threshold shifts were assessed. We observed that the auditory brainstem response threshold shift was significantly less in the quercetin group than in the vehicle control group. Furthermore, The survival rates of outer hair cells were significantly higher in the quercetin group than in the control group in the cochlear second turn

The results of our study indicate that quercetin can determine additional protective drugs for the inner ear.

PS 358

Inhibition of Dynamin Related Protein 1 Activity Reduces Noise Induced Hearing Loss

Teresa Wilson; Sarah Foster; Suzan Dziennis; Beth Kempton; Alfred L Nuttall; Alfred L. Nuttall
Oregon Health & Science University

Background

Mitochondria are highly dynamic organelles that are maintained by the opposing processes of fusion and fission, events which directly influence mitochondrial biogenesis, energy metabolism, autophagy, calcium and reduction/oxidation homeostasis, and cell death. Mitochondrial dysfunction, including the deregulation of fission and fusion processes, is implicated in many pathological conditions including hearing loss. Pharmacological inhibition of dynamin related protein 1 (DRP1), the key regulator of the fission process proven protective in animal model systems of neurodegeneration, retinal and renal ischemia and reperfusion injury, stroke, and myocardial infarction. In this study, we examined the role of DRP1 activity in noise-induced hearing loss.

Methods and Results

10 week old CBA/CaJ mice were used in this study. Exposure to a moderately damaging level of loud sound (103 dB (SPL)/8-16 kHz/2 hours) resulted in increased levels of phosphorylated DRP1 Ser616 (pDRP1) in whole cochlea extracts at 4 hours post-noise exposure, returning to baseline at 24 hours. Total DRP1 levels remained unchanged up to 48 hours post-noise exposure. Immunolabeling of both whole mount and vibratome-cut cochlea sections for pDRP1 revealed that high levels of

mitochondrial-associated pDRP1 are present in outer hair cells. Additionally, an increase in DRP1 phosphorylation in several different locations of the cochlea was observed following noise exposure. Pharmacological inhibition of DRP1 activity lead to a significant reduction in noise-induced loss of hearing sensitivity. Morphological analysis revealed that DRP1 inhibition protected against loss of outer hair cells following noise exposure.

Conclusion

This study demonstrated the important role of DRP1-mediated activity in noise-induced hearing loss and indicates a therapeutic potential for inhibition of DRP1 activity.

Funding: This work was supported by grants from the National Institute of Health NIDCD R01 DC000105 and the US Army DOD W81XWG-15-1-0560.

PS 359

A Role of Kinase in Hair-cell Death of the Zebrafish Lateral Line

Yosuke Takemoto¹; Yoshinobu Hirose²; Kazuma Sugahara²; Makoto Hashimoto²; Hiroshi Yamashita²; Yosuke Takemoto³

¹*Department of Otolaryngology, Yamaguchi University Graduate School of Medicine, Ube, Yamaguchi, Japan;*

²*Department of Otolaryngology, Yamaguchi University Graduate School of Medicine;* ³*Department of Otolaryngology*

Introduction

The lateral line which detects a stream exists in the body surface of a zebrafish, and it is consist of neuro-masts which have a hair cell. The zebrafish lateral line is a powerful system for studying hair cells and hair-cell death. Hair cells can be easily labeled and imaged in vivo with fluorescence microscopy. We have reported the hair-cell protection effect, using a zebrafish about antioxidants, such as a quercetin, an astaxanthin, and a kanpo-preparation.

We observed about the role of kinase in hair-cell death this time. A kinase phosphorylates a protein, and it has been reported that a part of kinase have an important role for hair-cell death. Then, we considered the relevance of kinase inhibitor and a hair-cell death as a collaboration with Cancer Research Institute of Kanazawa University.

Materials and Methods

Zebrafish embryos were used in this study. Zebrafish larvae were exposed to kinase inhibitor (0.1-10 ug/ml) for 1 hour before 100 uM neomycin to induce hair cell

death for 1 hour. We also created the group which does not prescribe a neomycin for the zebrafish. After that, they were fixed in 4% paraformaldehyde, incubated with anti-parvalbumin, Alexa 488, and hair cell damage was assessed.

Results and Conclusion

We identified the pharmacological agent which causes hair-cell death or protects from neomycin. We examined the relevance of kinase and hair-cell death in this time using the fry of a zebrafish. We were able to screen kinase inhibitors and were able to identify the pharmacological agent with which a relevance with hair-cell death is suggested. We will repeat the further investigation, we would like to reveal about the role of kinase in a cell death.

PS 360

A Novel Gene, UCH-L1 Sensitizes Cells to Gentamicin-induced Ototoxicity by Downregulating the Autophagic Flux in the Cochlea

Yun Yeong Lee; Yeon Ju Kim; Young Sun Kim; Beomyong Shin; Oak-sung Choo; Jeong Hun Jang; Yun-Hoon Choung

Department of Otolaryngology, Ajou University School of Medicine, Suwon, Republic of Korea

Background

Despite various efforts, the molecular pathogenesis associated with aminoglycoside-induced ototoxicity is still unclear. In our previous study, we revealed that autophagy may play a critical role in the process of aminoglycoside-induced delayed ototoxicity. In the following study, we investigated the possible link between autophagy process and hair cell protection against aminoglycoside-induced ototoxicity using the next generation sequencing (NGS). The present study aimed to identify the differentially expressed genes and functional modules from protein-protein interaction (PPI) data following gentamicin (GM)-induced ototoxicity.

Methods

Organ of Corti explants of Sprague-Dawley rats were cultured on tissue culture plates. The explants were exposed to: (a) Distilled water, (b) 50 μ M gentamicin and (c) 50 μ M gentamicin + 50 pM rapamycin (as an autophagy inducer) for 2 days. Transcriptome of organ of Corti cells were examined using RNA-sequencing. Differentially expressed genes were additionally verified with quantitative RT-PCR. Further experiments were followed to identify the role of specific genes using knock-down techniques and specific inhibitors.

Results

We were able to discover that ubiquitin carboxyl-terminal esterase L1 (UCH-L1), a gene acting as a deubiq-

uitinating enzyme, was significantly downregulated in GM-induced ototoxicity. Originally, UCH-L1 was predominantly expressed in the spiral ganglion neurons, afferent peripheral nerve terminals in hair cells, the third row of Deiters' cells and inner pillar cells. However, disruption of UCH-L1 by either a pharmacological inhibitor LDN-91946 or siRNA caused a significant increase in GM-induced cell death in the auditory cell lines. Furthermore, UCH-L1 knock-down resulted in the accumulation of autophagosomes indicating impaired autophagosome clearance.

Conclusions

A novel gene called UCH-L1 sensitizes cells to gentamicin-induced ototoxicity by downregulating the autophagic flux in the cochlea.

PS 361

Electrocochleography During Surgical Treatment of Meniere's Disease

Laura Stephens¹; W. Jason Riggs¹; Oliver Adunka²; Aaron Moberly¹; Michael Harris¹; Edward Dodson¹

¹Ohio State University; ²The Ohio State University

Background

Patients presenting with Meniere's disease (MD) like symptoms, suffering from episodic vertigo, progressive and fluctuating hearing loss, tinnitus and aural fullness, but who have not responded to dietary or pharmacologic treatments often undergo more invasive treatment options such as endolymphatic sac (ELS) surgery, among others (labyrinthectomy or vestibular nerve sectioning). ELS surgery can provide relief of vertiginous symptoms for patients but the physiologic changes that occur in the cochlea during ELS surgery is not completely understood. In this study we performed electrocochleography (ECoChG) to assess the changes in inner ear physiology that take place during ELS surgery.

Methods

Electrocochleography recordings were obtained from the round window of a cohort of subjects undergoing ELS surgery for treatment of MD. ECoChG measures were obtained using both click and tone burst stimuli prior to shunt placement/decompression and repeated immediately following placement/decompression.

Results

Analyses were performed on the compound action potential (CAP), summation potential (SP), and on-going hair cell/neural response (CM and ANN). Behaviors and patterns were identified across subjects. Growth functions were calculated and correlation analyses were carried out with audiometric and ECoChG findings.

Conclusions

Our results reveal a variety of physiologic changes that occur during surgical treatment Meniere's disease. Moving beyond the traditional SP/AP measure and including the on-going response of the ECochG can shed light on the effect Meniere's disease has on the mechanical properties of the inner ear and the impact ELS surgery has on both hair cell and neural generators.

PS 362

Kainic Acid-induced Degeneration of Auditory-nerve Fibers in the Budgerigar

Kenneth S. Henry¹; Joseph C. Holt²; Kristina Abrams²
¹Department of Otolaryngology, University of Rochester Medical Center; ²University of Rochester

Degeneration of auditory-nerve (AN) fibers occurs steadily with age and with exposure to loud sound, even when audiometric thresholds remain normal in some cases. AN degeneration is predicted to cause deficits in central coding and perception of complex sounds due to diminished information transfer to the brainstem. However, outside of compensatory changes in excitatory and inhibitory input in the auditory midbrain and cortex (increased "central gain"), these effects are relatively unexplored. The budgerigar is an interesting model species for studying consequences of AN degeneration because this small parrot species can discriminate a variety of complex sounds with human-like behavioral acuity. Here, we present the results of a preliminary study aimed at establishing techniques to induce permanent AN degeneration in the budgerigar using kainic acid. Kainic acid is a powerful glutamate analog that when infused into the cochlea in chickens, causes long-term damage to the AN with no adverse effects on sensory hair cells. Budgerigars were infused with varying quantities of kainic acid in artificial perilymph solution into the cochlea to induce degeneration of AN fibers. The functional status of the AN and hair cells were assessed using compound action potentials and cochlear microphonics, respectively, recorded from near the round window in anesthetized birds before and after kainic-acid infusion. Kainic acid caused immediate reduction of compound action potentials by up to 80%, consistent with impaired AN function. In contrast, stable cochlear microphonics showed no change in hair cell function following kainic acid. Auditory-brainstem responses were recorded from the scalp surface once per week for several months following kainic-acid infusion to determine the extent and time course of any recovery in wave I amplitude/gross AN activity. At the conclusion of these longitudinal studies, immunohistochemical analyses were conducted using antibodies against Na⁺,K⁺-ATPase, myosin7, and CtBP2 to clarify underlying anatomical and synaptic changes

in the cochlear neuroepithelium. The techniques established in this work will be used in upcoming studies on the effects of kainic-acid induced AN degeneration on central coding and behavioral sensitivity to complex signals, and will help clarify the perceptual consequences of this common problem. This work was supported by grant R00 DC013792 from NIDCD.

Interactions Between Spatial Acoustic Cues and Non-Spatial Aspects of Perception

PS 363

What the Visual Saccade System May Indicate About Auditory Targeting in the Superior Colliculus

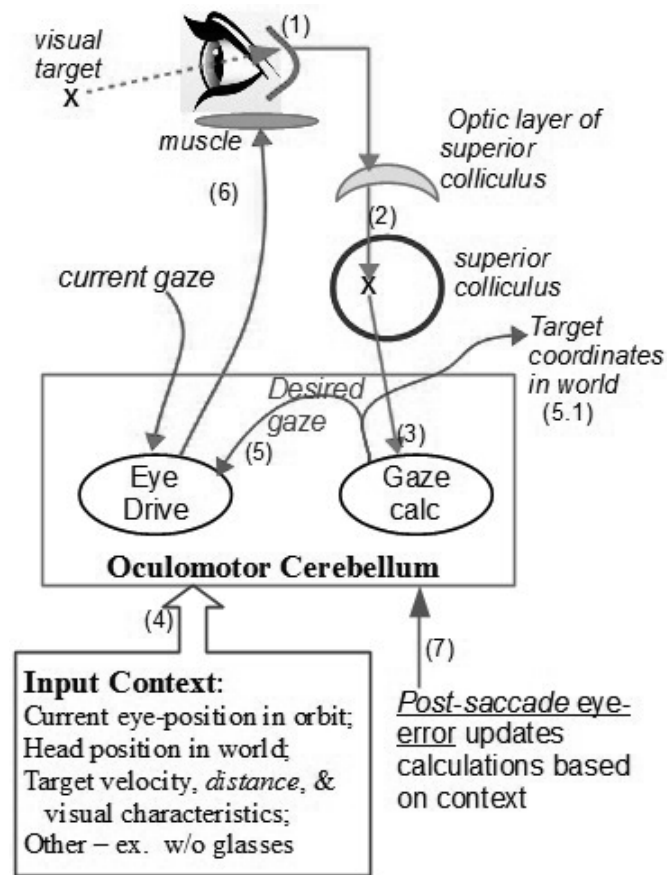
Mark Riggle

Causal Aspects LLC

Current theory for spatial hearing conjectures that localization of auditory stimuli occurs in the auditory midbrain, and then from that, a target is placed in the Superior Colliculus (SC) which accurately produces a saccade (or an orienting movement). This is based on a model of the SC where a SC stimulation location encodes a movement vector and then the SC executes the saccade. This model thus requires that the localization of auditory (and also tactile) stimuli be converted to an eye-based reference frame so that the SC can be correctly stimulated. How and where that reference frame conversion occurs has been a murky theory -- vague midbrain or forebrain processing has been suggested. This requirement for accurate SC stimulation was thought to parallel how the SC processes a visual saccade. For a visual saccade, a visual stimulus on the retina projects topographically to the SC and then that retinal position initiates the SC's fixed movement vector as a saccade. Surprisingly, it is now known that the visual saccade system actually works rather differently. The same visual stimuli (which creates the same fixed SC stimulation location) can produce very different saccades depending on many other conditions. This occurs because the SC only initiates a saccade, but, after that initiation, the oculomotor cerebellum (OMC) controls the saccade and makes it accurate. The OMC uses the retinal position of the stimulus (passed via the SC) plus various other inputs (such as eye-position and target velocity) to determine the actual saccade end point.

We show, by using evidence about visual saccades, that prior to the execution of the saccade, the OMC must produce a visual target's world coordinate; the OMC can then use the difference of that world coordinate and the current gaze to accurately drive the gaze to the correct saccade end-point. However, the computed target coordinate is also passed to the forebrain for additional functions. This OMC capability of using additional inputs to

calculate the actual location of visual targets can greatly simplify auditory localization. To simplify, instead of requiring vague mechanisms for reference frame transformations, auditory localization must reuse this known OMC capability for calculating where targets are in the world.



Visual saccade system – Superior Colliculus initiates a saccade but the OMC computes a target coordinate and drives the saccade to its accurate end point.

PS 364

Echolocating Bats Discriminate Landmark Features to Guide Spatial Navigation

Chao Yu; Cynthia Moss
Johns Hopkins University

Echolocating bats emit high frequency calls and process information carried by echo returns to navigate through the environment and avoid obstacles. Past research has demonstrated that bats can use acoustic landmarks to guide their navigation. However, it remains unknown whether echolocating bats are capable of discriminating acoustic landmarks that differ in physical characteristics (eg. shapes and materials), and associating specific landmarks with a clear navigation path. In this study, we trained echolocating big brown bats (*Eptesicus fuscus*)

to fly through a net opening to access a food reward. We presented the bat with one valid landmark (eg. a plastic multi-faceted object), which was placed to the left of the net opening in training trials; and one invalid landmark (eg. a foam cylinder), which was placed left to a barrier blocking access to the food reward. During each test session, we probed the bat's landmark-guided navigation by swapping the valid landmark with the invalid landmark, so that the multi-faceted plastic shape no longer provided a reliable cue for the bat to find the net opening, but instead led the bat to a barrier. We used high-speed IR motion capture cameras (Vicon) and high-speed video cameras (Miro) to record the flight behaviors of the bat, and a microphone array to reconstruct the duration, bandwidth, temporal patterning and beam aim of the bat's echolocation calls while it performed the navigation task. The preliminary data suggest the bat can discriminate between the two landmarks and can rely on landmark features over spatial location to find its way around an obstacle. The audio data will be further analyzed to understand how the bat adapts its sonar call design as it performs this navigation task.

PS 365

Spatial Representation of Speech in Human Auditory Cortex

Prachi Patel¹; Laura K. Long¹; Jose Herrero²; Ashesh Mehta²; Sameer Sheth³; Guy McKhann⁴; Nima Mesgarani¹

¹Columbia University; ²Feinstein Institute for Medical Research; ³The Neurological Institute, Columbia University; ⁴Department of Neurological Surgery, The Neurological Institute, Columbia University

Sound localization is an important ability that allows an organism to monitor its surroundings. While the neural mechanisms of sound localization have been extensively studied in nonhuman mammals, auditory spatial selectivity in human primary and nonprimary brain areas remains largely speculative. Moreover, it remains unclear how the auditory cortex jointly encodes spatial cues with the spectrotemporal features of speech that carry linguistic and non-linguistic information. In this study, we used invasive neurophysiological recordings in humans while they listened to speech from five different directions to study the spatial selectivity in human auditory cortex. We found distinct responses to spatial cues at the level of single electrodes in primary cortical areas, clearly revealing a spatially selective organization of responses. Moreover, a linear decoder was able to predict the direction of speech stimuli based on neural population data with accuracy significantly higher than chance. We characterized the joint encoding of spec-

trotemporal and spatial information and found a dissociated encoding of these cues; spectrotemporal feature selectivity was largely independent of the direction of the sound. We observed that the stimulus direction changes the baseline neural activity by addition of bias. These findings reveal the organization of responses in the human auditory cortex with implications for more accurate neurophysiological models of speech processing in the auditory pathway.

PS 366

Evaluations of Binaural-Cue-Based Speech Segregation and Ideal-Time-Frequency Speech Segregation in Multi-Talker Conditions

Jing Mi¹; H. Steven Colburn²

¹*Biomedical engineering department & Hearing Research Center, Boston University;* ²*Department of Biomedical Engineering and Hearing Research Center, Boston University*

How binaural cues contribute to source segregation is a long-standing question in auditory scene analysis. Some studies hypothesized that binaural cues are not the main cues for segregation of simultaneous presented stimuli because binaural cues are much distorted in real-world listening environments, such as rooms with substantial reverberation and/or diffuse noise. In order to test this hypothesis, the current study evaluates how effectively spatial cues can be used to segregate the source of interest in a complex listening environment. We proposed a binaural-cue-based source segregation algorithm and compared its segregation performance with the segregation performance of the ideal binary mask (IBM). The binaural-cue-based algorithm uses Target-based Equalization-Cancellation (TEC) processing with a binary decision rule to estimate a time-frequency binary mask. Then target is segregated by applying the estimated mask to the original mixture. For comparison, the "ground-truth" segregation is obtained by applying the IBM, which is calculated with prior knowledge of the target's and maskers' waveforms, to the original mixture.

Listening experiments were performed with normal-hearing listeners to evaluate the intelligibility of TEC-segregated and IBM-segregated speech. Performance with the unprocessed binaural mixture was also measured as a reference. Subjects were asked to identify the words spoken by the front target talker in three conditions: anechoic with two maskers, moderate reverberant with two maskers, and diffuse babble. The target and masker speech are from the same talker and the two maskers are symmetrically separated from target by 60 degrees. In the diffuse-babble condition, interferers were generated using 23 talkers

each separated by 15 degrees in the horizontal plane. Preliminary results show that the speech-reception thresholds (SRTs) of TEC-processed stimuli are significantly lower than the SRTs of unprocessed stimuli for both anechoic and reverberant conditions, which suggests that even in multiple talker and strong reverberant condition, source segregation can be done rather successfully with binaural cues as the only segregation cue. Thus, binaural cues provide useful information for segregation, even in difficult listening environments. Funding

Work Supported by NIH/NIDCD Grant DC000100.

PS 367

The Effect of the Number of Talkers on the Binaural Unmasking of Clean and Vocoded Speech

Daniel Eisenberg¹; Olga A. Stakhovskaya²; Joshua G.W. Bernstein³; Matthew J. Goupell¹

¹*Department of Hearing and Speech Sciences, University of Maryland, College Park;* ²*Walter Reed National Military Medical Center, Bethesda, MD;* *Department of Hearing and Speech Sciences, University of Maryland, College Park, MD;* ³*Walter Reed National Military Medical Center, Bethesda, MD*

Background

The goal of bilateral cochlear implants (BICIs) is to improve spatial-hearing abilities, including speech understanding in noise. BICI listeners receive fewer spatial-hearing benefits than normal-hearing (NH) listeners. One measure of spatial benefit is binaural unmasking of speech. For NH listeners, binaural unmasking increases as the masker becomes more similar to (and therefore more confusable with) the target, and as task complexity increases with a greater number of concurrent talkers [i.e., "informational masking" (IM)]. It is unclear if such a relationship occurs with BICIs. This study investigated binaural unmasking of speech as a function of the number of interfering talkers using BICI simulations (vocoded speech). We hypothesized that for vocoded speech, the amount of binaural unmasking would monotonically decrease with increasing number of interfering talkers, rather than following the pattern displayed for unprocessed speech, due to poor perceptual separation of individual talkers.

Methods

Ten NH listeners were presented sentences over headphones from the coordinate-response measure corpus ("Ready [call sign], go to [color] [number] now"). The target talker was always presented monaurally at 70 dB-A. One to four same-gender interferers were presented in the same ear as the target (monaural condition) or in

both ears (binaural condition) at target-to-masker ratios of -12 to +8 dB. Stimuli were either unprocessed or processed with a 16-channel vocoder.

Results

For all conditions, binaural performance was consistently better than monaural performance with any number of interferers (i.e., binaural unmasking occurred). For unprocessed speech, binaural unmasking increased from one (4.1 dB) to two (6.4 dB) then decreased for three (5.5 dB) and four interfering talkers (5.1 dB). For vocoded speech, binaural unmasking decreased monotonically with additional interferers (from 4.0 dB with one to 2.9 dB with four interfering talkers).

Conclusions

One interpretation of the results for unprocessed speech is that binaural unmasking increased when a second interfering talker was added because of increased IM. With additional interferers, other limitations appeared that reduced the effectiveness of binaural unmasking, such as a reduced ability to perceptually separate the concurrent talkers. In this context, the vocoder results suggest that reduced perceptual separation occurred with as few as two interfering talkers, decreasing the role of IM and contralateral unmasking. Poor BICI performance in complex auditory environments may be partially attributable to poor segregation of individual sources, possibly resulting from the removal of temporal fine-structure information and reduced spectral resolution.

[Work supported by NIH grant R01-DC014948 and the University of Maryland.]

PS 368

Modeling Spatial Release from Masking for a Wide Range of Target/Masker Spatial Configurations

Nathaniel Spencer¹; Douglas S. Brungart²; Brian Simpson³; Nandini Iyer³

¹Wright-Patterson Airforce Base; ²National Military Audiology and Speech Pathology Center, Walter Reed National Military Medical Center; ³U.S. Air Force Research Laboratory

Background

Spatial Release from Masking (SRM) describes the benefit found in speech intelligibility when the target and masker(s) are spatially-separated relative to when they are co-located. This benefit largely depends on how the different sources are spatially-distributed. The equalization-cancellation (EC) model (Durlach, 1963), based on a priori knowledge about the relative locations of the target and maskers, derives equalization parameters to optimize the signal-to-noise ratio post-cancellation with-

in each frequency-band, and can predict SRM. It was long assumed that the equalization parameters had to be fixed throughout a sentence; more recently, the short time equalization-cancellation (STEC) model (Wan et al., 2014) allowed them to be time-dependent. The STEC model does not predict the effects of specific types of masking (i.e., energetic versus informational) for a spatial configuration. It did however achieve improved predictions when speech was presented amid fluctuating, spatially-distributed maskers. In these conditions the spatial location at which the masker level was the highest was time-dependent. Spencer (2013) tuned individual STEC model parameters to explain some of the within-task variability in SRM. Two spatial configurations (target in front, two speech maskers) were explored: "symmetric" (maskers symmetric around target), and "anti-symmetric" (maskers co-located and off-midline). Increasing the time and intensity jitter parameters simulated poorer interaural difference sensitivity, while lengthening the time window simulated reduced frequency in ability to change the location at which the maskers were the most cancelled. Varying the jitter parameters captured a broader range of behavioral SRMs for the anti-symmetric condition, as opposed to varying the window for the symmetric condition. Model parameters can be fine-tuned to best predict performances for different spatial configurations.

Methods

We extend the approach and predict performance for more spatial configurations (Brungart et al., 2007). Three kinds of configurations (target in front) are of interest: 1) one masker in front (co-located with the target)/second masker at a different azimuth (e.g., 0/-50°), 2) two maskers at different locations within one lateral hemifield (e.g., +50/+90°), and 3) two maskers, one in either lateral hemifield, asymmetric around the target (e.g., +50/-90°).

Results

Predicted SRM did not vary with second-masker azimuth when the target and first masker were in front. Predicted SRM was higher when the maskers were at +10/+10° than at +50/+90° when the window was long, but not short.

Discussion

A set of model parameters will be selected for a wide range of multisource environments with speech maskers, and will capture the variability in behavioral SRM.

PS 369

Lungs Contribute More to Noise Cancellation than to the Directionality of Treefrog Ears

Mark A. Bee¹; Norman Lee¹; Jakob Christensen-Dalsgaard²

¹Department of Ecology, Evolution, and Behavior, University of Minnesota; ²Department of Biology, University of Southern Denmark

Sound source localization and segregation are critical functions of the auditory system that allow frogs to communicate acoustically in noisy social environments (breeding choruses). Frogs have air-filled middle ear cavities that are internally coupled through the mouth cavity and wide Eustachian tubes. This internal coupling renders the frog ear an inherently directional pressure-difference receiver. An additional source of acoustic input to the frog ear is the lungs, which are coupled to the mouth via the glottis. The lung input has long been considered to function in sound localization by enhancing directionality. However, in some species, the lung input both enhances directionality and reduces sensitivity at frequencies that are, paradoxically, not emphasized in the acoustic signals used for communication. The goal of this study of the green treefrog (*Hyla cinerea*) was to determine the primary function of the lung input. We tested the hypothesis that the lung input's primary function is to enhance directionality in the context of localizing conspecific calls versus the alternative hypothesis that it functions to achieve masking release by reducing sensitivity to noise generated by the calls of another frog species (the barking treefrog, *Hyla gratiosa*) that breeds in the same, mixed-species choruses as green treefrogs. Using laser vibrometry, we measured the tympanum's directionality and frequency response with the lungs in either an inflated or deflated state. The peak resonant frequency of the inflated lungs (measured as body wall vibration) was 1.5 kHz. Compared to the lung-deflated state, the tympanum was approximately 5-10 dB less sensitive to frequencies in the range of 1.5 to 2.3 kHz when the lungs were inflated, with the greatest reductions in sensitivity occurring in a frontal direction (-60° to +60° azimuth). Notably, this frequency range of maximally reduced sensitivity in *H. cinerea* encompasses the prominent spectral peak present between 1.7-2.2 kHz in the heterospecific calls of *H. gratiosa*. In contrast, changes in directionality between the lung-deflated and lung-inflated states for the two prominent spectral peaks emphasized in conspecific calls (0.8 kHz and 2.7 kHz) were much smaller and on the order of 1 dB. These results support the hypothesis that the lung input in green treefrogs functions in communication by reducing the potential for masking interference by heterospecific calls, especially in the frontal field, where localization of

conspecific calls is most acute. Precisely how the lung input achieves noise cancellation is currently under investigation.

PS 370

Modeling the Relevance of Low Signal-to-noise Ratio Target Components in a Spatial Multi-talker Auditory Scene Analysis Task

Angela Josupeit¹; Esther Schoenmaker¹; Volker Hohmann²

¹University of Oldenburg, Dept. of Medical Physics and Acoustics; ²Universität Oldenburg, Medizinische Physik and Cluster of Excellence Hearing4all, Germany

Human listeners are able to understand a talker of interest, even when other talkers are active at the same time. An interesting question is, which information is most important for a listener to solve such a complex task. A recent psychoacoustic study investigated the relevance of low signal-to-noise ratio (SNR) components of a target signal on speech intelligibility in a spatial multi-talker situation. For this, a three-talker stimulus was manipulated in the spectro-temporal domain such that target speech time-frequency units below a variable SNR threshold (SNR₀) were discarded while keeping the interferers unchanged [Schoenmaker and van de Par, in: Physiology, Psychoacoustics and Cognition in Normal and Impaired Hearing, Springer International Publishing, 2016, 73-81]. This way, time-frequency units with a local SNR below SNR₀ cannot contribute to intelligibility. Psychoacoustic data show that the speech reception threshold starts to drop close to SNR₀ = 0 dB, i.e., only target components at and above a local SNR of 0 dB contribute to intelligibility. The present study applies an auditory scene analysis model [Josupeit et al., ARO 2016] to the same manipulated stimuli to see the effect of the manipulation on model performance. The model is based on the extraction of salient auditory features ("glimpses") in the spectro-temporal domain. It is investigated if the model gives similar results as the subjects; in particular the following questions are relevant: (1) Does the model predict spatial masking release, i.e., the difference in threshold between the target being placed at the same location as the maskers versus being placed at a different location? This question is of particular interest, because the auditory model does not incorporate any mechanism to simulate a binaural masking level difference, such as equalization-cancellation. (2) Is the masking release constant across the different SNR₀? (3) At which SNR₀ does the model performance start to drop and how does this compare to the human data?

PS 371

Effect of Amplitude Modulation on Binaural Pitch Fusion

Yonghee Oh; Lina Reiss

Oregon Health & Science University

Background

Hearing-impaired adults, including both cochlear implant and bilateral hearing aid (HA) users, often exhibit broad binaural pitch fusion, meaning that they fuse dichotically presented tones with large pitch differences between ears (Reiss et al, JARO 2014; JARO 2016). These studies suggest that broadened binaural pitch fusion is one potential underlying cause of reduced binaural speech perception benefit in hearing-impaired listeners. The current study was designed to investigate how binaural pitch fusion can be influenced by amplitude modulation (AM) of the stimuli and give insight into how listeners might generally integrate spectrotemporally varying information between ears.

Methods

Six normal-hearing (NH) listeners and five bilateral HA users were tested using a dichotic pitch fusion measurement procedure. Both reference and dichotic comparison stimuli were presented simultaneously in a 1500-ms single interval. The reference stimulus was held constant in one ear and the comparison stimulus was presented in the contralateral ear with pseudorandom order across trials. In the unmodulated (control) condition, both reference and comparison stimuli had a constant envelope. In the AM condition, both reference and comparison stimuli were co-modulated at 2, 4, and 8-Hz modulation rates with the modulation depth ranging from 20% to 100% in 20% steps. Subjects were asked to indicate whether they heard a single fused sound or two different sounds in each ear.

Results

Coherent AM increases binaural pitch fusion ranges, the frequency ranges over which binaural pitch fusion occurs, to about 2 to 4 times wider than those in the unmodulated condition in both NH and bilateral HA subjects. Even small temporal envelope fluctuations (i.e., the 20% AM depth) significantly increased fusion ranges in all three AM rate conditions. For some NH subjects, the fusion range asymptoted with small modulation depths and did not increase with increased modulation depth; for other NH subjects, the fusion range continued to increase with modulation depth. Results from HA users showed similar AM effects on binaural pitch fusion, but greater inter-subject variability.

Conclusions

The findings suggest that the importance of temporal cues, specifically AM cues, in binaural pitch fusion may vary across subjects. Since speech sounds vary in both spectral and temporal domains, measurements of binaural pitch fusion with stimuli having both spectral and temporal characteristics may yield more realistic estimates of binaural fusion, and provide a better understanding of how fusion affects binaural speech perception benefits for hearing-impaired listeners.

Funding: Supported by NIH-NIDCD grant R01 DC013307.

Midbrain: Organization and Coding Properties

PS 372

Sustained Synaptic Transmission Produces Newly Synthesized Presynaptic Proteins at the Calyx of Held

Matthew Scarnati; Ken Paradiso; Kenneth Paradiso
Rutgers University

Sustained high frequency neurotransmitter release is required to process auditory information. The interaction of thousands of proteins are required to maintain sustained synaptic transmission. While some presynaptic and postsynaptic proteins, ion channels for example, are stable for days, others undergo faster turnover. The rate of protein synthesis that is required to replenish the proteins that are necessary to maintain ongoing synaptic activity is not fully understood. We examine this question using electrophysiological recordings at the Calyx of Held, a large synapse in the mammalian auditory brainstem that allows presynaptic and postsynaptic electrical recordings of synaptic transmission. To study synaptic activity, we stimulated the presynaptic axon of this nerve terminal and recorded the postsynaptic response. We find that blocking protein synthesis by bath application of cycloheximide increases the delay between the presynaptic stimulation time and the postsynaptic response. Compared to control recordings, we find an approximately 2-fold increase in the latency of the excitatory postsynaptic current (EPSC) at the end of a 20 Hz stimulation train. We also find an approximately 50% reduction in the expected peak amplitude of the EPSC and a reduction in the slope of the EPSC resulting in a smaller but prolonged EPSC compared to control recordings. These results appear to involve changes in the release of neurotransmitter, which indicates a presynaptic effect. To determine the location and relative change in the levels of protein synthesis, we used Fluorescent Non-Canonical Amino acid Tagging (FUNCAT) to label newly synthesized proteins. Under conditions where we evoke synaptic activity, we see evidence of fluorescent

labeling in the presynaptic terminal indicating the presence of newly synthesized proteins. We are currently determining if these proteins are synthesized locally in the presynaptic terminal.

PS 373

Genetically-targeted Calbindin Neurons Comprise Excitatory and Inhibitory Subtypes in the Central Nucleus of the Inferior Colliculus of Gerbils

Lauren J. Kreeger¹; Preeti Mehta¹; Boris V. Zemelman¹; Nace L. Golding²

¹*The University of Texas at Austin*; ²*Department of Neuroscience and Center for Learning and Memory, University of Texas at Austin*

Neurons in the central nucleus of the inferior colliculus (ICC) exhibit diverse morphologies, postsynaptic targets, endogenous neurochemical markers, and electrophysiological properties. Yet none of these individual parameters define functional classes of neurons. We hypothesize that ICC neurons will exhibit distinctive neurochemical markers, and that when combined with morphological and electrophysiological parameters, will define functional classes. Our goal is to use molecular-genetic and electrophysiological approaches to identify and target discrete classes of neurons in the ICC of the Mongolian gerbil and reveal their computational roles.

We used adeno-associated viruses to express fluorophores in neurons expressing calbindin D-28k, a calcium-binding protein previously found in the ICC and assumed to be a marker for inhibitory neurons. We developed viruses conditionally dependent on the activity of two native promoters, enabling us to target expression in either excitatory or inhibitory populations. For example expression was restricted to excitatory calbindin neurons by using a calbindin promoter element and a CaMKII α promoter element interdependently. Virus specificity for intended cell populations was confirmed using multiplexed in situ hybridization. Stereotaxic viral injections were made at ages P21-24, and after 10-16 days, 250 μ m acute slices were prepared and fluorophore tagged calbindin neurons were visualized and targeted for whole-cell current clamp recordings. In some experiments, channelrhodopsin was also expressed in calbindin neurons and activated with short pulses of blue light to find synaptic connections between calbindin neurons and other neurons in the local ICC circuit.

We found calbindin neurons have a homogeneous "adapting" firing pattern. The use of interdependent viruses with promoter elements that target excitatory or inhibitory neurons divided calbindin neurons into two

new classes of adapting neurons with distinct action potential signatures. Excitatory calbindin neurons have a single-phase afterhyperpolarization while the remaining, presumably inhibitory neurons have a dual-phase afterhyperpolarization. Anatomical reconstructions of calbindin neurons show branching axons with collaterals in the local ICC circuit and the medial geniculate nucleus. Optogenetic activation of calbindin neurons has confirmed excitatory and inhibitory synaptic connections from calbindin neurons within the intrinsic ICC circuitry. Light-driven activation of calbindin inputs drove both excitatory and inhibitory responses in both regular and onset firing types.

Calbindin D-28k neurons comprise two classes, containing excitatory and inhibitory neurons, based on endogenous neurochemical markers and electrophysiological properties. Ongoing experiments will continue to investigate the connectivity and functional role of these neurons in the intrinsic circuit of the ICC.

PS 374

Characterization of Ascending Synaptic Connections in the Core of the Central Nucleus of the Inferior Colliculus of the Chicken

Thomas Kuenzel; Jana Wolf; Sebastian Malinowski
RWTH Aachen University, Institute for Biology 2, Aachen, Germany

The core of the central nucleus of the inferior colliculus (ICCc) of birds receives ascending synaptic connections from neurons both in the contralateral nucleus laminaris and the contralateral dorsal nucleus of the lateral lemniscus. Neurons in the ICCc are sensitive to interaural time differences and show narrow frequency tuning. They project to the shell of the central nucleus of the inferior colliculus, where interaural time and intensity information first converges. In addition, the ICCc neurons also project to the thalamic nucleus ovoidalis. Thus the ICC is a major center for sound localization and processing in the auditory pathway of birds. Despite this, little information is available about the biophysical or basic synaptic properties of ICCc neurons or about the synaptic dynamics of the ascending connections.

We thus performed whole-cell recordings from ICCc neurons in acute E20 chicken brains slices with electrical stimulation of ascending auditory axons. We determined basic biophysical parameters, action potential firing behavior and quantified intrinsic adaptation of excitability in these neurons. Furthermore we recorded evoked synaptic events. Synaptic dynamics were analyzed by applying paired-pulse stimulation. Synaptic potentials evoked just above threshold were exclusively depolarizing (5.9 \pm 0.9 mV, n=8). They

were mainly mediated by AMPA receptors (38% +/- 12%, n=8, amplitude blocked by DNQX). However, NMDA receptors (26% +/- 13%, n=8, amplitude blocked by APV) and other receptors (36% +/- 10% residual amplitude after DNQX+APV wash-in) contributed a significant component. Accordingly, evoked synaptic currents showed a 10-90% risetime of 4.4 +/- 0.9 ms (n=16) and an exponential decay time-constant of 16.1 +/- 2.6 ms (n=16). Average amplitude was -410 +/- 157 pA (n=16). Upon paired-pulse stimulation we found evidence for a diversity of synaptic short term dynamics in ICCc. A number of synaptic connections we recorded from were dominated by short-term depression (6/16), short-term facilitation (4/16) or a complex mixture of both mechanisms (6/16). Surprisingly, we could not correlate the type of short-term synaptic plasticity of a neuron with biophysical parameters or action potential firing behavior, which may indicate a surprising homogeneity of post-synaptic neurons in the ICCc. However, total numbers of recorded cells are too low to allow strong statements about classes of neurons in the chicken ICC.

Averaged over all neurons and intervals a general tendency for short-term depression was evident, which could underlie slow adaptation phenomena reported from ICCc neurons in vivo.

PS 375

A Novel Class of Inferior Colliculus Stellate Cells Labeled in Vasoactive Intestinal Peptide-Cre Mice

Michael Roberts; Peter Malinski; Alexander George Kresge *Hearing Research Institute, Department of Otolaryngology-Head and Neck Surgery, University of Michigan*

The central nucleus of the inferior colliculus (ICC) is the hub of the ascending auditory system and a critical site for sound processing. To better understand how sounds are processed in the ICC, it is important to identify the classes of neurons that make up the ICC and determine how they function within neural circuits. Using conventional approaches, this has proven difficult to do. Both in vitro and in vivo electrophysiological studies have consistently shown that IC neurons exhibit diverse physiological properties. However, based on physiology alone, it has been difficult to delineate classes of neurons, much less associate their properties with specific functional roles. To overcome these issues, we are using a combination of genetics, physiology, and morphology to identify and characterize classes of ICC neurons. Here we report a novel class of stellate cells that are labeled in Vasoactive Intestinal Peptide (VIP)-IRES-Cre mice. We tentatively call these VIP neurons, as we are currently testing whether they express VIP. To visualize VIP neurons, VIP-Cre mice were crossed with Ai14 reporter

mice, resulting in tdTomato expression in Cre-expressing neurons. Whole cell recordings were targeted to fluorescent neurons in the central region of the IC in acute brain slices. The electrode solution contained biocytin, enabling post hoc staining and reconstruction of recorded neurons. VIP neurons exhibited a sustained firing pattern with relatively little spike frequency adaptation. Their input resistances ranged from 100 - 290 M Ω (median = 175 M Ω , n = 14) and membrane time constants from 8 - 25 ms (median = 16 ms, n = 14). They showed moderate to no hyperpolarization-activated cation current (I_h). VIP neurons had stellate morphologies, with 3 - 7 primary dendrites (mean = 4.7, n = 10) extending in multiple directions away from the soma. Histology showed that VIP neurons are distributed throughout the central region of the IC and a large population, possibly with different properties, are located in the caudal pole of the IC. In addition, at least some VIP neurons appear to project across the IC commissure. We propose that VIP neurons in the ICC constitute a distinct class of stellate cells with a limited range of physiological properties. We are currently working to identify whether VIP neurons are glutamatergic or GABAergic, to determine their sources of afferent input, and to identify their postsynaptic targets. These experiments will lay a foundation for determining how VIP neurons contribute to sound processing.

PS 376

Calretinin as an Extramodular Marker in the Lateral Cortex of the Inferior Colliculus in Developing Mouse

Seam M. Gay; Roxana Behrooz; Christopher H. Dillingham; Mark L. Gabriele
James Madison University

Background

The functional compartmentalization of the multimodal lateral cortex of the inferior colliculus (LCIC) has yet to be fully established. Mounting evidence suggests a modular framework with surrounding extramodular zones that provide an anatomical substrate for input-output arrays. Previously, we identified a variety of markers that highlight discrete modules in layer 2 of the LCIC. The present study builds upon these findings and establishes calretinin (CR) as a seemingly complementary marker, specifically labeling extramodular LCIC zones.

Methods

In addition to confirming prior modular staining, immunocytochemistry was performed for CR (SWANT, 1:5000) on a developmental series of C57BL/6J and CBA/CaJ mice. Brains were fixed, cryoprotected, and sectioned at 50 μ m on a sliding freezing microtome. A Nikon C1si TE2000 microscope was used to acquire Z-stacks that

were then subject to a deconvolution algorithm using Nikon Elements software. Three-dimensional reconstructions of LCIC compartments were performed using an MBF Biosciences NeuroLucida system.

Results

As previously reported, LCIC layer 2 modules were positive for acetylcholinesterase (AChE), cytochrome oxidase (CO), glutamic acid decarboxylase (GAD), nicotinamide adenine dinucleotide phosphate-diaphorase (NADPH-d), and parvalbumin (PV). CR-specific labeling was observed in the LCIC at all ages, albeit concentrated most heavily in areas surrounding presumptive layer 2 modules. CR staining was modest at birth and early developmental stages, with clearly defined extramodular fields not readily apparent until hearing onset. By postnatal day 20 (P20), LCIC calretinin labeling exhibited a distinct pattern of strikingly positive extramodular domains that encompass layer 2 negative patches. This finding is in contrast to previous results in developing rat in which LCIC calretinin patterns were most evident prior to hearing onset (Lohmann and Friauf, 1996).

Conclusions

The present findings identify calretinin as a reliable marker of LCIC extramodular fields. Ongoing multiple-labeling studies will assess the spatial arrangement of modular and extramodular domains with respect to each other, as well as how each align with similarly organized Eph/ephrin guidance expression patterns.

NIH DC012421-01, NSF DBI-0619207

PS 377

The Lateral Nucleus of the Inferior Colliculus – a Core or Belt Structure?

Kendall A. Hutson¹; Gilberto D. Graña¹; Douglas C. Fitzpatrick²

¹University of North Carolina at Chapel Hill; ²University of North Carolina Department of Otolaryngology-Head and Neck Surgery

Previous studies have subdivided the inferior colliculus (IC) into two broad structures – a central or ‘core’ nucleus (ICC) bounded by ‘belt’ areas - and shown that the ICC is innervated primarily by ascending projections, the ‘belt’ by descending projections. The lateral part of the ‘belt’ region is now generally divided into an external nucleus (EX) and a lateral nucleus (L), however L receives both ascending (core-like) and descending (belt-like) inputs, suggesting that based on afferent projections alone, L possesses both ‘core’ and ‘belt’ characteristics. Recently, based on connections, cytochrome oxidase (CO) activity and physiological properties, the

gerbil’s ICC was divisible into three regions (dorsal core 1, ventral core 1 and core 2); surrounded by a dorsal cortex (DC) and by L and EX along its lateral margin. Within the ICC there is a strong tonotopic organization where distinctions between regions can be made according to their sensitivity to interaural time differences (ITD), for example dorsal and ventral ‘core 1’ areas have a high proportion of ITD units but ‘core 2’ does not. Interestingly, units in L have features similar to those in ‘core 2’ in that they both prefer higher frequencies and both have a low proportion of ITD sensitive neurons, suggesting a possible functional relationship between the two areas. All parts of the ICC are known to project to the ventral division of the medial geniculate body (MGv). One way to assist in determining or categorizing L as a ‘core’ or ‘belt’ structure would be to look at its efferent projections to the medial geniculate (MG). A projection to the MGv would be evidence of L as a ‘core’ structure while a projection to the dorsal MG as evidence of a belt structure. However, little is currently known about the efferent projections of L neurons. To investigate the possibility of segregated functional pathways within the ascending auditory system, we made injections of biotinylated dextran amine into the MGv. We found that L does project to the MGv, particularly the anterior part including the rostral pole. The injections that labeled the highest number of cells in L also labeled cells in the ‘core’, yet few in EX or DC. Thus, unlike other areas of the ‘belt’, L contributes a projection to the MGv. Given its afferent and efferent projection patterns, L may represent a level of processing at the IC intermediate to that of ‘core’ and other ‘belt’ regions.

PS 378

Neural Coding of Temporally Jittered Pulse Trains in the Inferior Colliculus of Unanesthetized Rabbit

Yaqing Su¹; Dan Goodman²; Bertrand Delgutte³

¹Eaton Peabody Lab, Massachusetts Eye and Ear Infirmary; Dept. of Biomedical Engineering, Boston University; ²Dept. of Electrical and Electronic Engineering, Imperial College London; ³Harvard Medical School

Background

Periodic pulse trains evoke a strong pitch percept at their repetition rate, which is also their fundamental frequency when considered as harmonic complexes. However even a small amount of jitter in pulse timing deteriorates the pitch percept and rate discrimination for human listeners (Pollack, JASA 43:1113). In a previous study, we identified a non-tonotopic rate code to the envelope repetition rate of harmonic complex tones in the inferior colliculus (IC) of unanesthetized rabbit. Here we further test this potential code by measuring IC neuron responses to jittered pulse trains.

Method

Single IC neuron responses to rectangular pulse trains at 65 dB SPL with varying pulse rate (20-2560 Hz) and amount of jitter were recorded in 2 unanesthetized, normal hearing rabbits. To create jittered pulse trains, each interpulse interval (IPI) was drawn from a uniform distribution centered at the mean IPI, with a half-width equal to a certain percentage of the mean IPI. The jitter percentage was varied from 0% (periodic) to 90%.

Results

Of 74 neurons tested, 88% showed rate tuning to the mean pulse rate for at least one jitter condition, as determined by ANOVA ($p < 0.001$). In about half the neurons, the tuning observed for periodic pulse trains was degraded by introducing temporal jitter, while in the other half, tuning to the mean pulse rate was largely maintained even with large jitter. In general, the effects of jitter were most pronounced at high pulse rates (> 320 Hz). At these high pulse rates, many neurons only gave an onset response to periodic pulse trains. By introducing jitter, these neurons could fire throughout the stimulus duration. Such sustained activity degrades tuning by flattening the dependence of firing rate on mean pulse rate.

Conclusion

IC neurons demonstrate rate tuning to mean pulse rate. For some neurons this rate tuning is affected by temporal jitter. The effect of jitter is most prominent at high pulse rates, consistent with earlier results from deaf animals using electric stimulation through cochlear implants (Hancock et al., *J. Neurophysiol.* 108:714). The consistency of jitter effects on firing patterns in normal hearing and deaf animals suggests common neural mechanisms. Jitter-sensitive neurons may contribute to the vulnerability of pitch perception to temporal irregularity. On the other hand, neurons with rate tuning robust to jitter are not likely to convey pitch information, but could still code for mean repetition rate. Supported by NIH grants R01 DC002258 and P30 DC005209.

PS 379

Properties of Offset Facilitation in Duration Tuned Neurons

Roberto Valdizon-Rodriguez; Haichao Zhang; Paul A. Faure
McMaster University

Neurons selective for stimulus duration, called duration-tuned neurons (DTNs), are thought to be created de novo in the auditory midbrain. Previously, the paired tone stimulation paradigm was used to measure the strength and time course of the synaptic inhibition act-

ing on DTNs by randomly varying the onset time of a short, best duration (BD), excitatory probe tone relative to the onset of a longer duration, non-excitatory (NE) tone and noting when BD tone evoked spikes were suppressed by NE tone evoked inhibition. Here we describe the properties of an offset-evoked, spike facilitation response seen as a transient increase in BD tone evoked spiking during or directly following NE tone suppression. This spike facilitation is thought to correspond to an offset-evoked, excitatory synaptic input acting on the cell. We used paired tone stimulation and extracellular recording in the inferior colliculus of the big brown bat (*Eptesicus fuscus*) to examine the properties of offset-evoked, spike facilitation in DTNs as the NE tone duration/amplitude/frequency, BD tone amplitude, and ear stimulated by the NE tone were varied. Offset-evoked, spike facilitation was observed in 33 of 119 (27.7%) DTNs tested. When the duration of the NE tone was increased the latency of spike facilitation (re NE tone onset) also increased, demonstrating that the facilitated response was time-locked to stimulus offset. Interestingly, the first spike latency of the facilitatory response was tolerant to changes in NE tone frequency and amplitude, suggesting that such precise timing may play a role in duration tuning by encoding signal offset relative to other stimulus features. Offset-evoked, spike facilitation was also primarily observed during monaural, but not binaural, paired tone stimulation, demonstrating that the neural circuitry underlying the response originates from monaural central auditory pathways. Finally, we observed that the strength and timing of the offset facilitation was not related to the offset of the inhibition evoked by the NE tone, suggesting the mechanism that creates spike facilitation is a separate excitatory input instead of post-inhibitory rebound. These findings further our understanding of duration selectivity in the inferior colliculus and neural mechanisms of temporal processing in the central auditory system.

PS 380

Neural Responses in the Inferior Colliculus to Diotic Tone-in-Noise Stimuli Support Detection Based on Envelope and Neural Fluctuations

Langchen Fan; Laurel H. Carney
University of Rochester

Background

Tone-in-noise (TIN) detection is a classical experiment to understand signal detection. Previous psychophysical and modeling studies have shown that slow fluctuations within a frequency channel can be used to detect masked tones: adding a tone to a narrowband noise flattens the envelope, decreasing the fluctuations of auditory-nerve (AN) responses. Changes in fluctuations may be particularly important when AN fibers saturate, and

average rate alone does not encode masked signals. Rates of the inferior colliculus (IC) neurons are sensitive to amplitude modulations, thus we expect changes in fluctuations to affect the average rate in response to noise-alone (NA) and TIN stimuli.

Methods

Extracellular responses were recorded in awake Dutch-belted rabbits. Best modulation frequency was identified using a rate modulation transfer function (MTF). TIN stimuli were 1/3-octave narrowband noises centered on the tone frequency, which was generally matched the best frequency. Discharge rates were analyzed for a wide range of signal-to-noise ratios (SNRs) and overall noise levels. Temporal patterns were examined using two metrics: the correlation between post-stimulus time histograms (PSTHs) for NA and TIN conditions, and the split-half reliability of PSTHs within conditions.

Results

Changes in average rate with SNR were generally consistent with the features of neurons' MTFs. At moderate noise levels, as SNR increased, the rates of most neurons with bandpass MTFs decreased, whereas rates of other MTF types could increase. Rates of many neurons with complex MTFs (e.g. having both a peak and a trough) also decreased with increased SNR. For all cells, the direction of the rate change vs. SNR could vary with overall noise level. This level dependence is expected because saturation of both inner hair cells and AN synapses affect neural fluctuations, and also IC MTFs may change with sound level. For some neurons, MTFs were measured at multiple sound levels and were consistent with TIN responses at different noise levels. The temporal metrics examined here did not vary as consistently vs. SNR as the changes in average rate.

Summary

These results support the hypothesis that the IC encodes TIN stimuli based on changes in fluctuations that originate in the auditory periphery and are shaped by nonlinearities. Future work will continue to examine both rate and temporal metrics, and their relation to level-dependent modulation tuning.

This study was supported by NIH-DC-010813.

PS 381

Dual Recordings in the Auditory Brainstem and Midbrain Reveal Differences in the Processing of Vocalizations

Richard Felix II; Alexander Dimitrov; Christine V. Portfors

Washington State University Vancouver

Background

A normal functioning auditory system must rely on fast and precise neuronal responses in order to accurately represent temporal information in complex sounds. Impairments in temporal processing contribute to a variety of listening disorders, yet our understanding of mechanisms that govern these processes remains limited. We examined how enhanced spike timing at the level of the inferior colliculus (IC) in the midbrain might underlie efficient encoding of vocalizations compared to the cochlear nucleus (CN), an earlier site in the ascending auditory pathway.

Methods

We recorded neuronal responses to tones, frequency modulated sweeps, and conspecific vocalizations in the IC and CN of awake, normal-hearing mice that expressed Channelrhodopsin in VGlut2-positive neurons. We used an optrode that combined the recording of single unit activity with light delivery to the CN. Once a recording was established in the CN, a second electrode was placed in the IC and dual recordings were established at locations with matching frequency tuning. The CN was stimulated with light in the absence of sound to measure effects in the IC, and then responses to sound stimuli were simultaneously recorded at each site. We assessed the extent of functional connectivity between CN and IC recording sites, selectivity to vocalization stimuli, and the temporal precision of evoked spiking.

Results

We found that stimulating the CN with light evoked activity in the IC when the two recording sites had matched frequency tuning, suggesting that tonotopic organization reliably predicts functional connectivity between the sites. Despite matching frequency tuning, IC neurons exhibited greater selectivity a common set of vocalization stimuli compared to the DCN. Overall, CN responses had higher rates of evoked spiking, while IC responses were more transient and had enhanced spike timing, suggesting a shift toward the extraction of temporal information contained in vocalizations at the level of the midbrain.

Conclusion

Neurons in the CN often contributed to activity recorded in the IC. Dual recordings conducted under the same experimental conditions that have a degree of functional connectivity provide a strong paradigm for comparing processing at different stages of the auditory pathway. Enhanced selectivity to vocalizations and temporal precision of responses in the IC suggest that this region may be important for encoding biologically important sounds. When auditory processing is impaired, the IC may be a subcortical site for the generation of auditory disorders typically thought to arise in the cortex.

PS 382

The Contributions of Gabaergic and Glycinergic Inhibition in Shaping Selectivity to Vocalizations in the Mouse Auditory Midbrain

Elena J. Mahrt; Cameron Elde; Christine V. Portfors
Washington State University Vancouver

Background

Speech is one of the most important forms of human communication, and yet we have a poor understanding of how these social vocalizations are processed by the brain. Mice are a great model organism to study neural processing of social vocalizations because of their rich repertoire of vocalizations and because they are mammals with brain structures analogous to humans, such as the auditory midbrain nucleus, the inferior colliculus (IC). Vocalization encoding in the IC is dependent on a complex interplay between excitation and inhibition. While the combined roles of GABAergic and glycinergic inhibition on vocalization selectivity in the IC have been studied to a limited degree, the discrete contributions of GABAergic and glycinergic inhibition have not. The goal of this study was to determine the individual contributions of GABAergic and glycinergic inhibition in shaping selectivity for ultrasonic vocalizations in the IC of awake restrained mice.

Methods

We recorded responses of single neurons in the IC of normal hearing mice before, during and after pharmacologically blocking GABAA or glycine receptors. We used piggy-back electrodes to iontophoretically apply the GABAA and glycine receptor antagonists, gabazine or strychnine. We compared changes in response rate, frequency tuning curves, spike timing, and levels of selectivity to a suite of ultrasonic vocalizations before and after applying each drug, and also compared effects between the two drugs.

Results

As expected, blocking either GABAA or glycine receptors increased response rate to pure tones and vocalizations, although the increases were typically greater with GABAA receptor blockage. We found that neurons responded to more vocalizations (decreased selectivity) when inhibition was blocked but this result was more common with GABAA receptor blockage and the decreases in selectivity were stronger when GABAA receptors were blocked compared to glycine receptors. In addition, we observed greater changes in firing patterns in response to vocalizations after blocking GABAA receptors compared to blocking glycine receptors.

Conclusion

Our results suggest that GABAergic inhibition has a stronger influence on shaping selectivity to vocalizations than glycinergic inhibition, but glycinergic inhibition still plays a role. These results contribute to our understanding of the interplay between different types of inhibition in shaping selectivity to communication sounds in the auditory midbrain.

PS 383

Phase Processing of Complex Sounds in the Auditory System

Yingyue Xu¹; Maxin Chen²; Petrina LaFaire¹; Xiaodong Tan³; Claus-Peter Richter⁴

¹*Northwestern University*; ²*Department of Biomedical Engineering, Northwestern University*; ³*Department of Otolaryngology-Head and Neck Surgery, Feinberg School of Medicine, Northwestern University*; ⁴*Department of Otolaryngology-Head and Neck Surgery, Feinberg School of Medicine, Northwestern University & Resonance Medical, LLC, Chicago*

Background

The auditory system processes everyday speech like a mechanical Fourier transform: different frequencies are spatially mapped along the hearing organs. Within each frequency bands, auditory neurons have been found sensitive to two features: a slowly varying temporal envelope (TE) and a rapidly varying temporal fine structure (TFS). It has been suggested that speech recognition is well sustained by TE in quiet, but TFS plays an important role for pitch and music perception, and speech perception under demanding environments. TFS is retained throughout the auditory pathway by the timing of neural discharges, i.e. phase locking. Our study examined the TFS coding in response to natural speech sentences.

Method

Guinea pigs with normal hearing were tested. The inferior colliculus of guinea pigs was surgically accessed and a 16-channel electrode was used for single unit recordings. Acoustic stimuli were natural speech sentences, and sentences with various extent of TFS distortion. Neural activity was recorded from well-defined single units. In some circumstances, more than one unit were captured simultaneously with the 16-channel electrode. A Fourier transformation of the post-stimulus time histogram (PSTH) was performed to examine the phase locking patterns. Acoustic signals were processed through short-time Fourier transform to extract the TFS patterns. The phase locking and the TFS patterns were then compared.

Results

Spectra of neural PSTH evoked by natural speech sentences showed dominating frequency peaks for distinct low frequencies. These frequency peaks match the representative frequencies in the TFS of the acoustic stimuli. For speech sentences with distorted TFS, dominating frequency peaks were deteriorated in the corresponding PSTH spectra. Furthermore, the phase locking patterns were compared across multiple neurons with different best frequencies recorded simultaneously. When the PSTH from two neurons were summed, spectral analysis of the combined PSTH still revealed dominating frequency peaks that were comparable to the summation of each individual PSTH spectra. This indicates the timing of neural firing were aligned.

Conclusion

Our data showed that phase locking patterns to speech sentences were evoked mainly by the primary frequency components in the TFS. Phase locking patterns were deteriorated with TFS distortion. Neurons with different best frequencies showed alignment in the timing of discharges. The neural coding of TFS in speech will facilitate our understanding in complex sound processing. It might also provide guidelines to incorporate TFS in the TE-based coding strategy of contemporary cochlear implants.

Funded with federal funds from the NIDCD, R01 DC011855

PS 384

Distinct Effects of Task Engagement Across Subdivisions of the Marmoset Inferior Colliculus

Stephen V. David¹; Sean J. Slee²

¹Oregon Health and Science University; ²Oregon Health & Science University

Recent work shows that neurons in the inferior colliculus (IC) undergo receptive field changes during auditory behavior in ferrets (Slee and David, 2015. *J Neurosci.*). In this study, we tested for similar effects in the marmoset monkey, a highly vocal primate species. Two marmosets were trained to detect a pure tone target embedded in a background of random spectral shape (RSS) distractor stimuli. The level of the target was manipulated to vary task difficulty. Both marmosets accurately performed this task over a 5-octave range of target frequencies (0.625-20 kHz). As the signal to noise ratio of the target decreased, we found a significant decrease in hit rate and an increase in false alarm rate.

To measure the effects of task engagement on sound representation, we recorded single-unit activity in the central nucleus of the IC (ICC). Neural responses to both

targets and RSS distractors were compared between conditions when the marmoset performed the detection task or listened passively. The target frequency was presented near the best frequency (BF) of the neuron under study. We found that responses to the distractors were suppressed in about half of the neurons during task engagement relative to passive listening. Distractor suppression had two components: a global decrease in gain and a local decrease in the response at BF. Target responses were significantly modulated in a subset of neurons but suppression or enhancement was equally likely.

In addition, we measured the effects of task engagement from neurons in non-central divisions of the IC (NCIC). In one marmoset, we recorded in a region of the NCIC using a chronically implanted tetrode microdrive. Neural responses to the task stimuli were markedly different in this area compared to the ICC. Responses to the distractors were often sparse, unreliable across presentations, and equally likely to be enhanced or suppressed during behavior. In contrast, in approximately half of the neurons recorded in this region, target responses were strongly enhanced during behavior (median change=70%). Interestingly, we also found that a subset of the neurons selectively responded with an increase in firing rate during the period following the target sound, possibly encoding a reward-related signal.

This study replicates our previous finding that distractor responses are suppressed during auditory behavior in the ferret. In addition, we found an area in the NCIC with large enhancement of target responses during behavior, suggesting that task engagement produces distinct effects across subdivisions of the IC.

PS 385

The Effect of Noise Exposure on the Intelligibility of Speech Reconstructed from Recordings Made in Gerbil Auditory Midbrain

Jessica J. M. Monaghan¹; Jose Garcia-Lazaro²; Roland Schaette²; David McAlpine¹

¹Macquarie University; ²Ear Institute, University College London

Increasing evidence supports the view that acoustic noise insults can engender damage to neural processing in the absence of elevated hearing thresholds (so-called hidden hearing loss). We investigated changes in the neural representation of speech-in-noise induced by acoustic noise insult in the auditory midbrain of gerbils. To determine the degradation of speech information at this level of processing, we reconstructed speech stimuli from neural recordings and assessed intelligibility of these stimuli in human listeners.

Anesthetized gerbils with normal auditory brainstem recordings (ABRs) were exposed to high intensity (105 dB SPL) noise over a period of two hours. Subsequent ABRs demonstrated elevated thresholds following the noise insult. Four weeks later, ABRs were again measured to confirm recovery of thresholds to pre-exposure levels. In vivo electrophysiological recording were made in the inferior colliculus (IC), of ketamine/xylazine-anesthetized, normal-hearing and noise-exposed Mongolian gerbils using silicon-electrode arrays. Responses to 16 vowel-consonant-vowel (VCV) speech tokens spoken by a female talker were recorded. The speech was presented at two intensities (60 and 75 dB SPL) both in the absence of noise and at five different signal-to-noise ratios (SNRs) from -12 dB to +12 dB (in 6 dB steps). Responses were recorded from 190 units in the IC of NH animals and 270 from the IC of the noise exposed animals.

A vocoder approach was used to reconstruct the stimuli from the pooled neural recordings. For each VCV and SNR/intensity condition, speech envelopes for logarithmically spaced frequency bands were reconstructed from the PSTH for each unit with a characteristic frequency in that band. The reconstructed speech envelopes were used to modulate a tone at the centre of the corresponding band. The relative energy of each band was set to correspond to those of the original stimulus.

Speech testing will be carried out with 20 normal hearing listeners to determine the intelligibility of the reconstructed VCV tokens in each SNR and intensity condition.

Psychoacoustics: Modulation and Pitch in Tones and Speech: Individual and Groups

PS 386

Relation Between f₀ Discrimination, Amplitude-Modulation Detection and Frequency Selectivity

Sara M. K. Madsen¹; Torsten Dau¹; Brian C.J. Moore²; Sara M K. Madsen³

¹*Hearing Systems group, Department of Electrical Engineering, Technical University of Denmark, 2800 Kgs. Lyngby, Denmark;* ²*Department of Psychology, University of Cambridge, CB2 3EB, UK;* ³*Technical University of Denmark*

Fundamental frequency (f₀) discrimination of complex tones is better when they contain low harmonics than when they contain only high harmonics (Houtsma & Smurzynski, 1990). A possible explanation is that f₀ discrimination is better when some harmonics are spectrally resolved (Bernstein & Oxenham, 2006;

Moore & Glasberg, 2011). When a tone contains only unresolved harmonics, f₀ discrimination probably depends on temporal envelope and/or temporal fine structure cues. It is therefore possible that f₀ discrimination for complex tones with only unresolved harmonics is related to amplitude modulation (AM) detection. This study explored the relationship between f₀ discrimination, AM detection, and frequency selectivity. Older normal-hearing (NH) and hearing-impaired (HI) subjects were tested. f₀ difference limens (DLs) were measured for complex tones that were bandpass filtered between 2 and 4 kHz. A background noise was used to mask combination tones and components falling on the skirts of the filter. The baseline value of f₀ was manipulated to vary the harmonic number of the harmonics within the passband. AM detection was measured using a 2-kHz sinusoidal carrier and modulation frequencies from 20-150 Hz. Frequency selectivity was measured using the notched-noise method with a 2-kHz signal presented at at 10 dB sensation level. There was a significant correlation between the f₀DLs and frequency selectivity for the HI subjects. Also, the mean f₀DLs for complex tones with low f₀s (80 and 100 Hz), which contained only unresolved harmonics, were positively correlated with the mean AM detection thresholds for modulation rates of 50, 100 and 150 Hz. The correlation was significant for the HI subjects but not for the NH subjects. However, the two correlations did not differ significantly. The results support the idea that f₀DLs for complex tones with high harmonics depend strongly on the use of envelope cues.

Acknowledgements

Supported by the Carlsberg Foundation. BCJM was supported by the Rosetrees Trust.

References

- Bernstein, J.G.W. & Oxenham, A.J. 2006. The relationship between frequency selectivity and pitch discrimination: Sensorineural hearing loss. *J. Acoust. Soc. Am.*, 120, 3929–3945.
- Houtsma, A. & Smurzynski, J. 1990. Pitch identification and discrimination for complex tones with many harmonics. *J. Acoust. Soc. Am.*, 87, 304–310.
- Moore, B.C.J. & Glasberg, B.R. 2011. The effect of hearing loss on the resolution of partials and fundamental frequency discrimination. *J. Acoust. Soc. Am.*, 130, 2891–2901.

Using Individual Differences to Assess Modulation-processing Mechanisms

Nihaad Paraouty; Christian Lorenzi
Ecole normale supérieure, Paris Sciences et Lettres
Research University and CNRS, France

Background

Amplitude-modulation (AM) detection is assumed to rely on dynamic changes in excitation-pattern cues along the basilar membrane, i.e., temporal-envelope cues. Frequency modulation (FM) detection is also assumed to rely on envelope cues resulting from cochlear filtering. However, several studies suggest that low-rate FM detection relies on an additional mechanism using temporal-fine-structure (TFS) cues conveyed by changes in the neural phase-locking pattern over time. Still, the respective roles of envelope and TFS in low-rate FM detection remain unclear. This study aimed at finding additional evidence for the contribution of TFS cues in low-rate FM detection through a correlational approach. AM and FM sensitivity was assessed for a large cohort of listeners with a wide range of age in order to increase the variability in peripheral coding between listeners.

Methods

Data was obtained from 70 normal-hearing listeners aged between 20-70 years. AM and FM-detection thresholds (AMDTs and FMDTs) were measured using a forced-choice, adaptive procedure. Modulation rate was 5 Hz and the carrier was a 500-Hz sinusoid. FMDTs were also measured in the presence of an interfering AM at a 5-Hz rate to discourage the use of envelope cues. All stimuli were presented monaurally at 40 dB sensation level. In addition, frequency selectivity was assessed at 500 Hz using a simplified version of the notched-noise masking method.

Results

As expected, frequency selectivity at 500 Hz was not affected by age. Moreover, frequency selectivity was not correlated with either measure of FMDT. AMDTs were significantly correlated with FMDTs, but not with FMDTs measured with interfering AM. Both measures of FMDTs were significantly correlated with each other. This pattern of correlation remained when age, absolute threshold or frequency selectivity were controlled for. Moreover, when comparing the three correlations, a significant difference was found, suggesting that this pattern of correlation is a robust finding.

Conclusion

The correlation between AMDTs and FMDTs is compatible with the notion that envelope cues are used by listeners when detecting both AM and FM. The absence of

significant correlation between AMDTs and FMDTs measured with interfering AM is compatible with the notion that listeners use auditory cues distinct from the envelope fluctuations evoked by FM at the output of cochlear filters when FM detection is measured with interfering AM. Altogether, these findings are consistent with the idea that for low carrier frequencies, low-rate FM detection is based on two distinct types of sensory information: envelope and TFS cues.

PS 388

Can Musical Training Compensate for Reduced Pitch-discrimination Performance in Hearing-impaired Listeners?

Federica Bianchi¹; Sébastien Santurette¹; Torsten Dau²

¹Hearing Systems group, Department of Electrical Engineering, Technical University of Denmark, DK-2800, Kgs. Lyngby, Denmark; ²Hearing Systems group, Department of Electrical Engineering, Technical University of Denmark, 2800 Kgs. Lyngby, Denmark

Background

Hearing-impaired (HI) listeners typically have a reduced ability to discriminate the pitch of complex tones as compared to normal-hearing (NH) listeners. This perceptual deficit may be ascribed to a variety of factors, including reduced frequency selectivity, reduced ability to use temporal fine structure cues, and decreased neural synchrony. While hearing loss generally reduces pitch-discrimination abilities, several studies have shown that musical training leads to improved pitch discrimination for complex tones. This improvement has been shown to be associated with an enhanced neural representation of pitch at central stages of the auditory system, possibly due to an increased neural synchrony and/or cortical plasticity. This study aimed to clarify the effect of musical training on complex-tone pitch discrimination in HI listeners. We hypothesized that HI listeners who had undergone musical training would perform as accurately as NH listeners, provided that they still had access to some resolved harmonics.

Method

Fundamental frequency (F0) discrimination thresholds were obtained for harmonic complex tones filtered between 300 and 1500 Hz, with F0s ranging from 100 to 500 Hz. The complex tones were embedded in threshold equalizing noise and the level of each harmonic was adjusted to 12.5 dB sensation level relative to the noise. Thirty-one NH listeners (16 musicians) and 9 HI listeners (3 musicians) participated in this study. The recruited musicians had at least 8 years of formal musical education.

Results

Although both NH and HI listeners had access to some resolved harmonics, the pitch discrimination thresholds of the HI listeners were, on average, significantly larger (worse) than those of the NH listeners, even though audibility was compensated for. However, while hearing loss led to a decrease in performance, on average, by a factor of two, musical training increased performance similarly in NH and HI listeners by a factor of two. Thus, the mean thresholds of the HI listeners with musical training were similar to those of the NH listeners with no musical training.

Conclusion

Preliminary results from three musically trained HI listeners show that musical training increases pitch-discrimination performance regardless of cochlear damage and may lead to similar pitch-discrimination thresholds as in NH non-musicians. These results suggest that musical training could compensate for the degraded performance of HI listeners in pitch discrimination with resolved complex tones. Musical training may be beneficial to HI listeners also in other perceptual contexts, e.g., stream segregation and speech recognition.

PS 389

Modulation Detection Interference in School-age Children and Adults

Emily Buss¹; Lori Leibold²; John Grose¹; Christian Lorenzi³

¹University of North Carolina at Chapel Hill; ²Boys Town National Research Hospital; ³Ecole normale supérieure, Paris Sciences et Lettres Research University and CNRS, France

Background

Detection of amplitude modulation (AM) is immature in young school-age children, with a uniform developmental effect across AM rates (e.g., Hall & Grose, 1994). Little is known about age effects for AM detection in the presence of a modulation masker, however. The present study evaluated sensitivity to AM in children and adults using the modulation detection interference (MDI) paradigm. In this paradigm AM detection at one carrier frequency is evaluated with and without masker AM at another carrier frequency. Previous results in other paradigms indicate that children may be less adept than adults at listening selectively in frequency (Leibold & Neff, 2011). The prediction at the outset was therefore that young children would be more susceptible to off-frequency masker modulation masking than adults.

Methods

Listeners were normal-hearing adults and children (5-10 yrs). The task was to detect sinusoidal 16-Hz AM on a 4.3-kHz target tone. The masker was a 1-kHz tone or a 1-kHz tone modulated by a bandpass noise (8-24 Hz). Thresholds were estimated in a 3AFC by adjusting target AM depth. The target carrier was gated on in each of the three 500-ms intervals with 50-ms ramps, and the masker was either synchronously gated or played continuously. Performance was evaluated in four conditions: target alone (QUIET), with a continuous tonal masker (CONT-TONE), with a continuous AM masker (CONT-AM), and with a gated AM masker (GATED-AM). These conditions roughly follow those used previously by Oxenham and Dau (2001) to evaluate MDI in adults.

Initial Results: Thresholds tended to improve with child age in all conditions. For all listeners, thresholds were similar for the QUIET, CONT-TONE and CONT-AM conditions, and poorer for the GATED-AM condition. There was a trend for greater off-frequency modulation masking in children than adults, computed as the difference between QUIET and GATED-AM thresholds.

Conclusions

As observed previously, sensitivity to AM matures with age. There is some indication that off-frequency masker AM in the GATED-AM condition may have a larger detrimental effect on thresholds in younger listeners. This result will be discussed in the context of recent data on the effects of inherent carrier fluctuation for AM detection with an on-frequency masker in children and adults.

PS 390

Investigating the Fluctuating Masker Benefit Using Synthesized Vowel Sequences

Yi Shen

Indiana University Bloomington

Under masking from sinusoidally amplitude-modulated noises, the dependency of speech-recognition performance on masker modulation rate could be affected by (1) the probability of whole word being embedded in a masker peak, which depends on the word duration; and (2) the amount of modulation masking/interference, which depends on the fluctuation rate of speech envelope. Synthesized vowel sequences were adopted in the current study to separately manipulate the duration of each speech segment (by varying the vowel duration) and the speech fluctuation rate (by varying the vowel rate). Each vowel sequence consisted of five synthesized vowels; each vowel was selected randomly from /a/, /i/, /u/, /æ/, and /ə/. Two vowel durations (25 and 100 ms) and two vowel rates (1 and 6 Hz) were tested, and for each combination of vowel duration and vowel rate,

vowel recognition was measured as a function of signal-to-noise ratio (-10, -5, 0, and 5 dB) and masker modulation rate (from 0.5 to 16 Hz). The fluctuating masker benefit (FMB), i.e., the improvement in vowel recognition relative to the unmodulated masker condition, was only observed for the longer vowel duration and high masker modulation rates, when each vowel spanned across multiple masker modulation periods. There was no observable performance degradation when the vowel rate and masker modulation rate were close, reflecting a limited contribution from modulation masking/interference. The current results show that modulation masking/interference is not always the main determining factor for the FMB, therefore, it is possible that its origin is not limited to a hard-wired, bottom-up mechanism.

PS 391

Effects of Inharmonicity in Music and Speech Suggest Multiple Pitch Mechanisms

Malinda J. McPherson¹; Josh H. McDermott²

¹Harvard University Program in Speech and Hearing Bioscience and Technology; ²MIT

Pitch is generally defined as the percept corresponding to the fundamental frequency (F0) of a sound. However, many real-world tasks thought to rely on pitch could in principle be performed without computing the F0 of the sounds in question, and there is remarkably little evidence for the importance of F0-specific mechanisms. In order to investigate the extent to which pitch perception tasks depend on F0 extraction, we conducted a battery of pitch-related music and speech tasks, comparing performance for standard harmonic sounds with inharmonic sounds that lack a clear F0. The tasks included basic pitch discrimination, melodic contour discrimination, sour-note detection, probe-tone tonality ratings, interval recognition, interval discrimination, and familiar melody recognition (crowd-sourced through Amazon Mechanical Turk). Speech tasks, enabled by a modified version of the STRAIGHT speech analysis and synthesis method, included pitch contour discrimination, voice discrimination, and speaker recognition. Collectively, these studies indicate that F0 is not necessary to extract a pitch contour in speech or music, but does appear to be necessary for accurate interval estimates, in addition to aiding speaker recognition. These findings suggest that there may be two or three distinct systems responsible for what has conventionally been couched as pitch perception: one which tracks shifts in fine spectral patterns and does not rely on F0, another that is dependent on F0 for determining precise interval relationships between musical notes, and perhaps another associated with voice qualities.

PS 392

Infant Sensitivity to Fundamental Frequency as a Segregation Cue for Concurrent Vowels

Bonnie K. Lau¹; Lynne Werner²

¹University of Washington; ²Department of Speech and Hearing Sciences University of Washington

Listening in every day acoustic environments requires the perceptual segregation of simultaneous signals that overlap in time and frequency. Fundamental frequency (F0), or pitch, is a strong cue that can be used to segregate competing sounds. Adult listeners discriminate concurrent vowels with different F0s better than vowels with the same F0. However, whether infants can perceive such F0 differences is unknown. To investigate, F0 difference limens (F0DL) for two concurrent vowels were obtained in 3-month-old, 7-month-old, and adult listeners using a single-interval observer-based method. Seven $\Delta F0$ levels (2, 1, 1/4, 1/8, 1/16, 1/32, and 0 semitones) were varied adaptively to estimate an F0DL. The stimuli consisted of 520-ms-long vowels /i/, /u/, and /a/ recorded from one male (F0 = 100 Hz) and one female (F0 = 225 Hz) speaker. Half of the participants were tested in each talker condition. The concurrent vowel pairs consisted of two equal-level vowel tokens summed together with onsets and offsets aligned, presented at an overall level of 70 dB SPL. Listeners heard a series of randomly selected vowel pairs constructed with two of the same vowel token with a 500-ms interstimulus interval. They learned to respond when the F0 of the vowels in the pair were different. The vowel pairs with a pitch difference were created by manipulating only the F0 in the original vowel token to $F0 + \Delta F0$, keeping all other acoustic parameters the same. The participant's F0DL was defined as the smallest $\Delta F0$ level they could discriminate at 80% correct. Infants at both 3 and 7 months of age had F0DLs of less than a semitone. No threshold differences between 3- and 7-month-olds or between the male and female talkers were observed. That infants demonstrated sensitivity to F0 differences between two simultaneous vowels, suggests that infants as young as 3 months of age were able to use F0 as a segregation cue. Future work with the addition of electrophysiological measures will provide further insight into the development of underlying neural mechanisms.

Comparing the Effects of Age and Sensorineural Hearing Loss on Detection and Temporal Integration of Amplitude and Frequency Modulation

Nicolas Wallaert¹; Brian C.J. Moore²; Stephan Ewert³; Christian Lorenzi¹

¹*Ecole normale supérieure, Paris Sciences et Lettres*

Research University and CNRS, France; ²*Department of Psychology, University of Cambridge, CB2 3EB, UK;*

³*Medizinische Physik and Cluster of Excellence Hearing4All, Universität Oldenburg*

Background

The relative contribution of excitation-pattern and temporal fine-structure (TFS) information to modulation sensitivity is still a matter of debate. We addressed this issue by investigating the effects of age and sensorineural hearing loss on amplitude-modulation (AM) and frequency-modulation (FM) detection thresholds (AM-DTs and FMDTs, respectively) and temporal integration for AM and FM detection.

Methods

AMDTs and FMDTs were measured at 40 dB SL for young and older normal-hearing listeners (NH_y and NH_o, respectively) and for older listeners with sensorineural hearing loss (H_{lo}) using a 500-Hz sinusoidal carrier and modulation rates of 2 and 20 Hz. The number of modulation cycles, N, varied between 2 and 9. We also assessed whether a computational model of temporal-envelope processing based on the modulation-filterbank concept and a template-matching decision strategy could account for the data

Results

Mean results for each group are shown in the figure. For all groups, AMDTs and FMDTs were always lower (better) for the 2-Hz rate than for the 20-Hz rate and decreased (improved) with increasing N. AMDTs were higher for the NH_o than for the NH_y group, and higher for the NH_o group than for the H_{lo} group. The effect of increasing N was similar for the NH_y and NH_o groups, but was greater for the H_{lo} group. FMDTs were higher for the NH_o group than for the NH_y group for the 2-Hz rate only. FMDTs were higher for the H_{lo} group than for the NH_o group for both rates. The effect of increasing N was similar across the three groups. The computational model accounted relatively well for the AM data, but failed to account for the FM data, probably the model did not take account of the use of TFS information.

Conclusions

Taken together, the data show that the effects of age and hearing loss are different for AM and FM detection and for temporal integration in AM and FM detection, consistent with the notion that AM and FM detection rely on different information. In addition, the data suggest that:

- i) Greater age reduces sensitivity to both excitation-pattern and TFS cues, but more so for the latter.
- ii) Loss of amplitude compression in the impaired cochlea is responsible for the enhanced sensitivity and temporal integration of excitation-pattern cues found for hearing-impaired listeners.
- iii) Ageing and hearing loss spare memory and decision factors responsible for temporal integration of excitation-pattern and TFS cues.

PS 394

Amplitude Modulation Detection with a Short Pure-tone Carrier: Effects of a Noise Precursor and Hearing Loss

Jessica Chen¹; Skyler G. Jennings¹; Sara E. Fultz²; Jayne B. Ahlstrom²; Judy R. Dubno²

¹*University of Utah;* ²*Medical University of South Carolina*

Background

Amplitude modulation (AM) detection measures sensitivity to temporal envelope fluctuations, such as those in speech and speech-like maskers. Recently, we showed that AM detection thresholds for narrowband, high-frequency carriers increased significantly at moderate levels in adults with normal hearing. These poorer AM detection thresholds are consistent with cochlear compression, which is expected to reduce post-cochlear AM depth. When the same carrier was preceded by a notched-noise "precursor," AM detection thresholds decreased and remained relatively constant across carrier level. These results are consistent with a reduction in cochlear gain via the medial olivocochlear (MOC) reflex, which is expected to linearize cochlear response growth and increase post-cochlear AM depth.

The response growth of the basilar membrane is more linear with cochlear hearing impairment, which predicts better-than-normal AM detection for subjects with cochlear hearing loss and smaller improvements in AM detection with a precursor. The purpose of this experiment was to test these hypotheses by measuring AM detection thresholds as a function of carrier level with and without precursors in younger adults with normal hearing (YNH) and in older adults with mild-to-moderate hearing impairment (OHI).

Methods

A 2-kHz, 50-ms carrier was presented at 45, 55, 60, 65, 75, and 85 dB SPL and was immediately preceded by silence or by a 40 dB SPL, notched-noise precursor whose notch width extended from 1.8 to 2.2 kHz.

Results

Without a precursor, AM thresholds for YNH subjects increased from low-to-moderate carrier levels. AM thresholds decreased at the highest carrier levels, consistent with detecting AM through off-frequency auditory filters where response growth is expected to be more linear. With a precursor, AM detection thresholds in YNH subjects decreased at low-to-moderate carrier levels. Preliminary results from OHI subjects revealed that AM detection thresholds were similar with and without a precursor and were generally better than thresholds for YNH subjects.

Conclusions

Consistent with our previous findings in YNH subjects, cochlear compression may be responsible for poor AM detection thresholds at moderate levels for carriers preceded by silence. Better AM thresholds with than without a precursor are consistent with the effects of MOC feedback, which are expected to improve post-cochlear modulation depth by linearizing cochlear responses. Lower AM detection thresholds and smaller precursor effects in OHI than YNH subjects are consistent with more linear cochlear response growth with cochlear hearing loss.

PS 395

Medial Olivocochlear Reflex Effects on Amplitude Modulation Detection

Enrique A. Lopez-Poveda¹; Miriam I. Marrufo-Pérez¹; Luís E. López-Bascuas²; Almudena Eustaquio-Martín¹
¹University of Salamanca; ²Universidad Complutense de Madrid

Medial olivocochlear (MOC) efferents may be activated in a reflexive manner by ipsilateral and contralateral sounds. Their activation linearizes basilar membrane input/output curves, an effect that could enhance the sound envelope as represented in the mechanical response of the cochlea, and thus facilitate the detection of amplitude modulation. To investigate this possibility, amplitude modulation (AM) detection thresholds were measured monaurally in the presence and in the absence of a 60 dB SPL, 400-ms, wideband (0.1-10 kHz) noise. It was assumed that this noise activated the MOC reflex without activating the middle-ear muscle reflex. The probe was a 70 dB SPL, 1500 Hz tone modulated in amplitude at a rate of 40 Hz. MOC reflexes have an onset delay of about 25 ms and need about 300 ms

to be completely activated. A short (50 ms) probe was used for the probe to minimally activate the MOC reflex by itself and AM thresholds were measured for the tone presented at the noise onset (early condition) and 300 ms after the noise onset (late condition). The difference in AM threshold for the late and early conditions was regarded as indicative of the MOC reflex effect on AM detection. To assess the effects of ipsilateral, contralateral, and bilateral MOC reflex elicitors on AM detection, AM thresholds were measured for ipsilateral, contralateral, and diotic noises, respectively, as well as in quiet. AM thresholds were worse in noise than in quiet. In noise, however, thresholds were better for the late than for the early condition, and the difference was comparable for ipsilateral, contralateral, and diotic noises. The results suggest that the MOC reflex facilitates the detection of amplitude modulation in noise, and that the magnitude of the benefit is comparable for ipsilateral, contralateral, and bilateral elicitors. [Work supported by the University of Salamanca, Banco Santander, and MINECO (BFU2015-65376-P).]

PS 396

Behavioral Performance in FM Tone Perception Is Lateralized for Direction Discrimination but Not Duration Discrimination in Humans

Ann-Kathrin Riegel-Betz; Bernhard Gaese
Goethe University Frankfurt

Processing of frequency-modulated (FM) tones in humans is dependent on stimulus parameters such as modulation direction (upward/downward) or stimulus duration. Imaging studies (fMRI) investigating FM direction discrimination revealed a critical involvement of the right hemisphere in this process (e.g. Behne et al. *J. Neurophys.* 2005). Processing of stimulus duration, on the other hand, revealed no significant fMRI activation differences between hemispheres (e.g. Angenstein&Brechmann *Neuroimaging* 2013), in spite of a behavioral left-hemisphere lateralization during dichotic listening (e.g. Brancucci et al. *Neuropsychologia* 2008). In the presented study, unilateral FM stimuli combined with contralateral noise bursts (NB) were used to investigate if lateralized brain activity during FM direction or duration discrimination has consequences at the behavioral level.

Ten right-handed subjects (6 females, 4 males, 21–35 years) participated in this study. The point of subjective equality for FM and NB detection was determined in a pre-test in order to rule out any unspecific lateralization. All test paradigms were organized as two-alternative-forced choice tasks, with the NBs always at a steady SPL (60 dB SPL), whereas contralateral FM stimuli were presented in blocks with decreasing SPL. This allowed

determination of performance differences between ears at levels of comparable difficulty (fault rate above 20%) between subjects.

FM discrimination depending on modulation direction revealed a clear lateralization. Average fault rates (FRs) for right ears (40%) were significantly higher than for left ears (20%), while no significant differences were found for reaction times (RTs). Furthermore, FRs of all subjects and average RTs increased with decreasing SPL. Categorizing FM stimuli regarding their stimulus duration (short: 400 ms, long: 600 ms), revealed again that FRs of all subjects increased with decreasing SPL. There was, however, no visible trend for the RTs and no significant lateralization for average FRs and RTs. In summary, a clear left ear advantage for FM direction discrimination was observed, leading to the assumption that the right hemisphere is critically involved. This in turn confirms that an increased activity in the right hemisphere correlates to improved perceptual performance. The discrimination of different FM stimulus durations, however, revealed no advantage for one side. Consequently, it is assumed that both hemispheres are equally required for this task.

Sound Localization in Humans and Animals

PS 397

Visual and Auditory Localization Tasks in Marmosets: A Preliminary Report

Rachele McAndrew; Hannah Horeczko; Christopher Montagne; Kyle Labban; Yi Zhou
Arizona State University

In foveate species, coordinated eye and head movements enable gaze shifts that improve target tracking and target identification. Recently, significant progress has been made in unveiling the behaviors of marmoset monkeys in visual tasks (Mitchell et al., 2014). However, few previous attempts have succeeded in training marmoset monkeys to perform an auditory localization task based on natural orienting behavior, such as eye or head movement. In this study we trained two marmoset monkeys to direct their gaze towards a visual or auditory target using eye movement in a head-fixed setup.

An operant conditioning procedure was implemented with juice reward for correct response. For acoustic stimulation (noise bursts or monkey calls), sounds were delivered from two loudspeakers positioned at eye level, 45° to the left and right of midline. For visual stimulation (monkey faces), images were displayed on an acoustically transparent screen with a low-noise projector. The image was positioned laterally at either +10 or -10 degrees. Marmosets quickly mastered the visual localiza-

tion task and were able to discriminate by fixation between 2 or 3 different image positions. Their performance dropped considerably as the subjects transitioned from a visual to auditory task. We found that localization to the visual feedback image tended to dominate the behavior at the initial phase of transition. With training, both subjects showed improvement in detecting the sidedness of an auditory target, but the range of gaze movement was more restricted (+/- 7 degrees) than that in the visual localization task (+/- 10 degrees). These results suggest that marmoset monkeys can detect the direction of a visual/auditory target using eye movement. However, the limited oculomotor range of marmoset monkeys may require them to use head movement to orient their gaze towards targets at peripheral positions.

PS 398

Psychophysical Evidence for the Adaption of Hemispheric Interaural Time Difference Encoding

Nicholas Haywood¹; Jaime Undurraga¹; David McAlpine²; Nick R. Haywood¹

¹*MacQuarie University*; ²*Macquarie University*

One means by which mammals might encode interaural time differences (ITDs) is through the use of opposing, hemispheric spatial channels. ITDs at the fringe of the physiological range elicit a maximal neural population response, and so behaviourally relevant ITDs might be encoded via differences in firing on the rising slopes of these channels. Here, we use psychoacoustics techniques and an adaption paradigm to characterise such hemispheric tuning.

In an adaptive 2I-2AFC paradigm, listeners discriminated a 1-s, 42-Hz amplitude modulated (AM) 500-Hz tone with a rapidly 'alternating' carrier interaural phase difference (IPD) from an otherwise identical static-IPD reference tone (i.e., diotic throughout, both tones 65 dB SPL). The amplitude envelope was diotic, and IPD transitions were applied to the carrier of the target at minimum points in the AM cycle. IPD switches between 0° and 40° occurred at a rate of 7 Hz (i.e., every 6 AM cycles). Tones were presented in a background uncorrelated white noise, the level of which was varied adaptively. Threshold was taken as an index of sensitivity to the rapid IPD transitions. In different conditions, the sequences were each preceded by a 2 s adaptor tone. The adaptor was matched to the target, except having a fixed IPD – either 45°, 67.5°, 90°, 112.5°, 135°, 157.5°. Reductions in thresholds were taken as an index of the adaptation hemispheric channels.

Group-averaged performance was poorest in the 90° adaptor condition, and improved at greater or lesser

adaptor IPD values. This suggests a hemispheric channel maximal activated at 90°. However, some subjects showed progressively worsening performance as the adaptor IPD increased. In either case, results were not predicted by the proximity of the adaptor IPD to the target IPD (i.e., the closest adaptors did not have the greatest adaptation effect). A second experiment will examine the effect of the comparable adaptor conditions on target sequences with IPD values close to 90° (target = 70° to 110° IPD, reference = 90° IPD). Preliminary data suggests a similar pattern of adaptation, and so results cannot be explained simply in terms of any distraction/attentional effects that may be associated with the absolute IPD separation between the adaptor and target. On-going work using a comparable design will test adaptation effects for ITDs presented on the envelope of high-frequency tones. This will allow for comparisons of the mechanisms of channels encoding the ITDs high- and low-frequency signals.

PS 399

Metacognition in a Speeded Localization Task: Real vs. Artificial Head

Guillaume Andeol; Jean Christophe Bouy; Clara Suied

Institut de recherche biomédicale des armées

Background

In a sound localization task, listeners can point towards the target position in the wrong front-back hemisphere; this is called a “front/back reversal”. In a previous study (Andéol et al, ARO Midwinter Meeting, 2015), using a circular array of loudspeakers, we showed that listeners responded with slower Reaction Times (RT) for positions where front/back reversals were more frequent. Because RTs are often positively correlated with confidence, we hypothesized that confidence was lower for those positions. Therefore, our results were in favor of a metacognition of the listeners in their front/back discrimination ability. Front/back reversals are considerably larger when listening with non-individual localization cues (e.g. listening through an artificial head). That raises the question whether the effect observed with a real-head situation still persists with an artificial-head situation. In the present study, we investigate the metacognition of the listeners in a front/back discrimination task by using a RT paradigm, with an artificial head.

Methods

An artificial head was positioned at the center of a 12-loudspeakers ring (Azimuth: 0 to 360 by 30°step), inside an anechoic chamber. A wideband noise target was presented at 70 dB SPL with a 10 dB roving range. Listeners sat in the control room of the anechoic chamber. They had to indicate whether the target was in front

of or behind them by pushing a switch. They were asked to respond as quickly and as accurately as possible. For half of the participants, a confidence rating between 0 and 9 was asked after each trial, in order to check the relationship between RT and confidence. This measure was done both with real and artificial head.

Results

While a strong positive correlation between RT and performance was found in the previous study with real head, (Andeol et al, ARO, 2015), a very different pattern was revealed here, with artificial head. The correlation between RT and confidence was very weak, and significantly lower than the one with real head. It suggests that with artificial head, participants were not conscious of their errors.

Conclusion

These results suggest that the listeners' metacognition is reduced when they use non individual localization cues.

PS 400

Reaction Time of Horizontal Sound Localization Responses in Normal Hearing Adults

Martin Eklöf¹; Filip Asp²; Erik Berninger²

¹Karolinska Institutet, CLINTEC; ²Department of Clinical Science, Intervention and Technology, Karolinska Institutet, Stockholm, Sweden

Background

Eye gaze is an innate response to auditory events. Recent methodological advances allow quantification of such responses--resulting in a measure of sound localization accuracy--using a corneal reflection eye-tracking technique (Asp et al., 2016). In addition to accuracy, reaction time (RT) of sound localization responses may be studied using gaze as a measure of sound localization behavior. The aim of this study was to quantify RT and specifically as a function of the magnitude of azimuthal shifts in normal hearing listeners.

Method

Eight healthy, normal-hearing adults (aged 18 to 40 years) participated in this study. An array of twelve loudspeaker/display-pairs spanning ± 55 degrees azimuth in the frontal horizontal plane was used for measuring sound localization responses. An ongoing auditory-visual stimulus presented at 63 dB SPL(A) was shifted to randomly assigned loudspeakers nearly simultaneously (visual stimuli turned off 170 msec before sound shift) with 1.6 sec pauses of the visual stimulus (i.e. a sound-only period). The visual stimulus was automatically reintroduced at the azimuth of the sounding loudspeaker. The gaze behavior was sampled continuously at 20 Hz during 24 azimuthal shifts. The time from an

azimuthal shift of the sound to subject's saccade was modeled by fitting an arctangent-function to the gaze samples. The RT was defined as the time from sound shift to 50 % point of the arctangent-slope, i. e. halfway through the saccade.

Results

Data from eight normal hearing adult subjects were successfully fit with our model. Preliminary analyses shows that the mean (SD) RT was 230 msec (50 msec) ($n = 8$ subjects) for this certain stimulus, reflecting low inter subject variability. By contrast, the intra subject variability was relatively high, as reflected by a standard deviation of 110 msec. The RT was independent of the magnitude of the azimuthal shifts, as shown by a simple linear regression analysis, ($p > 0.1$, $n = 192$, $R^2 = 0.02$).

Conclusions

The short RT and low inter subject variability found in this study indicates that innate sound localization responses, such as eye gaze, are reflexive by nature and, thus, driven by subcortical processes. Furthermore, there is no effect of the magnitude of the azimuthal shifts on the latency of saccades larger than 10 degrees toward auditory events between ± 55 degrees azimuth. The intra subject variability in RT may be explained by the naturally occurring sound intensity variations in the ongoing auditory stimulus.

PS 401

Neural Correlates of Sound Externalization Based on Spectral Cues

Robert Baumgartner¹; Darrin Reed¹; Brigitta Tóth²; Virginia Best³; Piotr Majdak⁴; Gerald Kidd³; H. Steven Colburn⁵; Barbara Shinn-Cunningham¹

¹*Boston University*; ²*Hungarian Academy of Sciences*;

³*Department of Speech, Language & Hearing Sciences and Hearing Research Center, Boston University, Boston, MA 02215 USA*; ⁴*Austrian Academy of Sciences*;

⁵*Department of Biomedical Engineering and Hearing Research Center, Boston University*

Background

Sound sources in natural environments are usually perceived as externalized auditory objects that are located outside the head. In contrast, when listening via headphones or hearing-assistive devices, sounds are often heard inside the head, presumably because the acoustic filtering of incoming sound becomes inconsistent with normal experience. Although it is well-known that the high-frequency spectral cues mainly induced by the pinnae encode the sound direction, it is less clear how the salience of these cues affects sound externalization.

The present study was targeted to evaluate the consequence of changes in spectral cue salience on sound externalization and to identify neural correlates of the perceptual changes by means of electroencephalography (EEG).

Methods

Stimuli consisted of two consecutive noise bursts filtered with listener-specific head-related transfer functions (HRTFs) that were parametrically modified to vary spectral contrast. Fifteen normal-hearing listeners were monitored with EEG while judging differences in externalization between the two parts of the stimuli.

Results

Behavioral results showed strong individual differences, but, on average, HRTFs with less spectral contrast evoked less externalization. Onsets of spectral changes in the stimuli elicited event-related potentials characterized by an early fronto-central negativity (N1) around 120 ms and a later fronto-central positivity (P2) around 220 ms. P2 amplitudes were larger the more the spectral contrast changed with a bias towards decreased spectral contrasts. P2 amplitudes were also larger if the listeners judged that externalization decreased versus increased. The within-listener variability of P2 amplitudes tended to correlate with listener-specific externalization discriminability ($\rho = .50$, $p = .060$).

Conclusions

The fact that approaching sounds lead to larger neural responses than retreating sounds is consistent with previous reports on the perceptual salience of looming auditory objects, whereby an increase in sound intensity is perceptually more important than a decrease in sound intensity. Here we show a similar asymmetry for spectral cues, confirming that our spectral modifications influenced sound externalization in the distance dimension. Inter-individual differences in the effect of spectral cue distortions on sound externalization appear to be reflected by P2 amplitude variability.

PS 402

A Similarity Measure of Sound Source Positions Based on Head-Related Transfer Functions

Maïke Gerhard¹; Hartmut Führt¹; Hermann Wagner²; Patrick Schillberg³

¹*Lehrstuhl A für Mathematik, RWTH Aachen University*;

²*Institute of Biology II, RWTH Aachen University*; ³*Institute for biology II RWTH Aachen University*

Head-Related Transfer Functions (HRTFs) describe the direction dependent acoustic filtering of sounds by the listeners outer ear, head and body. It is well known that

in localization tasks there are sound source positions which are more difficult to distinguish than others, for example all points lying on a cone of confusion. HRTFs contain all spatial cues that are believed to play a role in sound localization, such as spectral notches, Inter-aural Time Difference (ITD) or Interaural Level Difference (ILD). Previous work in HRTF-based analysis of localization performance has mostly relied on methods of extracting these features from the HRTFs and using them to predict the sound localization performance. We developed a somewhat different approach. We present a measure for the acoustic similarity of two positions, called the Acoustic Distance that can be calculated explicitly from the positions HRTFs. We justify the validity of this measure using notions from signal detection theory. We also present a new HRTF-based localization algorithm that is closely related to the acoustic distance. It can be shown theoretically that the algorithm achieves the localization precision predicted by the acoustic distance. These theoretical findings are based on a worst case analysis, where the disruptive noise must have a specific structure to cause confusion of different positions. For these reasons we also tested the localization algorithm on signals with random noise, and found that the acoustic distance allows a good prediction of localization performance for this setting as well. Based on this result, we expect that the acoustic distance will also be useful for the prediction of the localization performance in human and animal psychophysics.

PS 403

Human Sensitivity to Binaural Cues for Sound Localization via Bilateral Bone Conduction: Predictions and Measurements

Andrew D. Brown; Daniel J. Tollin
Department of Physiology and Biophysics, University of Colorado School of Medicine

Stimulation of the inner ear via bone conduction (BC) offers an alternative means of hearing for individuals with outer and middle ear pathologies, for tactical communications applications (e.g., military and law enforcement), and for a growing number of consumer devices. While the use of two transducers (i.e., bilateral BC) potentiates access to binaural cues for sound source localization and segregation, previous physical and perceptual measurements suggest that binaural disparities are reduced under BC, limiting binaural fidelity and performance. Toward improved understanding of limitations on binaural performance under BC, we measured psychophysical sensitivity to static and dynamic interaural time and level differences (ITD and ILD) in normal-hearing human subjects using a series of discrimination and scaling tasks. While subjects were sensitive to both cue types under BC, sensitivity differed from that measured under air

conduction (AC). Measures of particular interest were (1) the cross-frequency trajectory of ILD sensitivity with respect to measures of transcranial attenuation for BC stimuli and (2) the interrelationship (within subjects) between ITD JNDs and ILD JNDs for AC versus BC stimuli. Measurements of sensitivity to binaural cues under BC were subsequently used to predict performance in an absolute sound localization task. Implications for BC technology are discussed. [Funding provided by NIH Grant Nos. F32-DC013927 (ADB) NIH R01-DC011555 (DJT)]

PS 404

Envelope Modulations Reduce Sensitivity to Binaural Differences in Young Normal-Hearing Listeners

Matthew J. Goupell¹; Olga A. Stakhovskaya²; Stephen Fong¹

¹*Department of Hearing and Speech Sciences, University of Maryland, College Park*; ²*Walter Reed National Military Medical Center, Bethesda, MD*; *Department of Hearing and Speech Sciences, University of Maryland, College Park, MD*

Introduction

Processing of interaural time differences (ITDs) is rate limited, meaning that performance decreases as the pulse rate increases beyond 200-300 pulses per second (pps) for high-frequency bandlimited acoustic pulses. Relatively slow second-order envelope amplitude modulations (i.e., the pulses are encoding a time-varying envelope, such as encoding sounds with a cochlear-implant sound processing strategy) restore ITD sensitivity at high rates. While rate limitation release is well documented, it is unclear if this release is limited by the symmetry in a listener's hearing. Normal hearing assumes binaurally symmetric hearing; however, small (< 10 dB) asymmetries in hearing thresholds and loudness growth functions likely occur and this could impact binaural processing. The purpose of this study was to determine how slow second-order envelope modulations impacted ITD processing in pulse trains in normal-hearing listeners.

Methods

Ten young normal-hearing listeners participated in the experiment. The listeners were presented bandlimited acoustic pulse trains that varied in pulse rate (50-500 pps), carrier center frequency (4, 8, or 12 kHz), and second-order envelope amplitude modulation (unmodulated=Flat, modulated and binaurally correlated=Correlated, or modulated and binaurally uncorrelated=Uncorrelated). The second-order envelopes were extracted from 50-Hz bandwidth narrowband noises. The pulse trains were presented at 70-dB sensation level. The listeners' task was to detect a target in a three-interval,

two-alternative forced-choice task. Targets had 180 degrees interaurally out-of-phase pulse trains (i.e., non-zero ITD); non-targets had in-phase pulse trains (i.e., zero ITD). Listeners were presented 100 repetitions per condition and the percentage of correct responses was measured in a method of constant stimuli.

Results

ITD discrimination performance decreased with increasing rate; performance increased with increasing center frequency. A rate by modulation-type interaction revealed that performance was better for the flat conditions at higher rates than performance for the correlated conditions. Finally, performance for the flat and correlated conditions was better than performance for the uncorrelated conditions, as would be expected because the uncorrelated second-order envelope modulations should obscure the target ITD information.

Discussion

Slow second-order envelope modulations are thought to restore ITD sensitivity at high pulse rates; however, our results suggest that the opposite may be true, which may be a result of the type of second-order modulation applied to the pulse train. These results can be explained by small interaural asymmetries in loudness growth and modulation processing that were not measured in our listeners. These results also motivate further studies of what types of subject-specific differences limit binaural processing of modulated stimuli.

PS 405

Reverberation Alters Listeners' Trading of Interaural Time and Level Difference Cues

G. Christopher Stecker; Anna Diedesch
Vanderbilt University School of Medicine

Binaural lateralization is primarily dependent on interaural time and level differences (ITD and ILD). The relative influence of each cue can be determined, in the form of ITD/ILD "trading ratios," from localization judgments made when the two cues disagree. An extensive literature demonstrates that trading ratios vary significantly with sound frequency, intensity, and across listeners.

A previous study in our laboratory (Stecker 2010; *Hear Res* 268:202-12) measured ITD/ILD trading ratios for trains of narrowband filtered clicks. Trading ratios increasingly favored ILD cues as the click rate increased. Stecker (2010) argued that reduced availability of ongoing ITD cues at high rates led listeners to rely on the remaining intact cues: ILD and onset ITD. Here, we assessed whether reverberation, which degrades ongoing cues, might also enhance the relative weighting of ILD over ITD cues.

Experiments were conducted in an anechoic chamber containing a 360° azimuthal loudspeaker array. In the first phase of testing, broadband noises were presented from target locations spanning $\pm 61^\circ$ while binaural probe-tube recordings (Etymotic ER-7) were made for each of 10 normal-hearing listeners. Target stimuli were presented from 2m distance, in anechoic space or in a simulated 10x10m room with moderately absorptive walls ($\alpha = 0.5$). Lateral reflections up to 13th order were calculated via the image method and delivered via loudspeakers at the corresponding azimuth, delay, and intensity values. Gammatone filtering, transduction, and binaural cross-correlation (Akeroyd 2001) were used to extract frequency-specific ITD and ILD values for each stimulus.

In the second phase, listeners were presented with 500 ms sixth-octave bands of noise centered at 500 Hz or 4000 Hz and asked to indicate the perceived location using a touchscreen interface. Data were analyzed by linear regression of response azimuth onto the frequency-specific ITD and ILD values obtained from binaural recordings in each listener. The ratio of response-ILD and response-ITD slopes was used to express the relative influence of each cue in the form of an interaural-cue [trading] ratio (ICR). Measured in this way, ICR values (in $\mu\text{s}/\text{dB}$) were generally higher for 500 Hz than for 4000 Hz targets, particularly in the simulated room where low-frequency ITD can be significantly distorted. At both tested frequencies, ICR values were significantly higher in the simulated room than in anechoic conditions, consistent with a shift toward ILD-based localization in reverberant situations.

Supported by NID R01 DC011548.

PS 406

A New Approach That Accounts for Several "problematic" Sets of Binaural Detection Data Obtained with Narrow-band, Partially Interaurally Correlated Maskers

Leslie R. Bernstein; Constantine Trahiotis
University of Connecticut Health Center

Background

For decades, investigations have shown that binaural detection is successfully characterized and understood within the general framework of interaural correlation. Still, there exist stimulus contexts that are problematic because correlation-based approaches have not been shown to provide adequate explanations. For example, we found that an otherwise successful stimulus-based correlation model overestimated performance by amounts inversely related to the bandwidth of the masker for maskers that were both narrow-band and

partially interaurally correlated. We were able to redress that difficulty for a limited set of such data, albeit with a quantitative model that incorporated somewhat ad hoc parameters, assumptions, and computational complexity [Bernstein and Trahiotis, *J. Acoust. Soc. Am.* 136, 3211-3220 (2014)]. Although that effort was successful, we sought a simpler, more general and thus, to us, more satisfying approach.

Methods

The goal was to account for several different sets of relevant data taken from experiments published over the past several decades. We began with an existing model that includes several stages representing peripheral auditory processing and a central stage that computes normalized interaural correlations. The inputs to the model were experiment-specific multiple tokens of masker-alone and signal-plus-masker waveforms. Following Fisher's *z* transformation of the values of correlation, a decision variable was formed by computing the difference between the means of the distributions of the interaural correlations of masker-alone and signal-plus-masker waveforms divided by their variance. To make predictions, we assumed that, for a given experiment, a constant value of the decision variable would yield a constant level of performance.

Results and Conclusions

We found that predictions made using the existing model with its new decision variable accounted quite well for 1) the data that posed the initial difficulty and 2) a host of other related binaural detection data published across the last five decades that, to our knowledge, have never been accounted for quantitatively. In our view, this enterprise adds greatly to the generality and validity of an interaural correlation-based model that operates on the stimulus waveforms as they are processed (rather than operating on only the external stimulus waveforms).

PS 407

Maturation of the Binaural Interaction Component of the Auditory Brainstem Response in the Guinea Pig, a Precocious Species

Kelsey L. Anbuhl¹; Victor Benichoux²; Alexander T. Ferber¹; Daniel J. Tollin²; Andrew D. Brown²

¹Neuroscience Training Program; ²Department of Physiology and Biophysics, University of Colorado School of Medicine

The binaural interaction component (BIC) of the auditory brainstem response (ABR) is a sound-evoked potential that is specifically representative of the activation of binaural circuits in the auditory brainstem. The BIC is computed as the residual evoked potential after

subtraction of the binaural click-evoked ABR waveform from the sum of monaurally-evoked ABRs. The BIC has great potential for clinical applications as a non-invasive measure of central binaural auditory function in newborn through aging populations. In this study, we track the maturation of the characteristics of the BIC waveform amplitudes and latencies and their dependence on the binaural cues to location, the interaural time (ITD) and level (ILD) differences, over the early weeks of development in an animal model, the guinea pig (*Cavia porcellus*). Guinea pigs are audiologically similar to humans in that they hear at birth (a precocious species) and over a similar range of frequencies. Here, we measured monaural ABRs in guinea pigs from birth (P1) through adulthood (P56 onward). Consistent with the precocious nature of guinea pigs, we find that the ABR can be reliably evoked in newborn subjects. We discuss the evolution of the ABR waveform across ages as a marker of the relative activation of monaural ascending auditory pathways. In addition, we measure the binaurally-evoked ABRs and observe that the BIC can also be reliably evoked at birth. This result indicates that the binaural brainstem circuits of the guinea pig are indeed functional at birth similar to that observed in studies in human infants. Finally, we track the evolution of the BIC waveform, its amplitude and latency and their dependence on ITD and ILD over the maturation of the subject. Altogether our results confirm that the guinea pig is precocious, and suggest that it has functional binaural auditory brainstem circuits at birth. Our results can serve as baseline measures to study the plasticity of auditory brainstem circuits during development in an animal model that shares similar auditory developmental trajectories as the human. For example, such animal models can be used to simulate chronic conductive hearing losses in early life, and understand their effects on the maturation of binaural hearing.

Support: R01-DC011555 (DJT), F31-DC014219 (KLA), F30-DC013932 (ATF)

PS 408

The Bird Auditory Midbrain Functions Not for Auditory Localization but for Source Streaming: Developing the Theory and Reviewing the Data

Mark Riggle

Causal Aspects LLC

In 1978, an auditory space map was found in the Barn Owl ICX. This finding was taken as confirmation that sound localization occurred via the mid-brain auditory ascending pathway [the auditory pathway to the ICC then to the ICX which then placed targets into the optic tectum to drive a correct saccade].

However, in 1993, lesions showed the ICX was unnecessary for accurate localization. This meant another localization pathway must exist and furthermore, that localization does not require a specialized neural structure like the ICC-ICX. Then, because the owl failed to orient to a sound only when both the forebrain and the mid-brain (OT) were lesioned, it was inferred that there must be two independent localization pathways -- both a mid-brain and a forebrain pathway. Critically, this inference requires assuming that only the ascending auditory pathway (through the ICC) could perform localization; however, this assumption is incorrect. This is because a single sound source can be accurately localized using ILD-vector processing, and that the Vestibular Origin of Hearing theory (VOH -- Riggle2016) demonstrates that, instead of the ascending auditory pathway, auditory localization could be through the connections of the cochlear nuclei to the cerebellum. The VOH theory also shows how this cerebellar pathway computes localization (in world frame) and then places the auditory targets into the OT and forebrain. Localization via this pathway implies that the ICX does not contribute to auditory localization; instead, the evidence suggests the ICX specialized for separating multiple auditory sources and then streaming only one selected source -- which is a difficult auditory problem. The strongest evidence showing the ICX does not contribute to localization (found in 2004) occurs with prism fitted older owls where the ICC-ICX did not adapt to the prism's visual offset. With auditory stimulation, the OT showed stimulation first at the unadapted site (as expected), but 10 ms later, the OT showed stimulation at the correct location (as if adapted) which could not be from the ICX. While this result is predicted by VOH, the result strongly implies the ICX is not performing localization even in the mid-brain. We review additional evidence and the theory for the above claims about the ICX, including why the Owl's ICX shows a map.

PS 923

Echolocating Bats Adjust Sonar Signal Design in Response to Jamming Signals

Jinhong Luo; Cynthia F. Moss
Johns Hopkins University

Echolocating bats show individual differences in sonar call design, which suggests that they operate with a selective listening window for self-generated echo returns from objects in their surroundings. This listening window, however, cannot be entirely private, as there is also a great deal of spectral overlap between the calls of individual bats of the same species. This suggests that bats may be vulnerable to interference from acoustic signals with characteristics similar to their own sonar vocaliza-

tions. Many species of bats adjust the frequency of their echolocation calls in response to calls from neighboring conspecifics or biosonar playbacks, which is commonly referred to as a jamming avoidance response (JAR). JAR in echolocating bats has been documented in field and laboratory studies, but details of the time course of JAR has not been well characterized. Here, we trained big brown bats to track approaching prey targets by echolocation from a platform. During the sonar tracking, we presented jamming signals, simulating calls of another bat, to selectively perturb sound production or echo receiving processes. We found that the bats exhibited the strongest JAR when the jamming sounds occurred during vocal production. Surprisingly, bats did not show a JAR when the jamming signals coincided with the arrival of target echoes. Furthermore, bats exhibited the JAR in the first call following the jamming sound, revealing a response latency of 66 ~ 94 ms. Thus, bat JAR represents an extremely rapid audio-vocal behavior.

Speech Perception I

PS 409

Individual Differences in Sensory Coding and Auditory Perception

Le Wang¹; Hari Bharadwaj²; Barbara Shinn-Cunningham¹

¹*Boston University*; ²*Purdue University*

Background

Prior studies have revealed large individual differences both in sensory representations of sounds and in auditory perception. Studies in recent years have begun to reveal how these individual differences are related to each other. Here, a battery of auditory experiments was conducted on the same cohort of subjects in order to further elucidate the processes that affect auditory perception, especially speech understanding in the presence of competing sound sources.

Methods

All subjects had pure-tone thresholds within 20dB of normal hearing level in both ears. Each subject participated in a subset or all of the following five experiments. In Experiment 1, envelope-following responses (EFRs) were measured in three frequency bands centered around 1kHz, 2kHz and 4kHz, while subjects were watching a silent movie with subtitles. In Experiment 2, the middle-ear muscle reflex (MEMR) was measured using three pure tone elicitors: 1kHz, 2kHz and 4kHz. Experiment 3 measured behavioral thresholds for ITD discrimination using narrow-band stimuli with center frequencies at 1kHz, 2kHz and 4kHz. Experiment 4 measured tone-detection threshold in the presence of noise

(tone-in-noise). Three pure tone probes were used in Experiment 4: 1kHz, 4kHz and 8kHz. In Experiment 5, speech understanding in the presence of competing noise was measured using the Listening in Spatialized Noise (LiSN) test. Correlation analysis was done between all possible pairs of the five experiments.

Results

A complex correlation pattern is observed among the measures in the five experiments. Specifically, the passive physiological measures (EFR and MEMR) correlate with speech-in-noise performance: EFR magnitude in 2kHz and 4kHz bands, MEMR amplitude using 1kHz and 2kHz elicitors. EFR magnitude in the 2kHz band also correlates with MEMR using 2kHz elicitor. For the two behavioral measures (ITD and tone detection), ITD thresholds do not show significant correlation with the speech performance in any frequency band, while tone detection thresholds for the 1kHz probe are correlated with speech performance. No correlation is observed between the behavioral measures and the passive measures. The two behavioral measures correlate with each other only in the 4k band.

Conclusions

These results highlight how speech understanding in competing noises depends on complex interactions between multiple factors in sensory coding and basic auditory perception. Specifically, speech understanding in noise is affected by the temporal coding fidelity reflected in the EFR measure. Speech-in-noise perception is also related to MEMR and tone-in-noise detection, both of which may be sensitive to the integrity of the auditory nerve.

PS 410

Cortical Auditory Evoked Potentials(CAEPs) Elicited by Vowels Reflecting Emotionality Salient Aspects

Seungwan Lee; Jinsook Kim; In/ki Jin
Department of Speech Pathology and Audiology, Graduate School, Hallym University, Chuncheon, Korea

Objective

The purpose of this study was to investigate CAEPs elicited by essential vowels(/u/, /a/, /i/) of Ling 6 sounds employed emotions of angry(A), happy(H), sad(S) and neutral(N). The study was conducted by analyzing latencies and amplitudes of P1, N1, P2 and N2.

Methods

Twenty young adults(Mean age : 22.1, range : 21-27) with normal hearing (10 male, 10 female) participated for recording CAEPs. The stimuli were /u/, /a/, /i/ representing low, middle and high frequencies from Ling 6 sounds

reflecting emotionality salient aspects of A, H, S and N. For measuring CAEPs, bipolar channels with channel A and B were utilized. The electrodes were attached on channel A for collecting auditory evoked potentials and on channel B for monitoring eye movements and blinking. The stimuli were presented at 70dB HL using rarefaction polarity with the rate of 1.1 stimuli per second. Bandpass filter was from 1 to 30 Hz, the sweep number was 200, and the gain was 50K and 10K for channel A and B, respectively. The participants were comfortably seated in bed at a quiet environment for testing. Three main effects of emotion, vowel, and gender and their interaction effects were analyzed.

Results

Latency showed statistical differences in P1 for gender, N1 for emotion, P2 for emotion and vowel, and N2 for emotion($p < .05$). Amplitude showed statistical differences in P1 for gender, P2 for vowel and N2 for all three main effects($p < .05$). Interaction effects were significant for latency of P1 with emotion and vowel, for amplitude of N1 with emotion, vowel, and gender, for amplitude of P2 and N2 with vowel and gender and amplitude of N2 with emotion and vowel($p < .05$).

Discussion/Conclusion

Although the stimuli were different, CAEPs showed significant differences according to emotions of stimuli in the literature. The authors reported the most sensitive component of CAEP was amplitude of P2(Kanskee et al., 2007) and N2(Xu Q et al., 2015) following emotional change of stimuli. The latter study was agreed to the results of our study. The P1 showed significant difference by gender of this study which was explained by the allocation of attention difference between male and female in the previous study(Jaušovec N et al., 2009). Conclusively, this study indicates that vowels reflecting emotional salient aspect show the sensitivity to the component of CAEP in P2 and N2 meaning that the emotion and vowel differences are perceived by acoustical aspects.

PS 411

Effect of Mouse Vocalization Playback on the Listener

Alexandra Niemczura¹; Alyssa Carvalho²; Jasmine M. S. Grimsley²

¹*Northeast Ohio Medical University, Kent State University*; ²*Northeast Ohio Medical University*

Adult mice emit four categories of vocalizations; ultrasonic (USV), low frequency harmonics (LFH), noisy and mid-frequency (MFV). Between different contexts, mice alter the proportions of vocalizations emitted in each category and spectrotemporal characteristics of vocal-

izations. Very little is known about what these sounds mean to a listener. The LFH and MFV calls are typically emitted by distressed mice and may be aversive to listeners. The noisy call is predominantly emitted by lone animals who are not undergoing a stressful situation and may be affiliative. USVs are emitted in many types of social interactions, including mating and aggressive interactions, and may have varied meanings to a listener depending on the context. We used male USVs in bouts with structures akin to mating situations, which may be attractive to females and aversive to male listeners. We hypothesized that these categories will differentially affect listeners' behavior.

Sounds were presented from one side of an open field chamber while an ultrasonic microphone recorded emitted vocalizations from the opposite side; the microphone and speaker location varied between sessions. 24 adult CBA/CaJ mice (12m, 12f) were presented with three randomized exemplars of all four categories of vocalization and a no vocalization control. A single category was presented per session in a counterbalanced design. Animal location and vocal behavior was recorded for 10 minutes prior to sound onset, after which stimuli were presented at a rate of 0.25Hz for 20 minutes. To assess plasma corticosterone levels, a physiological measure of stress, blood was collected via submandibular puncture after each session.

Preliminary analysis of corticosterone levels ($n = 7f$) indicates that the playback of all vocalization categories elevates the stress levels of female listeners ($p < 0.05$). Video tracking ($n = 11m$) revealed that male mice avoided the side of the chamber where sound was being presented for all four categories. The calling rate of female mice (mice = 12f, vocalizations = 8,155) reduced during the presentation of vocalizations (Kruskal-Wallis chi-square = 12.07, $p = 0.017$); the rate was reduced when LFH and Noisy vocalizations were presented ($p < 0.05$) but was not affected by the presentation of USVs or MFVs. The duration of emitted vocalizations increased when MFV vocalizations were presented and decreased when LFH vocalizations were presented ($p < 0.002$ for both). Preliminary analysis of these data support the hypothesis that the playback of four mouse vocalization types has differential effects on the listener.

PS 412

Mouse Model of Temporal Coding Deficits Induced by Early Life Stress

Emily G. Hazlett¹; Alexandra Niemczura¹; Ryan Longenecker²; Alexander Galazyuk²; Jasmine M. S. Grimsley³

¹Northeast Ohio Medical University, Kent State University; ²Northeast Ohio Medical University (NEOMED);

³Northeast Ohio Medical University

In a normal human or animal, the magnitude of a startle response to a loud sound is attenuated by a shortly preceding lower intensity sound. This prepulse inhibition (PPI) is reduced in individuals with sensory processing deficits (SPD) induced by maternal stress or infant neglect. Individuals with SPD have difficulty following repetitive sounds and filtering out irrelevant stimuli – perceptual abilities which are essential for speech recognition. They are often distressed by sudden sounds or loud voices, and are impaired in emotion-related tasks. We investigated whether a mouse strain commonly used in auditory research due to maintenance of good hearing into adulthood (CBA/CaJ) has temporal coding deficits induced by early life stress (ELS).

ELS was induced by housing mother and pups (p2-p9) in wire bottomed cages with no substrate material and limited bedding material. Control animals were raised in standard cages with sawdust substrate and ample bedding material. Acoustic startle, PPI, and gap detection thresholds were measured in adults (>p90) within Kinder Scientific startle chambers ($n=11$ control; 16 ELS). Startle stimuli at multiple intensities (60-120 dB SPL) were used to assess whether ELS animals have elevated startle responses. Prepulse stimuli at multiple delays (2-200 ms) were used to assess whether ELS alters the time course of prepulse inhibition. Gaps of multiple durations (2-200ms) were used to assess whether ELS alters the threshold of detectable pauses between sounds. PPI used a 20ms prepulse at 70 dB SPL, and gap detection used a pause in a 70 dB SPL background sound 80 ms prior to startle stimuli. Both PPI and gap detection used 105 dB SPL startle stimuli. Inhibition was computed by comparing the change in the animal's center of mass to startle stimuli with a preceding cue to those without a preceding cue.

ELS animals did not have altered startle magnitudes or altered probabilities of startling. PPI was highly variable in ELS mice, with some mice showing robust PPI at a broad range of prepulse distances and others showing no significant PPI. Most control animals (91%) showed significant PPI ($p < 0.05$) for at least one delay, compared to only 43% of ELS animals. Gap detection thresholds

were twice as long in ELS animals ($p=0.03$). Together these data indicate that early life stress induces temporal coding deficits. This provides a good model for future investigation of the mechanisms that contribute to the auditory processing abnormalities induced by early life stress.

PS 413

Prediction of Speech Intelligibility Based on a Correlation Metric in the Envelope Power Spectrum Domain

Helia Relaño-Iborra¹; Johannes Zaar¹; Tobias May¹; Christoph Scheidiger¹; Torsten Dau²

¹Hearing Systems group, Department of Electrical Engineering, Technical University of Denmark, DK-2800, Kgs. Lyngby, Denmark; ²Hearing Systems group, Department of Electrical Engineering, Technical University of Denmark, 2800 Kgs. Lyngby, Denmark

A speech intelligibility model, named sEPSMcorr, is presented, which combines modulation-frequency selective processing based on the (multi-resolution) speech-based envelope power spectrum model (mr-sEPSM; Jørgensen et al. 2013) with a cross-correlation based back end inspired by the short-time objective intelligibility measure (STOI; Taal et al., 2011). The sEPSMcorr model can accurately predict data obtained with normal-hearing (NH) listeners for a broad range of listening conditions, including effects of stationary and fluctuating additive interferers as well as effects of non-linear distortions, such as spectral subtraction, phase jitter and ideal binary mask (IBM) processing. The model has a larger predictive power than both the original mr-sEPSM (which fails in the phase-jitter and IBM conditions) and STOI (which fails to predict the influence of fluctuating interferers).

sEPSMcorr includes audibility thresholds, such that sensitivity loss can be incorporated based on the audiogram, but other types of impairment (e.g., loss of compression, reduced frequency selectivity) cannot be simulated using this framework. However, speech perception can vary greatly among listeners even when hearing sensitivity is similar. Thus, it remains a challenge for this model configuration to predict speech intelligibility data from hearing-impaired (HI) listeners.

Therefore, the predictive power of the sEPSMcorr back end was further investigated in combination with a more realistic auditory pre-processing front end adopted from the computational auditory signal processing and perception model (CASP; Jepsen et al., 2008). The CASP front end contains outer- and middle-ear filters, a non-linear auditory filterbank (DRNL, López-Poveda and Meddis,

2001), an adaptation stage and simulations of outer and inner hair-cell loss. CASP has previously been shown to successfully predict behavioral NH data obtained in conditions of, e.g., spectral masking, amplitude-modulation detection, and forward masking (Jepsen et al., 2008). Furthermore, CASP can be tuned to model data from individual hearing-impaired listeners in different behavioral experiments (Jepsen and Dau, 2011).

Here, predictions of speech intelligibility obtained with sEPSMcorr as well as with the extended CASP-based version of the model are presented and compared to speech intelligibility data measured in conditions of additive noise, phase jitter, spectral subtraction, ideal binary mask processing and reverberation.

PS 414

Test Agreement Between Two Speech Perception in Noise Measures

Hillary Snapp¹; Prashant Angara²; Sandra Prentiss³

¹University of Miami; ²University of Miami Miller School of Medicine; ³University of Miami Department of Otolaryngology

Assessment of speech perception abilities is a fundamental aspect of rehabilitation in the hearing impaired population. A primary complaint of hearing impaired listeners is the inability to understand speech in background noise. Understandably, evaluation of speech perception in noise ability has become a standard part of the assessment process for intervention with a hearing device or implant. Numerous tools exist to quantify this difficulty. In 2011 both the AzBio (Spahr et al., 2012) and BKB-SIN (Niquette et al, 2003) tests were recommended as part of the minimum speech test battery to determine cochlear implant candidacy. The AzBio sentences are spoken by different talkers with limited context and presented at a fixed level in 10-talker babble at a fixed signal-to-noise ratio. The BKB-SIN test on the other hand, uses a modified adaptive approach wherein sentences are presented at a fixed level while four-talker babble is presented at increasingly more difficult signal-to-noise ratios. Fixed measures result in a percent correct score for a given signal to noise ratio, whereas adaptive measures calculate signal to noise ratio loss which is the dB level required by the listener above the noise to understand speech 50% of the time (SNR-50). These tests are gaining popularity as tools to determine treatment, measure post-treatment benefit and predict benefit with hearing devices. It is unclear, however, if these two measures provide comparable outcomes for speech in noise performance. Further, improved understanding of an individual's SNR-50 and how it correlates to the AzBio will guide clinicians in appropriate selection

of fixed SNR levels for assessment of speech in noise performance. The aim of this study is to examine test agreement between the AzBIO and the BKB-SIN in normal hearing listeners.

Normal hearing individuals were recruited at an academic medical center, where the BKB-SIN test was used to identify the 50% signal-to-noise ratio. The AzBio sentences were then presented at the fixed SNR level obtained during BKB-SIN testing to determine agreement with 50% accuracy.

Preliminary results indicate that when normal hearing listeners are presented AzBio sentences at a fixed SNR determined by their SNR-50 on the BKB-SIN, participant's correctly identified 37% of the words correctly on the AzBio test. These results suggest little agreement between the AzBio and BKB-SIN and that the AzBIO may require increased SNR levels to reach threshold. Clinicians should take this into consideration when determining SNR presentation levels for hearing device and implant candidacy evaluations.

PS 415

Responses to Vocalizations in the Basolateral Amygdala Carry Information about Social Context

Emily G. Hazlett¹; Jasmine M. S. Grimsley²; Jeffrey J. Wenstrup³

¹*Northeast Ohio Medical University, Kent State University*; ²*Northeast Ohio Medical University*; ³*NEOMED*

Acoustic communication requires processing vocalizations within a social context determined by the multisensory external environment and dynamic internal state. Understanding which brain areas establish social context is critical for understanding how meaning is derived from vocalizations. The basolateral amygdala (BLA) is an important area for integrating multisensory information and for processing salience and emotional relevance. Big brown bats live in complex, dynamic social groups and use complex social vocalizations. Here, we assessed whether the presence of a cagemate alters activation patterns in the BLA to categories of social vocalizations in big brown bats (*Eptesicus fuscus*). We hypothesize that BLA responses to social vocalizations are modulated by social context.

Female bats (n=3) were implanted with custom multi-channel electrodes in their BLA and a subdermal electrode in their flank to monitor movement. Both alone and with a cagemate present, animals were presented with four categories of sounds comprising five duration-matched exemplars (broadband noise (BBN) and three vocalization types; appeasement, high aggression,

medium aggression). Local field potentials (LFP), spiking activity, and movement data were recorded via wireless telemetry from free moving animals, vocal behavior was recorded via an ultrasonic microphone, and interactions were monitored via infrared video. Trials with movement or emitted vocalizations were removed from analyses. LFP responses remained robust for more than one month post-implantation, allowing for repeated testing. Pearson's correlations on individual trials of the LFP were used to investigate how a cagemate's presence effects responses to sounds. These data were used to derive information pertaining to social context or sound category.

BLA responses to social vocalizations and BBN carried information about the social context in all three animals. Within each social context two of the four categories of sound were more likely to be correctly classified for all three animals. However, the categories which are correctly classified differed between the alone and social contexts and between animals. These preliminary data suggest that the robustness of LFP responses for a vocalization category is effected by social context. This may reflect an increase in salience for a particular vocal category in a specific setting. Future analyses will investigate whether these differences are also present at the single unit level.

PS 417

Predicting Speech-in-Noise Deficits from the Audiogram

Daniel E. Shub¹; Matthew J. Makashay²; Douglas S. Brungart¹

¹*National Military Audiology and Speech Pathology Center, Walter Reed National Military Medical Center*; ²*Army Hearing Division, Army Public Health Center (Provisional)*

Background

In the US Army, individuals with audiometric thresholds that exceed a predetermined set of criteria are referred for an auditory fitness-for-duty evaluation. Because communication in noise is so critical in military tasks, speech-in-noise testing is a major component of this evaluation. This study evaluated different strategies for identifying individuals who have functional deficits in their communication abilities.

Methods

Three large data sets that included both audiograms and speech-in-noise performance were used to evaluate different ways of using the audiogram to identify individuals with poor speech-in-noise performance (bottom 5% of normal). The data sets are from hearing-loss studies

and are not representative of the population as a whole or of the US Army. A variety of classification rules were examined, including the current US Army standard and rules based on individual frequencies, the all-frequency pure-tone average, the speech-intelligibility index, two generalized linear models (GLMs), and an optimized threshold-based procedures that compares the threshold at each frequency with a cutoff criterion. The more complicated second-order GLM included both additive terms for the individual frequencies and their pairwise interactions, while the first-order GLM did not include these interactions.

Results

Of the individuals included, 19.4% had normal hearing thresholds and 49.1% would be referred for a fitness-for-duty evaluation based on the current US Army hearing profiling system. In total, 74.3% of the individuals had speech-in-noise performance similar to that obtained by individuals with normal hearing thresholds. The current US Army standard statistically reliably outperforms rules based on individual frequencies, the all-frequency pure-tone average, and the speech-intelligibility index and performs similarly to the first-order GLM. Classification rules based on the second-order GLM and the optimized threshold-based procedure both statistically reliably outperform the current US Army standard.

Conclusions

The current US Army standard better identifies individuals with functional communication problems than simple classification rules and even a rule based on the speech-intelligibility index. Optimized classification rules, however, can outperform the current standard. A modest improvement in the efficiency of the military's audiometric monitoring program may be obtained by making small changes to the current threshold-based criteria. Substantial improvements in the sensitivity of the audiometric monitoring program, however, will probably require the inclusion of a speech-in-noise test as part of the annual testing.

[The opinions and assertions presented are the private views of the authors and are not to be construed as official or as necessarily reflecting the views of the Department of Defense.]

PS 418

The Spatial Release of Cognitive Load in Cocktail Party is Determined by the Relative Levels of the Talkers. A fNIRS Study

Guillaume Andeol¹; Sara Suied¹; Sebastien Scannel-la²; Frédéric D. ...

¹Institut de recherche biomédicale des armées; ²Institut Supérieur de l'Aéronautique et de l'Espace

In a multi-talker situation, spatial separation between talkers reduces cognitive processing load: this is the "spatial release of cognitive load". The present study investigated the role played by the relative levels of the talkers on this spatial release of cognitive load. An experiment was designed in which participants had to report the speech emitted by a target talker in the presence of a concurrent masker talker. The spatial separation (0° or 120° angular distance in azimuth) and the relative levels of the talkers (adverse, intermediate or favorable target to masker ratio) were manipulated. The cognitive load was assessed with a prefrontal functional near-infrared spectroscopy. Data from 14 young normal-hearing listeners revealed that the target to masker ratio had a direct impact on the spatial release of cognitive load. Spatial separation significantly reduced the prefrontal activity only when the levels of the talkers are close (intermediate target to masker ratio) and had no effect on prefrontal activity when the masker is much louder than the target (adverse target to masker ratio). Therefore, the relative levels of the talkers might be a key point to determine the spatial release of cognitive load, and more specifically the prefrontal activity induced by spatial cues in multi-talker environments.

PS 419

Simulation of Bimodal and Single-sided Deaf Cochlear Implant Listeners' Speech Intelligibility – How Realistic Can It Be?

Tim Jürgens¹; Ben Williges¹; Sven Kliesch¹; Thomas Wesarg²; Lorenz Jung²; Leontien Ingeborg Geven³

¹Medizinische Physik, Forschungszentrum Neurosensorik, and Cluster of Excellence "Hearing4All", Carl-von-Ossietzky Universität Oldenburg, Germany;

²Universitätsklinik für Hals- Nasen- und Ohrenheilkunde, Freiburg im Breisgau, Germany.;

³Universitätsklinik Hals-Nasen-Ohrenheilkunde am Evangelischen Krankenhaus, Carl von Ossietzky Universität Oldenburg, Germany.

Introduction

A growing number of patients with cochlear implants (CI) shows contralateral acoustic hearing with either

normal (single-sided deaf, SSD) or impaired audiometric thresholds, the latter may be supported by a hearing aid (bimodal CI users). The access to both acoustic and electric hearing provides improvements in speech intelligibility, especially in spatial situations, which, however, is considerably poorer than that of normal-hearing listeners.

Goals of the study:

The goal of this study is to compare speech-in-noise recognition of simulated and actual bimodal and SSD-CI listeners using different spatial separations of speech and noise.

Methods

Simulation of bimodal or SSD-CI users has been realized by presenting normal hearing listeners with vocoder-processed speech. A further development of the vocoder of Williges et al. (2015) was used for simulating electric hearing, including signal processing details of two CI manufacturers and physiologically plausible details that are present in CI listeners. These details include pulsatile sampling of the audio signal envelope, loudness-growth functions, electrode positions, and electric field spatial spread. Simulation of unilateral acoustic hearing has been realized using three possible hearing ability specifications: (i) (unaided) normal hearing, (ii) aided moderately impaired hearing and (iii) aided severely impaired hearing. The hearing impairment simulation included the reproduction of audiometric thresholds, loudness recruitment and a poorer representation of the speech envelope due to broadened auditory filters. Speech reception thresholds (SRTs) were assessed using an adaptive procedure in stationary noise with long-term speech spectrum. Three different noise azimuth angles and frontal speech were simulated using virtual acoustics. The same methods (without the simulations) were used to assess the speech-in-noise performance also in exemplary actual bimodal and SSD-CI listeners.

Results

Within the simulations, SRTs were generally higher for poorer acoustic hearing, but were very similar across the two CI manufacturers. A spatial separation of speech and noise showed significant improvement (decrease) in SRTs due to better-ear-listening. Normal contralateral hearing provided SRT-benefit compared to CI if the noise was facing the normal-hearing ear. Comparisons with actual bimodal and SSD-CI listeners revealed a very similar pattern of speech-in-noise performance.

Conclusions

Bimodal and SSD-CI listening can be plausibly simulated using the signal-processing and physiological restrictions present in the sound processing of actual listeners. The proposed simulation framework is a candidate for

investigating the impact of preprocessing algorithms on speech intelligibility without the need to involve actual bimodal or SSD-CI patients. This work is financed by DFG JU2858/2-1.

PS 420

The Spatial Release of Cognitive Load in Cocktail Party is Determined by the Relative Levels of the Talkers. A Pupillometry Study.

Guillaume Andeol¹; Annie Moulin²; Clara Suied¹

¹Institut de recherche biomédicale des armées; ²Centre de recherche en neurosciences de Lyon

Homing on one talker's voice whilst ignoring another talker can be helped by spatially separating the two talkers. However, other cues, such as the level difference between the two talkers can be used by the listeners. The present study aims to investigate the listening effort by the objective means of pupil dilation, in a two talker speech perception task, in two conditions of spatial separation (0° and 120°) and 3 levels of target to masker ratio (TMR)(-12, -4 and +4 dB). The protocol was as close as possible to Andeol et al. (ARO, 2017) to allow better comparison between both studies.

Twenty-three normally-hearing young subjects (aged 18 to 25), mostly undergraduate students, were involved in the experiment. Same equipment and stimuli were used as in Andeol et al. (ARO, 2017) for auditory stimuli presentation. In order to record pupil dilation for each one of the 32 trials, within each one of the 8 blocks of measures, the following modifications had to be made: a 4 seconds silent gap was added after each sentence, followed by a small auditory marker indicating to the subject that he could repeat the answer (a combination of a color (out of 4) and a single digit number (from 1 to 8)). The auditory stimulus and the subjects' answers were recorded for later quotation as correct and incorrect answers. During the task, the subjects were instructed to fix a cross in the center of a white board situated 55 to 65 cm in front of them, whilst the camera of an Eyelink 1000° eyetracking system was constantly monitoring their pupil size, with a sampling frequency of 500 Hz.

Preliminary results show that spatial separation yielded significantly greater scores, and significantly lower pupil dilation for each one of the TMR. In the most adverse TMR (-12 dB), the spread of the percent scores in the 0° condition lead us to identify two separate groups of subjects: 11 subjects had scores at -12 dB lower than at -4 dB, whereas 12 subjects had scores at -12 dB TMR greater than at -4 dB, showing a "U-shape" pattern similar to that of Andeol et al (ARO, 2017).

This study confirms that the TMR can play an important role in the spatial release of the cognitive load.

PS 421

Auditory-Cognitive Training Alters the Neural Encoding of Speech for Older Adults with Normal Hearing

Stefanie E. Kuchinsky¹; Alessandro Presacco²; Samira Anderson³; Jonathan Z. Simon⁴

¹*University of Maryland*; ²*University of California, Irvine*;

³*Department of Hearing and Speech Sciences, University of Maryland, College Park*; ⁴*University of Maryland, College Park*

Understanding speech in background noise is a challenging task that is supported by interactive auditory and cognitive processes. Indeed, magnetoencephalography (MEG) studies have shown that the encoding of speech information in auditory cortex is attention-modulated: superior temporal cortex activity exhibits greater phase-locking to the low-frequency envelope for an attended versus ignored speech signal. Age-related changes in such neural encoding have been investigated as a contributing factor to the speech-recognition challenges that older adults face. Specifically, older adults appear to over-represent speech information, exhibiting exaggerated (greater) cortical phase-locking compared to younger adults, which likely reflects an age-related imbalance between excitatory and inhibitory systems and inefficient cognitive processing.

Interventions that train top-down, executive functions within an auditory task have been hypothesized to more comprehensively target the processes that support speech recognition in noise than primarily auditory- or cognitive-focused training. Thus, the current study aimed to investigate the impact of combined auditory-cognitive training for improving speech understanding and the cortical encoding of speech for older adults.

Older (≥ 65 years old), normal-hearing adults completed Listening and Communication Enhancement (LACE™) training. Training involved ~8 hours of auditory-cognitive exercises, including auditory working memory, speech recognition in babble, speech recognition with a competing speaker, recognition of rapid speech, and filling in missing words based on sentence context. In pre- and post-test MEG sessions, participants listened to one-minute long stories in quiet and at four signal-to-noise ratios (SNRs) with either a relatively meaningful (English) or meaningless (Dutch) background speaker. The extent of neural encoding was quantified by the correlation between the actual and the neurally reconstructed speech envelope across participants.

Replicating previous studies of LACE™, trainees' accuracy on the Q-SIN test of sentence recognition in noise improved. These participants also exhibited patterns of neural encoding more similar to that of younger adults reported in previous studies, particularly in the most challenging listening conditions (i.e., a decrease in over-representation). Ongoing work compares the effectiveness of LACE™ to a closely aligned, active control training, which includes memory and attention exercises in the absence of auditory stimuli (BrainHQ, Posit Science). We discuss the results in terms of their support for the hypothesis that auditory-cognitive training drives changes in the neural encoding of the speech signal and in speech understanding.

PS 422

The Effect of Voice Familiarity and Memory Load on Speech Intelligibility in Multitalker Environments

Ysabel Domingo; Emma Holmes; Ingrid S. Johnsrude
University of Western Ontario

The ability to separate words spoken by a target talker from those of competing talkers is crucial for successful communication. Johnsrude et al. (2013) demonstrated that familiarity with a spouse's voice improves speech intelligibility during two-talker listening: in a Coordinate Response Measure (CRM) task, listeners achieved better speech intelligibility when either the target voice or masker voice was familiar than when both voices were unfamiliar. A follow-up experiment (Domingo, Holmes, & Johnsrude, ARO 2016) presented sentences from the Boston University Gerald (BUG; Kidd et al., 2008) corpus to young adults who had been friends for at least six months. The results showed improved speech intelligibility when the target voice was familiar but, unlike Johnsrude et al., no improvement when the masker voice was familiar. Different results between these experiments could either be explained by (1) lower memory load in the CRM task or (2) greater familiarity with a spouse's voice than that of a friend. The current experiment aimed to dissociate these possibilities by presenting the BUG task to participants whose familiar voice was their cohabiting spouse.

Fifteen participants (mean age = 59.8 years) completed a two-talker listening task with sentences from the BUG corpus (which follows the structure "Name Verb Number Adjective Noun"). The target sentence was identified by the Name word (Bob or Pat). Participants had to report the four subsequent words from the target sentence. In the Familiar Target condition, the target sentence was spoken by the participant's spouse and the masker sentence was spoken by an unfamiliar talker. In the Familiar Masker condition, the target sentence was spoken by an unfamiliar talker and the masker was the

participant's spouse. In the Both Unfamiliar condition, the talkers speaking the target and masker sentences were unfamiliar. We analysed the percentage of trials in which participants correctly identified all four words. As expected, listeners correctly reported the target sentence more frequently in the Familiar Target condition than in the other two conditions. However, there was no significant improvement for the Familiar Masker compared to the Both Unfamiliar condition.

These results, in combination with those of previous experiments in our lab, suggest that listeners more accurately identify words spoken by a familiar voice across different sentence corpora and for voices with different degrees of familiarity. However, only in the CRM so far (which has a lower memory load) is intelligibility of an unfamiliar voice improved by a familiar masker voice.

PS 423

The Impact of Bilingualism and Age on Understanding Vocoded Speech

Arifi Waked; Matthew J. Goupell

Department of Hearing and Speech Sciences, University of Maryland, College Park

Most studies on speech understanding in cochlear-implant (CI) users and normal-hearing (NH) individuals listening to vocoded speech have focused on monolingual English-speaking adults. Worldwide, however, most people are bi- or multilingual. For NH bi/multilingual listeners, there are many factors known to make speech understanding more difficult. These may be even more substantial for bi/multilingual CI users as the auditory input they receive is impoverished and distorted. Child CI users may face relatively greater difficulties compared to adult CI users because the latter have greater experience with language use and are also likely to have more fully-developed top-down language processing abilities. These factors give adults greater resources for understanding degraded speech signals, whereas younger listeners may not have reached these levels of development and experience. As such, we hypothesize that age and bi/multilingualism may interact with speech understanding for degraded signals, as would occur with a CI.

To begin exploring the effects of bilingualism on speech understanding with a CI, we examined how child (8-10 years) and adult (18+ years) NH monolingual English speakers and bilingual Spanish-English speakers learn to understand vocoded speech. Over a two-hour period, participants trained on understanding vocoded speech where there was a simulated shallow CI insertion depth (6-mm frequency-to-place mismatch) with both auditory and visual feedback. Between these training trials, participants were tested on standard (0-mm) or shal-

low (6-mm) simulated insertion depth without feedback.

Adult monolingual participants performed significantly better than monolingual children in the 0-mm shift condition, which might be a result of adults' better top-down abilities. In the 6-mm shift condition, adults and children performed similarly, which might be a result of an inability to apply top-down knowledge when signals are degraded and shifted. Addition of bilingualism is predicted to interact with age, removing the age differences for the 0-mm shift condition and causing lower accuracy scores in the 6-mm shift condition as compared to their monolingual peers. This is because both groups will have relatively fewer cognitive and linguistic resources available for speech understanding as compared to monolingual participants.

Results showing that bilingualism impacts degraded speech understanding would have important clinical and educational implications for bilingual CI users. Many bilingual CI users only receive education and therapy in English. As such, they may need extra time and attention from both educators and clinicians. [Work supported by NIH grant R01-DC014948 and the University of Maryland.]

PS 424

Age Effects on Perceptual Restoration of Degraded Interrupted Sentences

Brittany Jaekel; Rochelle Newman; Matthew J. Goupell

Department of Hearing and Speech Sciences, University of Maryland, College Park

Young normal-hearing listeners typically show a restoration effect, or an increase in speech recognition scores, when sentences interrupted with short silent gaps are instead interrupted with short noise bursts. Despite the slower auditory temporal processing associated with aging, older normal-hearing (NH) listeners appear to maintain this restoration effect as well, showing sentence intelligibility scores similar to young listeners only when silent gaps are filled with noise. Noise apparently facilitates the interaction of top-down mechanisms with the partial bottom-up information from interrupted speech streams, and older NH listeners utilize the top-down information to a greater extent than do young NH listeners.

When speech is degraded, the restoration mechanism is negatively affected. Older cochlear-implant (CI) users, who hear degraded speech signals through their processors, have typically shown only small or negligible restoration effects. Young NH listeners who are hearing degraded speech through a vocoder, which simulates

aspects of CI processing, also show less ability to utilize noise to restore speech: at least one study reported that young NH listeners needed as many as 32 spectral channels of information to show a restoration effect, which is well beyond the number of actual or functional spectral channels available to CI users. Though there appears to be a strong effect of spectral loss on the restoration mechanism, perhaps there is also an interaction with age. Under certain circumstances, older NH listeners may be able to obtain more benefit from the addition of noise in the silent gaps in the degraded speech stream than can young NH listeners because of their greater reliance on and utilization of context cues and linguistic knowledge.

Characterizing to what extent this restorative process is available to older listeners hearing degraded sentences will be helpful for better understanding how some CI users might be processing interrupted, noisy speech. The present study tested two groups of normal-hearing listeners (younger < 45 yrs and older >65 yrs) for restoration effects in interrupted sentences with various rates of interruption. Degradations in the speech signal were carefully controlled by manipulating vocoder parameters to analyze effects of spectral resolution, fidelity of speech envelope transmission, and similarity in spectral content of speech and noise bursts on restoration. [Work supported by NIH grant R01-DC014948 and the University of Maryland.]

PS 425

Effects of Presentation Level on Listening Performance in Noise

Roland Schaette; Sarah Kassem; Priya Singh
Ear Institute, University College London

Understanding speech in background noise is one of the toughest challenges for people with a hearing impairment. However, also normal-hearing people often struggle to understand speech, especially in loud environments. We therefore investigated whether presentation level has an effect on the ability to understand speech and detect tones in background noise.

Methods

15 volunteers (11 female, age-range 23-46 years) took part in our research. Pure tone audiometry was performed to confirm that all participants had clinically normal hearing thresholds, i.e. thresholds ≤ 20 dB HL from 125 Hz to 8 kHz. The QuickSIN test for speech in noise was administered at overall levels of 30, 50 and 70 dB HL in all participants, and additionally at 80 dB HL in 10 participants. Three lists were used per sound level. The QuickSin test gives results in terms of signal-to-noise ratio (SNR) loss. The remaining 5 subjects indicated that

80 dB HL was uncomfortably loud. Additionally, we also used the Threshold Equalising Noise (TEN) test (Moore et al., 2004), which was administered using 1, 2, and 4 kHz pure tones and noise levels of 30, 50, and 70 dB HL. TEN thresholds were measured with a 2-dB step size.

Results

Results of the QuickSin test showed a significant effect of presentation level on speech recognition performance in babble noise. SNR loss was lowest at 50 dB HL, with significantly higher values at 30, 70, and 80 dB HL, thus demonstrating a U-shaped curve of listening performance vs . In contrast, thresholds relative to the noise level in the TEN test were approximately constant at 1 kHz, and showed significant increases with noise level at 2 and 4 kHz. Correlation analyses showed weak but significant correlations between SNR loss and TEN thresholds at 1 kHz, but not for 2 and 4 kHz.

Conclusions

Even in normal-hearing people, there is a significant effect of overall sound level on listening performance in background noise, indicating that attenuation might improve the intelligibility of speech in challenging listening conditions. For hearing-impaired patients, determining their optimum-SNR-sound-level might be provide an important additional parameter for hearing aid fitting.

References

Moore BC, Glasberg BR, Stone MA (2004) *Ear Hear* 25(5):478-87

PS 426

Comparison of Consonant Recognition in Background Noise by Normal Hearing Young and Older Subjects

Christopher Boven¹; Robert Shepard²; Jont Allen³; Fatima T. Husain⁴; Robert Wickesberg²

¹Neuroscience Program, University of Illinois at Urbana-Champaign; ²Department of Psychology, University of Illinois at Urbana-Champaign; ³Department of Electrical and Computer Engineering, University of Illinois at Urbana-Champaign; ⁴Department of Speech and Hearing Science, University of Illinois at Urbana-Champaign

The intelligibility of most consonants decreases when presented above a certain intensity, especially with a background noise. For older adults who have trouble recognizing speech in loud, noisy environments, this is a particularly annoying problem, even though they may have normal hearing thresholds. This study compared how well these older adults recognize speech in back

ground noise with the ability of younger adults who have similar normal hearing thresholds.

We recruited 16 subjects between 45 and 70 years of age and 16 subjects between 18 and 22 years old. Both groups had normal hearing thresholds based on a standard audiometric evaluation. All older subjects complained of difficulty in understanding speech in noisy environments. Both groups of subjects were presented the same set of 6 plosive and 2 nasal CV pairings, spoken by 2 males and 2 females. Speech tokens were presented at signal-to-noise ratios of 0 and -6 dB and three intensities (45, 65, and 85 dBA).

At 0 dB SNR, the average recognition scores for the older and younger adults were almost identical at 45 and 65 dBA. For both groups, the recognition scores at 65 dBA were higher than at 45 dBA. At 85 dBA, the younger adults had slightly lower recognition scores while the older adults had noticeably lower scores (a “roll-over” effect).

For the -6 dB SNR condition, both the younger and older adults had lower average recognition scores at all three intensities. At 45 dBA, the scores from the two groups were similar. With an increase in the intensity to 65 dBA, the scores for the younger adults improved while those of the older adults stayed the same. The difference between the two groups in their average scores at 65 dBA was significant. At 85 dBA, the scores for both groups again declined.

The significant reduction in the ability of older adults to recognize speech under very noisy conditions (-6 dB SNR) compared to younger adults, although they do almost equally well with less background noise (0 dB SNR), represents a hidden hearing loss for the older adults. It is consistent with their complaints about difficulty recognizing speech in noisy environments. Because the difference in recognition scores at -6 dB SNR was not significant until the intensity reached 65 dBA, this hidden hearing loss may be due to a loss of higher threshold, lower spontaneous rate auditory nerve fibers either through age or noise damage.

PS 427

Recognition of Interrupted Speech with Competing Talkers: Effects of Age, Envelope Cues, and Cognitive Abilities

William J. Bologna; Kenneth I. Vaden; Jayne B. Ahlstrom; Judy R. Dubno
Medical University of South Carolina

Background

Speech communication often occurs in environments

where background sounds fluctuate and mask portions of the intended message. The auditory system groups together audible fragments of speech, fills in missing information, and segregates the glimpsed target from the background. Older adults, even those with normal hearing, are known to experience greater difficulty than younger adults with these challenging tasks. The purpose of this study was to determine the extent to which this age-related difficulty can be explained by declines in recognition of short glimpses of speech, perceptual restoration of missing speech segments, and/or segregation of glimpses from a competing talker background. An additional goal was to examine contributions from specific cognitive abilities to individual differences in recognition of interrupted speech.

Methods

Keyword recognition was measured for 20 younger and 20 older adults with normal hearing. Sentences were interrupted and filled with silence or intervening noise, leaving different proportions of the original sentence intact, and were presented in quiet and with a competing talker. When present, intervening noise was modulated by the broadband temporal envelope of the missing speech and facilitated keyword recognition (“phonemic restoration”). A battery of cognitive measures assessed inhibitory control (Stroop), short-term memory (Reading Span), processing speed (Connections), and linguistic closure (Text Reception Threshold).

Results

An item-level logistic regression of keyword recognition based on a generalized linear mixed model showed significant effects of speech proportion (0.40-0.70), background (quiet or competing talker), interruption (silence or noise), and group (younger or older). Older adults were poorer than younger adults at recognizing keywords based on short glimpses, but benefited more when envelope-modulated noise filled silent intervals. Recognition declined with a competing talker, but this effect did not interact with age. Faster processing speed and better linguistic closure were predictive of better recognition among older but not younger adults.

Conclusions

Older adults may be poorer than younger adults at grouping short glimpses of speech into a coherent message, and they may rely more on envelope cues to facilitate perception of missing speech. This pattern was similar with and without a competing talker, suggesting that age-related declines may not affect speech segregation. Among older adults with slower processing speed and poorer linguistic closure, glimpsing speech may place high demands on cognitive resources, which may limit performance.

PS 428

Attention Induces a Processing Tradeoff Between Midbrain and Cortex

Jennifer Krizman¹; Adam Tierney²; Trent Nicol¹; Nina Kraus¹

¹Northwestern University; ²University College London - Birkbeck

Attention profoundly influences how we experience our world, but the mechanisms by which this takes place in the auditory system are not fully understood. Previous studies in humans have found that attention enhances cortical, and suppresses cochlear, sound processing. Animal work suggests that active engagement with sound reduces auditory midbrain function; however, previous studies in human midbrain have yielded inconsistent findings. We hypothesize that there is a tradeoff in processing demand between the cortex and midbrain during active and passive listening. Thus, we predict that while active attention to sound enhances cortical processing, it suppresses midbrain processing. Employing a systemic approach to the investigation of attention's influence on auditory processing, we simultaneously recorded cortical and subcortical neurophysiological activity in fifty-nine adolescents and young adults during active and passive listening. We find that when actively attending to sentences, cortical phase-locking consistency over the theta, alpha, and beta bands increases relative to when passively listening to the same sentences. However, midbrain phase-locking consistency to the stimulus pitch contour declines in the active condition. The opposing effects of attention on human cortical and subcortical function align with a similar dissociation found in visual processing and suggest that the auditory cortex and midbrain play distinct roles during active and passive listening. Specifically, while the cortex may be central to active attention to sound, the midbrain's larger passive response could highlight a privileged role for the auditory midbrain in monitoring the auditory scene during passive listening, facilitating bottom-up, orienting attention. In sum, this study demonstrates distinct roles for these two processing centers and provides novel mechanistic insights into attention's impact on sensory function. This research is funded by F31 DC014221 to JK, the Mathers Foundation, and the Knowles Hearing Center, Northwestern University.

PS 429

Modeling Speech Intelligibility based on Envelopes derived from an Auditory Nerve Model

Christoph Scheidiger¹; Johannes Zaar¹; Jayaganesh Swaminathan²; Torsten Dau³

¹Hearing Systems group, Department of Electrical Engineering, Technical University of Denmark, DK-2800, Kgs. Lyngby, Denmark; ²Starkey Hearing Research Center, Berkeley, CA, USA; ³Hearing Systems group, Department of Electrical Engineering, Technical University of Denmark, 2800 Kgs. Lyngby, Denmark

Speech intelligibility models aim to predict the human ability to understand speech in adverse listening conditions. Most previous speech intelligibility models do not capture the detailed physiological transformation the acoustic signal undergoes in the auditory periphery. The goal of this study was to combine an established speech intelligibility model with the auditory signal processing of an auditory nerve (AN) model. Specifically, the back-end processing of the multi-resolution speech-based envelope power spectrum model (mr-sEPSM; Jørgensen et al., 2013) was combined with the auditory nerve model by Zilany and Bruce (2014). The presented work calculated signal-to-noise-ratios in the envelope domain (SNR_{env}) for normal-hearing listeners based on different envelope representations derived from the AN model: (i) instantaneous firing rates (ii) peristimulus time histogram (PSTH) of auditory nerve spike trains, and (iii) shuffled-correlogram based analyses of AN spike times (Heinz and Swaminathan, 2009). The SNR_{env} patterns showed good agreements compared to the SNR_{env} patterns calculated from the acoustic (i.e. Hilbert) envelope (Heinz, 2016). Furthermore, speech intelligibility for normal-hearing listeners based on envelopes derived from PSTHs for CLUE sentences (CLUE; Nielsen and Dau, 2009) was predicted accurately in speech shaped noise (SSN), sinusoidally amplitude modulated noise (SAM) and speech-like noise (ISTS; Holube et al., 2010). Effects of hearing loss resulted in poorer speech intelligibility predictions. The work provides a foundation for quantitatively modeling individual effects of inner and outer hair cell loss on speech intelligibility.

PS 430

The Effect of Acoustic Cue Weighting Strategy on Listening Effort in Acoustic Simulations of Cochlear Implants: A Pupillometry Study

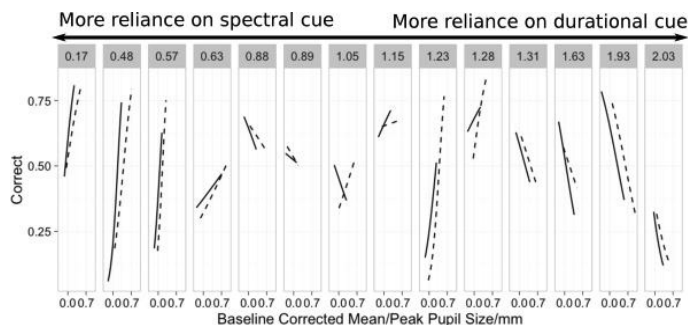
Yue Zhang¹; Stuart Rosen²

¹University College London; ²UCL, London, UK

This study examined the relation between cognitive effort and intelligibility of cochlear implant acoustic sim-

ulations at different levels of perceptual difficulty, and whether listeners' acoustic cue-weighting strategies affected the behavioural gain from any increase in cognitive effort. Normal hearing listeners were first tested with 8-band 4-mm frequency-shifted noise-vocoded sentences in quiet in order to determine their maximum performance level. Following that, adaptive procedures were used to determine two Speech Reception Thresholds (SRTs) for sentences in speech-shaped noise (also frequency-shifted and noise-vocoded). These were the speech-to-noise ratios (SNRs) required for each listener to obtain 40% and 80% of their performance in quiet. They were then tested with sentences fixed at these two SNR levels and both their percentage correct and cognitive load (measured by pupil mean dilation, peak dilation and peak latency) were recorded. Listeners' weighting strategies on duration and spectral cues were measured with a tense and lax vowel categorisation task in quiet, with stimuli processed in the same way.

When perceptual difficulty was high (SRT for 40% correct), higher listening effort was associated with better behavioural performance, but this effect was smaller compared to the perceptually easy condition (SRT for 80% correct). In addition, there was a significant interaction between individual acoustic cue-weighting strategy and pupil response on behavioural performance, suggesting that the acoustic cue-weighting pattern explained a significant amount of variance in the relation between listening effort and sentence recognition. Further trend analysis showed a significant linear trend for cue-weighting pattern in its interaction with pupil response: for individuals with more weighting on the duration cue, higher listening effort was associated with a lower level of performance; while for individuals weighting more on the spectral cue, higher listening effort was associated with a higher level of performance. This experiment indicated a dynamic relationship between changes in cognitive load and behavioural performance, with the behavioural gain from cognitive effort depending upon individual differences in cue-weighting strategy and levels of perceptual load.



Thalamus and Primary Auditory Cortex

PS 431

Parallel Ascending Pathways to the Avian Auditory Thalamus (*Gallus gallus*)

Yuan Wang¹; Diego Zorio¹; Harvey Karten²

¹Florida State University; ²University of California, San Diego

Birds serve as a suitable model for investigating brain mechanisms underlying auditory information processing. In avian and mammalian brains, acoustic features are encoded in separate ascending pathways at the brainstem and midbrain levels. In chickens (*Gallus gallus*), three pathways arise from the nucleus laminaris (NL), nucleus angularis (NA), and region intermedius (RI) in the brainstem, and innervate three distinct subdivisions of the nucleus mesencephalicus lateralis pars dorsalis (MLd) in the midbrain. These pathways are thought to encode time, intensity and very low frequency information of sounds.

The current study provides several lines of anatomic evidence supporting the segregation of these pathways in their subsequent projections to the nucleus ovoidalis (Ov) in the thalamus. Based on cytoarchitecture and myelin distribution, we identified seven Ov subregions, including five neuronal clusters within the Ov proper, the nucleus semilunaris paravoidalis (SPO), and the circum-ovoidalis (cOv) which surrounds the Ov proper and SPO. Immunocytochemistry further revealed that a ventromedial cluster of the Ov proper (Ov_{vm}) contains unique cell types that are immunoreactive to $\alpha 8$ subunit nicotinic acetylcholine receptor, while SPO and cOv are characterized with expression of calcitonin-gene-related peptide and cholecystokinin. SPO and cOv also differ from the Ov proper in a notably lower level of acetylcholinesterase activity. Cholera toxin B (CTB) injection into various MLd subdivisions demonstrated differential innervation of Ov subregions from the midbrain. Ov_{vm} is the major target of the NL-recipient zone of MLd, while the RI-recipient zone of MLd predominantly projects to a ventrolateral cluster of the Ov proper (Ov_{vl}). Afferent inputs to the remaining regions of the Ov proper mostly arise from the NA-recipient zone of MLd. SPO and cOv receive an input from the surrounding areas of MLd named the nucleus intercollicularis (ICo). The projections from MLd upon the Ov proper are bilateral, while the innervation from ICo upon SPO and cOv is either primarily ipsilateral or bilateral depending on specific cell groups in ICo. CTB injection into the forebrain revealed that all Ov subregions project upon the Field L, the avian analogues of the mammalian primary auditory cortex.

Taken together, these results demonstrate that the avian auditory thalamus is a highly heterogeneous structure in recipient of multiple ascending auditory pathways in a precisely organized manner. These observations are consistent with the notion that the auditory thalamus generates novel representations for specific acoustic features that are important for eventual auditory perception at the cortical level.

PS 432

Distributions of Cells from the Inferior Colliculus Projecting to the Ventral Division of the Medial Geniculate Body in the Gerbil

Gilberto D. Graña¹; Kendall A. Hutson¹; Brendan Lutz¹; Douglas C. Fitzpatrick²

¹University of North Carolina at Chapel Hill; ²University of North Carolina Department of Otolaryngology-Head and Neck Surgery

One of the least characterized parts of the auditory system is the ascending connection between the inferior colliculus (IC) and the ventral division of the medial geniculate (MGv). The longstanding view has been that the central nucleus of the IC is composed of a single tonotopic organization that projects to the MGv to produce a similar tonotopic organization. We previously used electrophysiological experiments combined with cytochrome oxidase (CO) histochemistry to characterize the functional organization of the central nucleus of IC in the gerbil in terms of its frequency responses and the processing of interaural time differences (ITD). The results showed the central nucleus to have a lateral region (C1) with dense CO activity and many ITD-sensitive neurons, and a medial region (C2) with less dense CO activity and few ITD-sensitive neurons. A common tonotopic axis spanned both regions. Here we used these results as a stepping-point to investigate the IC-MG pathway using anatomical techniques.

Biotinylated dextran amine injections were placed into different locations within the MG. The location and distribution of retrograde labeled cells in the IC were examined in 40 μm thick sections. As in the previous IC study, a magnetic resonance image (MRI) of a gerbil brain served as a digital framework to localize and aggregate the locations and sizes of the injection sites across cases, and to compare the locations of the labeled cell bodies with the previously obtained physiological recordings.

An injection was considered to predominantly label a subregion if at least 35% of all labeled IC cells were found in that region. Injections predominantly labeling C1 cells were clustered at the lateral edge of the dor-

soventral extent of the MGv, while injections predominantly labeling C2 cells were located medially in the MGv. Importantly, regardless of its size, each injection also labeled some cells in the less densely labeled part of the central nucleus, as well as other areas of the inferior colliculus including the lateral nucleus, the dorsal cortex, and the external cortex. These results suggest a generally topographic but also highly convergent pattern of projections from the central nucleus to each part of the MGv.

PS 433

Neuronal Nicotinic Receptor Dynamics within the Medial Geniculate Body Circuitry: Impact of Aging

Sarah Y. Sottile¹; Donald M. Caspary²

¹Department of Pharmacology, Southern Illinois University School of Medicine; ²Department of Pharmacology and Surgery, Southern Illinois University School of Medicine, Springfield, IL

Background

The medial geniculate body (MGB) is the auditory thalamic nucleus situated between the inferior colliculus (IC) and auditory cortex (AC). Originally thought of as a relay station for ascending auditory signals, we now know it is capable of significantly influencing incoming auditory information. As aging occurs, ascending auditory signals are degraded and acoustic information is less accurately coded. In order to compensate, additional cortical resources play a role in knowledge-based input optimization. Top-down processing is mediated in part, by cholinergic systems which direct attention to relevant incoming sensory information. This study describes the location of nicotinic cholinergic receptors (nAChR) in the MGB circuitry, their subunit composition, physiology, and how these properties are impacted with aging.

Methods

Studies used current and voltage clamp recordings in thalamocortical slices containing MGB from young adult (4-6mos) and aged (28-32mos) FBN rats. For excitatory/inhibitory inputs, relevant receptors were pharmacologically blocked. For ascending/descending inputs, a bipolar stimulating electrode was placed on the incoming fibers and a paired-pulse protocol was carried out. For inhibitory responses from TRN or IC, patched neurons were held at +20mV to better reveal inhibitory currents. For excitatory responses from AC or IC, neurons were held at -70mV. Acetylcholine was bath-applied to determine its effect on the responses from the above inputs.

Results

Bath application of ACh was found to increase the amplitude of the first response and decrease the paired-

pulse ratio at both the descending excitatory terminals from AC and the ascending inhibitory terminals from IC. When this protocol was repeated in the presence of DH β E, the cholinergic effect on the paired-pulse ratio was eliminated, suggesting that ACh was acting at α 4 β 2 nAChRs. When these receptors are activated by acetylcholine, they were capable of potentiating GABA release from terminals ascending from IC and glutamate release from terminals descending from AC. There was a significant age-related reduction of both the descending excitatory and ascending inhibitory response.

Conclusions

We have shown that α 4 β 2 nAChRs can regulate both excitatory and inhibitory inputs onto MGB neurons. By controlling synaptic strength, cholinergic inputs allow thalamic neurons to adapt to an ever-changing sensory environment by sharpening ascending temporal signals while amplifying signal strength to AC. In addition, nAChR efficacy is altered by aging, likely due to a change in receptor stoichiometry. These studies provide novel information regarding the location and physiology of nAChR's in the MGB as well as the impact of aging on this attentional circuit.

PS 434

Age-related Changes in Neural Gap-detection Thresholds in the Auditory Thalamus

Lucy A. Anderson¹; Shmma Quraishe²; Tracey A. Newman²

¹*UCL Ear Institute, University College London, UK;*

²*Clinical Neurosciences, Faculty of Medicine, Life Sciences Building 85, University of Southampton, UK.*

A common method of assessing the temporal acuity of the human auditory system is the gap-detection paradigm. Difficulty hearing brief gaps within on-going background noise is a common consequence of ageing, however, impaired performance in a gap-detection task can occur even when peripheral hearing sensitivity is completely normal. This impaired performance may reflect changes in neuronal inhibition within the auditory pathway, indeed gap-detection deficits are widely believed to reflect a general reduction in auditory temporal acuity. Similarly, recent evidence has suggested that reduced central auditory activity following sound offsets can result in a decreased neural sensitivity to brief gaps in background noise, while sensitivity to other rapidly changing sounds remains unchanged. Here, we will establish whether aged, normally hearing, male CBA/Ca mice show a neural gap-detection deficit at the level of the auditory thalamus, and whether such deficits can be accounted for by dissociable sound-onset sensitive and sound-offset sensitive channels. Additionally, we

will determine if the physiological changes are associated with an altered expression of GABAergic inhibitory interneurons, or their associated perineuronal net. Extracellular recordings were made from the three subdivisions of the auditory thalamus. Subjects were either young adult (3m), or aged but normally hearing (18m), anaesthetised CBA/Ca mice. Auditory brainstem responses (ABRs) were recorded from all animals to establish peripheral hearing sensitivity, and no differences in ABR threshold to click or tone stimuli were recorded between the two groups. Sections through the auditory thalamus were stained for cytochrome oxidase and using immunohistochemistry to determine subdivision boundaries and the distribution of GABAergic cells and perineuronal net.

Physiological changes in neural processing were observed at the level of the auditory thalamus in aged mice compared to young adults. In particular, neurons recorded from the ventral and medial subdivisions of the auditory thalamus in aged animals had significantly attenuated responses to brief gaps in noise, shorter response latencies and increased probability of firing compared to neurons recorded from young adults. Other aspects of thalamic processing, such as response thresholds, bandwidth and firing rate were normal, as were responses to other rapidly varying stimuli such as click trains.

These results suggest that age-related neural changes in auditory temporal processing arise in both lemniscal and polysensory pathways prior to more commonly observed threshold shifts. The results of this study will be used to understand neural changes that occur during ageing and to inform future diagnosis of central auditory hearing impairment.

PS 435

Types and Distribution of Multisensory Interactions in Auditory Thalamus

Michael Lohse¹; Victoria M. Bajo²; Andrew J. King¹

¹*University of Oxford;* ²*Oxford University*

Considerable attention has focused on the involvement of auditory cortex in multisensory processing. Although visual and somatosensory influences can arise via corticocortical pathways, it is likely that some aspects of multisensory cortical processing are inherited from the thalamus. However, we currently know much less about the origins and effects of visual and somatosensory inputs on the activity of neurons in the auditory thalamus.

We investigated the nature and distribution of multisensory interactions (somatosensory-auditory) across different divisions of the medial geniculate body (MGB)

of anaesthetised mice. We recorded extracellularly, using 32 or 64 channel Neuronexus silicon probes, in the MGB, while presenting 50 ms tones (2-64 kHz, 40-80 dB SPL) or 50 ms broadband noise (BBN) stimuli (60 and 80 dB SPL) with, or without, simultaneous deflection of the whiskers (50 ms single cosine wave deflection of all principal whiskers).

We found that stimulation of the whiskers can drive cells within the medial division of the MGB (MGBm), but not the ventral division (MGBv). We also found that whisker deflections increased firing rate responses to BBN, as well as inducing a positive scaling of the neurons' frequency response areas. We did not find that responses to tones or BBN were modulated by whisker deflections in the MGBv.

These results begin the mapping of multisensory properties across the MGB and provide a better understanding of the stimulus-related information the auditory cortex is likely to receive from thalamus.

PS 436

Input-specific Gain Modulation by Local Sensory Context Shapes Cortical and Thalamic Responses to Complex Sounds

Jennifer F. Linden¹; Ross S. Williamson²; Misha B. Ahrens³; Arne F. Meyer⁴; Maneesh Sahani⁴

¹*Ear Institute, University College London*; ²*Eaton Peabody Laboratories, Massachusetts Eye and Ear Infirmary*; ³*Janelia Research Campus*; ⁴*Gatsby Computational Neuroscience Unit, University College London*

The linearly-weighted receptive field has been used to describe central auditory responses to complex stimuli for decades, and one or more linearly-weighted fields also lie at the heart of more recent linear-nonlinear (LN) approaches to analysis of neuronal responses to complex sounds. However, the crucial assumption of linear weighting---that the sensitivity of the neuron to a local element of the stimulus is independent of the rest of the stimulus---is challenged by many reports of nonlinear combination sensitivity in the central auditory system. Such nonlinearities include forward suppression of the response to the second tone in a pair and more complex combination effects for spectrally offset tone pairs. How do these and perhaps other contextual nonlinearities combine over frequency and time to shape neuronal responses to complex sounds at different stages of auditory processing?

To address this question, we studied the impact of local acoustic context on mouse auditory cortical and thalamic responses using a nonlinear-linear (NL) model

(Williamson, Ahrens, Linden and Sahani 2016 *Neuron*), extending a multilinear framework developed previously (Ahrens, Linden and Sahani 2008 *J Neurosci*). We recorded neuronal responses to spectrotemporally rich dynamic random chord stimuli in two subdivisions of the auditory thalamus and two auditory cortical fields in anaesthetised mice. We also obtained additional data from auditory cortex of awake mice.

We show that in both auditory cortical and thalamic neurons, the weight of each element in the receptive field depends on the pattern of sound falling within a local neighbourhood surrounding it in time and frequency. This impact of local acoustic context manifests as a "contextual gain field" (CGF) for each neuron, which can be estimated from its responses to complex sounds. The CGF captures context-dependent changes in input gain within the receptive field, and improves predictions of both cortical and thalamic responses to stationary complex sounds. We find that CGFs vary between individual neurons, between thalamus and cortex, and between cortical areas AI and AAF, but there are strong shared qualitative characteristics. In a spectrotemporally rich soundscape, sound elements modulate neuronal responsiveness more effectively when they coincide with sounds at distant frequencies, and less effectively when they are preceded by sounds at similar frequencies. This input-specific gain modulation is evident in awake as well as anaesthetised animals.

We conclude that local-context-driven lability in receptive fields may be a widespread motif in sensory processing.

PS 437

Kotaro Ishizu¹; Masafumi Oizumi²; Tomoyo I. Shiramatsu³; Ryohei Kanzaki³; Naotsugu Tsuchiya⁴; Hirokazu Takahashi³; Kotato Ishizu⁵

¹*Department of Mechano-Informatics Graduate School of Information Science and Technology, The University of Tokyo*; ²*Laboratory for Mathematical Neuroscience, RIKEN Brain Science Institute*; ³*Research Center for Advanced Science and Technology, The University of Tokyo*; ⁴*Monash Institute of Cognitive and Clinical Neuroscience, School of Psychological Sciences, Monash University*; ⁵*The University of Tokyo*

The interaction between thalamus and sensory cortex plays critical roles in perception. This interaction is made by bottom-up and top-down pathways, which are defined as projections from thalamus to cortex, and from cortex to thalamus, respectively. In the present study, we attempted to information-theoretically characterize infor-

mation flow along these pathways from neural data in the rat thalamo-cortical system.

Five Wistar male rats were used in this study (11–13 weeks, 270–330 g) and were anesthetized with isoflurane during the experiments. A custom-designed micro-electrode array measured multi-unit activities (MUAs) and local field potentials (LFPs) simultaneously from the medial geniculate body (MGB: thalamus) and the primary auditory cortex (A1). The array was composed of three shanks with 6 mm in length, each of which has 15 recording sites for MGB at the distal edge and 17 recording sites for A1 at the proximal side. The test stimuli were tone bursts with frequencies from 1.6 to 6.4 kHz and intensities from 20 to 80 dB SPL. Each test tone was repeated 20 times in a pseudorandom order with an inter-tone interval of 600 ms. At each recording site, the characteristic frequency (CF), the most responsive frequency at the threshold of the sound intensity, was identified from MUA. The recording sites where CF was not identified were excluded from the further analyses. From LFP in response to click, the current source density analysis identified the cortical layer at a given recording site in the cortex. Transfer entropy (TE) between MGB and A1 (layers II/III, IV, V, VI) was estimated from MUA in all possible pairs of recording sites to define the optimal delay of TE in each pair. The time-course TE was then derived with a moving time window of 15 ms at the optimal delay.

Our analyses confirmed some significant information transfers in the thalamo-cortical system. First, the peaks of the bottom-up and top-down information streams were observed at 10 ms and 15 ms after the onsets of sound stimuli, respectively, the bottom-up stream being faster than the top-down. Additionally, the top-down stream showed the second peak at 35 ms. Second, the bottom-up flow was observed predominantly at layer IV and VI, and in addition to these layers, the top-down flow was observed at layer V. These results are consistent with existing anatomical facts, suggesting that our method is effective to investigate the thalamo-cortical interaction in sensory perception.

PS 438

Adenosine 1a Receptor (Adora1) Expression by Neuronal and Glial Phenotypes in the Auditory Forebrain

Troy Hackett

Vanderbilt University

In the brain, purines such as ATP and adenosine can function as neurotransmitters and co-transmitters, or serve as signals in neuro-glial interactions. Upon depolarization, adenosine is released from synaptic terminals

by vesicle-mediated exocytosis, binding to G-protein coupled purinergic receptors at pre-, post-, and non-synaptic sites. Recent studies of thalamocortical (TC) projections in sensory cortex revealed that adenosine functions as a negative regulator of glutamate release via activation of the presynaptic adenosine 1 receptor (Adora1). In the auditory forebrain, restriction of adenosine signaling in medial geniculate (MG) neurons is sufficient to extend LTP, LTD and tonotopic map plasticity in adult mice for months beyond the critical period (Blundon et al 2011, 2013; Chun et al 2013, 2016). In contrast, restricted adenosine signaling in neurons of the primary auditory cortex (A1) does not contribute to these forms of plasticity, suggesting that the effect is confined to presynaptic TC projections. Thus, presynaptic adenosine signaling in TC terminals reaching A1 appears to act as a gate that regulates glutamate release and plasticity at those synapses.

To advance understanding of the circuitry involved, in situ hybridization was used to localize neuronal and glial cell types in the auditory forebrain that express Adora1 using co-expression with cell-specific markers. Neuronal markers: vesicular glutamate transporters (VGluT1, VGluT2), GABA/glycine transporter (VGAT); Glial markers: astrocytes (Aqp4), oligodendrocytes (MBP), microglia (Itgam).

In A1, Adora1 transcripts were concentrated in L3/4 and L6, with lowest expression in L1 and white matter (WM). Transcripts were detected in nearly all VGluT1+ neurons, but infrequently in VGAT+ neurons. Expression by astrocytes and oligodendrocytes was most common in L3/4 or L6, and rare in microglia.

In MG, Adora1 was expressed by VGluT2+ neurons in all divisions, many of which co-expressed VGluT1. VGAT+ neurons were absent from MG, but coexpression with Adora1 was common in adjacent nuclei. Among glia, preliminary data suggest that the majority of astrocytes and oligodendrocytes express Adora1, compared to a minority of microglia (analysis ongoing).

The findings imply that the modulatory potential of adenosine on TC activity is not restricted to A1, but applies to all thalamorecipient areas of auditory cortex. Adenosine modulation may also impact glutamate release in the downstream projections of auditory cortical neurons. Widespread Adora1 expression by neuronal and glial subpopulations suggests that experimental manipulations could impact several cell types, depending on location. Strategies to target Adora1 in specific cell types can be developed from the data generated here.

Information Processing by Synchronized Neuronal Ensembles in the Primary Auditory Cortex

Christoph Schreiner; Jermyn See; Craig Atencio; Vikaas Sohal
UCSF

The primary auditory cortex (A1) contains interconnected populations of neurons that are responsible for auditory information processing. Most studies of information processing in A1 involve either single unit spectrotemporal receptive field (STRF) estimation or paired neuronal correlation analyses, and thus assume that A1 neurons filter auditory information either as individual entities or as pairs. However, mounting evidence suggests that sensory stimuli are processed by interconnected, co-activated populations of neurons. Therefore, determining how A1 encodes information will require an integrated approach that combines receptive field and multi-neuronal ensemble analyses.

To assess multi-neuronal information processing in A1, we performed multi-electrode extracellular recordings in rat A1 while presenting dynamic, broadband stimuli, which allowed us to construct STRFs. We then used dimensionality reduction techniques to identify distinct groups of A1 neurons (neuronal ensembles, or NEs) that reliably fired synchronously in A1. For each NE, we identified synchronous spiking events, and then used the events to assess spectrotemporal information processing. For neurons that were members of an NE, the spikes associated with the NE conveyed greater information than the spikes that were not associated with the NE. We also identified single neurons that participated in multiple NEs and found that the spikes associated with each NE represented receptive field properties that were significantly different from receptive field properties associated with other NEs, even though the spikes originated from the same neuron.

These findings challenge the classical idea that A1 neurons produce a homogeneous set of spikes that may be equally weighted to estimate a single STRF. Instead, A1 neurons can have multiple receptive fields based on contributions from different NEs, with each NE representing the convergence of thalamocortical, intracortical and top-down inputs into A1. For each A1 neuron, equally weighting all neuronal spikes to form a single STRF ignores this enhanced coding capacity. Therefore, by taking into account the stimulus preferences associated with each NE, we may gain a more complete evaluation of information processing in A1.

Hierarchical Emergence of Neuronal Mismatch Responses in the Auditory Brain

Javier Nieto-Diego¹; Guillermo V Carbajal¹; Gloria G Parras¹; Carles Escera²; Manuel S. S Malmierca¹
¹University of Salamanca; ²Universtiy of Barcelona, Institute of Neurosciences

A fundamental function of sensory systems is to automatically detect unexpected events, given their potentially relevant, high-informational content. In the auditory modality, this process of deviance detection is signaled by mismatch negativity (MMN), a long-latency (150–200 ms) deflection of the auditory event-related brain potentials elicited by sounds that do not match a regular background or otherwise predictable context. Over the past 40 years, the MMN has become a key tool in cognitive neurosciences for both basic and clinical research. Furthermore, the MMN is key electrophysiological evidence supporting the predictive coding framework of general brain function (Friston, 2010, *Nat Rev Neurosci* 11: 127–138), under which the MMN is interpreted as a prediction error signal. Stimulus-specific adaptation of single neuron responses closely resembles the MMN, and was proposed as its neuronal correlate. However, currently it is unclear whether SSA reflects a mere passive adaptation to repetitive stimulation, or rather, an active, memory-driven process of genuine mismatch detection. To tackle this question, we used recently developed controls for repetition effects (Ruhnau et al., 2012, *Cin Neurophysiol* 123:507–512), in addition to an oddball paradigm, and we recorded single units (N=207) in the inferior colliculus, auditory thalamus and auditory cortex of anesthetized rats, to test the neuronal sensitivity to deviant events along the auditory pathway. We used these controls to separate SSA into adaptation and deviance detection components, revealing a hierarchical emergence of deviance detection from lower- to higher-order processing stations along the auditory brain. Moreover, we found that the relative contribution of deviance detection actually supersedes that of adaptation in the higher-order auditory cortex. Finally, deviance detection in spiking responses of individual neurons correlates in time with a simultaneously recorded MMN-analog signal at the LFP level. Thus, we provide significant evidence that stimulus-specific adaptation is a genuine mismatch response, and a neuronal correlate of the MMN. Moreover, its hierarchical organization is consistent with the predictive coding account of the MMN. This result links single-neuron physiology to auditory cognitive neuroscience, and opens an invaluable opportunity for translational research.

Supported by: Spanish MINECO (Grant BFU2013-

43608-P to MSM and Grant PSI2013-49348-EXPLO-RA to CE and MSM), Spanish JCYL (Grant JCYL-SA343-U14 to MSM), the European Social Fund/ Spanish JCYL (Ph.D. Fellowship to JND under the Operational Programme ESF Castilla y León 2007-2013), and Spanish MINECO (Ph.D. Fellowship BES-2014-069113 to GGP).

Vestibular: VEMPs, SHIMPs, and Other Novel Approaches

PS 441

Comparative Characterization of Vertigo Associated Symptoms in a Preclinical Model Using Videonystagmography and Wireless Inertial Measurement of Head Kinematics

Cindy Gueguen¹; Jonas Dyhrfeld-Johnsen¹; Matthieu Pasquet²; Pierre Liaud¹; Guillaume Dugué³; Mathieu Petremann¹; Stéphanie Bressieux¹; Désiré Challuau¹; Christophe Tran Van Ba¹

¹Sensorion; ²Technical Consultant; ³Ecole Normale Supérieure, CNRS UMR 8197, IBENS S4.9

The successful selection of preclinical drug candidates for clinical development is strongly dependent on validated, quantitative translational endpoints. In the treatment of vestibular pathologies, the primary clinical endpoint of vertigo is subjective and not accessible in animal models, emphasizing the need for surrogate markers. One well-established vertigo associated symptom is spontaneous nystagmus, which can be evaluated quantitatively in both animal models and clinical populations, whereas eg. posturographic preclinical evaluations typically rely on scoring scales (Dyhrfeld-Johnsen et al., 2013; Beck et al., 2014). We report initial results comparing vertigo associated symptoms in a rat model of acute unilateral vestibular loss determined using infrared videonystagmography and wireless inertial measurement of head kinematics to determine posturographic deviations in head pitch and roll angles.

A head-post was surgically implanted on 9 adult female Long-Evans rats (200-225 g) under ketamine-xylazine anesthesia for head-fixation during VNG recordings and mounting of the 9-axis digital inertial sensor with onboard battery and Bluetooth transmitter. Following a baseline posturography recording (10 min), an excitotoxic vestibular lesion was induced using transtympanic injection of 40-45 mM kainate under isoflurane anesthesia. Videonystagmography and posturography recordings were subsequently performed at 1/3/5/24/48 hours after lesion induction. All rats developed spontaneous nystagmus with t=1h

frequencies ranging from 0-2.8 Hz bimodally distributed below or above 0.5 Hz. Mean pitch and roll angle deviations relative to baseline could be determined as early as t=1h post-lesion (0.1-15.4 deg and 0.6-10.8 deg respectively), but contrary to nystagmus frequency which generally peaked at t=1h, peak mean postural deviations were seen at t=3h (roll) and t=24h (pitch) post-lesion. There was no clear correlation between the degree of lesion reflected by nystagmus frequency and head angle deviations at early time-points, but rats initially displaying high (>0.5 Hz) spontaneous nystagmus frequency had higher degree of remaining postural deviations at t=48h. Furthermore, while mean spontaneous nystagmus frequency was already reduced to 13% of peak mean frequency at t=48h, both mean pitch and roll angle deviations remained above 80% of peak values at this time-point.

The described differential recovery time-course of spontaneous nystagmus and postural deficits is consistent with the clinical situation for eg. vestibular neuritis patients (Halamagyi et al., 2010) and suggest that wireless inertial measurement of head kinematics in animal models can provide complementary and relevant information for translational R&D efforts. Further experiments (including later time-points post-lesion) and analysis are required to complete the understanding and exploitation of the posturographic data in this model.

PS 442

Head Movements During Locomotion in Vestibular Schwannoma Patients: Decreased Variability After Unilateral Vestibular Lesion

Omid Zobeiri¹; Carol Zhang¹; Susan King²; Richard Lewis³; Kathleen E. Cullen¹

¹McGill University; ²MEEI, Harvard University; ³Harvard University

The vestibular system plays a key role in a wide range of functions from basic reflexes to high-level behaviors. By detecting head motion and then generating the appropriate reflexes, the vestibular system is vital for maintaining balance and stabilizing gaze. In turn, it is well known that immediately following unilateral vestibular loss, patients experience impaired balance, postural, and gaze control. However, to date, much less is known about the effects of vestibular loss on voluntary behavior. Here, to assess how vestibular loss alters voluntary behaviour, we analyzed locomotive behavior in a group of patients with a diagnosis of vestibular schwannoma (VS) who had undergone a primary surgical resection of their tumor via suboccipital craniotomy and retrosigmoid approach with

sectioning of the vestibular nerve. Head movements were recorded before the surgery, as well as two and six weeks after surgery using a micro-electromechanical systems (MEMS) module (Carriot et al., 2014), which contains three linear accelerometers (recording linear accelerations along the fore-aft, inter-aural, and vertical axes) and three gyroscopes (recording angular velocity about pitch, roll, and yaw). Patients were asked to complete the Functional Gait Assessment, and we focused our analysis on short, 15-to-30-second long gait tasks including: normal walking, walking with eyes closed, and walking backwards on a level surface. We then compared pre- and post-operative data to determine if and how patients' movements were altered. We quantified gait asymmetry, gait cycle speed, and gait variability. We found no significant changes in movement asymmetry. However, surprisingly, we found that even though locomotor speed decreased two weeks after surgery, it actually increased six-weeks post-surgery as compared to pre-operative testing. Furthermore, although previous studies using age-matched controls have found increased variability in gait, we found that this was not the case when using the patients' pre-operative measures as their own control. Instead, movement variability was lower two weeks as well as six weeks after the surgery than before the surgery. Specifically, the standard deviation of both linear acceleration and angular velocity in all dimensions consistently decreased after surgery. While variability is often seen as the result of noise in the nervous system, it has been shown that variability could contribute to motor learning. Taken together, our results suggest that variability is an important indicator of how patients adapt to altered motion and their recovery process.

PS 443

Cooperative Nucleocytoplasmic Shuttling of Merlin and p53 by nutlin-3 Treatment in Vestibular Schwannomas

Hao Wu¹; Hongsai Chen²; Zhaoyan Wang²

¹*Department of Otolaryngology Head & Neck Surgery, The Ninth People's Hospital, School of Medicine, Shanghai Jiao Tong University, Shanghai, China;* ²*1. Department of Otolaryngology Head & Neck Surgery,*

The Ninth People's Hospital, School of Medicine, Shanghai Jiao Tong University, Shanghai, China

Background

Vestibular schwannomas (VS) are benign tumors and attributed to the deficiency of NF2 gene product merlin. Current treatment options are limited to surgery and radiation, which may pose unacceptable risks; therefore, novel medical treatments are urgently needed. In current study, we analyse the inhibitory effects of Nutlin-3 (a

p53 activator) on the proliferation activities of VS cells, thus providing foundations for the clinical application of the drug in VS treatment.

Methods

The NF2 gene mutation rates of VS were evaluated by Direct Sequencing Analysis. The correlation between NF2 mutation and expression of merlin, p53 and cyclinD1 in tumor tissues was investigated by Western Blotting. RNA interference experiments were performed to knockdown merlin expression in Human Schwann Cell (HSC) to mimic VS tumorigenesis, and the change of cell cycle distributions was determined by Cell Cycle Analysis. The implication of cell growth in response to Nutlin-3 treatment in RT4 schwannoma cell lines and primary cultured VS cells was evaluated by CCK-8 assays. The resulting alterations in expression and subcellular localization of related proteins was investigated by Western Blotting and Fluorescence.

Results

Here we showed that NF2 gene mutation is a common event in the VS development. NF2 mutations resulted in merlin deficiency, which was concomitant with p53 downregulation, leading to elevated cyclinD1 levels. Likewise, silencing of merlin gene expression in HSC resulted in down-regulated p53 and up-regulated cyclinD1, suggesting that deregulated p53 pathway was a crucial process involved in VS tumorigenesis. Interestingly, p53 was required to maintain merlin levels in HSC cells. These data above pointed out the possibility to recover merlin level in VS through p53 activation. Nutlin-3 was found to induce dose-dependent cell growth inhibition in RT4 schwannoma cell lines and primary VS cells, and at protein level, render a recovery of p53 and merlin. Furthermore, nutlin-3 rendered a shuttles of merlin-p53 signalling from cytoplasm to the nucleus.

Conclusion

Our findings establish a position feed-back loop between merlin and p53 triggered by merlin deficiency may play a very important role in the pathogenesis of vestibular schwannomas, and provide a clue that nutlin-3 might be a potential therapeutic option to VS treatment.

PS 444

The Vestibular Implant: Hearing Preservation During Intralabyrinthine Electrode Insertion

Raymond Van de Berg¹; Robert Stokroos²; Joost Van Tongeren³; Nils Guinand⁴; Jean-Philippe Guyot⁴; Herman Kingma¹; Angelica Perez Fornos⁴

¹*Division of Balance Disorders, Department of Otorhinolaryngology and Head and Neck Surgery, Faculty of Health Medicine and Life Sciences, School for Mental*

Health and Neuroscience, Maastricht University Medical Center, Maastricht, The Netherlands; ²Maastricht university medical center, Maastricht, the Netherlands;

³Department of Otorhinolaryngology and Head and Neck Surgery, Faculty of Health Medicine and Life Sciences, School for Mental Health and Neuroscience, Maastricht University Medical Center, Maastricht, Netherlands; ⁴Service of Otorhinolaryngology and Head and Neck Surgery, Department of Clinical Neurosciences, Geneva University Hospitals, Geneva, Switzerland

Introduction

The vestibular implant seems feasible as a clinically useful device in the near future. However, hearing preservation during implantation remains a challenge. Sensorineural hearing loss can occur with the intralabyrinthine approach (electrodes inserted in the semicircular canals) as well as with the extralabyrinthine approach (electrodes directly on the nerves, without opening the labyrinth). It is hypothesized that endolymph leakage is the cause of the hearing loss. This case study investigated the feasibility of hearing preservation during the acute phase after electrode insertion in the semicircular canals.

Methods

A 40-year old woman with good hearing (modified Fletcher-index of 10dB on the right side and 5dB on the left side) underwent a translabyrinthine approach for a vestibular schwannoma Koos Grade IV. Hearing was monitored using brainstem evoked response audiometry (BERA). Video recordings were made of the surgery and the BERA-signals were recorded and time-linked with the video. During surgery, the lateral and posterior semicircular canals were bluelined and opened without disrupting the membranous labyrinth. Following the principles of soft-tissue surgery, a conventional dummy electrode was carefully inserted in the lateral semicircular canal for a couple of minutes and subsequently removed. The same procedure was then applied for the posterior canal. Finally, the labyrinthectomy was completed and the schwannoma was removed without complications.

Results

Hearing remained preserved during insertion and after removal of the electrodes from the semicircular canals. No leakage of endolymph was observed during these procedures. Hearing loss occurred when the canals were completely opened during the labyrinthectomy.

Conclusion

Hearing preservation is possible in the acute phase of electrode insertion in the semicircular canals. Up to now, hearing preservation seems to be possible when no en-

dolymph leakage is observed. The reproducibility of this short-term observation and the presence of long-term effects of intralabyrinthine vestibular implantation on hearing have to be assessed further.

PS 445

Evoked Potential Recording to Optimize Stimulation with a Vestibular Prosthesis

James Phillips; Warren Piehl; Leo Ling; Christopher Phillips; Amy Nowack; Kaibao Nie; Jay Rubinstein
University of Washington

Introduction

Electrical stimulation with a vestibular prosthesis should provide limited activation of the afferents of single end-organs within the vestibular labyrinth. Most current designs place stimulating electrodes near the afferents of the semicircular canals. The extent to which the electrical stimulation activates additional afferent inputs is typically inferred by behavioral or perceptual studies, i.e., deviation of electrically elicited eye movement direction from canal planes, disconjugate eye movements, or changes in subjective visual vertical. We utilized evoked potential recording to evaluate activation of otolith or cochlear afferents.

Methods

3 human subjects implanted with a vestibular prosthesis returned to the laboratory for evaluation of electrically elicited cervical vestibular evoked myogenic potentials (ecVEMP), ocular vestibular evoked myogenic potentials (eoVEMP), and electrically elicited vestibular/auditory brainstem responses (eVsEP/eABR). Biphasic pulse electrical stimulation (100 us per phase, 8 us gap) from the most distal site on each canal electrode was performed after standard responses to air conducted tone bursts or clicks were obtained. During ecVEMP and eoVEMP stimulation, stimuli were presented at a rate of 10 pps for 200 stimuli. During eVsEP/eABR stimulation, stimuli were presented at 20 pps for 1000 stimuli.

Results

Electrical stimulation of the lateral and anterior canals in three subjects elicited robust ecVEMP responses with waveforms similar to the waveform of air conducted cVEMP. In 2 of the 3 subjects, eoVEMPS were similarly recorded. ecVEMPS showed increasing amplitude with increasing current amplitude, while the latency of the response remained unchanged. 300 Hz stimulation at current amplitudes that elicited ecVEMP or eoVEMP responses also elicited a percept of roll tilt toward the stimulated ear in two of the subjects. eVsEP/eABR responses were also recorded in 2 subjects in response to lateral canal stimulation. The responses showed the same waveform peaks and latencies as expected for co-

chlear implant elicited eABRs, except for an additional biphasic peak possibly associated with vestibular stimulation. At current amplitudes which elicited eVsEP/eABR responses, subjects reported an ambiguous sensation of sound or vibration.

Conclusion

Electrically elicited evoked potentials can be recorded from the neck, extraocular muscles and brainstem in response to electrical stimulation via electrode sites near individual semicircular canal ampullae. Such responses suggest the possibility of current spread to the otolith organs and the cochlea during vestibular prosthetic stimulation, however more work must be done to fully define the source of these uniquely elicited potentials.

Acknowledgements: NIH 1 R01 DC014002-01

PS 446

Restoration of the Vestibulo-collic Reflex with a Vestibular Implant

Raymond Van de Berg¹; Angelica Perez Fornos²; Samuel Cavuscens³; Maurizio Ranieri⁴; Herman Kingma¹; Jean-Philippe Guyot²; Nils Guinand²

¹Division of Balance Disorders, Department of Otorhinolaryngology and Head and Neck Surgery, Faculty of Health Medicine and Life Sciences, School for Mental Health and Neuroscience, Maastricht University Medical Center, Maastricht, The Netherlands; ²Service of Otorhinolaryngology and Head and Neck Surgery, Department of Clinical Neurosciences, Geneva University Hospitals, Geneva, Switzerland; ³Unige; ⁴University of Geneva

Background

The vestibulo-collic reflex (VCR) is important for postural control. It can be assessed by recording cervical vestibular evoked myogenic potentials (cVEMPs), which are thought to reflect the functionality of the saccular part of the otolith organ. In this study, we explored the potential of the vestibular implant to artificially restore the VCR using electrical stimulation of the vestibular organ.

Methods

In 3 patients with BVL, fitted with a custom modified cochlear implant (Medel, Austria), cVEMPs were recorded according to a standard protocol, except for the stimulus, which consisted of 100 trials of single cathodic first, biphasic, charge balanced pulses delivered at a rate of 5 pulses per second to the vestibular nerve using intralabyrinthine electrodes located close to the ampullas of the superior (SAN) and lateral (LAN) semicircular canals in 2 patients and using an extralabyrinthine electrode

located in the vicinity of the posterior ampullary nerve (PAN) in the third patient.

Results

cVEMPs with its classical characteristics could be elicited in all 3 tested patients (see example in Fig. 1). In general, cVEMPs amplitudes increased as stimulus intensity increased.

Conclusion

Artificial restoration of the VCR in patients with a complete BVL is possible. This indicates that functionally useful motion information could potentially be delivered via the vestibulo-spinal pathways and thus could influence posture. Interestingly, it remains unclear whether it results from activation of the canal or of the otolithic system, or a combination of both.

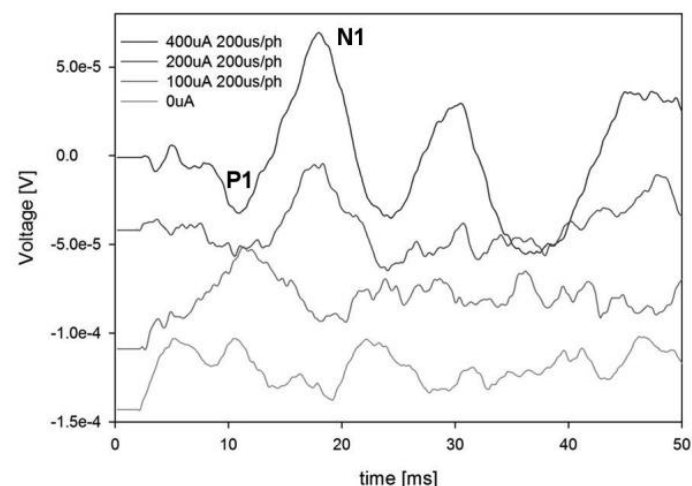


Figure 1. Example of cVEMPs signals recorded upon stimulation with the SAN electrode in one patient. Individual curves for different stimulation amplitudes are presented. The typical P1 and N1 waves can be easily identified in the signals obtained at the largest amplitude (topmost signal).

PS 447

Vertical and Torsional Alignment Nulling: A Rapid Quantification of Binocular Misalignment without Recording Eye Movements

Jennifer Millar¹; Yoav Gimmon¹; Jorge Serrador²; Michael C. Schubert¹

¹Johns Hopkins University; ²Rutgers biomedical health sciences

Background

Patients with otolith pathology may have abnormal vertical or torsional ocular alignment, known to differ when positioned supine vs upright. We have developed a handheld, portable technology that uses a perceptual measure to quantify ocular misalignment. Vertical Alignment Nulling (VAN) and Torsional Alignment Nulling (TAN) tests were assessed for stability across hours and days, in addition to being assessed for differences in up-

right versus supine position. We have started to examine for differences across healthy control, patients with vestibular hypofunction, and veterans with multisensory impairment.

Method

Subjects view one red and one blue line on a tablet computer while looking through color-matched red and blue filters. Subjects align the red and blue lines, initially vertically offset from one another during VAN or rotated relative to one another during TAN, until they perceive a single continuous line. Ocular misalignments are inferred from residual offsets in the final line position. During testing, all binocular visual cues that would otherwise confound the misalignment results are eliminated by utilizing OLED technology and testing in a completely darkened room. To date, 5 healthy control subjects and 6 patients performed VAN and TAN in both upright and supine positions. The healthy controls completed 20 trials each (upright and supine) once per hour, every 4 hours in 1 day; and separately once per day for 4 days. The patient subjects completed 1 set of VAN and TAN (20 trials each) in both upright and supine conditions.

Results

Both VAN and TAN were very stable within the same day and between different days with no significant differences ($p > 0.05$). The patients appear to have similar mean scores for VAN (0.05 ± 0.23 upright; 0.06 ± 0.24 supine) as the healthy controls (0.11 ± 0.28 upright; 0.17 ± 0.34 supine). However, the patients appear to have TAN scores that are 2-4 times worse with greater variability in both upright (patients 0.62 ± 1.98 vs healthy 0.27 ± 0.76) and supine (patients 0.45 ± 1.13 vs healthy -0.06 ± 0.92) positions.

Conclusion

Our data suggest that the VAN and TAN ocular misalignment tests are stable across days and hours. Our pilot data in patient subjects appears to suggest that TAN may be a better measure of ocular misalignment given the patients show a larger amount of error.

Funding supported by DoD Award W81XWH-15-1-442 (MCS)

PS 448

A Tool to Quantify the Impact of Oscillopsia on Functional Mobility

Eric Anson¹; Tim Kiemel²; John Jeka³; John P. Carey⁴

¹Johns Hopkins School of Medicine; ²University of Maryland; ³Temple University; ⁴Johns Hopkins University

Background

Individuals with vestibular hypofunction (VH) often report symptoms of oscillopsia during walking. Existing assessments of oscillopsia are limited to descriptions of severity and symptom frequency, neither of which provides a description of functional limitations or activity changes attributed to oscillopsia. A novel questionnaire, the Oscillopsia Functional Impact scale (OFI) was developed to describe the impact of oscillopsia on activity participation and mobility. Questions on the OFI ask how often individuals are able to participate in specific activities considered to depend on gaze stability in an effort to link functional mobility impairments to oscillopsia for individuals with vestibular loss.

Methods

Subjective reports of oscillopsia, dizziness, and balance confidence were recorded for 14 individuals with bilateral VH, 6 individuals with unilateral VH, and 29 healthy controls. Spearman correlation coefficients were calculated to determine the relationship between the OFI and other questionnaires that characterize oscillopsia, dizziness, and balance perception to demonstrate face validity. Chronbach's alpha was calculated to demonstrate internal validity. A one way MANOVA was conducted with post-hoc paired T-tests for group differences on all oscillopsia questionnaires.

Results

The OFI was highly correlated with measures of oscillopsia severity ($r = .84$) and frequency ($r = .88$) and also with the Dizziness Handicap Inventory ($r = .89$) and the Activities Specific Balance Confidence scale ($r = -.85$). Chronbach's alpha for the OFI was 0.97. Individuals with unilateral VH and bilateral VH scored worse on all measures of oscillopsia and dizziness handicap compared to healthy individuals ($p < .05$).

Conclusions

The OFI appears to capture the construct of oscillopsia in the context of functional mobility. Combining with oscillopsia metrics that quantify severity and frequency allows for a more complete characterization of the impact of oscillopsia on an individual's daily behavior. The OFI discriminated individuals with either bilateral VH or unilateral VH from healthy individuals.

Saccade Amplitude in the Suppression Head Impulse Paradigm (SHIMP) - a New Indicator of Semicircular Canal Function

Ian Curthoys¹; Catherine de Waele²; Qiwen Shen²; Christophe Magnani²; Georges Lamas³; Olivier Sterkers³

¹Univ of Sydney; ²Cognitive and Action Group; ³ENT department, Salpetriere Hospital Bd de l'Hôpital

Introduction

In the video head impulse test (HIMPs) (Macdougall et al 2009) the person is required to maintain fixation on an earth-fixed target during the brief abrupt unpredictable head turn and if their VOR is not adequate they make a corrective saccade to return fixation to the target. A new variant requires the person to maintain fixation on a head-fixed target during the head turn. This new variant is called the suppression head impulse test (SHIMP) (MacDougall et al 2016)). With SHIMPs it is healthy individuals who make a corrective saccade at the end of the head impulse because they do not suppress their VOR during the first 80ms or so of the head impulse. During that time their gaze is driven by their VOR off the head-fixed target, necessitating a corrective saccade at the end to regain the target. In contrast, for patients with total vestibular loss, their inadequate VOR does not drive their eyes off the head-fixed target so they do not make a corrective saccade. The occurrence and amplitude of the SHIMP saccade, as measured by peak velocity, should indicate the level of vestibular function.

Methods

35 normal subjects and 57 patients suffering from different vestibular pathologies associated with unilateral vestibular loss (UVL) or bilateral vestibular loss (BVL) were tested in both the HIMP and SHIMP paradigm. For each individual we measured the VOR gain and for SHIMPs the peak saccadic velocity, the percentage of the 10 trials completed with saccades and the latency of the saccades.

Results

Healthy subjects made a large SHIMP saccade at the end of the head turn. At the acute stage after a complete UVL, patients had zero or a few SHIMP saccades for head turns towards the lesioned side. There was a significant correlation between VOR gain and saccade amplitude. At the chronic stage, some of the patients recovered the ability to perform SHIMP saccades at each head turn towards the lesioned side. In BVL patients, no anti-compensatory saccades or only significantly smaller ones, could be detected for head turns to either side.

Conclusion

SHIMP is a specific and sensitive test to detect a complete horizontal canal loss at the acute stage. The SHIMP test is intuitive and much easier for subjects to understand since it is like watching a tennis game.

MacDougall HG et al. Neurology 2009, 73:1-9

PS 450

Toward Optimizing VEMP: Calculating VEMP Inhibition Depth (VEMPid) with a Generic Template

Kimberley S. Noij¹; Barbara S. Herrmann¹; Mark van Tilburg¹; Steven D. Rauch²; John J. Guinan³

¹Massachusetts Eye and Ear Infirmary, Harvard Medical School; ²Harvard Medical School, Mass Eye and Ear; ³Mass. Eye and Ear Infirmary; Harvard Medical School

Background

Cervical vestibular evoked myogenic potentials (cVEMP) indirectly reveal the response of the saccule to acoustic or vibrational stimuli through the inhibition of sternocleidomastoid muscle electromyographic (EMG) response. VEMP inhibition depth (VEMPid) is a metric that provides both normalization and better sensitivity at low response levels than amplitude-normalized cVEMPs (nVEMP). We advocate using VEMPid because past work indicates that VEMPid is more sensitive than cVEMP peak-to-peak amplitudes (VEMPPp) or nVEMP for assessing VEMP threshold and that threshold is better than VEMP amplitudes for clinical assessments. To calculate VEMPid, a template is needed; this method resembles a matched filter for the detection of a signal (cVEMP) in noise. The original VEMPid method used the subject's own cVEMP as a template but this can be problematic in patients who do not have robust cVEMP responses. We hypothesize that a "generic" template created by assembling cVEMPs from healthy subjects can be used to compute VEMPid, and would allow computing VEMPid in subjects with pathological conditions.

Methods

Twenty healthy subjects underwent cVEMP testing using 500, 750 and 1000Hz tone bursts, at levels 93-123dB peSPL, and with stimulus-off EMG measurements. From a second group of twenty healthy subjects multiple 123 dB peSPL recordings were collected at all frequencies and 93-123dB peSPL recordings were collected only at 500Hz. A generic template was made by averaging VEMP responses from six normal subjects. To compensate for the generic template's lack of latency information, VEMPid's were calculated for latencies -5 to +5 ms around the normal cVEMP latency, and the largest value was used for the VEMPid. The latency that yielded the

largest VEMPid at the highest sound level was used for calculating VEMPids at lower sound levels. VEMPid's were calculated both with the generic template and with the subjects own template. The ability of these metrics to determine whether a cVEMP was present or not was compared using Cohen's-D effect size.

Results

VEMPid using a generic template was larger than VEMPid using a subject-specific template at all levels above 93dB peSPL (60dB HL). Based on Cohen's-D effect size, the generic template was better than the subject-specific template at determining whether a VEMP is present or not. Within limits, the shape of the generic template did not affect these outcomes.

Conclusion

A generic template can be used instead of a subject-specific template to calculate VEMPid. This brings us a step closer to the use of VEMPid in patients.

PS 451

Toward Optimizing VEMP: Strong Muscle Contractions are Unnecessary

Kimberley S. Noij¹; Barbara S. Herrmann¹; Steven D. Rauch²; John J. Guinan³

¹Massachusetts Eye and Ear Infirmary, Harvard Medical School; ²Harvard Medical School, Mass Eye and Ear; ³Mass. Eye and Ear Infirmary; Harvard Medical School

Background

The cervical vestibular evoked myogenic potential (cVEMP) is an inhibitory reflex of the saccule measured in the ipsilateral sternocleidomastoid muscle (SCM) in response to acoustic or vibrational stimulation. Since cVEMP is a modulation of SCM electromyographic (EMG) activity, cVEMP response amplitude is proportional to muscle EMG amplitude. Thus stronger voluntary SCM contractions produce bigger cVEMP peak-to-peak amplitudes (VEMPPp). Calculations of normalized cVEMP amplitudes (nVEMP) or cVEMP inhibition depth (VEMPid) reduce the impact of variations in muscle contraction. Nonetheless, it is common practice to ask subjects to produce strong SCM contractions. It is unclear however, the extent to which contraction level influences the cVEMP metrics or their ability to distinguish cVEMP presence/absence. To determine the effect of contraction strength, cVEMP responses were gathered from healthy subjects across a range of muscle contractions.

Methods

Six healthy subjects underwent cVEMP testing at 500Hz while voluntarily contracting their SCM at three pre-

defined EMG levels: root mean square (rms) values of 45-65uV, 66-105uV, and >105uV. For each contraction level, we obtained cVEMP sound-level functions (93-123dB peSPL) and EMG responses with the sound off ("no-stimulus condition"). Responses for recordings contained at least 200 sweeps to acquire reliable cVEMPs. Data were obtained from both ears and were pooled across subjects.

Results

VEMPPp showed a significant interaction between muscle tension and stimulus level (ANOVA: $F=9.890$, $p < 0.001$), consistent with VEMPPp amplitudes being significantly greater at higher muscle tensions for all above-threshold sound levels. In contrast, nVEMP and VEMPid showed no significant effect of muscle tension (ANOVA: $F=0.023$, $p=0.977$ and $F=0.214$, $p=0.808$, respectively). The η^2 effect sizes (which measure how much muscle tension changed the cVEMP metrics), applied across levels were: large for VEMPPp (0.35-0.60), small to medium for nVEMP (< 0.01 -0.07) and small for VEMPid (< 0.01 -0.04). An alternate effect measure Cohen's D, which measures how well sound-evoked cVEMPs can be distinguished from no-stimulus EMG measurements, indicates that contraction strength produces little change in the ability to distinguish cVEMP presence/absence for the three cVEMP metrics.

Conclusion

Although muscle contraction level strongly affects VEMPPp amplitude, it has little effect on nVEMP or VEMPid. We found that cVEMP detection is reliable even with relatively weak SCM contractions (rms 45-65 uV). Clinically, this means there is no need for subjects to exert maximal or high muscle contraction effort, which is especially beneficial in patients for whom reaching high levels of SCM contractions can be challenging.

PS 452

Effects of High Sound Exposure during Air-Conducted Vestibular Evoked Myogenic Potential Testing in Young Adults and Children

Amanda I. Rodriguez; Megan Thomas; Denis Fitzpatrick; Kristen Janky

Boys Town National Research Hospital

Background

Cervical and ocular vestibular evoked myogenic potentials (c- and oVEMP, respectively) assess otolith organ function. However, there is concern for the high intensity stimuli required to elicit VEMPs (Young, 2006); Temporary changes in cochlear function in adults have been documented; Following cVEMP, an immediate reduction in distortion product otoacoustic emissions (DPOAEs) and aural fullness was observed (Stromberg et al., 2015;

Krause et al., 2013). Despite utility of VEMP in children, increased sound exposure may exist; Differences in ear canal volume (ECV) and stimulus parameters (e.g., stimulus duration and intensity) alter exposure levels delivered to a child's ear.

While evidence demonstrates hearing changes in adults following VEMP testing, similar findings in children are unknown. Therefore, the purpose of the present study was to: 1) measure sound pressure levels (SPL) in children and young adult ears using short duration VEMP stimuli, 2) calculate a safe exposure level for VEMP, and 3) assess whether cochlear changes exist following VEMP testing.

Methods

Phase I: 15 children with normal hearing (NH) and 10 young adults with NH participated. Equivalent ECV was measured. In one ear, SPL was recorded for 5 seconds at 105-125 dB SPL, in 5 dB increments for 500 and 750 Hz tone-bursts. Recorded SPL values (accounting for stimulus duration) were then used to calculate safe sound energy exposure values for VEMP testing in adults and children (Colebatch & Rosengren, 2014). Phase II: 15 children with NH and 10 young adults with NH are planned to participate. All subjects will complete tympanometry, audiometric threshold testing, DPOAEs, and a questionnaire addressing subjective otologic symptoms prior to VEMP testing. In one ear c- and oVEMP will be completed. Following VEMP testing, all subjects will complete DPOAEs, audiometric threshold testing, and otologic symptom questionnaire.

Results

Phase I: Adults had significantly greater ECV values compared to children. As ECV decreased, SPL increased. Recorded SPL values were then used to calculate safe sound exposure levels for VEMP testing. 125 dB SPL was deemed safe for young adults and 120 dB SPL was appropriate for children (Colebatch & Rosengren, 2014). Based on these results, data collection for phase II is underway.

Conclusions

Preliminary results suggest that children with smaller ECVs are at risk for unsafe sound exposure during routine VEMP testing. Stimuli should not exceed 120 dB SPL for children. Results from phase II will provide evidence regarding whether these stimuli result in cochlear function changes following VEMP testing.

Inner Ear: Damage and Protection I

PD 55

A High-throughput Screen Identifies Small Molecules and a Common Molecular Target for Protection Against Cisplatin- and Noise-induced Hearing Loss

Tal Teitz¹; Jie Fang¹; Asli N. Goktug¹; Justine D. Bonaga¹; Shiyong Diao¹; Luigi Iconaru¹; Marie Morfouace¹; Yinmei Zhou¹; Cheng Cheng¹; Robyn A. Umans¹; Michael R. Taylor¹; Jaeki Min¹; Burgess Freeman¹; Martine F. Roussel¹; Richard Kriwacki¹; Kip Guy¹; Taosheng Chen¹; Jian Zuo²

¹St. Jude Children's Research Hospital; ²Dept. of Developmental Neurobiology, St. Jude Children's Research Hospital, Memphis, TN, USA

Hearing loss due to chemotherapy, noise and aging affects nearly 10% world population but there are no FDA approved drugs for its prevention and treatment. To address this need, we screened a library of 4,359 small bioactive molecules using a cochlear cell line and identified 10 compounds that protected against cisplatin-induced outer hair cell damage in mouse cochlear explants. The top three hits had a common cellular target; cochlear explants isolated from mice deficient in this molecular target displayed enhanced resistance to cisplatin toxicity and mice with germline deficiency in this molecular target showed significant resistance to noise-induced cell death in the cochlea. We demonstrated in adult mice that local delivery (transtympanic injection) of the top prototype compound, SJZuo-4, offered protection against cisplatin- and noise-induced hearing loss. Pharmacokinetics studies showed that SJZuo-4 was effective within the inner ear fluid within approximately 6 hrs of administration. Through cheminformatics by determination of structure-activity relationships (SAR), we identified additional analogs that were more potent than our original hits. Our studies reveal a novel molecular target in the cochlea and small molecule compounds for potential therapeutic intervention of widespread hearing loss including cisplatin-treated cancer patients and noise-induced hearing loss in the military personnel and in the general population with age.

PD 56

Glucose 6-Phosphate Dehydrogenase Deficiency: A Novel Model for Noise-Induced Hearing Loss

Thomas Schrepfer¹; Lingchao Li²; Gabriel Corfas³; Jochen Schacht⁴

¹University of Michigan; ²Kresge Hearing Research Institute, University of Michigan; ³Kresge Hearing Research Institute, The University of Michigan; ⁴University of Michigan Medical School

The generation of reactive oxygen species resulting in the promotion of apoptotic and necrotic hair cell death has been suggested as an underlying mechanism of noise-induced hearing loss. In support, both endogenous and exogenous antioxidants can mitigate oxidative stress and limit the severity of noise trauma. In endogenous antioxidant systems, NADPH serves as the ultimate reductant for the redox activities of glutathione reductase and thioredoxin reductase by restoring their reduced state. The major cellular provider of NADPH is glucose 6-phosphate dehydrogenase (G6PD), the rate-limiting enzyme in the pentose phosphate pathway. We hypothesized that a decreased activity of G6PD should lead to a compromised ability to counter oxidative stress and thus aggravate the adverse effects of noise exposure.

Heterozygous and homozygous G6PD-deficient mice and their wild-type littermates were exposed for two hours to a wide-band noise from 2-20 kHz at 110 dB. Auditory performance was assessed before and after exposure by auditory brainstem audiometry and distortion product otoacoustic emissions at the frequencies of 5.6, 8, 11.3, 16, 22.6, 32 and 45.2 kHz. Baseline values were the same in all three groups. Two weeks after exposure significant differences were apparent in all measures between the wild-types and their G6PD-deficient littermates. While the wild type group sustained only a mild hearing loss for all frequencies, both mutant groups displayed a moderate to severe hearing loss for midrange and high frequencies. Histological studies showed an increased hair cell loss in G6PD-deficient mice compared to wild-type littermates.

These results establish a novel model to investigate noise-induced hearing loss. The data strongly support the involvement of ROS and the crucial role of NADPH and G6PD as endogenous protectants. Interestingly, G6PD-deficiency is the most common human enzymopathy rendering carriers sensitive to oxidative agents including common foods (e.g., fava beans; "favism") and, by extension of our results, possibly to noise.

[This research was supported in part by National Institute on Deafness and Other Communication Disorders Grant R01 DC 004820]

PD 57

Effects of Long-term Exercise on Age-related Hearing Loss in CBA/CaJ Mice

Shinichi Someya¹; Chul Han¹; Dalian Ding²; Senthilvelan Manohar³; Mi-Jung Kim¹; Hyo-Jin Park¹; Karessa White⁴; Richard Salvi³

¹University of Florida, Department of Aging and Geriatric Research; ²State University of New York at Buffalo; ³Center for Hearing & Deafness, Department of Communicative Disorders and Science, State University of New York at Buffalo; ⁴University of Florida, Department of Aging and Geriatric Research; Department of Speech, Language, and Hearing Science

Background

In older adults, an age-related decline in mobility is a major risk factor for mortality. Importantly, long-term physical activity prolongs mobility in the elderly, while leisure-time physical activity lowers the risk of 13 types of cancers and increases life expectancy. Consistent with human data, lifelong voluntary wheel running in animals increases the median lifespan. Nearly two thirds of adults aged 70 years or older develop significant hearing loss. Hearing loss is also associated with decreased physical function among older adults. The goal of this project was to investigate the effects of long-term voluntary wheel running on age-related hearing loss (AHL) in CBA/CaJ mice, a well-established model of AHL.

Methods

To investigate the effects of long-term voluntary wheel running, we conducted ABR hearing tests in non-wheel running control and wheel running (WR) CBA/CaJ mice at 3, 6 and 24 months of age. To investigate the effects of long-term exercise on age-related cochlear pathology, we performed histological analyses, including cochleograms, spiral ganglion neuron counting, stria vascularis thickness measurements, and strial capillary counting in the cochlea following ABR tests. To investigate the mechanisms by which regular exercise delays AHL, we performed DNA microarray and PCR array analyses of inner ear tissues from 6-month-old control and WR mice.

Results

Running activity peaked at 6 months of age (12280 meters/day) and gradually decreased over time. Twenty-four-month-old runners had less cochlear outer hair cell and spiral ganglion neuron loss, and had better ABR thresholds at the low and mid frequencies compared to

age-matched controls. Gene Ontology (GO) enrichment analysis of inner ear tissues from young control and WR mice revealed that wheel running resulted in a marked enrichment for GO gene sets associated with inflammatory response, vascular function, and apoptosis. In agreement with these results, there was reduced stria vascularis atrophy and reduced loss of capillaries in the stria vascularis of old runners versus old controls.

Conclusions

Taken together, these results show that regular exercise can significantly slow age-related hearing loss and cochlear degeneration in a well-established murine model. Our data also suggest that regular exercise delays the progression of AHL by reducing age-related loss of stria capillaries associated with inflammation.

Funding

Supported by NIH/NIDCD grants R01 DC012552 (S.S.), R01 DC014437 (S.S.) and R03 DC011840 (S.S.).

PD 58

A Small Molecule Mitigates Hearing Loss in a Mouse Model of Usher Syndrome Iii

Kumar N. Alagramam¹; Suhasini Gopal²; Ruishuang Geng²; Daniel Chen²; Ina Nemet³; Guilian Tian³; Masaru Miyagi³; Karine Malagu⁴; Christopher Lock⁴; William Esmieu⁴; Andrew Owens⁴; Nicola Lindsay⁴; Krista Ouwehand⁵; Faywell Albertus⁵; David Fischer⁵; Roland Bürl⁴; Angus MacLeod⁴; William Harte³; Krzysztof Palczewski³; Yoshikazu Imanishi³

¹Department of Otolaryngology - HNS, Case Western Reserve University; ²University Hospitals Cleveland Medical Center, Case Western Reserve University;

³Case Western Reserve University; ⁴Charles River Laboratories, UK; ⁵Charles River Nederland BV

Usher syndrome type III (USH3), characterized by progressive deafness and blindness, is caused by destabilizing mutations in the gene encoding the clarin-1 protein (CLRN1). Here we report a novel strategy to mitigate hearing loss associated with a common USH3 mutation, CLRN1-N48K that involves a cell-based high-throughput screening of small molecules stabilizing CLRN1-N48K whereas eliminating general proteasome inhibitors and optimizing structure-activity relationships. This resulted in the identification of BF844. To test the efficacy of BF844, a mouse model was developed that mimicked the progressive hearing loss of USH3. BF844 effectively attenuated progressive hearing loss and prevented deafness in this model. Because the human CLRN1-N48K

mutation causes both hearing and vision loss, BF844 could in principle prevent both sensory deficiencies in USH3. Moreover, the model strategy described here could help identify drugs for other protein-destabilizing monogenic disorders.

PD 59

Protection Against Noise-Induced Hearing Loss by HK-2, a Novel Multifunctional Antioxidant

Richard Salvi¹; Peter Kador²; Guang-Di Chen¹; Dalian Ding³; Haiyan Jiang³; Jerry Tseng⁴; Damian Daszynski⁵; Theodor Woolman⁵

¹Center for Hearing & Deafness, Department of Communicative Disorders and Science, State University of New York at Buffalo; ²University of Nebraska; ³State University of New York at Buffalo; ⁴Center for Hearing and Deafness, SUNY at Buffalo; ⁵University of Nebraska Medical Center

Background

Noise-induced hearing loss (NIHL) is a major hearing health care problem due to the ubiquitous presence of industrial, leisure and military noise. While noise regulation and hearing protection can clearly reduce the risk of NIHL, pharmaceutical agents that could further mitigate the risk of developing NIHL could be extremely useful. Recently a novel multifunctional antioxidant, HK-2, has been developed, which can not only scavenges free radicals but also independently chelates metals involved in the generation of highly toxic reactive oxygen species (ROS) that cause oxidative stress. Here we provide compelling electrophysiological and anatomical evidence showing that HK-2 substantially reduces the risk of NIHL from noise exposures similar to those found in the workplace.

Methods

Rats were exposed to an OBN (8-16 kHz) with total energy of ~95 dB SPL for 8 h/day for 21 days. One noise-exposure group (N, n=6) received normal food and the other noise-exposure group received HK-2-treated food (N+HK2, n=6) starting 5 days prior to the noise exposure and ending 10 day post-exposure. Based on food intake, each rat consumed ~38-43 mg HK-2/kg/per day. A Food-Control group (HK-2, n=6) received only HK-2 and the Control group (C, n=6) only untreated rat chow. The cochlear compound action potential (CAP) was recorded 3-4 weeks post-noise exposure for all 4 groups. Afterwards, the cochleae were harvested for hair cell counting.

Results

The noise exposure caused a significant reduction in CAP amplitude and significant increase in threshold. In the noise band frequency range, the exposure induced a CAP threshold shift (TS) of ~30-40 dB in the N-alone group whereas the TS was reduced to ~10 dB in the N+HK-2 group. In the high frequency range the noise exposure induced a 10-20 dB TS in the N group whereas there was no TS in the N+HK-2 group. Correspondingly, the noise exposure induced significant loss of outer hair cells (OHC) in the N group whereas there was little or no OHC in the N+HK-2 group.

Summary

Our data indicate that HK-2, a multi-functional antioxidant, is a highly effective otoprotective agent. It can be conveniently administered in food or water for long periods of time with little or no side effects and would presumably protect other sensory or organ systems.

PD 60

The Impact of Sex on the Response to Noise and Otoprotective Therapies Against Acoustic Injury in Mice

Sunayana Mitra¹; Virginia Drake²; Zachary Margulies²; Beatrice Milon²; Yang Song³; Didier Depireux⁴; Ronna Hertzano⁵

¹Department of Otorhinolaryngology, School of Medicine, University of Maryland Baltimore; ²Department of Otorhinolaryngology, University of Maryland School of Medicine; ³Institute for Genome Sciences, University of Maryland School of Medicine; ⁴Department of Otorhinolaryngology, University of Maryland School of Medicine; Institute for Systems Research, University of Maryland; ⁵Department of Otorhinolaryngology, Department of Anatomy and Neurobiology, and Institute for Genome Sciences, University of Maryland School of Medicine

Background

Hearing loss, both genetic and acquired, is a widespread health problem with very few options for prevention or reversal. Noise induced hearing loss (NIHL) affects both men and women and afflicts 15% of the adult US population. Controlled noise exposure is often used to induce hearing loss in animal models for research purposes. To date, most of the published studies testing otoprotective agents from NIHL used males only. In 2015 the NIH published guidelines requiring the use of both male and female animals in all studies. This can be accomplished by repeating experiments separately on male and female animals, or using an equal mix of both sexes as the experimental subjects.

Objective

To test the efficacy of treatment with Suberoylanilide Hydroxamic Acid (SAHA), a previously validated otoprotective agent from NIHL (validated in male mice only), now on mice from both sexes.

Methods

Thirty-two 10-week old B6CBAF1/J mice (16 of each sex), were injected with SAHA (100 mg/kg) or DMSO (Control) 3 days before as well as 2 hours after noise exposure. The mice were exposed to 101 dB SPL octave band noise (8-16 kHz) for 2 hours. Hearing thresholds were measured using auditory brainstem responses (ABR) a week before and 1, 8 and 15-21 days after exposure. Following the last ABR, the inner ears were procured for cytochrome c oxidase (COX) and synaptic ribbon counts using an antibody for CtBP2.

Results

When mice of both sexes were analyzed together treatment with SAHA did not result in a significant therapeutic effect. When each sex was analyzed separately, SAHA treatment significantly reduced the permanent threshold shift in male but not female mice. Further analysis using the control mice alone, showed a statistically significant difference in the permanent threshold shifts across most frequencies between male and female mice, with the male mice having significantly more hearing loss. However, the hearing thresholds of the male treated mice were similar to those of the treated and untreated females. No statistically significant differences were detected in the synaptic ribbon counts across all groups measured.

Conclusions

These data validate previous reports that show effectiveness of SAHA in reducing NIHL in male mice. However, we show here that the efficacy of SAHA is sex-dependent. A contributing factor may be the differential susceptibility to NIHL in male and female mice. Thus, experiments for NIHL should be performed on both sexes and analyzed both separately and combined.

PD 61

Hepatocyte Growth Factor Mimetic Protects from Aminoglycoside-induced Hair Cell Death

Phillip M. Uribe¹; Meiyang Jiang²; Leen Kawas³; Peter S. Steyger⁴; Joseph Harding⁵; Allison B. Coffin¹; Phillip Uribe¹

¹Washington State University, Vancouver; ²Oregon Health & Science University, Oregon Hearing Research Institute; ³M3 Biotechnology; ⁴Oregon Hearing Research Center; ⁵Washington State University

Loss of sensory hair cells from exposure to certain licit drugs (e.g., aminoglycoside antibiotics) can result in permanent hearing loss. Application of exogenous hepatocyte growth factor (HGF), a potent neurotrophic factor, promotes neuronal cell survival in a variety of contexts, including protecting hair cells from aminoglycoside ototoxicity. HGF itself is not an ideal therapeutic due to a short half-life and limited ability to cross the blood-brain barrier. MM-201 is a chemically stable, blood-brain barrier permeable, synthetic HGF mimetic that forms a functional ligand to activate the HGF receptor and consequently its downstream signaling cascade. We asked if allosteric activation of the HGF cascade via MM-201 prevented aminoglycoside damage in the larval zebrafish lateral line system and the explanted mouse utricle. MM-201 robustly protects lateral line hair cells from acute gentamicin or neomycin exposure in a dose-dependent manner and MM-201-mediated protection is attenuated by co-treatment with an HGF antagonist, evidence that HGF activation is a component of observed protection. Pharmacological inhibition of MEK, Akt, or TOR signals partially attenuates the MM-201-mediated protection, implicating reliance on these signals for hair cell protection. Addition of an amino group to the N-terminal of MM-201 also attenuates the protective response, suggesting that even small substitutions greatly alter the specificity of MM-201 for its target. MM-201 treatment also protects utricular hair cells from neomycin damage, with protection evident at 1pM MM-201.

Using either plate or liquid growth assays we found that therapeutically relevant concentrations of MM-201 did not alter the bactericidal efficacy of aminoglycoside antibiotics. Our data suggest that MM-201 confers protection of hair cells through an HGF-mediated mechanism and holds great clinical potential. Future studies will continue to test the efficacy of MM-201 using in vivo mammalian models.

Funding for this work was provided by Action on Hearing Loss.

PD 62

The Requirement for Glutamate in Pre- and Postsynaptic Trauma at Cochlear Ribbon Synapses

Mark Rutherford¹; Keiko Hirose²; Kevin K. Ohlemiller²; Kyunghye Kim³; Shelby Payne³; Aizhen Yang-Hood³; Song-Zhe Li³

¹Washington University School of Medicine; ²Washington University; ³Washington University in St. Louis

Cochlear perfusion with glutamate or other AMPA receptor agonists causes auditory nerve fiber (ANF) postsynaptic terminals to swell and burst (Puel et al., 1994;

Wang and Green, 2011), and perfusion with AMPA receptor antagonists protects these terminals against noise-induced trauma (Puel et al., 1998). Therefore, activation of AMPA-type receptors may be necessary and sufficient for damage to ANF terminals, which show evidence of disintegration from presynaptic ribbons on inner hair cells (IHCs) immediately after two hours of moderate sound over-exposure (Liberman and Liberman, 2015). This dissociation of pre- and post-synaptic elements is thought to be glutamate-induced but the excitotoxic mechanisms are unknown. Although glutamate is recognized as the afferent neurotransmitter (Seal et al., 2008; Ruel et al., 2008), the existence of other excitotoxic substances in synaptic vesicles seems plausible. Moreover, trauma to the presynaptic active zone may involve mechanisms upstream of glutamate release, such as voltage-gated Ca²⁺ influx at the ribbon synapse.

To address this, we studied mice lacking the vesicular glutamate transporter-3 (Vglut3). Despite the lack of glutamatergic transmission, many afferent synapses developed and were subsequently maintained as AMPA receptors juxtaposed with presynaptic ribbons. However, the ring-shaped arrays of AMPA receptors on ANF terminals from KO mice were larger and often more complex in structure. In wildtype mice aged 9 weeks, 2 hours of 8-16 kHz noise at 100 dB SPL caused a threshold shift at 1 day that partially recovered by 2 weeks post-exposure. This was accompanied by loss of approximately 50% of synapses at 1 day, which partially recovered by 2 weeks post-exposure. Noise-induced synaptopathy was evident as disintegration between the presynaptic ribbon and postsynaptic AMPA receptors. In Vglut3 KO littermates the same noise exposure resulted in no synaptic disintegration; AMPA receptors remained paired with ribbons.

Along with previous findings, these results imply that glutamate is necessary and sufficient for noise-induced synaptopathic excitotoxicity in the cochlea. Other chemical constituents of synaptic vesicles are likely insufficient to cause noise-induced synaptopathy in the absence of glutamate. These findings do not exclude the possibility of other neuropeptides as necessary cofactors for the excitotoxic actions of glutamate. In Vglut3 KO IHCs, voltage-gated calcium channels (CaV1.3) clustered at presynaptic active zones, as in wildtype. The lack of presynaptic damage after overexposure to sound in the Vglut3 KO IHCs suggests that presynaptic Ca²⁺ influx is not sufficient in this context, and that damage to the presynaptic active zone depends on glutamate release.

Regeneration

PD 63

Spatiotemporally Controlled Up-regulation of Cyclin D1 Triggers Generation of Supernumerary Cells in the Postnatal Mouse Inner Ear

Shikha Tarang¹; Umesh Pyakurel¹; Sarath Vijayakumar²; Timothy A. Jones²; Sonia M. Rocha-Sanchez³

¹Creighton Dental School; ²University of Nebraska-Lincoln; ³Creighton University School of Dentistry

Hair cell (HC) regeneration through manipulation of existing cell-cycle machinery continues to be an attractive strategy. The retinoblastoma family of pocket proteins (pRBs) (i.e. RB1, p107 and p130) play a pivotal role in the negative control of the cell cycle and HC proliferation. pRBs' activity is phosphorylation-dependent. They are hypo-phosphorylated (active) in quiescent cells and hyper-phosphorylated (inactive) in mitotically active cells. Active pRBs repress gene transcription, required for G1-to-S transition, by directly binding to E2F genes. On another hand, increasing phosphorylation of pRBs by the Cyclin D1 (CycD1)-CDK4/CDK6 complex, leads to the release of E2F transcription factors and starts cell proliferation. Loss of function of any individual member of the pRB family, triggers HC and supporting cell (SC) proliferation in the murine cochleae to different extents. However, the combined effects of manipulating the three pocket proteins (pRBs) at the same time, has not been addressed. Based on the knowledge on pRBs and CycD1 interaction, we hypothesized that spatiotemporally controlled up regulation of CycD1 gene in the postnatal inner ear is likely to lead to inactivation of members of the pRB family and trigger unscheduled cell proliferation. To test this hypothesis, we generated a tetracycline controlled Atoh1-Cre/CAG-bgeo-tTA/TetO-CycD1 mouse model. Consistent with our original hypothesis, characterization of this mouse model demonstrated that controlled CycD1 up regulation in the postnatal mouse organ of Corti leads to mitotic cell division and generation of supernumerary HCs, particularly at the inner hair cells (IHCs) region, not immediately followed by apoptotic cell death. Physiological analyses to assess the Atoh1-Cre/CAG-bgeo-tTA/TetO-CycD1 mouse hearing are currently underway.

Supported by NIH/NIDCD 5R21OD019745-02 (SMRS).

PD 64

Modulating Mitotic Regeneration via Activation of the Wnt/ β -catenin Pathway

Patrick J. Atkinson¹; Yaodong Dong¹; Shuping Gu¹; Alan Cheng²

¹Department of Otolaryngology-HNS, Stanford University; ²Stanford University, School of Medicine, Department of Otolaryngology

Background

Canonical Wnt signaling plays diverse roles in the developing inner ear including otic induction, proliferation, prosensory cell specification, and hair cell differentiation. During mammalian cochlear development, activation of Wnt signaling induces proliferation of prosensory cells and ectopic hair cell formation. In the damaged zebrafish lateral line neuromast and neonatal mouse utricle, Wnt activation promotes mitotic hair cell regeneration. However, it remains to be determined the effect of Wnt activation in the damaged neonatal and adult mammalian cochlea. Here we stabilized β -catenin, the central mediator of canonical Wnt signaling, after hair cell ablation in the immature and mature cochlea.

Methods

The transgenic mice lines Fgfr3-icre, Pou4f3-DTR and, Ctnnb1-flox(exon3) were used. Hair cells were ablated via diphtheria toxin injection at postnatal day 1 (P1) or P21 in Pou4f3-DTR mice. A cohort of adult mice was alternatively deafened using aminoglycosides. Tamoxifen and EdU were administered after damage. Neonatal animals were sacrificed at P5 or P7 and cochleae collected for histology; adult animals were sacrificed at P28 or P58 after functional hearing assessment.

Results

In the neonatal Fgfr3-icre; Ctnnb1-flox(exon3) mice, β -catenin stabilization failed to induce proliferation or ectopic hair cell formation. After hair cell ablation in Pou4f3-DTR mice, mitotic hair cell regeneration was detectable in the apical turn only. When β -catenin was stabilized after hair cell ablation, the number of EdU-labeled supporting cells and myosin7a-positive hair cells significantly increased, suggesting that Wnt enhances proliferation in the neonate cochlea. In comparison to P5, cochleae examined at P7 had more EdU-labeled hair cells and supporting cells, implying survival and expansion of proliferative cells at least in the short term. In the mature cochlea, no proliferation was observed after β -catenin stabilization alone. After hair cell ablation via aminoglycoside administration or diphtheria toxin injection to Pou4f3-DTR mice, no EdU-labeled cells were detected with or without β -catenin stabilization 1 week or 1 month later.

Conclusions

Damage as a result of hair cell loss acts as a permissive signal for spontaneous and Wnt-induced mitotic hair cell formation in the neonatal but not in the mature cochlea.

Funding

California Initiative in Regenerative Medicine RN3-06529; NIH/NIDCD RO1DC013910; Akiko Yamazaki and Jerry Yang Faculty Scholarship, Department of Defense MR130316, Garnett Passe and Rodney Williams Memorial Foundation.

PD 65

Three Signaling Pathways - VEGF, SHH, and BMP4 - Regulate Supporting Cell Division in Avian Auditory Organs After Aminoglycoside Treatment in Vitro

Liang Cai Wan¹; Mark Warchol²; Michael Lovett³; Jennifer Stone⁴

¹University of Washington, Seattle WA and Southern Medical University, Guangzhou, China; ²Dept of Otolaryngology, Washington University School of Medicine, St Louis MO; ³Imperial College London; ⁴University of Washington, Seattle, WA

Supporting cells serve as progenitors to regenerated hair cells in post-hatch chickens after aminoglycoside treatment. We are interested in identifying signaling pathways that regulate all aspects of avian hair cell regeneration. We used RNA-Seq to assess all transcriptional changes in supporting cells from the chicken basilar papilla during regeneration. We identified three specific pathways - vascular endothelial growth factor (VEGF), sonic hedgehog (SHH), and bone morphogenetic protein (BMP) - whose receptors were particularly transcriptionally dynamic after hair cell damage. These pathways represent potential regulators of supporting cell division or transdifferentiation during avian hair cell regeneration.

We tested the possible role of VEGF, SHH, or BMP4 signaling in regulating supporting cell division during regeneration of auditory hair cells. In initial experiments, we applied selective inhibitors of these pathways to cultured explants of cochlear ducts from post-hatch chickens. Cultures were first treated with 100 μ M streptomycin for 2 days to kill hair cells and were then maintained without streptomycin for one additional day. One of the following drugs was added to media for the entire culture period: SU5416 (VEGF inhibitor), cyclopamine (SHH inhibitor), or noggin (BMP4 inhibitor). Parallel negative controls consisted of vehicle-only. Bromodeoxyuridine was present in culture media for the last day, to measure effects on supporting cell division. We found that 1 and 10 μ M concentrations of VEGF and SHH inhibitors each

significantly decreased division of supporting cells in a dose-dependent manner, while 0.5 μ g/ml noggin had no effect. Additionally, we tested whether addition of recombinant VEGF or BMP4 to damaged cultures altered supporting cell division using the same culture methods. We found that 100 ng/ml VEGF caused supporting cell division to increase 1.8 fold, while 10 ng/ml BMP4 reduced supporting cell division to 35% of control; both effects were statistically significant. Our observations indicate that VEGF and SHH each promote supporting cell division, while BMP4 antagonizes supporting cell division. Currently, we are analyzing expression of receptors for each pathway in supporting cells and testing whether either pathway controls numbers of hair cells that regenerate. We are also assessing the supporting cell toxicity profiles of various inhibitors and agonists of the pathways we have identified. We anticipate that these studies will help to better define the specific mechanisms by which birds regenerate auditory hair cells.

PD 66

Activation of ErbB2 is Sufficient to Induce Cochlear Supporting Cell Proliferation in vivo

Jingyuan Zhang; Patricia White; Stephen Paquette
University of Rochester

Background

Hearing loss affects a large population, and sensory hair cell loss is a primary cause of hearing loss, as little regeneration occurs in the mammalian system. To achieve sensory hair cell regeneration, replacement from another cell type, such as supporting cells, is crucial. Overexpression of Wnt target gene β -catenin initiated proliferation and subsequent transient expansion of Lgr5+ supporting cells in the cochlea. Other studies have implicated ErbB family signaling in regeneration in avian models and dissociated mouse cochlear supporting cells; however, no evidence yet exists to support a role for ErbB family signaling in the mouse cochlea in vivo.

Methods

We bred transgenic mouse lines to overexpress a rat constitutively active (CA) ErbB2 in vivo. Transgenic CA-ErbB2 activation was accomplished by crossing Tet-on CA-ErbB2 line with a cochlear specific rtTA line, Sox10rtTA. We also built an adenovirus construct that expresses human CA-ErbB2 in conjunction with GFP. Neonatal mouse cochlear explants were cultured and infected by CA-ErbB2 virus and control viruses. Cell proliferation is revealed by EdU nuclear incorporation, and quantified using AMIRA 3D-reconstruction.

Results

Our transgenic strategy established a way to activate CA-ErbB2 signaling with spatial and timely control in

vivo. We found significant EdU labeling in supporting cells upon Sox10rtTA/ CA-ErbB2 48 hours activation compared to Sox10rtTA control at postnatal age Day 2 (P2). In cochlear organ culture, large numbers of cell expansion were found in supporting cells and cochlear greater epithelial ridge (GER) region upon transgenic CA-ErbB2 activation at 24 hours driven by Sox10rtTA.

CA-ErbB2 adenovirus was used to study the mechanism of supporting cell proliferation in vitro. Infection of mouse cochlear supporting cells with CA-ErbB2 adenovirus in organ culture drove EdU incorporation. Interestingly, CA-ErbB2 virus infection triggered paracrine proliferation in Jag1+ supporting cells. Dividing supporting cells from the cochlear culture were shown to down-regulate Sox2 protein 24 hours after CA-ErbB infection. Some EdU+ supporting cells re-express Sox2 later at 32 hours after the CA-ErbB signal.

Conclusion

We conclude that activated ErbB2 signaling is sufficient to cause neonatal mouse supporting cell proliferation in vivo and in vitro. Moreover, the mitotic effects from ErbB2 activation on supporting cells were non-cell autonomous. Sox2 was down regulated during proliferation in vitro. Taken together, these findings support a role for epidermal growth factor receptor (ErbB) signal in the induction of cochlear supporting cell proliferation in neonatal mice, and the possibility of cross talk between ErbB2 mediated signaling and other pathways.

PD 67

Loss of fgf3 Leads to an Increase in Hair Cell Regeneration Downstream of Notch Signaling

Mark Lush; Tatjana Piotrowski
Stowers Institute for Medical Research

Organ regeneration is a complex process involving integration of multiple cell signaling pathways. The zebrafish lateral line contains mechanosensory hair cells that respond to vibrations in the surrounding water and serve as a powerful model to decipher the signaling network underlying hair cell regeneration. Lateral line hair cells are surrounded by at least two groups of support cells, which together form a structure called the neuromast. Unlike mammals, the sensory hair cells of the lateral line regenerate after damage. We have previously shown that hair cell regeneration requires Notch downregulation and Wnt-dependent proliferation of a resident support cell population (Romero-Carvajal, *Dev Cell* 2015). Other signaling pathways, such as Fgf are also expressed in mature neuromasts. Fgf signaling is required for lateral line development, as it is for ear development of mouse, chicken and zebrafish, but its role in regeneration is not well understood. RNASeq and in situ hybridization anal-

yses show that fgf3, fgf10a, fgf10b and the receptors fgfr1a and fgfr2 are expressed in homeostatic neuromasts and are immediately downregulated after hair cell death. These findings suggests that downregulation of Fgf signaling may be required to initiate lateral line hair cell regeneration. Indeed, BrdU and in vivo single cell fate analyses revealed that in fgf3 mutants, hair cell regeneration is enhanced due to increased support cell proliferation. Increased hair cell regeneration and proliferation is mimicked by low dose treatment with pharmacological inhibitors of Fgf receptors. Surprisingly, high doses of Fgf inhibitors block support cell differentiation/regeneration, even though proliferation is still increased, suggesting that high levels of Fgf signaling are needed for differentiation. Therefore, proliferation and hair cell differentiation are regulated via different receptors or downstream targets. Inhibition of Notch signaling during regeneration also leads to increased cell proliferation suggesting that Notch and Fgf signaling might interact. Our results show that loss of fgf3 leads to the upregulation of Wnt signaling and that Notch signaling regulates Wnt signaling via the control of fgf3. Therefore, the individual or combined downregulation of these pathways should be explored in mammals to trigger proliferation and hair cell regeneration.

PD 68

Are Changes in Local Mechanical Tension the Initial Signal that Triggers Regenerative Responses in Hair Cell Epithelia?

Mark A. Rudolf; Jeffrey T. Corwin
University of Virginia

Background

As mammals mature, inner ear supporting cells exhibit sharp declines in proliferative capacity and reduced replacement of lost hair cells. Concurrently, these cells develop robust F-actin “belts” at their apical junctions characterized by exceptional thickness and stability in comparison to other known epithelia. Supporting cells in non-mammals retain the capacity to proliferate and replace lost hair cells throughout life, and their circumferential F-actin “belts” remain thin. Notch, Wnt, FGF, and other signaling cascades have vital roles in hair cell regeneration, but the initial signal that triggers regenerative responses remains undefined. In other epithelia, mechanical signals play a crucial role in maintaining the local balance of cell death and proliferation. It is unknown to what degree such mechanical signals influence hair cell epithelia. We hypothesize that the F-actin “belts” of mammalian supporting cells impede the transmission of mechanical signals that may initiate the regenerative response.

Methods

To compare levels of local mechanical tension in utricles of chicks and mice, we measured cell shape anisotropy via immunohistochemical labeling of cell junctions. Length:width ratios for each supporting cell were determined by fitting an ellipse to its apical surface and measuring the ratio of major and minor axes. Ellipse orientation provided a quantitative measure of intercellular alignment. Time-lapse microscopy in the presence or absence of pharmacological agents was used to assess the dynamics of cell shape and its dependence on myosin-II activity.

Results

In P0 chick utricles, supporting cells exhibited significant shape anisotropy (length:width ratio 3.1 ± 1.0 , mean \pm SD) and tight local alignment (SD = 9.5 degrees). In contrast, supporting cells in P0 mouse utricles exhibited substantially less elongation (length:width ratio 1.6 ± 0.6) and less intercellular alignment (SD = 45.6 degrees). Inhibition of myosin-II contractility induced dramatic shape changes in supporting cells of chick, but not mouse.

Conclusions

In chick utricles, supporting cell shape is distinctly anisotropic, locally aligned, and dependent on maintained myosin contractility. In contrast, supporting cells in mouse utricles are relatively isotropic and their morphology appears independent of myosin contractility. This suggests that supporting cells in the chick utricle behave as members of a mechanical syncytium, each in turn shaped by local mechanical forces, while supporting cells in the mouse utricle do not. This preliminary evidence is consistent with the hypothesis that local mechanical tension may be the initial signal that triggers regenerative responses to hair cell loss.

PD 69

CHD7 Decreases Cellular Noise During Otic Neuronal Differentiation

Kelvin Kwan¹; Azadeh Jadali¹; Jennifer Skidmore²; Donna M. Martin³

¹Rutgers University; ²University of Michigan; ³Department of Pediatrics and Communicable Diseases, University of Michigan

The sensory hair cells and the spiral ganglion neurons (SGNs) of the cochlea allow us to discriminate and hear complex sounds. Hair cells convert sound into neural signals, which are then relayed to the brain by spiral ganglion neurons (SGN). Since SGNs do not normally regenerate, loss of SGNs from loud noise exposure contributes to hearing loss. Stem cell replacement therapies for SGNs have shown great promise. Identification of

factors that promote SGN differentiation will accelerate efforts for replacement therapies.

Using an immortalized otic progenitor (iMOP) cell line, CHD7 was identified as a chromatin remodeling factor involved in early stages of SGN differentiation. Immunolabeling of CHD7 in the early developing inner ear shows CHD7 expression in SOX2 neurosensory progenitors. To determine the genome-wide downstream targets of CHD7, we identified direct target genes by chromatin immunoprecipitation followed by deep sequencing (ChIP-seq) in iMOP cells. A specific subset of microRNAs was identified as targets of CHD7. Using CHD7 mutant animals, a decrease in mir9-2 and mir124a-1 was validated by qPCR. In addition to regulating gene expression, microRNAs have been implicated in reduction of cellular noise. Using a dual fluorescent reporter containing microRNA 9 binding sites, fluorescent images were acquired using a high content microscope. Cellular noise was determined from the fluorescent images. We showed that cellular noise decreases as iMOP cells undergo neuronal differentiation. Knockdown of CHD7 increases noise and prevents neuronal differentiation.

We propose that CHD7 decreases cellular noise by promoting microRNA expression to ensure robust SGN differentiation. Mutations in CHD7 causes CHARGE syndrome. Patients with CHARGE show a signature of clinical symptoms including hearing impairment due in part to improper SGN development. One hallmark of CHARGE is the variable penetrance of the symptoms. We propose ablation of CHD7 increases cellular noise and contributes to the varied penetrance of phenotypes observed in patients with CHARGE.

PD 70

Functional Recovery of the Damaged Adult Mouse Utricle and Characterization of Regenerated Hair Cells

Zahra Sayyid¹; Tian Wang¹; Sherri Jones²; Alan Cheng³

¹Stanford University; ²University of Nebraska-Lincoln;

³Stanford University, School of Medicine, Department of Otolaryngology

Background

The utricle requires sensory hair cells to detect gravity. Although the neonatal mouse utricle has the innate ability to regenerate new hair cells after damage, this regenerative potential significantly declines with age. Prior work on adult mice showed an incomplete recovery of hair cell number months after damage. The time-course of regeneration, whether organ function is restored, and if enhanced hair cell regeneration improves function are

currently unclear. Here, we have investigated the relationship between hair cell number and vestibular function 1 week to 6 months after damage. Furthermore, we have examined fate-mapped regenerated hair cells and compared their molecular features to vestibular function. Lastly, we are examining the effects of Atoh1 overexpression on hair cell number and vestibular function after damage.

Methods

Mice (wild-type, Plp1CreERT/+; R26RtdTomato/+, and CAGfloxAtoh1-HA/+; Plp1CreERT/+) received IDPN on postnatal day 30 and tamoxifen on day 32. Linear VsEPs were recorded 1 week, 1 month, 3 months, and 6 months post-injection. Utricles were immunostained for hair cell, supporting cell, bundle, neuronal, and synaptic markers. Densities of hair cells, supporting cells, and traced hair and supporting cells were determined in the striola and extrastriola.

Results

As a group, IDPN-treated animals have significantly higher VsEP thresholds than saline-treated, age-matched controls one week after injection, with 85% of animals displaying absent or elevated thresholds not observed in controls (n=56 controls and 63 IDPN-treated). By 6 months, IDPN-treated animals have significantly improved thresholds relative to 1 week, with ~64% of animals (14/22) regaining thresholds comparable to controls. Moreover, animals that have regained thresholds exhibit significantly longer P1 latencies and lower P1-N1 amplitudes than those of controls, suggesting a partial recovery of vestibular function. Serial assessment of vestibular function of 12 individual mice across all 4 time points demonstrates that 58% had recovered thresholds by 6 months and 17% showed no improvement of vestibular function, while others (25%) displayed an initial functional improvement followed by a loss of function by 6 months. Furthermore, improved VsEP thresholds correlated with increased hair cell numbers over time. Using Plp1CreERT/+;R26RtdTomato/+ mice to fate-map supporting cells, we found increasing number of fate-mapped hair cells that displayed short, disorganized bundles, markers of type 2 hair cells, and pre- and post-synaptic proteins. Lastly, Atoh1 overexpressing mice had significantly more traced hair cells. The vestibular function and histology of these mice are currently being analyzed.

Conclusions

Mammalian vestibular hair cell regeneration correlates with recovery of organ function.

Bridging the Gap Between Hearing Sciences and Audio Technologies

SYMP 29

Perceiving Graphical and Pictorial Information Using Hearing and Touch

James West

Johns Hopkins University

A dynamic interactive touch screen system for conveying visual information via hearing and touch that allows the user to actively explore a two-dimensional space containing multiple objects using fingers while listening to auditory feedback is presented. Sound is used as the primary source of information for object location, identification and shape, while touch is used for pointing and kinesthetic feedback. The head-related transfer function is used for rendering directionality, while other properties of sound, intensity, duration and coloration are used for rendering proximity. The main focus is on conveying the shape of an object.

SYMP 30

Computers and the Auditory System: what Can They Learn from Each Other?

Hynek Hermansky

The Johns Hopkins University

It is easy to argue that speech recognition engineering should apply knowledge of properties of human auditory perception - both have the goal of extracting message from speech. However, hearing research can also learn from advances in speech technology: the knowledge that helps in engineering applications lends support to hearing theories. Further, fundamental difficulties that speech engineering still faces could indicate weakness in our current understanding of the human speech communication process and should guide further inquires into it. The talk mentions some properties of human hearing that were found useful to emulate in a machine and points to some of the remaining engineering problems where speech perception research could significantly help.

SYMP 31

Large-scale Applications of Machine Hearing Research for Audio Processing

Richard F. Lyon¹; Malcolm Slaney²

¹Google Inc.; ²Google

The principles of machine hearing provide a strategy for analyzing large-scale audio collections, including soundtracks of movies on online movie sharing sites

(such as YouTube) and personal video collections (such as on photo sharing sites and connected-camera sites). Knowledge of the human hearing system allows the design of systems that understand sounds in terms of what they “sound like,” in the sense of psychoacoustic similarity. A good similarity measure based on auditory representations is a good starting point for detection, classification, and matching tasks. Starting with an efficient frontend based on a cascade model of cochlear processing, our machines can perceive the wide dynamic range of sounds in natural environments and in recordings in much the same way that humans do. Subsequent processing to arrive at a stabilized auditory image, or auditory correlogram, provides a representation in which temporal pattern cues become more explicit, and in which different sound sources tend to separate along different dimensions. We have found such representations to be effective, when combined with machine-learning systems, in tasks such as song identification, content-based recommendation of movies and music, sound search from text queries, salient sound event detection and classification, robust speech recognition, and segmentation or diarization of long audio streams. In systems with multiple microphones, augmenting the representations to handle spatial effects, leveraging knowledge of binaural processing such as the precedence effect, leads to improved interpretation of sounds in complex environments. A remaining challenge in such systems is to incorporate knowledge from the frontiers of knowledge of higher levels of the auditory system, beyond primary auditory cortex, including saliency and attention.

SYMP 32

The Influence of Hearing Science on Hearing Aid Advancement

Brent Edwards
EarLens Corp

Hearing aid technology is advancing faster than it ever has in the history of amplification. Hearing aid capabilities are becoming more advanced with wireless technology, while audio wearables or “hearables” are taking on features normally only found in hearing aids. More medically focused hearing aids have also been developed that expand their capabilities for addressing hearing loss. While the fundamentals of hearing science have informed the development and potential benefits of these technologies, the application of hearing science to demonstrating the effectiveness of novel technologies has lagged. Technology developments with both traditional and nontraditional hearing technologies are driving new scientific questions on candidacy and benefit, which will lead to advancements in diagnostics and outcome measures. This talk will provide a perspective

on this intersection of hearing science and hearing technology, providing examples from traditional and non-traditional hearing aid technologies.

A Tribute to Norman M. Weinberger (1935-2016): A Bridge to the Future of Research on Auditory Cortical Functions

SYMP 33

Changes in the Conceptualization of Auditory Cortical Receptive Fields: Diamond and Weinberger 30 Years Later

Dexter Irvine

Monash University School of Psychological Sciences

In 1986, Diamond and Weinberger reported changes in the frequency response areas of neurons in non-primary areas of auditory cortex as a consequence of behavioral conditioning procedures. Shortly after, changes in neuronal frequency selectivity in primary auditory cortex (AI) were described as a consequence of both restricted cochlear lesions and of conditioning. This evidence for plasticity of auditory cortical spectral receptive fields triggered major changes in the way in which these fields are conceptualized. Rather than being a relatively simple reflection of input from a labelled line originating from a frequency selective point on the basilar membrane, the spectral receptive field of an auditory cortical neuron at any point in time is sculpted from an extraordinarily wide range of inputs from a wide range of sources. The sculpting process itself can be driven by a wide range of experiential variables. The early experiments, and the range of subsequent studies that have shaped our current understanding of spectral RFs, will be reviewed.

SYMP 34

Synaptic Mechanisms and Functional Consequences of Nucleus Basalis Stimulation: Bakin and Weinberger 20 Years Later

Robert C. Froemke

Skirball Institute of Biomolecular Medicine, Neuroscience Institute, Department of Otolaryngology, and Department of Neuroscience and Physiology, New York University School of Medicine

In 1996, Bakin and Weinberger published a landmark paper demonstrating how stimulation of the cholinergic nucleus basalis could lead to long-lasting shifts of frequency tuning in adult rat primary auditory cortex. Over the last decade, our lab has been examining the synaptic mechanisms and behavioral consequences of their important discovery. I will describe the historical context for these experiments that pair neuromodulator release with acoustic stimuli, and discuss our recent results

comparing and contrasting the effects of nucleus basalis pairing with stimulation of other neuromodulatory centers.

SYMP 35

Neuromodulatory and Sensory Inputs Integrated: Norman Weinberger's (1990) Model for Receptive Field Plasticity in A1

Raju Metherate

University of California, Irvine

In 1990, Norm Weinberger and colleagues published a seminal model that sought to integrate a decade of largely independent work on cholinergic modulation and learning-induced plasticity in the auditory system (Weinberger et al, 1990). The model and its updates (e.g., Weinberger, 2004) provided a theoretical framework for subsequent research from his lab and others. This talk will review some important developments that led to the model and those that followed, focusing on findings that altered how we think cholinergic neuromodulation regulates auditory cortex function and plasticity. In particular, the role of nicotinic acetylcholine receptors, which prior to 1990 were not thought to play much of a role in CNS function, now play an increasingly recognized role in attention and learning at the level of A1.

References

Weinberger, N. M. (2004). Specific long-term memory traces in primary auditory cortex. *Nature Reviews Neuroscience*, 5: 279-290.

Weinberger, N. M., Ashe, J. H., Metherate, R., McKenna, T. M., Diamond, D. M., & Bakin, J. (1990). Retuning auditory cortex by learning: a preliminary model of receptive field plasticity. *Concepts Neuroscience*, 1: 91-132.

SYMP 36

Norman Weinberger and High Frequency Brain Rhythms: Bridging 50 Years of Conceptual Progress

Drew Headley

Rutgers University

While Dr. Weinberger is best remembered for his investigations into associative plasticity in auditory cortex, throughout his career he also contributed to our understanding of high frequency (>30 Hz) oscillations in the brain. Through several key papers this talk will follow his journey. Indeed, his first paper examined the properties of auditory stimuli that elicit such oscillations. Midway through his career he and his students investigated their neurochemical basis and consequences for cortical function. Later, his lab directly probed how gamma oscillations (40-100Hz) in primary auditory cortex affect

associative plasticity and coordinate spiking activity for behaviorally relevant stimuli.

SYMP 37

Mnemonic Functions of Adult Cortical Plasticity: Rutkowski and Weinberger 10 Years Later

Kasia Bieszczad

Rutgers University

In 2005, Rutkowski and Weinberger published a landmark paper demonstrating that long-lasting tonotopic reorganization in adult rat primary auditory cortex could encode the behavioral importance of sound. A consequence of that publication has been to realize that there are functions of traditional "sensory" representations in the domain of memory. I will tell a story of the experiments that followed to further demonstrate auditory sensory cortical roles in learning, remembering and even forgetting. The sensory cortex may not be so "sensory" after all.

Vestibular Influences on Cognitive Function

SYMP 38

Hippocampal Contributions to Cognitive Dysfunction in Vestibular Disorders

Paul Smith

Univ. Otago Medical School

In recent years there has been increasing evidence that patients with vestibular disorders exhibit spatial memory deficits. There are now also a number of papers that have reported that patients with vestibular disorders exhibit hippocampal atrophy. Although one potential explanation for such atrophy is stress related to vestibular dysfunction, there are other possible explanations. Animal studies suggest that there are extensive synaptic connections between the vestibular nucleus and hippocampus and that, at least some of the neurophysiological changes that take place, may be independent of stress and related more to the evolutionary importance of the vestibular system for hippocampal function. Our recent studies suggest that bilateral loss of vestibular function (bilateral vestibular loss, BVL) is associated with major changes in the acetylcholine (ACh) pathways converging on the hippocampus. Using receptor autoradiography and flow cytometry we have found that over a period of 30 days following BVL in rats, the expression of M1 muscarinic ACh receptors significantly decreases in the hippocampus while the expression of M2/4 muscarinic ACh receptors significantly increases. Using in vivo microdialysis we found no significant change in the basal ACh release in the hippocampus, but a significant increase in the number of cholinergic cells in the pedunc-

culopontine tegmental nucleus, a major source of cholinergic input to the cholinergic theta-generating pathway to the hippocampus. These results suggest that cholinergic input to the hippocampus undergoes major changes following BVL and that this may be related to some of the cognitive deficits associated with vestibular dysfunction.

SYMP 39

Vestibular Cognition: From Sensory Predictions to Mental Imagery

Fred Mast

University of Bern

Vestibular cognition has recently gained attention. In this session we will discuss several studies involving vestibular patients that showed that imagined spatial transformations and the processing of real vestibular information share common mechanisms. We suggest that the mechanisms that are in the service of sensory predictions can also operate offline, such that they are drawn upon when people simulate body movements (e.g. during spatial perspective transformations). We will discuss how known vestibular pathways could be involved in offline operations, and how interactions between online sensorimotor processing and offline usage might occur.

SYMP 40

High-density EEG of the Human Vestibular System

Olaf Blanke

Laboratory of Cognitive Neuroscience at EPFL

The human vestibular cortex has been studied using brain imaging techniques (i.e. fMRI) along with well-accepted, but artificial, vestibular stimulation such as caloric or galvanic vestibular stimulation (cVS/gVS). I will present studies joining rotatory vestibular stimulation (rVS) with high-density EEG recordings, which show that rVS suppresses alpha power (8-13Hz) over temporo-parietal scalp regions, and that rVS modulates visual and somatosensory processing. I will argue that rVS-EEG is a powerful tool to study human vestibular cortex and its interactions with other cortical systems, has advantages over neuroimaging studies using gVS/cVS, and is an important technique to study brain mechanisms of vestibular disease.

SYMP 41

Drift in Upright Perception During Head Tilt and Ocular Torsion: Is there a link?

Amir Kheradmand

Johns Hopkins School of Medicine

Torsional eye movements tilt the visual scene orientation on the retina and thus play

a critical role in visual perception of upright. Here we simultaneously measured perceptual estimate of upright and ocular torsion during static head tilt (known as ocular counter-roll). There was a drift in upright estimates over time consistent with an adaptive, perceptual bias during head tilt. The ocular torsion, however, did not change significantly, nor did it correlate with the drift in upright estimates. Here we discuss these findings with regard to the sensory inputs and central neural mechanisms involved in perception of upright.

SYMP 42

Vestibular Loss and Spatial Cognitive Decline in Aging Adults

Yuri Agrawal

Johns Hopkins School of Medicine

Vestibular function declines with age. We will review recent evidence showing that in healthy older adults, lower vestibular function was specifically associated with reduced spatial cognitive skills, such as the ability to mentally rotate images or recall spatial relationships. Moreover, we will extend these associations to older adults with dementia, and review evidence that vestibular loss is more common among individuals with dementia relative to age-matched controls, particularly among individuals with dementia who exhibit spatial disorientation and abnormal motor behavior. Finally, we will discuss whether impaired spatial cognition mediates the relationship between vestibular loss and another feared geriatric outcome – falls.

In Vitro Model Technologies for Hearing Regeneration and Ototoxicity Protection

SYMP 43

Microengineered Physiological Biomimicry: Human Organs-on-Chips

Dan Dongeun Huh

University of Pennsylvania

A paucity of predictive models that recapitulate structural and functional complexity of human organs poses major challenges in virtually all areas of life science and tech-

nology. This talk will present interdisciplinary research efforts focused on leveraging unique capabilities of microfluidics and microfabrication to develop microengineered biomimetic models that reconstitute complex structure, dynamic microenvironment, and physiological function of living human organs. Specifically, I will talk about i) a bioinspired microsystem that mimics the structural and functional complexity of the living human lung, ii) an organ-on-chip microdevice that emulates the ocular surface of the human eye, and iii) microengineered physiological models of human reproductive organs

SYMP 44

An In Vitro Model of the Inner Ear

Else Vedula¹; Danielle R. Lenz²; Abigail Spencer¹; Brett Isenberg¹; Tj Mulhern¹; Albert Edge³; Erin E. Pararas¹; Jeffrey T. Borenstein¹

¹*Draper*; ²*Eaton-Peabody Laboratories, Massachusetts Eye and Ear Infirmary, Boston, MA, USA*; ³*Department of Otolaryngology, Harvard Medical School, Boston, MA, USA, and Eaton-Peabody Laboratory, Massachusetts Eye and Ear Infirmary, Boston, MA, USA*

Sensory hair cell (HC) physiology, including differentiation, functional mechanisms, and response to toxicity are poorly understood due to the challenge of studying them outside the body. An in vitro platform that supports primary HC viability, attachment and replication of the in vivo architecture of the inner ear is needed to better culture and study HCs. We have begun to explore the effect of controlled mechanical stimuli, such as surface topography and fluid flow, on primary inner ear progenitor cells in vitro. Engineered microenvironments were designed and fabricated using hot embossing and traditional soft lithography techniques. LGR5+ cochlea progenitor cells were expanded in vitro, cultured in the engineered microenvironments and differentiated into Myosin7a- and Atoh1-positive hair cells by targeting known signaling pathways with small molecules. We have previously reported that nanotopographic patterns on planar and porous substrates provide important cues to enhance progenitor cell adhesion in vitro. Here, we show that LGR5+ cochlea progenitor cells cultured in formats like topographically-patterned Transwell inserts differentiate and show significant increase in myosin7a and TMC1 when compared to non-differentiated controls. We aim to leverage our preliminary results to exploit an in vitro model of inner ear sensory epithelia to investigate mature HC function and response to external stimuli. This can include integrating electrical sensing to record changes in hair cell potential after exposure to fluid flow. It can also include quantification of HC viability and response to known ototoxic stimuli like aminoglycosides

or cisplatin. Our engineered microenvironment plus differentiated progenitor cells provides an in vitro model to develop robust assays, incorporate integrated functional metrics and control spatial differentiation of cells for tissue engineering and toxicity evaluation applications.

SYMP 45

In Vitro Studies of Intercellular Signaling in the Inner Ear

Lisa Cunningham¹; Lindsey May¹; Elyssa Monzack²; Andrew Breglio²; Shimon Francis²

¹*National Institute on Deafness and Other Communication Disorders, NIH*; ²*National Institute on Deafness and Other Communication Disorders*

Emerging data indicate that surrounding cell types, including supporting cells and macrophages play critical roles in the survival, death, function, and phagocytic removal of sensory hair cells in the inner ear. These cell-cell interactions require that supporting cells and macrophages are in constant communication with hair cells. Intercellular signaling can be mediated by diffusible signals and/or by signals requiring cell-cell contact. We have used a variety of techniques including co-cultures, live imaging, and cell type-specific manipulation of gene expression to examine intercellular signaling in whole-organ cultures of utricles from mature mice. The utricle preparation serves as an in vitro model system of mature mammalian hair cells, supporting cells, and resident macrophages in their native tissue architecture. The disadvantage of the utricle preparation is the small size of the organ, which results in low yields of cells and cellular components. Our current studies use the utricle model system to examine signaling via secretory exosomes as well as signals that mediate the phagocytic engulfment of dead hair cells. These in vitro techniques allow us to examine the intercellular signals that are required for hair cell survival and function.

This work is supported by the NIDCD Division of Intramural Research.

SYMP 46

The Extracellular Matrix Scaffold of the Scala Media in the Mouse and Human

Peter Santi¹; Alec Brown¹; Sebahattin Cureoglu¹; Helge Rask-Andersen²

¹University of Minnesota; ²Uppsala University

The Extracellular Matrix Scaffold of the Scala Media in the Mouse and Human

Peter A. Santi, Ph.D., Alec Brown, Sebahattin Cureoglu M.D., Helge Rask-Andersen M.D., Department of Otolaryngology, University of Minnesota, Minneapolis, MN 55455, Department of Surgical Sciences, Section of Otolaryngology, Uppsala University Hospital, Uppsala, Sweden, 751 85

It is well known in mammals that cochlear hair cells and spiral ganglion neurons are postmitotic and do not regenerate. Furthermore, loss of fibrocytes in the spiral limbus and ligament occurs after intense sound exposure and ototoxic drug administration, and their loss also diminishes hearing. In order to restore hearing after cell loss, various approaches are being explored to either induce remaining cells to regenerate, or to transform and implant stem cells to become functional auditory cells. In addition to sensory elements of the cochlea, the extracellular matrix (ECM) likely plays an important role in normal hearing. However, we know little about its 3D morphology or its interaction with cochlear cells. In other tissues, the ECM has been shown to be directly involved in proliferation, differentiation, and polarization of epithelial cells. The cochlear ECM underlies the organ of Corti, surrounds nerves and spiral ganglion neurons, and forms an extensive matrix around fibrocytes of the spiral limbus and ligament. In order to further investigate the cochlear ECM in the mouse and human, we have developed a new method involving the detergent extraction of cochlear cells while preserving the ECM. Decellularized cochleas were examined by scanning thin-sheet laser imaging microscopy (sTSLIM) and scanning electron microscopy. After decellularization, the basilar membrane, spiral limbus and spiral ligament, and the bony structures surrounding the membranous labyrinth are present and easily recognizable. The organ of Corti, spiral ganglion neurons, and the epithelial cells lining the endolymphatic surface of the scala media were not present. A novel, spirally distributed structure on the endolymphatic surface of the basilar membrane was revealed after decellularization. Cells of the stria vascularis were removed but the basement membrane of the capillaries of the stria vascularis was present. Notable differences in the ECM of the mouse and human cochleas were observed and will be presented and discussed in this presentation.

Funding: NIDCD U24-DC011968, OTOSTEM 603029

Hair Cells - Anatomy and Physiology

PD 71

Plastin 1 Widens Stereocilia by Transforming Actin Filament Packing from Hexagonal to Liquid

Peter Barr-Gillespie¹; Jocelyn Krey¹; Rachel Dumont¹; Evan Krystofiak²; Sarath Vijayakumar³; Francisco Rive-ro⁴; Bechara Kachar²; Sherri Jones³

¹Oregon Health & Science University; ²National Institute on Deafness and Other Communication Disorders;

³University of Nebraska-Lincoln; ⁴University of Hull

With their essential role in inner-ear function, stereocilia of sensory hair cells demonstrate the importance of cellular actin protrusions. Actin packing in stereocilia is mediated by crosslinkers of the plastin, fascin, and espin families. Indeed, espin (ESPN), plastin 1 (PLS1), and fascin 2 (FSCN2) have each been reported to be abundant in hair cells. Previous work showed that mutations in *Espn*, *Fscn2*, and *Pls1* all cause hearing loss, which manifests at different developmental ages for each mutant line. While deaf jerker mice—bearing a null mutation in *Espn*—lack vestibular function, little is known about mice lacking *Pls1* or *Fscn2*. To better understand the role of PLS1 and FSCN2 in stereocilia function, we used previously-described *Pls1*^{-/-} mice, as well as the B6.D2-*Fscn2*^{R109H} mouse line, referred to here as *Fscn2*^{R109H}, which produces a mutant form of FSCN2 that can bind to but cannot cross-link actin filaments. We also generated double mutant mice that lacked PLS1 and had no functional FSCN2 (*Pls1*^{-/-} *Fscn2*^{R109H/R109H}). We found that thresholds for vestibular evoked potentials were modestly elevated (sensitivity was decreased) in *Fscn2*^{R109H/R109H} mice but were more substantially elevated in *Pls1*^{-/-} mice. *Pls1*^{-/-} *Fscn2*^{R109H/R109H} mice were also strongly affected, with VsEP thresholds that were only slightly elevated beyond *Pls1*^{-/-} mice. Using targeted and shotgun mass spectrometry, we found that PLS1 was the second-most-abundant protein of utricular bundles, considerably more abundant than FSCN2 and ESPN, and that bundles lacking PLS1 had unaltered levels of other crosslinkers. Using confocal and super-resolution imaging, we found that stereocilia from *Pls1*^{-/-} mice were significantly thinner and shorter than those of wild-type mice; stereocilia from *Fscn2*^{R109H/R109H} mice, however, had wild-type dimensions. Double mutant stereocilia had dimensions that were similar to *Pls1*^{-/-} mice. The genotypes varied dramatically, however, in their actin-filament packing, which we examined using TEM imaging. While wild-type stereocilia had random liquid packing of their actin filaments, vestibular and auditory stereocilia from *Pls1*^{-/-} mice had actin packed in a hexagonal lattice. Actin packing in stereo-

cilia from Fscn2^{R109H/R109H} mice was similar to that of wild type, but packing of actin filaments from double mutants was also hexagonal. These results show that PLS1 generates liquid packing of stereocilia actin, even in the presence of FSCN2 and ESPN, and may be necessary for formation of stereocilia with larger diameters.

PD 72

The Usher Syndrome Type 1J Defective Protein, Cib2, is Involved in the Integrity and Functioning of the Auditory Hair Bundle

Aziz El-Amraoui¹; Vincent Michel¹; Matteo Cortese¹; Amel Bahloul¹; Alice Emptoz¹; Andrea Lelli¹; Typhaine Dupont¹; Michael R. Bowl²; Steve D.M. Brown²; Paul Avan³; Christine Petit⁴

¹*Institut Pasteur, Génétique et Physiologie de l'Audition, 2 INSERM UMRS-1120, Sorbonne Universités;* ²*MRC Harwell Institute, Mammalian Genetics Unit, Harwell Oxford;* ³*Laboratoire de Biophysique Sensorielle, Faculté de Médecine, Université d'Auvergne;* ⁴*Institut Pasteur, Génétique et Physiologie de l'Audition, 75015 Paris, France, 2 INSERM UMRS-1120, Sorbonne Universités, 5 Collège de France*

Defects in CIB2, the calcium- and integrin-binding protein 2, have been found to cause isolated deafness DFNB48, and deaf-blindness in Usher syndrome of type 1J (USH1J). Cib2/USH1J contains three predicted EF-hand domains, and has been shown to play key role in intracellular calcium signaling. So far, no Cib2-mutant mice have been reported, and the precise role of this protein in the inner ear is still elusive.

To investigate the role of Cib2 in the inner ear hair cells, and to clarify its contribution to the Usher syndrome, we generated two Cib2-deficient mice: one displaying an ubiquitous, early gene inactivation (Cib2^{-/-} constitutive knockout mice) and the other, a postnatal, hair cell-specific loss of Cib2 (Cib2^{fl/fl}Myo15-cre^{+/-} post-natal conditional knockout mice). Physiological, molecular, cellular and subcellular investigations were performed to achieve full characterization of these mice.

We found that both the ubiquitous deletion of Cib2 at embryonic stages, and its suppression in hair cells at postnatal stages result in profound hearing loss. Unlike in USH1 mutant mice, the absence of Cib2, however, does not impair the early shaping of the hair bundle. The mechano-electrical transduction is totally absent in the auditory hair cells at postnatal day 7, and various hair bundle anomalies (loss of staircase pattern, kinocilium defects) were observed from P7 onwards. We

show that Cib2 is localized in the stereocilia, its absence causing the mislocalization of key hair bundle proteins.

Altogether, our findings led us to suggest that Cib2 is essential for both the development and maintenance of hair bundle structure and functioning. The cellular specificity of these hair bundle anomalies and their impact on clinical features of Usher syndrome will be discussed.

Research Funding

European Research Council (ERC) advanced grant "Hair bundle" (ERC-2011-AdG 294570), FP7 HEALTH-F2-2010-242013 (TREATRUSH), the French Agence Nationale pour la Recherche (ANR) as part of the second Investissements d'Avenir program (ANR-15-RHUS-0001), and LABEX Lifesenses [ANR-10-LABX-65]. LHW-Stiftung, FAUN Stiftung, Fondation Raymonde & Guy Strittmatter, Conny Maeva Charitable Foundation.

PD 73

Stretch-sensitive Channels in Cochlear Hair Cells

Robert Fettiplace; Maryline Beurg
University of Wisconsin-Madison

Throughout post-natal maturation of the mouse inner ear, cochlear hair cells display at least two types of mechanically-sensitive ion channel: normal mechano-transducer (MT) channels at the tips of the stereocilia that are activated by tension in inter-ciliary tip links, and unconventional stretch-activated channels on the top surface of the cells responsible for the previously reported reverse-polarity current. During development, the unconventional channels are present in both inner and outer hair cells at birth, preceding the appearance of the normal MT channels by about two days, and they are down-regulated by the end of the first week as the normal MT current develops to attain its adult amplitude. The aim of the work was to examine in more detail these unconventional stretch-sensitive channels. Single channels were recorded in cell-attached patches on the apical membrane of outer hair cells in isolated cochleas of neonatal wild-type mice (P0 - P5), and mechanical stimuli were delivered with a high speed pressure clamp via the patch electrode. The recordings revealed two categories of stretch-sensitive cation channel with unitary conductances of about 30 pS and 50 pS whose probability of opening was modulated by suction pressure. These conductance values are smaller than the normal MT channel, which under similar conditions at this age is ~70 pS. The activity of the larger stretch-sensitive channel displayed inactivation, with a time constant between 8 and 30 ms depending on stimulus level, and resembled the macroscopic reverse-polarity current. Ac-

tivity of the smaller-conductance channel was sustained throughout the pressure stimulus. The reverse-polarity current evoked under a variety of conditions, but not the normal MT current, was suppressed by whole-cell recordings with pipette solution containing high Ca²⁺ concentration. This suggests that the unconventional channels are inhibited by Ca²⁺ influx via the newly-appearing normal MT channels. The roles of neither type of stretch-sensitive channel, nor their relationship to the normal MT channel, are known.

PD 74

Overstimulation-induced Damage to Stereocilia Tips Causes Loss of Resting Tension in the Mechano-transducer of the Mammalian Auditory Hair Cells

Gregory I. Frolenkov¹; Ruben Stepanyan²; Anthony J. Ricci³; Mike Grossheim⁴

¹*Dept Physiology, University of Kentucky;* ²*Department of Otolaryngology - HNS, Case Western Reserve University;* ³*Stanford University, School of Medicine, Department of Otolaryngology;* ⁴*Dept. Physiology, University of Kentucky*

It is presumed that the mechanosensory machinery in the stereocilia bundles of the inner ear hair cells is extremely vulnerable to intense mechanical stimulation. Damage to the stereocilia bundles has been identified as a hallmark of noise-induced hearing loss for more than two decades. Yet, it is still unknown what exactly is damaged within the hair cell mechanotransduction machinery and whether these damages are repairable. Here we investigated the effects of intense (>1 μ m) stereocilia deflections on the mechano-electrical transducer (MET) current and stereocilia ultrastructure in inner hair cells (IHCs) of organ of Corti explants from young postnatal mice. During overstimulation, we observed an abrupt decrease in the resting open probability of the MET channels, loss of so-called "slow adaptation", and gradual reduction of MET current amplitude. We also observed a gradual appearance of a "reverse" transduction, i.e. activation of the transducer channels by normally inhibitory deflections of the hair bundle. Under whole-cell patch-clamp conditions, we did not observe recovery of overstimulation-induced MET changes within at least an hour. However, these changes seem to recover after incubation at 37°C for 24 hours. Scanning Electron Microscopy (SEM) examination of similarly overstimulated IHCs revealed ~30% reduction in tip links, which was consistent with the overstimulation-induced reduction of maximal MET current. Imaging of calcium entry into individual stereocilia showed that MET current in the mechanically overstimulated IHCs is still mediated by transducer channels at the shorter row stereocilia, including a few cases of "reverse" transduction. To explore

the ultrastructural basis of overstimulation-induced MET changes, we used focused ion beam (FIB) milling and backscatter SEM imaging to obtain serial sections of stereocilia at 20 nm thickness in fast-frozen freeze-substituted organ of Corti explants. Three-dimensional FIB-SEM revealed an increased gap between the plasma membrane and underlying cytoskeleton at the sites of tip and side link attachments in mechanically overstimulated stereocilia, indicating disruption of either cytoskeletal linkages to the plasma membrane or stereociliar cytoskeleton. These visible damages may result in the loss of resting tension of the MET apparatus and re-distribution of mechanical forces in the plasma membrane, which could explain the observed changes of the MET current after overstimulation. Thus, ultrastructural damages to the stereocilia tips may represent the earliest event in noise-induced hearing loss, in addition to the potential loss of the tip links.

Supported by NIDCD (DC008861 and DC014658 to G.I.F., DC003896 to A.J.R., and DC015016 to R.S.)

PD 75

Inner Hair Cell Bundle Movements Characterized in situ with Mechanical Stimulation of the Stapes

Yanli Wang¹; Charles Steele¹; Sunil Puria²; Anthony J. Ricci³

¹*Stanford University;* ²*Massachusetts Eye and Ear, Harvard Medical School;* ³*Stanford University, School of Medicine, Department of Otolaryngology*

Introduction

The stimulation of inner (IHC) and outer hair cell (OHC) bundles drives IHC synaptic release and OHC electromotility. Recent data demonstrates that the mode of hair bundle stimulation dramatically effects the transducer currents generated and so is predicted to alter cell function. The in vivo stimulation mode is unknown for both IHC and OHC bundles. OHC bundles are embedded in the tectorial membrane (TM) and IHCs are not, suggesting that the mode of stimulation will be different for these cell types. Recent data demonstrating the lack of coherence between stereocilia of cochlear hair bundles, makes predicting hair bundles movements less reliable. Thus the goal of the current work is to directly measure bundle movements in situ where the natural anatomical relationships are retained.

Method

Mouse cochlea were excised and imaged under a bright field microscope equipped with a high-speed camera (Phantom Miro M320S). The basilar membrane (BM) was accessed from scala media and scala tympani by making holes on the top and bottom of the cochlea bone

respectively. Reissner's membrane was also opened from the stria vascularis. Hair bundles were visualized with high power 488 nm diode illumination, under 100x 1.0 NA objective (Olympus). BM motion was generated by pushing the stapes with a piezo stack at 1 kHz, while the high-speed camera recorded at 10k frames per second. Videos are recorded at different depths between TM and BM, and analyzed using Imaris (Bitplane 8.3.1) for IHCs stereocilia motion, with cross-correlation for stapes and cochlea bone motion.

Results

The stapes followed the piezo stack movement at 1 kHz. With magnitude of ~200 nm at the stapes, the magnitude of the IHC stereocilia is as high as 18 nm. The motion of the cochlear bone during stimulation is below the noise floor of the data processing algorithm. Data show that IHC bundles move in the direction aligned with the collagen fibers in the TM, and their stereocilia show a small degree of splay.

Conclusions

The natural stimulation of IHC bundles is not uniform throughout the bundle supporting the idea that hair bundle coherence will shape the transducer current output.

[Work supported by R01 DC07910 and R01 DC0003896 from the NIDCD of NIH.]

PD 76

Quantitative Optical Nanophysiology of Presynaptic Ca²⁺ Signaling at Inner Hair Cell Active Zones

Jakob Neef¹; Tzu-Lun Ohn¹; Nicolai T. Urban²; Thomas Frank¹; Stefan W. Hell²; Katrin Willig³; Tobias Moser⁴

¹Institute for Auditory Neuroscience, University Medical Center Goettingen; ²Department of NanoBiophotonics, Max Planck Institute for Biophysical Chemistry, Goettingen; ³Nanoscale Microscopy and Molecular Physiology of the Brain (Exc171/CNMPB) c/o Max Planck Institute of Experimental Medicine, Goettingen; ⁴Institute for Auditory Neuroscience and InnerEarLab, University Medical Center Göttingen

Background

In inner hair cells (IHCs), sound-evoked Ca²⁺-influx triggers the release of synaptic vesicles at the presynaptic active zones (AZs) to transmit the signal to the spiral ganglion neurons of the auditory nerve. A quantitative characterization of presynaptic Ca²⁺ signaling is critical for understanding synaptic transmission and the conversion of sound stimuli into firing patterns of the auditory nerve. However, this has remained chal-

lenging to establish at the required nm-scale resolution. Here, we have quantified the number and arrangement of Ca²⁺-channels and measured the local Ca²⁺ concentration at AZs of mouse cochlear IHCs, with novel techniques using confocal and stimulated emission depletion (STED) microscopy.

Methods

We measured the arrangement of Ca²⁺ channel clusters in fixed tissue using 2D- and 3D-STED microscopy. In two alternative approaches, we estimated the number of Ca²⁺ channels at individual AZs using either optical fluctuation analysis or local Ca²⁺ deprivation by iontophoretic application of EGTA. Establishing STED Ca²⁺-imaging we analyzed presynaptic Ca²⁺-signals at the nanometer scale in living cells. Additionally, we measured local Ca²⁺-concentrations at IHC AZs during depolarization by performing fluorescence lifetime analysis.

Results

We found Ca²⁺ channels to be arranged in mostly linear clusters of typically ~70 nm width and 100-600 nm length, containing 30-360 individual channels. Using STED Ca²⁺ imaging, we found confined elongated Ca²⁺-domains at normal AZs, whereas Ca²⁺-domains were spatially spread-out at the AZs of bassoon-deficient IHCs. We approximated the average Ca²⁺ concentration to reach ~17 μ M within the 2D STED point spread function, a value which was well matched by a mathematical model of the IHC AZ that was constructed based on the previous measurements.

Conclusions

We established several novel techniques to quantify the number and arrangement of Ca²⁺ channels at AZs and propose that IHCs form presynaptic Ca²⁺-channel clusters of similar density and layout but scalable length, thereby varying the number of Ca²⁺-channels among the AZs.

PD 77

GCaMP5G-tdTomato Transgenic Mice Reveal Calcium Microdomains and Modulation in Vestibular Hair Cells

Holly A. Holman; Micah Fereck; Richard D. Rabbitt
University of Utah

Introduction

We report on calcium signaling in hair cells and neurons of the crista ampullaris and utricle using a transgenic mouse line Gad2-Cre::GCaMP5G-tdTomato [1]. Swept field confocal microscopy was used to image [Ca²⁺] modulation in labyrinths ex vivo from adult mice, in response to physiological hair bundle deflection from ei-

ther micromechanical movement or chemical stimuli. In semicircular canals, spatially localized $[Ca^{2+}]$ transients were observed and quantified at the extreme tips of stereocilia, the apex of hair cells, in microdomains at the base of hair cells, and in postsynaptic terminals.

Methods

Hair bundles were either stimulated with a fluid jet directly attached to a picospritzer or by piezoelectric micromechanical indentation applied to mimic physiological head rotation [2]. TdTomato fluorescence and GCaMP5G were imaged using a custom upright Scientifica microscope configured with Olympus optics and a fast swept field confocal imaging system (Brucker Nano Technologies). Images were collected through the intact membranous labyrinth or, in some cases, through a fenestration in the membrane. Stimuli were repeated over multiple Z-positions to resolve stimulus-evoked fluorescence transients in 3D. Custom software was written (WaveMetrics) to extract GCaMP5G $\Delta F/F$ and estimate spatially localized $[Ca^{2+}]$ transients.

Results

In the semicircular canals, $\sim 1\mu m$ deflection of the intact cupula revealed punctate increases in GCaMP5G fluorescence ($\Delta F/F$) at the tips of stereocilia located $\sim 40\mu m$ above the cuticular plate. $[Ca^{2+}]$ transients were restricted to the tips of stereocilia where MET channels are located and were not present in kinocilia [3]. Cupula deflection also evoked large $[Ca^{2+}]$ transients just below the cuticular plate, putatively colocalizing with the striated organelle [4]. Signal to noise was high, with $\Delta F/F$ often exceeding 2. Depolarization with application of KCl revealed punctate $[Ca^{2+}]$ transients in microdomains at the base of hair cells, likely reflecting opening of voltage gated calcium channels modulating synaptic release. Simultaneous recordings in presynaptic type I hair cells and their postsynaptic calyces revealed a delay in $[Ca^{2+}]$ in the calyx relative to the hair cell.

Conclusion

Preliminary results using adult vestibular organs of Gad2-Cre::GCaMP5G-TdTomato mice revealed highly localized time-resolved $[Ca^{2+}]$ transients at the tips of stereocilia, in microdomains of hair cells, and at synaptic terminals. This approach offers unparalleled spatial and temporal resolution to study calcium signaling in the vestibular system.

Funding

NIDCD R01 DC006685 (Rabbitt)

[1] Holman et al. (2017) ARO

[2] Rabbitt et al. (1995) J. Neurophysiol 73(6):2237

[3] Delling et al. (2016) Nature 531:656

[4] Vranceanu et al. (2012) PNAS 109(12):4473

PD 78

Functional Heterogeneity Underlies Sensory Encoding in Zebrafish Hair Cells

Qiuxiang Zhang; Jenny He; Candy Wong; Katie Kindt
National Institutes on Deafness and other Communication Disorders, NIH

Hair cells are the sensory receptors of both the auditory system and the vestibular system in the ears of all vertebrates. In hair cells, function is shaped by summation of local calcium signals that ultimately trigger vesicle release in order to encode a sensory stimulus. In zebrafish, hair cells are located in the inner ear and the lateral line system. The lateral line is made up of superficial clusters of hair cells called neuromasts. The goal of this study is use neuromasts as a model sensory organ to understand how sensory information is encoded in vivo. Using this model we were able to investigate how all hair cells and synapses coordinate to detect and transmit sensory stimuli.

We have developed several transgenic lines that express genetically encoded calcium indicators that allow us to stimulate and monitor localized calcium signals that reflect mechanotransduction or synaptic calcium in hair cells, as well as activity in the postsynaptic afferents. In addition, we use SyHy, an indicator to monitor hair-cell vesicle release. Overall, this is a very powerful system, where we can simultaneously record presynaptic and postsynaptic activity in vivo.

Our experimental results show that in response to stimulus, all hair cells have robust mechanosensitive calcium signals. In contrast, the synaptic calcium are extremely heterogeneous within a neuromast organ, with a subset showing a more robust and persistent synaptic calcium influx. It is only in hair cells with robust synaptic calcium that we observe vesicle release. Upon further investigation we found that that the functional heterogeneity at hair cell synapses does not result from afferent or efferent modulation. In addition, it is not related with the variation of hair cell ribbon numbers either. Instead, our pharmacological results suggest gap junctions may facilitate communication among cells in the neuromast organ, resulting in functional heterogeneity. In addition, damage to hair cells with robust calcium signal enables other hair cells significantly increase their calcium response, which may indicate that all hair cells are primed and competent to encode stimuli. From these results we hypothesize that not all hair cells may be required to encode sensory signals. The heterogeneity within the neuromast may play an important role in development and maintaining a healthy balance for encoding sensory information.

PD 79

RiboTag-Seq: A Comparative Analysis of Library Prep Approaches for Sequencing Low Input Translatome Samples

Yang Song¹; Beatrice Milon²; Sandra Ott³; Xuechu Zhao³; Lisa Sadzewicz³; Anup Mahurkar¹; Ronna Hertzano⁴

¹*Institute for Genome Sciences, University of Maryland School of Medicine, Baltimore, Maryland 21201, USA;* ²*Department of Otorhinolaryngology, University of Maryland School of Medicine, Baltimore, MD 21201, USA;* ³*Institute for Genome Sciences, University of Maryland School of Medicine, Baltimore, MD, USA;* ⁴*Department of Otorhinolaryngology, Department of Anatomy and Neurobiology, and Institute for Genome Sciences, University of Maryland School of Medicine, Baltimore, MD USA*

Background

The import of a cell type-specific approach in gene expression analysis is now well recognized in the ear field, resulting in the popular use of approaches such as fluorescence-activated cell sorting, and single cell RNA-seq. Cell type-specific ribosome pulldown using the RiboTag mice offers two unique advantages over the dissociation-based approaches: 1) the experimental procedure uses intact tissue, thus avoiding changes in gene expression induced by tissue dissociation or delay from procurement to RNA-extraction; 2) monitoring of protein synthesis in-vivo. However, the amount of total RNA obtained is often low.

Objective: To determine the best library prep protocol for RiboTag-IP RNA, when only 4ng of total RNA are used.

Methods

We obtained total and RiboTag-IP RNA, in three biological replicates. We tested the NuGen Ovation RNA-Seq system V2 and Clontech SMARTer Stranded Total RNA-Seq Kit (designed for < 10ng of total RNA), as well as the TruSeq RNA Library Preparation Kit V2 and NEBNext® Ultra™ Directional RNA Library Prep Kit for which we adapted the protocol to 4ng of starting material. An additional set of samples was processed using the TruSeq kit with 70ng, as a 'gold standard' control.

Results

TruSeq-processed samples had the best metrics overall, with similar results for the 4 and 70ng samples. The results of the NEB-processed samples were similar to TruSeq (Pearson correlation > 0.8), although the NEB approach detected 10% fewer features. All RiboTag-IP

samples had an increase in the intronic reads compared with the corresponding whole tissue, suggesting that the IP captures some immature RNAs. However, while the TruSeq/NEB-processed samples had up to 11% intronic reads, this increased to 22 and 41% with the NuGEN and Clontech kits, respectively. The Clontech-processed samples also had robust representation of ribosomal and non-coding RNAs scoring high RPKMs, as well as poor mapping statistics to non-ribosomal and non-miRNA genes (< 55%), leading to a low RPKM for protein coding mRNA. Last, while excellent separation was obtained between whole tissue and RiboTag-IP samples from TruSeq/NEB/NuGEN kits, the Clontech-processed samples could not be separated using hierarchical clustering.

Conclusions

RiboTag mice are a powerful tool for cell type-specific translatome analysis. When applied to the inner ear, the small amounts of starting material benefit from modified library prep protocols for optimal sequencing results. We adapted the TruSeq and NEB protocols for successful sample prep from 4ng, resulting in significantly superior results to those obtained with NuGEN and Clontech.

PD 80

Next-Generation Genetic Testing for Hearing Loss by Whole Genome Sequencing

Jun Shen¹; Qinghui Li²; Rong Chen³; Gang Jin²

¹*Brigham and Women's Hospital, Laboratory for Molecular Medicine, Harvard Medical School Center for Hereditary Deafness,;* ²*Cloud Health Genomics, Ltd., Shanghai, China;* ³*Department of Genetics and Genomic Sciences, Icahn School of Medicine at Mount Sinai, New York, NY, USA*

Gene therapy holds the promise of curing hereditary hearing loss, and accurate genetic diagnosis is a prerequisite. More than 150 nonsyndromic hearing-loss loci and over 600 syndromes involving hearing loss have been reported. However, fewer than half causative genes are known. Available clinical genetic tests could only solve 30-40% of all childhood hearing loss cases in developed countries, where 80% are estimated to have a genetic etiology. The lower-than-expected diagnostic yield is due to (1) insufficient information to support pathogenicity of identified variants in known genes, (2) inability to detect certain types of variants, e.g. deep intronic variants, copy number variants (CNV), and structural variants (SV), by whole exome sequencing (WES) or microarray alone, and (3) unknown genes associated with human hearing loss. Whole genome sequencing (WGS) can overcome these limitations, because it re-

veals information regarding the significance of identified variants, non-coding and unusual types of variants, and variants of novel genes. In this study, we evaluated the performance of WGS in identifying different types of genetic variants in known hearing-loss genes, its application to gene discovery, and cost-effectiveness in comparison to existing testing approaches. Human WGS data generated by Illumina next-generation sequencing technology of an average depth of 30x or more were analyzed. Shallow WGS data were simulated through random sampling of deep WGS data. Variants including small nucleotide variants (SNV), CNV, and SV were called and underwent a tiered variant interpretation process for hearing loss: Tier 1, exonic and splice site regions of known hearing loss genes; Tier 2, variants in topological associating domains and regulatory elements of known hearing loss genes; Tier 3, candidate genes based on animal models, molecular pathway predictions, and inner gene expression. As the depth of WGS increased, the accuracy of SNV calls and resolution of CNV and SV calls increased. WGS detected types variants that were identified as well as missed by targeted gene panels, WES, or microarray. Shallow WGS data were sufficient for large CNV and single nucleotide polymorphism (SNP) detection. SNP data would be useful for genome wide association studies and linkage analyses to generate evidence for variant interpretation. WGS was more comprehensive but cost less than WES and microarray combined. In summary, WGS offers a cost-effective comprehensive approach to genetic diagnosis and genomic research.

PD 81

The Gear Portal – Sharing and Displaying Gene Expression Now Simplified and Diversified

Joshua Orvis¹; Dustin Olley¹; Amiel Dror²; Michael C. Kelly³; Beatrice Milon⁴; Yang Song¹; Rani Elkon⁵; Anup Mahurkar¹; Ronna Hertzano⁶

¹*Institute for Genome Sciences, University of Maryland School of Medicine, Baltimore, Maryland 21201, USA;* ²*Department of Human Molecular Genetics and Biochemistry, Sackler School of Medicine, Tel Aviv University, Tel Aviv 69978, Israel.;* ³*Laboratory of Cochlear Development, NIDCD, NIH;* ⁴*Department of Otorhinolaryngology, University of Maryland School of Medicine, Baltimore, MD 21201, USA;* ⁵*Department of Human Molecular Genetics and Biochemistry, Sackler School of Medicine, Tel Aviv University, Tel Aviv, Israel;* ⁶*Department of Otorhinolaryngology, Department of Anatomy and Neurobiology, and Institute for Genome Sciences, University of Maryland School of Medicine, Baltimore, MD USA*

Next generation sequencing as a tool for recording gene expression has increased in popularity over the past decade, now extending also to single cell RNA-seq. While tissue processing, library preparation and sequencing are now both faster and more affordable, data sharing and visualization remain challenging. We previously introduced the gEAR portal (gene Expression for Auditory Research) as a website for dissemination, presentation and cross-comparison of cell type-specific gene expression in the public domain. Since its conception, the gEAR has evolved to allow many new features, including: 1) multiple forms of data visualization (graph, cartoon and violin plots); 2) a user-friendly data uploader; 3) user-defined control of private dataset security and sharing; 4) customized layouts; 5) graphic support for single-cell RNA-seq data; 6) an online manual and many additional features and updates.

The gEAR is a home and a portal for all members of the hearing research community. For those actively generating gene expression datasets, it allows visualization of their data in the context of other datasets, including single cell RNA-seq. For all other researchers, the gEAR is a continually-updating portal that can be utilized to answer questions from as simple as 'where is this gene expressed in the ear' to 'how does it change in published datasets'. The gEAR portal provides direct links to a variety of other resources for each gene query, and will soon allow more complex data-query to expand the accessibility and utility of gene expression datasets relevant to the community.

The gEAR portal is publicly available and can be accessed through <http://gear.igs.umaryland.edu>.

PD 82

HEar-Seq for Determining the Spectrum of Inherited Mutations for Deafness in the Israeli Jewish Population

Zippora Brownstein¹; Fábio Tadeu Arrojo Martins¹; Nada Danial-Faran²; Suleyman Gulsuner³; Maria Birkan¹; Lara Kamal⁴; Silvia Casadei³; Ofer Isakov⁵; Noam Shomron⁵; Bella Davidov⁶; Moshe Frydman⁷; Michal Sagi⁸; Michal Macarov⁸; Tzipora Falik-Zaccai⁹; Reuven Sharony¹⁰; Tom Walsh³; Moien Kanaan⁴; Stavit Allon-Shalev¹¹; Mary-Claire King³; Karen B. Avraham¹
¹*Department of Human Molecular Genetics & Biochemistry, Sackler Faculty of Medicine, Tel Aviv University, Tel Aviv, Israel;* ²*Department of Human Molecular Genetics & Biochemistry, Sackler Faculty of Medicine, Tel Aviv University, Tel Aviv;* *Genetics Institute, Ha'Emek Medical Center, Afula;* *Faculty of Medicine, Technion, Haifa, Israel;* ³*Department of Medical Genetics &*

Department of Genome Sciences, University of Washington, Seattle, WA, USA; ⁴Department of Biological Sciences, Bethlehem University, Bethlehem, Palestine; ⁵Department of Cell & Developmental Biology, Sackler Faculty of Medicine, Tel Aviv University, Tel Aviv, Israel; ⁶Department of Medical Genetics, Rabin Medical Center, Petah Tikva, Israel; ⁷Danek Gertner Institute of Human Genetics, Sheba Medical Center, Tel Hashomer & Sackler Faculty of Medicine, Tel Aviv University, Tel Aviv, Israel; ⁸Department of Human Genetics & Metabolic Diseases, Hadassah-Hebrew University Medical Center, Jerusalem, Israel; ⁹Institute of Human Genetics, Western Galilee Medical Center Naharia & Faculty of Medicine Galilee, Bar-Ilan U, Safed, Israel; ¹⁰Genetics Institute, Meir Medical Center, Kfar Saba & Sackler Faculty of Medicine, Tel Aviv University, Tel Aviv, Israel; ¹¹Genetics Institute, Ha'Emek Medical Center, Afula & Faculty of Medicine, Technion, Haifa, Israel

Deafness, or hearing loss, is due to a large and varied number of genes and mutations. As a result of this clinical and genetic heterogeneity, high-throughput and cost effective methods for detection are essential for optimizing diagnosis in both research and clinical settings. We previously developed a multigene panel approach, HEar-Seq, for identifying variants in all known human genes and human orthologues of mouse genes associated with deafness. We have used HEar-Seq to determine the spectrum of genes and alleles responsible for deafness in the Israeli Jewish and Palestinian Arab populations. Our current goal was to determine the magnitude and features of hereditary hearing loss in Israeli Jewish populations. We evaluated 65 families with hearing loss (62 non-syndromic and 3 syndromic) of various Ashkenazi, Sephardic and Middle Eastern Jewish ancestries. For 45 families, we identified the causal gene and mutation. The current design targeted 367 genes, including protein-coding genes, microRNAs and the human orthologues of genes causing deafness in the mouse. Mutations were found in 21 known deafness genes, including missense, indel, splice, nonsense and CNV variants. Causality was assessed both by consequence of the mutation and by co-segregation of the mutation with hearing loss in the family. A splicing mutation was found to cause deafness for the first time in the SLC12A6 gene, previously implicated in inner ear abnormalities in the mouse and in agenesis of the corpus callosum with peripheral neuropathy (ACCPN). The 20 unresolved families likely represent new genes for hearing loss, which are being explored further. These results will facilitate a strategy for how best to implement genetic evaluations and subsequent management by otolaryngologists, audiologists and speech therapists in the daily care of these patients.

PD 83

A RiboTag Database of Translated Proteins in Hair Cells

Xudong Wu¹; Rory Kirchner²; Jun Shen³; Lingsheng Dong⁴; David P. Corey¹

¹Harvard Medical School; ²Harvard Chan School of Public Health; ³Brigham and Women's Hospital, Laboratory for Molecular Medicine, Harvard Medical School Center for Hereditary Deafness.; ⁴Harvard Medical School, Department of IT Research Computing

Understanding gene transcription and translation in cochlear hair cells and spiral ganglion neurons can provide important insights into the basic mechanisms of hearing. Although advances in next generation sequencing of mRNA have produced a wealth of information on transcription in the inner ear, it is thought that only about 40% of the variation in protein concentration can be explained by mRNA abundance. Here, we assess protein translation in the inner ear, using immunoprecipitation of ribosomes from hair cells and spiral ganglion neurons.

We crossed the RiboTag mouse (Sanz et al., 2009), in which Cre-dependent recombination adds a hemagglutinin tag to a key ribosomal protein, to mouse lines with hair-cell- or spiral ganglion-specific Cre expression. We then immunoprecipitated tagged ribosomes along with their associated mRNAs at P0, P2, P4, and P7. Translated mRNAs were recovered and sequenced to produce translatoome databases. Additionally, we determined the translatoome in cochlear hair cells from different tonotopic positions (apical, middle, and basal segments) at P2 and P7. All data were obtained in biological triplicates or quadruplicates.

Using these datasets, we found new proteins enriched in hair cells and spiral ganglion neurons. We also discovered new genes that are differentially translated in high and low frequency regions. One of these, Pkhd111, is a deafness gene encoding a hair bundle protein (see companion poster). In comparing the RiboTag-based translatoome to our FACS-sorted transcriptome, we found high correlation but also significant differences. This database may be a rich resource for understanding hair cell and ganglion cell development and function.

Constitutive Activation of DIA1 (DIAPH1) via C-terminal Truncation Causes Human Sensorineural Hearing Loss

Yuzuru Ninoyu¹; Takushi Miyoshi²; Hirofumi Sakaguchi³; Naoki Watanabe⁴; Shin-ichi Usami⁵; Naoaki Saito¹; Shin-ichiro Kitajiri²; Takehiko Ueyama¹

¹Laboratory of Molecular Pharmacology, Biosignal Research Center, Kobe University; ²Department of Otolaryngology, Head and Neck Surgery, Graduate School of Medicine, Kyoto University; ³Department of Otolaryngology-Head and Neck Surgery, Kyoto prefectural University of Medicine; ⁴Department of Pharmacology, Kyoto University Graduate School of Medicine; ⁵Department of Otorhinolaryngology, School of Medicine, Shinshu University School of Medicine

DIAPH1 is one of the three isoforms of human homologue of *Drosophila* Diaphanous and encodes human DIA1 protein, which is involved in straight actin elongation through binding with activated Rho family GTPases. Mutation in the DIAPH1 gene (c.3634+1G>T) is known as a cause of autosomal dominant non-syndromic sensorineural deafness (DFNA1) in large Costa Rican kindred. It was hypothesized that the mutation would interfere with proper maintenance of the actin cytoskeleton in hair cells (HCs), affecting either the amplification of sound by HCs or the structure of stereocilia. However, the molecular mechanisms underlying DFNA1 has been unclear since the pedigree was firstly reported in 1997 (Lynch et al, 1997).

Here, we identified a novel DIAPH1 point mutation (c.3610C>T: p.R1204X), which results in early termination prior to the 4 sequential basic amino acids (RRKR1204-1207) in the diaphanous autoregulatory domain (DAD). This R1204X mutation was found in two unrelated Japanese families, and showed autosomal dominant progressive hearing loss in the high frequency range that began in childhood. This clinical manifestation is different from that of Costa Rica kindred showing a low-frequency hearing loss.

To investigate the pathophysiology of R1204X mutant, we performed several in-vitro experiments and found that DIA1(R1204X) behaved as a constitutively active due to the disruption of the autoinhibitory intramolecular interaction between the diaphanous inhibitory domain (DID) and the DAD. Fluorescence single-molecule speckle microscopy (SiMS) was used to visualize the actin elongation activity of DIA1(R1204X): constitutive activity of DIA1(R1204X) reveals frequent directional movement in live cells. Furthermore, we generated transgenic (TG)

mice expressing FLAG-tagged DIA1(R1204X) under control of the CAG promoter, which showed progressive hearing loss that began in the high frequency range. Cochlea of DIA1 (R1204X)-TG mice showed OHC-dominant HC loss and various types of deformities in stereocilia in the basal turn, which is consistent with the auditory phenotype. These data indicated that the basic region of the DAD mediates DIA1 autoinhibition, and that the disrupted DID-DAD interaction due to R1204X mutation is followed by activation of DIA1(R1204X) causing novel DFNA1.

In summary, we identified a novel DFNA1 subtype caused by constitutively active DIA1 mutant, DIA1(R1204X), and revealed its pathogenesis using in-vivo and in-vitro models. Further study using R1204X-transgenic mice will provide a molecular basis for the clinical feature of DFNA1.

Young Investigator Symposium: Limiting Factors in Current Cochlear Implants

SYMP 47

Intensity and Temporal Resolution Limits on Channel Contribution to Speech Recognition

Adam Bosen; Monita Chatterjee
Boys Town National Research Hospital

Previous work in listeners with cochlear implants has demonstrated that speech recognition can be improved by using psychophysical properties (such as modulation detection thresholds) to select individual channels for inclusion or exclusion from a MAP. However, it is unknown to what extent individual channels' properties are correlated with their contributions to speech intelligibility. Two experiments were designed to explore this issue in depth. The first measured the importance of each channel within their clinical MAP for speech intelligibility. In the second study, we are measuring the temporal modulation transfer functions (TMTFs) of a subset of those channels at clinically relevant stimulation levels. Channel importance was measured using acoustic sentence materials that were filtered to contain only random subsets of channels on each trial, and regression across trials estimated the main effect of each channel's presence on speech intelligibility. Channel importance was averaged across a population of listeners, and channels that had the most and least importance relative to the group average within different regions of the electrode array were selected for subsequent TMTF testing for each listener. TMTFs are measured via an adaptive three-alternative, forced-choice procedure with stimulation parameters selected to closely match individual listeners' processor settings. Modulation rates are varied from low rates (10 Hz) that primarily measure intensity resolution to high

rates (200 Hz) that estimate both intensity and temporal resolution. Because channels were selected based on speech recognition with clinical MAPs, TMTF measurements were made with stimulation parameters that were based on those MAPs. We hypothesize that each channel's contribution to speech intelligibility will be partly predicted by a unique combination of that channel's intensity and temporal resolution, as measured via TMTFs. By characterizing the relationship between each channel's importance for speech perception and its intensity and temporal resolution, it should be possible to identify the necessary resolutions for good speech recognition on a band-by-band basis, which could be used to select clinical programming targets.

SYMP 48

Pitch as a Function of Current Amplitude in Cochlear Implant Users

Ann E. Todd¹; David M. Landsberger²

¹New York University; ²New York University School of Medicine

Background

For cochlear implant users, place pitch is thought to play an important role in speech perception. This is evidenced by the fact that performance with multi-channel cochlear implants is better than with single-channel cochlear implants, and that listeners report a general increase in pitch as electrodes are stimulated from the apex to the base of the cochlea. However, anecdotal reports have suggested that in addition to place (and rate) of stimulation, amplitude of pulse trains has an effect on pitch. If this is the case, the pitch of electrical stimulation may unintentionally shift with changes in loudness. In the following experiment, we examined the effect of amplitude on pitch perception.

Methods

Ten cochlear implant users completed a pitch scaling task at each of six electrodes and nine different current amplitudes. Electrodes tested were distributed across the electrode array. Current amplitude was presented at 20 to 100 percent of the listener's dynamic range in 10 percent steps. Stimuli were constant-amplitude pulse trains presented at 900 pulses per second with pulse phase durations of 54 μ s. Participants also completed a loudness scaling task with the same stimuli.

Results & Conclusion

Electrodes located more toward the base of the cochlea were rated as higher in pitch. Pitch shifts with current amplitude varied across listeners and electrodes. Typically, an increase in amplitude either shifted the pitch higher or had little effect on pitch. Basal electrodes tended to provide larger pitch shifts as a function of ampli-

tude than apical electrodes. The results of the cochlear implant users will be compared to those of normal-hearing listeners in order to evaluate whether the pattern of changes in pitch with current amplitude is specific to electrical stimulation.

Support provided by NIH grant R01 DC012152 (Landsberger).

SYMP 49

Complex Pitch Perception with Limited Spectral Resolution: Implications for Cochlear Implants

Anahita H. Mehta; Andrew J. Oxenham

University of Minnesota

Background

Cochlear-implant listeners typically perform poorly in complex pitch perception tasks. This limitation in performance is thought to be mainly due to the restricted number of active channels and the broad current spread that leads to channel interactions and subsequent loss of precise spectral and temporal information. This study explores the limitations of complex melodic pitch perception using vocoder-based simulations of both the number of channels and the degree of channel interactions.

Methods

A paradigm designed to tap into listeners' abilities to explicitly extract pitch was used in four of the experiments. The stimuli were noise vocoded and were designed to require that the pitch was extracted from low-order spectrally resolved harmonics, rather than the temporal envelope or the spectral edge of the stimulus. Across three behavioral experiments, the number of spectral channels and the degree of channel interaction were parametrically varied, using both symmetric and asymmetric filter slopes. Additional experiments using pitch matching were carried out to get a better understanding of the listeners' percept of the complex vocoded stimuli.

Results

Overall, the results indicate that the number of channels required to extract complex spectral pitch is greater than previous studies have suggested. However, the factor of greatest importance is the amount of spectral overlap between channels (equivalent to current spread in CI). For symmetric vocoder filters, even with 64 channels, melodic pitch perception was not achieved with filter slopes of 72 dB/octave or less. For the asymmetrically shaped channels, performance was good with at least 64 channels, so long as one of the filter slopes was very steep (>100 dB/octave).

Conclusions

The results suggest that spectrally based pitch is unlikely to be generated in CI users without a substantial change in technology or and/or site of stimulation. The results highlight the limitations of pitch perception in current cochlear implants, in addition to shedding light on the cues that the normal (acoustic) auditory system uses to perceive complex melodic pitch. [Supported by NIH grant R01DC005216.]

SYMP 50

Cochlear Implants and Binaural Hearing

Alan Kan

University of Wisconsin-Madison

Binaural hearing enables sound localization abilities and provides a benefit for understanding speech in noisy environments. For patients who use bilateral cochlear implants, the benefits of binaural hearing are much less when compared with normal hearing listeners. This difference in performance can arise from a number of different factors ranging from patient pathology to engineering and signal processing. In this talk, results from various psychoacoustic experiments that have been conducted to systematically examine a number of these factors will be reviewed. I will also discuss the implications these results may have on clinical practice and the development of new signal processing strategies to improve binaural hearing for bilateral cochlear implants.

Work supported by NIH-NIDCD (R03 DC015321 to Alan Kan, R01 DC003083 & R01 DC008365 to Ruth Litovsky) and NIH-NICHHD (P30HD03352 to the Waisman Center).

SYMP 51

Robust Sound Localization Coding in Bilateral Cochlear Implants

Ben Williges¹; Tim Jürgens¹; Hongmei Hu²; Regina M. Baumgärtel²; Mathias Dietz³

¹*Medizinische Physik, Forschungszentrum Neurosensorik, and Cluster of Excellence "Hearing4All", Carl-von-Ossietzky Universität Oldenburg, Germany.;*

²*1 Medizinische Physik, Forschungszentrum Neurosensorik, and Cluster of Excellence "Hearing4All", Carl-von-Ossietzky Universität Oldenburg, Germany.;*

³*National Centre for Audiology, School of Communication Sciences and Disorders, Western University, London, Ontario, Canada.*

Introduction

Sound localization is an important factor in everyday life. Normal-hearing listeners can localize even in adverse listening conditions utilizing interaural level (ILD)

and interaural time differences (ITD). Bilateral cochlear implant (CI) users can make use of ILDs, but show poor ITD sensitivity, due to factors related to the CI speech coding (e.g., unsynchronized pulse-timing across CIs) as well as physiologic factors (low rate limit for ITD sensitivity). Thus, preserving ITD information in low-rate pulse patterns, or presenting an enhanced ITD, might improve CI users localization abilities.

Goals of the study

The goal of the study is to systematically evaluate the localization abilities of bilateral CI users in noise, when encoding speech either with natural or enhanced ITDs and ILDs by using a novel binaural cue enhancement algorithm.

Methods

Localization abilities of bilateral MED-EL CI users were assessed in acute laboratory testing via a research interface box, using short speech tokens processed with two different strategies.: The continuous interleaved sampling at 800 pulses per second (providing ILD cues), and a low-rate "peak-picking" strategy, which preserves perceptually exploitable timing information in the pulses. Additionally, a binaural beamformer that preserves interaural cues, and an algorithm for enhancing ILDs or ITDs were used. Localization discrimination was measured using a two-interval-two alternative-forced-choice procedure. Two speech stimuli were presented subsequently from different angles, spaced 20° apart, in random order from either -55°, 0° and 55° degrees. An isotropic background noise at +5 dB signal-to-noise ratio was used. The participants indicated whether the second speech token was to the right or the left of the first one. Additionally, speech-in-noise performance was assessed using an adaptive sentence test.

Results

Frontal localization was found to be more accurate than lateral localization. At least in some subjects, lateral accuracy was improved by using the time-preserving low-rate strategy without compromising speech intelligibility. At all angles and for both strategies the binaural beamformer increased the accuracy significantly. Only some subjects appear to benefit from an additional enhancement of ILDs or ITDs.

Conclusion

Delivering coherent, reliable ITD and/or ILD cues enables localization in bilateral CI users, especially, when the signal is coming from lateral angles. Robust localization, even in noisy situations, is possible using only ITD-cues in low-rate coding strategies and appropriate pre-processing.

This work is supported by DFG cluster of excellence EXC 1077/1 "Hearing4all", Advancing Binaural Cochlear Implant Technology (ABCIT, No. 304912) and DFG JU2858/2-1.

SYMP 52

Neural ITD Sensitivity and Temporal Coding with Cochlear Implants in an Animal Model of Early-onset Deafness

Yoojin Chung¹; Brian Buechel¹; Bertrand Delgutte²

¹Eaton-Peabody Laboratories, Massachusetts Eye and Ear; ²Harvard Medical School

Background

Although bilateral cochlear implant (CI) users experience benefits in sound localization and speech perception in noise over unilateral CIs, their sensitivity to interaural time differences (ITD) is still poorer than normal. This problem is especially acute at the high stimulation rates used in clinical CI processors and in those who lost hearing in early childhood. Here, we characterize temporal coding and ITD sensitivity of single neurons in the inferior colliculus (IC) of unanesthetized rabbits that were deafened as neonates.

Methods

Three Dutch-belted rabbits were deafened as neonates with daily injection of neomycin and then bilaterally implanted at 2-3 months of age. Beginning at adult age (6 months), their cochleas were electrically stimulated in the laboratory during single-unit recording sessions from the IC. Stimuli were periodic trains of biphasic electric pulses with varying pulse rates (20 – 640 pps) and ITDs (-2000 to +2000 μ s). The results are compared to measurements from adult-deafened rabbits (Chung et al., *J Neurosci.* 36:5520) to understand the effect of early-onset deafness on neural ITD sensitivity.

Results

IC neurons in early-deafened rabbits showed decreased sustained responses to pulse-train stimulation. Fewer neurons showed synchronized responses to pulse train stimuli at any rate in the early-deaf group (66%) compared to the adult-deaf group (83%). However, the maximum pulse rates that could elicit synchronized responses were similar between the two groups when the analysis was limited to synchronized neurons (early-deaf: median = 202 pps, adult-deaf: median = 182 pps). Fewer neurons showed significant ITD sensitivity in their overall firing rate (62%) in the early-deaf group compared to adult-deaf animals (76%). ITD sensitivity was lower for pulse rates above 80 pps in early-deaf animals compared to adult-deaf animals. Neural ITD discrimination thresholds in the early-deaf group were

poorer than thresholds in adult-deaf group for all pulse-rates tested.

Conclusions

Fewer neurons show synchronized responses and ITD sensitivity to pulse train stimuli in rabbits that experienced early-onset, long-term deafness. The degradation in ITD sensitivity in early-deaf animals is most acute at high pulse rates. The overall degradation of neural ITD sensitivity is consistent with difficulties encountered by human CI users who lost hearing early in life.

Funding

NIH grants R01 DC005775 and P30 DC005209.

SYMP 53

Effect of Uncertainty in Site of Spike Generation on Envelope Coding in the Electrically Stimulated Auditory Nerve

Suyash N. Joshi¹; Torsten Dau²; Bastian Epp³

¹Hearing systems, Technical University of Denmark;

²Hearing Systems group, Department of Electrical Engineering, Technical University of Denmark, 2800 Kgs.

Lyngby, Denmark; ³Hearing Systems, Technical University of Denmark

Background

Cochlear implants (CI) stimulate the auditory nerve fibers (ANF) with a train of charge-balanced biphasic pulses that are amplitude modulated by the envelope of the acoustic signal. The injected current produces depolarizing- and hyperpolarizing regions throughout the cochlea, enabling both the anodic and the cathodic pulse phases of biphasic pulses to generate a spike. Physiological recordings have shown that the cathodic phase generates a spike along the peripheral axon of the ANF and exhibits longer spike-latencies than spikes evoked by the anodic pulse phase generated along the central axon. As a result, responses to pulse-train stimulation exhibit bimodal spike-time distributions, reflecting an uncertainty related to the site of spike generation. To what extent the uncertainty in the site of spike-generation affects the fidelity of envelope coding is still unknown.

Methods

A computational model of the electrically stimulated ANF was used to quantify the effect of the uncertainty in the site of spike generation on the fidelity of envelope encoding. The effects of carrier pulse rate (Condition 1), additive noise (Condition 2) and inter-pulse interval jitter (Condition 3) were investigated. The uncertainty in the site of spike-generation was quantified using entropy. The fidelity of envelope coding was quantified by predicting sinusoidal modulation detection thresholds (MDT)

using an ideal observer analysis that discriminated between responses to unmodulated and modulated pulse trains. The predicted MDTs were compared to available psychophysical data in CI listeners.

Results

The predictions show that the model can successfully account for the trends in psychophysical MDTs: (1) an increase in carrier pulse rate resulted in an increase of MDTs at low and moderate stimulus levels; (2) the addition of the noise resulted in a decrease of MDTs only at low stimulus levels but an increase at higher stimulus levels and (3) the introduction of inter-pulse interval jitter led to a decrease of MDTs at moderate carrier pulse rates (1000 to 4000 PPS) but to an increase at low pulse rates (250 and 500 PPS). Least-square regression fits, relating predicted MDTs to entropy in the site of spike-generation, showed a significant correlation.

Conclusion

The increase of uncertainty in site of spike-generation leads to an impaired envelope coding in electrically stimulated ANFs and hence an increase of MDTs. The development of stimulation strategies which reduce the uncertainty in site of spike-generation may improve the envelope coding in electrically stimulated ANFs and hence the perceptual performance of CI users.

SYMP 54

Electrode-neuron Interface as a Limiting Factor in Cochlear Implant Efficacy

Jaime Undurraga¹; Rajeev Mathew²; Deborah Vickers²; Astrid van Wieringen³; David McAlpine⁴

¹Macquarie University; ²University College London;

³KU Leuven; ⁴Macquarie University

Introduction

The ability to understand speech in the presence of noise still remains as an important limitation for cochlear implant (CI) listeners. These limiting factors start at the peripheral level of the cochlea where current spread, neural survival, stimulus polarity and level, among other factors reduce representation of speech signals at the level of the auditory nerve. Understanding the perceptual effects of these factors on electrical hearing is necessary to develop better stimulation strategies.

This study evaluates the perceptual effects of varying pulse shape and stimulation level on pitch ranking. Additionally, electrically evoked acoustic complex change (eACC) responses are evaluated as an objective measure of pitch discrimination.

Methods

Four users of the CII or HiRes90k CI (Advanced Bionics) took part in a pitch ranking experiment where they had to rank which of two pulse trains – presented at the same loudness – was higher in pitch at different percentage of the dynamic range (DR). Pulse shapes consisted of symmetric anodic-first (SYMA), pseudomonophasic anodic (PSA), pseudomonophasic cathodic (PSC), and alternating pseudomonophasic pulse (ALTPS; consisting of PSA and PSC pulses presented alternately).

Additionally, 10 Advanced Bionics users took part in objective and behavioral discrimination measures. eACC recordings were obtained using a 66 channels EEG system. Stimuli consisted of 800ms pulse trains with a change in stimulating electrode imposed at 400ms.

A behavioral task assessed whether participants could discriminate the change of electrode by means of a 3-interval 2-alternative forced choice task.

Results

Pitch ranking using different pulse shapes and stimulation levels revealed significant interactions between pulse shapes and percentage of DR.

ALTPS pulse trains elicited a lower pitch than PSA and SYMA presented at the same rate.

As the level decreased, ALTPS were ranked lower than PSA or PSC and these lower than SYMA pulses. PSA and SYMA pulse trains presented at the same rate elicited a similar pitch whereas PSC pulse trains tended to elicit a lower pitch than that produced by SYMA pulse trains presented at the same rate.

The eACC was reliably observed after the change of stimulation electrode and correlated well with the behavioral discrimination task where poor behavioral discrimination was associated with poor eACC responses.

Conclusions

These data demonstrate that both polarity and stimulation levels have significant effects on the perceived pitch of an electrical pulse train. These results also demonstrated that the eACC can be reliably obtained and used to assess electrode discrimination in CI users.

Auditory Cortex II

PS 453

Tonotopic, Field-specific and Layer-specific Information Processing of Long-lasting Sustained Activity in Rat Auditory Cortex

Tomoyo I. Shiramatsu¹; Kenji Ibayashi²; Hirokazu Takahashi¹

¹Research Center for Advanced Science and Technology, The University of Tokyo; ²Graduate School of Medicine, The University of Tokyo

Sustained activities in the auditory cortex play an important role in auditory perception. However, they have received less attention because they do not exhibit distinct and reproducible responses compared to transient activities. Therefore, cortical representation of the sustained activities remains elusive while that of the transient activities, e.g., cortical subfield and tonotopy, have been well characterized in each layer of the auditory cortex. In the present study, we investigated whether and how sustained activities represent sound information in each layer by using machine learning. A microelectrode array with 96 recording sites recorded local field potentials (LFPs) from layer 2/3 or layer 4 of the rat auditory cortex under isoflurane anesthesia. To record sustained activities, we presented long-lasting pure tones (30-s duration, 60 dB SPL) with five frequencies (8, 10, 13, 16 and 32 kHz) for the recording from layers 2/3, or with four frequencies (12, 22, 32 and 50 kHz) for the recording from layer 4. Each pure tone was repeated 7–12 times in a pseudorandom order and interleaved with a 30-s silence. The recorded LFPs were bandpass filtered in five bands (theta, 4–8 Hz; alpha, 8–14 Hz; beta, 14–30 Hz; low-gamma, 30–40 Hz; high-gamma, 60–80 Hz), and we extracted 60–100 samples of band-specific power or PLV in each band. Then sparse logistic regression (SLR) was applied to discriminate sound-induced power or PLV from preceding spontaneous power or PLV. After discrimination, we obtained the discrimination accuracy, which indicates the percentage of successful discrimination from the test data. In the case of layer 4, we also investigated the characteristic frequency and cortical subfields of the informative recording sites. As a result in layer 4, the highest discrimination accuracy was achieved in high-gamma band. However, in all bands, mean discrimination accuracy was lower in layer 2/3 than layer 4, indicating ambiguous sound representation in layer 2/3. Moreover, in layer 4, the informative recording site of SLR had a characteristic frequency close to the test frequency, and tended to locate in the belt than in the core region. These results indicate tonotopic, field-specific and layer-specific representation of the sustained activities in rat auditory cortex. This work

was partially supported by Tateisi Science and Technology Foundation and KAKENHI (16H01604, 26242040).

PS 454

The Effects of Anesthesia, and Different Anesthetics, on EEG and LFP Recordings in Guinea-pigs

Christian Sumner; Oscar Woolnough; Joel Berger; Ben Coomber; Mark Wallace; Alan Palmer
MRC Institute of Hearing Research, University of Nottingham

Anaesthesia is widely used in in vivo studies of sensory neural processing. Previous studies of the effects of general anaesthesia on neurons in the auditory cortex have shown significant changes to frequency tuning and responses to basic features within the stimulus such as onsets and offsets. Studies of this nature have typically used a single anaesthetic agent, comparing awake and anaesthetised states, and it remains unclear to what extent the choice of anaesthetic agent will affect basic response properties of cortical neurons to sensory stimulation.

Electrophysiological recordings were made with chronically implanted, extradural electrodes, positioned over auditory and visual cortices, and penetrating electrodes in auditory cortex. Recordings were made both while awake and under a range of anaesthetic regimes including opiates, NMDA antagonists and GABA potentiators.

Recordings of spontaneous oscillations replicate the results of previous human studies, showing a rapid increase in power of low-frequency (< 10Hz) oscillations at loss of consciousness, suppression of high frequency activity and a shift toward criticality, with a higher proportion of unstable oscillatory modes being observed - effects which appear mostly independent of anesthetic regime. Responses to a range of basic sensory stimuli, such as auditory clicks and tones, display substantive differences in population level processing of even basic auditory stimuli between anesthetic regimes. These modulations range from -20% to +50% changes in onset response amplitude, up to 25ms peak latency shifts and up to 600% increases in offset response amplitudes. Neural responses to visual flashes demonstrated universal suppression of visually evoked potentials under all anesthetics and we also observed, under all anesthetics tested, near total abolishment of auditory-visual cross-modal interactions. Adapter-probe stimuli were also tested showing substantial modulation of adaptation recovery time constants, with diazepam slowing the release from adaptation and ketamine allowing faster recovery than when awake. Local field potentials were used to isolate changes occurring in primary auditory cortex, helping to explain the phenomena seen in the

EEG recordings and show changes in frequency tuning resulting from each anesthetic.

In conclusion, we have demonstrated that anesthesia has significant effects on systems level sensory processing and that the choice of anesthetic used for recording can have grossly different effects on the response to even simple sensory stimuli.

PS 455

Resetting the Phase of Cortical Oscillations Through Cortical Inhibitory Circuits

Andrew T. Landau; Wei Guo; Daniel B. Polley
Eaton-Peabody Laboratories, Massachusetts Eye and Ear Infirmary

Background

Neural excitability and perceptual awareness are linked to the phase of low-frequency oscillations in the cortical electric field. Oscillatory phase can be 'reset' by high-contrast bottom-up stimuli or top-down cognitive signals related to selective attention. Adaptive phase control can accentuate target stimuli, dampen distracting stimuli, and mediate the competing demands of detection versus discrimination. The neural circuit mediating phase resets has never been identified. Here, we identify an intracortical circuit that can control the phase of cortical oscillations.

Methods

We recorded from all six layers of the auditory cortex (A1) in awake, head-fixed mice using linear, multi-channel probes. Transgenic and/or viral expression strategies were used to express channelrhodopsin in select types of cortical neurons: Layer 6 corticothalamic (L6 CT), L5 corticocollicular, or somatostatin-expressing GABAergic interneurons (SST+). The phase and frequency of cortical oscillations was computed from the trans-laminar current source density (CSD) signal. Single units were identified by laminar location, regular or fast spike width (RS and FS, respectively) and by optogenetically "phototagging" L6 CT, or SST+ neurons. By cross-correlating spike times between single units relative to abrupt transitions in the phase and analytical amplitude of the CSD, we were able to infer changes in the flow of activity preceding oscillation reset events.

Results

Optogenetic activation of L6 CT or SST+ units induced strong rhythmic oscillations in the CSD that persisted for several cycles after laser offset. Activating L5 corticocollicular neurons induced a brief volley of spikes across the column but did not initiate rhythmic activity. Analysis of the spontaneously occurring spike-triggered CSD phase indicated that FS and SST+ interneurons orchestrated

reset events. Whereas a sub-population of FS units reliably spiked immediately prior to phase resets, SST spikes occurred at the center of the reset, just before the CSD pattern flipped polarity. Cross-correlation analysis of SST+ units and FS units demonstrated that FS spikes tended to lead SST+ spikes at a range of latencies that matched their temporal relationship to the phase reset.

Conclusions

These results suggest that a subpopulation of FS neurons mostly in layers 4-6 could initiate abrupt shifts in the phase of low-frequency columnar oscillations. FS 'resetter' neurons could be driven by L6 CT neurons but tended to lead, rather than lag, SST+ spikes. Bottom-up or top-down inputs could adaptively control the phase of columnar oscillations by selectively recruiting this neural population.

PS 456

Pupil Size Predicts Single-neuron Response Variability in Primary Auditory Cortex

Zachary P. Schwartz; Stephen V. David
Oregon Health and Science University

Cortical neurons show high trial-to-trial variability in their response to repeated sensory stimuli, which is typically treated as unexplained noise. Recent research indicates that luminance-independent fluctuations in pupil size predict membrane potential dynamics of single neurons in mouse auditory cortex (McGinley, et al. Neuron 2015). This finding suggests that pupil size is a reliable indicator of large-scale changes in brain state that modulate activity in sensory cortex. However, understanding of the relationship between pupil-related state changes and auditory neural coding is limited. We recorded pupil size and extracellular spiking activity in the primary auditory cortex (A1) of awake ferrets over multiple repetitions of natural sounds and tone-pip stimuli. Our data indicate that pupil size predicts variability in neural responses to sound. A simple regression model shows that pupil-related effects can be broken down into two components: an additive change in baseline firing rate and a multiplicative gain change. Pupil-related changes in baseline firing rate during sound presentation are correlated with changes in spontaneous activity, suggesting that the same circuit mechanism modulates both processes. Analysis of spectral tuning measured from tone-pip responses suggests that pupil-related variability in evoked responses is primarily explained by changes in global gain and that frequency tuning is relatively stable across changes in pupil-indexed state.

PS 457

Layer 5 and 6 Neurons Projecting to the Inferior Colliculus Comprise Two Distinct and Heterogeneous Populations in the Cortex in Mouse

Georgiy Yuditsev; Daniel Adolfo. Llano
University of Illinois at Urbana-Champaign

Top-down modulation is a powerful mechanism by which the brain can disambiguate signals arriving from the sensory periphery, and descending projections are believed to be an important anatomical substrate by which this modulation may occur. One set of descending projections - the corticocollicular projection - has recently garnered much attention due to its potential to alter response properties of cells in the inferior colliculus (IC). However, the anatomical organization of this pathway remains poorly understood.

The corticocollicular neurons emanate from two distinct bands of the auditory cortex - layer 5 and deep layer 6 - and differ in their morphology and biophysical properties. The current mouse study from our laboratory demonstrates significant heterogeneity in the global distributions of layer 5 and 6 corticocollicular neurons, with layer 6 generally covering a broader area of the cortex than layer 5. As confirmed by more detailed analysis of serial reconstructions obtained in *NeuroLucida*, we found that layer 6 cellular distribution is centered more ventrally and anteriorly than layer 5, also forming a rostro-ventral area in the cortex consisting only of layer 6 cells. Combining in vivo imaging in GCaMP mice, followed by a retrograde tracer injection and post-hoc anatomical reconstructions, we found the rostro-ventral area of layer 6 cells to be acoustically unresponsive to pure tones, noise or species-specific mouse calls. Further, small injections of an anterograde tracer (BDA) or retrograde tracer (CTb) into this area revealed its connections with the amygdala and a number of subcortical structures, including paralaminae thalamic nuclei.

These data extend previous findings and suggest that layer 5 and layer 6 corticocollicular projections have different organizations and, presumably, different roles in modifying inferior colliculus function.

PS 458

Laminar Recordings from Primary Auditory Cortex (A1) and the Posterior Auditory Field (PAF) in Rat

Matthew Banks¹; Nicholas Moran²

¹*University of Wisconsin – Madison*; ²*UW Madison, Department of Anesthesiology*

Introduction

We seek to understand how stimulus representation

and connectivity vary across auditory cortical fields in rat. Although in primates the hierarchical organization of auditory cortex is well established, with clearly delineated core, belt and parabelt areas, this organization is less clear in rodents. In rats, previous studies have shown that the posterior auditory field (PAF) has longer latencies and is less responsive to tones than primary auditory cortex (A1), the spatiotemporal pattern of stimulus-evoked activity in columns in A1 versus PAF, and the relationship between this activity, is unknown. Here, we compared synaptic current flow and spiking activity across the cortical laminae in rat A1 and PAF.

Methods

Simultaneous recordings from A1 and PAF in female Sprague-Dawley rats (n = 5, 4-6 months old) were obtained using chronically implanted 16 channel (1x16, electrode spacing 100 microns) laminar probes inserted orthogonally to the surface of the brain. During implant surgery, A1 was identified by a sharp frequency tuning and 10-15 msec spiking latency to the best frequency. PAF was identified by poor and broadly tuned tone responses, but robust spiking responses to band pass noise. Electrode arrays were mounted on microdrives and their positions adjusted to span the cortical laminae in each area. Animals were allowed to recover 1 week following surgery before recordings commenced. Local field potentials recorded in response to acoustic stimuli were used to estimate synaptic current flow via current source density (CSD) analysis. Multiunit activity (MUA) was recorded simultaneously to investigate input-output relationships in each cortical area.

Results

Laminar CSD profiles in response to single click stimuli in A1 were characterized by short, early sinks in granular layers at a mean latency of ~14 msec. Click CSD profiles in PAF were distinct from those in A1, with weaker, short latency granular sink and a much larger long latency sink (~25 msec) in infragranular layers. Spiking responses in A1 were strongest in granular and infragranular layers and occurred at latencies of 8.5-10 msec. Spiking in PAF was also strongest in granular and infragranular layers; however it was sparser and occurred at latencies 3-5 ms longer than in A1.

Conclusions

Differences between tuning properties and tone responses in A1 and PAF are consistent with previous findings. Latency differences and distinct CSD profiles are consistent with a hierarchical relationship between the primary field A1 and PAF. The longer latency sink in infragranular layers in PAF could reflect intracortical connectivity/processing.

PS 459

Impacts of Millisecond-order Onset Timing Difference of High Frequency Component in Spectrally Complex Sounds on Cortical Activity and Sensation

Masataka Nishimura; Wen-Jie Song
Kumamoto University

Background:

Natural sounds including vocalizations often contain complex frequency components. If high frequency components of a sound are filtered out, such as music from radio, rich sensation of the sound will be lost, although the meaning of the sound will be mostly preserved. It remains to be elucidated that how the brain extracts delicate acoustic information from wide-band complex sounds. Because high frequency components theoretically can carry precise timing information, here we hypothesized that slight onset timing difference of high frequency component in spectrally complex sounds has impacts on brain activity and our sensation of sounds. To test the hypothesis, we conducted animal experiments and psychological experiments in human subjects.

Methods:

Adult guinea pigs were used for animal experiments. Cortical responses to synthesized complex sounds were recorded with voltage-sensitive dye imaging techniques (Nishimura and Song, 2014). Given onset timing difference of high frequency component was 0 - 8 msec. For psychological experiments, 10 normal-hearing subjects participated in the experiment approved by the ethics committee in Kumamoto University. A tablet computer and headphone were used to interactively present the synthesized sounds. The onset timing difference was randomly chosen from 4 msec to 64 msec, logarithmically stepped, in the test sounds. Mutual information was calculated from subjects' responses and it was used for statistical tests of sensation difference.

Results:

Animal experiments demonstrated that high frequency part of guinea pig primary auditory cortex (> 8 kHz) had sensitivity to millisecond-order change of onset timing difference of high frequency component with the response modulation ratio (-1.9 %/msec, $p < 10^{-6}$), measured at peak of response. Meanwhile, the low frequency part had no significant sensitivity to the change (0.16 %/msec, $p = 0.60$). Psychological experiments demonstrated that subjects had a significantly different sensation to synthesized sounds having 4 msec onset timing difference in the high frequency component compared to those having no onset timing difference (0.0518 bit, $p < 0.001$). Larger timing difference gave larger sensation

difference (0.110, 0.259, 0.511, and 0.655 bit for 8, 16, 32, and 64 msec, respectively).

Summary:

Millisecond-order onset timing difference of high frequency component had significant impacts on both animal cortical activity and human sensation. Such slight difference in sounds and cortical sensitivity to the difference may be involved in the extraction of delicate acoustic information from wide-band complex sounds.

PS 460

A Two-photon Imaging Investigation of Tonotopy in the Ferret Auditory Cortex

Quentin Gaucher; Mariangela Panniello; Johannes Dahmen; Andrew J. King; Kerry Walker
University of Oxford

Tonotopic organization of the primary auditory cortices in mammals has been a widely accepted property for more than fifty years. This property has been demonstrated in numerous electrophysiological studies in a wide range of mammals, including rodents, cats, ferrets, primates and cetaceans. Nonetheless, recent studies in mice have challenged this fact. Two studies using 2-photon calcium imaging (2PI) of the activity of single cortical cells have shown that although tonotopic organization is visible at a large scale, neighboring neurons can have vastly different tuning properties (Bandyopadhyay et al. 2010; Rothschild et al. 2012). Data from our lab in mice also confirmed this result (Panniello et al., in review), but Issa et al. (2014) reported less local variation in frequency tuning. As 2PI studies of auditory cortex to date have all been carried out in the mouse, it remains unclear whether the "salt and pepper" tonotopy is a general feature of mammalian auditory cortex, or a peculiarity of mice. To address this controversy, we have developed technique to carry out, for the first time, 2PI imaging of the auditory cortex of a carnivore - the ferret. Each ferret ($n=5$) was injected with 100nl of AAV1 expressing a genetically encoded calcium indicator (GCaMP6m; Penn Vector Core) at several (8-10) locations in the primary auditory cortex (AI and AAF). Four weeks later, a craniotomy was performed above the injection sites, and a custom-made glass well (1 mm diameter) was sealed in the craniotomy. Image acquisition was performed using a commercial two-photon laser-scanning microscope (ThorLabs B-scope). Our typical imaging field was $200\mu\text{m} \times 200\mu\text{m}$, and between 100 - $400\mu\text{m}$ deep (layer II/III). Pure tones ranging from 1.2 - 41 kHz and from 40 - 100 dB SPL were used to derive the frequency response area (FRA) of individual cortical neurons. Our results show that although the classical tonotopic organization is visible at the large scale across the cortical surface, at the finer scale (i.e. within an imaging field) nearby neurons are

more varied in their frequency preferences. This result shows that the salt and pepper tonotopy of the mouse auditory cortex reported by previous 2PI studies can be generalized to the ferret auditory cortex and presumably to other mammals.

PS 461

Critical Dynamics in A1 Networks During Sound Processing in the Awake Mouse

Daniel E. Winkowski¹; Zac Bowen²; Saurav Seshadri³; Dietmar Plenz⁴; Patrick O. Kanold²

¹University of Maryland; ²The University of Maryland;

³NIMH, NIH; ⁴NIH, NIMH

The ability to detect and encode sensory stimuli hinges on the encoding capability of neuronal populations. While individual neurons in primary auditory cortex (A1) can show selectivity to stimulus features (i.e., sound frequency), the representation of sound information in populations of A1 neurons and the nature of populations activated by sound stimuli is unresolved. Self-organized criticality is a theory that describes dynamic systems, which operate at or near a critical point (i.e., balanced between order and disorder). This theory has been gaining traction in neuroscience and describes complex cortical network activity patterns as a simple system operating near a critical point poised between synchronous and weak activity propagation. Cortical population activity takes on the form of neuronal avalanches which can be described as cascades of activity bounded by periods of quiescence. At the critical point, the probability distribution of neuronal avalanche sizes, durations, as well as other features exhibit power law relationships. Theoretical studies show that many aspects of network function including dynamic range and information capacity are maximal at the critical point (i.e., in the presence of neuronal avalanches). Here, we tested whether sound processing in A1 neuronal populations obeys critical dynamics. We characterized spontaneous as well as sound evoked activity in A1 of awake mice using in vivo 2-photon calcium imaging of neuronal populations. We explore the relationship between properties of sensory stimuli, single cell responses, and population responses with respect to avalanches. We investigate the spectral tuning properties of neurons participating in avalanches in order to probe the relationship between criticality and sensory coding. On the population level, we found that avalanche statistics varied depending on the stimulus frequency and intensity of the presented sound. We speculate that stimulus frequency and intensity dependence reflected in avalanche size suggests that stimuli are encoded in distinct local subpopulations; not just single neurons. Our investigation provides insight into how neural networks containing differing pop-

ulations of neurons with varying firing rates stably encode information about sensory stimuli in the context of self-organized criticality.

PS 462

Auditory and Neuromodulatory Projections to the Mouse Basolateral Amygdala: A Retrograde Transport Study

Calum A. Grimsley; Jeffrey J. Wenstrup

NEOMED

The basolateral amygdala (BLA) is an important brain center for learning and analyzing the significance of sensory stimuli. The BLA responds to acoustic stimuli including social vocalizations, which are modified by other sensory or contextual cues. Our overall goal is to provide a framework for optogenetic stimulation of both auditory and neuromodulator inputs to the BLA in order to assess their relative roles in the analysis of social vocalizations by the BLA. One aim of this study was to identify, in mouse, the auditory inputs to the BLA. A second aim was to identify neuromodulatory inputs that may provide the contextual cues for the processing of acoustic communication signals.

Male CBA/CaJ mice (P90-P250, n=5) underwent surgery to deposit retrograde tracers into the BLA in each hemisphere, one side receiving a deposit of Fluoro-Gold the other a deposit of red beads. The tracers were given 5 to 7 days of transportation time. Animals were then perfused, brains were cut in coronal sections, and transport was investigated using fluorescent microscopy.

Auditory cortical neurons projecting to the BLA were primarily located in the ventral portion of auditory cortex, with very few or no labeled cells in presumptive primary or dorsal cortical areas. In the thalamus, labeling was observed in the dorsal and medial divisions of the medial geniculate body (MG) and adjacent areas. No labeling was observed in the ventral division of MG.

Retrograde labelling was observed in several nuclei associated with neuromodulatory functions: locus coeruleus (LC), the ventral tegmental area (VTA), the raphe and substantia innominata (SI). LC may contribute a noradrenergic input, VTA a dopaminergic and/or serotonergic input, the raphe a serotonergic input, and SI a cholinergic input. The majority of the connections from these nuclei were ipsilateral, with the exception of LC, which provides a bilateral projection.

The auditory connections to the mouse BLA support previous studies in other species that have reported both a ventral AC and a dorsal and medial MG connection to the BLA. The relative strength of these connections is yet

to be investigated but their existence indicates at least two sources for auditory information entering the BLA. These BLA auditory inputs may have distinct responsiveness or selectivity for social vocalizations. Further, these multiple auditory inputs allow for more complex auditory processing in the BLA. Neuromodulator input to BLA neurons may provide for context-dependent alterations in the response to social vocalizations.

PS 463

Differential Release of Neurochemicals in Mouse Basolateral Amygdala in Response to Negative and Positive Social Vocalizations

Zahra Ghasemahmad¹; Anthony Zampino¹; Muhammad M. Hossain¹; Jason R. Richardson¹; Jeffrey J. Wenstrup²

¹Northeast Ohio Medical University (NEOMED);

²NEOMED

Introduction:

Vocalizations reflect the emotional state of a sender and influence the emotional state and behavior of a listener. Previous studies indicate that the basolateral amygdala (BLA) contributes to the analysis of vocalizations and other acoustic stimuli. For this role, the BLA receives inputs from acoustic and other sensory systems, as well as neuromodulatory centers. Thus, neuromodulators within the BLA may play an important role in defining the meaning of social vocalizations and influencing a listener's behavior. This study examines release of neurochemicals into BLA in response to negative and positive social vocal sequences. The neurochemical levels are then related to concomitant changes in sound-evoked behavior.

Method:

Subjects were CBA/CaJ mice aged 3-6 months (n=6). After 2 consecutive days experiencing periods of restraint or mating, mice were implanted with a microdialysis probe into the BLA. On the day after implantation, mice were tested for levels of neurochemicals using microdialysis while their behavior was monitored with video recording. Animals were introduced into the test arena and allowed to stabilize for 3 hours. Then, baseline levels of neurochemicals were measured for 60 mins followed by a 30 min period of acoustic stimulation. Sounds consisted of previously recorded sequences of either restraint- or mating-related vocalizations. Behaviors of the subject were recorded before, during and after stimulus presentation. The dialysate samples were analyzed using high-performance liquid chromatography (HPLC) with electrochemical detection.

Results:

Exposure to vocal sequences associated with restraint resulted in a gradual increase in the level of extracellular norepinephrine and of dopamine metabolites within the BLA. In the first 10 minutes of sound presentation, these mice showed increased duration of freezing and dramatically decreased self-grooming behavior compared to the pre-stimulus period. These changes persisted for at least 60 minutes after playback ended. In contrast, exposure to vocal sequences associated with mating resulted in transient changes in the level of NE and the dopamine metabolite DOPAC. These animals displayed less change in the observed behaviors after sound presentation began.

Conclusion:

Vocal signals with positive and negative affect evoke differential release of neurochemicals into BLA. Vocal signals associated with restraint increase stress-related behaviors, confirming the communication value of these recently described sounds (Grimsley et al., 2016). Further, change in the release of neuromodulators that accompanies these vocalizations is very likely to affect the processing of subsequent acoustic signals in a context-dependent manner.

PS 464

Interference Effects Between Acoustic Stimulation and Intracortical Microstimulation in the Auditory Cortex of Guinea Pigs

Mathias B. Voigt¹; Andrej Kral²

¹Institute for AudioNeuroTechnology (VIANNA), Hannover Medical School, Germany; ²Hannover Medical School, DFG Cluster of Excellence Hearing4all

The cortical column integrates different information streams from many cortical and subcortical sources. Previously it has been suggested that part of this function depends on hearing experience (Kral and Sharma, 2012, TINS). The present study investigated whether targeted stimulation of one cortical layer may modulate auditory processing in the cortical column. By combining intracortical microstimulation (ICMS) with extracellular recordings on the same shank of a linear multi-electrode array in vivo we can show that a focused activation of the cortical network is possible with single ICMS pulses of sufficiently low current. Building on this possibility to differentially activate separate cortical strata, we examined the modulating effects of ICMS pulses in combination with physiological, acoustical stimulation.

Responses were recorded from the auditory cortex of Ketamine/Xylazine anaesthetized guinea pigs using 15 electrodes of a linear Neuronexus electrode array. ICMS was performed with single current pulses (monopolar,

biphasic, charge-balanced, cathodic-leading, 0.1–45 μ A, 200 μ s/phase) on the remaining 16th electrode of the shank. This electrical ICMS was combined with acoustic click stimulation (50 μ s condensation clicks, 40 dB above ABR threshold) with varying time delays between ICMS and acoustic click onset.

Analysis of the local field potential patterns showed non-linear interactions between the responses to the auditory and the electric stimulus. Current-source density analysis of the underlying cortical activation revealed complex interference effects, depending among others on the delay between auditory and electric stimulation. Although important in the electric only condition, the depth of ICMS had less of an influence on the local field potential response during combined stimulation. However, using a Morlet wavelet analysis, the strongest effect of combining ICMS and acoustic clicks was found to be a pronounced gamma band activation several 100 ms post stimulus which was completely absent in the auditory only condition.

Together this shows that applying short electrical ICMS currents is not only able to directly activate cortical networks, but also to modulate processing on longer timescales than would be expected from such focused sub-millisecond pulses.

Supported by Deutsche Forschungsgemeinschaft (Cluster of Excellence Hearing4all)

PS 465

Interaction of Spatial and Non-Spatial Cues in Auditory Stream Segregation in the European Starling Forebrain

Naoya Itatani¹; Georg M. Klump²

¹Cluster of Excellence Hearing4all, Animal Physiology and Behavior Group, Department for Neuroscience, School of Medicine and Health Sciences, University of Oldenburg; ²Cluster of Excellence Hearing4all, Animal Physiology and Behaviour Group, Department for Neuroscience, School of Medicine and Health Sciences, University of Oldenburg, D-26111 Oldenburg, Germany

Integrating or segregating sounds based on their acoustic features in the auditory system is crucial for auditory object formation. Non-spatial cues such as frequency spectra, temporal fine structure and the signal envelope are important for auditory stream segregation. Previously, auditory streaming based on tone frequency was behaviorally and physiologically measured by using an objective onset time shift detection paradigm (Itatani and Klump 2014). In the natural environment, however, multiple auditory cues are present and they will interact

in forming the streaming percept. We behaviorally and physiologically investigated how tone frequency cue and spatial position cue of the sound source affect stream segregation in the European starling (*Sturnus vulgaris*). We conducted operant Go/NoGo experiments with a repeated background to obtain an objective measure of stream segregation. Background stimulus was a sequence of ABA- triplets, where A and B represent 40 ms pure tones separated by a 40 ms silent gap and – indicates 120 ms silent period (total duration of one triplet was 320 ms). For the target triplet, the B tone onset time was delayed by 4, 12, 20, 28 or 36 ms reducing the duration of following silent gap accordingly. Animals were trained to react to the target with a Go response. Time shift detection is easier when the tones are heard as one stream. The non-spatial cue for stream segregation was introduced by varying the frequency difference between A and B tones ($\Delta f = 0$ or $\Delta f = 6$ semitones). For generating varying spatial cues, the A tone was always presented from the front and the B tone position was either the same as the A tone position or shifted to the side. Spike responses in the auditory forebrain were recorded while behavioral experiments were carried out.

The behavioral results showed that the time shift detection was worse for Δf of 6 semitones than for $\Delta f = 0$ semitones confirming previous results (Itatani and Klump 2014). Spatial position of the B tone source affected detection performance, showing a decline of performance as separation increased. The spatial and frequency cues independently affected the performance. An analysis of neuronal responses recorded in parallel to the behavioral response will reveal whether an interaction between effects of spatial and spectral cues on the representation of streaming stimuli can be observed in the starling primary auditory cortical area that corresponds to the behavioral results. The study was funded by the DFG (TRR31).

PS 466

Active Auditory Stream Segregation in the Secondary Auditory Cortex of Ferrets

Kai Lu¹; Jonathan Fritz²; Shihab Shamma³

¹University of Maryland; ²1) Neural System laboratory, Institute for System Research, University of Maryland, College Park, Maryland, USA; ³1) Neural System laboratory, Institute for System Research, 2) Electrical and Computer Engineering Department, University of Maryland, College Park, Maryland, USA

In a complex acoustic soundscape, successful detection of an acoustic target in a noisy background requires segregating it from other sound sources. Previously, we have proposed that interaction of temporal coherence

and attention could play an important role in segregating sounds. According to our model, during attentive listening to temporal coherent sounds, excitatory interactions between neurons at different coherent frequency channels would become enhanced, while listening to non-coherent sounds would lead to suppressive interactions among neurons at different frequency channels. Consistent with this hypothesis, our earlier work in primary auditory cortex (A1) showed that, during attentive listening, neural responses to temporal coherent sounds were significantly enhanced, while responses to non-coherent sounds were suppressed. In the current work, we hypothesized that greater effects would be seen in higher auditory areas. We tested this hypothesis in the dorsal posterior ectosylvian gyrus (dPEG) of ferrets, a secondary auditory area. Two ferrets were trained to restrain their licking to a waterspout during presentation of two-tone sequences, and to lick freely after the onset of target stimuli consisting of a cloud of random tone pips. The two-tone sequences were either alternating tones or synchronized tones, allowing us to detect the effect of temporal coherence. Single-unit responses to these stimuli were recorded during the task performance and during a passive listening state. As we expected, our results in dPEG showed a significant suppression in responses to alternating tones during task performance. In addition, this attention-induced suppression of responses to alternating tones was most prominent when the two tones were separated in frequency. This suppressive effect was much stronger in PEG than the suppressive effects we have previously described in the primary auditory cortex (A1). Our results suggest that segregation becomes more clearly expressed in secondary auditory cortical areas and thus that the dPEG may be a higher stage for auditory segregation in the ferret. .

PS 467

A Crucial Test of the Population Separation Model of Auditory Stream Segregation in Macaque Primary Auditory Cortex

Yonatan Fishman; Mitchell Steinschneider
Albert Einstein College of Medicine

Background:

According to the 'population separation' (PS) model of auditory stream segregation, alternating 'ABAB' tone sequences are perceived as a single stream when frequency-tuned neural populations in primary auditory cortex (A1) respond to both 'A' and 'B' tones, and as two separate streams when they respond exclusively to 'A' tones or to 'B' tones (Fishman et al., 2001). In the latter case, which occurs when their frequency separation is large or their presentation rate is fast, 'A' and 'B' tones activate largely separate neuronal populations in A1.

While supported by several neurophysiological studies, the PS model was challenged by a study in ferrets comparing A1 responses to sequences where 'A' and 'B' tones were presented either synchronously or in alternation (Elhilali et al., 2009). Under synchronous (SYNC) and alternating (ALT) conditions, the sequences are perceived as a single stream and as two separate streams, respectively. Accordingly, if the PS model of stream segregation is correct, then a difference in response patterns should be observed under these two stimulus conditions, with a significantly larger 'dip' in neural activity occurring in-between tonotopic locations tuned to frequencies of the 'A' and 'B' tones in the ALT condition than in the SYNC condition. Contrary to predictions of the model, no significant difference in the depth of the 'dip' was observed between ALT and SYNC conditions. These findings suggested instead a predominant role for 'temporal coherence' in stream segregation. The present study attempted to replicate these results in macaque A1, and thereby crucially test the PS model.

Methods:

We recorded neuronal population activity in A1 of awake macaques elicited by ALT and SYNC tone sequences using a stimulus design similar to that of Elhilali et al. (2009).

Results:

In contrast to findings of Elhilali et al. (2009), a significantly larger 'dip' in neuronal activity patterns was observed under ALT than under SYNC conditions, thereby paralleling the perceptual organization of the sequences and vindicating the PS model of stream segregation.

Conclusions:

Findings suggest that the reason why SYNC sequences tend to be perceived as a single stream is that they lead to reduced separation of 'A' and 'B' tone responses in auditory cortex. Possible neuronal mechanisms accounting for the results are considered. We conclude that while the present findings are still consistent with the temporal coherence model, the population separation model is sufficient to account for the perceptual organization of ALT and SYNC sequences.

PS 468

Learning Mid-Level Codes for Natural Sounds

Wiktor Młynarski¹; Josh H. McDermott²

¹*Massachusetts Institute of Technology*; ²*MIT*

Along the ascending auditory pathway sensory neurons become sensitive to progressively more complex features of sound. Neural feature selectivity has traditionally been characterized by spectrotemporal receptive

fields (STRFs). Because they are single, linear functions of the spectrogram, STRFs are limited as descriptions of selectivity of auditory neurons in higher regions of the brain. In particular, recent studies have described cortical neurons that are sensitive to combinations of more than one spectrotemporal feature. The nature of these complex representations remains poorly understood.

In this work we attempt to develop intuitions and predictions about mid-level codes in the auditory system. A starting point of our considerations is the Efficient Coding Hypothesis, which suggests that sensory neurons are adapted to the structure of natural stimuli. Inspired by successes of this methodology in the visual domain, we developed a hierarchical, statistical model that learns combinations of spectrotemporal features from natural stimulus statistics. In the first layer the model forms a sparse, convolutional code of spectrograms. Features learned on speech and environmental sounds resemble spectrotemporal receptive fields (STRFs) of mid-brain and cortical neurons, consistent with previous findings. In order to generalize from specific STRF activation patterns and model higher-order selectivity, the second layer encodes patterns of the time-varying magnitude of first layer coefficients. High-level units become selective to STRF combinations, thus forming a more abstract representation of sound.

Representations learned by the model reflect some known properties of auditory cortical neurons and give rise to new predictions about cortical representations of sound. For instance, we have found that second-layer units pool activations from up to dozens of first-layer units. They also often encode “opposing-dimensions”, being respectively excited or inhibited by two types of stimuli with distinct spectrotemporal properties. To our knowledge, our model is the first attempt to predict mid-level auditory representations from high-order stimulus dependencies present in the natural acoustic environment.

PS 469

Revisiting Neural Connections in the Ferret Primary Auditory Cortex Using Adeno-associated Virus (AAV) Tagged with GFP

Victoria M. Bajo¹; Fernando R. Nodal¹; Alina Aaltonen²; Andrew J. King²

¹Oxford University; ²University of Oxford

The use of optogenetic tools in the ferret auditory cortex has provided an opportunity to review cortical connectivity by visualizing neurons expressing green fluorescence protein (GFP). Unilateral or bilateral AAV injections were performed in the primary auditory cortex (A1)

of anaesthetized ferrets using AAV8/CAG-ArchT-GFP or AAV8/CamkII-ArchT-GFP.

The survival time after injections ranged between 3 weeks and 30 months, with longer times corresponding to animals used for behavioural testing. GFP fluorescence in the brain tissue was visualized directly using fluorescent microscopy or after signal amplification using antibodies against GFP. In some sections GFP staining was made permanent using the ABC-DAB system.

Results were similar across cases independently of survival time, indicating that, in ferret tissue, 3 weeks is enough time for cortical cells to be transfected and express GFP in the cell soma, dendrites, axon and terminals, with no changes observed in GFP expression after longer survival times (at least up to 30 months).

Injections in A1 resulted in either homogenous staining throughout the cortical layers when AAV8/CAG-ArchT-GFP was used or a characteristic bi-laminar staining pattern, mainly concentrated in layers II/III and V/VI, when AAV8/CamkII-ArchT-GFP was used, revealing the transfection of either most of the neurons or only of excitatory pyramidal neurons when CAG or CamkII promoters were used, respectively.

Independently of the type of construct used, profuse terminal fields of corticofugal axons were observed in the medial geniculate body (MGB) and in the inferior colliculus (IC). Terminal fields in the MGB were exclusively ipsilateral, mainly concentrated in the ventral division and so profuse that it was possible to visualize axons and terminals surrounding putative thalamic cell bodies. Terminal fields in the IC were bilateral but with a clear ipsilateral predominance, with axons running parallel to the lateral surface of the IC in the external/lateral cortex and following the orientation of the fibrodendritic laminae in the central nucleus and dorsal cortex.

GFP-labelled axons in the ipsilateral auditory cortex created bands of terminal fields in the posterior pseudo-sylvian and suprasylvian fields, as previously described, and produced a mirror-like image of labelling in the contralateral auditory cortex.

Cortical labelling beyond auditory cortex was bilateral with a predominant ipsilateral component, and more profuse than previously reported with classical neural tracers, with terminal fields located in the orbital gyrus (dorsal), anterior (dorsal and lateral) and posterior sigmoid gyri, lateral gyrus (mainly dorsal and medial, but also posterior), and cingulate gyrus (medial).

PS 470

Analysis of the Representation of Interaural Phase Differences in Cortical Local Field Potentials

Joshua Goldwyn¹; Simon Jones²; David McAlpine³

¹Ohio State University; ²UCL Ear Institute; ³Macquarie University

Background

Interaural time differences (ITDs) are a critical cue for sound localization. Standard theories of binaural hearing (e.g. cross-correlation models) postulate ITD-based neural representations of sound location, but physiological constraints (the pi-limit) suggest that binaurally-sensitive auditory neurons may in fact represent interaural phase differences (IPDs).

Local field potentials (LFPs) can provide a population-level view of in vivo neural activity and shed light on the cortical representation of sound location. Here, we perform data analysis in combination with computational modeling to investigate the representation of ITDs/IPDs in cortical LFPs.

Methods

Stimulus and field potential recordings: We used an "adaptor+probe" paradigm in which adaptor sounds preceded probe sounds by one second. Probe and adaptor sounds were narrowband noise centered at 500 Hz with bandwidth of 400 Hz. Probe sounds had a fixed ITD and adaptor ITDs varied (-1500, -500, +500, or +1500 microsecond). Local field potentials (LFPs) in auditory cortex of anesthetized guinea pigs were recorded with a sixteen-channel NeuroNexus penetrating electrode. The electrode array was inserted in the low-frequency region of auditory cortex and spanned its depth.

Data analysis and modeling: We measured the amplitudes of responses to probe stimuli and their dependence on adaptor ITD at each channel in the sixteen channel recording electrode. We also sought to identify plausible generators of LFP responses by decomposing LFP responses into spatial and temporal modes that account for qualitative features of the data. We complemented our data analysis by developing a computational model to simulate spatio-temporal LFP patterns.

Results

We find evidence of adaptation patterns that are IPD-dependent. Specifically, we find recording sites at which LFP responses are strongly adapted in the case that probe and adaptor sounds share a common IPD, even though their respective ITDs differ substantially (2 ms difference between adaptor and probe ITD). Using modeling and data analysis we can tentatively separate slow and fast components of LFP responses and quantify

adaptation effects in these two channels. We speculate that the generators of these components are AMPA (fast) and NMDA (slow) synaptic inputs to thalamo-reipient pyramidal cells.

Conclusion

LFPs provide an essential view of in vivo cortical activity, but proper interpretation of these extracellular signals is a long-standing challenge. Using model-assisted data analysis we can identify likely neural generators of cortical LFPs and advance understanding of sound location processing in auditory cortex. Evidence of IPD-based representation of sound location could spur rethinking of standard models of binaural hearing.

Auditory Cortex: Human Studies I

PS 471

Vowel Discrimination in Infants Evidenced by Cortical Auditory Evoked Potentials

Barbara Cone; Diane Cheek

University of Arizona

Audiologists are tasked with detecting hearing loss at birth, diagnosing the type and degree of hearing loss and instituting habilitation, including fitting hearing aids, by 6 months of age. Methods of estimating thresholds from the auditory brainstem response and visual reinforcement audiometry are in widespread use, but there are no clinical methods for determining if infants can hear differences between different speech features. Such measures are important for ensuring that hearing aids or cochlear implants are providing sufficient access to the speech signal for the infant listener to discriminate between speech sounds.

The challenge of assaying infant speech feature discrimination abilities was met by employing cortical auditory evoked potentials (CAEP). 26 infants under the age of 12 months participated in an experiment in which CAEPs were measured in response to vowel tokens presented in an oddball paradigm, with a 75/25 % standard-to-deviant ratio. The vowel tokens were /a/, /i/, /o/ and /u/, each with 500 ms duration, presented at 70 dBA SPL in the sound field at two different rates: 1/s (mismatch negativity paradigm) and 2/s (acoustic change complex paradigm). Twelve vowel pairs were tested, including control conditions in which there was no token change. The peak-to-trough amplitudes of CAEP components, P1-N1, N1-P2 and P2-N2, were measured in a derived waveform obtained by subtracting the response to the standard token from the response to deviant. The differences between the derived waveform components in control and contrast conditions were used as a metric of vowel discrimination.

For responses obtained at 1/s, the mean amplitudes of P1-N1 and N1-P2 did not differ between control and test conditions, but the P2-N2 component in the contrast condition was 1.5 times the amplitude in the control condition, and this was statistically significant. The /u-/i/ contrast evoked the largest derived P2-N2 amplitude. For responses obtained at 2/s, each CAEP component demonstrated a statistically significant difference between control and test conditions. The contrast/control amplitude ratios were 1.8, 4.8, and 3.4 for P1-N1, N1-P2 and P2-N2, respectively. The /u-/i/ and /o-/i/ contrasts evoked the largest derived CAEP amplitudes.

The robust derived responses obtained with the acoustic change complex paradigm appear to be suitable for translation to clinical methods for estimating vowel discrimination abilities. Proof-of-concept will be illustrated with results from children with hearing loss who were tested using the paradigm, with and without their hearing devices (hearing aids or cochlear implant).

PS 472

Neural Reconstructions of Speech in Reverberant Multi-talker Environments

Søren Asp Fuglsang¹; Jens Hjortkjær¹; Torsten Dau²; Søren Asp. Fuglsang¹

¹Technical University of Denmark; ²Hearing Systems group, Department of Electrical Engineering, Technical University of Denmark, 2800 Kgs. Lyngby, Denmark

Research Background

Recent studies have shown that low-frequency amplitude modulations inherent in speech signals can be reconstructed from magnetoencephalographic (MEG) and electroencephalographic (EEG) recordings using spatial-temporal reconstruction filters. It has been shown that such reconstruction filters are sensitive to auditory attentional modulation, and that the neural reconstructions can be used to classify the identity of attended and ignored speakers in multi-talker listening scenarios.

Methods

The present study uses a stimulus-reconstruction filtering technique to estimate attended speech envelopes from 64-channel scalp EEG recordings in response to speech mixtures. EEG data were recorded from subjects listening attentively to one of two or more talkers in virtual auditory environments. Binaural room impulse responses from three different rooms were used to create virtual auditory environments consisting of two or more speakers simultaneously talking in anechoic, mildly reverberant and highly reverberant rooms.

Results and Conclusion

We showed that attentional selection can be successfully decoded in anechoic and reverberant multi-talker environments. High decoding accuracies were observed irrespective of convolutive stimulus distortions, suggesting a robust selective cortical representation of the attended speech streams. We further showed that the decoding accuracies remained high using only 10 scalp electrodes and short (< 30 s) test segments, which highlights the prospects of stimulus-response mapping functions in closed-loop brain computer interfaces.

PS 473

Neural Representations of Noisy Reverberant Speech in Human Auditory Cortex

Krishna C. Puvvada; Jonathan Z. Simon
University of Maryland, College Park

Natural listening conditions are challenging because of interference that degrades the acoustic signal before it even reaches the ear, with additive noise and reverberation being two major contributors. In reverberation, the direct target signal and its multiple reflections, with corresponding delays, are linearly superposed at the listener's ear, degrading the signal with temporal as well as spectral smear. Yet speech perception in such noisy and reverberant conditions is relatively effortless for normal hearing listeners, possibly due to the noise robust processing and representations of the speech by the auditory system. In spite of the apparent ease with which the human brain maintains the robustness of target speech across varying degrading sound environments, little is known about the mechanisms and the neural representations of noisy and reverberant speech. In this experiment, using magnetoencephalography (MEG) recordings from normal hearing listeners, we examine the cortical representations of continuous speech degraded by reverberation and also distorted by additive noise. In a separate experiment brainstem responses to short vowel sounds under various reverberation and noisy conditions are recorded using electroencephalography (EEG).

Twelve conditions were investigated (4 reverberant conditions x 3 noise levels) with MEG. The four reverberation conditions were anechoic, low, intermediate and severe reverberation, with corresponding RT20 values of 0 ms, 150 ms, 300 ms and 450 ms. The three noise conditions were clean speech, 6 dB SNR and 3 dB SNR. Stimulus envelope reconstruction from the neural responses was used to quantify the neural representation of the speech, and the correlation between actual and reconstructed envelope was used as the measure of fidelity.

In the delta band (1-4 Hz), the envelope of reverberant speech is shown to be better reconstructed than that of the clean version, indicating that, at this scale, the cortical representation explicitly maintains the reverberance, and correspondingly that the delta band preserves the reverberant timbre we perceive in such an environment. In contrast, for the theta band (4-8 Hz), no significant difference was found in the ability to reconstruct reverberant or the corresponding clean speech. Since the envelope of clean speech is less correlated with its reverberant version in the theta band than delta, these results imply that in the theta band (corresponding to phonemic rates), the neural representation of reverberant speech demonstrates restoration to a cleaned version.

PS 474

The Acoustic Change Complex and its Relation to Speech Perception in Noise in Hearing-Impaired Subjects

Bernard Vonck; Marc Lammers; Wouter Schaake; Wilko Grolman; Gijsbert van Zanten; Huib Versnel
University Medical Center Utrecht

Background

Cortical auditory evoked potentials (CAEPs) in response to changes within sounds (e.g., vowel transitions, or changes in level or frequency) may be suitable for assessing suprathreshold neural processes related to speech perception. These CAEPs evoked by sound changes are also referred to as acoustic change complexes (ACCs) and are composed of a typical P1-N1-P2 waveform morphology. Since frequency changes are a fundamental part in speech sounds, ACCs elicited by frequency changes may be related to speech perception. This study's objective was to investigate whether the ACC was related to psychophysical outcomes as frequency discrimination and speech reception in noise.

Methods

In 13 patients with sensorineural hearing loss and 12 normal hearing controls we recorded ACCs in response to frequency increases within stimuli. Stimuli were tones of 3300 ms with three components: a) a reference tone of 1000 Hz with a duration of 3000 ms, b) an FM sweep with a frequency change Δf , c) a tone with a frequency 1000- Δf or 1000+ Δf Hz and a duration of 300 ms. First ACCs were recorded in response to 12% Δf with respect to reference tones of 500, 1000, 2000 and 4000 Hz. Then the size of Δf was reduced in order to determine an ACC threshold. In addition, frequency discrimination thresholds were assessed using pure tones with reference frequencies of 500, 1000, 2000 and 4000 Hz in a 3-interval 2-alternative forced choice paradigm. Speech reception thresholds (SRTs) were measured in free-field speech-in-noise tests using Dutch standardized sentences.

Results

The ACCs of the hearing-impaired group showed higher thresholds, smaller N1-P2 amplitudes and longer N1 latencies compared to the normal-hearing controls. As expected, the hearing impaired group performed more poorly on the frequency discrimination and speech perception tasks than the normal-hearing controls. Unexpectedly, none of the ACC measures including ACC threshold were correlated to frequency discrimination. However, interestingly, subjects with better speech perception results showed shorter N1 latencies. Multiple regression analyses revealed that after hearing loss, ACC latency was a secondary predictor for speech perception.

Conclusion

ACC thresholds are poor indicators for hearing performance. Instead the suprathreshold ACC latency, in addition to hearing loss, appeared to be an indicator for speech perception in noise. The ACC might therefore hold clinical value as an objective measure to assess hearing performance in hearing-impaired subjects.

PS 475

Recurrent Representation of Acoustic Features in Neural Responses to Continuous Speech

Bahar Khalighinejad; Guilherme Cruzatto da Silva; Nima Mesgarani
Columbia University

Humans are unique in their ability to communicate using spoken language. However, it remains unclear how the speech signal is transformed and represented in the brain at different stages of the auditory pathway. In this study, we applied a novel analysis technique to electroencephalography (EEG) signals as subjects listened to continuous speech. We averaged the time-aligned neural responses to phoneme instances and calculated a phoneme-related potential (PRP) and showed that the PRPs for different phonemic categories have distinct profiles. We found that each instance of a phoneme in continuous speech produces multiple distinguishable neural events occurring as early as 50 ms, and as late as 400ms after the phoneme onset. Comparing the patterns of phoneme similarity in the neural responses and the acoustic signals confirms a repetitive appearance of acoustic distinctions of phonemes in the neural data. Analysis of the linguistic (phonetic) and non-linguistic (speaker) information in neural activations revealed that different time intervals jointly encode the acoustic similarity of both phonetic and speaker categories. These findings provide evidence for a sequential neural transformation of low-level speech features as they propagate along the auditory pathway, and form an empiri

cal framework to study the representational changes in learning, attention, and speech disorders.

PS 476

Intracranial Recordings Reveal Modulation of Primary Auditory Cortical Activity During Pop-out of Degraded Speech Based on Matching Visual Information

Alexander J. Billig¹; Ariane E. Rhone²; Phillip E. Gander²; Kirill V. Nourski²; Conor J. Wild¹; Matthew A. Howard²; Ingrid S. Johnsrude³

¹*Brain and Mind Institute, The University of Western Ontario*; ²*Human Brain Research Laboratory, The University of Iowa*; ³*University of Western Ontario*

Speech comprehension under adverse listening conditions can be enhanced by semantic context and visual information (Miller et al., *J Exp Psychol* 41:329-35, 1951; Sumbly & Pollack, *J Acoust Soc Am* 26:212-5, 1954). For noise-vocoded sentences lacking fine spectrotemporal detail, matching text facilitates perceptual “pop-out” such that the impoverished signal is reported as less noisy than when heard alongside meaningless letter strings (Wild et al., *Neuroimage* 60:1490-502, 2012). Wild et al. (2012) found an elevated BOLD response in primary auditory cortex associated with this effect, suggesting that early cortical stages of auditory processing can be modulated by non-auditory information in support of speech comprehension. In the current study, we analysed a more direct measure of neural activity. Intracranial recordings were made from a patient undergoing monitoring to establish the sources of epileptic activity. Coverage included depth electrodes in Heschl’s gyri (HG) of both hemispheres. In each trial, the subject was presented with an auditory sentence (clear or 3-channel noise-vocoded), then written text, followed by a repeat of the auditory stimulus. In the clear speech case, the text matched the auditory sentence; in the noise-vocoded cases, text could be matching or consist of meaningless letter strings. To engage attention, the subject was asked to detect occasional capital letters in the written text and warned that memory for the sentences would be tested at the end of the experiment. Changes in event-related high gamma (75-150 Hz) power were computed for each auditory presentation, relative to a pre-stimulus baseline. Responses to noise-vocoded speech were averaged over the six contacts in postero-medial HG (two left, four right), most likely to be recording from primary auditory cortex. A significant cross-over interaction between text type and presentation number reflected an increase in high gamma power from the first to the second presentation when the text was matching, compared to a decrease when text

was meaningless. The design rules out these effects being driven by acoustic differences or mere repetition. In further subjects, a control condition with meaningful but mis-matching text will clarify the contribution of any attention differences across conditions. Additional connectivity analyses will probe the role of non-auditory areas in facilitating perceptual pop-out. In summary, we show that the provision of informative written text results in increased high frequency neural activity within primary auditory cortex that may underlie perceptual pop-out of degraded speech. The findings have implications for predictive accounts of perception and its neural underpinnings.

PS 477

Neural Correlates of Variance in Speech-in-noise Understanding Performance

Subong Kim¹; Timothy D. Griffiths²; Phillip E. Gander³; Inyong Choi¹

¹*Department of Communication Sciences and Disorders, University of Iowa*; ²*Newcastle University*; ³*Human Brain Research Laboratory, The University of Iowa*

In noise, even people with normal hearing have difficulty understanding speech, showing varying performance among individuals. What factors can predict the variance in speech-in-noise (SiN) understanding performance? Given that traditional demographic variables only explain a limited amount of variance, we need to characterize neural substrates that may predict speech understanding ability in noise. We hypothesized that the interplay between inferior frontal gyrus (IFG), known as a “language processing area,” and Heschl’s gyrus (HG), where primary auditory cortex is placed, plays a key role in SiN understanding. We conducted a region-of-interest based analysis of high-density electroencephalographic (EEG) evoked activity rendered into source space. We found earlier and stronger HG and IFG activity in the higher signal-to-noise ratio (SNR) condition as well as later but stronger IFG activity in the lower SNR condition. Furthermore, in the same higher SNR condition, the lower performance group showed later but stronger frontal activity while the higher performance group showed earlier and stronger temporal and frontal activity. Together, our results suggest that the interplay between language-related frontal cortex and primary auditory cortex predicts the variance of SiN performance among normal hearing individuals. This work will lead to a better understanding of the neural substrates of individual differences in SiN performance.

PS 478

Changes in Pitch Height Elicits Both Language Universal and Language Dependent Changes in Neural Representation of Pitch in the Brainstem and Auditory Cortex

Chandan Suresh; Ananthanarayan Krishnan; Jackson Gandour
Purdue University

Language experience shapes encoding of information relevant to pitch at both brainstem and cortical levels of processing. Pitch height is a salient dimension that orders pitch from low to high. The aims of this study were to assess the effects of language experience (Chinese, English) on i) neural activity associated with pitch height in the brainstem and cortex, ii) presence of asymmetry in cortical pitch representation, and iii) patterns of relative changes in magnitude of pitch height. Stimuli were three nonspeech homologs of Mandarin Tone 2 varying in pitch height only. Brainstem frequency-following and cortical pitch-specific responses were recorded concurrently. Peak latency (Fz: Na, Pb, Nb) decreased with increasing pitch height for both groups. Peak-to-peak amplitude (Fz: Na-Pb, Pb-Nb) increased with increasing pitch height across groups. Chinese group advantage was limited to Na-Pb. At temporal sites (T7/T8), larger amplitude of Chinese listeners across stimuli was both limited to the Na-Pb component and right temporal site. In the brainstem, F0 magnitude decreased with increasing pitch height; Chinese had larger magnitude across stimuli. Direct comparison of cortical and brainstem responses revealed distinct patterns of relative changes in magnitude shared in common across groups. CPR amplitude increased and FFR amplitude decreased with increasing pitch height. Experience-dependent effects on CPR components vary depending on neural sensitivity to specific attributes of pitch (height) within a particular temporal window (Na-Pb). Differences between the auditory brainstem and cortex imply distinct neural mechanisms for pitch extraction at the brainstem and cortical levels.

PS 479

Classifying Attended Speech from EEG Using Canonical Correlation

Daniel D.E. Wong¹; Jens Hjortkjær²; Søren Asp Fuglsang²; Alain de Cheveigné¹
¹*École Normale Supérieure*; ²*Technical University of Denmark*

Background:

Recent studies probe the cortical response to ongoing speech using systems-identification methods, with the aim of understanding perceptual and attentive process-

es, and decoding which source is the focus of attention for engineering applications. Previous approaches either predict the response from the stimulus via a forward model (temporal response function, TRF), or reconstruct the stimulus from the response via an inverse model. In contrast, Canonical Correlation Analysis (CCA) maps both EEG and audio into a common space. This formulation produces multidimensional features that improve the robustness of the classification, and allows application of additional methods to adaptively suppress noise and unattended components.

Methods:

Ten subjects were presented with two Danish stories simultaneously from either of two loudspeakers positioned at ± 60 degrees azimuth, and requested to attend to one or the other story while 64-channel EEG was recorded. The position of the loudspeaker from which the attended story was presented was randomized, as well as the gender of the person talking. Stimuli were presented in 50s trials for a total of 60 trials. In a leave-one-out cross-validation analysis CCA was used to identify canonical components between a) the EEG and attended audio (attended decoder) and b) the EEG and unattended audio (unattended decoder). Correlation coefficients were computed between canonical component pairs for a range of analysis window durations, and a SVM classifier was used to classify the attended audio based on these coefficients.

Results:

CCA yielded higher classification scores compared to TRF methods. For 10s classification windows, TRF and CCA decoding on average yielded 70% and 77% accuracy respectively, and when additional noise suppression methods were applied, CCA accuracy reached 84%.

Conclusion:

CCA provides an audio-EEG decoding framework that allows the available data to be processed into multiple features that allow a classifier to provide better accuracy compared to prior methods. The approach can be implemented in real time, and can potentially be used to cognitively steer a hearing device.

PS 480

Comparing the Timescale of Cortical Speech and Music Analysis with Sound Quilts

Sam V. Norman-Haignere¹; Dana Boebinger²; Josh H. McDermott¹; Samuel V. Norman-Haignere³

¹MIT; ²Program in Speech and Hearing Bioscience and Technology, Harvard University; ³Howard Hughes Medical Institute Fellow of the Life Sciences Research Foundation; MIT; Boston Children's Hospital

Recent work suggests that human non-primary auditory cortex contains distinct neural populations that respond selectively to speech and music, respectively. However, little is known about what these neural populations compute. We have previously used “quilting” – a technique for scrambling sound waveforms at different durations – to investigate the sensitivity of speech-selective populations to sound structure at different timescales. Here, we apply the same technique to music, and compare the results to those for speech. We generated sound quilts from excerpts of music and speech by reordering sound segments of durations ranging from 31 ms to 2 seconds. Reordering segments preserves local structure within the segment but removes temporal structure at timescales longer than the segment duration. We used a previously established method (“voxel decomposition”) to estimate the fMRI response of speech- and music-selective populations to the sound quilts. Replicating prior findings, the response of speech-selective populations increased with increasing segment duration up to approximately 500 ms, after which the response plateaued. By contrast, the response of music-selective populations did not exhibit a plateau at 500 ms, and instead appeared to respond maximally to the longest duration quilts tested (comprised of 2-second segments). This pattern is consistent with the idea that the neural analysis of music occurs over longer timescales than does the neural analysis of speech.

PS 481

Attentive Tracking of Auditory Streams in the Presence of Static or Dynamic Distractors

Daniel Bates¹; Maria Chait²

¹University College London; ²Ear Institute, University College London, UK

Listeners' ability to selectively track a sound source through a busy scene deteriorates in the presence of distractor sounds. Previously, we demonstrated that attended streams are associated with enhanced brain response and that the magnitude of this effect depends on scene size.

In the current EEG experiment we quantify how in-

creasing distractor complexity affects attentive tracking. Scene are comprised of either 2 or 4 streams, with one allocated as the attended stream. Each stream is a sequence of pure tones with a different rate (3, 7, 13, 23Hz) and starting carrier frequency (CF, between 200 and 4248Hz). The CF of the attended stream remained constant. The CF of the non-attended streams either remained stationary or was allowed to fluctuate in frequency (the trajectory: up, down or static was randomly altered every 2 seconds). We utilise a detection task requiring participants to respond to tone omissions within the attended stream, whilst inhibiting responses to omissions within distractor sequences. To allow us to estimate brain activity associated with a 'neutral' state (i.e. scene components neither attended nor ignored), embedded within all scenes were two or three 100ms pure tones with frequency substantially above that of the scene. On a proportion of the trials, listeners were instructed to respond to those tones. This task was deliberately set to be very easy as appropriate for a 'neutral' condition.

Ongoing analysis of the EEG data demonstrates that attention boosts responses to the tracked source, manifested in EEG as enhanced spectral power at its AM rate. The strength of this effect depends on the number of competing sound sources within a scene. Further results pertaining to the effect of the complexity of the distractor will be reported.

Auditory Nerve III

PS 482

Level-dependence of Frequency Tuning in the Auditory Nerve

Mark Sayles¹; Bertrand Fontaine²; Philip H. Smith³; Philip X. Joris²

¹Purdue University; ²University of Leuven; ³University of Wisconsin - Madison

Auditory-nerve-fiber spiking responses provide a window onto the magnitude and phase response of “cochlear filters”. Typically, cochlear frequency resolution is quantified using threshold tuning curves (an iso-response measure of tuning). Superficially, threshold tuning curves suggest dramatic and systematic filter broadening with increasing sound level. Broadening of filters is often invoked to explain psychoacoustic phenomena. Spike-timing derived measures of the variation in phase with sound level have suggested phase may “pivot” around the filter center frequency, with a relative lag at low frequencies and a relative lead at high frequencies as sound level increases. Modelling studies have pro-

posed a role for these systematic phase cues in level discrimination.

We recorded auditory-nerve-fiber spike times from normal-hearing chinchillas. We gathered threshold tuning curves in response to tones, and responses to 0.01-20 kHz wideband noise over a wide intensity range from each fiber. Linear filter estimates were obtained from responses to noise at each sound level by reverse correlation. We characterized the magnitude and phase response of these filters to obtain iso-level measures of tuning for a broadband acoustic input at a range of sound levels to quantify the level dependence of tuning.

We considered responses from 175 fibers (CF range: [0.1, 3.0] kHz; all SR groups). Responses to noise were obtained with sound level varying over a 40 to 100-dB range. Reverse-correlation derived filter 10-dB bandwidth varied minimally with input sound level over a 40 to 50-dB range. Some fibers demonstrated phase pivoting with level; however, most did not follow this simple scheme.

Common teaching is “auditory filters broaden with level”, and threshold tuning curves are easily misinterpreted to indicate a widening of bandwidth with level. Here, gain functions constructed from responses to a fixed-level input show this broadening is not as severe as threshold tuning curves might suggest. Broadening is very subtle over a large range of input levels (< 50-dB SPL in ERB), before rapidly increasing at “high” levels (>60-dB SPL in ERB). Phase varies with sound level, often in unpredictable ways. Simple “pivoting” does not accurately describe the majority of these data.

Supported by: Research Foundation - Flanders (FWO) [post-doctoral fellowship, M.S.]; European Community Marie Skłodowska-Curie fellowship (MSCA-RI-655137 [B.F.]); NIH (R01 DC012782 [P.H.S. and P.X.J.]); FWO (G.091214N and G.0961.11[P.X.J.]); Research Fund KU Leuven (OT/14/118 [P.X.J.]).

PS 483

Long-term Fate of Auditory Neurons After Selective Hair Cell Ablation

Takaomi Kurioka¹; Min Young Lee²; Lisa A. Beyer³; Donald L. Swiderski³; Yehoash Raphael¹

¹Department of Otolaryngology-Head and Neck Surgery, Kresge Hearing Research Institute, University of Michigan, Ann Arbor, Michigan, USA; ²Department of Otolaryngology-Head & Neck Surgery, College of Medicine, Dankook University, South Korea; ³Kresge Hearing Research Institute, Department of Otolaryngology, University of Michigan

Background

In experimental animal models of cochlear hair cell (HC) loss, insults such as noise or ototoxic drugs often lead to primary and secondary degeneration in spiral ganglion neurons (SGNs). In contrast, using the diphtheria toxin (DT) receptor (DTR) mouse, the primary insult is specific to the HC. We and others have shown that selective HC loss in adult mice had no significant impact on SGN survival for at least 2 months (Golub et al. 2012; Tong et al. 2015; Kurioka et al. 2016). However, it is not clear whether SGNs survive in the long-term without HCs. SGN survival is important for studying functional implications of HC regeneration and cochlear implants. Here we investigated the long-term fate of SGNs in adult DTR mice after a complete loss of cochlear HCs.

Materials and Methods

We used mice expressing DTR selectively in HCs (Mice provided by Dr. Rubel from the University of Washington). DTR mice were injected with DT (15 ng/g) at 3 weeks of age and allowed to survive 2 or 4 months after DT injection. Cochleae were analyzed to confirm HC loss and assess SGN density.

Results

One week after injection, DTR mice were profoundly deaf. Following DT injection the mice exhibited complete HC loss. Their supporting cells remained intact 2 and 4 months after DT injection. Two months after DT injection, the size of SGNs decreased but their density did not. However, 4 months after DT injection, both the size and density of SGNs had decreased.

Conclusions

Although the reduction in neural density was not significant in the short-term, we did observe a significant decrease in cell size of SGNs 2 months after DT-induced HC loss. Moreover, this selective HC ablation led to secondary degeneration in SGNs density over the long-term. These results suggest that long-term survival of SGNs is not sustained in the absence of HCs. The data suggest that the DTR mouse model is useful not only for studying HC regeneration but also for studies on sustaining the neural components of the cochlea with electrical stimulation, neurotrophins or HC regeneration.

Supported by NIDCD grants R01-DC010412, R01DC014832 and P30-DC05188.

Coding of Temporal Information in the Auditory Nerve of Aging Gerbils

Lichun Zhang; Friederike Steenken; Christine Köppl
Cluster of Excellence H4A, Dept. of Neuroscience, Carl von Ossietzky University Oldenburg

Background

The coding of temporal fine structure (TFS) and envelope (ENV) information are important foundations of auditory central processing, e.g., for speech perception, and may degrade with aging. The Mongolian gerbil, having excellent low frequency hearing and a short life span, is a popular animal model for age-related changes in hearing. In this study, we are specifically interested in temporal processing at the level of individual auditory-nerve fibers and their potential changes with age in gerbils.

Methods

Single-unit recordings with glass microelectrodes were obtained from auditory-nerve (AN) fibers of quiet-aged gerbils under ketamine/xylazine anesthesia, via a posterior fossa approach. A range of standard tests were run, using pure tones delivered via a closed sound system. Broad-band frozen noise and anti-phase frozen noise were also presented to derive several measures of temporal synchrony (SAC, XAC, Difcor, Sumcor), according to Joris et al. (J Neurosci., 2003, 23:6345-6350) and Louage et al. (J Neurophysiol., 2004, 91(5):2051-2065). The ratio between the peak height of the XAC and SAC at delay zero was used as a metric for the transition from TFS phase locking to predominantly ENV locking.

Results

A total of 188 single units, with CF ranging from 400 Hz to 15.3 kHz, were collected from 20 young (2.7 to 11 months) and 5 old (23 to 30 months) gerbils. Threshold sensitivity (typically between 10 and 40 dB SPL) and spontaneous firing rates (SR, ranging from 0 to 131 spikes/s) of young gerbils were consistent with previous studies. In the quiet-aged gerbils, the range of SR was similar to the young animals; however, the thresholds of the middle-and-low SR fibers (≤ 18 spikes/s) suggested a mild increase (Mann-Whitney U test, $p=0.013$). Regarding temporal processing, our preliminary analysis did not reveal any differences between young and quite-aged gerbils. This was true for both the vector strength (VS) of pure-tone phase locking and the SAC to broad-band noise. The maximal VS declined from 0.9 at 500 Hz to 0.1 at 4 kHz. For both age groups, the transition from TFS phase locking to predominantly envelope locking occurred at about 3 kHz.

Conclusions

In conclusion, temporal coding at the level of AN fibers did not degrade in gerbils up to an age of around 2 years, an age where the sensitivity of hearing has already begun to decline. It remains open whether temporal coding eventually deteriorates at ages beyond 2 years.

PS 485

Auditory Nerve Coding Strategies in Noisy Conditions

Antoine Huet¹; Thomas Justal¹; Gilles Desmadryl¹; Régis Nouvian¹; Jean-Luc Puel²; Jérôme Bourien¹

¹UMR 1051, INSERM, University of Montpellier; ²Institute for Neurosciences of Montpellier-Inserm U1051; University of Montpellier, France

Background

Inner hair cells (IHCs) translate sound stimulation into the release of glutamate onto afferent auditory nerve fibers. A single IHC is innervated by 10-20 afferent auditory nerve fibers (ANFs) that vary in activation threshold and spontaneous rate (SR). Low sound levels activate the high-SR fibers whereas higher levels progressively recruit fibers with lower SR. While the coding properties of ANFs have been extensively investigated under resting silent conditions, the behavior of ANFs in the presence of background noise remains mostly unknown.

Methods

Here, we compared single-fiber response from the gerbil auditory nerve (tone burst presented at the fiber characteristic frequency) and behavioral audiometric data (prepulse inhibition startle reflex) with or without a continuous broad-band noise presented at 60 dB SPL.

Results

In quiet conditions, behavioral threshold is highly correlated with ANF threshold, which can be calculated from discharge rate or using temporal response precision (i.e., phase locking and first spike latency). In noisy conditions, the rate-based threshold of ANFs is severely altered. In contrast, the temporal-based threshold remains highly correlated with the behavioral threshold assessed in the same noisy conditions, notably below 3 kHz where the phase locking operates.

Conclusion

These results suggest that temporal response precision enables more effective sound coding in noisy conditions.

Complementary Metrics of Human Auditory Nerve Function Derived from Compound Action Potentials

Kelly C. Harris; Judy R. Dubno
Medical University of South Carolina

Background

The compound action potential (CAP) generated by the auditory nerve (AN) represents the summation of individual AN action potentials. Although latencies and amplitudes of individual fiber responses are conceptually independent, these measures can be confounded when responses are averaged. For example, it is expected that the onset time of the averaged CAP waveform reflects the onset of the earliest single-trial responses from the fastest AN fibers, whereas the latency of the averaged waveform peak reflects the latency of responses with average onset times. With increasing intensity, the response width of the averaged CAP waveform may be expected to increase, reflecting recruitment of fibers with longer latencies. Measures of peak amplitude may also be affected by signal averaging, such that the recruitment of fibers with slower onset times would be expected to lead to an increase in response area owing to their delayed response, with possibly minimal changes in peak amplitude. Finally, larger peak amplitudes with increasing intensity most probably result from an increased number of synchronized responses from fibers with similar onset times. We hypothesize that subjects who recruit more AN fibers, particularly those with slower response latencies, will have larger and broader CAP waveforms with longer peak latencies, and stronger phase locking.

Methods

CAP and wave V waveforms of the auditory brainstem response (ABR) were recorded from younger adults with normal hearing. Using tympanic-membrane electrodes, CAPs were elicited using alternating-polarity 100- μ s click trains presented at 70-110 dB pSPL. In Matlab, modified ERPlab functions estimated the onset of the averaged CAP response, the rectified response area, and the response width. Peak latency and amplitude of the averaged waveforms were recorded for N1 of the CAP and ABR wave V. EEGLab performed time-frequency analyses across trials and estimated phase locking value (PLV) at a given frequency for CAP and ABR wave V.

Results

Slopes of CAP amplitude-intensity functions varied widely across subjects, subjects with larger responses showed steeper amplitude-intensity slopes, longer peak latencies, and stronger PLVs. In contrast to longer peak latencies, onset latency was not associated with CAP amplitudes. CAP response amplitudes and widths were

positively correlated at higher but not lower intensities. CAP response measures were not associated with ABR wave V measures.

Conclusions

Preliminary results from younger adults suggest that use of complementary metrics will provide a more analytic approach to characterizing AN function in humans and changes with age and other pathology. Supported by NIH/NIDCD

PS 487

The Contribution of Peripheral Processes to the Electrically Evoked Compound Action Potential

Dyan Ramekers; Ferry Hendriksen; Sjaak F.L. Klis;
Huib Versnel
University Medical Center Utrecht

Background

A central question in cochlear implant research is whether the site of excitation is at the spiral ganglion cell (SGC) soma or at its peripheral process (PP), which is located more closely to the electrode array. This question has become more relevant since recent attempts to grow these processes onto the array, thereby possibly creating a gapless electrode-tissue interface. As the electrically evoked compound action potential (eCAP) may contain valuable information to address the question of action potential initiation, we have compared several relevant eCAP characteristics to detailed histological data of SGCs.

Methods

We have re-evaluated the eCAPs of a subpopulation of guinea pigs, of which at the time of the recordings the number of surviving SGCs was roughly similar, but the number of surviving PPs varied considerably. This group included normal-hearing and deafened guinea pigs, either with or without a four-week brain-derived neurotrophic factor (BDNF) treatment. eCAPs were analysed with respect to amplitude, latency and threshold of the N1 peak, and amplitude and latency of the N2 peak relative to the N1 peak.

Results

Twelve guinea pigs had SGC packing density ranging from 78-87% compared to normal-hearing animals, and PP packing density ranging from 37-99%. Animals with substantially better SGC than PP survival were long-term (6-14 weeks) deaf treated with BDNF. The maximum eCAP amplitude was positively correlated with the PP/SGC ratio (lower amplitude with higher relative PP loss). The N1 latency tended to be longer with more PP loss, as a possible result of demyelination. The eCAP threshold was not affected by PP loss.

Conclusion

An increase in eCAP amplitude with better PP survival suggests a functional role of PPs. However, a corresponding decrease in threshold was not observed. In order to obtain a study population with similar SGC count but with variable PP count, a heterogeneous group of normal-hearing, short-term and long-term deaf, with or without BDNF had to be created. We therefore cannot rule out that factors such as more pronounced demyelination of SGCs in long-term deaf animals may confound the observed patterns.

PS 488

Neurophysiological Evaluation of the Speech-based Envelope Power Spectrum Model

Satyabrata Parida; Michael G. Heinz
Purdue University

Patients with similar audiograms often have different speech-recognition abilities, providing great challenges to audiologists in diagnosing hearing loss and selecting treatment options. Individual perceptual differences may be explained by a better understanding of the differential effects of outer- and inner-hair-cell damage on neural coding of speech. Recently, the psychophysically motivated speech-based envelope power spectrum model (sEPSM) has shown that the signal-to-noise envelope power ratio (SNR_ENV) is an important metric that can predict overall speech intelligibility in many degraded conditions better than long-standing models. In the sEPSM, background noise is assumed to 1) reduce the envelope power of speech-in-noise by filling in the dips within clean speech, and to 2) introduce an envelope noise floor from intrinsic fluctuations in the noise itself. While SNR_ENV has been proposed based on normal-hearing conditions, it has not been tested for hearing-impaired listeners because our physiological knowledge of how sensorineural hearing loss (SNHL) affects envelope coding of speech in noise is limited. Here, we apply quantitative spike-train based analyses to compute a neural SNR_ENV based on auditory-nerve (AN) responses recorded from anesthetized chinchillas, for which the effects of SNHL on envelope coding can be studied directly. Spike trains were recorded from single AN fibers in response to clean speech, noisy speech, and noise alone at several acoustic SNRs. Envelope coding to non-periodic stimuli (e.g., speech in noise) was quantified from recorded neural spike trains using shuffled correlograms. Modulation-band power in neural responses was estimated from the modulation power spectral density, computed as the Fourier transform of the sumcor correlogram, which quantifies the strength of envelope coding. Spike-train analyses show strong similarities to the sEPSM in terms of modulation excitation patterns (modulation band power across modulation frequencies) for clean speech, noisy speech, and noise alone. As in the psychophysically based modeling, neural envelope SNRs were computed for a range of modulation frequencies by comparing the noisy-speech and noise-alone responses for each AN fiber. A total SNR_ENV value was computed by combining individual values across all modulation frequencies and evaluated as a function of acoustic SNR. The similarity in patterns of responses between neural and psychophysically based measures demonstrates the feasibility of computing a neural SNR_ENV. Future estimates of the neural SNR_ENV in animal studies with various forms of SNHL will provide valuable insight for understanding individual differences in speech-in-noise intelligibility.

lation frequencies) for clean speech, noisy speech, and noise alone. As in the psychophysically based modeling, neural envelope SNRs were computed for a range of modulation frequencies by comparing the noisy-speech and noise-alone responses for each AN fiber. A total SNR_ENV value was computed by combining individual values across all modulation frequencies and evaluated as a function of acoustic SNR. The similarity in patterns of responses between neural and psychophysically based measures demonstrates the feasibility of computing a neural SNR_ENV. Future estimates of the neural SNR_ENV in animal studies with various forms of SNHL will provide valuable insight for understanding individual differences in speech-in-noise intelligibility.

This work was supported by an International Project Grant from Action on Hearing Loss (UK).

PS 489

Envelope Following Responses to Schroeder-phase Harmonic Stimuli

Steven J. Aiken¹; **Ganesh Attigodu Chandrashekhara**¹; Jian Wang²

¹*School of Human Communication Disorders, Dalhousie University*; ²*School of Human Communication Disorders, FHP, Dalhousie University*

Background

The scalp-recorded envelope-following response (EFR) has electrical sources at multiple levels of the auditory neuroaxis, but the neural processes involved in the generation of the response are not fully understood. This limits the usefulness of the EFR as a non-invasive measure of auditory function and index of underlying pathophysiology. The neural encoding of the envelope is thought to arise initially as a result of non-linear processing in the auditory periphery. However, recent studies and new work in our lab suggest that peripheral nonlinearities only partially account for envelope-related activity recorded at the scalp, with additional contributions from more broadly tuned neurons in the central nervous system for low-frequency carriers, which support robust phase-locking in the auditory nerve and tend to be well-resolved in the cochlea. The present study investigated this hypothesis by measuring EFR to low and high frequency stimuli designed to 1) optimize within-channel phase synchrony to produce maximal envelope modulation depth on the basilar membrane, or 2) optimize phase synchrony across multiple frequency channels to maximize envelope-related activity arising in the central nervous system.

Methods

The EFR was measured to Schroeder-phase stimuli with harmonic components constrained to low and high frequency ranges, as well to multi-frequency sinusoidally amplitude modulated tones as a function of component phase. Stimulus phases were selected on the basis of individualized timing measures, with basilar membrane phase curvature assessed behaviorally using a rapid Bekesy-style Schroeder-phase masking paradigm (Rahmat & O'Beirne, *Hear Res* 2015), and basilar membrane latency estimated with physiological measures. All electrophysiology measurements were conducted with normal hearing listeners with both far-field and near-field recording channels.

Results

Behavioral and physiological estimates of basilar membrane phase and latency varied across individuals. Response amplitudes and phase-locking values for the EFR varied as a function of carrier frequency range and component phase. The present results are consistent with an understanding of scalp-recorded EFR as a measure of central envelope processing extending beyond the initial encoding of the stimulus envelope arising in the periphery.

Conclusions

The scalp-recorded EFR reflects central processes beyond the periphery and is thus not a direct index of envelope encoding in the auditory nerve. The results of the study contribute to our understanding of the neural processes involved in the generation of the EFR and will help in the design of ideal stimuli for assessing peripheral and central auditory dysfunction in research and in clinical applications.

PS 490

Using Signal-in-Noise Electrocochleography to Assess the Integrity of High-Threshold Auditory Nerve Fibers

Brian R. Earl¹; Hannah Reeg¹; Ivy Schweinzer¹; Simone Mariotti Roggia²

¹University of Cincinnati; ²Universidade Federal de Santa Catarina

Introduction

The action potential component of the electrocochleography (ECoChG) response represents the synchronous firing of peripheral auditory neurons and corresponds to wave I of the auditory brainstem response. ECoChGs have significant potential for the identification of noise-induced cochlear neuropathy due to the associated enhancement of wave I amplitude, and because the high stimulus intensities at which they are common-

ly recorded should reveal the integrity of the excitotoxicity-susceptible, high-threshold auditory nerve fibers. The objectives of this study are to examine the ECoChG amplitude growth patterns for broadband and octave-band chirp stimuli during simultaneous masking with noise at varying bandwidths and signal-to-noise ratios (SNRs).

Methods

CochGs were recorded from adults with normal hearing (N=22) and with mild sensorineural hearing loss (N=5) using a tympanic membrane electrode. Amplitude growth patterns for broadband and octave band (4 kHz) chirps at 100 dB SPL were constructed using simultaneous white noise that was high-passed in ½ octave intervals between 722 and 8944 Hz and by using various SNRs from +5 to +35 dB. The QuickSIN test (Etymotic) was used to assess speech-in-noise performance. Distortion product otoacoustic emissions (DPOAEs) were measured before and after the ECoChG measures.

Results

The amplitude of ECoChGs evoked with broadband and octave-band chirps were consistently larger than click and traditional tone-burst stimuli, respectively. ECoChG amplitude growth curves showed a general pattern of increasing amplitude as the high-pass masker cutoff frequency or the SNR increased. Preliminary analysis suggests a trend of lower ECoChG amplitudes and a decreased rate of amplitude growth in individuals with more SNR loss on the QuickSIN measure. DPOAEs following the masked ECoChG procedure were generally not significantly different than those measured before the procedure.

Summary

These data build on previous studies assessing the utility of signal-in-noise action potentials (SiNAPs) to assess the integrity of high-threshold auditory nerve fibers. The use of 4 kHz octave-band chirp stimuli theoretically has strong potential of uncovering a notch in neural function before an audiometric notch at 4 kHz appears. Further data collection from individuals with mild to moderate hearing impairment is ongoing with the aim of determining the co-occurrence of cochlear hair cell pathology and cochlear neuropathy.

PS 491

The Role of Extracellular Matrix Versican in the Formation and Maintenance of Myelin Sheath in the Mouse Auditory Nerve

Hainan Lang¹; Yazhi Xing¹; Jianning Zhang²; Hui Li³; Mary Bridges¹; Kenyaria Noble³; Clarisse Panganiban³; Jeremy Barth⁴; Corey Mjaatvedt⁵

¹Department of Pathology and Laboratory Medicine

- Medical University of South Carolina; ²Shanghai

Yueyang Hospital, Shanghai China; ³Department of Pathology and Laboratory Medicine, Medical University of

South Carolina; ⁴Department of Regenerative Medicine and Cell Biology - Medical University of South Carolina;

⁵Department of Regenerative Medicine and Cell Biology, Medical University of South Carolina

Background

Myelination is a biological process critical for the functional maturation of auditory nerve (AN) during postnatal development. Proper function of myelinating glial cells is also required for the functional and structural integrity of spiral ganglion neurons (SGNs) and the AN fibers in the adult cochlea. Versican (Vcan), an extracellular matrix (ECM) proteoglycan, is expressed in the glial cells of various nervous tissues. Recent studies have implicated Vcan in several aspects of nerve biology, including neural cell adhesion, migration, pattern formation, and regeneration. However, Vcan is an alternatively spliced gene, giving rise to multiple isoforms. Here our study aims to understand how specific Vcan isoforms contribute to the formation and maintenance of myelin sheath in the AN.

Methods

CBA/CaJ, Vcan mutation (V0/V2 isoform null; Vcantm1Zim), and wild type (WT) mice aged postnatal days (P) 0, 7, 10, and 2-3 months were used. Digital droplet PCR and quantitative real-time PCR were utilized to determine expression patterns of Vcan isoforms and myelin related genes in the ANs. Pathological alterations of the cochleas in WT and Vcantm1Zim mice were examined with auditory brainstem response (ABR) tests, immunohistochemistry and transmission electron microscopy.

Results

The expression levels of Vcan V0 and V1 isoforms peak at P0 and are down-regulated with age during postnatal development, while the V2 isoform peaks around P7, concurrent with the beginning of myelination. Ultrastructural examinations revealed that myelination was delayed in the SGN somas of Vcantm1Zim mice. The compact myelin lamellae were significantly reduced around the SGN somas of the adult Vcantm1Zim mice.

The g ratio of the AN significantly increased in the osseous spiral lamina of Vcantm1Zim mice compared to that in WT, indicating a reduction of the myelin sheath thickness. Downregulation of several myelin related genes was seen in the ANs of the adult Vcantm1Zim mice. The ABR measurements revealed that V0/V2 deletion resulted in a delayed onset of the auditory responses in the postnatal mice and a slightly elevated ABR threshold in the adult mice.

Conclusions

Our data demonstrate that ECM Vcan V0/V2 isoforms play an essential role in the formation and maintenance of myelin sheath in the AN.

Funding: The research project described was supported in part by NIH R01 DC7506 (H.L.), NIH P50 DC0422 (H.L.), NIH GM103342 (J.L.B.), and NIH GM103499 (J.L.B.)

PS 492

Macrophages Contribute to Auditory Nerve Refinement by Eliminating Excessive Glial Cells in the Postnatal Mouse Cochlea

LaShardai Brown¹; Yazhi Xing²; Jeremy Barth³; Clarisse Panganiban⁴; Nancy Smythe¹; Mary Bridges²; Hainan Lang²

¹Department of Pathology and Laboratory Medicine-

Medical University of South Carolina; ²Department of Pathology and Laboratory Medicine - Medical University of South Carolina; ³Department of Regenerative

Medicine and Cell Biology - Medical University of South Carolina; ⁴Department of Pathology and Laboratory

Medicine, Medical University of South Carolina

Background

Spiral ganglion neurons (SGNs) are the conduits for the transmission of auditory information from the hair cells to the brain. During development of the mouse cochlea, SGNs extend an abundance of nerve fiber connections to hair cells. Both SGNs and their auditory nerve fibers become ensheathed by myelinating or non-myelinating glial cells. Immature neural circuits are refined by elimination of excessive nerve and glial cells, however it remains undetermined how glial cell numbers are regulated during this auditory nerve refinement process. In other neural systems (e.g., retinogeniculate system, hippocampus and peripheral neuromuscular), extra synapses and axonal branches are eliminated during development by macrophage phagocytosis. Here, our study determines the extent to which macrophages eliminate excessive glial cells during auditory nerve refinement, contributing to the maturation of auditory function.

Methods

CBA/CaJ mice were used at postnatal day (P) 0, 3, 7, 14, and 21. Quantitative immunohistochemical analysis was used to quantify numbers of Sox10+ glial cells and IBA1+ macrophages during postnatal development. Neuron-glia-macrophage interactions were investigated using 3D confocal imaging and transmission electron microscopy. Microarray assay and Ingenuity Pathway Analysis (IPA) were used to identify key molecules that regulate macrophage activation and auditory nerve refinement. Mice with a diphtheria toxin (DT) receptor on CD11b, a surface integrin on the membranes of active macrophages, were used to selectively eliminate macrophages during nerve refinement. Auditory nerve function of DT-treated mice was measured by auditory brainstem response (ABR).

Results

Macrophage numbers peaked around P7, concurrent with the decrease of glial cells and auditory nerve refinement. Confocal imagery using 3D reconstruction and ultrastructural examinations revealed that macrophages engulf nerve fibers and glial cells during nerve refinement. Diminishing macrophage activity with DT treatment in CD11bDTR mice resulted in a significant increase in glial cells in the auditory nerve, supporting the hypothesis that macrophages are required for the elimination of excessive glia. Additionally, physiological tests revealed elevated ABR wave I thresholds in DT-treated CD11bDTR mice compared to control mice.

Conclusions

Our data demonstrate a novel role of cochlear macrophages in the formation of proper neural circuits and the maturation of auditory function in the cochlea.

Funding: The research project described was supported in part by Glenn/AFAR scholarship (L.N.B.), NIH T32 DC014435 (J.R.D.) NIH R01 DC7506 (H.L.), NIH P50 DC000422 (H.L.; J.R.D.), NIH GM103342 (J.L.B.), NIH GM103499 (J.L.B.) and NIH R25 GM072643.

PS 493

Three-Dimensional Visualization of Micro-Anatomical Structures of the Human Inner Ear

Raymond Van de Berg¹; Marc van Hoof¹; Thomas van den Boogert¹; Nils Guinand²; Jean-Philippe Guyot²; Herman Kingma¹; Angelica Perez Fornos²; Stephan Handschuh³; Lejo-Chacko Johnson⁴; Rudolf Glueckert⁴; Anneliese Schrott-Fischer⁴

¹*Division of Balance Disorders, Department of Otorhinolaryngology and Head and Neck Surgery, Faculty of Health Medicine and Life Sciences, School for Mental Health and Neuroscience, Maastricht University Med-*

ical Center, Maastricht, The Netherlands; ²*Service of Otorhinolaryngology and Head and Neck Surgery, Department of Clinical Neurosciences, Geneva University Hospitals, Geneva, Switzerland;* ³*VetCore Facility for Research, Veterinary University Vienna, Austria;* ⁴*Medical University of Innsbruck, Department of Otolaryngology, Anichstr. 35, 6020 Innsbruck, Austria*

Introduction

Knowledge of the neuro-anatomical architecture of the inner ear contributes to the improvement and development of cochlear and vestibular implants. The present knowledge is mainly based on two-dimensional images (histology) or derived models that simplify the complexity of this architecture. This study investigated the feasibility of visualizing relevant neuro-anatomical structures of the inner ear in a dynamic three-dimensional reproduction, using a combination of staining, micro-CT and a newly developed image processing algorithm.

Methods

Four fresh cadaveric temporal bones were postfixed with osmium tetroxide (OsO₄) to visualize membranes and myelinated nerve fibers and decalcified with EDTA. A micro-CT was used for scanning at a resolution of 10 micrometers (4 scans) and 5 micrometers (1 scan). A new image processing algorithm was developed and applied in Mathematica (version 10.4). The scans were visualized in 3D slicer.

Results

OsO₄ enhanced the contrast in all scans and the signal-to-noise ratio was substantially improved by the image processing algorithm. The three-dimensional models provided detailed visualization of the whole inner ear. Details were visible up to neurones, nerve crossings and the specific neuro-anatomical structures like the tunnel of Corti.

Conclusion

The combination of OsO₄ with micro-CT and the newly developed image processing algorithm provides an accurate and detailed visualization of the three-dimensional micro-anatomy of the human inner ear.

PS 494

The Three-dimensional Culture System with Matrigel Preserves the Structure and Function of Pure Spiral Ganglion Neuron in Vitro

Wenwen Liu; Wenqing Yan; Gaoying Sun; Xiaohui Bai; Zhaomin Fan; Jianfeng Li; Haibo Wang
tolaryngology-Head and Neck Surgery, Shandong Provincial Hospital Affiliated to Shandong University

The survival of cochlea spiral ganglion neurons (SGNs) is indispensable for the preservation of hearing, and damage to SGNs causes hearing loss. In vitro culture of SGNs is a useful approach to investigate numerous aspects of neuronal behavior, and to identify potential therapies for SGN protection, however, extraction and long-term culture of pure SGNs, as well as maintaining of the SGNs structure and function in vitro remains challenging. In this study, utilizing the crossed transgenic mice line Bhlhb 5 cre; tdTomato, we isolated pure spiral ganglion neurons and investigated the effect of three-dimensional (3D)-matrigel culture on SGNs. First, we isolated SGNs extracted from Bhlhb5-cre; tdTomato mice with flow cytometry and identified the purity, we then encapsulated the pure SGNs into matrigel and cultured the neurons in 3D system in vitro. Next, we found that 3D culture environment improved SGNs survivability, enabled long term cultivation of SGNs, suppressed apoptosis, and promoted the neurite extension of SGNs in vitro. 3D-matrigel culture also significantly increased the polarity and promoted the growth of growth cones in SGNs. Last, we found that 3D culture system elevated synapse density in SGNs, and more importantly, 3D matrigel culture promoted parts of the electrophysiological properties of SGNs. In conclusion, this system allows isolation and cultivation of pure SGN and 3D matrigel culture system promoted survival, morphological development and function of SGN in vitro.

Auditory Prostheses: Animal Models

PS 495

Miniature Pigs – An Experimental Model for Otological Research

Shi-ming Yang¹; Wei Sun²

¹Chinese PLA General Hospital; ²University at Buffalo, The State University of New York

Introduction

Animal models are critical for much clinical research regarding human diseases. Rodents are most commonly used laboratory animals. However, as the cochlear organs of rodents are much smaller than those of humans, it is difficult to use them for some otological studies, such as cochlear and middle ear implantation. Animals

that have middle and inner ear similar to human's are desirable for these otological researches.

Methods

Miniature pigs were a type of pig roughly one-fifth the weight and size of a normal pig. The morphology and electrophysiology of the middle and inner ear of miniature pigs, which were derived from small-size swine species from Guizhou Province in China, were studied in order to create a new animal model for otological research.

Results

The miniature pigs have a similar temporal bone structure compared to humans, including the squamous, mastoid, tympanic parts, and the styloid process. The petrous bone houses the cochlea and the vestibular system. The tympanic cavity and middle ears are also similar to that of humans. The cochlea and the three semi-circular canals can be easily identified. The cochlea of a miniature pig has three and half turns and the average length of the cochlea is 39 mm, 25% longer than a human cochlea. The cochlear implants designed for human can be fully implanted in the miniature pigs' cochleae without any modifications. The threshold and waveforms of the auditory brainstem response of miniature pigs are mature from birth. The hair cell bundle in the apical turn of the cochlea splits into multiple clumps and the length of hair cell stereocilia in the apical turn is longer than those in the basal and middle turns. The miniature pigs were found to be very susceptible to noise exposure, suggesting this may be an excellent model to study noise induced hearing loss. However, miniature pigs are resistant to ototoxic drugs. A congenital deafness model has also been developed using chemical mutagenesis which mimics Mondini dysplasia.

Conclusions

The miniature pig cochlea provides an excellent model for the human cochlea. Our study helps to establish miniature pigs as an animal model for future otological and audiological studies.

Acknowledgement

This work was supported by grants from the National Basic Research Program of China (973 Program) (#2012CB967900) and the National Natural Science Foundation of China (31101701)

PS 496

Cochlear Implantation in an Auditory Neuropathy Cell Transplant Model – a Conversation Between Cells and Electrodes

Leila Abbas¹; Daniela Cacciabue-Rivolta¹; Daniel Smyth²; Marcelo Rivolta¹

¹Centre for Stem Cell Biology, University of Sheffield;

²Cochlear Technology Centre

The cochlear implant has been seen as the success story of neural prostheses, bringing the gift of hearing to many for whom this sense was absent. However, in order for a favourable outcome, the patient must have at least the semblance of a functioning auditory nerve, in order to 'connect' the inner ear to the brain – thus for many people, this is not currently a therapeutic option.

A gerbil model has been developed with a two-pronged sensorineural hearing loss - auditory neuropathy is induced with topical ouabain and subsequently the hair cells are lesioned with a kanamycin/furosemide treatment. To recapitulate cochlear implantation, a fully-implantable rodent stimulator¹ is used, in which the electrode is activated by a magnetic field. In animals with hair cell loss only, using a three-dimensional field with waking animals allows us to establish a functional threshold for each animal – they show a characteristic behavioural changes when the field is applied. eABR measurements are also taken, whilst under anaesthesia to establish functional levels for the implant.

Current work has focussed on the rebuilding of the auditory nerve using human otic neural progenitors (hONPs) derived from embryonic stem cells; the line in question, H14-NopSox2-GFP, has been engineered to express a GFP construct which reports the expression of SOX2 under the control of specific otic/nasal placode enhancers, allowing the purification of hONPs in vitro prior to transplantation. A paradigm has been established in which the doubly-deafened animals simultaneously receive an implant and a cell transplant; their progress is monitored over the following three months to look for signs of behavioural change in the chronic stimulator and an eABR response. Histology suggests that the transplanted cells survive and differentiate in the implanted animals, with neural fibres tracking towards the implant.

1Millard R. E. and Shepherd R. K., *J. Neurosci Methods* (2007) 166(2): 168-77.

PS 497

Measurement of the Electrophonic Response in the Guinea-pig Inferior Colliculus

Attila Frater; Torsten Marquardt

UCL Ear Institute, University College London

In recent years, effort is made to improve surgical techniques of cochlear implantation to preserve residual hearing. Combined electrical and acoustical hearing (EAS) is known to enhance listening experience of cochlear implant users by providing acoustic low frequency information in addition to the electric stimulation. However, besides direct stimulation of auditory nerves, electrical currents also evoke an electro-motile excitation of the functioning cochlea, resulting in an acoustic-like response ("electrophonic effect", Nuttall & Ren, 1995), which travels to the low-frequency region of the cochlea (Sato et al, 2016), and there, potentially interfere with the residual acoustical hearing. We developed an experimental framework to investigate the interaction between electrical and acoustical stimulation using the guinea pig as a model: After each stage of the surgery (intact bulla, opened bulla, cochleostomy, electrode insertion), neural responses to acoustically presented tone pips are recorded with a linear 32-contact electrode array along the tonotopic axis of the inferior colliculus (IC) to monitor preservation of sensitivity along the cochlea. After implantation of a 4-contact stimulation electrode into scala tympany, the cochlea is stimulated with electric pulses of varying length, amplitude, polarity, repetition rate and electrode configurations. Their efficacy in evoking an electrophonic response are later analysed in an attempt to find electrical pulse shapes with minimal disruptive effects on the acoustical signal in combined hearing. First results show that good preservation of hearing sensitivity can be maintained after electrode insertion. Along the IC's tonotopy, distinct activation loci are observed: Neurons tuned to high frequencies are apparently directly electrically stimulated by the basally located stimulation electrode (CF ~ 10 KHz). Responses of neurons tuned to low-frequencies exhibit sharper tuning, longer latencies and appear activated via electro-motile response that travels mechanically along the basilar membrane to locations according to the pulse repetition rate.

We started also to simultaneously record acoustic responses in the ear canal (EEOAE) and will compare their behaviour to physiological manipulations, such as acoustical, electrical, or pharmacological biasing, with that of the electrophonic responses. This will test their potential as a non-invasive diagnostic tool to characterise the degree of remaining electromotility in cochlear implant patients.

Acknowledgements

Supported by Oticon Medical. AF received an AoHL travel award.

References

Nuttall & Ren (1995): Electromotile hearing: evidence from basilar membrane motion and otoacoustic emissions. *Hear. Res.*, 92, 170-177.

Sato et al. (2016): Cochlear implant stimulation of a hearing ear generates separate electrophonic and electroneural responses. *J. Neurosci.*, 36(1), 54-64.

PS 498

Bilateral Changes of Spontaneous Activity Within the Central Auditory Pathway upon Chronic Unilateral Intracochlear Electrical Stimulation

Dietmar Basta¹; Moritz Gröschel¹; Sebastian Jansen²; Patrick Boyle³; Arne Ernst¹

¹Department of Otolaryngology at Unfallkrankenhaus Berlin, University of Berlin, Germany; ²Department of ENT at ukb, University of Berlin, Charité Medical School; ³Advanced Bionics European Research Center, Hanover, Germany

In recent years cochlear implants have been applied successfully for the treatment of unilateral hearing loss with quite surprising benefit. One reason for this successful treatment, including the relief from tinnitus, could be the normalization of spontaneous activity in the central auditory pathway due to the electrical stimulation.

The present study therefore, investigated at a cellular level, the effect of a unilateral chronic intra-cochlear stimulation on key structures of the central auditory pathway.

Normal-hearing guinea pigs were mechanically single-sided deafened through a standard HiFocus1j electrode array (on a HiRes 90k® cochlear implant) being inserted into the first turn of the cochlea. Four to five electrode contacts could be used for the stimulation.

Six weeks after surgery, the speech processor (Auria®) was fitted, based on tNRI-values and mounted on the animal's back.

The two experimental groups were stimulated 16 hours per day for 90 days, using a HiRes®-strategy based on different stimulation rates (low-rate (275 pps/ch), high rate (5000 pps/ch)). The results were compared to those of unilateral deafened controls (implanted but not stimulated). All animals experienced a standardised free field auditory environment.

The low-rate group showed a significantly lower average spontaneous activity bilaterally in the dorsal cochlear nucleus and the medial geniculate body than the controls. However, there was no difference in the inferior colliculus and the primary auditory cortex. Spontaneous activity of the high-rate group was also reduced bilaterally in the dorsal cochlear nucleus and in the primary auditory cortex. No differences could be observed between the high rate group and the controls in the contra-lateral inferior colliculus and medial geniculate body.

Unilateral intra-cochlear electrical stimulation appears to facilitate the homeostasis of the network activity, since it decreases the spontaneous activity which is usually elevated upon deafferentation. The electrical stimulation per se appears to be responsible for the bilateral changes described above, rather than the particular nature of the electrical stimulation (e. g. rate).

The normalization effects of electrical stimulation found in the present study are of particular importance in cochlear implant recipients with single-sided deafness.

This study was supported by Advanced Bionics GmbH, Hanover, Germany.

PS 499

Endocochlear Potential and Lateral Wall Changes After Cochlear Implantation

Lina Reiss; Wenxuan He; Gemaine Stark; Tianying Ren
Oregon Health & Science University

Background

Hybrid or electro-acoustic stimulation cochlear implants (CIs) can provide high-frequency electric hearing while preserving residual low-frequency acoustic hearing for combined electric and acoustic stimulation in the same ear. However, a third of patients lose >30 dB of residual hearing after implantation (Gantz et al., 2010; Gstöettner et al., 2009) without hair cell or spiral ganglion cell loss (Tanaka et al., 2014; Reiss et al., 2015; Quesnel et al., 2016). Instead, hearing loss correlates with reduced vascular density in the stria vascularis, suggesting that hearing loss may be caused by a reduced blood supply and ability to maintain the endocochlear potential (EP) necessary for cochlear transduction. The goal of this study is to determine whether EP is reduced after cochlear implantation.

Methods

Endocochlear potentials were measured in three groups of guinea pigs: 1) control; 2) cochleostomy-only; 3) cochlear implant with cochleostomy. Animals in groups 2 and 3 were allowed to recover for 3 weeks after surgery.

Auditory brainstem responses (ABRs) to tones at 1, 2, 4, 8 and 16 kHz were used to measure baseline hearing thresholds in all groups and hearing changes in the experimental groups. At 9 weeks of age, all animals underwent EP recording using a ventral approach through the cochlear lateral wall, while leaving the CI electrode undisturbed in the scala tympani. After EP recording, cochlear sections were immunostained to quantify stria vascularis vascular density.

Results

Average EP values in four control animals were 83 ± 3 mV in the first turn and 76 ± 6 mV in the second turn. Preliminary findings in cochleostomy-only and CI animals indicate significant reductions ranging from 20-30 mV in EP values when ABR threshold shifts were present.

Conclusions

Preliminary results suggest smaller EP values in the experimental groups compared to the control group, especially when hearing loss was present. More data along with histology quantification will be presented. The research will indicate avenues to reduce implantation-induced hearing loss and maximize the benefits of EAS CIs.

Funding

Supported by a grant from the American Hearing Research Foundation.

PS 500

Temporal Characteristics of Electrophonic and Electroneural Excitation in the Inferior Colliculus

Mika Sato¹; Peter Baumhoff²; Andrej Kral³

¹*Institute of Audioneurotechnology and Department of Experimental Otolaryngology, ENT Clinics, Hannover Medical School, Germany;*

²*Hannover Medical School;*

³*Hannover Medical School, DFG Cluster of Excellence Hearing4all*

Electric stimulation of a hearing cochlea generates hair-cell responses (electrophonic, EP) and a direct neural responses (electroneural, EN). EP appears at the dominant frequency component of the electrical stimulus time function and the EN appears at the position of the active electrode (Sato et al., 2016, *J Neurosci*). To investigate the temporal characteristics of these two responses, normal hearing guinea pigs were implanted with a cochlear implant through a cochleostomy. A Neuronexus double-shank 32-channel electrode array was stereotactically placed with the inferior colliculus parallel to the tonotopic axis. The electrical stimuli were charge-balanced biphasic electric pulses (100 μ s/phase). Threshold and onset latency were computed from local field

potential and multiunit activity in the midbrain. The cochlea was subsequently deafened with the implant left in place. The post stimulus time histogram (PSTH) before and after deafening were compared.

The thresholds for responses to cochlear implant stimulation were compared at the CF of EP response (5 kHz) and at the CF of the EN response (9.5 kHz). The electrophonic threshold (mean 45.2 ± 2.6 dB attenuation, (40dB attenuation = 100 μ A pp)) was lower than the electroneural threshold (30.5 ± 5.1 dB attenuation). The mean latency at lowest thresholds in the deafened cochlea was 3.8 ms in both CF \sim 5kHz and 9.5kHz. In the hearing condition, at the same stimulus intensity, the latency was slightly smaller (3.2 ms). In contrast, in the hearing cochlea, the mean latency at the threshold was 5.6ms CF around 5kHz, indicating an EP, and 4.2ms in CF around 9.5kHz, indicating an EN.

The long onset latency and unsynchronized onset response at the 5 kHz region in hearing condition demonstrates that this response is predominantly hair-cell-mediated (EP). A direct neural response (EN) with short latencies and synchronized onset response was observed regardless of the CF in deafened condition, and also in the hearing condition at high stimulus levels (mainly around 9.5 kHz). The response in the hearing cochlea at stimulus levels below the threshold of the deaf condition suggests that the direct neural stimulation has lower threshold in the hearing cochlea and is generated more centrally (has shorter latency). Combined with one of the previous findings showing that the maximum response of deafened cochlea is larger than that of hearing cochlea, the data indicate an effect of deafening (hair cell loss) on the orientation and spread of electrical field generated by the cochlear implant.

Supported by Deutsche Forschungsgemeinschaft (Cluster of Excellence Hearing4All)

PS 501

An Objective Measure of Cochlear Health; Identifying Neural Dead Regions

Andrew K. Wise; Simone Classen; James B. Fallon
Bionics Institute

Background

Current focusing strategies are designed to improve cochlear implant performance by reducing current spread in the cochlea. However, clinical trials have not resulted in the expected improvements. It is thought that regions of relatively greater neural loss (known as neural dead regions) have a significant effect on the efficacy of focused stimulation strategies. This study used an animal model with well-defined neural dead regions to

determine the relationship between the neural electrical thresholds and neural survival. We examined the hypothesis that differences in neural thresholds using focused and unfocused electrical stimulation strategies could be used to identify neural dead regions.

Methods

Normal hearing adult guinea pigs were noise deafened using 10 kHz 130 dB SPL for two hrs. After 28 days the left cochlea was acutely deafened with local perfusion of neomycin and implanted with an intra-cochlear electrode array. The contralateral inferior colliculus (IC) was exposed and a multichannel silicone probe inserted along the tonotopic axis of the central nucleus of the IC. Neural activity was measured in response to electrical stimulation using focused and unfocused (monopolar) stimulation strategies. Cochleae were collected and the density of the auditory nerve fibres measured.

Results

Results showed that there was a significant correlation (Pearson correlation, $p < 0.02$) between electrodes with high thresholds for focused stimulation (compared to monopolar thresholds) and the regions of the cochlea that exhibited greater neural loss (ranging from 40-70% nerve fibre survival).

Conclusion

The results from this study have shown that threshold differences between focused and unfocused stimulation strategies could provide an objective method of determining the 'neural health' of the cochlea by identification of neural dead regions.

This work was funded by the Bionics Institute and supported by the Victorian Government through its Operational Infrastructure Support Program.

PS 502

Chronic Implantation of a Soft Flexible Auditory Brainstem Implant Electrode Array in Mouse

Osama Tarabichi¹; Shreya Narasimhan²; Ariel E. Hight²; Amelie Guex³; Vivek V. Kanumuri⁴; Elliott Kozin⁵; Stephanie Lacour³; Chris Brown²; Daniel J. Lee⁶
¹Harvard Medical School/Massachusetts Eye and Ear; ²Massachusetts Eye and Ear Infirmary; ³École polytechnique fédérale de Lausanne; ⁴Massachusetts Eye and Ear Infirmary/Harvard Medical School; ⁵Massachusetts Eye and Ear Infirmary; ⁶Harvard Medical School

Introduction

The auditory brainstem implant (ABI) provides hearing to deaf individuals who are not eligible for a cochlear implant due to anatomic constraints. Most ABI users have modest audiologic outcomes compared to cochlear implant users and often experience side effects from stimulation of non-auditory neurons. The current clinical ABI uses a stiff surface electrode array that is placed on or near the dorsal cochlear nucleus (DCN). We hypothesize that a flexible ABI electrode interface will improve performance by better molding to the surface anatomy of the DCN and reduce electrical current spread. Herein, we demonstrate chronic implantation of a novel micro-fabricated flexible 8-channel ABI electrode in mouse.

Methods

The surface of the left DCN was exposed by an occipital craniotomy in CBA/CaJ mice. An 8-channel flexible surface array was passed through a second craniotomy to stabilize the proximal lead, positioned on the DCN and secured to the surrounding skull. Sound-evoked auditory brainstem responses (ABRs) were recorded 1 week post-op. Multi-unit recordings from contralateral inferior colliculus (IC) were made in response to electrical stimulation of the DCN in acute experimental preparations. Revision craniotomy was performed two weeks following initial surgery to investigate position of the electrode and analyze electrode-brainstem interface.

Results

No extracranial infection was observed with chronically implanted arrays. Multi-unit recordings from contralateral IC confirmed stable responses to electrical stimulation of the DCN. Revision craniotomy confirmed stable orientation of the array along the DCN in all subjects. Sound-evoked ABRs were maintained following ABI surgery.

Conclusions

Chronic implantation of a novel flexible ABI electrode array in a mouse is associated with minimal tissue reaction and no adverse effects on acoustic hearing thresholds. These findings represent a step toward establishing whether flexible arrays are associated with improved outcomes compared to electrodes used in the clinic. Future studies will include use of a flexible array in a murine model following cochlear nerve transection to determine how electrically-evoked responses are influenced by retrocochlear deafness.

Supported by the Bertarelli Foundation and the NIH

PS 503

The Temporal Statistics of Electric Stimuli from a Cochlear Implant Modulate Auditory Temporal Processing and Plasticity in the Inferior Colliculus of Early Deafened Cats

Maïke Vollmer¹; Patricia A. Leake²; Ralph E. Beitel²

¹*Comprehensive Hearing Center, University Hospital Würzburg, Germany;* ²*Department of Otolaryngology-HNS, University of California, San Francisco, CA, USA*

The temporal patterns of sound in the acoustic environment are critically important for the development of neuronal temporal processing in the immature auditory system as well as for modifications in temporal processing in the adult system. The present study investigates whether the specific temporal statistics of intracochlear electric stimulation (ICES) delivered by a cochlear implant can modify neuronal temporal processing and plasticity in the deaf auditory midbrain.

Kittens were neonatally deafened by systemic injections of ototoxic drugs. At 6-8 wk of age, animals were implanted with a feline prosthesis in the left scala tympani, and a regimen of continuous, passive ICES was initiated (~4 h/day, 5 day/wk). The temporal fine structure (TFS) rates of passive ICES were selected to be either 1) low (30 or 80 pps, unmodulated); 2) intermediate (300 pps); or 3) high (500-800 pps) relative to the upper range (~300 pps) of temporal following capacity of neurons in the inferior colliculus. Intermediate and high rate carriers (300-800 pps) were 100% sinusoidally amplitude modulated at 30-60 Hz.

After several weeks of stimulation, responses of single neurons in the contralateral central (ICC) and external (ICX) nuclei of the inferior colliculus to unmodulated pulse trains of increasing rates were recorded with metal microelectrodes in anesthetized animals. The principal response parameters of interest were: best repetition rate (BRR), i.e., the stimulus rate that produced the maximum number of phase-locked spikes; cutoff rate (CR) at which the number of phase-locked spikes was 50% of the number at BRR; minimum neuronal response latency and response jitter. Prior normal hearing adult animals served as controls.

In the ICC, passive stimulation with an intermediate TFS rate of 300 pps was capable of significantly enhancing neuronal temporal processing, whereas stimulation with both low and high carrier rates had no significant effect on ICC temporal processing. In the multisensory ICX, temporal processing was not affected by the temporal characteristics of the applied signals.

Our findings indicate that the temporal characteristics of ICES modulate, i.e., maintain or enhance, auditory temporal processing and plasticity in the deaf cat ICC. Within a clinical setting, passive stimulation with appropriate stimulus repetition rates could provide a means of overcoming temporal processing deficits, particularly in individuals with poor speech discrimination abilities.

Support provided by NIH-NIDCD Contract HHS-N-263-2007-00054-C, Grant R01DC013067 and DFG Vo 640/2-2.

PS 504

3D X-ray Microscopy as a Tool for Non-destructive Imaging of Bony and Soft Tissue Elements of Mouse and Human Cochleae after Cochlear Implantation

Alexander D. Claussen¹; Christopher Kaufmann²; Rene Vielman¹; Elise Cheng¹; Brian Mostaert¹; Marlan R. Hansen²

¹*University of Iowa Hospitals and Clinics, Department of Otolaryngology-Head&Neck Surgery;* ²*University of Iowa Hospitals and Clinics, Department of Otolaryngology- Head & Neck Surgery*

Introduction

Modern cochlear implant research has greatly benefited from the recent advances in animals models as well as continued post-mortem temporal bone studies. Traditional histologic methods involving destructive sectioning of the cochleae with or without the implant in-situ have been used to provide great cellular and morphologic detail of the cochlea. However, successful histologic sectioning requires skilled personnel, time intensive protocols and is still subject to artifact. Here we present a non-destructive method of imaging post-mortem mouse and human cochlea with cochlear implants left in-situ with minimal sample preparation compared to classic histology methods and sub-micron resolution, available on a commercially available platform.

Methods

Samples included post-mortem, fixed human or mouse temporal bones with cochlear implants removed or left in-situ. Post-fixed samples were treated with a series of rinses and osmium tetroxide perfusion. Samples were mounted and imaged using the Xradia 520 Versa 3D X-ray Microscope (Zeiss, USA). Three dimensional reconstructions and artifact rejection were implemented within Scout and Scan Control System and XM Reconstructor – Cone Beam 10 software (Zeiss, USA). Image viewing and analysis were conducted within Visual SI (ORS, Canada).

Results

Resolution of cochlear scans varied from 700nm to 3µm per pixel for mouse cochleae and 12µm per pixel for human cochleae. Images of mouse cochleae with the cochlear implant left in-situ provided excellent bony and soft tissue detail of both the membranous labyrinths and peri-electrode tissue response. Nearly similar detail was attained in human cochlea, providing excellent approximations of implant trajectory, localizing sites of implant basilar membrane penetration and lateral wall penetration.

Conclusion

Here we demonstrate a non-destructive imaging modality for post-mortem human and mouse temporal bone specimens that allows for additional traditional histology after imaging. Time to imaging after fixation is relatively short compared to traditional histology and does not require personnel skilled in sectioning. The image acquisition hardware and software are commercially available. This technique has potential applications in studying cochlear implant related tissue response as well as assessing cochlear implant insertion trajectories in post-mortem tissue. Additionally, the availability of sub-micron resolution imaging of mouse cochleae allows the possibility of achieving targeted cellular contrast with gold-conjugated antibodies to provide even greater detail of specific cellular elements.

PS 505

A Mouse Model of Cochlear Implantation and Chronic Stimulation

Alexander D. Claussen¹; Jonathon R. Kirk²; Rene Vielman¹; Wolfram F. Dueck³; Brian Mostaert¹; Kristien JM. Verhoeven³; Marlan R. Hansen⁴

¹University of Iowa Hospitals and Clinics, Department of Otolaryngology-Head&Neck Surgery; ²Cochlear Americas; ³Cochlear Technology Centre; ⁴University of Iowa Hospitals and Clinics, Department of Otolaryngology- Head & Neck Surgery

Introduction

Cochlear implant (CI) technology continues to advance, restoring a functional level of hearing to an increasing number of patients with hearing loss. Notably, the recent development of the hybrid CI has extended the potential population of patients that benefit from cochlear implantation to include those with partial hearing loss. However, problems still exist that may hamper CI efficacy including loss of residual acoustic hearing after hybrid implantation post-implant intra-cochlear tissue response (Kopelovich et al., 2014; Kamakura & Nadol, 2016). The biologic significance and etiology of these problems is still incompletely understood, suggesting the utility of a

mouse CI model amenable to the vast array of molecular and genetic investigatory techniques available for mice. Here we provide an update of our mouse model of cochlear implantation that enables behaviorally significant chronic stimulation.

Methods

10 week old CBA/CaJ adult mice are unilaterally implanted in the left ear using a post-auricular approach (Soken et al., 2013). The device featured a 3-contact electrode array designed for the mouse cochlea (Cochlear, Australia) and two extracochlear ball electrodes attached to a percutaneously mounted connector. The connector allowed tethered communication to an implant emulator and sound processor for impedance testing, neural response telemetry (NRT) and programming via Custom Sound EP 4.2 (Cochlear, Australia). Custom housing supporting the tethered setup enabled chronic electric stimulation. Post-implant x-ray imaging as well as post-mortem histology and 3D X-ray microscopy were used to assess implant position and intra-cochlear changes.

Results

Impedance testing was performed serially on implanted mice starting between 2 and 7 days post-operative. We demonstrated repeatable acquisition of NRT growth responses and thresholds, which were used to program implants. Utilizing manual stimulation paradigms within Custom Sound EP 4.2, behavioral responses close to NRT threshold were obtained while mice were connected to a chronic stimulation cage. Post-operative x-ray allowed implant placement confirmation. Non-destructive 3D X-ray microscopy was used to assess post-mortem tissue response with the CI left in-situ. Final histology was performed after electrode removal showing varying degrees of intra-cochlear fibrosis and osteoneogenesis.

Conclusion

We demonstrate a mouse model of cochlear implantation that is programmable to behaviorally significant stimulation levels. Chronic, daily stimulation is deliverable via a stimulation cage that avoids daily mouse handling. Novel non-destructive 3D X-ray microscopy techniques allow sub-micrometer imaging of intra-cochlear tissue response with the CI in-situ. This mouse model and novel imaging techniques may be used to probe pertinent biologic questions in cochlear implantation.

PS 506

Development of Artificial Auditory Epithelium Implantable in the Cochlea

Juichi Ito¹; Takayuki Nakagawa²

¹Shiga Medical Center Research Institute; ²Dept. Otolaryngology, Head and Neck Surgery, Graduate School of Medicine, Kyoto University

Inner ear disorders such as sensorineural hearing loss are incurable in some occasion by conventional therapeutic strategies. New therapeutic strategies for protection or recover of inner ear function are therefore to be investigated. The aim of this project is to investigate a newly-invented artificial auditory epithelium (AAE) which is implantable in the inner ear.

Using piezoelectric material we fabricated inner ear implantable device, which is named as HIBIKI device. The project to develop this AAE device is named as Project HIBIKI.

The prototype of this device consists of a 40-micrometer-thick piezoelectric material. Piezoelectric material was fixed in a trapezoid-shape, which mimics the shape of the basilar membrane. It was made trapezoid so that it will possess frequency characteristics. The prototype was placed on a micro positioning stage. Pure tone was given to the prototype in the air at frequencies from 3 kHz to 20 kHz at 60 dB SPL. Oscillations of the prototype were detected by a laser Doppler vibrometer and voltages produced by the prototype were measured for each electrode. This device generated electrical potentials in response to sound stimuli.

Using deaf animal spiral ganglion neurons were stimulated by amplified output of electricity generated by the device and electrically-evoked ABR (eABR) was measured. In result eABR was recorded in deafened guinea pigs using this device.

AAE or HIBIKI device will become an effective tool for the treatment of highly hearing impaired patients.

PS 507

Miniature Pigs: A Large Animal Model of Cochlear Implantation

Weiwei Guo¹; Tao Cong²; Shi-ming Yang³; Wei Sun⁴

¹Department of Otolaryngology, Head & Neck Surgery, Institute of Otolaryngology, Chinese PLA General Hospital; ²Department of Otolaryngology, Head & Neck Surgery, Institute of Otolaryngology Of PLA, Chinese PLA General Hospital; ³Chinese PLA General Hospital; ⁴University at Buffalo, The State University of New York

Objective

To investigate the suitability of the miniature pig as a large animal model of cochlear implantation (CI).

Methods

Micro-CT scanning and three-dimensional reconstructions of the inner ear were completed in six miniature pigs. Photographs of the procedures and measurements of the inner ear were made. The CI procedure was simulated in 10 animals. Electrically evoked auditory brain stem responses (eABRs) and radiographic images were evaluated during or after the CI surgery.

Results

Morphological examination and measurements of inner ears of the miniature pigs were completed by micro-CT scanning. The capsule of the cochlea is a spiral tube coiled three and a half turns. The height of the scala tympani was 873.12 μm in the first turn, 641.46 μm in the second turn, 445.13 μm in the third turn and 339.19 μm in the fourth turn. The length of the cochlea was 38.6 mm which is similar to that in the human (36 mm) and larger than the rats (7.2 mm) and macaque (22 mm). Commercial cochlear implant electrodes used for humans (870 μm at the end and 630 μm at the tip in diameter) were tested in the pig's cochlea and eABRs were obtained. Radiographic images after the implant surgery revealed electrodes located in the scala tympani of the first and second turns of the cochlea.

Conclusion

Compared with traditional animal models, greater similarities of the inner ear between miniature pigs and humans make this animal a potentially useful model for CI studies.

PS 932

Spiral Ganglion Neurite Outgrowth on Electrospun Nanofibrous Piezoelectric Polymer Scaffolds

Hassan A. Zabalawi¹; Mohamed Jomaa²; Xiao Liu³; Wenhui Song³; Jonathan Gale¹

¹UCL Ear Institute; ²Co-Author; ³University College London

Sensorineural hearing loss (SNHL) is caused by hair cell loss and by the degeneration of spiral ganglion neurons (SGNs). Cochlear implants (CIs) restore hearing to profoundly deaf people by electrical stimulation of preserved SGNs. Thus, the extent of SGN degeneration dictates the efficacy of CIs. Progressive degeneration of SGN peripheral processes raises the thresholds needed for electrical stimulation, necessitating higher currents reducing battery life and the precision of frequency representation since a larger number of adjacent SGNs are

stimulated. The replacement and/or directed regrowth of auditory neurons would be an important step in any attempt to restore auditory function in patients with damaged SGNs or hair cells.

We examined the viability of oligosilsesquioxane-poly(ϵ -caprolactone) (POSS-PCL), polyhedral oligomeric silsesquioxane poly(carbonate-urea) urethane (POSS-PCU) and Polyvinylidene Trifluoroethylene (PVDF-TrFE) for SGN adhesion and survival. Due to its biocompatibility and piezoelectric properties, PVDF-TrFE was chosen to add directional growth cues through electrospinning aligned nanofibre scaffolds. We are testing the ability of these scaffolds to control and potentially enhance SGN neurite regrowth and alignment.

The effects of alignment on the length and orientation of re-growing SGN neurites and glia were tested in vitro using primary SGNs from C57BL/6 P5 mice. Firstly, two methods of SGN preparation were compared: SG explants and dissociated SGN cultures. After fixation and immunostaining, neural and glial cells were counted, the length and direction of the regrown neurites were measured. Primary SGNs showed preferential affinity to PVDF-TrFE nanofibres which were also found to promote SGN neurite regrowth compared to glass cover slips. The angles at which SGN neurites extended significantly correlated with the orientation of the nanofibres.

Our data show that electrospun aligned nanofibrous PVDF scaffolds can modulate SGN organization in vitro. The aligned piezoelectric nanofibrous scaffolds provide high mechanical and electrical versatility. We are currently optimising the mechanical and electrical properties of the nanofibres through incorporation of carbon nanotubes and graphene mini-sheets and testing their effects on SGN regrowth and alignment.

Brainstem Session III

PS 508

Nitric Oxide Donor Evokes Excitation in the Ventral Cochlear Nucleus

Xiao-Jie Cao; Donata Oertel

School of Medicine and Public Health, University of Wisconsin-Madison

T Stellate cells of the posteroventral cochlear nucleus (pVCN) are interconnected within isofrequency laminae through potentiating, glutamatergic synapses (Cao and Oertel, 2016, ARO Abstract). Several lines of evidence support the conclusion that potentiation requires retrograde signaling by nitric oxide (NO), a free radical and potent neuromodulator in the mammalian brain. Calcium

enters through NMDA receptors, activates neuronal nitric oxide synthase (nNOS) that crosses from the postsynaptic T stellate cell to the presynaptic cell where it is detected by soluble guanylate cyclase which in turn increases the probability of the generation of an EPSC (Burette et al., 2001; Coomber et al., 2015). We have made single and dual whole-cell patch recordings from T stellate cells in slices to measure responses to the bath application of an NO donor, 250 μ M propylamine-propylamine NONOate or PAPA NONOate. In every T stellate cell tested (n=6) PAPA NONOate evoked trains of EPSCs. The sizes and shapes of evoked EPSCs differed widely. In some cells (n=3), evoked EPSCs were relatively small, between 150 and 500 pA in amplitude, and their time course resembled the time course of EPSCs evoked by shocks to the auditory nerve (Cao and Oertel, 2010) and EPSCs evoked by stimulation of another T stellate cell (Cao and Oertel, 2016, ARO Abstract). These EPSCs are likely unitary EPSCs evoked by a single presynaptic neuron. In other cells (n=3), EPSCs evoked by the application of an NO donor were much larger, 900 to 1400 pA, and rose to a broader peak before decaying. Spontaneous EPSCs comprised mEPSCs of about 50 pA (Gardner et al., 1999). The NO donor did not alter the average amplitude of EPSCs in octopus cells. Our results are consistent with the interpretation that the larger EPSCs are compound EPSCs resulting from the roughly synchronous activation of multiple neurons. As T stellate cells are interconnected within an isofrequency lamina, the compound EPSCs likely reflect the synchronous firing in an isofrequency lamina.

PS 509

Hyperpolarization-activated Cation Conductances Are Tonotopically Distributed in the Chick Cochlear Nucleus

Lashaka Jones; Stephan Oline; R. Michael Burger
Lehigh University

Auditory stimuli are processed in parallel frequency-tuned circuits, beginning in the cochlea. Auditory nerve fibers (nVIII) impart 'tonotopic' organization onto nucleus magnocellularis (NM), a division of the cochlear nucleus specialized for phase-locking. Phase-locking precision is required for sound localization via a coincidence detection process in nucleus laminaris (NL), the sole target of NM output. While NM is a superficially homogenous structure, a large number of physiological properties vary systematically along the tonotopic axis. For example, low voltage-activated potassium currents (KLVA) (Fukui & Ohmori, 2004), length of the spike initiation zone (Kuba & Ohmori, 2009), number of synaptic inputs, and resting potential, all vary tonotopically. NL neurons exhibit similar tonotopically arranged features including expression of hyperpolarization-activated

cation channels (HCN), the channels that underlie Ih currents. HCN channels contribute to membrane excitability and resting potential. Cyclic adenosine monophosphate (cAMP) has been shown to modulate HCN channels by speeding up activation kinetics and shifting the voltage of activation to more depolarized potentials (Ohmori & Yamada, 2005). Within NM cAMP its thought to play a significant role in inhibiting the influx of calcium, thus preventing calcium apoptosis, via activation of metabotropic glutamate receptors (Lachica & Rubel, 1995). Within NL Ih sensitivity to cAMP is higher in high characteristic frequency (HCF) neurons, which have increased synaptic activity, compared to low and middle characteristic frequency neurons (LCF, MCF). As a first step, we have investigated whether HCN channels are indeed tonotopically distributed in NM as they are in NL. To examine Ih currents, we measured membrane responses using whole cell voltage clamp protocols in the presence or absence of the HCN antagonist ZD7288, and a cocktail of pharmacological agents to block synaptic or other voltage gated conductances. Our data show that the magnitude of Ih current is larger in low characteristic frequency (CF) neurons in comparison to high CF neurons. Interestingly, the activation voltage for both populations of NM neurons appears to be well matched to the resting membrane potential within that population where low CF neurons tend to rest at more depolarized potentials while high CF neurons rest at more hyperpolarized potentials. An intriguing unresolved question is whether cAMP is differentially modulating Ih in low CF, middle CF, and high CF NM neurons and more importantly, whether HCNs influence postsynaptic excitability by way of HCN channel composition, cAMP accumulation, or a combination of both within a particular tonotopic region.

PS 510

Descending Projections from the Ventral Tectal Longitudinal Column to the Dorsal Cochlear Nucleus in the Mouse

Giedre Milinkeviciute¹; Michael A. Muniak²; Kiera Grierson²; David K. Ryugo¹

¹Garvan Institute of Medical Research, University of New South Wales; ²Garvan Institute of Medical Research

Background

The ventral tectal longitudinal column (TLCv) is a relatively novel nucleus in the mammalian auditory system. It runs on both sides of the midline from the caudal limit of the commissure of the inferior colliculus (coIC) through to the rostral extreme of the commissure of the superior colliculus (coSC). The TLCv is traversed by these commissural fibers that bilaterally connect the inferior and superior colliculi. TLCv neurons most likely

sample auditory and visual information as well as inputs arising from other brain structures. Neurons in the TLCv are not sensitive to light but respond to acoustic stimuli with long first spike latencies and appear to be less selective to sound frequency. Tonotopic organization has not been observed along the rostrocaudal axis. Additionally, numerous TLCv neurons were labeled following retrograde tracer injections to the superior paraolivary nucleus. Together, these data suggest TLCv involvement in descending regulatory pathways rather than processing primary auditory information. In this report, we investigated the descending pathway from the TLCv to the dorsal cochlear nucleus (DCN).

Methods

The Golgi stain was used to characterize morphological neuron types. A cocktail of anterograde and retrograde tracer dyes was injected in the DCN of CBA/CaH and transgenic GAD67-EGFP mice after determining multiunit best frequency and threshold. Brains were processed using standard histologic methods for visualization and examination of neuronal tracer dyes using fluorescence and brightfield microscopy. Cells were plotted and reconstructed in 3D.

Results

Golgi-stained tissue revealed three neuronal populations comprising the TLCv—pyramidal, stellate, and elongate bipolar. Injections in the DCN resulted in retrogradely-labeled neurons throughout the length of the TLCv with an ipsilateral predominance. Occasional partial fills of dendrites by the retrograde tracer dye revealed that elongate bipolar and stellate cells participate in sending descending projections to the DCN. GABAergic neurons (EGFP-positive) were scarce in the TLCv, and none co-labeled with retrogradely filled neurons. BDA-labeled terminals arising from the DCN were present in the TLCv.

Conclusions

The TLCv receives input from the DCN and also projects back to it, creating a novel excitatory auditory feedback-circuit that is positioned to modulate and refine signal processing at the very beginning of the ascending auditory chain. Based on its location, the TLCv could serve as a platform to synchronize signals from different sensory modalities and participate in the localization of sounds along the vertical plane in the DCN by matching acoustic signals to gaze direction.

PS 511

Distinct Neuronal Mechanisms for Low Frequency Processing in the Chicken Nucleus Magnocellularis

Xiaoyu Wang¹; Hui Hong²; David Brown¹; Jason Sanchez²; Yuan Wang¹

¹Florida State University; ²Northwestern University

The avian cochlear nucleus magnocellularis (NM) and its mammalian analogue, the anteroventral cochlear nucleus (AVCN), are the first stations for temporal processing in the brain. Similar to AVCN, NM is tonotopically organized; neurons display gradually increasing characteristic frequency (CF) along the caudolateral to rostromedial axis. NM neurons with mid to high CFs are well studied and known to adopt a number of structural, synaptic and intrinsic specializations for optimized temporal processing. Neurons that encode sounds of very low to low frequencies in the caudolateral NM (NMc), however, display some distinct neuronal and synaptic morphologies with the underlying neuronal mechanisms for low frequency processing largely unknown.

To fill this gap, we characterized the organization and biophysics of the chicken (*Gallus gallus*) NMc in late embryos and hatchlings. NMc neurons display extensive dendrites as visualized with a somatodendritic marker, distinct from mostly adendritic NM neurons with higher CFs. Furthermore, based on cytoarchitecture and dendritic morphology, we first identified two subregions in NMc, named NMc1 and NMc2. 3D dendritic reconstruction of individually dye-filled NMc neurons further revealed that NMc2 neurons have significantly larger and more complex dendritic fields than NMc1. Tract tracing studies demonstrated that the auditory nerve forms small bouton-like terminals in NMc, distinct from large endbulb synapses on the adendritic NM neurons. NMc also receives inhibitory inputs from the superior olive nucleus, suggesting that inhibition is a common mechanism in NM. Importantly, NM neurons differ in the expression of calcium binding proteins and neuropeptide. Higher-CF NM neurons and most neurons in NMc1 are calretinin immunoreactive, while few express cholecystokinin. On the contrary, the majority of NMc2 neurons are calretinin negative but specifically express cholecystokinin.

A biophysical hallmark of higher-CF NM neurons is the generation of a single onset action potential (AP) in response to sustained depolarization, a response property critical for sound localization encoding. In contrast, we show that NMc neurons can generate multiple APs to suprathreshold sustained depolarization with slower kinetics and poorer reliability. This distinct firing phenotype may have a unique role in low frequency processing. In addition, NMc neurons are also spontaneously active. Interestingly, both evoked and spontaneous activity of

NMc neurons display a clear heterogeneity, likely due to multiple neuron types found in this region. Taken together, our data indicate that NMc contains multiple neuronal cell types with distinct structure, molecular signatures, and biophysical properties, emphasizing highly specialized and distinct mechanisms for processing sounds of low frequency.

PS 512

Corticotropin Releasing Factor Expression in the Cochlear Nucleus and Upstream Auditory Pathway Nuclei

Kathleen T. Yee; Douglas E. Vetter
University of Mississippi Medical Center

Introduction

We are interested in how gene expression and cell signaling contributes to the mature organization of the cochlear nucleus (CN). We have previously shown that hypothalamic-pituitary adrenal axis molecules are expressed in the cochlea (Graham et al 2010) and have also presented evidence that this signaling extends upstream to the first auditory synaptic target in the brain, the CN. We have extended the report of CRFR1 expression in the adult CN (CRFR1 BAC transgenic GFP mice, Justice et al. 2008) and show that in addition to CRFR1 expression in the molecular and granule cell layers of the CN and scattered cells in the ventral cochlear nucleus (VCN), CRFR1 in the CN is more broadly expressed during development and is down-regulated with maturity. Since CRFR1 has a dynamic spatial and temporal distribution, we were interested in identifying putative ligand-expressing cells and their morphologies; we report the expression of corticotropin releasing factor (CRF) here.

Methods

CRF-IRES-Cre mice and ROSA26-tdTomato mice, expressing a reporter preceded by a floxed STOP cassette, aka Ai14 line (purchased from Jackson Labs) were mated as homozygous crosses to generate CRF:tdTomato reporter mice. The progeny carry both transgenes and result in tdTomato expression in cells expressing CRF due to Cre recombinase activity. Reporter expression faithfully mirrors CRF expression patterns based on immunohistochemical procedures (Chen et al., 2015). Brains from cardiac perfused (4% paraformaldehyde) CRF-Cre tdTomato mice were sectioned, mounted, coverslipped and examined by fluorescence microscopy.

Results

Within the CN, expression of CRF (tdTomato) is associated predominantly with the granule cell layer of the dorsal CN (DCN) and VCN and the DCN molecular layer. In these regions, large tdTomato-positive cell bodies

with elaborate dendritic trees in the granule cell layer are prominent, notably in the DCN. TdTomato-positive terminal fields are also detected heavily, but not exclusively, within the DCN core. A small number of scattered cells within the VCN also express CRF. CRF is also expressed in other higher order auditory nuclei, including the inferior colliculus and medial geniculate.

Conclusions

These results show that CRF is expressed in the CN, and offers a signaling partner for CRFR1 in the CN. Furthermore, the presence of CRF in higher order auditory centers suggests that CRFR1 signaling may occur in those nuclei as well. Future studies will examine whether other CRFR ligands are localized in central auditory nuclei and whether noise alters CRF/CRFR1 expression.

Supported by: R21DC015124 (DEV)

PS 513

Developmental Changes in the Vesicular Content at a GABA/glycinergic Inhibitory Synapse in the Cochlear Nucleus

Jana Nerlich¹; Rudolf Rübsamen²; Ivan Milenkovic¹
¹University of Leipzig; ²Faculty of Biosciences, Pharmacy and Psychology, University of Leipzig, Germany

Background

Spherical bushy cells (SBCs) in the ventral cochlear nucleus integrate acoustically driven excitatory input from the auditory nerve (AN) with non-primary inhibitory inputs to precisely encode the temporal structure of sounds. During the first postnatal week, GABA and glycine have a depolarizing effect on SBCs thereby also triggering calcium signals. In mature rodents, hyperpolarizing slow glycine/GABAergic signaling exhibits an activity dependent conductance build-up, thus endowing inhibition with high-pass filter properties for large and well-timed excitatory inputs.

It remained elusive, whether GABA and glycine are released from distinct presynaptic vesicles or coreleased from the same vesicle. Here, we determined the glycinergic and GABAergic contribution to the inhibitory vesicle content by measuring spontaneous vesicle release during development.

Methods

Whole-cell recordings were performed on SBCs in acute slices of gerbils from P1 up to P25. Glycine- (GlyR) and GABAA-receptor mediated miniature inhibitory postsynaptic currents (mIPSCs) were recorded under pharmacological inhibition of glutamate receptors (50 μ M AP-5, 10 μ M NBQX), GABAB receptors (3 μ M CGP 55845) and NaV (0.5 μ M TTX). GABAAR- and GlyR-mediat-

ed mIPSCs were isolated by application of strychnine (0.5 μ M, GlyR) and SR95531 (15 μ M, GABAAR).

Results

Miniature IPSCs were first detectable at P2 in a small subset of neurons. The frequency, amplitude and rise time of mIPSCs showed a significant increase up to P25. The decay time constant was unchanged during maturation. In the first postnatal week, no purely glycinergic mIPSCs were detected, inferred by the lack of mIPSCs frequency change under strychnine. Thus, all mIPSCs contained a GABAergic component. The block of GABAAR, on the contrary, reduced the mIPSCs frequency, suggesting a large portion of presynaptic vesicles containing solely GABA. The remaining mIPSCs were consistent with a corelease of glycine and GABA in a subset of vesicles. During maturation, the frequency and amplitude of glycinergic mIPSCs increased, whereas the fraction of GABAergic events decreased. In P23-25 gerbils all mIPSCs exhibit a glycinergic component, while no pure GABAergic events were observed. Here, mIPSCs with large amplitudes feature GABAergic components, again suggesting a corelease of GABA and glycine in a subset of vesicles.

Conclusion

Before hearing onset, the inhibitory synaptic terminals predominantly release GABA, whereas glycine is coreleased only in a subset of presynaptic vesicles. With maturation, the glycinergic fraction increases and glycine becomes the major inhibitory transmitter after hearing onset. In juvenile gerbils, particularly large mIPSC are evoked by vesicles containing GABA in addition to glycine.

PS 514

Plasticity of Zinc-mediated AMPAR Inhibition in the Dorsal Cochlear Nucleus

Nathan Vogler; Thanos Tzounopoulos
Department of Otolaryngology and Neurobiology, University of Pittsburgh

In many brain areas, such as the neocortex, limbic structures, and the auditory brainstem, glutamatergic nerve terminals also contain zinc in their synaptic vesicles (synaptic zinc). In the dorsal cochlear nucleus (DCN), an auditory brainstem nucleus, synaptic zinc is released from glutamatergic parallel fiber synapses, and inhibits presynaptic glutamate release as well as postsynaptic NMDA and AMPA receptors (NMDARs/AMPA), thus functioning as a major inhibitory modulator of excitatory synaptic strength. Vesicular zinc levels are reduced following sound exposure, thus providing a novel mechanism of experience-dependent plasticity at excitatory synapses. However, the signaling mechanisms under-

lying this plasticity remain unknown. To study these mechanisms, we employed in vitro electrophysiological recordings in DCN slices. Application of the zinc chelator ZX1 (100uM) potentiates AMPAR EPSCs evoked by stimulation of zinc-rich parallel fibers, demonstrating inhibition of AMPAR by synaptic zinc. High-frequency stimulation (HFS, 3 x 100Hz) of parallel fibers eliminates potentiation by ZX1, indicating activity-dependent plasticity of zinc-mediated AMPAR inhibition (zinc plasticity). Application of intracellular BAPTA (Ca²⁺ buffer, 10mM) to the postsynaptic recording pipette preserves ZX1 potentiation after HFS, indicating that zinc plasticity requires increases in postsynaptic calcium. Bath application of APV (NMDAR antagonist, 50uM) before and during the HFS does not affect zinc plasticity, indicating that zinc plasticity does not require NMDARs. The lack of ZX1 potentiation after HFS is also associated with decreased paired-pulse ratio and increased 1/CV² (coefficient of variation analysis), suggesting that zinc plasticity is associated with increased presynaptic release probability (Pr). Together, these results demonstrate plasticity of zinc-mediated AMPAR inhibition at DCN parallel fiber synapses. The dependence of zinc plasticity on rises of postsynaptic calcium, as well as its association with changes in Pr, are consistent with the involvement of a retrograde signaling mechanism in zinc plasticity.

This work was supported by: R01-DC007905 (T.T.); T32-NS007322, F31-DC015924 (N.V.)

PS 515

Paired Auditory-somatosensory Stimulation Alters Temporal Processing in Bushy Cells

Susan E. Shore; Amarins Heeringa
Department of Otolaryngology, Kresge Hearing Research Institute, University of Michigan

Bushy cells of the ventral cochlear nucleus (VCN) receive auditory nerve input through somatic endbulb projections that help preserve and enhance auditory nerve spiking patterns. These neurons provide input to the superior olivary nuclei, which require accurate preservation of spike timing in order to encode sound location. Bushy cells also receive inputs from the somatosensory system, including the spinal trigeminal nucleus (Sp5) (Zhou and Shore, *J Neurosci Res*, 2004), the function of which is unknown. Here we investigate the long-term effects of bimodal auditory-Sp5 stimulation on bushy cell AM temporal coding by examining phaselocking to amplitude modulation (AM).

Recording and stimulating electrodes were stereotaxically placed in the VCN and Sp5, respectively, of normal-hearing guinea pigs. Single units from bushy cells

were identified by their primary-like or primary-like with notch responses to best frequency tone bursts. Bimodal stimulation consisted of a short burst of electrical deep-brain stimulation (10-60 μ A) in Sp5 followed by a 50ms noise burst (0-90 dB SPL). AM noise bursts (400 ms, 8-2048 Hz, 6-100% modulation depth) and unmodulated noise bursts were presented before and after bimodal stimulation, and their responses were compared.

Forty two percent of bushy cells showed altered vector strengths following bimodal stimulation, half of which were improved and half of which were degraded. Furthermore, best modulation frequency (BMF) was altered so that bushy cells with a high BMF had decreased BMFs, whereas bushy cells with a low initial BMF had increased BMFs after bimodal stimulation. A majority (76%) of bushy cells showed altered amplitude modulation detection thresholds, (neurometrically determined after Sayles et al., *J Physiol*, 2013), following bimodal stimulation. Both improvements and decrements of detection thresholds were observed in different bushy cells.

This study showed that bimodal stimulation differentially altered temporal coding of bushy cells. Previous studies indicate that changes in vector strength and best modulation frequency can occur when stimulus level is varied (Frisina et al., *Hear Res*, 1990), suggesting that bimodal stimulation may alter the set-point of bushy cells' firing patterns. Future studies will determine whether the change in temporal coding depends on the type of neurotransmitter used by Sp5 terminals on bushy cells or whether it depends on the involvement of inhibitory interneurons innervated by Sp5 terminals.

Supported by NIH RO1-DC004825 (SES) and NIH P30-DC05188

PS 516

Functional Development of Neurons in the Anteroventral Cochlear Nucleus of Laboratory Mice

Sasa Jovanovic¹; Maria Katharina Müller¹; Rudolf Rübsamen²; Ivan Milenkovic³

¹*Carl Ludwig Institute for Physiology, Faculty of Medicine, University of Leipzig, Germany;* ²*Faculty of Biosciences, Pharmacy and Psychology, University of Leipzig, Germany;* ³*University of Leipzig*

Background

In the cochlea, auditory information is encoded by series of action potentials (AP) which are conveyed to the cochlear nucleus. The two principal neuronal types in the anteroventral cochlear nucleus (AVCN) encode distinct features of sound: (i) bushy cells (BC) preserve the temporal structure of auditory nerve activity, which is cru-

cial for sound source localization in the superior olivary complex; (ii) stellate cells (SC) encode the sound intensity by monotonically increasing their firing rate. While development of AVCN neurons has been extensively investigated in slice preparations, the respective *in vivo* data is still lacking. Here we investigated the temporal profile of functional BC and SC development starting before hearing onset, through the phase of early acoustical experience, up to the adult-like developmental stages.

Methods

In vivo juxtacellular recordings of spontaneous and acoustically evoked activities were conducted to investigate the functional development of BCs and SCs. Experiments were performed on 8-30 days old CBA/J mice.

Results

BCs and SCs exhibit bursting activity before hearing onset, which gradually changes to Poisson-like activity up to P14, when bursts completely vanish. Bursting discharge pattern and the occurrence of bursts between P8 and P10 are more pronounced in SCs than in BCs. Along with the change in the activity pattern both synaptic transmission and APs become faster. Generally faster APs of SCs reach mature-like level at P13, while in BCs AP duration continues to decrease up to P18. Shortening of response times to acoustic stimulation and sharpening of frequency response areas progress in both neuronal types until P18. Thereafter, further changes were observed up to P25 with respect to an increase in spontaneous and acoustically evoked firing rates.

Conclusion

These data reveal that the synaptic inputs to BCs and SCs and the physiological properties of these neurons undergo prominent changes during first four postnatal weeks. Two neuronal types share similar maturation pattern, with the notable exception of AP duration which develops faster in SCs. Earlier maturation may be a consequence of more pronounced bursting activity in SCs compared to BCs. Physiological properties such as AP duration, firing rates and first spike latencies differ between BCs and SCs throughout development, reflecting their distinct roles in sound processing. In summary, this study describes in detail the developmental time-course of the physiological properties of BC and SC which can be used as a reference for future studies in genetically modified mouse models.

PS 517

Subunit Composition of Glutamate Receptors in Developing Avian Cochlear Nucleus Magnocellularis

Jason Sanchez; Ting Lu; Hui Hong
Northwestern University

Fast neural encoding of sound is essential for normal auditory functions, such as sound localization abilities and speech in noise discrimination. An example of fast neural encoding occurs in the cochlear nucleus. Here, AMPA-receptors (AMPA-Rs) mediate fast glutamatergic synaptic transmission and provide functions important for the perception of behaviorally relevant communication signals. Elsewhere in the developing brain, NMDA-receptors (NMDA-Rs) assist in regulating normal AMPA-R properties. These specialized functions of AMPA- and NMDA-Rs are defined by their subunit composition. In this study we investigate the subunit composition of both AMPA- and NMDA-Rs in the developing avian cochlear nucleus magnocellularis (NM), an analogous structure to the mammalian anteroventral cochlear nucleus.

Whole-cell voltage clamp recordings were performed from NM neurons in brainstem slices of developing chicken embryos before, during, and after hearing onset, corresponding to embryonic (E) days 10-12, E14-E16, and E19-E21, respectively. AMPA- and NMDA-R mediated currents were elicited either through synaptic stimulation using a concentric bipolar electrode, or puff application of corresponding agonist. Subunit specific antagonists were bath applied. Recorded E10-11 neurons were filled fluorescently (neurobiotin, 0.05%) to verify structure and location within the nucleus.

Between E10 and E21, AMPA-R currents become inwardly rectifying. AMPA-R current reduction by IEM-1460 (100 μ M), a highly specific antagonist to the GluA2-lacking AMPA-R, gradually increased from 20.18% to 83.21%. Ifenprodil (10 μ M), a selective antagonist of GluN2B-containing NMDA-R, blocked NMDA-R currents by about 60% at all ages. TCN-201 (10 μ M), an NMDAR inhibitor with selectivity against GluN2A-containing receptors had minimal effect on NMDA-R currents. The ratio of TCN-201 sensitive NMDA-R is 6.72%, 2.04%, and 7.7% for E10-12, E14-E16, and E19-E21 NM neurons, respectively. For E19-21 NM neurons, an increase in the NMDA-R/AMPA-R ratio was observed across the high-to-low frequency tonotopic regions.

Our results from the avian NM suggest a dramatic decrease in GluA2-containing AMPA-R during development, likely to accommodate rapid postsynaptic transmission. With age, the subunit composition of NMDA-R remains unchanged; GluN2B-containing receptor con-

tributes to the majority of the NMDA-R current throughout development. The relatively small effect of TCN-201 might be attributable to a basal level of Zn²⁺ in the extracellular solution; hence the contribution of GluN2A-containing receptors needs further confirmation. The larger NMDA-R/AMPA-R ratio in the low frequency region of NM suggests that NMDA-Rs may play an important role in low frequency postsynaptic transmission in the avian NM.

PS 518

Neuromodulation of Inhibitory Transmission by Group I mGluRs in Mouse MNTB Neurons

Rebecca Curry; Yong Lu

Northeast Ohio Medical University

The medial nucleus of the trapezoid body (MNTB) provides synaptic inhibition to many auditory brainstem nuclei and also receives inhibitory inputs. However, not much is understood of the inhibition the MNTB itself receives and it remains entirely unknown how this inhibition is regulated. Here, we investigated group I metabotropic glutamate receptor (mGluR I, consisting of two members, mGluR1 and mGluR5) modulation of the glycinergic and GABAergic inputs to MNTB neurons in both wildtype (WT) mice and a fragile X syndrome (FXS) mouse model, in which the fragile X mental retardation gene 1 is knocked out (Fmr1 KO). Loss of the FMR protein results in exaggerated activity of mGluR I, allowing for comparisons of mGluR I function under normal and altered conditions. The KO and WT mice (with a background of C57/B6) were purchased from the Jackson Laboratory and bred at NEOMED. Brainstem slices (250 μ m) were prepared from P14-P21 mice. Whole-cell voltage clamp was used to record spontaneous and electrically evoked IPSCs (sIPSC and eIPSC) in MNTB neurons at 35 °C. Glycinergic and GABAergic IPSCs were pharmacologically isolated with bath application of gabazine (10 μ M) and strychnine (1 μ M), respectively. Immunohistochemistry was performed to detect the mGluR5 antigen. Activation of group I mGluRs by 3,5-DHPG (200 μ M) increased sIPSC frequency and amplitude in both WT and KO neurons for glycinergic transmission, but did not modulate glycinergic eIPSCs. Bath application of the mGluR1 antagonist LY367385 (200 μ M) and mGluR5 antagonist MPEP (10 μ M) during 3,5-DHPG puff application (200 μ M) resulted in lower frequency and amplitude of glycinergic sIPSCs in WT, compared to 3,5-DHPG puff application without the antagonists. For GABAergic transmission, 3,5-DHPG did not increase sIPSC frequency or amplitude, but did suppress eIPSCs in a subset of WT and KO neurons. The differential modulation of sIPSC and eIPSC suggests that there may be differences in the vesicle pools responsible for spontaneous and evoked glycine release,

as well as the mechanisms underlying mGluR modulation of the two release machineries. Additionally, group I mGluRs may differentially regulate glycinergic and GABAergic inputs to the MNTB.

Supported by NEOMED Bridge Funding to YL.

PS 519

Axon Growth and Myelination of Trapezoid Body Fibers Require Sound-evoked Activity

James Sinclair¹; Matthew Fischl¹; Conny Kopp-Scheinpflug¹; James L. Sinclair²

¹Ludwig-Maximilians University, Munich; ²Ludwig Maximilian University

Background

Activity dependent change in myelination has been predominantly demonstrated in cortical regions. However, in the auditory nerve demyelination occurs following damaging acoustic trauma, as well as age-related hearing loss. Here we ask whether temporary, non damaging sensory deprivation will also influence the growth of axon calibre and myelination.

Methods

The trapezoid body (TB) is a large, myelinated auditory fibre tract connecting the two sides of the brainstem similar to the corpus callosum in the forebrain. Axon calibre and myelin thickness were measured in TB using immunolabeling for neurofilament and myelin basic protein, respectively. Mild sensory deprivation (20dB attenuation) was induced by raising the animals with bilateral earplugs between P10 and P20. Physiological measures of hearing thresholds and conduction velocity were taken from auditory brainstem responses (ABRs) and two-electrode axonal stimulation patch-clamp experiments.

Results

In this study we characterised the developmental change in myelination in TB fibres in mouse from P8-65. At P8, mean axon calibre was 1.14 \pm 0.19 μ m and the surrounding myelin sheath was 0.65 \pm 0.18 μ m. Axon calibre increased until reaching stable values of 2.60 \pm 0.11 μ m around P25, while the myelin sheath kept increasing further until reaching a plateau of 1.39 \pm 0.06 μ m around P35. Conduction velocity of individual TB fibres was slow in prehearing animals (4.56 \pm 0.68 m/s). It increased in speed until reaching a plateau of 8.14 \pm 0.99 m/s around P20. Raising animals with earplugs (EP) for the critical period from P10-20 limited the growth of axon calibre and myelin in the third and fourth post-natal week and causing a significant difference in calibre and myelin at P35 between EP reared and control animals. By P45 both

calibre and myelin sheath were back to control levels. Interestingly ABR thresholds were normal immediately after EP removal. Performing a similar manipulation in adult, hearing mice (EP reared between P55-65) had no effect on axon calibre or myelin sheath thickness.

Conclusions

Our data show that axon calibre and myelin thickness in TB fibres are only partly intrinsically programmed but require acoustically driven activity for accurate development. Restricting afferent firing during development resulted in a greater reduction in calibre and myelin relative to age-matched controls, than the reduction resultant from EP reared adults, implying a critical period for axonal growth and myelin plasticity in the auditory brainstem. The fact that conduction velocity matured before axonal growth suggests that increased axon calibre and myelin thickness are needed for transmitting additional parameters rather than speed alone.

PS 520

Cholinergic Input Modulates Sound Evoked Responses in MNTB of the Adult Gerbil

Chao Zhang¹; Michael Pecka²; Inka Leprince³; R. Michael Burger⁴

¹Lehigh University, Matthew Fischl; ²Ludwig-Maximilians-Universität München; ³Chao Zhang, R. Michael Burger; ⁴Lehigh University

The superior olive complex (SOC) functions as a major hub of ascending and descending auditory circuitry. Within SOC, principle neurons of the medial nucleus of the trapezoid body (MNTB) are devoted to reliably convert monaural contralaterally derived, temporally precise excitation to inhibition that is distributed to several postsynaptic targets, thus conveying phase-locked inhibition to nuclei involved in computation of sound location. MNTB neurons are known to preserve temporal information in their firing patterns upon sound stimulation, however, modulatory mechanisms underlying these response features have yet to be illuminated. One such modulatory system is the cholinergic system, which influences neural signaling throughout the brain. In the SOC, Happe and Morley (1998) showed intense labeling of nicotinic acetylcholine receptors (nAChRs), suggesting potentially strong cholinergic modulation of MNTB neurons. Despite this evidence, no physiological investigation of this input has been reported for MNTB neurons, and the putative cholinergic projections to this region have not been described.

In order to investigate the role of cholinergic input to the MNTB, we made in vivo extracellular recordings from anesthetized gerbil MNTB, using piggyback multibarrel

electrodes. This configuration allowed us to pharmacologically manipulate cholinergic input with iontophoresis of agonist and antagonists of nAChRs. Both treatments altered sound driven responses. Application of the ACh antagonist, mecamylamine (MEC), revealed evidence of the involvement of endogenous cholinergic signaling in modulating acoustically stimulated responses of MNTB. In the presence of ACh agonist nicotine (NIC), neurons exhibit complex patterns of modulation, suggesting a dose-related sensitivity to cholinergic inputs. These data are the first, to our knowledge, confirming that ACh provides a strong modulatory input to MNTB, one that functions to powerfully shape responses to acoustic input.

PS 521

Development of Inhibitory Inputs to the Superior Paraolivary Nucleus

Ezhilarasan Rajaram¹; Conny Kopp-Scheinflug²

¹Ludwig-Maximilians-University, Munich; ²Ludwig-Maximilians University, Munich

Background

Sound termination is an important key to detect gaps in tones and noises and is reliably encoded by superior paraolivary nucleus (SPN) neurons in the auditory brainstem. Strong inhibition is crucial to SPN neurons to generate their typical offset responses but the development of these input remains poorly understood. Here we provide a developmental profile for the inhibitory inputs to the SPN before, during and after hearing onset.

Methods

In C57BL/6J mice with ages ranging from postnatal day 9 to 22 (P9-22), we used in vitro whole cell patch clamp recording to study intrinsic and synaptic properties of SPN neurons. Inhibitory postsynaptic currents (IPSCs) were evoked by stimulating the medial nucleus of trapezoid body (MNTB), in the presence of the AMPA receptor antagonist DNQX (10 μ M) and NMDA receptor antagonist D-AP5 (50 μ M). We determined amplitudes, time constants, input-output functions, reversal potential, synaptic depression, and miniature IPSCs in the following age groups: P9-11, P12-14, P15-18 and P19-22. All experiments were performed in accordance with the German guidelines for the care and use of laboratory animals as approved by the Regierung of Oberbayern (AZ 55.2-1-54-2532-38-13, Bavaria, Germany).

Results

In coronal slices of the auditory brainstem (150-200 μ m), SPN neurons were contacted on average by 1-8 inhibitory synapses. The number of inhibitory input was stable from before hearing onset (P9) all the way to the end of the third postnatal week (P22). Application of the GABAA-antagonist SR95531 (10 μ M) reduced the IPSC

amplitudes in the younger age groups, but did not have a significant effect on the number of inputs in any age group. IPSCs stimulated with pulse trains of different frequencies revealed that SPN neurons were able to encode frequencies of up to 400Hz, but not at 800Hz. In response to trains of 100Hz and 400Hz IPSCs showed synaptic depression which was more pronounced with increasing postnatal age.

Conclusions

Inhibitory inputs to the SPN were found to be primarily glycinergic from the age of postnatal day 9 and did not show significant pruning during after P9, corroborating results from the neighboring lateral superior olive. The inability of SPN IPSCs to follow high frequency input trains is interesting and sets it apart from neurons in the MNTB which are known to follow stimulus frequencies of up to 1000Hz.

Causes and Effects of Tinnitus

PS 522

Musicians Hearing Handicap Index: A New Tool for Professionals Exposed to Music

Thanos Bibas¹; Aikaterini Vardonikolaki¹; Vasilios Pavlopoulos¹; Nikolaos Markatos¹; Ilias Papathanasiou²; George Papadelis³; Miltos Logiadis⁴

¹National and Kapodistrian University of Athens; ²Technological Educational Institute of Western Greece;

³Aristotle University of Thessaloniki; ⁴Ionian University

The aim of this study is to quantify the hearing difficulties music professionals could face in relation to their functional hearing. Musicians and other professional working with music are a special occupational group with a high prevalence of tinnitus and hyperacusis which could affect their work (Kähärit et al., 2003)(Schink et al., 2014). This is not always demonstrated by pure tone audiometry (PTA) (Schäette and McAlpine, 2011). Additionally, exposure to loud music could cause music-induced hearing loss, presenting initially with the development of notches at 3, 4 or 6 KHz (Phillips et al., 2010; Jansen et al., 2009). Although music induced hearing loss is preventable, it cannot be treated once it has been established (Chasin, 2009). This type of hearing loss is not always associated with symptoms. Due to the fact that it progresses through many years, patients can adjust their functionality and this may have little effect on their performance. Despite the fact that there are articles and questionnaires that evaluate the singing disability, the performance, the anxiety or the musculoskeletal pain of this special occupational group, no tool that has been developed so far to measure how the above symptoms

or hearing loss could affect the functional hearing of musicians (Cohen et al., 2007; Cirakoğlu and Sentürk, 2013; Brugués, 2009).

A musicians hearing handicap index (MHHI) questionnaire was therefore developed and tested in 147 professionals for the validity and reliability. All participants were professional musicians and sound engineers/music producers aged between 18 and 59 years old. The research was conducted in 3 steps. The first step included a pilot study, the second step included finalizing the questionnaire and interim analysis in order to estimate the sample size and the third step included the main study and factor analysis. All participants were divided in 3 groups: a control group, a group with auditory symptoms but no hearing loss and a third group of both auditory symptoms and abnormal audiogram. The items of the questionnaire were divided into 4 conceptual factors and test retest reliability was evaluated. Content validity for the total score and reliability was high (Cronbach α = 0.910 and Pearson $r(56)$ = 0,943; $p < 0,001$). We believe that MMHI is a valuable tool to quantify functional hearing in musicians. Our research also showed that auditory symptoms other than hearing loss may influence functional hearing more than expected by the pure tone audiogram thresholds

PS 523

Event-related Potentials of Tinnitus Listeners in a Selective-attention Task

Matthew Richardson¹; Selena Saromo²; Katie Turner¹; Fan-Gang Zeng³

¹Cognitive Sciences, University of California Irvine, Irvine, CA 92697 USA, Center for Hearing Research, Hearing and Speech Laboratory; ²Biomedical Engineering, University of California Irvine, Irvine, CA 92697 USA; ³Biomedical Engineering, Dept. of Anatomy & Neurobiology, Otolaryngology, and Cognitive Sciences, University of California Irvine, Irvine, CA 92697 USA, Center for Hearing Research, Hearing and Speech Laboratory

Recent studies suggest that attention plays an important role in generating and modulating neural activities related to chronic tinnitus. Here we use event-related potentials to study the role of auditory attention in the tinnitus percept or heightened awareness of tinnitus. Selective attention is controlled by instructing a listener to either attend or ignore one of two concurrent tone streams. One stream consists of 60-ms tone bursts at 5000 Hz that is within the tinnitus frequency region while the other stream consists of 60ms tone bursts at 500 Hz that is outside the tinnitus frequency region. Tone bursts are randomly interleaved with inter-stimulus intervals

between 200 and 400ms. Tone levels are adjusted for each listener to match the loudness of the 500 Hz stimulus at 65 dB SL. Listeners are instructed to focus attention to only one stream at a time while ignoring the other in order to detect (press a button) occasional target tones of the same frequency but longer duration. Target duration is adjusted to produce 80-90% correct performance across frequencies and subjects. Simultaneous 64-channel EEG is recorded while subjects perform the task in order to measure attentional modulation of cortical evoked-responses.

Consistent with previous findings, preliminary results at midline electrodes show a sustained negative deflection of the evoked response for attended tones compared to tones of the same frequency when ignored. Interestingly, listeners with chronic high-frequency tinnitus show significantly enhanced N1 (latency 80-120ms) for the 5000 Hz tones compared to the 500 Hz tones. Although a control group of age-matched listeners also shows attentional N1-enhancements, they fail to show significant differences between low and high frequencies. Similarly, longer-latency activity (latency 150-250ms) including the P2 component shows a negative deflection that is greater for high frequencies than low frequencies in tinnitus listeners but not controls. These findings support the hypothesis that the neurophysiological mechanisms of attention are over-regulated in auditory regions where tinnitus-related activity is known to occur. Attentional modulation of the sensory-evoked N1 is linked to a central gain mechanism that amplifies feature-sensitive neural populations in A1 and A2. In this case, cortical amplification may be expanded in tonotopically-organized regions affected by high-frequency hearing loss where aberrant neural activity putatively underlies tinnitus. Finally, longer-latency ERP effects specific to tinnitus patients may implicate higher-level processes of stimulus selection or top-down attentional control that also show greater sensitization for sounds in the tinnitus frequency region.

Funding

P30 DC008369; R01 DC015587

PS 524

Effect of Tinnitus Severity and Loudness on Speech-in-Noise Ability in Normal Hearing Tinnitus Patients

Yihsin Tai¹; Fatima T. Husain²; Anthony Tsao¹

¹University of Illinois at Urbana-Champaign; ²Department of Speech and Hearing Science, University of Illinois at Urbana-Champaign

Introduction

Studies investigating the impact of tinnitus on speech

understanding have indicated that tinnitus patients experience more difficulty discriminating speech in adverse listening conditions than in quiet, when compared to controls. This difficulty is not necessarily attributed to the accompanying hearing loss because tinnitus patients with normal hearing thresholds have also shown consistently reduced speech discrimination in noise. If tinnitus is indeed a factor affecting speech-in-noise, then degree of severity of tinnitus or loudness may have a variable effect on speech understanding. However, few studies have parsed the association of variable tinnitus severity and loudness with speech-in-noise performance. The aim of the study was to investigate the effect of tinnitus severity and loudness on speech-in-noise ability in normal hearing tinnitus patients.

Methods

Pure-tone audiometry and the Quick Speech-in-Noise (QuickSIN) test were performed on 10 subjects (mean age 41.4 years) with bilateral tinnitus and normal hearing sensitivity up to 8 kHz. Tinnitus Handicap Inventory (THI), visual analog scale (VAS) of tinnitus loudness, and psychoacoustic tinnitus loudness matching with a 500-Hz tone and white noise were included to describe the percept and the individual's reaction to it. Six non-tinnitus subjects (mean age 42.67 years) with normal hearing were enrolled as a control group. Comparisons were made between tinnitus dominant ear (or the ear with better hearing) of patients and the better ear of controls. Spearman correlation was used for correlation analysis; Kruskal-Wallis test of non-parametric analysis was used for between-group comparisons.

Results

Preliminary results showed no significant correlation between overall QuickSIN score and any measurement of tinnitus severity or loudness; however, THI (0 – 48, slight to moderate severity of tinnitus) showed a significant correlation ($r = 0.636$, $p < 0.05$) with VAS scores of loudness (2 – 80 out of 100). Tinnitus subjects showed poorer hearing sensitivity with pure-tone average of 500, 1000, 2000, and 4000 Hz compared to that of controls, although this difference was not statistically significant ($p = 0.274$). There were also no significant differences in overall QuickSIN score ($p = 0.911$) and % correct of each signal-to-noise condition between tinnitus patients and controls.

Conclusion

The dataset is part of an ongoing study. The preliminary results did not support a significant correlation between speech understanding in noise and perceptual or psychological factors associated with tinnitus. More data, including a range of tinnitus severity and loudness scores, are necessary to better understand the impact of tinnitus on speech understanding.

Tinnitus with a Normal Audiogram: Relation to Noise Exposure but No Evidence for Cochlear Synaptopathy

Hannah Guest¹; Kevin Munro¹; Garreth Prendergast¹; Simon Howe²; Christopher Plack¹

¹Manchester Centre for Audiology and Deafness (Man-CAD), University of Manchester; ²South Tees Hospitals NHS Foundation Trust

Introduction

In rodents, exposure to high-level noise can destroy synapses between cochlear inner hair cells and auditory nerve fibers, without causing hair cell loss or permanent threshold elevation. Such “cochlear synaptopathy” is associated with amplitude reductions in wave I of the auditory brainstem response (ABR) at moderate-to-high sound levels. Similar ABR results have been reported in humans with tinnitus and normal audiometric thresholds, leading to the suggestion that the tinnitus might be a consequence of cochlear synaptopathy. However, the ABR is an indirect measure of synaptopathy and it is unclear whether the results in humans reflect the same mechanisms demonstrated in rodents. Measures of noise exposure were not obtained in the human studies, and it is also possible that very high frequency audiometric loss impacted ABR amplitudes. The present study aimed to clarify the role of cochlear synaptopathy in tinnitus, controlling for high frequency thresholds, adding the envelope following response (EFR) as a supplementary measure of synaptopathy, and assessing relations to lifetime noise exposure.

Methods

Twenty young adults with tinnitus and clinically normal audiograms were matched closely with controls for age, sex, and audiometric thresholds up to 14 kHz. Electrophysiological measures of synaptopathy were click-evoked ABRs at 102 dB peSPL and EFRs at two modulation depths. Lifetime noise exposure was assessed by structured interview.

Results

In contrast to previous reports, tinnitus was not associated with reduced ABR wave I amplitude. In addition, tinnitus was not associated with significant effects on EFR amplitude or on the function relating EFR amplitude to modulation depth. Electrophysiological measures were not correlated with lifetime noise exposure. Tinnitus was, however, associated with significantly greater lifetime noise exposure.

Conclusions

Our ABR and EFR data provide no evidence for cochle-

ar synaptopathy in audiometrically normal young adults with tinnitus. Given the divergence from previous reports, it is possible that synaptopathy is a major tinnitus aetiology only in older adults, or is limited to very basal cochlear regions. The finding of greater noise exposure in tinnitus subjects is important in its own right, since audiometric thresholds were closely matched between groups. It appears that even in tinnitus sufferers with audiograms indistinguishable from those of controls, symptoms may arise from subclinical damage due to noise exposure.

Funding

Supported by the Marston Family Foundation, Action on Hearing Loss, and the Medical Research Council UK (MR/L003589/1).

PS 526

Plastic Changes in the Auditory Pathway and Limbic System on a Rat Blast-induced Tinnitus Model Induced by Laser-induced Shock Waves

Katsuki Niwa¹; Kunio Mizutani¹; Toshiyasu Matsui²; Takaomi Kurioka³; Takeshi Matsunobu⁴; Satoko Kawauchi⁵; Yasushi Satoh⁶; Shunichi Sato⁵; Akihiro Shiotani¹; Yasushi Kobayashi²

¹Department of Otolaryngology, Head and Neck Surgery, National Defense Medical College, Japan;

²Department of Anatomy and Neurobiology, National Defense Medical College, Japan; ³Department of Otolaryngology-Head and Neck Surgery, Kresge Hearing Research Institute, University of Michigan, Ann Arbor, Michigan, USA; ⁴Division of Otolaryngology, New Tokyo Hospital, Japan; ⁵Department of Biomedical Information Science, National Defense Medical College, Japan; ⁶Department of Pharmaceutical Science, National Defense Medical College, Japan

Background

Auditory deficiency, such as hearing loss or tinnitus, is one of the most frequently observed consequences after blast injuries.

We have already established an animal model of sensorineural hearing loss (SNHL) by laser-induced shock wave (LISW) (1). Utilized this model, we conducted tinnitus evaluation by gap detection test (GAP). We analyzed relationship between tinnitus and neuronal plasticity of the rat brain.

Methods

9 SD rats were exposed to LISWs generated by irradiating a YAG laser. 3 SD rats were used as control. We evaluated tinnitus repeatedly using GAP up to 4 weeks

accompanied by prepulse inhibition test (PPI) and ABR. Histological analysis at the brain was performed at 4 weeks after the LISW exposure. Brain expression of Arc, which is neuronal plastic markers, was evaluated by immunohistochemistry.

Results

The ABR threshold shifts at higher frequencies remained up to 4 weeks. Tinnitus at high frequencies aroused 1 or 2 weeks after LISW exposure. The number of Arc positive cells at the CN, IC and hippocampus CA1 of the no tinnitus rats were drastically increased compared to normal rat brain immediate after LISW exposure. The number of Arc positive cells at the CN and amygdala of the tinnitus rats were increased compared to the no tinnitus rats. On the other hand, the number of Arc positive cells at the Au1 of both no tinnitus and tinnitus rat was decreased compared to normal rat.

Conclusion

This research revealed that there are dramatic neuronal plastic changes in subacute phase tinnitus. We speculated that these neuronal plastic changes at CN, Au1 and amygdala might lead to tinnitus perception. Also, the balance between excitatory neuron activity and inhibitory neuron activity at the central auditory pathway and limbic system was thought to be related with tinnitus generation and disappearance. 1. Niwa K, Mizutari K, Matsui T, Kurioka T, Matsunobu T, Kawauchi S, et al. Pathophysiology of the inner ear after blast injury caused by laser-induced shock wave. *Sci Rep.* 2016;6:31754.

PS 527

Can Prolonged, Non-traumatic Noise Exposure Cause Tinnitus? A GIASR Study in CBA/CaJ Mice

Martin Pienkowski; Trevor Simones
Salus University

Noise trauma reduces spontaneous and sound-evoked firing rates in the auditory nerve, but increases them in the central auditory system, including primary auditory cortex (A1). Additionally, noise trauma increases the synchrony of neural firing in A1, and may lead to a reorganization of the A1 tonotopic map, such that sound frequencies near the edge of the hearing loss are “over-represented” at the expense of frequencies whose thresholds are elevated by the loss. These trauma-induced changes have also been linked with the presence of tinnitus, although the exact causes of tinnitus remain unclear.

Increases in A1 spontaneous firing rates, neural synchrony, and map reorganization have also been observed after prolonged exposure to noise in the 70 dB SPL range, in the apparent absence of damage to the cochlea (Pi-

enkowski & Eggermont 2009). In this study, we explore whether such long-term, moderate noise exposures can also give rise to tinnitus. Normal-hearing, adult CBA/CaJ mice are being exposed to an 8–16 kHz octave-band noise at 70 dB SPL for approximately 8 weeks, 24 h/day. The possibility of tinnitus is being assessed at 4, 6, 8, 11, 16, 23 and 32 kHz (i.e., within, at the edges of, and above and below the 8–16 kHz exposure band) using the gap inhibition of the acoustic startle reflex (GIASR).

PS 528

Acoustic Startle Reflex and Stress Hormonal Changes in a Mouse Model of Noise-induced Tinnitus

Shi-Nae Park¹; Min-Jung Kim²

¹*Department of Otolaryngology-Head&Neck Surgery, college of Medicine, Catholic Univ. of Korea;* ²*Department of Otolaryngology-Head&Neck Surgery, college of Medicine, Catholic Univ. of Korea*

Objectives

Gap-prepulse inhibition of the acoustic startle reflex (GPIAS) has been used in rats and mice for tinnitus screening and assessment. Tinnitus animal models previously demonstrated the development of deficits in GPIAS. In this study, noise-induced tinnitus (NIT) in mice was serially evaluated by GPIAS after different types of noise exposure to determine the most appropriate method for tinnitus development. To investigate the relationship between NIT and stress, we firstly evaluated the stress hormones in the plasma as a pilot study.

Methods

Male C57BL/6 mice aged 1 mo were exposed to three different noise stimuli: 110 dB SPL white noise for 1 hr once, 4 hrs once, and 4 hrs everyday for 5 days. Auditory brainstem response (ABR) thresholds and distortion product otoacoustic emissions (DPOAE) were serially recorded up to 3 months. Tinnitus was also assessed serially by GPIAS to obtain GPIAS ratios. All the audiological and GPIAS data of three NIT groups were compared with those of the control group. Plasma levels of norepinephrine (NE) and cortisol were compared among the four groups. Results: During the 3 mo follow-up period, hearing levels of three different NIT groups showed significantly elevated ABR thresholds with a mild increasing trend with time compared to the control group. DPOAE levels of the NIT groups were significantly lower than those of the controls without any inter-NIT-group differences. GPIAS ratios decreased in NIT groups up to 1 month, and subsequently, individual variations seemed to increase. NE level in the plasma of 1 hr NIT group and cortisol levels of all NIT groups were significantly higher than those of the controls.

Conclusion

NIT mouse models developed by different types of noise exposure and confirmed by GPIAS seem to be well established in this study. Elevated plasma level of stress hormone in NIT groups indicates its possible role as a biomarker in tinnitus-related stress condition, which still needs further investigation.

PS 529

Tinnitus Screening in CBA/CaJ Mice: Improving the Acoustic Startle Reflex Measurement and Analysis

Inga Kristaponyte¹; Ryan Longenecker²; Greg Nelson²; Jesse Young²; Alexander Galazyuk²

¹*Northeast Ohio Medical University (NEOMED), Kent State University;* ²*Northeast Ohio Medical University (NEOMED)*

Background

The most used method to assess tinnitus in mice utilizes gap-induced pre-pulse inhibition of the acoustic startle reflex (GPIAS). It has been assumed that a deficit in this gap-induced inhibition following an acoustic over exposure (AOE) reveals the presence of tinnitus. Due to high startle magnitude and gap-induced inhibition variability, this method would benefit from refinements to improve reliability. Thus, the goals of the current study were to: (1) determine the number of startles (before and after AOE) needed to ensure appropriate statistical power to detect a significant gap-effect; (2) examine efficacy and accuracy of utilizing shorter inter-trial intervals to reduce the time needed to test each mouse; (3) evaluate the effect of testing during the dark and light cycles on gap detection performance; (4) assess gap-induced facilitation and its impact on tinnitus detection.

Methods

To induce tinnitus we unilaterally exposed mice to a 116 dB SPL narrowband sound centered at 12.5 kHz for one hour under ketamine/xylazine anesthesia. The startle stimulus was 20 milliseconds (ms) 105 dB SPL wideband noise. 20 ms silent gaps were inserted in 65 dB SPL narrowband sound centered at six different frequencies and terminated 100 ms before the startle stimulus onset. For each background frequency, five startle stimuli preceded by a gap and five without gap were presented pseudorandomly, comprising one block of data. Nine such blocks were evenly distributed across the entire testing session for each background frequency. Custom software used a template matching approach to separate the startle response waveforms from unspecific animal movements. Gap detection performance at a given background frequency was assessed by comparing the difference between the average startle magnitudes in no-gap and gap trials instead of commonly used ratios.

Results

Preliminary analysis suggests that at least 30 startles at each background frequency are needed to evaluate gap detection performance with appropriate statistical power. Startle magnitudes and probabilities are affected by noise exposure, different inter-trial intervals, and light/dark cycle at the time of testing. We analyzed both gap-induced inhibition and facilitation and suggest that both indicate gap detection deficit.

Conclusions

A reliable mouse tinnitus model is of paramount importance for future tinnitus studies. The suggested acoustic startle reflex measurements and analyses provide an optimal way to test gap detection deficits and screen for tinnitus in CBA/CaJ mice.

PS 530

A Conditioned Behavioral Paradigm for Assessing Onset and Lasting Tinnitus in Rats

Edward Pace¹; Hao Luo²; Michael Bobian¹; Ajay Panekkad³; Xueguo Zhang¹; Huiming Zhang⁴; Jinsheng Zhang⁵

¹*Department of Otolaryngology, Wayne State University School of Medicine;* ²*School of Medicine, Wayne State University;* ³*Department of Electrical Engineering, Wayne State College of Engineering;* ⁴*Department of Biological Sciences, University of Windsor;* ⁵*Wayne State University School of Medicine*

Numerous behavioral paradigms have been developed to assess tinnitus-like behavior in animals. Nevertheless, they are often limited by prolonged training requirements, as well as an inability to simultaneously assess onset and lasting tinnitus behavior, tinnitus pitch or duration, or tinnitus presence without grouping data from multiple animals or testing sessions. To enhance behavioral testing of tinnitus, we developed a conditioned licking suppression paradigm to determine the pitch(s) of both onset and lasting tinnitus-like behavior within individual animals. Numerous behavioral paradigms have been developed to assess tinnitus-like behavior in animals. Nevertheless, they are often limited by prolonged training requirements, as well as an inability to simultaneously assess onset and lasting tinnitus behavior, tinnitus pitch or duration, or tinnitus presence without grouping data from multiple animals or testing sessions. To enhance behavioral testing of tinnitus, we developed a conditioned licking suppression paradigm to determine the pitch(s) of both onset and lasting tinnitus-like behavior within individual animals. Rats learned to lick water during broadband or narrowband noises, and to suppress licking to avoid footshocks during si-

lence. After noise exposure, rats significantly increased licking during silent trials, suggesting onset tinnitus-like behavior. Lasting tinnitus-behavior, however, was exhibited in half of noise-exposed rats through 7 weeks post-exposure tested. Licking activity during narrow-band sound trials remained unchanged following noise exposure, while ABR hearing thresholds fully recovered and were comparable between tinnitus(+) and tinnitus(-) rats. To assess another tinnitus inducer, rats were injected with sodium salicylate and then demonstrated high pitch tinnitus-like behavior, but later recovered by 5 days post-injection. Further control studies showed that 1): sham noise-exposed rats tested with footshock did not exhibit tinnitus-like behavior, and 2): noise-exposed or sham rats tested without footshocks showed no fundamental changes in behavior compared to those tested with shocks. Together, these results demonstrate that this paradigm can efficiently test the development of noise- and salicylate-induced tinnitus behavior. The ability to assess tinnitus individually, over time, and without averaging data enables us to realistically address tinnitus in a clinically relevant way. Thus, we believe that this optimized behavioral paradigm will facilitate investigations into the mechanisms of tinnitus and development of effective treatments.

PS 531

Spontaneous Behavior Is Not a Suitable Indicator of Tinnitus in Mice

Daniel O. J. Reijntjes¹; Alexander Pietrus-Rajman¹; Nick M. A. Schubert¹; Pim van Dijk¹; Sonja J. Pyott²

¹University Medical Center Groningen; ²Dept. Otorhinolaryngology/Head and Neck Surgery, University Medical Center Groningen, The Netherlands.

Research into the cellular, molecular, and genetic mechanisms underlying tinnitus demands mouse models that permit the detection of tinnitus perception. Existing animal models utilize either spontaneous or conditioned responses that are difficult to apply in mouse, have low throughput, and/or have questionable relevance to human tinnitus perception. As a result, the experimental advantages of mouse models have been largely untapped to study tinnitus. A recent study in guinea pigs identified a novel spontaneous behavior, changes in movement during silent gaps, that identified a subgroup of animals presumably suffering tinnitus (Heeringa et al., 2014). We tested the utility of this novel behavior to detect the perception of tinnitus in mice in the hopes of developing a rapid and reliable assay for examining tinnitus in mice. In this study, C57BL/6 mice underwent three trials (8.5 min each) in which spontaneous movement (free exploration in an open arena) was recorded in the presence of white noise (80 dB SPL) interrupted

with 6 silent gaps of either 0.5 or 1 s each. Movement was video recorded and analyzed offline. Movement metrics included velocity, head, torso, or tail movement. Before the third trial, mice underwent either sham or unilateral noise exposure (10 Hz, 120 dB SPL, 90 min) to induce hearing loss and tinnitus. ABRs before and after noise trauma confirmed normal hearing in sham-treated animals and unilateral hearing loss in the noise-exposed cohort. We found, unlike previous observations in guinea pig, no differences in the various metrics of movement were observed during the silent gaps either before or after sham/noise exposure. Previous observations also reported increased movement overall in guinea pigs identified as suffering tinnitus. In contrast, mice showed no differences in overall movement across trials or before and after sham/noise exposure. These results indicate that changes in movement during silent gaps are not suitable for the detection of tinnitus perception in mice. The behavioral differences in response to noise exposure may represent neuroethological differences in tinnitus presentation between guinea pigs and mice.

Hair Cells - Anatomy and Physiology III

PS 532

Compartmentalization of Antagonistic Ca²⁺ Signals in Developing Cochlear Hair Cells

Marcelo Moglie¹; Paul A. Fuchs²; Ana Belén Elgoyhen³; Juan D. Goutman¹

¹Instituto de Investigaciones en Ingeniería Genética y Biología Molecular; ²Johns Hopkins University School of Medicine; ³Instituto de Investigaciones en Ingeniería Genética y Biología Molecular "Dr. Héctor N. Torres" (CONICET) and Instituto de Farmacología, Facultad de Medicina, Universidad de Buenos Aires

Background

Before the onset of hearing (postnatal day 14 in rodents) cochlear inner hair cells (IHCs) fire sensory-independent action potentials, crucial for the normal development of the auditory pathway. Ca²⁺ influx through voltage-dependent channels triggers the release of glutamate onto afferent dendrites of the auditory nerve. At this stage, efferent cholinergic neurons from the brainstem also innervate IHCs. This efferent synapse combines the entry of Ca²⁺ through cholinergic $\alpha 9\alpha 10$ receptors with the activation of nearby SK2, Ca²⁺-dependent potassium channels, to hyperpolarize the IHC. Thus, efferent Ca²⁺ signals are inhibitory, opposing IHC transmitter release. The aim of our work was to investigate the mechanisms that allow segregation of excitatory versus inhibitory Ca²⁺ effects within the limited diffusional space of the IHCs synaptic pole.

Methods

We performed anatomical and functional IHC 3D reconstructions via electron microscopy (EM) of ultra-thin serial sections and swept-field confocal Ca²⁺ imaging of IHCs in cochlear explants. Electrophysiological recordings were combined with Ca²⁺ imaging measurements in IHCs from P9-P11 mice to investigate Ca²⁺ dynamics during synaptic transmission evoked by electrical stimulation of efferent axons. Electrophysiological recordings of type I afferent boutons were made while stimulating efferent synapses.

Results

Ca²⁺ imaging experiments revealed an average of 6±2 Ca²⁺ entry hotspots per IHC upon efferent fiber electrical stimulation. This value represents a lower limit of the functional synaptic contacts that could be successfully distinguished and differed from EM counts (17±8), which included all morphologically discernible synapses. Afferent hotspots were visualized following IHC depolarization and were spatially segregated from those encountered during efferent activation. We estimated an average distance between efferent hotspots and closest afferent neighbors of 1.45 μm. This value agreed with the distance measured between nearest neighbor sub-synaptic cisterns and synaptic ribbons in electron micrographs.

Finally, in order to establish a possible efferent to afferent crosstalk, recordings from afferent boutons were performed. Despite the close proximity, only high frequency (80 Hz) electrical stimulation of efferent fibers evoked an increase in the frequency of postsynaptic excitatory currents, attributable to glutamate release triggered by Ca²⁺ influx through α9α10 receptors.

Conclusions

Both morphological and Ca²⁺ imaging data provide evidence for close proximity between afferent and efferent synapses in developing IHCs. Although high frequency efferent stimulation could drive IHC transmitter release, physical barriers imposed by synaptic cisterns and/or strong Ca²⁺ buffering in IHCs prevent efferent to afferent synaptic crosstalk during lower frequency stimulation that is sufficient to suppress spontaneous action potentials in the IHC.

PS 533

What Is the Ribbon Needed For? Functional Deletion of RIBEYE Leads to a Mild Auditory Phenotype

Lars Becker¹; Sara Talaei²; Willy Sun³; Mark Ruthenford⁴; Michael Schnee⁵; Mamiko Niwa²; Stephan Maxeiner⁶; Bechara Kachar⁷; Anthony J. Ricci¹

¹Stanford University, School of Medicine, Department

of Otolaryngology; ²Stanford University; ³NIH/NID-CD Section on Structural Cell Biology; ⁴Washington University School of Medicine; ⁵stanford university; ⁶Medizinische Fakultät der Universität des Saarlandes; ⁷National Institute on Deafness and Other Communication Disorders

The gene for the C-terminal Binding Protein 2 (CtBP2) encodes for two distinct proteins. The N-terminal A-domain is specific for the protein named RIBEYE which in conjunction with the B-domain is found in specialized synapses of the retina, hair cells of the inner ear, and cells within the pineal organ. The B-domain composes the majority of the transcriptional repressor CtBP2, it possesses a NAD(H) binding capacity and, if connected to the A-domain, interacts with other components of the presynaptic terminal. RIBEYE has been proposed as the key organizer of synaptic ribbons and has been implicated as a conveyor to provide synaptic vesicles for sustained release, a coordinator for multivesicular fusion events, a structural component for organizing the active zone (AZ) (Matthews and Fuchs, 2010), and may also ensure continuous vesicle availability by limiting exocytosis of associated vesicles, influencing in turn temporal representation of sound in the auditory nerve. Here, we study the knockout of the RIBEYE-specific A-domain (Maxeiner et al., 2016), its function on synapse formation in the organ of Corti and its effects on hearing.

We studied hearing in young adult (P21) RIBEYE-knockout mice by measuring ABR and DPOAE thresholds. DPOAE thresholds, a read out of outer hair cell function, were unaffected in knockouts. RIBEYE-knockouts hear at slightly elevated ABR thresholds (~10 dB SPL), mainly due to a significant reduced first peak amplitude, while peak latencies are not affected. This suggests a role for RIBEYE in maintaining vesicle numbers, replenishment or filling.

Using Transmission electron microscopy, we confirmed the absence of electron dense ribbon structures in hair cells of knockout animals and quantified the number and size of synaptic vesicles in the AZ. Our data suggest a loss of synaptic vesicles, but a similar size distribution of vesicles compared to the wild-type situation.

We quantified several pre- and postsynaptic markers (Homer, Bassoon, Piccolo, CtBP1, Shank, CaV1.3, GluA2) using immunohistochemistry in the organ of Corti at P21-35. We used co-labeling of presynaptic Bassoon and postsynaptic Homer to quantify the number of synapses per inner hair cell. Synapse number did not vary significantly between the genotypes. In the absence of synaptic ribbons, CaV1.3 channel clusters remained

juxtaposed with AMPA receptors across the synaptic cleft. Similarly, the close association of CaV1.3 with the ribbon-anchoring protein Bassoon at the inner hair cell AZ was maintained.

This work was supported by NIDCD grants DC009913 and core grant P30 44992

PS 534

Examining the Contribution of Hair Cell and Afferent Neuron Mechanisms to Spike Train Adaptation

Josef G. Trapani; Thomas F. Sommers
Amherst College

Sensory adaptation is an important neurological process that allows organisms to appropriately respond to sensory stimuli by filtering out static or unchanging stimulus information. Sensory systems with hair-cell receptors, such as vertebrate auditory systems and lateral-line systems in fish, adapt robustly to constant stimuli, yet the exact mechanisms and their contribution to adaptation remain poorly understood. In order to examine the molecular contributions to spike-rate adaptation in hair-cell systems, we mechanically stimulated hair cells of the zebrafish lateral line while recording action potentials (spikes) from individual afferent neurons. We observed substantial adaptation of both first spike latency (FSL) and overall spike rate in response to a constant, saturating stimulus. By determining the time courses of recovery from adaptation for both FSL and spike rate, we observed that FSL recovers more quickly than spike rate. The differential recovery rates of FSL and spike rate suggested that two distinct mechanisms may underlie these forms of adaptation, as a shared mechanism would presumably return both parameters to their non-adapted values within a similar time course. As a thought experiment, we considered possible features of hair-cell systems that would account for the observed difference in recovery rates of FSL and spike rate and propose that mechanisms at the ribbon synapse best account for the portion of spike-rate adaptation that remains following the rapid recovery of FSL adaptation. These findings provide preliminary insight into the contributions of known hair cell and afferent neuron mechanisms for adaptation of spike trains.

PS 535

Voltage-gated Calcium Loads Synaptic Cisterns to Enhance Inhibition of Inner Hair Cells in the Postnatal Rat Cochlea

Stephen Zachary¹; Paul A. Fuchs²

¹*Johns Hopkins School of Medicine*; ²*Johns Hopkins University School of Medicine*

Background

Before postnatal day 14, cholinergic olivocochlear efferent neurons form synapses with inner hair cells (IHCs) in the rat cochlea. Acetylcholine released from efferent terminals activates postsynaptic nicotinic acetylcholine receptors (nAChRs), which flux calcium into the IHC. Calcium entry leads to inhibition via the activation of small conductance calcium-activated (SK) potassium channels. Efferent-IHC synapses feature a postsynaptic cistern that may regulate synaptic calcium signaling, and thus SK channel activation. Additionally, afferent and efferent contacts co-exist on IHCs during this period of development. We tested the hypothesis that cisternal calcium as well as calcium entering through voltage-gated (VGCa) channels (typically associated with afferent drive) shape efferent IPSC waveforms. We propose that voltage-gated calcium is sequestered in postsynaptic cisterns until it is deployed via calcium-induced calcium release (CICR) during efferent activation of nAChRs.

Methods

Serial electron microscopy (EM) sections were collected from P9 rat IHCs. Electrically evoked and spontaneous inhibitory postsynaptic current (IPSC) waveforms were analyzed using whole-cell tight-seal recording from IHCs in apical cochlear turns excised from young rats (P7-9).

Results

EM analysis revealed that postsynaptic cisterns accompany efferent contacts and that efferent and afferent contacts exist in close proximity to one another. Supporting the role of cisterns as calcium stores, high concentrations of ryanodine (which blocks CICR) shortened the decay time constant of IPSCs evoked at -40 mV, while low concentrations of ryanodine (which positively modulates CICR) prolonged time constants. The impact of voltage-gated calcium was demonstrated by application of nimodipine (to block L-type VGCa channels) and Bay K (which prolongs L-type VGCa channel open time), which shortened and prolonged IPSC decay time constants respectively. A comparison of decay time constants of synaptic events recorded at different holding potentials revealed that IPSCs were longer-lasting at potentials that recruit VGCa channel activation. Finally, we show that the response to brief 'puffs' of exogenous acetylcholine was altered following IHC depolarization, presumably through VGCa influx and subsequent release via CICR.

Conclusion

SK channel gating at the efferent-IHC synapse is determined by multiple calcium handling processes, including calcium flux through acetylcholine receptors, cisternal calcium release, and prior VGCa channel activity. Afferent and efferent pathways can interact at the level of the IHC such that prior afferent drive is encoded in subsequent cholinergic responses.

PS 536

Deletion of the RIBEYE Specific A Domain Reduces Synaptic Release in Mouse Inner Hair Cells

Michael Schnee¹; Mamiko Niwa²; Lars Becker³; Sara Talaei²; Willy Sun⁴; Mark Rutherford⁵; Bechara Kachar⁶; Anthony J. Ricci³

¹stanford university; ²Stanford University; ³Stanford University, School of Medicine, Department of Otolaryngology; ⁴NIH/NIDCD Section on Structural Cell Biology; ⁵Washington University School of Medicine; ⁶National Institute on Deafness and Other Communication Disorders

RIBEYE is a major protein component of synaptic ribbons, structures found at pre-synaptic terminals of many sensory receptor cells including the auditory hair cells. Deletion of RIBEYE A domain in mice resulted in complete elimination of ribbons in the retina and impaired fast and sustained vesicle release¹. Impairment of vision or auditory function was not reported.

Here we characterized auditory function in these RIBEYE knockout mice using electrophysiology including ABR and DPOAE measurements (P21), postsynaptic afferent bouton recordings (P17-19) and presynaptic capacitance (Cm) measurements (P10-14) as an indication of synaptic vesicle fusion. Release in bouton recordings was evoked by application of 40 mM K⁺. Absence of ribbons in inner hair cells was confirmed with inclusion of the Hylite tagged CTBP2 binding peptide in whole cell patch recordings.

The auditory phenotype consisted of mild (10dB) elevation in thresholds across frequencies and a strong (60%) reduction in peak 1 amplitude of ABR measurements without change in peak width or latency. DPOAE measurements were unaffected in the KO suggesting normal outer hair cell function.

Postsynaptic recordings demonstrate that the EPSC frequency was significantly reduced in KO (48.5% of WT; $p = 0.042$) while amplitude was normal (WT = 145 ± 39 pA, KO = 204 ± 59 pA; $p = 0.075$).

Presynaptic Cm measurements made in response to hair cell depolarization showed no difference in two components of release², a saturable linear component that scaled with Ca²⁺, WT 33 ± 13 fF (SD) vs KO 43 ± 26 fF, and a second larger component WT 263 ± 143 fF vs KO 258 ± 92 fF of higher constant release rate previously termed superlinear. Small depolarizations from hyperpolarization demonstrated that the time to release was unchanged 201 ± 194 vs 183 ± 185 ms however the time to the 2nd release component was significantly in-

creased ($p=0.017$) compared to WT 407 ± 165 vs 920 ± 605 ms. Ca²⁺ current amplitude, V_{1/2} and kinetics were unchanged in the KO. Endocytosis was also comparable between KO and WT.

These results indicate that the ribbon is unlikely to be involved in establishing multivesicular release. Rather, the ribbon is mostly likely involved in maintaining vesicles near to the synapse.

1. Maxeiner et. al. 2016 EMBO.35(10):1098
2. Schnee et. al. 2011 Neuron.70(2):326

Funded by NIDCD grant DC009913 to AJR and core grant P30 44992

PS 537

Cryptic Connections: Modes of Transmission Between Calyceal Afferents and Type I and Type II Hair Cells

Donatella Contini; Steven D. Price; Jonathan J. Art
Department of Anatomy and Cell Biology, University of Illinois at Chicago, Chicago, IL, USA

Background

Vestibular synaptic processing at calyceal endings is complex. Type I hair cells (HCs) are enveloped by afferents that form restricted volumes (clefts) where rapid excitatory synaptic transmission is modulated by the dynamics of K⁺ and H⁺ accumulation. This primary calyceal relation is augmented by outer-face synapses between the calyx and type II HCs. Relatively little is known about the calculus of synaptic transmission and the relative impact of quantal transmission and ionic modulation on afferent physiology.

Methods

Simultaneous patch-electrode recordings from either type I or type II HCs and their associated calyceal afferents were made with KF/KCl, dye-filled pipettes, in the epithelia of the posterior semicircular canal of the turtle, *Trachemys scripta elegans*. Both were examined under conditions of ionic substitution and pharmacological block. Steady-state and instantaneous I-V curves from the HC and afferent were used to analyze changes in conductance and driving force.

Results

HCs demonstrated a large, outward current when depolarized from -90 mV. Associated with outward HC current was an inward current in the calyx. This effect was symmetric, and depolarization of a calyx generated inward current in type I HCs. Substitution of Na⁺ for K⁺, and the addition of 20 mM 4-AP and 30 mM TEA-F in the HC recording pipette, was sufficient to block 99%

of the outward current in the type I HC, and abolish the associated inward current in the calyx, whilst leaving quantal transmission intact. With K⁺-based intracellular solutions in HC and afferent, increased extracellular pH buffering resulted in an increase in both the outward hair cell current, and the associated inward afferent current. Comparison of depolarization of type I and type II HCs revealed that the slow inward current in the afferent induced by type I HCs is 8X larger than that induced by type II hair cells. Increased K⁺ in the synaptic cleft following large depolarization of type I hair cells was sufficient to generate tonic, regular, high frequency discharge in the afferent.

Conclusions

Our experiments suggest that both type I HCs or calyx afferents can elevate [K⁺] in the synaptic cleft, and this dynamic change in [K⁺] acts as a slow modulator of rapid quantal transmission from either type I or type II hair cells. With sufficient type I HC depolarization, the [K⁺] in the cleft is sufficient to depolarize the afferent into a tonic discharge domain.

PS 538

Tonotopic Differences in the Coupling Between Ca²⁺ Entry and Vesicle Release at Mature Hair Cell Ribbon Synapses

Stuart L. Johnson¹; Jennifer Olt¹; Soyoun Cho²; Henrique von Gersdorff³; Walter Marcotti¹

¹University of Sheffield; ²The Vollum Institute; ³Vollum Institute, Oregon Health and Science University

Background

Synaptic vesicle fusion at hair cell ribbon active zones is triggered by Ca²⁺ entry through L-type (CaV1.3) Ca²⁺ channels in response to sound-induced graded receptor potentials. Although ribbon synapses become more Ca²⁺ efficient with maturation (Johnson et al. 2005 J Physiol 563:177), how Ca²⁺ is able to regulate exocytosis at mature ribbon synapses is still mostly undetermined. Calcium nanodomain coupling between a few Ca²⁺ channels and the readily releasable synaptic vesicles has been proposed to control exocytosis in vertebrate hair cells (Graydon et al 2011, J Neurosci 31:16637; Wong et al 2014, EMBO J 33:247). This tight-coupling has the advantage of providing accurate temporal encoding for phase-locking. However, another hypothesis is that the exocytotic coupling is controlled by many channels cooperatively (Ca²⁺ microdomain) and it is the molecules intrinsic to the synaptic machinery (Ca²⁺ sensors) that generate the highly Ca²⁺ efficient exocytosis at mature ribbon synapses (Johnson et al 2010, Nat Neurosci 13:45). These two release mechanisms may in fact co-exist along the same auditory or-

gan, thus emphasizing the different frequency components of the cell's in vivo receptor potential, respectively.

Method

Whole-cell patch-clamp recordings were used to investigate exocytosis in hair cells at specific characteristic frequencies (CF) of the mature gerbil, mouse and bullfrog auditory organs. The physiological coupling between Ca²⁺ influx and the synaptic machinery was investigated using different intracellular concentrations of EGTA, which buffers increases in intracellular Ca²⁺ only relatively far away from its source (Neher 1998 Neuron 20:389). Experiments were performed at body temperature and using 1.3 mM extracellular Ca²⁺ and following UK and USA animal regulations.

Results

We show that the coupling between Ca²⁺ channels and release sensors change as a function of the cell's frequency position. While low-frequency hair cells (< 2 kHz), which are phase-locked to sound stimuli, exhibit a tight, nanodomain, coupling between Ca²⁺ channels and synaptic vesicles, high-frequency cells (>2 kHz) have a much more loose coupling, which becomes progressively more microdomain (or more EGTA sensitive) along the gerbil cochlea. We also studied how the level of intracellular Ca²⁺ buffer affects the speed of recovery from paired-pulse depression.

Conclusions

Our findings show that both the nanodomain and microdomain coupling are present in mature auditory hair cells, the function of which is to preserve the precise temporal coding of sound in phase-locked low-frequency hair cells and stimulus intensity in high-frequency cells, respectively.

Supported by The Wellcome Trust (WM); NIDCD (HvG).

PS 539

Response Properties Of Calyx Terminals Are Modulated by Muscarinic Acetylcholine Receptors

Yugandhar Ramakrishna; Soroush G. Sadeghi
Center for Hearing and Deafness, Dept. of Communicative Disorders and Sciences

The mammalian vestibular pathway is divided into phasic and tonic pathways. The phasic pathway has high pass properties and includes vestibular-nerve afferents with irregularly firing resting discharges, which most likely receive their main inputs from vestibular calyx terminals. Calyx terminals also receive inputs from cholinergic vestibular efferents and contain KCNQ (Kv7) potassium channels. Here we investigated whether, similar

to other brain areas, muscarinic acetylcholine receptors (mAChRs) modulate KCNQ channel activity in calyx terminals of rats. Patch clamp recordings were performed from calyx terminals in central areas of the cristae of the horizontal and superior canals of 14 – 21 day old rats. First, KCNQ channel antagonists XE-991 and linopirdine dihydrochloride decreased voltage activated currents by ~30% and converted step-evoked firing of calyces from a single spike to more sustained (up to 20 spikes/s) firing. This supports the findings of previous studies that have shown contribution of Kv1 and KCNQ currents to changes in firing pattern in the vestibular ganglion. Second, mAChR agonist oxotremorine methiodide decreased KCNQ currents, with a shift of the activation curve to the right, resulting in changes in step-evoked responses similar to that observed with KCNQ blockers. Furthermore, in response to current steps, the first spike latency significantly decreased by ~40% after mAChR agonist or KCNQ antagonist application. Finally, application of these drugs also decreased the spike threshold by ~50% as evidenced by the minimum current step required for inducing a spike. Thus, mAChR activation increases the sensitivity and speed of response of calyx terminals. Together, these findings suggest that vestibular efferents can play a role in modulating the phasic peripheral vestibular pathway through modulation of KCNQ channels, resulting in an increased firing rate, decreased threshold, and faster response times.

PS 540

Presynaptic Voltage-dependent Ca²⁺ Channels Involved in Synaptic Transmission at the Mouse Medial Olivocochlear-outer Hair Cell Synapse at the Onset of Hearing

Eleonora Katz¹; Lucas G. Vattino²; Ana Belén Elgoyhen³

¹Instituto de Investigaciones en Ingeniería Genética y Biología Molecular “Dr. Héctor N. Torres” (CONICET) and Departamento de Fisiología, Biología Molecular y Celular, Facultad de Ciencias Exactas y Naturales, Universidad de Buenos Aires; ²Instituto de Investigaciones en Ingeniería Genética y Biología Molecular “Dr. Héctor N. Torres” (CONICET); ³Instituto de Investigaciones en Ingeniería Genética y Biología Molecular “Dr. Héctor N. Torres” (CONICET) and Instituto de Farmacología, Facultad de Medicina, Universidad de Buenos Aires

Medial olivocochlear (MOC) fibers begin to innervate outer hair cells (OHCs), the final targets of this efferent system, at postnatal day (P)6. From birth to hearing onset (P12 in altricial rodents) MOC fibers innervate inner hair cells (IHCs). At P9-11, ACh release at the transient MOC-IHC synapse is supported by P/Q- and N-type voltage-gated Ca²⁺ channels (VGCC). At this

age, Ca²⁺ flowing in through L-type VGCC activates large conductance Ca²⁺-activated potassium (BK) channels exerting a negative control on release, likely by curtailing the duration of the terminal action potential (Zorrilla de San Martín et al., 2010). At earlier more immature postnatal ages (P5), however, N-type VGCC are not involved and release is mediated by P/Q- and R-type VGCCs. Interestingly, at this earlier developmental stage, L-type VGCCs have a dual role: they activate BK channels, but also support release indicating less compartmentalization of presynaptic molecules involved in synaptic transmission (Kearney et al., ARO Abstracts 2014). So far, nothing is known concerning the presynaptic ion channels involved in transmitter release at the MOC-OHC synapse. Using isolated mouse cochleas at P11-13 we show, by whole-cell voltage-clamp recordings in OHCs while stimulating the efferent axons, that the quantum content of transmitter release (*m*) is very low (around 0.3-0.4) and mediated by both P/Q (200 nM ω -agatoxin VIA blocked ~74% of the control response *n* = 4, *p* < 0.03) and R-type VGCC (500 nM SNX482 blocked ~60% of the control response *n* = 7; *p* < 0.01). N-type VGCC, however, do not participate in evoked release at this synapse (500 nM ω -conotoxin IVA, had no significant effect on *m*; *n* = 7). In addition, we show that BK channels are functionally expressed at the MOC-OHC synapse as their block by iberiotoxin, a specific BK antagonist, significantly increased release (200 nM Ibtx caused a 188% increase in *m*; *n* = 6; *p* < 0.002). We also show that both the L-type VGCC antagonist nifedipine (3 μ M) and the agonist BayK (10 μ M) significantly increased *m* (154%, *p* < 0.02 and 216%, *p* < 0.05, respectively). Preliminary occlusion experiments with iberiotoxin and the dihydropyridines also indicate that Ca²⁺ flowing in through L-type VGCC is both activating BK channels and partially supporting ACh release. This resembles the MOC-IHC synapse at early immature stages (P5) and suggests that the MOC-OHC synapse is functionally immature at the onset of hearing. Support:UBA&ANPCyT:EK,ABE; NIH: PAF,ABE.

PS 541

Effects of Temperature on Exocytosis at the Bullfrog Hair Cell Ribbon Synapses

Minghui Chen; Henrique von Gersdorff
Vollum Institute, Oregon Health and Science University

Synaptic transmission from the auditory hair cell to afferent fiber is a fundamental step in hearing. Temperature dependence of exocytosis has been demonstrated in variety of preparations. In vivo single fiber recordings have shown that activities of frog auditory nerve fibers are temperature sensitive. To investigate the mechanisms of temperature-dependence of exocytosis from hair cell ribbon synapse, we performed whole-cell patch-

clamp recordings, obtained Ca²⁺ current (ICa) plus membrane capacitance changes (ΔC_m) in hair cells and spontaneous excitatory postsynaptic current (EPSC) of afferent fibers under both room (23-25°C) and high (30-33°C) temperature. Temperature was adjusted by heating bath perfusion with a temperature controller and measured by a miniature thermistor close to the bullfrog amphibian papillae that was recorded. An increase of temperature within this range increased peak amplitude and Ca²⁺ charge transfer (QCa) through voltage-gated calcium channels (Q₁₀ = 1.4 and 1.5), accelerated activation and inactivation of ICa, and enhanced 20-ms and 200-ms depolarizing steps-evoked synaptic release with larger temperature dependence (Q₁₀ = 2.4 and 2.0). The results indicate increase in release efficiency ($\Delta C_m/QCa$) of both fast and sustained release at elevated temperature. Ca²⁺ current transient block was temperature independent. Recordings from postsynaptic afferent fiber showed that both amplitude and frequency of spontaneous EPSC increased at high temperature. Furthermore, high temperature also quickened activation and decay of EPSC. Altogether, our results suggest that increased Ca²⁺ influx at high temperature does not only enhance evoked vesicle release by promoting vesicle fusion directly, but also playing a role in enlarging rapidly releasable pool of vesicles available at the active zone and accelerating replenishment of vesicles to sustain release through Ca²⁺-induced Ca²⁺ release. Besides temperature effect on hair cell exocytosis, temperature dependence of EPSC amplitude and kinetics may arise from the temperature dependence of postsynaptic AMPA receptors and glutamate transporters.

PS 542

Ribeye Protein is Intrinsically Dynamic but is Stabilized in the Context of the Ribbon Synapse

Zongwei Chen¹; Shih-Wei Chou¹; Brian M. McDermott²

¹Department of Biology, Case Western Reserve University; ²Department of Otolaryngology - HNS, Case Western Reserve University

Ribeye protein is a major constituent of the synaptic ribbon, an organelle that coordinates rapid and sustained vesicle release to enable hearing and balance. The ribbon is considered to be a stable structure. However, under certain physiological conditions such as acoustic overexposure that results in temporary noise-induced hearing loss or perturbations of ion channels, ribbons may change shape or vanish altogether, suggesting greater plasticity than previously appreciated. The dynamic properties of ribeye proteins are unknown. Here we develop a novel system to explore the behaviors of ribeye proteins within the ribbon and also their intrinsic

properties outside the context of the ribbon synapse in a control cell type, the skin cell. Using fluorescence recovery after photobleaching (FRAP) on transgenic zebrafish larvae, we test whether ribeye proteins are dynamic in vivo in real time. In the skin, a cell type devoid of synaptic contacts, Ribeye a-mCherry exchanges with ribbon-like structures on a minute timescale ($t_{1/2}$ = 3.2 min). In contrast, Ribeye a of the ear and lateral line and Ribeye b of the lateral line each exchange at ribbons of hair cells an order of magnitude slower ($t_{1/2}$ of 125.6 min, 107.0 min, and 95.3 min, respectively) than Ribeye a of the skin. These basal exchange rates suggest that long-term ribbon presence may require ribeye renewal. Our studies demonstrate that ribeye proteins are inherently dynamic but are stabilized at the ribbons of sensory cells in vivo.

PS 543

GABAA Protein-Protein Interactions Implicate GABAergic Regulation of Hair Cell Cyclic Nucleotide-Gated Ion Channels

Marian Drescher; Dakshnamurthy Selvakumar; Angela Vong; Neeliyath Ramakrishnan; Dennis Drescher
Wayne State University School of Medicine

Background

The neurotransmitter GABA originally was identified in the cochlea by its release into perilymph in response to sound stimulation (Drescher et al., 1983). Ultrastructural immunolocalization pointed to GAD, a source of GABA, in olivocochlear lateral efferents synapsing directly on both I spiral ganglion afferents and cochlear IHC, putatively in the adult configuration (Sobkowitz et al., 1997). We have determined that transcripts for GABAA channel subunits alpha1, alpha2, beta1, beta2, beta3 and gamma2 are expressed in the mammalian organ of Corti of the adult. Further, GABAA alpha1 is expressed in saccular hair cells (GenBank Accession No. KF644440). The question therefore concerns the molecular function of GABA and the ionotropic GABAA receptor in cochlear inner and outer hair cells, especially considering that GABAA subunits in retinal tissue were immunoprecipitated with the hair-cell synapse marker ribeye (Kantardzhieva et al., 2012).

Methods

We performed yeast two-hybrid mating and co-transformation of GABAA subunit protein interactions and studied cross-interaction with HCN1 and CNGA3 binding partners. Immunolocalization of GABAA alpha1 and LRP-1 was carried out with diaminobenzidine and fluorescence detection, the latter with confocal microscopy.

Results

Yeast two-hybrid mating analysis indicated that (1) GABARAP2L, which immunoprecipitates with TMC1 and interacts with GABAA gamma-2, also directly binds to the same moiety of protocadherin 15 CD3 as does HCN1. (2) CNGA3, targeted by GABAA alpha1-binding partner LRP-1, directly interacts with FKBP9, a modulator of immunosuppressant FK506, along with FKBP8, reported to interact with TMC1 (Labay and Griffith, 2009). (3) GABAA alpha-1 immunolocalizes to the IHC plasma membrane, the modiolus afferent synapse and to the stereocilia. (4) LRP-1, the GABAA alpha-1 binding partner in rat organ of Corti and teleost vestibular hair-cell models, localizes to IHC plasma membrane, perinuclear and stereociliary sites.

Conclusions

The immunolocalization sites emphasize that hair-cell stereociliary function and synaptic functions are linked, presumably through trafficking. The cyclic nucleotide-gated channels HCN1 (Ramakrishnan et al., 2012) and CNGA3 (Selvakumar et al., 2012), and GABAA alpha-1, are all localized to the stereocilia, a possible site for interaction, as is otoferlin (Ramakrishnan et al., 2013), the latter primarily considered in context of directing exocytosis. The perinuclear immunoreactivity for GABA alpha-1-binding partner LRP-1 points to additional nuclear regulation. The mechanism of action of GABAA within the hair cell synaptic ribbon remains to be elucidated, although GABAA operates through its PPI with both NSF and AP2, providing the opportunity to modulate dopaminergic D1A/otoferlin PPI at these sites (Selvakumar et al., 2016).

PS 544

Mitochondria Exhibit Structural Features That Differ Between Hair Cells and Afferents

Anna Lysakowski¹; Sofia Sobkiv²; Aashutos Patel²; Joseph Lesus²; Kevin Arias²; Meet Patel²; Laila Ghatah²; Vidya Babu³; Ashik Jayakumar²; Anuj Kambalyal⁴; Mark Ellisman⁵; Guy Perkins⁵

¹Department of Anatomy and Cell Biology, University of Illinois at Chicago, Chicago, IL, USA; ²Department of Biological Sciences, University of Illinois at Chicago, Chicago, IL, USA; ³Illinois Math and Science Academy; ⁴Department of Economics, University of Illinois at Chicago, Chicago, IL, USA; ⁵National Center for Microscopy and Imaging Research, University of California at San Diego, San Diego, CA, USA

In other organs in the body, the structure of mitochondria and their role in apoptosis and cell death is a topic of intense research interest. Such a framework of struc-

tural studies is missing in the inner ear. This study is an attempt to fill that gap by studying hair cell mitochondria for the ultimate purpose of addressing hair cell damage and death in mitochondrial-associated forms of deafness (both non-syndromic and antibiotic-induced). We wanted to know if variations in the physical structure and corresponding molecular composition in various sub-populations of hair-cell mitochondria could cause mitochondria to be affected differently by ototoxic insults, such as aminoglycoside antibiotics and chemotherapeutics.

Using electron microscope (EM) tomography and 3D-reconstructions, we have found that mitochondria in vestibular endorgans come in different sizes (large, medium and small) and exhibit different internal structures (lamellar vs. tubular cristae). The mitochondria found in hair cells are mostly medium-sized with lamellar cristae; those found in afferents (both calyces and boutons) are also medium-sized but they have tubular cristae. Efferent boutons are small with tubular cristae. Finally, the largest mitochondria, which have lamellar cristae, are found in the subcuticular plate region in central type I hair cells. We have analyzed the internal structure of these various types of mitochondria and find differences in the surface areas and volumes of their cristae, which can affect their ATPase-carrying capacity. In addition, they appear to be not only tethered to various hair cell organelles, but also to be arranged in particular orientations in relation to these organelles. As previously shown in mitochondria in the auditory brainstem (Perkins, Spirou, et al., 2010), mitochondrial cristae have openings to the inner mitochondrial membrane termed "crista junctions" and there are 1.5-2X more crista junctions on the side of the mitochondria facing toward structures relevant to hair cell function than on the side away from these structures. These crista junctions may be a way of directing ATP and Ca²⁺ toward energy-requiring organelles, such as ribbon synapses, stereociliar rootlets, striated organelles, etc. We have produced several short animations that illustrate these structural differences.

Supported by NIH R21 DC-013181-01.

Ultrastructural Investigation of Assembly, Maturation and Heterogeneity of Mouse Inner Hair Cell (IHC) Ribbon Synapses

Susann Michanski¹; Rituparna Chakrabarti¹; Christian Fischer²; Christian Vogl¹; Tobias Moser¹; Carolin Wichmann¹

¹Institute for Auditory Neuroscience and InnerEarLab, University Medical Center Göttingen; ²Georg-August-University of Göttingen

Background

Ribbon synapses are specialized glutamatergic contacts between inner hair cells (IHCs) and spiral ganglion neurons (SGNs). These presynaptic electron-dense structures tether synaptic vesicles (SVs) and transmit acoustic information via Ca²⁺-dependent exocytosis (Nouvian et al., 2006; Matthews & Fuchs, 2010; Wichmann & Moser, 2015). In murine IHCs, immature and mature ribbon synapses differ morphologically (Sobkowicz et al., 1986; Stamatakis et al., 2006; Wong et al., 2014) and undergo developmental refinement to achieve functional maturation. To date, developmental aspects including ribbon synapse assembly, maturation and targeting ribbon precursors to the active zone (AZ) are not well understood. Moreover, the correlation between ribbon position, morphology and function, factors that contribute to the synaptic heterogeneity observed within the individual IHC, remains elusive.

Methods

We used transmission electron microscopy and electron-tomography to study ultrastructural changes at IHC ribbon synapses at different developmental stages (E14-P48) of C57Bl6 wild-type mice before and after the onset of hearing. We quantified size and number of SVs and ribbons as well as the postsynaptic density (PSD) length across all age groups. Moreover, we used pre-embedding immunogold labelings against AZ and cytoskeletal proteins combined with confocal and stimulated emission depletion microscopy to identify the intracellular trafficking pathways of ribbon material. Additionally, we utilized serial-block-face scanning electron microscopy to reconstruct IHCs and their innervating SGNs in 3D to correlate the location and diameter of SGNs to attributes like ribbon and PSD size as well as number of ribbons and SVs.

Results

Our study reveals changes in the number and size of ribbons and SVs as well as in PSD arrangement during development. Interestingly, our results indicate that microtubules might play an important role in targeting ribbon precursors towards AZs and that fusion events of

synaptic ribbons may present at least one mechanism of confining the AZ/PSD complex around the onset of hearing (P12) and finally establish the typically 1:1 relationship between presynaptic ribbon and postsynaptic SGN bouton. However, multiple ribbons at one AZ could still be observed at synapses of mature ears, suggesting that they may present the structural correlate of large and complex ribbon synapses to contribute to functional heterogeneity in IHCs. Further, we detected dense-core vesicles close to IHC AZs in pre- and postnatal immature age groups, possibly containing neurotrophins to regulate maturation processes (Fritzsche et al., 2004, 2015).

Conclusions

These results significantly contribute to the understanding of ribbon synapse maturation and synaptic heterogeneity of murine cochlear IHCs.

PS 546

The Compact Active Zone Topography of Mature Mammalian Auditory Hair Cell Ribbon Synapses Promotes a Fast Proton-mediated Block of Ca²⁺ Current

Philippe Vincent¹; Didier Dulon²; Henrike von Gersdorff³

¹Johns Hopkins School of Medicine; ²University of Bordeaux; ³Vollum Institute, Oregon Health and Science University

Background

A synaptic cleft pH regulation of presynaptic Ca²⁺ currents appears as a general feature of sensory ribbon synapses. This process, described in the retina (DeVries et al., 2001; Palmer et al., 2003) and in auditory hair cells (Cho and von Gersdorff, 2014; Vincent et al., ARO 2016), is explained by the acidified content of the synaptic vesicles that is released concomitantly with glutamate in the synaptic cleft. The exocytosed H⁺ rapidly bind to the mouth of the nearby Ca²⁺ channels, containing glutamate residues, and produce a transient block of the Ca²⁺ conductance (ICaTB). Intriguingly, ICaTB has not been described in conventional glutamatergic synapses such as those of the Calyx of Held. The aim of the study was to determine the vesicular release mechanisms that underlie ICaTB at hair cell ribbon synapses.

Methods

Freshly dissected organs of Corti from pre-hearing (P7) and post-hearing (P14-P18) mouse IHCs were continuously perfused with a 95% O₂, 5% CO₂ bubbled extracellular solution in the presence of the physiological pH buffer bicarbonate (25 mM). Ca²⁺ currents and time-resolved changes in membrane capacitance (exocytosis)

were recorded in the whole-cell voltage-clamp configuration from IHCs. The topographical organization of the Ca²⁺ channels at IHC ribbons was assessed using fluorescence-immunochemistry under high resolution confocal microscopy.

Results

In bicarbonate solutions, Ca²⁺ currents of post-hearing mouse IHCs typically showed a single initial large transient block (ICaTB) that was followed by smaller transient notches (or spikelets). When switching the intracellular Ca²⁺ buffer from 1 mM EGTA to 5 mM BAPTA, IHCs displayed largely reduced exocytotic responses (from 31.9 ± 1.9 fF (n = 17) to 9.1 ± 2.1 fF (n = 6) and a significantly reduced initial ICaTB (from 29.3 ± 3.2 pA, n = 17 to 7.0 ± 1.5 pA, n = 12). Notably, small secondary transients in the Ca²⁺ current (spikelets) were still present with BAPTA, suggesting that they originate from asynchronous release events. Remarkably, we found that ICaTB is absent in P7 pre-hearing IHCs, when Ca²⁺ channels are spatially organized in large clusters loosely coupled to the ribbon-associated sites of release.

Conclusions

We propose that ICaTB occurs only in synapses that operate via Ca²⁺ nanodomain-triggered multivesicular release events that are orchestrated within a compact active zone. This H⁺ regulation of Ca²⁺ channels provides a fast feedback mechanism that efficiently reduces Ca²⁺ current and transmitter release, thus contributing perhaps to the fast adaptation of spike rates at auditory nerve fibers.

PS 547

Prehearing Efferent-inner Hair Cell Synaptic Strength and Afferent Synapse Maturation Are Not Altered in Mice Lacking the BK Channel

Eleonora Katz¹; Graciela Kearney²; Lucas G. Vattino²; Daniël O. J. Reijntjes³; Carolina Wedemeyer²; Andrea Meredith⁴; Sonja J. Pyott³; Ana Belén Elgoyhen⁵

¹Instituto de Investigaciones en Ingeniería Genética y Biología Molecular "Dr. Héctor N. Torres" (CONICET) and Departamento de Fisiología, Biología Molecular y Celular, Facultad de Ciencias Exactas y Naturales, Universidad de Buenos Aires; ²Instituto de Investigaciones en Ingeniería Genética y Biología Molecular "Dr. Héctor N. Torres" (CONICET); ³Dept. Otorhinolaryngology/Head and Neck Surgery, University Medical Center Groningen, The Netherlands.; ⁴University of Maryland School of Medicine; ⁵Instituto de Investigaciones en Ingeniería Genética y Biología Molecular "Dr. Héctor N. Torres" (CONICET) and Instituto de Farmacología, Facultad de Medicina, Universidad de Buenos Aires

Before the onset of hearing, inner hair cells (IHCs) receive efferent input from cholinergic medial olivocochlear (MOC) neurons. This input inhibits spontaneous activity of the IHCs and is thought to refine maturation of the afferent auditory system. Efferent inhibition before the onset of hearing has been hypothesized to drive pruning of supernumerary afferent (ribbon) synapses contacting the IHCs. However, the evidence to date has been limited and contradictory. Recent work combining pharmacology, electrophysiology, and immunofluorescence shows that L-type VGCCs suppress ACh release by activating BK channels expressed at MOC terminals. BK channel activation likely suppresses release by curtailing the duration of the terminal action potential. These observations suggest that mice lacking the BK channel (BK α ^{-/-} mice) should have enhanced efferent inhibition of the IHCs and, therefore, provide an in vivo model in which to test the hypothesis that efferent inhibition of IHCs contributes to the pruning of supernumerary afferent synapses. To probe the role of BK channels in efferent synaptic function, we isolated cochleas from BK channel knockout mice and their wild-type littermates (BK α ^{-/-}, BK α ^{+/+}) at P9-11 and measured evoked release during whole-cell voltage-clamp recordings from IHCs. We found no significant differences between genotypes in quantum content (BK α ^{+/+} 0.69±0.17, BK α ^{-/-} 0.69±0.14, p=0.97; n=10) nor in the short term plasticity pattern upon high frequency stimulation. In addition, the number and size of IHC ribbons were tracked by immunofluorescence. In both genotypes, ribbons are smaller and greater in number at P6 compared to their mature morphology at P21. The number of ribbons/IHC decreased from P6 to P21 from 33 ± 1 (n=3) to 21 ± 1 (n = 4) in wildtype mice and from 34 ± 2 (n = 3) to 22 ± 0.7 (n = 5) in knockout mice. The size of individual ribbon synapses increased from P6 to P21 from 0.24 ± 0.03 (n = 4) to 0.33 ± 0.03 (n = 4) μm² in wildtype mice and from 0.23 ± 0.03 (n = 3) to 0.33 ± 0.02 (n = 4) μm² in knockout mice. These results suggest that the lack of BK channels at efferent terminals might be compensated for by other regulatory mechanisms that prevent synaptic strength and pruning of supernumerary afferent synapses from being altered by this genetic modification.

Support:UBA&ANPCyT: EK,ABE; UMCG:SJP

Differential Inhibition Of Vestibular Nerve Afferents By Optical Stimulation

Vishal Raghu¹; Yugandhar Ramakrishna²; Senthilvelan Manohar³; Richard Salvi³; Soroush G. Sadeghi²

¹Neuroscience Program; ²Center for Hearing and Deafness, Dept. of Communicative Disorders and Sciences;

³Center for Hearing & Deafness, Department of Communicative Disorders and Science, State University of New York at Buffalo

Optical stimulation of neurons has been widely used in various parts of the peripheral and central nervous system. Different methods of neuronal stimulation (e.g., cell-targeted gold nanoparticles, optogenetics, and ligand uncaging) have gained popularity due to their fast kinetics and high specificity. Here, we report the effect of direct optical stimulation on vestibular nerve afferent activity in wild type C57BL/6 mice. A standard 460 nm LED fiber optic (10 Hz, duty cycle = 0.9 stimulation) was used in one month old animals. First, the activity of vestibular nerve fibers were monitored using in vivo extracellular recordings. Afferents showed spontaneous resting discharges (mean: 17 ± 2 spikes/s, range: 1 – 40 spikes/s, $n = 63$) and were divided into two groups based on their discharge regularity. Optical stimulation differentially affected the two types of afferents: while 97% of irregular afferents ($CV^* > 0.1$) showed 40-100% decrease in resting rate, most regular afferents (85.7%) showed < 40% inhibition. This effect started at ~ 500 ms after stimulation onset and plateaued at ~5.5 s. The firing rate returned to baseline ~10 s after stimulus termination. Notably, all irregular (but not regular) afferents could be silenced with substantially strong stimuli. Silenced irregular afferents failed to fire action potentials even under strong rotational stimulation (1 – 7 Hz, 20 – 100 deg/s). Next, in vitro voltage clamp recordings from calyces of the crista ampularis showed an outward current during the optical stimulation at the resting membrane potential. A current was present even with single pulses of light and a cumulative effect was observed with multiple pulses. Increasing extracellular potassium concentration from 5.8 mM to 30 mM shifted the reversal potential from ~ -70 mV to ~ -40 mV, suggesting the involvement of potassium channels. These findings show that optical stimulation can be used for exclusive inhibition or silencing of irregular afferents in the vestibular periphery in vivo. This can be a powerful tool for studying the differential roles of the peripheral phasic and tonic pathways involved in processing of vestibular information.

Biophysical Properties of the Posterior Lateral Line Ganglion of Developing Zebrafish in Vivo

Katherine Hardy; Walter Marcotti
University of Sheffield

Background

The afferent fibres of the zebrafish posterior lateral line (pll) form synapses with mechanosensory hair cells clustered together in neuromasts along the flank of the zebrafish. These fibres transmit the sensation of external water movement from the hair cells to the brain via the pll ganglion that lies posterior to the inner ear. The spontaneous activity of these afferent fibres has been studied at larval stages. However it is not known if the biophysical profiles of this activity are retained in older fish, at a time when afferent fibres undergo extensive growth and reorganization, which is essential for the fine-tuning and increased sensitivity to movement of adult zebrafish (Haehnel et al 2012 J Comp Neurol 520:1376; Liao & Haehnel, 2012 J Neurophysiol 107:2615).

Method

The firing activity of the afferent fibres was investigated using the zebrafish line NeuroD, which enable visualisation of neurons within the pll ganglia. Zebrafish, aged 2-21 days post fertilisation (dpf), were immobilized onto a thin layer of Sylgard 184 using tungsten wire (< 5.2 dpf: Olt et al 2016 J Physiol doi: 10.1113/JP271794) or restrained with agarose (5.2-21 dpf). Extracellular, loose-patch recordings of afferent neurons were performed as previously described (Olt et al 2016 Methods Cell Biol 133:253). The Mini Analysis Program was used to detect spike events in loose-patch, to calculate their frequency and to analyse interspike intervals (ISI). All experiments were performed in accordance with Home Office and following approval by the University of Sheffield Ethical Review Committee.

Results & Conclusions

We have developed a technique to obtain extracellular recordings in the zebrafish pll past protected larval stages (European Directive 2010/63/EU). Spontaneous firing activity was observed from when the lateral line becomes functional at 2 dpf and persists into older developmental stages. Preliminary data also suggests that neurons within each ganglion show a large variability in both the ISIs and spiking frequencies. Bursting activity was also seen in some neurons. This preparation will give us a unique insight into the in-vivo properties of hair cells and afferent neurons in a mature system.

Supported by Action on Hearing Loss

Hair Cells Use Active Zones with Different Voltage-dependence of Ca²⁺ Influx to Decompose Sounds into Complementary Neural Codes

Mark Rutherford¹; Tzu-Lun Ohn²; Zhizi Jing³; Sangyong Jung³; Carlos Duque-Afonso³; Gerhard Hoch³; Magdalena Picher³; Anja Scharinger³; Nicola Strenzke³; Tobias Moser⁴

¹Washington University School of Medicine; ²Institute for Auditory Neuroscience, University Medical Center Goettingen; ³University of Goettingen; ⁴Institute for Auditory Neuroscience and InnerEarLab, University Medical Center Göttingen

For sounds of a given frequency, spiral ganglion neurons (SGNs) with different thresholds and dynamic ranges collectively encode the wide range of audible sound pressures. Heterogeneity of synapses between inner hair cells (IHCs) and SGNs is an attractive candidate mechanism for generating complementary neural codes covering the entire dynamic range. Here, we quantified active zone (AZ) properties as a function of AZ position within mouse IHCs by combining patch clamp and imaging of presynaptic Ca²⁺ influx and by immunohistochemistry. We report substantial AZ heterogeneity whereby the voltage of half-maximal activation of Ca²⁺ influx ranged over ~20 mV. Ca²⁺ influx at AZs facing away from the ganglion activated at weaker depolarizations. Estimates of AZ size and Ca²⁺ channel number were correlated and larger when AZs faced the ganglion. Disruption of the deafness gene GIPC3 in mice shifted the activation of presynaptic Ca²⁺ influx to more hyperpolarized potentials and increased the spontaneous SGN discharge. Moreover, Gipc3 disruption enhanced Ca²⁺ influx and exocytosis in IHCs, reversed the spatial gradient of maximal Ca²⁺ influx in IHCs, and increased the maximal firing rate of SGNs at sound onset. We propose that IHCs diversify Ca²⁺ channel properties among AZs and thereby contribute to decomposing auditory information into complementary representations in SGNs (Ohn et al., 2016).

Ohn, T.L., Rutherford, M.A., Jing, Z., Jung, S., Duque-Afonso, C.J., Hoch, G., Picher, M.M., Scharinger, A., Strenzke, N., and Moser, T. "Hair Cells Use Active Zones with Different Voltage Dependence of Ca²⁺ Influx to Decompose Sounds into Complementary Neural Codes." PNAS 113(32): E4716 (2016) PMID: 27462107

WDR1 Presence in the Mouse Organ of Corti

Henry J. Adler¹; meiyang Jiang²; Yuan Zhang²; Peter S. Steyger³

¹SUNY - Buffalo, Center for Hearing and Deafness;

²Oregon Health & Science University, Oregon Hearing Research Institute; ³Oregon Hearing Research Center

Background

Previously, Song et al., (2013; J Comp Neurol 521:1470-81) described the cochlear expression of WD40 repeat protein-1 (WDR1) among hair cells and supporting cells in the rat cochlea, with increased expression of WDR1 after noise exposure. Also, we have shown that cell lines treated with gentamicin treatment revealed significant changes in the association of WDR1 with organelles such as Golgi bodies of COS7 cells, as well as actin filaments in HEI-OC1 cells, where WDR1 may be an important player in actin dynamics.

Aim

To localize the subcellular distribution of WDR1 in whole mounts of the mouse cochlea.

Methods

Adult C57 mice were intracardially perfused and fixed with 4% paraformaldehyde. Excised pieces of mouse organ of Corti were permeabilized and immunolabeled with rabbit anti-WDR1 antibody (Ab) and visualized with Alexa Fluor 568-conjugated goat anti-rabbit Ab. Specimens were counter-labelled with Alexa Fluor 488 phalloidin, post-fixed and examined by confocal microscopy.

Results

Higher resolution confocal imaging revealed WDR1 labeling in the stereocilia and the cytoplasmic channel through the cuticular plate of hair cells that was not apparent in mouse immunofluorescent controls, nor in prior cryostat sections of the rat cochlea.

Conclusion

WDR1 presence in both the stereocilia and the cytoplasmic channel through the cuticular plate of hair cells is suggestive of a role in cellular maintenance and survival following trauma. Stereociliary expression of WDR1 is not surprising because of WDR1's known association with actin. However, based on previous observations that WDR1 localization with Golgi bodies of COS7 cells, it is interesting to find such localization in the organelle-rich cytoplasmic channel through the cuticular plate and close to the location of the Hensen's body in outer hair cells. Further studies will determine if oxidative

stress or drug treatments alter the expression of WDR1 in hair cells.

Supported by R01s DC04555 (PSS), DC012588 (PSS), and DC005983 (P30)

PS 552

Data Management Plan To Curate Electrophysiological Data Obtained From The Mammalian Cochlea

Brenda Farrell¹; Jason Bengtson²

¹Baylor College of Medicine; ²Kansas State University

Background

Traditionally, scientists publish reports that describe their findings. Data collected to uncover these findings are not typically reported nor are they made readily available to their scientific peers, despite their value for further discovery and public education and awareness. Our first goal is to facilitate sharing of electrophysiological data obtained from cells or tissues within the cochlea for further discovery. This is incumbent because making electrical recordings from hair cells and supporting cells within the mammalian cochlea is a slow through-put process and requires the sacrifice of mammals. In collaboration with a data architect, we provide a prototype design to transform electrophysiological data for public use, this example data set describes the electrical properties of outer hair cells isolated from the mammalian cochlea.

Data Management Plan (DMP)

We will describe our approach and philosophy which adopts the FAIR (i.e., findable, accessible, interoperable and reusable) principles. The data is currently stored as proprietary MATLAB files; this software must be licensed at a significant cost, and is not accessible to everyone. We have transformed this data set to Hierarchical Data Format (version 5, HDF5) that was developed for storage of large or complex data sets. We use expansive metadata to preserve as much as feasible the context and relationships within the data, and developed a variant ontology that makes use of the ontology of biological investigation (OBI) and foundational model of anatomy (FMA). This ontology is then used to design and arrange the data in this HDF5 format. Like directories in a computer, each specimen (i.e., a recording from an outer hair cell) is displayed with a tree configuration consisting of three main branches that describes: the organism used to extract the cells; the characteristics of the native cell; and the electrical recordings. This data can be viewed by tools freely available from HDF group (<https://www.hdfgroup.org/>) which also offer capabilities to export the data into other formats. We will discuss workflows needed to access the stored data and to transform it for re-analysis by accessory software (e.g., HDF5 to MATLAB back-flow).

Product

This data set will be placed in the Code Analysis, Repository & Modelling for E-Neuroscience (CARMEN) and Kansas State University REsearch eXchange (K-Rex) repositories. This DMP will be available to the community to manage similar data sets; such methodologies are becoming mandatory to promote more efficient use of publicly-funded collections. This work was funded by NLM and NIDCD R01DC000354-S1.

PS 553

Deletion of Auxiliary Ca²⁺ Channel Ssubunit $\alpha 2\delta 3$ Specifically Reduces P/Q (Cav2.1) But Not L-type Ca²⁺ Currents of Spiral Ganglion Neurons

Jutta Engel; Friederike Stephani

Dept. of Biophysics and Center for Integrative Physiology and Molecular Medicine (CIPMM), Saarland University

Introduction

Spiral ganglion (SG) neurons connect hair cells with central auditory neurons and therefore are indispensable for auditory signal transmission. Myelinated type I SG neurons comprise 95% of all SG neurons and make a precise 1 to 1 connection with inner hair cells. Proper function and morphology of auditory nerve fiber synapses require the auxiliary Ca²⁺ channel subunit $\alpha 2\delta 3$ (Pirone et al., *J Neurosci* 2014). To determine the role of $\alpha 2\delta 3$ for SG neurons, we analyzed Ca²⁺ currents in cultured SG neurons isolated from $\alpha 2\delta 3$ +/+ and $\alpha 2\delta 3$ -/- mice before (P5) and after the onset of hearing (P20).

Methods

Patch-clamp recordings of Ca²⁺ currents were performed on enzymatically dissociated SG neurons isolated from neonatal (P5) or juvenile (P20) mice (cf. Lv et al., *J Neurosci* 2012). Mice deficient with a targeted deletion of the CACNA2D3 gene coding for $\alpha 2\delta 3$ ($\alpha 2\delta 3$ -/-) generated by Deltagen (Neely et al., *Cell* 2010), were used. Cochleae were transversally cut in the middle, and SG neurons from the apical and basal halves of the cochlea were cultured separately for 2-3 days.

Results

Ca²⁺ currents of SG neurons were isolated by blocking voltage-gated K⁺ currents by TEA (30 mM), 4-AP (15 mM) and linopirdine (100 μ M) in the bath and by 110 mM Cs⁺ in the pipette solution. Large voltage-gated Na⁺ currents were fully suppressed by extracellular NMDG (110 mM). L-type Ca²⁺ currents were blocked by superfusing SGNs with 10 μ M nimodipine. The fraction of L-type currents amounted to 30 - 35 % of the total Ca²⁺ current in both $\alpha 2\delta 3$ +/+ and $\alpha 2\delta 3$ -/- mice. P/Q-type Ca²⁺ currents were blocked by superfusion with 1 μ M ω -agatoxin IVA. Cav2.1-mediated currents

were very small in SG neurons isolated from neonatal mice. However, in SGNs isolated from P20 $\alpha 2\delta 3$ +/+ mice, Cav2.1 currents contributed 50 – 55 % to the total Ca²⁺ current. Cav2.1 channels of P20 SG neurons had a clear preference for $\alpha 2\delta 3$ because their Cav2.1-mediated current was reduced to 20-25% of the total Ca²⁺ current in $\alpha 2\delta 3$ -/- mice.

Conclusion

Our data show that proper sizes of Cav2.1 Ca²⁺ currents in P20 SG neurons required the presence of $\alpha 2\delta 3$, whereas expression of L-type Ca²⁺ currents was independent of $\alpha 2\delta 3$. The role of $\alpha 2\delta 3$ for other Ca²⁺ current subtypes and a potential compensatory up-regulation in $\alpha 2\delta 3$ -/- SG neurons remains to be determined.

Supported by DFG-PP1608.

PS 554

Opposing Gradients of Tyrosine Hydroxylase and CGRP α Expression in Type II Afferent Neurons of the Mouse Cochlea

Jingjing Sherry Wu¹; Pankhuri Vyas¹; Amanda Zimmerman²; Paul A. Fuchs¹; Elisabeth Glowatzki¹; Jingjing Wu³

¹Johns Hopkins University School of Medicine; ²Harvard Medical School; ³Johns Hopkins School of Medicine

Type I and type II afferent neurons are classified by their morphology and innervation patterns. Despite their distinct anatomical features, little is known about differences in their molecular profiles. Peripherin, an intermediate neurofilament protein, has been reported to be preferentially expressed in type II versus type I neurons (Hafidi, 1998). However, with peripherin being the only candidate marker available so far, it is difficult to assess whether it labels all or a subset of type II neurons. To identify other candidate genes for studying type II neurons, we examined the expression patterns of several genes in the cochlea that are specifically expressed in small-diameter DRG neurons. In an accompanying abstract, Vyas et al. "Tyrosine hydroxylase expression in Type II cochlear afferents in mice", we describe one such gene, Th, to be preferentially expressed by type II versus type I neurons. Because type II neurons have been hypothesized to be the cochlear 'nociceptor', we also tested the expression pattern of Calca/CGRP α , a gene that is specific for pain-sensing DRG neurons.

Whole-mount cochlear preparations from 1-2 month old CGRP α -EGFP and CGRP α CreER; Rosa26LSL-EYFP mice showed expression of CGRP α in a subset of SGNs. Labeled fibers showed the typical morphology

of type II dendrites, with a radial fiber that crosses the tunnel of Corti and a long spiral process running along the outer hair cells. Double labeling with other molecular markers confirmed that the labeled SGNs were type II and not type I afferent neurons. At early postnatal age, in both mouse lines the expression level of CGRP α in type II fibers was higher, and at this age, a small population of type I afferent neurons was also labeled. However, antibody staining at a perinatal age only revealed CGRP labeling in type II afferents.

Interestingly, the expression patterns of Th and CGRP α in type II afferent neurons formed opposing gradients, with Th being preferentially expressed in apical and CGRP α in basal type II afferent neurons, indicating heterogeneity among the type II afferent neurons. The expression of Th and CGRP α was not mutually exclusive and co-expression could be observed, most abundantly around the medial turn.

In summary, Th and CGRP α are both preferentially expressed in type II versus type I afferent neurons. Their expression in type II afferent neurons showed opposing tonotopic gradients. Noise exposure experiments are currently in progress, to test if the expression gradients of these two genes are subject to experience-dependent modulation.

PS 555

Tyrosine Hydroxylase Expression in Type II Cochlear Afferents in Mice

Pankhuri Vyas¹; Jingjing Sherry Wu¹; Amanda Zimmerman²; Paul A. Fuchs¹; Elisabeth Glowatzki¹

¹Johns Hopkins University School of Medicine; ²Harvard Medical School

Background

Acoustic information is transduced from ear to brain by afferent neurons that innervate hair cells in the cochlea. The more abundant (95%) myelinated type I axons carry auditory information from inner hair cells and fewer (5%) unmyelinated type II axons carry information from outer hair cells. The anatomical distribution, synaptic connections and physiological properties of these afferent fibers have been studied largely without the benefit of genetic tools to distinguish between type I vs type II neurons. Here we describe Tyrosine Hydroxylase (TH) as a novel marker that specifically distinguishes type II from type I afferents. We demonstrate that this mouse model can be used to identify and study the morphology and development of type II afferent fibers in the cochlea.

Methods

We crossed TH2a- CreER mice with Rosa26LSL-EYFP (Ai3) or Rosa26LSL-tdTomato (Ai9) mice, treated with tamoxifen and immunolabeled for cell-specific markers that can identify type I and II afferents, medial and lateral efferents in cochlear whole-mounts.

Results

Cochlear whole-mounts from TH2a- CreER; Ai3 or TH2a- CreER; Ai9 mice showed expression of fluorescent label in a small subset of spiral ganglion neurons with type II-like morphology and trajectory. These TH2a- CreER expressing neurons were not labeled by antibodies against $\alpha 3$ Na/K ATPase that specifically labeled type I afferents and medial efferents, but were immunolabeled for TH. These afferents only partially co-labeled with antibodies against peripherin, a previously reported marker of type II afferents. TH expression was also observed in lateral olivocochlear (LOC) efferents and sympathetic neurons. TH2a- CreER afferents studied between 4-8 weeks of age formed on average 11.6 + 4.6 terminal branches onto outer hair cells, with typically one or two zones of arborization. Several type II fibers were observed to make synaptic boutons onto a single outer hair cell but not every bouton was associated with a pre-synaptic ribbon.

Conclusion

These results show that TH provides a selective marker to identify type II versus type I afferents and can be used to describe the morphology and arborization pattern of type II cochlear afferents, particularly in the apex of the mouse cochlea (see abstract from Wu et al. Opposing Gradients of Th and CGRP α Expression in Type II Afferent Neurons of Mouse Cochlea). Thus TH-dependent Cre-recombinase would enable genetic manipulation of type II cochlear afferents and will be useful in establishing the function of TH-expressing type II cochlear afferents in experimental models of cochlear development and damage.

PS 556

AMPA Receptors of Auditory Nerve Fiber Postsynaptic Densities appear to have Nanodomains that Lack the Ca²⁺-limiting GluA2 Subunit

Mark Rutherford

Washington University School of Medicine

Each mature mammalian auditory nerve fiber receives synaptic input from an inner hair cell via a single ribbon-type synapse, with a single postsynaptic density. Each postsynaptic density expresses the Ca²⁺-limiting AMPAR subunit GluA2 (Jing et al., 2013; Liberman and Liberman, 2016). Here, we show that these synapses all co-express the GluA3 and GluA4 subunits, along with

GluA2. We simultaneously labeled these three subunits via immunohistochemistry. Total postsynaptic volume was calculated for each synapse by thresholding a virtual channel created by summing the 3 individual confocal channels (GluA2 + GluA3 + GluA4). Total volume ranged from 0.09 – 0.85 μm^3 . We calculated intensity by summing the pixel values within each synaptic volume. Intensity per synapse scaled with volume over a similar relative range of approximately one order of magnitude for GluA2, GluA3, GluA4, and their sum, suggesting differences among synapses in postsynaptic molecular abundance.

In addition to this 10-fold range in total AMPA receptor immunofluorescence, we found considerable differences among synapses in fluorescence ratios for the 3 subunits. We calculated fluorescence intensity ratios for each subunit at each synapse as GluAX divided by GluASum. Although fluorescence ratios do not indicate relative subunit abundance at a given synapse, comparisons of these ratios among synapses provide a measure of the heterogeneity of subunit relative abundance among synapses. Histograms of fluorescence ratios for GluA2, 3, and 4 show that the three subunits were expressed in different ratios at different postsynaptic densities. Differences in fluorescence ratios generate the appearance of synapses with different hues in merged color panels. At some synapses GluA2, 3, and 4 appear to occupy very similar overlapping regions. Within other synapses, the subunits appear to occupy partially non-overlapping domains. Analysis with line profiles revealed GluA2-lacking regions, suggesting the presence of Ca²⁺-permeable AMPA receptors at some synapses.

PS 557

Regulation of Cochlear Rhythms and Circadian Expression of Core Clock Genes

Barbara Canlon; Jung-sub Park; Christopher Cederroth; Vasiliki Basinou; Rocio Paublete
Karolinska Institute

Circadian rhythms have been shown to regulate a large number of bodily functions including metabolism and inflammatory responses. The mammalian circadian clock system is hierarchically organized with the suprachiasmatic nucleus (SCN) functioning as the master clock that orchestrates peripheral clock rhythms, through behavioral, neuroendocrine and autonomic pathways, in order to regulate the physiological function of many organs. We recently identified robust self-sustained clock machinery in the cochlea and the inferior colliculus using mice that express a luciferase protein coupled to the circadian PERIOD 2 (PER2) protein (PERIOD2::LUCIFERASE (PER2::LUC)) (Meltser et al., 2014; Park et al., 2016). Here we describe the role of the SCN for

the cochlear rhythmicity Bmal1 is an essential component of the molecular clock machinery and its loss of function causes behavioral and molecular arrhythmicity. To assess the effects of a specific cochlear Bmal1 deletion on cochlear oscillations we crossed Bmal1^{fx/fx};Pax2:Cre mice with PER2::LUC expressing mice (Bmal1;Pax2:Cre;Per2Luc) in order to track PER2::LUC bioluminescence. The absence of PER2 rhythmicity in the cochlea from cBmal1(d/d) confirm that the cochlear clock relies on Bmal1 for maintaining self-sustained oscillations. We next examined the influence of light and the potential involvement of the SCN in the regulation of cochlear rhythms in normal light/dark cycles (LD) and inverted dark/light cycles (DL). The circadian patterns of cochlear mRNA transcripts of Per2, Rev-Erba, Rev-Erbb and Bmal1 were inverted in a DL cycle and support the hypothesis of a direct influence of the SCN on cochlear rhythms. To directly determine whether the SCN is required for cochlear rhythmicity, we performed bilateral SCN electrolytic lesions. In the cochlea, the circadian expression of the clock genes was abolished in absence of the SCN in both LD and DL conditions. Thus, the SCN maintains the phase of cochlear rhythms and circadian expression of core clock genes. Taken together, these results indicate that the SCN is required for the coordination of core clock and clock-dependent gene regulation in the cochlea.

PS 558

CAMSAP3 Plays Important Roles In Hearing

Jing Zheng; Aisha Ahmad; Satoe Takahashi; Mary Ann Cheatham

Northwestern University

Calmodulin-regulated-spectrin-associated protein 3 (CAMSAP3), also called Marshalin, is a microtubule (MT)-minus-end binding protein associated with centrosomal-independent MTs. CAMSAP3 is widely expressed in different types of cells in almost every tissue, including the organ of Corti and spiral ganglion neurons of the auditory nerve. To study CAMSAP3 function(s), we obtained a transgenic mouse model for CAMSAP3, Camsap3^{tm1a}, which was created in the C57BL/6N line as part of the Sanger Institute Mouse Genetics Project using the “knockout-first” conditional allele targeting strategy (Skarnes et al., 2011). In this model, the promoter-driven cassette, including a splice acceptor site (SA) and an internal ribosome entry site, was inserted between exons 6 and 7 of the CAMSAP3 gene to create a truncated transcript through RNA processing, thereby resulting in a functional null. Although our RT-PCR data show that CAMSAP3 transcripts are indeed decreased in homozygous Camsap3^{tm1a} mice, CAMSAP3 protein is still found in Camsap3^{tm1a}/C57BL/6N mice by Western blot. Hence, the Camsap3^{tm1a}/C57BL/6N mouse

model is likely hypomorphic for Camsap3 but not a functional null. Camsap3^{tm1a}/C57BL/6N mice show increased mortality before weaning, reduced size, and infertility in both sexes. These observations are consistent with the fact that CAMSAP3 is widely expressed and that it performs important functions in multiple tissues. To overcome the low reproduction rate and small litter size on the original C57BL/6N background, we re-derived this line on FVB and CBA/CaJ murine backgrounds to increase survival of Camsap3^{tm1a} homozygotes. Increased survival rates were indeed observed in both Camsap3^{tm1a}/FVB and Camsap3^{tm1a}/CBA/CaJ homozygotes. Even though homozygotes from both re-derived strains remained smaller than their wildtype littermates, homozygotes from Camsap3^{tm1a}/FVB retained their reproductive capability. Whether or not homozygotes on the CBA/CaJ background are fertile remains to be determined. Consistent with characterization of the original Camsap3^{tm1a}/C57BL/6N animals (Steel et al., ARO, 2016), hearing impairment was also observed in Camsap3^{tm1a} homozygotes independent of genetic background, indicating that CAMSAP3 plays an important role in hearing. However, the degree of hearing loss was variable. We suspect such variation may be associated with the degree of “leakiness” of CAMSAP3 mRNA expression. Currently, we are investigating the relationship between CAMSAP3 mRNA expression and hearing function among Camsap3^{tm1a} homozygotes on both FVB and CBA/CaJ backgrounds. (Work supported by NIDCD grants DC000089 and DC011813).

PS 559

Schroeder-Phase Complex Masking Effects on the Auditory Brainstem Response of Chinchillas

Ryan Harrison; Niall Klyn; Eric Bielefeld

The Ohio State University

The phase structure of auditory signals has a strong influence on auditory responses in normal hearing listeners due to the nonlinear response of the cochlear amplifier. This nonlinear response is relevant to the masking effect of Schroeder-phase complexes. The positive Schroeder complex (+SCHR) elicits a nonlinear response from the basilar membrane that increases signal detection despite the presence of a masker. Conversely, the negative Schroeder complex (-SCHR) does not elicit this response, thereby making it a more effective masker. This difference is present only in normal-hearing listeners; in hearing impaired listeners, both +SCHR and -SCHR mask with the same level of effectiveness. This change is thought to be directly related to the damage to the organ of Corti, specifically the outer hair cells, that underlies much sensorineural hearing loss. The current study explored the anatomical basis for the change in perception of Schroeder maskers. The difference in per-

ception of stimuli in the presence of Schroeder maskers before and after noise-induced hearing loss was examined by analyzing input-output functions from masked auditory brainstem response tests modified to a Schroeder masking paradigm. Chinchillas were tested at 2, 4 and 8 kHz with +SCHR and -SCHR masking conditions in which the stimulus level was fixed at 40 dB SPL and the masker varied from +55 dB SPL to -20 dB SPL. Animals were then exposed to a .5-6 kHz band noise at 98 dB SPL for 60 minutes. At week 1 and week 2 after the exposure, the +SCHR and -SCHR conditions were re-tested. Analysis revealed that, for the normal-hearing animals, the difference in masking response occurred once the masker reached levels of 20 dB SPL and higher. Above 20 dB SPL, the difference between the maskers in ABR P1 wave amplitude reduction generally increased with the level of the masker. After noise exposure, there were no differences between +SCHR and -SCHR at 2 kHz and little difference at 4 kHz. At 8 kHz, the differences between the maskers did not change compared to pre-exposure recordings. Post-mortem cochlear analyses indicated significant outer hair cells loss in the mid-frequency cochlear regions.

PS 560

Sound Exposure Induces Tyrosine Hydroxylase Expression in Cholinergic Intrinsic Lateral Olivocochlear Neurons

Jingjing Sherry Wu¹; Elisabeth Glowatzki¹; Jingjing Wu²

¹Johns Hopkins University School of Medicine; ²Johns Hopkins School of Medicine

Lateral olivocochlear (LOC) neurons innervate the dendritic endings of auditory nerve fibers (ANFs) that contact the inner hair cells (IHCs). Immunostaining studies in mice have suggested two cytochemical groups of LOC neurons: tyrosine hydroxylase (TH)-positive, presumably dopaminergic LOC shell neurons and choline acetyltransferase (ChAT)-positive cholinergic LOC intrinsic neurons (Darrow et al. 2006).

Immunostaining of whole-mount cochlear preparations and brainstem sections of 1-2 month old C57BL/6J WT mice showed TH expression in LOC shell neurons, as expected. However, sporadic expression of TH was also observed in a subset of cholinergic LOC intrinsic neurons. Along the cochlear coil, TH-positive terminals appeared in patches underneath the IHCs, as described before (Darrow et al. 2006). These TH-positive terminals co-immunolabeled with vesicular acetylcholine transporter (VAcHT), suggesting that they represented a subset of the cholinergic LOC neuron terminals that also expressed TH. In comparison, TH-positive LOC shell neu-

rons formed extensive spiral fibers that spanned the entire cochlear coil with sparse terminal branches, which were distinct from those large varicosities formed by LOC intrinsic neurons.

When comparing TH staining of individual cochleas from different animals, patches of TH-positive terminal regions seemed to appear randomly along the cochlear coil, with a slight preference towards the base. However, in Th2A-CreER;Rosa26LSL-EYFP mice, after multiple doses of tamoxifen delivered over several weeks, EYFP-positive terminals appeared all along the cochlear coil, suggesting that over time, TH-positive patches could shift to different locations. To investigate whether sound exposure affects the expression of TH in LOC neurons, a large dose of tamoxifen was injected into Th2A-CreER;Rosa26LSL-EYFP mice, followed by sound exposure (1 octave band centered at 12000 Hz, ~90 dB, 12 hour exposure for 5 days). Tamoxifen injection before sound exposure mainly labeled the TH-positive LOC shell neurons that had a relatively stable expression of TH. However, after sound exposure, antibody staining against TH in the same mice showed an increased number of TH-positive LOC intrinsic neurons, suggesting that the TH expression in cholinergic LOC intrinsic neurons can be induced by sound.

In summary, TH expression in LOC intrinsic neurons is dynamically regulated by acoustic experience in mice. In vitro electrophysiology experiments are underway to test the hypothesis that dopamine expression can be induced in cholinergic LOC intrinsic neurons by sound exposure, possibly to protect ANF dendrites against damage due to excitotoxicity.

PS 561

The Cochlea is an Extra-adrenal Steroidogenic Tissue

Douglas E. Vetter; Kathleen T. Yee
University of Mississippi Medical Center

Introduction

We have previously demonstrated that the mouse cochlea expresses numerous proteins classically considered as part of the hypothalamic-pituitary-adrenal (HPA) axis. Such molecules include corticotropin-releasing factor (CRF), the CRF receptors CRFR1 and CRFR2, pro-opiomelanocortin (POMC) and its cleavage product adrenocorticotrophic hormone (ACTH), and the ACTH receptor melanocortin receptor 2 (MC2R). Given that the cochlea is also subject to blood-borne hormonal regulation via the classic HPA axis, a significant question arises as to the degree of independence of the cochlear HPA-like signaling system from the classic HPA axis.

Methods

To isolate the cochlea from confounding blood-borne hormones, explant cochlear cultures were produced at P7 and P30 wild type and CRFR1 null mice. Cultures were stimulated with various concentrations of ACTH or CRF, and media was collected prior to stimulation (baseline), and at various times between 3 and 48 hours after stimulation. Release of corticosterone and aldosterone were individually analyzed by ELISA. Standard immunohistochemistry was performed on whole mounts, cryostat or paraffin embedded adult cochleae using antibodies to steroidogenic acute regulatory (StAR) protein (imports cholesterol into the mitochondria for use in producing numerous steroids), cyp11B1 and cyp11B2 (key synthetic enzymes responsible for the last steps in the production of corticosterone and aldosterone, respectively). Western blot was used to examine expression levels of 11-beta HSD2 (a key enzyme for degradation of corticosterone).

Results

Stimulation of wild type cultures by ACTH and CRF produced a robust release of both corticosterone (600pg/ml in response to CRF) and aldosterone (18pg/ml in response to ACTH) into the culture media. No ACTH was detected following CRF stimulation in explants from CRFR1 null mice. Additionally, the corticosterone degradation enzyme 11-beta HSD2 showed an increased expression following exposure to noise (95dB, 8-16kHz, 2 hrs) via western blot. We next sought to define expression and localization of enzymes important for the biosynthesis of corticosterone and aldosterone. Initial immunohistochemical analysis of StAR, cyp11B1, and cyp11B2 revealed localization for all of these proteins in Deiter's cells and support cells along the lateral and inner sulcus regions of the cochlea.

Conclusions

The cochlea harbors a signaling system essentially identical in form and function to the classic HPA axis. Additionally, immunohistochemistry reveals that the steroidogenic process largely, and perhaps exclusively, occurs within the support cell population of the cochlea. The ability of sound to drive steroid hormone production in the cochlea is currently being assessed.

Supported by: R21DC015124 (DEV)

PS 562

β 1- and β 2-adrenergic Stimulation-induced Electrogenic Transport by Human Endolymphatic sac Epithelium and Its Implications in Meniere's Disease

Bo Gyung Kim¹; Jin Young Kim²; Jinsei Jung³; Jae Young Choi³; Sung Huhn Klim³

¹Sooncheonhyang University College of Medicine; ²The Airway Mucus institute, Yonsei University College of Medicine; ³Yonsei University College of Medicine

The endolymphatic sac (ES) is a cystic structure connected to other inner ear organs, such as the cochlea and vestibule. The ES has been reported to play a role in regulating inner ear fluid volume and ion homeostasis for the maintenance of hearing and balance. If the inner ear fluid volume and ion homeostasis regulation are disrupted, inner ear disorders with hearing loss and dizziness, such as Meniere's disease, can develop. In this study, we attempted to investigate for the first time the functional evidence for the roles of β 1- and β 2-adrenergic receptors in electrogenic ion transport by human ES epithelium and in the development of Meniere's disease, using electrophysiological/pharmacological and molecular biological methods. The β adrenergic agonist isoproterenol induced significant apical electrogenic transport in the human ES epithelium. Electrogenic transport was dependent on the K⁺ and Cl⁻ ion transport in that the current was nearly completely inhibited by 1 mM Ba²⁺ and 100 μ M 4,4'-diisothiocyano-2,2'-stilbenedisulfonic acid. Isoproterenol-induced electrogenic transport was partially (~50%) inhibited by selective β 1- and β 2-adrenergic receptor inhibitors (100 μ M CGP-20712A and 100 μ M IC118551), indicating that the electrogenic transport was mediated by β 1- and β 2-adrenergic receptors simultaneously. However, the isoproterenol-induced electrogenic transport was absent or very weak in the ES epithelium of Meniere's disease patients. The results of this study suggested that adrenergic stimulation via β 1- and β 2-adrenergic receptors in the human ES was involved in the regulation of ion homeostasis of the inner ear and that impairment of this response could be one of the pathologic mechanisms of Meniere's disease.

PS 563

Localization of Corticotropin-Releasing Factor in Vestibular Hair Cells

Douglas E. Vetter; Kathleen T. Yee; Hong Zhu; Wu Zhou
University of Mississippi Medical Center

Introduction

We recently presented evidence that vestibular peripheral end organs express corticotropin-releasing hormone receptor 1 (CRFR1) in calyx endings surrounding Type I hair cells. Additionally, we previously showed that a cochlear CRF-based signaling system is protective against metabolic insult induced by exposures to loud sound, and that CRFR1 null mice express abnormal levels of glutamate receptor subunits (Graham et al., 2010). This suggests that activation of CRFR1 may be important for normal afferent neurotransmission. Since the vestibule

lar periphery can be activated by sound, investigating a role for CRF signaling may help define mechanisms by which modulation of afferent fiber activity occurs. Here, we localized a CRFR1 ligand in vestibular end organs.

Methods

Briefly, CRF-IRES-Cre mice and ROSA26-tdTomato mice, in which the reporter is preceded by a floxed STOP cassette (also known as the Ai14 line) were purchased from Jackson Labs. CRF:tdTomato reporter mice were produced by mating homozygous CRF-IRES-Cre mice with homozygous Ai14 ROSA26 tdTomato mice. The offspring carry both transgenes and result in tdTomato expression in cells expressing CRF due to Cre recombinase activity. Reporter expression faithfully mirrors CRF expression patterns previously defined using immunohistochemical procedures (Chen et al., 2015). Double transgenic mice were perfused (4% paraformaldehyde), and inner ears were processed and sectioned. tdTomato was visualized via immunofluorescence microscopy.

Results

Expression of CRF (tdTomato) was limited to scattered hair cells in the vestibular end organs at P22. Although currently qualitative, the location of the early expressing hair cells was often observed in the peripheral regions of the maculae and cristae. With increasing age, more central (maculae) or apical (cristae) regions of the end organs become labeled. Significantly, little or no tdTomato label was observed in cells other than hair cells.

Conclusions

While our previous work demonstrated expression of CRFR1 in the vestibular periphery, the source of the ligand responsible for activating CRFR1 remained unknown. We show here that the source of CRF, the major ligand for CRFR1, is the hair cell population. Unlike the cochlea, where CRF is expressed in some support cells as well as hair cells, the vestibular end organs seem to have a more restricted pattern of CRF expression. However, CRFR1 can also be stimulated by other peptides that are part of the CRF family, including urocortin. Further work is being conducted to more completely define sources of other potential ligands of CRFR1 in the vestibular periphery.

R01DC012060 (HZ), R01DC014930 (WZ), R21EY025550 (WZ), R21DC015124 (DEV)

PS 564

Spiking and Transmission in Calyceal Terminals in Different Zones of the Mouse Utricular Epithelium

Omar Lopez Ramirez; Ruth Anne Eatock
University of Chicago

Vestibular primary afferents form calyceal endings surrounding type I hair cells, bouton endings contacting type II hair cells, or both. In the utricular epithelium, functional differences between afferents are correlated with zones (striola, S, and extrastriola, ES): ES afferents have more regular spike timing and more tonic responses than S afferents. Low-voltage-activated K (KLV) channels of the Kv1 and Kv7 families and HCN channels have been implicated in vestibular afferent spike regularity. Calyceal HCN channels have also recently been implicated in a novel form of non-quantal (NQ) transmission from hair cells to calyx (Contini et al. ARO Abstr. 2016). To assess the contributions of KLV and HCN (h) currents to zonal variations in function, we record from calyces (postnatal days, P, 10-27, n=68) in an excised, intact preparation of the mouse utricle and map the locations.

S calyces had significantly larger KLV ($p < 0.001$) and HCN currents ($p < 0.01$) than ES calyces. KLV current difference was accounted for the larger size of S calyces, more of which are complex (surround multiple type I hair cells). For Ih there may be greater current density in S. Spike rate was similar across zones (22.5 ± 5.6 spikes/s, 33 calyces). As in vivo, spiking was more irregular in S calyces than in LES calyces: CV 1.1 ± 0.25 (4) vs. 0.6 ± 0.09 (12), $p = 0.02$; Fano factor, FF, 0.8 vs. 0.04, $p = 0.002$. In 6 LES calyces, ~60% block of KLV current with a Kv7 blocker (10 μ M XE991) increased spike regularity (CV 0.11 ± 0.01 , $p = 0.007$; FF 0.0007, $p = 0.037$), without significantly altering rate. This result supports the hypothesis that KLV channels contribute to spike irregularity in the rodent afferent nerve.

Previously we demonstrated NQ transmission in S calyces from the rat saccule in the first postnatal week (Songer & Eatock 2013). We have extended these findings to include mouse utricular calyces, ES calyces, and older calyces (P13-P26). 15/17 calyces driven by deflection of an enclosed type I hair bundle had clear NQ responses. At 2 Hz, NQ currents were 10-150 pA (peak-to-peak; median 18 pA) and NQ potentials were 2-16 mV (median 4 mV). Comparison of hair cell and calyceal responses to similar stimuli shows synaptic modifications of the signal. In contrast to reports from turtle, we find that NQ responses are faster than conventional quantal responses and drive afferent spiking with high vector strength up to 100 Hz.

Funding: NIDCD R01DC012347.

PS 565

Mouse Model with a DFNB59 Variant Unravels the Genetic Underpinning of Unfavorable Cochlear Implantation Outcomes

Ying-Chang Lu¹; I-Shing Yu²; Shu-Wha Lin²; Chen-Chi Wu¹; Chuan-Jen Hsu³

¹National Taiwan University Hospital; ²National Taiwan University; ³Taichung Tzu Chi Hospital

Background

Cochlear implantation is currently the treatment of choice for patients with profound sensorineural hearing impairment. However, the outcomes with cochlear implants (CIs) vary significantly among recipients. In our previous study, we identified that variants in DFNB59 and PCDH15 are associated with unfavorable CI performance. To explore the molecular mechanisms and therapeutic strategies, we recently generated knock-in mouse models with these genetic variants using the CRISPR/Cas9 technology. Herein, we presented the audiovestibular features and inner ear pathology of mice with DFNB59 p.G292R, the most common genetic variant related to unfavorable CI outcome in our previous series.

Methods

Mice with Dfnb59 p.G292R were generated and maintained in the C57BL/6 background. Homozygous, heterozygous and wild-type mice were then subjected to a battery of audiological assessments, vestibular evaluations, morphological studies, and electrophysiological examinations. The expression of pejvakin, the protein encoded by Dfnb59, was examined using immunolocalization.

Results

Dfnb59G292R/G292R mice showed significantly higher hearing thresholds than Dfnb59G292R/WT and Dfnb59WT/WT mice at clicks, as well as 8k, 16k and 32 kHz pure tones on auditory brainstem response (ABR). Further analysis of the waveforms revealed prolonged latencies of all the ABR waves, indicating the presence of retrocochlear lesions. In accordance with the audiological findings, pathological changes in hair cells and spiral ganglion neurons (SGNs) were observed in Dfnb59G292R/G292R mice at 3 weeks. In addition to the hearing phenotypes, Dfnb59G292R/G292R mice also demonstrated equilibrium deficits suggesting pathologies involving both the vestibular organ (circling) and the central nervous system (nodding).

Conclusions

Characterization of audiological and histological results in mice with Dfnb59 p.G292R revealed both cochlear

and retrocochlear lesions, indicating that unfavorable CI outcomes related to DFNB59 variants might be attributable to pathology in SGNs and/or brainstem auditory nuclei. These findings unravel the genetic underpinning of unfavorable CI outcomes and provide insight into therapeutics for improving CI performance in the future.

Funding This research was supported by grants from Ministry of Science and Technology, Taiwan.

PS 566

Generation and Phenotypic Characterization of Prps1 p.Ala87Thr Mouse Knock-in Model for Human DFN2 Deafness

Rahul Mittal¹; Qi Ma²; Denise Yan¹; M'hamed Grati¹; Xuezhong Liu¹

¹Department of Otolaryngology, University of Miami Miller School of Medicine, Miami, FL 33136, USA; ²Department of Otolaryngology, University of Miami Miller School of Medicine, Miami, FL, USA

Background

Mouse models are invaluable tools to understand the genetic basis of human diseases including Hearing loss (HL). Knock-in mice are preferred models to study the pathological consequence of a mutation as compared to knock-out animals where there is a complete gene depletion. Mutations in phosphoribosylpyrophosphate synthetase (PRPS1) gene have been demonstrated to cause X-linked nonsyndromic HL in humans. A c.G259A transition at in PRPS1 which causes p.Ala87Thr, has been demonstrated to cause HL. The aim of the present study was to generate the transgenic knock-in mice with Prps1 missense mutation p.Ala87Thr and to characterize their auditory phenotype.

Methods

Transgenic Prps1 knock-in (KI) mice with missense mutation p.Ala87Thr were generated through injection of recombinant embryonic stem cells. Auditory thresholds were evaluated by auditory brainstem recordings (ABRs) in response to pure tone stimuli at 8, 16 and 32 kHz over a period of 48 weeks.

Results

KI mice at 4-12 weeks of age presented comparable hearing thresholds to their littermate/age-matched mice at 8 and 16 kHz. However, a slight but significant increase in auditory thresholds was detected at 32 kHz (average of 10 – 15 dB SPL; P < 0.05). At 16-24 weeks of age, the gap between hearing thresholds of Prps1 KI mice and age-matched wild type animals became wider showing even more significant hearing defect at high frequencies. Interestingly, at 48 weeks of age, the de-

tected progressive hearing loss trend in Prps1 KI mice continued to become quite significant ($P < 0.05$) at all three tested frequencies. Experiments are in progress in our laboratory to determine the effect of this mutation on hair cell and neuron survival. Organ of Corti preparations from WT and KI mice will be subjected to immunostaining with apoptosis detection kits and caspase-3 to determine the extent of cell survival. Prps1 levels will be determined in urine and erythrocytes of WT and KI mice using ELISA kits and HPLC.

Conclusions

The results of our study suggest that Prps1 p.Ala87Thr KI mice exhibit mutation specific progressive HL similar to the findings reported in human patients, and therefore, it is an ideal model to study the pathogenicity of the mutation. We also observed that the KI mouse has more severe HL in high frequencies as compared to low and middle frequencies. Further studies employing genome editing tools to rescue the function of Prps1 will help in designing effective therapeutic strategies to prevent HL.

PS 567

Generation and Phenotypic Characterization of P2rx2 p.Val61Leu Mouse Knock-in Model for Human DFNA41 Deafness

M'hamed Grati¹; Qi Ma²; Rahul Mittal¹; Abhiraami Kannan-Sundhari³; Denise Yan¹; Xuezhong Liu¹

¹Department of Otolaryngology, University of Miami Miller School of Medicine, Miami, FL 33136, USA;

²Department of Otolaryngology, University of Miami Miller School of Medicine, Miami, FL, USA; ³University of Miami Miller School of Medicine

Introduction

The high prevalence/incidence of hearing loss (HL) in humans makes it the most common sensory defect. We previously identified p.Val60Leu mutation in P2RX2 purinergic receptor as the cause of human DFNA41 form of progressive HL, and also a likely cause for increased vulnerability to noise. Our in vitro data showed that p.Val60Leu mutation severely disrupts the ATP binding and therefore the ionic permeability of the receptor.

Goal

The generation of the human P2RX2 p.Val60Leu orthologous mutation in the mouse (p.Val61Leu in NP_700449.2) and the characterization of its effect on mouse cochlea hair cell (HC) function and survival.

Methods

We used homologous recombination in mouse stem cells (ES) and microinjection of targeted ES cells to generate p.Val61Leu P2rx2 knock-in model on C57BL/6 and

129/sv mixed background. We used auditory brainstem recordings (ABRs) in response to pure tones to evaluate hearing thresholds at several ages in both heterozygous P2rx2V61L/+ and homozygous P2rx2V61L/V61L mice. We evaluated mouse vestibular function by behavioral examination and swimming test. We performed whole-mount immunofluorescence (WMIF) and scanning electron microscopy (SEM) to examine cochlea and vestibular HCs.

Results

Heterozygous P2rx2V61L/+ and homozygous P2rx2V61L/V61L mice are overall healthy and viable. Homozygous mutant P2rx2V61L/V61L mice exhibited severe to profound HL at the earliest stage at which we start performing ABRs (3-4 weeks of age), as well as severe vestibular dysfunction, reflected by head-bobbing, circling and swimming incapability. WMIF and SEM of cochlea preparations revealed mild outer HC death and sickening, reflected by nuclear swelling, partial stereocilium hair bundle fusion/internalization and hair bundle disorganization, starting at around the onset of hearing. This phenotype became more severe at 4 weeks of age. Moreover, heterozygous P2rx2V61L/+ mice exhibited almost no HL up to 6 weeks of age, but acquired progressively a moderate to severe hearing loss by the age of 24 weeks. The effect of noise on the severity of the phenotype in these mice is also being evaluated.

Conclusions

P2rx2V61L/+ mice exhibit similar pattern of HL to that described in P2RX2 p.Val60Leu carrier patients in Chinese families, and so are ideal model for studying DFNA41 form of human deafness and for searching for therapy. P2rx2V61L/V61L mice exhibited severe vestibular dysfunction and a much more severe and earlier onset HL than that previously described in P2rx2-/- null mice, suggesting upregulation/compensation of other P2RX members in the null mice.

Research Funding – The National Institutes of Health - NIDCD.

PS 568

Maturation of Mechanoelectrical Transducer Channels in Mouse Cochlear Hair Cells

Adam Goldring¹; Robert Fettiplace²

¹University of Wisconsin- Madison; ²University of Wisconsin-Madison

Introduction

Hair cells convert vibrations into electrical signals through action of mechanoelectrical transducer (MET) channels located in their hair bundle. The molecular identity of these channels remains unclear. However,

the biophysical properties of the channel have been extensively characterized in mice near or after the maturation of transduction. The MET channel is a large cation channel with high permeability to Ca^{2+} , which is blocked by extracellular Ca^{2+} . Macroscopic currents in hair cells exhibit a stimulus dependent change in their current-displacement relationship, referred to as adaptation, which has been proposed to operate at or near the MET channel. We set out to determine if these properties are constant from the onset of transduction or vary with age, and thus whether the channel complex changes throughout maturation.

Methods

We recorded MET currents from CD1 mouse outer hair cells (OHC) between embryonic day 18 and postnatal day (P) 7 in response to fluid-jet stimulation of hair bundles. Single channel currents were recorded in whole cell mode by stimulating the hair bundle after exposure to sub-micromolar Ca^{2+} buffered with BAPTA.

Results

We found significant changes in macroscopic current amplitudes, the extent of adaptation, and MET channel unitary conductance, while channel Ca^{2+} -permeability was constant and Ca^{2+} -block was maintained. In OHCs, macroscopic MET current amplitudes grew several-fold at the apex of the cochlea from P1 to P6 and at the base two days earlier. This developmental phenomenon has been described previously (Waguespack et al. 2007, Lelli et al. 2009) and may be partly explained by changes to bundle architecture during this time. However, in addition, we found an increase in single-channel conductance over the same period. At P1 there was an absence of the known tonotopic gradient in unitary conductance with conductances in apical and basal outer hair cells being near 50 pS. Associated with the developmental growth in current amplitude, there was also a significant increase in fast adaptation from the onset of transduction to P5. Both the Ca^{2+} -permeability of the channel and its block by the ion were constant throughout development.

Conclusions

These results imply that there are changes in the molecular machinery underlying mechano-electrical transduction during development of cochlear hair cells. These changes occur, at least in part, at the level of the transducer channel as indicated by changes in single channel conductance with time. Moreover, changes in unitary conductance alone are insufficient to explain changes in other aspects of transduction.

PS 569

Interdental Cells generate spontaneous Calcium Transients during the Critical Period of Cochlear Development

Thore A. D. Schade-Mann; Jutta Engel; Tobias Eckrich
Dept. of Biophysics and Center for Integrative Physiology and Molecular Medicine (CIPMM), Saarland University

Introduction

The tectorial membrane (TM) is essential for a normal hearing function. It is attached to the spiral limbus and the stereocilia of the outer hair cells, stretching across the whole organ of Corti and spiraling along the longitudinal axis of the cochlea. It consists of collagens and glycoproteins (α - and β -tectorin and otogelin), the latter accounting for about 50 % of TM material and exclusive to the inner ear. Mutations of these proteins not only lead to aberrant TM formation but also to severe hearing loss or deafness. During the first postnatal week IDCs massively secrete TM proteins into the extracellular space. So far, little is known about the physiology of IDCs and about how they build up the TM.

Methods

Live cell imaging of inner ear explants using FM4-64 or CellMask Deep Red was performed to elucidate the anatomy of IDCs and the spiral limbus. We performed Ca^{2+} imaging experiments of acutely dissected inner ear explants at postnatal day 1 (P1) to P18 using a Ca^{2+} sensitive indicator and a confocal laser scanning microscope (Zeiss LSM 710).. Specimens were bathed with standard buffer that partially contained ATP or UTP at 1 – 10 μM .

Results: 5 - 20 % IDCs generated spontaneous Ca^{2+} transients at a low rate (≥ 1 event/10 min). Two principal types of spontaneous IDC Ca^{2+} transients were observed: a) single peaks with fast upstroke and decay and (b) longer, complex transients with double or multiple peaks. Both rate of activity and types of signals changed as a function of developmental age. Ca^{2+} transients were confined to single IDCs and did not propagate to neighbouring cells. Applying 1-10 μM ATP/UTP evoked Ca^{2+} responses in nearly all IDCs at all ages. Responses to ATP and UTP were similar before P12, but differed significantly after the onset of hearing.

Conclusion

Spontaneous Ca^{2+} signals in IDCs varied in shape and duration as a function of development and were confined to individual IDCs. Differential responses to ATP/UTP indicate a change in purinergic receptor expression during postnatal development. Mechanisms

behind the Ca²⁺ transients remain to be elucidated.

Supported by the DFG, SFB1027.

PS 570

Both the Surface-anchorage and the Release of GPI-anchored Proteins Are Required for the Formation of the Tectorial Membrane

Sungjin Park¹; Dong-Kyu Kim¹; Ali Almishaal²

¹*Department of Neurobiology and Anatomy, University of Utah*; ²*Department of Communication Sciences and Disorders, University of Utah*

The tectorial membrane (TM) is formed extracellularly and exhibits a defined shape and characteristic ultrastructure. However, the mechanism for how the exquisite structure is assembled outside the cells is not known. The TM is composed of both secreted proteins and glycosylphosphatidylinositol-anchored proteins (GPI-APs) including alpha-tectorin, beta-tectorin and otoancorin. While GPI-anchorage of the TM components is conserved in vertebrates, the role of the GPI-anchor in the formation of the TM structure is poorly understood. GPI-APs are localized in the outer leaflet of the plasmamembrane and are released from the producing cells by members of glycerophosphodiester phosphodiesterase (GDE) enzyme family. Since the Tectorins bind to multiple TM components, we hypothesize that (1) surface-localization of GPI-anchored Tectorin prevents the diffusion of other secreted molecules into the Scala media space and is required for the formation of the molecular network of the TM at the early developmental stage. (2) Release of the GPI-anchored TM components by a releasing enzyme plays a role in growing and detachment of the TM. To test the hypothesis, we utilized two mouse mutant lines. (1) To reveal the surface role of GPI-anchorage, we generated Tecta knock-in mice where alpha-tectorin is constitutively secreted without GPI-anchorage. We are currently characterizing the structure and function of the TM of Tecta-sec mice. (2) To prevent Tectorin release, we used Gde3 KO mice. GDE3 is the major GDE family member that is expressed in the developing cochlea and facilitates the release of alpha- and beta-tectorin when overexpressed in heterologous cells. In Gde3 knockout mice, the structure of the TM is abnormal and auditory brainstem response (ARO) and distortion product otoacoustic emissions (DPOAE) are reduced, indicating that release of GPI-anchored TM components by GDE3 is necessary for auditory function. Electron microscopy of the TM of the specific mutant mice will reveal the molecular mechanism by which the unique ultrastructure of the TM is formed and maintained outside the cells. Taken together, the pres-

ent study suggests important roles of GPI-anchor in the formation of the TM.

PS 571

Computer-aided Detection of Endolymphatic Hydrops in Vivo Using Optical Coherence Tomography Imaging

George Liu¹; Jinkyung Kim¹; Brian E. Applegate²; John S. Oghalai³

¹*Stanford University*; ²*Department of Biomedical Engineering, Texas A&M University*; ³*Department of Otolaryngology - Head & Neck Surgery, Stanford University*

The lack of a method to conclusively make the diagnosis of Meniere's disease remains a significant challenge in the treatment of dizziness. A presumed diagnosis of Meniere's disease is currently based on clinical symptoms that suggest the presence of endolymphatic hydrops, the abnormal accumulation of fluid in the scala media. Using non-invasive cochlear imaging with optical coherence tomography (OCT), we have found that endolymphatic hydrops occurs in mice after noise exposure. To improve the interpretation of cochlear OCT images for detecting endolymphatic hydrops, we developed image analysis software to identify cross-sectional image features that predict endolymph volume and hydrops severity. We found that bulging of Reissner's membrane correlated with endolymph volume, and exhibited well-separated distributions of values for different levels of hydrops severity. We then implemented computer-aided detection software to automatically classify endolymphatic hydrops in cross-sectional OCT images using this metric. Using a decision threshold of 7.4 μm displacement of Reissner's membrane in the transverse direction away from the scala media, which maximized the F1 score in a training set of more than 3000 OCT images, our computer-aided detection software achieved classification sensitivity and specificity of 83% (AUC=0.87) on a test set of more than 900 previously unseen OCT images of cochlea. Averaging displacement measurements across five images from the same cochlea increased the sensitivity to 88% and specificity to 91% (AUC=0.96). These results suggest that measuring Reissner's membrane displacement in cochlear OCT images could serve as an objective, automatable, and accurate test for detecting endolymphatic hydrops to aid the diagnosis of Meniere's disease.

Supported by NIH-NIDCD DC014450, DC013774, and DC010363.

PS 572

Centerline-based Automatic Measurement of Inner Ear in Different Laboratory Animals

Qingqing Jiang¹; Shi-ming Yang²; Wei Sun³

¹*Institute of Otolaryngology Of PLA, Chinese PLA General Hospital;* ²*Chinese PLA General Hospital;* ³*University at Buffalo, The State University of New York*

Objective

The aim of this research is to develop an accurate and automatic measuring method based on the aid of centerline to construct three dimensional models of inner ear in different mammals and to assess the morphological variations.

Methods

Three adult healthy mice, three adult guinea pigs, three adult mini pigs and one left temporal bone of human were included in this research. All eighteen animal specimens and the human sample were scanned with the use of Micro-CT. After being segmented, three-dimensional models of the inner ear in different mammals were reconstructed using Materialise Mimics – a medical 3D reconstruction software. A novel method with the use of centerline was established to estimate the properties of 3D models and to calculate the length, volume and angle parameters automatically.

Results

Morphological models of inner ears in different mammals have been built which can be used to describe the detailed shapes of cochlea and vestibular organs (the semicircular canals and the common crus). The mean values of the lengths and the volumes of cochlea and three semicircular canals increased with the body size of the examined species. Mini pigs showed a very similar size of cochlea and vestibular organs with human both on total length and volume. The angles between the semicircular canal were different between species. The angle of the semicircular canals of mice and mini pigs were closely resembled the structure of human.

Conclusion

The automatic measurement of the inner ear based on centerline builds an effective way to assess length, volume and angle of three-dimensional structures. This study provides a theoretical basis for mechanical analysis of inner ear in different mammals. Our results found the similarity of the inner ear structure between mini pigs and humans.

PS 573

Nano-based Contrast Agents for Inner Ear Imaging

Mohammad N. kayyali¹; Alexander C. Wright²; Lee Brake¹; Daqing Li³

¹*Department of Otorhinolaryngology- Head & Neck Surgery, University of Pennsylvania School of Medicine, Philadelphia, Pennsylvania;* ²*Department of Radiology, University of Pennsylvania, Philadelphia, Pennsylvania;* ³*Department of Otorhinolaryngology- Head & Neck Surgery, Perelman School of Medicine at the University of Pennsylvania, Philadelphia, PA*

With current technology, it is difficult to distinguish various pathologies at the cellular molecular level of the sensorineural hearing loss. This is largely due to the challenging anatomy structure of the inner ear and contrast agents for diagnostic imaging. Conventional CT scanning is limited by its inability to visualize the morphology of detailed soft tissue structures in the cochlea, such as the Organ of Corti, whereas MRI imaging provides poor information of the bony landmark structures of the inner ear. Neither imaging modality is currently able to detect the cellular and molecular pathology for the different diagnosis of the sensorineural hearing loss. This may negatively impact the personalized treatment of such inner ear diseases which requires precise determination of inner ear pathology at a cellular molecular level.

The current study aims to develop a CT-based molecular imaging strategy, utilizing targeted nanoparticles as a contrast agent, for potential clinical application in the diagnosis of inner ear disorders with varying molecular genetic etiologies. Initially, spherical gold nanoparticles were tested. Using our novel hydrogel delivery method, these gold nanoparticles were shown to successfully pass through the round window membrane and were able to enter the inner ear as shown by confocal microscopy, with no severe toxicity identified by histological analysis. However, CT scan contrast and image resolution were not significantly improved.

To further address this, liposomal iodine nanoparticles have been studied and developed as targeted contrast agents for the CT-based molecular imaging. Using the same hydrogel delivery system shown to be successful with the gold particles, liposomal iodine was able to diffuse through the round window membrane and reach the inner ear cellular structures, and were able to be detected using a standard microCT machine. This novel approach enables the visualization of the inner ear structures that current CT technology cannot achieve. Furthermore, no significant toxicity was seen after histological analysis, as well as through an in vitro MTT assay. The results indicate that by targeting these lipo-

somal iodine particles to inner ear biomarkers, we will be able to detect molecular genetic defects of specific inner ear structures. The clinical application of this approach will significantly improve our diagnosis and potential treatment for the inner ear diseases.

PS 574

Usefulness of Intravital Multi-photon Microscopy in Visualizing Study of Mouse Cochlear Imaging and Non-invasive Analysis of Volume Changes in the Scala Media

Young Joon Seo; Yoon Ah Park; Hyun Mi Ju; Sun Hee Lee

Yonsei Wonju University College of Medicine

Currently, no vestibular or auditory diagnostic test is available for endolymphatic hydrops or dilation of the scala media. Clinical diagnosis is based on the physician's observations and the patient's history, symptoms, and symptom pattern. By using near-infrared lasers for multi-photon excitation, intravital multi-photon microscopy (MPM) can detect endogenous fluorescence and second harmonic generation of tissues. In this study, we used intravital MPM to visualise various cochlear microstructures without any staining and non-invasively analyse the volume changes of the scala media without removing the overlying cochlear bone. The intravital MPM images revealed various tissue types, ranging from Reissner's membrane to dense bone, as well as the spiral ganglion beneath the cochlear bone. The two-dimensional cross-sectional and serial z-stack intravital MPM images also revealed the spatial dilation of the scala media in the temporal bone of pendrin-deficient mice. These findings suggest that intravital MPM might serve as a new method for obtaining microanatomical information regarding the cochlea, similar to standard histopathological analyses. Given the capability of intravital MPM for detecting an increase in the volume of the scala media in pendrin-deficient mice, it might be a promising new tool for assessing the pathophysiology of hearing loss.

PS 575

Inner Ear Fluid Movement Visualized with Light Sheet Fluorescence Microscopy

Daniel J. Brown¹; Christopher J. Pastras¹; Lieke Van Roon²; Ian Curthoys³

¹*The University of Sydney*; ²*Utrecht University*; ³*Univ of Sydney*

Background

A clear understanding of where endolymph is absorbed is vital to our understanding of Meniere's disease. Tech-

niques for investigating endolymph dynamics include micropipette recordings of fluid tracers in vivo, or imaging tracer diffusion in histological sections or MRI scans.

Objective

To visualize endolymph movement throughout the inner ear of guinea pigs using Light Sheet Fluorescence Microscopy (LSFM), in both normal and pathological ears.

Method

Via a glass micropipette, fluorescein isothiocyanate (FITC)-dextran dissolved in artificial endolymph was injected into scala media in anaesthetized guinea pigs. Functional measures were continuously performed throughout the injection. Alternatively, Tetramethylrhodamine (TRITC)-dextran was infused through the vasculature, with membrane permeability modulators used to investigate changes in the blood-labyrinth barrier. In select animals, lipopolysaccharide was injected into scala media via a glass micropipette, with subsequent recovery of the animal for a period of weeks. Temporal bones were harvested and processed for imaging on our custom-built LSFM.

Results

A substantial amount of the FITC-dextran appears to be transported into the endolymphatic sac, utricle and semicircular canals once endolymph volume had more than doubled, a volume associated with a sudden reduction in endolymphatic pressure. No FITC-dextran is observed in the perilymphatic compartments, suggesting that the membranous labyrinth remains intact. Blood-infusions of fluorescent markers demonstrate changes in the vasculature permeability in animal models of pathology. LPS injection into scala media results in the excessive production of protein within the endolymphatic duct, and moderate endolymphatic hydrops in the cochlea.

Conclusion

Whilst this technique can only provide a post-mortem 'snap-shot' of fluid dynamics, it provides high-resolution 3D images of biomarker distribution and morphological changes. The presence of FITC-dextran in the utricle following sudden hydrops pressure relief supports theories that the utriculo-sacculus duct opens suddenly in the presence of severe endolymphatic hydrops. The remarkable uptake of FITC-dextran into the periductal channels of the endolymphatic duct suggests that the duct is the primary region endolymph is absorbed. The blockage of this duct with immune activity supports suggestions that endolymphatic hydrops results from a blockage of the endolymphatic duct, where absorption of endolymph normally occurs.

PS 576

Fluid Pressure at the Sensory Tissue of a Tonotopical Insect Ear

Manuela Nowotny¹; **Elizabeth Olson**²; Sushrut Kale²; Michael Carapezza²

¹*Institute of Cell Biology and Neuroscience, Goethe University Frankfurt am Main, Germany;* ²*Columbia University*

Like the hearing organs of mammals, the hearing organ of katydids (bushcrickets), called the crista acustica, features a smooth anatomical gradient along its length. Upon sound stimulation the crista responds with mechanical traveling waves and tonotopic frequency tuning. The interaction between sound-induced fluid pressure and organ motion is unknown. In this study we measured the sound-induced crista motion and fluid pressure above the crista. The fluid pressure decreased with increasing distance above the surface of the crista, and using two different measurement positions, we calculated the fluid velocity perpendicular to the crista. This allows for simultaneous pressure and velocity measurements. These measurements were made at several positions along the tonotopic longitudinal axis of the hearing organ. We also measured the crista motion with a laser-Doppler vibrometer before and after pressure.

Both sound-induced fluid pressure and motion responses were tonotopically organized along the longitudinal axis of the crista. We only measured the fluid pressure close to the upper side of the crista because the tracheal pressure below the organ was inaccessible. Thus, the data were inadequate to quantify the mechanical impedance of the crista. However, based on the anatomy, the distal region that is tuned to high frequencies is expected to be relatively stiff and the proximal region that is tuned to low frequencies relatively compliant. The fluid pressure can be used to quantify the effective mechanical impedance of the overlying fluid, which is another useful quantity for understanding the crista's mechanical response to sound. The data indicate mass-dominated impedance for the fluid, but without the frequency dependent increase of a simple mass, presumably due to the frequency-dependent wavelength of the crista's wave response.

PS 577

Cochlear Spiral

Andrej Kral¹; Markus Pietsch²; Lukas Aguirre Davila³; Peter Erfurt⁴; Ersin Avci³; Thomas Lenarz⁵

¹*Hannover Medical School, DFG Cluster of Excellence Hearing4all;* ²*physician;* ³*Medical University Hannover;*

⁴*Hannover Medical School;* ⁵*Department of Otolaryngology, Hannover Medical School and DFG Cluster of Excellence Hearing4all*

The present study analyzed the cochlear form in 108 human temporal bones post mortem. For this purpose, frozen human temporal bones were used. After filling the cochlea with epoxy and exposing these to vacuum for 5 min., the bones were stored for 8 hrs. under room temperature to harden the epoxy. Subsequently, the bone was removed by storing the specimen in alkali solution for 3 weeks. The resulting corrosion casts were mechanically cleaned and photographed in 3 orthogonal directions using a custom-made micromechanical holder with laser-controlled positioning and a Keyence VHX 600 digital microscope. The resulting resolution was 12 μm per pixel. The images were analyzed using VHX-600 software and ImageJ. More than 60 different parameters were manually measured in each cochlea. The data were compared to data obtained with 30 temporal bones that were imaged in μCT with similar resolution. The data obtained from the corrosion casts were used to fit a mathematical 3D spiral model.

The μCT s and corrosion casts corresponded very well and demonstrated that the corrosion cast data were reliable. As in previous study, also the present study demonstrated a high variance in many parameters including absolute metric and angular length, as well as in wrapping factor. Notably, the B ratio, a parameter characterizing where the modiolar axis cuts the base width axis of the cochlea, appeared to be partly related to the course of the basalmost vertical profile: if the ratio was small, the vertical profiles had more pronounced roller-coaster course (vertical minimum in the first 180°), if it was large and close to 0.5, this vertical minimum was small or absent. Furthermore, factor analysis revealed a relation between cochlear base width and length with absolute metric length, but not with height of the cochlea. Finally, the analytical model allowed us to fit the cochlear 3D shape with residuals < 1 mm using the cochlear length and width and their intersection with the modiolar axis. The model was validated using the leave-one-out cross-validation technique and demonstrated excellent fit already using few parameters of a real cochlea. This demonstrates that the analytical model can be used to predict the length (angular and metric) and the shape of the human cochlea from data obtained in imaging with high precision.

Supported by Deutsche Forschungsgemeinschaft (Cluster of Excellence Hearing4all).

PS 578

Mitochondrial Calcium Uniporter Knockout Protects from Noise-Induced Cochlear Synaptopathy

Yuanping Zhu; Su-Hua Sha; Zhiqi Liu
Medical University of South Carolina

Background

Mitochondrial calcium overload has been speculated to play an important role in noise-induced hearing loss (NIHL). Calcium overload in mitochondria resulting in cell death is one of the central mechanisms of NIHL. Mitochondrial calcium uniporter is the main specific calcium channel on the inner mitochondrial membrane allowing calcium uptake into mitochondria from the cytosol. Recently, we have proved that traumatic noise exposure increases the expression of MCU in cochlear cells and blockage of MCU via the specific pharmacological inhibitor Ru360 or MCU siRNA attenuates NIHL. Here, we further investigated the role of MCU in NIHL using MCU knockout mice.

Methods:

Both MCU knockout mice and wild-type littermates were bred from a hybrid CD1 background of MCU heterozygous mice. Since CD1 mice have a known predisposition for high-frequency hearing loss, mice were exposed to an octave band noise with a central frequency of 4 kHz at 116 dB SPL for 2 hours at 4.5 weeks of age, when hearing is expected to be intact at 8 kHz. Hearing thresholds of 4–7 week-old mice and noise-induced auditory threshold shifts were measured by auditory brainstem response (ABR). Morphology of hair cell stereocilia was evaluated by scanning electronic microscopy (SEM). Outer hair cell loss was assessed by immunolabeling with myosin VII and staining with DAB. Inner hair cell synapses were counted and ABR wave I amplitudes were measured 14 days after noise exposure.

Results

Hereditary hearing loss was noted in both MCU knockout mice and wild-type littermates at 32 kHz with wide variation at 16 kHz, but the thresholds remained normal at 8 kHz. Surface preparations showed that outer hair cell (OHC) loss appeared in a base-to-apex gradient with complete loss in the base, while the apex remained intact. There was no inner hair cell (IHC) loss throughout the cochlear spiral. Noise exposure induced permanent threshold shifts in both wild-type and MCU knockout mice at 8 kHz compared to their non-noise-exposed littermates. Although noise-induced threshold shifts were not significantly different between MCU knockout and wild-type littermates, extensive loss of OHC stereocilia was observed in wild-type mice. Furthermore, noise-di-

minished ABR wave I amplitude and loss of IHC synapses were well averted in MCU knockout mice.

Conclusions

These results indicate that knockout of the MCU gene blocks calcium uptake into mitochondria and effectively prevents noise-induced cochlear synaptopathy, which may provide a novel route to protection from NIHL.

PS 579

Evidence for Noise-Induced Hidden Hearing Loss in Veterans

Naomi Bramhall; Dawn Konrad-Martin; Garnett McMillan; Susan Griest
VA RR&D National Center for Rehabilitative Auditory Research

Background

Animal studies have demonstrated that cochlear synaptopathy, a partial loss of inner hair cell-auditory nerve synapses, can occur in response to noise exposure without any permanent auditory threshold shift. In animal models, synaptopathy is associated with a reduction in the amplitude of wave I of the auditory brainstem response (ABR). This study examines whether higher levels of self-reported lifetime noise exposure in young people with clinically normal pure tone thresholds are associated with lower ABR wave I amplitudes.

Methods

Sixty-four young military Veterans and non-Veterans (19–35 years of age) with pure tone thresholds of 20 dB HL or better were assigned to 1 of 4 groups based on their self-reported lifetime noise exposure history and Veteran status (Veterans with high noise exposure, Veterans with low noise exposure, non-Veterans with low noise exposure, and non-Veterans with a history of firearm use). Suprathreshold ABR measurements in response to alternating polarity tone bursts were obtained at 1, 3, 4 and 6 kHz with gold foil tiptrode electrodes placed in the ear canal. Wave I amplitude was calculated from the difference in voltage at the positive peak and the voltage at the following negative trough. Distortion product otoacoustic emission (DPOAE) input/output (I/O) functions were collected in each subject at the same 4 frequencies to assess outer hair cell (OHC) function.

Results

After controlling for individual differences in sex and DPOAE amplitude, the groups containing subjects with higher reported histories of noise exposure had smaller ABR wave I amplitudes at suprathreshold levels across all 4 frequencies as compared to the groups with less history of noise exposure.

Conclusions

Suprathreshold ABR wave I amplitudes were smaller in Veterans reporting high levels of military noise exposure and in non-Veterans reporting any history of firearm use as compared to Veterans and non-Veterans with lower levels of reported noise exposure history. The lower ABR wave I amplitudes in the groups with higher levels of noise exposure cannot be accounted for by sex or variability in OHC function. The observed group differences are similar to the decreased ABR wave I amplitudes observed in animal models of noise-induced cochlear synaptopathy. These data suggest that cochlear synaptopathy or “hidden hearing loss” may occur in response to noise exposure in humans, although post-mortem examination of the temporal bone would be necessary for confirmation.

PS 580

A Descriptive Analysis and Critique of Pharmaceutical Interventions for Hearing Loss Study Methods and Reporting in the Literature

Tanisha Hammill¹; Carlos Esquivel¹; Martin D. Slade²
¹DOD Hearing Center of Excellence; ²Yale University School of Medicine

While pharmaceutical interventions for hearing loss (PIHL) research has been ongoing for over 30 years, there are no standards for methods employed in PIHL research studies. The literature shows that PIHL research is largely conducted with heterogenic methodologies, precluding the conduct of meta-analysis of PIHL drugs outcomes.

Aims

This study conducts of a novel type of descriptive systematic review of peer-reviewed PIHL studies to understand the various elements of study methodologies being employed across this field. Analyses to identify any correlations among study methodology variables and injury outcomes are conducted. This assessment will not focus on the safety or efficacy outcomes of the compounds being studied but instead will focus on the research designs in PIHL investigations, including identification of trends among the data, to craft criterion standards and best practices for future study design selection. These outcomes will be translated into policy recommendations for the consideration of the Food and Drug Administration, Federal funding agencies and primary peer-reviewed journal editorial boards as part of an overall knowledge dissemination, implementation and adoption strategy.

Methodology

Using PIHL literature attained through systematic review search strategies and methods consistent with current

standards, this effort will identify, characterize, evaluate and correlate the methodological variables across the full translational scope of PIHL studies, from animal to human. The review will document, describe and critically assess study methods, including analyses of correlations between study method elements – e.g., design, inclusion/exclusion criteria, species model, level of injury induced and intervention characteristics – as well as reporting quality of reporting. Publications which report findings from original reports of pre-clinical animal or human controlled trials of interventions to prevent or treat hearing loss or tinnitus caused by noise or blast exposure will be included. Subgroup analyses among like studies (e.g., within human studies for noise exposed population) will be conducted to identify, evaluate and summarize any trends of correlation between methodologies utilized in study designs.

Discussion

Critical review and understanding of the state of current study methodology outcomes and trends will provide the evidence-base to set norms and standards to best protect study subjects and provide useful recommendations for drug approval authorities, funding agencies, future investigators and the scientific community at large.

PS 581

Roles of Glucose-6-Phosphate Dehydrogenase in the Maintenance of NADPH Redox Status, Glutathione and Thioredoxin Antioxidant Defenses, and Cellular Survival in Mouse Cochlea

Karessa White¹; Mi-Jung Kim²; Chul Han²; Hyo-Jin Park²; Dalian Ding³; Zaimary Meneses⁴; Jonathan Hirst⁵; Paul Linser⁶; Richard Salvi⁷; Shinichi Someya²
¹University of Florida, Department of Aging and Geriatric Research; Department of Speech, Language, and Hearing Science; ²University of Florida, Department of Aging and Geriatric Research; ³State University of New York at Buffalo; ⁴University of Florida, Department of aging and Geriatric Research; ⁵University of Florida, Department of Speech, Language, and Hearing Science; ⁶University of Florida, Whitney Lab; ⁷Center for Hearing & Deafness, Department of Communicative Disorders and Science, State University of New York at Buffalo

Background

NADPH is a major cellular reductant and is central to cellular redox homeostasis, survival, and antioxidant defenses because NADPH is required for regeneration of reduced glutathione (GSH) from oxidized glutathione (GSSG), and reduced thioredoxin (redTXN)

from oxidized thioredoxin (oxiTXN), and for the activity of catalase that decomposes hydrogen peroxide. Glucose-6-phosphate dehydrogenase (G6PD) is the first rate-limiting enzyme of the pentose phosphate pathway and is thought to be the principal source of NADPH for cellular antioxidant defenses and survival. The overall goal of this project is to investigate the roles of G6pd in maintaining redox homeostatic, glutathione and thioredoxin antioxidant defenses, and cellular survival in the cochlea of CBA/CaJ mice.

Methods

To investigate the roles G6pd in auditory function, we performed auditory brainstem response (ABR) tests to measure ABR thresholds, wave I amplitudes, and wave I latencies in young G6pd wild-type and G6pd deficient mice that have been backcrossed onto the CBA/CaJ mouse strain for 4 generations. To confirm these physiological test results, we performed histological analyses, including cochleograms, spiral ganglion neuron counting, and stria vascularis thickness measurements in the cochlea from G6pd wild-type and G6pd deficient mice. To investigate the roles of G6pd in maintaining cellular redox homeostasis, glutathione and thioredoxin antioxidant defenses, and cellular survival in the cochlea, we measured the ratios of GSH/GSSG and NADPH/total NADP, antioxidant defense parameters (glutathione reductase, thioredoxin reductase, catalase and superoxide dismutase) and oxidative damage parameters (protein carbonyl and 8-oxoguanine) in the cochleae.

Results

Our results showed no significant changes in ABR thresholds at 4, 8, 16, 32, 48 or 64 kHz between wild-type and G6pd deficient male or female mice at 3-5 months. There were no differences in the mean numbers of cochlear inner hair cells, outer hair cells or spiral ganglion neurons between wild-type and G6pd deficient mice. Our results also show no differences in the ratios of GSH/GSSG and NADPH/total NADP ratio, levels of antioxidant defense markers or levels of oxidative damage markers between wild-type and G6pd deficient mice.

Conclusions

Taken together, these results show that G6pd is not essential for the maintenance of redox homeostasis, glutathione and thioredoxin antioxidant defenses or cellular survival in the cochlea of CBA/CaJ mice.

Funding: Supported by R01 DC012552 (S.S.) and McKnight Doctoral Fellowship Program (K.W.).

PS 582

Role of the Guanylate Cyclase in Auditory Function

Katrin Reimann¹; Dorit Möhrle¹; Nicole Eichert¹; Steffen Wolter¹; Markus Wolters²; Evanthia Mergia³; Doris Koesling³; Andreas Friebe⁴; Robert Feil²; Marlies Knipper¹; Lukas Rüttiger¹

¹University of Tübingen, Department of Otolaryngology, Tübingen Hearing Research Centre (THRC), Molecular Physiology of Hearing; ²Interfakultäres Institut für Biochemie, University of Tübingen; ³University of Bochum, Department of Pharmacology and Toxicology; ⁴University of Würzburg, Department of Physiology

In the inner ear, the cGMP signaling pathway has been described to facilitate protective processes in response to traumatic events. The aim of this study was to investigate the role of two cGMP coupled receptors, the soluble guanylate cyclase (NO-GC) or particulate guanylate cyclase-A (GC-A) and their ligands (nitric oxide (NO) or atrial and brain natriuretic peptide (ANP, BNP) in these otoprotective processes and auditory function. Mice with the deletion of either one of the α -subunits of NO-GC (NO-GC1 KO or NO-GC2 KO) as well as GC-A KO mice were tested for hearing function and recovery from acoustic trauma. We performed immunohistochemistry and PCR for NO-GC, GC-A, ANP and BNP expression. FRET measurements were used for visualization of intracellular cGMP. Auditory brainstem responses (ABRs) and distortion product of the otoacoustic emissions (DPOAEs) were recorded before and after acoustic trauma. Our results show that the NO-GC- β 1 protein is expressed in IHCs, pericytes and endothelial cells and that NO-GC mRNA is expressed in IHCs, but not in OHCs. Accordingly, FRET measurements showed an increase in intracellular cGMP during NO incubation in IHCs but not in OHCs. GC-A mRNA is expressed in OHCs, while ANP and BNP are expressed in OHCs and IHCs. Before acoustic trauma, there was no difference in hearing thresholds and OHC function and phenotype between WT, NO-GC1 KO and NO-GC2 KO mice. After acoustic trauma, the OHC phenotype showed similar KCNQ4 downregulation and loss of OHC function in all three genotypes. However, NO-GC1 and NO-GC2 KO mice maintained better ABR thresholds in correlation with better preserved auditory nerve function by preserving more IHC ribbons. This indicates that absence of either isoform has a protective effect on the inner hair cells and their synapses. In contrast, GC-A KO mice showed distinct vulnerability of OHCs after acoustic trauma, suggesting a protective effect of the ANP and BNP/GC-A/cGMP pathway.

This work was supported by grants from the Deutsche Forschungsgemeinschaft (FOR 2060 project FE 438/5-

1) and by Fortüne 2339-0-0 (University of Tuebingen, Tuebingen, Germany).

PS 583

Distinct Cellular Targets Account for Epigallocatechin 3-gallate (EGCG)-induced Protection Against Cisplatin Ototoxicity and Anti-tumor Efficacy

Vikrant Borse¹; Tejbeer Kaur²; Kelly Sheehan³; Debashree Mukherjee¹; Srinivasan Tupai³; Raheem Al-aameri¹; Sandeep Sheth³; Sumana Ghosh³; Asmita Dhukhwa¹; Michelle Lowy¹; Leonard P. Rybak⁴; Vickram Ramkumar¹

¹*Southern Illinois University School of Medicine;*

²*Washington University School of Medicine Saint Louis Missouri;* ³*Southern Illinois University, School of Medicine;* ⁴*SIU School of Medicine*

Background

Cisplatin-induced ototoxicity is one of the major limiting factor for cisplatin chemotherapy. Multiple studies have reported that cisplatin has profound damaging effect on the outer hair cells (OHCs) present in the basal turns of the cochlea, with negligible effect on inner hair cells (IHCs). In addition, cisplatin also damages spiral ganglion neurons (SGN), stria vascularis (SV) and fibrocytes of spiral ligament (SL). Recently, we have shown that robust activation of reactive oxygen species (ROS) and STAT1 by cisplatin contributes to cochlear inflammation and apoptosis in hair cells, leading to permanent hearing loss. Oral administration of EGCG protected against cisplatin ototoxicity. In this study, we identified multiple cellular targets underlying EGCG otoprotective role and its efficacy as an antitumor drug.

Methods

Adult male Wistar rats (200-250g) were treated with oral EGCG (100mg/kg), followed by cisplatin (11mg/kg, i.p.). Auditory brainstem responses (ABRs), scanning electron microscopy (SEM) and cochlear whole mount were performed to assess hearing loss, OHC morphology and ribbon synapse loss. Immunohistochemical studies evaluated the activation of pEK1/2, pSTAT1/5, apoptosis and loss of type II and V fibrocytes in cochlea. Squamous cell carcinoma (UMSCC) 10B cells were used to examine potential antitumor interference by EGCG in a xenograft mouse model. Organ of Corti-derived cells (UB/OC-1) and UMSCC 10B cells were treated with cisplatin in the presence and absence of EGCG to determine effects on ROS, pEK1/2, pSTAT1/5 activity and cell apoptosis. Cell ROX and Annexin V assays were used to assess cisplatin activation of ROS and apoptotic processes, respectively. Western blots were performed to determine pEK1/2, pSTAT1 activation and apoptotic proteins.

Results

In vivo studies in male Wistar rats showed that oral EGCG significantly protected animals from cisplatin-induced ABR threshold shifts at all frequencies tested. This was associated with reduced OHC damage, loss of IHC ribbon synapses and loss of type II and V fibrocytes in the basal turn of the cochlea. In SCID mice, oral EGCG did not interfere with cisplatin mediated anti-tumor action but possessed intrinsic anti-tumor properties. In vitro studies in UB/OC-1 and UMSCC10B cells showed that EGCG significantly inhibited cisplatin-induced ROS, pEK1/2, and pSTAT1/5 phosphorylation and the expression of apoptotic proteins. Interestingly, EGCG inhibited cisplatin-mediated apoptosis in UB/OC-1 while potentiating apoptosis of UMSCC 10B cells in vitro by inhibiting similar targets in both cell types.

Conclusions

This study shows that oral EGCG reduces cisplatin ototoxicity without compromising its chemotherapeutic efficiency by interacting with similar cellular targets.

PS 584

Behavioral Assays for Evaluating Hair Cell Function of Zebrafish Larvae

Chen Fangyi¹; Sun Peng¹; Wang Changquan¹; Zhang Yingla²; Liu Dong³

¹*Department of Biomedical Engineering, South University of Science and Technology of China;* ²*School of Life Sciences, Peking University;* ³*School of Life Sciences, Peking University*

Due to its ototoxic drug sensitivity and genomic similarity to human being, zebrafish has become an effective and economical model for drug/gene screening in auditory system. However, lack of approaches to quantify its auditory function has limited its application. Here we implemented two behavioral measurement systems for quantifying the drug-induced hair cell functional change of the zebrafish larvae.

Vestibular ocular reflex (VOR) is a compensatory eye movement to stabilize retinal images. VOR is evoked by the vestibular receptors, so it can be used to evaluate vestibular and thus auditory function, since both systems share the same sensory cell, hair cell. An instrument system, including a rotational platform, a digital microscopic system and image processing software, was built to measure the gravity-induced linear VOR of zebrafish larvae.

Acoustic startle response is an innate, reliable and robust behavior of zebrafish. An instrument system was implemented with a vibrator for delivering acoustic

stimulus and a digital video system to record the larval movement. In each test, 10 fish larvae were placed in a petri dish, which is stimulated by the vibrator underneath. Two features were extracted from the video to quantify the startle responses: the average moving distance and the number of fish that demonstrated typical C-shape bending after each stimulus.

With the two systems, we first measured the fish behavior under different concentration of the ototoxic drug. 6 pdf zebrafish larvae were treated with ototoxic drugs, neomycin and cisplatin, of different concentrations. Testing results from both systems showed that the magnitude of behavioral responses decreases with rising drug concentration and demonstrated the capability and possibility of both systems for ototoxicity drug screening. We also tested the impact of several gene manipulation to the hair cell functions using the VOR system. The results demonstrated significant difference between the wild type zebrafish larvae and the mutant, which was difficult with traditional methods such as hair cell staining and counting.

PS 585

Reduced TRMU Expression Increases the Sensitivity of Hair-cell-like HEI-OC-1 Cells to Neomycin Damage in Vitro

Renjie Chai¹; Zuhong He²; Shan Sun³; Fuping Qian¹; Cheng Cheng⁴; Shasha Zhang¹; Mingliang Tang¹; Yongming Wang⁵; Xiaoli Zhang⁶; Mingshu Zhang⁷; Huawei Li⁸

¹MOE Key Laboratory of Developmental Genes and Human Disease, State Key Laboratory of Bioelectronics, Institute of Life Sciences, Southeast University, Nanjing 210096, China.; ²MOE Key Laboratory of Developmental Genes and Human Disease, Institute of Life Sciences, Southeast University, Nanjing 210096, China.; ³Department of Otorhinolaryngology, Hearing Research Institute, Affiliated Eye and ENT Hospital of Fudan University, Shanghai; ⁴St. Jude Children's Research Hospital; ⁵Department of Otorhinolaryngology, Hearing Research Institute, Affiliated Eye and ENT Hospital of Fudan University, Shanghai 200031, China; ⁶Department of Otolaryngology, the Affiliated Drum Tower Hospital of Nanjing University Medical School; ⁷Medical School, Southeast University; ⁸The EENT Hospital of Fudan University

Aminoglycosides are ototoxic to the cochlear hair cells, and mitochondrial dysfunction is one of the major mechanisms behind ototoxic drug-induced hair cell death. TRMU (tRNA 5-methylaminomethyl- 2-thiou-

ridylate methyltransferase) is a mitochondrial protein that participates in mitochondrial tRNA modifications, but the role of TRMU in aminoglycoside-induced ototoxicity remains to be elucidated. In this study, we took advantage of the HEI-OC-1 cell line to investigate the role of TRMU in aminoglycoside-induced cell death. We found that TRMU is expressed in both hair cells and HEI-OC-1 cells, and its expression is significantly decreased after 24 h neomycin treatment. We then down-regulated TRMU expression with siRNA and found that cell death and apoptosis were significantly increased after neomycin injury. Furthermore, when we down-regulated TRMU expression, we observed significantly increased mitochondrial dysfunction and increased levels of reactive oxygen species (ROS) after neomycin injury, suggesting that TRMU regulates mitochondrial function and ROS levels. Lastly, the antioxidant N-acetylcysteine rescued the mitochondrial dysfunction and cell apoptosis that was induced by TRMU downregulation, suggesting that ROS accumulation contributed to the increased aminoglycosides sensitivity of HEI-OC-1 cells after TRMU downregulation. This study provides evidence that TRMU might be a new therapeutic target for the prevention of aminoglycoside-induced hair cell death.

PS 586

Inhibition of Arc Decreases the Survival of HEI-OC-1 Cells After Neomycin Damage in Vitro

Renjie Chai¹; Ming Guan²; Qiaojun Fang¹; Zuhong He³; Yong Li²; Fuping Qian¹; Xiaoyun Qian⁴; Ling Lu⁴; Xiaoli Zhang⁵; Dingding Liu⁴; Jieyu Qi¹; Shasha Zhang¹; Mingliang Tang¹; Xia Gao⁴

¹MOE Key Laboratory of Developmental Genes and Human Disease, State Key Laboratory of Bioelectronics, Institute of Life Sciences, Southeast University, Nanjing 210096, China.; ²Department of Otolaryngology, Hangzhou First People's Hospital, Hangzhou 310006, China.; ³MOE Key Laboratory of Developmental Genes and Human Disease, Institute of Life Sciences, Southeast University, Nanjing 210096, China.; ⁴Department of Otolaryngology, Nanjing Drum Tower Hospital, The Affiliated Hospital of Nanjing University Medical School, Nanjing 210008, China.; ⁵Department of Otolaryngology, the Affiliated Drum Tower Hospital of Nanjing University Medical School

Hearing loss is a common sensory disorder mainly caused by the loss of hair cells (HCs). Noise, aging, and ototoxic drugs can all induce apoptosis in HCs. Apoptosis repressor with caspase recruitment domain (ARC) is a key factor in apoptosis that inhibits both intrinsic and extrinsic apoptosis pathways; however, there have

been no reports on the role of ARC in HC loss in the inner ear. In this study, we used House Ear Institute Organ of Corti 1 (HEI-OC-1) cells, which is a cochlear hair-cell-like cell line, to investigate the role of ARC in aminoglycoside-induced HC loss. ARC was expressed in the cochlear HCs as well as in the HEI-OC-1 cells, but not in the supporting cells, and the expression level of ARC in HCs was decreased after neomycin injury in both cochlear HCs and HEI-OC-1 cells, suggesting that reduced levels of ARC might correlate with neomycin-induced HC loss. We inhibited ARC expression using siRNA and found that this significantly increased the sensitivity of HEI-OC-1 cells to neomycin toxicity. Finally, we found that ARC inhibition increased the expression of pro-apoptotic factors, decreased the mitochondrial membrane potential, and increased the level of reactive oxygen species (ROS) after neomycin injury, suggesting that ARC inhibits cell death and apoptosis in HEI-OC-1 cells by controlling mitochondrial function and ROS accumulation. Thus the endogenous anti-apoptotic factor ARC might be a new therapeutic target for the prevention of aminoglycoside-induced HC loss.

PS 587

The Effect of LLLT on Synaptopathy Induced by Acoustic Overexposure

Jae-Hun Lee¹; Min Young Lee²; Phil-Sang Chung²; Jae Yun Jung³

¹*Beckman Laser Institute Korea, College of Medicine, Dankook University, South Korea;* ²*Department of Otolaryngology-Head & Neck Surgery, College of Medicine, Dankook University, South Korea;* ³*Department of Otolaryngology-Head & Neck Surgery, College of Medicine, Dankook University, South Korea*

Background and Objective

Noise can cause hearing loss by destructing the hair cell. While, certain degree of noise can cause hearing problems without the permanent change of hearing threshold, which is called transient threshold shift (TTS). In this particular circumstance, hearing abilities such as temporal processing and sensitivity, could be decreased without hearing loss. It has been reported that low level laser therapy (LLLT) has protective effect on the hair cell after noise trauma. In this study, we evaluated the effect of LLLT on temporal coding after TTS in rat model.

Materials and Methods

SD Rats were divided into laser treat group and noise only group. Narrow band noise 105 dB, centered at 16 kHz (1 kHz of bandwidth) was generated and exposed to the animals for 2 hours. ABR was measured before and immediately after noise exposure, 3 days, a week,

and two weeks after noise exposure. In laser group, low level laser was irradiated to the right ear for 7 days after noise exposure. ABR recordings using paired-click was also acquired before and after two weeks of noise exposure. To evaluate the synaptic connection between the hair cell and auditory nerve fiber, pre-synaptic ribbon density was evaluated.

Results

Two weeks after noise exposure, ABR threshold was recovered in both groups and laser treated group showed faster recovery. However, density and distribution of synaptic ribbons were significantly different between laser treat group and noise only group. The result of paired click ABR also showed that the recovery of temporal coding is reduced after noise exposure. In addition, laser treat group show enhanced recovery of temporal coding than noise only group.

Conclusion

This study suggests that TTS by noise exposure can damage the temporal coding of hearing despite normal hearing threshold. Furthermore, we showed that LLLT has protective effect in synaptic connections against noise exposure. The underlying protective mechanism of LLLT against to noise is not reported yet. Nevertheless, this result could shed a light to the clinical application of laser therapy for noised induced hearing loss.

This study was supported by a grant of the Ministry of Science, ICT and Future Planning grant funded by the Korea government (NRF-2012K1A4A3053142).

PS 588

Behavioral Consequences of Cochlear Histopathology Following Noise Overexposure in Nonhuman Primates

Samantha Hauser; Jane Burton; Ramnarayan Ramachandran; Evan Mercer
Vanderbilt University

Noise exposure is one of the most common etiologies of hearing loss. Detailed anatomical and physiological data from nonhuman animals exposed to noise complement the extensive behavioral data collected in humans with hearing loss. A nonhuman primate model of noise induced hearing loss is necessary as it allows for studies of anatomy, physiology, and behavior within the same subjects under controlled exposure conditions. Exposure to a 146 dB SPL 50 Hz bandwidth of noise centered at 2 kHz for four hours caused permanent physiological changes in toneburst auditory brainstem response (ABR) thresholds and otoacoustic emissions (OAE), as well as related anatomical changes to ribbon synapse number (synaptopathy), outer and inner hair cell (OHC,

IHC) count, and auditory nerve fiber numbers. The purpose of the present experiment was to investigate the behavioral consequences of the exposure and to correlate these findings with the previously documented anatomical and physiologic data.

Two macaque monkeys (*Macaca mulatta*, *Macaca radiata*) were trained to perform a lever release Go/No-Go behavioral detection task. Behavioral and physiological assessments were obtained before and after the noise exposure. Physiological measures included ABRs and distortion product OAEs. Behavioral measures included audiograms, masked detection in steady state and modulated noise, and critical band measurements.

Physiologic measurements in these subjects mirrored previous results, with elevated ABR and DPOAE thresholds at all frequencies tested. Audiograms showed frequency specific changes, with the greatest threshold changes (up to 64 dB) above the exposure frequency, and little change in threshold at lower frequencies. Masked detection was affected in a similar frequency specific manner, and threshold shift rates were lower than pre-exposure. Post-exposure critical bandwidths were found to be significantly larger than baseline. Each of these changes was well correlated with the frequency specific loss of IHCs and OHCs. Detection in modulated maskers post-exposure showed no difference from steady state noise, whereas pre-exposure results show better detection in the presence of low frequency modulations. Such temporal processing impairments were likely related to IHC ribbon synaptopathy following overexposure to the high level stimulus.

These results reveal that behavioral effects of noise exposure in macaques are similar to those seen in humans and provide preliminary information on the relationship between noise exposure and perceptual changes in hearing. These studies are a prelude to studies of lower sound level exposures that cause hidden hearing loss and the establishment of an animal model to test therapeutic interventions prior to human trials.

PS 589

Inhibition of Histone H3 Lysine 9 Dimethylation Protects from Noise-induced Hearing Loss

Hao Xiong; Haishan Long; Yuanping Zhu; Kayla Hill; Su-Hua Sha

Medical University of South Carolina

Introduction

Post-translational modification of histones alters their interaction with DNA and nuclear proteins, influencing gene expression and cell fate. In this study, we investigated the protective effect of inhibition of histone H3 ly-

sine 9 dimethylation (H3K9me2) against noise-induced hearing loss in adult CBA/J mice.

Methods

CBA/J male mice at the age of 12 weeks were exposed to an octave band noise with a frequency spectrum from 8–16 kHz for 2 hours at 103 dB sound pressure level with or without BIX-01294 treatment. Hearing threshold shifts were monitored by auditory brainstem response (ABR). Alteration of H3K9me2 expression in the cochlea was evaluated by immunohistochemistry. The numbers of hair cells and inner ear synaptic ribbons after noise exposure were also counted.

Results

H3K9me2 was increased in the nuclei of outer hair cells and marginal cells 1 hour after exposure to a traumatic noise paradigm known to induce permanent threshold shifts. G9a, a major histone methyltransferase responsible for H3K9me2, was increased in the inner hair cells, outer hair cells, spiral ganglion cells, and marginal cells examined 1 hour after the noise exposure. Inhibition of G9a with its specific inhibitor BIX-01294 significantly attenuated the noise-induced increase of H3K9me2 in the outer hair cells and reduced the noise-induced loss of outer hair cells and inner hair cell synaptic ribbons, ABR wave I amplitude, and subsequent noise-induced hearing loss.

Conclusions

These findings suggest that methylation of histone H3 at lysine 9 is involved in the pathogenesis of noise-induced hearing loss. Pharmacological targeting of histone methylation may afford a strategy for protection against noise-induced hearing loss and cochlear synaptopathy.

Acknowledgements

The research project described was supported by R01 grant DC009222 from the National Institute on Deafness and Other Communication Disorders, National Institutes of Health.

PS 590

Dynamic Activation of Basilar Membrane Macrophages in Response to Chronic Sensory Cell Degeneration in Aging Mouse Cochleae

Mitchell D. Frye¹; Weiping Yang²; Celia Zhang¹; Binbin Xiong¹; Bo Hua Hu²

¹University at Buffalo, The State University of New York; ²Center for Hearing and Deafness, University at Buffalo

Background

Cochlear immune cells, particularly macrophages, are central to cochlear immune and inflammatory activities. In the sensory epithelium, macrophages have been identified on the scala tympani side of the basilar membrane. These basilar membrane macrophages are the spatially closest immune cells to sensory cells and are able to directly respond to and influence sensory cell pathogenesis. While basilar membrane macrophages have been studied in acute cochlear stresses, their behavior in response to chronic sensory cell degeneration is largely unknown.

Methods

Cochleae from C57BL/6J, a mouse model of age-related sensory cell degeneration, were collected at 1, 3-5, and 10-12 months of age, and a systematic observation of the variance in phenotypes, the changes in morphology and distribution of resident basilar membrane macrophages was undertaken for these three age groups.

Results

This study reveals that resident macrophages, not infiltrating monocytes, are the major macrophage population for immune responses to chronic sensory cell death. These macrophages display dynamic changes in their numbers and morphologies as age increases, and the changes are related to the phases of sensory cell degeneration. Notably, macrophage activation is characterized by changes in the cell shape from stingray to amoeboid, enlargement and fusion of cell bodies, and formation of intracellular vacuoles. Macrophage activation precedes sensory cell pathogenesis, and the enhanced activities persist until sensory cell degradation is complete.

Conclusion

Resident macrophages of the basilar membrane are a dynamic group of cells that are capable of vigorous adaptation to changes in the local sensory epithelium environment influenced by sensory cell status. These cells are a sensitive immune sensor for sensory cell homeostasis and are likely to play roles in modulating hair cell degeneration.

PS 591

Cochlear Synaptopathy in the Noise-exposed and Aging Rhesus Macaque (*Macaca Mulatta*)

Michelle D. Valero¹; Jane Burton²; Samantha Hauser²; Gregg Recanzone³; Troy Hackett²; Ramnarayan Ramachandran²; M. Charles Liberman¹

¹Massachusetts Eye and Ear Infirmary, Harvard Medical School; ²Vanderbilt University; ³U.C. Davis

Cochlear synaptopathy can occur as a consequence of various insults, including acoustic trauma, aging, ototoxicity, conductive hearing loss, and possibly others, regardless of whether outer hair cells (OHCs) are lost. Recent work in mice and guinea pigs, for example, demonstrates that moderate noise overexposure can cause a permanent loss of up to ~50% of cochlear synapses without affecting OHCs or threshold, because the synaptopathy is selective for high-threshold auditory nerve fibers. However, the fiber loss likely impairs temporal processing and speech comprehension in noise, a classic complaint of those with sensorineural hearing loss. When OHCs are spared, these deficits hide behind a normal audiogram, creating a "hidden hearing loss." When OHCs are also lost, understanding speech may be challenging in all environments.

Due to possible species differences, a non-human primate model, in which behavioral detection and discrimination testing can be paired with electrophysiology and histopathology, may prove to be valuable in the development of diagnostics and therapeutics. Here, we describe the establishment of the macaque model of noise-induced and age-related cochlear synaptopathy: we compared the normal innervation pattern of cochleas from young, post-pubescent monkeys to those of noise-overexposed or aging macaques from Vanderbilt University, Boston University, and U.C. Davis.

Noise-exposed monkeys were presented bilaterally with narrowband noise centered at 2 kHz (108 or 146 dB SPL for 4 hrs) under isoflurane anesthesia. Cochlear function was assayed for up to 8 weeks following exposure. As previously reported in lower-order mammals, there were fewer synapses on inner hair cells (IHCs) surviving acoustic trauma when compared to unexposed controls. With higher exposure levels, synaptopathy was more severe, and widespread OHC loss correlated with elevated cochlear thresholds. Aging monkeys with no history of purposeful noise exposure had up to 36% missing OHCs in high-frequency regions and some missing IHCs. However, up to 50% fewer synapses (re young) remained in surviving IHCs.

In both groups, there were regions with significant synaptopathy and no OHC loss, suggesting that synapses are the most vulnerable element in noise-exposed and aging primates. Variations in the severity of synaptopathy may explain why two individuals with the same audiogram can have widely divergent performance on speech-in-noise tests. In future work, we will test this hypothesis by training macaques on a variety of auditory discrimination tasks, and we will use this model as a platform to test emerging therapies to elicit neurite extension and synaptogenesis in the adult inner ear.

PS 592

Ototoxic Effects of Loop Diuretics

Dalian Ding¹; Hong Liu²; Haiyan Jiang¹; Yongqi Li³; Xuewen Wu²; Hong Sun²; Kenneth Gross⁴; Richard Salvi⁵

¹State University of New York at Buffalo; ²Xiangya Hospital of Central South University; ³The Third Affiliated Hospital of Sun Yat-Sen University; ⁴Roswell Park Cancer Institute; ⁵Center for Hearing & Deafness, Department of Communicative Disorders and Science, State University of New York at Buffalo

Over the past two decades considerable progress has been made in understanding the ototoxic effects and mechanisms underlying loop diuretics. As typical representative of loop diuretics ethacrynic acid or furosemide only induces temporary hearing loss, but rarely permanent deafness unless applied in severe acute or chronic renal failure or with other ototoxic drugs. Loop diuretic induce unique pathological changes in the cochlea such as formation of edematous spaces in the epithelium of the stria vascularis, which leads to rapid decrease of the endolymphatic potential and eventual loss of the cochlear microphonic potential, summing potential, and compound action potential. Loop diuretics interfere with strial adenylate cyclase and Na⁺/K⁺-ATPase and inhibit the Na-K-2Cl cotransporter in the stria vascularis, however recent reports indicate that one of the earliest effects in vivo is to abolish blood flow in the vessels supplying the lateral wall. Since ethacrynic acid does not damage the stria vascularis in vitro, the changes in Na⁺/K⁺-ATPase and Na-K-2Cl seen in vivo may be secondary effects results from strial ischemia and anoxia. Recent observations showing that renin is present in pericytes surrounding stria arterioles suggest that diuretics may induce local vasoconstriction by renin secretion and angiotensin formation. The tight junctions in the blood-cochlea barrier prevent toxic molecules and pathogens from entering cochlea, but when diuretics induce a transient ischemia, the barrier is temporarily disrupted allowing the entry of toxic chemicals or pathogens.

PS 593

The JNK/c-Jun Stress Response in the Traumatized Cochlea

Anni Herranen¹; Tommi Anttonen²; Ulla Pirvola²

¹PhD student; ²N/A

The cellular stress response network guides cells to initiate protective responses upon stressful stimuli. But if stress is too strong or prolonged, cellular stress signaling feeds into cell death pathways. Inhibition of detrimental processes or boosting protective processes of the stress response network offer protective therapeutic potential in many biological contexts. In the inner ear, inhibition of activation of the MAPK pathways has been studied as a pharmacotherapeutic approach to protect hair cells against traumas. Inhibition of the JNK pathway has been shown to confer protection of auditory hair cells against noise and ototoxic drugs, but the cellular mechanisms of JNK signaling in the inner ear are poorly understood. This understanding would benefit the development of safe and efficient therapeutic interventions against hearing loss.

In the noise- and ototoxic drug-challenged cochlea, we have characterized the rapid and transient activation of the c-Jun transcription factor, the major downstream effector of stress-activated JNKs. Interestingly, rather than in the vulnerable outer hair cells, c-Jun is phosphorylated in several non-sensory populations of the cochlea. These results suggest the the c-Jun stress response regulates OHC death by non-autonomous mechanisms. As c-Jun phosphorylation is a dynamic event, still unidentified stress molecules seem to interact with JNK/c-Jun signaling, and the interplay between these responses is likely to ultimately determine the extent of cellular loss.

PS 933

Polyphenols Play a Role in the Chemosensitization and Protection Against Cisplatin Induced Ototoxicity

Anna Rita Fetoni¹; Rolando Rolesi²; Fabiola Paciello³; Sara M.L Eramo⁴; Antonella Di Pino⁴; Daniele Mezzogori⁵; Diana Troiani⁵; Gaetano Paludetti⁴; Anna R Fetoni⁶

¹Catholic University School of Medicine; ²Catholic University of Rome; ³Institute of Otolaryngology, Catholic University School of Medicine; ⁴Institute of Otolaryngology Catholic University of Rome; ⁵Institute of Physiology Catholic University of Rome; ⁶Catholic University of Rome - School of Medicine

Antioxidant supplementation during conventional chemotherapy based on cisplatin is a controversial topic. It

is well established that antioxidants may play a role in limiting side effects induced by cisplatin in the cochlea. However in oncology, an emerging paradigm emphasizes molecularly targeted approaches for cancer prevention and therapy and the use of adjuvant chemotherapeutics to overcome cisplatin limitations. In addition antioxidant supplements may play a dual roles performing as double edged swords. On such basis, we explore the effectiveness of two well known antioxidants, Curcumin and Ferulic Acid (FA) as chemotherapeutic adjuvant to cisplatin in vitro (oral squamous cell carcinoma) and as protective drugs against cisplatin induced cochlear damage in vivo. For the in vitro procedures, the oral squamous cell carcinoma (PE/CA-PJ15) were treated with curcumin (0,5, 1,0, 3.37 or 6.75 μM and), FA (10, 100 or 600 μM) cisplatin (1,56 μM) and cisplatin + curcumin or cisplatin +FA. Cell growth and proliferation, apoptosis activation and pSTAT3 and Nrf2 signaling were evaluated. In vivo experiments were performed in the Wistar Rat treated with cisplatin (16 mg/kg, i.p.) and curcumin (100, 200, 400 mg/kg) or FA (150, 300 or 600 mg/kg) 1h before cisplatin injection and for 3 consecutive days) were used. Functional (ABR), morphological analyses were performed. Curcumin administration significantly decreases cancer cell survival and promotes apoptosis with a dose dependent manner. On the contrary, FA given alone did not activates apoptotic pathway and when administered with cisplatin did not potentiate the amount of apoptotic cancer cells affected by cisplatin. Curcumin prevents pSTAT3 and Nrf2 nuclear translocation when administered in conjunction with cisplatin indicating that curcumin targets the anticancer response of cisplatin decreasing chemo-resistance signaling pathways. Conversely, FA promotes pSTAT3 and Nrf2 nuclear translocation with a dose dependent manner either when administered alone or in conjunction with cisplatin. FA in particular at higher doses increases chemoresistance in cancer cells. Curcumin as well as FA systemically administered in the animals treated with cisplatin significantly prevent cisplatin induced hearing loss as shown by auditory threshold shift values measured by ABR at day 3 and 5 after cisplatin treatment and morphological analyses and cell count. In conclusion the effectiveness of polyphenols is dose dependent. Curcumin decreases the chemoresistance and prevents ototoxicity. FA may interfere with the anticancer activity of cisplatin. Beneficial effects of polyphenols offer strong preliminary data for clinical studies in humans, possibly by using novel target for drug delivery systems

Inner Ear: Damage & Protection IV

PS 594

A Combinatorial Approach to Protect Sensory Tissue Against Cisplatin-Induced Ototoxicity

Nicole Febles¹; Robert D. Frisina¹; Bo Ding¹; Nathan D. Gallant²

¹Global Center for Hearing and Speech Research, University of South Florida, Tampa, FL, USA; ²Mechanical Engineering Department, University of South Florida, Tampa, FL, USA

Introduction

Sensorineural Hearing Loss (SNHL) is a multi-factorial neurodegenerative disorder often involving permanent damage/loss to the inner ear's mechano-sensory hair cells, needed for proper auditory transduction and perception. Ototoxic drugs are one of the major contributing causes to SNHL, including Cisplatin (CDDP), a very effective treatment for cancer resulting in irreversible neurosensory hearing loss, has an average incidence of 62% of patients being effected overall. Since there is currently no FDA approved prevention and/or treatment for SNHL, attenuation of ototoxicity is a major area of focus in oncology and hearing research. Through a combinatorial approach of utilizing multiple otoprotective agents, we observed an in-vitro otoprotective effect against CDDP on an immortalized epithelial organ of Corti cell line.

Methods

HEI-OC1 cells were grown in permissive conditions, as previously described. Following permissive growth, HEI-OC1 cells were seeded in 96 well plates for 24 hours. On Day2, experimental pretreatment conditions or IFN- γ -free growth media were added. On Day3 respective wells were incubated with CDDP treatment for 24 hours. ATCC MTT Cell Proliferation Assay was initiated and evaluated on Day4. All statistical analysis was done with a one-way analysis of variance and Holm-Sidak all pairwise multiple comparison procedure using SigmaPlot (See Table 2).

Results

We confirmed that CDDP at a final concentration of 200 microM for 24 hour administration on HEI-OC1 cells does induce cell death. When analyzed by MTT assay, our cocktail of agents (ALL Prot + CDDP) had significantly increased cell viability when compared to CDDP only ($t= 3.403$; $P=0.011$; Figure 1 and Table 2). Additional findings via this MTT analysis revealed more information in regards to the cytotoxicity of our otoprotective agents alone. Specifically, NT3 alone is not cyto-toxic to cells, but D-methionine and PFT-alpha had some cytotoxicity, with PFT-alpha having the highest degree of cytotoxic-

ity of the three otoprotective agents. To further investigate these cytotoxic findings in regards to PFT-alpha, a DMSO control was added to this experiment revealing a significant decrease in cell viability when compared to control. Thus, we believe that the decrease in viability found in the PFT-alpha only conditions could be due to the use of DMSO as a solvent.

Conclusions

These findings reveal an otoprotective effect when our combination of otoprotective agents is used as a pre-treatment prior to CDDP administration. We plan to optimize the otoprotective effect of this biotherapeutic cocktail of agents, while minimizing any changes to the anti-tumor efficacy of Cisplatin.

PS 595

Hearing Preservation in Guinea Pigs With and Without Intracochlear Corticosteroid Treatment After Cochlear Implantation

Huib Versnel; Sarah Havenith; Dyan Ramekers; Sjaak F.L. Klis
University Medical Center Utrecht

Background

For cochlear implantation it is regarded important to preserve cochlear structures, in particular when the patient has residual hearing, which may be used in combination with the cochlear implant (CI). Often, corticosteroids are applied to the cochlea during implantation to boost preservation, however, it is not well known whether corticosteroid treatment has a clinically relevant effect. We investigated whether intracochlear corticosteroid treatment prevents inner ear damage after cochlear implantation in guinea pigs.

Methods

The right ears of 14 guinea pigs were implanted with a custom-made electrode (MED-EL), with a flexible tip and insertion depth of 5 mm. Six of those animals were implanted with an electrode coated with 10% dexamethasone with slow release of dexamethasone into the cochlea after implantation. Auditory brainstem responses (ABRs) and compound action potentials (CAPs) were recorded to click and tone stimuli. Pre-operatively, only ABRs were recorded, and post-operatively, both ABR and CAP recordings were performed (including electrically evoked ABRs), up to 4 weeks after implantation. After 4 weeks all animals were sacrificed and the cochleas were processed for histological analysis.

Results

The degree of insertion trauma ranged from elevation of the basilar membrane to total rupture of the basilar membrane and/or the spiral lamina. There were no

differences in hair cell and/or spiral ganglion cell loss between dexamethasone-treated and control animals. Dexamethasone did not cause additional damage and/or an infection in the cochlea. The insertion trauma after implantation, based on the CAP and ABR threshold shifts, was found in the 4 to 16 kHz region. Electrophysiological data showed a greater threshold shift directly after implantation in the dexamethasone-treated group (35 dB) than in the control group (25 dB). One day after implantation thresholds of the two groups were comparable; accordingly, animals with greater insertion trauma showed greater recovery. Thresholds were stable during the 4 weeks follow-up. Electrically evoked ABRs did not show differences in threshold, amplitude or latency between both groups. Surprisingly, threshold shifts after implantation were not correlated to the degree of structural insertion trauma.

Conclusion

We found no significant protective (or negative) effect of intracochlear corticosteroid treatment.

PS 596

Evaluating the Ototoxicity of Novel Platinum(II) Chemotherapy Compounds Using a Zebrafish Inner Ear Model

Jerry D. Monroe¹; Kevin M. Williams²; Michael E. Smith¹

¹*Department of Biology, Western Kentucky University;*

²*Department of Chemistry, Western Kentucky University*

Background

Recently synthesized heterocyclic- and triamine-ligated platinum(II) compounds bind DNA differently than traditional diamine-ligated platinum chemotherapy drugs and could produce reduced hearing side-effects by signaling through different cellular pathways. This project uses electrophysiological and fluorescent staining techniques in a zebrafish inner ear model to investigate whether novel platinum-based chemotherapy drug candidates damage hearing and auditory tissue.

Methods

Four novel platinum(II) compounds, phenanthriplatin, pyriplatin, Pt(dien)Cl, and Pt(Et2dien)Cl, were tested in five cancer cell lines [HTB-16 (glioma), Saos-2 (osteosarcoma), A549 (lung), MCF-7 (breast), Caco-2 (colorectal)] and a non-cancer control line [IMR-90 (fibroblast)]. The 3-(4,5-dimethylthiazol-2-yl)-2,5-diphenyltetrazolium bromide (MTT) assay was used to quantify cellular viability. Zebrafish were injected with platinum compounds or a 0.9% NaCl vehicle control and after 24 or 48 hours were given hearing tests (100, 250, 400, 600, 800, 1000,

1500, 3000 Hz) using the auditory evoked potential technique. After hearing testing, two auditory inner ear end organs, the utricle and saccule, were dissected out for fluorescent staining. Left end organs were stained using terminal deoxynucleotidyl transferase dUTP nick end labeling (TUNEL) and the number of apoptotic cells was quantified. Right end organs were stained with phalloidin and an epifluorescent microscope was used to quantify hair cells in the striolar and extrastriolar regions of the utricle and in four regions of the saccule to determine hair cell loss.

Results

Our preliminary findings suggest that these novel platinum-based compounds target cancer cells but can also produce hearing side-effects and damage auditory tissue. We found that hearing thresholds are generally shifted upwards at most frequencies for all of the compounds except pyriplatin. However, unlike zebrafish injected with cisplatin, those injected with the novel compounds exhibited minimal hair cell loss in both the utricle and saccule.

Conclusions

We show that the zebrafish inner ear is an effective model for screening novel platinum-based chemotherapy compounds and that some of the new compounds cause hearing loss. However, because a reduction in hair cell numbers is generally not observed, this suggests that a physiological mechanism may be responsible for the hearing deficits produced by these compounds.

Supported by INBRE grant, NIGMS 8P20GM103436-12, and NIH grant, 1 R15 CA188890-01A1.

PS 597

The Detrimental Effects of Caffeine Consumption on Hearing in the Rat Model of Cisplatin Ototoxicity.

Sandeep Sheth¹; Kelly Sheehan¹; Michelle Lowy²; Vikrant Borse²; Asmita Dhukhwa²; Raheem Al-aameri²; Debashree Mukherjee²; Leonard P. Rybak³; Vickram Ramkumar²

¹*Southern Illinois University, School of Medicine;*

²*Southern Illinois University School of Medicine;* ³*SIU School of Medicine*

Background

Cisplatin is a commonly used chemotherapeutic drug which produces a major side effect of permanent hearing loss. Adenosine A1 receptors (A1AR) are well characterized for their role in cytoprotection. These receptors are expressed in the cochlea where they have shown

to suppress inflammatory response initiated by cisplatin to attenuate hearing loss. Caffeine, a widely used psychoactive substance, is a non-selective antagonist of the A1AR. We reasoned that caffeine intake could antagonize the endogenous protective role of the A1AR in cochlea and potentiate cisplatin-induced hearing loss. In the current study, we demonstrate that caffeine exacerbates cisplatin ototoxicity in a rat model.

Methods

Auditory brainstem responses (ABRs) in naïve male Wistar rats were recorded before and 3-days following cisplatin (11mg/kg), oral caffeine (15mg/kg) and transtympanic R-PIA (1µM) treatment to assess auditory threshold shift for hearing loss. Cochlea were then isolated for whole mount preparation to check for the loss of OHCs using myosin VIIa staining and ribbon synapses using CtBP2 and glutamate receptor-2. The expression of inflammatory genes were studied in cochlea and UB/OC-1 mouse derived organ of Corti cells through qRT-PCR. UB/OC-1 cells were also used to study protein expression of apoptotic markers using Western blotting. Immunohistochemistry was performed on mid-modiolar sections on cochlea to determine TNFα and p-STAT1 staining.

Results

After single oral administration of caffeine and cisplatin, one of the three frequencies (32 kHz) tested showed statistically significant greater hearing loss as compared to cisplatin or caffeine alone groups. Interestingly, exacerbation in OHC damage was not seen in these groups. However, caffeine with cisplatin decreased the number of ribbon synapses and increased orphan synapses. Caffeine also enhanced cisplatin-induced expression of inflammatory genes, such as iNOS, COX-2 and TNFα in the cochlea as well as UB/OC-1 cells. Immunohistochemical analysis of the mid-modiolar sections revealed that caffeine significantly increased cisplatin-induced TNFα staining, but not p-STAT1, in spiral ganglion cells, stria vascularis and spiral ligament but not in OHC. These effects of caffeine were mediated by its blockade of A1AR, as co-administration of R-PIA, an A1AR specific agonist, reversed the detrimental actions of caffeine and cisplatin on hearing loss.

Conclusion

Our findings indicate that oral administration of caffeine sensitizes the cochlea to cisplatin by inhibiting the endogenous protection afforded by the A1AR. These studies point to a possible drug-drug interaction between caffeine and cisplatin and suggest that caffeine consumption should be cautioned in cancer patients on a chemotherapeutic regimen containing cisplatin.

PS 598

Outer Hair Cell (OHC) Loss in Prestin Knockout/ Tecta C1509G Heterozygous Mice

Yingjie Zhou; Kylie McLaughlin; Kazuaki Homma;
Mary Ann Cheatham
Northwestern University

Introduction

Following the discovery of prestin, several mouse models were developed to test its function. Although unexpected, OHC loss was observed in the basal region of the cochlea (Liberman et al., 2002; Wu et al., 2004). Because OHCs lacking prestin are short and compliant, this study sought to investigate the mechanisms underlying premature OHC death by manipulating extrinsic factors to reduce mechanical stress. Using mice that express a mutation in the tectorial membrane (TM) protein alpha tectorin (Tecta), we created double mutants that also lacked prestin. Because mice that are heterozygous (het) for Tecta C1509G display a short TM that couples only to row 1 OHCs (Xia et al., 2010), we sought to learn if increased survival is observed for OHCs in rows 2 and 3.

Methods

Prestin knockouts (KO), either WT or het for Tecta C1509G, were euthanized at postnatal day 42. Following fixation and decalcification, the cochleae were dissected and stained with anti-prestin to facilitate the counting of OHCs.

Results

Prestin KOs with a short TM suffered greater loss of OHCs in row 1 (ANOVA, post-hoc t-tests) but only in the mid-apical region of the cochlea. Although there was basal OHC loss it was not influenced by shortening the TM. Surprisingly, prestin KOs that were WT for Tecta also showed considerable loss of row 1 OHCs in the mid-apical region albeit less than for the Tecta C1509G hets. Although the initial Wu et al. paper commented on greater OHC loss in row 1, the effect was small and documented only in the basal half of the cochlea. Because of the apical loss in prestin KOs that were WT for Tecta, we reexamined OHC loss in the original prestin KO line. Again, we observed mid-apical loss of row 1 OHCs. In contrast, Tecta C1509G hets did not suffer OHC loss as reported previously (Liu et al., 2011).

Conclusion

Prestin KO mice with a shortened tectorial membrane displayed greater row 1 OHC loss in the mid-apical region of the cochlea. Because OHCs coupled to the TM produce transducer currents, this enhanced loss may be activity dependent and could relate to higher shear forces predicted in cochlear models for first row OHCs (Liu

et al., 2011). If true, row 1 OHC loss may vary depending on the degree of background noise in the vivariums where the mice are housed.

(Work supported by NIDCD (DC000089) and by the Capita Foundation).

PS 599

Rapid Cochlear Dysfunction and Outer Hair Cell Loss after Treatment with 2-Hydroxypropyl- β -Cyclodextrin, a Potential Therapeutic Drug for Niemann-Pick Type C Disease

Keith Duncan¹; Mark Crumling¹; Su-Hua Sha²

¹Kresge Hearing Research Institute, University of Michigan; ²Medical University of South Carolina

With its ability to bind cholesterol, 2-hydroxypropyl- β -cyclodextrin (HPBCD) is being tested for treatment of Niemann-Pick Type C disease, a lethal cholesterol storage disorder. Within the last few years, ototoxicity of HPBCD has been described in animals at doses comparable to those used in human patients. In mice, HPBCD kills outer hair cells (OHCs) specifically. However, the mechanism of cell death is unknown, and experiments have revealed little involvement of oxidative stress and apoptotic pathways. Knowing the timing of critical events in HPBCD ototoxicity would aid in uncovering the death mechanism and finding otoprotectants. To learn how fast HPBCD has its ototoxic effects, we investigated functional and anatomical consequences of HPBCD administration within hours of a subcutaneous injection of HPBCD (8,000 mg/kg) in mice. OHC loss began around 6 hours and was about 70% by 8 hours, similar to one week after HPBCD. Preceding cell loss, ABR and DPOAE amplitudes decreased beginning 3 to 3.5 hours after injection. For both anatomy and physiology, the effect began at high frequencies and progressed toward low. The physiological effects before OHC disappearance could be due to cyclodextrin's effect on membrane lipids and proteins. The potassium channel, KCNQ4, is of particular interest. It provides the dominant conductance setting the OHC resting potential, and we have found that its current is decreased in OHCs after beta-cyclodextrin treatment. Decreased KCNQ4 conductance would depolarize the OHC resting potential, making it more likely for voltage-gated calcium channels to open. HPBCD may therefore act via KCNQ4 and voltage-gated calcium channels to kill OHCs by an excitotoxic process. In an initial look at KCNQ4 after HPBCD injection, immunohistochemical detection showed no difference in localization and protein level between control and HPBCD cochleae 3 hours after injection. So, HPBCD does not appear to affect the subcellular localization of KCNQ4, but it remains to be

seen if altered channel properties underlie a change in conductance. Finding that HPBCD eliminates hair cells very rapidly and that physiological effects are evident even hours before this will guide the investigation of the cellular mechanism of toxicity both in vitro and in vivo, because efforts of cellular study and mitigant testing can be focused when cochlear physiology is declining.

Funded by Support of Accelerated Research for Niemann-Pick Type C (SOAR-NPC)

PS 600

Characterization of Auditory Injury in Mice Exposed to Blast Overpressure in an Advanced Blast Simulator

Kamren Hollingsworth¹; Ying Wang²; Stephen McInturff¹; Amy Northrop³; Yanling Wei²; Yan Su²; Donna Wilder²; Chang Weise³; Peethambaran Arun²; Irene Gist²; Rodrigo Urioste²; Stephen Van Albert²; Sajja Venkatasivasaisujith²; Elizabeth C. Driver⁴; Tracy Fitzgerald⁵; Joseph Long²; Matthew W. Kelley⁴

¹Laboratory of Cochlear Development, NIDCD, NIH;

²Walter Reed Army Institute of Research; ³Laboratory of Cochlear Development, NIDCD, NIH, Bethesda, Maryland;

⁴Laboratory of Cochlear Development, NIDCD, NIH, Bethesda, Maryland, USA; ⁵Mouse Auditory Testing Core Facility, NIDCD, NIH, Bethesda, Maryland, USA

Background

The use of explosive devices continues to increase in modern combat, and many veterans who have been exposed to blast have developed permanent hearing loss, vertigo, and/or other balance-related problems. A lack of postmortem histological exams of the central and peripheral auditory and vestibular systems in blast-affected individuals has limited our understanding of the damage resulting from blast exposure. Past studies with animal models that attempted to recapitulate blast exposure with ordinary shock tubes failed to accurately simulate blast waveforms, which has led to the development of the Advanced Blast Simulator (ABS). This study seeks to characterize the effects of blast exposure on the vestibular and cochlear function of adult CBA/J mice.

Methods

Morphological changes in the cochleae and utricles of blast or sham exposed animals were assessed at 4hrs, 1 day, 7 days, 15 days, 1 month, and 3 months post-exposure, using both hair cell and supporting cell markers. Functional changes were assessed by distortion product otoacoustic emission (DPOAE) and auditory brainstem

response (ABR) of mice subjected to either single blast or repeated blasts, and compared to sham-treated controls.

Results and Conclusions

We observe significant damage and hair cell loss in the cochleae of blast-exposed animals, but an increase in hair cell density in the utricles as compared to sham controls. DPOAE signals are undetectable shortly after mice are exposed to blast overpressure, and are still absent at least 15 days post-exposure. In addition, the ABRs of animals subjected to blast showed significant increases in threshold and wave latency, and a reduction in ABR wave amplitude. These results confirm morphological and functional changes to the peripheral auditory region that highlight the vulnerability of the inner ear to damage caused by blast overpressure, simulated by the ABS. This animal model should aid in furthering our understanding of underlying mechanisms in hearing impairment, vertigo, and other inner ear-related health issues seen in veterans who have been exposed to blast.

PS 601

Aldosterone Modulates NKCC1 Currents In Vitro – Implications for Age-Related Hearing Loss

Parveen Bazard¹; Harish Chittam¹; Bo Ding²; Venkat R. Bhethanabotla³; Robert D. Frisina²; Joseph P. Walton⁴

¹Global Center for Hearing and Speech Research, University of South Florida; ²Global Center for Hearing and Speech Research, University of South Florida, Tampa, FL, USA; ³Department of Chemical & Biomedical Engineering, University of South Florida; ⁴Communication Sciences and Disorders, University of South Florida, Tampa FL, USA

Introduction

Among the top three chronic medical conditions of the elderly, yet there are no medical treatments for age-related hearing loss (ARHL). Degeneration of the stria vascularis (SV) has been implicated in ARHL. The SV is a specialized organ located on the lateral wall of scala media and is responsible for maintaining the endolymphatic potential, which powers the receptor transduction. Marginal cells contain Na⁺-K⁺-2Cl⁻ co-transport protein (NKCC1), which generates the potassium rich endolymphatic fluid. Recently, we have demonstrated that NKCC1 activity is involved in ARHL and long-term treatment with aldosterone (ALD) can slow the progression of ARHL in aging mice, possibly by increasing SV sodium-potassium transport, and up-regulation of NKCC1 protein expression. The present study investigated the biophysical mechanisms of how ALD alters

NKCC1 currents in an in-vitro model using whole cell electrophysiology.

Methods

The SH-SY5Y neuroblastoma cell lines were used because these cells become differentiated, like neurons, with use of retinoic acid in the culture media. To confirm NKCC1 protein expression, semi-quantitative reverse-transcription-polymerase chain reaction (RT-PCR) and western blotting were performed. Electrophysiology experiments were done at room temperature using standard in-vitro patch clamp techniques, utilizing a 700-B Multiclamp amplifier and 1440-A data acquisition unit from Molecular Devices.

Results

RT-PCR and Western Blot experiments confirmed that both undifferentiated and differentiated cells express NKCC1 protein. Subsequently, differentiated cells were used for whole-cell patch clamp experiments. In the dish, cells were continuously perfused with extracellular solution containing 1 μ M ALD. An increase in outward K⁺ currents was observed after approximately 10 minutes following 1 μ M of ALD, which was completely reversed by washout of ECS. These K⁺ currents were sensitive to tetraethyl ammonium (TEA), a potassium channel blocker, with 1 μ M of TEA blocking the increase in whole currents elicited by ALD. To test the role of NKCC1 in ALD activity-elicited currents, experiments were designed to inhibit NKCC1 action or expression by using bumetanide – NKCC1 channel blocker and by using small interfering RNA (si-RNA) techniques. Preliminary experiments suggest that ALD was not as effective in the presence of bumetanide, with decrease in currents at positive holding potentials, as compared to control– no bumetanide. Further experiments are underway to quantify the role of NKCC1 in ALD-elicited ion currents.

Summary

This study helps elucidate the cellular and molecular mechanisms by which ALD modulates NKCC1 channel function, and our long-term goal is to determine the therapeutic potential of ALD in the treatment of ARHL.

PS 602

Fate of Human Induced Pluripotent Stem Cell-derived otic Progenitors Transplanted into the Cochlea of a Guinea Pig Model of Ototoxic Drug-induced Hair Cell Death and Hearing Loss

Azel Zine¹; Alejandra LOPEZ¹; Hanae Lahlou¹; Arnaud Fontbonne¹; Alain Toneto²; Jean Michel Brezun¹; Yves Cazals³

¹CNRS UMR 7260; ²FR1739 Chemistry federation

Aix-Marseille university; ³Aix-marseille University and CNRS, LNI A UMR7260

In mammals, auditory hair cells (HCs) and supporting cells are only generated during embryonic development and loss of HCs due to environmental stresses, ototoxicity, genetic factors, or aging is irreversible. Stem cell therapy approach for inner ear damage has received considerable attention over the past decade; however, two major challenges remain to be addressed i) to obtain a sufficient number of characterized human otic progenitors in vitro and ii) to promote their survival and migration within damaged cochleae in vivo. Recently, our group was able to direct in vitro induction of human induced pluripotent stem cells into human otic progenitor cells (hOPCs). Then, the long-term in vitro differentiation of these hOPCs resulted in differentiated cells up-regulating a subset of HC associated markers (Pou4F3, MyosinVIIA,) as revealed by qPCR and immunostaining analyzes.

The aim of this study was to analyze the capacity of hOPCs to survive, migrate and differentiate within damaged organ of Corti in vivo. To this end, we developed a partial hearing loss model in the guinea pig using amikacin ototoxic drug. The level of hearing loss was evaluated both histologically by HCs count and functionally by auditory brainstem response (ABR) measurements. We observed that amikacin treatment at 400 mg/kg for a period of 15 days was sufficient to induce a partial hearing loss. The ABR thresholds of amikacin-treated animals increased by about 20-30 dB at 8-32 kHz and three of amikacin-treated animals did not have any response at 16-32 kHz as compared to ABR measured before amikacin exposure. Furthermore, HCs count along the cochlear epithelium showed a partial and significant loss of OHCs within the corresponding tonotopic areas. For engraftment purpose, the hOPCs were pre-labeled with VybrantTM dye to track their fate in our established guinea pig model of ototoxicity induced hearing loss. After transplantation through cochleostomy in amikacin-damaged cochleae, VybrantTM positive-hOPCs were observed to migrate at different turns and tissues along the entire cochlear duct of damaged guinea pig cochleae at least 14 days after xenografting.

Our preliminary engraftment data suggest the amikacin-induced hearing loss as one valuable model to track the in vivo migration, integration and differentiation of hOPCs for extended periods post-engraftment within ototoxic damaged mature cochleae.

PS 603

Transplatin, a Novel Treatment for Cisplatin Ototoxicity

Asmita Dhukhwa¹; Debashree Mukherjea¹; Sumana Ghosh²; Kelly Sheehan²; Vikrant Borse¹; Sandeep Sheth²; Peter S. Steyger³; Leonard P. Rybak⁴; Vickram Ramkumar¹

¹*Southern Illinois University School of Medicine;*

²*Southern Illinois University, School of Medicine;* ³*Oregon Hearing Research Center;* ⁴*SIU School of Medicine*

Background

Cisplatin chemotherapy is used for the treatment of various solid tumors. However, its use is compromised by dose-limiting toxicities such as ototoxicity, nephrotoxicity and peripheral neuropathy. A number of studies have documented that the ototoxic and nephrotoxic potentials of cisplatin is due to its ability to generate reactive oxygen species (ROS) in the cochlear and renal tissues which promote lipid peroxidation, DNA damage, inflammation and apoptosis of cells in the cochlea. We have previously shown that transplatin, the inactive analog of cisplatin, prevents cisplatin ototoxicity by presumably by inhibiting TRPV1 channels in the organ of Corti, spiral ganglion neurons and other sites. This study further characterized the mechanism of action and efficacy of transplatin in otoprotection.

Methods

Male Wistar rat model is used for cisplatin ototoxicity. ABR were recorded in rats 72 h following vehicle or cisplatin. Cytokines were analyzed simultaneously by Luminescence assays. Explants were isolated from pups aged P3-5 of C57/BL6 mice and separated as organ of Corti (OC) and stria vascularis/spiral ligament. Entry of FM-143 and GTTR was tracked in the OC and stria vascularis by confocal microscopy. SCID mice injected with human head and neck cancer cells were used to determine potential interference of transplatin against cisplatin anti-tumor action.

Results

We now show that transplatin (1 μ M) inhibits the entry of styryl dye, FM-143, and gentamicin tagged with Texas Red (GTTR) in freshly isolated mouse explant cultures of organ of Corti at room temperature, presumably by blocking TRPV1 and/or MET channels. Effective blockade was maintained over the duration of the study (10 min for FM-143 or 30 min for GTTR). Similar findings were obtained using explant cultures of stria vascularis and spiral ligament. Rats pre-treated with transplatin showed less cisplatin-induced ABR threshold shifts and reduced induction of cytokines detected by 4 h in se-

rum and kidney (IL-10, IL-18, CXCL1, MCP1, MIP-1 α and TNF- α). Transplatin also reduced the induction of cytokines (IL10, CXCL1, IL-1beta, MIP-3 α , GCSF and RANTES) in the cochlea at 24h. Changes in the cochlea were associated with reductions in cisplatin-mediated activation of signal transducer and activator of transcription 1 (STAT1), iNOS and COX-2 in the cochlea. Studies performed in a mouse xenograft model of head and neck tumor showed that transplatin did not inhibit cisplatin tumor killing.

Conclusions

These data suggest that transplatin is effective against cisplatin-induced inflammation and ototoxicity, presumably by limiting entry of the drug into cochlear cells.

PS 604

Loss of Sirt3 has Little Effect on Noise Recovery in Mice

Patricia White; Sally Patel; Bao Dang; Stephen Paquette; Felicia Gilels
University of Rochester

Research Background

Noise induced hearing loss affects up to 70% of combat soldiers, depending on deployment, and costs the Veterans' Administration over a billion dollars annually in disability payments and medical care. Understanding the genetic mechanisms underlying susceptibility to noise damage has important implications for public health. Activation of Sirtuins using nicotinamide riboside has the effect of mitigating the effects of noise damage on auditory thresholds as well as reducing neurite retraction, in a Sirt3-dependent manner. We hypothesized that exposing Sirt3-KO mice to noise would result in reduced numbers of auditory synapses compared to wild-type littermates.

Methods

Sirt3-KO mice were bred to FVB/nJ for three generations and heterozygotes were interbred to create Sirt3-KO and wild-type littermates. Their hearing was tested using ABR and DPOAE. Mice were randomly assigned to control or 30 minutes of 105 dB octave band noise centered on 12 kHz, which is sufficient to induce a temporary threshold shift, but not induce high-frequency synaptic loss. Their hearing was tested 1 and 14 days after noise exposure. Both thresholds and voltage rise were calculated for the ABR. Tissue was analyzed with cochleograms and confocal synaptic analysis, including 3D reconstruction. Sirt3 protein expression was also analyzed with immunofluorescence.

Results

ABR thresholds in Sirt3-KO before and after noise were not different from wild-type littermates. Curiously, prior to noise exposure Sirt3-KO had significantly less ABR voltage rise compared to wild-type littermates. Wild-type littermates displayed the expected loss in ABR voltage rise; however, Sirt3-KO voltage rise was unchanged after noise damage. No increase in outer hair cell loss was observed after noise exposure in the Sirt3-KO. No increase in synaptic loss was observed after noise exposure in the Sirt3-KO.

Conclusions

Sirt3-KO mice may have developmental differences compared to wild-type mice prior to noise exposure. Absence of Sirt3 does not apparently predispose FVB/n mice to synaptic loss as predicted.

PS 605

In Vitro Model to Test the Effects of Electrical Stimulation Within the Inner Ear

Christopher O'toole; Jorge Bohorquez; Jeenu Mittal; Kadri Ila; Carolyn Garnham; Adrien A. Eshraghi
University of Miami

Introduction

There is a new trend to implant patients with residual hearing. However, we know that cochlear implantation may cause loss of this residual hearing. The direct effect of implantation of the electrode in macroscopic structures of the inner ear is well described. The initiation of programmed cell death post cochlear implantation is also currently under evaluation by many centers. However the role of electrical stimulation on hair cells is not well established.

Materials and Methods

Design – Design of a custom stimulator circuit that allows us to study several parameters, including stimulation amplitude, pulse width, and total stimulation duration. In vitro - Neonatal (P3-P5) rat pups were used. Animals were anesthetized and the organs of Corti dissected out. Organs were placed in culture solution in a microchannel flow slide. Stimulation was applied with varying parameters, to determine the effect of the stimulation on the survival of hair cells. Survival was quantified by counting hair cells using confocal microscopy.

Results

A compact and easily-adjustable stimulator circuit was produced. It has sufficient flexibility to imitate a wide range of cochlear implant settings. By varying the amplitude, pulse width, and time parameters, we are able to achieve the simulation required for the electrical effects similar to a cochlear implant. In vitro testing re-

vealed the possibility of testing the effects of changing various stimulation parameters on hair cell survival. **Conclusions:** Studying the effect of electrical field on organ of Corti is feasible and has the potential to protect residual hearing and to help screen otoprotective approaches.

Funding

MED-EL Corporation, and HERA Foundation to Dr. AA Eshraghi

PS 606

Electrocochleography during Translabyrinthine Approach for Resection of Vestibular Schwannoma

W. Jason Riggs; Oliver Adunka; Aaron Moberly; Michael Harris; Edward Dodson; Laura Stephens
Ohio State University

Hypothesis

Utilizing electrophysiologic measures obtained from the round window during various stages of the drilling portion of a translabyrinthine approach for resection of vestibular schwannomas will be a feasible yet efficacious technique to monitor the progression of changes in cochlear physiology.

Background

Patients undergoing a translabyrinthine approach for resection of a vestibular schwannoma are left with an ipsilateral profound hearing loss as a result of the surgery. It remains unclear, however, how the progression of the drilling of the inner ear labyrinth affects cochlear function and mechanics during this procedure; especially since only the vestibular portion of the inner ear is removed but the cochlear portion is left intact. Furthering our understanding of this process may ultimately shed light on possible modifications that can be made to possibly preserve residual cochlear function in this patient population.

Methods

Electrocochleography (ECoChG) utilizing tone burst stimuli was recorded from the round window using a monopolar probe during surgery in an adult cohort. Recordings were obtained at various times throughout the drilling of the labyrinth. Various subcomponents of the ECoChG signal were analyzed and Fourier analysis was used to extract spectral features of the on-going response.

Results:

Measureable ECoChG responses were obtained from more than 80% of subjects. The results demonstrate that there is a general trend of loss of cochlear function as the drilling stage of the labyrinth progresses. Patients'

with better preoperative audiometric thresholds appear to maintain measurable physiology longer throughout the procedure.

Conclusion

Electrocochleography obtained from the round window during translabyrinthine approach for resection of a vestibular schwannoma allows for monitoring the progression of changes in cochlear physiology at various stages in the drilling process. Further investigations utilizing this monitoring technique while providing exploratory hearing preservation interventions during the drilling process should be considered.

PS 607

Damage and Recovery of the Stereocilia Actin Core After Mechanical Overstimulation.

Mike Grossheim¹; Gregory I. Frolenkov²; J Mike Grossheim³

¹Dept. Physiology, University of Kentucky; ²Dept Physiology, University of Kentucky; ³University of Kentucky

Background

The core of auditory hair cell stereocilia consists of beta and gamma actin filaments (Furness et al., 2005). These filaments are crosslinked into a paracrystalline structure to provide life-long stability and rigidity to the shafts of stereocilia. Intense noise causing permanent hearing loss disrupts the actin core of stereocilia (Liberman, 1987; Avinash et al., 1993). However, it is yet unclear whether this disruption is produced directly by mechanical overstimulation or occurs later, when temporary hearing loss progresses into permanent hearing loss. In vitro, mechanical overstimulation of mammalian auditory hair cells elicits a transient decrease of hair bundle stiffness (Saunders et al., 1986) which may indicate damage to the tip links, stereocilia core, or both. The goal of this study was to explore the acute effects of mechanical overstimulation on the ultrastructure of the hair bundle.

Methods

Using a fluid-jet, we produced ~20 large (>1 µm) positive and negative deflections of the inner hair cell (IHC) stereocilia in young postnatal cultured murine organ of Corti explants in a small, demarcated region of the explant until video recordings of the bundle displacements indicated the decrease of hair bundle stiffness. The unstimulated IHCs near that region served as undamaged controls. Explants were fixed, fast-frozen, and freeze-substituted for transmission electron microscopy (TEM) or focused ion beam milling backscatter scanning electron microscopy (FIB-SEM).

Results

TEM examination of the explants immediately after overstimulation revealed sub-micron breaks in the actin core of overstimulated IHC stereocilia which were not found in the unstimulated control IHC stereocilia. The breaks were formed mostly at the base of stereocilium, at the site of the largest bending forces. FIB-SEM serial sections revealed that these breaks occur more often at the periphery but not in the center of the stereocilium actin core. Incubation of the explants for 24 hours at 37°C after overstimulation resulted in partial recovery of the hair bundle stiffness. The actin core of the overstimulated and later recovered stereocilia showed no breaks but displayed some small areas with reduced actin filament density. These areas were not present in the unstimulated control IHCs.

Conclusion

The loss and recovery of hair bundle stiffness after mechanical overstimulation may occur due to sub-micron breaks in the actin filaments near the base of the stereocilia and their subsequent repair. The repair mechanism may involve gamma actin since similar gaps were observed in noise damaged stereocilia labeled for gamma actin (Belyantseva et al., 2009).

PS 608

Genetic Activation of the HSF1-Mediated Stress Response for Protection Against Noise-Induced Hearing Loss

David Kohrman¹; Catherine A. Martin¹; Ariane Kanicki¹; Danielle Dejournett¹; Pamela Song¹; Lisa Kabara¹; David Dolan¹; Richard Altschuler²

¹University of Michigan Medical School; ²University of Michigan

Experimental activation of the classic heat shock stress response through up-regulation of heat shock proteins (HSPs) is very effective in protecting the inner ear from noise-induced hearing loss (NIHL) in animal models as well as other traumas such as aminoglycoside- and cisplatin-induced ototoxicity (e.g., J. Neurosci 19:10116-10124, 1999; Cell Stress Chaperones 14:427-437, 2009). Conversely, the loss of heat shock pathway induction through the inactivation of HSF1, the master transcriptional regulator of the heat shock response, results in greater sensitivity to NIHL and ototoxicity (e.g., J Neurosci Res 81:589-596, 2005; JARO 9:277-289, 2008). We have recently evaluated the effects on hearing of a small molecule that relieves the feedback inhibition of endogenous HSF1 and thus efficiently up-regulates multiple HSPs (PLoS Biology, 8:e1000291, 2010). This molecule, HSF1A, activates HSF1 without causing proteotoxicity, thereby mitigating the cellular patholo-

gies associated with neurodegenerative disease in cultured cell and fruit fly models (Cell Reports, 9: 955–966, 2014). Systemic delivery of HSF1A to FVB/NJ mice induces multiple HSP genes in the cochlea and decreases the threshold shift subsequent to a damaging noise exposure.

We are also evaluating two types of transgenic mouse lines for their ability to augment the HSF1-mediated stress response in the cochlea. One transgenic line carries a genomic copy of the full length normal human HSF1 gene. The higher levels of HSF1 protein and target HSP genes expressed in this line have previously been associated with reductions in the cellular, molecular, and systemic pathologies present in genetic models of amyotrophic lateral sclerosis and Alzheimer's disease (J. Neurochemistry 124: 880–893, 2013; Molecular Neurodegeneration, 8:43, 2013). The second type of transgenic line carries a mouse cDNA encoding a version of the HSF1 protein that is missing a central regulatory domain. This mutant HSF1 isoform is constitutively active and also induces higher baseline levels of HSP genes. We are currently evaluating the upregulation of HSF1 target gene expression in the cochlea in both types of transgenic lines and testing their abilities to protect auditory function from noise trauma.

PS 609

Neuroprotectant Nampt Inhibitor P7C3 Demonstrates Otoprotection in an Age Related Hearing Loss Model

Geraldine Cabrera; Michael Poon; Alejandro Dearie; Karin Stebbins; Daniel Lorrain; Peppi Prasit
Inception Sciences

Age related hearing loss (presbycusis) is the dominant cause of sensorineural hearing loss that usually begins around 18 years of age at the highest frequencies. Sensorineural hearing loss is attributed to degeneration of sensory cells in the inner ear, damage to the vestibulocochlear nerve or neural connections. Regeneration or protection of sensory cells has been an approach to target hearing loss. P7C3 is an orally bioavailable brain penetrant NAMPT inhibitor that is known to promote neuroprotection and neurogenesis in neurodegenerative disorders. C57BL/6N mice were dosed with P7C3 per os once daily beginning at 2 months of age, before the onset of age related hearing loss to evaluate if P7C3 would act as an otoprotectant, monthly ABR recordings were taken - thereafter. Animals treated with P7C3 showed a decreased threshold shift over time at 4, 8, and 16kHz significant from vehicle treated animals. P7C3 protects from age related hearing loss and a may represent a novel therapeutic strategy for presbycusis.

PS 610

The Targeted Antioxidant, Catalase-SKL, Protects Against Aminoglycoside-Induced Outer Hair Cell Loss in Organotypic Cultures

John J. Kelly¹; Anna Tyker¹; Stanley R. Terlecky²; Paul A. Walton¹; Brian L. Allman¹

¹University of Western Ontario; ²Seton Hall University

Background

The accumulation of reactive oxygen species in cochlear hair cells is thought to contribute to hair cell death in response to ototoxic drugs, such as the aminoglycoside antibiotic, kanamycin, as well as in noise-induced and age-related hearing loss. Within the cochlea, there are two groups of antioxidant enzymes that attempt to neutralize free radicals; those involved in glutathione metabolism, and others that breakdown superoxide anions and hydrogen peroxide, such as catalase. Found within the peroxisome of cells, catalase plays an important role in protecting cochlear integrity, as transgenic mice that over-express catalase were found to be resistant to age-related hair cell death and hearing loss, and over-expression of catalase via an adenoviral vector in the guinea pig inner ear was found to protect against aminoglycoside ototoxicity. Overall, our research program endeavors to take advantage of the otoprotection offered by catalase, while avoiding the need to genetically manipulate its expression in the cochlea. Thus, in the present study, we investigated whether our novel antioxidant, CAT-SKL—a stable, cell-penetrating, peroxisome-targeted derivative of catalase—is able to increase catalase activity in cochlear hair cells, and offer protection against kanamycin-induced cell death.

Methods

Organotypic cultures from P3-4 rats were cultured for 24 hours, after which time, CAT-SKL was transduced for 24 hours. The following day, cultures were exposed to 1mM kanamycin or control media for another 24 hours. Cultures were fixed and immunostained for the hair cell marker myosin VI and counterstained with phalloidin. Confocal images of basal, mid-basal, mid-apical and apical turn regions were analyzed and hair cell counts quantified.

Results: CAT-SKL was well-tolerated in organotypic cultures at various concentrations up to 50 μ M. As expected, kanamycin induced considerable inner and outer hair cell loss in a basal-apical gradient after 24 hours of exposure. In cultures pre-treated with CAT-SKL (1 μ M), there was significantly less outer hair cell death in the basal turn compared to kanamycin treatment alone. In contrast, however, the number of inner hair cells surviving after kanamycin treatment was not affected by CAT-SKL.

Conclusion

Pre-treatment of organotypic cultures with our targeted antioxidant, CAT-SKL, reduced kanamycin-induced ototoxicity in basal turns of the rat cochlea. Future studies will investigate whether CAT-SKL is protective against hair cell loss in vivo in response to aminoglycoside antibiotics or loud noise exposure.

Funding: Supported in part by a CIHR Open Operating Grant to BLA.

Inner Ear: Mechanics & Modeling II

PS 611

Saddle Shape of the Round Window Membrane Stabilizes Dynamic Properties Against Static Pressure Change

Hirobumi Watanabe; Anil Lalwani; Jeffrey Kysar
Columbia University

Round window membrane (RWM) is a membrane separating the middle and inner ears and releases sound waves in response to the oval window. Recently, we showed a guinea pig (GP) RWM has a unique saddle shape that improves the stability and reliability in sealing perilymph from the middle ear without compromising the compliance to release dynamic pressure. Though this stability as a seal efficiently minimizes the intrascalar quasi-static volume change, static pressure does deform a RWM and consequently the dynamic properties can be affected by quasi-static pressure change seen in normal or pathological conditions including head movements, middle ear pressure change or Meniere's disease.

Here, the dynamic behaviors of a deformed RWM under various range of static pressure were simulated. Using finite element modeling, a GP RWM was modelled as a hyperbolic paraboloid (hyper) shell under static pressures ranging from 0.1 to 100kPa. To clarify the advantage of the hyper, a flat shell was used as a control. In turn, the deformed shells were used to extract eigenmodes and to determine the resonant frequencies of RWMs within 54~50,000Hz. Steady state dynamic analysis was performed to calculate the vibration dynamics of the whole membranes upon uniform sinusoidal pressure and to determine the volume flow rate and acoustic impedance.

Histograms of the numbers of eigenmodes (Figure 1) and impedance curves (Figure 2 and 3) showed clear contrasts between hyper and flat shells. As the pressure increases, histograms showed that the flat shell loses eigenmodes in the low frequency range from 0.1kPa consistently through 100kPa. Conversely, histograms of

hyper showed little change up to $\pm 1\text{kPa}$ (10cmH₂O). The impedance curves showed that the pressure increase from 0 to 0.1kPa made the flat shell 10-fold impedance increase in the low frequency from 0 to 0.1kPa and drastic increase through 100kPa. Conversely, the impedance curves of the HP shell showed virtually no change until 10kPa.

From our previous study, the saddle shape was expected to show stability in the acoustic impedance against the static pressure change due to the low compliance within \pm a few kPa compared to a flat shell. The stability was seen in wider pressure range and indicates a further mechanism that stabilizes the acoustic impedance of a GP RWM. Because a deformed saddle shaped RWM maintains a similar double arched shape, the deformed shape still can retain acoustic characteristics strikingly close to the undeformed RWM.

PS 612

Head Specimen Models of Oval Window and Round Window Occlusion and Laser Doppler Vibration Measurements

Kegaung Chen¹; Lin Yang¹; Tianyu Zhang¹; Peidong Dai²; Kegaung Chen³

¹Eye&ENT Hospital, Fudan University, Shanghai, China; ²EENT Hospital of Fudan University; ³Department of Otorhinolaryngology Head&Neck Surgery, Eye&ENT Hospital, Fudan University, Shanghai, China

Objective

To explore the feasibility of medical adhesive in the molding of oval window occlusion and ear mold glue in the molding of round window occlusion in head specimens and study their effect on bone conduction hearing.

Methods

(1) One head specimen (two ears) was selected. Medical adhesive was used to immobilize stapes footplate in the oval window occlusion group. Ear mold glue was used to immobilize round window niche in the round window occlusion group. The vibrations of stapes footplate (VFT) in round window occlusion model and round window membrane (VRW) in oval window occlusion model, stimulated by sound pressure, were measured by using laser Doppler vibrometer before and after molding. (2) Seven head specimens (fourteen ears) were selected. The vibrations of stapes footplate (VFT) in round window occlusion model and round window membrane (VRW) in oval window occlusion model, and promontory (VPR) in every group stimulated by transducer B71, were measured by using laser Doppler vibrometer before and after molding.

Results

(1) The vibration of stapes footplate (VFT) in round window occlusion model decreased by about 15dB among the 0.5 kHz, 1 kHz, and 2 kHz frequencies, and the vibration of round window membrane (VRW) in oval window occlusion model decreased by about 30dB among above frequencies.(2) The relative vibration of round window membrane (VRW-VPR)/VPR in oval window occlusion model decreased in bone conduction pure tone for the frequency of 3 kHz with significant statistical differences ($P<0.05$).The relative vibration of stapes footplate (VFT-VPR)/VPR in round window occlusion model decreased in bone conduction pure tone for the frequency of 4 kHz with significant statistical differences ($P<0.05$).The decrease of the relative vibration of round window membrane in oval window occlusion model exceeded the decrease of the relative vibration of stapes footplate in round window occlusion model. <

Conclusions

(1) Medical adhesive was available for the immobilization of stapes footplate in head specimens and ear mold glue was available for the immobilization of round window niche in head specimens, respectively. (2) The relative vibration of round window membrane in oval window occlusion model decreased in bone conduction pure tone for the frequency of 3 kHz. (Fig.1) The relative vibration of stapes footplate in round window occlusion model decreased in bone conduction pure tone for the frequency of 4 kHz. (Fig.2)

PS 613

The Effects of Cochlear Implantation Surgery on Power Absorbance and Stapes Velocity to Air and Bone Sounds in Cadavers Temporal Bones

Yona Vaisbuch¹; Joseph Attias²; Koka Kanthaiah³; Yanju Liu³; Leonid Litvak⁴

¹Stanford University; ²University of Haifa; ³Advancedbionics; ⁴Advanced Bionics

Background

Recent reports on live animals and patients showed that cochlear implantation surgery might be associated with immediate or delayed conductive hearing loss.

Methods

To explore the possible mechanism for this type of hearing loss, measurement of Laser-Doppler Vibrometry (LDV) of the stapedial and of the promontorium velocities to air and bone conduction sounds were performed before and after CI electrode insertion. In addition, wide band Tympanometry, utilized power absorbance (PA) measurement, that were collected before and after each stage of CI surgery.

Results

Ten fresh human temporal bones were studied. With respect to baseline LDV measurement, we observed 3 to 5 dB, statistically non significant differences between pre and post CI across all frequencies and for AC and BC stimulations.

However, PA changed significantly across surgical stages and frequencies. A significant change in PA was noticed after opening the antrum and the facial recess, where a notch loss in absorbance may reach up to 20 dB at mid frequencies.

Mastoid cortex opening did not influence the PA significantly.

PA began to change gradually when opening the mastoid air cells, antrum and facial recess.

Specifically, PA increased at low and high frequencies and decreased at mid frequencies (1000-2500 Hz) in a notch pattern. Round window opening preserved the same pattern of changes.

Insertion of a CI electrode significantly changed the pattern in the mid frequencies to an increase of the PA with absence of the notch. Furthermore, filling the mastoid cavity with cement glue, caused a partially recovery of the original baseline PA values.

Conclusions

Power absorbance measurements may add insights to the middle/inner ear mechanism associating with acoustic energy changes in patients undergoing CI surgery. The LDV measurements of stapes velocity to air conduction and promontory to bone conduction didn't reflect any changes after electrode array insertion. We propose a further investigation of Air and bone conduction by combining PA and electro-cochleography (ECoG) in order to characterize the hearing changes following CI insertion.

PS 614

Estimated Auditory Performance Limits of Simulated Acoustic, Electric and Optogenetic Hearing

Astrid Klinge-Strahl¹; Stefan Strahl²; Tobias Moser³

¹Institute for Auditory Neuroscience, University Medical Center Göttingen, Germany; ²MED-EL Medical Electronics GmbH, Research & Development; ³Institute for Auditory Neuroscience and InnerEarLab, University Medical Center Göttingen

Optogenetic cochlear implants (oCI) are considered as a promising approach to overcome the frequency and intensity resolution limits of currently available cochle-

ar implants. Electrically stimulating CIs suffer from a wide current spread around each electrode leading to a recruitment of a large number of auditory nerve fibres (ANF). Thus, the number of useful frequency channels is limited. As an alternative, oCIs would make use of focused optical stimulation, thereby increasing the number of independent stimulation sites, reducing the number of activated ANFs and widening the dynamic range. However, not much is known about the effect of the respective spatial resolution limits on auditory performance limits.

In this study, we estimated psychophysical performance limits for acoustic, electric and optogenetic stimulation using a signal detection theory approach. Excitation patterns of auditory nerve fibers are simulated using computational auditory nerve (AN) models for humans, marmosets and gerbils. A range of excitation patterns is generated by sampling the parameters spread of excitation and phase locking for the electric and optogenetic stimulation in order to obtain data to optimize stimulation parameter settings. Performance limits are then estimated based on the AN discharge times and discharge counts (all-information vs rate place).

Besides the verification of the apparent working hypothesis that an increased spatial resolution is beneficial for psychophysical tasks like mistuning detection, the model further allows for an optimization of the number and position of stimulation sites along the cochlea.

PS 615

Intracochlear Pressures and Impedances of the Middle and Inner Ear in Normal Human Temporal Bones

Darcy Frear¹; Xiying Guan²; Hideko H. Nakajima²
¹Harvard University; ²Dept. of Otolaryngology, Harvard Medical School & Massachusetts Eye & Ear, Boston, MA USA

We have measured intracochlear pressures and velocities of stapes and round window (RW) evoked by air conduction (AC) stimulation in many fresh human cadaveric specimens for over seven years. Our techniques have improved; for example, we take important steps to avoid introduction of air into the inner ear, make measurements for the existence of air, and confirm that fluid leaks at the pressure-sensor insertion sites do not occur. Air can easily leak into the inner ear during extraction of specimens, freezing/defrosting of specimens, and insertion and sealing of intracochlear pressure-sensors. To determine if air leaked into the inner ear, the phase ratio between stapes and RW velocities ($V_{\text{stap}}/V_{\text{rw}}$) is confirmed to be $\frac{1}{2}$ cycle at low frequencies before and after sensor insertion and throughout the experiment. Next,

the magnitude and phase of stapes and RW velocities (V_{stap} and V_{rw}) with respect to ear canal pressure are confirmed to be within normal limits and stable throughout the experiment. We have also developed methods to accurately correct for sensor calibration drift that occasionally occur during an experiment. Finally, we set the criterion that the signals should be at least 6dB above noise in order to be included for analysis.

With these criteria, we aim to ensure our data is reliable and can be used as a basis for computational models of the middle and inner ear. We have obtained updated normal ossicular velocities and intracochlear pressures for AC and RW stimulation that have undergone strict screening. These data sets are further used to determine the impedances of the middle and inner ear, thereby creating a lumped element model. The impedances of the middle ear, cochlear partition, RW, and physiological leakage impedance in scala vestibuli are calculated using the averaged experimental data. This model will be useful as a tool to understand complex sound transmission, like bone conduction, and diseases such as superior canal dehiscence.

PS 616

Evaluation of Cochlear Duct Length Computations Using Synchrotron Radiation Phase-contrast Imaging

Robert W. Koch¹; Mai Elfarnawany¹; Ning Zhu²; Sumit K. Agrawal³; Hanif M. Ladak¹
¹Western University; ²Canadian Light Source Inc., Saskatoon, SK; ³London Health Sciences Centre

Background

Cochlear duct length (CDL) is important for the success of cochlear implants as the suitable electrode must be preoperatively selected to achieve proper cochlear coverage. Current methods to estimate CDL include measuring the A-value [i.e. the largest distance from the round window to the lateral wall (LW)] from a preoperative image and using a linear relationship between 'A' and CDL to find the total length. Validation of these relationships are required in order to be used clinically. Synchrotron radiation phase-contrast imaging (SR-PCI) provides excellent visualization of the cochlear anatomy and therefore, would be effective in evaluating the accuracy of these relationships.

Objective

To validate A-value-based methods for calculating CDL using SR-PCI.

Methods

Ten cadaveric temporal bones were scanned using SR-PCI. Three dimensional (3D) models were reconstructed from the images and the A-value of each sample was measured. Points were placed at three locations [LW, organ-of-Corti (OC) and end of basilar membrane (I)] along the length of the cochlea (Figure 1). CDL at each location was computed as the cumulative distance between successive points, and used as reference for evaluating CDL computations from measured A-values. The mean difference between CDL values were computed and tested for significance using paired t-tests. The differences were compared to clinically significant differences of $\pm 1.5\text{mm}$. From these results, modifications to the existing relations between 'A' and CDL were proposed and tested.

Results

The mean difference between CDL estimates were 0.7mm, 1.4mm and -1.5 mm for LW, OC and I, respectively. The CDL values at the LW were not statistically different ($p = 0.18$) and their differences were within the clinically accepted range. The CDL computations for OC were also not statistically different ($p = 0.06$) but were on the boundary of the clinical range. By adjusting the equation to reflect an observed larger distance between LW and OC than previously assumed, the revised equation yielded more accurate CDLs (mean difference of 0.33 mm, $p = 0.61$). The CDL values at I were statistically different ($p = 0.02$) for which corrections would require a larger sample size.

Conclusions

SR-PCI provides high visualization capability to validate previously published equations to compute CDL from a single simple measurement. The equations for CDL at LW yield accurate approximations of CDL, whereas a revised equation produce better approximations of CDL at OC. Therefore, these equations can provide quick and accurate preoperative estimates of CDL for improving electrode-to-cochlea length matching.

PS 617

The Effect of Superior Canal Dehiscence on Wide-band Acoustic Immittance in Fresh Human Cadaveric Specimens

Salwa F. Masud¹; Stephen T. Neely²; Stefan Raufer¹; Hideko H. Nakajima³

¹The Harvard Speech and Hearing Bioscience and Technology Program; ²Boys Town National Research Hospital, Omaha, NE USA; ³Dept. of Otolaryngology, Harvard Medical School & Massachusetts Eye & Ear, Boston, MA USA

Superior canal dehiscence (SCD) is a hole in the bony wall of the superior semicircular canal, which can cause auditory and/or vestibular symptoms such as hearing loss, aural fullness, autophony, and pressure- and sound-induced vertigo. Currently in the clinic, diagnosis of SCD involves assessment of symptoms, directed otologic exam, audiogram, stapedial reflex test, CT scan, and vestibular evoked myogenic potential (VEMP). SCD patients frequently have conductive hearing loss at low frequencies due to hyper-sensitivity to bone conduction and decreased sensitivity to air conduction. Sensitivity to low-frequency air-conducted sounds appears to decrease due to a "third window" in which an SCD shunts the oval-window volume velocity (in response to sound stimuli) away from the cochlea. In general, SCD seems to decrease the impedance of the inner ear.

To observe mechanical changes due to an SCD, we measured wideband acoustic immittance (WAI) and extracted the reflectance (R)—the ratio between the reflected sound from the tympanic membrane and the forward sound stimulus. WAI is a potential non-invasive, cost-effective diagnostic tool that can be used to distinguish various middle-ear pathologies. In a controlled soundproof chamber, we measured WAI in five fresh human cadaveric temporal bones before and after simulating a superior semicircular canal. As a control, the dehiscence was then patched with dental impression material to reverse SCD-induced changes in WAI.

In all five experiments, there was a decrease in power reflectance ($PR = |R|^2$) due to SCD between 300 Hz and 800 Hz, and an increase in PR between 800 Hz and 1500 Hz. Consistent SCD-induced changes across all five experiments show potential in using WAI as a non-invasive diagnostic tool to detect SCD. Experimentally manipulating the inner-ear system with SCD allows for further development of phenomenological models to better understand the auditory and vestibular symptoms and to aid in SCD diagnosis.

PS 618

A Microfluidic Device with Conformal Printed Electrodes for Integrated Monitoring of Inner Ear Sensory Epithelium

Abigail Spencer¹; Else Vedula¹; Tj Mulhern¹; Danielle R. Lenz²; Peter Lewis¹; Albert Edge³; Erin E. Pararas¹; Jeffrey T. Borenstein¹

¹Draper; ²Eaton-Peabody Laboratories, Massachusetts Eye and Ear Infirmary, Boston, MA, USA; ³Department of Otolaryngology, Harvard Medical School, Boston, MA, USA, and Eaton-Peabody Laboratory, Massachusetts Eye and Ear Infirmary, Boston, MA, USA

As the field of cochlear regeneration evolves, methods for sensing and assaying cellular health throughout the process of differentiation are needed to directly quantify cell and tissue phenotype and function. One unique marker of a mature auditory hair cell is its resting receptor potential and its dynamic change in response to a mechanical stimulus. This is typically measured on an individual cell level via patch-clamping, a tedious process that is challenging to integrate with hair cells in vitro and provides data on individual cells alone. We are developing a method for culturing and differentiating LGR5+ cochlear progenitor cells (LCPs) using an enclosed microfluidic environment with integrated electrodes that are designed to record potential differences in a population of electrically active cells. We have previously reported that nanotopographic patterns on either planar substrates or porous semipermeable membranes provide important cues to guide cellular function and differentiation pathways. Here we demonstrate planar electrodes printed onto nanoembossed substrates within a microfluidic device, which allows us to monitor cell behavior in-situ without disrupting the LCPs during differentiation. The electrodes are printed onto the substrate using a silver nanoflake ink and an Optomec Aerosol Jet 300 Series. The Optomec atomizes the ink, directs it through a print nozzle, and deposits metal traces on the order of 25µm wide and 1µm thick. These metal electrodes are photonic annealed, locally curing the printed ink into a conductive trace without damaging the low temperature substrate. This technology allows us to print precise, low profile electrodes in virtually any pattern and on a wide range of substrates suitable for cell culture. The electrode design comprises of a current source electrode spanning the length of the microfluidic channel, with several voltage-sensing electrodes spaced at intervals along the opposite edge of the channel. This configuration allows the sensing electrodes to pick up changing potentials in the media surrounding the LCPs or other tissue type as the layer is stimulated with flow.

PS 619

Noninvasive Acoustic Force Spectroscopy Method for Measuring Apical Surface Tension and Intercellular Adhesive Forces in Polarized Epithelium

Alexander X. Cartagena-Rivera¹; Christina M. Van Itallie²; James M. Anderson³; Richard S. Chadwick¹

¹National Institute on Deafness and Other Communication Disorders; ²National Heart, Lung and Blood Institute; ³National Heart, Lung, and Blood Institute

Epithelial tissue integrity requires stability between cell-cell adherens, tight junctions (TJ), and the perijunctional actomyosin cytoskeleton. The perijunctional actomyosin

cytoskeleton lies just inside the lateral plasma membrane near the apical junctions, and mainly consists of filamentous actin, NM myosin II motor proteins, and crosslinking proteins. Changes in the actomyosin cortical cytoskeleton directly translate into modification of mechanical properties of single cells (Cartagena-Rivera et al. *Biophys. J.* 110, 2016). The ZO-1 and -2 proteins bind both TJ transmembrane proteins and the F-actin cytoskeleton, suggesting that ZO-1 and -2 could influence both the epithelial physical parameters and the actomyosin cytoskeleton. Here we used the atomic force microscope to address the hypothesis that the alterations in TJ structure and remodeling of the perijunctional cytoskeleton can modify the epithelial tension and the intercellular adhesive forces. We developed a method using noncontact frequency modulation atomic force microscopy frequency shifts to determine the intercellular tension in polarized epithelium. We then measured the tension in confluent polarized monolayers of Madin-Darby canine kidney cell lines. Our results shows that TJ structural changes in ZO-1/ZO-2 double knockdown (dKD) monolayers dramatically elevates the apical epithelium tension, consistent with the previous observations that there is a major reorganization of the perijunctional cytoskeleton with recruitment of NM myosin II and F-actin into large arrays just inside the adherens junction complex and myosin II forming a contractile sarcomeric belt-like distribution (Fanning et al. *MBoC* 23, 2012). Additionally, we measured the tensional force along the cell-cell junctions and the epithelium intercellular adhesion forces. As expected the tensional force along junctions are elevated with increase in contractility. Surprisingly, the intercellular adhesive forces of dKD cell lines are equal to control forces suggesting that the monolayer balances the forces to be maintained below levels that will avoid catastrophic epithelium damage and rupture. In conclusion, this method enables the physiological and quantitative study of relevant physical parameters on biological tissues and should be of broad application for deciphering the molecular regulation relevant to cellular organization and epithelial morphogenesis.

PS 620

Effect of Round Window Reinforcement on Hearing – Experimental and Modeling Results

Xiying Guan¹; Song Y. Cheng¹; Deepa Galaiya¹; John J. Rosowski²; Hideko H. Nakajima¹

¹Dept. of Otolaryngology, Harvard Medical School & Massachusetts Eye & Ear, Boston, MA USA; ²Eaton-Peabody Laboratory, Mass. Eye & Ear Infirmary; Department of Otolaryngology and Laryngology, Harvard Medical School; Speech and Hearing Bioscience and Technology program, Harvard and M.I.T.

Introduction

Recently, some surgeons are treating a variety of inner-ear conditions, such as superior canal dehiscence syndrome, presumed perilymph fistula and hyperacusis with “round window (RW) reinforcement”. However, outcomes are quite variable: some patients report symptoms are reduced while others complain of worsened symptoms. While this experimental surgery is emerging, the basic understanding of how RW reinforcement changes the mechanics of the inner ear and hearing is lacking. The aim of this study is to clarify the effect of RW reinforcement on hearing by comparing the cochlear input drive (ΔP) – the differential sound pressure across the cochlear partition – before and after reinforcing the RW in normal fresh human temporal bones.

Methods

Intracochlear pressures in scala vestibuli (P_{sv}) and scala tympani (P_{st}) at the basal turn of 7 fresh human cadaveric ears were measured using micro-fiberoptic sensors. The cochlear input drive (ΔP) was determined as the difference between P_{sv} and P_{st} ($\Delta P = P_{sv} - P_{st}$). Velocity of the stapes (V_{stap}) was measured with a laser Doppler vibrometer. RW reinforcement was performed using perichondrium, fascia, cartilage, or a combination of these tissues. P_{sv} , P_{st} , ΔP , and V_{stap} in response to air-conducted sound from 25 Hz to 10 kHz were measured at baseline and after RW reinforcement. These measurements were normalized by the sound pressure in the ear canal.

Results

After RW reinforcement, V_{stap} was decreased by up to 10 dB below 1 kHz. P_{sv} was increased by 5-10 dB from 25 Hz to a few hundred Hz while P_{st} was increased by 10-20 dB over 25 Hz-2 kHz. Changes in ΔP (an estimate of hearing) were frequency-dependent. Below 100-200 Hz, ΔP either increased (up to 10 dB) or did not change. From 100-200 Hz to 1 kHz, ΔP sometimes decreased slightly (< 5 dB). Above 1 kHz, ΔP was not affected. Analysis suggests that reinforcement of the RW increases RW impedance, resulting in increased P_{sv} and P_{st} . With RW reinforcement, normal high-impedance paths of the inner ear, such as the cochlear aqueduct, may become important in sound transmission. With larger scalae pressures, this path may allow significant volume velocity flow to maintain ΔP and near normal hearing function.

Conclusion

Reinforcing the RW results in no change or increased hearing at low frequencies, thus can worsen low-frequency hyperacusis. The reinforcement shows little effect at higher frequencies.

Acknowledgement

This study is supported by NIH/NIDCD R01DC004798 and R01DC013303, and Hearing Health Foundation emerging research grant (2016).

PS 621

Near Real-time Volumetric Optical Coherence Tomography and Vibrometry (VOCTV)

Brian E. Applegate¹; Scott Mattison²; Patrick Raphael³; Sangmin Kim¹; John S. Oghalai³

¹Department of Biomedical Engineering, Texas A&M University; ²Department of Otolaryngology - Head & Neck Surgery, Stanford University and Department of Biomedical Engineering, Texas A&M University; ³Department of Otolaryngology - Head & Neck Surgery, Stanford University

In recent work, we have quantitatively measured vibrations within the inner ear of animal models using techniques collectively termed Volumetric Optical Coherence Tomography and Vibrometry (VOCTV). This technique permits 3-D spatially resolved measurements of the vibratory response to sound stimuli with sub-nanometer sensitivity. Ultimately, we would like to simplify the measurement of vibratory responses for every voxel (x,y,z) within a defined volume to pure tone stimuli over a range of frequencies (f) and intensities (I). Currently, acquiring this 6-D (x,y,z,f,I,t) data set has been very time consuming due to hardware/software limitations that prevented us from fully parallelizing data collection and processing. As an example, at one x,y position, the vibratory response along a line (z) in depth measured at 20 frequencies and 10 amplitudes with 50 ms stimuli could be acquired in ~120 s using our current combination of hardware/software. However in principle this acquisition should only require 10 s. Developing a software/hardware solution that can process data at the same rate as collection and in parallel holds the promise of reducing data acquisition time by over an order of magnitude. Such time savings would maximize the number of vibratory measurements that could be performed on each animal and reduce motion artifact in the data due to respiration and other animal movement. Our approach uses a combination of high speed digitizers, a field programmable gate array (FPGA), and a graphical processor unit (GPU), along with custom software that takes advantage of parallelization and pipelining of the processing so that data is being processed as it is being collected. Because the data is processed nearly at the rate of data collection, the results of the experiment can be displayed with only a small time latency, i.e. in near real-time. Consequently, the acquisition parameters for an entire 6-D data set can be pre-set, and then collected all at once. Using this new software/hardware

combination, we have reduced the time required to collect a series of tuning curves for 20 frequencies and 10 amplitudes down to 14 s. With additional modifications to address inefficiencies in display and memory management, we expect to get even closer to the 10 s limit. Thus, by taking advantage of the latest advances in hardware and software, the experimentalist can quickly test and modify experimental protocols on the fly in order to maximize his/her productivity, collect more accurate data, and minimize the use of experimental animals.

PS 622

Elasto-hydrodynamic Model of the Deformable Semicircular Canals

Richard D. Rabbitt; Marta Iversen
University of Utah

Introduction

Classical models of the semicircular canals assume the membranous labyrinth is perfectly rigid and moves in synchrony with the temporal bone [1,2]. This model is adequate for modest low-frequency stimuli [3,4], but fails to capture responses to high accelerations, acoustic stimuli, or vibration. Here, we present a simple one-dimensional model of the deformable canal that captures both the low-frequency responses as well as high-frequency responses to sound and vibration. Results address biomechanical origins of Tullio Phenomenon, canal responses to acoustic stimuli [5,6], and residual responses of surgically plugged canals [7].

Methods

We combined an established approach used to model waves in elastic arteries [6,8], with a morphologically descriptive approach used previously to model rigid semicircular canals [1,2]. Conservation of momentum was applied to the endolymph and perilymph tangent to the duct centerline under unsteady laminar flow conditions [9]. The membranous labyrinth was modeled as a thin elastic shell, and the cupula as a visco-elastic gel. Equations were solved for head rotations and acoustic stimuli under normal and pathological conditions in frequency-domain for the linear case, and time-domain for the nonlinear case.

Results

The model can be written as a dispersive wave equation, similar to one-dimensional cochlear models but lacking local turning points key to the cochlear place principle. For low-frequency head rotations, equations reduce to the rigid-canal model and reproduce previous results [4]. At high frequencies, the membranous duct deforms, obscuring the upper-corner frequency present in classical models. Simulations reproduce residual plugged-canal responses [10], and the relationship between mechan-

ical indentation and head rotation [7,11]. Results for acoustic stimuli and vibration predict the presence of both standing and traveling waves, that are small under normal conditions but increase with canal dehiscence. These waves are predicted to cause phase locking to acoustic stimuli in sensitive irregularly-discharging afferents [12], and to induce tonic asynchronous afferent responses through fluid streaming [6] and nonlinear impedance pumping.

Conclusion

Results further confirm membranous labyrinth deformability is key to responses of canals to sound and vibration. Amplified sensitivity in the compromised labyrinth is consistent with canal dehiscence syndrome as well as normal responses to loud sounds and vibration. The model predicts that standing and traveling waves underlie cycle-by-cycle cupula vibration and phase locking of afferent discharge, and that nonlinear endolymph pumping underlies rectified cupula displacement and slow changes in afferent discharge during maintained acoustic or vibrational stimuli.

Funding

NIDCD R01 DC006685 (Rabbitt)

PS 623

Measurement of Fluid Movement in Scala Vestibuli

Eli Elyas¹; William E. Brownell²; Anders Fridberger¹

¹*Linköping University, Linköping, Sweden;* ²*Baylor College of Medicine, Houston, TX, USA*

Experimental measurement of fluid motion in cochlea has always presented a technical challenge, and the spatial resolution of currently available data is therefore relatively limited. This limits our understanding of fluid-structure interactions in the cochlea, especially for the low-frequency parts, which are most critical for speech perception.

Here we have applied the 'nano-ear' method to measure fluid movement in scala vestibuli. A small orifice was made at the cochlear apex of an excised temporal bone mounted onto a holder filled with oxygenated cell culture medium. The outer ear was kept isolated for sound stimulation. 50nm gold nanoparticles were introduced into the perilymph and were trapped with optical tweezers. A digital video camera was used to detect the vibration of trapped particles and their 3D movement was subsequently analysed using an in-house written software. The displacement of Reissner's membrane was measured by time-resolved confocal imaging and optical flow techniques.

We found the movement of the trapped nanoparticle peaked between 160 and 250Hz at a frequency that cor-

responded to the maximal displacement of Reissner's membrane at that location. The amplitude of the Reissner's membrane oscillation was smaller than the movement of the nanoparticles. There was a consistency in the depth profile of fluid movement and in that closer to the membrane the movement of the nanoparticles approached that of the Reissner's membrane. As expected, the movement of the nanoparticle was smaller at higher attenuations.

These initial findings show promise for a better understanding of cochlear fluid dynamics. In the next step we will use the developed technique to measure fluid motion at various depths in scala media.

PS 624

Intracochlear Pressures in Simulated Otitis Media with Effusion: A Temporal Bone Study

Mohamed A. Alhussaini¹; Nathaniel T. Greene²; Victor Benichoux³; Renee M. Banakis Hartl¹; Herman A. Jenkins¹; Daniel J. Tollin³; Andrew D. Brown³

¹*Department of Otolaryngology, University of Colorado School of Medicine*; ²*U.S. Army Aeromedical Research Laboratory*; ³*Department of Physiology and Biophysics, University of Colorado School of Medicine*

Background

Otitis media with effusion is a common cause of conductive hearing loss in children and adults and can produce deficits up to 30-40 dB. Previous studies have measured the effects of simulated effusion on middle ear mechanics, yet no study has assessed its effects on intracochlear pressures. Here, we measure intracochlear sound pressure levels, as well as umbo velocities, in cadaveric temporal bone before and after a simulated effusion.

Methods

Temporal bones of seven cadaveric hemi-cephalic specimens were prepared by complete mastoidectomies with facial recess approach to expose the ossicles and the cochlea. Sound pressure levels in scala tympani and scala vestibuli were measured with fiber optic pressure probes. Acoustic stimuli were applied to the ear canal via a speculum modified to accommodate speaker and microphone tubing, and sealed with a glass coverslip to provide a closed acoustical environment, while allowing umbo velocity measurements via laser Doppler vibrometry. Stimuli were pure tones presented between 100 Hz – 12 kHz. Effusion was simulated by filling the mastoid cavity and middle ear space with water.

Results

Acoustic stimulation with middle ear effusion resulted in mean decreases in umbo velocities of ~14 dB for low

(0.1-1 kHz), ~24 dB for mid-range (1-3 kHz) peak ~26 dB at 1kHz and 10 dB for high frequencies (3-10 kHz). Pressure levels in scala vestibuli were reduced by 8 dB for low frequencies, 12 dB for mid-range frequencies, and 6 dB for high frequencies. This attenuation was greater than in the scala tympani, which was reduced by 1 dB for low frequencies, 5 dB for mid-range frequencies and 3 dB for high frequencies. We finally computed the differential pressure between the two cavities, and found that it followed a similar trend with a peak attenuation due to effusion of ~20 dB at 1kHz.

Conclusion

Differential intracochlear pressure, the main driving force for the basilar membrane, displayed attenuation due to the simulated effusion comparable in magnitude to the change in umbo velocity. Additionally, this decrease in differential pressure appears to result from a decrease in scala vestibuli rather than a change in scala tympani pressure. Our results are consistent with previous studies measuring basilar membrane movements in animal models and with clinical data characterizing hearing loss due to otitis media with effusion.

PS 925

Mode Conversion and Activation of the Cochlear Amplifier: are They One and the Same?

Richard Chadwick

NIDCD

Mode conversion is a wave phenomenon studied in other fields such as plasma physics, geophysics, and optics. It occurs when the wave numbers of two non-orthogonal modes approach each other, and coincides with a breakdown of the passive energy conservation equation with a defined place-frequency map. In a dual wave model of the cochlea, this occurs when the tectorial membrane vibration (TM) leads the basilar membrane (BM) vibration by $\frac{1}{4}$ cycle. Recent OCT and simultaneous pressure/voltage measurements indicate that the onset of nonlinear compression may occur when the phase of the TM leads the phase of the BM by approximately a $\frac{1}{4}$ cycle. Thus the breakdown of the passive energy conservation equation may signal the activation of the cochlear amplifier.

PS 625

Cholinergic Receptor Expression in Primary Auditory and Rostral Belt Cortices After Noise Damage

Gregory J. Basura¹; Taylor Forest²; Tim J. Desmond³; Peter Scott⁴

¹Dept of Otolaryngology; Center for Human Growth and Development; University of Michigan; ²Dept of Otolaryngology; University of Michigan; ³The University of Michigan; ⁴Dept of Radiology, Division of Nuclear Medicine, the University of Michigan, MI, USA

Background

Hearing loss leads to increased spontaneous firing rates, neural synchrony and changes in response to bimodal (somatosensory-auditory) stimulation in auditory cortex (A1) and a region known to modulate A1 activity, the adjacent dorsal rostral belt (RB). Modulation is pairing order and interval dependent; a process consistent with spike-timing dependent plasticity (STDP; Basura et al., 2015). Acetylcholine has been shown to modulate STDP in other cortical areas including visual and pre-frontal through receptor-mediated mechanisms. Plasticity in A1 following noise-damage may reflect changes in cholinergic receptor expression. Here we investigated muscarinic (mAChR) and nicotinic (nAChR) expression in both A1 and RB following unilateral noise damage and a temporary threshold shift in hearing.

Methods

Three weeks following unilateral (left ear) noise-exposure (97dB SPL; narrowband at 7kHz for two hours) or anesthesia only for sham-controls, animals were sacrificed and brains sectioned through A1 and RB. Using radioligand binding to map muscarinic ([³H]scopolamine) and nicotinic ([¹⁸F]flubatine) receptors respectively, optical density was measured in both A1 and RB across all cortical layers (supra-granular, granular, infra-granular). Receptor density was measured using densitometry and results were analyzed using MatLab.

Results

[³H]Scopolamine binding to map mAChRs three weeks following noise damage was significantly decreased in both RB and A1 as compared to sham controls. Specifically, expression was decreased only in the right hemisphere (contralateral to noise exposure) across all layers in RB (supragranular, $p=0.0011$; granular, $p=0.0438$; and infragranular, $p=0.0468$) and in A1 (supragranular, $p=0.0180$; granular, $p=0.0209$; and infragranular, $p=0.0426$). No significant changes in [³H]scopolamine binding were seen in the left hemispheres (ipsilateral to noise-exposure) in either region or layer. [¹⁸F]Flubatine

binding to map nAChRs showed a non-significant increase in the right RB and A1 cortices, however neither hemisphere or region or layer were significantly changed following noise-exposure.

Conclusion

This study shows a conserved down-regulation of mAChRs in both A1 and RB cortices contralateral to unilateral noise-damage, with no significant changes in nicotinic receptor expression despite an upward trend. The mechanism by which mAChRs are reduced is currently unknown and may reflect pruned neurons secondary to noise, post-translational processing, or activity dependent down-regulation. Regardless, these data demonstrate that noise-damage may preferentially influence auditory cortical interneurons that are typically populated by muscarinic receptors versus nicotinic receptors that are traditionally found on thalamocortical projections. This differential response to noise may ultimately influence cortical plasticity and function.

PS 626

Transcriptional Shifts in Genes for Excitatory and Inhibitory Neurotransmission Predict Functional Recovery of Cortical Sound Processing After Near-complete Cochlear Denervation

Pooja Balaram; Daniel B. Polley
Eaton-Peabody Laboratories, Massachusetts Eye and Ear Infirmary

Background

Lesioning cochlear afferent neurons depresses sound-evoked activity early in the auditory pathway but causes a paradoxical increase in sound-evoked responsiveness at the level of the auditory cortex (ACTx). In some animals, enhanced cortical gain contributes to the recovery of normal behavioral detection thresholds and supports neural decoding of rudimentary sound features (Chambers et al., 2016). In other animals, cortical sound processing never fully recovers despite an equivalent loss of cochlear afferent synapses and ABR amplitude. What are the mechanisms underlying these different functional endpoints? We addressed this question by eliminating ~95% of Type-I cochlear afferents and then compared sound-evoked cortical responsiveness against the expression levels of genes that encode excitatory (E) and inhibitory (I) neurotransmitter receptors.

Methods

We characterized functional recovery with chronic wide-field calcium imaging in awake, head-fixed adult mice that expressed a genetically encoded calcium indicator (GCaMP6) in cortical pyramidal neurons. After establishing baseline levels of sound-evoked activity, ouabain was applied to the contralateral cochlear round window,

which eliminates the ABR and ~95% of cochlear afferent synapses. Thirty days following denervation, when individual mice had staged various degrees of functional recovery, their brains were extracted and transcript counts for AMPA and GABAA postsynaptic receptor subunits were quantified in individual neurons using fluorescent in situ hybridization. Individual differences in transcriptional E/I balance were then compared to individual differences in central gain.

Results

Across individuals, ACtx neurons express higher levels of AMPA receptor transcripts and lower levels of GABAA receptor transcripts, which could contribute to increased central gain. E/I shifts were more pronounced in ACtx than the inferior colliculus. Sound-evoked cortical activity recovered slowly, and to variable degrees in different mice. Our ongoing analysis seeks to align the functional recovery in a given region of ACtx against the E/I transcription balance in the underlying neurons.

Conclusions

Significant and opposite shifts in gene expression for AMPA and GABAA receptors were observed after a near-complete loss of cochlear afferent synapses. We present a new approach to relate homeostatic regulation of E/I gene transcription to the status of functional recovery in individual mice. Our ongoing analysis will reveal how much of the variance in functional recovery and central gain can be predicted from E/I transcription shifts and not, for example, to changes in protein expression or intrinsic excitability.

PS 627

Resting State Networks of Tinnitus Patients Are Replicable: A Preliminary Study

Sara Schmidt¹; Fatima T. Husain²; Yihsin Tai¹

¹University of Illinois at Urbana-Champaign; ²Department of Speech and Hearing Science, University of Illinois at Urbana-Champaign

Recently, resting state functional magnetic resonance imaging (fMRI) studies of tinnitus have revealed that tinnitus, independent of hearing loss, affects the connectivity within and across resting state networks. These networks are defined by correlations in the spontaneous fluctuations of the blood oxygenation level-dependent (BOLD) response across the brain. In our own work, we have previously noted decreased correlations between the Default Mode Network (DMN) and the precuneus, as well as increased correlations between the Auditory Network (AUD) and the parahippocampus in tinnitus patients when compared to hearing loss or normal hearing control groups. While most resting state fMRI studies of tinnitus have indicated that its presence does change

network connectivity, across research groups, there is little consistency in the specifics of these changes. To determine why results have been variable, it is first important to establish the replicability of resting state networks in tinnitus. While resting state networks have been shown to replicate well in a non-tinnitus, normal population, this has not been directly assessed in tinnitus patients.

In this preliminary study, we examined the replicability of three resting state networks (the DMN, AUD, and Dorsal Attention Network) in 10 participants with chronic tinnitus using a seed-to-voxel connectivity analysis. Resting state fMRI data were collected from participants twice, in two visits separated by exactly one week. Tinnitus severity of the participants, as measured by the Tinnitus Functional Index, was an average of 30.61 across both visits (std: 22.81, range: 0.85-72). Individual scores did differ on each scan day, ranging from a 0.2 to an 11.1 point difference between visits, but the group average TFI score was similar across visits (average visit 1: 30.53, visit 2: 30.69). The pure tone average (measured at 0.5, 1, 2, 4 kHz) of participants ranged from 5-30.625 dB (average 16.5 dB, std: 7.80 dB). When participants' first scans were compared to their second, no significant differences in connectivity were noted in any of the networks examined. This suggests that resting state networks of tinnitus patients are replicable, and that differences across resting state fMRI studies of tinnitus are likely due to differences in analysis technique and the populations examined. This study is ongoing; additional data from tinnitus patients and control participants without tinnitus but matched hearing profiles is currently being collected and analyzed.

PS 628

Remediation of Deprivation-induced Gap Detection Deficits by Passive Stimulus Exposure

Yi Ye¹; David B. Green²; Michelle Mattingly¹; Jen Gay¹; Merri J. Rosen¹

¹Northeast Ohio Medical University; ²NEOMED

In childhood, partial hearing loss, such as that induced by otitis media, can produce prolonged deficits in speech perception and temporal processing. Early therapeutic interventions that target temporal processing may improve later speech-related outcomes in this population. Gap detection, a measure of temporal processing ability, relies on local circuitry within auditory cortex (ACx), and auditory deprivation alters intrinsic and synaptic properties in ACx, particularly during critical periods of development. Thus, early deprivation should induce deficits in gap detection abilities, and this should be reflected in ACx gap sensitivity.

Here, we tested whether early auditory deprivation, induced by ear-plugging, caused correlated deficits in behavioral and cortical gap detection, and whether these could be remediated by brief exposure to gaps in background noise. We compared Mongolian gerbils that were ear-plugged from P11-24 with non-plugged controls. Short gaps were inserted into a bandpass (2.5-20kHz) 50dB background noise. After earplug removal, for three hour-long sessions across 7 days, animals were placed in small restrainers in an acoustic startle apparatus, and exposed to either Silence or the bandpass noise containing gaps (i.e., no acoustic startle sounds were presented). Gap detection ability was then measured using three sessions of gap-prepulse inhibition (gap-PPI) of the acoustic startle response in the same testing apparatus, followed by single- and multi-unit recordings from ACx under urethane anesthesia. Gap-PPI detection thresholds (GDTs) were significantly higher in ear-plugged Silence-Exposed animals than in Silence-Exposed controls. Gap-Exposure eliminated this detection deficit. Cortical GDTs were also increased in the ear-plugged Silence-Exposed group compared with Silence-Exposed controls, and Gap-Exposure eliminated this difference. This was primarily due to a reduction in the proportion of cells with high sensitivity to short gaps. Furthermore, both first-spike latency and first-spike jitter were increased in ACx cells of ear-plugged Silence-Exposed animals, an effect which was not present in ear-plugged Gap-Exposed animals. Thus early transient hearing loss induced a gap detection deficit that was remediated by three brief, passive sessions of exposure to gaps in background sound. Auditory cortical neurons reflected both the detection deficit and the effect of remediation. The increase in first-spike latency and jitter suggests there may be broader temporal processing deficits than those measured here. Furthermore, the remediation of first spike timing by passive gap exposure suggests that brief stimulus exposure, perhaps in a salient context such as the unfamiliar placement into the testing apparatus, may improve not only gap detection, but also general deficits in temporal processing.

PS 629

Maladaptive Gain Control Along the Central Auditory Pathway Following Acoustic Trauma

Benjamin D. Auerbach¹; Mostafa Gobadi²; Guang-Di Chen¹; Kelly Radziwon¹; Ehsan Esfahani²; Richard Salvi¹

¹*Center for Hearing & Deafness, Department of Communicative Disorders and Science, State University of New York at Buffalo;* ²*Human in the Loop System*

Laboratory, Department of Mechanical and Aerospace Engineering, State University of New York at Buffalo

Auditory neurons must adapt their response properties to a constantly varying stream of sensory input in order to optimize the encoding of sound intensity over a wide-range of conditions. Recent evidence indicates that the auditory system compensates for diminished auditory input associated with hearing loss by increasing neuronal gain at multiple sites along the central auditory pathway. Excessive central gain enhancement, however, can lead to maladaptive intensity coding and aberrant sound perception. Indeed, hearing loss is often associated with a paradoxical enhancement of sound-evoked responses in central auditory structures which likely contributes to auditory perceptual disorders like tinnitus and hyperacusis. Determining where this hyperactivity originates and which structures most contribute to these disorders has remained elusive due to the complex and interconnected nature of the auditory system, which engages in extensive bottom-up and top-down processing via recurrent connectivity. In order to gain new insights into the progression of central gain enhancement, we performed concurrent multi-electrode extracellular recordings from multiple levels of the auditory system before and after mild acoustic trauma. We found a progressive recovery of sound-evoked responses at ascending auditory stations, demonstrating that sound intensity coding can be restored along the central auditory pathway via increased neuronal gain. Interestingly, we observed a robust hyperactivity in the auditory cortex, due mainly to increased intra-cortical processing as assessed by current source density analysis. These results suggests that neural activity is not passively transmitted from lower to higher levels of the central auditory system, but undergoes progressive amplification at each successive stage of processing. In order to determine how information transfer along the central auditory pathway is affected by acoustic trauma and the resulting gain changes, we applied multivariate autoregressive modeling (i.e., Granger causality) to the electrophysiological recordings. Our results show that causality patterns along the ascending auditory pathway are intensity and frequency dependent and follow expected tonotopic and laminar distributions. Following acoustic trauma, we observed complex changes in the pattern of causality indicative of changes to both intra-structure information transfer and inter-structure communication. These results suggest that central gain enhancement is associated with complex dynamics in activity throughout the central auditory pathway, which likely contributes to maladaptive intensity coding and aberrant loudness perception associated with hearing loss.

PS 630

Event-Related Potential Correlates of Auditory Discrimination in Children with Mild to Moderate Sensorineural Hearing Loss

Axelle Calcus¹; Outi Tuomainen¹; Stuart Rosen²; Xiaowen Wang¹; Lorna Halliday¹

¹University College London; ²UCL, London, UK

Introduction

This study aimed to investigate the effects of mild to moderate sensorineural hearing loss (MMHL) on auditory discrimination of speech, speechlike and nonspeech stimuli in children, using the Mismatch Negativity (MMN).

Methods

We tested 46 children with MMHL and 44 normally-hearing controls, aged between 8-16 years. All children were monolingual British English native speakers and had normal nonverbal IQ. Children were presented with a passive two-deviant oddball paradigm, using three different types of stimuli. In the “nonspeech” condition, the standards were 1-kHz pure tones, and the deviants were frequency-modulated pure tones at a rate of 40 Hz that varied in modulation depth (1%: small deviant; 10%: large deviant). In the “speech-like” condition, the standards were complex periodic sounds and the deviants were modulated in f0 at a rate of 4 Hz around a centre frequency of 100 Hz. (20 Hz: small deviant; 200 Hz: large deviant). In the “speech” condition, the standards were consonant-vowel /ba/ syllables, and the deviants were taken from a /ba/-/da/ continuum (/ba/-like sound: small deviant; /da/-like sound: large deviant).

Results

Preliminary results suggest that control children had larger responses than children with MMHL as evoked by all types of deviants. Latency and amplitude of the MMN will be compared across groups and types of deviants, with respect to the size of the deviant.

Discussion

Results will be discussed with respect to the developmental effects of hearing loss on auditory processing of speech, speechlike and nonspeech stimuli in children.

PS 631

Changes in Corticocollicular Feedback Following Cochlear Synaptopathy

Meenakshi Asokan¹; Ross S. Williamson²; Daniel B. Polley¹

¹Eaton-Peabody Laboratories, Massachusetts Eye and Ear Infirmary; ²Eaton Peabody Laboratories, Massachusetts Eye and Ear Infirmary

Background

Layer 5 cortico-collicular (CCol) neurons are a prominent component of the corticofugal pathway and provide a major source of descending feedback for neurons in the inferior colliculus (IC). Despite the density of corticofugal projections, little is known about their role in auditory stimulus processing and plasticity following hearing loss. In mice, CCol axons form a dense plexus on the dorsal cap of the IC, between the cerebral cortex and cerebellum, thereby providing easy optical accessibility. Here, we expressed a genetically encoded calcium indicator, GCaMP6, in cortical neurons and imaged changes in sound-evoked activity in CCol axons before and after a moderate loss of cochlear afferent synapses that causes only a temporary shift in auditory brainstem response (ABR) thresholds.

Methods

CBA/CaJ mice aged 4-6 weeks were injected with a viral vector to induce expression of GCaMP6s in cortical neurons. A 3mm glass cranial window was installed atop the ipsilateral inferior colliculus. Sound-evoked CCol axon activity was repeatedly imaged in awake, head-fixed mice with a widefield epifluorescence microscope. Central gain was estimated from the growth of CCol axon activity for tone bursts and noise bursts ranging from 10-80 dB SPL. Temporary Threshold Shift (TTS) was induced by acoustic exposure to an octave band of noise (8-16 KHz) presented at 99 dB SPL for two hours. Auditory brainstem responses (ABR) and distortion product otoacoustic emissions were measured pre-exposure and periodically post-exposure.

Results

CCol axon activity increased monotonically with SPL within a circumscribed region atop the dorsal surface of the IC. No changes were observed in neighboring regions of the cerebellum. Central gain in CCol axons was relatively stable from one day to the next prior to noise exposure. Central gain in CCol axons was reduced immediately following TTS but then increased above baseline levels on subsequent days. Our ongoing analysis is focusing on the precise time course of central gain changes in CCol neurons as they relate to the growth of early and late waves in the ABR.

Conclusion

We implemented a chronic imaging approach to isolate population activity from corticofugal neurons and tracked changes in their sound-evoked activity before and after cochlear synaptopathy. The findings suggest that there is a robust acoustically driven response that originates from the cortex and spreads down through the descending projections to provide feedback to IC. Changes in the strength of cortical feedback could contribute to central gain changes in the IC after hearing loss.

PS 632

Presbycusis related Plasticity Changes in the Hippocampus

Marlies Knipper; Angelika Kübler; Chengfang Chen; Hyun-Soon Geisler; Lukas Rüttiger; Wibke Singer
University of Tübingen, Department of Otolaryngology, Tübingen Hearing Research Centre (THRC), Molecular Physiology of Hearing, Elfriede-Aulhorn-Str. 5, 72076 Tübingen, Germany

Age related hearing loss is one of the most common disabilities in humans. In rodents we could show that age related hearing loss occurs mainly in the last third of the lifespan. Before disturbed OHC function becomes obvious, an elevation of hearing thresholds for higher frequencies is already detectable. Such changes were found in old, but also already in middle aged animals.

We recently reported that, as long as sufficient compensatory neuronal gain is preserved, suprathreshold temporal coding of amplitude modulated stimuli was maintained, independent of age. However, in old animals central neuronal gain was reduced and temporal coding failed (Möhrle et al. 2016). We also observed that central auditory circuit changes affect hippocampal circuits (Singer et al., 2013; Rüttiger et al., 2013; Chumak et al., 2015). We here use a new generated BLEV mice model to investigate plasticity changes in the hippocampus linked to presbycusis.

Möhrle et al. Loss of auditory sensitivity from inner hair cell synaptopathy can be centrally compensated in the young but not old brain. *Neurobiol Aging*. 2016 May; 44:173-184.

Singer et al. The function of BDNF in the adult auditory system. *Neuropharm* 2014 Jan; 76: 719-728.

Rüttiger et al. BDNF mRNA expression and protein localization are changed in age-related hearing loss. *Neurobiol Aging* 2007 Apr; 28(4):586-601

Chumak T, Rüttiger L, Lee SC, Campanelli D, Zuc-cotti A, Singer W, Popelář J, Gutsche K, Geisler HS, Schraven SP, Jaumann M, Panford-Walsh R, Hu J, Schimmang T, Zimmermann U, Syka J, Knipper M (2015) BDNF in Lower Brain Parts Modifies Auditory Fiber Activity to Gain Fidelity but Increases the Risk for Generation of Central Noise After Injury. *Mol Neurobiol*. 2015

Acknowledgments:

This study was supported by grants from the Deutsche Forschungsgemeinschaft DFG-Kni-316-10-1, KN316/12-1, and RU713/5-1), and the Hahn Stiftung (Index AG).

PS 633

Prolonged Exposure to Moderate-Level Noise Induces Selective Plasticity in Rat Auditory Cortex

Guang-Di Chen¹; Benjamin D. Auerbach¹; Xiaopeng Liu²; Jerry Tseng²; Richard Salvi¹

¹Center for Hearing & Deafness, Department of Communicative Disorders and Science, State University of New York at Buffalo; ²Center for Hearing and Deafness, SUNY at Buffalo

Background

Urban environments are noisy most of the time. In New York City, the Leq ranges from 50-90 dBA; during the night the city-wide average is between 65 and 70 dBA and during the day the levels are above 70 dBA. The effects of moderate intensity continuous noise on the peripheral and central auditory system are poorly understood. In cats, long-term exposure to moderate intensity, narrowband noise induces frequency dependent hypo-activity in the noise band and hyperactivity at the edges of the noise. In rats the observations showed an expanded representation in central auditory centers at the exposure frequency. Whether these changes result from peripheral hearing loss versus central auditory plasticity are unclear. To address this question, we made electrophysiological recordings from both the cochlea and auditory cortex (AC) following continuous, long duration exposure to an octave band noise (OBN) presented at a moderate-level.

Methods

Sprague-Dawley rats were continuously exposed to an OBN (10-20 kHz) at 75 dB SPL for 6-8 weeks. Control rats were only exposed to ambient noise in the colony. The effects of the noise exposure were assessed by recording the cochlear compound action potential (CAP) and electrophysiological recordings (16-channel micro-electrode array) from several subdivisions of the AC 0-10 h and 3 weeks post-exposure.

Results

The 75-dB noise significantly reduced the CAP amplitude at frequencies within the noise band; however, the CAP amplitude completely recovered 3 weeks post-exposure. In contrast to the reduced cochlear response, sound-evoked hyperactivity was observed immediately after the noise exposure in the AAF of AC whereas sound-evoked activity in other AC regions around AI and VAF/SRAF were generally reduced or unchanged. The noise-band-related hyperactivity in the AAF disappeared when measured 3 weeks post-noise, when the CAP was recovered.

Summary

Continuous exposure to low level noise similar to that found in urban environments temporarily reduced the neural output of the cochlea. The cochlear reduction was associated with transient hyperactivity only in the AAF, but not other AC-regions. The sound-evoked activity in the AAF subdivision overcompensates for the reduced output from the cochlea. The heightened activity in the AAF, thought to be important for the detection and analysis of communication sounds, may increase the salience and importance of biologically relevant warning signals. The functional changes observed in the cochlea (hypoactivity) and AAF (hyperactivity) completely recovered 3 weeks post-exposure providing evidence of neuroplastic changes in both the central and peripheral auditory system.

PS 634

Prolonged Development of Temporal Integration in Auditory Cortex

Jen Gay; Merri J. Rosen; Jennifer Gay
Northeast Ohio Medical University

Auditory perception has a varied developmental timeline, as some percepts reach maturity early in life while others show a more prolonged course of maturation that can last throughout adolescence. Behavioral studies have shown prolonged developmental trajectories for detecting silent gaps in noise, and for detecting short duration stimuli, indicating immature temporal integration abilities. Immature performance in adolescents occurs well past the time point in development where the peripheral auditory system has adult-like function, implying that more central mechanisms are involved. Consistent with this, cortical inhibition, which contributes to processing temporally-varying stimuli, has a prolonged developmental trajectory, with IPSC amplitudes and decay rates reaching adult-like levels very late in development. Despite these data, many neural studies of temporal processing in the central auditory system have focused either on adult responses or on the robust changes that occur during early critical periods.

To examine temporal integration differences between adolescent and adult neurons, single- and multi-unit recordings were made from the left primary auditory cortex of awake, head-fixed Mongolian gerbils in adolescents (P25-30) and mature adults (P90-P130). We presented sound bursts of varying durations at the best frequency for each cell. Compared to adults, adolescent cells showed sustained firing responses to tones of short durations, along with decreased discriminability across tones of different durations. Given that our adolescent population had more sustained firing to short tones, we hypothesized that a gap presented after a short lead

burst would be more difficult for adolescent neurons to detect than adult neurons. This is supported by behavioral evidence in humans, where gaps presented early in a background noise are more difficult to detect than those presented later, presumably due to the close apposition of the initial response and the response to the gap. To test this idea, we presented gaps of varying durations inserted at several delays relative to signal onset. Consistent with previous data, neural adult gap detection thresholds were higher as gaps were presented closer to signal onset. Adolescent gap detection thresholds showed the same pattern, but the increased thresholds for short delays between signal onset and gap were significantly higher than in adults. These differences may be due to immature cortical inhibition, and suggest a potential neural substrate for immature performance on temporal integration tasks in adolescents.

PS 635

Neonatal Hypoxia-ischemia Causes Functional Circuit Changes in Developing Auditory Cortex

Aminah Sheikh¹; Xiangying Meng¹; Ji Liu¹; Patrick O. Kanold²

¹University of Maryland; ²The University of Maryland

Embryonic brain development is crucial for the proper maturation of neural circuits. While in-utero, the embryo is vulnerable to injuries that have potential to cause long-term health problems and disorders such as epilepsy and cerebral palsy. For example, premature white matter brain injury results in disruption of normal brain maturation and consequently increases risk of developing neurological disorders in infants. Neonatal hypoxia-ischemia (HI) in the preterm human results in damage to subcortical developing white matter, a condition referred to as periventricular leukomalacia (PVL). One population of neurons that HI injures are the developing neurons in the subcortical white matter region of the brain, the subplate. Subplate neurons (SPNs) are among the first cortical neurons to be born and lesion studies showed that SPNs are necessary for proper functional development of the cerebral cortex. Thus, while it is clear that SPNs play a major role in the maturation of developing brain circuitry, the amount of circuit changes in subplate and cortical plate consequent to developmental injuries is unknown.

We address these issues by using a rodent stroke model of HI to induce either Mild HI or Severe/Moderate HI (Sev/Mod HI). We used laser-scanning photostimulation (LSPS) in acute thalamocortical slices of rat auditory cortex during P5-10 to study the functional connectivity of subplate and layer 4 neurons in both injuries. We find that while Sev/Mod HI results in noticeable gross

histological abnormalities likely to loss of SPNs, Mild HI brains seemed normal. We next analyzed the spatial differences in excitatory and inhibitory synaptic circuits. Both severities of HI result in hyperconnectivity of excitatory and inhibitory circuits to SPNs. Sev/Mod HI results in hypoconnectivity of excitatory and inhibitory connections to layer 4 while Mild HI did not alter connectivity within layer 4. Our results suggest that Sev/Mod HI is detectable on the gross anatomical level, unlike Mild HI. However, both severities of HI alter synaptic connectivity as well as the strength of these connections of subplate and layer 4 in distinct manners. Importantly mild injuries seem to selectively affect subplate neurons. Funded by NIDCD RO1DC009607

PS 636

Cross-modal Plasticity of Excitatory Intracortical Circuits in A1 Requires Arc

Xiangyang Meng¹; Hey-Kyoung Lee²; Patrick O. Kanold³

¹University of Maryland; ²Johns Hopkins University;

³The University of Maryland

Sensory systems do not work in isolation but interact with each other. For example the interactions between the auditory and visual systems become evident during sensory loss. For example, cross-modal compensation in blind individuals leads to functional enhancements of the remaining senses, including enhanced frequency discriminations in the auditory domain. Previous results in mice show that short-term visual deprivation (dark exposure, DE) leads to improvement in frequency selectivity and synaptic changes in primary auditory cortex (A1). On the cortical circuit level, DE leads to refinement of intra- and inter-laminar excitatory and inhibitory connections A1. However, the underlying pathways that are engaged by DE in A1 are not known. Arc is a single copy gene that is a main effector molecule downstream of many pathways leading to synaptic changes. Since Arc is required for long-term synaptic changes and learning we tested whether Arc is also required for the circuit effects of DE. To address this question, we dark exposed trans-genetic Arc knock-out mouse (ArcKO). Since Arc is almost exclusively expressed in CaMKII-positive glutamatergic neurons in the hippocampus and neocortex and since Arc is involved in AMPA receptor trafficking, we hypothesized that changes in visual experience can cause refinement only in inhibitory but not excitatory synaptic connections within A1.

We investigated this hypothesis by comparing intracortical connections to Layer 2/3 neurons in dark-exposed ArcKO mice to those from normally reared ArcKO mice. We study the spatial pattern of excitatory and inhibition

connections in acute slices of A1 using laser-scanning photostimulation (LSPS). We find that inhibitory but not excitatory circuits related to layer 2/3 neurons are different in dark exposed ArcKO mice than those from normally reared ones.

Our results show that the cross-modal plasticity of excitatory connections in A1 involves Arc.

PS 637

Whole-Brain Functional Connectivity in Hearing and Early-Deaf Cats Using High-Field Functional MRI

Daniel Stolzberg; Blake E. Butler; Stephen G. Lomber
Department of Physiology and Pharmacology, University of Western Ontario

Magnetic Resonance Imaging (MRI) permits the simultaneous study of whole-brain networks. Identifying how these networks are altered in models of hearing loss and deafness will lead to novel insights guiding how to best approach aural rehabilitation and auditory prosthetic devices. High-field functional MRI (7T) was used to image whole-brain blood-oxygen level dependent (BOLD) fluctuations of mature normal hearing and postnatally deafened (early chronic aminoglycoside antibiotic treatment) cats under light anesthesia at a resolution of 1 mm³. Group independent component analysis (ICA; GIFT implementation with Icasto validation) was used to identify distinct spatiotemporal patterns in whole-brain BOLD fluctuations during resting state scans. ICA uncovered several distinct bilateral resting-state networks in eight normal hearing mature cats, including separate components for a dorsal auditory network and a ventral auditory network. Somatosensory, somatomotor, visual, and limbic networks were also uncovered using ICA in normal hearing cats which exhibited strong similarity to human and non-human primate resting-state networks. ICA was also performed on resting state functional MRI data for five mature early-deafened cats. Differences between ICA networks and other functional connectivity measures are contrasted between normal hearing and early-deafened cats.

PS 638

A Probabilistic Model of Absolute Auditory Threshold: Key Components and Parameter Values

Peter Heil; Artur Matysiak; Heinrich Neubauer
Leibniz Institute for Neurobiology

The detection of sounds in quiet is among the simplest tasks performed by the auditory system. Detection thresholds, specified in terms of sound level, depend on the temporal envelope of the stimulus and decrease with increasing stimulus duration in every species studied. The neural mechanisms underlying these observations are not fully understood. They are frequently thought to involve the operation of a leaky integrator of sound intensity, but the long time constants required are at variance with the exquisite temporal resolution of the auditory system. We used a forced-choice procedure to measure thresholds from 227 human ears for 3.125-kHz tones differing in the shape of the temporal envelope and duration. We grouped ears according to their mean threshold, with ears in groups 1 and 5 having the lowest and highest thresholds, respectively. We find that the differences in group-mean thresholds for different stimuli decrease from group 1 to group 5. Thresholds increase slightly when the duration of silent gaps between successive tone bursts is prolonged beyond a few milliseconds, as studied in 16 ears. The data are well described by a probabilistic model in which the stimulus gives rise to stochastic neural detection events and threshold is reached when a criterion number of events have occurred (probability summation). Because no long-term integration is required, the model is consistent with the high temporal resolution of the auditory system. The model assumes that detection events occur with a probability proportional to the bandpass-filtered time-varying amplitude, above some lower bound, raised to an exponent. The gain decreases slightly over time to account for the effects of gap duration. Model fits show that, from group 1 to group 5, the filter bandwidth and lower bound increase and the time-dependent gain decrease becomes less pronounced. The exponent is approximately 3, consistent with our previous studies. Our model provides a physiologically plausible description of absolute threshold and its dependence on stimulus parameters and challenges models in which stimulus intensity is the relevant physical quantity for the auditory system.

Supported by the Deutsche Forschungsgemeinschaft (SFB-TR31 A6 to PH).

PS 639

Implications of Novel Logical Premises on Accuracy of Estimation of Sensory Threshold by Psychophysics

Amitava Biswas

University of Southern Mississippi

Determination of sensory threshold is often necessary for variety of diagnosis and treatment in otolaryngology and pathology. A common example is the audiologic evaluation of an individual who needs a hearing aid. Unlike motor behavior such as running speed that can usually be observed and quantified directly, sensory acuity such as hearing capability is normally quantified with some kind of psychophysical trial and error approach. Usually, very simple rough estimation of threshold calculations have been traditionally adopted for day to day clinical needs. Nevertheless, for the purpose of futuristic research, to obtain the most precise estimates, it may sometimes be necessary to apply various logical principles to extract the underlying model behavior from empirical data that are usually corrupt with variety of perturbations. For example, psychophysical data of stimulus strength versus detection rate usually appear nonmonotonous when known to be essentially monotonous in principle. An often confusing and usually avoided, Probit algorithms are traditionally needed to iteratively calculate an optimal regression curve for such nonmonotonous data and then deduce the 50% detection threshold level. A few logical premises are presented that enable monotonicity even with nonmonotonous observed rates. Monte-Carlo simulation demonstrated that this strategy not only finds a monotonic relation between detection rate versus stimulus intensity, but also significantly improves accuracy of estimation of the 50% threshold level. In conclusion, these logical premises can help to obtain uniform monotonicity of the sigmoid shaped psychometric regression curve, even without using conventional probit iterations, leading to faster and simplified estimation of the 50% threshold point with greater accuracy.

PS 640

Will Bayesian Adaptive Procedures Improve the Efficiency of Loudness Balancing?

Yi Shen¹; Celia Zhang²

¹*Indiana University Bloomington*; ²*University at Buffalo, The State University of New York*

Balancing the loudness of stimuli across a number of experimental conditions could be a time-consuming but necessary process in many auditory psychophysical experiments. This usually involves having the listener compare the loudness of each stimulus to a common reference sound and adjusting the stimulus intensity on

a trial-by-trial basis according to an adaptive procedure. For this purpose, one of the most commonly adopted adaptive procedures is the interleaved staircase (ISC) procedure (Jesteadt, 1980, *Atten. Percept. Psychophys.* 28). The current study uses the equal-loudness-level contour as an example to compare the efficiency and accuracy of the ISC procedure to two Bayesian adaptive procedures. Throughout the two experiments, a 1-kHz, 60-dB SPL pure tone was used as the reference stimulus. To achieve equal loudness to the reference tone, the intensity of the test tones were estimated as a function of the test tone frequency between 250 and 4000 Hz. Two Bayesian adaptive procedures were implemented. One of the Bayesian procedures, namely the interleaved maximum likelihood (IML) procedure, conducts loudness matching on a frequency-by-frequency basis. The second Bayesian procedure, the interleaved threshold contour (ITC) procedure, randomly picks a test frequency from trial to trial and optimizes the stimulus intensity for the selected frequency. Experiment I was conducted to validate the ITC procedure using naïve, normal-hearing listeners. The equal loudness level was estimated twice using the ITC procedure. During the second ITC run, a 10-dB attenuation was applied to test stimuli below 500-Hz. The artificial shift of the loudness level contour was well captured by the ITC procedure. The ITC procedure also demonstrated satisfactory test-retest reliability. Experiment II ran the ISC (~500 trials per run, two runs), IML (~500 trials per run, two runs), and ITC (200 trials per run, one run at the end of data collection) procedures for each listener. The equal-loudness-level contours from individual procedures were compared to a best estimate based on the pooled data across the two experiments and three procedures (~2600 trials). Results show that the reliabilities and accuracies of the ISC and IML procedures are comparable. The ITC procedure could provide a reliable estimate of equal-loudness-level contour with improved efficiency for experienced listeners but not for naïve listeners.

PS 641

Pitch-Trained Neural Networks Replicate Properties of Human Pitch Perception

Ray Gonzalez¹; Josh H. McDermott²

¹*MIT, Department of Brain and Cognitive Sciences, Cambridge, MA;* ²*MIT*

Pitch perception is among the most studied aspects of human hearing, and exhibits well established dependencies on a number of stimulus characteristics. In human listeners, pitch is predominantly determined by low-numbered harmonics that are resolved by the cochlea, but is also conveyed to a lesser extent by high-numbered harmonics that are individually unresolved. Moreover, the

relative phases of harmonics influence pitch perception only when the stimulus consists of unresolved harmonics. To better understand if these dependencies arise from information constraints intrinsic to the problem of extracting pitch from peripheral auditory representations, we trained neural networks to estimate the pitch of tones in noise. The tones were intended to mimic properties of mammalian vocalizations, being the product of a harmonic source signal with several coarsely tuned bandpass filters whose peak frequencies varied randomly across sounds. These tones were embedded in noise whose spectrum and relative level was also varied randomly across sounds. The networks were trained to classify the cochleagram of each sound in the training set according to its F0. We trained several neural network architectures, and then tested the best performing architecture on complex tones that varied in harmonic composition and phases (as in classic psychoacoustic experiments). The network qualitatively replicated several features of human pitch perception, including better performance for tones containing resolved harmonics and worse performance for random phase harmonics when the harmonics were unresolved. The results are consistent with the notion that human pitch perception exhibits near-optimal performance characteristics for the task of estimating fundamental frequency from peripheral auditory representations.

PS 642

Lossy Compression of Uninformative Stimuli in the Auditory System

Wiktor Młynarski¹; Josh H. McDermott²

¹*Massachusetts Institute of Technology;* ²*MIT*

Despite its high temporal precision, the auditory system appears to not encode the fine detail of some classes of natural sounds. Sounds known as “auditory textures” instead seem to be encoded in a compressed, “lossy” representation consisting of a set of time-averaged statistics. One explanation of this phenomenon is that the auditory system compresses stimuli that exceed its informational bandwidth. Alternatively, compression could reflect an efficient coding strategy in which the auditory system maximizes information about the environment while minimizing energy expenditure. In such a scenario the optimal strategy is to decrease encoding accuracy (i.e. coding cost) of stimuli that carry little or no information about the state of the environment. Stimuli originating from a known and predictable distribution, such as auditory textures, whose statistical properties are typically stationary, should be therefore compressed with a loss.

In order to distinguish between the two hypotheses it is necessary to characterize stimuli in terms of 1) the re-

sources required to accurately encode them and 2) their stationarity (i.e. how quickly their properties change over time). We thus introduced practical measures to quantify these concepts. We measured the representation cost (or entropy) as the number of spikes required to encode the sound with a simple model of the auditory nerve. We quantified stimulus stationarity by measuring the degree of change to the sound spectrum across successive time windows. We then assessed the fidelity of encoding in human listeners by asking them to discriminate exemplars of the same texture, for a range of textures. We found that human listeners' ability to discriminate sound exemplars was predicted by stationarity rather than representation cost – discrimination of sounds generated by a homogenous source was consistently poor regardless of the number of spikes needed to encode them.

Our results are consistent with the hypothesis that compressing auditory textures via statistical representations is an adaptive coding strategy aimed at minimization of neural resources allocated to represent uninformative stimuli.

PS 643

The Effect of Contralateral Noise on Behavioral Thresholds in Human is Low-Frequency Biased

Eric Verschooten¹; Elizabeth A. Strickland²; Philip X. Joris¹

¹University of Leuven; ²Purdue University

Noise presented to one ear has been shown to increase behavioral thresholds and decrease otoacoustic emissions in the other ear, which could be consistent with the action of the medial olivocochlear reflex (MOCR). In our previous electrophysiological study in human we found almost no effect of contralateral noise on the compound action potential for a tone at 4 kHz, but a clear effect on the neurophonic at low frequencies (500-700Hz), suggesting that the contralateral evoked MOCR is low-frequency biased. This would be consistent with previous OAE results. Moreover, we found similar trends in psychophysical measurements in the same group of subjects. In the present psychophysical study, we examine the low-frequency hypothesis more closely and assess the frequency-dependence (e.g., frequency-limit) of effects of contralateral noise over a wide frequency range.

The effect of contralateral broadband noise (0.1-8kHz) on threshold for short probe tones was measured for frequencies between 0.5-6.5kHz. Thresholds were obtained with a 3-alternative forced-choice method using the PsyAcoustX research package. Stimuli were delivered with ER-2 insert earphones and Lynx-TWO soundcard. All subjects had audiograms and

tympansograms within the normal range. Threshold for acoustic reflex (middle ear muscle) were obtained for 1 kHz tones and broadband noise. All measurements were performed in acoustically shielded rooms. First, the change in threshold as a function of contralateral noise level was assessed for a signal at 800 Hz. Next, averaged ($n \geq 3$) change in threshold for sequentially measured pairs (with and without contralateral noise) were obtained at different frequencies. Contralateral noise levels were fixed at 60/65 dB SPL, which was at least 10 dB below the acoustic reflex threshold.

All subjects ($n=10$), except one, showed contralateral-noise-evoked increases in threshold at low frequencies. These began to emerge at 45 dB SPL and increased linearly with level. Between subjects, a large variability in magnitude was noted with a maximum threshold change of 8 dB. Most increases in threshold showed a low-pass frequency dependence with a steep roll-off of up to ~ 6 dB/oct and a frequency-limit between 1.5-4.0 kHz. The maximum threshold-change of the population was 4 dB at 800 Hz, the minimum was < 1 dB at the highest frequency measured (6.4 kHz). The roll-off of the low-pass slope was ~ 1.5 dB/oct.

In humans, we observed a low-frequency bias for threshold-increases in response to contralateral noise. These have a low-pass characteristic with a steep roll-off and a frequency-limit around 2.5 kHz.

Supported by FWO(G.0961.11),BOF(OT-09-50&OT-14-118) and NIH(NIDCD)R01 DC0008327.

PS 644

Modeling Individual Differences in Tracking Changes in Complex Sound Sequences

Ben Skerritt-Davis; Mounya Elhilali
Johns Hopkins University

Many natural sound sources are not perfectly predictable, but are governed by some unknown probability distribution that adds uncertainty to the sound environment. Auditory scene analysis tasks become more difficult with these complex sound sources, where an unexpected sound event can be considered an outlier of the existing scene or it can be attributed to a change in the scene (and the unknown distribution governing it). Change detection is then not a matter of identifying a single event that deviates from the previous context, but rather tracking some statistics over time that indicate a change in the environment.

Previously, we have shown that humans can detect such changes in randomness with fractal melodies, which exhibit long-range statistical dependence ($1/f^\beta$)

power-law spectrum) while being inherently random, with the amount of randomness determined by the spectral exponent β . While average behavior scaled with the degree of change in β (as expected), there was a wide range in performance across subjects. Here, we present a model operating on the same task in order to investigate the statistics sufficient to perform the task, as well as explain individual differences in performance.

PS 645

Suprathreshold Processing Deficits in Listeners with Hyperacusis

Katie Turner¹; Matthew Richardson¹; Fan-Gang Zeng²

¹*Cognitive Sciences, University of California Irvine, Irvine, CA 92697 USA, Center for Hearing Research, Hearing and Speech Laboratory;* ²*Biomedical Engineering, Dept. of Anatomy & Neurobiology, Otolaryngology, and Cognitive Sciences, University of California Irvine, Irvine, CA 92697 USA, Center for Hearing Research, Hearing and Speech Laboratory*

Introduction

Hyperacusis is typically defined by decreased sound tolerance or even pain response to normal sounds. Hyperacusis may develop after noise exposure, possibly as a result of damage to the auditory nerve and subsequent overcompensation by the brain. Despite recent attention to hyperacusis, little is known about its perceptual consequences, particularly in suprathreshold processing and speech perception in noise.

Methods

We recruited listeners who complained about hyperacusis, as well as normal-hearing control listeners. First, we used surveys and audiometric measures to define listeners by their degrees of hyperacusis and hearing loss if present. Participants with a complaint of hyperacusis and scores of 25 or greater out of 42 on the Khalfa Hyperacusis questionnaire were included. Second, we obtained physiological measures in otoacoustic emissions and auditory brainstem responses to determine potential sites of lesion. Finally, we measured frequency-specific temporal acuity and speech recognition in noise to assess perceptual deficits related to hyperacusis. Assessments included temporal modulation detection thresholds and speech reception thresholds (SRTs) in noise. Detection of modulated pure tones was measured using an adaptive 3 alternative forced choice task and several combinations of carrier and modulator. Carriers were sinusoids of 250, 2000, and 8000 Hz; modulation frequencies were 4 Hz, 41 Hz, and 80 Hz. Speech reception in noise was measured using English sentences spoken by a male talker, masked separately with speech-spectrum-shaped noise, a female talker, and a male talker.

Results

With an initially limited sample size, listeners with hyperacusis appeared to require a greater percentage of modulation for detection than normal controls did. Listeners with hyperacusis also appeared to have higher speech recognition thresholds in noise, particularly when the signal and masker were both male talkers.

Discussion

The preliminary results suggest that hyperacusis has a perpetual consequence in impaired suprathreshold processing. Effective management of hyperacusis needs to consider this impaired processing component.

Funding

Supported by NIH grants P30DC008369, R01DC015587, and T32DC010775

PS 646

Behavioral Measures of Hidden Hearing Loss in Audiometrically Normal Young Listeners.

Garreth Prendergast¹; Kevin Munro¹; Karolina Kluk²; Agnès Léger²; Deborah Hall³; Michael G. Heinz⁴; Christopher Plack¹

¹*Manchester Centre for Audiology and Deafness (ManCAD), University of Manchester;* ²*Manchester Centre for Audiology and Deafness, University of Manchester, Manchester Academic Health Science Centre, UK.;*

³*NIHR Nottingham Hearing Biomedical Research Unit;*

⁴*Purdue University*

Cochlear synaptopathy (“hidden hearing loss”) refers to the loss of synapses between inner hair cells and auditory nerve fibers caused by noise exposure or aging. Despite clear evidence for this pathology in various rodent models[1,2], the evidence from humans is limited and mixed. Previously we have shown that brain-evoked auditory potentials correlate poorly with lifetime noise exposure[3], thus suggesting that hidden hearing loss is not prevalent in healthy young listeners.

Here, we describe the results of a number of psychophysical tasks, including frequency and intensity discrimination, modulation detection, interaural phase difference discrimination, speech-in-noise tasks, and self-reported estimates of listening abilities (via the SSQ Hearing Scale[4]). Measures were made at two different levels and frequencies, based on the assumption that synaptopathy should affect performance most at high levels and high frequencies. 141 listeners aged 18-36 years were tested and the main predictor variable was the total lifetime noise exposure estimated via a structured interview.

Listeners with high levels of noise exposure in this cohort tend to work in high-noise music entertainment venues. Surprisingly, these listeners tend to have a higher subjective opinion of their hearing, as measured by the SSQ Hearing Scale, compared to listeners with significantly lower levels of noise exposure. This raises the question of whether listeners with high noise exposure in the current cohort are better trained at performing auditory tasks and thus are able to compensate for any reduction in audibility which they may have due to noise-induced cochlear synaptopathy. The results of the behavioral psychophysics show that lifetime noise exposure is a poor indicator of performance on the behavioral and speech-in-noise tasks. There are some relations of interest but the strength of these indicate that they are unlikely to be a viable tool for the identification of noise-induced synaptopathy. If noise-induced cochlear synaptopathy does affect audiometrically normal young humans, it is not simply waiting to be uncovered using standard psychophysical paradigms.

1. Furman et al. 2013. Noise-induced cochlear neuropathy is selective for fibers with low spontaneous rates. *J. Neurophysiol.* 110, 577-586.

2. Kujawa et al. 2009. Adding insult to injury: cochlear nerve degeneration after “temporary” noise-induced hearing loss. *J. Neurosci.* 29, 14077-14085.

3. Prendergast et al. Effects of noise exposure on young adults with normal audiograms I: Electrophysiology. Submitted for review.

4. Gatehouse et al. 2004. The speech, spatial and qualities of hearing scale (SSQ). *Int. J. Audiol.* 43, 85-99.

Spatial Hearing in Listeners with Hearing Loss

PS 648

Children with Congenital Unilateral Sensorineural Hearing Loss: Effects of Late Hearing Aid Amplification

Marlin Johansson; Filip Asp; Erik Berninger
Department of Clinical Science, Intervention and Technology, Karolinska Institutet, Stockholm, Sweden

Background

Children with unilateral hearing loss are at risk of experiencing academic, social-emotional and speech-language difficulties. Reduced neural stimulation in one auditory pathway to the brain can cause maladaptive cortical reorganization and effortful listening (Sharma & Glick, 2016). Two major perceptual challenges for children with unilateral hearing loss are sound-source localization and understanding speech in the presence of

multiple interfering speech signals, e.g. playground and school settings. The aim was to analyze how hearing aid use affects 1) perceived real life function, 2) sound localization accuracy, and 3) speech understanding in competing speech, in a group of children with congenital unilateral sensorineural hearing loss.

Methods

Eligible subjects were 7 children (6-12 yrs of age) with non-syndromic congenital unilateral sensorineural hearing loss and hearing aid use > 6 months in the impaired ear (Stockholm County Council). Six subjects (9.7-10.8 yrs of age) with first hearing aid fitting between 4.8-8.9 yrs of age agreed to participate. All had pure tone thresholds ≤ 20 dB HL in the normal ear (0.125-8kHz) and their 4 frequency pure-tone average (PTA; 0.5-4kHz) was better than 90 dB HL in the impaired ear.

Hearing aid function was verified with real ear measurements and aided hearing threshold. Aided and unaided perceived real life function was measured with the abbreviated profile of hearing aid benefit (APHAB) and parents' evaluation of aural/oral performance of children (PEACH) questionnaires. Speech understanding in (non-correlated) competing speech (SCS, 63 dB SPL_{Ceq}) originating from multiple sound-sources, and an objective test of sound localization accuracy (SLA, 63 dB SPL_{Aeq}) were measured aided and unaided.

Results

Average PTA was 45.0 dB HL (30.6–52.4 dB HL) and 5.6 dB HL (-0.5–10.2 dB HL) in the impaired and normal ear, respectively (n=6). Preliminary analyzes showed worse SLA and SCS compared to normal-hearing subjects. All subjects could localize sound better than chance in the unaided and aided conditions. On group level, aided SLA was significantly worse than unaided SLA ($p < 0.05$). No significant difference between aided and unaided SCS existed. APHAB scores for Ease of communication and total PEACH scores were significantly better in the aided condition ($p < 0.05$).

Conclusions

Preliminary results indicate that late hearing aid intervention (>4.8 yrs of age) in children with congenital unilateral sensorineural hearing loss may disrupt horizontal sound localization. Furthermore, results suggest that these children and parents nevertheless can experience benefit with a hearing aid fitted late—displayed by higher aided scores in self-report questionnaires.

Duration of Temporary Hearing Loss During Development Influences Severity of Behavioral and Neural Impairments to Sound Localization

Kelsey L. Anbuhl¹; Andrew D. Brown²; Victor Benichoux²; Nathaniel T. Greene³; Alexander T. Ferber¹; Daniel J. Tollin²

¹Neuroscience Training Program; ²Department of Physiology and Biophysics, University of Colorado School of Medicine; ³U.S. Army Aeromedical Research Laboratory

Children who experience conductive hearing loss (CHL) early in life often display binaural hearing impairments that persist long after CHL is resolved. These impairments are particularly strong and long-lasting in individuals that have substantial cumulative CHL experience during the first five years, suggesting abnormal central auditory development that scales with duration of hearing deficit. Previous data has shown that CHL (e.g., due to an ear infection) can attenuate sound in the affected ear by >30 dB, thus dramatically distorting the interaural level difference (ILD) cues used for high-frequency sound localization. We hypothesize that abnormal neural coding of ILDs resulting from chronic CHL during development underlies the binaural hearing impairments. We induced a unilateral CHL using custom-made silicone earplugs and simultaneously quantified its effects on 1) behavioral spatial acuity, 2) the binaural interaction component (BIC) of the auditory brainstem response (ABR), and 3) neural information processing in the auditory midbrain (inferior colliculus, IC). The duration of developmental CHL was variable, analogous to the fluctuations of CHL observed in children with recurring ear infections. The CHL experience was quantified as the percentage of earplug retention over time, and the average and maximum duration of consecutive ear-plugged days. All animals raised with CHL showed behavioral and physiological impairments. Behaviorally, animals displayed larger minimum audible angles for high-pass noise compared to age-matched controls (~2x worse-than-controls), suggesting impaired ILD sensitivity. Physiologically, animals displayed abnormal BICs of the ABR (e.g., reduced BIC amplitude) indicating altered binaural processing in the auditory brainstem. To examine alterations of binaural processing in more detail, extracellular recordings were made in the IC contralateral to the previously occluded ear, and ILD discrimination thresholds for single neurons were determined using Fisher Information. Across the population of CHL-exposed animals, neural ILD discrimination was moderately impaired (~2-3 dB worse-than-control). Further analysis revealed that animals that experienced high rates of CHL (>50%) during the first 30 days after birth (corresponding to the period with the

fastest head-growth) were more severely impaired compared to other animals with lower CHL rates during that period. Our data suggests that experiencing a temporary unilateral hearing loss alters the normal development of spatial hearing, which may be attributed to impaired binaural processing at the level of the brainstem and IC.

Support: R01-DC011555, T32-DC012280, F31-DC014219

PS 650

The Effect of Acute, Reversible, Unilateral Hearing Loss on Spatial Hearing

Filip Asp¹; Erik Berninger¹; Anne-Marie Jakobsson²

¹Department of Clinical Science, Intervention and Technology, Karolinska Institutet, Stockholm, Sweden;

²Karolinska Institutet

Background

Individuals with unilateral hearing loss generally show worse than normal ability to localize sounds and understand speech in the presence of multiple spatially separate competing talkers. The aim of this study was to characterize the degraded performance in spatial hearing resulting from systematically and experimentally elevated hearing thresholds in one ear of normal hearing (NH) listeners.

Subjects and Methods

Eight healthy, otologically normal, and NH adult volunteers (7 females) aged 18 to 40 years participated in this study. Two experimental conditions were achieved by monaural, acute, and reversible sound attenuation using an ear plug (NA1), and the combination of an ear plug and a circum-aural hearing protector (NA2) in the right ear, respectively. The subjects participated in three sound field measurements--sensitivity to frequency-modulated tones, speech recognition in spatially separate multi-source competing speech (SCS, 63 dB SPL_{Ceq}), and horizontal sound localization accuracy (SLA, 63 dB SPL_{Aeq})--under binaural and experimental conditions. SCS was expressed as a signal-to-noise ratio (SNR), and overall SLA was quantified by an error index (EI) ranging from 0 (perfect performance) to 1.0 (chance performance).

Results

The configuration of the unilateral induced hearing loss in the NA1 condition showed a more pronounced effect of the ear plug at high than low frequencies (e.g. the mean absolute threshold was 25.3 dB HL and 39.0 dB HL at 0.5kHz and 4kHz, respectively). In the NA2 condition, the most distinct effect on absolute thresholds existed at low frequencies (e.g. 41.8 dB HL at 0.5kHz and

50.7 dB HL at 4kHz). The mean(SD) SNR for binaural SCS was -15.1dB (1.6dB). A mean increase in SNR of 2.0 dB (NA1:p=0.008), and 3.0 dB (NA2:p=0.004) existed in the experimental conditions, reflecting an elevated speech recognition threshold and a relatively small additive effect between the NA2 and the NA1 condition. The listeners revealed an EI close to 0 in the binaural condition (mean(SD)=0.054(0.021)), demonstrating near perfect SLA. The mean EI increased significantly in experimental conditions (NA1: EI=0.21, $p < 0.0001$; NA2: EI=0.54, $p < 0.001$), showing the largest effect in the NA2 condition.

Conclusions

Experimentally induced unilateral hearing loss has a distinct effect on spatial hearing. The configuration and the level of the hearing loss dictate the magnitude of the effects on sound localization accuracy and speech recognition in spatially distributed competing speech.

PS 651

Auditory Motion Perception of Individuals with Single Sided Deafness

Keng Moua¹; Alan Kan²; Ruth Y. Litovsky³

¹University Of Wisconsin-Madison; ²University of Wisconsin-Madison; ³Waisman Center, University of Wisconsin, 1500 Highland Avenue, Madison, Wisconsin 53705, USA

A growing number of individuals with single sided deafness (SSD) have been implanted with a cochlear implant (CI) in the ear with severe-to-profound hearing loss, despite having normal hearing (NH) in their contralateral ear. Little is known about how individuals with SSD who are implanted with a CI, benefit from processing two different modalities (CI + acoustic ear) and how it effects their spatial hearing ability. We are particularly interested in spatial hearing abilities in realistic situations, such as when a sound source is moving. In this work, we assessed the auditory motion perception ability of adults with SSD who received a CI in their deaf ear. One hypothesis was that these individuals may perform as well as a normal hearing (NH) listener because of access to acoustic cues through their NH ear. Alternatively, the degraded auditory input from the CI may interfere with the ability to perceive a moving sound and performance may be similar to that of a bilateral cochlear implant (BiCI) user.

We conducted an experiment where subjects reported the perceived trajectory of a moving sound source, as well as the location of stationary targets. Stationary targets were located 10 degrees apart, and moving sound sources traversed through angular ranges of 10, 20 and 40 degrees. Moving sounds were simulated using an

array of thirty-seven loudspeakers in the frontal hemisphere (spaced 5 degrees apart from left to right) using vector-based amplitude panning. The data was analyzed to assess patients' ability to identify the location of stationary sounds, distinguish between stationary and moving sounds, and their ability to correctly identify the direction of motion.

Results to date showed that SSD patients who are implanted with a CI in their deaf ear have stationary sound localization abilities comparable to that of BiCI users. However, their ability to detect sound source movement and direction was better compared to BiCI users. Overall performance was still poorer than that of NH listeners. These results suggest that SSD patients are able to track the location of a moving sound source by integrating the input from a NH ear and a CI. This result demonstrates a positive outcome of intervention when an SSD patient is provided with a CI in their deaf ear.

Work supported by NIH-NIDCD (R01 DC003083 & R01 DC008365 to RYL, R03 DC015321 to AK) and NIH-NICHD (P30HD03352 to the Waisman Center).

PS 652

Cortical Electrophysiological Markers of Phonemic Discrimination in Single Side Deafness Patients: A Mismatch Negativity Study

Elsa Legris¹; Sylvie Roux²; John Galvin³; Marie Gomot²; Jean-Marie Aoustin⁴; Frederique Bonnet-Brilhault²; Mahieu Marx⁵; David Bakhos⁶

¹Service d'ORL et CCF, CHU Tours, Tours, France; ²UMR-S930, Tours, France; ³Université François-Rabelais de Tours, CHRU de Tours, UMR-S930, Tours, France.; ⁴DGSOM, Department of Head and Neck Suregery, SPAPL; ⁵Service ORL et CCF, CHU Purpan, Tours, France; ⁶Service ORL et CCF; Université François-Rabelais de Tours, CHRU de Tours, UMR-S930, Tours, France.

Background

For spatially separated speech and noise, binaural listening offers an advantage over monaural listening. Auditory processing of interaural time and level differences to allows listeners to better segregate speech and noise that originate from different locations. For patients with single-sided deafness (SSD), speech perception in noise can be difficult due to the loss of binaural listening. Cortical auditory evoked potentials (AEPs) may provide insight into the neural encoding of speech in noise under conditions of unilateral hearing loss. The aim of this study was to compare behavioral performance (speech

recognition in quiet and in noise) to objective measures (cortical AEPs) in SSD patients.

Methods

Eight right-handed native French-speaking adults (3 women, 5 men; mean age = 60 years, ranging from 48 to 65 years) with unilateral deafness in the right ear participated in this study. The mean pure-tone average threshold was 113 dB HL (± 15.19) for the deaf ear and 25 dB HL (± 3) for the better ear. Etiology of hearing loss included sudden deafness ($n=3$), Meniere's disease ($n=2$) and progressive hearing loss ($n=3$). Sentence recognition was measured in quiet and in noise; in different conditions:

the dichotic condition with the signal presented to the poorer ear and the noise to the contralateral best ear; the diotic condition with both the signal and the noise presented from the loudspeaker located in front of the subject, and the reverse-dichotic condition with the signal presented to the best ear of the subject and the noise to the poor ear. The speech recognition threshold was measured in terms of dB signal-to-noise ratio (SNR) yielding a 50% correct word score. Cortical AEPs were collected using a mismatch negativity (MMN) paradigm for stimuli presented in quiet and in noise.

Results

A significant delay in MMN latency was observed for speech in noise, relative to speech in quiet at the frontal and occipital sites; no difference was observed between the quiet and noise conditions for MMN amplitude. Scalp map potentials showed a posterior distribution of the MMN for speech in noise, relative to speech in quiet. A correlation was observed between SRT in diotic condition and MMN amplitude in noise.

Conclusion

These preliminary data suggest that MMN could be an objective marker with which to investigate binaural squelch. Future studies could investigate the evolution of MMN measures in SSD patients after interventions such as cochlear implants.

PS 653

Frequency Dependence of the Head-shadow Benefit for Single-Sided Deaf and Bilateral Cochlear Implantees

Sterling W. Sheffield¹; Matthew J. Goupell²; Nathaniel Spencer³; Olga A. Stakhovskaya⁴; Joshua G.W. Bernstein⁵

¹National Military Audiology and Speech Pathology Center, Walter Reed National Military Medical Center, Bethesda, MD; ²Department of Hearing and Speech

Sciences, University of Maryland, College Park;

³Wright-Patterson Airforce Base; ⁴Walter Reed National Military Medical Center; ⁵Walter Reed National Military Medical Center, Bethesda, MD

Background

For bilateral (BI) and single-sided deafness (SSD) cochlear-implant (CIs) users, having two ears improves speech recognition in noise, primarily when the head shadows sound to create a signal-to-noise ratio advantage at one ear. BI-CI and SSD-CI listeners can also benefit from binaural interactions, although these benefits may be partly limited by an interaural place-of-stimulation mismatch. Reprogramming the frequency-to-electrode allocation to minimize interaural mismatch could remove frequency content from a CI signal, potentially decreasing head-shadow benefit. This study evaluated how much frequency content could be removed from the poorer-ear CI without sacrificing head-shadow benefit.

Methods

BI-CI, SSD-CI, and normal-hearing adults performed sentence recognition in noise. Matrix sentences were presented over circumaural headphones with head-related transfer function simulations of the free field. The speech originated from the poorer-ear side (-70° azimuth) and a speech-shaped noise from the better-ear side ($+70^\circ$). Stimuli presented to the poorer ear (CI) were filtered with a range of cutoffs. BI-CI listeners were presented lowpass or highpass filtered stimuli. SSD-CI listeners were presented only highpass filtered stimuli because of the expected direction of the interaural place-of-stimulation mismatch. Normal-hearing listeners were presented with vocoder simulations of BI-CI and SSD-CI listening without a place-of-stimulation mismatch. Head-shadow benefit was calculated as bilateral minus better-ear performance. Results were compared to an existing model of head-shadow benefit for CI listeners.

Results

Preliminary results from 3 of 8 planned listeners in each group showed sigmoidally decreasing head-shadow benefit as frequency content was removed from the poorer ear. For all listeners, highpass-filter cutoffs up to 1000 Hz had little effect on speech-reception thresholds (performance reduction < 2 dB). For the BI-CI listeners (and associated simulations), the same was true for lowpass-filter cutoffs down to 5000 Hz. There was a moderate correlation between model predictions and measured benefit within each group ($r=0.8$), although the model predicted more immunity to filtering than was observed. The model fit might improve by adjusting the speech-intelligibility index frequency-importance function to more heavily weight low frequencies.

Discussion

For BI-CI and SSD-CI listeners, frequencies below 1000 Hz and above 5000 Hz can be removed from the poorer CI ear without sacrificing much head-shadow benefit. This will allow leeway in CI reprogramming to reduce interaural place-of-stimulation mismatch and potentially improve binaural hearing. [The views expressed in this article are those of the authors and do not reflect the official policy of the Department of Army/Navy/Air Force, Department of Defense, or U.S. Government.]

PS 654

Predicting Sensitivity to Differences in Concurrent, Across-Channel Amplitude Modulation Rates from Single-Channel Sensitivity

Sean R. Anderson¹; Alan Kan²; Ruth Y. Litovsky¹

¹Waisman Center, University of Wisconsin, 1500 Highland Avenue, Madison, Wisconsin 53705, USA; ²University of Wisconsin-Madison

In cochlear implant (CI) users, access to cues that are used to segregate sound sources may be limited by the electrode-neuron interface. A single channel on a CI array that transmits information poorly may cause performance to be worse in across-channel tasks, like speech in noise. The purpose of the present study was to investigate whether increased amplitude modulation (AM) rate discrimination thresholds on a single channel predicted discrimination of AM rates presented simultaneously across channels in normal-hearing (NH) and CI listeners. NH listeners were included to simulate cases of good and poor electrode-neuron interface by reducing the stimulus dynamic range. It was hypothesized that if the threshold for AM rate discrimination increased on one channel, then the ability to detect differences in concurrent AM rate across channels would increase relative to other pairs of channels.

Single-channel AM rate discrimination thresholds were tested using an oddball discrimination task. In NH listeners, or electrode-neuron interface was simulated by decreasing the depth of AM, reducing the AM dynamic range and rendering the AM rate less salient to the listener. In CI users, the electrode-neuron interface was expected to vary across channels in the electrode array. Across-channel AM rate discrimination thresholds were tested using a single presentation, same-different judgment task. Distantly spaced cochlear channels were chosen in each ear to limit channel interaction. Stimuli for NH listeners were sinusoidal AM tones presented at 65 dB SPL in 4 channels: carrier frequencies of 4000 and 7260 Hz in the left and right ear. Stimuli for CI users were sinusoidal AM pulse trains presented at a pulse

rate of 3000 pulses per second in 4 channels: electrodes 4 and 16 in the left and right ear.

Results from NH listeners indicate that when AM depth in one channel was reduced, threshold for AM rate comparisons across channels increased. Preliminary results from CI users suggest that higher thresholds on the single-channel task from the poorer channel predicted higher thresholds for comparisons across pairs of channels. Results suggest that when thresholds for AM rate increase on a single channel, ability to compare AM rates simultaneously across channels worsens. These findings imply that when the electrode-neuron interface is poor at a single cochlear channel, ability to compare information across channels in order to segregate sound sources is impaired.

Work supported by NIH-NIDCD (R01 DC003083 to RYL and R03 DC015321 to AK) and NIH-NICHD (P30HD03352 to the Waisman Center).

PS 655

Access to Binaural Cues in Noise and Reverberation with Bilateral Electrical Stimulation

Kostas Kokkinakis; Natalie Pak
University of Kansas

Background

To a large extent the prevalence of binaural mechanisms in bilateral fittings of clinical processors (e.g., head-shadow, squelch, and spatial release from masking) depends on the optimal processing of interaural level differences and faithful access to robust interaural timing differences. Access to such binaural cues allows individuals wearing bilateral cochlear implants (BCIs) to understand and localize speech well, even in difficult scenarios, such as noisy restaurants, reverberant classrooms, and group meetings. Prior research has revealed that in noisy and anechoic environments, BCI listeners will often benefit from a robust head-shadow effect and may also occasionally demonstrate access to spatial release from masking. However, even with no additive reverberant energy present, the contributions due to binaural squelch and binaural interaction are relatively small, and sometimes entirely absent. In reverberation, the interaural cues, which may aid in the detection and identification of direct sounds (i.e., target and maskers), are either reduced or distorted by indirect sounds (i.e., acoustic reflections) present in the reverberant environment. The purpose of this study was to investigate the extent to which increased acoustic complexity due to the combination of noise and reverberation affects speech intelligibility in individuals who rely on bilateral devices.

Methods

Speech perception by bilateral cochlear implant listeners was measured adaptively using BKB-SIN sentences in competing four-talker babble and moderate reverberation (RT60 = 0.2 s). By systematically controlling reverberation and noise inputs to the two devices, speech reception thresholds were measured in sound-field under various speech and noise spatial configurations, as well as different listening conditions (e.g., monaural, binaural).

Results

The presence of the binaural effects of head-shadow, squelch, summation, and spatial release from masking in noise and reverberation were determined using non-parametric statistical analysis. The results in the bilateral population tested, indicated significant effects of head-shadow and summation, while binaural squelch contributed no statistically significant benefit to bilateral performance. The benefit provided due to spatial release from masking was also not found to be significantly different from zero in noise and reverberation.

Conclusion

These findings are consistent with those of previous studies, which have demonstrated that head-shadow yields the most pronounced advantage, while summation contributes to a somewhat smaller degree. The findings that spatial release from masking and binaural squelch effects produced little to almost no benefit in bilateral listeners are consistent with the hypothesis that reverberation degrades spatial cues and negatively impacts overall binaural performance.

PS 656

Evaluating the Time Course of Binaural Sensitivity Using Stimuli That Mimic Cochlear Implant Processing

Taylor N. Fields¹; Alan Kan²; Ruth Y. Litovsky³

¹Neuroscience Training Program, University of Wisconsin-Madison, Madison, WI, USA; ²University of Wisconsin-Madison; ³Waisman Center, University of Wisconsin, 1500 Highland Avenue, Madison, Wisconsin 53705, USA

Bilateral cochlear implant (BiCI) users have shown significant improvements in sound localization abilities compared to unilateral implantees, but performance is still generally poorer than that of normal hearing (NH) listeners. One reason for this disparity is that CI processors use high stimulation rates which reduce sensitivity to interaural timing differences (ITDs), but are important for good speech encoding. Mixed-rate, multi-electrode stimulation strategies have been proposed as a means of improving BiCI users' ITD sensitivity while retaining speech intelligibility. This strategy uses high-rate stim-

ulation on some electrodes and low-rate stimulation on others. This study aimed to determine the optimal number and location of these low-rate electrodes, and was conducted in NH listeners to avoid some of the variability in ITD sensitivity inherent in BiCI users.

An eye gaze paradigm was used to capture the time course of the decision-making process, as well as ITD sensitivity. Each trial consisted of two stimulus intervals, the first with a 0 us ITD and the second with a left/right-leading ITD. Subjects were instructed to fix their gaze in the center of a computer display, and then shift their gaze to one of two target locations (left/right). The correct answer was revealed 2s after stimulus offset. Two types of stimuli were used: (1) Single transposed tone (4 kHz center frequency, 126 Hz modulation rate); (2) Complex of eight sinusoidally amplitude-modulated (SAM) tones with fixed center frequencies between 4 and 7 kHz. The transposed tone was chosen as a well-studied stimulus to provide a reference for interpreting the eye gaze data. The SAM tone complexes simulated the systematic introduction of low-rate channels in a mixed-rate strategy, with high- and low stimulation rates simulated by 1000 and 100 Hz modulation, respectively.

Preliminary results indicate that the introduction of low rate channels in a mixed-rate strategy can improve ITD sensitivity over an all-high rate strategy. In some cases, introducing one low rate channel led to sensitivity comparable to that of the all-low condition. In these conditions, the time to make left/right judgements was also faster, suggesting the strength of certainty in the decision-making process. However, there was inter-subject variability in the number and cochlear location of low-rate channels that produced maximal improvement, suggesting that individualized clinical fitting of mixed-rate stimulation will likely be necessary to maximize performance with such strategies.

Work supported by NIH-NIDCD (R01DC003083 to RYL; R03DC015321 to AK), NIH-NICHD (P30HD03352 to Waisman Center), and NRSA T32 GM007507.

PS 657

Using the Acoustic Signal to Time-lock the Pulses in the Left and Right Cochlear Implant

Ann E. Todd¹; Justin Aronoff²; Hannah Staisloff²; Daniel Lee²; David M. Landsberger³

¹New York University; ²University of Illinois at Urbana-Champaign; ³New York University School of Medicine

Background

Although bilateral cochlear implants (CI) have led to a significant improvement in performance compared to

unilateral CIs, bilateral CI users still do not receive the same benefits from having two ears that normal hearing listeners do. One of the main limitations is that bilateral CI users are generally not sensitive to interaural time difference (ITD) cues when using their clinical processors. Work with research interfaces suggests that it is possible for CI users to perceive ITDs. However delivering precise ITDs may require synchronized processors. An alternative to physically synchronizing the left and right processors is to use the acoustic signal, which is already naturally time-locked at the two ears, to synchronize the processors. By delivering stimulation at each zero-crossing of a signal, it is possible to time-lock the pulses in the two ears. However, the accuracy of this time-lock depends on the sampling rate used to detect the zero-crossings. The goal of this experiment was to determine a) if ITD sensitivity can be improved by using the acoustic signal to time-lock the pulse trains, and b) how that improvement is affected by the sampling rate.

Methods

ITD sensitivity was measured using a four interval, two alternative forced-choice task. Participants were presented with four stimuli. The first and last stimuli always had an ITD of 0 microseconds. One of the middle two stimuli had a non-zero ITD. Participants were asked to indicate which stimulus was different. ITD was varied adaptively.

Results

Preliminary data with two subjects indicated that ITD sensitivity was best when the pulses in the two ears were manually time-locked. Additionally, ITD sensitivity was comparable when the acoustic stimulus was used to time-lock the two ears, but only when a high sampling rate was used. Performance decreased with decreasing sampling rates.

Conclusions

The results indicate that it is possible to use the acoustic signal to time-lock the pulses in the two ears and yield good ITD sensitivity. However, high sampling rates may be needed.

Speech Perception II

PS 658

The Cortical Entrainment Response to Speech Shows No Effect of Stimulus Intensity

Lucas S. Baltzell; Ramesh Srinivasan; Virginia Richards
University of California, Irvine

Recent studies have uncovered a neural response that appears to track the envelope of speech, and have

shown that this tracking process is mediated by attention. However, the underlying neural mechanisms that generate this tracking response, often called the “entrainment” response, remain unclear. One possibility is that abrupt changes in stimulus energy generate auditory evoked potentials (AEPs) that concatenate to form the entrainment response. In other words, the entrainment response may merely reflect a combination of transient AEPs associated with the processing of low-level acoustic properties of the stimulus. Consistent with this hypothesis, Doelling et al. (2014) showed that entrainment to click trains, which carry no linguistic information but contain maximally abrupt changes, was significantly higher than entrainment to natural speech. Under this hypothesis, we might expect the entrainment response to parallel changes in the AEP under low-level acoustic manipulations. Accordingly, it is well known that the magnitude of the N1 component of the AEP increases with stimulus intensity (Rapin et al., 1966; Billings et al., 2007), and if the entrainment response is reducible to a sum of AEPs, we should expect a similar change in magnitude as a function of stimulus intensity. Presenting sentences at 50, 60, 70, and 80 dB, we failed to find an effect of stimulus intensity on the entrainment response, suggesting that neural generators underlying the entrainment response are distinct from those underlying the AEP.

PS 659

Taking Attention Away from the Auditory Modality: Subcortical Representation of Speech Signals During Inattentive Deafness

Zilong Xie¹; Bharath Chandrasekaran²

¹*Department of Communication Sciences and Disorders, The University of Texas at Austin;* ²*Department of Communication Sciences and Disorders, Department of Psychology, Department of Linguistics, Institute for Neuroscience, Institute for Mental Health Research, The University of Texas at Austin*

Imagine conversing with a friend who is texting on their phone. You asked a question, but his/her puzzled expression indicates they were not attentive. This scenario, termed “inattentive deafness”, refers to the inability to perceive auditory stimuli, such as speech, under an increased perceptual load. Mechanistically, withdrawing attention from the auditory modality leads to reduced auditory processing at auditory cortical levels (Molloy et al., 2015). To date, the extent to which the auditory modality is impacted by perceptual load remains controversial (Murphy, Fraenkel, & Dalton, 2013). Mechanistically, the impact of elevated perceptual load on the auditory system, beyond the auditory cortex has not been examined.

Speech processing involves a dynamic interplay between auditory cortical and subcortical structures (Kraus & White-Schwoch, 2015). An emerging view posits that auditory cortices modulate sound processing at auditory subcortical structures in a continuous, online fashion via corticofugal pathways (Chandrasekaran, Skoe, & Kraus, 2014). If the input signal is predictable, predictions at the cortex are likely to be accurate, as a result, subcortical representation of the signal is enhanced (Chandrasekaran et al., 2009).

Here we examine the impact of withdrawing attention away from the auditory modality on the subcortical representation of speech sounds. Adult native Mandarin speakers ($n = 20$) performed a visual search task of high (target similar to distractor) and low (target dissimilar to distractor) perceptual load. On a random subset (50%) of trials, task-irrelevant linguistic-relevant pitch patterns (Mandarin tones: level, rising, and falling pitch patterns) were presented concurrently with the visual stimuli in either predictable or random contexts. In the predictable context, the pitch patterns were presented in blocks within which the each tone was presented repetitively. In the random context, the pitch patterns were presented in a pseudo-random order. Subcortical electrophysiological responses to the pitch patterns were recorded during the visual search task.

We found enhanced subcortical decoding (using data-driven machine learning metrics) of pitch patterns in the predictable context (versus the random context) under low visual perceptual load ($b = -1.006$, $SE = 0.469$, $Z = -2.146$, $p = 0.032$). Intriguingly, a reverse pattern of context-dependent effects (random > predictable) was observed under high perceptual load ($b = 0.887$, $SE = 0.433$, $Z = 2.047$, $p = 0.041$).

These findings demonstrate a dynamic interaction between stimulus regularity and perceptual load in determining the fidelity of auditory subcortical representation.

PS 660

EEG Alpha Rhythms Are Associated with Listening Effort While Listening to Speech in Noise in Cochlear Implant Users

Andrew Dimitrijevic

Sunnybrook Hospital ENT University of Toronto

Background

Cochlear implant (CI) users often struggle while listening to a conversation in adverse listening environments such as a noisy room and often report that they feel exhausted after a day of listening. In order to follow conversations, especially in the presence of noise, attention and effort must be exerted and may be related to

listening effort (LE). The physiological mechanisms of LE are not well understood. This study relates LE rating to physiological processes as measured by the electroencephalogram (EEG) in CI users while performing a speech perception in noise task. We have previously shown that EEG alpha power recorded over parietal regions is related to speech perception in noise in normal hearing adults and children. We therefore hypothesized that alpha power would show a similar relationship in CI users and would additionally be related to LE.

Methods

Ten adult CI users were tested in free field using their everyday CI setting while performing the Digit Triplet Test (DTT). The DTT presents trials of three digits in speech-shaped noise. In an initial behavioral task, the signal to noise ratio (SNR) was varied adaptively until 50% of digits were identified correctly, the Speech Reception Threshold (SRT). Afterwards, 64 channel EEG recordings were made during DTT listening at individualized suprathreshold levels. After each recording block, participants were asked to rank the difficulty of performing the DTT task (i.e., LE).

Results

Listening to speech in noise was associated with increased alpha power, in both normal hearing individuals and CI users. CI users had greater alpha power compared to normal hearing individuals. Significant correlations were observed between parietal alpha power and LE in CI users. Additionally, significant correlations were observed between performance (number of correctly identified digits) and alpha recorded over left temporal regions.

Conclusions

CI users and normal hearing have similar cortical oscillation patterns while listening to speech in noise. Given that alpha power was significantly correlated to LE and that CI users had greater alpha power compared to normal hearing individuals, alpha may represent an objective measure of LE in CI users.

PS 661

Error-driven Learning in Online Speech Perception

Yunan Wu; Lori Holt

Carnegie Mellon University

The mapping from acoustic signal to speech category is notoriously complex, with variability arising from different talkers, accents, and dialects, among other sources like environmental noise. A great deal of recent behavioral research documents listeners' ability to adapt quickly to systematic deviations in short-term speech input. But, the mechanisms underlying this adaptive plasticity re-

main unresolved. A recent human neuroimaging study (Guediche et al. 2014) suggests the possibility that cerebellum-guided error-driven learning may play a role. By this proposal, incoming acoustic information can be sufficient to at least partially activate existing speech representations for phonemes, or words, even when the input is distorted or otherwise deviates from the norm. This activation is posited to generate expectations about other signal attributes consistent with long-term experience. When the incoming acoustic speech does not meet these expectations (due to signal distortion, noise, talker idiosyncrasies, or accent etc), the discrepancy may generate an error signal that drives adaptive plasticity to rapidly adjust the acoustic-to-category mapping. Guediche et al. provide evidence that such adjustments may take place via cortico-cerebellar loops. Here we test a specific prediction of this account. Namely, acoustic dimensions that robustly signal categories should be more effective at generating appropriate predictions, and thus should elicit more robust error-driven teaching signals to drive adaptive tuning of speech categorization. Therefore, among the multiple acoustic dimensions that typically signal speech categories, the dimensions most highly diagnostic of category membership should be the most effective at eliciting adaptive tuning. We test this prediction using noise-vocoding to manipulate the effectiveness with which a spectral acoustic dimension signals vowel category membership. Comparing vowel categorization among the same group of listeners categorizing clear and noise-vocoded speech reveals opposite patterns of adaptive plasticity, with the results patterning as a function of the acoustic dimension that most robustly signals vowel category in a particular listening context. In each case, the secondary, non-dominant, dimension is perceptually down-weighted upon introduction of an 'artificial accent' with acoustic dimension correlations that are opposite those of English, consistent with prior findings. These findings underscore the dynamic mapping of acoustics to speech categories and the rapidity with which the mappings are 'tuned' by short-term stimulus regularities. At the broadest level, the results are consistent with a role for error-driven supervised learning in speech categorization and support the possibility that cortico-cerebellar learning may be important in 'tuning' the mapping of input to established auditory and speech categories.

PS 662

Frontal P2 Cortical Evoked Potentials in Response to Ongoing Speech

Andrew Liu¹; April Hubbard²; Subong Kim²; Inyong Choi²

¹Department of Otolaryngology-Head and Neck Surgery, University of Iowa Hospitals and Clinics; ²Department of Communication Sciences and Disorders, University of Iowa

Understanding speech in noisy environments can be quite challenging for hearing impaired listeners. Speech in noise performance cannot be predicted directly from an audiogram alone and cortical ERP modulation by SNR has been linked to performance on speech in noise tasks. We propose testing the interaction between listening effort and predictability with sentences embedded in noise. In this study we validated the computation of event related potentials for ongoing speech stimuli.

We presented subjects with 26 sentences, representing 13 pairs of high and low context sentences associated with the same final word of the sentence taken from the R-SPIN stimulus set. High-density EEG responses were recorded from the subjects during passive listening.

Preliminary ERP analysis of the data show predominantly early left temporoparietal responses, approximately 90-100 ms after stimulus onset, and late right frontal responses approximately 200 ms after stimulus onset. These findings in right frontal areas are suggestive of P2 cortical evoked responses and are broadly consistent with reported latency differences in STG vs IFG activity for speech in noise tasks.

PS 663

Development of Perception and Perceptual Learning for Low- and High-pass Filtered Speech

Julia Jones. Huyck¹; Merri J. Rosen²

¹Kent State University; ²Northeast Ohio Medical University

Slow changes in speech are preferentially processed by the right hemisphere, where information is extracted from long (~200 ms) temporal integration windows, while the left hemisphere extracts information from short (~30 ms) windows (Poeppe 2003). Indeed, Saoud et al. (2012) showed a perceptual advantage when each hemisphere received the information to which it is tuned: speech intelligibility was better when low-pass filtered speech was presented to the left ear (thus more to the right hemisphere) and high-pass filtered speech to the right, rather than vice versa. However, this study, con-

ducted in adults, did not account for perceptual learning of speech over time, or any variability in speech comprehension with age. Here we examined perceptual learning on these filtered (and thus degraded) speech stimuli in children and adolescents.

Three age groups (ages 8-11, 12-15, and 16-19 years) were presented with 2- and 3-syllable words, filtered to include only slow (0-4 Hz, F-Low) or fast (22-40Hz, F-High) modulations, and overlaid with bandpass noise to avoid ceiling performance. Words were presented in four counterbalanced conditions: matched (F-Low to left ear, F-High to right), mismatched (F-Low to right, F-High to left), F-Low to both ears, and F-High to both. Groups were tested for accurate word repetition before and after four sessions of training on all conditions.

For all age groups, performance was best when F-Low was presented to one ear and F-High to the other, but surprisingly with no ear order advantage. Performance was poorest when F-High was presented diotically to both ears, and intermediate when F-Low was presented diotically. A developmental trajectory for speech recognition was apparent, as the 8- to 11-year-olds had poorer performance than the 16- to 19-year-olds, and the 12- to 15-year-olds did not differ from either of the other age groups. In terms of perceptual learning, the 8- to 11-year-olds learned the most, and all groups improved more on diotic F-High than on any other condition.

We were unable to reproduce Saoud et al.'s perceptual advantage for hemisphere-matched filtering in any age group, likely due to the presence of background noise with the speech signal, though possibly due to the younger age of our participants. Nevertheless, the results show that speech intelligibility is dependent on the form of degradation and the age of the listener. Moreover, perceptual learning of degraded speech might be greater for younger listeners and for more difficult conditions because there is more room for improvement.

PS 664

Benefit of Bilateral Input for Monaural Listeners

Hillary Snapp¹; Xue Liu²; Michael E. Hoffer³; Ozcan Ozdamar⁴; Suhud M. Rajguru⁵

¹University of Miami; ²Department of Otolaryngology, University of Miami Miller School of Medicine, Miami, FL; Dr. John T. Macdonald Foundation Department of Human Genetics, and John P. Hussman Institute for Human Genomics, University of Miami, Miami FL; ³Department of Otolaryngology and Neurological Surgery, University of Miami; ⁴University of Miami Department of Biomedical Engineering; ⁵Departments of Biomedical Engineering and Otolaryngology; University of Miami; FL

Studies have estimated that only 5% of individuals with bilateral profound sensorineural hearing loss (PSNHL) receive bilateral implants and that a maximum of 36% of cochlear implant (CI) patients are bilateral recipients. At present, more than 60% of current CI recipients function as monaural listeners, thereby subject to the deficits inherent to monaural listening. These deficits include reduced localization ability and speech perception in noise. Monaural listeners lose access to critical timing and level cues provided through binaural hearing. Providing bilateral input, however, for monaural listeners (MLs) has the potential to overcome some of these limitations. The present study aimed to 1) compare the benefits of non-invasive CROS technology to the more invasive bone-anchored implant system for MLs, and 2) determine if CROS technology results in improved hearing outcomes in unilateral CI patients and provides similar gains in speech perception in noise to traditional monaural listeners.

Speech perception in noise and localization ability was assessed in the unaided (normal ear only/CI only) and aided condition (normal ear +BAI, normal ear + CROS, CI + CROS) condition. Speech in noise stimuli were presented in a sound booth utilizing four speech/noise configurations (Figure 1a). Localization stimuli were presented in a soundbooth utilizing 19 loudspeakers at a radius of 1.3m and spatially separated by 10°, +/- 90° (Figure 1b). Stimuli consisted of a broadband - 189-ms male-voiced 'hey', narrowband - 350-ms 1/3 octave noises centered at 500 Hz and at 4000 Hz.

Results

A prospective clinical trial was conducted to compare the performance of 3 monaural listening groups in the unaided (monaural) and aided (BAI/CROS/CI+CROS) conditions. For measures of speech perception in noise, significant improvement from the unaided to aided condition for both BAI and CROS groups ($p < 0.0001$) was observed, with no significant difference for aided performance between subject groups ($p > 0.05$) (Figure 2). In the unilateral CI group significant benefit was observed from unaided to aided (CI+CROS) condition when noise is masking the CI and speech is directed at the non-implanted ear (Figure 3). For tasks of localization there was no observable benefit in the horizontal plane for any of the subject groups (BAI, CROS or CI+CROS) and no significant difference between systems. These results indicate the use of CROS stimulation in unilateral cochlear implant recipients provides increased benefit and an additional rehabilitative option for this population when bilateral implantation is not possible.

Performance of Monolingual and Bilingual Speakers of English on Speech Recognition Tasks in a Real-World Environment

Calli Fodor¹; Mikayla Abrams¹; Julie Cohen²; Douglas S. Brungart³; Sandra Gordon-Salant¹

¹Department of Hearing and Speech Sciences, University of Maryland; ²Henry M. Jackson Foundation for the Advancement of Military Medicine; ³National Military Audiology and Speech Pathology Center, Walter Reed National Military Medical Center

Background

People often have difficulty attending to one talker in the presence of background noise (Cherry, 1953), and this task becomes more challenging when the talker and listener have different native languages. In laboratory settings, non-native speakers of English perform more poorly on speech recognition tasks in noise than native speakers of English (Mayo et al., 1997). Additionally, native speakers of English have more difficulty understanding accented than unaccented English in both quiet and noise conditions (Gordon-Salant et al., 2010). To date, little research has compared speech recognition performance by native (monolingual) and non-native (bilingual) speakers of English in everyday listening situations. The purpose of this study is to determine the extent to which native language influences speech recognition performance in real world noisy environments.

Method

Participants 18-43 years old (n=65) with pure-tone thresholds ≤ 20 dB HL were evaluated in a noisy cafeteria in groups of four, while seated around a table with a touch-sensitive tablet computer in front of them. Participants acted as speakers and listeners throughout the study on a trial-by-trial basis. When acting as the speaker, the participant received a prompt on their tablet to read a sentence from the Modified Rhyme Test (MRT), the Oldenberg Matrix Test (OMT) or a modified matrix test that contained real words and nonsense words, after which the listeners selected the word or sentence from a set of choices. Listeners also rated talkers on degree of difficulty at the end of each block of 52 sentences.

Results

Preliminary data analyses indicate that bilingual speakers exhibited somewhat lower scores on the MRT and OMT in noisy environments than the monolingual speakers of English. Differences in response time between the two groups were observed, with bilingual speakers exhibiting longer response times than monolingual speakers. Both listener groups obtained poorer performance scores when the talkers were bilingual speakers.

Conclusions

Preliminary results suggest that bilingual speakers of English have more difficulty understanding speech in typical noisy environments than native speakers of English. The findings also indicate that monolingual speakers of English have more difficulty understanding speech when the talker is bilingual than when the talker is monolingual, as measured by accuracy scores and response time. The implications of these findings for communication performance by monolingual and bilingual speakers will be discussed.

Funding in part provided by Create, Inc in conjunction with the Department of Defense.

PS 666

Direct and Indirect Methods of Measuring Visual Contribution in Real-World Listening Environments

Mikayla Abrams¹; Calli Fodor¹; Julie Cohen²; Douglas S. Brungart³; Sandra Gordon-Salant¹

¹Department of Hearing and Speech Sciences, University of Maryland; ²Henry M. Jackson Foundation for the Advancement of Military Medicine; ³National Military Audiology and Speech Pathology Center, Walter Reed National Military Medical Center

Background

Listeners recognize speech in noise more accurately with auditory and visual cues compared to auditory cues alone. These laboratory findings may not reflect performance in real-world environments. Recent investigations of speech understanding in real-world environments have not examined listener benefit from visual cues. This presentation compares four methods of quantifying the effect of visual cues in natural settings.

Method

Normal-hearing listeners participated in a series of speech intelligibility experiments in which four participants with touch-sensitive tablets sat around a table in a noisy public restaurant. In each trial, one participant was randomly selected as the "talker" and prompted to say a phrase, and the other three were assigned as "listeners" and asked to use the tablet to identify the phrase. Four different methods were used to assess the contribution that visual cues made to speech intelligibility in each case: 1) using a surgical mask to physically obstruct visual cues from the talker; 2) using a headtracker to measure head motion cues on each trial; 3) using an eyetracker to measure eye-gaze on each trial; and 4) analyzing the incorrect responses to determine how frequently incorrect responses contained the same viseme as the target word. Most trials were conducted with un-

constrained head motion, but some validation trials were included where subjects were instructed to look toward or away from the target talker.

Results

As expected, preliminary analyses indicate that listeners tend to perform worse when visual cues are eliminated either through the use of a surgical mask or by instructing the listener to look away from the talker. Headtracking data alone does not appear to be a reliable measure of visual contribution, because participants often moved their head without looking at the talker or used their eyes to look at the talker without moving the head. Visemic analysis also indicated some differences in error patterns between trials conducted with and without visual cues.

Conclusions

Visual cues provide some benefits for speech perception, but the results of this experiment suggest that the listeners did not consistently utilize visual cues unless prompted to do so. Possible explanations include visual distractions in the environment and/or an ambient noise level that was too low to require visual cues. Further studies are needed to more fully explore the factors that influence the contribution that visual cues make in real-world environments.

Funding in part provided by Create, Inc in conjunction with the Department of Defense.

PS 667

Effects of Temporal Segmentation Depend on Smallest Meaningful Unit Size

Sierra Broussard; Gregory Hickok; Kourosh Saberi
University of California, Irvine

Temporal segmentation is a necessary part of auditory processing, whether the stimulus consists of speech units, musical notes, or pseudo-rhythmic environmental sounds. With speech, particular attention has been given to phoneme and syllable length temporal windows, and previous studies have demonstrated that the amount of intelligibility information provided by amplitude and phase spectra depends primarily on temporal window size. In order to fully understand the effect of different lengths of temporal segmentation, it is useful to investigate how a signal's amplitude and phase spectra affect units of language, such as phonemes and syllables, and musical units.

This study investigated how temporal window size affects frequency and temporal smearing (decorrelating amplitude and phase spectra). Listeners in our experiment heard either degraded sentences and identified

words or they heard degraded melodies and performed a same-different judgement. Sentences were either normal speed or time-compressed. Each stimulus was degraded by first dividing it into segments; then for each segment, the amplitude and phase spectra were decorrelated independently relative to those of the original segment. Finally, segments were recombined into their original full length to present to the listener.

Preliminary results show that for the longest window lengths, phase spectrum information is most helpful for both speech intelligibility and music recognition. As window size decreases, normal speech becomes unintelligible when the phase spectrum correlation is 0.4 or less, even when the amplitude spectrum is unaltered. Conversely, music only becomes unrecognizable in the syllable length condition when the amplitude spectrum correlation is below 0.5. In the shortest temporal window size, speech is unintelligible whenever the amplitude spectrum is completely decorrelated, while music remains recognizable. Results for compressed speech appears to follow a similar pattern to uncompressed speech, but with predictable differences related to how speech units are affected by temporal compression.

These results not only support recent findings that the effects of amplitude and phase spectra decorrelation on speech intelligibility depend on temporal window size, but also suggest that this relationship is due to the size of the smallest meaningful unit in the stimulus.

PS 668

Accent and Listening Effort in Speech Recognition with Competing Talkers: Cerebral-acoustic Coherence, P1-N1-P2, and N400

Paul Iverson; Emma Brint; Jieun Song; Mengfan Wu
University College London

Focused attention to a speech signal (e.g., in the presence of a distractor) has diverse effects on auditory and lexical processing. For example, low-frequency modulations (1-8 Hz) in cortical activity track the amplitude envelope of attended speech, and auditory evoked potentials (P1-N1-P2) become greater for an attended auditory stream. However, listeners can rely less on lexical constraints with greater attention to the acoustic signal. The present study examined how these effects are modulated by accent and listener background. The listeners were native speakers of southern British and Glaswegian English, and Chinese second-language English speakers. Listeners heard sentences spoken in southern British and Glaswegian accents, either with single or competing talkers. The results demonstrate that difficult accents and competing talkers have similar effects at a lexical level, increasing the amount of

lexical search for native listeners and disrupting lexical search for non-native listeners. In contrast, accent had little effect on cerebral-acoustic entrainment, although entrainment was increased for target talkers in competing-talker conditions.

Vestibular: Central Circuits

PS 669

Bilirubin Potentiates Acid-Sensing Ion Channel 1A/2A Heteromers in Medial Vestibular Nucleus Neurons

Haibo Shi¹; Ke Lai²; Haosong Shi²; Yaqin Wu²; Shankai Yin¹; Hai B. Shi³

¹Department of Otorhinolaryngology-Head & Neck Surgery Affiliated Sixth People's Hospital, Shanghai Jiao Tong University, 600 Yishan Road, Shanghai 200233, P.R.China; ²Department of Otorhinolaryngology Head & Neck Surgery, The Sixth People's Hospital Affiliated to Shanghai Jiaotong University; ³The Sixth People's Hospital Affiliated to Shanghai Jiaotong University

Purpose

To investigate the effect of bilirubin on ASIC channels (Acid-Sensing Ion Channel) in neurons from MVN (medial vestibular nucleus) of rats.

Methods

Acute dissociation of neurons from MVN of rats was performed. Briefly, brainstem slices were made using a microtome and the MVN region was located using a dissecting microscope. For dissociation, the MVN neurons were triturated using a mechanical device incorporating a fire-polished glass pipette. ASIC currents were recorded with the conventional patch-clamp technique and a "Y-tube" perfusion system was used to achieve a rapid exchange of extracellular solutions within 20 ms.

Results

Here we show that the activation of ASICs in medial vestibular nucleus neurons is positively modulated by perfusion bilirubin at micromolar concentrations (control: 744.95 ± 141.03 pA; $9 \mu\text{M}$ bilirubin: 1249.16 ± 225.66 pA; $n=7$, $P < 0.01$). The bilirubin potentiation of proton-induced currents is large extent from heteromeric ASIC2a/1a channels. The pharmacological properties of ASIC channels are confirmed by blockers for different subunits of ASICs. With BAPTA loaded into these neurons, an underlying mechanism of intracellular signal transduction involved in bilirubin potentiation may be the activation of NMDARs-CaMKII cascade. Current-clamp recordings exhibited that bilirubin enhances acid-induced membrane depolarization from the holding

potential of -60 mV to -16.31 ± 2.07 mV ($n=6$, $P < 0.01$) which is partially inhibited by TEA-Cl (-33.04 ± 2.13 mV, $n=6$, $P < 0.05$).

Conclusion

Our studies suggest that bilirubin may play an important role in potentiation of ASICs, leading to a synergistic effect for the increased neuronal excitation and neurotoxicity in pathological conditions.

PS 670

Bilirubin Enhances Medial Vestibular Nuclei Voltage-gated Sodium Channel Currents by Dephosphorylation

Haibo Shi¹; Haosong Shi²; Ke Lai²; Yaqin Wu²; Shankai Yin¹; Hai B. Shi³

¹Department of Otorhinolaryngology-Head & Neck Surgery Affiliated Sixth People's Hospital, Shanghai Jiao Tong University, 600 Yishan Road, Shanghai 200233, P.R.China; ²Department of Otorhinolaryngology Head & Neck Surgery, The Sixth People's Hospital Affiliated to Shanghai Jiaotong University; ³The Sixth People's Hospital Affiliated to Shanghai Jiaotong University

Neonatal unconjugated hyperbilirubinemia and jaundice affect nearly 85% of newborns. Acute bilirubin encephalopathy may ensue to kernicterus which would result in movement disorders, hearing loss, oculomotor pareses and etc. Although hyperexcitability may contribute to the deficits, the accurate mechanism underlying neural impairment by bilirubin are ambiguous. Medial vestibular nuclei(MVN) plays an important role in the processing of body motion-related multisensory signals and their transformation into motor commands for gaze and posture control. Evidences have shown MVN will be infected during kernicterus. Voltage-gated sodium channels(VGSCs) mediate the generation of action potential, their kinetics including half-activation voltage, current density and etc will determine the excitability and response mode of cell, thus it's significant to elucidate the role of VGSCs in hyperbilirubinemia.

Postnatal day 5 Sprague-Dawley rats were anesthetized with sodium pentobarbital and then decapitated. The brain was removed and placed into oxygenated, ice-cold artificial cerebrospinal fluid. Transverse slices were cut at a thickness of 300 μm with a microslicer. Slices containing the MVN were maintained in oxygenated ACSF at 37°C for at 20-30min, neurons were mechanically isolated using fire-polished glass pipettes and placed on 35-mm-diameter dishes containing standard external solution and visualized using the phase-contrast mode of an inverted microscope. Whole cell patch-clamp recordings were made with the aid of an amplifier. All data

were recorded in voltage clamp mode at a holding potential of -70 mV. Recording solution was continuously buffered to the cells for at least 3 min, the solution contains 50mM NaCl in order to reduce the voltage error owing to the large sodium current.

Bilirubin could enhance VGSC currents by dephosphorylation resulting from inhibition of PKA and PKC kinase. Besides, bilirubin would hyperpolarize activation V_{half} , accelerate activation and hyperpolarized the inactivation V_{half} , all these imply other modulation forms or sites could interact with bilirubin. Further work shall be done.

PS 671

The Role of the Vestibular Nuclei in Congenital Disorders of the Inner Ear

Sigmund J. Lilian¹; Kenna D. Peusner²

¹GWU; ²George Washington University School of Medicine

In congenital disorders producing malformed vestibular inner ear structures, children experience delayed motor development and posture and balance problems. What happens to the brain regions processing vestibular signals is not known in these children. We hypothesize that improper vestibular signals are transmitted to the vestibular nuclei, the first brain centers processing the input, leading to their abnormal development.

In our lab, we are implementing a new animal model, the chick embryo, to determine what happens in the CNS of children with congenital vestibular disorders. As published by other labs, our lab found that rotating the developing ear, or otocyst, 180 degrees in two-day-old chick embryos (E2) most commonly produced a large sac or an inner ear missing one or more semicircular canals. After hatching, the experimental chicks showed abnormal vestibular-mediated behaviors, including head tilt, stumbling while walking, delayed righting reflex, and a tendency to close one or both eyes. In the brainstem, we study the chick tangential nucleus because this is a rather unique vestibular nucleus with an orderly arrangement of its principal cells. Also, considerable information is available on the structure and function of the developing tangential nucleus. From preliminary otocyst rotations, we found that the number of principal cells decreased inconsistently due to differences in the inner ear pathologies resulting from otocyst rotation. To study how abnormal vestibular inputs impact on brain development, it is necessary to have a reproducible chick model with consistent inner ear defects. Therefore, we revised the otocyst rotation protocol to produce inner ears lacking only the lateral canal, the most common defect found in many congenital disorders (e.g., CHARGE Syndrome).

To make the model reproducible, otocyst rotations were performed only on chick embryos at Hamburger-Hamilton stage E15, and the rotated otocysts were photographed before and two hours after rotation to confirm that the rotated otocyst maintained a stable position. With the reproducible chick model, we will determine what happens to the structure/function development of the tangential nucleus and the remaining central vestibular neural circuitry when the lateral canal fails to develop. Understanding developmental processes is crucial to reassessing how the disorder is treated and to design new treatments.

PS 672

Plasticity Within Vestibular Reflex Pathways: Implications for Use of Vestibular Prostheses

Diana E. Mitchell¹; Charles C. Della Santina²; Kathleen E. Cullen¹

¹McGill University; ²Johns Hopkins University School of Medicine

Whether it is the generation of a simple reflex behavior or an elaborate gymnastic routine, plasticity within motor pathways is required for the accurate execution of movements. Linking synaptic plasticity with changes in motor performance requires understanding how synaptic efficacy influences behavioral responses. The vestibular system plays a vital role in gaze and postural stabilization, through the vestibulo-ocular reflex (VOR) and vestibulo-spinal reflexes, respectively. Notably, the relative simplicity of vestibular pathways and their precise behavioral readout make it an excellent model system for studying the mechanisms underlying the fine tuning of motor performance. Here, we examined the neural correlates of behavioral plasticity induced by applying temporally precise stimulation to the vestibular periphery in alert rhesus monkeys. To link changes in neuronal activity with changes in motor performance, we recorded eye and head movements driven by the VOR and vestibulo-spinal reflexes, respectively, as well as the activity of neurons that drive these reflexes during behaviorally relevant stimulation of the vestibular nerve.

Responses of neurons within direct VOR and vestibulo-spinal pathways were decreased following behaviorally relevant patterns of vestibular nerve activation in awake behaving animals. Specifically, stimulation of the vestibular nerve resulted in a decreased efficacy of the synapse between vestibular afferents and first-order central neurons (i.e. long term depression (LTD)). The attenuation of these pathways was sufficient to cause a reduction in evoked VOR and vestibulo-spinal reflex responses. Interestingly, we found evidence of nearly instantaneous complementary changes in the strength

of indirect inhibitory brainstem pathways, which worked to offset the reduced sensitivity of first-order central neurons. Therefore, rapid plasticity at the first central vestibular synapse can fine-tune motor performance, while complementary plasticity within indirect inhibitory brainstem pathways ultimately contributes to ensuring a robust behavioral output. Taken together, these findings provide evidence that vestibular prosthetic stimulation induces LTD at the synapse between vestibular afferents and first-order central neurons. Fortunately, our additional finding that the changes induced at this synapse are rapidly offset by the enhancement of local inhibitory pathways within the vestibular nuclei, suggests that complementary brainstem mechanisms are also evoked which in turn function to ensure a relatively robust behavioral performance.

PS 673

The Neuronal Potentiation of the Neurons in the Vestibular Nucleus (VN) by Galvanic Vestibular Stimulation (GVS)

Kyu-Sung Kim¹; Gyutae Kim²; EunHae Jeon¹; Hyun Ji Kim¹; Sangmin Lee³

¹*Dept. of Otolaryngology-Head & Neck Surgery, Inha University Hospital, Incheon, Korea;* ²*Institute for Information and Electronics Research, Inha University, Incheon, Korea;* ³*Department of Electronic Engineering, Inha University, Incheon, Korea*

Background

The study for plasticity has focused on some specific regions, such as hippocampus and olfactory bulb, in the brain, and that in the vestibular nucleus (VN) has been rarely investigated. However, the plasticity shown as the neuronal potentiation in the VN is strongly related with vestibular compensation, and it might exhibit in the early structural level. Here, we explored the neuronal potentiation in the VN by analyzing the vestibular-related neurons responding to galvanic vestibular stimulation (GVS).

Method

From eighteen guinea pigs, we recorded twenty four neuronal responses to repeated GVS in the VN. The anesthetized animal's head was positioned in a motorized stereotaxic apparatus, and was placed on the top of a rotatory table. Using a tungsten electrode (5-12M Ω , A-M System, US), the extracellular potentials of vestibular neurons were recorded. The applied GVS was direct current (100 μ A, 2-3 sec, repeated five times) and the stimulated region was the temporal bone and around its muscles. The neuronal responses were selected before and after GVS (1 sec duration for each), and the means

of peak-to-peak spike amplitudes were compared. In addition, the average values of inter-spike-interval, minimum, and maximum of spikes were examined for further investigation of plasticity.

Result

The amplitudes of the spikes were strengthened after the repeated GVS in four neurons (16.7%). The neuronal potentiation was emerged through the comparisons among the amplitudes before GVS. A similar observation was made comparing the amplitudes of spikes after GVS, and the minimum increase in amplitude was 10.3%. On the other hand, the inter-spike intervals before and after GVS showed no significant changes ($p=0.58$).

Conclusion

The neuronal potentiation by the repeated GVS was observed in the VN. The peak-to-peak amplitudes in neuronal spikes increased as the stimulus repetition proceeded, which implied the plasticity in the VN existed by the external electrical stimulus. In the VN, however, only a little portion of vestibular-related neurons exhibited the potentiated activities.

[This research was supported by Basic Science Research Program through the National Research Foundation of Korea (NRF) funded by the Ministry of Education (2010-0020163) and the Ministry of Science, ICT & Future Planning (NRF-2016R1C1B2014826).]

PS 674

Local Field Potentials (LFPs) Reveal Vestibular Signal Processing in Brainstem

Stephanie Haggerty¹; W. Michael King²

¹*University of Michigan;* ²*Department of Otolaryngology - Head and Neck Surgery, University of Michigan*

Introduction

Research using local field potentials (LFPs) has mostly been confined to the cortex where they are generally thought to reflect the local network activity. Though little has been published on LFPs in brainstem, there has been growing interest in how local networks play a role in processing information at these lower centers. In particular, it has recently been shown that a subset of secondary vestibular neurons known as vestibular-only (VO) cells encode head velocity only when the head movement is unexpected despite receiving an afferent head velocity signal from primary afferents. One explanation for this phenomenon is that these cells reflect the output of a network which compares the expected head velocity to feedback received from vestibular and proprioceptive afferents.

Methods

To further explore this question, we recorded local field potentials and neuronal spiking activity from the vestibular nuclei of guinea pigs using chronically implanted stereotrode arrays. The array was oriented stereotaxically towards the vestibular nuclei. A head post and eye coil were also surgically implanted to monitor head and eye movements. During testing, the animal was placed on a servo-controlled turn table such that his body was constrained to the turn table but his head was free to move. The animal was subjected to sinusoidal and constant velocity steps. To distinguish vestibular related activity from proprioceptive inflows, we compared whole body (WBR), head on body (HOB) or body under head (BUH) rotations.

Results

We found that during sinusoidal rotations, LFPs encoded head movement as expected, with ipsilateral and contralateral movement encoded as increases and decreases in magnitude, or vice versa. However, during constant velocity steps, an increase in velocity, either ipsilateral or contralateral, was always encoded as an increase in magnitude. Further, we found that LFPs did not strictly encode head velocity but also appeared to encode body in space acceleration, suggesting the use of proprioceptive inputs.

Conclusions

While further analysis is needed to determine the exact nature of LFPs in the vestibular nuclei, it is clear from our preliminary findings that they do not simply reflect the afferent inputs from the peripheral vestibular organs but rather a local network which integrates proprioceptive and other inputs.

PS 675

Localization of Vestibular Nuclear Neurons that are Activated by Pulsed, Focused Infrared Stimulation of Vestibular End Organs

Gay R. Holstein¹; Darrian Rice²; Weitao Jiang³; Suhru M. Rajguru²; Giorgio P. Martinelli¹

¹*Depts of Neurology and Neuroscience; Icahn School of Medicine at Mount Sinai, NYC;* ²*Departments of Biomedical Engineering and Otolaryngology; University of Miami; FL;* ³*University of Miami Department of Otolaryngology*

The vestibulo-sympathetic reflex (VSR) mediates proactive, direct and rapid modulation of blood pressure (BP), initiating blood redistribution in the body at the onset of movement or a postural adjustment in order to assure consistent cerebral perfusion. The VSR conveys vestibular end organ signals to a region of the caudal vestibular nuclei (VNC) that projects to key pre-sympathetic sites for integration of cardiovascular signals in the rostral and caudal ventrolateral medulla (RVLM and CVLM, respectively). We have previously shown that there are direct projections from VNC to RVLM and CVLM, that neurons in these pathways are activated by sinusoidal galvanic vestibular stimulation (sGVS), and that there are both glutamate-immunoreactive and GABAergic components of the VSR. However, sGVS is a global vestibular stimulus that activates the entire vestibular nerve. The goal of the present study was to compare the locations of vestibular nuclear neurons activated by sGVS and by pulsed infrared neural stimulation (INS) that is focused on individual end organs, within the context of the VSR.

All experiments were approved by the Institutional Animal Care and Use Committees at University of Miami or Mount Sinai Medical Center. Subjects were adult male Long-Evans rats. For the INS, a head post was cemented to the skull of the anesthetized rats and attached to a stereotaxic frame. BP and heart rate were measured while frequency modulated stimuli (1863nm, 200us, 100-250pps, varied radiant exposure) were delivered to vestibular end organs using 200 or 400 μm optical fibers at 0.01Hz in the right ear.

In response to the INS, BP and heart rate were altered in all rats. To determine whether INS activation of the VSR resulted in cFos protein accumulation in VNC and other VSR-related neurons, rats were euthanized by cardiac perfusion with aldehydes 90 min after the cessation of the INS. The brains were harvested, postfixed overnight, sectioned and stained. Immunostained brainstem sections from these rats demonstrated specific cFos immunolabel in neurons of VNC as well as RVLM and CVLM. In contrast to the findings obtained using sGVS and tilt, the INS-activated vestibular neurons were concentrated in small discrete regions of medial and spinal VNC. In addition, there were substantially fewer cFos-stained neurons in RVLM and CVLM than observed following sGVS and tilt. These observations suggest that the higher spatial resolution of INS can be used to identify VSR neurons activated by individual end organs.

Supported by NIDCD grants 1R01DC008846 (GRH) and 1R01DC013798 (SMR).

PS 676

Pulsed Infrared Stimulation of Vestibular System Evokes Vestibulo-Sympathetic Reflex Responses

Darrian Rice¹; Weitao Jiang²; Gay R. Holstein³; Giorgio P. Martinelli³; Suhrud M. Rajguru¹

¹*Departments of Biomedical Engineering and Otolaryngology; University of Miami; FL;* ²*University of Miami Department of Otolaryngology;* ³*Depts of Neurology and Neuroscience; Icahn School of Medicine at Mount Sinai, NYC*

Background

Galvanic stimulation (GVS) of the vestibular end organs has been shown to alter blood pressure (BP) and heart rate (HR), however the cardiovascular responses are not well understood. Infrared neural stimulation (INS) is an alternative to GVS that has been shown to produce afferent responses in the vestibular system and can be focused to activate individual vestibular endorgans. In the present study, we investigated changes in BP and HR evoked when the vestibular sympathetic reflex pathway (VSR) was stimulated by INS in a rat model.

Method

The University of Miami Institutional Animal Care and Use Committee approved all procedures. Changes in BP and HR were studied in adult male Long-Evans rats weighing 300-500 g, anesthetized with ketamine (44mg/kg) and xylazine (2.5 mg/kg). A head post was cemented to the skull of each rat and attached to a custom-designed stereotaxic frame to restrict movement during stimulation. BP and HR were measured using a non-invasive tail cuff-based BP monitor (CODA, Torrington, CT). Frequency modulated INS (1863nm, 200us, 100-250pps, varied radiant exposure and frequencies) was delivered to vestibular endorgans using 200 or 400 μ m optical fibers in the right ear. Following the measurements, the fiber was fixed in place and orientation and distance of the typical optical fiber placement relative to vestibular structures were determined using Microcomputed Tomography (Micro-CT).

Results

Sinusoidal INS at 0.01Hz induced oscillations in BP and HR. In addition, we observed both increases and decreases in BP during INS at infrared radiation energies between 120-450 μ J. Most notably, an initial decrease in BP followed by a gradual increase to baseline during IR stimulation was observed in several rats. MicroCT image analysis highlighted the spatial selectivity of IR and showed the posterior canal ampullary region to be the primary target of stimulation.

Conclusions

The INS-evoked responses compared well to previous studies that report both an increase and decrease in cardiovascular response with stimulation of the vestibular endorgans. We hypothesize that INS activated neurons that provide inputs to the vestibulo-sympathetic reflex upon changes in head position relative to gravity. Results are suggestive of selective activation of the vestibular system by pulsed infrared, which can be used to detail the functioning of the VSR pathways activated by individual end organs.

Funding

[NIH NIDCD 1R01DC008846 (GRH) and 1R01DC013798 (SMR)]

PS 677

Identification of MicroRNAs Related with Vestibular Compensation

Mun Young Chang¹; Sohyeon Park²; Jun Jae Choi²; Eun-bit Bae²; Young Ho Kim³; Moo Kyun Park⁴

¹*Department of Otorhinolaryngology-Head and Neck Surgery, Chung-Ang University College of Medicine, Seoul, Republic of Korea;* ²*Department of Otorhinolaryngology-Head and Neck Surgery, Seoul National University College of Medicine, Seoul National University Hospital, Seoul, Republic of Korea;* ³*Department of otorhinolaryngology, Seoul National University College of Medicine, Seoul National University Boramae Medical Center;* ⁴*Department of Otolaryngology-Head and Neck Surgery, Seoul National University Hospital, Seoul National University College of Medicine, Seoul, Republic of Korea*

Background

Vestibular compensation is the functional recovery that follows unilateral peripheral vestibular lesions, which is a good model for the neuroplasticity of the central nervous system. Several studies have been performed to identify the cellular and molecular mechanisms involved in vestibular compensation. MicroRNA is an important regulator of biological processes. In the previous study, we reported that miR-218a-5p, 219a-5p, 221-3p and 1298 were the candidate microRNAs related in vestibular compensation based on the results from microarray and qRT-PCR analysis. In the present study, we validated which microRNAs affected the vestibular compensation using agomir or antagomir of these microRNAs.

Method

We performed two experiments. Forty SD rats were randomly divided into 5 groups: the control group (n = 8) receiving artificial cerebrospinal fluid (aCSF), the 218a-5p group (n = 8) receiving miR-218a-5p antagomir, 219a-5p

group (n = 8) receiving miR-219a-5p antagomir, 221-3p group (n = 8) receiving miR-221-3p agomir and 1298 group (n = 8) receiving miR-1298 antagomir. Five animals in each group were used for the first experiment (rotarod test) and the three animals were used for the second experiment (immunohistochemistry (IHC) for 5-bromo-2'-deoxyuridine (BrdU)). In both experiments, animals underwent labyrinthectomy with intracerebroventricular infusion of aCSF or agomir or antagomir of miR-218a-5p, 219a-5p, 221-3p and 1298. Then, in the first experiment, rotarod test was performed postoperatively to check the behavioural recovery. The scores of rotarod test were expressed as a percentage of the previous best record during training. In the second experiment, BrdU were injected to animals and IHC for BrdU was performed to evaluate neurogenesis at vestibular nucleus.

Results

In the first experiment, the rotarod test was performed daily for 11 days after surgery. The mean rotarod score of the control group reached plateau up to 100% at 4 days after labyrinthectomy. However, the mean rotarod scores of the 218a-5p, 219a-5p and 221-3p groups were less than 60% for 10 days after labyrinthectomy. The rotarod scores were analyzed among the groups using mixed model. The 218a-5p, 219a-5p and 221-3p groups showed statistically significantly lower scores than control group. In the second experiment, the number of BrdU-immunoreactive cells was statistically significantly lower in the 218a-5p, 219a-5p and 221-3p groups than the control group.

Conclusion

We suggested that miR-218a-5p, 219a-5p and 221-3p might be regulators in vestibular compensation. This study could pave the way for the study which identifies the role of microRNA in the neuroplasticity of the central nervous system.

PS 678

M2 Subtype Controls Synaptic Glutamatergic Input of Cerebellum-Projecting Medial Vestibular Nucleus Neurons

Yun Zhu¹; Shaorui Chen²; Weijia Kong³; Huilin Pan²

¹Union Hospital of Tongji Medical College of Huazhong University of Science and Technology; ²Center for Neuroscience and Pain Research, Department of Anesthesiology and Perioperative Medicine, The University of Texas MD Anderson Cancer Center, Houston, TX 77030, USA; ³Department of Otolaryngology, Union Hospital of Tongji Medical College, Tongji Medical College

Neurons in the vestibular nuclei have a vital function in balance maintenance, gaze stabilization, and posture. Although muscarinic acetylcholine receptors (mAChRs) are expressed and involved in regulating vestibular function, it is unclear how individual mAChR subtypes regulate vestibular neuronal activity. In this study, we determined which specific subtypes of mAChRs control synaptic glutamatergic input of medial vestibular nucleus (MVN) neurons that project to the cerebellum. Cerebellum-projecting MVN neurons were labeled by a fluorescent retrograde tracer and then identified in rat brainstem slices. The mAChR agonist oxotremorine-M significantly inhibited the amplitude of glutamatergic excitatory postsynaptic currents evoked by stimulation of vestibular afferents, and this effect was abolished by the M2-preferring antagonist AF-DX 116. Presynaptic M2 mAChR regulates excitatory glutamatergic input from vestibular primary afferents, which in turn regulates the excitability of cerebellum-projecting MVN neurons. This new information has therapeutic implications for treating vestibular disorders with mAChR subtype-selective agents.

PS 679

Unipolar Brush Cells in the Vestibulocerebellum Receive Mossy Fiber Inputs from Primary and Secondary Vestibular Sources

Timothy Balmer¹; Laurence O. Trussell²

¹Oregon Hearing Research Center, Oregon Health and Science University; ²Vollum Institute, Oregon Hearing Research Center, Oregon Health and Science University

Unipolar brush cells (UBCs) are glutamatergic interneurons of the vestibular cerebellum and dorsal cochlear nucleus (DCN) that receive mossy fiber synaptic inputs to their elaborate brush-like dendrites and project to granule cells and other UBCs. The mossy fiber excitatory input is converted to either an increase or decrease in spiking that outlasts the input, depending on their expression of mGluR2 receptors and AMPA receptors. OFF UBCs have high mGluR2 expression, which activates an outward current mediated by G-protein coupled inward rectifying potassium channels, and are thus inhibited by glutamatergic input. Synaptic currents in ON UBCs, which express lower levels of mGluR2, are dominated by AMPARs. The mossy inputs to cerebellum and DCN have diverse origins, and it is not known which innervate the different UBC subtypes. To understand how the UBCs' prolonged increase or decrease in activity contributes to auditory or vestibular processing the origins of the mossy fibers must be identified. The goal of this project was to identify whether primary and secondary vestibular mossy fibers project directly to UBCs, and if so, whether they target specific UBC subtypes. We

utilized a mouse line that expressed Cre-recombinase in the vestibular ganglion in order to breed the light-activated ion channel channelrhodopsin-2 (ChR2) along with EYFP into these primary projections of the vestibular organ. To express ChR2 specifically in secondary vestibular afferents, an AAV-mCherry-ChR2 viral construct was injected into the medial vestibular nucleus. Using a combination of immunohistochemistry, acute slice physiology and super-resolution imaging we found that fibers from the vestibular ganglion project to ON UBCs. Activation of these primary afferents with light stimulation showed that the synaptic currents were almost completely mediated by AMPARs. In contrast to these primary inputs to ON UBCs, ChR2 expression in the medial vestibular nucleus revealed that secondary vestibular afferents may project to both ON and OFF UBCs. 3D reconstructions of several of these mossy fiber-UBC synapses recovered after patch clamp recordings reveal the complex intertwining of the mossy fiber and dendritic brush, and suggest a correlation between the size of the contact and the size of the synaptic signal.

PS 680

The Status of Vestibular and Optokinetic Reflexes in a Mouse Model of Spinocerebellar Ataxia Type 6

Hui Ho Vanessa Chang; Sriram Jayabal; Alanna J. Watt; Kathleen E. Cullen; Hui Ho Chang
McGill University

Spinocerebellar Ataxia Type 6 (SCA6) is a mid-life onset neurodegenerative disease that affects motor coordination. Notably, patients with SCA6 experience progressive ataxia, dysarthria, and nystagmus. This autosomal dominant disease is caused by the expansion of a CAG repeat tract in a CACNA1A gene that encodes the $\alpha 1A$ subunit of the P/Q type voltage-gated Ca^{2+} channel. A hyper-expanded polyglutamine (84Q) mouse model of SCA6 (84Q/84Q), is characterized by impaired locomotive function. Using both in vitro and in vivo recordings, we have recently shown that, in this same mouse model, the firing precision of cerebellar Purkinje cells in lobule 3, areas of the cerebellum generally associated with locomotion, is significantly reduced (Jayabal et al., 2016).

A recent study has further demonstrated an impairment in eyeblink conditioning in a different, Purkinje-cell specific SCA6 mouse model, likely due to alteration in the cerebellar circuitry (Mark et al., 2015). Accordingly, we hypothesized that SCA6 (84Q/84Q) mice would likely show deficits in other cerebellar-dependent behaviors. To test this hypothesis and to understand the pathophysiology of SCA6 mice in more detail, we characterized their vestibular-ocular reflex (VOR) and optokinetic reflex (OKR) by quantifying their eye movements. Vestibular stimuli were delivered to a head-restrained

mouse by head rotations at frequencies and velocities that are similar to those in natural behaviors (0.2-3 Hz and 16 and 8 deg/s). VOR eye movement responses were measured in both dark and light conditions. OKR were evoked by rotation of visual stimulus at the same frequencies and velocities. Our preliminary data shows that SCA6 mice had approximately 20% reduction of both the VOR and OKR gain without a change in phase compared to litter-matched control WT mice. Based on this, we speculate that neuronal responses may be altered in the floccular lobe of SCA6 (84Q/84Q) mice, a region of the cerebellum known to play a vital role in the calibration of the VOR pathway as well as the generation of the optokinetic responses.

PS 681

Pontomedullary Reticular Formation Neurons Integrate Inputs from Limb and Labyrinth in an Additive Manner

Derek M. Miller; Andrew A. McCall; Carey D. Balaban; William M. DeMayo; George H. Bourdages; Bill J. Yates
University of Pittsburgh

The maintenance of balance is an inherently multimodal process, as no one sensory system provides all the inputs needed to accurately estimate body position and movement in space. For example, while the vestibular system exquisitely signals head position and the direction and velocity of head movements, it alone cannot indicate the relative positions of the head, trunk, and limbs. Previous research has shown that the central nervous system integrates vestibular and neck proprioceptive afferent information to distinguish whole-body from head-on-body motion, and it uses this information to execute corrective postural responses that account for head-on-body position. However, much less is known about how limb state alters the processing of vestibular inputs, which is surprising given that the limbs are the sole actuators responsible for the execution of postural reflexes. We recently demonstrated in both decerebrate and conscious cat preparations that hindlimb somatosensory inputs converge with vestibular afferent input onto neurons in multiple CNS locations that participate in balance control. While it is known that head and limb movements modulate postural reflexes, presumably through vestibulospinal and reticulospinal pathways, the combined influences of the two inputs on the activity of neurons in these brainstem regions is unknown. Therefore, in the present study, we compared the responses of pontomedullary reticular formation (pmRF) neurons to vestibular and hindlimb stimuli delivered separately and together in conscious cats. The pmRF was chosen because of its well-established role in postural control. Extracellular single-unit recordings were obtained from

pmRF neurons. Sinusoidal whole body rotation in the roll plane was used as the search stimulus. Units responding to the search stimulus were tested for their responses to 10° ramp-and-hold body rotation in the roll plane (vestibular stimulation), 10° extension hindlimb movement delivered in the rostral-caudal plane, and both movements delivered simultaneously. Composite response histograms were generated and fit by a model of low and high pass filtered limb and body position signals using least squares nonlinear regression. A subpopulation of neurons that responded to both vestibular and limb stimulation did so in an additive fashion. We speculate that the pmRF neurons which integrate inputs from the labyrinth and limb likely participate in adjusting reticulospinal outflow in response to the mechanical state of the limb.

PS 682

Is VOR Gain an Adequate Measure of Semicircular Canal Function?

Ian Curthoys¹; Hamish MacDougall²; Leigh McGarvie³; Michael Halmagyi AO³; Catherine de Waele⁴; Leonardo Manzari⁵; Julia Dlugaiczyk⁶

¹Univ of Sydney; ²Sydney Human Factors Research, School of Psychology, University of Sydney, NSW, Australia; ³Department of Neurology, Royal Prince Alfred Hospital, Sydney, Australia; ⁴Cognitive and Action Group, UMR 8257, 45 rue des Saints Pères, 75006 Paris; ⁵MSA ENT Academy Center – Cassino, Italy; ⁶Department of Otorhinolaryngology, Saarland University Medical Center, Homburg, Germany

Introduction

Whilst a global measure such as VOR gain is effectively used for diagnosing many vestibular disorders, recent evidence has again questioned the adequacy of this measure. Intratympanic gentamicin (ITG) selectively attacks type I receptors and so degrades the response of irregular afferents from the semicircular canals and the otolithic maculae. These receptors are jerk detectors and so respond well to changes in acceleration at the onset of stimuli. The effectiveness of each ITG injection is now assessed clinically by measuring the semicircular canal response to an abrupt rotational stimulus – the video head impulse test (vHIT) - which shows a decline in the very early eye velocity response even after a single ITG injection. In sharp contrast are the eye velocity response profiles on vHIT of other patients who report dizziness. In some of these patients there can be enhanced eye velocity at the early part of their eye velocity response. This study contrasted the eye velocity response profiles of healthy subjects against these two patient groups.

Methods

The ICS Impulse system measured vHIT using the HIMP paradigm where the subject or patient was instructed to maintain fixation on an earth-fixed target during small, abrupt, passive, unpredictable head turns (head impulses) in the plane of the horizontal canal.

Results

There are systematic differences in the way the eye velocity of patients tracks head velocity. These responses are reliable and are not artifacts, such as due to goggle slippage or errors in calibration or hardware defects in the particular glasses used or misunderstanding the instructions or malingering. The usual measure of performance - VOR gain - is a global measure which does not reveal such detailed differences in the exact time series of eye velocity response shown here. In some patients with enhanced eye velocity, the overall VOR gain was 1.0, whereas the time series of eye velocity systematically departed from the usual response profile of healthy subjects

Discussion and Conclusion

VOR gain is a global measure which has been designed to minimize artifacts due to goggles slippage etc. The results reported here are due to changes in exactly how the eye velocity response takes place. We conclude that in addition to VOR gain we need new measures of canal performance to quantify the exact form of the response to abrupt stimuli.

PS 683

Vision Has Minimal Impact on Set-point Adaptation During Magnetic Vestibular Stimulation

Bryan K. Ward; Dale C. Roberts; Michael C. Schubert; David S. Zee; Jorge Otero-Millan
Johns Hopkins University

Background

Strong static magnetic fields such as those in an MRI machine can induce sensations of self-motion as well as nystagmus. The proposed mechanism is a Lorentz force resulting from the interactions between strong static magnetic fields and ionic currents in the inner ear endolymph and causing displacement of the semicircular canal cupulae. The nystagmus persists (although partially adapts) throughout an individual's exposure to the magnetic field. After leaving the magnetic field an aftereffect occurs in which the nystagmus and sensations of rotation reverse direction, reflecting adaptation that occurred while inside the MRI. The influences of visual fixation and head movements inside the MRI on this vestibular adaptation are unknown.

Methods

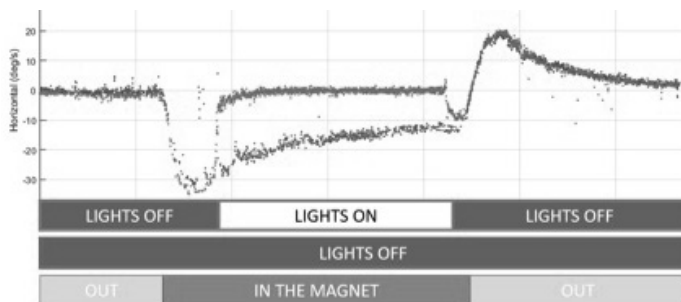
Three-dimensional video oculography was performed on 6 individuals before, during and after exposure to a 7T MRI scanner. Subjects entered the MRI bore head-first and supine and eye movements were recorded in darkness with infrared illumination for 5 minutes and then for 4 minutes after exiting. The trials were then repeated with subjects entering the magnetic field in darkness, followed by either light with visual fixation or yaw head rotations (2 Hz) in the dark while inside the MRI, beginning 60 seconds after entering the magnetic field. Subjects were placed in darkness again 30 seconds before exiting the bore.

Results

Similar with prior studies, all subjects developed horizontal nystagmus inside the magnetic field, with slow-phase eye velocity that partially decreased inside the magnetic field. All subjects exhibited an aftereffect upon exiting the magnet, developing nystagmus in the opposite direction. During the fixation trials, nystagmus was suppressed with visual fixation; however, when again placed in darkness just before exiting the magnet, nystagmus resumed with velocity close to that of the control condition and after exiting the magnet, the aftereffect was also the same as the control condition (figure). Similar effects occurred with yaw head rotations.

Conclusions

Visual fixation and head shaking inside a strong static magnetic field have minimal impact on short-term set point adaptation of magnetic field-induced nystagmus and suggest that the pathways for adaptation to a vestibular lesion differ from that of dynamic adaptation.



PS 684

Effect of Eccentric Gaze Position on Visual-vestibular Heading Perception

Benjamin T. Crane

University of Rochester

Visual heading perception is strongly eye position dependent while vestibular or inertial headings are not. This study examined visual and inertial heading integration with eccentric eye positions in 7 humans (3 male,

age 22-57). Experiments had randomly interleaved trials in which eye position was centered, 25° left, or right. A fixation was monitored using a binocular video eye tracking. The fixation point disappeared during the stimulus and eye position was maintained at the location. The stimulus was 2s of visual motion through a star field or analogous inertial motion. After each stimulus, subjects reported whether they felt each stimulus was consistent with motion left or right of the midline. In the visual only condition with eccentric viewing positions the average point of subjective equality (PSE) in which motion was equally likely to be perceived as left or right of center was 10.3° in the direction of gaze. Thus, visual heading perception was shifted in the direction opposite gaze, a shift consistent with retinotopic coordinates. When the experiment was conducted with an inertial stimulus in darkness, eccentric viewing positions had a smaller and opposite effect than they had with visual stimuli. The PSE with inertial stimuli in darkness was 4.6° in the opposite direction of gaze. Since eye position had opposite effects on the perceived directions of visual and inertial headings, provided a novel method of studying visual-vestibular multisensory integration without the sensory stimuli artificially offset from each other. Visual and inertial integration was studied by varying the coherence of the visual stimulus. Varying the visual coherence alone had no effect on the PSE (Fig. 1A). Visual stimuli with coherences of 0%, 35%, 50%, 70%, 80%, 90%, and 100% were combined with inertial stimuli. Thresholds increase with decreasing visual coherence (Fig. 1B). At coherences of 50% and lower the eye position bias of PSE was predicted by Bayesian weighting (Fig. 1A). However, at higher coherences the inertial stimulus had more influence than would be predicted based on reliability (Fig. 1A). These findings were consistent with a Bayesian integration at low visual coherence but suggested closer to ideal performance (e.g. less eye position bias than would be predicted) than Bayesian predictions at high visual coherence.

Support: R01 DC013580; K23 DC011298

PS 685

Development of Original Real-time 3D Video-oculography and Image Filing System, yVOG

Makoto Hashimoto¹; Takuo Ikeda²; Hironori Fuji¹; Kazuma Sugahara¹; Yoshinobu Hirose¹; Hiroshi Yamashita¹

¹Department of Otolaryngology, Yamaguchi University Graduate School of Medicine; ²Tsudumigaura medical center for children with disabilities

Background

It is essential to use an infrared CCD camera in clinical examination of the vestibular system. Devices are currently available that can quite accurately record human eye movements, based on the principle of video-oculography (VOG). We devised an original VOG (HI-VOG) system using a commercialized infrared CCD camera, a personal computer and public domain software program (ImageJ) for data analysis. In the present study, we revised the VOG and image filing system for real-time 3D quantitative analysis of nystagmus, yVOG.

Methods

The video image from a commercialized infrared CCD camera was captured at 30 frames per second at a resolution of 640*480 pixels. For analysis of the horizontal and vertical components, the X-Y center of the pupil was calculated. For analysis of torsional components, the whole iris pattern was overlaid with the same area of the next iris pattern, and the angle at which both iris patterns showed the greatest match was calculated.

Results

Accurate measurements of horizontal, vertical and torsional eye movement were taken while recording the video image in real-time. For quantitative analysis, the slow phase velocity of each occurrence of nystagmus and the average value of the slow phase velocity were analyzed automatically.

Conclusion

Using the revised yVOG system, it was possible to perform real-time quantitative 3D analysis of nystagmus from video images recorded with a commercialized infrared CCD cameras.

PS 929

The Neuronal Potentiation of the Neurons in the Vestibular Nucleus (VN) by Galvanic Vestibular Stimulation (GVS)

Kyu-Sung Kim¹; Gyutae Kim²; EunHae Jeon¹; Hyun Ji Kim¹; Sangmin Lee³

¹Dept. of Otolaryngology-Head & Neck Surgery, Inha

University Hospital, Incheon, Korea; ²Institute for Information and Electronics Research, Inha University, Incheon, Korea; ³Department of Electronic Engineering, Inha University, Incheon, Korea

Background

The study for plasticity has focused on some specific regions, such as hippocampus and olfactory bulb, in the brain, and that in the vestibular nucleus (VN) has been rarely investigated. However, the plasticity shown as the neuronal potentiation in the VN is strongly related with vestibular compensation, and it might exhibit in the early structural level. Here, we explored the neuronal potentiation in the VN by analyzing the vestibular-related neurons responding to galvanic vestibular stimulation (GVS).

Method

From eighteen guinea pigs, we recorded twenty four neuronal responses to repeated GVS in the VN. The anesthetized animal's head was positioned in a motorized stereotaxic apparatus, and was placed on the top of a rotatory table. Using a tungsten electrode (5-12M Ω , A-M System, US), the extracellular potentials of vestibular neurons were recorded. The applied GVS was direct current (100 μ A, 2-3 sec, repeated five times) and the stimulated region was the temporal bone and around its muscles. The neuronal responses were selected before and after GVS (1 sec duration for each), and the means of peak-to-peak spike amplitudes were compared. In addition, the average values of inter-spike-interval, minimum, and maximum of spikes were examined for further investigation of plasticity.

Result

The amplitudes of the spikes were strengthened after the repeated GVS in four neurons (16.7%). The neuronal potentiation was emerged through the comparisons among the amplitudes before GVS. A similar observation was made comparing the amplitudes of spikes after GVS, and the minimum increase in amplitude was 10.3%. On the other hand, the inter-spike intervals before and after GVS showed no significant changes ($p=0.58$).

Conclusion

The neuronal potentiation by the repeated GVS was observed in the VN. The peak-to-peak amplitudes in neuronal spikes increased as the stimulus repetition proceeded, which implied the plasticity in the VN existed by the external electrical stimulus. In the VN, however, only a little portion of vestibular-related neurons exhibited the potentiated activities.

This research was supported by Basic Science Research Program through the National Research Founda-

tion of Korea (NRF) funded by the Ministry of Education (2010-0020163 & NRF-2016R1D1A1B03930657) and the Ministry of Science, ICT & Future Planning (NRF-2016R1C1B2014826).

Binaural Hearing & Sound Localization

PD 85

Experience-Dependent Plasticity In The Nucleus Laminaris Of The Barn Owl

Catherine E. Carr¹; Tiffany Wang¹; Anna Kraemer²; Go Ashida³; Christine Köppl⁴; Hermann Wagner⁵

¹*Univ Maryland*; ²*University of Maryland College Park*;

³*Cluster of Excellence "Hearing4all", Department of Neuroscience, Faculty 6, University of Oldenburg*;

⁴*Cluster of Excellence H4A, Dept. of Neuroscience, Carl von Ossietzky University Oldenburg*; ⁵*Institute of Biology II, RWTH Aachen University*

Detection of interaural time differences depends on precise coding of delay. In the barn owl, myelinated axons from the first order nucleus magnocellularis act as delay lines to create maps of interaural time difference in the nucleus laminaris (NL). Myelination of the delay lines is timely, coinciding with the attainment of adult head size (Cheng and Carr, 2007, *DevNeurobiol* 67:1957-1974). Since myelination coincided with stable ITD cues, we hypothesized that conduction velocity could be modified by experience. To test this, we had previously fitted 8 young owls (from P21) with unilateral ear-canal inserts designed to introduce a time delay to inputs from that ear (Gold and Knudsen, 1999, *JNeurophysiol* 82:2197-2209). In the adult map of ITD in the barn owl, the phase of a monaurally or binaurally evoked neurophonic shifts in an orderly fashion that reflects the map of delays (Carr et al., 2015, *JNeurophysiol* 114:1862-1873). We hypothesized that, if NL adjusts for the temporally altered input, the maps of ITD would be shifted compared to normal. However, the manipulated owls did not show any such shifts at a minimum age of 3 months. Reasoning that P21 might be past a critical period for adjustment of conduction velocity in NL, we raised 10 owls from P14 with unilateral earmold plugs.

Plugs, instead of the previously used custom inserts, were used because the ear canals were too narrow for the inserts. Owls experienced this altered auditory input for 3 months and their maps of ITD were later measured without the plug, when they reached adulthood. Neurophonic responses were recorded in NL and small electrolytic lesions were placed at selected recording sites, to recover their precise position and determine whether the map of ITD was altered by experience.

We hypothesized that plasticity would induce complementary shifts in ITD representation on the two sides, i.e. on the side ipsilateral to the ear plug, the point of zero ITD should shift ventrally, and dorsally on the contralateral side. We found that the positions of zero μ s ITD shifted in the predicted direction, but only ipsilaterally, while the contralateral map did not change.

Thus, experience-dependent plasticity of conduction delay occurs in the owl NL. Remarkably, it appears that the ipsilateral and contralateral maps are independently regulated.

PD 86

Does "Reverberation Constancy" Alter the Temporal Weighting of Auditory Spatial Cues?

G. Christopher Stecker; Travis Moore; Monica Folkerts; Julie Stecker
Vanderbilt University School of Medicine

A rich literature now demonstrates that exposure to a consistent reverberant context can alter listeners' subsequent perception. Examples include the buildup of the precedence effect, in which pre-exposure to a consistent echo enhances the fusion of source and echo sound (Clifton 1987 *JASA* 82:1834-5, Brown & Stecker 2013 *JASA* 133:2883-98), loudness and duration judgments of exponentially decaying envelopes, which are reduced following exposure to consistent envelope decays (Stecker & Hafter 2000 *JASA* 107:3358-68; Ries et al. 2008, *JASA* 124:3772-83), and alterations of reverberant speech perception following exposure to consistent synthetic reverberation (Watkins & Makin 2007 *JASA* 121:257-66, Brandewie & Zahorik 2010 *JASA* 128:291-9). Each of these cases is consistent with the notion of "reverberation constancy" (Stecker & Hafter 2000) that compensates for the perceptual effects of reverberation when they can be estimated from the timing, geometry, and envelope characteristics of ongoing sound.

Despite clear evidence that pre-exposure alters qualitative aspects of sound perception, impacts on sound localization are not well established. In fact, there is some evidence that buildup affects the perception of source-echo fusion much more than it impacts localization dominance (Brown & Stecker 2013). In the current study, we considered whether pre-exposure to a consistent anechoic or reverberant context could alter the temporal weighting of auditory spatial cues, for example by magnifying or reducing the importance of sound-onset cues for localization.

Temporal weighting functions (TWFs) were measured for 4-kHz Gabor click trains presented in anechoic space using the method of Stecker & Hafter (2002 *JASA*

112:1046-57). Stimuli were presented anechoically or in a simulated 10x10m room, with ~700 lateral reflections (image method, $\alpha=0.5$) spanning 360° azimuth. In separate conditions, localization judgments were made for (a) single stimulus presentations, or following a series of 12 click-trains presented from a different location in (b) anechoic or (c) simulated-room contexts. For baseline measurements (a), TWFs revealed strong onset dominance in simulated reverberation and flat weighting—consistent with previous studies—in anechoic listening. Pre-exposure to reverberation (c) reduced onset dominance but did not return it to anechoic levels. The results suggest a stronger role of onset dominance in reverberant localization than previously suspected based on anechoic measurements, an effect that is only partly mitigated by reverberation constancy.

Supported by NIH R01DC011548.

PD 87

Neural Coding of Time-varying Interaural Time Differences (ITD) in the Inferior Colliculus: Relation to Human Performance in Motion Direction Identification and Binaural Gap Detection

Nathaniel Zuk¹; Bertrand Delgutte²

¹Massachusetts Eye and Ear; ²Harvard Medical School

Background

Identifying the presence and direction of moving sounds may be important for parsing a complex acoustic scene, but how motion direction is encoded in the auditory system is still unclear. Previous studies have suggested that the inferior colliculus (IC) is the first nucleus in the ascending auditory system to show direction selective neurons, but isolating a neuron's direction selectivity from firing rate adaptation is challenging. Additionally, humans can detect a brief burst of diotic noise flanked by interaurally uncorrelated noise (so-called "binaural gap"), at shorter burst durations than they can identify the direction of brief moving sounds. It is unclear why threshold durations are different for these two tasks.

Methods

We recorded from single neurons in the IC of unanesthetized rabbits in response to broadband noise at 65 dB SPL. The noise contained a brief (31-1000 ms), linearly time-varying ITD (a "sweep") that was flanked by interaurally uncorrelated noise for a total stimulus duration of 2 s. We used a point process model to separate the neural responses into three components: (1) the neuron's ability to follow the sweep's instantaneous ITD, (2) selectivity to motion direction, and (3) the dependence of the neural response on previous spiking history. In parallel perceptual experiments, the same stimuli were presented to 33 normal-hearing human listeners in two

separate tasks. In the first, participants identified the direction of the ITD sweeps. In the second, participants detected the presence of a sweep, similar to a binaural gap detection task.

Results

Across our sample of neurons, the ITD-following component captured more of the response variability than the direction selectivity component, suggesting that neurons are primarily sensitive to the instantaneous ITD rather than exhibit true direction selectivity. Neurons could follow the ITD for sweep durations shorter than human thresholds for direction identification. However, using an optimal classifier to decode the single-neuron responses, we found that neural threshold durations for direction identification were larger than threshold durations for detection. Furthermore, the range of neural threshold durations for both tasks overlapped with the corresponding human perceptual thresholds.

Conclusions

IC neurons can follow time-varying ITDs for the shortest ITD sweep durations we measured. Nevertheless, the similarity between neural and perceptual thresholds suggests that the inherent randomness of firing may limit the ability to identify the direction of moving ITDs.

Funding

NIH grants R01 DC002258, P30 DC005209, T32 DC000038, and an Amelia-Peabody Scholarship from the MEE.

PD 88

Uncertainty in Binaural Hearing Linked to Inherent Envelope Fluctuations

Gabrielle O'Brien¹; Matthew Winn²

¹University of Washington; ²University Of Washington

It was recently shown that supra-threshold changes in interaural level differences (ILDs) in 1/3-octave bands of noise were more quickly and reliably perceived when carried by high-frequency (4000 Hz center-frequency) rather than low-frequency (500 Hz center-frequency) noise. For fixed-octave ratio noises however, center frequency differences are accompanied by differences in inherent envelope modulations stemming from differences in absolute bandwidth, presenting a confound in the stimuli. We propose that envelope fluctuations (rather than frequency differences) are a more parsimonious explanation of response latency and certainty, and are therefore an essential component of a model of ILD perception.

In the current study we investigate the hypothesis that for noisier envelopes, there is less certainty that an

ILD is a true deviation from noise perceived at center. Differences in inherent envelope modulation strength were controlled using three types of stimuli: low-noise noise (with negligible envelope fluctuations), high-noise noise, and an equal mixture of the two, producing medium-noise noise.

Perception was measured using anticipatory eye movements elicited by ILD changes. Results confirm that sensitivity and response latency to ILD changes were affected by degree of envelope fluctuation, such that ILDs that were perceptible with low-noise noise were rendered entirely imperceptible when the stimulus had more pronounced envelope fluctuations. In addition, high-noise noise provoked more phantom percepts, which were nearly absent for low-noise noise.

Two computational models of evidence accumulation were used to distinguish distinct mechanisms of ILD change detection in this study. Evidence accumulation models are well suited to reaction time tasks, as they predict distributions of response latencies in addition to overall performance scores for continuously varying stimuli. In the first model, new evidence is acquired independently at each time sample, using temporal integration windows of varying length. In the second model, the deviation (rather than raw magnitude) of the instantaneous ILD was measured in relation to the prior distribution. Hence, the rate of evidence accumulation was influenced by past signal statistics. Of the two models, only the second was able to capture the relationship between envelope fluctuations and uncertainty in judging an ILD change.

The role of prior signal statistics in binaural perception has not always been obvious in classic psychoacoustic studies because of the tradition of presenting stimuli in intervals separated by silence. Here, we show that when an ILD emerges in an ongoing signal, prior signal statistics will affect the accuracy and latency of ILD perception.

PD 89

Comparison of Visual Influence on Timing-based Summing Localization Among Listeners with Normal Hearing, Symmetric and Asymmetric Hearing Loss

Yi Zhou; Emily Venskytis; Christopher Montagne
Arizona State University

Unilateral or asymmetric hearing loss (HL) interrupts binaural processing and causes difficulty in sound localization. Recently, we show that for normal hearing listeners light stimulus caused a large misjudgment in the location of a phantom sound source created by timing-based

stereophony (Montagne and Zhou, JASA, 2016). In this study we extended this testing paradigm to examine the extent of “visual capture” in listeners with various configurations and lengths of HL. Since the timing-based stereophonic stimulus offers no level cues and requires a sensitivity to interaural time difference to localize it, we hypothesized that hearing loss, especially asymmetric hearing loss, may cause degraded performance and greater visual capture relative to normal hearing.

Five subject groups, divided by hearing levels, were tested in the sound localization task. This includes one group with normal hearing, three groups with chronic unilateral or bilateral hearing loss, and one group with acute unilateral hearing loss by wearing a monaural ear-plug. We found that HL listeners responded with a different degree of accuracy in localizing a stereo sound. Listeners with chronic severe unilateral HL (>40 dB) and acute unilateral HL completely failed the task, whereas the performances of listeners with either chronic moderate bilateral or unilateral HL (< 40 dB) were almost indistinguishable to the performances of normal hearing listeners. The addition of a light stimulus further interrupted sound localization performance. The listener’s performance was least affected for normal hearing and moderate bilateral HL, but became noticeably compromised and moved towards the light direction for unilateral HL.

These results suggest that accurate localization of a timing-based stereo “phantom” sound source requires an intact binaural system. When the binaural system fails, as in the case for severe and abrupt unilateral hearing loss, sound localization succumbs to visual capture. However, when the binaural system is not completely damaged, i.e., moderate HL, plasticity and learning may help a listener recalibrate weakened and unbalanced binaural cues to enable near-normal sound localization performance, even in the presence of conflicting visual information.

PD 90

Predicting Spatial Release from Masking Using Electrophysiology

Frederick Gallun; Melissa Papesch; Robert Folmer
VA RR&D NCRAR

When sounds sources are spatially separated, intact auditory systems can utilize the subtle differences in the acoustic information between the two ears to improve detection of signals of interest. However, conditions such as aging and hearing loss can degrade such binaural cues, leading to poorer auditory perception in environments with multiple sound sources. This likely contributes to the greater difficulty understanding speech in

noisy environments reported by many hearing-impaired and older listeners. Thus, the ability to assess the robustness with which binaural cues are encoded by the auditory system is likely to provide important information regarding individual differences in hearing-in-noise perception, including the effects of aging and hearing loss. In the present study, we investigated the use of cortical auditory evoked potentials (AEPs) to rapidly assess encoding of interaural phase differences (IPD), and examined the ability of this measure to predict spatial release from masking in a behavioral speech perception task. IPD stimuli consisted of amplitude-modulated tones with a 180° interaural phase shift embedded during a low-amplitude time point within the stimulus.

Participant groups included young and middle-aged listeners with normal or near-normal hearing thresholds, and older listeners with typical presbycusis hearing losses. AEP measures revealed that younger participants were more likely to have discernable responses to higher frequency IPD stimuli compared to middle-aged and older participants, indicating that decreased binaural temporal precision begins as early as middle age even in the absence of significant hearing loss. Further, AEP measures of IPD were well correlated with behavioral Spatial Release from Masking (SRM) measures and accounted for a substantial and significant portion of the variance in behavioral performance. This relationship was particularly strong among older presbycusis listeners for whom evoked potential IPD measures were better predictors of behavioral performance than either participant age or hearing loss.

Overall, the present work shows that objective measures of the encoding of interaural phase information can be readily obtained using commonly available AEP equipment, allowing accurate determination of the effects of age and hearing loss on binaural sensitivity in individual listeners. Further, objective measures of interaural phase encoding are better predictors of SRM in speech-in-speech conditions than are age, hearing loss, or the combination of age and hearing loss.

Supported by VA RR&D Merit Review Award C77551, Service Award C8016P, and a Career Development I award C1820M, and NIH R01 DC015051.

PD 91

Impact of Verbal and Spatial Short-term Memory Load on Auditory Spatial Attention Gradients

Edward Golob¹; Jenna Winston²; Jeffrey Mock¹

¹University of Texas, San Antonio; ²Tulane University

Attentional biases are known to influence perception over a wide range of timescales, from milliseconds to

hours. Thus there is a need to consider how retaining information in short-term memory (STM) influences attention control. Here we used an auditory spatial attention task to test whether auditory attention gradients are influenced by STM, and if so whether verbal vs. spatial information in memory have differential effects. Young adults performed short blocks of an auditory spatial attention task under two STM load conditions, either by maintaining verbal (3 words) or spatial (1 sound location) information, and a no-load control. After memory encoding (STM condition), or passive viewing (no load condition), subjects attended to a standard location and discriminated the amplitude modulation rate of noise (25 or 75 Hz button press, 90% AM depth). Stimuli were presented using insert headphones at 5 virtual locations in the frontal azimuth plane (-90°, -45°, 0°, +45°, +90°). Stimuli came from the standard location on most trials ($p=.84$), but occasionally shifted to one of the other four locations ($p=.04/\text{location}$). The verbal task included 3 standard locations separated by blocks (left (-90°), midline (0°), right (+90°)). The spatial STM task only used the midline location as a standard because the relation between locations in memory and stimulus locations were examined. Reaction times and accuracy were analyzed as a function of stimulus location (5) and memory load (no load, STM), standard location (verbal task), and memory location (spatial task). No load conditions replicated prior results showing that reaction times increased on shift trials but decreased for farthest shifts, specific to the left and midline standard conditions ($p's < .001$). In the verbal memory task load tended to increase reaction times when attending to left and midline standards but not to the right ($p < .07$). In the spatial memory task load increased reaction times at lateral locations, with no effect at the attended midline location ($p < .001$). The load effect was greater in the left vs. right hemisphere ($p < .05$). There was no significant association between memorized and stimulus locations. Comparison of verbal and spatial load effects in the 0° standard showed opposite load effects among tasks. The maximal load effect was at midline for verbal memory but at lateral locations for spatial memory ($p < .02$). Findings show that short-term memory influences the distribution of auditory attention over space; and that the specific pattern depends on the type of information in short-term memory.

Improvements in Dynamic Gait and Balance with Hearing Aids and Cochlear Implants

Corey S. Shayman¹; Bahir Chamseddin²; Martina Mancini³; Timothy E. Hullar¹

¹Department of Otolaryngology-Head & Neck Surgery, Oregon Health & Science University; ²UT Southwestern Medical School; ³Department of Neurology, Oregon Health & Science University

Background

Vestibular, visual, and proprioceptive inputs help maintain balance, but recent evidence indicates that audition contributes additional valuable information. This novel finding could open up new methods for treating imbalance and broaden indications for cochlear implantation or hearing aid use, in addition to developing new insights into the basic neuroscience of maintaining balance. Wearing hearing aids has been shown to reduce postural sway in the presence of sound, but no research has been done to see if cochlear implant recipients experience these same benefits. Additionally, no attempt has been made to quantify the effect of sound on gait, which is a potentially more important outcome than simply standing in place.

Methods

Nine cochlear implant users wore head-mounted inertial sensors (measuring RMS sway acceleration) while standing 30 seconds in the dark in the presence and absence of broadband white noise (0-4 kHz). Gait performance during an 8 meter walk during normal and tandem walking was assessed in hearing impaired listeners aided with bilateral hearing aids or cochlear implants in the dark. Lumbar and shank mounted inertial sensors quantified gait cycle parameters including cadence (strides/minute), variability (difference in seconds/stride), and symmetry (left vs right leg velocity) in sound and silence.

Results

The overall head sway of cochlear implant recipients was less with spatial sound than in silence (mean difference = 0.03 m/s², $p = 0.06$). This was accompanied by a significant ($p = 0.04$) reduction in anteroposterior RMS head sway (mean difference = 0.03 m/s²). This corresponds to a clinical improvement in fall risk. Participants wearing hearing assistive devices demonstrated reduced gait variability during normal ($p=0.02$) and tandem ($p=0.005$) walking. They also increased their cadence (steps/minute) an average of 3.18% during normal walking and 1.36% during tandem walking. No systematic changes were seen in gait symmetry.

Conclusions

Adult recipients of hearing assistive devices may be able to use spatial auditory cues to improve their balance and reduce their risk of falling. These devices can be seen as balance aids in addition to hearing aids. This is critical given that falling is currently the leading cause of accidental death in people older than 65 years. This effect is likely to be most important in patients with losses in other balance-related sensory modalities and may be most important in elderly patients subject to falls. The neural processes underlying auditory integration with other balance-related sensory inputs remain to be studied.

Genetics B: General

PD 93

A High-throughput Workflow for CRISPR/Cas9 Mediated Targeted Mutagenesis to Model Non-syndromic Deafness Genes in Zebrafish

Gaurav Varshney¹; Blake Carrington²; Raman Sood²; Shawn Burgess²

¹Functional & Chemical Genomics Program, Oklahoma Medical Research Foundation, Oklahoma Cit, OK;

²National Human Genome Research Institute, NIH, Bethesda, MD

Advances in sequencing technologies have enabled the rapid identification of human disease genes by GWAS or whole exome sequencing techniques. There is a large-gap between identification of human disease genes and their functional validation. Numerous publications have demonstrated the efficacy of gene targeting in zebrafish using CRISPR/Cas9 including a variety of tools and methods for guide RNA synthesis and mutant identification. While all the published techniques work, not all approaches are readily scalable to increase throughput. In addition, zebrafish have been shown to effectively recapitulate disease phenotypes, however models that fail to generate relevant phenotypes are rarely reported. We recently described a CRISPR/Cas9 based high-throughput mutagenesis and phenotyping pipeline in zebrafish. Here we present a complete workflow including target selection, cloning-free single guide RNA (sgRNA) synthesis, microinjection, validation of the target-specific activity of the sgRNAs, founder screening to identify germline transmitting mutations, determination of the exact lesion by PCR and next generation sequencing (including software for analysis), and genotyping in the F1 or subsequent generations. We used this high throughput pipeline to target all published human genes linked to non-syndromic deafness in zebrafish. We will present phenotyping data from homozygous mutants, and the rate of successful modeling in zebrafish.

NLRP3 Mutation and Cochlear Autoinflammation Cause Syndromic and Nonsyndromic Hearing Loss DFNA34

Hiroshi Nakanishi¹; Yoshiyuki Kawashima²; Kiyoto Kurima¹; Jae Jin Chae³; Astin Ross¹; Gineth Pinto-Patarroyo³; Seema Patel⁴; Julie Muskett¹; Jessica Ratay¹; Parna Chattaraj¹; Carmen Brewer⁵; Michael Hoa⁶; H. Jeffrey Kim¹; John Butman⁷; Lori Broderick⁸; Hal Hoffman⁸; Ivona Aksentijevich³; Daniel Kastner³; Raphaela Goldbach-Mansky⁹; Andrew Griffith¹

¹NIDCD/NIH; ²Department of Otolaryngology, Tokyo Medical and Dental University; ³NHGRI/NIH; ⁴NIAMS, NIH; ⁵National Institute on Deafness and Other Communication Disorders, NIH; ⁶Office of the Clinical Director, Otolaryngology Surgeon-Scientist Program, Auditory Development and Restoration Program, Division of Intramural Research, NIDCD, NIH, Bethesda, Maryland, USA; ⁷RIS/NIH; ⁸UCSD; ⁹NIAID/NIH

Background

The NLRP3 inflammasome is an intrinsic intracellular immune sensor expressed in innate immune cells including monocytes and macrophages. Activation of the NLRP3 inflammasome triggers the maturation and secretion of interleukin-1 β (IL-1 β), a potent proinflammatory cytokine. Gain-of-function mutations of NLRP3 cause cryopyrin-associated periodic syndromes (CAPS) that can include recurrent fevers, episodic skin rashes, arthritis and sensorineural hearing loss (SNHL). Peripheral blood mononuclear cells (PBMCs) from CAPS subjects show increased IL-1 β secretion at rest or in response to lipopolysaccharide (LPS) stimulation. Here, we report that a novel mutation in NLRP3 causes SNHL, without the other clinical signs and symptoms of CAPS that are associated with other mutations of NLRP3, at the DFNA34 locus.

Methods

We ascertained two unrelated families, LMG113 and LMG446. In family LMG446, SNHL is accompanied with autoinflammatory signs and symptoms but none of the family members met the criteria for CAPS. In family LMG113, SNHL segregates without any other clinical signs and symptoms associated with CAPS. Clinical evaluations, magnetic resonance imaging and IL-1 β blockade therapy were performed in the family members.

Results

A genome-wide linkage analysis of family LMG113 revealed a novel DFNA locus designated as DFNA34 on

chromosome 1q44. The DFNA34 interval includes 36 protein-coding genes, one of which is NLRP3. Dideoxy sequencing of NLRP3 detected a heterozygous missense substitution, c.2753G>A (p.Arg918Gln). p.Arg918Gln completely co-segregated with SNHL in family LMG113. In family LMG446, the same nucleotide substitution was identified. The levels of IL-1 β secreted from PBMCs from these patients were elevated. Pathologic enhancement of the cochlea was identified on postcontrast MRI FLAIR. Six months of treatment with Anakinra, an IL-1 β blocker, improved hearing thresholds in affected members of family LMG446, but not in those of family LMG113. These findings indicate that SNHL is associated with cochlear autoinflammation that is possibly induced by resident macrophages/monocytes-like cells in the cochlea via activation of the NLRP3 inflammasome. In mice, we identified tissue-resident macrophage-like cells scattered throughout the cochlear tissues. In these cells, Nlrp3 expression was detected. In response to LPS and ATP stimulation, cochlear tissues secreted IL-1 β , indicating the NLRP3 inflammasome could be activated in the cochlea. Pro-IL-1 β was predominantly expressed in macrophage-like cells, indicating that the NLRP3 inflammasome exists in these cells.

Conclusion

The p.Arg918Gln mutation of NLRP3 causes DFNA34 SNHL by cochlear autoinflammation. The inflammation may be induced by cochlear resident macrophage-like cells via unregulated activation of the NLRP3 inflammasome.

PD 95

A Missense Variant in PRKCB gene Segregates Low-frequency hearing loss in Autosomal Dominant Meniere's Disease

Jose Antonio Lopez-Escamez¹; Teresa Requena²; Carmen Martin-Sierra²; Lidia Frejo²; Steven D. Price³; Angel Batuecas-Caletrio⁴; Sofia Santos-Perez⁵; Andres Soto-Varela⁵; Anna Lysakowski³; Jose A. Lopez-escamez⁶

¹Otology & Neurotology Group CTS495 GENYO
²Department of Otolaryngology, Granada University Hospital, ibs.GRANADA, Granada, Spain; ³Otology & Neurotology Group CTS495, Department of Genomic Medicine, GENYO - Centre for Genomics and Oncological Research - Pfizer/University of Granada/ Junta de Andalucía, Granada, Spain; ⁴Department of Anatomy and Cell Biology, University of Illinois at Chicago, Chicago, IL, USA; ⁵Department of Otolaryngology, Hospital Universitario de Salamanca, Salamanca, Spain; ⁶Division of Otoneurology, Department of Otorhinolaryngol-

ogy, *Complejo Hospitalario Universitario, Santiago de Compostela, Spain*; ⁶*Center for Genomic and Oncology (GENyO) Pfizer-Universidad de Granada-Junta de Andalucía*

Introduction

Familial Meniere's disease (FMD) is a rare autosomal dominant (AD) disorder characterized by recurrent attacks of spontaneous vertigo, sensorineural hearing loss (SNHL), and tinnitus with incomplete penetrance and variable expressivity. It is associated with an accumulation of endolymph in the membranous labyrinth, and the hearing loss usually onsets at low-to-middle frequencies with progression to high frequencies.

Methods

We performed whole-exome sequencing in an AD-MD kindred consisting of 2 patients with MD and a third one with SNHL without vestibular symptoms. DNA samples were sequenced in a SOLiD 5500xl platform. After alignment and annotation, variants were filtered by our in-house control database and minor allelic frequency (MAF) < 0.0001 according to dbSNP 142, Exome Aggregation Consortium and 1000 genome project. To reduce the list of possible candidate variants, we prioritized using different criteria. qPCR and immuno-labelling were performed to confirm the expression in human and rat tissue as well as to define which cell types express the candidate gene in the cochlea. By using mouse gene expression data in the cochlea, we selected base-to-apex differentially expressed genes and performed pathway analyses including to search for tonotopic-related pathways.

Results

We identified a novel missense variant in the PRKCB gene segregating low-to-middle frequency SNHL. Confocal imaging showed strong PKC II protein labelling in non-sensory cells, the tectal cells (TCs) and inner border cells (IBCs) of the rat organ of Corti with an expression gradient along the cochlea. PKC II signal was more pronounced in apical turn TCs of the cochlea compared with the middle and basal turns. In rat tissue we found that PKC II protein labelling was much higher in cochlear than in vestibular tissue. In silico analyses extracted the significant PKCB-related signaling pathways: "Axonal Guidance Signaling", "Alpha-Adrenergic Signaling", "14-3-3-mediated Signaling" and "CXCR4 Signaling".

Conclusions

PRKCB is a novel candidate gene for SNHL in FMD and the gradient of expression in TC along the cochlea may explain the onset of hearing loss as well as the progression from low to high frequencies SNHL in MD. In addition, the role of TCs in K⁺ recycling within the endolymph could explain endolymphatic hydrops development.

Funding

This study was funded by Grants from FPS PI0496-14, Meniere's Society, UK and National Institutes of Health DC013181.

PD 96

PIIP5K2, an Acid Phosphatase Protein, Is Essential for Hearing in Human and Mouse

Rizwan Yousaf¹; Zubair Ahmed²; Shaheen N. Khan³; Thomas B. Friedman⁴; Sheikh Riazuddin⁵; Saima Riazuddin¹

¹*Laboratory of Molecular Genetics, Department of Otorhinolaryngology Head & Neck Surgery, School of Medicine, University of Maryland, Baltimore, MD, USA.;*

²*Department of Otorhinolaryngology Head & Neck Surgery, School of Medicine University of Maryland, Baltimore, MD, 21201, USA;* ³*National Center for Excellence in Molecular Biology, University of the Punjab, Lahore, Pakistan;* ⁴*Section on Human Genetics, Laboratory of Molecular Genetics, National Institute on Deafness and Other Communication Disorders, National Institutes of Health, Bethesda, MD, USA.;* ⁵*Shaheed Zulfiqar Ali Bhutto Medical University, Pakistan Institute of Medical Sciences, Islamabad, Pakistan*

Hearing loss is a genetically heterogeneous disorder. Linkage and candidate genes screening in large families have been fruitful in deciphering the cause of recessively inherited hearing loss. With the advent of innovative technologies like massive parallel sequencing (MPS), there has been a rapid increase in the identification of causative genes for Mendelian disorders, including hearing loss in humans. In this study, through linkage studies we mapped a novel non-syndromic recessive hearing loss locus DFNB100 on chromosome 5q21.1-q21.3 in two large consanguineous Pakistani families. Using MPS technique we screened all of the candidate genes within the linkage region and have identified a transition mutation (c.2510G>A) in PPIIP5K2 gene segregating with hearing loss in both families. PPIIP5K2 encodes an Inositol hexakisphosphate and diphosphoinositol-pentakisphosphate kinase 2 protein. The DFNB100 allele results in a change of an evolutionarily conserved arginine residue at position 837 with a histidine (p.Arg837His). This mutation was not identified among the 180 control chromosomes from normal control Pakistani individuals, in the 1000 Genome, and NHLBI-ESP exome databases. However, it is present in the ExAC database at a very low frequency of 0.0001406.

In the mouse inner ear, PPIIP5K2 is ubiquitously expressed and is found in the sensory hair cells and supporting cells of the organ of Corti, as well as in the spiral

ganglion, stria vascularis and vestibular end organs. Our preliminary studies revealed progressive hearing loss in mice homozygous for Ppip5k2 knockout allele. We have also generated a ppip5k2 knock out zebrafish model system utilizing the CRISPR/CAS9 technology and current studies are underway to understand the resulting inner ear pathophysiology. The PPIP5K2 protein has two predicted domains, a kinase and an acid phosphatase domain and the p.Arg837His allele is located in the acid phosphatase domain of the protein. PPIP5K2 is known to have kinase activity that results in the generation of high energy Inositol Pyrophosphates IP7 & IP8, which act as cell signaling molecules and regulate many cellular processes, including endocytosis, vesicle trafficking, apoptosis and DNA repair. We anticipate that further studies using animal models and biochemical assays will elucidate the function and role of PPIP5K2 in the inner ear development and hearing function, a protein indispensable for hearing in humans and mice.

PD 97

Acsl4 Mutation Leads to Early and Fast Progressive Hearing Loss in Mice

Elisa Martelletti¹; Neil J. Ingham²; Annalisa Buniello¹; Jacqueline K. White³; Karen P. Steel⁴

¹Wolfson Centre for Age-Related Diseases, King's College London, Guy's Campus, London SE1 1UL, UK;

²King's College London, Guy's Campus, London SE1 1UL, UK; ³Wellcome Trust Sanger Institute, Hinxton, Cambridge CB10 1SA, UK; ⁴King's College London; Wellcome Trust Sanger Institute

Acsl4 (Acyl-CoA synthetase long-chain family member 4) transfers a coenzyme A molecule to free fatty acids in order to activate the metabolic processing of the lipids. It prefers arachidonic and eicosapentaenoic acids as substrates. This project is focused on elucidating the effect of Acsl4 mutation and lipid metabolism on auditory function.

The Acsl4tm1a(EUCOMM)Wtsi mutant mice were generated as part of the Sanger Institute Mouse Genetics Project and exhibited high frequency hearing loss. However, these mice showed severe viability problems, therefore Acsl4tm1d conditional knockout mice were generated to delete the gene in the inner ear. The Sox10-Cre mouse line was used because Sox10 is known to be activated early in development in neural tissues that contribute to the otic vesicle. We found that Acsl4 is expressed in both inner and outer hair cells, spiral ganglion and stria vascularis. ABR measurements in response to click stimuli and tone pips ranging from 3-42kHz were performed at different ages in order to determine the onset of the hearing impairment. Acsl4tm1d mutant mice

have normal hearing sensitivity at 2 weeks old, but only one week later they dramatically lost hearing sensitivity starting from the high frequencies and by 4 weeks old the thresholds at all frequencies were severely impaired. Further analysis at 3 weeks revealed that Acsl4tm1d mutant mice have increased DPOAE thresholds, but normal endocochlear potential. Acsl4tm1d mutant mice revealed no major abnormalities in the overall structure of the middle and inner ear. However, degeneration of the hair bundles of both inner and outer hair cells was observed using scanning electron microscopy starting from the base of the cochlea at 3 weeks and getting worst by 4 weeks. Loss of hair cell nuclei was detected by confocal imaging in the basal and middle turns of the cochlea at 4 weeks. No obvious innervation or synaptic defects were found in Acsl4tm1d mice at 2, 3 and 4 weeks in the remaining hair cells.

Our results suggest that Acsl4 has a pivotal role for normal hearing function locally within the inner ear. Moreover, although its mutation does not affect the development of hearing, it causes an early and fast progressive hearing loss.

PD 98

Methionine Sulfoxide Reductase B3 Is Indispensable for Hair Bundle Integrity and Auditory Function in Mice

Elodie M. Richard¹; Gowri Sarangdhar²; Bruno Manta³; Inna A. Belyantseva⁴; Byung C. Lee³; Thomas B. Friedman⁵; Zubair Ahmed⁶; Vadim N. Gladishev³; Saima Riazuddin¹

¹Laboratory of Molecular Genetics, Department of Otorhinolaryngology Head & Neck Surgery, School of Medicine, University of Maryland, Baltimore, MD, USA.;

²Cincinnati Children's Hospital Research Foundation, University of Cincinnati, Cincinnati, OH, USA.; ³Division of Genetics, Department of Medicine, Brigham and Women's Hospital and Harvard Medical School, Boston, MA 02115, USA.; ⁴Laboratory of Molecular Genetics, National Institute on Deafness and Other Communication Disorders, National Institutes of Health;

⁵Section on Human Genetics, Laboratory of Molecular Genetics, National Institute on Deafness and Other Communication Disorders, National Institutes of Health, Bethesda, MD, USA.; ⁶Department of Otorhinolaryngology Head & Neck Surgery, School of Medicine University of Maryland, Baltimore, MD, 21201, USA

Methionine sulfoxide reductases (MSR) are enzymes responsible for catalyzing the reduction of methionine-sulfoxides in damaged proteins. Previously, we demonstrated that MSRB3, an MSR family member, is

associated with human profound autosomal recessive prelingual non-syndromic hearing loss DFNB74. To decipher the role of MsrB3 in the auditory pathway, we generated a MsrB3 knock out mouse model. ABR and DPOAE measurements showed that the homozygous mutant mice were profoundly deaf by P16 with outer hair cell abnormalities. A closer look at the organ of Corti epithelium revealed stereocilia bundle shape abnormalities as early as P4. In the mutant mice, MSR3 deficiency leads to the degeneration of the stereocilia followed by complete hair cell loss via apoptosis. Despite its specific localization at the base of the stereocilia, transmission electron microscopy revealed no obvious alterations of the rootlet morphology in the MsrB3 mutant mice at P14. Considering the known role of MSR3 as an antioxidant repair protein, we investigated the oxidative stress status of the cochlea of the mutant mice compared to their wild-type (WT) littermates before the degeneration of hair cells. No differences in oxidative stress markers were detected at the cochlear level. Our biochemical studies revealed that MSR3 prevents oxidation of actin filaments, while the DFNB74 allele abolishes this ability. Consistent with our in vitro data, we observed imbalanced reduced/oxidized actin ratio in the cochlear samples from MsrB3 mutant mice. Taken together with the stereocilia degeneration, our data suggest a possible role for MSR3 in regulating the levels of reduced actin needed to maintain the actin filaments in the cochlear hair cells. In summary, our data show that the loss of MSR3 results in deafness and a specific hair bundle defect in the homozygous mutant mice. This study provides insight into the mechanisms underlying the crucial role of MSR3 in the hearing pathway and particularly the importance of a built-in antioxidant mechanism in the inner ear for maintenance of the hair bundle.

Inner Ear: Anatomy & Physiology

PD 99

Immunofluorescent Staining in Celloidin Embedded Sections of the Human Temporal Bone

Ivan Lopez; Gail Ishiyama; Dora Acuna; Fred Linthicum; Akira Ishiyama
UCLA School of Medicine

Background

A reliable identification of the different cell populations and structures of the human inner ear is key to understand the pathophysiology of numerous inner ear diseases, and normal aging. We recently described an immunofluorescent technique to identify hair cells and supporting cells in archival celloidin embedding sections of the human cochlea using double immunolabeling (Lopez et al 2016, *Histochem Cell Biol*, DOI:1007/

s00418-016-1471). We present further improvements to this technique that allow also to reliably identify cells of the spiral ligament, spiral ganglia neurons and their processes innervating hair cells.

Methods

We used specific antibodies and immunofluorescence to identify outer hair cells (prestin), supporting cells (acetylated tubulin), spiral ligament fibrocytes (connexin-26), and spiral ganglia neurons (neurofilaments) in celloidin embedded tissue sections. A critical step to colocalize several proteins using secondary antibodies tagged with different fluorophores is to subject the celloidin section to UV exposure, before and after celloidin is removed in addition to antigen retrieval steps. We tested different times of UV radiation (from 2 to 12 hrs.), and we compared the immunohistochemical results with those obtained using celloidin sections and 2nd antibodies labeled with HRP-DAB and formalin fixed frozen sections of the human cochlea.

Results

By exposing celloidin sections to UV radiation before and after it is removed the intrinsic auto-fluorescence of the human temporal bone sections is quenched allowing reliable identification and colocalization of several cell components on the human cochlea. Results are comparable to those obtained using formalin frozen sections of the human cochlea, and matches to previous reports in the several animal models.

Conclusions

These results represent the first steps to reliably identify major cellular populations and components in the human ear using the valuable resource of celloidin embedded sections. In addition, a decrease or increase in several proteins detected by immunofluorescence in different inner ear pathological conditions may help to understand their underlying pathophysiology. It is expected that this methodology will encourage basic inner ear researchers to use this valuable resource to contrast and compare findings in the human inner ear and animal models.

Funding

This work was supported by the National Institutes of Health Grant U24 DC011962-05

Imaging the Mammalian Cochlea with Micro-optical Coherence Tomography

Janani S. Iyer¹; Shelley A. Batts²; Kengyeh K. Chu³; Mehmet I. Sahin⁴; Hui Min Leung³; Guillermo J. Tearney³; Konstantina M. Stankovic⁵

¹*Eaton-Peabody Laboratories and Department of Otolaryngology, Massachusetts Eye and Ear Infirmary;*

²*Program in Speech and Hearing Bioscience and Technology, Harvard Graduate School of Arts and Sciences;* ²*Eaton-Peabody Laboratories and Department of Otolaryngology, Massachusetts Eye and Ear Infirmary;* ²*Analysis Group, Inc., Health Economics and Outcomes Research;* ³*Wellman Center for Photomedicine, Massachusetts General Hospital;* ²*Department of Pathology, Harvard Medical School;*

⁴*Eaton-Peabody Laboratories and Department of Otolaryngology, Massachusetts Eye and Ear Infirmary;*

⁵*Eaton Peabody Laboratories, Department of Otolaryngology, Massachusetts Eye and Ear, Harvard Medical School*

Although sensorineural hearing loss is prevalent worldwide, our understanding of how specific physiological defects within the cochlea translate to impairment in auditory perception is limited. This gap in our understanding of the etiology of hearing loss exists in part because of a) the cochlea's fragility, small size, complex 3D structure, and deeply embedded position within the temporal bone, which make it difficult to access for imaging, and b) the limited capabilities of available clinical imaging technologies (e.g. CT and MRI), which preclude resolving micron-scale cellular details. We recently demonstrated the ability of micro-optical coherence tomography (μ OCT), a non-contact, low-coherence interferometric imaging technique that improves upon its predecessor (OCT) in resolving capability and depth of focus, to reveal microanatomy and physiological mechanisms involved in atherosclerosis and mucociliary clearance. Here, we demonstrate μ OCT's ability to resolve cellular structures such as neuronal fiber bundles, hair cells, and supporting cells within the mammalian organ of Corti. Guinea pig cochleae were extracted, fixed, and imaged with μ OCT via 0.5-1 mm cochleostomies placed in the basal and apical turns. 3D volumetric reconstructions of raw image stacks enabled unique forms of visualization, such as endoscopic perspective 'fly through' videos and virtual sectioning across specific planes of interest. The present acquisition methods demonstrate significant improvements to current clinical OCT imaging in both resolution and focal depth. These are the first μ OCT images resolving intracochlear microanatomy in situ, and motivate further investigation into μ OCT's po-

tential utility as an imaging tool in otologic research and clinical practice.

PD 101

Tonotopic Network of Cellular Oscillators in the Cochlea

Barbara Canlon¹; Vasiliki Basinou¹; Renate Buijink²; Stephen Michel²; Gabriella Lundqvist³; Christopher Cederroth¹

¹*Karolinska Institute;* ²*Leiden University Medical Center;* ³*Max Planck Institute for Ageing*

Recently, the cochlea was found to express circadian rhythms in core clock genes, such as Bmal1, Rev-Erb α , Per1 and Per2. Using mPer2Luc mice expressing the PER2 protein fused with luciferase (PER2::LUC), real-time tracking of PER2::LUC rhythms were captured from whole cochlea revealing a robust and self-sustained molecular clock. PER2 is primarily expressed in inner and outer hair cells of the cochlea, as well as in spiral ganglion neurons (SGN). However, there is no knowledge on the temporal order or dependencies between the cells types that could suggest functional clusters within the cochlea. Using bioluminescence imaging of whole cochlear explants we were able to directly determine the location of cellular oscillators in the cochlea and their activity within the tissue. We describe how cellular oscillators in the cochlea show a distinct spatial and temporal organization suggesting that inter-cellular coupling and synchronization within the organ is needed for the generation of robust tissue circadian rhythms. Interestingly, the cellular clocks were tonotopically arranged along the cochlea. The PER2::LUC rhythms began at low frequencies (apex) and traveled towards higher frequencies (base). This resulted in a 3 hour phase difference between cells in the apical and middle turns. These findings indicate that cellular networks organize rhythms along the tonotopic axis. Cochlear circadian rhythms were disrupted in the presence of tetrodotoxin (TTX), demonstrating that Na⁺-dependent action potentials are required to coordinate a coherent rhythm. Thus, synaptic communication is crucial for the synchronization and maintenance of circadian oscillations in the cochlea.

PD 103

NMDA Receptors Modulate Glutamatergic Transmission at the Hair Cell Afferent Synapse

Joy Y. Sebe¹; David W. Raible²

¹University of Washington, Seattle; ²University of Washington, Seattle

We have recently shown that synaptic transmission and excitotoxic damage at the hair cell synapse is mediated by Ca²⁺ permeable AMPA receptors (CP-AMPA). Using a combination of in vivo Ca²⁺ imaging and immunohistochemical approaches in the zebrafish lateral line system, we visualized afferent terminal structure and responses to hair cell activation. We used transgenic zebrafish larvae (6-7 days post fertilization) expressing the fluorescent calcium indicator GCaMP5 in afferent neurons to monitor postsynaptic terminal responses to hair cell activation. We show that hair cell activation causes Ca²⁺ influx into afferent terminals that is primarily mediated by CP-AMPA. Blocking AMPAR desensitization with cyclothiazide increases afferent terminal Ca²⁺ responses. However, blocking NMDARs significantly enhances terminal Ca²⁺ responses. Immunohistochemical studies show NR1 subunit localization to the postsynaptic marker MAGUK. In the developing hair cell synapse, NMDAR activation prolongs glutamatergic postsynaptic currents and promotes spontaneous activity. In contrast, our studies indicate that as the synapse matures NMDAR activation limits glutamatergic transmission.

PD 104

Deafness Mechanisms Underlying Digenic Cx26 (GJB2) and Cx30 (GJB6) Mutations – Reduction of Endocochlear Potential (EP) by Impairment of Heterogeneous Gap Junctional Coupling in the Cochlear Lateral Wall

Ling Mei; Hong-Bo Zhao; Liang Zong; Jin Chen; Yan Zhu; Chun Liang

Dept. of Otolaryngology, University of Kentucky Medical Center

Background

The digenic connexin26 (Cx26, GJB2) and Cx30 (GJB6) heterozygous mutations are the second most frequent cause of recessive deafness in humans. However, the underlying deafness mechanism remains unclear.

Methods

In this study, double Cx26 and Cx30 heterozygous (Cx26^{+/-}/Cx30^{+/-}) mice were used to investigate the underlying deafness mechanisms for Cx26 and Cx30 heterozygous mutations induced hearing loss. ABR, DPOAE, and endocochlear potential (EP) were record

ed. Cochlear development and cell generation were also examined.

Results

Double Cx26 and Cx30 heterozygous (Cx26^{+/-}/Cx30^{+/-}) mice had hearing loss. However, sole Cx26^{+/-} or Cx30^{+/-} mice appeared normal hearing. The cochlea in Cx26^{+/-}/Cx30^{+/-} mice displayed normal development and also had no apparent hair cell degeneration. Gap junctions in the cochlea form two independent networks: the epithelial cell network in the organ of Corti and the connective tissue network in the cochlear lateral wall. We found that mice of only conditional heterozygous deletion of Cx26 in the cochlear supporting cells with heterozygous deletion of Cx30 (Prox1-Cx26^{+/-}/Cx30^{+/-} mice) had no hearing loss, suggesting that hearing loss in double heterozygous Cx26^{+/-}/Cx30^{+/-} deletion mainly results from impairment of gap junctional function in the cochlear lateral wall. We found that most of Cx26 and Cx30 in the lateral wall showed heterozygous coupling and were co-expressed in the same gap junctional plaques. Positive endocochlear potential (EP), which is a driving force and required for generation of auditory receptor current/potential, is generated in the cochlear lateral wall. EP in Cx26^{+/-}/Cx30^{+/-} mice was reduced. However, EP in Prox1-Cx26^{+/-}/Cx30^{+/-} mice was normal.

Conclusions

These data suggest that digenic Cx26 and Cx30 mutations may mainly impair heterozygous coupling of Cx26 and Cx30 in the cochlear lateral wall and EP generation, thereby leading to hearing loss.

Supported by NIH R01 DC 05989 and R56 DC 015019.

PD 105

Hearing Loss in an ABCG1 Knockout Mouse

Karen Pawlowski¹; Joyce J. Repa²; Nancy Gonzalez³; Elena Koulich⁴

¹UT Southwestern Medical Center Department of Otolaryngology; ²UT Southwestern Medical Center Departments of Physiology and Internal Medicine; ³UT Southwestern Medical Center Department of Physiology; ⁴UT Southwestern Medical Center Department of Otolaryngology

Dysregulation of lipid homeostasis within the central nervous system is involved in various neurodegenerative disorders. Sterol homeostasis within the tissues of the central nervous system is essential for proper cellular function. Therefore, it is possible that dysregulation of lipid homeostasis at the level of the inner ear tissues may also contribute to hearing disorders.

Hearing loss has been associated with increased plasma lipid levels, suggesting hearing loss can be a possible secondary outcome of vascular disease. Our previous work with a mouse model of Niemann Pick Disease type 1 (NPC1, a model of aberrant cellular cholesterol trafficking and lysosomal storage) supports a role for sterol/lipid regulation in hearing. To further investigate the role of cellular lipid dysregulation within the inner ear tissues and hearing loss, we studied a mouse model with a null mutation of ABCG1 (ATP-binding cassette G1) - a mutation associated with increased cellular sterol levels but without a corresponding increase in levels of plasma lipoproteins. Unlike NPC1-/- mice, the ABCG1 mouse model has normal viability and growth.

ABCG1 plays a critical role in controlling lipid levels within tissues through the transfer of cholesterol from the intracellular lipid pool to the extracellular pool via an association with high density lipoprotein (HDL). At 15-24 weeks of age, Abcg1-null mice accumulate neutral lipid, multinucleated giant cells, and lymphocytes in tissue, indicating ABCG1 plays a critical role in regulating lipid homeostasis. The lack of a corresponding increase in plasma lipid levels suggest ABCG1 has no significant role in regulating levels of plasma lipoproteins. Determining the effect of the loss of Abcg1 on hearing function allows us to separate changes secondary to lipid-associated vascular disease from that of changes brought on by the disruption in cellular lipid function within inner ear tissues.

By 2.5 months (10 weeks) of age, significant hearing loss is present in Abcg1-null/lacZ knockin mice fed a low-fat chow diet (Teklad 7001). Auditory brainstem response thresholds are elevated in affected mice, showing moderate hearing loss in all frequencies tested (14 dB at 4 kHz, 14 dB at 16 kHz, and 17 dB at 32 kHz). Mild but significant outer hair cell loss (5-10%) is seen in the base and mid cochlear regions of the affected mice. Our results suggest that ABCG1 is critical for regulating lipid homeostasis within tissues of the inner ear.

Auditory Implants: Improving Auditory Function from Pre-processing to Peripheral and Central Mechanisms (Honoring Bob Shannon)

SYMP 55

How the Brain Hears

Robert Shannon

USC

For more than 50 years auditory research has primarily focused on the cochlea, while the role of the brain in hearing was seriously underrepresented. The success of cochlear implants changed this focus because CI patients were able to recognize speech at a high level even though the pattern of neural activity produced by a CI is highly impoverished compared to an acoustic ear. Research over the last 25 years has shown which cues a CI presents and which cues are most important for speech and music. This research has led to a new understanding of the role of ear and brain in hearing. Some auditory tasks depend critically on spectral detail (harmonic pitch) while other tasks only require broad spectral representations changing dynamically in time (speech). Comparing the level and type of cues required for different tasks provides insight into the ear-brain system and the different demands on peripheral representation for different tasks. Not all fine details of the spectral/temporal representation at the cochlea are equally important for all tasks. Speech recognition in quiet can be accomplished with a few broad bands representing broad regions of spectral energy changing in time. Voice quality and emotion require a much richer spectral representation. In music the rhythm can be conveyed with broad band temporal cues while melodic pitch requires more spectral resolution than present day CIs can provide. Localizing sounds in space can be accomplished with coarse spectral representation, but improves as spectral resolution improves. However, some CI users can localize sounds almost as well as normally hearing listeners and even achieve some binaural improvements in speech recognition in noise. Comparisons across simple and complex auditory tasks and across degrees of peripheral degradation due to hearing loss provide new insights into the requirements of the brain for hearing.

SYMP 56

SEDA-RT: A Real-time Multi-talker Babble Noise Reduction Algorithm for Cochlear Implant Devices

Roosbeh Soleymani

New York University

Cochlear implant users have difficulty understanding speech in the presence of the background noise. Several single-channel de-noising algorithms have been de-

signed to address this problem. Nevertheless, designing a de-noising algorithm which is capable of performing well for non-stationary noise (e.g. Multi-talker babble) still remains a difficult task. The problem becomes even more challenging if it must function in real-time and have a low latency.

Being real time requires avoiding computationally costly operations such as iterative or other complex algorithms. In other words, a simple and fast algorithm capable of performing multi talker babble reduction is needed. Moreover, the algorithm should be designed to function on devices with limited computational power including a cell-phone or a DSP chip embedded into a cochlear implant sound processor.

The primary challenge associated with having a low latency is the duration of the audio frames (i.e. buffer duration). To prevent a noticeable delay in the audio signal, the buffer duration should not exceed few tens of milliseconds. As a result, there is relatively little information (because of the correspondingly small number of samples) within a frame for the de-noising algorithm to extract.

We have designed a low latency, real-time babble noise reduction which maintains its efficiency for devices with limited processing power such as a smart phone. Preliminary data on the effectiveness of the algorithm has been collected on both cochlear implant users and normal hearing subjects suggesting the algorithm is effective.

In the presentation, the details of the noise reduction algorithm will be presented. Further, performance with the algorithm will be shown for cochlear implant users at various signal-to-noise ratios.

SYMP 57

Dynamic Current Steering with Phantom Electrode

Xin Luo

Arizona State University

Introduction

Partial bipolar stimulation of the most apical electrode in a cochlear implant (CI) can generate an extra low-frequency channel called phantom electrode (PE). Previous studies of PE processing strategies used a fixed compensation coefficient σ (i.e., returned a fixed proportion of current to the basal flanking electrode) and only explored temporal coding of low-frequency information on PE. It is possible to change the stimulation place of PE by continuously adjusting σ over time. This study tested pitch contour identification (PCI) using such dynamic current steering with PE.

Methods

Seven adult users of the Advanced Bionics CII and HiRes90k implants participated in this study. The experiment started with loudness and pitch perception of 300-ms static PE stimuli on EL1 with a fixed σ (0, 0.2, 0.4, and 0.6). After measuring the dynamic range for each σ , static PE stimuli with different σ were balanced in loudness at the most comfortable level and ranked in pitch with an σ interval of 0.2. Dynamic PE stimuli were created based on the perceptual results of static PE stimuli. Over 300, 500, 750, and 1000 milliseconds, σ was either linearly increased from 0 to 0.6, decreased from 0.6 to 0, or kept at 0.3, to generate falling, rising, and flat pitch contours, respectively. The current level was changed as a linear function of σ to maintain equal loudness. PCI was tested with these dynamic PE stimuli.

Results

The loudness-balanced most comfortable level of static PE stimuli was roughly a linear function of σ , which validated the method of loudness control in dynamic PE stimuli. On average, subjects perceived a lower pitch as σ increased by 0.2 for 67% of the time. The cumulative d' of pitch ranking for σ from 0 to 0.6 in a step of 0.2 ranged from -0.24 to -8.49 across subjects. Subjects scored 74 to 96% correct in PCI with dynamic PE stimuli. The PCI performance slightly but not significantly improved with duration. Across subjects, the PCI performance with 1000-ms dynamic PE stimuli was significantly correlated with the cumulative d' of pitch ranking with 300-ms static PE stimuli.

Conclusions

CI users were able to perceive time-varying pitch cues created by dynamic current steering with PE. Future studies should test the integration of place and temporal cues on PE as a potential way to enhance pitch perception with CIs.

SYMP 58

Processing of Electrical Stimulation by ABI and CI Users: Implications for Speech Coding Strategies

Mahan Azadpour

NYU School of Medicine

Auditory brainstem implants (ABIs) stimulate auditory pathways via electrodes placed on the surface of the cochlear nucleus, and provide an opportunity to restore hearing to profoundly deaf individuals who cannot benefit from cochlear implants (CIs). Current ABI devices use the same coding strategies as those developed for stimulating auditory nerve in CIs: temporal envelopes of frequency bands of the signal modulate levels of electric pulses delivered to tonotopically ordered electrodes. However, the simple place and amplitude codes may

not adequately convey the important auditory information in majority of ABI users. That is because the cochlear nucleus is located higher in the auditory processing hierarchy than the auditory nerve, and its anatomy is complex and contains different types of neurons. Some ABI electrodes may not be in the optimal anatomical and physiological location, particularly for NF2 patients in whom tumors and tumor removal may cause damage to the neural structures of the cochlear nucleus. In fact, speech perception performance is generally poor with ABIs with only a small percentage of brainstem implantees achieving the level of performance comparable to that of the average cochlear implantees. In this presentation we will compare perception of the same stimulation patterns that are delivered to cochlear nucleus and auditory nerve in ABIs and CIs respectively. The findings will be interpreted with respect to neural processing mechanisms that are inferred from electrically-evoked compound action potentials obtained in the two patient groups. Implications for designing ABI-specific coding strategies will be discussed.

SYMP 59

Difficulties of Cochlear-implanted Children in Utilizing Voice Pitch Information

Mickael L. D. Deroche¹; Shu-Chen Peng²; Hui-Ping Lu³; Yung-Song Lin³; Charles J. Limb⁴; Monita Chatterjee⁵

¹*McGill University Montreal*; ²*Food And Drug Administration*; ³*Chi Mei Medical Center*; ⁴*University of California - San Francisco*; ⁵*Boys Town National Research Hospital*

Children who have recovered hearing through cochlear implants (CI) can display remarkable spoken language, and yet they face major deficits in their reception of voice pitch information. In a first step, we collected basic psychophysical data on the sensitivity of CI children to static and dynamic changes in fundamental frequency for broadband complexes. Compared to their normally-hearing (NH) peers who - for a d' of 0.77 - exhibited static thresholds of about 10-20 cents and dynamic thresholds of 4-8 semitones/sec, with relatively little variability across subjects, CI children exhibited static thresholds of 2-3 semitones and dynamic thresholds of 32 semitones/sec, on average, with considerable variability across subjects. Unexpectedly, these results were largely independent of whether children were implanted at an early or late age, whether they had little or extensive experience with their device, and whether they were brought up in a tonal or non-tonal language environment. In a second step, we studied voice emotion recognition (English-speaking children) and lexical tone

recognition (native speakers of Mandarin), attempting to determine from acoustic analyses of the stimuli what cues subjects used primarily. Here again, CI children performed more poorly than their NH peers. Poor reception of F0 information was found to be a strongly limiting factor for these prosody-related tasks. In a third step, we recorded CI children producing contrasts in emotion (happy/sad) and lexical tone contrasts in Mandarin. On one hand, acoustic contrasts between happy and sad productions were smaller in the CI children than their NH peers. On the other hand, CI children exaggerated the duration and intensity contrasts in production of lexical tone contrasts compared with their NH peers. Overall, these data suggest that sensory deficits, largely due to the spectro-temporal degradation in CIs, may contribute to deficits in both linguistic and social aspects of communication.

SYMP 60

Low-Frequency Harmonicity Cues Facilitate Top-Down Processing in Bimodal Hearing

Ying-Yee Kong¹; Gail S. Donaldson²; Soohee Oh³

¹*Northeastern University*; ²*University of South Florida*;

³*Audiology Institute, Hallym University of Graduate Studies*

For cochlear implant users, access to low-frequency residual hearing in the implanted and/or non-implanted ear can improve speech recognition in quiet and noisy listening conditions. Previous studies on the benefit of combined electric and acoustic (bimodal) stimulation have focused mainly on the acoustic properties of low-frequency cues that support the bottom-up aspects of speech perception, such as enhanced segmental cues that support phoneme identification and voice pitch cues that support lexical segmentation and talker identification. However, speech perception also involves higher-level processes that are likely to influence the magnitude of bimodal benefit observed across individuals and for different speech materials. In the case of bimodal stimulation, listeners are required to combine spectrally-degraded speech information from the cochlear implant with low-frequency acoustic cues transmitted via residual hearing, integrate the two sources of information over time and across speech segments, and apply linguistic and world knowledge to fill in missing information. This talk will describe a series of experiments from our laboratory that examined the role of top-down processing for speech recognition with simulated bimodal hearing. Vocoded speech was presented to one ear, and either low-pass speech or low-frequency fine-structure information was presented to the opposite ear. Findings indicated that listeners were better at using linguistic context for speech perception with simulated bi-

modal hearing than with vocoded speech alone. Further, findings suggested that a continuous representation of low-frequency harmonicity cues facilitated the listeners' ability to reconstruct the original sentence when the vocoded speech was temporally interrupted.

SYMP 61

Cortico-acoustic Alignment in EEG Recordings with CI Users

Anita Wagner¹; Natasha Maurits²; Deniz Baskent³

¹University Medical Centre Groningen; ²University of Groningen, University Medical Centre Groningen, Department of Neurology, Groningen, The Netherlands;

³University of Groningen, University Medical Centre Groningen, Department of Neurology/ Head and Neck Surgery, Groningen, The Netherlands

Regularities in the temporal amplitude modulations of speech entrain neural oscillations. Such alignments between cortical and acoustic signals appear to play a role in speech processing, and to reflect automatic feature extraction or active comprehension. In electroencephalographic (EEG) recordings with cochlear implant (CI) users, however, cortico-acoustic alignment is also a device-induced artifact. In order to disentangle the sources of cortico-acoustic alignment in EEG recordings with CI users, we combine measures of cortico-acoustic alignment with online measures of speech processing, and relate these also to the manifestation of the CI artifact, as it is recorded in EEG with a dummy head.

We compared EEG recordings of experienced CI users, normal-hearing (NH) controls and NH listeners presented with acoustic CI simulations (8-channel noise vocoded speech). Listeners were presented with sentences of 3 to 6 seconds duration. The first 2 seconds of each sentence were used to compute the coherence between the acoustic and the cortical signal within the range of 2-20Hz. Our experimental design elicited also ERPs of phonological and semantic processing, these measures were free of the CI artifact. Individual measures of ERPs and of cortical-acoustic coherence were then ranked based on individual's performance in a series of behavioral and eye-tracking experiments. The behavioral measures allowed us to establish groups of good (similar performance to NH) and poor perceivers amongst the CI users.

We found significant coherence in the delta and theta ranges (2-8 Hz) for electrodes on the bilateral temporal lobes and on midline electrodes for NH listeners. When presented with vocoded speech, coherence was smaller in magnitude. For CI users, coherence was overall greater in magnitude, in particular in the theta range (4-8

Hz) on bilateral temporal electrodes. The recordings on the dummy head showed a coherence that is similar in magnitude to the one obtained for CI users but present over a wide range of frequency bands. Our pairing with behavioral and ERP measures showed that CI listeners categorized as good perceivers have increased coherence in the delta range (< 4 Hz) on midline central electrodes.

These results speak to the idea that cortico-acoustic coherence in EEG recordings with CI users is more than an artifact. As assumed for NH listeners, cortico-acoustic alignment found for CI users can represent a measure of active speech comprehension, in particular if present on midline frontal electrodes within the delta range (< 4Hz).

Symposium to Honor Contribution of John Niparko

SYMP 62

Considering the "Whole Child:" Key Outcomes of the Childhood Development after Cochlear Implantation (CDaCI) Study

Alexandra Quittner

University of Miami

Background

The CDaCI study is the largest, nationally representative 15-year longitudinal study of the outcomes in young children with cochlear implants and was led by Dr. John Niparko. The conceptual framework underlying this study was an evaluation of the effects of CIs on the "whole child" which included multiple domains of functioning, including oral language, auditory skills, and cognitive, behavioral and social development. Importantly, we measured the quality of parent-child interactions and their effects on oral language and other developmental outcomes.

Methods

The sample included 188 deaf children from 6 implant centers who underwent implantation before 5 years of age and 97 hearing children recruited from 2 preschools. Participants completed a multidimensional battery of assessments which captured several domains of functioning. Quality of parent-child interactions were evaluated in videotaped tasks and coded using the NICHD Early Childcare codes. Both the CI and hearing children completed assessments every 6 months for the first 3 years and then on an annual basis.

Results

Improvements in oral language and auditory skills were documented 3-4 years after implantation. Findings indicated that implanting children before age 2 years is important for optimal outcomes on several domains

of functioning. In addition, maternal sensitivity coded during parent-child interactions predicted growth in oral language 4 years after implantation. Significant differences between the CI and hearing groups were also found for externalizing behavior problems, visual selective attention, novel noun learning at baseline and after implantation.

Discussion

This is a landmark study of cochlear implant outcomes and was guided by Dr. Niparko's vision of the dynamic and multi-factorial impact of implantation. It is one of the few studies to examine behavioral, social and cognitive outcomes in relation to oral language. Results of this study have also highlighted the importance of parental input and sensitivity early in this process, which has implications for early interventions that address the quality of parent-child interactions. Highlights of study findings and future results will be presented.

Acknowledgements

The CDaCI was supported by grant R01 DC004797 from the National Institute on Deafness and Other Communication Disorders, the CityBridge Foundation, and the Sidgmore Family Foundation. Warranties on the implant devices used by children with implants in this study were discounted by 50% by the Advanced Bionics Corporation, Cochlear Corporation, and the MedEl Corporation. Implant centers included: Johns Hopkins, University of North Carolina, University of Miami, University of Michigan, University of Texas-Dallas, and University of Southern California.

SYMP 63

Hearing Loss in Older Adults - A Public Health Perspective

Frank Lin

Johns Hopkins University

Age-related hearing loss in older adults is often perceived as being an unfortunate but relatively inconsequential part of aging. However, the broader implications of hearing loss for the health and functioning of older adults are now beginning to surface in epidemiologic studies. I will discuss recent epidemiologic research demonstrating that hearing loss is independently associated with accelerated cognitive decline, incident dementia, and poorer physical functioning. Current and planned studies to investigate the impact of hearing rehabilitative interventions on reducing cognitive decline and the risk of dementia in older adults will be discussed. Finally, I will discuss current initiatives from the White House and the National Academies of Science, Engineering, and Medicine that are approaching hearing loss as a critical public health problem and have made recommendations

for the disruptive changes needed to bring about more accessible and affordable hearing healthcare.

SYMP 64

A Tribute to John K. Niparko

David K. Ryugo

Garvan Institute of Medical Research, University of New South Wales

John K. Niparko was a friend and colleague. He was a man of contradictions, very private on the one hand yet gregarious on the other. He was a dedicated clinician and loved his patients; he wanted the best for them and so, impressed his standards upon all of his students. As such, he was ferociously demanding and often harshly critical, a dedicated practitioner of tough love. Underneath it all, however, he was warm and had great sense of humor. I'll talk a bit about our collaboration with congenitally deaf white cats and cochlear implants, and I'd like to tell some funny stories about John.

SYMP 65

Multi-center Study of Cochlear Implant Outcomes in Children

Nae-Yuh Wang

Johns Hopkins University

This presentation summarizes the conception, design, and execution of the first prospective, multi-center study of cochlear implant outcomes in children: the Childhood Development after Cochlear Implantation (CDaCI) Study. Building on his academic and administrative record demonstrating deep curiosity and commitment, Dr. John Niparko assembled a world-class team of researchers and clinicians to address fundamental questions regarding the determinants of speech, language, psychosocial, behavioral, and quality of life outcomes following pediatric cochlear implantation. A few personal observations and some CDaCI study results demonstrate Dr. Niparko's tireless dedication to excellence and rigor, even through his final days, in finding answers to alter practice and reduce variability in the success of children with cochlear implants.

SYMP 66

John's Vision in Founding the American Cochlear Implant Alliance

Teresa Zwolan

University of Michigan Department of Otolaryngology

John Niparko was instrumental in founding the American Cochlear Implant Alliance (ACIA) - a not-for-profit membership organization created with the purpose of

eliminating barriers to cochlear implantation by sponsoring research, driving heightened awareness and advocating for improved access to cochlear implants for patients of all ages across the US. to establish a group of professionals who could work together to prioritize and address the needs of patients and professionals in the cochlear implant community. ACIA is unique in that its strength lies in the collaborative efforts of people from many different professions who make cochlear implants so successful, Membership includes surgeons, audiologists, SLPs, researchers, and educators, to name a few, as well as cochlear implant recipients and their families. John was very proud of ACIA and its accomplishments. This session will provide an overview of John's essential role in establishment of ACIA with a focus on recent programs and accomplishments that can be attributed to his amazing vision and the change he knew was possible with establishment of such an organization.

SYMP 67

Niparko Legacy at the University of Southern California

Laurie S. Eisenberg¹; Carolina Abdala²

¹*Keck School of Medicine of the University of Southern California*; ²*University of Southern California*

At a turning point in his life, Dr. John K. Niparko was named Chair of Otolaryngology-Head & Neck Surgery at the University of Southern California's (USC) Keck School of Medicine. Perhaps the decision to leave Johns Hopkins University seemed a risky one, but in three short years Dr. Niparko turned a relatively small clinical department into a major program of medical training, patient care, and hearing research. By 2014, with the addition of seven hearing researchers and their labs, the Otolaryngology Department at USC rose into the top ten programs for NIH-sponsored research funding. On the heels of this initial growth, Dr. Niparko recruited three additional hearing researchers and two neurotologists to the renamed Tina and Rick Caruso Department of Otolaryngology. The hearing research group at USC is currently among the largest auditory science groups on the West coast. Motivated by his personal interest in pediatric hearing loss and his drive to improve pediatric programs in Southern California, John also forged a thriving relationship with Children's Hospital Los Angeles and built the Caruso Family Center for Childhood Communication at USC. In this tribute, we highlight John's remarkable legacy at USC with a summary of accomplishments and personal remembrances.

SYMP 68

A Tribute to John K. Niparko, Md, Mentor, Advocate and Friend

Douglas Backous

Center for Hearing and Skull Base Surgery

With privilege I will pay tribute to John Niparko, my mentor as I was the first formal Neurotology fellow at Johns Hopkins. On his arrival to Johns Hopkins, Dr. Niparko envisioned a Neurotology fellowship which has become one of the true benchmarks fellowship training in our field. John was able to instill in his fellows a human approach to patient care, clear methods for building a large tertiary referral practice, a full understanding of what it means to "contribute to the field", and how to partner with basic scientists to create real-time translational research opportunities. I miss him and work each day to fulfill his legacy.

SYMP 69

River School Tribute to John Niparko

Nancy K. Mellon

The River School

Even as a young surgeon, John Niparko had a remarkably sophisticated understanding of child development and thought holistically about the cochlear implant as an intervention. He saw the CI as a tool, something that could facilitate human connection. He knew the surgery wasn't curative, and he recognized that the technology had outpaced the programs needed to optimize its use.

He wanted his pediatric patients to fit in seamlessly with their siblings, their neighbors, and their classmates. They needed not only to hear and speak well, but to learn the lingo, or as he put it—to know how to be "cool." That was going to take a village, in clinical terms a full multidisciplinary team, working alongside the surgeons, and he was determined to build that team.

John founded The Listening Center at Johns Hopkins to bring rehabilitation services into the medical model, and he initiated parent support and education programs at Johns Hopkins. He intuitively understood that maternal sensitivity was an important predictor of CI outcomes long before the field acknowledged a connection.

Still, John worried that therapy alone wasn't enough. He believed that pediatric patients needed access to hearing peers at school—children who would serve as language and social models. In 1999 John became a founding board member of The River School an inclusive program in Washington, DC. For 16 years, The Listening Center and The River School worked together to

help parents negotiate those critical early years—from a child's diagnosis, through surgery and rehabilitation at Johns Hopkins, and finally early education and support at River.

John's compassion and capacity for work were legendary—the holiday hours in the operating room, the Sunday afternoons spent editing journal articles. The constant calls on his cell phone from patients, parents or colleagues. It seemed that with each year his work grew exponentially, yet he never lost his trademark soft touch with patients—the gentle manner, his great humility and his talent for listening intently.

As a tireless advocate for early implantation and intervention, rehabilitation, and inclusive education, John spoke frequently about the role played by parents and schools in optimizing CI outcomes. By directing his gaze outside the hospital setting and building alliances with parents, educators, clinicians and policymakers, John Niparko leaves behind a lasting legacy that has moved the field forward, and benefitted thousands of patients and their families.

Auditory Pathways: Brainstem

PD 106

Auditory Processing Deficits in Genetic Knockout Models of Dyslexia

Jane Mattley¹; Luiz G. Guidi²; Anthony P. Monaco³; Antonio Velayos-Baeza³; Zoltan Molnar⁴; Jennifer F. Linden¹

¹*Ear Institute, University College London*; ²*Dept. Physiology, Anatomy & Genetics / Wellcome Trust Centre for Human Genetics, University of Oxford*; ³*Wellcome Trust Centre for Human Genetics, University of Oxford*; ⁴*Dept. Physiology, Anatomy & Genetics, University of Oxford*

Dyslexia, a common reading disability, is a highly heritable neurodevelopmental disorder. Genetic linkage and association studies have repeatedly identified KIAA0319 and subsequently KIAA0319-Like as candidate susceptibility genes in humans. Downregulation of either Kiaa0319 or Kiaa0319-Like expression in rats, using RNA-interference techniques, has been shown to produce cortical migration abnormalities and (in some cases) deficits in auditory processing. However, no cortical migration abnormalities have been found in recently developed Kiaa0319 and Kiaa0319-Like knockout mice, nor in mice with double-knockout of both Kiaa0319 and Kiaa0319-Like (Martinez-Garay et al. 2016 and unpublished observations). Here we investigated auditory pro-

cessing in mice with knockouts of Kiaa0319, Kiaa0319-Like, or both Kiaa0319 and Kiaa0319-Like.

To assess auditory processing in these mice, we measured auditory brainstem responses (ABRs) to clicks and to clicks following noise. We tested 11 Kiaa0319 knockout mice, 12 Kiaa0319-Like knockout mice, and 13 mice with double-knockout of both Kiaa0319 and Kiaa0319-Like, along with appropriately age-matched controls (25 wildtype animals total).

ABR thresholds did not differ between any of the groups, and there were no significant differences between Kiaa0319 knockout and wildtype animals in amplitudes or latencies of ABR waves I-IV after correction for multiple testing. However, in Kiaa0319-Like knockout mice, amplitude of the late ABR wave III (but not wave I) was significantly reduced and latency increased. In the double-knockout animals, amplitudes of early as well as late ABR waves were significantly reduced.

These results suggest that knockout of Kiaa0319-Like disrupts the strength or synchrony of neural activity in the auditory brainstem, while double-knockout of both Kiaa0319 and Kiaa0319-Like produces more profound deficits in early auditory processing.

References

Martinez-Garay I, Guidi LG, Holloway ZG, Bailey MAG, Lyngholm D, Schneider T, Donnison T, Butt SJB, Velayos-Baeza A, Molnár Z and Monaco AP (2016). Normal radial migration and lamination are maintained in dyslexia-susceptibility candidate gene homolog Kiaa0319 knockout mice. *Brain Struct Funct*, in press.

PD 107

Attentional Modulation of Envelope Following Responses Only for Lower Frequencies

Emma Holmes¹; David Purcell¹; Robert P. Carlyon²; Hedwig Gockel²; Ingrid S. Johnsrude¹

¹*University of Western Ontario*; ²*MRC Cognition and Brain Sciences Unit*

In complex acoustic environments, listeners must direct attention flexibly to sounds of interest when other sounds are present. Directing attention to sounds of different frequencies modulates activity in auditory cortex; however, whether frequency-specific attention modulates activity at lower, brainstem, levels of the auditory system is unclear. Envelope following responses (EFRs) originate primarily from the human brainstem, although, recent evidence has called into question the assumption that EFRs at frequencies above 70 Hz reflect brainstem activity with minimal influence from cortex. We per-

formed two experiments investigating the effect of attention on EFRs recorded using electroencephalography (EEG): one within the range of frequencies commonly used for EFR recordings (90–150 Hz) and one using a higher range for which cortical contributions can be ruled out (> 200 Hz). If brainstem responses are affected by frequency-specific attention, attentional modulation of EFRs should occur for both sets of frequencies.

We measured EFRs elicited by three simultaneous sequences of amplitude-modulated (AM) sinusoids. Each sequence had a unique carrier frequency and contained tones with unique durations and inter-stimulus intervals so that tone onsets for the sequences were different. The highest and lowest carrier frequencies were tagged with unique AM rates, which differed between the two experiments: Experiment 1 used 93 and 109 Hz; Experiment 2 used 217 and 233 Hz. In both experiments, we compared EFRs in three different attentional conditions with identical acoustic stimuli. In the Attend Low condition, participants detected shorter-length deviant tones in the sequence with the lowest carrier frequency. In the Attend High condition, participants detected shorter-length deviants in the sequence with the highest carrier frequency. In the Attend Visual condition, participants performed an N-back task on visual digits presented concurrently with the acoustic sequences.

For the lower rates used in Experiment 1, the amplitude and phase coherence of EFRs were greater for each of the two different AM rates when the corresponding stimulus frequency was attended than when it was unattended. This was not the case for the higher rates used in Experiment 2. The interaction between experiment and attentional modulation was significant. This dissociation may reflect cortical contributions to EFRs at lower, but not higher, AM rates rather than modulation of brainstem responses. Our results suggest that the envelope rate may critically determine outcomes of EFR studies: EFRs may reflect different processes (including cortical processes) for rates below 200 Hz, which are common in the literature, than for higher rates.

PD 108

Encoding of Surprise Magnitude along the Human Auditory Hierarchy

Carles Escera; Teresa Ribas; Natàlia Gorina-Careta
Universitat de Barcelona, Institute of Neurosciences

Encoding of surprise in the auditory environment has been associated with a specific cortical, long-latency component of the human auditory evoked potentials (AEP) termed mismatch negativity (MMN), peaking at 100–200 ms from the sound onset. However, human electrophysiological correlates of surprise encoding

have been recently found at much shorter latencies, by the middle-latency response (MLR), and in lower anatomical stations as indicated by the subcortical frequency-following response (FFR). These results parallel those obtained in animal studies recording single and multi-unit neuronal activity, which have disclosed stimulus-specific adaptation (SSA) at different stations of the auditory system as the neuronal mechanism subserving surprise encoding. Together, these two parallel lines of research have supported the emerging view that surprise detection based on regularity encoding is a common property of the entire auditory system. For example, both the MMN and SSA have been shown to be related to the magnitude of the physical difference between the auditory stimuli establishing a common background (the “regularity”) and those yielding the surprise. The aim of the present experiment was therefore to assess the effects of the magnitude of the frequency difference between a repetitive standard tone and different deviant stimuli in the human MMN as well as subcortically through measurements of the FFR obtained to stimuli delivered in oddball sequences. Pure tones of a standard frequency of 269 Hz and deviant tones of 289, 329 and 409 Hz were delivered in separated oddball blocks to 19 healthy human adult participants. To oversee refractoriness confounds a control condition delivered these very same stimuli with identical probability. EEG recordings were carried out with open filters, and subsequently filtered out in the long-latency (0.5–30 Hz) and FFR (120–1500 Hz) ranges. As expected, MMN increased as a function of deviance when compared to the standard, but MMN to the different magnitudes of frequency difference were similar when compared to the corresponding control stimuli. On the other hand, deviant stimuli yielded a significant effect on the FFR, which however was similar irrespective of deviance magnitude. These results suggest that the encoding of surprise is present along the auditory hierarchy, and that its magnitude is parsed out at cortical level, by a mechanism that is not associated to true deviance detection.

PD 109

Topographic Distribution of Frequency Components of the Human Frequency-following Response (FFR) Monaurally and Binaurally Evoked by Missing-fundamental Complex Tones

Qin Gong; Xiaochen Zhang
Tsinghua University

The neural origins underlying the human frequency-following response (FFR) are still unclear. The FFR is conventionally assumed to reflect subcortical phase-locking, which is supported by the topographic distribution and the source estimation of the peaks and troughs in speech-evoked FFRs revealed in a recent study based

on electroencephalography. However, another recent study based on magnetoencephalography of FFR topographic distribution supports the dominance of cortical contribution to FFR generation. Apart from these two studies, we find it difficult to reach another study describing FFR topographic distribution, which provides vital information about its origins, as most previous FFR studies involve only a few, if not one, recording channels. This study aims to describe the topographic distribution of FFR components at the fundamental frequency (F0) and at the second harmonic (H2) under monaural and binaural stimulation. In ten subjects with normal hearing, we recorded FFRs evoked by three missing-fundamental complex tones with pitch at 264, 330, and 393 Hz, which are respective pitches of musical tones C4, E4 and G4. The stimuli were composed of harmonics at integer multiples (> 4) of F0. Each type of stimulus was repeatedly presented monaurally on left or right side, or binaurally, for at least 2000 trials. After artifact rejection, the rest trials were averaged. The data were recorded from 34 channels, re-referenced to the average of all channels, and transformed into the frequency domain by Fourier transform. We found that i) topographies obtained under left monaural stimulation were basically mirrored version of those obtained under right stimulation; ii) F0 components of FFRs monaurally evoked by C4, E4 but not G4 tones showed laterality in topography, while H2 components of monaurally-evoked FFRs, regardless of stimulus pitch, showed laterality in topography to the contralateral side compared with F0 components; iii) topographies obtained under binaural stimulation were basically symmetrical about the central line, except that the topography of the F0 component of FFRs evoked by C4 tones showed laterality; the center of the vertex region where the power of F0 component concentrated moved forward as the stimulus pitch increased (from Cz to Fz), while the center of the vertex region where the power of H2 component concentrated stayed frontal (Fz or FCz-Fz midpoint) for all three stimuli. Our findings suggest that different neural origins underlie F0 and H2 components of FFRs, and those underlying F0 components may vary with stimulus pitch.

PD 110

Transmission of Auditory Information Deteriorates at the Auditory Nerve Terminal During Age-related Hearing Loss

Ruili Xie

Department of Neurosciences, University of Toledo

Age-related hearing loss (ARHL) is largely attributed to structural changes and functional declines in the peripheral auditory system, which include synaptopathy at the inner hair cell/spiral ganglion cell (SGC) connection as well as the loss of SGCs. However, functional changes

at the central terminals of SGCs, namely the auditory nerve synapses in the cochlear nucleus, are not yet fully understood during ARHL. Our previous studies with voltage clamp recordings showed that synaptic transmission at the endbulb of Held is compromised during aging, which is expected to decrease the sensory inputs from the auditory nerve to the central auditory system during ARHL. In cochlear nucleus slices from young (1-3 months) and old (25-30 months) CBA/CaJ mice, this study used current clamp recording to evaluate the intrinsic properties of the bushy neurons postsynaptic to the endbulb of Held synapses, and the firing properties of these neurons to direct current injections as well as to synaptic inputs from the auditory nerve. Results showed that bushy neurons in old mice are more excitable, and are able to fire spikes at similar rate and timing to direct current injections as those in young mice. In response to synaptic inputs, however, bushy neurons from old mice fired spikes with significantly decreased rate and reduced temporal precision to stimulus trains at 100 and 400Hz, with the drop in firing probability more profound at 400 Hz. It suggests that transmission of auditory information at the endbulb is declined in both rate and timing during aging, which signifies the loss of sensory inputs to the central auditory system under ARHL. The study proposes that, in addition to damages at the peripheral terminals of SGCs as well as the loss of SGCs, functional decline at the central terminals of the surviving SGCs is also an essential component of ARHL.

KV3, KV2 and Resurgent NaV Currents Shape Burst Firing for Low Frequency Processing in the Avian Cochlear Nucleus MagnocellularisHui Hong¹; Xiaoyu Wang²; Yuan Wang²; Jason Sanchez¹¹Northwestern University; ²Florida State University

Low-frequency nucleus magnocellularis neurons (< 500 Hz, termed caudolateral NM or NMc) present with multiple dendritic processes and receive small bouton synapses from the auditory nerve. In contrast, higher-frequency NM neurons are mostly adendritic and form large axosomatic endbulb of Held synapses. Consistent with their structural differences, we previously showed that NMc neurons display enhanced excitability as well. Here we report distinct response properties of NMc neurons to varying sinusoidal current injections and their underlying ion channel mechanisms.

Brainstem slices from low frequency NM were obtained from embryonic (E) chickens at E19-21. Whole-cell current clamp was used to record voltage responses to suprathreshold sinusoidal current injections from 5 to 200 Hz. Whole-cell voltage clamp was used to document voltage dependent ion channel properties.

We found that NMc neurons act as a low-pass filter in response to sinusoidal current injections. They fire bursts of action potentials (APs) within each cycle of low frequency stimuli (i.e., 5 and 10 Hz) but fail to phase lock reliably to stimuli > 50 Hz. In contrast, higher-frequency NM neurons act as a band-pass filter and prefer frequencies between 75-100 Hz. Voltage clamp recordings show that NMc neurons have significantly lower amount of total KV current than higher-frequency NM neurons. Pharmacological studies show that ~40% of the total KV current in NMc is mediated by KV3, while KV2 and KV1 account for ~30% and 20%, respectively. Blockade of KV3 and KV2 channels increase AP duration and significantly reduce AP firing probability in response to low frequency current injections. However, blockade of both channels did not abolish burst firing and suggests other regulating factors.

Indeed, we observed resurgent NaV current in NMc neurons, likely induced by specific open channel blockers. We hypothesized that resurgent NaV current is an additional factor that regulates burst firing. To test this, we documented the recovery of NaV current after conditioning NMc neurons to prefer either an "open-channel blocked" state (+30 mV, 5 ms) or a classical inactivation state (-30 mV, 40 ms). NMc neurons conditioned to the "open-channel blocked" state recover significantly faster and have more available NaV channels during recov-

ery. This suggests resurgent NaV current permits native NaV channels to recover quickly from inactivation immediately following an AP, promoting burst firing. Taken together, the interaction between KV3, KV2 and resurgent NaV currents regulate burst firing of NMc neurons. Ongoing studies are investigating distribution pattern of KV channels in NMc.

Auditory Nerve

PD 114

Synaptic Repair and the Effects of Noise Induced Hidden Hearing Loss

Jian Wang¹; Kegan Stephen²; Hengchao Chen²; Steven J. Aiken³

¹School of Human Communication Disorders, FHP, Dalhousie University; ²School of human communication disorder, FHP, Dalhousie University; ³School of Human Communication Disorders, Dalhousie University

Background

The synapse between inner hair cells (IHCs) and spiral ganglion neurons (SGNs) has been found to be a sensitive target in noise induced cochlear damage: brief exposure to moderate-level noise can cause massive synaptic damage without permanent threshold shift. Functional deficits have been found in such cases and are called noise induced hidden hearing loss (NIHHL) due to the lack of threshold shift. While synaptic disruption results in disuse of innervated auditory neurons, there has been prolonged debate as to whether damaged synapses can be repaired. Our previous experiments have shown partial re-establishment of synapses in guinea pigs and the development of coding deficits associated with the repair, suggesting that repaired synapses are abnormal. Here we provide more evidence for synaptic repair and extend our evaluation of the functional consequences of synaptic damage and repair. We also observe whether damage to presynaptic ribbons is secondary to the loss of postsynaptic terminals or directly caused by noise.

Methods

Guinea pigs were subjected to a brief noise exposure at 105 dB SPL to produce NIHHL. Morphological changes to synapses were observed using a transmission electronic microscope (TEM) and confocal microscope. Potential changes in synaptic proteins were observed in Western blot and qRT-PCR with a focus on the protein composition of pre-synaptic ribbons and a marker of axon growth. Suprathreshold deficits in hearing were evaluated using envelope following responses (EFR).

Results

An equal loss of ribbons and PSD immediately following noise exposure suggests that ribbon damage is directly caused by noise, and is not secondary to post-synaptic terminal damage. Confocal image counts of both pre-synaptic ribbons and post-synaptic terminals (stained against post-synaptic density) showed recovery following the massive initial loss. Evidence of plastic reorganization and regeneration of presynaptic ribbons was provided by changes in the size, location and number of ribbons in each synapse (TEM). Synapse re-establishment was further supported by recovery of the compound action potential and up-regulation of GAP43 (a marker of axon growth). Analysis of the impact of NI-HHL on the EFR is currently in process.

Conclusions

Synapses damaged by noise are partially repairable. New methods need to be explored to identify functional deficits at suprathreshold levels.

PD 115

P2X7 ATP-purinergic Receptor Deficiency Increases Susceptibility to Noise Stress

Yan Zhu; Hong-Bo Zhao; Ling Mei

Dept. of Otolaryngology, University of Kentucky Medical Center

Background

The cochlear efferent reflex is well-known to play an important role in the adjustment of outer hair cell electromotility and active cochlear amplification as well as in the attenuation of noise stress. P2X7 is an ATP-gated, purinergic ionotropic (P2X) receptor, and predominantly expresses at the post-synaptic nerve endings under outer hair cells. In this study, we have tested whether P2X7 participates in the adjustment of outer hair cell electromotility and active cochlear amplification to attenuate noise-stress.

Methods

P2X7 knockout (KO) mice were used. Hearing function was examined by auditory brainstem response (ABR) and distortion product otoacoustic emission (DPOAE) measurements. Mice were also exposed to noise to examine the susceptibility to noise-stress.

Results

In comparison with wild-type (WT) mice, hearing function measured as ABR threshold in P2X7 KO mice had no significant changes. However, DPOAE in P2X7 KO mice was significantly increased, especially, in high-frequencies. After being exposed to middle levels of white noise (~ 90 dB SPL, 1-2 hr), both of WT and P2X7 KO mice had similar initial temporary threshold shift (TTS).

However, P2X7 KO mice showed less recovery than WT mice and had permanent threshold shift (PTS).

Conclusions

P2X7 deficiency can increase susceptibility to noise stress. Based on P2X7 location, this may result from the reduction of the regulation of active cochlear amplification through the cochlear efferent reflex.

Supported by NIH R56 DC 015019

PD 116

Localizing Cochlear Neuropathy Using Signal-in-Noise Action Potentials (SiNAPs)

Brian R. Earl¹; Maggie Schad¹; Chun Liang²; Lauren Meyer³; Ivy Schweinzer¹

¹University of Cincinnati; ²Dept. of Otolaryngology, University of Kentucky Medical Center; ³Ohio University

Introduction

The interest in noise-induced cochlear neuropathy has been intensified by recent research showing a reduction in the amplitude of electrocochleography responses in noise-exposed adults with speech-in-noise listening difficulties. The utility of amplitude measures in localizing the cochlear location of the neuropathy may be improved by tracking CAP amplitude growth while systematically limiting the region of neural firing with a high-pass masking paradigm. Previous experiments have indicated that the pattern of CAP amplitude growth for high-level stimuli is independent of outer hair cell pathology and is sensitive to neural lesions in the basal region of the cochlea. The objective of this study was to determine if the CAP growth pattern is also sensitive to noise-induced neuropathy in the gerbil cochlea.

Methods

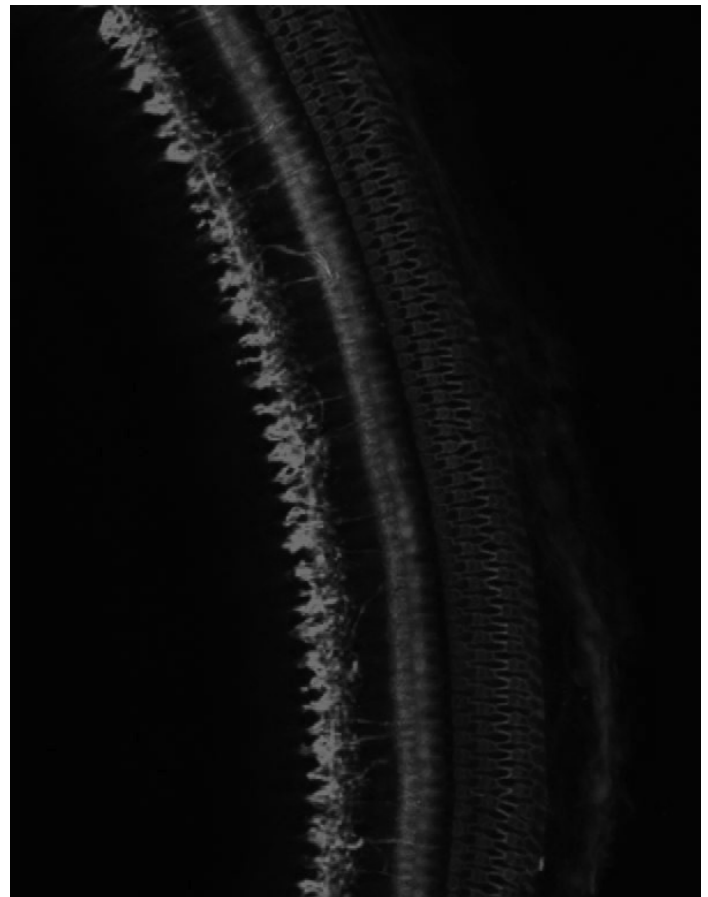
Gerbils (N=44) were exposed to one or two-octave bands of noise between 1 and 16 kHz at levels ranging from 97 to 106 dB SPL RMS for a period of two hours and were compared to a group of normal-hearing, age-matched gerbils (N=23) at the following time-points post exposure: 1 hour, 1 week, 1 month, 2 months, 6 months. CAP thresholds generally returned to normal for the majority of gerbils by 1 month post-exposure. SiNAPs were evoked with broadband chirps at 60 and 90 dB SPL during simultaneous white noise that was high-passed in 1/3 octave intervals between 0.4 and 63 kHz. Cumulative amplitude functions were constructed by plotting the amplitudes of the masked CAPs as a function of masker cutoff frequencies. Cochlear hair cell and peripheral auditory nerve anatomy were analyzed using confocal microscopy.

Results

In the majority of noise-exposed gerbils, the cumulative amplitude functions were lower in amplitude in select cochlear regions compared to those for normal-hearing gerbils for the 90 dB SPL condition. Cumulative amplitude functions for 60 dB SPL condition were generally within the normal range. Confocal microscope images of a subset of noise-exposed cochleae revealed a decrease in staining intensity of afferent neurons in regions above the upper frequency of the noise band.

Summary

These data suggest that the frequency location of abnormalities in CAP-derived cumulative amplitude functions may predict the cochlear location of noise-induced neuropathy impacting high threshold auditory nerve fibers. This finding in a gerbil model is especially relevant because of the closer low-frequency overlap in hearing sensitivity between humans and gerbil than between humans and mice or rat species in which cochlear neuropathy has been studied.



Macrophages Influence Noise-Induced Cochlear Synaptopathy and Neuropathy Via Fractalkine Signaling

Tejbeer Kaur¹; Kevin K. Ohlemiller²; Angela Schrader¹; Mark Warchol³

¹Washington University School of Medicine Saint Louis Missouri; ²Washington University; ³Dept of Otolaryngology, Washington University School of Medicine, St Louis MO

Background

The fractalkine ligand (CX3CL1) is a transmembrane protein and chemokine involved in the adhesion and migration of leukocytes by binding to its exclusive receptor CX3CR1. Fractalkine-mediated interactions between macrophages and spiral ganglion neurons (SGN) influence the survival of auditory neurons after cochlear damage (Kaur et al., 2015; Kaur et al., ARO 2016). Promoting the long-term survival of SGNs after cochlear injury is of great interest, because their survival is essential for the success of cochlear prosthetics. Notably, the role of macrophages in neuronal survival after noise-exposure is unknown. The present study examined the role of fractalkine signaling in the survival of auditory neurons after noise-induced cochlear damage.

Methods

Adult CX3CR1^{+/+}, CX3CR1GFP^{+/+} and CX3CR1GFP/GFP mice (~6 week post-natal), on a C57BL6 background were exposed for 2 hour to an octave band (8-16 kHz) noise at either 90 or 120 dB SPL intensity. Animals were allowed to recover for 1, 7, 14, 30, 60 days. The CX3CR1GFP^{+/+} line retains fractalkine signaling, while CX3CR1GFP/GFP lack the fractalkine receptor. Auditory brainstem response (ABR) thresholds were characterized prior to noise exposure, immediately after noise exposure, at two weeks recovery, and immediately prior to sacrifice. Temporal bones were fixed and processed for immunohistochemistry to label hair cells, macrophages, neurons or synapses. Animals exposed to ambient noise levels served as controls.

Results

Exposure to 120 dB noise led to permanent shifts in ABR thresholds, loss of hair cells and prolonged increase in the numbers of cochlear macrophages. In addition, deletion of CX3CR1 resulted in increased loss of SGN cell bodies, when compared to noise exposed CX3CR1GFP^{+/+} littermate controls. In contrast, exposure to 90 dB SPL noise caused elevated ABR thresholds in both CX3CR1GFP^{+/+} and CX3CR1GFP/GFP mice without any evident hair cell loss. These elevated thresholds returned to the baseline within two weeks in CX3CR1G-

FP/+ mice but not in CX3CR1GFP/GFP mice. We also observed increased macrophage migration towards the inner hair cell synaptic region shortly after moderate noise exposure. Immunolabeling for synaptic elements revealed synapses in CX3CR1GFP/+ mice had recovered at 2 months after moderate noise exposure, while CX3CR1GFP/GFP mice displayed an enhanced loss of synapses and hair cell damage compared to control animals.

Conclusions

Results indicate that disruption of fractalkine signaling leads to enhanced degeneration of cochlear synapses and SGNs after noise exposure. Such findings point to a crucial role for macrophages in promoting synapse recovery and long-term survival of neurons after cochlear injury.

PD 118

The Role of Auditory Attention and Different Sound Stimuli During Exposure Resulting in Temporary Threshold Shifts

Lou-Ann Christensen Andersen¹; Ellen Raben Pedersen²; Ture Andersen³; Bjørn Petersen⁴; Peter Vuust⁴; Jesper Hvass Schmidt⁵

¹Department of Audiology, Odense University Hospital, DK-5000 Odense, Denmark, Department of Clinical Research, University of Southern Denmark, DK-5230 Odense, Denmark; ²The Maersk Mc-Kinney Moller Institute, University of Southern Denmark, DK-5230 Odense, Denmark; ³Department of Clinical Research, University of Southern Denmark, DK-5230 Odense, Denmark; ⁴Center for Music in the Brain, Aarhus University, DK-8000 Aarhus C, Denmark, Department of Clinical Medicine, Aarhus University, DK-8000 Aarhus C, Denmark/The Royal Academy of Music, DK-8000 Aarhus/Aalborg; ⁵Department of Audiology, Odense University Hospital, DK-5000 Odense, Denmark, Department of ENT Head and Neck Surgery, Odense University Hospital, DK-5000 Odense, Denmark, Department of Clinical Research, University of Southern Denmark, DK-5230 Ode

Background

Temporary hearing loss in connection with excessive short-term exposure to sound is described as temporary threshold shift (TTS). The auditory cortex has neural pathways, which directly affect the medial olivocochlear system (MOCS) via the descending efferent auditory system. One of the functions of MOCS may be to protect the inner ear from noise exposure. Objective: The purpose of this crossover randomized controlled trial was: (1) To investigate the effect of auditory attention on TTSs

measured with auditory brainstem responses (ABRs) and distortion product otoacoustic emissions (DPOAEs); (2) To investigate the influence of the character of the sound using three different sound stimuli (noise, familiar, and unfamiliar music) on TTSS.

Method

20 normal-hearing individuals were randomized to the task of auditory attention or non-auditory attention. For each of the two tasks the participants were exposed to the three different sound stimuli in randomized order on separate days. Each stimulus was 10 minutes long and the average sound level was 100 dB SPL. ABRs (4 kHz tone burst) and DPOAEs (2, 3, and 4 kHz) were measured pre-exposure and immediately after the sound exposure.

Results

An increase in ABR wave I amplitude, a decrease in the amplitude difference between wave V and wave I, and a decrease in DPOAE amplitudes were found - all for the left ear immediately after sound exposure, with an opposite effect of the DPOAE amplitudes for the right ear. Non-auditory attention showed a decrease in wave I amplitude, and an increase in the amplitude difference between wave V and wave I. Music listening induced an increase in DPOAE amplitude on the left ear compared to noise. Level of music aptitude (AMMA score) was correlated with ABR wave V-I amplitude differences. A possible learning effect was observed throughout the experiment.

Conclusion

We found that ABR wave I amplitudes were reduced when measured after exposure with non-auditory attentions leading to a TTS. Furthermore, our results suggest a possible effect of musical training in the full extent of the auditory pathway, and a clear lateralization towards the left ear which is currently unexplained but maybe due to a dominant activation of cochlear efferents favoring one side. These results can further explain that the size of the TTS is dependent on auditory attention, but whether or not this affects the permanent hearing thresholds is not known.

PD 119

The Expression of AMPA Receptors and NMDA Receptors of the Inner Hair Cell Ribbon Post-synapse in Type I Afferent Dendrite After Ototoxicity

Juan Hong¹; Yanping Zhang²; Yan Chen³; Peidong Dai⁴

¹Affiliated Eye & ENT Hospital of Fudan University;

²Affiliated Eye & ENT Hospital of Fudan University;

³Department of Otorhinolaryngology, Hearing Research

Institute, Affiliated Eye and ENT Hospital of Fudan University, Shanghai; ⁴EENT Hospital of Fudan University

Background

Cochlear inner hair cell(IHC) ribbon synapses played an important role in sound encoding and neurotransmitter release. The change of the number and size of synaptic ribbons was related to the hearing restoration after ototoxicity withdrawn. By comparison, the molecular architecture of the inner hair cell-spiral ganglion neurons(IHC-SGN) post-synapse and SGNs afferent dendrite after ototoxicity was much less resolved. Although the excitatory post-synaptic currents of the SGNs afferent dendrite was convincingly mediated by AMPA receptors, it was recently suggested that NMDA receptors enhance spontaneous activity and promote neuronal survival in the developing cochlea.

Purpose

To study the role of AMPA receptors and NMDA receptors of the IHC-SGN post-synapse in SGNs afferent dendrite after ototoxicity.

Materials and Methods

Ten C57L/B6 mice were injected intraperitoneally with a low dose of gentamicin (100 mg/kg) once a day for 7 days. Double and triple immunostaining with antibodies against AMPA receptors(GluA2), NMDA receptors(-GluN1) and ribbons(Ctbp2) were used to identify IHC ribbon synapses and glutamate receptors in SGN afferent dendrite; the hearing threshold shifts and wave 1 amplitude were recorded by auditory brainstem response examinations.

Results

Under physiological conditions the AMPA receptors were distributed around the base pole of the IHCs, the NMDA receptors were distributed laterally and above the IHCs. The quantity of the co-localization of the AMPA receptors and the NMDA receptors was little. But after ototoxicity their location was reversed. Accompanied the SGN afferent dendrites, the NMDA receptors were retracted to the base pole of the IHCs, the AMPA receptors climbed upside to the lateral and above the IHCs. Interestingly, at the base pole of the IHCs the quantity of co-localization of the AMPA receptors and the NMDA receptors was increased ($p < 0.05$), but the pairs of ribbon synapses double stained with Ctbp2 and GluA2 were decreased ($p < 0.05$).The total quantity of the GluA2 was not significant different with ototoxicity($p > 0.05$). The distribution tendency of the Ctbp2 was consistent with the AMPA receptors. Correspondingly, the elevated hearing threshold and the declined wave 1 amplitude were consistent with the quantity of the pairs of ribbon synapses.

Conclusions

The AMPA receptors and the NMDA receptors changed the location in SGNs afferent dendrites after ototoxicity, especially in base turns and middle turns of cochlear. The AMPA receptor in SGNs afferent dendrites selectively combined the NMDA receptor or presynaptic ribbons with ototoxicity. It seemed that the AMPA receptor indicated for the location of presynaptic ribbons in the IHC-SGN synapse after ototoxicity.

PD 22

Formes Frustes of Pathognomonic Tinnitus Percepts

Robert A. Levine

Tel Aviv Medical Centre

The tinnitus percept can vary in multiple dimensions including: loudness, quality (including pitch), location, temporal pattern, and how it interacts with activation of both the auditory and non-auditory neural systems (e.g. acoustic masking and somatic testing). From this matrix of possibilities has emerged two pathognomonic tinnitus percepts that have specific (1) etiologies, (2) generating mechanisms, and (3) treatments. The two pathognomonic tinnitus percepts are as follows:

[A] Clicking (“Typewriter”) Tinnitus: its percept is pathognomonic (monaural, staccato, irregular, and intermittent); it is caused by auditory nerve distortion usually from vascular compression, that results in ephaptic cross-talk between individual auditory nerve fibers. It can be suppressed by (a) carbamazepine or (b) vascular decompression of the auditory nerve.

[B] Somatosensory Pulsatile Tinnitus Syndrome: its percept is pathognomonic (cardiac synchronous pulsations that can be abolished by intense head or neck muscle contractions). It is caused by a somatic myofascial dysfunction that leads to abnormal CNS interactions between the somatosensory and auditory systems. In some cases it can be abolished by (a) dry needling of head and neck trigger points or (b) auricular electrical stimulation.

A case series will be presented, supporting the notion that when a constant non-specific tinnitus percept is intermixed even intermittently with a forme fruste of one of these two types of pathognomonic tinnitus, detection of the pathognomonic component will point to the underlying cause of the constant non-specific percept, which in turn will lead to treatment that can abolish both percepts.

For monaural non-specific tinnitus, if typewriter-like clicking is also present, then the etiology is auditory nerve distortion, which will then lead to specific treatment options.

For any kind of non-specific tinnitus, if sometimes there are pulsations that can be suppressed somatically, then the etiology is head or neck somatic myofascial dysfunction.

Plasticity, Learning & Adaptation to Hearing Impairment

PD 120

Amplitude Modulation Detection in Children with a History of Temporary Conductive Hearing Loss

Margo McKenna Benoit¹; Kenneth S. Henry¹; Mark S. Orlando¹; Paul Allen²

¹Department of Otolaryngology, University of Rochester Medical Center; ²University of Rochester Medical Center

Otitis media with effusion (OME) has been considered a form of sensory deprivation during the critical period of speech and language acquisition; however, there remains considerable debate in the literature about whether OME in early childhood has lasting effects on processing of complex sounds. Amplitude modulation (AM) is recognized as a critical feature of speech, but little is known about the development of AM sensitivity, or whether early temporary impairments in hearing during childhood can affect acquisition and maturation of AM detection abilities. Animal studies have demonstrated that moderate reversible hearing loss during early development can result in elevated thresholds for an AM detection task, even after restoration of normal hearing. AM detection in humans with a history of OME-associated hearing loss has not been previously investigated. We hypothesized that temporary hearing loss in otherwise healthy children between the ages of 6 months to 3 years can result in measurable deficits in AM detection that persist into later childhood, even after restoration of normal audiometric thresholds. In this study, children between the ages of 4 and 7 years with normal hearing but either a documented history of OME-related conductive hearing loss or no such loss, underwent audiometric testing of both ears, followed by an experimental session requiring them to listen to a series of amplitude modulated sounds, presented in a two alternative forced choice paradigm. AM thresholds were measured at modulation frequencies of 8 and 64 Hz using a noise carrier signal and an interactive computer program designed for use in young children. Testing was conducted in a standard, double-walled audiometric test booth with acoustic stimuli presented diotically through calibrated audiometric headphones. Children in this age range showed a significant maturation of AM detection thresholds, with older children achieving lower thresholds particularly at the 8 Hz modulation frequency. Large individual differences in

AM detection thresholds were observed within each age group. Limited behavioral sensitivity to low modulation frequencies, as seen here in young children, has also been observed in animal studies. Comparison of AM detection thresholds between individuals with a history of OME and individuals with a history of normal hearing will provide insight into the effects of this common condition on auditory processing of complex sounds. Results from this study may have implications for the treatment of children with OME.

PD 121

Effects of Language Experience and Long-term Training on the Neural Weighting and Categorical Perception of Pitch Dimensions

Rachel Reetzke¹; Han Gyol Yi¹; Zilong Xie¹; Bharath Chandrasekaran²

¹*Department of Communication Sciences and Disorders, The University of Texas at Austin;* ²*Department of Communication Sciences and Disorders, Department of Psychology, Department of Linguistics, Institute for Neuroscience, Institute for Mental Health Research, The University of Texas at Austin*

There is now overwhelming evidence that auditory subcortical processing is plastic even in adulthood. However, the neural mechanisms underlying experience-dependent plasticity in humans remains unclear. We examined subcortical decoding of linguistically relevant pitch patterns to better understand the time-scale and mechanisms underlying experience-dependent plasticity. Across two experiments scalp-recorded frequency-following responses (FFRs), which capture phase-locked responses from subcortical neural ensembles, were elicited while adult participants passively listened to the four Mandarin linguistic pitch patterns. In addition to the FFRs, we also assessed the extent to which experience modulated participants' categorical perception (CP) of a seven-step pitch continuum (level to rising tone). In experiment 1, FFRs were recorded from native speakers of Chinese ($n = 15$) and English ($n = 15$). In experiment 2, English participants ($n=20$) were trained over multiple days ($M = 17.5$ days) to reach Mandarin tone categorization accuracy and reaction time performance equal to that of Chinese participants. A data-driven support vector machine (SVM) learning approach was implemented to classify FFRs to the four Mandarin tones. SVM learning output was then used to generate dissimilarity matrices that were subjected to a multidimensional scaling (MDS) model. In both experiments, a two dimensional MDS solution emerged that subjectively corresponded to "pitch height" and "pitch direction" of the Mandarin tones. In experiment 1, we found that stimulus decoding was strongly influenced by long-term lin-

guistic experience, with poorer decoding of the four pitch patterns in English, relative to Chinese participants. Chinese participants additionally demonstrated more robust CP for the pitch patterns of the Mandarin tonal space. In experiment 2 we found that training enhanced decoding of the falling pitch pattern, which also showed the maximal improvement with training. MDS revealed that, initially, pitch direction was weighted more by the Chinese participants relative to the English participants. Notably, following long-term training to native-like Chinese performance, relative weighting on pitch direction was found to increase in the English participants. Native-like performance was further reflected behaviorally, as English participants demonstrated native-like CP for the pitch continuum. However, when participants returned after 2 months of no training, behavioral performance and categorical perception remained native-like, but subcortical plasticity reverted to pre-training language specific norms. These results suggest that long-term training leads to the formation of categories of pitch patterns, which persist after 2 months of no training. Subcortical plasticity as a function of training relates to initial learning, but not behavioral stabilization.

PD 122

Evidence for Extended High Frequency Hearing Loss in Children with Listening Difficulties (aka APD)

Lisa L. Hunter¹; Chelsea Blankenship²; Allison Bradley¹; Nicholette Smith¹; Audrey Perdeu¹; Morgan Bamberger¹; David R. Moore¹

¹*Cincinnati Children's Hospital;* ²*University of Cincinnati*

Background

Listening difficulties (LiD) in childhood that are unexplained by hearing threshold elevation have been termed "auditory processing disorder". These difficulties have recently been explained on the basis of attention or cognition (Moore, Pediatrics, 2010) and often coexist with other language learning problems in a constellation of neurodevelopmental disorders (Moore & Hunter, Hear Bal Comm, 2013). However, the role of the auditory periphery is poorly understood. Cochlear neuropathy or "hidden hearing loss" could be an explanation for listening difficulties (Kujawa & Liberman, J Neurosci, 2009). Alternatively, undetected sensory or conductive hearing loss could also cause listening difficulties.

Methods

Prospective study of children aged 6-12 years with complaints of listening difficulties (LiD, $n=51$) on a validated questionnaire (ECLIPS, Barry and Moore, MRC, 2014), some also diagnosed through an audiologic test battery of speech in noise, dichotic words and sentences, com-

pared to age and gender-matched typically developing children (TD, n=63). All children underwent comprehensive peripheral auditory tests, including standard and extended high frequency (EHF) audiometry, wideband tympanometry and acoustic reflexes (tonal and broadband stimuli), distortion product otoacoustic emissions (DPOAE), Transient Evoked OAE using chirps, ear canal recordings of the auditory nerve compound action potential (CAP), and speech-in-noise tasks (LiSN-S, SCAN 3:C). Differences between LiD and TD groups were measured, as well as hypothesized relationships among these measures.

Results

Pure tone thresholds for standard audiometric frequencies (0.25-8 kHz) were not significantly different between groups. However, significantly poorer hearing thresholds in the LiD group were obtained from 12-16 kHz. Abnormal EHF hearing (> 30 dB HL) was found in 9 of the LiD group (18%) and 1 of the TD group (2%). Poorer DPOAE levels were found in the APD group between 4-10 kHz. A non-significant trend to higher acoustic reflex thresholds in the LiD group for tonal activators was found. The amplitude and latency of the CAP was not significantly different. Correlations between tests showed that EHF hearing thresholds were significantly related to parental report of listening difficulties on the ECLiPS questionnaire, and between EHF hearing and speech in noise (LiSN-S low cue, high cue, spatial advantage, and total advantage). There was no relationship between EHF thresholds and the SCAN scores.

Conclusion

Preliminary evidence indicates a relationship between EHF hearing sensitivity, listening difficulties and spatial speech in noise performance in children.

Supported by NIH R01DC014078.

PD 123

Age, Hearing and the Perceptual Learning of Time-Compressed Speech: A Glass Half Empty or a Glass Half Full?

Karen Banai; Limor Lavie; Maayan Manheim
University of Haifa

Background

Rapid speech rates pose disproportionate difficulties to older adults whether they have normal hearing or a hearing loss. This difficulty was attributed to difficulties in processing brief acoustic events or to age-related declines in processing speed. Another alternative is that age and/or hearing loss interfere with the rapid perceptual learning that takes place when listeners encounter rapid or otherwise distorted speech. This study was

designed to test the hypotheses that age and hearing loss are associated with impairments in the rapid perceptual learning of time-compressed speech, and that prolonged training with time-compressed speech might help overcome this impediment with compressed as well as with naturally-fast speech.

Methods

Normal hearing young adults (n = 55, ages 20-38), older adults with normal hearing (n = 52, ages 65-86) and older adults with mild to moderate sensory-neural hearing loss (n = 36, ages 65-81) participated in this study. Recognition of time-compressed and naturally-fast speech was assessed, and an index of rapid learning of time-compressed speech was calculated from the data. Subsequently, half the listeners in each group completed 45 minutes of training on the semantic verification of time-compressed sentences. Finally, all listeners were tested again on the recognition of time-compressed and naturally-fast speech.

Results

Age and hearing loss were associated with less accurate recognition of naturally-fast speech as well as with reduced rapid perceptual learning of time-compressed speech. This was true even when compression was adjusted to yield comparable performance across the three groups. Further practice resulted in robust learning in all three groups, but training-induced gains in the recognition of compressed speech were smaller in older, normal-hearing listeners than in young-adult listeners, especially when assessed with sentences not encountered during practice. Training-induced gains in the recognition of naturally-fast speech were also observed. These were unaffected by age, but limited to sentences that were encountered during practice. In contrast to its detrimental effect on rapid learning, hearing loss had little influence on training-induced learning and its generalization to naturally-fast speech.

Conclusions

Age and hearing loss both appear to impede the rapid perceptual learning that allows listeners to adapt to harder-to-understand speech over the time-frame of daily communicative situations. Although age is associated with reduced training-induced gains, hearing loss doesn't seem to reduce them any further. Moreover, the generalization of learning to naturally-fast speech was similar across groups.

PD 124

Neural Plasticity in the Presbycusis Hearing Aid User: Spectral Rebalancing.

Ludovic Bellier¹; Evelyne Veuillet²; Jean-François Vesson³; Virginie Durin⁴; Amélien Debes⁵; Anne Caclin⁶; Hung Thai-Van²

¹Lyon Neuroscience Research Center, currently in UC Berkeley; ²Lyon Neuroscience Research Center / Hospices Civils de Lyon; ³Hospices Civils de Lyon; ⁴Sonova; ⁵Phonak France / Sonova; ⁶Lyon Neuroscience Research Center / DYCOG team

The effect of hearing aid use on auditory pathways activity in the presbycusis patient is still poorly understood. Here, we followed the evolution of an electrophysiological marker of speech encoding, namely the Speech Auditory Brainstem Response (Speech ABR), across the first months of hearing aid use. Our hypothesis was that hearing aid use enables a rebalancing of spectral encoding in the auditory nervous system, as low frequencies have been shown to be overrepresented in presbycusis patient's auditory pathways, thus undermining speech understanding by masking high frequencies.

Speech ABRs were recorded through five sessions spread across the first four months of hearing aid use, in 11 presbycusis patients using hearing aids for their first time (mean age 70 ± 7 years, 3 females). To control for any training effect, the same protocol was run with six normal-hearing participants (mean age 64 ± 1 years, 4 females). At the beginning of the first recording session, each participant performed a phoneme identification task with /ba/-/da/ and /ba/-/ma/ continuums; the results were used to determine five syllables as stimuli for the electrophysiological recordings. Stimuli were delivered binaurally through hearing aids, using the initial hearing aid fitting in all five recording sessions for presbycusis patients, or neutral hearing aid fitting for normal-hearing controls. Thus, any evolution of neural activity observed in presbycusis patients but not in normal-hearing controls could only result from hearing-aid-induced neural plasticity. To study the evolution of spectral encoding, the spectrum of the Frequency-Following Response (FFR), a component of the Speech ABR which encodes spectral characteristics of speech sounds, was first computed; then, the amplitude of the spectral peak at the fundamental frequency (f_0) of the five syllables (namely 170 Hz) was measured.

Our analysis highlights a longitudinal decrease of f_0 encoding, only in presbycusis hearing aid users ($p = 0.044$). This result is in line with a decrease of the abnormal over-encoding of low frequencies in the presbycusis patient, and therefore with a rebalancing of spectral encoding.

Our longitudinal study allows for the first time to highlight an effect of hearing-aid-induced neural plasticity in a time period as short as four months. It is also the first time that consequences of hearing aid use on the central processing of speech sounds' spectral characteristics are described. The spectral rebalancing observed in this study could underlie the improved speech discrimination usually observed using vocal audiometry across the first months of hearing aid use.

PD 125

Coordinated Homeostatic Modifications Enable Cortical Compensation for Auditory Nerve Damage

Jennifer Resnik¹; Daniel B. Polley²

¹Massachusetts Eye and Ear Infirmary Harvard Medical School; ²Eaton-Peabody Laboratories, Massachusetts Eye and Ear Infirmary

Background

Cortical neurons remap their receptive fields and rescale sensitivity to spared peripheral inputs following sensory nerve damage. Cortical reorganization is thought to reflect homeostatic mechanisms that normalize spiking by rapidly reducing local inhibitory tone and scaling up sensitivity to weak excitatory inputs. In the auditory system, loss of cochlear hair cells and afferent nerve fibers can occur following exposure to intense noise, ototoxic drugs, or normal aging. Deafferented central auditory neurons become hyperexcitable, exhibiting elevated spontaneous firing rates and increased central gain. It is unclear how these distinct biomarkers of cortical reorganization are coordinated over the days and weeks following varying degrees of sensory nerve injury. Nor is it certain whether these plasticity processes precede or follow homeostatic regulation of intracortical inhibition.

Methods

We addressed these unanswered questions by recording from single units in awake, head-fixed adult mice before and after selective elimination of Type-I auditory nerve fibers while monitoring the strength of feedforward inhibition from fast-spiking parvalbumin-expressing GABAergic interneurons. By implanting an optetrode assembly into the primary auditory cortex of adult PV-Cre:Ai32 mice, we could isolate regular spiking putative pyramidal neurons and track the dynamic regulation of feedforward inhibition over a 50 day period surrounding profound or moderate cochlear afferent neuropathy induced by round window ouabain application or sound exposure, respectively.

Results

Following an immediate threshold elevation, sound-evoked cortical thresholds returned over days (moder-

ate afferent loss) or several weeks (profound afferent loss). Cortical inhibition was lost but then partially recovered as auditory responsiveness returned. Inhibitory dynamics scaled with the extent of denervation. Moreover, whereas brainstem-evoked potentials did not predict the status of cortical processing, homeostatic adjustments in local inhibitory tone during the first days following injury could predict the recovery of cortical sound processing months later.

Conclusions

These findings underscore the central importance of inhibitory dynamics in the recovery of function after sensory nerve damage. A sharp reduction in cortical inhibition may be necessary to enhance structural synaptic plasticity, modulate gain and allow the cortex to maintain rudimentary cortical sound processing. This approach would allow the cortex to adapt to the reduced auditory input and to normalize behavioral detection thresholds in the long term. However, of all the biomarkers of cortical plasticity, inhibitory tone was the only measure that never fully returned to baseline following moderate or profound cochlear denervation. Thus, recovery of sound sensitivity might introduce unstable circuit dynamics associated with tinnitus or hyperacusis.

PD 126

Quantifying the Impact of Early-Onset Hearing Loss on Stimulus-Directed Behavior: An Analysis of Corticotectal Projections in the Deaf Cat

Blake E. Butler¹; Julia K. Sunstrum²; Stephen G. Lomber¹

¹Department of Physiology and Pharmacology, University of Western Ontario; ²University of Western Ontario

The onset of hearing loss initiates structural and functional changes in the brain that can be measured anatomically and/or behaviorally. Much of the focus on anatomical changes has been placed on ascending thalamocortical projections, and on connectivity within the auditory cortex and between sensory cortices. However, it remains unknown what effect deafness has on descending projections from sensory cortices to the superior colliculi – the structure responsible for orienting toward environmental stimuli. We recently provided the first comprehensive quantitative description of sensory and motor corticotectal projections within a single species (Butler, Chabot, and Lomber 2016). In the current study we examine the effect of hearing loss by depositing the retrograde neuronal tracer BDA into the superior colliculus of cats ototoxically deafened shortly after birth, around the time of hearing onset. Coronal sections were taken at regular intervals and observed under a light microscope. Neurons showing a positive retrograde

labeling were counted. Labelled neurons were assigned to functional cortical areas according to published criteria. The proportion of labelled neurons in each area was determined in relation to the total number of labeled neurons in the brain. The relative proportions of labelled cells arising from each sensory cortical region are compared, with special attention to those associated with orienting behaviors. Moreover, comparisons between early-deaf animals and those with normal hearing are discussed in an effort to quantify the shift in corticotectal inputs that occurs following sensory loss.

PD 127

Differential Cross-modal Sensitivity of Visual Areas in the Hearing and Congenitally Deaf Brain

Rüdiger Land¹; Jan-Ole Radecke¹; Andrej Kral²

¹Hannover Medical School; ²Hannover Medical School, DFG Cluster of Excellence Hearing4all

Congenital deafness can lead to cross-modal plasticity in the deprived auditory cortical regions during brain development. The absence of auditory input in congenital deafness may induce additional changes in non-auditory areas. Specifically, the presence of modulatory auditory input to visual areas, which might be present in the hearing brain, may be altered by congenital deafness.

Here we studied visual areas and adjacent auditory areas in the cortex of congenitally deaf and hearing cats. We recorded cortical neuronal activity with multi-electrode arrays in response to visual and cochlear implant stimulation in the dorsal auditory cortex, and in the visual areas of the lateral suprasylvian cortex.

We found slight differences in responses to cochlear implant stimulation in visual areas between hearing and congenitally deaf cats. Whereas hearing cats showed sparse responses in the visual cortex to cochlear implant stimulation, these responses were reduced in congenitally deaf cats. In contrast, no notable differences were found for visual stimulation in the visual areas in both groups. Whereas in a previous study we showed modest cross-modal plasticity in the dorsal auditory cortex in congenitally deaf cats, the present results shows an additional differential effect in responsiveness in the adjacent visual areas in congenital deafness.

In conclusion, the results demonstrate the influence of the presence of functional sensory input in connection with the plasticity of the cortex during normal development. However, in combination with previous results this also indicates a surprising general functional conservation between sensory areas in the congenitally deaf brain, given the sparse changes even in the presence of lifelong deafness with respect to general responsiveness.

Aging: Animals Models and Mechanisms of Aging

PS 686

oboe – A New Model of Age-Related Hearing Loss Identifies a Role for Wars2 in Normal Auditory Function

Michael R. Bowl¹; Carlos Aguilar¹; Thomas Agnew¹; Anna Morgan²; Michelle M. Simon¹; Sara Wells³; Paolo Gasparini⁴; Roger Cox¹; Steve D.M. Brown¹

¹MRC Harwell Institute, Mammalian Genetics Unit, Harwell Oxford, OX11 0RD, UK; ²University of Trieste, Trieste, Italy; ³MRC Harwell Institute, Mary Lyon Centre, Harwell Oxford, OX11 0RD, UK; ⁴University of Trieste, Trieste, Italy; Sidra medical research, Doha, Qatar

Background

Age-related hearing loss (ARHL), also called presbycusis, is the most common sensory deficit experienced by the elderly. It is a complex disorder that is not fully understood, although onset and progression of the condition are known to be influenced by environmental factors and genetic susceptibility. Currently our knowledge of the genes underlying ARHL is very limited, as such we have utilized age-challenged mutagenized mice to help elaborate upon the genetics of ARHL.

Methods

At the MRC Harwell Institute we have undertaken a large-scale N-ethyl-N-nitrosourea (ENU) mutagenesis screen to generate mouse models of age-related disease. G3 pedigrees, of ~100 mice, were bred and entered a phenotyping pipeline comprising recurrent assessment across a wide range of disease areas. Auditory screening consisted of recurrent Clickbox and Auditory-Evoked Brainstem Response phenotyping.

Results

To date our phenotype-driven screen has identified 26 hearing loss models of which 8 displayed progressive late-onset phenotypes. Investigation of one late-onset hearing loss model, employing genome mapping, whole genome sequencing, and a complementation test, identified a c.349G>T mutation in the nuclear gene Wars2, which encodes the mitochondrial-localized Tryptophanyl-tRNA synthetase (mt-TrpRS) protein. This line was named oboe. In addition to causing a missense substitution (p.V117L), RT-PCR of cochlear RNA demonstrated the Wars2oboe allele also causes skipping of exon 3. At 1-month of age Wars2oboe/oboe mice have hearing thresholds similar to wild-type and heterozygous mice. By 3-months of age Wars2oboe/oboe mice have elevated low frequency thresholds. By 6-months of age Wars2oboe/oboe mice exhibit ~60 dB SPL thresholds at all frequencies tested (8, 16 and 32 kHz), and by 12-months

of age their thresholds have further increased to ~80 dB SPL. Ultrastructural studies of the sensory epithelium found that Wars2oboe/oboe mice have a normal complement of outer hair cell bundles at 1-month of age, but these are gradually lost by 12-months of age with an apical-to-basal increase in severity. In contrast, assessment of histological sections found loss of apical spiral ganglion neurons, but not basal, in aged Wars2oboe/oboe mice.

Conclusion

Our findings establish that mt-TrpRS, which is essential for mitochondrial protein synthesis and viability, is required for normal auditory function in aging mice. Investigation of oboe, and the other 7 late-onset hearing loss models, will increase our understanding of the genetics and pathobiology of ARHL.

PS 687

Loss of Lysosomal Mucolipins 3 and 1 in Hair Cells Causes Early Onset Age-Related Hearing Loss Due to Outer Hair Cell Death

Teerawat Wiwatpanit; Natalie Remis; Aisha Ahmad; Yingjie Zhou; Mary Ann Cheatham; Jaime Garcia-Anoveros

Northwestern University

Background

Mucolipins are lysosomal calcium channels that regulate endolysosomal trafficking. While mucolipin 1 is expressed in all cells, we discovered that mucolipin 3 was expressed in a small subset of cochlear cells (i.e. hair cells and marginal cells of stria vascularis) and very few other cell types. This selective co-expression of mucolipins suggests that they contribute to hair cells' unique characteristics, one of which is longevity. Cochlear hair cells are remarkably resilient as they can withstand constant high-energy demands and mechanical stimulations, and yet they survive for decades and up to a century in humans. However, hair cells do degenerate, causing age-related hearing loss, which is the most prevalent neurodegenerative condition. Given that lysosomes have protective roles in many neurodegenerative diseases, we hypothesize that hair cells utilize specialized lysosomes for their long-term survival.

Methods

We accessed auditory functions using DPOAEs and ABRs from mice lacking mucolipin 3 (Trpml3^{-/-}), mucolipin 1 (Trpml1^{-/-}), and both in all cells (Trpml3^{-/-}; Trpml1^{-/-}), along with mice conditionally lacking mucolipins in hair cells only (Gfi1Cre^{+/+}; Trpml3^{Flox/Flox}; Trpml1^{-/-}), at ~1 and ~3 months of age. We examined cochlear anatomy and constructed cytochleograms to determine the extent of hair cell loss. We also examined lyso-

somes and other organelles in hair cells using immunohistochemistry and electronmicroscopy.

Results

Mice lacking both mucolipins 3 and 1 in all cells, but not either one alone, experienced high-frequency (27kHz) hearing loss as early as at 1 month of age. The severity of hearing loss progressed towards lower frequency (12kHz) and increased with age. Hearing loss especially at high frequencies was accompanied by outer hair cell (OHC) loss in the base of cochlea. Mice conditionally lacking mucolipins in hair cells exhibited the same phenotypes suggesting that hearing loss and OHC death are due to mucolipin co-absence in hair cells. Furthermore, we observed that OHCs lacking mucolipins contained aberrant lysosomal aggregates at the apical third of the cell, while other organelles (peroxisomes, autophagosomes and mitochondria) appeared normal. Ultrastructure observations revealed the presence of vesicle aggregates and multivesicular bodies at the apex of OHCs lacking mucolipins.

Conclusions

Mucolipin 3 and 1 co-absence caused an early onset of hearing loss from high to low frequencies due to OHC death. Conditional ablation of mucolipins in hair cells indicates that these cells, especially OHCs, require these channels for their remarkable resilience and longevity. The pathological lysosomal augmentation further confirms that hair cells require specialized mucolipins 3 and 1-endowed lysosomes for their longevity.

PS 688

Aging of Mammalian Cochlear Hair Cells

Jing-Yi Jeng; Matthew Holley; Walter Marcotti
University of Sheffield

Background

Mammalian auditory hair cells are crucial for detecting sound stimuli and transducing them into electrical signals. They degenerate irreversibly with age, which is one of the main problems associated with age-related hearing loss (ARHL). Despite ARHL affecting millions of people worldwide, the underlying mechanisms are still largely unknown. We propose that a functional analysis of the changes in hair cell physiology and whole cochlear function with age will provide a better understanding of the progression of ARHL.

Methods

We performed whole cell patch clamp recordings from inner hair cells (IHCs) and outer hair cells (OHCs) in acutely dissected organs of Corti from ARHL mouse models. To represent early and late onset ARHL we are studying the mouse strains C57BL/6N and C57BL/6N

Cdh23-repaired, respectively. Depolarizing and hyperpolarizing voltage steps were applied to elicit potassium and calcium currents; and resting membrane potentials were recorded in current clamp. We recorded from male and female mice to investigate potential differences in ageing between genders. Comparisons between the strains should reveal age-related differences that may or may not be linked to the Cdh-23 repair.

Results and Conclusions

We have defined an electrophysiological baseline for IHCs and OHCs in healthy adult male and female mice of both strains at up to 1 month of age. We recorded no obvious deficits in the hair cells and there were no significant differences either between strains or between males and females. We are now recording from hair cells at 3 months and 6 months, ages at which increased hearing thresholds have been observed in C57BL/6N mice but not in the Cdh-23 repaired mice (Li & Borg, 1991, *Acta Oto-Laryngologica* 111(5): 827–834; Mianné et al., 2016, *Genome Medicine* 8:16). Thus we will present data on the possible correlation between changes in the electrophysiological properties of hair cells and increased hearing thresholds.

Supported by The University of Sheffield & The Wellcome Trust

PS 689

Mitochondrial Protein Fus1 Protects from Premature Hearing Loss via Regulation of Oxidative Stress, Autophagy, Nutrient and Energy Sensing Pathways in the Inner Ear

Alla Ivanova¹; Winston Tan¹; Lei Song²; Dhasakumar Navaratnam³; Joseph Santos-Sacchi⁴

¹*Yale School of Medicine, Department of Surgery*; ²*Ear Institute, Shanghai No. 9 Hospital, Shanghai Jiao Tong University Medical School*; ³*Yale School of medicine, Department of Neurology and of Neuroscience*; ⁴*Yale Medical School, Surgery, Cellular and Molecular Physiology, and Neuroscience*

Aims. Acquired hearing loss is a worldwide epidemic that affects all ages. It is multifactorial in etiology with poorly characterized molecular mechanisms. Mitochondria are critical components in hearing. Here, we aimed to identify the mechanisms of mitochondria-dependent hearing loss using Fus1 KO mice, our novel model of mitochondrial dysfunction/oxidative stress. Results. Using Auditory Brainstem Responses (ABRs) we characterized the Fus1 KO mouse as a novel, clinically relevant model of Age-Related Hearing Loss (ARHL) of metabolic etiology. We showed that early decline of the Endocochlear Potential (EP) is the major cause of ARHL and

that it occurs due to severe mitochondrial and vascular pathologies in the cochlear stria vascularis. We showed that pathological alterations in antioxidant (AO), autophagy, and nutrient and energy sensing pathways (mTOR and PTEN/AKT) occur in cochleae of young *Fus1* KO mice prior to major hearing loss. Importantly, short-term AO treatment corrected pathological molecular changes, while longer AO treatment restored EP, improved ABR parameters and delayed the development of hearing loss in the aging mouse. Innovation. Currently, no molecular mechanisms linked to metabolic ARHL have been identified. We established pathological and molecular mechanisms that link the disease to mitochondrial dysfunction and oxidative stress. Conclusion. Since chronic mitochondrial dysfunction is common in many patients, it could lead to developing hearing loss that can be alleviated/rescued by AO treatment. Our study creates a framework for future clinical trials and introduces the *Fus1* KO model as powerful platform for developing novel therapeutic strategies to prevent/delay hearing loss associated with mitochondrial dysfunction.

PS 690

RNA-Sequencing Identifies Temporal Gene Expression Changes in the Aging Mouse Cochlea

Anne Giersch¹; Jun Shen²; Nahid Robertson³; Cynthia Morton⁴

¹*Brigham and Women's Hospital, Harvard Medical School, Harvard Medical School Center for Hereditary Deafness;* ²*Brigham and Women's Hospital, Laboratory for Molecular Medicine, Harvard Medical School Center for Hereditary Deafness,;* ³*Brigham and Women's Hospital;* ⁴*Brigham and Women's Hospital, Harvard Medical School, Harvard Medical School Center for Hereditary Deafness, Broad Institute of MIT and Harvard, University of Manchester*

Background

Age-related hearing loss is the most common sensory disorder in the aging population. Despite the discovery of many deafness genes, the pathophysiology of progressive hearing impairment due to the normal aging process remains poorly understood. We hypothesize that gene expression profiling of the mouse cochlea with advancing age will reveal some of the molecular mechanisms of age-related hearing loss and inform potential target selection for prevention and treatment.

Methods

We performed gene expression profiling of mouse cochlea by next-generation sequencing of messenger RNA (RNA-Seq), using cochlear tissues from mouse strains with good hearing past one year of age (CBA/CaJ and B6.CAST-Cdh23Ahl+) and strains with known

age-related hearing loss (C57BL/6J and Coch gene mutants on a CBA/CaJ background). Cochlear tissues were collected from whole litters (6-10 animals, males and females) at 1 week, 3 weeks, 12 weeks, 32 weeks, 52 weeks, 62 weeks and 82 weeks for total RNA extractions. PolyA-selected mRNAs were fragmented and reverse-transcribed, and the derived cDNA samples were, indexed, pooled, and sequenced on the Illumina HiSeq platform. Biological replicates were obtained for all time-points. We evaluated expression levels of all transcripts, and performed differential gene expression analyses.

Results

We have obtained gene expression profiles of mammalian cochlea at various ages by RNA-Seq. With at least 30 million total reads per sample, more than 16,000 genes were detected in each sample, and expression levels were highly reproducible. We observe significant systematic differences in gene transcriptomes between C57BL/6J and CBA/CaJ strain backgrounds, regardless of age. Hundreds of genes also show significant temporal changes in the aging mouse cochlea. Gene interaction analyses reveal several pathways with significant changes in gene expression levels prior to the onset of measurable hearing impairment.

Conclusions

We have surveyed gene expression in mammalian cochlea by RNA-Seq, in different mouse strains and at various ages, throughout the life-span. Systematic transcriptome differences were present in mouse strains with different hearing loss profiles. Analyses of temporal gene expression profiles in the aging cochlea identify potential candidate gene and pathway targets for prevention or treatment of age-related hearing loss.

PS 691

Changes of Mitochondrial Function in Age Related Hearing Loss Animal Model

Yong-Ho Park¹; Ah-Ra Lyu²

¹*Department of Otolaryngology, Chungnam National University;* ²*Department of Medical Science, Chungnam National University*

The aim of this study was to investigate the morphological and functional changes of mitochondria in the cochlea of age related hearing loss mice. C57BL/6J male mice were divided into young age group (2 months old) and old age group (20 months old). Auditory brainstem response (ABR) threshold and cochlear blood flow (CBF) were measured from both group and morphologic study including immunohistochemistry and transmission electron microscope (TEM) were conducted to compare

the differences of mitochondria in the cochlea of young mice and ARHL mice. To compare the function of mitochondria in both groups, quantitative real time polymerase chain reactions (qRT-PCR) for the mitochondrial OxPhos complexes, markers of oxidative stress and mitochondrial unfolded protein response (UPRmt) and endoplasmic reticulum (UPRER) were conducted. Significantly increased ABR thresholds and decreased CBF were observed in the old age group compared to the 2 months old group ($p < 0.05$). Almost all the auditory hair cells (HCs) in the basal turn of the cochlea were destroyed in the old age group. Nerve fibers in the zona pectinata were markedly decreased throughout the entire cochlea of the old age group compared to the young age group. Wide ranges of mitochondrial damage were observed in the HCs and in the middle layer of the stria vascularis (SV) of old age mice compared to those of young age mice. The expression of OxPhos complex I was significantly decreased and the oxidative stress markers were significantly increased in the old age group compared to the young age group. Some of the markers of UPRmt and UPRER were increased in the old age group compared to the young age group. This study demonstrated that defects of OxPhos complex I and increased oxidative stress may be associated with ARHL in old age mice. The various changes of UPRmt and UPRER were engaged in ARHL in old age mice without dominance.

This work was supported by the Basic Science Research Program through the National Research Foundation of Korea (NRF), funded by the Ministry of Education (NRF-2015R1D1A3A01018881 for Yong-Ho Park)

PS 692

Cholesterol Homeostasis Is Required to Maintain Cochlear Microvascular Integrity and Auditory Function

Fred A. Pereira¹; Michelle L. Seymour²; Sarah Pfannenschmidt²; Hsin-I Jen³; Allyson Munneke²; Teggy Vadakkan⁴; Andy Groves³

¹Department of Molecular & Cellular Biology, Huffington Center on Aging, Department Otolaryngology–HNS, Baylor College of Medicine; ²Department of Molecular & Cellular Biology, Huffington Center on Aging, Baylor College of Medicine; ³Baylor College of Medicine; ⁴Department of Molecular Physiology & Biophysics, Baylor College of Medicine

Diseases of cholesterol metabolism affect hearing function; however, fundamental information about the temporal nature of the relationship between systemic cholesterol homeostasis and auditory function, the involvement of cochlear cholesterol homeostasis, and the underlying pathophysiology is lacking. We have used

the LDLR null mouse model of hypercholesterolemia to discover that systemic hypercholesterolemia results in ABR threshold elevations, increased focal permeability in the cochlear blood-labyrinth barrier (cBLB), and altered stria vascularis organization that appear as early as one month of age. ABR threshold elevations progressively worsen by four months of age when the cBLB barrier integrity is lost and cholesterol accumulates within cochlear tissues. Re-expression of LDLR in the LDLR null mouse normalizes systemic cholesterol levels, but does not fully restore hearing function or cBLB integrity by two months after treatment, although there is evidence of vascular remodeling in the stria vascularis. These findings suggest that hearing loss in LDLR null mice is due to dysfunction of the stria vascularis with cholesterol accumulation in cochlear tissues occurring secondary to loss of cBLB integrity.

This work was funded by DC00354 and DC009622 (FAP), NIH/NIA 5T32 Training Grant AG00183 (MLS) and NIDCD/NIH NRSA F31DC012503 (MLS).

PS 693

Sestrin-2 Deficiency Potentiates Early Onset of Age-related Sensory Cell Degeneration in the Cochlea

Celia Zhang¹; Wei Sun¹; Ji Li²; Binbin Xiong¹; Mitchell D. Frye¹; Bo Hua Hu³

¹University at Buffalo, The State University of New York; ²University of Mississippi Medical Center; ³Center for Hearing and Deafness, University at Buffalo

Introduction

Age-related hearing loss (ARHL) is the most common cause of hearing dysfunction in the elderly. The main pathological basis of ARHL is sensory cell degeneration. While sensory cell pathogenesis has been linked to oxidative stress in the cochlea, the biological mechanisms that lead to the oxidative stress is not clear. Sestrin-2 is a stress inducible protein that has been shown to protect tissues from oxidative stress by suppressing the production of reactive oxygen species (ROS). ROS activities can interact with other pathological activities, such as inflammatory responses, to potentiate the age-related pathologies. This study investigated the role of sestrin-2 in age-related cochlear degeneration.

Methods

Sestrin-2 knockout and age-matched C57BL/6J mice were examined at 4–6 weeks, 3 months and 5 months for auditory brainstem responses and hair cell quantification. Sensory epithelial distribution of sestrin-2 and basilar membrane macrophages were examined using immunolabeling and age-related changes in sestrin-2

expression were measured using qRT-PCR and Western blotting. To determine whether sestrin-2 deficiency provokes inflammatory activity in the sensory epithelium, we examined the transcription expression of five proinflammatory genes, i.e., tumor necrosis factor (Tnf), chemokine ligands 2, 3 and 4 (Ccl2, Ccl3, Ccl4), interleukin 1 beta (Il1b).

Results

Strong expression of sestrin-2 was observed in the sensory epithelium, particularly in outer hair cells, of the mouse cochlea. The expression is reduced at both the transcriptional and protein levels with aging. Sestrin-2 knockout leads to an early onset of hearing loss starting from high frequencies and accelerated age-related sensory cell degeneration beginning from the basal end of the cochlea. This cochlear degeneration is accompanied by the increased expression of proinflammatory genes and the activation of basilar membrane macrophages, suggesting that loss of sestrin-2 function enhances proinflammatory activities.

Conclusions

Sestrin-2 plays a protective role in sensory cell homeostasis. Sestrin-2 expression decreased with aging and knockout of sestrin-2 gene exacerbates ARHL in C57BL/6J mice. The effect of sestrin-2 on protecting ARHL is likely to be mediated by the suppression of cochlear inflammatory activities.

PS 694

Deafness Model Phenotypes with Impaired Cellular Calcium Sequestration Implies Pathways Contributing Progressive Deafness

Osamu Minowa¹; Hideaki Toki¹; Hiroshi Suzuki²; Kazusaku Kamiya³; Kazuhisa Ikeda⁴; Tetsuo Noda¹
¹RIKEN Bioresource Center; ²Department of Biochemistry, Asahikawa Medical University; ³Juntendo University; ⁴Juntendo University

Background

Murine deafness models will greatly facilitate our understanding of the mechanisms underlying hearing impairments including age-related such disorders [1]. We have used an ENU-mutagenesis platform to identify mice with hearing impairments, aiming to develop novel mouse models of human progressive deafness.

Methods

We screened mice by observing the startle responses evoked by a click box and then measuring the auditory brainstem responses (ABR) [2-3]. The isolated mutants showed a phenotype that was not accompanied by other traits, which is a characteristic typical of human diagnos-

tic-type nonsyndromic deafness. To prove a possible defect in hair cell calcium-ion mobilization, we performed Ca-decay measurement on cells expressing the mutant product.

Results

The mutations in four of the lines were mapped to the distal region of chromosome 6. Direct sequencing showed that these lines harbored missense mutations in different domains of pmca2 [4]. We observed clear phenotypic variations in the four lines harboring mutations in pm, including differential increases in the ABR threshold at the early stage of deafness, followed by the eventual loss of hair cells and spiral ganglion cells at different time points.

Conclusion

This phenotypic variation seems to result from the enzymatic activity differences of the mutated gene products. The pathway through which these phenotypes evolve is thought to branch into two parts: one to functionally impair hair cells and the other to threaten their survival. To clarify these pathways may help to understand the pathogenesis of human age-related hearing disorders.

[1] Brown SD, Hardisty-Hughes RE, Mburu P. *Nat Rev Genet*, 9, 4, 277-90, 2008.

[2] Bull KR et al., *PLoS Genet*.9, 1, Epub 2013 Jan 31.[3]

[3] Gondo Y, *Nat. Rev. Genet.*, 10, 803 – 810, 2008.

[4] Spiden SL, Bortolozzi M, Leva FD, Angelis MH, Fuchs H, Lim D, Ortolano S, Ingham NJ, Brini M, Carafoli E, Mammano F, Steel KP. *PLOS Genetics*, 4,10, e1000238, 2008

PS 695

Aging May Differentially Impact Neuronal Nicotinic Acetylcholine Receptors in the Inferior Colliculus and Auditory Cortex

Brandon C. Cox¹; Lynne Ling²; Donald M. Caspary³

¹Department of Pharmacology & Department of Surgery Southern Illinois University School of Medicine;

²Department of Pharmacology, Southern Illinois University School of Medicine; ³Department of Pharmacology and Surgery, Southern Illinois University School of Medicine, Springfield, IL

Background

Acetylcholine (ACh) plays a critical role in attention and in assigning salience to environmentally important stimuli. Aging negatively impacts top-down and bottom-up processing of acoustic information. Neuronal nicotinic acetylcholine receptor (nAChR) density and subunit composition determines the efficacy and affinity of ACh

released from brainstem pedunculo-pontine tegmental nuclei (PPTg) and basal forebrain cholinergic projections to inferior colliculus (IC) and auditory cortex (AC) respectively. nAChRs are present within IC and AC but receptor density, subunit composition, and the impact of aging have not been examined.

Methods

Experiments were completed using Fischer Brown Norway (FBN) male rats supplied by the NIA rodent resource colony. Procedures were performed in accordance with protocols approved by the Laboratory Animal Care and Use Committee of Southern Illinois University School of Medicine.

Pooled homogenates from IC and AC were obtained from young adult (4-8 mos) and aged (28-35 mos) rats. nAChR saturation binding studies were performed using [³H]epibatidine to determine the number (BMAX) and affinity (Kd) of heteromeric nAChRs composed of alpha (α) and beta (β) subunits in IC and AC. Competition binding curves, as described in Turner and Kellar (2005) used pooled homogenates from IC and AC. Iodo-A85380 was used to compete for [³H]epibatidine-labeled binding sites to distinguish between β2- and β4-containing nAChRs.

Results

Saturation analysis revealed higher levels of nAChRs in AC than in IC (BMAX fmol/mg protein =105 AC; 51 IC). In AC, there was an age-related decrease in nAChR density (BMAX), but no significant change in BMAX was detected in IC. Competition binding studies in young AC and IC showed one-site high affinity binding, suggesting that most nAChRs in these structures contain the β2 subunit. Competition binding studies in aged IC showed two-site binding suggesting a significant decrease in the number of β2-containing nAChRs, with a significant age-related increase in β4-containing nAChRs. In contrast, aged AC showed one-site binding, suggesting no change in nAChR subunit composition.

Discussion

The present saturation analysis in AC supports earlier [³H]epibatidine binding studies which showed high levels of heteromeric nAChRs in whole cortex, which were negatively impacted by aging. We found that nAChRs in IC show age-related changes in competition binding, which suggests subunit changes, not seen for AC. Collectively, the loss of nAChR density in AC and the change in nAChR subunit composition in IC could underpin a loss of normal functioning, resulting in decreased ability to attend to important communication signals.

Funding

Supported by NIDCD.

PS 696

Enhanced p-Tau Expression and Neural Degeneration in the Hippocampus of Mice Showing Cognitive Dysfunction After Noise-induced Hearing Loss

Shi-Nae Park¹; Min-Jung Kim²

¹Department of Otolaryngology-Head&Neck Surgery, college of Medicine, Catholic Univ. of Korea; ²Department of Otolaryngology-Head&Neck Surgery, college of Medicine, Catholic Univ. of Korea

Objectives

Previous clinical studies demonstrated that hearing impairment is a potential risk factor, and even mild or moderate hearing loss as well as severe loss is associated with cognitive decline or dementia. This study was performed to investigate the effect of hearing loss on cognitive function during a long-term follow-up period and to evaluate neural degeneration and phosphorylated-Tau (p-Tau) expression in the hippocampus, the memory center, of mouse brain to show more direct evidence of the relationship between hearing and cognition.

Methods

P1mo male C57BL/6 mice were used. Mice of the noise-induced hearing loss (NIHL) group were exposed to 110 dB SPL white noise for 60 min everyday for 20 days. ABR thresholds were serially measured up to 18mo. The cognitive function of the mice was measured by a radial arm maze (RAM) and novel object recognition (NOR) task. P-Tau expression in the hippocampus of the mouse brain was investigated by western blot assay, immunohistochemical staining, immune-transmission electron microscope (TEM) study. Lipofuscin expression in the hippocampus was also evaluated by TEM.

Results

During the 18mo follow-up period, hearing levels of the mice with noise-induced hearing loss remained, while those of the control mice slowly increased and the gap between two groups became closer from post-noise 12month. Most of the RAM performances improved gradually within each group across five trials, probably due to learning effect, but NIHL group showed lower performance scored than the control group at several different time points of the study period. NOR task also revealed the decreased function of cognition in NIHL group (p < 0.05). Enhanced p-Tau expression measured by western blot assay and immunohistochemical staining was observed in the hippocampus of the mice with NIHL compared to those of the control mice (p < 0.05). Intracellular lipofuscin was overexpressed in the hippocampus in mice with NIHL.

Conclusion

Moderate hearing loss induced by noise in mice resulted in cognitive impairment and enhanced expression of p-Tau as well as neural degeneration in the hippocampus of the mice, which provide the more direct causal relationship between hearing loss and cognitive dysfunction.

PS 697

Aging in the Auditory System of the Sprague Dawley Rat : A Study from the VIIIth Nerve to the Auditory Cortex

Boris Gourévitch¹; Florian Occelli¹; Florian Hasselmann²; Jérôme Bourien²; Jean-Luc Puel³; Nathalie Samson¹; Bernadette Wiszniowski¹; Jean-Marc Edeline¹

¹UMR9197, CNRS, Univ. Paris-Sud; ²UMR 1051, INSERM, University of Montpellier; ³Institute for Neurosciences of Montpellier-Inserm U1051; University of Montpellier, France

In human, age-related hearing loss, called presbycusis, is one of the most prevalent and important pathology which deteriorates the quality of life and is associated with depression, anxiety and social isolation. In human and mammals in general, the deficits classically described are threshold elevation, degraded spectral and temporal resolution as well as impaired processing of sounds drowned in noise. In human, those results stem from psychoacoustic studies. In animals, most of the studies described the aging effects on the cochlea, the 8th nerve and the lower stages of the auditory system. Relatively few studies have described the effects of aging in the upper stages of the auditory system, particularly at the cortical level.

Here, we describe the impact of aging on responses obtained from the 8th nerve (CAP), brainstem (ABR) and primary auditory cortex (A1) on groups of female Sprague Dawley rats aged of 6, 9, 15 and 21 months (5-9 animals/group). At the cortical level (300-400 recordings/group), we tested parameters derived from spectro-temporal receptive fields (STRF), temporal modulation transfer function (TMTF), and responses to vocalization presented in quiet, in noise, and with small gaps at the middle of the vocalizations.

We found moderate signs of aging in the auditory system. Both at the brainstem (ABR) and cortical level, auditory thresholds were increased by less than 30dB for the 21month rats, with CAP thresholds and amplitudes which were little or not affected. At the cortical level, the response latency, duration and bandwidth were affected when analyzing STRF and the spike-timing of

responses to communications sounds was reduced at 21months only. A deficit in gap detection was found for high frequency neurons (but a facilitation was found for low frequency neurons); there was no obvious deficit when analyzing TMTF. There were small, but significant, changes in the number of GABAergic neurons across cortical layers. At the behavioral level, the detection of the depth in amplitude modulation was impaired at 21months only.

Overall, signs of aging were moderate especially at the cortical level and a multiparameter analysis could neither separate aged neurons from younger ones nor emphasize a specific aging pattern. Our results suggest that, in contrast with other strains such as the Fisher 344, the auditory system of Sprague Dawley rat ages relatively well.

PS 698

Linear Combination of Auditory Steady-state Responses Evoked by Co-modulated Tones

François Guérit¹; Jeremy Marozeau²; Bastian Epp²
¹MRC Cognition and Brain Sciences Unit; ²Hearing Systems, Technical University of Denmark

The auditory steady-state response (ASSR) is an auditory evoked potential obtained by presenting a carrier modulated at a given modulation frequency while recording the neural response with scalp electrodes. At low- and medium intensities, the neural response to a multi-tone carrier modulated with a different modulation frequency for each carrier component is similar to the sum of the responses to each component presented individually. At high intensities, the ASSR deviates from such a linear superposition, supposedly because of phase interactions of the stimulus components in different regions of the basilar membrane. Here, this hypothesis was investigated by studying responses to a medium intensity stimulus composed of two tones modulated with the same modulation frequency, and where the phase difference between modulators was varied. Nine normal-hearing (NH) listeners were presented with: (1) a sinusoidally amplitude modulated tone with a carrier frequency of 1 kHz, (2) a sinusoidally amplitude modulated tone with a carrier frequency of 4 kHz, and (3) a dual-frequency carrier of 1 and 4 kHz. The modulation frequency was 88 Hz for all conditions. For the dual-frequency carrier stimulus, the same modulation frequency was used (co-modulated), and the relative modulator phase was set to five values uniformly distributed around the unit circle. The neural response was recorded using scalp electrodes (Biosemi ActiveTwo with active electrodes). The results showed that the ASSRs evoked with either a 1 or a 4 kHz carrier differed in phase by a mean delay

of 3.3 ms, consistent with basilar membrane dispersion. With the dual-frequency carrier, the relative modulator phase had a significant effect on both phase and magnitude of the evoked ASSRs. The resulting phase was well predicated by a linear superposition of the ASSRs for the two tones measured in isolation. The measured amplitudes ranged from values that approximated the sum of the amplitudes of the isolated tones, to values too low to give a significant response, even after 10 minutes of recording. This study suggests that the ASSR at 88 Hz with co-modulated carriers is a linear sum of the responses to each modulated carrier in isolation. This finding contributes to the understanding of the deviations from linearity in multi-frequency ASSR applications at high intensities. This study was funded by the Oticon Centre of Excellence for Hearing and Speech Sciences.

Auditory Cortex: Human Studies II

PS 699

The Impact of Visual Gaze Direction on Human Auditory Scene Analysis

Ulrich Pomper¹; Maria Chait²

¹*UCL Ear Institute*; ²*Ear Institute, University College London, UK*

In everyday life, we constantly change the direction of our visual gaze, depending on our current tasks and goals. Animal research has suggested that neural responses in auditory cortex are increased to sounds coming from the direction of gaze, as compared to another direction. How this direction of gaze influences auditory processing in humans is not understood. Here, we recorded Electroencephalography (EEG), eyetracking and behavioural data to investigate how gaze direction impacts the processing of either attended or unattended sounds from different locations. We presented rapid (~4 Hz; random inter-tone-interval) streams of pure tones from three speakers (left, central, right). Participants (N=19) gazed at one of the speakers, and responded to occasional targets from either the same or a different speaker. We found significantly faster response times when gaze and attention were directed towards the same location, as compared to when they were directed to different locations. In addition, both spatial attention and gaze modulated EEG activity in the alpha-band (8-14 Hz). In conditions where gaze and attention were not spatially aligned, alpha-band activity was significantly increased contralateral to the direction of gaze, indexing a suppression of distracting sensory input. Interestingly, auditory spatial attention but not gaze direction modified event-related potentials to individual sounds. In summary, our data suggest that gazing towards the source of a sound facilitates processing of that sound. When spatial

attention and gaze are not spatially aligned, alpha-band activity acts to suppress task irrelevant input, resulting in similar event-related neural responses to gazed-at and non gazed-at sounds.

PS 700

Sensitivity to Non-Deterministic Pattern Change in Rapid, Stochastic Tone Sequences

Sijia Zhao¹; Yinuo Zhou¹; Fred Dick²; Maria Chait¹

¹*Ear Institute, University College London, UK*; ²*Birkbeck-UCL Centre for NeuroImaging, Birkbeck, University of London, UK*

Much of the mismatch negativity literature has focused on measuring listeners' sensitivity to deterministic (precisely repeating) auditory patterns. In this series of experiments, we aimed to understand what information the auditory brain extracts from non-deterministic (random frequency) tone-pip patterns and how this depends on attention. The basic signal was a rapid sequence of abutting 50 ms tone pips with frequencies randomly sampled from a pool of 20 values. Some trials contained a change in this fluctuation pattern partway through the signal. This change was manifest as a reduction in the size of the pool from which frequencies are drawn, such that detection of the change must be based on sensitivity to the statistics of the fluctuating pattern. Across a number of different conditions, the distribution and number of the retained frequencies was systematically manipulated.

We recorded EEG brain responses from naïve human participants exposed to these signals while watching a silent subtitled documentary. There were significant changes in EEG activity associated with changes in sequence patterning, even when listeners were not actively attending to the unfolding sound. The latencies at which brain activity changes were first observed was taken as an estimate of the computation time required to detect the change in statistics. Transitions characterised by increased signal predictability were associated with increased sustained response amplitude. This is consistent with previous findings in our lab suggesting that the brain tracks the statistics of unfolding auditory signals and rapidly increases responses to more reliable (predictable) inputs as a means of focusing resources on stable aspects of the environment.

PS 701

The Effect of Spectro-Temporal Coherence and Selective Attention on Auditory Sensory Memory

Darrin Reed¹; Brigitta Tóth²; Barbara Shinn-Cunningham¹

¹*Boston University*; ²*Hungarian Academy of Sciences*

Background

Identifying the neural mechanisms related to sensory memory representations of auditory objects can reveal how the auditory system tracks changes attributed to a sound source in an auditory scene. Investigations into how selective attention influences these mechanisms can inform us about which types of auditory objects are processed automatically. The current study presented stimuli composed of a repeating inharmonic tone complex (figure) that is perceptually segregated from simultaneous randomly varying tones (background). This figure-background stimulus enabled us to investigate (1) whether or not the auditory system is equally sensitive to changes attributed to the figure versus to the background and (2) whether selective attention to whichever object, i.e. the figure or the background, is task-relevant facilitates the neuronal registration of changes attributed to that object.

Methods

We compared figure-background and background-only stimuli, like those in Tóth et al. (2016). Listeners were asked to detect a “change.” Specifically, six of ten total tonal components making up either the figure (in figure-background stimuli) or part of the background (in background-only stimuli) were reduced in intensity, while the remaining four tonal components increased in intensity to preserve overall energy. In total, four stimulus configurations were possible: figure change, background change, figure control, and background control. For a given block, the task of the subjects was to detect either a figure change or a background change. Both behavioral performance and an electroencephalogram were measured simultaneously for twelve normal-hearing subjects.

Results

Listeners were more sensitive to changes attributed to the figure versus those attributed to the background. Change detection was accompanied by N200 (early fronto-central negativity) and P300 (late centro-parietal positivity) event-related potentials (ERPs). The amplitudes of N200 and P300 were larger for figure changes than for background changes. Compared to task-irrelevant changes, task-relevant changes of the figure were associated with larger N200 and P300 amplitudes. However, task relevance had no effect on ERP amplitudes for changes applied to the background.

Conclusion

Our results suggest: (1) The N200 reflects enhanced violation detection of the memory representation for the figure. This indicates that the spectro-temporal coherence of the figure results in a specialized memory representation as compared to that of the background. (2) The enhanced P300 for task-relevant objects implies that selective attention further facilitates the change-detection processes. The effect of attention on N200 only for the figure object indicates enhanced, early automatic change detection.

PS 702

Repetition Increases Cross-Frequency Coupling in Human Auditory Cortex

Urszula Malinowska¹; Magdalena Zieleniewska²; Piotr Franaszczuk³; Dana Boatman-Reich⁴

¹*Department of Neurology, Johns Hopkins School of Medicine*; ²*Department of Biomedical Physics, University of Warsaw, Warsaw, Poland*; ³*Human Research and Engineering Directorate, US Army Research Lab*; ⁴*Departments of Neurology and Otolaryngology, Johns Hopkins School of Medicine*

Background

A hallmark of sensory cortex is that neural responses decrease with stimulus repetition, a form of short-term plasticity known as adaptation or repetition suppression. In auditory cortex, adaptation is thought to improve sound detection and facilitate perception in noisy environments. Effects of stimulus repetition on cortical auditory network dynamics, including cross-frequency coupling, are not known. We used electrocorticographic (ECoG) recordings to investigate repetition effects on phase-amplitude coupling (PAC) in human auditory association cortex.

Methods

Participants were ten normal-hearing patients (ages 15-56 yrs; 7 female) with 8x8 electrode arrays implanted over the left (6 patients) or right hemisphere for clinical purposes of seizure localization. ECoG recordings were acquired using 300-trial passive auditory oddball paradigms in which one stimulus, either a tone (1000 Hz) or speech syllable (/ba/), was presented consecutively (1-12 trials) and frequently (82% trials; inter-stimulus interval = 1500 ms), with a different tone (1200 Hz) or speech (/da/) stimulus interspersed infrequently. Time-frequency matching pursuit analysis was performed to identify sites with significant ($p < 0.05$) auditory-related increases in high-gamma power (HG, 70-150 Hz). HG sites were designated as adapting using a repetition suppression index computed from mean log power density estimates. For all HG adapting sites, PAC measurements

were based on phase-locking values of theta (4-7 Hz) phase and HG amplitude across repeating trials. Repetition-related changes in theta-HG coupling were measured by coefficient of linear regression fitted to averaged PAC values.

Results

A total of 53 HG adapting sites were identified, located mainly in posterior perisylvian auditory areas of the left (33) and right (20) hemisphere. The number of HG adapting sites for speech and tones was comparable across hemispheres. More than 50% of HG adapting sites (N=29) showed repetition-related increases in phase-amplitude coupling. Positive PAC linear regression trends were significant across patients, sites and hemispheres ($p < 0.05$). The strongest PAC increase was for speech in the left hemisphere: 1.5% per repetition; the increase for tones was 1.3%. For the right hemisphere, the opposite trend was observed: tones yielded the strongest PAC increase (0.9% per repetition), with a weaker increase for speech (0.7%).

Conclusions

Cross-frequency theta-HG coupling increases significantly with auditory repetition in the left and right hemisphere. PAC trends were stimulus- and hemisphere-specific. Results suggest that increased cross-frequency coupling may reflect optimization of local cortical networks involved in processing repetitive auditory information.

Funding

Supported by The U.S. Army Research Laboratory under Cooperative Agreement W911NF-10-2-0022, and U.S. Army Research Office Grant W911NF-14-1-0491.

PS 703

The Magnetoencephalographic Spectrotemporal Response Function in Auditory Cortex

Francisco Cervantes Constantino; Jonathan Z. Simon
University of Maryland, College Park

The spectrotemporal response function (STRF) model of neural encoding may relate the response of a single auditory neuron, or network of neurons, to the stimulus input expressed as a spectrogram. The STRF is most often used to ascertain statistical features in the input that effectively drive or elicit change in neural activity, but can also quantify the explanatory power of an experimental parameter as a coding variable on neural activity. We show that the linear STRF model applied to noninvasive magnetoencephalography (MEG) recordings, a whole-brain recording technique with high temporal resolution, can account for 20-70% of auditory stimulus-explained

power for long-durations acoustic stimuli. This compares well to analogous single/multiunit recordings in primary auditory cortex (A1), which explain 20-40% of the stimulus-explained statistical power. Furthermore, the spectrotemporal structure of the MEG STRF provides a qualitative analog to the neuromagnetic evoked response to an impulsive stimulus. For auditory stimuli consisting of random spectrotemporal clouds composed of pure tone pips, an inverse relationship is found between the magnitude of the model's principal structural features and the temporal density of the tones, similarly to A1 single/multiunit STRFs. The emergence of STRF features for noise-like stimuli, akin to pre-attentive sensory gating in evoked potentials and to inhibitory processes in the receptive field literature, is also discussed.

Support to JZS from NIH R01 DC 014085, and to FCC from CONACYT (Mexico)

PS 704

Sequence Predictability Is Associated with Enhanced Error Responses – a Mismatch Negativity Study

Rosy Southwell¹; Maria Chait²

¹University College London; ²Ear Institute, University College London, UK

How are responses to surprising events affected by the preceding context? In this series of behavioural and EEG experiments we measure responses to deviants in regular or random sequences.

Stimuli were sequences of 50-ms tone-pips, whose frequencies varied in either a regular (REG) or random (RAND) pattern. For each trial, 10 frequencies were randomly chosen from a pool of 26 logarithmically spaced values. REG patterns were created by repeating the 10 frequencies in the same order; RAND patterns were created by shuffling the entire resulting sequence. Therefore, REG and RAND patterns were generated in 'matched' pairs, but presented in a mixed order within the experiment. RAND sequences were thus overall matched to REG for frequency content, and were controlled to contain no adjacent repeating tones.

Deviant occurred on 50% of trials. These were single tones inserted into the sequence, but at least 2 whole-tones higher or lower than the other frequencies used in the same stimulus. Therefore, deviants were equally divergent (in terms of frequency distance) relative to both REG and RAND sequences. Consequently, our paradigm is free from confounds due to adaptation of frequency-selective units, which are expected to be similar in both REG and RAND.

Behavioural experiments demonstrate that listeners were faster and significantly more accurate at detecting deviants embedded in REG relative to RAND patterns. An EEG experiment in naïve participants demonstrated sensitivity to regularly-repeating patterns, manifest as a sustained increase in the evoked response to REG compared to RAND – a finding consistent with previous EEG, MEG and fMRI work from our lab. This is interpreted as reflecting increased weighting of the neural responses to regular (highly precise) sounds, as a means of focusing processing resources on stable aspects of the environment. Importantly, over and above this difference, the mismatch response (MMN) evoked by deviants was significantly larger in REG, relative to RAND sequences.

These findings demonstrate the sensitivity of the MMN to the level of regularity in the preceding context. The results are consistent with predictive coding accounts, according to which prediction errors are weighted according to the confidence, or precision, of the predictions.

PS 705

Auditory Figure-ground Segregation Can Be Impaired by High Visual Load

Katharine Molloy¹; Nilli Lavie¹; Maria Chait²

¹*Institute of Cognitive Neuroscience, University College London, UK;* ²*Ear Institute, University College London, UK*

When listening to an auditory scene, one of the crucial roles of the hearing system is to separate objects of interest out from background noise. Several studies have demonstrated that figure-ground segregation occurs in the absence of explicitly directed attention, even when this requires integration of spectro-temporal information from a rapidly changing, complex scene (O'Sullivan et al., 2015; Teki et al., 2016). However, this is a process with potentially high computational demands, and capacity limits on sensory processing could mean that under very high processing load there are not enough resources available for it to be performed optimally. Here, we measure neural responses to the presence of auditory objects while attention is actively directed towards visual tasks with a range of demands.

Auditory Signals ('stochastic figure-ground': SFG; Teki et al., 2016) were comprised of a sequence of brief broadband chords containing random pure tone components that vary from one chord to another. We used very short (200ms overall; 25ms chords) stimuli, 50% of which contained repeated frequency components which are perceived as 'figures' popping out of a stochastic 'ground'. Passive MEG responses to the scenes were recorded during active visual search (where 200ms visual stimuli

were presented at precisely the same time as the auditory scenes) of both low and high visual perceptual load.

The results demonstrate the presence of a neural signature for segregation in both the high and low load conditions, suggesting that segregation was not completely abolished under high load. However, this signature was significantly smaller during the high load search task than the low load one. Behavioural data show that detection accuracy for the figures within the auditory scene was also reduced during the high visual load task compared to low load.

These data highlight the auditory system's impressive ability to respond to regularities within a scene, even when those scenes are extremely short and attention is not directed towards them. However, we show that the process can be disrupted when an active visual task places a high demand on processing resources. This suggests that while scene segregation is carried out by default when there are resources available, it is not truly 'automatic'.

References:

- O'Sullivan, J. A., Shamma, S. A., & Lalor, E. C. (2015). *JoN*, 35(18), 7256-7263.
Teki, S., Barascud, N., Picard, S., Payne, C., Griffiths, T. D., & Chait, M. (2016). *Cereb Cortex*, 26(9), 3669-3680.

PS 706

Contextual Influence on Auditory Target Search

Marissa L. Gamble; Barbara Shinn-Cunningham
Boston University

On a daily basis we encounter situations where we may need to search our environment for relevant auditory information while simultaneously rejecting and suppressing irrelevant distractors. Maintaining a representation of the stimulus enables us to achieve this rapidly. Approximately 60 ms after an auditory stimulus, a deviant-related event related potential (ERP), the Early Bilateral Negativity (EBN), reflects this rapid target/nontarget differentiation: the EBN is larger for relevant targets compared to irrelevant nontargets (Gamble & Woldorff 2015a; 2015b). In the current experiment, we focus on how the larger experimental context impacts early processing and how the presence or absence of a second irrelevant deviant sound affects target processing, in both the time and frequency domains.

Trials consisted of a visual cue (H or L) followed by a stream of ten diotically presented tones. The target tone, as indicated by the visual cue, was imbedded in the stream of standard, middle tones. Participants had

to focus on the target and then identify whether it was a pure or amplitude modulated tone. In the Single-Search condition, trials contained one deviant (one-deviant trials), either the high or low tone. The Inter-Mixed condition consisted of one-deviant trials intermixed with two-deviant trials (streams containing both a target and nontarget).

Identical one-deviant trials were identified less rapidly and accurately in the more difficult, Inter-Mixed condition than in the Single-Search condition. Target identification was slowest and least accurate overall in two-deviant trials (within the Inter-Mixed condition). Moreover, responses in Two-Deviant trials were slower when the target deviant came first compared to when it was second (though accuracy did not depend on presentation order).

Between 80-120 ms post-deviant, there was a large deviant-related activity (EBN). In the Inter-Mixed condition, the EBN was larger for the target than the nontarget, suggesting that in the Inter-Mixed condition, participants focused attention toward the target before the stream of sounds began. In contrast, in the Single-Search condition, target identification can be reactive, negating the need to inhibit irrelevant information.

Preliminary time-frequency analyses show similar decreases in alpha (~10 Hz) after the cue for both the Inter-Mixed condition and the Single-Search condition. This may reflect the maintenance of the stimulus representation during the cue-stream interval. Post-Deviant time-frequency analyses show more alpha and beta (15-20Hz) to the nontarget, compared to the target, suggesting increased suppression of the irrelevant deviant information.

PS 707

Neural Underpinnings of Auditory Saliency Using Natural Scenes

Nicholas Huang; Mounya Elhilali
Johns Hopkins University

The saliency of a stimulus is defined by how likely it is to draw our attention towards it. We rely on this property to help us allocate mental resources towards important sensory information and away from stimuli that are less likely to be relevant. Visual saliency has been studied extensively, with eye tracking being an accepted standard method of determining ground truth. In contrast, there is no such standard for studies of auditory saliency which remain few and far. Additionally, many of the methods used to measure auditory saliency have a slower response time than eye tracking, allowing for greater confounding influence of top-down attention.

The purpose of the present study is to discover electroencephalogram (EEG) features that could serve as physiological markers of auditory saliency.

EEG recordings were obtained using a 128-channel Biosemi Active Two system. Stimuli consisted of an existing set of natural auditory scenes with associated salient events obtained using a behavioral method. These natural scenes served as distractors while listeners performed a tone amplitude modulation detection task. A decrease in the phase-locked neural response to the attended tone stimuli was observed as result of salient events in the background scene. The event related potentials in response to the task stimuli were also perturbed by the presence of concurrent salient events. These changes were more pronounced when the distracting event was of a higher degree of saliency, and may be used in concert to identify portions of auditory scenes that are particularly salient without conscious user input.

PS 708

Robust Capabilities of Auditory Cortex Neurons to Discriminate Between Vocoded Communication Sounds

Jean-Marc Edeline¹; Samira Souffi²; Christian Lorenzi³; Chloe Huetz²

¹UMR9197, CNRS, Univ. Paris-Sud; ²NeuroPSI UMR 9191; ³Ecole normale supérieure, Paris Sciences et Lettres Research University and CNRS, France

Cochlear implants are neuroprosthetic devices designed to restore hearing in the case of severe deafness by stimulating directly auditory-nerve fibers. Cochlear implants incorporate a "speech processor" that transforms acoustic stimuli into electrical stimulation. The speech processor operates as a "vocoder" that splits the input signal into a limited number of frequency bands and extracts temporal-envelope fluctuations from the narrow-band stimuli. Although many efforts has been made to improve electrical-stimulation strategy and determine how auditory neurons respond to these stimuli, very few studies have investigated how auditory cortex neurons respond to envelope-vocoded stimuli.

Here, we have tested neuronal responses to original and vocoded vocalizations in the primary auditory cortex (AI) of anesthetized guinea pigs. A set of four conspecific vocalizations (Whistle) were processed by a tone vocoder using several levels of spectral resolution (10, 20 and 38 frequency bands). The original and vocoded vocalizations were presented either in quiet or in noisy conditions using two types of noise: a "chorus" noise mimicking the effect of a hubbub in a restaurant, and

a wide-band unmodulated noise. Three signal-to-noise ratios (SNR) were tested: +10, 0 and -10 dB.

Based on a total of 176 recordings which vigorously responded to the original vocalizations in quiet, we found that the evoked firing rate and the temporal reliability of cortical responses were slightly and progressively reduced by the vocoding process as the spectral resolution decreased. The mutual information quantified from the temporal spike patterns significantly decreased when the number of frequency bands was reduced from 38 to 10. In other words, the ability to discriminate between the four vocalizations decreased when using 10 frequency bands in quiet. Surprisingly, the effects of the two types of noise were similar for the normal and vocoded vocalizations: The lower the SNR, the higher the reduction in evoked responses and in mutual information. Interestingly, the effects of the two types of noise were much larger than the vocoding effect itself.

These data indicate robust coding of the temporal-envelope cues delivered by vocoders in the primary auditory cortex. They also suggest that it is important to increase the spectral resolution of speech processors beyond 10 independent frequency bands to preserve accurate neural representation of vocalization cues.

Auditory Cortex: Human Studies III

PS 709

Cortical Processing of Interaural Time and Level Differences Is Abnormal in Children with Simultaneously Implanted Bilateral Cochlear Implants Despite Long-term Experience

Vijayalakshmi Easwar¹; Hiroshi Yamazaki²; Michael Deighton³; Blake C. Papsin⁴; Karen A. Gordon⁵

¹Archie's Cochlear Implant Lab, The Hospital for Sick Children; ²Department of Otolaryngology, Head and Neck Surgery, Graduate School of Medicine, Kyoto University; ³Archie's Cochlear Implant Lab; ⁴Cochlear Implant Program (The Hospital for Sick Children), University of Toronto; ⁵The University of Toronto, The Hospital for Sick Children

Infants have access to interaural time (ITDs) and level differences (ILDs) which are important for sound localization and speech-in-noise perception. Sensitivity to these cues increases over the first 4 to 5 years of life but this development is disrupted by deafness. The present study aimed to: 1) define normal cortical processing of binaural cues in children and 2) how this processing might be restored through early bilateral cochlear implantation. Early work indicated that brainstem

integration of bilateral input is retained in children using cochlear implants (CIs); however, behavioral measures reveal poorer-than-normal sensitivity to binaural cues. We thus hypothesized that mature patterns of binaural processing will be evident in normal hearing children but disrupted in children with CIs despite early simultaneous bilateral implantation and long-term (~ 4 years) device experience.

Sixteen children with CIs ($M \pm SD = 6.13y \pm 0.79$) and 16 normal hearing children ($M \pm SD = 5.24y \pm 0.95$) participated in the ITD experiment. Thirteen children with CIs ($M \pm SD = 6.19y \pm 0.70$) and 15 normal hearing children ($M \pm SD = 5.15y \pm 0.92$) participated in the ILD experiment. Children in both groups had similar length of hearing experience. Cortical activity to 36 ms-long bilateral stimuli was recorded using a 64-channel electrode cap in three conditions: 1) baseline with no ITD and ILD, 2) ITDs ($\pm 400, \pm 1000 \mu s$) introduced at stimulus onset, and 3) ILDs (± 10 dB/CU) created by increasing and decreasing the stimulus level by 5 dB/CU in either ear. In children with CIs, biphasic pulse trains were delivered to electrodes at the apical end of the array and in normal hearing children, click trains were delivered through insert earphones. Cortical activity was localized using the time restricted artifact and coherent source suppression beamformer.

Children with normal hearing and bilateral CIs demonstrated stronger right hemispheric activity across all bilateral conditions, providing evidence for protected binaural pathways through early simultaneous bilateral implantation. As previously reported in normal hearing adults, responses in each auditory cortex were smallest to ipsilaterally-leading ITDs in normal hearing children. A similar pattern was evident for ipsilaterally-weighted ILDs, but in the right cortex only. This is consistent with preferential processing of fine timing cues in the left cortex. No similar evidence of cortical processing of either cues was found in children with bilateral CIs. Moreover, they had reduced activity in spatially sensitive non-auditory cortical areas. These findings confirm cortical binaural processing deficits despite early bilateral implantation suggesting persistent effects of prelingual deafness and inaccurate/inconsistent provision of binaural cues from independent auditory prostheses.

New Views on the Anatomy of Planum Temporale

Barrett V. St. George¹; Andrew T. DeMarco¹; Frank Musiek²

¹The University of Arizona; ²University of Arizona

The planum temporale (PT) is a workhorse for auditory processing. It is considered to be one of the most important brain regions for audition and the overlaid processes of speech and language. Specifically, the PT processes spectrotemporal patterns that make up the acoustic signals of speech, music and environmental sounds (Price et al., 2010; Griffiths & Warren, 2002). Considering the functional importance of the PT, its anatomy has been studied extensively in both healthy and disordered populations (Shapleske et al., 1999). The PT reliably demonstrates the most pronounced hemispheric asymmetry out of all structures in the human brain (Toga and Thompson, 2003; Van Essen, 2005), often larger in the left hemisphere. This anatomical asymmetry has been related to the left-hemisphere dominance of language function (Geschwind & Levitsky, 1968).

Occupying the posterior portion of the dorsal plane of the superior temporal gyrus, the PT is concealed within the Sylvian fissure. It is bounded anteriorly by Heschl's gyrus, and posteriorly by the posterior ascending ramus (PAR) of the Sylvian fissure. However, these two anatomical boundaries are considerably variable in their morphology. PARs vary significantly in length and angle, and sometime are absent (St. George et al., 2016). In addition, Heschl's gyrus often demonstrates a partial or complete duplication (Marie et al., 2015).

Although the literature quantifying PT has considered some of these complexities, it has not considered the effects of new research refining its boundaries. Specifically, recent work has suggested that duplications of Heschl's gyrus constitute a part of primary auditory cortex (Da Costa et al., 2011; De Martino et al., 2014; Moerel et al., 2014). As such, we argue that Heschl's duplications should not be included in the anatomical measurement of planum temporale. Recent efforts have also developed specific criteria for what is to be considered a PAR, which in the past has been loosely described (St. George et al, 2016).

Here we measure the influence of these bounding structures on the size of the PT in light of this new evidence. We hypothesized that duplications of Heschl's gyrus and the presence of prominent posterior ascending rami would both reduce PT size. We hoped this information might clarify the sources of structural PT asymmetry in the human brain.

Altered Resting State Functional Connectivity in Tinnitus Subjects Measured by Functional near Infrared Spectroscopy (fNIRS)

Juan San Juan¹; **Gregory J. Basura**¹; Mohamad Issa¹; Xiaosu Hu²; Silvia Bisconti²; Ioulia Kovelman²; Paul Kileny¹

¹Dept of Otolaryngology; Center for Human Growth and Development; University of Michigan; ²Center for Human Growth and Development; University of Michigan

Background

Tinnitus is the phantom perception of sound in the absence of a stimulus. Tinnitus percepts are thought to arise from aberrant central auditory circuits. Putative physiologic correlates (increased spontaneous firing rates and neural synchrony) in animal models have not been translated in human brains with tinnitus. This is due, in part, to inadequate technology to measure real-time neural activity without modifying the tinnitus environment. Functional Near-Infrared Spectroscopy (fNIRS) is an ideal tool to measure neural activity in humans with tinnitus as it is virtually silent. We have shown maintained and increased hemodynamic activity in auditory and non-auditory cortices in humans with tinnitus during auditory stimulation and at baseline; the later response potentially akin to animal correlates of tinnitus. Here we investigate another possible correlate; resting state functional connectivity (RSFC) in the same brain regions in human subjects with and without tinnitus.

Methods

Near-normal hearing subjects with bilateral tinnitus (n=10) and non-tinnitus controls (n=8) were measured with fNIRS. Oxygenated hemoglobin was monitored over the region of interest (ROI, primary auditory cortex) and non-ROI (adjacent non-auditory cortices) and brain connectivity was measured during a 60 second baseline/period of silence before and after a passive auditory challenge consisting of alternating pure tones (750 and 8000Hz), broadband noise (BBN) and silence.

Results

Pre-stimulation connectivity from ROI to temporal (p=0.0034) and parietal lobes (p=0.0323) differed among tinnitus and control subjects. ROI connectivity remained markedly unchanged from pre- to post-stimulation in tinnitus subjects compared to controls ($\chi^2 = 23.3$, p< .00001). In tinnitus subjects, pre- to post-stimulation connectivity decreased in the parietal, occipitoparietal, and occipitotemporal lobes (p< 0.0001, p= 0.0240, p= 0.0195), but increased in frontotemporal lobe (p= 0.0164). Conversely, controls demonstrated a decrease in connections involving frontotemporal and

temporal ($p= 0.0017$, $p= 0.0064$) lobes, but increased in the frontal, frontoparietal, parietal and occipitoparietal ($p= 0.0033$, $p= 0.0001$, $p< 0001$, $p= 0.0114$).

Conclusions

These data demonstrate that tinnitus leads to RSFC changes within auditory and non-auditory regions. RSFC involving auditory cortex is vastly unaffected by passive, unimodal auditory stimuli, while the control connectivity changes to stimulation. This suggests that dynamic changes in tinnitus may render central auditory circuits unresponsive to unimodal stimuli leading to permanence of effect and ultimately phantom perception. Our data also supports fNIRS as a translational tool in measuring pathologic states including tinnitus and implicates RSFC as a possible objective measure/correlate of tinnitus in humans, akin to those described in animal models.

PS 712

Effects of Obstructive Sleep Apnea-hypopnea Syndrome on Central Auditory Processing

Hui Wang; Hongliang Yi; Shankai Yin

Department of Otolaryngology Head and Neck Surgery, Shanghai Jiao Tong University Affiliated Sixth People's Hospital

Backgrounds

Obstructive sleep apnea-hypopnea syndrome (OSAHS) is associated with detrimental neurocognitive and behavioral consequences. The long term impact on central auditory processing is unknown. We aimed to explore the effects of OSAHS on central auditory processing abilities.

Methods

Fifteen right-handed patients with severe OSAHS (apnea hyponea index, $AHI>30$) were enrolled in the study. Thirty right-handed volunteers with normal hearing and without OSAHS participated as controls. Central auditory processing tests including speech in noise test, competing sentences test, dichotic listening, gap detection and auditory brainstem response to complex sounds (CABR) were performed in both groups. Brain responses were recorded with a 256-channel high-density electroencephalogram equipment on (Event Related Potential, ERP) components, i.e., the Mismatch Negativity (MMN) and the P3.

Analysis

Repeated-measures analysis of variance (ANOVA) was used for the analysis of data.

Results

OSAHS in all patients was of 5-7 years duration and the mean AHI values were 47.35 ± 11.12 . There was no significant difference in the auditory behavior performance between severe OSAHS patients and control subjects. Severe OSAHS patients had smaller amplitudes and longer latency of P3 and MMN than control subjects at Fz, Pz and Cz ($p < 0.05$). Poor performance of pitch tracking in speech detected by CABR in OSAHS patients compared with control subjects.

Conclusions

An early-level cortical sound-discrimination dysfunction and decreased in cognition was shown in severe OSAHS individuals, as evidenced by the decreased MMN and P3 response. Long-term OSAHS degrades central auditory processing ability.

PS 713

Intracranial Electrophysiology of Auditory Selective Attention During Semantic Classification Tasks

Mitchell Steinschneider¹; Kirill V. Nourski²; Ariane E. Rhone²; Matthew A. Howard²

¹Albert Einstein College of Medicine; ²Human Brain Research Laboratory, The University of Iowa

Auditory selective attention is a crucial component of speech perception, wherein acoustic-to-phonetic and phonetic-to-lexical/semantic transformations must occur within one processing stream amidst competing sound sources. An electrocorticography (ECoG) study by Chang et al. (J Cogn Neurosci 23:1437-46, 2010) revealed that high gamma (70-150 Hz) activity within posterolateral superior temporal gyrus (STG) was modestly enhanced for target syllables in a phonetic target detection task. Here, we examined ECoG activation during semantic classification tasks within and beyond auditory cortex.

Subjects were nine neurosurgical patients undergoing chronic invasive monitoring for treatment of medically refractory epilepsy. Four subjects had left hemisphere electrode coverage, four had right coverage, and one had bilateral coverage. Research was approved by The University of Iowa IRB and the NIH. Informed consent was obtained from all subjects, research participation did not interfere with clinical data acquisition, and subjects could rescind consent at any time. Stimuli were 300 ms monosyllabic words, spoken by different male and female talkers, or complex tones. There were three categories of words (animals, numbers, colors). Subjects were instructed to press a button whenever they heard a target (tones, animals, numbers). Data analysis focused on high gamma activity simultaneously recorded from

Heschl's gyrus (HG), STG, middle temporal and supra-marginal gyri (MTG, SMG), and prefrontal cortex (PFC).

Posteromedial HG (auditory core cortex) was neither task nor target-modulated, while posterolateral STG was task, but not target-modulated. Activity in MTG and SMG, which began later than that on the STG, showed target-specific modulation. PFC exhibited multiple response patterns, ranging from non-specific activation, to graded responses (target > non-target word in semantic task > non-target word in tone task), to target-specific responses that preceded the button press. Significant task effects (at $p = 0.01$) were more prominent in the left temporal cortices (STG, MTG, SMG) (27/282 sites) than in the right (12/263) (Chi-square $p = 0.036$). Target effects occurred later than task effects and were also more prominent in the left hemisphere (15/282 sites) than in the right (1/263) (Chi-square $p = 0.002$).

To our knowledge, this is the first ECoG evidence of hemispheric asymmetry in speech and language processing. Tasks requiring speech decoding more prominently engage the language-dominant hemisphere than a tone target detection task. Target effects require the words to be phonemically decoded, lexically identified and semantically classified. This provides direct evidence that the MTG and the SMG in the language-dominant hemisphere are involved in tasks requiring semantic processing.

PS 714

Combined Effects of Interaural Time and Level Differences in Human Auditory Cortex

Nathan Higgins; G. Christopher Stecker; Sandra Da Costa

Vanderbilt University School of Medicine

Interaural time and level difference (ITD and ILD) cues are initially extracted in the auditory brainstem. Their representations are partly integrated in neural activity within the inferior colliculus, but not fully integrated even at the level of the auditory cortex (AC). In humans, AC activity assessed using blood-oxygen-level-dependent (BOLD) fMRI is sensitive to sound-source location conveyed in binaural recordings, but it is not known whether such responses reflect sensitivity to ILD, ITD, or both. Previous work suggests that AC BOLD responses are dominated by ILD and only weakly tuned to ITD cues. Here, we measured BOLD sensitivity to ITD and ILD independently and in combination (ILD+ITD) to determine the unique contributions of each cue to spatial tuning of AC responses.

A phase-encoding approach was used to modulate binaural cues during continuous, whole-brain, fMRI at 3T.

Ten normal-hearing subjects listened passively to a series of complex tone bursts presented during 8.5-minute scanning runs. Binaural cues swept repeatedly from left to right or right to left over 34 s. Separate runs manipulated ITD (-700 μ s to 700 μ s in 100 μ s steps), ILD (-21 dB to 21 dB in 3dB steps), or both cues (using the same ranges). We hypothesized that the latter condition would produce greater modulation of BOLD responses. Data were analysed using BrainVoyager and MATLAB. Regions of interest (primary auditory areas A1 and R, and posterior superior temporal gyrus pSTG) were defined anatomically and functionally with a separate tonotopic localizer scan. We computed response-ITD and response-ILD functions in each region. The maxima, slopes, and cross-correlations of these functions were then used to quantify voxel selectivity.

Both the BOLD response functions and their maxima indicated stronger contralateral dominance for ILD and ILD+ITD conditions than for ITD alone, consistent with previous human imaging studies (McLaughlin et al., 2016; Stecker et al., 2015). Response magnitudes were greater in primary auditory cortex (A1 and R) compared to pSTG. Analysis of response-function slopes revealed the steepest changes in response across midline cue values for all three conditions, consistent with opponent-channel coding of ITD and ILD cues (Stecker et al., 2005). The greatest binaural modulation was observed in voxels that preferred contralateral cue values. Overall, our results confirm strong BOLD modulation by ILD, which was only slightly enhanced by ITD modulation. Little to no modulation of the BOLD responses was observed for manipulations of ITD alone.

Supported by NIH R01DC011548 and Swiss National Foundation P2LAP3_158671

PS 715

Noise and Pitch Interact During the Cortical Segregation of Concurrent Speech Sounds

Amy Fehrenbach; Anusha Yellamsetty; Gavin M. Bidelman

University of Memphis School of Communication Sciences & Disorders

Behavioral studies reveal that listeners exploit differences in voice fundamental frequency (F0) to segregate concurrent speech sounds, the so-called "F0-benefit." More favorable signal-to-noise ratios (SNRs) in the acoustic environment similarly benefit the parsing of simultaneous speech. Here, we examined the neurobiological substrates and interaction of these two cues in the perceptual segregation and neural encoding of multiple speech signals. To elucidate the mechanisms underlying concurrent speech segregation, we recorded event-re-

lated brain potentials (ERPs) while listeners performed a speeded double-vowel identification task. Listeners heard two concurrent vowels whose F0 differed by zero or four semitones presented in either clean (no noise) or noise-degraded (+5dB SNR; noise babble) conditions. Behavioral results showed that listeners were more accurate in correctly identifying both vowels for larger F0 separation but that this improvement interacted with noise; F0-benefit was more pronounced at higher, more favorable SNRs. Analysis of the ERPs revealed that N1 latency (~100 ms) showed a similar F0*SNR interaction, particularly at frontocentral electrode sites. Paralleling behavior, modulations in neural activity with changes in F0 were larger for clean compared to noise-degraded speech. F0 effects were also observed in later time windows (~400 ms) suggesting the recruitment of additional processing related to pitch segregation. The earlier timing of SNR compared to F0 effects at a neural level implies that the cortical extraction of speech from noise is more efficient than differentiating speech based on F0 cues alone. Our findings demonstrate that both noise and pitch differences interact relatively early (few hundred milliseconds) in cerebral cortex as the brain navigates the auditory scene and arrives at the identity of concurrent speech signals.

PS 716

Classification of Auditory Stimuli Using Event-related Potentials

Nikolas Blevins¹; Matthew Fitzgerald¹; Steven Losorelli¹; Gabriella Musacchia²; Blair Kaneshiro¹
¹Stanford University; ²University of the Pacific

Sound classification is the process of assigning auditory stimuli to one of many categories, or classes, based on acoustic characteristics. The ability to correctly classify sound, which consists of finding an appropriate relationship between the brain response to acoustic features and memory-encoded class boundaries, is a crucial step for speech identification. This process is seamlessly automatic for individuals with normal hearing (NH) but can be a significant challenge for individuals with cochlear implants (CIs), who receive acoustic input that differs tremendously from that of individuals with NH. As a result, many individuals with cochlear implants have difficulty describing what they hear with their device. This can make programming the device more challenging for audiologists, and potentially limit patient performance. There may therefore be benefit to an objective method to determine whether an individual receives sufficient neural signals to categorize a given sound independent of the patient's reporting ability.

Electroencephalography (EEG) methods have success-

fully categorized different visual and auditory stimuli. For example, event-related potential (ERP) methodology has been used to discriminate between visual presentation of a human face, animal face, or inanimate object and differentiate speech sounds or musical instruments. More recently, event-related oscillations (EROs), which examine both spectral and temporal characteristics of the brain response, have demonstrated the brain's fine-grained acoustic resolving power.

In this pilot investigation, 256-channel EEG data were recorded in listeners with NH to eight auditory stimuli via insert earphones presented at a comfortable listening level. Stimuli were divided into three major functional categories (speech, musical instrument, and non-musical sounds) and subdivided into acoustic categories of easily distinguishable stimuli (e.g., da vs. ta, a trumpet vs. a piano, and a click vs. a pure tone). In this way, we could evaluate the ability for brain activity to distinguish across major functional categories, and between different acoustics within a given category. Brain responses were subjected to a classification algorithm using two factors: the latency and amplitude of various ERP components across the global waveform, and ERO activity within individual frequency components (e.g., gamma, theta, beta, and alpha activity). While preliminary, our data suggest that ERPs and EROs can categorize auditory stimuli at a greater than chance level in listeners with NH. We are presently refining our classification algorithm to improve its accuracy, and determining which EEG components are likely to yield the best data for brain-based categorization.

PS 717

Influence of Structural and Functional Asymmetries on Pitch-Relevant Neural Activity in Auditory Cortex

Chandan Suresh; Ananthanarayan Krishnan; Jackson Gandour
Purdue University

Long-term language experience enhances pitch-relevant neural activity in the auditory cortex, as reflected by the components (Na-Pb and Pb-Nb) of the cortical pitch response (CPR). Previous results have consistently shown that this neural activity shows a relative rightward asymmetry in Chinese only. These experience-dependent results have been interpreted to suggest that extrasensory processes modulate early sensory level processes to optimize representation of temporal attributes of pitch that are behaviorally relevant. However, it is not known how structural asymmetries—characterized by contralateral dominance—in the ascending auditory pathways interplay with functional hemispheric asymmetries at the cortical level. We recorded cortical

pitch responses (CPR) from native speakers of Mandarin and English in response to speech (S; /i/) and nonspeech (NS; iterated rippled noise) sounds, both of which carried a pitch homolog of Mandarin high rising Tone 2. Stimuli were presented under diotic (either S or NS in both ears), dichotic (S-LE/NS-RE; S-RE/NS-LE), and monotic (S-RE; NS-RE; S-LE; NS-LE) conditions. Irrespective of the mode of stimulation, the magnitude of CPR components in the Chinese group was greater compared to the English; the Chinese group also showed a rightward asymmetry. In contrast, the English group showed no asymmetry when either speech was presented in the LE or nonspeech in the RE; and only a weak rightward asymmetry when speech was presented to the RE or nonspeech to the LE. In monotic conditions, the Chinese group showed a rightward asymmetry only, when speech or nonspeech was presented to the LE, with no asymmetry when speech or nonspeech was presented to the RE. In contrast, the English group showed the largest response in the contralateral hemisphere regardless of stimulus type (S, NS). These findings suggest that the rightward asymmetry observed in the Chinese group mostly represents an experience-dependent functional asymmetry. A right-sided preference with LE monaural stimulation further suggests that long-term experience may also influence structural asymmetry. In monotic conditions, the English group's responses more likely reflect a structural asymmetry in which the dominant contralateral pathway suppresses activity of the ipsilateral pathway. Based on these pattern of results for diotic, dichotic, and monotic conditions in the two groups, long term language experience in the Chinese group not only enhances representation of pitch relevant information in the auditory cortex, facilitated by selective reinforcement of structural asymmetries along the ascending auditory pathway to deliver the optimal input to the preferred pitch processing site in the auditory cortex.

PS 718

How Far down Does the Top-down Control of Speech Processing Go?

Heivet Hernández-Perez¹; Catherine McMahon¹; Sri-ram Boothalingam²; Sumitrajit Dhar²; David Poeppel³; Jessica J. M. Monaghan¹

¹Macquarie University; ²Northwestern University; ³New York University

The perception of speech sounds in humans requires a fast and accurate integration of both bottom-up and top-down information carried by the auditory afferent and efferent pathways respectively. However, it remains poorly understood whether during speech perception the top-down control reaches the level of the brainstem or even the cochlea via the auditory efferent pathway.

There is evidence that this efferent control may play a role in extracting signals from noise (Giraud et al., 1997; Maison et al., 2001; Garinis et al., 2011) and the detection of target sounds (Scharf et al., 1997; Tan et al., 2008). Here we evaluated the role of attention on the auditory efferent control of the brainstem (using auditory brainstem responses; ABRs) and the cochlear gain (using otoacoustic emissions; OAEs) during passive listening and a task of variable difficulty. We hypothesised that both the ABRs and OAEs would be modulated by attention and that the degree of suppression of OAEs (relative to the passive condition) would increase with increasing task difficulty.

Thirty normal-hearing, English speakers between 18-35 years old were assessed using lists of monosyllabic words and non-words presented in a natural or noise-vocoded (less-intelligible) conditions. Participants were tested during active and passive listening conditions. In the active condition, the participants were instructed to press a button every time they heard a non-word. A synchronised 64 channels-EEG and click evoked-OAE (CEOAEs) recording system allowed the measurement of speech onset auditory event-related potentials (ERPs), click-auditory brainstem responses (ABRs), CEOAEs and behavioral responses. Click evoked-OAE were obtained from the contralateral ear to the speech stimuli with a probe in the external ear canal.

Preliminary results suggest that auditory attention modulates the activity of the cochlear activity, brainstem and cortical responses. Click evoked-OAE amplitudes were inhibited during lexical decision tasks relative to passive listening, in contrast, ABR-wave V amplitude increased and latency decreased in the active listening condition. Behavioral results showed that the accuracy (d') decreased as the number of vocoder channels decreased. This task-difficulty effect was reflected in the early ERP components, as well as in the CEOAE data where the less intelligible condition showed stronger inhibition. These data suggest that the accurate classification of speech sounds engage not only bottom-up processing but also top-down control mechanisms that influences the auditory brainstem and the cochlear gain via the auditory efferent system.

Auditory Prostheses: Objective Measures

PS 719

Objective Identification of Simulated Cochlear Implant Settings in Normal-hearing Listeners via Auditory Cortical Evoked Potentials

Gavin M. Bidelman; Sungmin Lee

University of Memphis School of Communication Sciences & Disorders

Providing cochlear implant (CI) patients the optimal signal processing settings during mapping sessions is critical for facilitating their speech perception. Here, we aimed to evaluate whether auditory cortical brain potentials (ERPs) could be used to objectively determine optimal CI parameters. While recording neuroelectric potentials, we presented a set of acoustically vocoded consonants (aKa, aSha, and aNa) to normal hearing listeners (n=12) that simulated speech tokens processed through four different combinations of CI stimulation rate and number of spectral maxima. Parameter settings were selected to feature relatively fast/slow stimulation rates and high/low number of maxima; 1800 pps/20 maxima, 1800/8, 500/20 and 500/8. Speech identification and reaction times did not differ with changes in either the number of maxima or stimulation rate indicating ceiling behavioral performance. Similarly, we found that conventional univariate analysis (ANOVA) of N1 and P2 amplitude/latency failed to reveal strong modulations across CI-processed speech conditions. In contrast, multivariate discriminant analysis based on a combination of neural measures was used to create “neural confusion matrices” and identified a unique parameter set (1800/8) that maximally differentiated speech tokens at the neural level. This finding was corroborated by information transfer analysis which confirmed these settings optimally transmitted information in listeners’ neural and perceptual responses. Translated to actual implant patients, our findings suggest that scalp-recorded ERPs might be useful in determining optimal signal processing settings from among a closed set of parameter options and aid in the objective fitting of CI devices.

PS 720

Neural Facilitation in 8th Nerve Fibers: Its Possible Impact on Fiber IO Functions

Mark White¹; Jason Boulet²; Leon F. Heffer³; James B. Fallon⁴; Ian C. Bruce²

¹unaffiliated; ²McMaster University; ³The University of Melbourne; ⁴Bionics Institute

In a study of 8th nerve responses to electrical stimulation [1], fiber input-output (IO) functions were measured for pulse-trains of 100 ms duration at pulse-

rates of 200, 1000, 2000, and 5000 pps. Here, we examine evidence that “neural facilitation” may be responsible, at least in part, for the shallow fiber IO-functions observed at higher stimulus pulse-rates.

Psychophysical measures of temporal integration, multi-pulse integration, intensity discrimination, modulation detection threshold, and spread-of-excitation are probably all related to the steepness of fiber IO functions [2],[3].

For charge-balanced pulsatile stimulation, “facilitation” is primarily due to a non-linear neural mechanism in which “residual excitation,” resulting from one or more prior sub-threshold pulses, builds-up enough to enable the subsequent pulse to elicit a discharge.

For the stimulus intensity range analyzed in Fig. 7 by Heffer et al [1], we hypothesize that fiber IO-functions are shallower for higher pulse-rate stimuli due to neural facilitation. Our reasoning is straight-forward: at low stimulus levels and high pulse-rates, facilitation substantially “raises” the neuron’s discharge probability but, at somewhat higher stimulus levels, facilitation does little to “raise” the already high discharge probability.

Is neural facilitation sufficient to quantitatively account for the impact of pulse-rate on the steepness of measured fiber IO-functions? In an effort to answer this question, we will present simulation results using an 8th-nerve fiber model that simulates neural facilitation. This work was supported by NSERC Discovery Grant 261736 (ICB)

[1] Heffer LF, Sly DJ, Fallon JB, White MW, Shepherd RK and O’Leary SJ (2010) “Examining the Auditory Nerve Fiber Response to High Rate Cochlear Implant Stimulation: Chronic Sensorineural Hearing Loss and Facilitation,” *J Neurophysiol* 104:3124-3135.

[2] Bruce IC (1997) “Spatiotemporal coding of sound in the auditory nerve for cochlear implants,” PhD Thesis, The University of Melbourne, Australia.

[3] Zhou N, Pfungst BE (2016) “Evaluating multipulse integration as a neural-health correlate in human cochlear-implant users: Relationship to spatial selectivity,” *J Acoust Soc Am* 140(3):1537-1547.

PS 721

Electrophysiological Changes in the Cochlea During Cochlear Implantation

Adrian Dalbert¹; Flurin Pfiffner¹; Marco Hoesli¹; Christof Roosli¹; Alexander Huber²

¹Department of ENT, Head and Neck Surgery, University Hospital Zurich, Switzerland; ²1, Department of Otorhinolaryngology – Head and Neck Surgery, University Hospital Zurich, Zurich, Switzerland

Introduction

The aim of this study was to assess at which point during cochlear implantation measurable electrophysiological changes in the cochlea occur. Electrophysiological changes in the cochlea were assessed by electrocochleography (ECoG).

Methods

ECoG responses to tone bursts at 250, 500, 750, and 1000 Hz and to click stimuli were recorded. The recording electrode was placed on the promontory and left in an unchanged position for all recordings. ECoG recordings were conducted before, during, and after insertion of the cochlear implant electrode array and after intraoperative suprathreshold electrical stimulation.

Results

After cochleostomy or incision of the round window membrane, an increase of high- and low-frequency ECoG responses was observed regularly. No decrease of ECoG signals occurred after opening of the cochlea. During insertion, no decrease of low-frequency ECoG signals was observed until the cochlear implant electrode array was inserted half-way into the cochlea. Afterwards, two different patterns occurred: 1) Low-frequency ECoG responses remained stable until the last ECoG recording after suprathreshold electrical stimulation; 2) A decrease of low-frequency ECoG responses began and continued until the last ECoG recording after suprathreshold electrical stimulation. During insertion, a decrease of high-frequency ECoG responses to click stimuli occurred without detectable changes of low-frequency ECoG responses. A complete loss of high-frequency ECoG responses was associated with a decrease of low-frequency ECoG responses.

Conclusions

Electrophysiological changes in the cochlea during cochlear implantation can be monitored using extracochlear ECoG. Electrophysiological changes in the low frequencies may occur with insertion of the cochlear implant electrode array beyond the basal turn. If a decrease of low-frequency ECoG responses is detectable during insertion, the decrease continues after comple-

tion of the insertion, suggesting ongoing deterioration of the cochlear function in the early postoperative phase. Electrophysiological changes in the high frequencies occur without detectable changes in low-frequency ECoG recordings, suggesting limited trauma to high-frequency regions of the cochlea during insertion of the cochlear implant electrode array.

PS 722

Acoustic Change Complex (ACC) Evoked By Pitch Changes in Cochlear Implant Users and Normal Hearing Listeners

Chun Liang¹; Lisa Houston²; Ravi Samy²; Jing Xiang³; Fawen Zhang²

¹University of Cincinnati; ²university of cincinnati; ³cincinnati children's hospital medical center

Pitch change detection may play a crucial role for speech and music perception. Cochlear implant (CI) users typically perform poorly in pitch perception, which is the main reason for their poor performance in speech perception in noisy environment and music perception (Chen & Zeng, 2004; Won et al., 2007; Gfeller et al., 2012; Gifford et al., 2014). However, it is unclear about the neural mechanisms underlying pitch change detection. The neural responses, if confirmed to be related to behavioral performance on pitch change detection, may serve as an objective tool for assessing the auditory training effects and providing training guidance. The aim of the current project is to better understand how the auditory brain processes pitch changes in CI users and normal hearing listeners using both psychoacoustic and electroencephalographic (EEG) measures.

Method

Ten CI users and 12 normal hearing (NH) young listeners participated in this study. A psychoacoustic test and EEG recordings were administered in each participant. For the psychoacoustic test, stimuli were a series of 160 Hz base frequency tones containing different magnitudes of upward frequency changes at 0.5 sec after the tone onset. The frequency change occurred for an integer number of cycles of the base frequency and the change occurred at 0 phase (zero crossing). Therefore, the onset cue was removed and it did not produce audible transients (Dimitrijevic et al., 2008). An adaptive, 2-alternative forced-choice procedure was employed to measure the minimum pitch change the participant was able to detect. For EEG recording, the stimuli are similar to those in the psychoacoustic test, but the base frequencies examined were 160 Hz and 1200 Hz. The magnitude of frequency changes was 0% (no change), 5%, and 50% change for each base frequency. Subjects were asked to ignore the stimuli during EEG recording.

Results

Data collection is ongoing. With the existing data from 5 CI users and 12 NH listeners, the results showed that CI users exhibited a much higher threshold (a greater percentage of pitch change from the base frequency, $M=4.43\%$) for pitch change detection compared to NH listeners ($M=0.72\%$). There was a trend that the threshold for pitch change detection was related to the ACC measure (N1 amplitude).

Conclusions

The results suggested that the ACC might be an objective tool for assessing the capacity of CI users to detect pitch changes, which is critical for speech perception performance.

PS 723

Modifying the 'PECAP' Method to Estimate Neural Excitation Patterns from Evoked Compound Action Potentials of Cochlear Implant Users

Stefano Cosentino; John Deeks; Richard Turner²; Robert P. Carlyon¹; Stefano Cosentino¹

¹MRC Cognition and Brain Sciences Unit; ²University of Cambridge

Panoramic ECAP ('PECAP', Cosentino et al. 2015, IEEE Trans.) is an algorithm to extract neural excitation patterns from evoked compound action potentials (ECAPs) measured in cochlear implant users using a forward masking paradigm. The algorithm is based on a model where the amplitude of the ECAP signal is directly related to the neural excitations of the probe and the masker. Specifically, it is assumed that, for any combination of masker and probe electrodes and at any given current level, the ECAP amplitude measured with a forward masking paradigm will depend on the overlap of the individual neural excitations produced by the masker and by the probe electrodes.

In previous work, the PECAP algorithm could reliably estimate the underlying excitation pattern from ECAP amplitudes that were either generated through simulation or measured. Of particular interest was its ability to detect instances of neural "dead regions" or cross-turn stimulations. The operating signal-to-noise ratio (SNR) for the proposed algorithm was 5 dB or higher, which matched well the SNR measured from human physiological data.

In the present work, PECAP was modified in the following three ways. First, the relationship between neural excitation patterns and ECAP amplitudes ("the model") was modified non-linearly so that all equations would express quantities in physical units of voltage. Second,

the neural excitation patterns were modeled using two components corresponding to current spread and variations in neural efficiency, e.g. dependent on the presence of "dead regions". This allows access to information about the neural layer, which in version 1 of PECAP (v1) was undistinguishable from the current spread within the cochlea. Finally, the symmetry assumption in the neural excitation patterns was removed, thus allowing variations in the neural efficiency along the cochlea to influence multiple excitation patterns in a more physiologically-plausible manner. Both versions (v1 and v2) of PECAP perform constrained nonlinear optimization where neural excitation patterns with different characteristics are adaptively adjusted to reduce the fitting error with measured ECAP patterns.

The new version of the PECAP was compared to v1's predictions across 20 simulated conditions involving both asymmetric and symmetric neural excitation patterns. In the first scenario, v2 showed better performance due to its ability to capture asymmetries in the data. Conversely, for symmetric scenarios, the gaussian assumption in v1 provides more robust predictions compared to v2. Further developments will aim to improve robustness of v2 whilst retaining the advantages of its increased physiological and physical validity.

PS 724

Electrically Evoked Auditory Brainstem Responses and Acoustic Change Complexes in Adolescent Cochlear Implant Users with Long Inter-Implant Intervals

Bernard Vonck; Marc Lammers; Geerte Ramakers; Huib Versnel; Gijsbert van Zanten; Wilko Grolman
University Medical Center Utrecht

Background

A prolonged interval between the first and the second cochlear implant (CI) in children is known to negatively affect auditory performance with the second CI. The relatively poor performance with the second implant (CI2) might be due to an impaired maturation of the auditory pathway of the later implanted ear caused by unilateral hearing with the first CI (CI1). To study possible maturational differences, we compared electrically evoked auditory brainstem responses (eABR) and acoustic change complexes (ACC) in children with long inter-implant intervals.

Methods

In 14 sequentially implanted adolescents (age 10-19) with varying inter-implant intervals (range 4 to 15 years), eABRs and ACCs were obtained 12 months after the first activation of CI2. ACCs are cortical auditory evoked potentials in response to change within an ongoing

sound; in the current study frequency changes were used. ACC stimuli consisted of three components: A) pure tone in the center frequency of a middle electrode B) a frequency modulation sweep C) a pure tone in the center frequency of a more basal electrode, accounting for a higher frequency. eABR stimuli consisted of an electrical biphasic pulse on a middle electrode.

Results

The consonant vowel consonant (CVC) phoneme scores were significantly lower in CI2 compared to CI1 (means 56% vs 91%, $P < 0.01$). Latencies of eABR waves III and wave V were significantly longer for CI2 than for CI1 (means 2.01 vs 1.91 ms and 3.88 vs 3.68 ms respectively, $P < 0.05$). There were no significant differences in ACC N1 and P2 latencies between CI2 and CI1. ACC N1-P2 amplitudes were significantly smaller for CI2 than for CI1 (means 5.8 vs 8.2 μV , $P < 0.05$). These various differences in eABRs and ACCs between CI2 and CI1 did not correlate with the inter-implant interval.

Conclusion

The longer eABR latencies and the smaller ACC amplitudes found for the CI2 ear indicate an impaired maturation of the auditory pathway of the CI2 ear, explaining the inferior hearing with CI2. One year of using a second CI does not restore deficiencies.

PS 725

ECAP-Based Measures for Assessment of Cochlear Health

Kara Schwartz-Leyzac; Christopher J. Buswinka; Deborah Colesa; Aaron P. Hughes; Bryan Pflugst
University of Michigan

Introduction

Previous studies demonstrated that more than 50% of the variance in SGN density in the deaf implanted guinea pig cochleae can be accounted for by the slopes of ECAP amplitude growth functions. Related studies have also shown that the proportion to which the ECAP AGF slope changes with increasing the IPG is also related to cochlear health. Both of these measures have been shown to vary across stimulation sites in human subjects who use multichannel cochlear implants. It has been hypothesized that variables other than neural health that affect the ECAP AGFs for short and long IPG stimuli equally would cancel and not be reflected in the magnitude of the IPG effect. The current study examined the across-site variation in both of these ECAP measures and their relationship with simple impedance measures in human and animal subjects.

Methods

Human participants were adult cochlear implant recipients who had been implanted for at least 6 months. ECAP responses were recorded from each individual electrode in each ear using a forward-masking technique with a leading cathodic phase. Animals included 40 adult male SPF pigmented guinea pigs. A 6-channel cochlear implant was implanted into the basal turn of the scala tympani. Deafening and post-deafening treatments were varied across the animals to create diversity of cochlear health. ECAPs were recorded in the awake state from an implanted electrode using alternating phase polarity. In both humans and animals, ECAP amplitude-growth functions were collected using two interphase-gap conditions.

Results

Results showed that the ECAP AGF slope and the proportional change in slope as a function of IPG varied across-electrodes within each human subject. For AGF slope, the across-site impedance measures were correlated in 37.5% of the cases whereas for the proportional-change measure the impedance measures were only correlated in 2.5% of the cases. The first measure was significantly correlated with duration of hearing loss, whereas the latter was not. For the guinea pigs, we observed a positive and significant relationship across animals between SGN density and the proportional change in ECAP slope as the IPG increased.

Conclusions

The subject-specific across-site variation in ECAP measures suggests that they are dependent on variables within the cochlea near the electrodes. Some measures seem to be sensitive to neural health and some are influenced by other variables such as those related to impedance. Additional experiments are needed to determine the relative contributions of the variables underlying each ECAP measure.

PS 726

Assessing Electrode Differentiation Using the Electrically Evoked Acoustic Change Complex

Deborah Vickers¹; Rajeev Mathew¹; Jaime Undurraga²; Guoping Li¹; Patrick Boyle³

¹*University College London*; ²*MacQuarie University*;

³*Advanced Bionics European Research Center, Hannover, Germany*

Introduction

Poor differentiation between electrodes may be indicative of large current spread, damage to the auditory nerve or inappropriate electrode placement. It is known that there is a relationship between poor electrode differ-

entiation and speech perception abilities, particularly for electrodes in the apical end of the array. There is some evidence that de-activating indiscriminate electrodes may lead to improvements in speech perception.

This research looked at the potential for using an objective measure to determine electrode differentiation. The electrically evoked acoustic change complex (eACC) encodes auditory change at the cortical level and could potentially be used to guide CI mapping and rehabilitation strategy without requiring a response from the participant. The study validated eACC against behavioural measures of electrode differentiation and determined if there was a relationship with speech perception.

Method

Ten adult unilateral users of the HiRes90k (Advanced Bionics) device participated. They underwent objective assessments (eACC), behavioral electrode differentiation tests, and speech perception measures.

The stimulation for the eACC was delivered using direct electrode stimulation, 800ms pulse train with change in stimulating electrode at 400ms, at 0.51 Hz. The electrodes were loudness balanced.

The electrocochleography measurements used a 64 channel cap with 2 ocular electrodes and 2 mastoid electrodes. For the analysis the artefact was removed with filtering and denoising source separation (DSS)

A behavioral 3-interval 2-alternative forced choice task using direct stimulation assessed whether participants could discriminate between electrodes. Each pair of electrodes were compared 20 times and binomial significance levels were used to determine discriminability.

Four most apical electrodes were tested with each measure.

Sentence perception in quiet was assessed using the Bamford-Kowal-Bench sentences presented at 70 dBA and vowel perception was assessed in quiet using the vowel section of the Chear Auditory Perception Test, which is a 4-alternative forced choice monosyllable test presented at 50 dBA.

Results

Average eACC amplitude was correlated with average behavioral d' for electrode differentiation ($r = 0.79$, $p = 0.01$). The Cohen's Kappa score between the two measures of electrode differentiation was high ($\kappa = 0.80$, $p = 0.001$). For individuals with poor electrode differentiation (< 2 electrodes passing) the speech perception scores were significantly worse than for individ-

uals with good electrode differentiation (> 2 electrodes passing) for both sentence and vowel perception.

Conclusions

These results showed that the eACC can reliably be used as an objective measure of electrode differentiation. Further work will be conducted to determine if the eACC can be used to guide fitting.

PS 727

Systemic Ancestral Adeno-associated Viral Vector Delivery Improves Opsin Expression in Auditory Pathways

Maria Duarte¹; Sumi Sinha¹; Shreya Narasimhan¹; Ariel E. Hight¹; Vivek V. Kanumuri²; Elliott Kozin³; Chris Brown¹; Daniel J. Lee⁴

¹Massachusetts Eye and Ear Infirmary; ²Massachusetts Eye and Ear Infirmary/Harvard Medical School;

³Massachusetts Eye and Ear Infirmary; ⁴Harvard Medical School

Introduction

Optogenetics is a powerful tool that uses pulsed light stimulation to modulate responses of photosensitized neurons with millisecond precision both in vitro and in vivo. Optogenetic approaches have been proposed as a stimulation paradigm for next-generation auditory neuroprostheses. Stable and robust opsin expression in the auditory pathway is crucial towards the development of an optically-based implant. Most optogenetic animal models use transgenic approaches or viral vector injections directly into the target tissue, making translation to the clinic challenging. In addition, efficiency of gene transfer is modest with existing viral vectors. Ancestral adeno-associated viral vector (Anc80) is a novel construct with greater transduction efficiency and lesser immunotoxicity than adeno-associated viral vector (AAV2/9). The use of Anc80 as a vector for opsins has not been studied, nor has its transduction efficiency along the auditory pathways. Herein, we compare expression patterns of opsins in cochlear and central auditory pathways following systemic delivery of AAV2/9 or Anc80.

Methodology

AAV2/9 or Anc80 carrying Chronos opsin with a GFP reporter was injected into lateral tail vein or superficial temporal vein of wild type CBA/CaJ mice. Neuronal-specific promoter Synapsin (SYN) or nonspecific CAG promoter was utilized. Multiunit responses from inferior colliculus (IC) were measured in response to pulsed light stimulation of photosensitized auditory neurons. Histologic analysis of cochlear nucleus (CN), superior olivary nucleus (SO), IC, medial geniculate body (MGB), and

auditory cortex (AC), as well as the spiral ganglion neurons of the cochlea, was performed.

Results

Histology from tail vein and temporal vein injections of AAV2/9-Chronos with SYN and CAG promoters demonstrated strong GFP expression in CN, SO, IC, and MGB. Opsin expression was lower in AC. Expression was also observed in the cochlea spiral ganglion. Preliminary histology from Anc80-Chronos mice demonstrated greater opsin expression throughout the auditory pathway compared to AAV2/9-Chronos treated mice. Preliminary neurophysiology demonstrated multiunit IC firing in response to optical stimulation of the CN following systemic injection. Control tail vein injections with saline showed no GFP expression and no evoked responses.

Conclusion

This is the first study to demonstrate successful transduction of central auditory pathways via systemic injection of novel ancestral adeno-associated viral vector. Optically-induced responses demonstrate that expression levels of opsins in our model are physiologically relevant. Transducing auditory neurons using this minimally-invasive approach offers a translatable model of a future auditory implant based on light. Supported by the Bertarelli Foundation and the NIH.

PS 728

Myographic Recordings of the Electrically and Acoustically Elicited Stapedial Reflex with a Chronically Implanted Recording Electrode

Moritz Gröschel¹; Rolf-Dieter Battmer¹; Patrick Boyle²; Arne Ernst¹; Dietmar Basta¹

¹Department of Otolaryngology at Unfallklinik Berlin, University of Berlin, Germany; ²Advanced Bionics European Research Center, Hanover, Germany

The electrically elicited stapedial reflex threshold (ESRT) correlates very well with the maximum comfortable level (C- or M-Level) and thus, is a viable tool with which to set upper stimulation limits when fitting cochlear implant (CI) recipients. Postoperative evaluation of the muscle response using an impedance bridge is very time consuming and in many cases not possible due to middle ear disturbances of the contralateral ear. The aim of this study was to investigate the feasibility of making myographic recordings via a chronically implanted intramuscular micro needle electrode in guinea pigs. Different recording electrodes were developed to suit the anatomical requirements and to easily penetrate the stapedial muscle. The ideal electrodes were prepared from a silicone coated Pt/Ir-wire which was uninsulated for

1mm and sharpened at the tip to 5µm. The reflex was elicited intraoperatively by either, contra-lateral acoustic stimulation, or by an ipsilateral dual biphasic pulse from a cochlear implant electrode. The recording electrode was left in place for 3 months. After 3 months the measurements were repeated and muscles were removed for histological investigation.

Myographic recordings of the stapedial reflex could be obtained in the monopolar and bipolar setup intraoperatively as well as after 3 months of chronic implantation. No migration of the electrode or macroscopic damages of the muscle were observed. Microscopic changes could be detected mainly at the insertion site. The present study demonstrates that myographic signals can be reliably recorded via a chronically implanted electrode placed into the stapedial muscle.

This work was supported by Advanced Bionics GmbH, Germany.

PS 729

Electrode Position and Physiological and Behavioral Measures of Channel Interaction in Cochlear Implant Listeners

Lindsay DeVries¹; Rachel Schepeler²; Julie A. Bierer¹
¹University of Washington; ²Montclair State University

Speech understanding abilities vary widely among cochlear implant (CI) listeners. A potential source of this variability is channel interaction, likely caused by poor electrode position and/or neural integrity. Electrode position can be estimated via CT imaging, but that can be costly and exposes patients to additional radiation; therefore, it is often not available. Alternate methods for assessing electrode position may be obtained using physiological and/or behavioral measures. Using the electrically evoked compound action potential (ECAP), we have measured channel interaction to accurately predict poor electrode placement in some CI listeners. However, the ECAP has some limitations as the measurement can contain electrical artifact and not all CI listeners have a measurable response. In this study, we explore the relationship between electrode position and a behavioral measure of channel interaction, psychophysical tuning curves (PTCs). This comparison may provide a detailed assessment of local variations in channel interaction. PTCs have the advantage that the response is not affected by electrical artifact and that most CI listeners have measurable PTCs. Conversely, PTC data collection can take longer than the ECAP because of the nature of the task. Therefore, the purpose of this study was to 1) compare degree of channel interaction measured with both ECAP and PTC methods to each other, and 2) to relate the degree of interaction to

electrode-to-modiolus distance and focused behavioral thresholds. Five unilaterally implanted adults with the Advanced Bionics HiRes90K device participated. CT scans were obtained reconstructed in three-dimensions to estimate electrode position. PTCs were collected using a forward-masking paradigm that employed a focused masker followed by a brief monopolar probe stimulus. For ECAP experiments, only monopolar stimulation was used. Channel interaction was quantified with an equivalent rectangular bandwidth (ERB). Results show a positive correlation between electrode-to-modiolus distance and the ERB of PTCs and ECAPs, suggesting poorer electrode placement may cause broader neural activation; broader tuning was also associated with higher behavioral thresholds. In both comparisons, the PTC measurement more robustly predicted electrode placement and focused thresholds, suggesting that PTC ERBs are more sensitive to electrode position. The correlation between ERB measured with ECAP and PTCs was weak, but statistically significant. The long-term goal of this research is to develop a fast, non-radiologic method for estimating electrode position to improve device programming by reducing unwanted channel interaction.

PS 730

Neural Decoding of Attentional Selection in Multi-Speaker Environments Without Access to Separated Sources

James O'Sullivan¹; Zhuo Chen¹; Sameer Sheth²; Guy McKhann³; Ashesh D. Mehta⁴; Nima Mesgarani¹

¹*Columbia University*; ²*The Neurological Institute, Columbia University*; ³*Department of Neurological Surgery, The Neurological Institute, Columbia University*;

⁴*Hofstra Northwell School of Medicine and Feinstein Institute for Medical Research*

People suffering from hearing impairments can find it extremely difficult to follow a conversation in a noisy environment. Modern hearing aids can suppress certain types of background noise, but they do little to help a user attend to one speaker amongst many, because they cannot determine to whom a user is attending, and they cannot selectively amplify that speaker while suppressing all others. It has recently been shown to be possible to decode the attentional focus of a listener using both invasive and non-invasive neural recordings. This has led to a surge in research in this area, with the ultimate goal of developing a cognitively controlled hearing aid. However, current attention-decoding algorithms require explicit access to the isolated sound sources in the environment, which is not realistic. Beamforming has been proposed as a possible solution. However, this method has three major limitations: (1) it requires multiple microphones that are spatially distant from each other,

(2) it requires knowledge of the target's spatial location, and (3) it fails when the target and interfering speakers are in the same location. What is needed is a means of automatically segregating one speaker from another, regardless of their spatial location, and with a single microphone. Here, we address these challenges by using state-of-the-art single-channel automatic speech separation algorithms in which deep neural networks (DNNs) are used to separate the sound sources. The output of the speech separation algorithm can then be used to decode the attentional focus of the listener, and to subsequently amplify the attended target. Using invasive electrocorticography (ECoG) and stereotactic electroencephalography (sEEG) data, we successfully decoded the attention of users in seconds, and could quickly and reliably detect switches in attention. We show that the separation algorithm used produces a speech signal that is objectively cleaner (8.97 dB increase in Signal-to-Distortion-Ratio (SDR), and 40% relative increase in the Perceptual Evaluation of Speech Quality (PESQ) score). Such an improvement has shown to significantly improve the subjective experience for the hearing impaired.

PS 731

The Cognitive P300 Auditory Event-Related Potential: a Method to assess Bimodal Benefit?

Lindsey N. Van Yper¹; Ingeborg Dhooge¹; Katrien Vermeire²; Eddy De Vel¹; Andy J. Beynon³

¹*Department of Otorhinolaryngology, Ghent University Hospital, De Pintelaan 185, 1P1, B-9000 Ghent, Belgium*; ²*NYU Steinhardt, Department of Communicative Sciences and Disorders, 665 Broadway, 9th Floor, New York, NY 10012, USA*; ³*Radboud University Medical Centre, Donders Institute for Brain, Cognition and Behaviour Centre for Neuroscience, Department of Otorhinolaryngology, Head and Neck Surgery, Philips van Leijdenlaan 15, 6525 EX Nijmegen, The Netherlands*

Background

Bimodal hearing refers to the combination of a cochlear implant (CI) in one ear and residual hearing in the other ear. The contralateral residual hearing usually requires amplification by a conventional hearing aid (HA). Although most CI-users benefit from bimodal hearing, others seem to perform worse in bimodal compared to CI-only listening. This unexplained outcome variability impedes clinicians to provide evidence-based counseling regarding post-operative HA-use. There is thus a need for measures of bimodal benefit. This study explores whether bimodal benefit can be assessed using the cognitive P300 auditory event-related potential (ERP).

Methods

Five bimodal listeners were included in the study. Cognitive P300 ERPs were recorded using an oddball paradigm with a low-frequency tonal contrast. Subjects counted the amount of deviant stimuli. The accuracy of the stimulus count served as a measure of behavioral performance. To assess the benefit of wearing a contralateral HA, the CI-only and bimodal conditions were compared.

Results

In four out of five bimodal listeners, the P300 ERP improved in bimodal versus CI-only listening. In these subjects, morphology improved, latencies decreased, and amplitudes increased in the bimodal condition. Interestingly, the subject with the largest improvement in the P300 ERP also showed the largest improvement in behavioral performance. Conclusions: The present study suggests that CI-users generally benefit from wearing a contralateral HA in order to discriminate low-frequency tonal contrasts. In addition, these preliminary data suggest that the P300 ERP may be a valuable technique to objectify bimodal benefit.

PS 732

The Summating Potential is a reliable Marker of Electrode Position in Intra-cochlear Electro-Cochleography (ECochG)

Peter Baumhoff¹; Victor Helmstaedter²; José Santos Cruz de Andrade³; Peter Erfurt¹; Andrej Kral⁴

¹Hannover Medical School; ²Hannover Medical School, DFG Cluster of Excellence Hearing 4 All; ³Universidade Federal de São Paulo, UNIFESP / CAPES Foundation; ⁴Hannover Medical School, DFG Cluster of Excellence Hearing4all

Subjects with residual hearing are increasingly considered for cochlear-implantation. Thus hearing preservation during cochlear implantation is required. Monitoring of the position of the cochlear implant (CI) relative to the intact cochlear region during surgery could help to preserve residual hearing. We tested the reliability of positional information from intra-cochlear ECochG recorded through an implant in an animal model.

We implanted 40 cochleae in 20 normal hearing, anaesthetized guinea pigs (Dunkin Hartley) with custom CIs (MedEL, Innsbruck). The cochleae were implanted through a cochleostomy ~800 µm below the round window edge. ECochGs were recorded from the 6 CI contacts (spacing: 700 µm) during acoustic stimulation either simultaneously in monopolar recording configuration (n=18) or sequentially in bipolar configuration

(n=22).

Following the experiments, the ECochG signal was processed offline to analyze frequency-tuning, threshold and amplitude of compound action potentials (CAPs), cochlear microphonics (CMs) and summing potentials (SPs), separately. Additionally the intra-cochlear position of the CI was accessed by post-mortem histology and µCT imaging.

CAPs and CMs are suitable measures for the physiological integrity of the cochlea. CAP properties varied little along different intracochlear recording positions. Frequency and sound level dependent changes in CMs were complex and ambiguous. Both measures were strongly affected by cochlear damage. SPs were most sensitive to electrode position in monopolar and bipolar recordings. The most apical contact was identified to be located at a median of 8.98 kHz, while the most basal contact had a median of 22.63 kHz. The place-frequency function sloped on average with 2.30 mm per octave. The deviation from the slope of the Greenwood function (1991, 2.59 mm/oct) was less than half the distance between neighboring contacts.

After the experiments the implanted cochleae were harvested and the location of the electrodes of the CI was reconstructed using Micro-CT or a grinding technique (Stöver et al., 2005). Anatomically the length adjusted place-frequency function sloped with 1.74 mm/oct. Despite the considerably steeper slope only 2 datapoints deviated more than ½ octave between electrophysiological and anatomical reconstruction. The electrophysiologically determined intra-cochlear positions were in agreement with the post-mortem anatomical reconstructions of CI positions and the Greenwood-function. The results of our experiments point to intra-cochlear bipolar ECochG recordings and an analysis of the SP changes as suitable method for an intra operative monitoring of the position of an inserted CI.

This project was supported by the DFG within the Cluster of Excellence "Hearing4All" and MedEL Company (Innsbruck).

Gapless Interface Between Cochlear Implant and Auditory Neurons

Marcus Müller¹; Masaaki Ishikawa¹; Monika Kwiatkowska²; Pascal Senn³; Hubert Löwenheim⁴

¹University of Tübingen; ²University Tübingen; ³Department of clinical neurosciences, Service ORL and CCF, HUG, Geneva; ⁴University Tuebingen

Deafness can be cured by surgically implanting a cochlear implant. Electrical current is used to stimulate auditory neurons bypassing the function of cochlear hair cells. A critical part of the system is the cochlear implant electrode array in the scala tympani, spatially distant from the peripheral processes of the auditory nerve. This anatomical gap between the electrode array and the nerve fibres results in high current consumption and a low spatial stimulation specificity, resulting in variability of sound quality and speech understanding. Recent research findings indicate that peripheral processes can grow under neurotrophin stimulation towards the electrodes. The project aims at developing a neuroprosthesis with a gapless interface to auditory nerve fibres. Gel-like matrix candidates with adequate physico-chemical and biological properties were selected from in vitro experiments testing compounds and matrices for neurite outgrowth and physiological properties. The concept was tested in a series of in vivo experiments using guinea pigs deafened using a local application of a kanamycin/furosemide mixture. One week later a cochleostomy was performed and the scala tympani was filled with a hydrogel mixed with BDNF. Then a 4 channel cochlea implant provided by MedEl was inserted. Six weeks after implantation eCAP was measured and ears were fixed for histology. Application of the BDNF-gel resulted in improved physiological responses and, in rare cases, neurite outgrowth onto the cochlear implant. We observed neurite outgrowth to the position of the former organ of Corti, beyond that position neurites turned into the scala tympani and grew onto the cochlea implant. Our result that auditory neurons can be guided into the scala tympani onto the cochlear implant validates the concept to bridge the gap between the electrode array and the nerve fibres. Lowered eCAP threshold furthermore validates the concept of a potential decrease in energy consumption.

Pressure Difference Receiving Ears Influence ITD Detection In The Auditory Brainstem Of Alligators. (A. Missispiensis)

Lutz Kettler¹; Catherine Carr²

¹University of Maryland, College Park; ²University of Maryland College Park

The difference between the timing of sounds at both ears (interaural time difference, ITD) is a key feature for sound source localization. In archosaurs, the detection of ITD is assumed to be consistent with the Jeffress model, which consists of coincidence detectors and delay lines. Coincidence detectors receive input from both ears and respond maximally if the inputs converge simultaneously. Delay lines compensate for the range of external delays and innervate arrays of coincidence detectors, leading to the formation of a map or place code of ITD. A structure that resembles the Jeffress model has been found in the nucleus laminaris (NL) of archosaurs, including alligators and birds. Alligators, like most birds, are sensitive to ITDs at low frequencies, where coupled ears allow transmission of sounds through the dorsal and ventral sinuses that connect both middle ears. This internal coupling could increase the range of interaural time differences, and thus compensate for small head sizes. It also opens an additional way to detect ITDs, since the eardrum vibration in response to sound becomes directional, which may lead to spatial tuning in monaural nuclei, as for example in lizards. We hypothesized that alligator first order nuclei might be spatially tuned, since their eardrum responses have been shown to be directional. We therefore performed in vivo extracellular recordings in the auditory brainstem in American alligators. Neurons in the monaural nucleus magnocellularis (NM), which carry precise information about the stimulus phase, were tuned to interaural time difference. However, the amplitude of NM tuning curves was much smaller than the amplitude in NL. ITD tuning in NL also deviates from a classic delay line model, because we found many units with characteristic phases around 0.5, which means that the characteristic delay lies in the trough of the ITD tuning. Additionally, some recording sites within NL had characteristic delays that differed for low and high frequencies, with a cutoff frequency around the resonance frequency of the interaural canal, above which ear drum directionality drops. Thus, directional sensitivity in nucleus magnocellularis might influence ITD detection in NL.

Activity-dependent Changes in Calcium Signaling in the Medial Superior Olive (MSO) During Late Postnatal Development

Delwen L. Franzen¹; Sarah Gleiss¹; Christian J. Kellner¹; Felix Felmy²; Louise Delwen Franzen³

¹*Department Biologie II, Ludwig-Maximilians-Universität, Munich;* ²*Institut für Zoologie, Stiftung Tierärztliche Hochschule Hannover, Germany;* ³*Ludwig-Maximilians-Universität München*

Binaural coincidence detector neurons of the gerbil MSO encode sound localization cues with microsecond precision by integrating excitatory and inhibitory inputs. The inhibitory input to these neurons has been shown to refine around hearing onset in an experience-dependent manner, and is accompanied by severe developmental changes in the cell's biophysical properties. To further understand how MSO neurons refine and mature, we investigated their developmental regulation of calcium entry. Calcium is an important second messenger associated with neuronal refinements.

Whole-cell recordings were carried out in acute slices from Mongolian gerbils around hearing onset at postnatal day (P) 10 - 18 and at mature stages (P60) to simultaneously image calcium transients evoked by synaptic and action potential (AP) stimulations. Before and during hearing onset, a strong calcium influx was evoked by both APs and EPSCs. However, from P13 onwards the AP-evoked calcium influx decreased rapidly and was undetectable at P60, as a result of a developmental decrease in AP amplitude and T-type calcium currents. Moreover, the NMDAR component of the EPSC declined drastically from P13 onwards. At mature stages a significant dendritic calcium transient was only driven locally through AMPARs. Thus, our findings show that calcium entry shifts from a pre- and postsynaptic activity dependence to predominantly a presynaptic activity dependence.

Previous studies have shown that depriving gerbils of correlated binaural inputs around hearing onset prevents the refinement of the inhibitory input to the soma of MSO neurons, suggesting that the refinement of the MSO circuit depends on experience. Therefore, we repeated our experiments in gerbils (P13 - P18) raised from P8 - P9 in omnidirectional white noise, and found that both AP-evoked and synaptically induced calcium signals resembled that of more mature stages in gerbils raised normally. Similarly, the loss of the T-type calcium current occurred slightly earlier in noise reared animals. The decay time constant of both evoked synaptic inputs and miniature EPSCs was faster in P14 gerbils exposed

to noise. In turn, while the size of single inputs at P14 increased to values characteristic of more mature stages, the size of miniature EPSCs remained unchanged, resulting in an effective increase in quantal content following noise exposure. Taken together, our data suggest that the synaptic properties and calcium signaling of MSO neurons in gerbils raised in omnidirectional white noise display characteristics of accelerated maturation.

PS 735

Activity Dependent Long-term Potentiation of MNTB-LSO Connections

Eva Bach¹; Karl Kandler²

¹*University of Pittsburgh, Department of Otolaryngology;*

²*University of Pittsburgh School of Medicine*

The lateral superior olive (LSO) in the mammalian brainstem receives tonotopically organized, inhibitory inputs from the medial nucleus of the trapezoid body (MNTB). During early postnatal development, the MNTB-LSO pathway is topographically refined through synaptic strengthening and silencing of connections. Activity-dependent changes in synaptic strength, such as long-term potentiation (LTP) or long term depression (LTD) are thought to represent the first steps in the activity-dependent reorganization of neuronal circuits, but LTP at MNTB-LSO synapses prior to hearing onset has not been demonstrated. We revisited LTP in this pathway by taking into account the characteristic temporal firing patterns of neonatal MNTB neurons. By mimicking in-vivo patterns to stimulate MNTB fiber tracts in auditory brainstem slices of prehearing mice (P5-8), we were able to reliably induce LTP in LSO neurons. Tetanic stimulation at 100 Hz, commonly used to induce LTP in other circuits, or equally spaced stimuli over a duration equivalent to that used for semi-natural pattern stimulation failed to induce LTP. Further variations of the temporal structure of the stimulus patterns revealed that stimuli with interstimulus-intervals of 5 ms (200 Hz) are essential and sufficient for the induction of LTP. Semi-natural-pattern stimulation was effective in inducing LTP when GABA-A and inotropic glutamate receptors were inhibited, implicating that LTP in the MNTB-LSO pathway potentiates glycine receptor mediated transmission. LTP was calcium dependent, but N-Methyl-D-aspartate (NMDA) receptors were not essential for its induction. Blocking GABA-B receptors, mGLURs, or activation of intracellular G-proteins with GDP- β -s prevented the induction of LTP. The potentiation of glycine-mediated transmission that we observed in this study is in congruence with the transition from a predominantly GABAergic to an almost exclusively glycinergic MNTB-LSO synapse that accompanies synaptic strengthening during development. Our results suggest that the transient

GABAergic and glutamatergic phenotype of MNTB-LSO synapses is important for tonotopic refinement by enabling the induction of LTP resulting in synaptic strengthening via an increase of glycinergic transmission.

NIDCD DC-011499 DSF Charitable Foundation Fellowship, 132RA03 (EB)

PS 736

FMRP in Dendritic Development and Axonal Guidance of Developing Auditory Brainstem

Xiaoyu Wang¹; Diego Zorio¹; Leslayann Schecterson²; Hitomi Sakano²; Edwin Rubel²; Yuan Wang¹

¹Florida State University; ²University of Washington

Fragile X syndrome (FXS) is the leading cause of inherited mental retardation and autism, characterized by a constellation of visual, auditory and motor dysfunction. FXS results from the absence of fragile X mental retardation protein (FMRP), an mRNA-binding protein that pleiotropically regulates protein translation. It is known that FMRP is important for proper wiring and function of neuronal circuits. However, it is not known exactly how FMRP regulates auditory development and how its loss leads to auditory dysfunction in FXS.

In this study, we characterize the function of FMRP in the developing auditory brainstem of birds. The chicken nucleus magnocellularis (NM) and nucleus laminaris (NL), analogues to the mammalian anteroventral cochlear nucleus (AVCN) and medial superior olive (MSO), are important for temporal processing and binaural hearing, two functions that are compromised in FXS.

Western blotting on micro-dissected tissue samples from NM and NL, reveals significantly stronger expression of FMRP during development than in mature systems. Importantly, immunocytochemical studies further revealed an accumulation of FMRP at dendritic branch points, implying a role of FMRP in dendritic branching. We next examined the effect of knocking down FMRP expression on the development of NM/NL circuit by introducing shRNAs into unilateral neural tube via in ovo electroporation. Consistent with previous studies, non-transfected NM neurons display dendrites before embryonic day 15 (E15) with progressive loss of dendrites afterwards. In contrast, transfected neurons with reduced FMRP protein level exhibit extensive dendrites at E15 with persistence of dendrites in some neurons until E19, indicating delayed dendritic pruning. Moreover, transfected NM neurons display abnormal axonal projection. Normally, NM axons projecting to the contralateral NL are restricted to the ventral dendrites of NL. Axons of transfected NM neurons terminate in both dendritic layer as well as

the somatic layer of contralateral non-transfected NL, suggesting presynaptic desensitization to repulsive signal in NL.

These data demonstrate that normal FMRP expression is required for correct dendritic development and axon guidance of NM neurons. To start exploring the underlying mechanisms, we examined the effect of FMRP knock-down on the protein level of calretinin. Calretinin is a FMRP targeted calcium binding protein, deletion of which leads to increased neuronal excitability. We found significantly lower calretinin immunoreactivity in transfected NM neurons as compared to neighboring non-transfected neurons. Ongoing studies are investigating how FMRP knockdown caused structural and protein expression deficits affect the biophysics and function of NM neurons in temporal processing and binaural hearing.

PS 737

Characterization of Possible Fmrp Substrates in Chicken Nucleus Laminaris

Hitomi Sakano¹; Xiaoyu Wang²; William Noble¹; Michael MacCoss¹; Edwin Rubel¹; Yuan Wang²

¹University of Washington; ²Florida State University

The avian nucleus laminaris (NL) is an auditory brainstem nucleus, analogous to the mammalian medial superior olivary nucleus (MSO), and essential for binaural temporal processing of low frequency sounds. Recent evidence suggests that fragile X mental retardation protein (FMRP) (loss of which leads to fragile X syndrome (FXS)) is concentrated in the dendritic branch points of NL neurons, suggesting a possible role of FMRP in NL dendritic regulation. FXS is a common hereditary autism spectrum disorder with sensory and speech abnormalities. It is known that patients exhibit behavioral abnormalities to repeated auditory stimulation and in temporal processing, however, the underlying mechanisms are not known. Evidence in other systems suggest that FMRP affect dendrites by regulating local translation of mRNA transcripts and such regulation appears to be cell-type specific. Studying the proteins whose expression is regulated by FMRP in NL is expected to shed lights on understanding the mechanisms of FMRP regulation in normal brains and auditory dysfunction of FXS.

Here we present a proteomic characterization of the NL. NL tissue was specifically collected from brainstem cryosections using laser micro-capture. Following protein extraction and digestion, 657 proteins are identified by chromatography tandem mass spectrometry. These proteins were represented highly by those involved in mitochondria, translation and metabolism, consistent with a

highly metabolic environment of NL neurons. By comparative analysis, we identified a subset of 96 proteins that are putative protein products of FMRP substrates. Gene ontology analysis reveals that these proteins are represented highly by pathways involved in cytoskeleton and intracellular transport, consistent with the proposed role of FMRP in structural dynamics of NL dendrites. Using immunohistochemistry and specific antibodies, we confirm the localization of a number of these candidates in NL dendrites and continue to evaluate more. This study provides a promising list of potential targets for studying the mechanism of FMRP regulation of auditory neurons.

PS 738

A Role for Glycine in Altered Excitation and Inhibition in the Auditory Brainstem of Fragile X Mice.

Elizabeth McCullagh A. McCullagh; Achim Klug;
Molly M. Huntsman; Elizabeth A. McCullagh
University of Colorado Anschutz

The sound localization pathway, in the auditory brainstem, helps us to make sense of a conversation in situations where distracting background sounds are present, and forms the neural basis for our cognitive ability to focus on the sound source of interest. Being unable to localize the source of a sound, and to focus on a conversation when distracting noises are present, is a cardinal symptom in autistic patients. This autism related auditory dysfunction is most noticeable as impairments in communication skills, social difficulties and sound localization. A recent theory posits that autism spectrum disorders may be caused by an imbalance in the ratio of excitation to inhibition, particularly in sensory systems. Since sound localization relies heavily upon the synaptic ratio of excitation and inhibition (E/I ratio) in the auditory brainstem, we hypothesized that these neural circuits may be altered in a mouse model of autism, the Fragile X mouse (Fmr1^{-/-}).

We investigated differences in presynaptic and markers for the neurotransmitters glutamate, glycine and GABA in the nuclei of the mammalian sound localization pathway, specifically the medial nucleus of the trapezoid body (MNTB), cochlear nucleus (posterior (PVCN), dorsal (DCN) and anterior (AVCN)) and the lateral superior olive (LSO). These centers receive substantial excitatory and inhibitory inputs and relay sound information to each other through.

Recently, it has been shown that there are more presynaptic GABAergic synapses in the MNTB of Fmr1^{-/-} mice as indicated by vesicular GABA transporter (VGAT). This study, however, did not investigate the effect of glycine, which, in the MNTB, becomes the primary inhibito-

ry neurotransmitter in adulthood. The main reason why glycine has not been studied in the context of Fragile X is that the current E/I model of Fragile X assumes most changes occur in GABAergic inhibition. Here we address the role of glycine in Fmr1^{-/-} mice by anatomical studies examining changes in number and organization of glycinergic neurons and synapses in the MNTB. Our results suggest that the glycinergic E/I ratio in Fmr1^{-/-} mice is altered, suggesting that not only GABAergic but also glycinergic inhibition may play an important role in auditory impairments seen in Fragile X.

PS 739

Principal Neurons in the Medial Superior Olive Form Two Subtypes with Contrasting Functional Properties

Brian J. Bondy; Nace L. Golding
Department of Neuroscience and Center for Learning and Memory, University of Texas at Austin

Interaural time differences (ITDs) are critical cues for localizing sounds in the azimuthal plane. To detect ITDs, the principal neurons (PNs) of the medial superior olive (MSO) exhibit biophysical specializations that confer selectivity for coincident, fast fast-rising synaptic depolarizations. However, these specializations make them poorly suited for detecting ITDs generated by low-frequency envelopes of high-frequency sounds, such as AM stimuli. In analogous neurons in birds, tonotopic differences in the morphology and electrical properties of cells in the high-frequency region impart functional properties better suited for envelope ITD detection. However, whether such tonotopic specializations exist in mammals is unclear.

We performed whole cell patch clamp recordings of MSO neurons in gerbil brainstem slices (P18-P80, 35° C) to correlate intrinsic membrane properties with topographic location within the nucleus. Cells were filled with biocytin, and all slices were saved so the entire MSO, as well as the recorded cells, could be reconstructed with NeuroLucida. This allowed us to determine the position of each cell within the MSO. Additionally, in some cells the responses of MSO neurons to bilateral cochlear nucleus axon stimulation was investigated.

We recorded from over 300 identified MSO neurons, 200 of which were characterized as PNs. PNs showed no differences in intrinsic membrane properties as a function of location within the MSO. The remaining cells were either the multipolar nonprincipal neurons (which, in fact, project out of the MSO,) or a previously undescribed subgroup of PNs clustered at the high- and low-frequency regions of the MSO that we have named oscillator neurons (ONs). Although the morphology of

ONs exhibited significant overlap with PNs, ONs could be distinguished from other neuron types by the presence of sub-threshold oscillations that drive repetitive spiking during long depolarizations. Like PNs, ONs received bilateral excitation and inhibition, but had input resistances and membrane time constants that were 4-5 times higher than those of PNs. Accordingly, in response to synaptic coincidence detection paradigms, ONs had 3-4-fold broader ITD-like response functions. In response to current injections that mimicked AM envelopes, PNs displayed a band-pass filtering response, firing best to 300-500Hz envelopes (range: 200-1000 Hz). By contrast, ONs acted as an all-pass filter, firing phase-locked action potentials at a relatively stable rate regardless of envelope frequency. Based on these results we hypothesize that both ONs and PNs jointly enable the MSO to encode sound localization information about both acoustic fine structure and envelopes.

PS 740

Developmentally Restricted Long-term Potentiation of Glycinergic Inhibition onto Neurons of the Medial Superior Olive

Bradley D. Winters; Nace L. Golding

Department of Neuroscience and Center for Learning and Memory, University of Texas at Austin

Medial superior olive (MSO) neurons are coincidence detectors that signal minute interaural time differences (ITDs) used for sound localization. Glycinergic inhibitory inputs onto MSO neurons are critical for sharpening their ITD responses. The inhibitory synaptic inputs are dramatically refined after hearing onset; supernumerary inhibitory inputs are pruned and the few that remain are well timed with binaural excitation and restricted to the soma and proximal dendrites. Little is known about the cellular mechanisms that guide these experience-dependent refinements.

We used whole-cell recordings in acute brain slices at 35°C from Mongolian gerbils (P12-32) to explore inhibitory synaptic plasticity in the MSO. To induce inhibitory plasticity, we isolated glycinergic IPSPs with AMPAR blocked (15 μ M NBQX), then paired glycinergic and NMDAR mediated PSPs (200 Hz bilateral stimulation) with action potentials (APs) triggered by 1 ms current injections. Plasticity relative to a 10 minute baseline was evaluated from the average of 24-34 minutes after induction.

The induction protocol resulted in a robust long-term potentiation of inhibitory potentials (iLTP) in MSO neurons early in the first week of hearing (P13.5; 44 \pm 8% increase). Neither APs nor electrical stimulation alone were sufficient to induce iLTP, suggesting synapse

specificity. Intracellular application of the calcium chelator BAPTA (15 mM) blocked induction of iLTP, as did both external and internal application of the use-dependent NMDAR antagonist MK-801. Thus, calcium influx through postsynaptic NMDARs is a critical mechanism underlying iLTP.

We found that iLTP was age-dependent (P19: 20 \pm 10% increase; P30: -1 \pm 7%) and mirrored the decline in AP amplitude over development. Indeed, in dual somatic-dendritic recordings (up to 84 μ m from soma) just before hearing onset (P10) APs reached +25 mV and backpropagated effectively into the dendrites, but just a week later (P17), APs at the soma reached only -19 mV and exhibited robust attenuation in the dendrites. To test whether the lack of iLTP at older ages results from the inability of smaller APs to sufficiently relieve the Mg²⁺ block on NMDARs, we delivered our iLTP induction protocol with the APs replaced with larger, wider depolarizations in voltage clamp. This manipulation rescued iLTP (P30: 57 \pm 14% increase).

Our data indicates that calcium influx through NMDARs triggered by backpropagating APs selectively reinforces the strength of inhibitory synapses that are well timed with binaural excitation. Further, the decrease in AP amplitude and backpropagation over the first two weeks of hearing places developmental limits on this plasticity.

PS 741

Targeted Presynaptic Loss of DRP1 at the Calyx of Held Results in Altered Ca²⁺ Homeostasis, and Enhances Depletion of the Readily-releasable Pool

Robert Renden¹; Mahendra Singh¹; Henry Denny¹; Heinz Horstmann²; Thomas Kuner³

¹*University of Nevada, Reno School of Medicine;*

²*Universität Heidelberg, Institut für Neuroanatomie und Zellbiologie;* ³*Universität Heidelberg, Institut für Anatomie und Zellbiologie*

Synaptic transmission at glutamatergic synapses during repetitive trains of stimuli is affected when presynaptic mitochondrial function or localization is disrupted, but the underlying mechanism is poorly understood. In this study we investigate the role of mitochondria in synaptic vesicle (SV) recycling at the calyx of Held, by eliminating Dynamin-Related Protein-1 (DRP1) selectively in the presynaptic terminal. DRP1 mediates mitochondrial fission. In other neuronal systems, DRP1 loss results in larger, and sometimes mislocalized presynaptic mitochondria. However, glutamatergic synapses are maintained, and postnatal DRP1 loss does not result in neuronal cell death. Floxed-DRP1 (DRP1^{fl/fl}) mice were injected with AAV-cre-GFP at postnatal day 1 (P1) to inhibit DRP-1 expres-

sion presynaptically, and morphology and physiology of the calyx synapse examined at P16 – P18. Infected (GFP+) cell soma in the ventral cochlear nucleus lacked any discernable DRP1 signal, and the calyx of Held terminal in the contralateral medial nucleus of the trapezoid body showed reduced DRP1 protein via anti-DRP1 staining, generating a presynaptic-specific DRP1-KO (DRP1-preKO). Volumetric reconstruction of the calyx terminal using confocal microscopy showed presynaptic mitochondria were present in DRP1-preKO calyces, and that mitochondrial size was significantly increased. We also observed a relative mislocalization of SV within the presynaptic terminal, as loss of ‘donut’ structures. Post-synaptic recordings from innervated Principal cell nuclei showed that DRP1-preKO resulted in increased release probability, and a 3-fold increase in spontaneous synaptic activity (mEPSC). However, quantal size was unaffected. In response to high-frequency stimulation, we observed 3-fold faster depression, and reduced steady-state transmission. RRP recovery following depression was also strongly depressed in DRP1-preKO synapses. Estimates of the readily-releasable pool (RRP) size suggest that DRP1-preKO contain half the normal population of SVs. Taken together, these results suggest that decreased mitochondrial health due to loss of DRP1 at the presynaptic terminal results in failure in several mechanisms, including: management of free cytosolic Ca²⁺, SV recycling, and RRP size. Ongoing experiments aim to determine the specific mechanism underlying the presynaptic defect in synaptic transmission.

PS 742

In-vivo Intracellular Characterization of ITD Sensitivity in the Dorsal Nucleus of the Lateral Lemniscus

Mark Sayles¹; Philip X. Joris²; Philip H. Smith³

¹Purdue University; ²University of Leuven; ³University of Wisconsin - Madison

Sensitivity to micro-second inter-aural timing differences (ITDs) emerges in specialized neurons in the medial superior olive (MSO), and underlies many aspects of spatial hearing. Axonal projections from MSO neurons ascend in the lateral lemniscus. Their post-synaptic targets include the dorsal nucleus of the lateral lemniscus (DNLL) and inferior colliculus (IC). We characterized the in-vivo intracellular responses of neurobiotin-labelled DNLL neurons to binaural sounds, and compared their responses to those obtained from MSO axonal recordings.

We used high-impedance (150-200 MΩ) sharp pipettes to record from axons and cell bodies in the lateral lemniscus of the anesthetized chinchilla. The pipette internal solution included neurobiotin, allowing labelling of

recorded neurons by injection of current pulses during intra-axonal or intra-cellular recording. We presented binaural-beat stimuli (typically, 1-Hz beat with a range of carrier frequencies), and broadband noise at a range of ITDs. Several DNLL cells were recovered anatomically.

In contrast to responses from MSO axons, DNLL responses are very broad in frequency tuning and often show areas of inhibition. Intracellular voltage records from DNLL cells could show an “iceberg” effect during presentation of binaural-beat stimuli. Periods of depolarization and spiking synchronized to the beat ride on sustained hyperpolarization of unknown origin. Excitatory post-synaptic potentials phase-locked to the carrier frequency were present in most cases. Similar sustained hyperpolarization was also present in DNLL cells’ responses to broadband noise at some ITDs. Depolarization could overcome this at other ITDs to give robust spiking to inter-aurally delayed noise, and therefore a strongly modulated firing-rate vs. broadband ITD function.

Supported by a postdoctoral fellowship of the Research Foundation - Flanders (FWO) [M.S.], NIH (R01 DC012782 [P.H.S. and P.X.J.]), FWO (G.091214N and G.0961.11[P.X.J.]) and Research Fund KU Leuven (OT/14/118 [P.X.J.]).

PS 743

Role of Low and High Frequency Cues in Subcortical Neural Representation of Envelope and Temporal Fine Structure

Saradha Ananthakrishnan; Danielle Yurjevich; Laura Grinstead

Towson University

Background

Auditory electrophysiology studies have established that brainstem neural representation of important acoustic features such as envelope and temporal fine structure cues is altered in sensorineural hearing loss (SNHL). Envelope cues are low frequency in nature and correspond to fundamental frequency of the speech stimulus, while TFS cues are higher frequency in nature, corresponding to harmonics and formants in the speech stimulus. Previous research indicates that in individuals with normal/near-normal low frequency hearing and mild-moderate high frequency hearing loss, brainstem envelope representation was reduced as compared to normal hearing listeners at equal sound pressure levels (SPL) but not at equal sensation levels (SLs). On the other hand, brainstem TFS cue representation remained affected in these listeners as compared to those with normal hearing, regardless of whether the stimuli were presented at equal SL or SPL. Collectively, these findings suggest that high

frequency audibility may play an important role in subcortical representation of envelope but not TFS cues. The aim of the current study is to describe the nature of subcortical envelope and TFS representation in listeners with normal hearing as high and low frequency cues in the stimulus are systematically varied using low- and high-pass filtering.

Methods

FFRs were collected in normal hearing adult listeners in response to a steady state speech stimulus presented in an intact and various high- and low-pass filtered conditions (cut-off frequencies ranged from .125-8 kHz). For each condition, envelope and spectral FFRs were extracted, and subjected to temporal and spectral analyses, including an examination of waveform amplitudes, autocorrelation analysis, and Fast Fourier Transform (FFT) analysis.

Results

Preliminary results indicate that brainstem envelope representation increases as a function of low-pass filter setting; the relationship between brainstem TFS representation and the low-pass filter setting seems more variable. Pilot data suggests that increasing the high-pass filter setting has a comparatively lesser effect on envelope representation, while strength and precision of TFS representation appear to reduce.

Conclusions

Initial results suggest that high-frequency cues may drive subcortical envelope representation to a greater extent than low-frequency cues, while low-frequency cues strengthen brainstem representation of TFS cues. A bigger sample size and detailed statistical analysis are needed to confirm these findings.

PS 744

Evidence That the Tinnitus-inducing Agent Salicylate Has a Direct Effect on Neural Activity in the Inferior Colliculus

Bas Olthof-Bakker; Dominika Lyzwa; Sasha Gartside; Adrian Rees
Institute of Neuroscience, Newcastle University

High doses of sodium salicylate induce tinnitus in humans and animals. Salicylate reportedly increases spontaneous firing rates in neurons in the inferior colliculus (IC), although it is unclear whether these effects are mediated up-stream of the IC, or directly within the IC. We addressed this question by comparing the effects of systemic and locally applied salicylate on IC neuronal activity.

Pigmented guinea pigs (350-650 g) were anaesthetised (Urethane 1g/kg i.p., Fentanyl 0.3 mg/kg i.p. and Midazolam 5mg/kg i.m.) a microdialysis probe and a single shank 32-channel recording electrode were implanted in the right IC. Spontaneous and sound-evoked multiunit activity was recorded at sites through the IC at baseline and after salicylate administration. In 7 animals the microdialysis probe was perfused with artificial cerebrospinal fluid throughout and salicylate was administered systemically (200mg/kg i.p.). In the other 3 animals the microdialysis probe was perfused with artificial cerebrospinal fluid followed by salicylate at increasing concentrations (0.1mM (2h), 1mM (2h) and 10mM (1h)).

Following systemic injection of salicylate, spontaneous activity remained unchanged for the first three hours, but then increased rapidly to more than double six hours post salicylate administration. In contrast, local delivery of salicylate into the IC reduced spontaneous activity in a time/concentration-dependent manner. Frequency response areas (FRAs) recorded following systemic salicylate showed a reduction in driven multiunit activity on the low frequency side of the CF during the first two hours. Later, an increase in driven activity was observed across the entire FRA. These changes resulted in an increase of the compound CF. Local administration of salicylate also increased driven activity across the FRA. Again this resulted in an increase in the measured CF. It was notable that neither mode of application of salicylate altered the minimum threshold for driven responses.

These results confirm previous findings of increased spontaneous rate and sound-driven activity in response to systemic salicylate. Since salicylate applied locally in the IC decreased rather than increased spontaneous activity, we conclude that the elevation of spontaneous firing by salicylate is mediated outside the IC. Similarly, the initial effect of systemic salicylate in reducing sound-driven activity in a frequency-selective manner was not mirrored by locally applied salicylate and hence likely originates elsewhere. However, the finding that both locally applied and systemic salicylate raised the CF and increased sound driven activity, suggests that these effects are, at least in part, mediated directly within the IC.

Supported by Action on Hearing Loss

PS 745

Subcortical and Cortical Encoding of Complex Tones in Informational Masking

Axelle Calcus¹; Leonard Varghese²; Barbara Shinn-Cunningham²

¹University College London; ²Boston University

Introduction

In everyday auditory scenes, listeners have to perform the challenging task of focusing on a relevant sound source while ignoring ongoing, possibly irrelevant sounds. Both peripheral (i.e., sensory) and central (i.e., cognitive) interference, or masking, contribute to the difficulties encountered in noisy backgrounds. "Informational masking" (IM) occurs at the central level of the auditory pathway, and reflects interference that cannot be explained by simple spectrotemporal overlap of auditory sources. Previous studies have shown that the neural correlates of release from IM are present in the representation of the auditory scene at the level of the auditory cortex (e.g., Gutschalk, Micheyl & Oxenham, 2008). The aim of this project was to determine whether neural correlates encoding of release from IM are also present at the subcortical stages (i.e., brainstem) of the auditory pathway.

Methods

We utilized subcortical and cortical EEG recordings to evaluate the neural encoding of sounds under informational masking in adults with normal hearing thresholds. Listeners ($n = 23$) were asked to detect a regularly repeating complex tone that was embedded in a randomly varying background of complex tones. There was no spectral or temporal overlap between the target and masker. This design choice minimized interference in the peripheral representation ("energetic masking"), while maximizing central interference between targets and maskers (IM). Targets were classified as detected or undetected based on behavioral responses. We hypothesized that in the absence of any peripheral interference between the target and masker, a larger N1 response would be evoked by detected compared to undetected targets. A larger subcortical envelope-following response (EFR) for the detected targets would either reflect an early enhancement of the target, or an efferent modulation of the subcortical response.

Results

Larger N1 responses were observed for detected targets compared to undetected targets. However, no such differences were observed in subcortical EFRs.

Discussion

The observation of larger N1s for detected targets is in agreement with previous studies. While the absence of

significant differences in subcortical results does not rule out their presence, it supports that view that any such differences are modest compared to more central effects.

PS 746

Perineuronal Nets in Subcortical Auditory Nuclei of Species with Different Hearing Ranges: A Study Using Multiple Markers

Nichole L. Beebe; Brett R. Schofield
Northeast Ohio Medical University

Perineuronal nets (PNs) are aggregates of extracellular matrix that inhibit structural plasticity and support fast-spiking in the cells they surround. PN distribution is believed to vary depending on species but this assumption is based on the use of different markers and staining protocols. We applied two widely-used markers to examine PNs in auditory nuclei of four species with different frequency ranges of hearing: low frequency (naked mole rats), wide range (guinea pigs) and high frequency (rats, CBA/CaJ mice). PNs were stained with Wisteria floribunda agglutinin (WFA) and anti-aggregan (AGG) (AB1031; Millipore).

PN distribution was nucleus- and species-dependent. PNs were more or less common in the ventral cochlear nucleus, but PNs were striking in the dorsal cochlear nucleus of guinea pigs whereas they were absent in this nucleus in the other species. The medial nucleus of the trapezoid body (MNTB), was strikingly similar across all species. PNs in the MNTB stained heavily using both markers. The medial superior olivary nucleus (MSO) showed intense, even staining with AGG and minimal staining with WFA. The lateral superior olivary nucleus (LSO) had PNs stained with WFA, AGG or both markers; the PNs were not distributed uniformly, but did not appear related to the tonotopic axis. PNs in lemniscal nuclei stained with WFA and AGG (most intensely in guinea pigs and least so in naked mole rats). PNs in the inferior colliculus (IC) stained with both markers. The medial geniculate body (MG) is devoid of PNs except for a pocket of AGG stained PNs in the medial MG in guinea pigs, mice and rats.

In conclusion, PNs were observed in many areas across all species examined. Some areas consistently stained for PNs (esp. MNTB, MSO, medial MG); others had almost no staining (e.g., most of MG). We found no consistent relationship between PN distribution and sound frequency. This was true when comparing 1) species with different hearing ranges, 2) nuclei with different frequency biases (e.g., LSO vs. MSO) or, 3) cells in different tonotopic regions of a single nucleus. From a technical perspective, neither WFA nor anti-aggregan can be

considered a “universal” marker for PNs in auditory nuclei. In some regions, most PNs stain with both markers, in other areas most PNs stain with one marker or the other. In short, the best PN marker for a particular nucleus has to be determined experimentally. Supported by R01 DC004391

Development II

PS 747

Drop-Seq as a Lower-Cost, High-Throughput Method for Single-Cell Gene Expression Profiling of Cochlear Cells

Joseph C. Mays¹; Joseph C. Burns²; Matthew W. Kelley³; Michael C. Kelly¹

¹Laboratory of Cochlear Development, NIDCD, Bethesda, Maryland, USA; ²Decibel Therapeutics; ³Laboratory of Cochlear Development, NIDCD, NIH, Bethesda, Maryland, USA

The mammalian cochlea is comprised of diverse cell types that vary significantly in structure and function. Single-cell mRNA sequencing (scRNA-seq) is able to provide transcriptomic profiles of individual cochlear cells to help to characterize the genetic heterogeneity between cell types. While this is a powerful method for studying complex tissues, commercial platforms for scRNA-seq can be prohibitively costly and low-throughput, preventing the generation of data sets from a sufficient number of cochlear cells of each type. Here, we utilize the Drop-Seq technique (Macosko et al., 2015) as a lower-cost, high-throughput method for performing single-cell RNA-seq on cochlear tissue. Drop-Seq allows for the generation of transcriptomes from individual dissociated cells by capturing mRNA from each cell with barcoded beads contained in nanoliter droplets. mRNA is reverse-transcribed and unique barcodes are used to map sequenced reads back to individual cells in order to efficiently generate expression data for each cell.

While the depth of coverage is lower than that of commercial platforms, Drop-Seq allows for a broad survey of cells to be processed at once. Utilizing this method, we have generated expression data from cochlear cells at late embryonic and early postnatal time points. We have compared these transcription profiles to existing scRNA-Seq data generated using the Fluidigm C1 platform and find that we can identify the same major cell types. The lower relative cost of droplet-based scRNA-Seq methods, such as Drop-Seq, make it a reasonable gene expression profiling technique to assess transcriptional changes at single-cell resolution in various

experimental paradigms. To demonstrate this, we have compared Drop-Seq scRNA-Seq data from control cultured or HDAC-treated cochlear explants, which show cell type-specific morphological and molecular changes. Differential expression analysis shows transcriptional profile changes both at the whole-tissue level, and unique changes within individual cell types following HDAC inhibitor treatment, providing insight into the role that histone dynamics play in cochlear development and maintenance of cell states.

These results illustrate the potential use of droplet-based scRNA-Seq methods for surveying normal and perturbed gene expression profiles of cells within the mammalian cochlea. Though some trade-offs are made in sensitivity and ease of use, the lower cost and higher-throughput make Drop-Seq attractive for a variety of applications. In addition to using these methods to characterize transcriptional changes in mutant and drug-treated tissue, we also hope to utilize transcriptional profiles to help optimize culture conditions so that our in vitro models best represent in vivo conditions.

PS 748

Technical Comparison of Four Single-Cell RNA-Seq Methodologies in Newborn Mouse Cochlea

Kathy So¹; Matthew Nguyen¹; Michael C. Kelly²; Hanna Sherrill³; Joseph C. Mays³; Matthew W. Kelley⁴; Joseph C. Burns¹; Adam Palermo¹

¹Decibel Therapeutics; ²Laboratory of Cochlear Development, NIDCD, NIH; ³Laboratory of Cochlear Development, NIDCD, Bethesda, Maryland, USA; ⁴Laboratory of Cochlear Development, NIDCD, NIH, Bethesda, Maryland, USA

A variety of new methodologies are emerging for profiling the levels of transcripts in dissociated single cells, several of which have been applied to inner ear biology. Whole transcriptome profiling of single cells with RNA-Seq is particularly attractive since it allows for unbiased identification of genes that have not been previously implicated in the model under study. There are a number of considerations when evaluating the pros and cons of these methods, including, but not limited to, throughput of single cell capture, fraction of input cells captured, protocol duration, fraction of the transcriptome recovered, and cost per cell. We have systematically compared these parameters for newborn mouse cochlea cells captured on four different platforms: Fluidigm C1 (microfluidics), FACS-based single-cell sorting, Drop-Seq (droplet microfluidics), and 10X Genomics Chromium (droplet microfluidics). The chemistry used for RT-PCR of single-cell mRNA is a major determinant of transcript yield and cost, so we also compared multiple RT-PCR

chemistries using the FACS system. RT-PCR was performed according to published protocol with the non-FACS methods. We found that the Fluidigm C1 system has the greatest sensitivity, detecting the highest number of expressed genes per cell on average. However, the Fluidigm system had the lowest throughput, the longest capture duration, and the highest cost. Drop-Seq and the 10X Genomics Chromium systems detected the fewest numbers of genes per cell, but also had the highest throughput and lowest costs per cell. For droplet microfluidics systems, the 10X Genomics Chromium had several important advantages over Drop-Seq, such as higher numbers of genes detected per cell, 10-fold shorter capture durations, and a 4:1 ratio of input cells to captured cells. Interestingly, we found that resolution of cellular heterogeneity appeared to be more dependent upon the number of cells captured than the number of genes detected per cell, suggesting that sequencing large numbers of cells at shallow depth is advantageous for detecting distinct cell types and subtypes. Finally, we found that RT enzyme type and efficient removal of residual primers are critical parameters that should be considered when reverse transcribing and amplifying single-cell mRNA. In summary, we present an in-depth technical guide that should help researchers to select the appropriate methodology for experiments that could be aided by single-cell RNA-Seq.

PS 749

Single-cell RNA-Seq Reveals Transcriptional Diversity in the Spiral Ganglion

Hanna Sherrill¹; Michael C. Kelly¹; Tessa Sanders¹; Joseph C. Burns²; Robert Morell³; Matthew W. Kelley⁴
¹Laboratory of Cochlear Development, NIDCD, Bethesda, Maryland, USA; ²Decibel Therapeutics; ³Genomics and Computational Biology Core, NIDCD, NIH, Bethesda, Maryland, USA; ⁴Laboratory of Cochlear Development, NIDCD, NIH, Bethesda, Maryland, USA

Spiral ganglion (SG) neurons convey auditory information from the cochlea to the brainstem. Despite the importance of this structure for normal hearing and cochlear implant function, our understanding of the development and diversity of neuronal phenotypes within the SG is still limited, in part because the total number of neurons within the ganglia is relatively limited. The development of methods to isolate and transcriptionally profile single cells using RNA sequencing has led to the identification and characterization of cellular heterogeneity in a variety of tissues including the sensory epithelia of the inner ear. Based on these studies, it seems likely that a similar approach could be used to address questions related to cellular diversity and development within the SG.

As a first step, fluorescent SG neurons from MapT-EGFP mice were dissected and isolated at E16 or P1. Individual neurons were then captured using two different platforms, the microfluidics-based Fluidigm C1 system and FACS-based single cell sorting. A minimum of 40 cells were profiled at each age. Initial results indicated wide transcriptional heterogeneity at E16 stemming from cellular differentiation and maturational processes, and more discrete transcriptional heterogeneity at P1. At P1, three transcriptionally distinct groups of neurons were identified by unbiased clustering. The most transcriptionally distinct group corresponds to ~15% of SGN cells collected, but these cells do not express Prph, indicating that they are not type II neurons. The three groups are thus far not easily defined transcriptionally by known type I and type II markers such as Prph or EphA4.

PS 750

Time Course of Macrophage Numbers and Morphology in the Developing Mouse Cochlea

Ashley Hinton¹; Tejbeer Kaur²; Mark Warchol³

¹University of South Florida and Washington University School of Medicine; ²Washington University School of Medicine Saint Louis Missouri; ³Dept of Otolaryngology, Washington University School of Medicine, St Louis MO

Background

During the development of the cochlea, auditory neurons and hair cells undergo a series of changes before achieving their final pattern of synaptic innervation. Normal development also requires precise coordination of cell proliferation, differentiation and programmed cell death (PCD). In many developing tissues, clearance of apoptotic corpses relies on resident macrophages. In addition, recent work in the developing CNS has demonstrated that selective synaptic pruning involves the activity of microglia (the resident macrophages of the brain). However, the numbers, phenotype and function of resident macrophages in the developing inner ear remain largely unknown. The aim of this study is to describe the time course of macrophage numbers and morphology in a neonatal mouse-developing cochlea.

Methods

Mice expressing GFP under the CX3CR1 promoter were used for the study. CX3CR1 (the receptor for fractalkine) is expressed by all macrophages and microglia. Mice were sacrificed either by quick decapitation or deep anesthesia, followed by fixation with 4% paraformaldehyde. Specimens were obtained at various time points from P3 to P30. The temporal bones were isolated and subjected to either mid-modiolar frozen sectioning or whole mount dissections. Tissue was processed for im-

munohistochemistry to label macrophages and neurons. Images were captured on a confocal microscope and post-processing and quantification of immune cells was completed using Volocity software.

Results

Quantitative data indicate that the numbers of GFP-positive cochlear macrophages are higher during first two weeks of postnatal development, when compared to mature cochleae (P30). Macrophage numbers in the sensory epithelium peaked at ~P7, while the number of macrophages associated with the spiral ganglion peaked at P10. In the sensory epithelium, we observed more macrophages in the apical region of the cochlea than in the basal region. In addition, macrophages in the developing cochlea were round, while those in the mature cochlea usually possessed a ramified morphology.

Conclusion

The enhanced numbers and distinct morphology of macrophages in the developing cochlea suggest that they may be actively involved during maturation and development, but the precise function of these macrophages during development is under further investigation.

PS 751

Site-specific Transformation and Re-organization of Tissue Macrophages in the Sensory Epithelium During the Postnatal Development

Bo Hua Hu¹; Youyi Dong¹; Weiping Yang¹; Bohua Hu²
¹Center for Hearing and Deafness, University at Buffalo; ²The Center for Hearing and Deafness, University at Buffalo

The sensory epithelium contains immune cells. In mature cochleae, these cells reside in the scala tympani side of the basilar membrane. We have demonstrated that the basilar membrane macrophages display site-specific phenotypes with the apical macrophages being dendritic and the basal macrophages being amoeboid. At present, it is not known when and how this mature pattern of macrophage distribution and phenotypes are formed. The current study aims to define the postnatal development of immune cells in the sensory epithelium.

Methods

Cochleae of C57BL/6J mice were collected at the ages from P1 to P21 as well as from mature mice (4-6 weeks). The cochleae were fixed and the sensory epithelia were collected. The tissues were immunostained for CD45, a pan-leucocyte marker, or for F4/80, a macrophage-specific marker. The stained tissues were examined using confocal microscopy. Macrophages were identified

based on their CD45 immunoreactivity and unique morphologies, and were confirmed by the presence of strong F4/80 immunoreactivity.

Results

Two subsets of macrophages are identified. One resides in the scala tympani side of the basilar membrane. These primitive cells are in a round shape at P1 and start to undergo site-specific differentiation from P4. In the apical section, the cells obtain a dendritic shape. In the basal section, the cells transform to mature cells first with an irregular shape at P21, and then with an amoeboid shape at the age of 4-6 weeks. These cells persist into adulthood. The other set of macrophages resides above the basilar membrane, either beneath the cells of organ of Corti or along the spiral vessel of the basilar membrane. As the maturation of the sensory epithelium, these cells gradually degrade via apoptosis. Similar to the basal-to-apical progression of sensory epithelium maturation, the degradation progresses from the basal to the apical end of the sensory epithelium, suggesting that these cells are development-dependent. At mature cochleae, residual bodies of these degraded cells are still visible in the sensory epithelium.

Conclusion

Two sub-populations of macrophages are present in the neonatal sensory epithelium and these cells have distinct developmental fates. The presence of short-lived macrophages above the basilar membrane suggests a developmental role for the immune system in postnatal remodeling of the sensory epithelium. The primitive immune cells that are populated beneath the basilar membrane are the origin of the mature basilar membrane macrophages observed in adult cochleae.

PS 752

Development of Resident Macrophage in the Mouse Cochlea

Ippei Kishimoto; Takayuki Okano; Koichi Omori
Department of Otolaryngology, Head and Neck Surgery, Graduate School of Medicine, Kyoto University

Background

The inner ear was once believed to be "immune-privileged", but a new era of inner ear immunology started by the findings of intimate contact between the lymphocytes and macrophages in the endolymphatic sac of guinea pigs (Rask-Andersen and Stahle, 1979). In addition, recent studies have demonstrated presence of immune-competent cells in the specific parts of the inner ear such as the spiral ganglion and the spiral ligament, which is referred to as resident macrophages in cochlea. However, the role of cochlear macrophages and the mechanisms of macrophage migration into the cochlea

still remain largely unknown. In this study, we investigated the distribution of macrophages in various developing stages by immunohistochemistry to reveal development of the immune system in the mouse cochlea.

Methods

The temporal bones of C57BL/6 mice, between embryonic day (E) 9.5 and postnatal day (P) 3, were dissected out, and the specimens were perfused with 4% paraformaldehyde in phosphate buffer overnight and cryoprotected with 30% sucrose. Specimens were prepared for cryostat sections (10 μ m in thickness), and midmodiolar sections were provided for histological analyses. Immunohistochemistry was performed for CD68 and Iba1 as surface marker of macrophage.

Results

CD68- or Iba1-positive cells were observed in cochlea between E11.0 and P3. They were distributed in the mesenchyme of presumptive area for the scala tympani and scala vestibule in earlier stage of cochlear development. In the cochlea of E16.5 onward, CD68- or Iba1-positive cells are gradually restricted to the spiral ligament and spiral ganglion, which demonstrated similar patterns of known distribution of cochlear resident macrophages shown by the previous reports. Especially in spiral ganglion, macrophage distribution became more apparent in neonatal stages than embryonic stages. On the other hand, CD68- or Iba1- positive cells were not observed in any area of cochlea at E9.5.

Conclusion

Macrophage was considered to be introduced in the developing cochlea of mice between E9.5 and E11.0, suggesting that cochlear resident macrophages might be originated from hematopoietic progenitors in the yolk sac.

PS 753

Septin7 Regulates Apoptosis to Achieve Gross Morphogenesis During the Development of Inner Ears

Norio Yamamoto¹; Hiroko Torii¹; Atsuhiko Yoshida²; Tatsuya Katsuno³; Takayuki Nakagawa¹; Juichi Ito⁴; Makoto Kinoshita⁵; Koichi Omori⁶

¹Dept. Otolaryngology, Head and Neck Surgery, Graduate School of Medicine, Kyoto University; ²Department of Otolaryngology, Kurashiki Central Hospital; ³Dept. Otolaryngology, Head and Neck Surgery, Kyoto University Graduate School of Medicine; ⁴Shiga Medical Center Research Institute; ⁵Division of Biological Science, Graduate School of Science, Nagoya University; ⁶Department of Otolaryngology, Head and Neck Sur-

gery, Graduate School of Medicine, Kyoto University

Septins are GTP-binding proteins that are evolutionally conserved in all eukaryotes other than plants.

There are 13 and 14 septin genes in mouse and human, respectively. They are divided into 4 subgroups and septin proteins canonically exert their effects as a multimeric complex that are composed of 4 septin proteins from each subgroup. Septin7 (SEPT7) is a core protein of multimeric septin complex because SEPT7 belongs to a subgroup which contains only SEPT7. Septin multimeric complexes interact with membrane lipids, actomyosin, and microtubules. Based on these interactions, septins play essential roles in the morphogenesis and physiological functions of many mammalian cell types including the regulation of microtubule stability, vesicle trafficking, cortical rigidity, planar cell polarity, and apoptosis.

The inner ear that contains highly differentiated hair cells to perceive auditory and equilibrium sensation has a complicated gross morphology. The hair cells and supporting cells have high polarity and are composed of rich actin and microtubule. Furthermore, inner ear development including morphogenesis is dependent on various molecular mechanisms, such as apoptosis, convergent extension that requires planar cell polarity, and cell fate determination. These suggest the important roles of septins in the inner ear development.

To examine how septins affect the development of the inner ear, we deleted Sept7, the non-redundant subunit in the canonical septin complex, specifically in the inner ear at two different times during development. Foxg1Cre-mediated deletion of Sept7, which achieved the complete knockout of Sept7 within the inner ear at E9.5, caused cystic malformation of inner ears and a reduced numbers of sensory epithelial cells although differentiated hair cells exist within inner ears. Excessive apoptosis was observed at E10.5, E11.5 and E12.5 in the whole inner ear epithelial cells as well as at E10.5 and E11.5 in Sox2-positive prosensory epithelial cells of the Sept7 deleted inner ears. In contrast with apoptosis, cell proliferation in the inner ear did not significantly change between control and mutant mice. Deletion of Sept7 within the cochlea at a later stage (around E15.5) with Emx2Cre transgene did not result in any apparent morphological anomalies. These results suggest that SEPT7 regulates gross morphogenesis of the inner ear and maintains the size of the inner ear sensory epithelial area by regulating apoptosis and exerts its effects at an early developmental stage of the inner ear.

PS 754

Characterization of Slc52a3, a Riboflavin Transporter Expressed in Hair Cells and Linked to Human Hearing Loss

Elizabeth C. Driver¹; Stephen McInturff²; Tracy Fitzgerald³; Rani Elkon⁴; Ronna Hertzano⁵; Matthew W. Kelley¹

¹Laboratory of Cochlear Development, NIDCD, NIH, Bethesda, Maryland, USA; ²Laboratory of Cochlear Development, NIDCD, NIH; ³Mouse Auditory Testing Core Facility, NIDCD, NIH, Bethesda, Maryland, USA; ⁴Department of Human Molecular Genetics and Biochemistry, Sackler School of Medicine, Tel Aviv University, Tel Aviv, Israel; ⁵Department of Otorhinolaryngology, Department of Anatomy and Neurobiology, and Institute for Genome Sciences, University of Maryland School of Medicine, Baltimore, MD USA

Background

Differentiation and early survival of the mechanosensory hair cells (HCs) of the inner ear are dependent on the transcription factor Atoh. Although the importance of Atoh1 in the development of HCs is well-established, only some of the Atoh1-dependent downstream targets involved in subsequent HC differentiation have been characterized.

Methods

To identify more genes involved in early HC development, as well as potential Atoh1 targets, we compared the transcriptomes of cochlear epithelia from Atoh1 wild-type and Atoh1 null mouse embryos at embryonic day 15. We identified several previously unreported HC-specific genes and determined their expression patterns in the developing inner ear.

Results

One such gene is Slc52a3, a recently reported riboflavin transporter. Mutations in SLC52A3 in humans are linked to riboflavin transporter deficiency syndrome (formerly Brown-Vialetto-Van Laere syndrome), which includes juvenile onset cranial nerve degeneration and sensorineural hearing loss. We find that Slc52a3 is expressed in all HCs of the inner ear during HC development. To examine the role of Slc52a3 in HC function, we obtained Slc52a3 mutant mice, and while the homozygous null mutation results in perinatal lethality, we observed no obvious defects in cochlear or vestibular HCs at that stage. To circumvent the early mortality caused by the null allele, we also generated tissue-specific mutants using Emx2-cre, which is expressed throughout the cochlear epithelium. Emx2-cre; Slc52a3 fx/del animals are viable, and their auditory function was assessed by ABR

and DPOAE testing. Auditory testing of conditional mutants indicated that thresholds in Emx2-cre; Slc52a3 fx/del animals were not significantly different from those of non-mutant litter mates. Preliminary results also indicate that neonatal cochlear explants cultured in riboflavin-depleted media have a similar number of HCs as explants grown in 500 nM riboflavin-supplemented media. However, when explants grown with or without riboflavin were subjected to neomycin treatment, more HC death was observed in riboflavin-depleted explants.

Conclusions

Although Slc52a3 is clearly necessary for overall viability, it may be dispensable for normal HC function in mice. Riboflavin depletion sensitizes HCs to neomycin ototoxicity, suggesting that riboflavin transport into HCs plays a role in protecting HCs against ototoxic stress. We are investigating other ways in which riboflavin transport and metabolism may influence HC viability.

PS 755

Cellular Senescence During Early Development of the Chicken Inner Ear: IGF-1 and TGF β

Marta Magarinos¹; Alejandro Gibaja²; María R. Aburto²; Raquel Barajas²; Isabel Varela-Nieto³

¹"Alberto Sols" Biomedical Research Institute (CSIC-UAM), Madrid, Spain; Centro de Investigacion Biomedica en Red de Enfermedades Raras, Madrid, Spain; Department of Biology, Autonomous University of Madrid, Madrid, Spain.; ²"Alberto Sols" Biomedical Research Institute (CSIC-UAM), Madrid, Spain.; ³Instituto de Investigaciones Biomedicas 'Alberto Sols' CSIC-UAM, Madrid, Spain; Centro de Investigacion Biomedica en Red de Enfermedades Raras, Madrid, Spain.

Embryonic development requires the strict regulation of cellular processes including proliferation, survival, autophagy and differentiation. Senescence is a cellular process classically associated with cancer and ageing, but also it is a novel developmental process. In this work, we show that senescence contributes to the early development of several neural and sensory structures of the chicken embryo in vivo, including the inner ear.

Further studies showed that TGF β and IGF-1 modulate senescence in the otocyst. To understand signalling pathways underlying these actions, ex vivo cultures of chicken otic vesicles were treated or not with pharmacological inhibitors of signalling pathways. The inhibition of the targets was confirmed by Western blotting. Senescence was assessed by detection of the senescence marker SA β G (senescence-associated β -galactosidase). Proliferation and apoptosis were assessed by EdU and TUNEL labelling, respectively.

In the developing inner ear, senescence showed a highly regulated temporal and region-specific pattern. The endolymphatic sac primordium showed programmed cell death and senescence associated to reduced proliferation. Senescence in the otocyst is mediated by the RAF-MEK-ERK, PI3K-AKT and canonical TGF β signaling pathways. TGF β signalling was also involved in the neurogenesis and differentiation of the acoustic-vestibular ganglion.

Taken together, these results show that senescence is a natural occurring process during the early development of the chicken inner ear that is modulated by the joint actions of TGF β and IGF-1.

This work was supported by the SAF2014-53979-R project to MM and IVN

PS 756

Expression of Endothelins During the Development of the Stria Vascularis

Martin L. Basch; William J. Davis

Case Western Reserve University School of Medicine

Endothelins are family of small peptides ET-1, ET-2, and ET-3, which transduce their effect through two G-protein coupled receptors: Ednra and Ednrb. Activation of these receptors in a variety of tissues mediates many functions throughout development including angiogenesis, vasoconstriction, cell proliferation, cell migration, cell differentiation, and regulation of Na⁺/K⁺ exchange. Targeted or spontaneous mutations in Ednrb or ET-3 affect the migration of neural crest that give rise to enteric neurons and melanoblasts. In humans, Ednrb mutations are responsible for Waardenburg syndrome type 4 and Hirschsprung disease, which affects 1 in 5000 births. Both these syndromes include pigmentation anomaly and lack of enteric ganglia in addition to congenital hearing impairment. Mouse models show that Ednrb signaling is necessary during a critical window of time after the onset of neural crest migration and before the cells reach their target tissues. However, because there is no increase in cell death in the migratory cells of Ednrb mutants, it has been proposed that in addition to migration, Ednrb is necessary for proliferation and differentiation of melanoblasts. Since Ednrb mutants lack intermediate cells altogether, the postnatal function of Ednrb in intermediate cells has not been studied. Our preliminary studies show that expression of Ednrb in intermediate cells, in contrast to skin melanocytes, is maintained throughout development and also postnatally. Here we describe the developmental expression of endothelins and their receptors during the embryonic and postnatal development of the

stria vascularis, as a first step to determine their potential role or roles in these processes.

PS 757

The Effect of Early Postnatal Neurotrophin 3 Gene Delivery on Hearing Acquisition

Yong-Ho Park¹; Ah-Ra Lyu²

¹Department of Otolaryngology, Chungnam National University; ²Department of Medical Science, Chungnam National University

The purpose of this study was to investigate the effect of early postnatal NT-3 (NT3) support on hearing acquisition. Adenoviral (Ad) vectors expressing green fluorescence protein (GFP) alone or in combination with NT3 were injected into the scala tympani (ST) through the round window of 5 postnatal day old (P5) rats. Changes in NT3 mRNA level, hearing thresholds and morphological studies were done after the viral vector injection. NT3 mRNA was significantly increased in the Ad-GFP-NT3 group compared to the normal developmental group and Ad-GFP alone group. GFP was widely expressed in the cochlea such as in the hair cells, supporting cell area, and spiral ganglion neurons. Auditory brainstem response (ABR) thresholds were significantly lower in the Ad-GFP-NT3 group compared to the normal developmental group and Ad-GFP alone group at 15 postnatal days (P15). These results show that early postnatal NT3 expression may have a critical role in normal hearing acquisition in rats.

This work was supported by the Basic Science Research Program through the National Research Foundation of Korea (NRF), funded by the Ministry of Education (NRF-2015R1D1A3A01018881)

PS 758

Neurotrophic Factors as Potential Regulators of Inner Ear Development During the Human Gestational Weeks 8 to 12

Lejo Johnson. Chacko¹; Elisabeth Pechriggl²; W Dietl¹; Rudolf Glueckert³; Anneliese Schrott-Fischer³; J Dudas¹

¹Medical University of Innsbruck; ²Dept of Anatomy, Histology & Embryology, Medical University of Innsbruck; ³Medical University of Innsbruck, Department of Otolaryngology, Anichstr. 35, 6020 Innsbruck, Austria

Introduction

Previous research (Vega et al., 1999, Vazquez et al., 1996) had demonstrated the differential expression of the Trk and p75 receptors in the developing human foe-

tal inner ear. Here we provide detailed insights into the staining patterns of these receptors during the human gestational weeks 8 to 12 versus their expression pattern in the adult human inner ear specimens. Differential expression profiles of these receptors would be helpful in identifying sites of neurotrophin expression.

Methods

Foetal temporal bones were excised from 8 legally aborted human embryos with prior parental consent and aged between 8 and 12 weeks after conception corresponding to the anatomical age. The embryological ages were differentiated by quantification of the crown-rump length, external and internal morphology and the estimated gynaecological age. Protein expression of neurotrophic receptors were then studied by immunohistochemistry and in situ hybridisation in embryonic as well adult inner ear specimens.

Results

Immunostaining is positive for the Trk B, Trk C & p75 receptors while Trk A is negative in the inner ear of all the gestational stages examined. Specific staining for TrkA though shows up in the facial nerve. P75 neurotrophic receptor is strongly expressed with positive fibres penetrating the Kollikers organ while the same stains the vestibular ganglion and nerve fibres. Trk B and Trk C staining was apparent in all the gestational stages examined, with Trk C in both the Spiral and the Scarpa ganglia while Trk C is confined to the nerve fibres of the ganglia. The immunostaining pattern for the Trk receptors seems to follow a tonotopic gradient in the cochlea with the gradient decreasing from the basal to the apical turn. Additional in situ hybridisation with BDNF showed reactions in the nerve fibres surrounding the cochlear ganglions at week 12.

Conclusion

Previous research from murine specimens has shown that that neurotrophins and their tyrosine receptor kinases are required for inner ear ganglion survival and their innervation (Fritsch et al., 1999). The predominant necessity for neurotrophins and their receptors in murines, towards the later embryonic stages to regulate this ganglion survival as well as innervation patterning at the later embryonic stages (Bitsche et al., 2011) could be analogous to that in the human inner ear developmental stages. However since the human inner ear development is completed by the 20th week of gestation this innervation may be regulated via neurotrophins and their receptors.

PS 759

Characterization of the Initial Stages of Myelination in the Maturing Auditory Brainstem

Douglas Kolson¹; Ashley Brandebura¹; George Spirou¹; Peter Mathers¹; Jun Wan²; Jiang Qian²

¹Sensory Neuroscience Research Center and Centers for Neuroscience, WVU School of Medicine; ²Wilmer Institute, Johns Hopkins University School of Medicine

The roles for glia in regulating neural circuit formation and maturation are still not well-understood. In order to examine the genetic programs that are interacting among various cell types during these events, we conducted an extensive microarray study, utilizing the early postnatal medial nucleus of the trapezoid body (MNTB) as our model system. The MNTB offers several advantages for studying genetic regulation of neural circuit maturation. The large presynaptic nerve terminals onto MNTB neurons, the calyces of Held, grow very quickly between postnatal day (P)2 and P6 and are mostly refined to monoinnervation within the first postnatal week. Furthermore, the astrocytes and oligodendrocytes in the MNTB have been found to increase in number and begin to exhibit morphological maturation within the same time window. For this study, we performed microarray analyses on micro-dissected MNTB tissue at P6 and P14 and found 775 genes that are significantly changing between these time points. Quantitative real-time PCR was performed on a subset of genes at P4, P6, P9 and P14, confirming the validity of the microarray results. Gene Ontology analysis identified numerous dynamic processes between P6 and P14, including myelination, ion channel activity, and calcium ion binding. To correlate these genetic data with observable structural changes within the MNTB, we used an extensive collection of serial block-face electron microscopy (SBEM) data sets and immunofluorescence to identify and systematically characterize the stages of oligodendrocyte maturation and myelination. The stages that we used to characterize the myelination of calyceal axons were unmyelinated, a single glial wrap, two or more loose glial wraps, and compaction of the myelin sheath. Many of the calyceal axons were receiving single glial wraps by P4 with compaction of the myelin sheath being prevalent by P9. This study provides a genetic and structural basis for future research investigating the coordinated maturation of neurons and glia in a developing neural circuit.

PS 760

Regulation of Hair-cell Ribbon Synapse Formation by Intracellular Calcium Stores

Candy Wong; Katie Kindt

National Institutes on Deafness and other Communication Disorders, NIH

Sensory hair cells rely on specialized ribbon synapses to facilitate rapid and sustained vesicle release. Calcium plays a critical role in signaling for synaptic vesicle release at the ribbon synapse. The major source of synaptic calcium influx is the L-type calcium channel Cav1.3. Previous work has shown that loss of Cav1.3 function during a critical period of development in hair cells leads to enlarged ribbons. How Cav1.3a-dependent synaptic calcium levels are regulated in developing hair cells is not clear. Several storage locations such as the endoplasmic reticulum (ER) and mitochondria may actively modulate synaptic calcium concentration during ribbon formation. We aim to investigate how ER and mitochondrial calcium stores regulate ribbon synapse formation.

To study the effects of calcium stores on ribbon synapse development, we examined hair cells in the zebrafish lateral line. Lateral line hair cells resemble mammalian vestibular hair cells in structure and are easy to access for in vivo pharmacology, stimulation and visualization. Our work uses pharmacology to disrupt ER-mitochondrial-synaptic calcium cycling in the developing hair cells. We also use transgenic zebrafish lines that express mitochondria, ER or synapse localized fluorescent calcium sensors to visualize calcium dynamics in hair cells during pharmacological treatments. Synaptic ribbon morphology is quantified by immunofluorescence staining of its main constituent, the protein Ribeye.

Similar to pharmacological inhibition of Cav1.3, blocking mitochondrial calcium uptake in developing hair cells causes an increase in synaptic ribbon size and Ribeye accumulation. Our pharmacological manipulations of ER calcium are underway. Because blocking Cav1.3 and mitochondrial calcium uptake both increase ribbon size, we predict that the mitochondria may act to mediate Cav1.3-dependent synaptic calcium and regulate synaptic ribbon development. We predicted that mitochondrial calcium might regulate cellular bioenergetics and increase levels of NADH; this could alter Ribeye self-assembly via its NAD-binding domain (NBD). To test this, we overexpressed either the NBD of Ribeye, or the bacterial NADH/NAD⁺ redox sensor protein REX in hair cells, to act as a NADH sink. The presence of a NADH sink resulted in less Ribeye accumulation and smaller ribbons. This indicates NADH can facilitate localization of Ribeye to the presynaptic ribbon body in vivo.

These result suggests that Cav1.3-dependent mitochondrial calcium uptake may control ribbon assembly through levels of NADH in the cytosol of developing hair cells. This mechanism couples synaptic function to synapse formation in the hair cell through changes in cellular metabolism in a manner similar to those of neuronal synapses.

PS 761

A Novel Cell Polarity Program During Innervation of a Non-Laminar Nucleus in the Auditory Brainstem

Paul S. Holcomb¹; Thomas Deerinck²; Mark Ellisman³; George Spirou¹

¹*Sensory Neuroscience Research Center and Centers for Neuroscience, WVU School of Medicine*; ²*National Center for Microscopy and Imaging Research, University of California, San Diego*; ³*National Center for Microscopy and Imaging Research, University of California at San Diego, San Diego, CA, USA*

Laminar sensory structures, such as rod and cone cells of the retina and the hair cells of the cochlea, restrict potential sites of innervation through both polarized expression of synaptic proteins and structural segregation of cells into apical and basal regions. Many cells in the central nervous system, however, lack the lateral cell-cell connectivity necessary to make such a polarized distinction. Is cellular polarity still evident in these systems, and if so, does it influence terminal placement irrespective of the lack of structural limitations evident in laminar systems? We utilized the calyx of Held (CH) – principal cell connection in the medial nucleus of the trapezoid body (MNTB) of the mouse, one such non-laminar system, to explore these questions. By applying serial block-face scanning electron microscopy (SBEM), three-dimensional reconstruction of neurons and terminals, and morphological measurement techniques, we showed polarity in the principal cells of the MNTB at early postnatal (P2-P9) ages; specifically, the nuclei of these cells are asymmetrically located, defining a nucleus-poor “cytoplasmic” pole and a nucleus-filled “nuclear” pole and establishing what we refer to as “intrasomatic polarity”. The asymmetric location of the nucleus increases significantly during development due to principal cell growth away from the position of the nucleus. Additionally, the nucleus structure itself is polarized, possessing a smooth surface on the hemisphere closest to the cell membrane and a highly invaginated surface on the opposite hemisphere facing the cytoplasmic pole. Terminal placement was assayed using the apposed surface area (ASA) between vesicle-filled contacts and the principal cell membrane as a measure of terminal size. As development proceeds, we found that the CH:MNTB connection not only becomes larger but also more po-

larized, with greater than 80% of the ASA of the largest terminals at P6 occupying the cytoplasmic pole surface opposite the nucleus. Competing inputs (2-3 inputs/cell with less than 1:5 ratio in size) fell into three categories: (1) the largest terminal is most polarized, (2) the second largest terminal is most polarized, or (3) the two largest terminals are equally polarized. This implies either a “flip-flop” of largest for second largest terminal or polarized growth towards the cytoplasmic pole or both. These findings suggest that the non-laminar MNTB still exhibits polarity on the cellular level that influences the placement and growth potential of terminals in the formation of the CH:MNTB circuit.

PS 762

Does Self-generated Noise Affect Low-frequency Audiometric Thresholds in Children?

Ryan McCreery¹; Emily Buss²; Lori Leibold¹

¹Boys Town National Research Hospital; ²University of North Carolina at Chapel Hill

Introduction

Recent evidence suggests that children’s audiometric thresholds at low frequencies may be elevated compared to adults due to the inability to control self-generated noise (Buss et al. 2016). Clinically, the presence of self-generated noise could reduce the accuracy of threshold estimation in children and lead to errors in the prescription of amplification at low frequencies. The goal of this study was to determine if there is evidence of low. We hypothesized that 250- and 500-Hz thresholds would improve with age among children with normal hearing or mild hearing loss, due to elevated levels of audible low-frequency self-generated noise in younger children. Such a finding would be consistent with the idea that children learn to suppress low-frequency self-generated noise as they get older.

Methods

Retrospective analyses of audiometric threshold data from the longitudinal Outcomes of Children with Hearing Loss study were analyzed. Data from 256 children between 6 months and 5 years of age were included. Pure-tone audiometric thresholds were obtained at octave frequencies between 250 Hz – 8000 Hz using age-appropriate behavioral methods. Children with audiometric thresholds measured at a minimum of two consecutive visits with normal middle ear function were analyzed. Linear mixed models with random intercepts for each child and random slopes across study visits were used to examine the pattern of threshold change over time for children with normal hearing or mild hearing loss (≤ 40 dB HL) and children with moderate or greater hearing loss (> 40 dB HL).

Results and Discussion

Thresholds at 250 Hz and 500 Hz were lower for older children, but thresholds at 1000 Hz, 2000 Hz and 4000 Hz did not vary as a function of age. These results are consistent with previous results for normal-hearing children (Buss et al. 2016; Trehub et al. 1988). For children with 250-Hz thresholds >40 dB HL, thresholds rose by about 1 dB / year, consistent with expected changes in thresholds with insert earphones related to ear canal growth. However, there was no increase in thresholds for children with 250-Hz thresholds < 40 dB HL, suggesting that effects of ear canal volume may be offset by maturation in the ability to suppress self-generated noise. The magnitude of the effect over the course of the study was not sufficient to alter a child’s diagnosis of hearing loss, but could have implications for the prescription of amplification.

PS 763

Developmental Effects in the Ability to Benefit from Target/Masker F0 Differences

Mary M. Flaherty¹; Emily Buss²; Lori Leibold¹

¹Boys Town National Research Hospital; ²University of North Carolina at Chapel Hill

Introduction

The current study investigated the extent to which children can benefit from fundamental frequency (F0) differences between target words and competing sentences for speech-on-speech recognition. Introducing a difference in the F0 of target and masker speech has been shown to benefit adults’ speech-on-speech recognition (e.g., Darwin et al., 2003; Mackersie, 2011), but it is unknown whether children show a similar benefit. Other studies investigating children’s abilities to use acoustic cues to improve speech-on-speech recognition have been mixed, but some indicate immature performance well into adolescence. For example, Wightman et al. (2003) showed children in the age range of 4-13 years had little to no improvement in performance when the target and masker were presented to different ears, compared to very large improvements for adults. It was hypothesized that age impacts the ability to benefit from F0 differences between the target and masker.

Methods

Listeners were 5- to 16-year olds and 19-to 35-year olds with normal hearing. Recognition thresholds for spondee words were measured in a continuous, 60-dB-SPL two-talker speech masker. The same male talker produced both the target and masker speech. The F0 of the target was either matched to the masker’s F0 (i.e., unaltered), or shifted higher than the masker by 3, 6, or 9 semitones. The level of the target words was adaptively

varied to estimate the level associated with 71% correct identification. The procedure was a four-alternative forced-choice with a picture pointing response.

Results and Discussion

Preliminary results suggest a developmental effect in the ability to use F0 differences between target and masker speech. Performance improved, often dramatically, in adults and older children for F0 differences of 6 or 9 semitones. There was no improvement in performance for children younger than 9 years old, and benefits of F0 separation generally increased with increasing age. Our findings suggest the ability to use target/masker differences in F0 is not evident until adolescence and may not fully mature until adulthood. Individual differences found for the older children (ages 9-16 years) are consistent with previous findings suggesting that the ability to use segregation cues in speech-on-speech recognition may be influenced by the rapid changes that occur in higher-order auditory development during adolescence. These results support the hypothesis that age affects the ability to benefit from the F0 differences that aid the separation of target from background speech.

PS 764

Exploring Individual Differences in Infant Speech Processing and Its Relationship with Later Language Skills

Paul Iverson¹; Kathleen McCarthy¹; Katharine Mair¹; Katrin Skoruppa²

¹University College London; ²Université de Neuchâtel

Background

In our recent work, we created detailed perceptual maps of infant vowel development using the Acoustic Change Complex (ACC) within EEG. More specifically, we showed that vowel perception development seems to be driven by the low frequency aspects of the speech signal. Such findings could be explained by early auditory experience of low frequencies in utero (Kisilevsky et al., 2009), and possibly explain the developmental trajectory of vowels being acquired earlier than higher frequency consonant sounds such as fricatives (Werker & Gervain, 2013). The aim of the present study was to explore this hypothesis further by detailing individual differences in vowel and fricative perception throughout the first year of life. A secondary aim was to investigate the relationship between this early auditory processing and later language outcomes.

Methods

Eighty monolingual English infants (4-5, 7-8 and 10-11 months old) took part in the study. Vowel and fricative sensitivity was assessed using the ACC within EEG,

which for infants typically evokes a positivity about 150-200 ms after a spectral change. The ACC was measured for three vowel pairs and three fricative pairs, that were presented in runs of five per pair before switching to a new random pair. ERPs were averaged across epochs for each pair, with the magnitude of the response for each pair being used as a comparison measure. Each infant was tested for an average of 18 minutes, resulting in around 250 trials per pair. In addition, the infants' language skills were assessed at 16, 20, and 24-months using the Oxford CDI.

Results

Preliminary results show individual differences in vowel and fricative perception. Infants initially show a greater sensitivity to the vowel contrasts, with fricative sensitivity increasing with age. Further analysis will be conducted to explore which spectral features are driving the infants' perceptual sensitivity. These findings display a more detailed pattern of the speech perception than has been shown before, and demonstrate how the ACC can be used to explore developmental trajectories. The results will be discussed with respect with the infants' later language outcomes, and the possible application of this method in a clinical setting.

PS 765

Modulation Masking and Temporal Integration for Amplitude Modulation in Childhood

Laurianne Cabrera¹; Stuart Rosen¹; Emily Buss²; Christian Lorenzi³

¹UCL, London, UK; ²University of North Carolina at Chapel Hill; ³Ecole normale supérieure, Paris Sciences et Lettres Research University and CNRS, France

Introduction

The capacity to detect amplitude modulation (AM) appears to reach adult levels at around 10 years of age. The reasons for this are still unclear, because other data suggest that the sensory encoding of AM may be mature as early as 3 months of age. This may suggest that the improvement in AM sensitivity with age reflects changes in higher-level processing ("processing efficiency") rather than changes in low-level processing (sensory encoding). This study tested this assumption by characterizing the contribution of sensory factors (modulation filtering) vs cognitive factors (memory and decision) to the development of AM sensitivity between 6 and 11 years. The ability of children and adults to detect AM i) as a function of AM rate (with or without masking AM fluctuations) or ii) as a function of the number of AM cycles, was evaluated to assess AM sensitivity, AM masking, and temporal integration for AM detection.

Method

3IAFC adaptive tasks were used to measure AM detection thresholds for 12 normal-hearing children from 6 to 11 years and 21 adults. In the first experiment, thresholds were measured at AM rates of 4, 8 and 32 Hz using three carriers: a 1027-Hz sine tone (TONE); 4-Hz wide random narrowband noises centered at 1027 Hz were generated and noises with small AM fluctuations as measured by the standard deviation of temporal-envelope amplitudes were selected (NOISE-LOW); or only those with larger AM fluctuations were selected (NOISE-HIGH). In the second experiment, thresholds were assessed in the TONE condition at 4 or 32 Hz using either N=2 or 8 AM cycles.

Results/Conclusions

Results of the first and second experiment are shown in Figures 1 and 2, respectively. In the first experiment, no difference was observed across ages in the TONE condition suggesting that low-level sensory mechanisms constraining AM processing may be mature by 6 years. However, differences across age groups were observed in NOISE-LOW, suggesting that some aspects of processing efficiency (e.g., the magnitude of internal noise limiting AM processing) may mature beyond 6 years. In the second experiment, no effect of age, AM rate, nor any interaction was observed, suggesting that higher-level factors constraining temporal integration do not mature beyond 6 years.

These findings suggest that changes in AM sensitivity during childhood are more related to changes in late internal noise rather than changes in AM sensitivity (temporal-envelope encoding), echoic memory and decision making.

PS 924

Otocyst Transplantations in Amphibians Reveal Sensory Afferent Navigation in the CNS

Bernd Fritzscht; Clayton Gordy; Karen Elliott-Thompson
University of Iowa, Dept of Biology.

Background

Developmental navigation of sensory afferents in the central nervous system establishes necessary connections for proper perception. Navigation has been extensively studied in the visual system, including transplantation of developing eyes onto the spinal cord and afferent tracing to the midbrain. Ectopic development is not exclusive to the visual system; the developing otic vesicle is capable of growth in ectopic locations and offers testing of sensory neuron afferent navigation. Previous work in generating three-eared frogs displayed the ability of the grafted ear to project afferents into the ves-

tibular nucleus of the hindbrain. Here we transplant the frog otocyst to the spinal cord to examine the extent to which otic sensory afferents can navigate along the dorsal column afferents of the spinal cord to the hindbrain and redirect to the vestibular nuclei. Additionally, we also investigate the timeline for the capacity of the otocyst to navigate to and in the nervous system by heterochronic otocyst transplantations of younger otocysts to either the spinal cord or replacing the native ear of later stage frogs to determine remaining capability for the otocyst fibers to reach the hindbrain.

Methods

Otocysts from stage 26 unlabeled or tdTomato-labeled donors either were transplanted to the spinal cord of same stage or older stage *Xenopus laevis* embryos or were used to replace the native ear of stage 43-44 embryos. Axonal projections from tdTomato-expressing donor ears or dye-labeled ears were visualized at stage 46-47 with a confocal microscope. We also transplanted ears between *Xenopus* and axolotl.

Results

Otocysts transplanted to the spinal cord show fibers in the dorsal column, which project rostral toward the hindbrain boundary. Otocysts transplanted to Stage 43-44 frogs, replacing the native ear, show fibers projecting into the hindbrain in the region of the vestibular nucleus. We are currently identifying the precise location in the hindbrain of axon terminals from both spinal cord and heterochronic ear replacement transplantations.

Conclusions

Here we show an ability of inner ear sensory afferents to navigate the CNS as shown by projections extending from the spinal cord toward the hindbrain when transplanted to the spinal cord. Heterochronic transplantations to replace native ears show projections into the vestibular region of the hindbrain, which suggest the opportunity to receive afferents by the vestibular nucleus is not restricted to very early stages in development. We are currently analyzing heterochronic, heterotopic and xenoplastic transplants between *Xenopus* and axolotl.

PS 767

Activity-dependent Regulation of the Hair Cell Stereocilia Actin Core in Vertebrates

A. Catalina Velez-Ortega¹; Patricia M. Quiñones²; Mary J. Freeman³; Sebastiaan W.F. Meenderink⁴; Artur Indzhykulian⁵; Mike Grossheim⁶; Dolores Bozovic⁴; Gregory I. Frolenkov⁷

¹*Department of Physiology, University of Kentucky, Lexington, KY, USA;* ²*University of California Los Angeles;* ³*Department of Physiology, College of Medicine, University of Kentucky, Lexington, KY, 40536-0298, USA;* ⁴*Dept. of Physics and Astronomy;* ⁵*Harvard Medical School;* ⁶*Dept. Physiology, University of Kentucky;* ⁷*Dept Physiology, University of Kentucky*

The sensory organelles of the inner ear hair cells are microvillus-like projections known as stereocilia. Unlike in microvilli, the actin core in stereocilia is remarkably stable. Only the tips of stereocilia exhibit active actin remodeling (Zhang et al., 2012; Narayanan et al., 2015; Drummond et al., 2015), which may underlie the changes in stereocilia tip shape after tip link disruption (Rzadzinska et al., 2004; Indzhykulian et al., 2013).

To study the contribution of mechanotransduction on the remodeling of the actin core at the stereocilia tips, we exposed early postnatal mouse and rat cochlear explants to known blockers of transduction channels. Scanning and transmission electron micrographs showed that incubation with these blockers induced thinning of stereocilia tips followed by stereocilia shortening. These changes were observed exclusively in the transducing stereocilia (i.e. the shorter row stereocilia, which harbor mechanotransduction channels; Beurg et al., 2009) but not in the non-transducing tallest row stereocilia or in any of the rows of stereocilia from mutant mice lacking hair cell mechanotransduction. Tip links remained intact and, as expected, mechanotransduction recovered immediately after blocker washout. We observed a similar decrease in hair cell stereocilia height after the breakage of tip links with BAPTA-buffered calcium-free medium. Notably, the restoration of mechanotransduction—after channel blocker washout or tip link regeneration—led to stereocilia regrowth. Moreover, an increase in intracellular calcium buffering—using the membrane permeable calcium chelator BAPTA-AM—also induced thin stereocilia tips and subsequent stereocilia shortening. To test whether this type of mechanotransduction-dependent regulation of the stereocilia actin core is limited to mammals, we incubated adult frog sacculus and amphibian papilla with transduction channel blockers. Similar to

mammalian hair cells, frog hair cell stereocilia shortened and exhibited abnormally thin tips. However, most tip links were broken and we did not observe the re-appearance of spontaneous bundle oscillations or mechanotransduction currents after blocker washout.

Our results demonstrate (i) the hitherto unknown activity-dependent regulation of the actin cytoskeleton at the stereocilia tips, (ii) the dependence of this regulation on the calcium influx via the mechanotransducer channels, and (iii) its presence in two different vertebrate classes. Our data, however, suggest different mechanisms for tip link maintenance during stereocilia shortening between mammals and amphibians.

Supported by NIDCD/NIH R01DC008861 & R01DC014658 to G.I.F, and NIDCD/NIH R01DC011380 to D.B.

PS 768

CIB2 Regulates Stereocilia Length in the Auditory Hair Cells and Is Essential for Mechanotransduction

Michael R. Bowl¹; Zubair Ahmed²; Arnaud P.J. Giese²; Yi-Quan Tang³; Ghanshyam P. Sinha⁴; Andrew Parker⁵; Mary J. Freeman⁴; Steve D.M. Brown¹; Saima Riazuddin⁶; William Schafer³; Gregory I. Frolenkov⁷

¹*MRC Harwell Institute, Mammalian Genetics Unit, Harwell Oxford, OX11 0RD, UK;* ²*Department of Otorhinolaryngology Head & Neck Surgery, School of Medicine University of Maryland, Baltimore, MD, 21201, USA;* ³*Division of Neurobiology, MRC Laboratory of Molecular Biology, Cambridge Biomedical Campus, Cambridge, CB2 0QH, UK;* ⁴*Department of Physiology, College of Medicine, University of Kentucky, Lexington, KY, 40536-0298, USA;* ⁵*MRC Harwell Institute, Mammalian Genetics Unit, Harwell Oxford, UK;* ⁶*Laboratory of Molecular Genetics, Department of Otorhinolaryngology Head & Neck Surgery, School of Medicine, University of Maryland, Baltimore, MD, USA.;* ⁷*Dept Physiology, University of Kentucky*

Previously, we identified the CIB2 gene as the cause of Usher syndrome type 1 (USH1J) and non-syndromic deafness (DFNB48) in 58 human families. Usher syndrome (USH) is a neurosensory disorder defined by a bilateral sensorineural hearing loss (HL) and a loss of vision due to retinitis pigmentosa (RP). CIB2 encodes a Calcium and Integrin Binding protein 2 (CIB2). In the inner ear CIB2 is localized toward the tips of the hair cells' stereocilia, near the tip link-MET complex. However, the exact role of CIB2 in the inner ear remained elusive. Here, we report that mechanotransducing short-

er row stereocilia overgrow in the auditory hair cells of mice lacking CIB2 and in mice carrying a deafness-related Cib2 mutation, p.F91S. Both these mutants are deaf. CIB2 also binds to the components of mechanotransduction complex, and this interaction is disrupted by deafness-causing mutations. Correspondingly, mechanotransduction is lost in the auditory hair cells of both Cib2 mutants. We concluded that CIB2 function is essential for regulation of the stereocilia core elongation complex and for the mechanotransduction apparatus in the mammalian cochlear hair cells.

Support: This work was supported by the NIDCD/NIH grants R01DC012564 (Z.M.A.), R01DC014658 (G.I.F.), R01DC011803 (S.R.) and partly by the Medical Research Council, UK grants MC-A022-5PB91 (W.R.S.), and MC-A390-5RX80 (S.D.M.B.) and a Wellcome Trust Investigator Award (W.R.S.).

PS 769

Stimulation of Hair Bundles with Ultraviolet Light

Julien Azimzadeh¹; Brian Fabella¹; A J Hudspeth²
¹Rockefeller University; ²The Rockefeller University

Hair cells are the mechanosensory detectors that underlie our senses of audition and balance.

Their mechanosensitivity arises from direct gating of force-sensitive channels by the tension in tip links located at the tops of the stereocilia. The study of hair cells and their mechanically gated channels has heretofore required physical displacement of a hair bundle to open its mechanotransduction channels. Here we present a novel method of hair-bundle stimulation: irradiation with ultraviolet light.

Exposing a hair cell to light at wavelengths near 400 nm leads to rapid motion of its hair bundle towards the tall edge, a movement typically associated with depolarization. The response originates less than 300 us after the onset of stimulation and rises to a plateau level within milliseconds. Tight-seal, whole-cell recording discloses that the motion is associated with equally rapid opening of mechanotransduction channels. Both the light-evoked movement and the channel gating disappear when tip links are ruptured, indicating that the mechanotransduction apparatus is involved in a hair cell's response to light. Blockage of the mechanotransduction channels in their open state with gentamicin abolishes the light-evoked electrical response but only partially reduces the light-evoked displacement, suggesting that channel gating is only partially responsible for light-evoked hair-bundle motion.

We sought to identify the cellular components underlying light-evoked hair-bundle motion. Using an illumination system containing a digital micromirror device, we localized the absorptive element responsible for hair-bundle motion to the region directly below the bundle. This region contains the cuticular plate, an organelle that anchors the hair bundle, surrounded by a belt of cytoplasm rich in mitochondria. The light-evoked response is maximal near 400 nm and has an action spectrum similar to the absorption peaks of several cellular constituents, including NADH, cytochromes, and flavin-based enzymes. Many of these molecules reside in mitochondria. We are investigating the role of these absorbers and of heat production in the generation of light-evoked hair-bundle motion.

PS 770

TRIOBP5 Deficient Mouse is Deaf but Hair Cells Develop Stereocilia Rootlets

Inna A. Belyantseva¹; Tatsuya Katsuno²; Gavin P. Riordan³; Atteeq U. Rehman⁴; Ayesha Imtiaz³; Eva L. Morozko³; Joseph A. Duda³; Elizabeth Wilson³; Ronald S. Petralia⁵; Tracy Fitzgerald⁶; Thomas B. Friedman⁷; Shin-ichiro Kitajiri⁸

¹Laboratory of Molecular Genetics, National Institute on Deafness and Other Communication Disorders, National Institutes of Health; ²Dept. Otolaryngology, Head and Neck Surgery, Kyoto University Graduate School of Medicine; ³Laboratory of Molecular Genetics, NIDCD/NIH; ⁴Department of Molecular and Human Genetics, Baylor College of Medicine; ⁵NIDCD/NIH; ⁶Mouse Auditory Testing Core Facility, NIDCD, NIH, Bethesda, Maryland, USA; ⁷Section on Human Genetics, Laboratory of Molecular Genetics, National Institute on Deafness and Other Communication Disorders, National Institutes of Health, Bethesda, MD, USA.; ⁸Department of Otolaryngology, Head and Neck Surgery, Graduate School of Medicine, Kyoto University

Mutations of TRIOBP cause DFNB28 human deafness. In mouse, there are at least three isoforms encoded by Triobp and expressed in the inner ear. TRIOBP5, the longest isoform, consists of 1,968 residues. Two shorter isoforms, TRIOBP4 and TRIOBP1, have no amino acid sequence in common. The sequence of TRIOBP4 is identical to the first 980 residues of TRIOBP5. We previously showed that a C-terminal gene trap (Bay Genomics, YHB226) affects only TRIOBP1 and TRIOBP5 and causes early embryonic lethality of homozygous mice, while heterozygotes are viable and have normal hearing. Mutations that affect simultaneously both TRIOBP4 and TRIOBP5, but not TRIOBP1, cause profound deaf-

ness due to a failure to form hair cell stereocilia rootlets. We also showed that in vitro, purified TRIOBP4 protein and F-actin form unusually tight bundles of filaments resembling rootlets. Deafness of *Triobp4/5* mutant mice suggest the possibility that both isoforms may be important for rootlet development, structure and normal hearing. However, the specific role of each isoform is currently unknown. To reveal only the function of TRIOBP5, we mated homozygous *Triobp4/5* mutant mice with *Triobp1/5* heterozygotes and generated compound heterozygotes, which have one wild-type copy encoding TRIOBP1 and one wild-type copy of TRIOBP4, while both copies of the sequence encoding TRIOBP5 are mutant. ABR analyses of compound heterozygous mice (i.e., no wild-type TRIOBP5) show that these mice are profoundly deaf by 3 month of age, but have some residual hearing before this time. Morphologically, confocal fluorescence microscopy and SEM studies reveal that auditory hair cells develop normally, but degenerate in the adult mouse. Surprisingly, anti-*Triobp4/5* and anti-*Triobp5* specific antibodies both show a signal in stereocilia rootlets indicating their presence at P8 and P15. However, ultrastructural analysis using TEM shows that at P8 rootlets appear to have a nearly normal length, although some of them are unusually bent or splayed, indicating possible problems with the bundling of F-actin. Our data suggest that TRIOBP4 and TRIOBP5 have non-redundant functions since the compound heterozygotes are deaf in presence of wild-type TRIOBP4. Based on morphological observations, TRIOBP5 also appears to be an actin-bundler, and the C-terminal domain of TRIOBP5 is necessary for reinforcement or maintenance of rootlet structure and function, while TRIOBP4 is important for rootlet development.

PS 771

Is XIRP2 Involved in Maintenance and/or Repair of F-actin in Stereocilia of Mechanosensory Hair Cells?

Elizabeth Wagner¹; Tingting Du²; Shimon Francis³; Jung-Bum Shin²

¹*University of Virginia*; ²*University of Virginia, Neuroscience Department*; ³*National Institute on Deafness and Other Communication Disorders*

The Shin lab studies the molecular basis of hearing and hearing loss, focusing on proteins important for the function and maintenance of the mechanotransducing hair bundle in sensory hair cells of the inner ear. A novel bundle protein, Xin Actin Binding Repeat Containing 2 (XIRP2), was identified in a previous utricular hair bundle proteomics study. XIRP2 was shown to be highly enriched in the bundle and to colocalize with filamentous actin (F-actin).

Genetic deletion of *Xirp2* by CRISPR/Cas9 causes progressive hearing loss in mice, but the underlying mechanism remains unknown. Unpublished data suggests that XIRP2 localizes to sites of F-actin damage in the stereocilia. XIRP2 may therefore be facilitating the repair and maintenance of the stereocilia F-actin. To test this hypothesis, we will knock-in a fluorescent protein into the endogenous *Xirp2* locus to determine whether GFP-XIRP2 is recruited to sites of mechanical damage in the stereocilia. Alternative splicing of *Xirp2* results in the expression of several isoforms, likely performing multiple functions within the hair cell. A short isoform of XIRP2 is localized specifically in the hair bundle, while longer isoforms are preferentially localized to the cuticular plate and cell-cell junctions. The short isoform contains a 3' exon (Exon 9) that is not included in the longer isoforms. It is also missing exon 7, which encodes the Xin repeats for which the protein is named. In addition to our *Xirp2* exon 2 KO mouse, which abolishes all isoforms, we used CRISPR to remove the exon 9 tail of the short isoform. The resulting truncated XIRP2 variant maintained its bundle localization. However, Auditory Brainstem Response measurements demonstrated that these mice still develop hearing loss. We hypothesize that the short XIRP2 isoform, specifically the exon 9 tail, is necessary for hair bundle maintenance. This study thus is expected to reveal a novel mechanism by which the F-actin cores of stereocilia are preserved throughout the life of the organism.

PS 772

Supervillin Is a Component of the Hair Cell's Cuticular Plate and the Head Plates of Organ of Corti Supporting Cells

Brian M. McDermott¹; Lana Pollock²; Nilay Gupta²; Xi Chen²

¹*Department of Otolaryngology - HNS, Case Western Reserve University*; ²*Case Western Reserve University*

The organ of Corti has evolved a panoply of cells with extraordinary morphological specializations to harness, direct, and transduce mechanical energy into electrical signals. Among the cells with prominent apical specializations are hair cells and nearby supporting cells. At the apical surface of each hair cell is a mechanosensitive hair bundle of filamentous actin (F-actin)-based stereocilia, which insert rootlets into the F-actin meshwork of the underlying cuticular plate, a rigid organelle considered to hold the stereocilia in place. Little is known about the protein composition and development of the cuticular plate or the apicolateral specializations of organ of Corti supporting cells. We show that supervillin, an F-actin cross-linking protein, localizes to cuticular plates

in hair cells of the mouse cochlea and vestibule and zebrafish sensory epithelia. Moreover, supervillin localizes near the apicolateral margins within the head plates of Deiters' cells and outer pillar cells, and proximal to the apicolateral margins of inner phalangeal cells, adjacent to the junctions with neighboring hair cells. Overall, supervillin localization suggests this protein may shape the surface structure of the organ of Corti.

PS 773

Different Role of Myosin-15a in the Development of Inner and Outer Hair Cells: Stereocilia Number and Diameter

Shadan Hadi¹; Andrew Alexander¹; A. Catalina Velez-Ortega²; Gregory I. Frolenkov³

¹*Department of Physiology, University of Kentucky;*

²*Department of Physiology, University of Kentucky, Lexington, KY, USA;* ³*Dept Physiology, University of Kentucky*

Myosin-15a is essential for the normal growth of stereocilia in the mammalian hair cells. There are two isoforms of myosin-15a with different functions and expression profiles. The short isoform of myosin-15a is expressed early in postnatal development and is responsible for normal stereocilia growth, while the long isoform with an N-terminus extension is expressed later and is responsible for the maintenance of transducing, shorter row stereocilia in the hair bundle (Fang et al., 2015). However, the role of Myosin-15 in the formation of other features of the hair bundle such as the number and diameter of stereocilia has not been investigated. Therefore, we are exploring the role of myosin-15a in the hair bundle development using two mice strains: (i) shaker2 mice where both isoforms are affected, and (ii) isoform-specific "deltaN" mice lacking the long isoform.

We used scanning electron microscopy to image the stereocilia of inner (IHC) and outer (OHC) hair cells at mid-cochlear location at postnatal days (PD): 1, 3, 6, 25, and 35. We found that the number of stereocilia per bundle decreases between PD1 and PD6 in both control heterozygous and mutant homozygous shaker2 mice, in both IHCs and OHCs. This decrease followed the normal developmental program, in which nascent hair bundles are formed by supernumerary stereocilia and are shaped later by retraction of redundant stereocilia. After PD6, however, we found that redundant stereocilia continue to retract in control hair cells and in shaker2 OHCs, but not in shaker2 IHCs.

We did not observe differences in the developmental changes of stereocilia diameter between control and shaker2 OHCs. Stereocilia in different rows of OHCs

have similar diameters, increasing between PD1 and PD6, and showing minimal changes afterwards. In contrast, stereocilia of normal IHCs are thick in the first (tallest) and second row, and thin in the third row. In control IHCs, first and second row stereocilia diameters increase gradually until ~PD25. In shaker2 IHCs, stereocilia grow in thickness until PD6, but there are minimal differences among rows.

We conclude that myosin-15a is essential for the retraction of redundant stereocilia and the formation of stereocilia diameter differences in IHC but not in OHC bundles. These differences between IHCs and OHCs may be related to the long isoform of myosin-15a, which was observed at the tips of all stereocilia rows in OHCs but only in the shorter row stereocilia in IHCs (Fang et.al, 2015).

Supported by NIDCD (R01DC014658).

PS 774

PKHD1L1, a New Hair-bundle Protein Required for High Frequency Hearing in Mouse

Xudong Wu; Artur Indzhykulia; Maryna Ivanchenko; David P. Corey
Harvard Medical School

From analysis of a hair-cell RiboTag database of translated proteins, we identified a novel protein highly enriched in hair cells, PKHD1L1. PKHD1L1 is a large protein of 4249 amino acids. It has a single transmembrane protein, and an extracellular domain that includes 14 IPT/TIG domains, 10 PbH1 repeats, and 2 G8 domains. The intracellular C-terminus is very short. PKHD1L1 is homologous to PKHD1, a gene mutated in autosomal-recessive polycystic kidney disease (ARPKD). However, PKHD1L1 itself is not associated with ARPKD. Previous research has suggested that PKHD1L1 is involved in the regulation of the cellular immunity. We investigated its role in hair cells.

Immunofluorescence staining revealed that PKHD1L1 expression has an apical to basal gradient along the cochlear coil, throughout the period from postnatal (P) day 0 to P7. In hair cells, PKHD1L1 is located in the hair bundle, primarily in the top half. We generated a PKHD1L1 conditional knockout mouse line. Disruption of the Pkhd1l1 gene in hair cells leads to loss of high frequency hearing as early as P21 but the loss did not progress with age. Planar cell polarity is not affected. Further detailed characterization of PKHD1L1 mutant mice may reveal PKHD1L1's specific function in hearing.

PS 775

Pejvakin, a Candidate Stereociliary Rootlet Protein, Regulates Hair Cell Function in a Cell-Autonomous Manner .

Martin Schwander¹; Marcin Kazmierczak¹; Piotr Kazmierczak²; Anthony W. Peng³; Suzan Harris¹; Prahar Shah¹; Jean-Luc Puel⁴; Marc Lenoir²; Santos Franco⁵
¹*Department of Cell Biology and Neuroscience, Rutgers the State University of New Jersey, Piscataway, New Jersey 08854*; ²*Inserm U1051, Institute for Neurosciences of Montpellier, 34091, Montpellier cedex 5, France*; ³*Department of Physiology and Biophysics, University of Colorado School of Medicine, Aurora, CO 80045*; ⁴*Institute for Neurosciences of Montpellier-Inserm U1051; University of Montpellier, France*; ⁵*Department of Pediatrics, University of Colorado School of Medicine, Aurora, CO 80045*

Auditory neuropathy spectrum disorder (ANSO) is a rare hearing disorder characterized by impaired neural transmission but normal function of cochlear outer hair cells (OHCs). Mutations in the Pejvakin (PJVK) gene are thought to cause ANSD and hearing loss of cochlear origin by affecting noise-induced peroxisome proliferation in auditory hair cells and neurons (Delmaghani et al., 2015). Here, we demonstrate that mice with conditional inactivation of pejvakin in auditory neurons have normal hearing and sensitivity to noise-induced hearing loss. By contrast, selective ablation of pejvakin in sensory hair cells causes profound hearing loss and OHC degeneration. Pejvakin binds to and co-localizes with the rootlet component TRIOBP at the base of stereocilia in injectoporated hair cells, a pattern that is disrupted by deafness-associated PJVK mutations. Hair cells of pejvakin-deficient mice develop normal rootlets, but hair bundle morphology and mechanotransduction are affected prior to the onset of hearing. In particular, some mechanotransducing shorter row stereocilia are missing, while the remaining ones exhibit over-extended tips and a greater variability in height and width. In degenerating hair bundles, stereocilia of all rows are successively resorbed. Unlike previous studies of Pjvk alleles with neuronal dysfunction, our findings thus reveal a cell-autonomous role of pejvakin in maintaining stereocilia architecture that is critical for hair cell function.

PS 776

Investigating Proteins Involved in Potential Modulation of Stereocilia Length and Stiffness

Sonal Prasad¹; Anders Fridberger²

¹*Department of Clinical and Experimental Medicine, Linköping University*; ²*Linköping University, Linköping, Sweden*

Background

Previous data (Hakizimana et al 2012) indicate that the length and stiffness of outer hair cell stereocilia are actively regulated. To find the mechanisms that underlie this stiffness modulation, we studied the membrane-cytoskeleton linker protein radixin, which is present in high concentration in stereocilia. The quinocarmycin analog DX-52-1 binds strongly and specifically to radixin and has previously shown considerable selectivity and faster kinetics for radixin over the other ERM proteins.

Methods

Temporal bones were excised from young normal hearing guinea pigs, and a small opening was made at the cochlea's base and at the apex. The basal opening was used to perfuse scala tympani with oxygenated tissue culture medium, whereas the apical opening provided an outlet for the perfusion solution and also allowed the organ of Corti to be observed using time-resolved confocal imaging. Special double-barreled electrodes were used for cochlear microphonic recording, electrical stimulation, staining of the bundle membrane with the membrane dye Di-3-ANEPPDHQ, and delivery of radixin inhibitor DX-52-1 (1.0mM). Quantitative confocal imaging was performed on a Zeiss LSM 780. In order to visualize the sound-evoked motion of stereocilia, sequences of confocal images were acquired during sound stimulation. Pixels acquired during the same phase of the stimulus were extracted using a Fourier series technique, and arranged into movies showing the sound-evoked motion of the bundle. Image acquisition triggered acoustic and electric stimulus. The extracellular potentials are tuned to a particular sound stimulus frequency near 220 Hz to get maximum response. The acquired image sequences were low-pass filtered and motion quantified through optical flow analysis using Matlab.

Results

When the DX-52-1 radixin blocker was introduced, the amplitude of the sound - evoked electrical potentials decreased substantially, and a pronounced change in the sound-evoked bundle deflections was observed. Motion at both the base and the tip of the bundle decreased, and there was a paradoxical increase in electrically evoked motion suggesting the function of radixin protein is important role for the bundle movements. Inhibition of radixin also led to a change in the properties of the ste-

reocilia membrane, as evidenced by using fluorescence recovery after photobleaching to measure the diffusion of Di-3-ANEPPDHQ within the stereocilia membrane.

Conclusions

Radixin influences several aspects of hair cell function, including sound-evoked stereocilia deflections and electromotility. Inhibition of radixin affect the bundle movement which might lead to reduced hearing.

Funding

Funded by the Swedish Research Council, the Söderberg Foundation and County Council of Östergötland.

PS 777

Refinement of Lipoma Hmgic Fusion Partner-like 5 to the Shorter Stereocilia Tips Occurs During Development in Mouse Cochlear Hair Bundles

David Furness¹; Shanthini Mahendrasingam¹; Robert Fettiplace²

¹Keele University; ²University of Wisconsin-Madison

The hair-cell mechanoelectrical transducer channel (MET) complex consists of the tip link, composed of CDH23 and PCDH15, with LHFPL5 (aka TMHS) associated with PCDH15 and TMC1 at its lower end. LHFPL5 is required for targeting of TMC1 and PCDH15 to the stereociliary tips (Xiong et al., 2012; Cell 151:1283-95; Beurg et al., 2015, PNAS 112:1589-94). Developmentally, the MET current is initially reversed in polarity, becoming normal by P2 to P4. It is uncertain whether this reflects developmental changes in location of the MET complex, expression of different channels (Fettiplace, 2016, Biophys J. 111:3-9) or the involvement of the kinocilium (Kindt et al, 2012, Dev Cell. 23:329-341). We have examined LHFPL5 distribution using transmission electron microscopy (TEM) to track developmental changes and whether these offer clues to changes in the MET current.

Cochleae from CD/1 mice (P0 to P21) were fixed using 4% paraformaldehyde, dissected, incubated in antibodies to LHFPL5 (Aviva Systems Biology) followed by 10 nm gold-conjugated secondary antibodies, postfixed and embedded in Spurr resin. Sections cut from comparable apical locations were examined by TEM and gold particle distributions quantified in three samples at each age.

At P0 bundles have thin stereocilia, approximately half of roughly equal height (0.5 – 0.75 mm) and half beginning to form ranked rows, and a kinocilium. LHFPL5 is dispersed throughout the bundle, including the kinocilium. By P3, 5 – 6 rows of ranked stereocilia are evident,

with scattered short stereocilia (0.2 – 0.5 mm) that are unranked in the centre with links between them. LHFPL5 localises to the tips of all ranked rows (including the tallest) and to lateral links on lower shafts, with some on unranked stereocilia and kinocilium. By P12 the bundle has three ranked rows but no unranked stereocilia or kinocilium. LHFPL5 localises to the tips of primarily shorter but not the tallest rows. Total gold-particle number in the bundle and kinocilium increases from P0 to P3 then decreases to a low level at P6. The proportion of tips labelled is reduced at P21 compared with P12.

These data suggest that the LHFPL5 is refined to the adult location of the MET over the first 12 days of post-natal development in mice and remains as a MET component in adults. Initial localisation on unranked stereocilia and lateral links, if accompanied by the MET, could explain the anomalous currents.

PS 778

TRIOBP Isoform Distribution Affects Stereocilia Rootlet Structure and Function

Tatsuya Katsuno¹; Inna A. Belyantseva²; Makoto Ikeya³; Kazuya Ono⁴; Kohei Segawa⁵; Juichi Ito⁶; Thomas B. Friedman⁷; Shin-ichiro Kitajiri⁸

¹Dept. Otolaryngology, Head and Neck Surgery, Kyoto University Graduate School of Medicine; ²Laboratory of Molecular Genetics, National Institute on Deafness and Other Communication Disorders, National Institutes of Health; ³CiRA; ⁴Laboratory of Molecular Biology, National Institute on Deafness and Other Communication Disorders, National Institutes of Health; ⁵Kyoto University Hospital; ⁶Shiga Medical Center Research Institute; ⁷Section on Human Genetics, Laboratory of Molecular Genetics, National Institute on Deafness and Other Communication Disorders, National Institutes of Health, Bethesda, MD, USA.; ⁸Department of Otolaryngology, Head and Neck Surgery, Graduate School of Medicine, Kyoto University

Background

TRIOBP is an actin-bundling protein necessary for hearing. Mutations of human TRIOBP are associated with nonsyndromic deafness DFNB28. In mouse inner ear hair cells, TRIOBP protein is localized in stereocilia rootlets. TRIOBP provides durability and rigidity for normal mechanosensitivity of the stereocilia bundle (Kitajiri et al., Cell 2010). TRIOBP encodes three major splicing isoforms: TRIOBP1, TRIOBP4 and TRIOBP5. The exact function and mechanism of action of each isoform in hair cells remain obscure. Here we investigate the physiological roles of each TRIOBP isoforms by using Triobp isoform-specific mutant mice.

Methods

In order to learn more about the functional significance of TRIOBP isoforms, we generated a TRIOBP5 null mutant mouse and an EGFP-TRIOBP4 transgenic mouse. Distribution of the TRIOBP isoforms was evaluated by immunocytochemistry and transmission electron microscopy to elucidate the morphology of stereocilia rootlets. The impact on the hearing sensation in each mutant mouse was evaluated by auditory evoked brainstem responses (ABR). Hair bundle morphology was examined by SEM.

Results

Immunocytochemistry revealed that TRIOBP4 is distributed from the top to the bottom of stereocilia rootlets, while TRIOBP1 and TRIOBP5 are localized in the part of the rootlet embedded in the cuticular plate. An EGFP-TRIOBP4 transgenic mouse has normal ABR responses suggesting that EGFP does not interfere with normal rootlet function or native localization of TRIOBP4. TRIOBP5 specific KO mice showed a severe hearing loss but were not profoundly deaf at 5 weeks of age. Stereocilia rootlets of the mutant mice were underdeveloped at P16 and especially malformed in the bottom part of rootlets located in the cuticular plate. Hair bundles of inner and outer hair cells undergo fusion and progressive degeneration beginning around one month of age.

Conclusion

TRIOBP isoforms have different distribution patterns along stereocilia rootlets and differentially alter the structure of rootlets and hearing.

PS 779

A Complex Transcriptional Landscape Underlies Regulation of the Stereocilia Actin Core by MYO15A

Jonathan E. Bird¹; Melanie Barzik¹; Randall J. Harley¹; Atteeq U. Rehman²; Thomas B. Friedman³

¹NIDCD/NIH; ²Department of Molecular and Human Genetics, Baylor College of Medicine; ³Section on Human Genetics, Laboratory of Molecular Genetics, National Institute on Deafness and Other Communication Disorders, National Institutes of Health, Bethesda, MD, USA.

Stereocilia are microvilli-derived organelles that elongate and thicken as they assemble into the mature hair bundle. These remarkable shape changes are driven by plasticity of the underlying actin cytoskeleton that comprises the stereocilia core. The molecular mechanisms regulating actin polymerization within stereocilia are poorly understood, but are critical for the acquisition and maintenance of mechanosensitivity. We recently report-

ed that two isoforms of the actin-based molecular motor myosin 15 (MYO15A) separately control elongation (isoform 2) and maintenance (isoform 1) of stereocilia lengths [1]. We hypothesize that MYO15A is a master orchestrator of the actin cytoskeleton within stereocilia, and that changes in isoform composition control polymerization/depolymerization kinetics that ultimately sculpt hair bundle architecture.

Isoform 1 of MYO15A differs from isoform 2 by inclusion of a giant exon 2 (~3,600 kb) encoding a 133 kDa N-terminal domain. To investigate whether additional diversity in MYO15A isoforms might further contribute to hair bundle architecture, we report here the discovery of two additional MYO15A isoform classes using 5'-RACE. The first new class utilizes multiple, internal transcriptional start sites (TSS) within giant exon 2 that are predicted to produce a series of isoform 1-like molecules with truncated N-terminal domains. The second new transcript class (designated isoform 3) utilizes a novel TSS in an unannotated, but highly conserved exon located within intron 2. This novel exon is predicted to encode a 50 residue N-terminal domain of unknown structure and function. Affinity-purified antisera specific to this novel N-terminal domain reveal that isoform 3 accumulates at stereocilia tips in mouse cochleae, similar to isoforms 1 and 2. A mouse model with a deletion of this exon is being generated to study the specific function of isoform 3 in hearing. Our data indicate yet further diversity in MYO15A protein isoforms and show that multiple TSS are engaged to generate a spectrum of N-terminal domains. How these different domains alter the biochemical properties of MYO15A to ultimately regulate actin polymerization at stereocilia tips [2] is the focus of ongoing investigations.

Acknowledgements: This work is funded by the intramural program of the NIDCD to T.B.F.

References:

- [1] Fang et al., (2015). The 133-kDa N-terminal domain enables myosin 15 to maintain mechanotransducing stereocilia and is essential for hearing. *Elife* doi:10.7554/eLife.08627
- [2] Drummond et al., (2015). Live-cell imaging of actin dynamics reveals mechanisms of stereocilia length regulation in the inner ear. *Nature Comms* doi:10.1038/ncomms7873

PS 780

Effects of the Hair Cell Soma on the Characteristics of Spontaneous Bundle Oscillations

Sebastian W.F. Meenderink¹; Patricia M. Quiñones²; Dolores Bozovic¹

¹Dept. of Physics and Astronomy; ²University of California Los Angeles

Hair bundles in the frog sacculus may exhibit spontaneous oscillations. These oscillations can be modelled as the result of the tension in the intervillar tip links and therewith associated open probability of the mechano-sensitive ion (MET) channels. Tip-link tension is changed by the opening/closing of the MET channels, as well as some intracellular adaptation mechanism. Although the exact adaptation mechanism(-s) is not established, it seems evident that it is affected by intracellular calcium. With this, the cell's membrane potential (V_m) can affect spontaneous oscillations, since the driving force for calcium into the cell depends on both the electrical and chemical gradient across the membrane. We demonstrated that, indeed, the cell's V_m can control the presence/absence of spontaneous bundle oscillations, and that several of their characteristics systematically vary with V_m . Here, we elaborate on these experiments by augmenting the constant membrane potential (DC) with various AC components. These were used to explore the dynamical aspects of the membrane potential's "feedback" to the mechanically oscillating hair bundle.

For the experiments, sacculi from the American bullfrog (*R. catesbeiana*) were used. These were freshly dissected from the ear, and placed in a two-compartment chamber such that a fluid separation between the apical and basolateral surfaces of the hair cells was maintained. We obtained simultaneous optical and electrophysiological recordings from hair cells that had spontaneously oscillating hair bundles. Hair bundle position was tracked using a high-speed video camera system, and the hair cell membrane potential was controlled (voltage-clamp) or monitored (current-clamp) using conventional whole-cell, patch-clamp techniques. Stimuli controlling the cell's membrane potential consisted either of sinusoidal waveforms or band-limited noise, presented at several different DC potentials.

Using a range of different stimulus frequencies and amplitudes we reconstructed receptive field maps showing the 1:1 phase-locked response of bundle position and the synchronously obtained electrophysiological recording. These are clearly correlated, and both reveal a tuned response. Moreover, the tuning to AC fluctuations in the membrane potential seems to match the frequency of the spontaneously oscillating hair bundle. In a similar fashion, noise as a stimulus also suggests that the cell

soma provides a frequency selective, voltage-mediated feedback to the hair bundle. By matching the frequencies that are dominant in the soma's and in the bundle's response, their coupling may actually enhance the hair bundle sensitivity to mechanical stimuli.

This work was supported by NIDCD, grant number RO1DC011380 and R21DC015035.

PS 781

Mechanically Tuned Responses of Spontaneously Oscillating Hair Bundles

Patricia M. Quiñones¹; Sebastian W.F. Meenderink²; Dolores Bozovic²

¹University of California Los Angeles; ²Dept. of Physics and Astronomy

Hair cells of the vertebrate vestibular and auditory systems show spontaneous bundle oscillations which are presumed to arise from the coupling of mechano-electrical transduction (MET) channel activation and some active feedback mechanism (adaptation) which keeps the MET channels at their most sensitive operating range. Previously, we combined high-speed video imaging of hair bundle motility and voltage-clamp of hair cells and showed that the membrane potential (V_m) of the hair cell can fully suppress or modulate several properties of the innate oscillations, thus controlling the dynamic state of the bundle. Here, we elaborate on these previous experiments by adding a piezo-driven mechanical stimulus probe to our simultaneous optical and electrophysiological recordings. This allows us to examine if V_m affects the mechanical tuning of the hair bundle.

Freshly dissected sacculi from the American bullfrog (*R. catesbeiana*) were mounted such that the fluid separation between the apical and basolateral surfaces of the hair cells was maintained. A combination of mechanical stimulation, using a floppy, mechanical probe and electrical stimulation via patch-clamp in either voltage- or current-clamp were used to probe the tuning of the hair bundle. The bundle position was tracked by calculating the bundle's center of gravity in each frame of a movie that was recorded using a high speed video camera system. Mechanical stimuli, sent to the hair bundle, consisted of a series of discrete sinusoids, the responses to which were used to construct receptive field maps for the 1:1 phase-locked component. In conjunction with the mechanical stimulus, the membrane potential was either actively maintained (V-clamp) or monitored (I-clamp) via the patch electrode.

The frequency of spontaneous bundle oscillations decreases as the membrane potential is depolarized. Our

preliminary data suggest that the mechanical tuning shows a similar shift in such a way that the frequencies of spontaneous bundle oscillations and highest mechanical sensitivity match. Moreover, differences in mechanical tuning obtained in voltage- or current-clamp exist. The transduction current that follows from mechanically opening the MET channels cannot change the membrane potential in voltage-clamp, while it can during current-clamp.

Furthermore, comparison of responses obtained in voltage- and in current-clamp indicate that the dynamical aspects of the voltage-mediated channels in the soma play a role in the bundle's mechanical response.

This work was supported by NIDCD, grant number RO1DC011380 and R21DC015035 to DB.

PS 782

Fascin-2 Crosslinks Turn over Much Faster Than Actin Filaments in Stereocilia

Benjamin Perrin; Pallabi Roy

Indiana University - Purdue University Indianapolis

Sensory hair cells have numerous protrusions known as stereocilia. The length of a stereocilium depends on the regulation of its actin core, which is a bundle of exceptionally stable parallel actin filaments. The actin filaments are heavily crosslinked by several proteins including fascin-2, an abundant actin crosslinking protein that is critical for stereocilia length maintenance. To better understand stereocilia homeostasis, we sought to measure the dynamics of fascin-2 using a novel transgenic mouse where GFP-fascin-2 expression is induced by cre recombinase. Overexpression of fascin-2 caused a slight increase in stereocilia length, but did not otherwise perturb stereocilia morphology or auditory performance. We assessed GFP-fascin-2 dynamics in stereocilia of hair cells from explants of early postnatal transgenic mice by measuring fluorescence recovery after photobleaching (FRAP). GFP-fascin-2 fluorescence recovered by uniformly incorporating along the entire length of stereocilia. The rate of fluorescence recovery was faster in outer hair cell stereocilia compared to inner hair cell, with half maximal recovery times in both cases of several minutes. These results contrast with photobleaching of GFP-actin, which did not recover fluorescence along the stereocilia length but instead recovered only at the tips over an hours-long timecourse. Therefore, actin and the actin crosslinker fascin-2 have markedly different behavior in stereocilia with fascin-2 being turned over much more rapidly compared to actin filaments.

PS 783

Reconciling Adaptation Mechanisms in Mammalian Cochlear Hair Bundles

Anthony W. Peng¹; Anthony J. Ricci²

¹*Department of Physiology and Biophysics, University of Colorado School of Medicine, Aurora, CO 80045;*

²*Stanford University, School of Medicine, Department of Otolaryngology*

In the auditory system, sensory hair cells convert mechanical stimuli into electrical signals at the hair bundle and pass the information onto the central nervous system. A key mechanism in this mechanotransduction process is adaptation to sustained deflection of the hair bundle. Calcium has long been thought to drive this process, but we recently challenged the calcium dependence of adaptation (Peng et al., 2013). However, others have subsequently shown calcium dependent adaptation in mammalian hair cells (Beurg et al., 2015; Corns et al., 2014, 2016), raising a bit of a controversy. Using new high-speed imaging of the hair bundle to track the position of the hair bundle during stimulation, we attempt to reconcile the differences in the various studies. Using fluid jet stimulation (force steps) of the mammalian hair bundle, we find that different states of the cell can result in differing amounts of current decline. This current decline during a force step appears to contribute to a calcium dependent version of adaptation, however another version of adaptation persists that does not manifest as a current decline during a force step. The multiple mechanisms of adaptation help to reconcile the seemingly contradictory results and indicate that calcium dependent and calcium independent adaptation mechanisms exist.

Beurg, M., Goldring, a. C., and Fettiplace, R. (2015).

The effects of Tmc1 Beethoven mutation on mechanotransducer channel function in cochlear hair cells. *J. Gen. Physiol.* 146, 233–243.

Corns, L.F., Johnson, S.L., Kros, C.J., and Marcotti, W. (2014). Calcium entry into stereocilia drives adaptation of the mechano-electrical transducer current of mammalian cochlear hair cells. *Proc. Natl. Acad. Sci. U. S. A.* 111, 14918–14923.

Corns, L.F., Johnson, S.L., Kros, C.J., and Marcotti, W. (2016). Tmc1 Point Mutation Affects Ca²⁺ Sensitivity and Block by Dihydrostreptomycin of the Mechano-electrical Transducer Current of Mouse Outer Hair Cells. *J. Neurosci.* 36, 336–349.

Peng, A.W., Effertz, T., and Ricci, A.J. (2013). Adaptation of Mammalian Auditory Hair Cell Mechanotransduction Is Independent of Calcium Entry. *Neuron* 80, 960–972.

PS 784

Structural and Biophysical Characterization of Inner-Ear Tip Link Variants

Yoshie Narui; Marcos Sotomayor
The Ohio State University

Human hearing relies upon the tip-to-tip interaction of two unique non-classical cadherins, protocadherin 15 (Pcdh15) and cadherin 23 (Cdh23). Together, these two proteins form a fine filament called the tip link that connects neighboring stereocilia on the apical side of mechanosensitive hair cells. As sound waves enter the cochlea, the stereocilia deflect and tension is applied to the tip link resulting in the opening of nearby transduction channels. Disruption of the tip link caused by loud sound or calcium chelators eliminates transduction currents and illustrates that tip link integrity is critical for mechanosensing. Recent studies have found that remodeling of the tip link after disruption is a dynamic process, which can lead to the formation of atypical complexes that may incorporate alternatively spliced variants of Pcdh15. Our current work focuses on understanding these unusual tip links and comparing them with the canonical tip link. Here, we present the crystal structure of a new complex formed from the first two extracellular cadherin repeats of Cdh23 and Pcdh15, CD1-2 refined at 2.3 Å resolution (PDB code:4XXW). While the molecular structure reveals subtle differences between the two complexes, the binding affinity between Cdh23 and Pcdh15, CD1-2 is ~8 times weaker than Cdh23 and Pcdh15, CD1-1 as determined by surface plasmon resonance analysis. In addition, steered molecular dynamics simulations reveal that the unbinding force of the Cdh23-Pcdh15, CD1-2 complex is notably lower than the canonical tip link. Three additional variants of Pcdh15, with differences in the extracellular domain, were included in this study. Our results demonstrate that alternative heterotypic tip link structures form stable protein-protein interactions in vitro and provide no evidence to support the existence of homotypic Pcdh15-Pcdh15 tip links.

PS 785

Homeostatic Enhancement of a Hair Bundle's Ability to Detect Sound

Andrew Milewski; Daibhid O Maoileidigh; Joshua Salvi; A J Hudspeth
The Rockefeller University

Introduction

Our sense of hearing boasts exquisite sensitivity, precise frequency discrimination, and a broad dynamic range. However, mathematical and computational models imply that the auditory system achieves this performance for only a narrow range of parameter values. As a result,

minuscule changes in certain parameters could compromise a hair cell's ability to detect sound. How might hair cells ensure operation at the requisite performance level? We propose that, rather than exerting precise control over parameters, hair cells employ a homeostatic mechanism that increases the robustness of their operation to changes in parameter values.

Methods

We evaluate this hypothesis by developing mathematical models of hair-bundle dynamics and endowing each with a specific homeostatic mechanism. We examine two models in which we confer dynamics upon the rate of adaptation to stimulation or upon the strength of the adaptation force. Through analytical techniques and computer simulations we investigate whether each homeostatic mechanism renders the model's signal-detection ability more robust to changes in two experimentally accessible parameters.

Results

The sensitivity, sharpness of tuning, and dynamic range in both models are more robust to changes in parameter values when the homeostatic mechanism is operational. For example, the range of values for which one of the models exhibits sharp frequency selectivity increases sixfold. The models also make experimentally testable predictions. For example, the homeostatic mechanism engenders delays in the hair bundle's response to force-pulse stimuli that are absent when the mechanism is inactive.

Conclusions

We show that, by widening the range of parameter values over which a hair bundle can attain the desired level of performance, a homeostatic mechanism can render signal detection by a hair cell more robust. The responses to mechanical stimuli predicted by the models provide a means to determine through experiment whether such a mechanism is actually employed by hair cells.

PS 786

Intracochlear Responses to Acoustic Stimuli during Cochlear Implantation

Christopher K. Giardina¹; Tatyana E. Fontenot¹; Kevin D. Brown¹; Craig Buchman²; Oliver Adunka³; Harold C. Pillsbury¹; Douglas C. Fitzpatrick¹

¹University of North Carolina Department of Otolaryngology-Head and Neck Surgery; ²Washington University in St. Louis Department of Otolaryngology; ³The Ohio State University

Background

Electrode selection and surgical considerations are taken to minimize damage to the cochlea during cochlear implantation (CI). Objective measures of cochlear health throughout CI insertion would be useful in detecting and possibly minimizing trauma. Additionally, accounting for overall trauma could aid in accounting for the wide range in speech and hearing outcomes. One approach to monitor residual cochlear activity is with electrocochleography (ECochG), or measurements of the sound-evoked responses of the cochlea. Specifically, we play a loud, low frequency tone and record intracochlear responses from the apical contact using a clip that connects standard recording equipment directly to the CI. This approach is distinct from other methods which are performed completely through the CI's telemetry.

The goal of this study was to characterize response changes throughout CI insertion. The hypothesis tested was that response magnitudes would increase with insertion depth as the apical contact approached surviving generators.

Methods

Twenty-one subjects of all ages receiving Cochlear Corporation or Advanced Bionics electrode types were included. Just before CI insertion, a standard monopolar probe was used to measure the ECochG at the RW to a 500 Hz, 107 dB SPL tone. Next, the CI was seated, manufacturer-provided telemetry software was used to create a digital short between the apical CI contact and a case reference electrode, and the clip to the recording system (Biologic from Natus, Inc) was attached to the CI reference contact. Responses to the 500 Hz stimulus were then collected during CI insertion.

Results

Responses through the CI/clip combination were detectable in 17 of the 21 subjects. The RW responses generally correlated with initial response through the CI (R2 = 0.55). Throughout CI insertion, response magnitudes

increased by more than 5 dB in 6 subjects, was within 5 dB of starting response in 10 subjects, and fell by more than 5 dB in one subject. Interestingly, in five subjects temporary deflections either increasing or decreasing by 5 dB reversed by the end of CI insertion. These waveforms demonstrated changes in latency and/or phase, suggestive of changing proportions of neural and hair cell contributions. Only one subject with changes in phase did not have an associated change in magnitude throughout insertion.

Conclusions

During CI insertion the intracochlear response magnitudes could increase, stay steady, or fluctuate. Reaching conclusions about whether a drop in response is due to trauma requires a more detailed analysis of the waveforms than simple measurements of magnitudes.

PS 787

Inhibition of Focal Adhesion Kinase Reduces Loud-Sound Induced Stress Response in the Cochlea

Qing Yu; Sarah Foster; Teresa Wilson; Alfred L Nuttall; Alfred L. Nuttall

Oregon Health & Science University

Background

Focal adhesion kinase (FAK) is a cytoplasmic protein-tyrosine kinase that is activated in response to integrin clustering, growth factors and ROS. It is involved in multiple cellular functions such as cell proliferation, motility, survival, invasion, metastasis and angiogenesis. FAK activity in endothelial cells (ECs) is important for regulating vascular permeability by promoting the phosphorylation, internalization and degradation of VE Cadherin and β -catenin, leading to increased vascular permeability. FAK signaling also promotes activation of the MAPK signaling cascade, which leads to upregulation of pro-inflammatory factors. Here, we examined the role of FAK in modulating the loud sound-induced stress response in the cochlea.

Methods and Results

10 week old CBA/CAJ mice, males and females, were used in this study. Immunolabeling of isolated spiral ligament (SL) and stria vascularis (SV) tissues revealed that, in endothelial cells (ECs), FAK was present in the nucleus, cytoplasm, and at the plasma membrane where it overlapped with VE-Cadherin. Next, we found that VS-4718, a small molecular FAK kinase activity inhibitor, attenuated both VEGF and H2O2-induced increases in pFAK Y397 phosphorylation levels in whole mount preparations of SV and SL tissues. Exposure of mice to loud sound (105 dB SPL, 8-16 kHz, 2 hours) resulted in increased levels of FAK Y397 phosphorylation in SV ECs and type I fibrocytes of the SL. To determine wheth-

er FAK kinase inhibition would attenuate noise-induced loss of hearing sensitivity, mice were treated with VS-4718 (30mg/kg, IP) or vehicle (PEG 400/2.25% DMSO/saline) at 1hr prior and 24 hrs post-loud sound exposure. Auditory brainstem response analysis revealed that VS-4718 treatment significantly reduced loss of hearing sensitivity as compared to controls. Quantitative RT-PCR analysis showed that FAK kinase inhibition also reduced the upregulation of several pro-inflammatory factors following noise exposure.

Conclusions

Pharmacological inhibition of FAK activity proved protective against loud sound-induced increase of inflammatory factor expression and hearing threshold shifts, establishing a role for FAK activity in loud sound-induced hearing sensitivity loss.

Funding

Supported by grants 5R01DC000105 (ALN) and P30DC005983.

PS 788

Role of Outer Hair Cell-Specific Signal Transducers and Activators of Transcription 3 in Protection Against the Noise-Induced Stress

Suzan Dziennis; Teresa Wilson; Sarah Foster; Alfred L Nuttall; Alfred L. Nuttall
Oregon Health & Science University

Background

Signal transducers and activators of transcription 3 (STAT3), part of Janus kinase/signal transducer and activator of transcription (JAK/STAT) signaling pathway, is a mechanism for transducing extra-cellular signals into a transcriptional response. We previously reported that although NE induced STAT3 translocation to the nucleus in other cell types, it remained in the cytosol of outer hair cells (OHCs). Recently the importance of non-genomic activities of STAT3 in preserving mitochondrial function and autophagy under stress conditions have been described. Here, we generated OHC-specific STAT3 knock-out mice to better understand the function of STAT3 in OHCs as well its role in the noise-induced stress response.

Methods and Results

Floxed STAT3 mice were crossed with prestin-CreERT2 mice for several generations to produce STAT3^{fl/fl} x prestin-CreERT2^{+/-} (STAT3^{fl/fl}) mice. Tamoxifen treatment resulted in STAT3 deletion specifically in OHCs (STAT3OHC Δ/Δ). The OHCs of 8 week old STAT3OHC Δ/Δ mice appeared morphologically normal and a full complement of OHCs was present. Ex vivo cochlea from STAT3^{fl/fl} and STAT3OHC Δ/Δ mice were

treated with IL-6, antimycin A or corresponding vehicle and nuclei stained with Hoechst. IL-6 or antimycin A treatment resulted in contrasting effects on nuclear morphology based on the loss of STAT3 demonstrating the importance of STAT3 in the noise-induced cellular stress response. Auditory brainstem response (ABR) analysis demonstrated that STAT3OHC Δ/Δ mice had normal hearing thresholds relative to STAT3^{fl/fl} and wildtype C57Bl/6 mice. The mice were exposed to a loud sound protocol of 96 dB SPL, 8-16 kHz for 1 hour. At 2 weeks post-NE, ABR thresholds were assessed and mice were sacrificed for cytochocleogram analysis. ABR analysis revealed that the STAT3OHC Δ/Δ group had significant loss of hearing sensitivity at 24 and 32 kHz relative to STAT3^{fl/fl} mice. Furthermore, cytochocleograms from NE STAT3OHC Δ/Δ mice revealed reduced survival of OHCs relative to STAT3^{fl/fl} mice.

Summary

OHC-specific STAT3 deletion decreased hearing sensitivity after noise exposure, and altered nuclear morphology in response to two distinct cellular stress pathways, IL-6 and antimycin A. Taken together, these data suggest STAT3 contributes to protection against noise-induced injury in OHCs, likely due to multiple and diverse activities of STAT3 including protector of mitochondrial function, and mediator of oxidative stress injury.

Funding

Supported by grants 5R01DC000105 (ALN) and P30DC005983.

PS 789

Effect of Mitochondrial-Targeted Peptide on Aminoglycoside-Induced Ototoxicity and Transient Threshold Shift in the Cochlea

Michael Brenner¹; Peng Jiang²; Mark Crumling³; Lisa Kabara⁴; David Dolan⁴; Keith Duncan³

¹Kresge Hearing Research Institute, Dept of Otolaryngology, University of Michigan; ²University of Michigan, KHRI; ³Kresge Hearing Research Institute, University of Michigan; ⁴University of Michigan Medical School

Introduction

Most cellular reactive oxygen species are formed in the mitochondria, suggesting the mitochondria as potential targets for protection from acquired hearing loss. Peptides that localize to inner mitochondrial membrane can stabilize mitochondrial cristae and promote oxidative phosphorylation. The possibility of improving bioenergetics and preventing cellular injury has prompted clinical trials of these peptides for skeletal, ocular, cardiac, and renal diseases. Such peptides are unstudied in the ear. We investigated SBT-20, a mitochondrial-target-

ed peptide, as a potential protectant from noise- and drug-induced injury.

Methods

SBT-20 protection from gentamicin ototoxicity was investigated in P2-P3 neonatal murine organ of Corti explants. Gentamicin (4.2 μ M) was administered alone or in combination with SBT-20 at 1-100 μ M and cytochrome c assays performed. SBT-20 was also studied with hydroxypropyl- β -cyclodextrin (HPBCD), another ototoxic drug. FVB/NJ mice received daily 5 mg/kg SBT-20 dosing for 5 days and 8000 mg/kg HPBCD for 4 days, with ABRs at 8, 16, and 32 kHz recorded at 7-10 days after HPBCD injection. In guinea pigs, a transient threshold shift model was used to evaluate potential SBT-20 protection from noise, with animals exposed to a 7 kHz centered, half-octave noise at 97 dB SPL for 2 hours. Animals received vehicle, 1 mg/kg SBT-20, or 5 mg/kg SBT-20. DPOAEs and ABRs at 8, 12, and 16 kHz were recorded at baseline and immediately, 3, and 14 days post-noise.

Results

SBT-20 was well tolerated in explants up to 30 μ M but did not confer protection from 4.2 μ M gentamicin. SBT-20 concentrations above 10 μ M increased gentamicin-induced hair cell loss. The HPBCD regimen induced 40-60 dB threshold shift across frequencies. No toxicity or elevation in ABR thresholds was observed with SBT-20 in treated or untreated FVB/NJ mice. ABR threshold elevations were similar among animals receiving HPBCD regardless of SBT-20 therapy. In the guinea pig noise model, transient threshold shift was demonstrated, with 40-60 dB SPL transient threshold shift across frequencies and recovery of thresholds to near normal levels at day 14. SBT-20 was not associated with hearing loss or toxicity on ABR/DPOAE, and determination of any potential protection awaits further enrollment and analysis.

Conclusion

Mitochondrial-targeted peptides that stabilize bioenergetics have intuitive appeal as tools to mitigate oxidative stress; but, their potential to preserve normal energy production and redox balance in mitochondria is predicated on successful peptide entry. Further research is needed to investigate uptake patterns in the inner ear and potential of peptides for inner ear delivery.

PS 790

Increase in Resistance Against Oxidative Stress in Inner-ear Hair Cells by the Use of Cobalt Chloride

Jong Woo Chung¹; Chan Ju Yang¹; Jhang Ho Pak¹; Christopher Chung²; Jeonghee Lim²

¹Dept. of ORL-HNS, Asan Medical Center, University of Ulsan College of Medicine; ²Dept. of ORL-HNS, Asan Medical Center

Introduction

Noise-induced hearing loss refers to a decrease in hearing due to noise exposure. Accumulation of HIF-1 by CoCl₂ before noise exposure may inhibit the damage of inner ear. The aim of this study is to elucidate the signal pathway of CoCl₂ in mouse inner ear cell line.

Methods

CoCl₂ was applied in the inner ear hair cell line (HEI-OC1) and the expression of transcription factors and cellular proliferation was measured by western blotting and CCK assay.

Results

Nuclear accumulation of HIF1a was evident by CoCl₂ application. Under 100 mM CoCl₂ exposure, expression of HIF-1a was gradually increased, reaching a maximal level at 9 h, and declined to basal level at 24 h. When the cells were incubated with CoCl₂ for 9 hours, HIF-1a expression increased in nucleus and Nrf2 expression increased in 50 and 100 mM of CoCl₂. In cytoplasm, PrDx6 expression reached maximal relative density at 100 mM of CoCl₂. Cytoplasmic Keap1 expression decreased at the CoCl₂ incubation.

Conclusions

The mechanism of the protective role of CoCl₂ preconditioning may depend on the activation of anti-oxidant mechanism with PrDx-6 and Nrf-2.

PS 791

Use of STR001 in Hearing Preservation Following Cochlear Implant: A Phase II Study Update

Arne Ernst¹; Claudia Berger²; Viktor Boerlin²; Alexander Bausch²; Jacques Gaudreault²; Daniel Bodmer³

¹Department of Otolaryngology at Unfallklinik Berlin, University of Berlin, Germany; ²Strekin AG; ³University Hospital Basel

Despite the advances in surgical techniques, the loss of residual hearing following Cochlear Implant (CI) Surgery remains an issue in CI eligible patients. STR001 is a new formulation of pioglitazone which has shown in vitro and in animals to preserve hair cells and protect

animals from hearing loss. We are conducting a randomized, multi-center, placebo-controlled Phase II study where patients with residual hearing (average PTA of \leq 80 dB in the 125-750 Hz) will be randomized to receive either placebo (N=55) or STR001 (N=55), administered by intratympanic injection. The first dose is administered within 24 to 12 hours prior to the CI surgery and the 2nd administration following insertion of the electrode. Patients are followed for a 6 week period for safety, tolerability and hearing capacity by audiometry with the primary endpoint as the average PTA (125-750 Hz) at Week 6. This study is enrolling patients in several countries and approximately 20% of the patients have been enrolled. For the first 10 patients enrolled, 6 were female and 4 male with a mean age of 52 years (range 30-67) with a baseline average PTA (125-750 Hz) mean (SD) of 58 (17) dB (range 30-78). A round window approach was used on all patients. Further details of the study design, update on the study progress and baseline characteristics of the study population will be presented.

PS 792

Treatment Window for Oral Administration of the Clinical Drug Candidate SENS-401 after Acoustic Trauma in Rat

Mathieu Petremann; Jonas Dyhrfeld-Johnsen; Laurianne Beynac; Pierre Liaud
Sensorion

Currently no approved pharmaceutical treatment exists for sudden sensorineural hearing loss and recent meta-analysis of the standard-of-care, off-label use of corticosteroid therapy has concluded that neither systemic nor intratympanic administration has any significant treatment effect (Crane et al. 2015, *Laryngoscope* 125(1):209-17). Noise-induced hearing loss is among the most common types of permanent hearing loss for adults (American Speech-Language-Hearing Association - ASHA; Hearing Loss Association of America - HLAA) and animal models of acoustic trauma are the most validated preclinical model of sudden sensorineural hearing loss.

SENS-401 is small molecule, orally administered clinical drug candidate and achieves significant local exposure in perilymph (50-500 nM) and inner ear tissue (50-800 nM) lasting at least 8 hours after a single oral administration in naïve rats.

Following baseline audiometry (ABRs at 8/16/24 kHz; DPOAEs at 4/8/16/24/32 kHz), 7 week old awake and behaving male Wistar rats were exposed to 120 dB octave band noise (8-16 kHz) for 2 hours. Daily oral SENS-401 treatment at 18.2 mg/kg base-equivalent was initiated either immediately after acoustic trauma or with a

delay of 24h or 48h and compared to oral placebo controls.

At D14, placebo treated animals (n=6) displayed ABR threshold shifts of 50 ± 7 dB to 62 ± 4 dB and DPOAE amplitude loss of 12 ± 4 dB to 34 ± 4 dB depending on stimulus frequency. Initiation of SENS-401 oral treatment immediately after acoustic trauma induction (n=6 rats) or with 24h delay significantly reduced ABR threshold shifts (immediate: 33-52 dB mean reduction, $p < 0.001$, n=6; 24h delay: 7-22 dB mean reduction, $p=0.009$, n=5) and enhanced ABR amplitude recovery from 24h to D14 post-trauma (immediate: 21-29 dB mean gain, $p < 0.001$, n=6; 24h delay: 12-14 dB mean gain, $p=0.016$, n=5) while treatment initiation with a 48h delay (n=6) only reached significant results at 8 kHz. All treatment initiation delays resulted in significant reduction of DPOAE amplitude loss (immediate: 13-26 dB mean reduction, $p < 0.001$, n=6; 24h delay: 12-14 dB mean reduction, $p < 0.001$, n=5; 48h delay: 2-10 dB mean reduction, $p < 0.001$, n=6) and enhanced DPOAE amplitude recovery from 24h to D14 post-trauma (immediate: 3-12 dB mean gain, $p=0.004$, n=6; 24h delay: 8-10 dB mean reduction, $p < 0.001$, n=5; 48h delay: 1-7dB mean reduction, $p=0.024$, n=6).

These results demonstrate that daily, oral administration of SENS-401 leads significant treatment benefits in rats suffering from severe, acute noise-induced hearing loss when administered up to 48 hours after acoustic trauma, consistent with clinical treatment requirements.

PS 793

Precision Medicine for Hearing Loss: Zebrafish Based Drug Screen

Alaa Koleilat¹; Aaron Lambert²; Tim Wiggin³; Mark Masino⁴; Stephen Ekker¹; Lisa Schimmenti¹

¹Mayo Clinic; ²University of Minnesota, Twin Cities, Harvard University; ³University of Minnesota, Twin Cities, Brandeis University; ⁴University of Minnesota, Twin Cities

Background

Hearing provides the basis of human speech. Current treatment to restore hearing consists of hearing aids and cochlear implants. We hypothesize that precision medicine principles can be used to identify pharmacologic therapies for hereditary hearing loss using zebrafish as a model organism. Homozygous recessive pathogenic variants in MYO7A are a common hereditary form of human hearing loss causing Usher Syndrome Type 1, characterized by profound congenital deafness and retinopathy. MYO7A encodes an unconventional myosin involved in maintaining the tension in hair cell stereo-

ilia. The mariner mutant is a zebrafish model of Usher Syndrome Type 1 caused by homozygous *myo7aa* mutations. Mariner zebrafish exhibit deafness and abnormal circular swimming. The objective of this study is to identify specific drugs that rescue the mariner swimming behavior.

Methods

We developed a quantitative method to assess wildtype and mariner mutant swimming by measuring average global change in body orientation (AGC). This methodology was used to evaluate the efficacy of various drugs to restore proper swimming behavior in the mariner mutants. Videos were acquired at either 120 or 180 fps using Flycap 2.0 software and the Point Grey Flea high-speed camera. Processing was performed using Ctrax and analysis using in-house scripts in Matlab. Comparisons for the mean global change in body orientation between treated and untreated groups were conducted using a student's t-test with an $\alpha=0.05$. Statistical analyses were performed with Sigma Plot 13.0 software for Windows.

Results

The AGC for wildtype fish was 670 +/- 180 radians/second. In contrast, the mariner fish had an AGC of 1100 +/- 300 radians/second ($p < 0.001$). Using two different L-type calcium channel agonists, (\pm)-Bay K 8644 and Nefiracetam, the AGC was 780 +/- 200 and 920 +/- 180 radians/second, respectively. Neither drug had any adverse effects on swimming in wildtype fish. The AGC of the mariner fish incubated in 5 μ M of (\pm)-Bay K 8644 differed from the control untreated mariner fish ($p < 0.001$) and did not differ from wildtype untreated fish ($p=0.114$). The AGC of the mariner fish incubated in 250 μ M of Nefiracetam differed from the untreated mariner controls ($p=0.006$).

Conclusions

These preliminary studies support that treatment with L-type calcium channel agonists shifts swimming behavior towards wildtype swimming. Further studies for sound response are required; however, this represents a step towards discovering compounds to treat hearing loss caused by mutations in MYO7A.

PS 794

Emerging Concepts for Otoprotection and Early Detection of Cisplatin-Induced Ototoxicity

James Naples¹; Kourosh Parham²; Gregory Bonaiuto¹

¹University of Connecticut Health Center; ²Un

Background

The chemotherapeutic agent, cisplatin, causes ototoxicity through calcium-mediated apoptosis of the outer hair

cells. Damage caused by cisplatin is permanent and irreversible. Current methods for detection of ototoxicity are available only after damage has occurred, and there are no otoprotective agents currently available. Diltiazem has shown promise as an otoprotectant and the concept of serological biomarkers in otology is an emerging concept. We use a guinea pig model to assess diltiazem as an otoprotective agent and explore use of a novel, serum biomarker, prestin, for early detection of cisplatin ototoxicity.

Methods

2 groups of guinea pigs were used to evaluate auditory brainstem response (ABR) thresholds to click- and pure-tone stimuli.

All animals had baseline ABR thresholds recorded and serum prestin levels obtained. A cisplatin bolus (8mg/kg) was given followed by 5 consecutive days of intratympanic diltiazem (2 mg/kg) (n=9) or saline (n=10). Serial ABR thresholds and prestin levels were obtained at 24, 48, 72hr, Day 7, and Day 14.

Results

Mean ABR thresholds showed significant elevation as a function of time after cisplatin administration in saline-treated animals ($p < 0.001$). In contrast, mean ABR thresholds in diltiazem-treated animals were not significantly different from baseline values at Days 7 and 14. Mean serum prestin levels showed significant early rise at 24, 48, and 72 hrs ($p < 0.001$, $p=0.022$, $p < 0.001$ respectively). While in the diltiazem group, mean prestin values remained near baseline.

Conclusion

Diltiazem demonstrates otoprotective effects against cisplatin ototoxicity, and prestin shows promise as a biomarker for early detection of inner ear damage. The guinea pig model appears to be a reliable model with which to study these concepts of early detection and protection of cisplatin ototoxicity.

PS 795

Using Mouse Stem Cell-derived 3D Inner Ear Organoids to Understand the Cellular and Molecular Mechanisms Underlying Hair Cell Degeneration

Pei-Ciao Tang; Rick Nelson

Indiana University School of Medicine

Hair cells are the key constituents of the mechanotransduction apparatus in auditory and vestibular systems, and their degeneration leads to hearing loss and vestibular dysfunction. Hair cell degeneration results from many causes, including genetic defects, aging, noise, or ototoxicity, and the molecular and cellular mechanisms

underlying such degeneration vary depending on the proximate cause of damage. Understanding the mechanisms underlying hair cell degeneration in mammals is a necessary first step for the development of therapeutics. Herein, a new system for studying hair cell degeneration using mouse embryonic stem cell (ESC)-derived 3D inner ear organoids is demonstrated. We targeted the type II transmembrane serine protease 3 (Tmprss3) locus of mESC using CRISPR/Cas9. Mutations throughout the human TMPRSS3 gene are known to cause non-syndromic autosomal recessive deafness (DFNB8/10), and Tmprss3 mutant mice (Tmprss3^{Y260X}) exhibit cochlear and vestibular hair cell degeneration without affecting hair cell development. Preliminary data from Tmprss3 mutant organoids demonstrates normal hair cell development followed by hair cell degeneration. Further proteomic and transcriptomic studies are being conducted in this organoid system to provide further insight into the protease targets of TMPRSS3 and the transcriptional mechanisms implicated in Tmprss3-mediated hair cell degeneration in the cochlear and vestibular systems. These data combined with future use of human ESC-derived organoids will increase our understanding of hair cell degeneration in humans and the development of therapeutics for hearing loss and vestibular dysfunction.

PS 796

IGF-1 Effects for Hair Cell Protection Against Neomycin is Mediated by Paracrine of Netrin-1 in Supporting Cells

Takayuki Nakagawa¹; Kohei Yamahara²; Juichi Ito³; Koichi Omori⁴; Norio Yamamoto¹

¹Dept. Otolaryngology, Head and Neck Surgery, Graduate School of Medicine, Kyoto University; ²Kyoto University; ³Shiga Medical Center Research Institute;

⁴Department of Otolaryngology, Head and Neck Surgery, Graduate School of Medicine, Kyoto University

Background

IGF-1 exerted hair cell protection in animal models of acute hearing loss, and clinical trials of topical IGF-1 therapy indicated the efficacy of IGF-1 for hearing recovery in patients with sudden deafness. It is important to understand mechanisms of IGF-1 action on cochlear hair cells, especially what are down-streams of IGF-1 signaling in cochleae. Our previous studies using cochlear explants have demonstrated that netrin-1 is a down-stream of IGF-1 signaling in cochleae damaged by neomycin. The aim of the present study was to examine whether netrin-1 is a mediator of IGF-1 protective effects on hair cell protection against neomycin.

Methods

Postnatal day-2 (P2) cochleae were used in this study. Pharmacological actions of IGF-1, netrin-1 or associated molecules on cochlear epithelia were examined using cochlear explant cultures. Neomycin was used as a toxin for hair cells. In situ hybridization (ISH) for netrin-1 receptor mRNAs was examined in P2 cochleae. Apoptosis was assessed by immunostaining for cleaved caspase 3, and cell proliferation was tested by BrdU labeling assay.

Results

Netrin-1 showed hair cell protection against neomycin similarly to IGF-1. Hair cell protection by IGF-1 was attenuated by application of a blocking antibody to netrin-1. IGF-1 induced upregulation of netrin-1 mRNA in supporting cells of cochlear epithelia damaged by neomycin. The expression of several netrin-1 receptors was found in P2 cochleae. Among netrin-1 receptors, Unk5b exhibited intense expression in cochlear epithelia. A blocking antibody to Unk5b showed significant reduction of IGF-1 or netrin-1 protective effects on hair cells against neomycin. Interestingly, netrin-1 reduced numbers of apoptotic hair cells similarly to IGF-1, while netrin-1 showed no effect on cell proliferation unlikely IGF-1.

Conclusions

Present findings indicate that IGF-1 protective effects on hair cells are partly mediated by paracrine of netrin-1 from supporting cells.

PS 797

Peroxisome Proliferator Activated Receptor -gamma and -alpha Agonists Protect Auditory Hair Cells from Gentamicin-induced Oxidative Stress and Apoptosis

Matthew B. Wright¹; Marijana Sekulic Jablanovic²; Alexander Bausch¹; Vesna Petkovic²; Daniel Bodmer²
¹Strekin AG; ²University Hospital Basel

The thiazolidinedione (TZDs, e.g. pioglitazone) and fibrate (e.g. fenofibrate) drugs are employed for the medical treatment of diabetes and dyslipidemia. These agents are agonists of the peroxisome proliferator-activated receptors, PPAR-gamma and PPAR-alpha, which function as transcriptional regulators of genes controlling glucose and lipid metabolism. PPARs have emerged as potential targets in several indications involving oxidative stress, inflammation, and metabolic dysfunction.

No information on the role of PPARs in the inner ear has been reported. We explored the ability of PPAR agonists to prevent gentamicin-induced auditory hair cell death. Organ of Corti (OC) from 5-day old mice were

exposed to gentamicin +/- either pioglitazone, tesaglitazar, or fenofibric acid in vitro, followed by detection and counting of hair cells (HCs). Immunohistochemistry and Western blots were performed to study the expression of PPAR-gamma and PPAR-alpha protein in mouse cochlea. Finally we measured effects of treatments on PPAR target gene and redox gene expression, levels of ROS, lipid peroxidation products and activated caspases.

Gentamicin (50 microM) led to reproducible losses of 50% of inner and outer HCs. Pioglitazone, tesaglitazar, and fenofibric acid all provided >90% protection of HCs from gentamicin toxicity. All agents demonstrated a dose-efficacy relationship, which roughly paralleled their potency to agonize PPAR receptors. Western blots detected high levels of PPAR-gamma and PPAR-alpha protein in mouse OC lysates. Immunofluorescence experiments detected PPAR-gamma and PPAR-alpha protein in auditory HCs and other cell types in the organ of Corti. Gentamicin treatment increased ROS, lipid peroxidation, and altered redox gene expression in mouse OCs. Pioglitazone treatment almost completely prevented the increase in ROS induced by gentamicin, inhibiting subsequent formation of 4-HNE (4-hydroxy-2-nonenal). Lipid peroxidation products, such as 4-HNE, have been shown to trigger apoptotic cell death through activation of caspases. Pioglitazone treatment substantially opposed caspase activation triggered by gentamicin, most likely through reduction in 4-HNE.

Together these data suggest that PPAR agonists may be effective treatments for hearing loss by reducing oxidative stress, lipid peroxidation and hair cell death.

PS 798

Experimental Studies, Theoretical Modeling and Simulations of Localized Therapeutic Hypothermia to Preserve Residual Hearing Against Electrode-induced Trauma

Ilmar Tamames¹; Jennifer Pineros¹; Charles Huang¹; Fred F. Telischi¹; Michael E. Hoffer²; Suhru M. Rajguru³

¹University of Miami; ²Department of Otolaryngology and Neurological Surgery, University of Miami; ³Departments of Biomedical Engineering and Otolaryngology; University of Miami; FL

Introduction

Insertion trauma during cochlear implantation has been shown to lead to hair cell apoptosis and loss of residual hearing. We have shown in an experimental model that localized hypothermia protects cochlear hair cells and residual hearing function against surgical and electrode

implantation trauma. For successful clinical translation, the surgical approach and efficacy of the custom-designed hypothermia delivery system need to be optimized which are the focuses of present work.

Methods

Using finite element analysis, we investigated the efficacy of our hypothermia probe and resulting heat distribution across human cochlea and surrounding tissues. A 3D model of the cochlea and temporal bone derived from CT images was created in COMSOL and placement of hypothermia probe next to the round window niche via the facial recess or myringotomy approaches were simulated. The model predictions were compared with temperature measurements carried out in cadaver temporal bones (n=5). The facial recess was approached by canal wall up mastoidectomy. The round window membrane was exposed and pierced using Rosen needle. The hypothermia probe was placed anteroinferior to the round window via a myringotomy. The bones were perfused via the round window with egress via a cochleostomy on the apical surface with warm saline. A custom device was used to lower the temperature of the cochleae. A microthermistor was placed on the surface of the mastoid. Two other microthermistors were placed at on the bone covering apical surface (via middle fossa approach) and another one near the round window membrane for continuous temperature measurements during hypothermia delivery.

Results

The numerically calculated temperature distribution was validated with experimentally measured temperature in human cadaver models. With hypothermia probe, the cochlear temperature was lowered by 4-6 °C on the 3 separate measurement locations from a baseline of 37 °C within 12-14 minutes, while the overall temperature of the temporal bone did not change during treatment (~1°C). The simulations confirm that the cooling was uniformly distributed across the cochlea with the position of the probe critically affecting the heat distribution in the tissue.

Conclusions

Overall, the results suggest that our custom-designed system can efficaciously deliver mild to moderate hypothermia treatment to the human cochlea during the implant procedure. Our results suggest strong translational potential of therapeutic hypothermia into patients with an aim to preserve residual hearing.

Acknowledgements

NIDCD 1R21DC014324.

Deciphering Hearing Loss Mechanisms Using an Innovative Nanoproteomic Approach ?

Akil KADERBAY¹; Sébastien Schmerber²; François Berger³; Ali Bouamrani⁴; Matthieu Dreyfus⁵; Magali Court⁶; Adrien Mombun⁷; Céline Leclec'h⁸; Eric Boyer⁹; Philipp Mitariu⁹

¹University Grenoble Alpes; ²University Grenoble Alpes, INSERM1205; ³Université Grenoble Alpes; ⁴CEA-LETI, Clinatec; ⁵Inserm Unit 1205; ⁶INSERM; ⁷CEA-Clinatec; ⁸CEA; ⁹Grenoble University Hospital

Background

Sensorineural hearing loss (SHL) is a major public health issue. The molecular mechanisms underlying many hearing loss-related diseases are not clearly understood and the diagnosis relies mostly on clinical data. Given the confined anatomy of the inner ear, the pathological processes are more accurately reflected in the protein profile of perilymph. Deciphering hearing loss molecular mechanisms is also a crucial opportunity for audioprotective therapies.

Objectives

Our aim was to investigate hearing loss long term molecular changes in perilymph using rodents hearing loss models and to identify the common and distinct pathways that mediate SHL. The goal is to build a spectral library specific of inner ear pathologies and to identify proteomic patterns or biomarkers of hearing loss mechanisms.

Methods

We investigated the proteomic content of perilymph in rats exposed to different deafness protocols. We implemented two models of deafness and we evaluated their consequences. 14 rats received combined injection of kanamycine and furosemide, 14 rats were exposed to a noise injury and the two groups were compared to 14 control rats. Perilymph samples were obtained during microsurgery and prepared for proteomic analysis. We used nano-interface strategies to enrich the proteomic content and access the deep proteome of perilymph before analyzing it with 2 mass spectrometry methods.

Results

Based on Auditory Brainstem Responses (ABR) we demonstrate that the two models are clinically different and that they induced different threshold shifts. The toxic deafness model induced a more profound hearing loss than the noise induced model.

Using nanoporous chips prior to MALDI-ToF mass spectrometry, we are able to access the deep proteome in

perilymph and classify the animals according to their hearing loss mechanism. Using nanoparticles combined to nanoLC-MS/MS, we identified 836 different proteins in perilymph. Among them, we found 47 proteins whose abundance is significantly different in the 2 models of deafness compared to the control group. This study allows us to identify potential molecular biomarkers of hearing loss mechanisms. These proteins of interest have to be further validated.

Conclusion

Perilymph proteomic analysis opens new perspectives in the understanding of profound sensorineural hearing loss. Nano-technologies allow us to reach the deep proteome that would not be detected by conventional analysis. This approach could lead to the diagnosis of hearing loss mechanisms, to the discovery of specific drug therapies, to the potentiation of cochlear implant within its protein environment or to the development of audio protective strategies.

PS 800

Furosemide Opens up the Intrastrial Fluid -blood Barrier for Gadolinium-containing Contrast Agents— an Experimental Study in the Mouse

Göran Laurell¹; Sahar Nikkhou Aski²; Peter Damberg³; Wei Liu⁴; Pernilla Videhult Pierre⁵; Allen Counter⁶

¹Department of surgical sciences, Uppsala university, Uppsala, Sweden; ²Department of Clinical Neuroscience, Karolinska University Hospital, Stockholm, Sweden; ³Department of Clinical Neuroscience, Karolinska Institute, SE-171 76, Stockholm, Sweden; ⁴Section of Otolaryngology, Department of Surgical Sciences, Uppsala University; ⁵CLINTEC, Karolinska institutet, Stockholm, Sweden; ⁶Department of Neurology, Harvard university

Background

To develop an effective pharmacological treatment of a well-defined inner ear disorder more knowledge is needed about inner ear drug trafficking. The two blood-labyrinth barriers greatly limit the bioavailability of medications. Experimental magnetic resonance imaging (MRI) is a tool that can be used to study in vivo the integrity of the blood-perilymph and intrastrial fluid-blood barriers. Under normal conditions the blood-perilymph barrier is rather leaky for gadolinium-containing contrast agents (GdCAs) while the intrastrial fluid-blood barrier is mainly impermeable. It has been known for a long time that high doses of the loop diuretic furosemide can induce a decrease of the endocochlear potential and cause a transient hearing loss. In concomitant treatment with aminoglycoside antibiotics or cisplatin the ototoxic effects are

enhanced by furosemide. The hypothesis: furosemide increases the permeability of the intrastrial fluid-blood barrier for Gds.

Methods

Balb/C mice were used for the MRI study. The tail vein was cannulated and a high single dose of furosemide was injected 20 min prior to the imaging. Gadoteric acid (Dotarem®), gadobutrol (Gadovist®) or gadopentetic acid (Magnevist®) were administered intravenously as a bolus injection during one minute. For the image acquisition, the animals were placed in a Milleped coil. High resolution T1 images of GdCA uptake were acquired with a horizontal 9.4 T Agilent magnet equipped with a 12 cm inner diameter gradient system with maximum gradient strength of 1000 mT/m. G3D images were collected every 10 minutes from the moment of GdCA injection for a period of 240 minutes. Signal intensity was used as a metric of GdCA delivery and distribution to the perilymphatic and endolymphatic spaces.

Results

Kinetic estimates of GdCA transport in the inner ear were achieved. The three contrast agents penetrated the perilymphatic compartments and endolymphatic compartment of the cochlea with increased concentration and minimal variability over a period of 95-165 minutes. For the three GdCAs no significant difference was found between the three compartments. In the control animals not given furosemide before GdCA injection, the ultra-high field MRI showed minimal if any penetration of the intrastrial fluid-blood barrier.

Conclusion

MRI is a noninvasive tool for estimation of GdCA kinetics in the inner ear. The most striking result was the enhanced delivery of all three GdCAs to the endolymphatic space. We speculate that the increased permeability could be attributed to alterations of furosemide-sensitive ion channels and transporters (e.g. inhibition of Na-K-Cl cotransporter NKCC1) in the stria vascularis.

PS 801

Targeting Nitratative Stress to Mitigate Cisplatin-induced Ototoxicity

Samson Jamesdaniel¹; Rajamani Rathinam¹; Rita Rosati¹; William Neumann²

¹Wayne State University, Detroit, MI; ²Southern Illinois University Edwardsville

Background

Cisplatin-induced ototoxicity remains a primary dose-limiting adverse effect of this highly effective anticancer drug. The clinical utility of cisplatin could be enhanced

if the signaling pathways that regulate the toxic side-effects are delineated. In previous studies, we reported cisplatin-induced nitration of cochlear proteins and provided the first evidence for nitration and downregulation of cochlear LIM domain only 4 (LMO4) in cisplatin ototoxicity. Here, we extend these findings to define the critical role of nitratative stress in cisplatin-induced downregulation of LMO4 and its consequent ototoxic effects.

Methods

UBOC1 cells derived from sensory epithelial cells of the inner ear and CBA/J mice were treated with cisplatin or cisplatin plus SRI110, a peroxy-nitrite decomposition catalyst. Nitratative stress and apoptosis were assessed by determining nitrotyrosine and active caspase 3 levels. Cytotoxicity was assessed by a count of viable cells after staining with trypan blue or MTT assay. Hearing loss was assessed by recording auditory brainstem responses.

Results

Cisplatin treatment increased the levels of nitrotyrosine and active caspase 3 in UBOC1 cells, which was detected by immunocytochemical and flow cytometry analysis, respectively. The cisplatin-induced nitratative stress and apoptosis were attenuated by co-treatment with SRI110 ($P < 0.001$, $n=3$), which also attenuated the cisplatin-induced downregulation of LMO4 in a dose-dependent manner. Furthermore, transient overexpression of LMO4 in UBOC1 cells prevented cisplatin-induced cytotoxicity while repression of LMO4 exacerbated cisplatin-induced cell death, indicating a direct link between LMO4 protein levels and cisplatin ototoxicity. Finally, auditory brainstem responses (ABR) recorded from CBA/J mice indicated that co-treatment with SRI110 mitigated cisplatin-induced hearing loss ($p < 0.05$, at 8 kHz, $n=5$).

Conclusion

Together, these results suggest that cisplatin-induced nitratative stress leads to a decrease in the levels of LMO4, downregulation of LMO4 is a critical determinant in cisplatin-induced ototoxicity, and targeting peroxy-nitrite could be a promising strategy for mitigating cisplatin-induced hearing loss.

PS 802

Cochlear Oxidative Stress Detection In Vivo using Quench-Assisted MRI

Andre Kuhl¹; Avril Genevieve Holt²; Angela Dixon³; Mirabela Hali³; Aaron K. Apawu⁴; Antonela Muca¹; Bruce Berkowitz¹

¹Wayne State University School of Medicine; ²Wayne State University School of Medicine/ JD Dingell VAMC;

³Wayne State University; ⁴Wayne State University Medical School

Introduction

We have previously used MEMRI to demonstrate spatial and temporal changes in neuronal activity following a single noise exposure. Noise driven increases in cochlear activity results in pathogenic excessive free radical production (eFRP), when measured ex vivo. Quench-assisted MRI is a new approach for studying paramagnetic eFRP in neurons as measured by anti-oxidant quenchable increases in 1/T1. Here, we generated eFRP in the cochlea using noise to test the hypothesis that acoustic trauma will result in eFRP detectable in vivo using quench-assisted MRI.

Methods

Sprague Dawley rats were divided into three groups (n=5/group): (1) exposed to a 10 kHz, 118 dB SPL, 1/3 octave sound, for 4 hours; (2) exposed to sound but administered antioxidants (methylene blue 1 mg/kg and α -lipoic acid 50 mg/kg) and (3) not exposed to sound. The left ear of each noise-exposed animal was blocked with silicone. Forty-eight hours after acoustic trauma, high-resolution 1/T1 MRI images were obtained with a 7-T MRI scanner (Bruker ClinScan, Billerica, MA) using a receive-only surface coil (1.0-cm diameter) positioned on the head of anesthetized animals (isoflurane 5% induction, 2% maintenance). Images were analyzed using custom scripts from R, an open source software program. The software program ImageJ was used to delineate cochlear regions and generate cochlear 1/T1 values using customized algorithms.

Results

Cochleae from the normal hearing group, had lower mean 1/T1 values (0.29 ± 0.01 sec⁻¹, mean \pm SEM) compared to those from the unblocked ear (right) of noise-exposed animals (2.5 ± 1.3 sec⁻¹); in silicone blocked ears (left) from noise exposed animals mean 1/T1 values (0.5 ± 0.1 sec⁻¹) were normal. Noise exposed animals treated with antioxidants normalized the mean 1/T1 values (0.26 ± 0.01 sec⁻¹) confirming the presence of eFRP.

Conclusion

The results highlight a new and clinically-relevant imaging approach that does not require administering a contrast agent to detect cochlear eFRP non-invasively, using quench-assisted MRI. Conventional methods cannot detect eFRP in vivo. Thus, future studies will focus on using quench-assisted MRI to detect pathogenic eFRP in auditory brain regions following acoustic trauma. Experimental models of hearing loss and tinnitus will be used to develop and optimize antioxidant treatments.

Inner Ear: Drug Delivery

PS 803

Synthetic Adeno-Associated Viral Vector Enables Safe and Efficient Cochlear Gene Transfer

Lukas D. Landegger¹; Bifeng Pan²; Charles Askew³; Sarah Wassmer⁴; Sarah Gluck³; Alice Galvin³; Ruth Taylor⁵; Andrew Forge⁶; Konstantina M. Stankovic¹; Jeffrey R. Holt³; Luk H. Vandenberghe⁴

¹Eaton Peabody Laboratories, Department of Otolaryngology, Massachusetts Eye and Ear, Harvard Medical School; ²Department of Otolaryngology, Boston Children's Hospital, Harvard Medical School; ³Department of Otolaryngology, F.M. Kirby Neurobiology Center, Boston Children's Hospital, Harvard Medical School; ⁴Grousbeck Gene Therapy Center, Schepens Eye Research Institute, Massachusetts Eye and Ear, Harvard Medical School; ⁵Centre for Auditory Research, UCL Ear Institute; ⁶Centre for Auditory Research, University College London, London, UK.

Background

Hearing loss is the most common sensory disorder worldwide. While the first cochlear gene therapy for hearing loss is underway (ClinicalTrials.gov identifier: NCT02132130), early results, as well as data from pre-clinical models, indicate a need for improved gene delivery vehicles for safe and efficient targeting of relevant cell types in the cochlea. In particular, outer hair cells (OHCs) have been a challenging target for adeno-associated viruses (AAVs). OHCs are important for auditory sensitivity and frequency selectivity, key parameters for complex and sophisticated hearing function in humans.

Methods

Here, we evaluated several common AAV serotypes as well as Anc80L65, an in silico designed AAV based on evolutionary modeling, for its ability to target the neurosensory cells in the inner ear, particularly inner (IHCs) and outer hair cells. Cochlear explants of both CBA/CaJ and C57Bl/6 mice were exposed to equal doses of

iodixonal purified preparations of AAV1, 2, 6, 8, 9, and Anc80L65 that encoded eGFP. After 48h, explants were evaluated either immediately or after an additional 5 days of culture. In both animal model explants, Anc80L65 demonstrated highly efficient IHC and OHC transduction (60-100% at 48h, and 100% at 48h+5d). AAV2 in this setting was also efficient, although to a lesser extent. Most serotypes targeted supporting cells and the spiral limbus, to a moderate extent, with AAV8 being least efficient. GFP expression was present from apex to base, with moderately increased targeting for basal hair cells. Next, we tested Anc80L65 in vivo using a clinically relevant round window injection approach. C57Bl/6 mice received 1µl injection of vector at postnatal day 0/1 (p0/p1) and cochleae were dissected between p6 and p30.

Results

Results demonstrate transduction from base to apex of IHCs, OHCs, and supporting cells at rates of close to 100% for IHCs, and ranging from approximately 50-100% of OHCs, although at lesser fluorescent intensity. Animals injected at p1 retained similar levels of GFP hair cell positivity at p30 day of sacrifice. Animals in our study were monitored for function of single cells electrophysiologically, hearing function by ABR and DPOAE measurements, vestibular function by rotarod tests, ectopic expression, and immunological parameters.

Conclusion

In conclusion, the properties of Anc80L65 may enable gene transfer to various therapeutic cell targets in the cochlea. Its unique ability to target both inner and outer hair cells is desirable for strategies that seek to restore higher level hearing function in genetic forms of deafness.

PS 804

Comparison of CRISPR/Cas9 Delivery Methods to the Mouse Inner Ear

Hong Jun Wang¹; Kevin Isgrig²; Joan Guitart¹; Wade W. Chien³

¹NIH/NIDCD; ²Division of Intramural Research, NIDCD, NIH, Bethesda, Maryland, USA; ³Office of the Clinical Director, Otolaryngology Surgeon-Scientist Program, Inner Ear Gene Therapy Program, Division of Intramural Research, NIDCD, NIH, Bethesda, Maryland, USA

Background

Genome editing is a powerful tool which can make permanent modifications to the genome. CRISPR/Cas9 is the most widely used genome editing method due to the ease in which it allows for gene targeting. This technology can potentially be applied to treat inner ear disease processes in the form of gene therapy. In this study, we

evaluate the efficacy of CRISPR/Cas9 delivery to the mouse inner ear using two different techniques: viral delivery vs. direct protein delivery.

Methods

Neonatal GF11-GFP mice were used in this study. An adeno-associated virus serotype 2 was constructed to carry a guide RNA (gRNA) which targets the GFP gene, as well as a Cas9 nuclease (AAV2-CRISPR). One group of animals received AAV2-CRISPR via posterior canal injections. The other group of animals received injections of Cas9 nuclease (protein) and gRNA as well as lipofectamine through the posterior semicircular canal. The efficiency of genome editing was assessed by counting the number of hair cells without GFP expression. ABR was performed at P30 to assess auditory function.

Results

Both viral delivery and direct protein delivery of CRISPR/Cas9 can induce genome editing in the GF11-GFP mouse inner ear. Both methods of CRISPR/Cas9 delivery resulted in minimal ABR threshold shifts in these mice.

Conclusions

Both viral delivery and direct protein delivery of CRISPR/Cas9 can induce genome editing in the mouse inner ear.

PS 805

Inner Ear Transduction with Intravenous rAAV2/9 Injection in Neonatal and Adult Mice

Hidekane Yoshimura¹; Seiji B. Shibata¹; Paul T. Ranum²; Alexander T. Goodwin³; Shin-ichi Usami⁴; Richard JH. Smith¹

¹Department of Otolaryngology, Molecular Otolaryngology and Renal Research Laboratories, University of Iowa; ²Interdisciplinary Graduate Program in Molecular & Cellular Biology, The University of Iowa Graduate College, University of Iowa, Iowa City, IA 52242, USA;

³Molecular Otolaryngology and Renal Research Laboratories, Carver College of Medicine, University of Iowa, Iowa City, IA 52242, USA; ⁴Department of Otorhinolaryngology, School of Medicine, Shinshu University School of Medicine

Background

Hereditary hearing loss is a heterogeneous condition caused by over 80 different genes and affecting 1 of every 500 newborns. Current treatment is relegated to hearing aids or cochlear implantation. For over one decade, we have worked on developing RNAi mediated gene therapy as a strategy by which to restore or prevent hereditary hearing loss. Many studies have demonstrat-

ed the feasibility of using adeno-associated virus (AAV) for gene transfer, with recent reports showing rAAV2/9 and other serotypes traversing the blood-brain barrier (BBB) and transducing cells in the central nervous system following systemic injection. The goal of this study was to assess transgene expression of rAAV2/9 in the inner ear of neonatal and adult mice following systemic intravenous (IV) injection.

Methods

We used systemic IV injection to inoculate P0-1 and P14-15 mice with rAAV2/9. At P0-1, 50µl of rAAV was injected into the superficial temporal vein. At P14-15, 200µl of rAAV was injected via the jugular vein. In all animals, auditory thresholds were assessed by ABR at P30. Animals were then euthanized and cochlear histologically was evaluated.

Results

Robust bilateral transgene expression in the cochleae and vestibular organs was noted in P0-1 mice. Cochlear transduction was greater in the apex than in the base, with overall transgene expression in cochlea hair cells much greater in P0-1 animals than in P14-15 animals. Auditory thresholds in the P0-1 group were comparable to non-injected controls. Off target transduction in brain, muscle and kidney was also noted following systemic rAAV2/9 delivery.

Conclusions

Our data demonstrate the feasibility of rAAV2/9 mediated cochlear gene transfer by systemic IV injection although only in P0-1 animals. This approach offers the advantage of bilateral therapy following a single injection but the potential disadvantage of wide-spread off-target tissue transduction.

PS 806

Posterior Semicircular Canal Injection Is an Effective Method for Mouse Cochlear Gene Delivery

Kevin Isgrig¹; Bovey Zhu²; Andrew Breglio³; Lisa Cunningham⁴; Wade W. Chien⁵

¹Division of Intramural Research, NIDCD, NIH, Bethesda, Maryland, USA; ²NIH/NIDCD; ³National Institute on Deafness and Other Communication Disorders; ⁴National Institute on Deafness and Other Communication Disorders, NIH; ⁵Office of the Clinical Director, Otolaryngology Surgeon-Scientist Program, Inner Ear Gene Therapy Program, Division of Intramural Research, NIDCD, NIH, Bethesda, Maryland, USA

Background

Cochlear gene therapy is an exciting and rapidly evolving field. Most cochlear gene therapy studies in mouse

models of hereditary hearing loss have used round window (RW) injection or cochleostomy as the surgical delivery approach of choice. Unfortunately, the infection efficiency can be variable and direct surgical manipulation of the cochlea can sometimes lead to hearing loss. In this study, we evaluated the efficacy of posterior semicircular canal (PSCC) injection for cochlear gene delivery in the mouse inner ear.

Methods

Neonatal R26R tdTomato reporter mice were separated into two groups. One group received AAV-Cre injections through the RW, and the other received AAV-Cre injections through the PSCC. Three AAV-Cre serotypes were used in this study: AAV1-Cre, AAV2-Cre, and AAV8-Cre. Injection of AAV-Cre took place before age P5. ABR testing was performed around P30. Confocal microscopy was used to assess the tropism and inner hair cell (IHC) infection efficiency of the three AAV serotypes.

Results

In all three AAV serotypes tested, PSCC injection resulted in at least equal if not superior IHC infection efficiency compared to RW injection. Mice that received PSCC injections had greater IHC infection efficiency at the cochlear apex, whereas mice that received RW injections had greater IHC infection efficiency at the cochlear base. Both PSCC and RW injections resulted in minimal ABR threshold shifts in neonatal mice.

Conclusions

PSCC injection is an effective method for cochlear gene delivery in the mouse inner ear. It offers superior IHC infection efficiency compared to RW injection and causes minimal ABR threshold shift.

PS 807

Rescue of Outer Hair Cells with Antisense Oligonucleotides in Usher Mice Is Dependent on Age of Treatment

Jennifer J. Lentz¹; Abhilash Ponnath²; Frederic Depreux³; Hamilton Farris¹; Frank Rigo⁴; Michelle L. Hastings⁵

¹Department of Otorhinolaryngology, Neuroscience Center for Excellence, LSUHSC; ²Neuroscience Center for Excellence, LSUHSC; ³Rosalind Franklin University; ⁴Ionis Pharmaceuticals, Carlsbad, CA, USA; ⁵Department of Cell Biology and Anatomy, Chicago Medical School, Rosalind Franklin University of Medicine and Science, North Chicago, IL, USA

Outer hair cell functional loss is a component of several forms of hereditary hearing impairment, including Usher

syndrome, the most common cause of concurrent hearing and vision impairment. Antisense oligonucleotides (ASO) designed to correct gene expression from the Usher syndrome associated mutation in Ush1c c.216G>A, significantly improves inner and outer hair cell (OHC) bundle morphology and auditory-evoked brainstem responses (ABRs) in mice treated with the drug. Here we investigate whether rescue of OHC function contributes to the hearing rescue by ASOs in Usher mice. Ush1c c.216AA mutant and control littermates were treated systemically by intraperitoneal injection with 300 mg/kg-1 body weight of ASOs. For a single treatment regimen, mice were given one dose in the first week of life on postnatal day 1, 5 or 7. For a multiple treatment regimen, mice were given two doses in the first week of life on postnatal days 1 and 3 (P1-3), or four doses in the first week on postnatal days 1, 3, 5 and 7 (P1-7). Hearing function was assessed by auditory evoked brainstem response (ABR) and distortion product otoacoustic emission (DPOAE) analyses at 1 and 3 months of age. Ush1c c.216AA mutant mice have little or no ABRs or DPOAEs, confirming inner and outer hair cell functional loss. Treatment with ASOs significantly improved ABRs for all ASO treatment regimens given in the first week of life. Treatment also significantly improved DPOAEs, however, only when treatment began before postnatal day 5. This improvement in DPOAEs did not correlate with an increase in ASO efficacy suggesting that rescue of both IHC and OHC function with ASOs is dependent on age of treatment that may be related to the developmental requirement for Ush1c expression.

PS 808

Novel Surgical Infracochlear Approach for Drug Delivery to the Human Internal Auditory Canal

Judith S. Kempfle¹; Elliott Kozin²; Aaron Remenschneider³; Benjamin Fiorillo⁴; Samuel R. Barber⁵; Andreas H. Eckhard⁶; Albert Edge⁷; Daniel J. Lee⁸
¹2, *Department of Otolaryngology, Massachusetts Eye and Ear Infirmary, Boston, MA, USA.* ³ *Department of Otolaryngology and Laryngology, Harvard Medical School, Boston, MA, USA.* ⁵ *Department of Otolaryngology, University Tübingen Medical Center, Tübingen, G;* ²*Massachusetts Eye and Ear Infirmary;* ³*University of Massachusetts / Massachusetts Eye and Ear Infirmary;* ⁴*Tufts Medical School;* ⁵2, *Department of Otolaryngology, Massachusetts Eye and Ear Infirmary, Boston, MA, USA;* ⁶1, *Department of Otorhinolaryngology – Head and Neck Surgery, University Hospital Zurich, Zurich, Switzerland;* ⁷*Department of Otolaryngology and Laryngology, Harvard Medical School, Boston, MA, USA, and Eaton-Peabody Laboratory, Massachusetts Eye*

and Ear Infirmary, Boston, MA, USA; ⁸*Harvard Medical School*

Background

To date, no cure is available for sensorineural hearing loss (SNHL). New advances in auditory research have enabled regeneration of neurons in animal models. Gene therapy, small molecules, growth factors, as well as stem cell therapies offer new treatment options for SNHL. Delivery of these new therapies into human remains challenging due to the complex anatomy of the temporal bone and the desire to avoid violation of the cochlea. Most surgical approaches to the inner ear result in loss of residual hearing. Novel surgical techniques such as endoscopic ear surgery and otologic navigation for the first time enable minimally invasive approaches to the internal auditory canal (IAC). We have developed an experimental surgical approach to access the human internal auditory canal for drug delivery to the cochlear nerve with preservation of the bony inner ear.

Methods

Computed tomography (CT) studies of 38 adult patients without pathology were used to quantify distances and evaluate position of carotid artery, jugular bulb and infracochlear air cells using Synapse and OSiriX. Surgical approach: Cadaveric heads (n=3) with bone-anchored fiducials underwent CT scan for CT-based electromagnetic image guidance (Medtronic) prior to surgery. Rigid endoscopes were used for transcanal visualization. Commercially available curved burs and a stapes curette were used for infracochlear tunnel and access to IAC. Cochlear preservation and successful access were confirmed with histology and CT.

Results

Radiographic analysis of normal temporal bones revealed favorable anatomy in 80% of patients. Endoscopic transcanal hypotympanic approach allowed for minimally invasive infracochlear access and visualization of the medial temporal bone. A minimum diameter of 2.5 mm was required for instrumentation within the infracochlear tunnel, and surgical navigation allowed for high accuracy during surgical access to the IAC. Flexible cannulas for drug delivery with a lumen up to 2mm could be accommodated. Histologic analysis following each dissection revealed no evidence of trauma to the cochlea.

Conclusion

Based on CT imaging and radiographic measurements, the majority of adult subjects have favorable anatomy that could safely accommodate a transcanal, infracochlear hearing preservation approach to the IAC for drug delivery.

Otoprotection Using a Combination of L-NAC and Dex in an in Vitro Model of Inner Ear Trauma

Jeenu Mittal; Joshua Tillinger; Kadri Ila; Carolyn Garnham; Mayank Aranke; Christopher O'toole; Fred F. Telischi; Adrien A. Eshraghi
University of Miami

Background

The inner ear trauma caused by cochlear implant electrode insertion trauma (EIT) initiates multiple molecular mechanisms in hair cells or support cells resulting in initiation of programmed cell death within the damaged tissues of the cochlea which leads to loss of residual hearing. In earlier studies L-N-acetylcysteine (L-NAC) (an antioxidant), and dexamethasone (Dex) (a steroid) have been shown independently to protect the HCs loss against different types of inner ear trauma. Dexamethasone is a glucocorticoid with anti-inflammatory and anti-apoptotic characteristics. L-NAC is a free radical scavenger, as well as a precursor to the antioxidant glutathione. Glutathione is an important step in the clearance of reactive oxygen species. These molecules have different otoprotective effects. Goal of this preliminary study is to test the efficacy of a combination of these molecules to enhance the otoprotection against EIT.

Methods

OC explants were dissected from P-3 rats and placed in serum-free media. Explants were divided into control and experimental groups. Control group: 1) untreated controls 2) EIT. Experimental groups: 1) EIT+ L-NAC (different concentrations) 2) EIT+ Dex (different concentrations) 3) EIT+ L-NAC+ Dex. In EIT Groups, a 0.28-mm diameter monofilament fishing line was introduced through the small cochleostomy located next to the round window area, allowing for an insertion of between 110° and 150°. After EIT was caused, explants were cultured in media containing L-NAC alone, or Dex alone at decreasing concentrations. Concentrations of L-NAC and Dex that showed 50 percent protection of hair cell loss individually were used as a combination in the experimental group 3. After incubation, the explants were fixed and stained with FITC-phalloidin, imaged by fluorescence microscopy, and viable HCs were counted.

Results

There was decrease of total hair cell count in the EIT explants compared with control group or combination therapy. We identified the dosage of L-NAC, and Dex for survival of 50% protection of hair cells in-vitro. This combination therapy may be beneficial in other type of inner ear trauma that can result in hair cell loss.

Conclusion

EIT involves oxidative stress and lipid peroxidation early on after the implantation. L-NAC, and Dex are effective alone in protecting the sensory cells in-vitro at high doses. A combination containing L-NAC, and Dex at much lower doses of each compound, is effective in protecting sensory cells. These compounds can be combined with synergistic effect allowing a decrease of potential side effects of each compound.

Funding

MED-EL Corporation, and HERA Foundation to Dr. AA Eshraghi

PS 810

Drug Development Towards Treatment of Sensorineural Hearing Loss by the REGAIN Horizon 2020 Consortium

Joanne Palmer¹; Anne GM Schilder¹; Helmuth Van Es²; Shakeel Saeed¹; Helen Blackshaw¹; Thanos Bibas³; Leonie Middelink²; Dimitris Kikidis⁴; Stephan Wolpert⁵; Marcus Müller⁵

¹UCL; ²Audion Therapeutics; ³National and Kapodistri-an University of Athens; ⁴The National and Kapodistri-an University of Athens; ⁵University of Tübingen

Introduction

Hearing loss affects over 328 million adults worldwide, with sensorineural hearing loss (SNHL) due to loss of auditory hair cells being the most common cause. This is considered irreversible; however, preclinical studies have demonstrated that pharmacological inhibition of Notch signalling with a gamma-secretase inhibitor (GSI) can regenerate outer hair cells and partially restore hearing capacity. The international REGAIN (REgeneration of inner ear hair cells with GAMMA-secretase INhibitors) consortium has been awarded €5.8 million by the EU Horizon 2020 Research and Innovation Programme to translate these preclinical findings into human proof of concept using a locally administered GSI. This translation is a crucial step in the development of a regenerative therapy for hearing loss.

Methodology

Preclinical development includes candidate selection from a library of potent third generation GSIs; synthesis optimisation, GMP production and full chemical characterisation; developing a formulation suitable for local delivery; inner ear pharmacokinetics and preclinical safety and toxicology studies. This information will be used to obtain regulatory approval to deliver: 1) an open label multi-ascending dose safety study; and 2) an open label randomised efficacy study of two doses taken for-

ward from the safety study, in adult patients with mild to moderate sensorineural hearing loss. The studies will be conducted in the UK, Germany and Greece. The GSI will be administered locally to the worst hearing ear; outcome assessments will include systemic and local safety, and subjective and objective hearing tests.

Conclusion

Small molecule drugs targeting the underlying biological causes of hearing loss in a safe way may meet a medical need for millions of patients, who currently rely on the limited benefits provided by hearing devices. REGAIN aims to advance the first highly promising pharmaceutical treatment of sensorineural hearing loss through rigorous clinical testing.

The REGAIN consortium consists of seven dedicated partners, coordinated by Audion Therapeutics and involving eminent scientists at the UCL Ear Institute, the Eberhard Karls University of Tübingen, National and Kapodistrian University of Athens, Eli Lilly, Nordic Biosciences and ttopstart.

This project receives funding from the EU Horizon 2020 Research and Innovation Programme (No 634893) and JP has received a conference bursary from Action on Hearing Loss.

PS 811

Development of a Drug Eluting Electrode System for the Prevention of Hearing Loss During Cochlear Implant Electrode Insertion

Erik Pierstorff¹; Wan-Wan Yang¹; Yen-Jung Angel Chen²; Fererico Kalinec²; Ya Lang Enke³; Christopher Miller³; Jonathon R. Kirk⁴; William Slattery¹

¹O-Ray Pharma; ²David Geffen School of Medicine at UCLA; ³Cochlear; ⁴Cochlear Americas

Background

Cochlear implants have restored hearing in thousands of patients over the past two decades. However, because residual hearing is damaged in the process of cochlear implantation, this valuable procedure has been restricted to those patients with profound or total deafness. Many patients with severe hearing loss, a far larger group, are not currently implanted for fear of losing their residual hearing. As of December 2010, approximately 219,000 people worldwide had received cochlear implants. However, these numbers are increasing rapidly each year; should a method be developed to allow implantation in patients with severe hearing loss but who retain some residual hearing, it is possible that as many as 10 times the number of patients might benefit from cochlear implantation. For this reason many researchers and the

manufacturers of cochlear implants are investigating the possibility of developing implants to be used in the setting of residual hearing. There is evidence that the addition of a steroid at the time of implantation may allow preservation of residual hearing.

We have developed multiple extended release steroid formulations in various dose-ranges utilizing sustained release polymer formulations. To test the activity of one of these formulations (extended release dexamethasone), drug delivery system was attached to Cochlear dummy H14 animal electrodes. These modified electrodes were implanted directly into the cochleae of guinea pigs. Unmodified dummy electrodes were used as a control.

Methods and Results

Pre- and post- treatment ABRs were performed to assess hearing. In all cases, significant hearing improvement was observed in ears implanted with electrode containing the steroid drug delivery system. Histological analysis was performed to determine the extent of damage in the cochlea following implantation and to see if the presence of the steroid eluting system had any effect on the extent of damage to the structures of the cochlea. Significant hearing loss and damage to various regions of the cochlea were observed following implantation of dummy electrodes. The inclusion of the steroid delivery system prevented hearing loss and substantially decreased the damage (i.e. lesions) following implantation.

Conclusion

These results demonstrate that the sustained release steroid system appears to be safe and effective in preserving hearing from trauma induced by the implantation of cochlear implant electrodes.

Grant Support from Cochlear, LTD

PS 812

Drug Delivery through a Cochlear Implant in Guinea Pigs for up to 7 Days: Pharmacokinetic, Functional and Morphologic Evaluation.

Alec Salt¹; Jared Hartsock¹; Daniel Smyth²; Jonathon R. Kirk³; Kristien JM. Verhoeven²

¹Washington University in St Louis; ²Cochlear Technology Centre; ³Cochlear Americas

Background

Application of drugs to the ear during or following cochlear implantation has the potential to help reduce inflammation and bone growth, preserve residual low frequency hearing, and maintain neural function. In this study we measured perilymph levels achieved when

drug was delivered from a cannula incorporated into a cochlear implant.

Methods

Cochlear implants incorporating a polyimide cannula were inserted into the basal turn of scala tympani (ST) through a cochleostomy near the round window. Artificial perilymph containing FITC-dextran marker was injected using a syringe pump or implantable micropump (iPrecio SMP-200) at 10 or 100 nL/min. After applications of two hours, 24 hours or 7 days duration, ST perilymph was sampled from the cochlear apex with a technique allowing drug gradients along ST to be quantified. Fluid sample data were interpreted with an inner ear fluids simulation program. Functional measures (CAP thresholds) and morphologic changes were also evaluated.

Results

In 5 animals, perilymph was sampled after 2 hours injection of 10 mM FITC-dextran at 10 nL/min. Dextran concentration was highest in perilymph from the basal turn, and a large basal-apical gradient of dextran was present along ST. The distribution was consistent with simulations based on kinetic parameters for dextran established in a prior study. Injections of longer duration (24 hrs or 7 days) were performed as recovery experiments. Gradients of dextran along ST were reduced at both time points relative to 2 hr injections, but were still present in most animals. Following implantation, cochlear sensitivity decreased over a frequency range of 2.5 – 13 kHz. The greatest losses (~25 dB) occurred at 5-6 kHz. Hearing loss was stable over the 7 day period and did not differ between dextran injected and non-injected ears, demonstrating minimal influence of the injected solution. Histology showed the cannula remained unobstructed over the 7 day period.

Conclusions

An implant incorporating a drug-delivery cannula provides a valuable research tool to study therapies that could improve cochlear implant performance over time. This study shows that a test compound (FITC-dextran) can be delivered quantitatively to perilymph. Longitudinal drug gradients became smaller as injection times were prolonged. Dextran distribution as a function of time is currently being modeled. Hearing losses generated by implantation of the normal ear were comparable with prior studies. The absence of hearing loss with low-frequency stimuli makes this a suitable model to evaluate therapies designed to preserve low frequency hearing.

Study supported by Cochlear Corp.

PS 813

Long Term in Vivo Release Profile of Dexamethasone from Silicone Rods Implanted into the Scala Tympani of Guinea Pigs

Arne Liebau¹; Ilona Schön¹; Bernd Kammerer²; Sören Schilp³; Kenneth Mugridge³; Susanne Braun⁴; Stefan Plontke¹

¹Martin Luther University Halle-Wittenberg; ²Albert-Ludwigs-University Freiburg; ³MED-EL Headquarters, Innsbruck; ⁴MED-EL Deutschland GmbH, Starnberg

The reliable function of cochlear implants may deteriorate by a tissue reaction e.g. with fibrosis around the cochlear electrodes. When cochlear implants are used in patients with partial deafness, (i.e. profound high frequency hearing loss but residual low-frequency hearing), damage of residual hearing in the low frequency range due the insertion of the electrode carrier into the cochlea should be prevented. The purpose is to reduce inflammatory reaction and cochlear tissue response due to insertion trauma by means of glucocorticoid administration.

It is known, that after intralabyrinthine application of the antiinflammatory, antioxidative, and antiapoptotic substance dexamethasone, its presence in the perilymph is short due to fast elimination half-time. The aim of the study was to determine the long term in vivo dexamethasone levels in the perilymph of guinea pigs which is released from silicone rods functioning as dummies for cochlear implant electrode carriers.

Silicone rods were loaded with various concentrations of dexamethasone and implanted into the basal turn of scala tympani of guinea pigs. Dexamethasone concentrations in perilymph were measured at several time points over a period of up to 7 weeks. The perilymph kinetics showed a burst release for all DEX-loaded silicone rods regardless of their dexamethasone concentrations. The initial burst release was followed by nearly constant drug concentrations during the whole observation period.

The results show that dexamethasone is released from the silicone rods in a sustained way over a period of several weeks leading to constant drug concentrations in the scala tympani perilymph.

PS 814

Therapeutic and Adverse Effect of Hyaluronic Acid Crosslink and Microcapsules for Intratympanic Dual-drug Delivery

Myung-Whan Suh¹; Jung-A Cho¹; Yujung Hwang¹; Tae-Soo Noh²; Ji Hun Park³; Moon Suk Kim³

¹Department of Otorhinolaryngology, Seoul National University Hospital; ²Department of Otorhinolaryngology, Seoul National University Hospit; ³Department of Molecular Science and Technology, Ajou University

Background

If the Intratympanic (IT) drug can be delivered through a vehicle that lasts longer in the middle ear, more drug may be delivered into the inner ear. In this study we evaluated the effect of hyaluronic acid (HA) crosslink and microcapsules. We verified the hearing outcome in noise induced hearing loss animals and compared the incidence of adverse inflammatory reaction.

Methods

A total of 22 male (44 ears) SD rats were used. IT dexamethasone (dex, 5mg/ml) and/or IGF1(1.25mg/ml) was delivered via six different HA vehicles according to the amount of crosslinks: H1 (1:10000), H2 (1:150), H3 (1:100), H4 (1:50), and H5 (no crosslink). Medications mixed in normal saline served as the control group: S1 (dex+GF) and S2 (dex without GF). Rats were exposed to noise and rats were treated with drug/vehicle injection. ABR threshold was measured before and after treatment for 2 months. Serial micro CT and endoscopy of the TM was performed to evaluate the adverse reaction.

Results

The drug lasted in the middle ear for 7.7 ± 5.1 d in the H group and 0.9 ± 0.3 d in the S group. The tympanic membrane perforation completely healed after 16.5 ± 16.0 d in the H group and 12.7 ± 7.6 d in the S group. Regardless of the amount, crosslinked HA (H group) was related with higher chance of infection (0-66.7%) compared to the S group (0-9.1%). The amount of crosslink did not correlate with the incidence of infection. The microcapsule did not increase the incidence of infection. GF did not increase the incidence of infection either. The onset and offset of infection were 7.0 ± 2.0 d and 31.3 ± 10.3 d after injection in the H group. And they were 11.3 ± 10.3 and 32.5 ± 17.9 d in the S group. The hearing was not different between the two groups. Hearing outcome and hair cell count was nearly identical between the two groups.

Conclusions

The vehicle/drug sustained 7-8 times longer in the middle ear when it was carried in various types of cross-

linked HA. But crosslinked HA may be related with higher chance of post-injection infection. Microcapsules and dual-drug delivery (dex+GF) is still valid since these factors does not seem to be the cause of increased incidence of infection. High molecular weight HA with higher viscosity may be a better option than crosslinking the HA for a longer durability.

PS 815

Protection from Noise-induced Hearing Loss in Mice Using a Non-invasive Nanohydrogel Drug Delivery System

Mei Lin; Julian Wooltorton; Daqing Li

Department of Otorhinolaryngology- Head & Neck Surgery, Perelman School of Medicine at the University of Pennsylvania, Philadelphia, PA

Hearing impairment is the most prevalent sensory disability and commonly attributed to sensorineural hearing loss (SNHL). Causes of SNHL include congenital deafness, noise-induced hearing loss and drug-induced ototoxicity. Although sound amplification devices and cochlear implants are the currently available remedies to this type of the hearing loss, the treatment outcome is often not satisfied. Therefore, it is important to develop alternate drug/biomaterial-based approaches for preventing SNHL. A successful inner ear drug/biomaterial delivery has to overcome two major obstacles: non-invasive access to the inner ear structures and the blood-inner ear barrier, which limits systemic drug administration. Our lab has developed a stable, safe, and controllable chitosan-hydrogel based nanoparticle delivery system which allows for reliable delivery of drugs/biomaterials into the inner ear with improved outcomes. We used this system to deliver nanoparticles (liposomes) containing the JNK inhibitor, D-JNKi-1, in an attempt to protect cochlear hair cells from noise-induced hearing loss (NIHL). Although delivering D-JNKi-1 using an invasive surgical approach may preserve hearing during acoustic trauma (Wang et al., 2003, J Neurosci. 23:8596 8607), the invasive nature of this approach may limit its clinical application.

The current study used the non-invasive nanohydrogel delivery system to deliver D-JNKi-1 for preventing NIHL. Liposomes were prepared with molar composition: 55% hydrogenated soy phosphatidylcholine (Avanti Polar Lipids, Alabaster AL) / 39.9% cholesterol (Sigma-Aldrich, St. Louis MO) / 4% 1,2-distearoyl-sn-glycero-3-phosphoethanolamine-N-[methoxy(polyethylene glycol)-2000] (18:0 PEG2000, Avanti) / 1% 1,2-distearoyl-sn-glycero-3-phosphoethanolamine-N-[dibenzocyclooctyl(polyethylene glycol)-2000] (DSPE-PEG(2000)-DBCO, Avanti) / 0.1% 1,2-dioleoyl-sn-glycero-3-phosphoethanolamine-N-(lissamine rhodamine B sulfonyl) (Avanti).

The D-JNKi1 was loaded into liposomes by hydrating with NaHCO₃ buffer (0.1M, pH9) containing 120 µm/ml D-JNKi1. Loaded liposomes were incorporated in the nanohydrogel in the ratio 1:5 V/V. C57BL/6 mice were used for this study. After exposure of the round window niche (RWN), nanohydrogel containing either D-JNKi-1-loaded liposomes or empty liposomes was carefully applied to the RWN. Acoustic trauma was induced by a continuous broadband tone (6 kHz-20 kHz) at 100 dB SPL for at least 2 hr. Hearing thresholds were evaluated using auditory brainstem response (ABR) at frequencies between 4 kHz and 32 kHz with intensities 20 to 100 dB before and after noise exposure. Preliminary results demonstrate that mice receiving D-JNKi-1 pre-treatment had a smaller hearing threshold shift than the untreated control group after noise exposure. This suggests that D-JNKi-1 can be delivered to the cochlea via the non-invasive nanohydrogel delivery system and protect hair cells from acoustic trauma and reduce NIHL.

PS 816

Optimization of Active Peptide Transport Across the Tympanic Membrane

Allen F Ryan¹; Arwa Kurabi²; Allen F. Ryan²

¹Department of Surgery, Division of Otolaryngology, University of California, San Diego; ²University of California, San Diego

Introduction

We previously employed phage display to identify 12-mer peptides that mediate rapid, active transport of large (1 µm) particles across the tympanic membrane (TM) into the middle ear (ME) for local therapeutics delivery. The choice of 12-mer peptides was based on sufficient sequence diversity to have biological activity. However, it was unclear whether this peptide length was optimal. We therefore engineered and screened 18-mer phage libraries, using the two top 12-mer first-generation peptides as backbones (termed X and Z).

Methods

For each screen, rat MEs were inoculated with non-typeable Haemophilus influenza (NTHi) to induce otitis media (OM). 48 hours later, an aliquot of one of the two libraries was applied to the external surface of the TM for 15 minutes or 1 hour, followed by extensive rinsing of the external ear canal. The ME effusions were then harvested, amplified and re-applied for three additional rounds. Twenty of the phage recovered from the ME for each library were then sequenced. Candidate 18-mer peptides were then applied to the TM and trans-TM transport compared to that of the parent 12-mer peptide. Transport rates for each 18-mer library across the TM

and into the ME were compared to those seen with the original 12-mer backbone peptides.

Results

Compared to its parent 12-mer peptide, the average transport for one 18-mer library (X plus 6) was slightly higher, while for the other library (Z plus 6) was ~10-fold lower, suggesting a range of effects of peptide extension. When the X plus 6 library was sequentially screened to enrich for trans-TM transport, sequencing revealed a highly diverse population peptides, with little evidence of collapse to a superior sequence. In contrast, sequential screening of the Z plus 6 resulted in almost complete collapse to one sequence. When trans-TM transport of this 18-mer peptide was compared to that of the X and Z 12-mer peptides, it was found to be nearly 80-fold greater than its parent 12-mer peptide, and 8-fold greater than the X 12-mer peptide.

Conclusions

The results indicate that the peptide-based active transport mechanism originally discovered using a 12-mer phage display library responds preferentially to a longer peptide sequence. This suggests that interaction of the peptide with the transport mechanism is enhanced by structural conformations that are beyond the range of 12-mer peptides. Characterization of potential structural motifs of the 18-mer peptide may provide clues regarding the mechanism of active trans-TM transport. [TRIH, NIH/NIDCD, VAMC]

PS 817

Permeation Enhancers for Intratympanically-applied Drugs Studied Using Fluorescent Dexamethasone as a Marker

Wei Li¹; Jared Hartsock²; Chunfu Dai¹; Alec Salt²

¹Fudan University; ²Washington University in St Louis

Background

The perilymph concentration achieved with an intratympanically-applied drug is typically variable and substantially below the applied concentration. This is due to a limited, and variable, entry of drug through the round window (RW) membrane and stapes. The present study explores the use of chemical manipulations to increase entry permeability and make it more consistent.

Methods

Dexamethasone-fluorescein (F-dex; Life Technologies Corp.) was used as an entry marker as it has a very low rate of entry at the RW membrane and stapes. F-dex was applied to the RW niche of guinea pigs as 20 µL bolus of 1 mM solution. Following 1 hr application, 10 samples of perilymph were collected sequentially from the lateral semi-circular canal, a technique that allows F-dex

distribution throughout the perilymph to be quantified. Entry was measured with F-dex dissolved in PBS (control) and with the medium containing dimethyl sulfoxide (DMSO), N-methylpyrrolidone (NMP), saponin, benzyl alcohol (BA) or poloxamer 407 (P407). Combinations of saponin or BA with P407 were also used.

Results

F-dex entered the inner ear slowly at both the RW and stapes, reaching an average of 0.086 μM in samples 1-3 (originating from the vestibule) and 0.16 μM in samples 6-9 (originating from scala tympani). F-dex entry into the inner ear is given below for groups ranked in increasing order of perilymph concentration. In each case, concentration achieved is given as a percentage of the applied concentration. Perilymph reached 0.011% for controls, 0.142% for 20% poloxamer, 0.157% for saponin, 0.16% for 2% BA%, 0.164% for NMP, 0.184% for DMSO and 0.324% for 4% BA, all of which were statistically significant (ANOVA) relative to the controls. Entry with 1% BA or 17% P407 was not changed significantly with respect to controls. In combination with 17% P407, 1% or 2% BA did not increase entry but 5% BA in 15% P407 did (0.22%). The gelling properties of P407 were affected by BA. Entry with saponin in 15% P407 was not significantly increased.

Conclusions

Similar to other drugs, intratympanically-applied F-dex enters the inner ear at both the RW and the stapes. 4% BA most effectively increased F-dex entry into the inner ear at both locations. However, BA is problematic when used in combination with P407, being less effective at a specific concentration and markedly disturbing the gelling properties of the poloxamer.

Study supported by NIH/NIDCD R01 DC001368 (AS) and NSF 81570917 (CFD)

PS 818

The Effect of Dexamethasone/CPP Nanoparticles on Gene Delivery for Inner Ear Therapy

Dong-Kee Kim¹; Keum-Jin Yang¹; Ji young Yoon²; Shi-Nae Park³; Jong-Duk Kim²

¹Department of Otolaryngology, College of Medicine, The Catholic university of Korea; ²Department of Chemical and Biomolecular Engineering (BK 21 Plus Program), KAIST; ³Department of Otolaryngology-Head&Neck Surgery, college of Medicine, Catholic Univ. of Korea

Background

Dexamethasone (Dex)-loaded PHEA-g-C18-Arg8 (PCA) nanoparticles (PCA/Dex) were developed for the deliv-

ery of genes to determine the synergistic effect of Dex on gene expression.

Method

The cationic PCA nanoparticles were self-assembled to create cationic micelles containing an octadecylamine (C18) core with Dex and an Arg8 peptide shell for electrostatic complexation with nucleic acids. For evaluation of synergistic effect of Dex on gene expression, HEI-OC1 cells treated with PCA/Dex/GFP DNA, PCA/GFP DNA, or Lipofectamine/GFP DNA were analyzed by FACS. For comparison of the levels of inflammatory cytokines after treatment of these particles, mRNA levels of IL1b, IL12, and INF γ were investigated by quantitative real time-PCR. Finally, for functional application of siRNA or DNA to HEI-OC1 cells, connexin 26 (Cx26) siRNA, or brain-derived neurotrophic factor (BDNF) pDNA were complexed with PCA/Dex nanoparticles, and after treating these particles to HEI-OC1 cells, its effects were also evaluated.

Result

The PCA/Dex nanoparticles conjugated with arginine 8 (Arg8), a cell-penetrating peptide (CPP) that enhances permeability through a round window membrane in the inner ear for gene delivery, was observed to have high uptake efficiency in HEI-OC1 cells. This potential carrier co-delivering Dex and the gene into inner ear cells has a diameter of 120-140 nm and a zeta potential of 20-25 mV. Different types of genes were complexed with the Dex-loaded PCA nanoparticle (PCA/Dex/gene) for gene expression to induce additional anti-inflammatory effects. PCA/Dex showed mildly increased expression of GFP and lower mRNA expression of inflammatory cytokines (IL1b, IL12, and INF γ) than did Dex-free PCA nanoparticles and Lipofectamine[®] reagent in HEI-OC1 cells. In addition, after loading Cx26 siRNA onto the surface of PCA/Dex, Cx26 gene expression was down-regulated according to real time PCR for 24 h, compared with using Lipofectamine[®] agent. After loading BDNF DNA into PCA/Dex, increased expression of BDNF was observed for 30 h, and its signaling pathway resulted in an increase in phosphorylation of Akt, observed by Western blotting. Conclusion: Dex within PCA/Dex/gene nanoparticles created an anti-inflammatory effect and enhanced gene expression in HEI-OC1 cells.

An Implantable Peristaltic Micropump with Direct-Write-Printed Features for Inner Ear Drug Delivery Under Wireless Control

Farzad Forouzandeh¹; Kyle E. Smith²; Meng-Chun Hsu²; Chaitanya Mahajan²; Jing Ouyang²; Robert N. Carter²; Xiaoxia Zhu³; Bo Ding⁴; Ahmed Alfadhel²; Joseph P. Walton⁵; Denis R. Cormier²; Robert D. Frisina⁴; David A. Borkholder²

¹Rochester Institute of Technology, Kate Gleason College of Engineering; ²Rochester Institute of Technology; ³University of South Florida; ⁴Global Center for Hearing and Speech Research, University of South Florida, Tampa, FL, USA; ⁵Communication Sciences and Disorders, University of South Florida, Tampa FL, USA

Biomedical engineering advances in protective and restorative inner ear biotherapies have created new opportunities to address vestibular disorders, deafness, and noise induced-, sensorineural, and age-related hearing loss. To avoid unwanted, systemic side-effects, controllable, programmable drug delivery systems are essential for therapeutic development in animal models, and for future human translation with implantable, subcutaneous or behind-the-ear systems. The mouse animal-model system offers significant advantages for studies involving specific transgenic, knock-in, and knockout variants that model different human diseases and communication disorders. However, the small size of the mouse necessitates key advances in pump miniaturization for implantation and scaling of flow rates and volumes to match cochlear anatomy. Here we present a biocompatible, fully implantable, scalable, and wirelessly controlled peristaltic micropump. The microfluidic core is based on commercially available catheter microtubing (250µm OD, 125µm ID) providing a leak-free, biocompatible flow path while avoiding complex microfluidic interconnects. Direct write micro-scale printing provides structure around the microtubing for mechanical support and actuation. Micropump features are fabricated directly on the backside of a printed circuit board assembly providing control electronics for sequenced actuation and wireless control. Peristaltic flow is achieved by compressing the microtubing via expansion and contraction of a thermal phase-change material integrated adjacent to the microtubing and within the printed micropump structure. A refillable reservoir was integrated with the micropump while maintaining a form factor optimized for subcutaneous implantation in the mouse. Pump characterization results and initial in vivo implantation tests are presented. Initially targeting the small murine cochlea, this low-cost design and fabrication methodology is in-

herently scalable to larger animals and for clinical applications in children and adults by appropriate scaling of the microtubing size and actuator volume.

Supported by the National Institute On Deafness and Other Communication Disorders of the National Institutes of Health, under Award # R01 DC014568.

PS 820

Dexamethasone (DXM) Coated Poly(lactic-co-glycolic Acid) (PLGA) Microneedles as an Improved Drug Delivery System for Intracochlear Biodegradable Devices

Stefania Goncalves¹; Devon Pawley²; Esperanza Bas³; Emre Dikici²; Neil Nayak⁴; Sapna Deo²; Sylvia Daunert²; Fred F. Telischi⁵

¹Jackson Memorial Hospital / UHealth System; ²Department of Biochemistry and Molecular Biology, Miller School of Medicine, University of Miami, Miami, FL, 33174, USA; ³University of Miami-Miller School of Medicine; ⁴University of Miami Ear Institute, Department of Otolaryngology, Miller School of Medicine, Miami, FL, 33136, USA; ⁵University of Miami

Background

The development of new techniques for drug delivery into the inner ear is a challenging field that has been hindered by cochlear anatomy, which limits molecular transportation. Biodegradable polymers allow continuous release of bioactive molecules and are promising in this field; however, some authors have reported ototoxicity, which may be due to the delayed release profile of the biopolymeric blends.

Methods

Biopolymer microneedles were prepared as described below, and their drug release and ototoxicity profiles were determined. The needles were prepared by dissolving 25 mg of 50:50 PLGA copolymer and 2.5 mg of dexamethasone in 100 µL of dimethyl sulfoxide. The solution was then cast into a custom polydimethylsiloxane elastomer (PDMS) mold shaped as the desired microneedles. Then, the DMSO was evaporated at 65 °C in a vacuum oven. The needles were removed from the mold and coated with additional dexamethasone by dipping the needles into a 10% solution of dexamethasone in DMSO. In order to study the drug release profile, a fluorescent compound, rhodamine B, was used instead of dexamethasone. The prepared microneedles were then placed in a quartz cuvette containing an artificial perilymph solution. The absorbance of the perilymph solution was checked every 30 min until the absorbance of the solution at 552 nm was constant.

Ototoxicity assessment was performed using whole organ of Corti (OC) explants dissected from 3-day-old rat cochleae, and the OC explants were exposed to the dexamethasone coated and non-coated microneedles in a 72 hour culture. Fluorescent microscopy for viable hair cell (HC) counts (FITC-phalloidin) was performed. ANOVA and Bonferroni post hoc testing were used for statistical analysis.

Results

The needles' drug release profile was determined by measuring the absorbance of the rhodamine B dye at 552 nm. The results showed a total release of the dye within 6 hours from the time of immersion into the artificial perilymph solution. The ototoxicity assessment of the dexamethasone coated microneedles showed a significant reduction of inner and outer HCs losses when compared to the non-coated prototype ($p < 0.0001$) and a similar efficacy in protecting from HCs loss when compared to DXM solution.

Conclusions

We have shown that the dexamethasone coating of the needles improves the effectiveness of the intracochlear needles, and also protects the hair cells from the ototoxicity.

PS 821

Computational Models of Pharmacokinetics for Micropump-Driven Intracochlear Drug Delivery

Vishal Tandon¹; Andrew M. Ayoob¹; Marcello Peppi¹; Erin E. Pararas¹; Mark Mescher¹; William F. Sewell²; Jeffrey T. Borenstein¹

¹Draper; ²Massachusetts Eye and Ear Infirmary

Introduction

Accurate prediction of pharmacokinetics is crucial for development of drug delivery systems for the inner ear. Direct delivery methods, such as intracochlear injection with a precision micropump, offer more controlled delivery kinetics. In addition, direct intracochlear delivery avoids systemic toxicity and is compatible with a range of drug sizes and types. When a drug is deposited directly into the cochlea, confounding factors such as transmembrane transport or travel through the blood-cochlear barrier are avoided.

Accurate transport models enables prediction of drug distribution for different sizes/classes of drugs, various cochlear anatomies, and a range of delivery schemes. Here we incorporate cochlear anatomy data and known drug properties into computational fluid dynamics simulation to predict spatiotemporal drug distribution patterns. Our model aims to optimize micropump-mediated

intracochlear delivery for maximal apical drug penetration.

Methods

Drug transport was modeled using a transient pseudo-1-D convection-diffusion-reaction equation, where terms were corrected for the varying cross-sectional area of the cochlea. Drug-protein binding interactions and drug clearance were modeled as chemical reactions with first-order kinetics. Rate and time constants, diffusion coefficients, and other physical parameters were informed by experimental data. The equation was solved using a finite difference scheme implemented in MATLAB. The scheme allows for an arbitrary number of sequential infusion, withdrawal, and diffusion steps. In order to determine the velocity field, a fluidic circuit model for the cochlea was constructed and solved in MATLAB. Simulation results were compared to our published experimental data for intracochlear delivery of DNQX in guinea pigs, and our ongoing experiments involving histological analysis of intracochlear delivery of fluorescent tracers, where drug is delivered via a cannula placed in the 12 to 16 kHz region.

Results

In order to compare results to our previous experiments, we simulated intracochlear delivery of DNQX, an AMPA receptor antagonist, in guinea pigs. The drug was infused via a cochleostomy into the 12-16 kHz region. The simulation data was qualitatively consistent with trends observed in experiments, showing fast convective distribution of drug from the infusion site toward the base (due to the open aqueduct), and slower diffusive distribution of the drug toward the apex. Histological analysis of cochlear tissue after direct intracochlear injection of a single bolus of a fluorescent hair-cell stain (FM1-43) showed a gradient of staining from base to apex that is consistent with predominantly diffusive transport, which is recapitulated by the model.

Modeling and Extraction of Diffusion, Permeability and Clearance Parameters for Drug Delivery in the Murine Cochlea

Kevin Wilson¹; Sanketh S Moudgalya²; Zhenlin Xu³; Xiaoxia Zhu⁴; Gary Martinez⁵; Mikalai Budzevich⁵; Robert D. Frisina⁶; Joseph P. Walton⁷; Nathan Cahill¹; David A. Borkholder¹

¹Rochester Institute of Technology; ²Chester F. Carlson Center for Imaging Science, Rochester Institute of Technology; ³Chester F. Carlson Center for Imaging Science, RIT; ⁴University of South Florida; ⁵H Lee Moffitt Cancer Center; ⁶Global Center for Hearing and Speech Research, University of South Florida, Tampa, FL, USA; ⁷Communication Sciences and Disorders, University of South Florida, Tampa FL, USA

An essential component in the study of inner ear drug delivery is cochlear fluid pharmacokinetics. A popular method for simulating the drug diffusion in the inner ear (Plontke et al., *Audiology and Neurotology*, 12:37-48, 2007) uses a finite element method model that relies on assumed values of the diffusion coefficients within the scala tympani (ST), scala vestibuli (SV), scala media (SM), and spiral ligament (SL), as well as parameters describing the permeability between them and clearance to other regions. In this work, we investigate inverting this model to estimate diffusion parameters given empirical concentration values derived from micro-computed tomography (μ CT) imagery of the mouse cochlea. Solving the inverse problem over the entire set of 3-D regions can be computationally intensive, so we focus instead on inverting the reduced 1-D problem proposed by Plontke et al. Given initial estimates of the diffusion, permeability, and clearance parameters, we use an iterative nonlinear least-squares technique to minimize the mean-squared error between the predicted concentration values and those derived by averaging over regional cross-sections of the μ CT scans. Extracting the appropriate cross-sectional data from each of the four regions in the μ CT scans is a difficult task that requires accurately identifying/segmenting the regions. So, we employed a 3-D subject-atlas image registration technique (Z. Xu, MS Thesis, Rochester Institute of Technology, 2016). This aligns the high-resolution atlas with pre-identified regions to the μ CT scans, enabling labels for the regions to be propagated. However, voxels are inherently discrete, hence the registration will not be perfectly accurate, so it is likely that the labeled regions may include data from bones near the region boundaries. For this reason, we weight voxels based on their proximity to the center of their labeled region, so voxels that may contain bone have less influence on the de-

rived concentration values. Using a set of μ CT scans comprising a baseline scan and subsequent scans of a mouse during micro-infusion delivery of a contrast agent (ioversol) to its cochlea, we illustrate how our techniques can be used to robustly estimate diffusion, permeability, and clearance parameters for Plontke et al.'s reduced 1-D problem. These results will accelerate pre-clinical and clinical development of infusion paradigms, to facilitate optimal drug delivery to the cochlea, for preventing or treating acute and chronic types of hearing loss.

Supported by the National Institute On Deafness and Other Communication Disorders of the National Institutes of Health, under Award # R01 DC014568.

PS 823

Quantitative Pharmacokinetics of Fluorescent Tracer Substances in the Cochlear Sensory Epithelia

Andrew M. Ayoob¹; Marcello Peppi¹; Vishal Tandon¹; Erin E. Pararas¹; Michael McKenna²; Sharon G. Kujawa³; Robert Langer⁴; William F. Sewell²; Jeffrey T. Borenstein¹

¹Draper; ²Massachusetts Eye and Ear Infirmary; ³Harvard Medical School and Eaton-Peabody Labs, Massachusetts Eye and Ear Infirmary, Boston MA; ⁴MIT

Introduction

Localized methods of drug delivery to the inner ear are being developed to improve control of cochlear drug concentration and to avoid side effects associated with systemic delivery. Validation of these methods requires quantitative assessment of spatiotemporal drug distribution in the target tissue, primarily the organ of Corti, including the sensory hair cells, supporting cells, and dendrites of the spiral ganglion neurons. Challenges associated with current methods for assessment of cochlear pharmacokinetics include poor spatial resolution of drug concentration along the tonotopic axis and contamination of perilymph samples with CSF from the cochlear aqueduct.

We have developed and demonstrated a method of pharmacokinetic analysis in the cochlea by measuring levels of fluorescent tracers in the organ of Corti with confocal imaging. Fluorescent substances known to accumulate in cochlear hair cells, FM 1-43 and Texas-Red labeled gentamicin, were selected as surrogate drug markers.

Methods

In Guinea pigs, an artificial perilymph solution containing either FM 1-43 or Texas-Red-labelled gentamicin was injected into the scala tympani via a cannula inserted 3 mm apically through a cochleostomy near the cochlear

base. The inner ear was harvested for fixation and decalcification 1 hr, 3 hr, or 72 hr after fluorophore delivery. Distribution of fluorescence intensity along the length of the organ of Corti was analyzed in confocal images of whole mounts with ImageJ and Matlab (Mathworks).

Results

Both FM 1-43 and labelled gentamicin accumulated in hair cells with a strong gradient from base to apex, demonstrating the versatility of the approach for pharmacokinetic analysis of clinically relevant drug substances. Diffuse cytoplasmic staining of the inner and outer hair cells was observed at all time points tested. Fluorescence can be detected over a large dynamic range, spanning more than 5 orders of magnitude, but the sensitivity to fluorophore detection in the whole mount tissue was limited by autofluorescence. The autofluorescence was constant along the tonotopic axis with no intensity gradient for either the fluorescein or Texas Red channels. Fluorophore distribution along the tonotopic axis was measured with a spatial resolution of 10-15 μm , using a moving average filter to process the raw intensity signal. FM 1-43 concentration levels in the base were highest at the 1-hour post-delivery time point and were reduced substantially by 3 hours. Labelled gentamicin was observed with strong signal intensity at 3 hours.

Midbrain: Auditory and Non-Auditory Modulation and Plasticity

PS 824

Electrophysiological and Behavioral Characterization of Mice Missing the Inferior Colliculus

Simone Kurt¹; Tingting Gao²

¹Saarland University; ²Ulm University

A way to characterize brain structures and their function is to generate mouse models with specific genetic mutations that lead to well defined phenotypes. Ap-2 transcription factors comprise a family of 5 closely related sequence-specific DNA binding proteins that play pivotal and non-redundant roles in embryonic organogenesis. The transcription factor Ap-2 δ is exclusively expressed in the central nervous system. Interestingly, gross anatomical inspection of HE-stained brain section revealed a complete lack of the inferior colliculus (IC). Despite this lack Ap-2 δ -deficient mice showed no obvious behavioral deficits.

We examined auditory function of the Ap-2 δ -deficient mice by behavioral and electrophysiological methods. In the behavioral experiment, an auditory discrimination paradigm was used (pure tone discrimination, 7kHz vs. 12 kHz, 75 dB SPL). Multiunit recordings were per-

formed in the caudal part of the temporal cortex with pure tone stimulation. All experiments were performed in Ap-2 δ -deficient mice and wildtypes.

Ap-2 δ -deficient mice showed no discrimination learning performance at all compared to wildtype mice. Despite the missing IC, the presence of neuronal responses to sounds in the auditory cortex (AC) indicated that auditory information still reached the neocortex. Neuronal responses of Ap-2 δ -deficient mice showed changes in response characteristics, such as shorter latencies and lower evoked rates. The temporal cortex area, where neuronal responses were recorded, was significantly smaller in size compared to wildtype mice.

These changes may reflect that auditory function in Ap-2 δ -deficient mice can be mediated via a possible rewiring within the auditory pathway with partial restoration of inferior colliculus function. Further studies are required to clarify the ascending connections to the AC in Ap-2 δ knockout mice.

In summary, our data define Ap-2 δ -deficient mice as a new and valuable animal model to study auditory functions in case of auditory midbrain loss.

PS 825

Neuroplastic Changes in the Ear and Brainstem Following Low-Level Noise

Adam Sheppard¹; Guang-Di Chen²; Dalian Ding³; Richard Salvi²

¹University at Buffalo; ²Center for Hearing & Deafness, Department of Communicative Disorders and Science, State University of New York at Buffalo; ³State University of New York at Buffalo

Background

Many individuals live or work in environments in which they are continuously exposed to low-level noise. We previously demonstrated that a 5-week, 75 dB SPL broad band noise depressed the compound action potential (CAP), but paradoxically enhanced IC spike discharge rates (SDR) and local field potentials (LFP), changes indicative of Central Gain. To determine if similar changes would occur at lower intensities, we reduced the exposure intensity to 65 dB SPL.

Methods

Rats, all housed in their home cage in the vivarium, were divided into two groups: (1) Control group (n=6) and (2) Low-level noise (n=6, 10-20 kHz, 65 dB SPL, 24 h/d for 5 weeks). Cochlear function was assessed by measuring CAP I/O functions. LFPs and multiunit SDRs were recorded from the central nucleus of the inferior collic-

ulus (CIC) using 16-channel microelectrodes. Cochleae were evaluated for histological damage.

Results

The low-level noise exposure caused: (1) a very mild shift in CAP threshold between 10-20 kHz, but had no effect on CAP thresholds below or above the exposure frequency. (2) Surprisingly, CAP supra-threshold amplitudes were reduced roughly 50% at supra-threshold levels. These results indicate that low-level noise exposure can greatly reduce the neural output of the cochlea. (3) Paradoxically, sound evoked neural activity LFPs and multiunit SDRs in the CIC were enhanced at test frequencies from 10 to 20 kHz. These results suggest that the central auditory system increases its gain in the 10-20 kHz region to compensate for the reduced cochlear output at these frequencies. (4) Histologically, there was no evidence of hair cell loss in the 10-20 kHz region of the cochlea.

Conclusion

Our results indicate that continuous exposure to noise levels as low as 65 dB SPL can induce neuroplastic changes within the auditory system. While these low-levels of noise are considered “safe”, we demonstrate that they can cause a mild CAP threshold shifts and greatly reduce the neural output of the cochlea. Despite a large reduction in cochlear output, sound evoked responses in the CIC are greatly enhanced within the exposure frequency band. These results are consistent with models of Enhanced Central Gain in which the central nervous system compensates for a reduced cochlear output. Clinically, these findings are relevant to long-term, low-level noise therapies use to treat tinnitus and hyperacusis.

Research supported in part by NIH grants R01DC011808, R01DC014693, R01DC014452 and F31DC015933)

PS 826

Quiet is the New Loud: Insights into the Effects of Hidden Hearing Loss on Listening Performance in Noise

Jose Garcia-Lazaro¹; Roland Schaette¹; Jaime Undurraga²; Richard Windle¹; Jennifer F. Linden¹; David McAlpine³

¹Ear Institute, University College London; ²MacQuarie University; ³Macquarie University

For many people, the first indication they might have a hearing problem comes from difficulties they experience following conversations in background noise. Often, however, their audiogram indicates normal hearing

thresholds. Recently, hearing problems not evident in the audiogram have been linked to cochlear synaptopathy, i.e. damage to the synaptic contact between inner hair cells and auditory nerve fibres (ANFs). Noise-induced synaptopathy effectively disconnects a substantial fraction of ANFs from the hair cells (Kujawa and Liberman, 2009), and high-threshold ANFs appear particularly vulnerable (Furman et al., 2013). Colloquially described as ‘hidden hearing loss’ (HHL), peripheral synaptopathy could contribute to tinnitus (Schaette and McAlpine, 2011) and disrupt performance on complex listening tasks such as processing speech in background noise.

Here we demonstrate evidence for a link between ANF damage and increased neural gain in the central auditory pathways, both in the midbrain of gerbils exposed to a single, controlled noise insult and in human listeners. In gerbils, exposure to octave-band noise (2-4 kHz, 105 dB SPL, 2 hours) caused a temporary increase in hearing thresholds, consistent with ANF damage. Four weeks after the noise exposure, neural responses were recorded from the inferior colliculus during presentations of ‘vowel-consonant-vowel’ stimuli (VCVs) in background noise (+12 to -12 dB signal-to-noise ratios). Neural responses to VCVs were stronger in noise-exposed animals than control animals for 60 dB SPL VCVs, whereas there was no difference between the groups for 75 dB SPL VCVs. Discrimination of VCVs based on neural population activity was better for 60 than 75 dB SPL VCVs in noise-exposed animals, but conversely, better for 75 than 60 dB SPL in control animals. A comparable pattern was evident in human listeners: a marker for HHL and central gain in the auditory brainstem response (ratio of wave V to wave I) showed a significant negative correlation with the change in listening performance for VCV stimuli at -6 dB SNR when the intensity of the background noise was increased from 60 to 80 dB SPL. These data suggest that HHL degrades neural output from the cochlea at higher sound levels, but increases central gain, which could explain differences in listening performance in different levels of background noise.

Acknowledgements

This study was supported by the Medical Research Council UK (MR/L022311/1)

Furman AC, Kujawa SG, Liberman MC (2013) *J Neurophysiol* 110:577-586.

Kujawa SG, Liberman MC (2009) *J Neurosci* 29:14077-14085.

Schaette R, McAlpine D (2011) *J Neurosci* 31:13452-13457.

PS 827

Noise Induced Changes in Dopamine Receptor Production and Trafficking in Central Auditory Pathways

Aaron K. Apawu¹; Avril Genene Holt²; Bozena Fyk-Kolodziej¹; Brittany Adams¹; Mirabela Hali³

¹Wayne State University Medical School; ²Wayne State University School of Medicine/ JD Dingell VAMC;

³Wayne State University

Introduction

Previous studies have reported that hearing loss, tinnitus and hyperacusis can result in temporal and spatial changes in spontaneous neuronal activity. However, the neural underpinnings of these changes are not fully understood. We have also demonstrated that deafness related changes in dopamine (DA) receptor (Drd) gene expression are region and time specific. Recently, we reported that inhibition of D1 receptors in the inferior colliculus (IC) attenuates noise induced hearing loss and enhances hearing sensitivity, suggesting that DA receptor function may be class specific (Drd1 or Drd2) as well as activity dependent. Therefore, we examined whether exposure to a tone resulting in a temporary threshold shift causes persistent changes in Drd localization and calcium dependent association with the trafficking protein NSF-1.

Methods

Gene expression, protein levels and localization of DA receptor subtypes were examined in adult male Sprague Dawley rats (n = 10) that were either normal hearing or exposed to a tone (16 kHz, 106 dB, SPL, 1 hour). Several brain regions were examined including auditory cortex (AC), cochlear nucleus (CN), and IC. Real time RT-PCR was used to investigate the expression of DA receptors while Western blotting was used to probe DA receptor proteins in the regions of interest. Immunocytochemistry was used to determine the distribution of DA receptors in brain sections throughout the AC, IC, and the medial geniculate body (MGB). Co-immunoprecipitation was used to determine DA receptor/NSF-1 interaction within the CN, IC and AC.

Results

The presence of D1 and D2-like receptors were observed throughout the AC, CN, IC, and the MGB. There was no significant change in expression of DA receptors in the AC 24 hours following noise exposure. In the IC, our immunoblots suggest differential production of Drd1 and Drd2 one year following the noise exposure. Immunocytochemistry data revealed differential distribution of D1 and D2 receptors within IC subdivisions. In the CN, IC and AC, co-immunoprecipitation revealed that both

Drd1 and Drd2 form complexes with NSF-1 which are calcium dependent following noise exposure.

Conclusions

Our data suggest that NSF interaction with Drd1 and Drd2 occurs across central auditory brain regions. Furthermore, noise exposure causes persistent changes in Drd localization and calcium dependent association with NSF-1. Future studies will further delineate the role of Drd distribution and trafficking in susceptibility to hearing loss, tinnitus and hyperacusis.

PS 828

Distribution of Tyrosine Hydroxylase and Dopamine Receptors in the Auditory Brainstem and Midbrain

Alexander A. Nevue¹; David J. Perkel²; Christine V. Portfors¹

¹Washington State University Vancouver; ²University of Washington

Background

Neuromodulators may affect the way we process sounds. For example, dopamine modulates neural response properties throughout the auditory system, from the inner ear to the cortex. We have previously identified the subparafascicular thalamic nucleus (SPF) as the dopaminergic source to the auditory brainstem and inferior colliculus (IC). This suggests that the SPF is modulating auditory processing via dopamine at multiple levels of the auditory pathway. However, the type of dopamine receptors present in these auditory nuclei is largely unknown. The purpose of this study was to determine the distribution of D1-like and D2-like receptors, both of which can convey neuromodulatory signals, and how those those receptors relate to the distribution of dopaminergic puncta in the auditory brainstem and midbrain.

Methods

We sectioned the brains of adult CBA/CaJ mice from the dorsal cochlear nucleus (DCN) to the inferior colliculus (IC). We then immunostained for DRD1, DRD2, and tyrosine hydroxylase (TH), the rate limiting enzyme in dopamine synthesis. Using a confocal microscope, we identified and imaged labeled receptors and fibers in the cochlear nucleus, the various nuclei in the superior olivary complex (SOC), and the IC.

Results

We found that D1 and D2 receptors were expressed in the DCN and superior olivary complex (SOC). We observed differential expression of dopamine receptors in the nuclei of the SOC. In the medial nucleus of the trapezoid body (MNTB), most if not all neurons expressed dopamine receptors, likely both D1 and D2 on the same

cells. Far fewer neurons in the superior paraolivary nucleus and lateral superior olive were immunoreactive for dopamine receptors compared to the MNTB. We found that only D2 receptors were expressed in the IC. Interestingly, in the IC, we observed more clusters of labeled dopamine receptors than TH-positive puncta.

Conclusion

We found that dopamine receptor expression is different in the brainstem and midbrain nuclei. D1 and D2 receptors are expressed in the auditory brainstem whereas only D2 receptors are expressed in the inferior colliculus, the principal auditory midbrain nucleus. More clusters of dopamine receptors than TH-positive puncta suggests that dopamine release acts over a longer timescale.

Funding

This project was funded by NIH NIDCD R01DC013102

PS 829

Dopamine Modulates Intrinsic and Synaptic Properties of Neurons in the Mouse Inferior Colliculus

Charles A. Williams¹; Agata Budzillo²; Christine V. Portfors³; David J. Perkel¹

¹University of Washington; ²Allen Institute for Brain Science; ³Washington State University Vancouver

Background

Auditory processing can change depending on intrinsic and extrinsic factors and these changes are likely mediated by neuromodulators. One such neuromodulator is dopamine (DA), as dopamine depletion is associated with disrupted auditory processing. One locus of modulation is likely the inferior colliculus (IC), which expresses DA receptors and receives dopaminergic input from the subparafascicular nucleus of the thalamus. In addition, application of dopamine to neurons in the central nucleus of the IC in mice alters responses to auditory stimuli. Such changes could be mediated through altered electrophysiological properties of individual neurons and/or altered synaptic strengths. Here we asked how dopamine affects the intrinsic and synaptic properties of IC neurons in vitro.

Methods

We made blind or visualized whole cell recordings from neurons in the central nucleus of the IC in brain slices prepared from CBA/CaJ mice on postnatal day 15-30. Recordings were made at 30-32 °C with potassium based internal solutions. Current-clamp recordings were used to examine intrinsic properties. Voltage-clamp recordings were used to examine synaptic properties, focusing on excitatory postsynaptic currents. Synaptic events were evoked by electrical stimulation to the lat-

eral lemniscus or IC commissure. We applied dopamine agonists and antagonists to assess dopamine's effects on intrinsic and synaptic properties.

Results

Neurons in the central nucleus of the mouse IC can be segregated into four classes based on their intrinsic spiking properties. Different classes fire action potentials in response to depolarizing current injection in sustained, adapting, onset, or intermittent patterns. These neuronal classes were similar to those identified in rats. Dopamine affected both intrinsic and synaptic properties of IC neurons. Dopamine application caused a depolarization resulting from an inward current and increased input resistance. Dopamine also reduced evoked excitatory postsynaptic currents in ~30% of IC neurons. In 50% of neurons that exhibited spontaneous synaptic events (~40 cells), dopamine reduced the frequency of excitatory events by 33%.

Conclusions

In parallel with the diverse effects of dopamine on auditory responses in vivo (Gittelman et al. 2013), we found diverse actions of dopamine on IC neurons in vitro. The combined excitatory and inhibitory effects of dopamine on intrinsic and synaptic properties in the IC are well placed to contribute to complex auditory modulation.

Funding

This project was funded by NIH NIDCD R01DC013102 and T32DC005361.

PS 830

Dopamine Reduces Global Auditory Responses via D2-like Receptors in the Inferior Colliculus of Freely Behaving Mice

Jeffrey M. Hoyt¹; David J. Perkel²; Christine V. Portfors¹

¹Washington State University Vancouver; ²University of Washington

Background

The ability to understand speech relies on accurate auditory processing of complex sounds. Individuals with Parkinson's disease suffer from speech perception deficits, suggesting that dopamine is involved in the encoding of complex sounds. The inferior colliculus (IC) is rich in both dopaminergic fibers and D2-like receptors, and recent studies from our lab demonstrated that dopamine has heterogeneous effects on the responses of many IC neurons in mice. The strongest effect in the IC, however, is to suppress neural activity. It is currently unknown whether D2-like receptors are involved in heterogeneously modulating neuronal responses, and

whether the observed preponderance of depressive effects reflects the global effect of dopamine in the IC. In this study, we tested whether dopamine acts via D2-like receptors to heterogeneously alter responses of individual IC neurons, and to globally depress responses of populations of IC neurons.

Methods

Single-unit experiments: We recorded extracellular responses of single IC neurons in awake, restrained mice. We compared responses to tones and natural mouse vocalizations before and after iontophoretic application of dopamine and D1- or D2-like agonists. We quantified how activating dopamine receptors changed the rate and timing of responses. **Freely behaving experiments:** We recorded multi-unit activity and local field potentials (LFP, 3-50 Hz) in the IC of freely behaving mice in response to tones natural mouse vocalizations before and after pressure injection of dopamine or a D2-like agonist into the IC. We quantified how activating dopamine receptors changed the rate and timing of multiunit activity, as well as the amplitude and timing of averaged LFP peaks.

Results

The effects of dopamine and a D2-like agonist on spiking rate and timing of single IC neurons were heterogeneous as both either increased or decreased individual neuronal responses to tones and vocalizations. Dopamine reduced responses in the majority (71%) of cells, and D2-like agonist application produced similar effects. In freely behaving mice, dopamine and a D2-like agonist reduced responses at the population level as both decreased multi-unit spike rate and peak LFP amplitude while increasing latency.

Conclusions

We found that dopaminergic neuromodulation in the IC alters responses to sounds while mice are freely behaving, and that such modulation occurs via D2-like receptors. Understanding how dopamine modulates auditory processing will ultimately inform therapies targeting mechanisms underlying disorders of auditory processing and communication.

Funding

NIH NIDCD R01DC013102

PS 831

Cholinergic Projections from the Pedunculo-pontine Tegmental Nucleus to the Inferior Colliculus

William A. Noftz; Nichole L. Beebe; Jeffrey G. Mellott; Brett R. Schofield

Northeast Ohio Medical University

Acetylcholine (ACh) modulates sound processing in the inferior colliculus (IC). Cholinergic inputs to the IC originate from the pedunculo-pontine tegmental nucleus (PPT), laterodorsal tegmental nucleus and lateral paragigantocellular nucleus. We showed previously that cholinergic boutons contact GABAergic and non-GABAergic IC cells, but these targets have not been associated with specific sources of cholinergic input. Here we injected an adeno-associated viral vector (rAAV/EF1a-DIO-EYFP or rAAV/EF1a-DIO-mCherry; UNC Vector Core) into transgenic rats (LE tg (CHaT-Cre) 5.1 Deis; RRRRC) to label cholinergic projections from the PPT. Sections were stained with antibodies to glutamic acid decarboxylase (GAD) to label GABAergic neurons and vesicular glutamate transporter 2 (VGLUT2) to label glutamatergic terminals.

Cholinergic axons were more numerous ipsilaterally than contralaterally. On both sides, labeled axons entered the IC via two main routes: 1) medial axons entered the ventromedial border of the central nucleus (ICc), and 2) lateral axons entered the IC with the lateral lemniscus to reach the ICc or the lateral cortex (IClc). Once in the ICc, axons branched infrequently, providing en passant boutons as they traveled across laminae. Some axons continued into the dorsal cortex where they provided additional boutons. Axons in the IClc branched extensively and formed complex terminal fields.

In all IC subdivisions, boutons were more numerous in the neuropil, but a substantial number appeared to contact neuronal somas. A minority of the contacted somas were GAD+. GAD+ cells in the IC can be categorized according to whether they are surrounded by a perisomatic ring of VGLUT2+ boutons. Cholinergic boutons appeared most often to contact cells that lacked VGLUT2 rings.

We conclude that cholinergic PPT axons enter the IC via multiple routes and contact cells in each of the major IC subdivisions. Within each subdivision, the cholinergic boutons contact GABAergic and non-GABAergic somata, suggesting that ACh acts on both excitatory and inhibitory cells. Moreover, ACh may act on multiple GABAergic cell types, albeit with one type (the "GAD-only") possibly playing a dominant role.

Retinal Projections to Auditory Nuclei in the Guinea Pig

Jeffrey G. Mellott; Matthew A. Smith; Samuel D. Crish; Brett R. Schofield
Northwest Ohio Medical University

We used axonal tracing techniques to identify projections from the retina to auditory nuclei in the diencephalon and brainstem of guinea pigs. We injected 5 µl of tracer (1% cholera toxin subunit B conjugated to Alexa Fluor-488 or Alexa Fluor-647) into the vitreal chamber of each eye in 6 adult guinea pigs. After 5-7 days we fixed the brain by perfusion with 4% paraformaldehyde and cut the brain into transverse or parasagittal sections for examination.

The lateral geniculate nuclei, the superior colliculus and numerous accessory optic nuclei were well labeled. Smaller projections, predominantly contralateral, were observed in auditory nuclei. In the thalamus, labeled retinal boutons were observed most often in the suprageniculate, medial, dorsal and shell divisions of the medial geniculate nucleus (MGsg, MGm, MGd, MGs). In the midbrain, labeled boutons and axons were most numerous in the dorsal cortex and lateral cortex of the inferior colliculus (ICd and IClc), where they were densest in the outer layers. The small axons tended to travel parallel to the layers whereas the largest axons were often oriented perpendicular to the layers. Labeled axons with en passant boutons were also identified in the sagulum, just ventral to the IC (and lateral to the dorsal nucleus of the lateral lemniscus). We did not observe retinal inputs within the nuclei of the lateral lemniscus or in more caudal auditory nuclei.

We conclude that the guinea pig retina projects directly to a set of auditory nuclei in the diencephalon and midbrain. We presume that all of these areas are involved in multisensory integration. Several of these regions – the IClc, sagulum and MGsg – are connected directly with the superior colliculus, and may serve specific roles in orienting behavior, auditory attention and possibly audiovisual motor interactions associated with the superior colliculus. The ICd and MGd are not connected with the superior colliculus and are not routinely associated with visual inputs. However, these areas have been implicated in auditory attention and, along with the sagulum, are all targets of dense, direct descending projections from auditory cortex. These connections suggest a potential for convergence of visual inputs with modulatory top-down auditory cortical projections. The role of such convergence, if it occurs, awaits further insight into the type of visual information conveyed by the retinal inputs. It will be of particular interest to identify the types of retinal ganglion cells that provide these inputs.

Light Field Otoscope Three Dimensional Imaging of Diseased Ears in an Alaska Native Population

Philip Hofstetter, Au.D¹; John Kokesh, MD²; Samantha Kleindienst, AuD, PhD, CCC-A¹; Noah Bedard³; Harshavardhan Binnamangalam³; Tiffany Romain³; Ivana Tomic³

¹Norton Sound Health Corporation; ²Alaska Native Medical Center; ³Ricoh Innovations Corporation

The prevalence of ear diseases is high in the Alaska Native population, yet diagnosis and management can be challenging even for the most experienced clinicians. Furthermore, the use of telemedicine is required to assess many of these conditions due to the majority of the population living in remote villages off the road system. This creates more reliance on static images of the tympanic membrane (TM) and subjective interpretation of the color and shape of image features. Misdiagnosis of diseases such as TM retractions and otitis media (OM) can lead to increased morbidity and over-prescription of antimicrobial agents, contributing to the worsening problem of antibacterial resistant strains in the United States. Light field imaging is a rapidly advancing technology that uses a microlens array in combination with a main lens to capture both spatial and angular distribution of light reflected from an object, in this case the TM. Based on this technology, a Light Field Otoscope (LFO) has been developed by Ricoh, which is capable of single-snapshot three-dimensional (3D) and spectral imaging of the TM without physically contacting the middle ear. The goal of this study was to evaluate the value and feasibility of the LFO by collecting preliminary image and 3D data on a diverse set of middle ear diseases in the Alaska Native population. Data were collected during a routine otolaryngology field clinic at Norton Sound Health Corporation (NSHC), in Nome, Alaska. A senior otolaryngologist examined all enrolled (n = 20) patients referred into the clinic for management of ear disease using a standard binocular microscope. His clinical impressions were recorded. Patients were then imaged by trained audiologists with a standard 2D video otoscope and with the Ricoh LFO. Two focus groups were held with the participating otolaryngologist, audiologists, and Ricoh research team to visually compare LFO 2D+3D images to standard 2D digital otoscope images, and discuss the relation of these to the binocular microscope findings. Insights from those discussions suggest that the 3D reconstruction rendered from the LFO image data (see Figure 1) provided important information, especially in cases of retracted TMs. This presentation will demonstrate and review the current LFO technology, clinical

applications, and the iterative process implemented between the clinical and research development teams for advancing and investigating the diagnostic capability of a technology that has the potential to improve the management of middle ear diseases, particularly when using a telemedicine medium.

PS 834

Middle Ear Responses Measured at the Tympanic Membrane during the Acoustic Reflex: A Comparison to Clinical Impedance Measures

Heath G. Jones; Nathaniel T. Greene; Stephanie Karch; Sean A. Hollonbecck; William A. Ahroon
U.S. Army Aeromedical Research Laboratory

Repetitive exposure to high-level acoustic impulses, such as those from firearms, increases the susceptibility for hearing loss. Over the past several years, recommendations have been made to update and/or replace current military standards and regulations intended to protect individuals exposed to high-level acoustic impulses from hearing injury. One method recently implemented by the Department of Defense for determining the risk of hearing injury from impulsive noise exposures is the Auditory Hazard Assessment Algorithm for Humans (AHAH). The AHAH is an electrical equivalence model of the human ear designed to reproduce sound transmission through the ear in order to predict potential hearing injury from a given sound exposure; however, several key assumptions involving the effects of middle-ear muscle contraction (MEMC) on sound transmission through the middle ear during the acoustic reflex have not been validated. In particular, the AHAH model presumes that, once activated, the effect of the MEMC is identical (i.e., a 20 dB decrease in transmission) across all frequencies. While it is known that the MEMC generally has a high-pass filter effect on sound transmission through the middle ear, studies are needed to fully characterize these filter characteristics. In the current study, we used laser-Doppler vibrometry (LDV) to measure tympanic membrane (TM) motion in response to an acoustic reflex-eliciting impulse as a proxy for assessing ossicular chain motion in human participants. The laser was mounted on a surgical microscope and focused on the TM near the umbo. A continuous probe tone of varying frequencies was delivered to the ear measured by the LDV transducer. An elicitor stimulus (i.e., a short tone pip presented at 110dB SPL) was delivered to the contralateral ear via an insert earphone. Using this approach, we directly measured the time course and magnitude of engaging the MEMC on middle ear movement. Changes in ossicular chain motion during MEMC were thus observed as frequency-dependent increases or decreases in TM velocity. These measurements were compared to acoustic impedance mea-

surements made using comparable stimuli and standard clinical techniques. Findings establish the effect of the MEMC on middle ear movements following high-intensity acoustic stimulation. Results also suggest a more nuanced, across-frequency potential for middle ear gain or attenuation during the acoustic reflex. Knowledge gained from this study indicates the need for updates to hearing health hazard assessments, and increases our understanding of the potential for hearing injury in individuals routinely exposed to high-level impulsive noises.

PS 835

Novel Experimental model for Negative Pressure in the Middle Ear and Effects of Epithelial-cell Proliferation in the Tympanic Membrane

Naotaro Akiyama¹; Tomomi Yamamoto-fukuda²; Haruo Takahashi³; Hiromi Kojima²

¹*Department of Otorhinolaryngology, Jikei University School of Medicine and Department of Otorhinolaryngology, Toho University School of medicine;* ²*Department of Otorhinolaryngology, Jikei University School of Medicine;* ³*Department of Otolaryngology-Head and Neck Surgery, Nagasaki University Graduate School of Biomedical Sciences*

Background

Negative pressure in the middle ear was thought to be closely related to the etiology of retraction-type cholesteatoma. Recently, it has been detected that physical forces translate them into biochemical and biological responses in cells. Continuous negative pressure in the middle ear may possibly accelerate the proliferation of epithelial cells of the tympanic membrane (TM). To investigate the influence of negative pressure in the middle ear, we analyzed experimental model in which continuous negative pressure was loaded in the middle ear.

Methods

To produce negative pressure, we utilized the negative pressure of the supply route of an iPRECIO® micro-injection pump.

For this study, nine male rats (6-10 weeks old, 220-470 g) were divided into three groups: a negative pressure group; a catheter placement into the middle ear with negative pressure load (n=3) and two sham groups; a small hole in the middle ear (n=3) or a catheter placement without negative pressure load (n=3). All left ears were used as control. Seven days after surgery, an otoscopic examination and micro-CT analysis, H&E staining and immunohistochemistry were performed. The degree of proliferation and differentiation of epithelial cells of the TM was investigated immunohistochem

ically using anti-keratin-5 (K5), anti- keratin -10 (K10) and anti- Wnt5a antibody.

Results

In the otoendoscopic examination, retraction of the pars flaccida (PF) and serous effusion behind the TM were detected in all negative-pressure group. Conversely, the sham groups showed no retraction of the PF. Through micro-CT analysis, all ears in the negative-pressure group showed soft-tissue-density (STD) areas in the hypotympanum. H&E staining revealed the thickened PF in all ears of the negative-pressure group. Immunohistochemistry demonstrated that K5 positive cells tended to increase in the basal cells of the epidermal layer of the PF into which negative pressure was loaded, as compared to the PF of the normal ears. On the other hand, K10 positive cells increased in the upper layer of the epidermis of the PF into which negative pressure was loaded. Moreover, Wnt5a positive cells was detected in epithelial cells of the thickened epithelium of the negative-pressure group.

Conclusions

We analyzed experimental model in which continuous negative pressure was loaded in the middle ear. As a result, it was revealed that the epithelium of PF was thickened under continuous negative pressure in the middle ear. Moreover, it was suggested that negative pressure might affect the proliferative activity of epithelial cells of PF in the TM.

PS 836

Functionally Designed Nano-scaffolds for Regeneration of Chronic Tympanic Membrane Perforations

Beomyong Shin¹; Hoon Seonwoo²; Kyoung-Je Jang²; Yeon Ju Kim¹; Young Sun Kim¹; Yun Yeong Lee¹; Oak-sung Choo¹; Mi Jin Choi¹; Yeong Cheol Kim¹; Jong Hoon Chung²; Yun-Hoon Choung¹

¹Department of Otolaryngology, Ajou University School of Medicine, Suwon, Republic of Korea; ²Department of Biosystems & Biomaterials Science and Engineering, Seoul National University, Seoul, Republic of Korea

Aim

Various patches releasing growth factors have been developed to treat chronic tympanic membrane (TM) perforations. However, nanostructures influencing cellular functions have never been applied to patches before. Aligned anisotropical nanostructures, directed toward the center, are anticipated to help the wound healing of TM. Thus, we developed a radially aligned electrospun patch scaffold that releases epidermal growth factor (EGF) and applied it to animal models.

Materials and methods

EGF-releasing radially aligned patch scaffolds (EGF-A) were fabricated by electrospinning and compared with electrospun EGF-releasing random patch scaffolds (EGF-R). Both patches were observed by scanning electron microscopy (SEM), and their alignments were analyzed by Image J. Also, the incorporation of EGF on scaffolds was confirmed by Fourier transform infrared spectroscopy (FTIR) and their release efficacies were evaluated by enzyme-linked immunosorbent assay (ELISA). The cell viability of all the patches was assessed with primary TM cells isolated from Sprague-Dawley (SD) female rats (4 weeks, 50-100g). In vivo, SD female rats (7 weeks, 200-250g) were used, and patches were applied to the perforated ears. Then, their healing status were checked and imaged once a week for 8 weeks. Non-treated group which induced spontaneous healing was set as the control group. For histological analysis, TMs to which patches were applied for 8 weeks were obtained and were analyzed with hematoxylin and eosin staining.

Results

Fibers of EGF-A were well organized and aligned toward centroid. FT-IR spectroscopy confirmed the presence of EGF in all patches. Proliferation of EGF-A group were significantly higher than those of the other group, and the TM cells of EGF-A group showed elongated morphology and alignment toward centroid. In animal studies, the EGF-A group showed 36.3% healing (12/33), while control group and EGF-R group revealed 14.2% (2/14) and 29.7% healing (11/37), respectively. Histological studies of regenerated TM in the EGF-A group were thinner than EGF-R group, indicating better qualitative results.

Conclusion

The radially nano-patterned EGF patch, a novel scaffold for regeneration of chronic TM perforation, showed efficacious wound-healing capability from our study. Thus, we expect that this nano-patterned EGF patch can be provided as a superior nonsurgical treatment for regeneration of chronic TM perforation.

Otopathologic Evaluation of Temporalis Fascia Grafts Following Successful and Failed Tympanoplasty

Elliott Kozin¹; Iman Ghanad¹; Nicole L. Black²; Reuven Ishai³; Aaron Remenschneider⁴

¹Massachusetts Eye and Ear Infirmary; ²Harvard John A. Paulson School of Engineering and Applied Sciences; ³Massachusetts Eye and Ear Infirmary, Harvard Medical School; ⁴University of Massachusetts / Massachusetts Eye and Ear Infirmary

Background

Success following tympanoplasty necessitates the complete healing of the tympanic membrane (TM) and restoration of conductive hearing. Unfortunately, tympanoplasty outcomes remain variable. The structure and composition of graft materials utilized in tympanoplasty directly affect the success of the procedure. The incorporation of allografts, such as temporalis fascia into new tympanic membranes is not well understood. The histologic structure and cellular composition of tympanoplasty graft materials have not been previously described. Herein, we aim to describe the pre- and post-operative histologic microstructure of temporalis fascia and compare findings to normal TM controls.

Methods

An otopathologic review of tympanoplasty specimens from a national human temporal bone repository was undertaken. Temporal bone specimens having undergone successful total drum replacement using temporalis fascia were identified (n=3). Specimens from patients having undergone failed tympanoplasty were similarly reviewed (n=3). Histopathologically prepared pre-implantation temporalis fascia (PreTF, n=4) and normal TMs taken from contralateral ears, when available, (n=5) were used as controls. Multiple measurements of thickness of PreTF and TMs at the mesotympanum and hypotympanum were obtained. Collagen and elastin fiber thickness and orientation of normal and grafted TMs were analyzed.

Results

In cases of fascia tympanoplasty, the average duration from time of surgery to death was 16 years (range 8-28). Three cases contained an aerated middle ear without residual perforation and three contained perforated, significantly thickened TMs. There was no significant difference between the thickness of PreTF and the successful tympanoplasty specimens (289 +/- 230 vs 226 +/- 105, p=0.4). Temporalis fascia in successful tympanoplasty cases did not change its perpendicular, longitudinal fibrous structure over time, with preserved inner and outer

collagen layers. Grafts from failed tympanoplasty cases contained mucinous glands, a thickened stroma and an absence of an identifiable fibrous structure. The normal TMs were thinner than the PreTF and both successful and failed tympanoplasty cases (p=0.002, p=0.01, respectively).

Conclusion

Temporalis fascia does not significantly change in thickness or fibrous structure following successful tympanoplasty within an aerated middle ear. In failed cases, temporalis fascia structure is unidentifiable, being replaced by mucinous components surrounding a persistent perforation. These studies have implications for novel grafting materials that must account for both the structural properties of the TM as well as biologic healing properties needed to close a persistent perforation.

PS 838

Quantification of the Effects of Stapes Fixation via a Novel 3-axis Force Sensor

Ivo Dobrev¹; Baktash Aqtashi²; Jae Hoon Sim¹; Alexander Huber³; Thomas Linder²; Christof Roosli¹

¹Department of ENT, Head and Neck Surgery, University Hospital Zurich, Switzerland; ²Department of ENT, Head and Neck Surgery, Cantonal Hospital Luzern, Switzerland; ³1, Department of Otorhinolaryngology – Head and Neck Surgery, University Hospital Zurich, Zurich, Switzerland

Background

Intra-operative quantification of the ossicle mobility could provide valuable feedback for the current status of the patient's conductive hearing. However, current methods for evaluation of middle ear mobility are mostly limited to the surgeon's subjective impression through manual palpation of the ossicles. This study applies novel methods for study of the effect on middle ear transfer function, in human temporal bones, due to: 1) stapes fixation; 2) stapes immobilization; 2) controlled palpation force.

Methods

A controlled palpation force was applied at the ossicular chain, while the middle ear transfer function, defined as the ratio of the stapes footplate velocity versus the ear canal sound pressure, was measured with a single point LDV, and the corresponding quasi-static displacement of the contact point was measured, via a 3-axis micrometer stage. The palpation force was applied sequentially, step-wise in the range of 0.1 – 20 gF (1 – 200 mN), at the stapes head in two in-plane (superior-inferior or posterior-anterior) directions, and at the incus lenticular process, near the incudostapedial joint, in the piston (lat-

eral-medial) direction. Each condition was repeated with various stages of stapes fixation, simulated by drying of the temporal bone, and with severe ossicle immobilization, simulated by gluing of the stapes footplate. The palpation force was controlled via a novel 3-axis PalpEar force sensor (Sensoptic, Switzerland) with a noise floor and resolution of < 10mgF (0.1 mN) and 1 mgF (0.01 mN), respectively.

Results

Simulated stapes fixation (drying time of 5 – 7 hrs.) increases (5-10dB) the high frequency (>3kHz) and decreases (3-5dB) the low frequency (< 1kHz) response of the middle ear. Stapes immobilization severely reduces (20-30dB) the low and mid frequency response (< 4kHz) but has lesser effect (< 10dB) at higher frequencies. Even moderate levels of palpation force (< 3gF, < 30mN) have negative effect (10-20dB) on the low frequency (< 2 kHz) response, but no significant effect at higher frequencies. Force-displacement measurements around the incudostapedial joint showed quasi-static stiffness in the range of 200-400 N/m.

Conclusion

Effects of the palpation force and stapes fixation have been analyzed based on the measurement of the stapes footplate motion, and controlled application of 3D force and displacement.

PS 839

Normative Measures of Ossicular Chain Compliance Using the Otopen Surgical Device

Tyler S. Okland¹; Mohamed A. Alhussaini¹; Justin T. Casey¹; Renee M. Banakis Hartl¹; Victor Benichoux²; Jameson K. Mattingly¹; Nathaniel T. Greene³; Herman A. Jenkins¹; Daniel J. Tollin²; Andrew D. Brown²

¹Department of Otolaryngology, University of Colorado School of Medicine; ²Department of Physiology and Biophysics, University of Colorado School of Medicine;

³U.S. Army Aeromedical Research Laboratory

Background

Conductive hearing loss is a common hearing pathology, sometimes caused by mechanical disruption of ossicular chain movement; however, no objective criteria currently exist to evaluate ossicular chain function in the intraoperative setting. This presents a problem when deciding potential surgical repair, as well as in evaluating intervention success. Our Device is a linear actuator coupled with a highly sensitive load cell that can be used to measure ossicular chain compliance intraoperatively, both before and after an intervention.

Methods

Seven fresh frozen hemi-cephalic cadaveric specimens were prepared with a canal-wall-up mastoidectomy and extended facial recess to optimize middle ear access. To confirm normal middle ear function, we used Laser Doppler vibrometry to measure umbo and stapes velocities to acoustic stimulation by tones of different frequencies. The Device was then used to displace the ossicular chain and measure compliance at various positions along the chain, including the umbo, the incus long process following surgical fixation of the middle ear, and the umbo and incus long process after surgical reconstruction of the middle ear.

Results

We demonstrate that the device is able to simultaneously measure force and displacement of the ossicular chain, and obtain results comparable with previously published data. We inferred stiffness and compliance of the ossicular chain in order to provide normative ranges in intact, normally functioning middle ears as well as those that have undergone reconstruction. Finally, using repeated measurements in the same specimens, we assess the reproducibility of device measurements.

Conclusion

Our device is capable of measuring ossicular chain force-displacement curves, and thus stiffness and compliance in the human middle ear. Results were found to be highly repeatable within a specimen, yet some across-specimen variability remains. Further studies are required to determine the utility and accuracy of ossicular chain compliance measurements for hearing outcomes.

PS 840

Analysis of Clinical Characteristic of Simple Congenital Ossicular Malformation and Ossicular Chain Reconstruction

Dong-Dong Ren¹; Xiao-Yu Yang²; Jing Yu²; Xin-Wei Wang²; Meng Zhao²; Fanglu Chi¹; Dongdong Ren²

¹Department of Otolaryngology and Skull Base Surgery, Eye, Ear, Nose and Throat Hospital; Fudan University, Shanghai, China; ²EYE & ENT Hospital of Fudan University

Object

To study of simple congenital ossicular malformation clinical and audiological characteristics, and to discuss options to different auditory ossicles in ossicular chain reconstruction.

Methods

Ossicular chain malformations in 75 cases (79 ears) were studied involving 43 males and 32 females, aged from 6 to 57 years old (average 23.5 ± 14.5 years old). There are four cases of bilateral conductive deafness and 71 cases of unilateral conductive deafness (39 left ears and 32 right ears). Results of preoperative audiometry showed that air-bone gap was 38.7dB of speech frequency. We operated exploratory tympanotomy in 79 ears (4 cases of bilateral). Among them, ossicular chain reconstruction was performed in 71 cases, while in six cases not done because of facial deformity, and in two cases ossicle joints'activities were good after incudostapedial joint release.

Results

According to Teunissen classification (1993), we divided 79 ears into four groups, including 5 (6.3%,5/79) ears of type I (Ankylosis or isolated congenital fixation of the stapes), 11(14%,11/79) ears of type II (Stapes ankylosis associated with other malformations of the ossicular chain), 47(59.5%,47/79) ears of type III (Congenital anomalies of the ossicular chain with mobile stapes footplate), 16(20.3%,16/79) ears of type IV (Congenital aplasia or severe dysplasia of the oval and round windows). Intraoperative findings demonstrated deformity types including: absence of long process of incus or in connection with the stapes soft tissues, absence of suprastructure of stapes, stapes muscle attached in lenticular process or long process of incus, crura separating from footplate, patial crura of stapes, incudostapedial joint ankyloses, stapes ankylosis, and absence of suprastructure of footplate with dyplasia of the oval window. 5 cases of type I were implanted with Kurz-Piston(2), Spiggle-Piston(2), Xomed-Piston(1). 11 cases of type II were implanted with Kurz-Piston(3), Spiggle-Piston(5), Xomed-Piston(3). For type III, 23 cases were implanted with partial ossicular replacement prosthesis (PORP), including Kurz-PORP(6), TTP-PORP(5), Xomed-PORP(12); 2 cases were implanted with autologous incus; 20 cases were implanted with total ossicular replacement prosthesis (TORP), including TTP-TORP(7), Spiggle-TORP(2), Xomed-TORP(10), autologous incus(1); and 2 cases were performed with incudostapedial joint release. 10 cases of type IV had done oval window drill-out occicular reconstruction, including 8 cases with Piston, 2 cases with TORP. The average air-bone gap was 21.5dB in two weeks post-surgery.

Conclusion

Ossicular chain reconstruction with selection of different types of artificial ossicular depending on types of ossicular chain malformations is an effective method to improve hearing and decrease air-bone gap.

PS 841

Novel Banked Bone Ossicular Replacement Prostheses with Ergonomic and Functional Geometry

Mario Milazzo¹; Serena Danti²; Francesco Inglese¹; Andrea De Vito³; Luca Bruschini⁴; Stefano Berrettini⁵; Cesare Stefanini⁶

¹The BioRobotics Institute, Scuola Superiore Sant'Anna, Pontedera (PI), Italy.; ²The BioRobotics Institute, Scuola Superiore Sant'Anna, Pontedera (PI), Italy; Dept. of Civil and Industrial Engineering, University of Pisa, Pisa, Italy.; ³Operative Unit of Otorhinolaryngology, Audiology and Phoniatics, Azienda Ospedaliero-Universitaria Pisana (AOUP), Pisa, Italy.; ⁴Operative Unit of Otorhinolaryngology, Audiology and Phoniatics, Azienda Ospedaliero-Universitaria Pisana (AOUP), Pisa, Italy ; Dept. of Surgical, Medical, Molecular Pathology and Emergency Medicine, University of Pisa, Pisa, Italy; ⁵Operative Unit of Otorhinolaryngology, Audiology and Phoniatics, Azienda Ospedaliero-Universitaria Pisana (AOUP), Pisa, Italy; Dept. of Surgical, Medical, Molecular Pathology and Emergency Medicine, University of Pisa, Pisa, Italy; ⁶The BioRobotics Institute, Scuola Superiore Sant'Anna, Pontedera (PI), Italy ; Dept. of Biomedical Engineering and Robotics Institute, Khalifa University of Science Technology and Research, Abu Dhabi, United Arab Emirates.

This work addresses the fabrication of innovative ossicular replacement prostheses (ORPs), both partial and total ORPs (PORPs and TORPs), manufactured from banked cortical bone via computer numerically controlled (CNC) ultraprecision micro-milling. Our aim was to combine optimal middle ear compatibility and surgical manageability in a single device, by releasing off-the-shelf homograft ORPs provided with the appealing features of synthetic ORPs, such as lightness, accuracy, surface decoration geometric plasticity (Fig. 1a).

Bone ORPs were microfabricated with holed head plates to facilitate their surgical positioning while reducing their mass. The TORP prototype was 13.1 ± 0.1 mg, leading to 81% weight reduction with respect to the previous model available in literature. In addition, surface annular motifs of the head plates were applied to prevent slipping and migration after surgery (Fig. 1b). Using scanning electron microscopy (SEM), we demonstrated that the chosen groove structure (~ 0.1 mm) showed the lowest debris on the bone surface. Debris may cause irritation with the coupled tissue under vibratory motion. On the other areas, the surface roughness was kept low to avoid friction with other structures. Finite element modeling (FEM) was used to evaluate the displacement occurring between the patterned PORP and the tym-

panic membrane under load-simulated conditions. Our estimation calculated a 0.74 nm displacement in case of patterned surface, that is about 70% less than the one evaluated with smooth surface.

Comparative measurements of acoustic responses of bone versus synthetic PORPs, the latter made of titanium and hydroxyapatite (HA), were conducted in the 250-8000 Hz frequency range with a patented acoustic apparatus (patent request #PCT/IB2015/059621). Differences were investigated by a one-way analysis of variance (ANOVA) with post-hoc Tukey's test with statistical significance set at 0.05. Results highlighted a better behavior of bone PORPs in particular at low and high frequencies with p-values 0.006 for "bone vs. HA" at 250 Hz and 7.8×10^{-7} for "bone vs. titanium" at 8000 Hz (Fig. 2).

Concluding, this study showed that banked compact bone can be optimally manufactured, standardized to produce highly performant ORPs, both from the acoustic and structural points of view.

The new bone ORPs may represent the ideal combination of biocompatibility and technology which can ultimately accomplish unmet otosurgical needs.

PS 842

Augmented Reality Combining Otoendoscopy and High-resolution CT-scan for Minimally Invasive Otological Procedures

Alexis Bozorg Grayeli¹; Roberto Enrique Marroquin Cortez²; Alain Lalande²; Angela Lavedrine³; Caroline Guigou³; Jean-Paul Camuset⁴

¹Otolaryngology Dept., Dijon University Hospital and Le2i, CNRS UMR-6306, Dijon, France; ²Le2i, CNRS, UMR-6306, Université Bourgogne Franche Compté;

³Otolaryngology Department, Dijon University Hospital, Dijon, France; ⁴Point Medical Imaging Center, Dijon, France

Introduction

The aim of this study was to develop and to test an augmented reality software combining otoendoscopy views and the high-resolution CT-scan data in order to visualize the middle ear content through an intact tympanic membrane.

Materials and Methods

Four human temporal bone specimens were included. The external auditory canal and the tympanic membrane were visualized and filmed by a 30 ° angled otoendoscope (Storz, Tittingen, Allemagne). The endoscope was rotated and translated inside the auditory

canal slowly (< 5 mm/sec) and rapidly. The specimens were also analyzed by CT-scan (Newtom 5G, Verona, Italy). Dicom data was imported into Osirix (Freeware, v 5.6, 32 bits, www.osirix-viewer.com) running on an iMac (quad-core Intel Core i7 CPU at 4 GHz, 8 Go RAM). The virtual endoscopy function was employed to obtain a 3D reconstruction of the middle ear and the labyrinthine windows. An extension module was developed for Osirix to implement the augmented reality function. The initial registration between the video recordings and the 3D CT-scan was conducted by a manual selection of 4 corresponding points on the rim of the tympanic membrane and the malleus handle. Several registration algorithms were employed to maintain correspondance between CT-scan and video during endoscope movements: one based on optical flow (Features from Accelerated Segment Test, FAST) and 3 others based on image features (Scale Invariant Feature Transform, SIFT; Speed Up Robust Features, SURF; Oriented FAST and Rotated BRIEF, ORB). The mean target error (MTE) was measured during the endoscope movements and compared between these algorithms.

Results

SURF and SIFT yielded higher precision than other methods with a MTE of 0.5 ± 0.60 mm and 0.6 ± 0.50 after 30 sec of rapid endoscope movements and a refresh rate of 17 and 10 frames per second (FPS) respectively. FAST produced the largest error (2.1 ± 2.0 mm at the beginning but with a higher refresh rate (28 FPS).

Conclusion

Augmented reality combining 3D CT-scan and dynamic otoendoscopy can be obtained by image-based techniques without the use of conventional neuronavigation. It will potentially enable the surgeon to visualise the middle ear content through an intact tympanic membrane in the operating room.

PS 843

Otitis Media in Mice with a Human Hematolymphoid System

Arwa Kurabi¹; Kwang Pak²; Allen F Ryan³

¹University of California, San Diego; ²Veterans Affairs San Diego Healthcare System, La Jolla CA; ³Department of Surgery, Division of Otolaryngology, University of California, San Diego

Introduction

Otitis media (OM) is a common infectious disease with significant morbidity especially in children. Recent results implicated innate immune responses in OM etiology, pathogenesis and resolution. We hypothesized that using "humanized mice," engrafted with human immune

cells, would address human-specific immunologic questions and provide a novel disease model.

Methods

OM was induced by inoculation of nontypeable *Haemophilus influenzae* (NTHi) into the middle ears (MEs) of NOD-Scid-IL2R γ null (NSG) severely immunodeficient mice that were previously transplanted with human hematopoietic CD34+ progenitor cells. Blood, bone marrow, and ear tissue were collected 48 hours and 7 days after OM induction, and human inflammatory cell mobilization was analyzed by flow cytometry and immunohistochemistry. The ME inflammatory response, leukocyte infiltration, tissue hyperplasia, bacterial clearance and OM recovery were compared to that in wild type (WT) BALB/c mice.

Results

48 hrs after NTHi inoculation into WT and humanized mice MEs, equivalent mucosal hyperplasia and inflammatory cell infiltration were observed. Similar to WT, the humanized mice were able to clear bacterial infection by day 7. In the humanized mice, we observed the mobilization of human CD45+ immune cells into the ME cavity, suggesting that the human cells are participating in both ME inflammation and NTHi bacterial clearance.

Conclusions

This study is the first to demonstrate the suitability of humanized mice for OM research. As NSG mice lack leukocytic immune responses to bacterial and fungal pathogens, the results indicate that the human immune cells of engrafted animals are able to enter into and function in the murine ME. They offer the possibility to address specific research questions not amenable to traditional mouse models, including the role of that subset of human-specific immune genes that are either significantly altered or totally absent from the mouse genome. The ability to study human immune cells in an animal setting will allow us to address human-specific immunity in OM, while preserving the many advantages of an animal model.

[Supported by NIH/NIDCD grants R03DC014801-01A1, DC000129 and the Veteran Affairs Administration Research Service.]

PS 844

Detection of Bacteria in Middle Ear Effusions Based on the Presence of Allergy: Does Allergy Augment Bacterial Infection in the Middle Ear?

Jeong-Hoon Oh; Woo Jin Kim; Ki-Hong Chang
Department of Otolaryngology-Head and Neck Surgery

Background and Objectives

Bacterial infection, Eustachian tube dysfunction, allergies, and immunologic factors are major causes of otitis media with effusion (OME). However, the exact pathogenesis of OME is still unclear. This study evaluated whether allergy influences bacterial growth in middle ear effusions.

Materials and Methods

Fifty-four samples were obtained from OME patients 3–10 years of age who underwent ventilation tube insertion and were divided into two groups based on the presence of allergy as determined using the multiple allergosorbent test (MAST). *Streptococcus pneumoniae*, *Haemophilus influenzae*, and *Moraxella catarrhalis* bacterial DNA in the middle ear effusions was analyzed using polymerase chain reaction. Overall detection rates and those for each species were compared between the two groups.

Results

Of the 54 middle ear effusion samples, 38 (70.4%) contained bacterial DNA and 14 (36.8%) of these contained DNA from multiple species. *S. pneumoniae* was detected in 27 samples (50%), *H. influenzae* in 17 samples (31.4%), and *M. catarrhalis* in 9 samples (16.6%). There was no significant difference in the bacterial detection rates between the middle ear effusions of the MAST-positive and MAST-negative groups.

Conclusion

The rate of bacteria detection in middle ear effusions did not differ between allergic and non-allergic children.

Comparative Analysis of the Expression of E-cadherin, β -catenin and β 1 Integrin in Congenital and Acquired Cholesteatoma

Chul Won Park¹; Dong Wook Lee²; Jae Ho Chung²; Seung Hwan Lee³

¹Department of Otolaryngology-Head and Neck Surgery, School of Medicine, Hanyang University, 222-Wangshimni-ro, Seongdong-gu, Seoul 133-792, Korea; ²Department of Otolaryngology-Head and Neck Surgery, School of Medicine, Hanyang University; ³Hanyang University

E-cadherin, β -catenin and β 1 integrin are important cell adhesion molecules to maintain epithelial structure and function. We investigated the expression of these cell adhesion molecules in cholesteatomas to understand the role of cell-cell and cell-extracellular matrix interaction in cholesteatomas. An immunohistochemical investigation was carried out on 35 cholesteatoma tissue samples (14 congenital, 21 acquired cholesteatomas) and 10 normal retroauricular skin (RAS) tissues which are obtained during middle ear surgery. The expression rate was measured to find out differences between retroauricular skin and cholesteatoma, as well as between congenital and acquired cholesteatoma. E-cadherin expression rate was significantly lower in the cholesteatoma (spinous layer 88.7 \pm 17.9%, granular layer 54.6 \pm 22.6%) than in the RAS(100%, 74.4 \pm 7.4%), and in the acquired(83.3 \pm 19.4%, 48.1 \pm 22.9%) than in the congenital (96.7 \pm 12.0%, 64.4 \pm 18.8%). β -catenin expression rate was significantly lower in the cholesteatoma (spinous layer 84.1 \pm 17.2%, granular layer 28.7 \pm 30.8%) than in the RAS (100%, 75.9 \pm 6.1%), and in the acquired (78.1 \pm 17.0%, 17.1 \pm 22.3%) than in the congenital (93.2 \pm 13.5%, 46.1 \pm 34.2%). The expression pattern of β -catenin is similar to that of E-cadherin. In β 1 integrin, there was no significant difference of the expression rate between RAS and cholesteatoma, as well as between congenital and acquired cholesteatoma. In conclusion, the expression of E-cadherin and β -catenin was reduced in cholesteatoma, and the reduction is more pronounced in acquired cholesteatoma than in congenital cholesteatoma. Acquired cholesteatomas showed more aggressive characteristics than congenital cholesteatomas in terms of cell-cell adhesion.

Neural Crest Cell Might Be Origin of Middle Ear Cholesteatoma

Tomomi Yamamoto-fukuda¹; Norifumi Tatsumi²; Masahiro Takahashi³; Naotaro Akiyama⁴; Masataka Okabe²; Hiromi Kojima¹

¹Department of Otorhinolaryngology, Jikei University School of Medicine; ²Department of Anatomy, The Jikei University School of Medicine; ³Department of Otorhinolaryngology, The Jikei University School of Medicine; ⁴Department of Otorhinolaryngology, Jikei University School of Medicine and Department of Otorhinolaryngology, Toho University School of medicine

Research background

Middle ear cholesteatoma is a gradually expanding destructive epithelial lesion within the middle ear, which leads to extensive tissue destruction in the temporal bone. In the previous studies the expression of cellular and inflammatory pathways cytokines were analyzed in middle ear cholesteatoma tissues, and as results cytokine network (e.g. IL-1, IL-1, IL-6, KGF, GM-CSF, EGF, TNF-, PDGF, and TGF-), is important in the growth of cholesteatoma. Current tumor therapies, based largely on targeting the growth factor pathway, show limited clinical benefits, thus necessitating the discovery of alternative targets. To analyze the origin of middle ear cholesteatoma is need for establishing new therapy. Here we show for the first time the presence of a novel stem cell-like cell population in our animal model of middle ear cholesteatoma.

Methods

All experiments were performed in accordance with the guidelines of the local ethics committee of the Jikei University School of Medicine. Wnt1-Cre/Floxed-EGFP mice (Shimada K et al. 2012) were used in this study. Based on the role of KGF in the development of cholesteatoma, Flag-hKGF cDNA driven by CMV14 promoter was transfected through electroporation into the right ear 5 times on every fourth day (Yamamoto-fukuda T et al. 2015). Left ears transfected with empty vector were used as controls. Cholesteatoma formation was evaluated by otoendoscopy. At 7 days after final injection, mice were sacrificed and temporal bones were removed en bloc. The paraffin sections of middle ear were used for H&E and immunohistochemical analysis.

Results

As a result, all mice were formed middle ear cholesteatoma in the rights ear. NC cells were found lining the middle ear cavity on the attic region in the vicinity of the ossicles and lining medial wall covering the otic capsule/cochlea. We found NC cells were expanded into middle

ear and formed middle ear cholesteatoma. Especially in the otic capsule/cochlea area, NC cells were formed stratified squamous epithelium solitary as like a congenital cholesteatoma formation.

Conclusions

These findings indicated that NC cell is an origin of middle ear cholesteatoma. In the recent study, Thompson H et al. (2013) showed that the mammalian middle ear develops through cavitation of a NC and the epithelium lining the middle ear cavity is roughly half NC and half endodermal. It suggests that mesenchymal NC cells migrated into the tympanic membrane have undergone a mesenchyme-to-epithelium transformation and formed middle ear cholesteatoma.

PS 847

Depth of the Sinus Tympani Is Unrelated to Mastoid Pneumatization: A Cartesian Coordinate Study

N Wendell Todd
Emory University

Background

Cholesteatoma involving the sinus tympani is notoriously difficult to assess and control. Otologists would be happy for every sinus tympani to be shallow. Correlates of sinus tympani depth are unknown, although some suggest that increased depth correlates with large mastoid pneumatization.

Objective

To describe the depth of the sinus tympani, relative to both the adjacent facial nerve and distance from the round window, and how depth correlates with mastoid size.

Methods

Ten clinically ear-normal crania underwent computed tomography in a custom non-metallic positioning device that referenced the Frankfort horizontal plane. The crania, from a series of 41, were the five with the largest mastoids, and the five with the smallest mastoids, as assessed by plain lateral radiograph. Each landmark (midst of round window [RW], apex of sinus tympani [ST] and midst of facial nerve [FN] is that slice) was twice independently identified in xyz Cartesian space. The midst of the facial nerve was chosen even though not surgically accurate, so as to better consistently landmark the facial nerve for this study.

Results

The mean direct distance from RW to ST ranged from 3.4 to 7.7 mm, median 6.1 mm for right ears; 4.1-8.0, 5.0 left. For FN to ST, the range was 1.6-4.0 mm, me-

dian 3.2 right; 1.8-3.2, median 2.5 left. Neither bilateral symmetry nor relationship with mastoid size was found.

Discussion

Using a technique free of proximity bias, the depth of the sinus tympani is variable and unpredictable.

Conclusion

From one ear to another ear, the depth of the sinus tympani varies and is not predictable.

PS 848

Augmented Reality as a Novel Tool for Teaching Middle and Inner Ear Anatomy

Kevin Wong¹; Brian A. Xavier²; Shivkumar C. Bhadola³; Gregory Grillone⁴

¹Department of Otolaryngology-Head and Neck Surgery, Boston Medical Center; ²Department of Radiology, Boston Medical Center; ³University of Massachusetts Memorial Medical Center; ⁴Boston Medical Center

Background

Augmented reality combines real-world environmental elements with computer-generated sensory input such as sounds, text, and graphics. Current applications focus on architecture, video games, and the visual arts, however, such navigation systems have potential for use in medical education. This technology allows students to visualize human structures beyond the limited planar views of traditional pictures or videos, which can be particularly useful for anatomical areas that may be difficult to visualize or conceptualize such as the middle and inner ear. Herein, we describe our experience designing a readily accessible augmented reality environment to aid students learning ear anatomy.

Methods

Computerized tomography and magnetic resonance imaging of the head and neck in DICOM format were opened in 3D Slicer (www.slicer.org) and volume rendered into 3D models. The 3D models were exported into the Unity 3D game engine (Unity Technologies, San Francisco, CA) and incorporated stereoscopically into an interactive 3D "game environment". This was converted into augmented reality using Vuforia software development kit (PTC Inc., Needham, MA), which positioned anatomic models in real space based on the user's orientation towards real world images so that a user's perspective of the virtual 3D models corresponded to their orientation towards the real world image. Data was exported onto an iPhone 6 (Apple Inc., Cupertino, CA) and fitted into a virtual reality viewer (Unofficial Cardboard, La Jolla, CA) worn by the user.

Results

Figure 1 displays the modifications made to the cardboard viewer to accommodate an iPhone equipped with augmented reality. Figure 2 demonstrates a user's perspective of a 3D skull and middle ear ossicles (red circle) in augmented reality using the above methodology.

Conclusions

The creation of an augmented reality environment was achieved using the 3D Slicer model generator, Unity game engine, and Vuforia augmented reality software development kit. All three programs are free and/or open source, and coupled with a mobile device and virtual reality viewer, provide a cheap, readily accessible way for students to visualize and conceptualize head and neck anatomy. Future prototypes can improve ergonomics of the head-mounted displays, incorporate clipping planes, and introduce a user interface to allow students to rotate, magnify, and manipulate 3D images in real time. Future applications in the diagnosis and surgical planning for ear and head and neck disorders may also be considered.

Plasticity, Learning and Adaptation: Behaviour

PS 849

Action Audio Game Training Enhances Speech Perception in Older Adults with Sensorineural Hearing Loss: A Randomized, Double-blind, Placebo Controlled Study

Jonathon Whitton¹; Kenneth Hancock²; Jeffrey Shannon³; Daniel B. Polley¹

¹Eaton-Peabody Laboratories, Massachusetts Eye and Ear Infirmary; ²Eaton-Peabody Labs, Mass. Eye and Ear; ³Hudson Valley Audiology Center

Background

Sensorimotor training with action videogames provides a transfer of learning to a wide range of selective attention and feature detection tasks. Boosting generalized perceptual processing abilities through action videogame training could have far-ranging therapeutic potential for individuals with sensory processing disorders. However, the essential features of effective action games are unknown and the possible influence of placebo effects have been called into question. Here, we programmed an audio game that 'closed the loop' between motor actions and sensory feedback, a key feature of action games, and asked whether it was sufficient to drive generalized perceptual improvements beyond those found with a 'placebo' auditory working memory game.

Methods

Subjects (N = 24, mean age = 70 years) were randomly assigned to train for 3.5 hours per week over an 8-week period from home on either the closed-loop audiomotor (C-L) or memory task (Mem). Both games were matched for complexity, learning and expectations of benefits. Psychophysical tests were administered at three time points: before training, immediately after training and again eight weeks after the conclusion of training. Psychophysical tests were designed to measure frequency discrimination, speech recognition in noise, inhibitory control and working memory.

Results

We employed a randomized, double-blind, placebo controlled study design in a population of elderly hearing-aid users and determined that closed-loop audiomotor game training drove clinically significant, generalized improvements in their ability to understand speech in noisy backgrounds. No changes in speech processing were observed in subjects trained on the Mem game. Transfer of learning was specific to perceptual tasks that involved tracking a signal over time, as C-L training i.) did not generalize to an isolated word recognition in noise test that was procedurally identical to the sentence tests, but ii.) did transfer to a digit streaming task devoid of linguistic context. Audiomotor training provided subjects approximately 3 times more benefit than their hearing aids for speech recognition in high levels of background noise (0-5 dB SNR). Improved speech processing following C-L training was not accompanied by enhanced spectro-temporal processing, memory capacity, or inhibitory control.

Conclusions

Closed-loop audiomotor training provided significant, but short-term, gains on various measures of sentence comprehension in background noise, the most common hearing complaint of older age for which assistive devices offer variable benefit. Thus, training in a simplified action audio game can provide generalized benefits for real-world perceptual challenges in sensory-impaired adults that cannot be attributed to placebo effects.

PS 850

The Effect of Passive Stimulus Exposures on Perceptual Learning of Distorted Speech

Steven Losorelli¹; Aliza Frankel-Segal²; Matthew Fitzgerald¹

¹Stanford University; ²Montclair State University

In auditory training programs, the ability to maximize learning with minimal amounts of practice has the potential for significant clinical importance. In young adults

with normal hearing (NH), combining periods of active practice with periods of passive stimulus exposure can result in learning that is more rapid and of greater magnitude than learning resulting solely from active practice. We have previously shown, however, that recipients of cochlear implants (CI) fail to benefit from passive stimulus exposures when learning to identify phonemes that are not native to the English language. One key difference between listeners with NH and those with CIs is that the signal heard by recipients of CIs is substantially degraded relative to that heard by NH. Here, we investigated whether the combination of active training and passive exposures yielded learning in individuals with NH listening to stimuli degraded through a simulation of a cochlear implant.

24 participants between the ages of 19 and 35 with NH participated in this experiment, which took place in a single training session. In this session, participants received training on speech identification when the stimuli were distorted with an 8-channel simulation of a cochlear implant. The 24 participants were then divided into three groups. All groups received a pre-test, a training phase, and a post-test. The active-only group completed 8 lists of training on AzBio sentence recognition with feedback. The active-passive group completed 4 lists of training on AzBio sentence recognition with feedback, and 4 lists of passive stimulus exposures while performing a written task. The control group completed 4 lists of training on AzBio sentence recognition with feedback.

Both the active-only and active-passive groups improved significantly between the pre- and post-tests by the same magnitude. In contrast, the control group showed no statistical improvement between the pre- and post-tests. Taken together, these results suggest that passive stimulus exposures can facilitate learning when combined with active practice on a speech-identification task, even when the signal is distorted. We plan to re-examine the effects of passive stimulus exposures by training listeners with NH to identify the same non-native phonemes previously utilized in individuals with CIs. If passive stimulus exposures continue to benefit learning of distorted speech, this suggests that the differences in patterns of perceptual learning between individuals with NH and those with CIs may result at least in part from the auditory deprivation caused by hearing loss.

PS 851

Cortical Activity in Children with Single-Sided Deafness Pre- and Post-Implantation

Melissa J. Polonenko¹; Blake C. Papsin²; Karen A. Gordon¹

¹The University of Toronto, The Hospital for Sick Children; ²Cochlear Implant Program (The Hospital for Sick Children), University of Toronto

The objectives of this study are to examine effects of single-sided deafness (SSD) on cortical development in children with early onset deafness and utility of cochlear implantation in this population. Bilateral deafness treated with one cochlear implant abnormally strengthens pathways from the stimulated ear in both kittens and children. We thus hypothesized that similar cortical changes: 1) occur in children with SSD, particularly when the impaired ear is deaf from birth, and 2) are avoided when function is restored as soon as possible to the impaired ear with a cochlear implant.

Thirteen children aged 4.0 ± 2.8 years participated in this study. Severe to profound sensori/neural hearing loss was measured by pure tone audiometry in either the left ($n = 9$) or right ($n = 4$) ears. Six of these children received a cochlear implant in their deaf ear. Thirteen age-matched normal hearing children were also recruited. Electroencephalographic measures of cortical activity were recorded across 64-cephalic electrodes in response to monaurally presented clicks via an insert earphone to the normal hearing ear. For implanted children, responses from the deaf ear were evoked by biphasic electric pulses from the apical (#20) electrode on the implanted array within a week and after a month of device activation. The time-restricted artifact and coherent source suppression (TRACS) beamformer was used to locate underlying activity of the immature cortical peaks.

Preliminary analyses indicated activity in both the left and right temporal auditory cortices in children with normal hearing and children with SSD. Activity lateralized to the contralateral cortex in children with normal hearing but was more bilateral or lateralized to the ipsilateral cortex in 8 of the 13 children with SSD (6 of 9 left SSD; 2 of 4 right SSD). Clear cortical responses were evoked by electric stimulation in all 6 implanted children. Further analyses will include: effects of etiology and duration of unilateral deafness on the extent of cortical reorganization; cortical sources evoked by the deprived ear; and effects of duration of implant use on cortical sources.

Initial results suggest that cortical reorganization occurs in many young children with single sided deafness but

that implantation of the deaf ear provides access to bilateral input.

PS 852

Tracing the Origins of Speech-In-Noise Perceptual Improvement: An Auditory Training Study in Normal-Hearing Listeners

Leonard Varghese¹; Jonathon Whitton²; Sara Beach³; Dana Boebinger³; Justin Fleming³; Daniel B. Polley²
¹*Boston University*; ²*Eaton-Peabody Laboratories, Massachusetts Eye and Ear Infirmary*; ³*Program in Speech and Hearing Bioscience and Technology, Harvard University*

Recent work has found that older adults trained with a tablet-based 'audiogame' that emphasized continuous discrimination of dynamic auditory stimuli acquired an improved ability to accurately process sentences embedded in high levels of babble noise. No benefits were observed in a control group that played a challenging auditory working memory game (Whitton et al., submitted). Improved speech processing was thought to reflect an improved ability to direct and maintain selective attention. Here, we characterize changes in the neural and perceptual correlates of selective attention before and after younger individuals with "normal hearing" abilities acquired expertise with this immersive audiomotor game.

Methods

Training paradigm: We implemented a double-blind, randomized, placebo-controlled study design that assigned participants to train for eight weeks from home on a game that emphasized either closed-loop audiomotor discrimination (treatment condition) or auditory working memory (placebo condition). In this design, neither the subject nor the experimenters are aware of whether training is carried out with the treatment or placebo game. Data from the previous cohort of older listeners indicates that subjects' expectations for an auditory-related benefit were matched for both training conditions.

Electrophysiology

Prior to the start of training, and after the tablet training regime is complete, participants undergo a series of EEG recordings during both passive and active listening. Active listening tasks involve AM discrimination or pitch discrimination during selective attention. The stimuli used in these EEG sessions (diotic presentation of two concurrent streams of amplitude-modulated (AM) complex tones) are designed to test auditory sensory acuity and attention without placing strong demands on memory. Cortical event-related potentials (ERPs), cortical auditory steady-state responses (ASSRs), and

subcortical envelope following responses (EFRs) are derived from the EEG responses obtained during the active and passive paradigms.

Preliminary results

Initial results from the pre-training active EEG task indicate that ERPs to tone onsets, ASSRs, and EFRs can be obtained with sufficient signal-to-noise ratio to be useful correlates of potential neural encoding changes arising from gameplay. These correlates of basic sensory encoding and auditory attentional modulation may help explain the efficacy of auditory-sensorimotor gameplay in improving speech-in-noise perceptual abilities, and may aid in developing more highly targeted gameplay-based interventions for individuals with hearing impairment.

PS 853

Corruption Rather Than Destruction of Learning on Interaural-level-difference Discrimination from Anterograde Interference

Robert B. Baudo¹; Beverly A. Wright²

¹*Department of Communication Sciences and Disorders, Northwestern University*; ²*Department of Communication Sciences and Disorders, and Knowles Hearing Center, Northwestern University*

Listeners improve on perceptual tasks with practice, providing a means to enhance normal perceptual abilities and treat perceptual disorders. Development of optimal training strategies requires an understanding of perceptual learning processes, including the circumstances that disrupt learning. We recently observed that across-day learning on an interaural-level-difference (ILD) discrimination task was disrupted when training on that task was immediately preceded by training on an interaural-time-difference (ITD) discrimination task (TL) but not when the order of the tasks was reversed (LT), indicating anterograde but not retrograde learning interference. One potential explanation for this outcome is that training on the ITD task prevents the processes necessary for the subsequent acquisition of learning on the ILD task. If so, then training on the TL complex should not affect learning induced by subsequent training on the ILD task alone. To test this prediction, we trained a group of normal-hearing adults on the TL complex and then on a second, isolated, bout of the ILD task 30 minutes later (TL30minL; n=8). Contrary to the prediction, performance on the ILD task did not improve from the initial bout to a final bout the next day (P=0.871). To determine whether this lack of learning was due to anterograde interference from the ITD task extending to the isolated bout of the ILD task, we trained another group on only the ITD task 30 minutes before the ILD task (T30minL; n=8). Although no learning occurred on

the ILD task from the initial to the final bout ($P=0.812$), starting threshold on the ILD task was lower for the T30minL group than for the TL30minL group ($P=0.01$). Thus, training on the ITD task did not harm, but instead enhanced, performance on the isolated bout of the ILD task 30 minutes later. Together, these results suggest that training on the ITD task does not prevent the acquisition of learning on the ILD task. An alternative explanation is that performance on the ITD task contaminates the encoding of the ILD task in the TL complex and this contaminated memory is reactivated by performance of the ILD task in isolation. This proposal is consistent with evidence in other learning domains that during recall, memories are retrieved from a stable state back into a labile state in which they can be modified and must then be re-consolidated. Thus, a lack of improvement from perceptual training may reflect corrupted learning rather than no learning at all.

PS 854

Evidence for Independent Processing of Rhythms with Different Tempos

Ruijing Ning¹; Samuel Trosman¹; Andrew T. Sabin¹; Beverly A. Wright²

¹*Department of Communication Sciences and Disorders, Northwestern University;* ²*Department of Communication Sciences and Disorders, and Knowles Hearing Center, Northwestern University*

Rhythm is fundamental to music and speech, yet relatively little is known about how even simple rhythmic patterns are processed. Here we investigated the processing of an isochronous rhythm using a perceptual-learning paradigm. We asked (1) whether anisochrony detection at a single tempo marked by tones of a single frequency improved with practice and, if so, (2) whether this improvement generalized to anisochrony detection with an untrained tempo or untrained marking frequency, or to a temporal-interval discrimination task. We also examined the relationships among the pre-training thresholds for all of the tested conditions. Trained listeners ($n=8$) practiced anisochrony detection 720 trials per day for 7-8 days using an adaptive, two-alternative, forced choice procedure. In each trial, listeners discriminated an isochronous sequence of six brief 1-kHz tones with a standard inter-onset interval (IOI) of 100 ms from an anisochronous sequence in which one of the middle four tones was randomly presented late. Between pre- and post-training tests, trained listeners improved significantly more than controls (no training; $n=8$) on the trained anisochrony-detection condition: IOI=100 ms, frequency=1 kHz. Remarkably, trained listeners got worse than controls—negative generalization—on anisochrony detection with the trained frequen-

cy but an untrained IOI (200 ms vs. 100 ms). There was no generalization to anisochrony detection with the trained IOI but an untrained marking frequency (4 kHz vs. 1 kHz) or frequencies (variable vs. fixed frequency), and no generalization to an untrained temporal-interval discrimination task with the trained IOI and frequency. Further, pre-training thresholds for all of the conditions with 100-ms IOIs were at least marginally correlated with each other, but not with the condition with the 200-ms IOI. Thus, the learning on anisochrony detection was specific to the trained tempo and frequency and did not transfer to temporal-interval discrimination, and pre-training performance was correlated across different frequencies for the same tempo, but not across different tempos. These results provide behavioral evidence for independent processing of rhythms of different tempo, of rhythms of common tempo marked by different frequencies, as well as of rhythms and the individual temporal intervals of which they are composed.

PS 855

Auditory Brainstem and Envelope Following Responses in Children with and Without Listening Difficulties

Allison Bradley¹; Audrey Perdew¹; Nicholette Smith¹; Andrew Dimitrijevic²; Leonard Varghese³; Barbara Shinn-Cunningham³; Lisa L. Hunter¹; David R. Moore¹
¹*Cincinnati Children's Hospital;* ²*Sunnybrook Hospital* *ENT University of Toronto;* ³*Boston University*

Background

Some children report listening difficulties (LiD) despite clinically normal hearing thresholds. Recent evidence has indicated that loss of auditory nerve fibers and IHC synapses, 'cochlear neuropathy' (CoN), could cause suprathreshold deficits such as those reported in LiD, without affecting behavioral hearing thresholds. We hypothesized that CoN underlies some of the deficits experienced by children with LiD. Two neural response measures proposed for the detection of CoN in humans are the auditory brainstem response (ABR) and envelope following response (EFR). ABR Wave I amplitude, reflecting cumulative activity of auditory nerve fibers (ANFs), is diminished in mice with CoN. EFRs evoked by AM transposed tones may be a sensitive indicator of CoN as they are hypothesized to be influenced by loss of high threshold ANFs (Bharadwaj, *Front Sys Neurosci*, 2014).

Methods

ABRs and EFRs were recorded in 96 children aged 6-12 years. Based on parent's perception of their child's listening difficulties (ECLiPS questionnaire) participants were classified as either typically developing (TD, $N=51$), or

as having listening difficulties (LiD, N=45). ABRs evoked by clicks (75, 80, 85 and 90 dB nHL) were recorded between 'tiptrodes' placed in each ear canal and an electrode on the forehead. Tiptrodes enhance ABR Wave I amplitude. EFR stimuli were transposed tones (100 Hz modulation, 4kHz carrier signal, 100%, 63% and 40% modulation depth). EFRs were recorded using 64-channel EEG. PCA was used to combine channels and reduce recording time. EFR amplitude and 'phase-locking value' (PLV) were calculated as SNR. ABR Wave I amplitude and latency and EFR amplitude and PLV were compared between groups, and tested for relationships with ECLIPS score and behavioral audiometry thresholds.

Results

Eleven participants (5 TD, 6 LiD) were excluded from EFR analysis due to poor signal quality. No difference in any response measure was found between the TD and LiD groups. EFR amplitude and PLV increased slightly with better behavioral audiometry thresholds, with the strongest correlation at 4000 Hz ($r^2 = 0.13$, $p < 0.001$). Parent report of listening difficulties did not correlate significantly with EFR amplitude or PLV.

Conclusion

No evidence was found of cochlear neuropathy underlying childhood listening difficulties.

PS 856

Behavioral Measures Reveal Central Auditory and Cognitive Contributions to Childhood Listening Difficulties (APD)

David R. Moore¹; Allison Bradley¹; Nicholette Smith¹; Audrey Perdew¹; Andrew Dimitrijevic²; Lisa L. Hunter¹
¹Cincinnati Children's Hospital; ²Sunnybrook Hospital
ENT University of Toronto

Background

Despite clinically normal pure-tone thresholds, some children experience listening difficulties (LiD) including reduced understanding, attention and recall of speech, especially in noisy environments. Some of these children are diagnosed with 'auditory processing disorder' (APD). The causes of LiD are poorly understood; both top-down (cognitive) and bottom-up (sensory) mechanisms have been proposed. Our objectives were to examine validity of APD diagnosis, and reliance of listening tests on cognitive ability. As part of a program including audiology and physiology, we tested 6-12 y.o. children on a clinical 'APD' battery, using speech-in-noise and cognitive measures.

Methods

Children were classified typically developing (TD; n=60) or LiD (n=51) based on parent report (ECLIPS questionnaire on listening and related skills; Barry et al, Ear Hear, 2015) and clinical evaluation. For this presentation overall ECLIPS scores were the "gold standard" for LiD. Clinical APD testing was the SCAN 3:C (Auditory Figure/Ground, Filtered Words, Competing Words, Competing Sentences). Other measures were sentence listening in competing speech (LiSN-S), and cognition assessment of NIH Toolbox (NIH-TB). Linear modeling related these tests to LiD, as measured with ECLIPS. Further modeling determined interactions between listening and cognition.

Results

Scores on SCAN 3:C, LiSN-S, and NIH-TB all correlated significantly with parental report of LiD (ECLIPS). NIH-TB, particularly the list sorting working memory and oral reading tests, predicted parental report of LiD better than SCAN or LiSN-S. SCAN predicted LiD better than LiSN-S. However, SCAN results also correlated well with NIH-TB, confirming a strong relationship between the SCAN, LiD and cognitive ability. LiSN-S spatial and total advantage measures were not significantly correlated to NIH-TB. However, a significant correlation was found between the spatial advantage measure of the LiSN-S and behavioral measures of extended (very high) frequency hearing loss ($r^2 = 0.18$, $p < 0.01$).

Conclusions

Cognitive abilities contribute significantly both to LiD and currently used clinical tests of APD. LiSN-S advantage measures were not dependent on cognitive abilities, and predicted less of the variance in LiD. However, LiSN-S may be measuring an independent auditory contributor to LiD. Such a mechanism would be additional to the cognitive influences measured by the SCAN and other tests of hearing. LiSN-S advantage measures thus appear to partial out cognitive influences on performance, as previously hypothesized. Overall, our results provide new evidence for impaired peripheral and central auditory processing, and confirm impaired cognition as contributions to LiD (APD) in children. Supported by NIH R01DC014078.

A Randomized Controlled Crossover Study of the Impact of Online Music Training on Pitch and Timbre Perception in Cochlear Implant Users

Nicole T. Jiam¹; Mickael L. D. Deroche²; Patpong Jiradejvong³; Charles J. Limb³

¹Johns Hopkins University School of Medicine; ²McGill University Montreal; ³University of California - San Francisco

Cochlear implant (CI) related biomechanical constraints result in impoverished spectral cues and poor frequency resolution, making it difficult for users to perceive pitch and timbre perception. There is emerging evidence that music training therapies may improve CI-mediated music perception, however, most of the previous studies on the effects of music training with CI users involve intensive one-on-one in-person structured music training programs over extended periods of time. Online resources for auditory rehabilitation remain an untapped potential resource for CI users. Establishing immediate value from an acute music training program may encourage CI users to adhere to post-implantation rehabilitation exercises, therefore improving overall performance with CI-mediated music perception. In this study, we evaluated the benefits of an acute online music training program on CI-mediated pitch and timbre perception. We conducted a randomized controlled crossover study. 20 CI users and 21 normal hearing (NH) adults were assigned to one of two arms. Arm-A underwent one month of online self-paced music training (intervention) followed by one month of audiobook listening (control) and Arm-B underwent one month of audiobook listening (control) followed by one month of music training (intervention). Pitch and timbre performance scores were taken across three visits: (1) baseline, (2) after one month of intervention or control, (3) after crossover and one month of intervention or control. All participants were required to meet a minimum of 2 hours a week of exercises or audiobook listening over the course of 4 weeks. We found that acute music training improved pitch sensitivity ($F(1,28) = 5.0$, $p = 0.033$) and timbre discrimination (d' gain of 0.3, $p = 0.000$) relative to audiobook listening. These findings held regardless of hearing status and Arm. As expected, CI subjects performed much more poorly than NH subjects in all tasks. A small procedural effect was observed in the timbre task that likely contributes, to some degree, to the main effect of online music training. In conclusion, online music training programs offer an opportunity to provide cost-effective and accessible post-implantation rehabilitation for CI users. Acute participation in these programs demonstrate benefit in overall pitch and timbre perception for CI users, and may potentially lead to overall improved levels of satisfaction with music listening.

Speech in Noise Perception as a Marker of Cognitive Decline in HIV Infection

Yi Zhan¹; Abigail Fellows²; Tangkai Qi³; Odile Clavier⁴; Sigfrid Soli⁵; Xiudong Shi⁶; Yuxin Shi³; Jay C. Buckey²

¹Shanghai Public Health clinic center, Fudan University njjiooo; ²Geisel School of Medicine at Dartmouth; ³Shanghai Public Health Clinical Center, Fudan University; ⁴Creare, LLC; ⁵University of British Columbia; ⁶Shanghai Public Health Clinical Center

Background

HIV+ individuals report hearing difficulties, but standard audiological tests show little or no changes in peripheral hearing ability. The hearing complaints may reflect central nervous system (CNS) auditory processing deficits, rather than middle or inner ear problems, and may result from HIV- related CNS damage. If central auditory task performance and cognitive deficits in HIV+ individuals are related, then central auditory tests might serve as a “window” into CNS function in these patients.

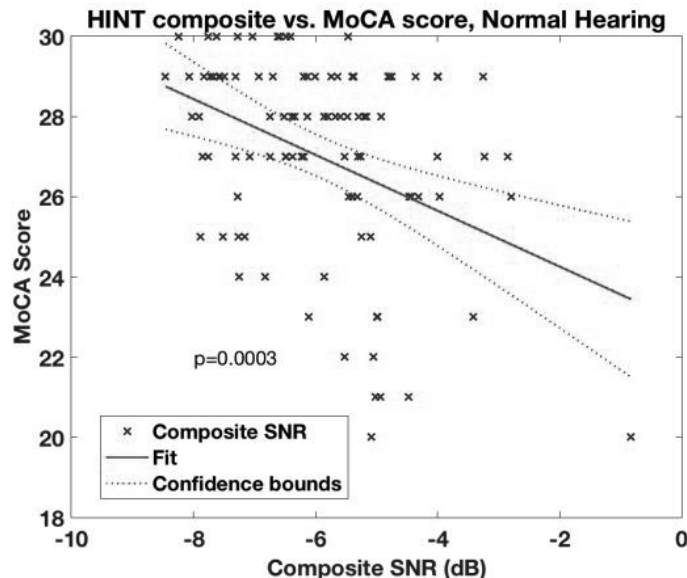
Methods

We measured cognitive performance (Mandarin Montreal Cognitive Assessment (MoCA)) and speech-in-noise perception (Mandarin hearing-in-noise test (HINT)) in 98, normal-hearing HIV+ individuals (95 men, 3 woman, average age 38) at the Shanghai Public Health Clinical Center in Shanghai, China. Data collection included audiometry, tympanometry, and the Amsterdam Inventory of Auditory Handicap (AIAH), which assesses the subjective ability to understand speech and localize sound.

Results

Subjects had no middle ear disease and had a pure tone average (500, 1000, 2000, 4000 Hz) < 25 dB HL bilaterally. The composite speech recognition signal to noise ratio (SNR) was significantly worse in those with abnormal performance on the MOCA ($p < 0.003$), and a significant negative relationship between SNR and MOCA scores ($r^2=0.13$, $p < 0.001$) existed (Figure 1). AIAH and MOCA scores were also related ($p < 0.05$). Those with worse MOCA scores reported more problems on the AIAH. Although age was also significantly related to the composite SNRs ($R^2=0.31$, $F=42.4$, $p < 0.001$), the average age for the abnormal cognitive status group (41 ± 11.5 years) was not significantly different from the normal cognitive status group (37 ± 9.8 years). Also, there was no significant relationship between MoCA scores and age found in this cohort ($R^2=0.02$, $F=2.2$, $p = 0.14$). Conclusions: Understanding speech in noise was inversely related to cognitive abilities, despite normal ability to hear soft sounds. Speech perception involves cortical and subcortical centers and is a demand-

ing neurological task. Problems interpreting speech in noise may reflect HIV-related central nervous damage, suggesting that central nervous system complications in HIV+ individuals could be diagnosed and monitored using simple central auditory tests.



PS 859

Individual Differences in Adaptation to the Signal Transmitted via Cochlear Implants in Experienced CI Users

Anita Wagner¹; Deniz Baskent²

¹University Medical Centre Groningen; ²University of Groningen, University Medical Centre Groningen, Department of Neurology/ Head and Neck Surgery, Groningen, The Netherlands

Cochlear implant (CI) users need to adapt their processing of speech to a strongly degraded signal. Although on average this adaptation appears successful [1], speech perception outcomes vary greatly between individuals. Perceptual adaptation to degraded speech can include re-weighting of phonetic cues, and stronger reliance on higher-level lexical processing. None of these adaptation strategies alone may be optimal for each CI users [2], and knowing individual's strategies may allow individualising rehabilitation to obtain greater benefit from the device. We investigate CI users' ability to use higher-level processes of integrating information from sentential context during lexical access. By means of the visual world paradigm we capture the course of lexical decision-making, and focus on individual differences between experienced CI users, and on how these differences relate to increased mental effort when processing speech.

In an eye-tracking experiment we measured the time-course of lexical decision making - reflected in gaze fixations -, and the mental effort involved - measured in pupil dilation. Participants' ocular responses to pictures on a screen were recorded while listening to sentences containing target words (baby), which were either preceded or followed by context disambiguating them (crawl). The displayed pictures contained the target (baby), a competitor that phonetically overlapped with the target (bay), a word that was viable given the context (worm given the context crawl), and an unrelated distractor. Sixteen experienced CI users were compared to age-matched normal hearing (NH) listeners.

The gaze fixations for NH show a fast uptake of context information, which leads to a decrease in mental effort involved in lexical decisions. The gaze fixations of the CI users showed a similar pattern on average. Individual data, however, showed that the ability to use contextual information to make early and certain lexical decisions varies between CI users. CI users' pupil dilation data complements the gaze fixations showing individual differences in release from mental effort during lexical decisions. Combining gaze-fixations with pupillometry has the potential to capture CI users' individual adaptation strategies and to individualise their hearing rehabilitation as to reduce the effort involved when processing speech.

[1] Farris-Trimble, A., et al., (2014). The process of spoken word recognition in the face of signal degradation. *J Exp Psychol Hum Percept Perform*, 40(1), 308.

[2] Moberly, A. C., et al., (2014). Do adults with cochlear implants rely on different acoustic cues for phoneme perception than adults with normal hearing? *J Speech Lang Hear Res*, 57(2), 566-582.

PS 860

Behavioral Model of Loudness Intolerance

Senthilvelan Manohar; Jaclyn Spoth; Kelly Radziwon; Benjamin D. Auerbach; Richard Salvi
 Center for Hearing & Deafness, Department of Communicative Disorders and Science, State University of New York at Buffalo

Intense noise exposure not only causes hearing loss, but can also induce hyperacusis, an inability to tolerate moderate-intensity sounds either because they are perceived as too loud, annoying or, in some cases, painful. Growing evidence suggests that loudness intolerance arises from hyperactivity within the central auditory pathway to compensate for reduced neural output from the cochlea. In addition, non-auditory areas may contribute to the emotional aspects of hyperacusis. Since escaping

from a loud sound is indicative of an aversive reaction, we developed an Active Loudness Avoidance paradigm (ALAP) test in which rats shifted their place preference from a dark, enclosed box to a bright, open space when intense sounds were presented in the dark box. To determine if noise-induced hearing loss would make moderately intense sounds more aversive, we used ALAP to measure the shift in dark-light place preference after inducing a high-frequency hearing loss in adult rats. The ALAP test is based on a rodent's innate aversion to a bright (Light Box) open space and preference for a dark (Dark Box), enclosed space. We first determined the baseline Light/Dark preference with ambient sound. In the second phase, we measured the Light/Dark preference when sounds of different intensity and frequency were presented in the dark box. Active avoidance was the difference between the percentages of time spent in the dark during baseline versus various sounds. To determine if high-frequency, noise-induced hearing loss would cause a change in light/dark preference, rats were exposed to 16-20 kHz noise at 102 dB for 21 days and then retested on the ALAP. (1) During baseline ALAP testing without sound, rats spent 80-90% of time in the Dark box. (2) When ALAP testing was conducted with sound stimulation in the dark box, the percentage of time spent in the dark box decreased as intensity increased. These results suggest that as sound intensity increased the sounds became more aversive. (3) After inducing a high-frequency noise-induced hearing loss, rats spent significantly less time in the dark box when low-frequency sounds were presented compared to pre-noise exposure measurements. Suggest that when rats develop high-frequency hearing loss, they become less tolerant to low-frequency sounds where hearing thresholds are normal i.e., they become loudness intolerant and find moderate-intensity sounds aversive. Supported by NIH/NIDCD (R01DC014452 & R01DC014693) and HHF (72364).

PS 928

Functional Consequences of a Hidden Hearing Loss

James B. Fallon; Andrew K. Wise
Bionics Institute

Background

Recent animal studies have demonstrated that moderate sound exposure can damage up to half the auditory nerves and their synapses, without damaging hair cells. As only a small number of the highly sensitive low-threshold auditory nerve fibres are required for sound detection in quiet environments, there is no loss in auditory sensitivity. Normal auditory sensitivity, despite the significant loss of auditory nerve fibres, has led to this type of damage being termed a 'hidden hearing

loss'. To date, the only reported functional consequence of the loss of auditory nerves and their synapses is an increase in median spontaneous firing rate of the auditory nerve fibre population, indicative of a preferential loss of low spontaneous rate fibres. However, modelling of the loss of functional auditory nerves and their synapses suggests a reduction in temporal fidelity. This project aimed to quantify temporal processing deficits using both behavioural and electrophysiological techniques in a guinea pig model of hidden hearing loss.

Methods

Guinea pigs were exposed to 105 dB SPL octave-band noise centred around 10kHz for 2 hours that produced a significant temporal threshold shift, but no permanent threshold shift. Behavioural psychophysics used a variant of the 'pre-pulse inhibition' of the startle reflex, where a 100ms period of 100 Hz amplitude modulation of the octave-band background noise centred around 10kHz was used as the pre-pulse stimulus. Temporal processing was quantified by determining the minimum modulation amplitude that could elicit a significant suppression of the startle response. Electrophysiology involved recording single- and multi-unit clusters from a multi-channel silicon recording array inserted into the central nucleus of the inferior colliculus in response to amplitude modulation of octave-band noise centred around 10kHz. Temporal processing was quantified by using vector strength analysis to determine modulation detection thresholds (minimum modulation depth to produce a significant vector strength, Rayleigh's test $p < 0.01$).

Results

Following noise exposure, there was an increase in the minimum modulation amplitude required to produce a significant suppression of the startle response from 13.5% (± 1.1) to 21.5% (± 3.3), which just failed to reach significance (paired t-Test; $p = 0.06$) Noise exposure resulted in modulation detection thresholds of neurons in the inferior colliculus of 46.8% (± 5.9) which was significantly higher than in normal hearing animals (25.5% ± 3.9 ; t-Test; $p < 0.01$).

Conclusion

Despite no change to auditory thresholds, moderate noise exposure results in temporal processing deficits.

Memory for Time Intervals across Sensory Modalities: Audition, Vision, and Touch.

HiJee Kang; Denis Lancelin; Daniel Pressnitzer
Laboratoire des Systèmes Perceptifs (CNRS UMR 8248), École normale supérieure, Paris, France

The present study probes perceptual learning of purely time-domain information. It uses a paradigm previously used to demonstrate fast learning in audition, based on the detection of repetitions within random noise (Agus et al., 2010; Andrillon et al., 2015) or random click trains (Kang et al., 2015). The click trains essentially conveyed a sequence of time intervals, so the technique can be extended to other modalities: time intervals can be conveyed by e.g. light flashes or touch pulses. Here, we asked whether the learning of temporal information was specific to audition, or if it could also be observed in vision and touch. Also, we tested for transfer of learning across modalities.

For the auditory stimulus, click trains were used, with Poisson-distributed random inter-click intervals (average rate of 7 Hz and refractory period of 60 ms). Listeners had to distinguish 2.4s-long random click trains from click trains containing two abutting repeats of the same, 1.2s-long sequence. Moreover, unbeknownst to the listeners, some sequences re-occurred identically over several trials. Perceptual learning was measured as an improvement in performance for those sequences re-occurring across trials. Stimuli were presented as click trains over headphones for the auditory task, as light flashes of a green LED light for the visual task, and as tangential motion pulses to the fingertips for the touch task. Parameters were chosen so that the shortest possible time intervals were detectable in all modalities with our apparatus. We observed perceptual learning for all three modalities, with a similarly fast time course. A second experiment tested for transfer. In one half of a test block, click trains were presented in the auditory modality. In the second half, the task was performed in a different modality, vision or touch. We observed that a sequence learnt in the auditory modality led to high performance from its very first presentation in the other modality, suggesting transfer from audition to vision or touch.

Performance was generally highest for the auditory case, followed by the tactile and visual cases. Transfer was more efficient from audition to touch than to vision. These observations may simply result from our choice of stimuli. They could also follow from links between audition and touch for temporal processing (Yau et al.,

2009). In any case, the results demonstrate qualitatively similar memory processes for temporal information in different sensory modalities, possibly subserved by common neural plasticity mechanisms (Gütig & Sompolinsky, 2006).

PS 862

Head and Eye Movement Behavior in Realistic Virtual Audiovisual Environments for Hearing Aid Research

Volker Hohmann¹; Maartje Hendrikse¹; Gerard Llorach²; Giso Grimm¹

¹*Universität Oldenburg, Medizinische Physik and Cluster of Excellence Hearing4all, Germany;* ²*Interactive Technologies Group, Universitat Pompeu Fabra, Barcelona, Spain*

The long-term goal of this project is to develop an interactive space-aware hearing aid, which is interacting with the spatial acoustic surrounding and the hearing aid user. Promising applications include head motion compensation to improve speech signal processing, e.g., improved direction of arrival estimation and improved speech enhancement, and to (interactively) determine the “hearing wish”, i.e., the sound source currently attended by the user, by jointly analyzing the gaze direction and head motion.

For the development of the space-aware hearing aid, realistic motion data is required. Therefore head and eye movement behavior was measured in a variety of virtual audiovisual environments in normal-hearing listeners. Realistic audiovisual environments using a 3D loudspeaker setup and animated visual cues (“avatars”) were created for this purpose. Preliminary results of two studies will be presented. The first study focused on the effect of different visual cues on user engagement, which was rated by looking at differences in head and eye movement behavior, speech intelligibility and localization performance and questionnaires. Real video was compared to an animated scene with avatars with and without lip syncing and gaze direction towards the active speaker. The second study also measured head and eye movement behavior in such realistic audiovisual environments. Different environments that are considered important in daily life were used. Head movement behavior was analyzed, and the effect of the head movement on the performance of hearing aid algorithms was evaluated. The evaluation was done by recreating the virtual acoustic environment with a virtual listener making the recorded head movements, and a virtual hearing aid system processing the signals recorded with virtual behind-the-ear microphones placed behind the ears of the virtual listener. Using this completely virtual system

makes it possible to process target and noise separately, so that the signal-to-noise ratio, speech intelligibility index and spatial cues of the hearing aid algorithm output can be calculated during the movement recorded in subjects.

PS 863

The Influence of Word Sequence Length and Source Segregation on Serial Recall of Masked Speech

Elin Roverud¹; Virginia Best²; Christine R. Mason²; Gerald Kidd²

¹Department of Speech, Language & Hearing Sciences, Boston University; ²Department of Speech, Language & Hearing Sciences and Hearing Research Center, Boston University, Boston, MA 02215 USA

Human listeners have a limited capacity for recalling serial items, but this capacity may depend on the processing demands of the listening condition [Rönnerberg et al. (2013), *Frontiers in Systems Neuroscience*, 7, 31]. Many studies examining speech intelligibility in the presence of interference require the participant to recall the words spoken by a target talker to measure performance. Generally the number of items to be recalled in these tasks is small and therefore the memory capacity limitations are not a major consideration. However, factors often explored in speech in noise studies such as spatial separation of target and maskers (relative to no spatial separation, i.e., collocated condition), type of interference (e.g., noise or speech maskers), and expectation (e.g., whether or not the target words follow a known syntax) are assumed to vary in the processing demands placed on the listener. As such, the recall capacity may also vary across levels of these factors (e.g., between collocated and spatially-separated masker conditions). Put differently, the measured effects of these factors may depend on the number of items the participant must recall. The focus of the present study was to examine the influence of sequence length on the effects of and interactions between these different factors. In this study, normal-hearing listeners were presented with sequences of words ranging from 1 to 10 items in quiet and in various types of masking. The target sequences were constructed using words drawn from six word categories (names, verbs, numbers, adjectives, nouns, conjunctions) arranged either in an expected sentence-like order or random order. The maskers were either two independent speech-shaped speech-modulated noises (SSSMN) or two competing talkers speaking words chosen from the same corpus as the target. The maskers were either collocated with the frontal target or spatially separated (at +/- 45 degrees azimuth). All three sources were presented at the same level and percent words

correct was measured. Participants responded by selecting the target words in order from a closed set of 8 exemplars in the same category. Preliminary results indicate that the improvement in performance for the main comparison conditions (spatially separated vs. collocated maskers, SSSMN vs. speech maskers, and expected vs. random target order) depended on the sequence length and interacted with other factors. [Supported by NIH/NIDCD]

PS 864

Perceptual Priors on Musical Rhythm Revealed by Iterated Reproduction

Nori Jacoby¹; Josh H. McDermott²

¹Columbia University; ²MIT

Probability distributions over external states (priors) are essential to the interpretation of sensory signals. Priors for cultural artifacts such as music and language remain largely uncharacterized, but critically constrain cultural transmission, because only those signals with high probability under the prior can be reliably reproduced and communicated. Extending previous research on concept learning and language (Bartlett 1932, Griffiths and Kalish 2005, Xu & Griffiths 2010), we developed a method to estimate priors for simple rhythms via iterated reproduction of random temporal sequences. Listeners were asked to reproduce random “seed” rhythms; their reproductions were fed back as the stimulus, and over time became dominated by internal biases, such that the prior could be estimated by applying the procedure multiple times. Our method can be applied irrespective of the participant’s musical or cultural background, and is hypothesis-neutral, allowing any possible pattern of results to be detected.

We measured listeners’ priors over the entire space of two- and three-interval rhythms, examining Westerners with different level of musical expertise as well as members of the Tsimané, a native Amazonian society with very limited exposure to Western music. We found that priors in Westerners showed peaks at rhythms with simple integer ratios, but only those that are prevalent in Western music. Priors were similar for musicians and nonmusicians, suggesting that they are shaped primarily by passive exposure to the music of a culture. Priors in a native Amazonian society also exhibited modes at integer ratios, but were otherwise qualitatively different from priors in Westerners, in ways that are consistent with the structures prevalent in their music. The results were similar for several different modes of reproduction (for example, finger tapping versus rhythmic vocalization of a repeated syllable), but did not extend to the reproduction of spoken phrases, indicating that integer ratio

priors are at least somewhat specific to music. Our results are consistent with biological constraints that favor integer ratios, but indicate that any such constraints are strongly modulated by experience. Our method holds promise for characterizing of priors for a range of other auditory domains including phonetics, speech rhythms, and musical melodies.

PS 865

Determining the Energetic and Informational Components of Speech-on-speech Masking in Listeners with Sensorineural Hearing Loss

Gerald Kidd¹; Christine R. Mason¹; Virginia Best¹; Elin Roverud²; Jayaganesh Swaminathan³; Todd Jennings⁴; H. Steven Colburn⁵

¹*Department of Speech, Language & Hearing Sciences and Hearing Research Center, Boston University, Boston, MA 02215 USA;*

²*Department of Speech, Language & Hearing Sciences, Boston University;*

³*Starkey Hearing Research Center, Berkeley, CA, USA;*

⁴*Department of Biomedical Engineering and Hearing Research Center, Boston University, Boston, MA 02215 USA;*

⁵*Department of Biomedical Engineering and Hearing Research Center, Boston University*

The ability to identify the words spoken by one talker masked by two or four competing talkers was tested in a group of young-adult listeners with moderate bilateral sensorineural hearing loss (SNHL). In the reference condition, the masking speech was colocated with the target speech (presented directly in front of the listener at 0° azimuth), the target and masker talkers were all female, and the masker speech was presented naturally (intelligible). In three comparison conditions, the maskers were manipulated in a manner intended to produce a release from masking. These masking release variables included replacing the female masker talkers with male masker talkers, time-reversal of the masker speech (rendering it unintelligible) and spatial separation of the masker talkers from the target talker (spaced symmetrically at $\pm 90^\circ$ for two maskers and $\pm 45^\circ$ and $\pm 90^\circ$ for four maskers). All three of these variables produced significant release from masking. To determine performance after controlling for energetic masking (EM) the stimuli were subjected to ideal time-frequency segregation analysis resulting in stimuli comprising only the time-frequency units in which the target energy exceeded that of the masker. The subjects were tested with these resynthesized “glimpsed stimuli” for all conditions. For either two or four maskers, the range of speech reception thresholds across the four conditions for the glimpsed stimuli was only about 2 dB suggesting that EM was roughly equal. Compared to a similar group of normal-hearing

(NH) listeners tested in an earlier study (Kidd et al. J. Acoust. Soc. Am., 140, 132-44, 2016), the listeners with hearing loss demonstrated both higher glimpsed thresholds and greater “additional masking” (difference between thresholds for the natural speech stimuli and the glimpsed speech stimuli - thought to reflect primarily informational masking, IM). Large individual differences in both groups were observed that were correlated across masking release conditions suggesting that listeners could be categorized according to their general ability to solve the task. The results of acoustic analysis, including estimation of the proportion of available glimpses/energy, and auditory nerve-based modeling (estimating the information available in the temporal fine structure and envelopes), of these conditions were compared with the trends found for human performance. Overall, both peripheral and central factors appear to contribute to the differences in performance between NH and SNHL groups. [Work supported by NIH/NIDCD]

PS 866

Binaural Unmasking and Executive Function in Older Adults

Sara M. Misurelli¹; Rachael Jocewicz²; Ruth Y. Litovsky¹

¹*Waisman Center, University of Wisconsin, 1500 Highland Avenue, Madison, Wisconsin 53705, USA;* ²*University of Wisconsin-Madison*

There is some evidence to suggest aging negatively impacts auditory processing, even for those with normal audiograms. However, little is known about auditory attention and source segregation abilities in this population. The main goal of this study was to investigate the ability to attend to target speech in noise in older, normal hearing (NH) adults. Specifically, we were interested in: (1) examining source segregation and auditory attention in younger vs. older adults with NH, and (2) the potential contribution of aging to the lack of unmasking demonstrated by older adults with bilateral cochlear implants (BiCIs). To explore these questions, we compared performance of older NH adults listening to unprocessed or vocoded stimuli on a speech-in-noise task with results from younger NH adults and older adults with BiCIs (Goupell, Kan, and Litovsky, 2016, J Acoust Soc Am, 140, 1652-1662).

The current study uses methods similar to those used in Goupell et al., 2016. Adults with NH (55+years) were tested. Participants were instructed to identify target speech, spoken by a female talker, in the presence of interfering speech spoken by a male talker. Stimuli, either unprocessed or vocoded, were presented via headphones at various target-to-masker ratios. Partici-

pants listened to the target in the right or left ear in four conditions: (1) no interferer; (2) contralateral interferer; (3) ipsilateral interferer; and (4) ipsilateral+contralateral interferer. Measures of executive function were also obtained.

Results thus far show that older and younger adults demonstrate similar trends in performance; however, older adults need the target to be played 4–9 dB louder, even when no interferer is present. When the stimuli are unprocessed, the older adults demonstrate comparable performance in the ipsilateral (3) and ipsilateral+contralateral (4) conditions, similar to the younger adults. This may be because NH listeners are able to use the voice-pitch cues between the female target and male interferer to perceptually segregate two sources even when played ipsilaterally. When the stimuli are vocoded, initial results indicate that some older adults do demonstrate unmasking, similar to the younger adult group. This suggests that other factors besides age, such as limitations of the CI devices, have a greater impact on the lack of unmasking demonstrated by adults with BiCIs. Additional findings will be discussed in regards to the relationship between executive function and auditory attention.

Funded by NIH-NIDCD (R01 DC003083 to RYL, P30HD03352 to Waisman Center).

PS 867

Musicians Have Enhanced Audiovisual Multisensory Binding: Experience-dependent Effects in the Double-flash Illusion

Gavin M. Bidelman

University of Memphis School of Communication Sciences & Disorders

Musical training is associated with behavioral and neurophysiological enhancements in auditory processing for both musical and non-musical sounds (e.g., speech). Yet, whether the benefits of musicianship extend beyond enhancements to auditory-specific skills and impact multisensory (e.g., audiovisual) processing has yet to be fully validated. Here, we investigated multisensory integration of auditory and visual information in musicians and nonmusicians using a double-flash illusion, whereby the presentation of multiple auditory stimuli (beeps) concurrent with a single visual object (flash) induces an illusory perception of multiple flashes. We parametrically varied the onset asynchrony between auditory and visual events (parametrically varied between leads and lags of ± 300 ms) to quantify participants' "temporal window" of integration, i.e., stimuli in which auditory and visual cues were fused into a single percept. Results show that musically trained individuals were both faster and more accurate at processing concurrent audiovisual

cues than their nonmusician peers; nonmusicians had a higher susceptibility for responding to audiovisual illusions and perceived double flashes over an extended range of onset asynchronies compared to trained musicians. Moreover, temporal window estimates indicated that musicians' temporal integration windows (< 100 ms) were ~ 2 - 3 x shorter than nonmusicians' (~ 200 ms), suggesting more refined multisensory integration and audiovisual binding. Collectively, findings indicate a more refined binding of auditory and visual cues in musically trained individuals. We conclude that experience-dependent plasticity of intensive musical experience extends beyond simple listening skills, improving multimodal processing and integration of multiple sensory systems in a domain-general manner.

PS 868

Sensitivity to Physical Regularities in Auditory Event Sequences

Maddie Cusimano¹; Josh H. McDermott²

¹*MIT Brain and Cognitive Sciences*; ²*MIT*

Sensitivity to physical regularities in auditory event sequences

Maddie Cusimano, Josh H. McDermott

Department of Brain and Cognitive Sciences, MIT

Background

Perception relies on regularities in sensory data that are caused by physical laws. In audition, the physical laws governing object interactions constrain the structure of real-world sounds, and an internal model of these constraints and their interactions could underlie auditory inferences about the world. To investigate whether these constraints are modeled by the auditory system, we tested whether people are sensitive to the consistency of physical cues in sequences of impacts produced by a bouncing ball.

Methods

We recorded audio produced by balls of various materials being dropped. We measured the timing and amplitude of the sound produced by each bounce impact, and extracted the individual impact sound tokens. The amplitude and inter-impact time intervals decreased from bounce to bounce due to energy dissipation, but the rate of decrease varied depending on the material, as did the timbre of the impact sounds. We then synthesized sequences of impact sounds in which the tokens and the timing/amplitude pattern were matched (derived from the same ball) or mismatched (derived from different balls). Thus, the acoustic information from the tokens could be consistent or inconsistent with the motion information from the timing/amplitude pattern. We com

pared participants' ability to distinguish real recordings from the matched and mismatched synthetic signals.

Results

When the token and temporal pattern were mismatched, participants were better at distinguishing the synthetic sequences from real recordings. Furthermore, participants classified mismatched synthetics as having mismatched information more often than the matched synthetics or real recordings.

Conclusion

Human listeners can identify when there is a mismatch between the material that is implied by individual impact sounds and the pattern formed by a sequence of impacts. This result is consistent with the idea that physical constraints on sound are modeled by the auditory system.

PS 869

Subjective Time Estimations of Music, Noise, and Pure Tone Sequences

Juan Huang¹; Yue Ding²; Yang Zhang²; Xiaoqin Wang³

¹*Department of Biomedical Engineering, Mind and Brain Institute, The Johns Hopkins University, Baltimore, MD, USA;* ²*Department of Biomedical Engineering and Tsinghua-Johns Hopkins Joint Center for Biomedical Engineering Research, Tsinghua University, P.R. China;* ³*Department of Biomedical Engineering, The Johns Hopkins University, Baltimore, MD, USA*

Temporal information is one of the most important characteristics of auditory stimuli. Auditory perception is not possible without temporal processing. However, to what degree that the spectrum information of an auditory stimulus influences the temporal processing of the same stimulus remains unclear. In this study, we examined the time estimation of musical note sequences, pure tone sequences, and noise burst sequences using an immediate recall paradigm. Results show that the time estimation was significantly determined by the duration of auditory materials. The error of time estimation varied as a function of the duration of auditory material, from being positive (over estimate) to negative (over estimate) with the stimulus duration increases. Significant difference was observed between the time estimations of musical note and pure tone sequences. Meanwhile, the time estimations of pure tone and noise burst sequences were significantly correlated. However, such a correlation was not observed between the estimations of musical note sequences and that of pure tone or noise burst sequences. Our findings indicate that the content of spectrum information influences the time estimation of the duration of an auditory sequences. Furthermore,

the dependency of the time estimation error on the duration of auditory stimuli suggests the co-existence of expansion and compression mechanisms in auditory temporal processing.

PS 870

A Multi-second Adaptive Integration Process Underlies Sound Texture Perception

Richard McWalter¹; Josh H. McDermott²

¹*Technical University of Denmark;* ²*MIT*

Background

Sound textures – as produced by rain, fire or insect swarms – are a category of sound defined by their temporal homogeneity. The perception of such textures is thought to be mediated by time-averaged statistics of early auditory representations, but little is known about the averaging process that might compute such statistics. We probed the averaging process involved in sound texture perception using synthetic signals whose statistics changed at some point in time, the idea being that judgments should be biased by the stimulus history included in the averaging process. We investigated the conditions in which such biases occurred, and examined whether they depended on the stationarity of the texture, as might be expected from an integration process that could adapt its averaging to the signal characteristics.

Methods

We extended the McDermott and Simoncelli texture synthesis algorithm (2011) to create texture steps – synthetic textures whose statistical properties underwent a change at some point in time. Listeners were presented with two sounds, a texture step and a probe texture (with constant statistics). Listeners were asked to compare the endpoint of the texture step to the probe and to select the sound that was most similar to a familiar reference texture. We compared performance for texture steps that underwent a change at either 1 or 2.5 seconds from the end of the stimulus. We divided the textures that were used according to the variability of their texture statistics over 1-second analysis windows. We separately analyzed more and less homogenous textures to evaluate whether any averaging window might be adaptive to the texture statistics (integrating over longer periods of time for signals that are more variable).

Results

Listeners were biased by the presence of a step in the texture statistics, suggestive of an averaging process. Biasing effects were larger when the step occurred 1 second prior to the stimulus endpoint than when it occurred 2.5 seconds from the endpoint, but the bias from the step at 2.5 seconds was substantially larger for

less-homogenous textures, suggesting that their statistics were averaged over a longer window.

Conclusion

The results suggest a texture integration process operating over several seconds, but whose integration window is adapted to the homogeneity of the sound texture, averaging over longer periods of time for signals that are more variable.

PS 871

Auditory Perception of Material and Force from Impact Sounds

James Traer¹; Josh H. McDermott²

¹Massachusetts Institute of Technology; ²MIT

Background

Humans can identify physical attributes of objects from audio recordings of bouncing, scraping and rolling. Because the sound produced by such events depends on multiple independent factors (mass, size, material, motion, room reverberation etc.), the inference of any single such parameter is ill-posed. To determine which of two dropped balls is heavier, or bigger, or harder, listeners likely use knowledge of how different physical factors affect sound. We investigated the physical mechanisms of sound generation from colliding rigid objects and measured how physical properties affected the sound waveform. We then synthesized sounds from simple physical models to investigate the acoustical structure underlying human listening abilities.

Methods

We measured the vibrational impulse responses (IRs) of a large set of everyday objects to assess the distribution of object acoustics that humans encounter in daily life. We examined effects of material on the IR. We also derived theoretical estimates of the forces that act between objects when they collide, and simulated the effects of different impact velocities and material on the forcing function (the variation in force between two objects over time). We then generated collision sounds by convolving IRs with synthesized forcing functions, and tested how properties of the IRs and forcing function affected perception of material and impact velocity.

Results

We found object IRs to decay exponentially with frequency-dependent decay rates and sharply peaked spectra. Both decay rates and spectra varied with material, size and shape, and listeners could associate IRs with material. Large perceptual effects also resulted from varying the forcing functions – small hard objects recoil quickly and large soft objects spend more time in contact, and we found this variation in impact time to have a large

effect on the perceived size and hardness of the object, even if the object IR remained unchanged.

Conclusion

Simple parameterizations of physical impacts can replicate the perceptual experience of material properties. The time course of collisions is particularly important for the perception of object weight and hardness, but the object IR also matters – altering the object IR decay rates alters the perception of material and size. The results are consistent with the idea that humans use these acoustic cues to infer the causes of sounds.

Funding

NRSA post-doctoral fellowship awarded to JAT; McDonnell Scholar Award to JHM.

PS 872

Effect of Reverberation and Its Presentation Context on Material Perception Based on Impact Sounds.

Takuya Koumura¹; Shigeto Furukawa²

¹NTT Communication Science Laboratories; ²NTT Communication Science Labs

Sound emitted from a source is usually modulated by reverberation caused by the environment surrounding us before it reaches our ears. Reverberation alters the short-term spectrum and the temporal decay of sound, which are important cues for identifying materials based on impact sounds (Aramaki et al. 2011). The present study examined the extent to which reverberations affect material perception and the contribution of presentation context to the reverberation effect.

Participants were presented with various impact sounds and were asked to categorize them into one of three material classes, namely wood, metal, or glass. The stimuli included synthesized impact sounds of wood, metal and glass and sounds generated by morphing between pairs of these materials (Aramaki et al. 2011). These samples were presented as “dry” or convolved with impulse responses recorded in reverberant rooms. We tested three types of reverberation represented by impulse responses recorded in three different rooms. The existence or the type of reverberation was fixed (block condition) or randomized (random condition). In either condition, the order of the stimuli (the original and morphed samples) was randomized within a block.

The presence of reverberation generally altered the reported material categories, although the pattern of the effect varied depending on the listeners, original materials, and impulse responses. The magnitude of the reverberation effect was evaluated by the proportion of

sounds categorized into different materials due to reverberation. The effect of reverberation was generally smaller with block presentation than with random presentation (Figure 1). This suggests that the effect of the reverberation was reduced during repeated exposure to sounds with the same reverberation.

Our result is consistent with the finding of a previous study on speech recognition in reverberation (Watkins 2005). The study showed that category boundaries between speech sounds are affected by reverberation, but that the effect is reduced when the target word and the embedding sentence have the same reverberation. The present study suggests the existence of a context-dependent compensation mechanism for reverberation that functions when perceiving general sound objects as well as speech. This work was supported by JSPS KAKENHI Grant Number JP15H05915 (Grant-in-Aid for Scientific Research on Innovative Areas “Innovative SHITSUKSAN Science and Technology”).

References:

Aramaki, M. et al., 2011. *IEEE Transactions on Audio, Speech and Language Processing*, 19(2), pp.301-314.
Watkins, A.J., 2005. *The Journal of the Acoustical Society of America*, 118(1).

PS 873

Eye-metrics a Measure of Auditory Distraction?

Makoto Yoneya¹; Sijia Zhao²; Maria Chait²; Shigeto Furukawa¹; Makio Kashino¹

¹*NTT Communication Science Labs*; ²*Ear Institute, University College London, UK*

In this series of behavioral and eye tracking experiments we seek to understand whether information from eye-metrics (i.e., pupillometry and micro-saccades) can be used to measure and quantify distraction in the context of an auditory task.

We used a behavioral paradigm developed in our earlier work (Petsas et al, 2016). Stimuli were artificial acoustic ‘scenes’ composed of several concurrent tone-pip streams (‘sources’). A gap (2000ms) was inserted partway through the ‘scene’. Changes in the form of an appearance of a new source or disappearance of an existing source, occurred after the gap in 50% of the trials. Listeners were instructed to monitor the unfolding ‘soundscapes’ for these events and respond as quickly as possible when a scene change had been detected. Half of the trials contained a distractor (one of eight 600 ms long environmental sounds) inserted in the gap. Listeners were instructed to ignore the distractor sounds and focus on the change detection task. Simultane-

ously, we measured eye activity during the gap (shortly before, and after the presentation of the distractor).

Trials containing a distractor were associated with increased pupil amplitude as well as a lower micro-saccade rate during the gap (after the presentation of the distractor sound). Interestingly, microsaccade rate distinguished successful (correct response) from unsuccessful (incorrect response) distractor trials: The mean micro-saccade rate during the silent gap was higher in trials where participants eventually responded correctly. These preliminary results suggest that eye-metrics may be used to infer the presence of distracting sounds and could provide a measure for quantifying the perceptual disruption caused by a distractor.

References:

Petsas T, Harrison J, Kashino M, Furukawa S, Chait M (2016) The effect of distraction on change detection in crowded acoustic scenes. *Hearing Research*

Authors MC, MK, and SF contributed equally to this work.

PS 874

The Effect of Distraction by Brief Transients on Auditory Change Detection

Mathilde de Kerangal; Maria Chait
Ear Institute, University College London, UK

Change detection is a core capacity of hearing. The auditory system is widely assumed to serve as an ‘early warning system’ which continuously scans the unfolding acoustic scene for behaviourally-relevant events (e.g. those that could indicate the approach of predators or prey). In this series of behavioural experiments we investigate how listeners’ ability to detect abrupt changes in crowded acoustic scenes, manifested by the disappearance of an existing source or appearance of a new source, is affected by brief distractors occurring in close proximity to the scene change.

Stimuli are artificial acoustic ‘scenes’ composed of 10, 2 ERB spaced, concurrent streams (‘sources’), each consisting of a sequence of tones characterized by a unique frequency and rate. Listeners are instructed to monitor the unfolding ‘soundscapes’ for appearance or disappearance of a source. Distractors (henceforth referred to as ‘splashes’; nomenclature from the visual change blindness literature) are 50 ms chords of four, concurrently presented, pure tones amplitude modulated at 100 Hz (depth of 0.5). The AM was useful for making the ‘splash’ stand out from the rest of the scene. Splash frequencies varied from trial to trial and were spaced at least 2 ERBs away from any scene source. Splashes

occurred unpredictably in 50% of the trials and were placed at 0, 100, 200, 300, 500 ms after or before the change.

For both appearance and disappearance changes, results demonstrate that splashed occurring between -200 - +200 ms from the change resulted in substantially reduced change detection performance (as measured by d' and reaction time). Namely, despite the fact that the interruption was brief and did not mask any scene sources, the presence of the splash resulted, in a proportion of the trials, in 'change deafness'. These results suggest a role for sensitivity to transients in the process of auditory change detection, similar to what has been demonstrated for visual change detection. To further understand the temporal dynamics of the 'splash' effect, MEG brain imaging data with these stimuli will also be presented.

PS 875

Alpha Oscillatory Activities During Auditory Spatial Attention: Topography Specificity and Inter-/intra-individual Differences in Peak Frequency

Yuqi Deng¹; Inyong Choi²; Barbara Shinn-Cunningham¹

¹*Boston University*; ²*Department of Communication Sciences and Disorders, University of Iowa*

Hemispheric lateralization of alpha oscillation (8-14Hz) can be induced by spatial attention in multiple modalities, including in audition. In visuospatial and somatosensory spatial attention, alpha oscillations are topographically specific with respect to the attended location. However, the specificity of alpha topography with respect to the attention focus of auditory spatial attention has not been reported. Moreover, most studies on alpha oscillation used the average of a fixed spectral band (typically 8-14Hz) uniformly across cortical areas; there may be variability of alpha peak frequencies across cortical regions, supporting the idea that there are multiple independent cortical generators of alpha. We recorded electroencephalography in human subjects while they were performing a variation of the Posner paradigm, in which they were cued to attend to certain spatial locations. We examined the lateralization of alpha power and found specific alpha topography with respect to attention focus during an attentional preparation period (after listeners knew where to focus attention, but prior to the sound stimulus beginning). We also studied alpha activity in multiple cortical areas. We found intra-individual differences in peak alpha frequency between parietal and central cortex. In addition, we measured behavioral performance and related behavioral results to alpha activity and auditory object formation using spatial cues. These

findings further our understanding of the role of alpha oscillation when listeners deploy auditory spatial attention.

PS 876

Can Perceptual Oscillations Be Influenced by Attention?

Sierra Broussard; Gregory Hickok; Kourosh Saberi
University of California, Irvine

Slow-rate temporal modulations (~3-8 Hz) are prevalent in speech, music, and environmental sounds. Recent findings have suggested that there may be a neural basis for rhythm detection ability. Additionally, rhythmic information has been shown to modulate auditory excitability. This excitability modulation could either indicate a potential parsing mechanism for auditory stimuli, or be a top-down driven attention mechanism. Our study attempted to determine whether this oscillation is a perceptual parsing mechanism or an attentional mechanism.

We used amplitude modulated noise to induce a perceptual oscillation. Our stimulus consisted of modulated noise followed by one second of unmodulated noise. On half of the trials, there was a 1 kHz tone within the unmodulated noise, placed at one of nine time points. Listeners were given a dual attention task. In the attend fine structure (AFS) condition, they were first asked to determine whether the carrier noise was relatively high or low pitched, and in the attend envelope (AE) condition, they were asked to judge whether the modulation rate was relatively fast or slow. In both conditions, listeners were then instructed to indicate whether or not they heard a tone.

When participants were not specifically directed to attend to either the fine structure or envelope, their behavior modulation matched the induced oscillation in frequency but was delayed in phase. Listeners were poorer at detecting tones where there would have been a peak in the modulation and detection improved where there would have been a dip. Preliminary results of the directed attention tasks suggest that listening strategy can also how alter how the induced modulation affects the tone detection.

These results support recent findings that auditory perception can be influenced by inducing rhythmic contexts and suggest that attention may play a role in this phenomenon.

PPI Audiometry Can Assess Both Threshold and Suprathreshold Features of Hearing Performance

Ryan Longenecker; Alexander Galazyuk
 Northeast Ohio Medical University (NEOMED)

Background

Most behavioral methods which assess animal hearing are time consuming. One of the most common tools of hearing assessment performance is ABR threshold or amplitude. Alternatively prepulse inhibition of the startle reflex can also be effectively used to measure hearing thresholds in rats (Fechter et al. 1988) and more recently in mice (Longenecker et al. 2016). The goal of this study was to compare these methods of hearing assessment in mice.

Methods

CBA/CaJ mice were tested with PPI audiometry before and after sound exposure [narrowband noise centered at 12.5 kHz presented at 116 dB SPL unilaterally for 1 hour under general anesthesia (Ketamine/Xylazine)]. The startle stimulus consisted of a 20 ms white noise presented at 100 dB SPL, with a 1 ms rise/fall time, while prepulse stimuli were 20 ms pure tones (4 to 31.5 kHz) presented at 10 to 80 dB SPL 100 ms before the startle stimulus. The magnitude of the startle responses at different sound levels of the prepulse were measured and an inhibition function for each frequency of the prepulse was constructed. Statistical analysis of this function was used to determine the threshold: the minimal level of the prepulse at which the startle response was significantly different than the startle without a prepulse. The amount of inhibition obtained at each stimulus level was used to determine suprathreshold inhibition deficits. ABRs thresholds and wave I amplitudes were directly compared to corresponding PPI values in the same animal.

Results

When compared to ABR thresholds, PPI thresholds demonstrated a characteristic notch deficit three months after sound exposure. Interestingly, PPI suprathreshold deficits were detected at the same frequencies as ABR wave one deficits, however to a greater degree. This pattern was especially true for the frequencies which had the greatest threshold changes after sound exposure.

Conclusions

PPI audiometry could be a useful tool for fast and reliable assessment both threshold and suprathreshold hearing for laboratory animals. Data suggests that PPI audiometry can assess peripheral and central components of hearing loss, but

more testing needs to be conducted to confirm this. This research was supported by grant R01 DC011330, R01 DC013314, and 1F31DC013498-01A1 from the National Institute on Deafness and Other Communication Disorders of the U.S. Public Health Service.

PS 878

How the Eyes Detect Acoustic Transitions: A Study of Pupillary Responses to Transitions Between Regular and Random Frequency Patterns

Hsin-I Liao¹; Sijia Zhao²; Maria Chait²; Makio Kashino³; Shigeto Furukawa³

¹NTT Communication Science Laboratories; ²Ear Institute, University College London, UK; ³NTT Communication Science Labs

The auditory system is sensitive to stimulus patterning and rapidly detects transitions in the fluctuation statistics of unfolding sound sequences. In an MEG study on naïve, distracted, listeners, Barascud et al (2016) demonstrated cortical responses to transitions from regular-to-random as well as random-to-regular frequency patterns. In the present study we use eye tracking to measure pupillary responses to similar transitions. Emerging work suggests these to be sensitive to surprising (oddball) and salient auditory events (Liao et al, 2016a,b).

Participants listened to sequences of abutting 50 ms tone pips (adapted from Barascud et al, 2016) which contained transitions from random to regularly repeating frequency patterns and vice versa. To ensure that participants paid attention to the auditory stream but not to the transition per se, they were instructed to detect occasional silent gaps (presented in 16.7% of trials) within the sequence. This task encouraged attentive listening but was independent of sequence regularity. Trials which contained gaps or when a response was made were discarded from the analysis.

We demonstrate that despite the fact that both transition directions (regular-to-random and random-to-regular) are clearly detectable behaviorally and both evoke strong MEG (Barascud et al, 2016) and EEG (Southwell et al, 2016) responses, only the regular-to-random transition evokes a measurable pupillary dilation response (PDR). To the extent that PDR can be interpreted as reflecting surprise or attentional capture by a salient event, this result is consistent with previous behavioural work (Southwell et al, 2016) demonstrating that the emergence of a regular pattern does not exogenously capture attention, despite evoking sizeable changes in EEG/MEG activity.

References:

- Barascud, N., Pearce, M. T., Griffiths, T. D., Friston, K. J., & Chait, M. (2016). Brain responses in human reveal ideal observer-like sensitivity to complex acoustic patterns. *PNAS*, 113(5), E616-E625.
- Liao, H.-I., Yoneya, M., Kidani, S., Kashino, M., & Furukawa, S. (2016a). Human pupillary dilation response to deviant auditory stimuli: Effects of stimulus properties and voluntary attention. *Frontiers in Neuroscience*, 10:43.
- Liao, H.-I., Kidani, S., Yoneya, M., Kashino, M., & Furukawa, S. (2016b). Correspondences among pupillary dilation response, subjective salience of sounds, and loudness. *Psychonomic Bulletin & Review*, 23(2), 412-425.
- Southwell, R., Baumann, A., Gal, C., Barascud, N., Friston, K., & Chait, M. (2016). Is predictability salient? A study of attentional capture by auditory patterns. *Philosophical Transactions of the Royal Society B: Biological Sciences*

PS 879

Event-related Potential Correlates of Confidence in an Auditory Probe-signal Task

Alexandria Zakrzewski¹; Matthew G. Wisniewski²; Nandini Iyer²; Brian Simpson²

¹University of Richmond; ²U.S. Air Force Research Laboratory

Background

Recent cognitive science research has focused on measuring neural correlates of metacognitive judgments during decision and post-decision processes. The tasks used in these studies are often memory retrieval or visual categorization tasks. However, many other paradigms (e.g., sound detection) likely require monitoring of earlier perceptual processing.

Methods

Here, participants (n = 14) were tasked with detecting 80-ms pure tones presented in noise at a signal-to-noise ratio 3 dB above their predetermined ~70.7% correct detection threshold. A two-interval, two-alternative forced-choice probe-signal method was used (Sharf, 1998). One tone frequency (the 'primary') was presented on ~80% of all trials, while another frequency (the 'probe') was presented on ~20% of trials. Frequencies of tones were 1000 Hz and 2500 Hz. Assignments of these frequencies to either the 'primary' or 'probe' were counterbalanced across participants. Participants rated their confidence after each trial on a 6-point Likert scale.

Results

Detection accuracy, confidence ratings, and auditory N1 amplitudes in the event-related potential (ERP) were greater on 'primary' compared to 'probe' trials. Tone-locked auditory N1 and P3b amplitudes were larger for trials rated with high-confidence than low-confidence. These effects remained even when controlling for detection accuracy and tone probability. Additionally, differences between 'primary' and 'probe' confidence varied significantly with differences between 'primary' and 'probe' N1 as well as P3b amplitudes. Although an analysis of response-locked ERPs revealed larger error positivity (Pe) for 'probe' trial than 'primary' trial responses, there was no clear relationship between these post-decisional ERPs and confidence judgments.

Conclusions

We suggest that metacognitive judgments can track both sensory- and decision-related processes, at least in auditory detection. Given a large body of work showing parallels between processing at several stages and metacognitive judgments, we propose that the particular processes on which confidence judgments are based depends upon the task. Tasks in which an individual is required to use information at sensory stages of processing will reveal parallels between metacognitive judgments and the quality of information at these stages.

Regeneration II

PS 880

Inflammation Linked Mechanisms of HSP60-mediated Tissue Repair

Jason Sinclair¹; Wuhong Pei¹; Shawn Burgess²

¹National Human Genome Research Institute/NIH;

²National Human Genome Research Institute, NIH, Bethesda, MD

~15%, or 26 million Americans between the ages of 20 and 69 may have the symptoms of noise-induced hearing loss (NIHL), significantly reducing their ability to hear[1]. The main cause of NIHL is damage or death to the hair cells, the sensory receptors of the auditory system. In mammals, hair cells do not regenerate after injury, thus NIHL is generally permanent. However, evidence suggests that hair cells are not unconditionally incapable of regeneration. Therefore, it is possible that hair cell regeneration can be induced in mammals if we better understood the mechanisms involved. To define the regulatory pathways that govern hearing regeneration, we exploit the model organism zebrafish (*Danio rerio*). Remarkably, the hair cells of the zebrafish mechanosensory organs, the inner ear and the lateral line, can fully regenerate following cell death. Understanding

how these sensory receptor cells regenerate in zebrafish may lead to novel therapies for hearing impairment or other injury-related pathologies in humans.

Although it is known that the immune system plays an important role in regeneration, the molecular cues that guide the immune system to initiate inflammation and subsequently transition to a pro-regeneration state have not been well characterized. Through large-scale forward genetic screening, we have uncovered an unanticipated role for Heat shock 60kD Protein 1 (HSP60, *hspd1*) in the recruitment and activation of immune cells to stimulate tissue regeneration. In the absence of HSP60, immune cell infiltration is attenuated and hair cell regeneration is completely blocked. Additionally, injection of exogenous HSP60 results in increased immune cell infiltration and enhanced regeneration. Moreover, topical application of exogenous bacterial HSP60 (GroEL) dramatically improved skin wound healing in a diabetic mouse model, suggesting that HSP60 is required for tissue repair across all cell types in all vertebrates. Data from our laboratory indicates that HSP60 influences tissue regeneration by stimulating the expression of specific receptors and growth factors associated with M2 macrophages, which are involved in inflammation resolution and tissue repair

Currently, we are using zebrafish genetics to understand how HSP60 and the immune system stimulate hair cell regeneration. Through Clustered Regularly Interspaced Short Palindromic Repeats (CRISPR)/Cas9 mediated genetic screening, macrophage ablation, and tissue-specific mutations we aim to determine how HSP60 recruits macrophages to the point of injury and influences macrophage phenotype and gene expression.

PS 881

Building New Blood Vessels in the Inner Ear from NG2-Derived Cell Migration-Trans-Endothelial Formation

Xiaorui Shi

Oregon Health & Science University

Normal cochlear blood flow (CBF) is critical for generating the endocochlear potential (EP) on which transduction in hair cells depends. Disruption of CBF is seen in a wide variety of hearing disorders including loud sound-induced hearing loss (endothelial injury), ageing-related hearing loss (lost vascular density), and genetic hearing loss (e.g., Norrie disease: strial avascularization). Progression in CBF pathology can parallel progression in hair cell and hearing loss. To sustain hearing acuity, a healthy CBF must be maintained including a normal function of blood-labyrinth-barrier (BLB) must be maintained in the ear. This is particularly true since gener-

ation of the endocochlear potential (EP), the essential driving force for hair cell transduction, is so metabolically demanding. We seek to learn whether damaged strial vessel function can be restored via angiogenesis. Angiogenesis in the ear has not been studied, nor has the role of angiogenesis in hearing been investigated. In this study, using an in vivo pericyte depletion animal model in association with a newly established ex vivo strial tissue based-model, we demonstrate for the first time that damaged vascular function (blood labyrinth barrier) can be regenerated by activating the vascular endothelial growth factor signal pathway. Using transgenic neural/glial antigen 2 (NG2) fluorescent reporter mice, we have shown the progenitors of "de novo" strial vessels are pre-existing ECs and converted perivascular NG2-derived cells. Most important, the pattern of the newly formed vessels resembles the natural 'mesh pattern' of in situ strial vessels, with both lumen and expression of tight junctions. Taken together, our data shows that damaged strial microvessels can be regenerated by reprogramming angiogenic cells. The restoration of functional vasculature may be crucial for restoration of vascular dysfunction related hearing loss.

ACKNOWLEDGMENTS: This work was supported by National Institute of Health grants NIH NIDCD R01-DC010844 (XS), and NIHP30-DC005983 (P.B.G)

PS 882

Strial Vascular Regeneration by Reprogramming of NG2-derived Angiogenic Cells

Xiaohan Wang; Xiaorui Shi

Oregon Health & Science University

Can damaged or degenerated vessels be regenerated in the ear? The question is important as disruption of cochlear blood flow is seen in a wide variety of hearing disorders including loud sound-induced hearing loss (endothelial injury), ageing-related hearing loss (lost vascular density), and genetic hearing loss (i.e., Norrie disease: strial avascularization). Progression in CBF pathology can parallel progression in hair cell and hearing loss. However, new vessel growth in the ear has not been studied, nor has the role of angiogenesis in hearing. In this study, using a vascular damage model created by depleting pericytes (PC) in the cochlea which is in conjunction with an established ex vivo tissue explant model, we demonstrate for the first time that damaged vascular function (blood labyrinth barrier) can be restored by activating the vascular endothelial growth factor signal. Moreover, using transgenic neural/glial antigen 2 (NG2) fluorescent reporter mice, we have shown the progenitors of "de novo" strial vessels are pre-existing ECs and converted perivascular NG2-derived cells. Most important, the pattern of the newly formed vessels resembles

the natural 'mesh pattern' of in situ strial vessels, with both lumen and expression of tight junctions. Taken together, our data shows that damaged strial microvessels can be regenerated by reprogramming of NG2-derived angiogenic cells. The restoration of functional vasculature may be crucial for restoration of vascular dysfunction related hearing loss.

ACKNOWLEDGMENTS: This work was supported by National Institute of Health grants NIH NIDCD R01-DC010844 (XS), and NIHP30-DC005983 (P.B.G)

PS 883

Generation of Otic Progenitors from iPSCs Derived from Deaf Patients with P2RX2 c.178G>T (p.V60L) Mutation

Yunpeng Dong¹; Tao Peng¹; Bing Zou²; Rahul Mittal³; M'hamed Grati³; Dinghua Xie¹; Xue Liu⁴

¹*Department of Otolaryngology and Head & Neck surgery, Second Xiangya Hospital, Central South University, Changsha, Hunan, 410011, China.*; ²*University of Miami Miller School of Medicine, Department of Otolaryngology*; ³*Department of Otolaryngology, University of Miami Miller School of Medicine, Miami, FL 33136, USA*; ⁴*Department of Otolaryngology, University of Miami Miller School of Medicine, Miami, FL*; Dr. John T. Macdonald *Foundation Department of Human Genetics, and John P. Hussman Institute for Human Genomics, University of Miami, Miami FL*

Background

Hearing loss (HL) affects ~10% of the global population, and ~50% of HL cases have a genetic etiology. Although cochlear implants are so far the most effective approach for treating severe to profound sensorineural HL, long-term strategies such as gene therapy and cell therapy are essential for its comprehensive treatment. Restoring the normal function and providing a rich source of hereditary HL patients-derived induced pluripotent stem cells (iPSCs) that were induced from their somatic cells and genome-edited using CRISPR/Cas9 tools holds great clinical potential for treating genetic diseases. Previously, we have demonstrated that c.178G>T mutation in P2RX2 (p.V60L) causes autosomal-dominant progressive HL DFNA41 in two Chinese families. The aim of the present study is to generate otic progenitor cells from the iPSCs derived from the urine samples of affected individuals and transplant GFP-labeled iPSCs into mouse cochlea to test the cell survival and tumorigenicity.

Methods

Primary epithelial cells were isolated from the urine samples of two carrier patients of DFNA41 Chinese family and were induced to iPSCs (P-iPSCs) via lenti-

ral transduction of four Yamanaka factors. iPSCs were characterized by immunostaining and by teratoma test, and further differentiated into hair cell-like cells (HCLCs). GFP reporting iPSCs were transplanted into mouse ears by direct delivery into the modiolus.

Results

P-iPSCs induced from urinary samples showed expression of OCT4, SOX2, SSEA4, TRA-1-60, confirming their stem cell type. HCLCs induced from P-iPSCs showed no significant differences in the process of differentiation into HCLCs compared with normally-hearing individual-derived iPSCs, demonstrating that P2RX2 is likely not involved in hair cells development. We observed that iPSCs could survive in the cochlea for up to four weeks. We also did not observe any tumorigenesis during the 6 months after cochlea injection.

Conclusions and perspectives

Our study demonstrates that urinary cells could be reprogrammed to iPSCs capable of surviving in the cochlea for weeks with absent tumorigenicity and can be differentiated into otic progenitor cells. This study will provide novel avenues to design cell-based therapies for the treatment of genetic HL.

PS 884

Predifferentiation of Human Embryonic Stem Cells into Placodal Progenitors Enhances the Efficiency of Neurog1-Induced Neuronal Differentiation

Keith Duncan; Sandra Hackelberg; Benjamin Loomis; Liqian Liu
Kresge Hearing Research Institute, University of Michigan

Neurogenin-1 (Neurog1) is a proneural transcription factor that is important in several central and peripheral neuronal lineages with subtypes that include glutamatergic and GABAergic fates. Overexpression of Neurog1 and other members of the Neurogenin gene family induces neuronal differentiation in embryonic stem cells (ESCs), but the derived phenotypes include features of both central and peripheral nervous system neurons (Velkey and O'Shea, *Dev Dyn*, 2013, 242:230-253). Here, we sought to examine the impact of Neurog1 overexpression in human placodal progenitors in an effort to bias subtype specification toward cranial sensory neurons. Adenoviral vectors encoding a GFP-reporter alone (Ad.GFP) or GFP and human Neurog1 (Ad.Neurog1) were used to transduce human ESCs and placodal progenitors. Predifferentiation toward a placodal fate was achieved by modulation of BMP signaling, a major factor in ectoderm specification. As such, a high to low gradient in BMP ex-

pression during development is responsible for regional specification of epidermis (high BMP) to placodes and neural crest (moderate-to-low BMP) to neural plate (very low BMP). Quantitative PCR results indicated that manipulation of BMP levels in our culture paradigm mimicked developmental requirements of BMP with, for example, added BMP4 upregulating the epidermal marker TP63 and BMP inhibition with LDN212854 suppressing TP63. A moderate concentration of LDN212854 (20 nM) was chosen for further study, as this concentration optimized the combined expression of placodal markers Six1, Pax2, and Gata3 while minimizing TP63. Nearly 85% of these predifferentiated cells were immunopositive for Six1 and Pax2. Adenoviral transduction was highly efficient in the human ESCs and placodal cells (~90% GFP+). Likewise, Neurog1 gene expression increased more than 10,000-fold in both human ESCs and placodal cells exposed to Ad.Neurog1, and this overexpression was sustained for more than 8 days, though to a smaller extent. Interestingly, NeuroD1, a direct target of Neurog1 and a major factor in specifying a neural fate, was induced by Ad.Neurog1 in placodal cells but not human ESCs. Consequently, neurodifferentiation was more efficient in Ad.Neurog1 placodal cells than transduced ESCs. Moreover, overexpression of Neurog1 in the placodal cells produced neuronal cells co-expressing Brn3a, Gata3, and vGlut1, suggesting a sensory neuronal lineage. This protocol, which requires less than 2 weeks for terminal differentiation, may be advantageous for stem cell-replacement of damaged spiral ganglia. (Supported by Department of Defense grant W81XWH-12-1-0492)

PS 885

Is the Lack of Mammalian Hair Cell Regeneration Linked to Evolutionarily Dependent Amino Acid Changes Within Functional Protein Domains?

Robert Boney; Allison B. Coffin; Phillip M. Uribe
Washington State University, Vancouver

Sensory hair cells are vulnerable to multiple insults, such as noise and ototoxins. In mammals, hair cell loss is permanent because mammals cannot regenerate lost hair cells, leading to permanent hearing impairment. In contrast, non-mammalian vertebrates exhibit robust regeneration. We set out to characterize amino acid-level differences between regenerating and non-regenerating species, thereby identifying conserved protein sequences in regenerators that are not present or altered in mammals and may contribute to differential regenerative capacity. In this study, we used bioinformatics analysis to compare 265 proteins that have previously been described as expressed within the regeneration window. Then we examined MUSCLE alignments from two non-regenerating species (NRS) and 5 hair cell regener-

ating species (RS) to identify conserved amino acid sequences amongst RS that were divergent from the NRS. We then analyzed these conserved sites to determine the overall proportion of the protein that was conserved between RS and to identify conserved regions that fell within known functional domains. From this query, Ataxin-7-Like-3, which is involved in histone acetylation, contained the highest percentage of conserved amino acids within RS (46%). Sox3 also demonstrated a high degree of conserved amino acids in RS (27%). Sox3 is involved in inner ear specification during development and may be important for neuronal regeneration in other tissues, but a role in hair cell regeneration has not been previously established. We then took our 265 protein sequences from NRS and RS and queried them against predictive functional protein domains to determine if any of the hits from the conserved site analysis also demonstrated a lower number of predicted protein domains in NRS compared to RS. From this analysis, Robo3 rose high on our list of proteins of interest because it ranked as the eighth most conserved between RS's and demonstrated a loss of 2 predicted functional domains in NRS when compared to RS. As with Sox3, Robo proteins have also been implicated in neuronal development within the inner ear but do not have a known role in regeneration. Our analysis suggests novel candidate genes that may be manipulated to facilitate hair cell regeneration.

PS 886

MicroRNA Effects on Hair Cell Transdifferentiation by ATOH1

Michael D. Weston¹; Shikha Tarang²; Umesh Pyakurel²; Sonia M. Rocha-Sanchez³

¹*Creighton University*; ²*Creighton Dental School*;

³*Creighton University School of Dentistry*

Studies over the past 15 years have underscored the role of ATOH1 in hair cell (HC) fate determination. However, as demonstrated more recently, ATOH1-mediated supporting cell (SC) transdifferentiation in the mouse organ of Corti (OC) creates phenotypically immature HCs that lack functional synapses with afferent cochlear neurons (Liu et al., *J. Neuro.* 2014). Recent research supports the utility of small interfering RNAs (siRNAs) to downregulate specific targets of Notch signaling and induce SC-to-HC transdifferentiation (Du et al., *Hearing Res.* 2013). The endogenous microRNA Mir96 gene acts as a master regulator, controlling multiple genes and coordinating HC maturation (Kuhn et al., *PNAS* 2011). The miR-183 cluster of miRNAs (i.e., Mir96, Mir182 and Mir183 genes) are abundantly expressed in newly differentiated HCs whose expression persists long term in healthy adult mouse HCs. Ectopic miR-183 cluster misexpression in SCs is likely to oppose its evolutionarily selected

absence to promote SC-to-HC transdifferentiation. To address this question and shed light on the role of miRNA manipulation on postmitotic SC-to-HC transdifferentiation and maturation, we had generated a transgenic mouse, Tg(GFAP-183-96-182)1MDW (Tg1MDW), that constitutively expresses the miR-183 cluster in OC SCs. Tg1MDW mice demonstrate a modest increase in cochlear HCs with occasional MYO6+ Dieter's cells. This evidence suggests the miR-183 cluster influences intercellular signaling to affect HC/SC identity in the mammalian OC. As ATOH1 and miR-183 miRNAs are positive regulators of HC fates, we sought to identify whether a synergistic effect on SC-to-HC transdifferentiation and subsequent HC maturation would occur from simultaneous ATOH1 and miR-183 cluster expression. Towards that goal, we are currently comparing SC-to-HC transdifferentiation and HC maturation in PLP-CreERT+;Atoh1-HAloxP OCs with and without the genetic addition of Tg1MDW. Results generated from our studies should be beneficial to, and better inform, therapeutic efforts to renew damaged or diseased cochlear sensory epithelia. Supported by NIH/NIDCD 1 R15 DC014813-01A1 (MDW).

PS 887

NEUROG1 Activity is Dependent on Changes in Chromatin State

Zhichao Song; Azadeh Jadali; Kelvin Kwan
Rutgers University

Introduction

Loss of spiral ganglion neurons (SGNs) due to loud noise significantly contributes to hearing loss. Currently, there are no viable treatments for loss of SGNs. Understanding how key transcription factors promote SGN differentiation in stem cells will accelerate efforts for replacement therapies. During inner ear development, a pro-neural transcription factor, NEUROGENIN1 (NEUROG1), is highly expressed in the neurosensory domain (NSD) of the developing inner ear. NEUROG1 expressing cells from the NSD give rise to spiral ganglion neurons (SGNs).

Results

Using an immortalized multipotent otic progenitor (iMOP) cell line that can self-renew and differentiate into otic neurons, we showed that changes in the H3K4me3 and H3K27me3 marked promoters altered the transcriptional activity of NEUROG1. ChIP-seq with H3K4me3 and H3K27me3 antibodies revealed bivalent domains in the promoter region of the cyclin dependent kinase 2 (CDK2). Overexpression of NEUROG1 increased CDK2 expression to drive proliferation while knockdown of NEUROG1 decreased CDK2 and reduced proliferation. In contrast, changes in NEUROG1 levels in post-mitotic

iMOP cells undergoing neuronal differentiation did not affect CDK2. Instead overexpression of NEUROG1 increased levels of neuronal differentiation genes (NEUROD1 and POU4F1) while NEUROG1 knockdown decreased levels of these genes.

Conclusions

Our findings showed that the ability of NEUROG1 to promote proliferation is dependent on the bivalent chromatin state of the CDK2 promoter. We propose that NEUROG1 is a lineage dependent transcription factor that promotes proliferation in otic progenitors.

PS 888

siRNA Therapeutics for Hair Cell Regeneration in Adult Mammalian Cochlea

Swetlana Adamsky¹; Rivka Levron²; Esperanza Bas³; Dalian Ding⁴; Sharon Avkin-Nachum¹; Hagar Kalinski²; Hagit Ashush²; Richard Salvi⁵; Thomas R Van De Water³; Elena Feinstein⁶

¹Quark Pharmaceuticals, Inc; ²Quark Pharmaceuticals, Inc.; ³University of Miami-Miller School of Medicine; ⁴State University of New York at Buffalo; ⁵Center for Hearing & Deafness, Department of Communicative Disorders and Science, State University of New York at Buffalo; ⁶Quark Pharmaceuticals Inc

Background

Accumulating evidence suggests that sensory hair cells in the inner ear of newborn mammals can be regenerated upon division and trans-differentiation of supporting cells, via developmental mechanisms that are silenced in the adult mammalian cochlea. Modified siRNA can be efficiently delivered to various inner ear structures in both large and small mammals and, hence, used for manipulating gene expression. Because studies to date inhibiting single genes and/or pathways to evoke the mechanisms of interest in adult mammals have been inconclusive, we used a cocktail of several siRNAs to investigate whether simultaneous inhibiting specific genes in divergent pathways regulating proliferation and differentiation of auditory epithelium can restore auditory function in a rat ototoxic hearing loss model.

Methods

An ototoxic model using transtympanic aminoglycoside was conducted in 3-month old rats (n = 10 per group). Four days later, when hearing function was confirmed lost, a specific cocktail of synthetic chemically stabilized siRNAs or vehicle were placed onto the round window membrane through surgical access. Functional hearing assessments were performed by repeated Auditory Brainstem Response (ABR) threshold measurements

over 12 weeks. Prior to termination at 12 weeks, Distortion Product of the Otoacoustic Emissions (DPOAE) measurements were performed. Subsequently, harvested cochleae whole mounts were stained with the FM1-43FX dye for mechanotransduction and with a Myosin7a antibody and DAPI for hair cell counts.

Results

Treatment of animals with the siRNA cocktail caused small (10-20 dB) but significant ($p < 0.05$), frequency-dependent decreases in ABR thresholds compared to control vehicle-treated animals. DPOAE testing corroborated the ABR results. Morphological examination showed more Myosin 7a-positive outer hair cells (OHC) throughout the cochleae of siRNA-treated animals compared to control. Control animals had complete OHC and substantial inner hair cell (IHC) loss in basal cochlea turns, while these were present in siRNA-treated ears. Unlike in control animals, a number of siRNA-treated cochleae contained well-organized rows of hair cells that were also positive for mechanosensory transduction sensitive staining.

Conclusions

Our data suggest that local inner ear delivery of specific multi-pathway targeting siRNA cocktail in adult animals potentially represents an effective therapeutic approach to hearing function restoration.

PS 889

Astrocyte Conditioned Medium Promotes Synaptogenesis Between Stem Cells-derived Neuron and the Cochlea Nucleus in Vitro

Zhenjie Liu¹; Zhengqing Hu²; Xiaoyang Li³

¹Wayne State University, School of Medicine; ²Wayne State University; ³Department of Otolaryngology-HNS, Wayne State University

Spiral ganglion neurons (SGNs) conduct sound signals from hair cells to the cochlea nucleus (CN). However, SGNs are vulnerable to a number of insults, which cause irreversible hearing loss. We have demonstrated that SGN-neural stem cell-derived neurons (ScNs) possess SGN-like features and they are electrophysiologically functional. However, whether ScNs are able to form neural connections with the CN is obscure. To address this issue, we co-culture ScNs with mouse CN tissues in the presence of astrocyte conditioned medium (ACM) or thrombospondin-1 (TSP1) to identify novel approaches to stimulate synapse formation. eGFP-ScNs were generated as previously reported (Li et al 2016 Stem Cell Dev) and co-cultured with postnatal wild-type mouse CN tissues. Wild-type ACM, TSP1-immunodepleted-ACM, ACM from TSP1-knockout (TSP1-KO)

mice, and purified TSP1 protein were supplied to the ScNs-CN co-cultures for 4-6 days, followed by immunofluorescence using antibodies specific for synapses, including synaptic vesicles (SV2), synapsin I and PSD93. FM4-64 synaptic recycling test was used to identify the synaptic vesicles in co-cultures. Synapse-like structures were found in ScN and CN co-cultures by SV2 immunostaining and quantification study showed: (a) significant more SV2 staining was found in the co-cultures supplied with ACM than those without ACM ($p < 0.05$, Student's t-test); (b) 10 nM TSP1 exerted the highest SV2 immunostaining; (c) TSP1-immunodepleted-ACM had less SV2 immunostaining compared to the wild-type ACM, and supplementation of exogenous TSP1 to the TSP1-immunodepleted-ACM group rescued SV2 immunostaining; (d) Fewer SV2 immunostaining was found in the TSP1-KO-ACM group, whereas supplement of exogenous TSP1 to TSP1-KO-ACM group rescued SV2 immunostaining. These data suggest that ACM is able to stimulate SV2 synaptic vesicle formation and TSP1 seems to play a critical role in synaptogenesis. Newly-formed synaptic-like structures were labeled by pre- and post-synaptic markers including synapsin I and PSD93, and confocal microscopy-based co-localization showed apposition of synapsin I and PSD93 immunostaining. Further, new synapses were labeled with glutamatergic markers VGlut1 and GluR2, indicating glutamatergic synapse formation. FM4-64-based synapse recycle test showed remarkable synaptic vesicles in co-cultures supplied with ACM or TSP1, which suggests that new synapses possess functional synapse vesicles and potential synapse function. This research demonstrates that ScNs can form neural connections with the CN in vitro and ACM is able to stimulate synaptogenesis via TSP1. The results of this study will promote the research of auditory pathway regeneration using stem cell-based approaches.

PS 890

Sox2 and Lin28 Influence Proliferation and Cell Fate of Cochlear Glial Cells Cultured as Spheres

Marco Petrillo¹; Judith S. Kempfle²; Ngoc-Nhi Luu³; Albert Edge⁴

¹Massachusetts Eye and Ear Infirmary; ²Department of Otolaryngology, Massachusetts Eye and Ear Infirmary, Boston, MA, USA. ³Department of Otolaryngology and Laryngology, Harvard Medical School, Boston, MA, USA. ⁵Department of Otolaryngology, University Tübingen Medical Center, Tübingen, G; ³2, Department of Otolaryngology, Massachusetts Eye and Ear Infirmary, Boston, MA, USA. ³Department of Otolaryngology and Laryngology, Harvard Medical School, Boston, MA, USA; ⁴Department of Otolaryngology, Harvard Medical School, Boston, MA, USA, and Eaton-Peabody Laboratory, Massachusetts Eye and Ear Infirmary, Boston, MA, USA

Background

The transcription factor Sox2 is crucial for proliferation of progenitor cells and neurogenesis. Sox2 directly interacts with RNA binding protein Lin28 in human neural precursors to maintain optimal levels of Lin28 and to promote proliferation and early neurogenesis. In the postnatal inner ear, Sox2 is expressed in supporting cells and peripheral glial cells and has previously been associated with expansion of sensory progenitors that develop into hair cells. We found that proteolipid protein 1 (Plp1), a marker for glial cells that can act as progenitor cells for neurons in the CNS, is co-expressed with Sox2 in peripheral spiral ganglion glia. Plp1-positive cochlear glial progenitors was dependent on Sox2 and Lin28 for progenitor activity.

Methods

Spiral ganglion stem cells were isolated from cochleae of neonatal Plp-Cre-ER;Sox2flox/flox, and Plp-Cre-ER;Lin28aflox/flox mice or from Plp-Lin28TetO/+ and Plp-Sox2TetO/+ mice. Single cell suspensions of spiral ganglion tissue were cultured with growth factors to obtain proliferative spheres. Neurosphere formation was then quantified by immunohistochemistry after 3 passages. Under differentiation-promoting conditions, plated neurospheres were quantified after 8 days in vitro and analyzed for neural progenitor and glial cell marker expression by quantitative RT-PCR and immunohistochemistry.

Results

Plp1-positive glial cells from the spiral ganglion required Lin28 and Sox2 to maintain proliferation in vitro. Downregulation of Lin28 or Sox2 in Plp1-positive neurospheres showed reduced proliferation in vitro and failed

to initiate neurogenesis upon differentiation. Transient overexpression of Sox2 or Lin28 led to increased proliferation and neurogenesis from Plp- positive progenitors in vitro.

Conclusions

Sox2 interacts with Lin28 in cochlear glial progenitors to promote proliferation and influence cell fate.

PS 891

Ciliary Neurotrophic Factor Promotes Synapse Regeneration after Noise-Induced Cochlear Synaptopathy

Sepand Bafti¹; S.M Mirghorbani²; Stephanie Peterson¹; Steven H. Green³

¹Department of Biology, University of Iowa; ²University of Iowa; ³Department(s) of Biology and Otolaryngology

Background

Noise exposure destroys cochlear afferent synapses between inner hair cells (IHCs) and spiral ganglion neurons (SGNs), even in the absence of hair cell loss or permanent threshold shift. This cochlear "synaptopathy" is a result of excess release of the neurotransmitter glutamate from IHCs and consequent glutamate excitotoxicity. Noise induced cochlear synaptopathy in animal models can be detected as a reduction in the number of synapses on the IHCs. Few, if any, synapses normally regenerate but application of neurotrophic factors such as BDNF or NT-3 promotes regeneration. NT-3 is normally expressed in the organ of Corti (OC) and appears necessary for regeneration. Ciliary Neurotrophic Factor (CNTF) is also normally expressed in the OC (Bailey & Green, 2014) and we ask here whether CNTF can promote cochlear synapse regeneration after synaptopathy resulting from excitotoxic trauma.

Methods

Effects of CNTF on SGN survival and neurite growth were assessed in dissociated spiral ganglion cultures. For synapse regeneration, cochlear explant cultures from postnatal day 5 rat pups were prepared as described by Wang et.al, 2011. These cultures maintain intact a portion of the organ of Corti, associated SGNs, and synaptic connections. Synaptopathy is caused by addition of the glutamate agonist kainic acid (KA) for 2 hours (equivalent to the duration of noise exposure used in vivo). Exposure was to 0.5 mM or 0.03 mM KA that, respectively, cause nearly complete synapse loss or synapse loss comparable to that seen after noise exposure in vivo. The cultures were then incubated for three days after KA exposure, with CNTF and/or NT-3 or no neurotrophic factors. Labeling was with anti-Ribeye (presynaptic ribbons), anti-PSD95 (postsynaptic densi-

ties) and anti-Myosin 6 (IHCs). Synapse counts were compared among experimental conditions and controls. To facilitate the process of quantifying synapse loss/regeneration in confocal image stacks we are developing software that automates it, rapidly and accurately counting synapses. Results. CNTF promotes SGN survival and neurite growth in vitro similarly to NT-3. Following exposure to 0.5 mM KA, which leaves 1-2 synapses/IHC, regeneration of cochlear synapses is significantly enhanced by CNTF, nearly as well as by NT-3; the difference between CNTF and NT-3 is not significant. Nearly half of the synapses were restored.

Conclusions

Our data shows that CNTF has the ability to promote synapse regeneration after excitotoxic trauma and may be useful for synapse regeneration after noise exposure in vivo.

PS 892

Reprogramming Spiral Ganglion Non-neural Cells into Induced Neurons

Teppei Noda¹; Koji Nishimura²; Steven Meas³; Yutaka Amemiya³; Alain Dabdoub⁴

¹Sunnybrook Research Institute; ²Shiga Medical Center Research Institute, Moriyama, Japan; ³Sunnybrook Research Institute, Toronto, Canada; ⁴Biological Sciences, Sunnybrook Research Institute, University of Toronto

Background

Primary auditory neurons (PANs) play a critical role in hearing as they transmit sound information from the inner ear to the brainstem. Their progressive degeneration is associated with excessive noise, disease and aging. Due to their inability to recover, the loss of PANs is permanent leading to hearing impairment.

Spiral ganglion non-neural cells (SGNNCs), comprised mainly of glia, are an excellent target cell population for replacing damaged neurons by cellular reprogramming. SGNNCs are resident within the modiolus, continue to survive and divide after neuron loss, and have a partially overlapping phenotypic profile to PANs; bipolar morphology, sub-sets of regulatory receptors, and some classes of relevant voltage-gated ion channels.

In order to replace PANs we overexpressed the proneural pioneer factor *Ascl1*, and the PAN differentiation factor *NeuroD1* in vitro to directly reprogram endogenous SGNNCs into induced neurons.

Method

Cochleae were isolated from postnatal day 1 Tau-GFP mice (neuron reporter), and the spiral ganglia were dis-

sected from the modiolus. Tau-GFP positive neurons and Tau-GFP negative SGNNCs were sorted using fluorescence activated cell sorting (FACS). The Tau-GFP negative fraction was transfected with a combination of *Ascl1-IRES-DsRed-Express2*, and *NeuroD1-IRES-DsRed-Express2*, or a *DsRed-Express2* control vector. Total RNA was extracted and sequenced to compare the transcriptome of induced neurons arising from *Ascl1/NeuroD1* transfected SGNNCs, endogenous Tau-GFP positive neurons and control transfected SGNNCs.

Results

Overexpression of *Ascl1* and *NeuroD1* resulted in SGNNC expression of several neuronal markers including β III-tubulin, MAP2, a glutamatergic marker VGLUT1, and the PAN specific transcription factors *Gata3* and *Prox1*.

Utilizing RNA-Seq and gene ontology enrichment analysis we compared gene expression related to neurogenesis, neuron differentiation and neuron maturation detailing the transition to induced neurons. Gene expression data were further validated by droplet digital PCR (ddPCR), investigating four genes (β III-tubulin, *Peripherin*, *Sox2*, and *Tenascin C*) as two neuronal markers, a glial marker, and a mesenchymal marker, respectively.

Conclusion

We generated induced neurons from SGNNCs that resemble endogenous PANs, as evidenced by positive immunostaining for neuronal markers and transcriptomic data that detail a change in cellular lineage.

PS 893

Identifying Therapies to Promote Hair-Cell Reinnervation: A Pilot Study in the Zebrafish Lateral Line

Lavinia Sheets

Eaton-Peabody Lab/ MEEI/ Harvard Medical School

Auditory neuropathy—a hearing condition in which sound information is not properly transmitted from the cochlea to the brain—is a common form of hearing impairment. In patients where auditory neuropathy is caused by cochlear nerve-fiber loss, great benefit could be derived from therapies that promote nerve fiber regeneration and hair-cell reinnervation. While the secreted growth factor neurotrophin-3 (NT-3) has shown promising therapeutic value in regenerating damaged cochlear nerve contacts, its partial effectiveness indicates that more biological pathways need to be identified in order to fully restore cochlear hair-cell innervation.

To identify potential therapies that promote nerve regeneration, one effective strategy would be to perform a large-scale screen of chemical libraries containing bioactive compounds. The zebrafish lateral line has been successfully used in multiple large-scale drug screens to identify compounds that modulate hair-cell regeneration and that protect against ototoxic hair-cell death. A similar strategy could therefore be used to identify compounds that promote reinnervation of hair cells and restoration of hair-cell synaptic contacts.

To demonstrate the utility of the zebrafish lateral line in screening for compounds that promote cochlear nerve-fiber reinnervation, I performed a pilot study whereby I ablated transgenic zebrafish lateral-line organs via exposure to copper sulfate (CuSO₄) — a treatment that causes both loss of lateral-line hair cells and considerable retraction of afferent nerve terminals—then treated the fish with known trophic factors or drug delivery vehicle alone. I observed that application of NT-3 post-CuSO₄ exposure enhanced regeneration of lateral-line afferent innervation relative to the vehicle-treated control based on both the number of innervating nerve fibers and the number of dendritic branch points. These results indicate similar biological pathways promote reinnervation in both zebrafish and mammals, and support that novel biological mechanisms uncovered in the zebrafish will provide information toward regenerating innervation in the mammalian cochlea. This assay will now be used to perform a large-scale bioactive molecule screen for drugs that modulate hair-cell reinnervation and synaptogenesis.

PS 894

Using Multi-Electrode Arrays to Stimulate and Record from Stem Cell-Derived Sensory Neurons In Vitro

Bryony A. Nayagam¹; Abdullah Alshawaf²; Wanzhi Qiu³; Stan Skafidas³; Mirella Dottori³

¹The University of Melbourne. The Bionics Institute;

²University of Melbourne; ³The University of Melbourne

Research Background

In severe cases of sensorineural deafness where the numbers of hair cells and auditory neurons are significantly depleted, stem cell-derived neurons may provide a potential source of replacement cells. In the absence of functional hair cells, these stem cell-derived neurons would require appropriate depolarization from a cochlear implant in order to precisely relay sound information to the brainstem. Unlike acoustic stimulation, electrical stimulation of the auditory nerve causes significantly higher firing rates in auditory neurons. This raises important considerations for the development of a stem

cell replacement therapy, including: can stem cell-derived neurons faithfully transmit electrical signals to the target neurons in the cochlear nucleus, and will they be able to respond to the high stimulus rates delivered by a cochlear implant? As a first step, we are investigating whether electrical stimulation of stem cell-derived neurons using multi-electrode arrays (MEAs), can improve overall firing rates of these neurons in vitro.

Methods

We utilised our previously published protocols to derive functional sensory neurons from human pluripotent stem cells. These stem cell-derived neurons were cultured on MEAs (Multichannel Systems, Germany) for up to 6 weeks in vitro and exposed to 2 Hz biphasic voltage pulses (± 800 mV, 200 μ sec per phase) fo

Results

Stem cell-derived neurons expressed numerous sensory- and neural-specific markers, were spontaneously active after 9 days differentiation, and generated action potentials in response to membrane depolarization after 14 days differentiation. In vitro electrical stimulation of stem cell-derived neurons using MEAs produced a maximum average array-wide rate of 195.8 ± 110.3 spikes/sec and spontaneous firing activity developed into trains of spikes and bursting, reaching a maximum number of 1021.3 ± 626.1 bursts.

Conclusions

The electrical activity and network forming capacity of stem cell-derived neurons can be measured and quantified using MEAs. In vitro electrical stimulation may assist in the functional maturation of stem cell-derived sensory neurons in vitro. This has important implications for developing a combined stem cell/cochlear implant therapy for severe-to-profound sensorineural hearing loss. Current experimentation includes comparing a number of different ES regimes for enhancing firing activities in these cell populations.

Acknowledgements

This work is sponsored by the Garnett Passe and Rodney Williams Memorial Foundation, The NHMRC (Australia), The Australian Research Council, and a travel grant from the CASS Foundation, Australia.

PS 895

Neuroglobin Is Important for the Regeneration of Auditory Processing After Acoustic Trauma

Lenneke Kiefer¹; Daniel Andre²; Thomas Hankeln²; Stefan Reuss³; Manuela Nowotny¹

¹*Institute of Cell Biology and Neuroscience, Goethe University Frankfurt am Main, Germany;* ²*Institute of Molecular Genetics, Johannes Gutenberg-University Mainz, Germany;* ³*Department of Nuclear Medicine, University Medical Center, Johannes Gutenberg-University, Germany*

Many questions are open in the understanding of oxygen homeostasis in the hearing process. This study deals with the importance of Neuroglobin (Ngb), an oxygen-binding protein which is comprehensively expressed in auditory neurons (Reuss et al., *Mol. Neurobiol.*, 2016). We investigated the impact of Ngb on hearing and regeneration following a noise trauma by measuring distortion product otoacoustic emissions (DPOAE) and auditory brainstem responses (ABR) in Ngb-knock-out (Ngb-KO) and normally hearing, wild-type mice (WT).

Experiments were performed on eight wild type (C57Bl/6) and nine Ngb-KO mice (*Mus musculus*). Hearing ability was investigated by means of ABRs measured at 5, 8, 10, 18 and 28 kHz. Furthermore, we measured DPOAEs from the left ear. During DPOAE measurements, we apply a broad band noise (10 kHz \pm 2 oct) into the right ear to activate the efferent system and to modulate the DPOAE amplitude measured from the contralateral ear. These measurements were conducted before, four days after and four weeks after intense noise trauma (center frequency 10 kHz, \pm 0.25 oct., 120 dB SPL).

Measuring DPOAEs (2f₁-f₂), we found significantly increased hearing thresholds at 8 and 10 kHz in Ngb-KO mice. Activation of the efferent system resulted in an increased distortion product f₂-f₁ amplitude only in WT mice. ABR responses to tone pips were not found to be different between WT and Ngb-KO mice before noise trauma. However, we detected a slower regeneration of ABR thresholds after acoustic trauma in Ngb-KO mice. After four weeks, in Ngb-KO-mice a permanent threshold shift covered a frequency range from 10 to 28 kHz, while in WT mice only frequencies from 18 to 28 kHz were affected.

We conclude that the lack of neuroglobin impairs hearing on the level of the inner ear but only slightly influence the processing of auditory information along the auditory pathway under physiological conditions. We found a strong effect of noise trauma on the efferent pathway in Ngb-KO mice, activated by a third stimulus in the contra-

lateral ear. Hearing in Ngb-KO-mice seemed to regenerate slower, and a pronounced permanent threshold shift that covered a large frequency range from 10 to 28 kHz was found.

PS 927

A Systems Biology Approach to Understanding Hearing Regeneration in Zebrafish

Shawn Burgess¹; Wuhong Pei²; Jason Sinclair²; Erin Jimenez²; Gaurav Varshney³; Lisha Xu²; Chunxin Fan²; Zelin Chen²; Alberto Rissone²

¹*National Human Genome Research Institute, NIH, Bethesda, MD;* ²*National Human Genome Research Institute/NIH;* ³*Functional & Chemical Genomics Program, Oklahoma Medical Research Foundation, Oklahoma Cit, OK*

Tissue regeneration is the result of a complex integration of injury signals, stem cell activation, inflammation responses, reactivation of developmental programs and regeneration-specific processes. We have developed a systematic approach to dissect and analyze the various pathways involved in hearing regeneration by using zebrafish as a model organism. By using a high-throughput "guided" genetics and chemical genomics screen to identify the key genes and pathways involved in hearing regeneration, we have significantly enriched our success rate for identifying regeneration-specific genes. From our previous work, we had collected 2000 candidate genes involved in hearing regeneration by transcriptionally profiling regenerating zebrafish adult inner ears after sound damage. We've built an efficient gene knockout pipeline, first using retroviral mutagenesis but now using CRISPR/Cas9 targeting and we are systematically inactivating the 2000 candidate genes and testing their role in both normal hair cell development and hair cell regeneration. In addition, we have screened a broad number of well-characterized pharmacological inhibitors to identify genes that cannot be easily tested by KO because of their important roles in early development. From our first two hundred and fifty genes and twenty chemical inhibitors tested, we have identified seven genes that reduce the number of hair cells in a normal embryo, and we have identified an additional seven genes and three chemical inhibitors that specifically disrupt regeneration of the hair cells without affecting normal development. We will present data on the genetic strategy used to generate and screen hundreds of zebrafish gene knockouts for hearing regeneration defects, the pathways emerging from our genetic and chemical genomic analysis, and the deeper phenotypic characterization of a RNA splicing complex and how two genes in the complex are key regulators of hair cell regeneration.

PS 930

Ciliary Neurotrophic Factor Promotes Synapse Regeneration after Noise-Induced Cochlear Synaptopathy

Sepand Bafqi¹; S.M Mirghorbani²; Stephanie Peterson¹; Steven H. Green³

¹Department of Biology, University of Iowa; ²University of Iowa; ³Department(s) of Biology and Otolaryngology

Background

Noise exposure destroys cochlear afferent synapses between inner hair cells (IHCs) and spiral ganglion neurons (SGNs), even in the absence of hair cell loss or permanent threshold shift. This cochlear “synaptopathy” is a result of excess release of the neurotransmitter glutamate from IHCs and consequent glutamate excitotoxicity. Noise induced cochlear synaptopathy in animal models can be detected as a reduction in the number of synapses on the IHCs. Few, if any, synapses normally regenerate but application of neurotrophic factors such as BDNF or NT-3 promotes regeneration. NT-3 is normally expressed in the organ of Corti (OC) and appears necessary for regeneration. Ciliary Neurotrophic Factor (CNTF) is also normally expressed in the OC (Bailey & Green, 2014) and we ask here whether CNTF can promote cochlear synapse regeneration after synaptopathy resulting from excitotoxic trauma.

Methods

Effects of CNTF on SGN survival and neurite growth were assessed in dissociated spiral ganglion cultures. For synapse regeneration, cochlear explant cultures from postnatal day 5 rat pups were prepared as described by Wang et.al, 2011. These cultures maintain intact a portion of the organ of Corti, associated SGNs, and synaptic connections. Synaptopathy is caused by addition of the glutamate agonist kainic acid (KA) for 2 hours (equivalent to the duration of noise exposure used in vivo). Exposure was to 0.5 mM or 0.03 mM KA that, respectively, cause nearly complete synapse loss or synapse loss comparable to that seen after noise exposure in vivo. The cultures were then incubated for three days after KA exposure, with CNTF and/or NT-3 or no neurotrophic factors. Labeling was with anti-Ribeye (presynaptic ribbons), anti-PSD95 (postsynaptic densities) and anti-Myosin 6 (IHCs). Synapse counts were compared among experimental conditions and controls. To facilitate the process of quantifying synapse loss/regeneration in confocal image stacks we are developing software that automates it, rapidly and accurately counting synapses.

Results

CNTF promotes SGN survival and neurite growth in vitro similarly to NT-3. Following exposure to 0.5 mM KA, which leaves 1-2 synapses/IHC, regeneration of cochlear synapses is significantly enhanced by CNTF, nearly as well as by NT-3; the difference between CNTF and NT-3 is not significant. Nearly half of the synapses were restored.

Conclusions

Our data shows that CNTF has the ability to promote synapse regeneration after excitotoxic trauma and may be useful for synapse regeneration after noise exposure in vivo.

Tinnitus: Treatments and Mechanisms

PS 896

Treatment Effects of Antioxidants on Tinnitus-related Biomarker Expression in the Central Auditory System after Blast Exposure

Xiaoping Du; Matthew B. West; Weihua Cheng; Jianzhong Lu; Donald Ewert; Richard D. Kopke
Hough Ear Institute

Background

Sensorineural hearing loss (SNHL) and tinnitus resulting from blast-induced trauma are prevalent disabilities among military personnel. Our previous studies demonstrated that antioxidants have the potential to simultaneously treat blast-induced injuries in the brain and the auditory system. In the present study, we examined tinnitus-related biomarker expression in the brain after blast exposure and evaluated the potential therapeutic efficacy of antioxidants on mitigating blast-induced tinnitus and manifestations of its underlying pathology.

Methods

Neural plasticity biomarkers (activity-regulated cytoskeleton-associated protein, ARC, and growth associated protein 43, GAP-43) were immunohistochemically examined in the brain of non-transgenic rats after single shock tube blast exposures (8 psi) in animals that were either left untreated or were subsequently treated with a regimen of antioxidants. The therapeutic antioxidants evaluated in the present study were a combinatorial regimen of 2,4-disulfonyl α -phenyl tertiary butyl nitron (HPN-07) and N-acetylcysteine (NAC). Acoustic startle reflex, including GAP and prepulse inhibition (PPI), were used for tinnitus measurement before and 7-8 weeks after blast exposure.

Results

The blast exposure model induced down-regulation of ARC and up-regulation of GAP-43 in the auditory sys-

tem, including the auditory cortex (AC), the inferior colliculus (IC), the dorsal cochlear nucleus (DCN) and the cochlea. Therapeutic intervention with the combinatorial antioxidant regimen significantly reduced down-regulation of ARC and up-regulation of GAP-43, particularly in the AC, the IC and the DCN. A negative correlation ($r = -0.48$) was observed between ARC density in the IC and PPI score at a frequency (20kHz) in all animals examined.

Conclusions

The combination of HPN-07 and NAC administered shortly after a blast exposure can reduce manifestations of maladaptive neural plasticity in the auditory system. Reduced ARC expression in the IC may be associated with blast-induced tinnitus. In conclusion, potent antioxidant formulations, such as combinatorial HPN-07 and NAC, represent a promising approach for treating broad-spectrum auditory injuries, including SNHL and tinnitus, that result from damaging blast exposures.

Funding

This research was supported by grant AR14-020 from The Oklahoma Center for the Advancement of Science and Technology (OCAST).

PS 897

Development and Characterization of a MRI Capable, Targeted Nanoparticle Platform for Receptor Mediated Transcytosis Over an In Vitro Blood-Brain-Barrier Model

Magnus Bergkvist¹; Stephanie Curley¹; Avril Genee Holt²; James Castracane¹; Angela Dixon³; Anthony Cacace³

¹SUNY Polytechnic Institute, College of Nanoscale Science and Engineering; ²Wayne State University School of Medicine/ JD Dingell VAMC; ³Wayne State University

Tinnitus is a prevalent problem with no effective treatments. Tinnitus has been linked with spatial and temporal spontaneous changes in neuronal activity even after a single exposure to a noise resulting in a temporary hearing loss. Targeting these susceptible brain regions via delivery of theranostic nanoparticle (NP) agents could facilitate diagnostics and delivery of drugs to normalize neuronal activity and alleviate symptoms of tinnitus.

Fundamental challenges remain to deliver functional nanoparticles to brain regions implicated in tinnitus onset. One substantial challenge is to design functional NPs that cross the blood-brain-barrier (BBB) and target specific brain regions. Thus, a multifunctional NP sys-

tem is needed that can be 1) loaded with functional molecules, 2) transported across the BBB, and 3) localized to relevant regions in the brain.

We are currently developing a multifunctional nanoparticle platform for brain delivery that utilizes cellular transport mechanisms. Angiopep-2 (AP2) is a 3 kDa peptide capable of receptor-mediated transcytosis across the BBB. Here we report on the development of a multifunctional NP utilizing AP2 conjugated to MS2 bacteriophage capsids and evaluate transport over an in vitro BBB model. Furthermore, we evaluate nucleotide mediated loading of a MRI contrast agent into MS2 NPs based on psoralen and DOTA-Gd3+.

Two AP2-MS2 NP constructs were prepared using a heterobifunctional reagent with/without a PEG linker (SMCC or SM (PEG)24). Confluent 2D monolayers of RBE4 cells on Transwell inserts were used as an in vitro BBB model to evaluate the effect of linker and AP2 ligand density on the transcytosis efficiency. Nanoparticle transport across the BBB model was monitored over 24 hours by fluorescence; 4.4 kDa TRITC-dextran was used as a paracellular transport control. Previously, loading of cargo into MS2-NPs has been demonstrated using fluorescent dyes and photosensitizers. Here we investigate a strategy to load NPs with the MRI contrast agent DOTA-Gd3+ via nucleotide driven interactions. DOTA was conjugated to a psoralen molecule, which is known to intercalate with RNA/DNA. Subsequently, exposure to UV-light can covalently link the psoralen to the nucleotides. We evaluate loading efficiency of psoralen-DOTA-Gd3+ into the MS2 NP using spectroscopic titration and inductively coupled plasma mass spectrometry (ICP-MS).

Preliminary results show that both MS2-AP2 constructs are capable of transport from the basolateral domain, across the BBB, with little transport of untargeted MS2 particles. Furthermore, ICP-MS analysis shows that MS2 can be loaded with the psoralen-DOTA-Gd3+ complex.

PS 898

Effects of the Cochlear Electrical Stimulation of the Tinnitus Suppression: Behavioral and Neural Activity Studies in Rats

Hao Luo¹; Syed Ahsan²; Eric Kim³; Maricel Pabustan Gener⁴; Yong Xu³; Jinsheng Zhang⁴

¹School of Medicine, Wayne State University; ²Henry Ford Health Systems, Department of Otolaryngology/Head and Neck Surgery; ³Wayne State University College of Engineering; ⁴Wayne State University School of Medicine

Cochlear implantation for hearing restoration has been reported to have favorable effects on coexisting tinnitus, and can significantly or totally suppress tinnitus in 45-78% of patients. However, cochlear implants and their speech processors are mainly designed for hearing restoration, and cochlear electrical stimulation (CES) has not been specifically designed or used to modulate tinnitus. In addition, the underlying mechanisms of (CES)-induced tinnitus suppression remain unclear. To address these questions, we successfully developed a cochlear implantation rat model. We induced tinnitus by exposing rats to intense noise (2 hours, 8-16 kHz, 115 dB SPL), monitored tinnitus status before, during and after CES using gap-detection acoustic startle reflex paradigm, and measured neural activity in the auditory cortex before and after CES. The stimulus consisted of 1 mA biphasic current pulses presented at 10 pulses per second (pps) for 30 minutes at the high frequency region (basal) of the cochlea. Our results showed significant CES-suppression of high-frequency pitch tinnitus behavior, with suppression lasting for up to two days. We also observed significant neural activity change in the auditory cortex immediately after CES, including spontaneous firing rate decrease, neural synchrony reduction at middle and high frequency areas, and bursting activity increase at all frequency areas. Such results confirm that CES can suppress tinnitus, and that CES can modulate neural activity in the auditory cortex. This suggests that modulation of the afferent pathways by CES is responsible for the central effects observed in the auditory cortex, which indicates that bottom-up modulation contributes to tinnitus related neural activity management.

PS 899

Bimodal Stimulation Desynchronizes the Tinnitus Circuit in Guinea Pig Dorsal Cochlear Nucleus

David T. Martel; Calvin Wu; Susan E. Shore

Department of Otolaryngology, Kresge Hearing Research Institute, University of Michigan, Ann Arbor, MI 48109, USA

Introduction

Synchrony across neuronal assemblies transforms spiking into perception and is dependent on dynamic learning mechanisms, such as synaptic plasticity. Spike-timing-dependent plasticity (STDP) theoretically regulates synchrony by modulating neural connectivity via synaptic strength adjustment. However, despite various computational models (eg, Tass and Popovych, 2012), it remains to be shown that STDP plays a role in perceptual coding.

Tinnitus, or phantom auditory perception, provides a model for testing STDP regulation of synchrony. Dorsal cochlear nucleus (DCN) fusiform cells, putative tinnitus generators, exhibit the in vivo equivalent of STDP: stimulus-timing-dependent plasticity (STDP). In tinnitus, STDP “learning rules,” i.e., temporal- and order-dependent plasticity functions, show enhanced long term potentiation (LTP: persistent increase in synaptic strength following high-frequency stimulation) and diminished long term depression (LTD) (Koehler and Shore, 2013). Theoretical models predict that increased LTP would result in hypersynchrony and tinnitus. If STDP triggers synchrony-driven tinnitus, then shifting STDP towards LTD and de-synchrony, could reverse tinnitus.

Methods

Guinea pigs were exposed to unilateral narrow band noise (1/2 octave, centered at 7 kHz, 97 dB SPL) for two hours to induce temporary threshold shifts. Tinnitus was assessed with gap-prepulse inhibition of acoustic startle paradigm (Turner et al, 2016). A bimodal stimulus paradigm consisting of somatosensory stimuli (via transdermal stimulating electrodes placed dorsal to the cervical vertebrae) presented within 20 ms of 40 dB SL sounds matching the tinnitus spectra. Animals were treated with this bimodal stimulus daily for 20 minutes for four weeks concurrently with biweekly tinnitus assessments. Following bimodal treatments, single unit recordings were obtained using electrodes placed into the DCN fusiform cell layer after ketamine/xylazine anesthesia. Responses were analyzed for neurons with best frequencies ranging from 4 kHz to 32 kHz. Neural synchrony was assessed via spike train cross-correlation.

Results

Bimodal stimulation with an interstimulus interval targeting the LTD window reversed STDP timing rules and synchrony in fusiform cells and reduced behavioral evidence of tinnitus.

Conclusion

The results suggest that non-invasive, long-term alteration of DCN neural activity through bimodal stimulation can be utilized to alleviate tinnitus in humans. Further, STDP plays a fundamental role in regulating neural synchrony, providing a framework for treating diverse synchrony disorders such as Parkinson's disease or epilepsy.

Funding

R01-DC004825 (SES)

T32-DC00011 (CW,DTM)

Wallace H. Coulter Translational Research Partnership

PS 900

Auditory-Somatosensory Stimulation Alleviates Tinnitus in Human Subjects

Susan E. Shore¹; Kendra Marks²; David T. Martel¹; Gregory J. Basura³; Larry E. Roberts⁴; Kara Leyzac²

¹Department of Otolaryngology, Kresge Hearing Research Institute, University of Michigan, Ann Arbor, MI 48109, USA; ²University of Michigan; ³Dept of Otolaryngology; Center for Human Growth and Development; University of Michigan; ⁴McMaster University

Background

A majority of tinnitus subjects are able to modulate their tinnitus by moving or applying pressure to their head or neck, so called, 'somatic' tinnitus [1]. This ability is mediated, at least in part, by the dorsal cochlear nucleus (DCN), which integrates auditory and somatosensory information [2]. DCN circuitry is altered in tinnitus to produce hypersynchrony and heightened spontaneous firing rates in output neurons [3]. Pairing auditory- with somatosensory stimuli can induce long-term increases or decreases in firing rates and synchrony in these neurons, depending on the precise timing of the bimodal intervals [3]. By presenting bimodal intervals that depressed firing rates and synchrony, we were able to decrease physiological and behavioral evidence of tinnitus in animals [4]. Here, we extend these findings to a human population.

Methods

Twenty human subjects with constant, bothersome somatic tinnitus were recruited to participate in a double-blinded, sham-controlled, cross-over study. Subjects were randomly assigned to sham (auditory only)

or active (bimodal auditory-somatosensory) stimulation treatment. Somatosensory stimulation was achieved by pads placed on the face or neck. Using a take-home device, treatments consisted of 30 minutes a day of auditory only (sham) or bimodal (auditory-electric) stimulation for four weeks. Each sham or active period was followed by a four-week washout period. Throughout the sixteen-week study, subjects completed the Tinnitus functional Index (TFI) and loudness matching tasks to monitor their tinnitus on a weekly basis.

Results

Bimodal but not unimodal stimulation resulted in significant reductions in loudness matching (mean decrease of -7.334 dB) and total TFI score (mean decrease of 6.11 points), with 11 of the subjects showing greater than a 13 point reduction in their TFI scores.

Conclusion

Bimodal auditory-somatosensory stimulation alters tinnitus circuitry to alleviate tinnitus in human subjects and could be a safe and effective treatment for a large number of tinnitus patients.

1. Levine, R., Somatic modulation of Tinnitus appears to be a fundamental attribute of tinnitus. Proceedings of the 6th International Tinnitus Seminar, Cambridge UK., 1999. 1: p. 93-197.
2. Koehler, S.D. and S.E. Shore, Stimulus timing-dependent plasticity in dorsal cochlear nucleus is altered in tinnitus. *Journal of Neuroscience*, 2013. 33(50): p. 19647-56.
3. Wu, C., D.T. Martel, and S.E. Shore, Increased Synchrony and Bursting of Dorsal Cochlear Nucleus Fusiform Cells Correlate with Tinnitus. *J Neurosci*, 2016. 36(6): p. 2068-73.
4. Martel, D., C. Wu, and S. Shore, Bimodal stimulation desynchronizes the tinnitus circuit in guinea pigs. *ARO Abstracts*, 2017.

PS 901

Increased Density of Inhibitory Synapses in the Dorsal Cochlear Nucleus of a Rat Model of Noise-Induced Hearing Loss and Tinnitus

Christopher Neal; Andrea Freemyer; Jennifer Nelson-Brantley; Hinrich Staecker; Dianne Durham
University of Kansas Medical Center

Background

Tinnitus is the perception of sound with no corresponding external stimulus. A probable neural correlate of tinnitus is hyperactivity in central auditory nuclei, including the dorsal cochlear nucleus (DCN). Hyperactivity can be the result of a loss of inhibition and/or an increase in excitation. In a rat model of noise induced hearing loss

(NIHL) and tinnitus, we labeled pre-synaptic (Vesicular GABA/Glycine Transporter, VGAT) and post-synaptic (Gephyrin) components to examine frequency-specific changes in inhibitory synapse density related to NIHL deficits and/or tinnitus.

Methods

Adult male, Long-Evans rats were anesthetized using isoflurane; unilaterally exposed to a 118dB, 16 kHz pure-tone for 4 hours; and then allowed to recover for two weeks. Pre-exposure and post-exposure auditory brainstem response (ABR) and gap detection data (GD) were also collected for all rats. Following the 2-week recovery period, rats were sacrificed, perfused and brain tissue was collected. The DCN ipsilateral to the sound exposed ear was serially sectioned, and the median section was processed for immunohistochemical labeling using antibodies against VGAT and Gephyrin. Labeled tissue was imaged using confocal microscopy. The density of puncta with co-localized labels was quantified as a function of layer location and (molecular, fusiform, or deep) and frequency (low ~ 2 kHz, mid ~ 16 kHz, and high ~48 kHz).

Results and Conclusion

Animals were sorted into tinnitus negative and tinnitus positive groups based on their startle reflex (intact reflex = tinnitus negative, n=5; impaired reflex = tinnitus positive, n=5). A subgroup of animals (n=3) demonstrated severely impaired start reflexes (>2 standard deviations above control, n=4). All tinnitus positive rats demonstrated impaired startle reflexes at 16 kHz and 20 kHz backgrounds, but not 12 kHz. All sound exposed rats, regardless of tinnitus status, exhibited significantly elevated hearing thresholds, relative to their baseline ABRs, at 11.3, 16, 22.6, and 32 kHz. Tinnitus positive rats exhibited significantly elevated thresholds at 8 kHz. At 16 kHz rats with severely impaired startle reflexes had significantly increased thresholds relative to tinnitus negative rats. For all tinnitus positive rats, we observed significant increases in the density of inhibitory synapses in the molecular layer of the DCN in both high and mid frequency regions. In the mid frequency fusiform layer, all tinnitus positive rats showed significant increases in inhibitory synapses over controls and tinnitus negative animals. These unanticipated findings may be clarified by analogous, in-progress work quantifying excitatory synapse density.

PS 902

Expression of NMDA Receptor Subunit 2B After Administration of Korean Red Ginseng in Salicylate-induced Ototoxic Rat Model

Jae Joon Han¹; Woongsang Sunwoo¹; Mun Young Chang²; So Young Kim³; Young Ho Kim¹

¹Department of otorhinolaryngology, Seoul National University College of Medicine, Seoul National University Boramae Medical Center; ²Department of Otorhinolaryngology-Head and Neck Surgery, Chung-Ang University College of Medicine, Seoul, Republic of Korea; ³Department of Otorhinolaryngology, Bundang CHA Medical Center

Background

Sodium salicylate (SS) is often used to make the tinnitus animal model. The protective effect of Korean Red Ginseng (KRG) against the salicylate-induced ototoxicity has not been studied previously. The present study was performed to investigate changes of expression levels of N-methyl D-aspartate receptor subunit 2B (NR2B) protein in inferior colliculus (IC) after administration of SS and/or KRG in rats, and to evaluate the protective effect of KRG in salicylate induced tinnitus.

Methods

Male Sprague-Dawley rats were divided into 4 groups and treated as follows: control group (vehicle); SS group (sodium salicylate, 300 mg/kg, 5 days, IP); KRG-SS group (KRG gel extract, 200 mg/kg, 12 days, PO). Auditory brainstem responses (ABRs) were recorded at pre-treatment and 12 days posttreatment. Whole brains and inferior colliculus were harvested for immunohistochemical staining and Western blot assay using anti-NR2B antibody.

Results

There was no significant difference of mean ABR thresholds among groups before and after treatment. Western blot assay for anti-NR2B antibody of IC in SS group and KRG-SS group demonstrated the higher expression compared to in control group. However, the expression level in SS group did not show the significant difference compared to that in KRG-SS group. Immunohistochemical staining for anti-NR2B antibody in IC showed a higher expression level in SS group compared to in control group, whereas there was no difference between SS group and KRG-SS group.

Conclusion

Salicylate-induced ototoxic rat model demonstrated over-expression of NR2B protein in IC. However, the administration of KRG did not show the significant reduction of protein expression level of NR2B in IC in re-

sponse to administration of salicylate. These findings suggest that KRG may not have the protective effect on salicylate induced tinnitus and NMDA receptor expression.

PS 903

The Mechanisms of Noise-Induced Insulin Resistance in Skeletal Muscle in Mice

Lijie Liu¹; Shuangfeng Cao²; Yongfang Wang¹; Shengwei Li¹; Jun Sha¹; Mingming Zha¹; Min Guo¹; Cong Fang²; Yi Huang²; Guang-Di Chen³; Jian Wang⁴

¹Medical College, Southeast University; ²Institute of Life Sciences, Southeast University; ³Center for Hearing & Deafness, Department of Communicative Disorders and Science, State University of New York at Buffalo; ⁴School of Human Communication Disorders, FHP, Dalhousie University

Background

Epidemiological studies have revealed that noise exposure may increase risk of type 2 diabetes mellitus (T2DM). We have found that noise exposure induced insulin resistance in skeletal muscle in mice. However, the underlying mechanisms are still elusive. The aim of the present study is to explore noise-induced processes underlying the impaired insulin sensitivity.

Methods

192 male ICR mice were randomly assigned into four groups for noise exposure. The N20D-group (n=48) were exposed to the broadband noise at 95 dB SPL for 4 h per day for 20 days; N10D-group (n=48) for 10 days; N1D-group (n=48) for 1 day. The control group (n=48) received no noise exposure. Each group of mice were further divided into 3 subgroups for systemic insulin sensitivity evaluation at 1 day, 1 week, and 1 month post-noise exposure by insulin tolerance tests (ITT). Several insulin-related processes including phosphorylation of Akt (the pleiotropic kinase essential for most of the metabolic actions of insulin), IRS1 (insulin receptor substrate 1, the main mediator of insulin signaling in skeletal muscle) and JNK (stress-responsive Jun-N-terminal kinase which has been recognized as a crucial link between stress and insulin resistance) in skeletal muscle of the animals were examined by standard immunoblots in each animal. Meanwhile, circulatory levels of corticosterone (a biomarker of stress), TNF- α and IL-6 (inflammatory cytokine), and levels of SOD, CAT, MDA (oxidative stress) in skeletal muscle were also measured by chemical analysis.

Results

(1) While a transient systemic insulin resistance was observed in N1D-group, a prolonged insulin resistance

was observed in N10D- and N20D-groups. (2) The noise exposure lead to an enhanced JNK phosphorylation and IRS1 serine phosphorylation and a blunted Akt phosphorylation in response to exogenous insulin stimulation. (3) Plasma corticosterone level was significantly increased in all noise groups. (4) The levels of plasma inflammatory cytokines (TNF- α and IL-6), activity of CAT and concentration of MDA in skeletal muscle were elevated after noise exposure, but no change for SOD.

Summary

Noise exposure induced insulin resistance in mice. The noise-induced insulin resistance may be mediated by JNK, IRS1, and Akt-involved signaling pathways. The noise-induced oxidation and stress may initiate the processes.

PS 904

How to Best Measure Physiologically Tinnitus Induced by Salicylate in Rats?

Sylvie Cosnier-Pucheu¹; Philippe PLC. Larroze-Chicot¹; Aurore Marie²; Veronique Baudoux¹; Noelia Montejo³; Maïda Cardoso⁴; Amandine Laboulais⁴; Christophe Coillot⁵; Guillaume Dupont⁴; Pauline de Pellegars⁴; Eric Alibert⁴; Yves Cazals⁶; Arnaud Norena³; Christophe Goze-Bac⁴; Sergio Gonzalez¹
¹CILcare; ²Cilcare; ³Aix-marseille University and CNRS; ⁴BionanoNMRI, CNRS, University of Montpellier; ⁵L2C-BionanoNMRI, CNRS, University of Montpellier; ⁶Aix-marseille University and CNRS, LNIA UMR7260

Tinnitus, the perception of a “phantom” sound in the absence of external stimulation, is a common consequence of damage to the auditory periphery. It affects around 15% of the population and may induce intolerable discomfort. Today, no treatment exists to cure tinnitus. Some candidate drugs are in the process of being developed and several have to be tested in animal models but it remains very difficult to detect tinnitus objectively and quantitatively in animals.

Objectives

The objective of this study is to search for reliable and valid experimental measures of the presence of tinnitus in order to promote the development of treatments against tinnitus. Aspirin consistently induces tinnitus at high doses. Using this salicylate model, we explored three different techniques to detect salicylate-induced alterations. Salicylate was administered in Long Evans rats by i.p. administration during 4 days.

Preliminary results

The silent gap prepulse inhibition of acoustic startle reflex (GPIAS) was measured (Turner et al., 2006). In control animals, a silent gap in a constant acoustic background inhibited the subsequent startle response to a very loud sound burst. Two hours after salicylate treatment we observed less silent gap induced inhibition of the acoustic startle.

Tinnitus must be associated with alterations in brain functioning. In this perspective we examined electrophysiological alterations at the auditory cortex using recordings of spontaneous activity and evoked responses from microelectrodes in ketamine anesthetized rats. Our results showed an increase in amplitude of cortical responses evoked by tone bursts over a wide range of frequencies and intensities, changes in spectral profile of local potentials, and an increase of spontaneous spike rates after salicylate administration.

Finally, using MEMRI together with local 0.2mg/kg transtympanic MnCl₂ administration (24h before) at the cochlear round window, we observed that salicylate increased MRI signals in different brain structures as compared with controls.

Conclusion

We obtained reproducible results with each technique. We intend to further develop our research and to finally validate our measures by comparison with operant conditioning experiments in the same animals. Psychophysical equivalents of GPIAS may be used in humans. New chemical developments of Manganese compounds for administration in MRI suggest a putative translation to humans.

Vestibular: Physiologic Drivers of the Vestibular Periphery

PS 905

High Frequency Threshold Dependence in Bone Conduction Vibration Indicates the Possible Mechanism of Vestibular Hair Cell Stimulation

Wally Grant¹; Ian Curthoys²

¹Dept. Biomedical Engineering and Mechanics, VA Tech, Blacksburg, VA; ²Univ of Sydney

Introduction

Vibrator stimulus head acceleration and frequency were measured in Bone Conduction Vibration (BCV). Neurons activated by BCV are irregular neurons emanating from the striolar region of utricle and saccule from Type I Hair Cells (HC). These HC bundles are free standing in endolymph fluid or weakly bound to the Otoconial Layer

(OL), and can be freely moved by the endolymph fluid movement that is initiated by the sinusoidal BCV stimulus.

Methods

Neural data was extracellular recordings of irregular primary utricular afferents (Curthoys et al. 2016) to multiple frequencies. Vibration stimulus was delivered by a Radioear B-71 that was cemented to the skull. A triaxial accelerometer, also cemented to the skull, measured BCV accelerations. The vector sum of the three components of accelerations formed the rms-acceleration stimuli values. At each frequency the threshold acceleration was measured from extrapolating of a linear firing rate-BCV intensity function down to no response. Sinusoidal BCV acceleration stimulus was integrated twice to obtain HC deflection δ where the amplitude is A/ω^2 . Threshold bundle deflection δ_t accompanied by threshold acceleration stimulus amplitude A_t is $\delta_t = A_t/\omega^2$; as ω increases, the stimulus amplitude A_t for threshold detection by the hair cell bundles must increase in order to reach the threshold stimulus bundle deflection δ_t . For any given Type I HC bundle the value of the quotient A_t/ω^2 will remain a constant.

Results

Threshold BCV stimulus accelerations at frequencies from 300 - 2000 Hz were measured and the mean value was $\delta_t = A_t/\omega^2 = 6.27E-8 \text{ m} = 1.783E-7 \text{ g-rms/Hz}^2$. The bundle deflection for threshold stimulation = 5 nm (Geleoc et al. 1997)) and using the stimulation frequency, the mean threshold acceleration stimulus magnitude is $(A_t)_{\text{Bundle}}/(\omega)^2 = 1.422E-8 \text{ g-rms/Hz}^2$. The mean threshold acceleration amplitude A_t to mean BCV threshold bundle acceleration stimulus ratio is $(A_t)_{\text{Bundle}}/(A_t)_{\text{BCV}} = 0.08$, or approximately 92% of the initial BCV acceleration is attenuated in its conduction to the Type I bundles.

Conclusions

The amplitude of the threshold stimulus $\delta_t = A_t/\omega^2$ proves to be constant from 300-2000 Hz. That suggests: (1) that at high frequencies it is fluid displacement that is driving the Type I bundles, not fluid velocity, or acceleration; (2) the stimulus amplitude is attenuated by approximately 92% in the transmission from skull to HC bundle.

PS 906

5 MHz Pulsed Ultrasound Activates Vestibular Organs Through Acoustic Radiation Force

Marta Iversen; Jessica Chen; Douglas Christensen; Dennis Parker; Micah Fereck; Holly A. Holman; Richard D. Rabbitt
University of Utah

Introduction

Packets of 5 MHz ultrasound focused on vestibular organs through the perilymph evoke action potentials in first-order vestibular afferents that track stimulus strength, direction, and timing. In the present study, we examined the mechanism(s) responsible for vestibular activation by ultrasound. High intensity focused ultrasound delivers heat to tissue and is used to ablate regions of tissue through thermal necrosis. Ultrasound also generates a mechanical radiation force arising from both ultrasound absorption and reflection by changes in tissue acoustic impedance. Results determine the relative contributions of the mechanical and thermal components, and provide a new method to selectively activate vestibular organs.

Methods

Focused ultrasound packets were delivered to the utricle, saccule, and crista ampullaris in the oyster toadfish using a focused ultrasound transducer. Ultrasound packets at 5 MHz were delivered at rates of 0.1-2000 pps over a range of stimulus strengths (0.5-1000 kPa). Single-unit afferents were recorded in vivo and analyzed for vector strength and discharge rate. The acoustic radiation force and temperature were measured as functions of ultrasound parameters in excised tissue by directing focused ultrasound at each organ.

Results

Saccular afferents responded robustly, often phase locking to the onset (or off-time) of each ultrasound packet. Phase locking was to packet repetition rate, not to 5 MHz ultrasound. Responses of utricular afferents were weaker, and rarely detectable in semicircular canals. The lack of robust responses in canals, sensitivity to direction, and the small size of the temperature rise, ruled out heat as the primary mechanism. The delay to action potential was less than 1 ms, also implying direct mechanical activation of transduction currents. The acoustic radiation force measured due to ultrasound was three orders of magnitude greater on the saccular otolith than the utricular otolith and canals, and two orders lower in the canals alone. The magnitude and direction of the acoustic radiation force was sufficient to explain afferent responses.

Conclusion

Otolith organs were activated by pulsed 5 Mhz ultrasound with primary afferents phase locking at high vector strength. Afferent responses were sensitive to the ultrasound direction and occurred primarily in the otoliths, consistent with acoustic radiation force origin. The radiation force arose primarily from the ultrasound reflection at the acoustic impedance mismatch of endolymph and the otolithic mass rather than absorption. Focused ultrasound provides a new means to selectively activate vestibular organs with potential applications in basic science, clinical assessment, and therapeutics.

Funding

NIDCD R01 DC006685 (Rabbitt)

PS 907

Characterization of Vestibular Microphonic Recordings in Guinea Pigs

Christopher J. Pastras¹; Ian Curthoys²; Daniel J. Brown¹

¹*The University of Sydney*; ²*Univ of Sydney*

Background

The Cochlear Microphonic (CM) and Vestibular Microphonic (VM) were first reported in 1930 and 1934, respectively. The CM has been used extensively in auditory research to study auditory physiology and pathology. Conversely, the VM has only featured in a handful of publications mostly involving non-mammalian and ex vivo models. Trincker (1959) was the first to report in vivo mammalian recordings of the VM, detailing the effects of recording location, stimulus frequency, depth, surgical destruction, and cooling. Apart from a hand-full of other studies, mostly performed ex vivo, much remains to be learnt about the vestibular system from studying the VM.

Objective

To further develop, characterise, and investigate features of the VM, measured in vivo in guinea pigs.

Methods

The VM was recorded from the basal surface of either the utricular or saccular macula, after surgical removal of the cochlea, recorded either via low impedance glass micropipettes or AgCl electrodes. Responses were evoked by Bone-Conducted Vibration (BCV), of various frequencies and levels, delivered via a Radioear B-81 tightly secured into the ear-bar.

Results

The VM persisted after vestibular nerve blockade with TTX, but was completely abolished following destruction of the maculae, or death of the animal. The VM reversed polarity as the electrode was tracked across the utric-

ular or saccular macula surface, suggesting that either the VM is a highly-localized response whose polarity is determined by the orientation of the kinocilium at the recording location, or that the VM is the summated response of spatially distant hair cells, whose response properties differ. That the polarity of the VM reversed as the glass micropipette electrode penetrated through the utricular macula, supports the VM being a localized response. Similar to the results reported by Trincker, we found the VM could be evoked by BCV stimuli of frequencies greater than 2kHz, although in our experimental setup, the response was most sensitive to vibrations of 700Hz. Our preliminary recordings demonstrate changes in the VM with potassium toxicity, displacement of the maculae, rupture of the utricular membrane, whole-body tilt, and galvanic stimulation.

Conclusions

VM recordings in guinea pigs can be performed with relative ease. The frequency response supports recent studies which demonstrated the vestibular hair cells are sensitive to vibrations of several kilohertz. Changes in the response with displacement of the macula, or ruptures of the otolithic membrane, suggest hydrops of the utricle may alter its sensitivity due to either mechanical or ionic changes.

PS 908

Analysis of Vestibular Function in Calcium and Integrin Binding Protein 2 (CIB2) Mutant Mice, a Model for Usher Syndrome Type I Gene.

Arnaud P.J. Giese¹; Naoki Shimizu²; Beau Vandiver²; Rebecca Cook²; Saima Riazuddin³; Tomoko Makishima²; Zubair Ahmed¹

¹Department of Otorhinolaryngology Head & Neck Surgery, School of Medicine University of Maryland, Baltimore, MD, 21201, USA; ²Department of Otolaryngology, University of Texas Medical Branch; ³Laboratory of Molecular Genetics, Department of Otorhinolaryngology Head & Neck Surgery, School of Medicine, University of Maryland, Baltimore, MD, USA.

Background

A mutation in CIB2 gene causes Usher syndrome type 1 characterized by pre-lingual deafness, vestibular ataxia, and pre-adolescent development of visual dysfunction (Riazuddin et al, 2012). CIB2 plays a crucial role in maintaining mechano-electrical transduction in the cochlear hair cells (see accompanying presentation by Giese et al. ARO 2017). Our goal here was to characterize the vestibular function in a transgenic strain of Cib2 mice (Cib2F91S), which contains a mutation that leads to hearing loss in humans.

Methods

Vestibular function of Cib2F91S mice was assessed by vestibular ocular reflex (VOR). Results were compared among genotypes. Vestibular hair cells (VHCs) were observed in whole mount preparations and their mechanotransduction function assessed by FM1-43 uptake. Expression of Cib genes (Cib1-4) was analyzed by RT-qPCR in Cib2 mutant mice, while the immunostaining followed by confocal microscopy was performed for protein localization.

Results

VOR gain and phase was similar in all groups. In the homozygous mutant mice, VHCs were intact. The stereociliary bundle morphology was not affected and the staircase pattern of stereocilia was maintained. Consistent with VOR results, the mechanotransduction function of VHCs was maintained and VHCs were able to uptake the FM1-43 dye in Cib2F91S vestibular explants. RT-qPCR analysis revealed that, in contrast to the cochlear tissues, Cib3 is significantly up-regulated in the vestibular system of Cib2 mutant mice. Immunolocalization studies for CIB3 revealed that it is localized in the VHCs and at some extent present in the VHC stereociliary bundle.

Conclusions

Cib2F91S mutant mice do not have vestibular dysfunction at 3 month of age, and are comparable to wild type mice. The up-regulation of Cib3 in Cib2 mutant mice suggests that there may be functional redundancy among the CIB family members.

Supported by NIDCD/NIH (K08DC011540 to T.M., and R01DC012564 to Z.M.A.)

PS 909

Characterizing Vestibular Efferent Innervation Patterns in alpha4, alpha6, or beta2 nicotinic ACh Receptor Knockout Mice

Joseph C. Holt; Paivi M. Jordan; Mosaheb Mujeeb; Zijie Sha
University of Rochester

The efferent vestibular system (EVS) begins as a modest number of neurons in the dorsal brainstem, whose axons project to the vestibular periphery to give rise to numerous varicosities synapsing on hair cells and afferent terminals. A preponderance of pharmacological data in several vertebrate species including mice, indicate that the response of vestibular afferents to EVS stimulation relies on the activation of distinct cholinergic mechanisms at each one of these synaptic locations. The rapid excitation of vestibular afferents is thought to require the activation of $\alpha 4\alpha 6\beta 2$ -containing nicotinic ACh receptors

while efferent-mediated inhibition of vestibular afferents utilizes $\alpha 9\alpha 10$ nAChRs and SK2 potassium channels in type II vestibular hair cells. Not surprisingly, the ablation of $\alpha 9$, $\alpha 10$, or SK2 proteins in the peripheral auditory system of mice is associated with a change in the size and number of presynaptic efferent terminals on cochlear hair cells and a loss of function. However, similar studies have not been done in the EVS. To gain further insight into the functional organization of the mammalian EVS, we have begun to characterize peripheral EVS innervation patterns in transgenic mice lacking either the $\alpha 4$, $\alpha 6$, or $\beta 2$ nAChR subunit.

Standard fluorescent immunohistochemical studies were performed on both whole and sectioned vestibular end organs to determine if the peripheral morphology of EVS neurons was altered in these mutant animals. In this study, we used antibodies to choline acetyltransferase (ChAT) to stain EVS neurons and a number of other antibodies to selectively counterstain hair cells and afferents. Visual inspection of stained specimens demonstrated that the vestibular end organs of $\alpha 4$ -, $\alpha 6$ -, or $\beta 2$ nAChR subunit-deficient mice expressed a robust and extensive ChAT-positive EVS innervation. Preliminarily, ChAT-positive staining in $\beta 2$ nAChR knockout mice suggested that the size and number of efferent varicosities differed from controls, while there were no obvious distinctions between EVS terminal fields of either $\alpha 4$ - or $\alpha 6$ nAChR knockout (KO) and control animals. We are currently quantifying the number and size of EVS varicosities in each strain to determine if they, in fact, do vary. More work is needed to confirm our preliminary observations, but provided that these subunits are used to construct functional nAChRs on vestibular afferents, changes in peripheral EVS innervation may be more distinct in $\beta 2$ nAChR-KO animals given its obligatory requirement for the assembly of functional neuronal nAChRs. In contrast, loss of the $\alpha 4$ nAChR unit may be compensated by $\alpha 6$ nAChR subunits, or vice versa.

PS 910

Expression of Kir4.1 Channels in Vestibular Epithelia

Kenny D. Rodriguez¹; Frances L. Meredith¹; Katherine J. Rennie²

¹University of Colorado School of Medicine; ²UC Denver School of Medicine

Background

Kir4.1 channels mediate weak inwardly rectifying currents and serve to remove excess extracellular potassium in several cell types including central glia and supporting cells in the cochlea. Immunohistochemical data suggest Kir4.1 is localized to calyx terminals encasing

type I hair cells in vestibular neuroepithelia (Udagawa et al. 2012). It is also known that in Kir4.1 knockout mice there is a degeneration of type I hair cells, without loss of type II cells (Rozengurt et al. 2003). We investigated the expression of Kir4.1 channels that may mediate potassium buffering at vestibular hair cell synapses.

Methods/Approach

Utricles and cristae were removed from the vestibular system of Mongolian gerbils (postnatal days 8-33) and adult mice. Immunohistochemistry was performed with antibodies to Kir4.1, beta-tubulin III and calretinin to determine the location of Kir4.1 channels with respect to afferent nerve terminals in vestibular epithelia. Whole cell patch clamp recordings were made from isolated cells or cells within vestibular slices. ZD 7288 (100 μ M) was used in some recordings to block known hyperpolarization-activated cyclic nucleotide-gated currents in calyx terminals and hair cells (Horwitz et al. 2014; Meredith et al. 2012) and barium (0.5 mM) was used to test for the presence of inward rectifiers. The tricyclic anti-depressants (TCAs) desipramine and nortriptyline selectively inhibit channels containing Kir4.1 subunits (Su et al. 2007) and were applied extracellularly at 100 micromolar. At higher concentrations TCAs may also block Kir2.1-mediated currents.

Results

Whole cell currents were recorded in voltage clamp in hair cells and calyx terminals. Desipramine and nortriptyline blocked inward currents in both type I and type II hair cells by 51-63 %, consistent with the expression of potassium-selective inward rectifiers. Inwardly rectifying currents in calyx terminals were enhanced when external potassium was increased from 5 to 40 mM, however these currents were not blocked by barium or desipramine. Using confocal fluorescent microscopy, Kir4.1-like immunoreactivity was seen at the type I hair cell/calyx synapse as described previously. In addition, immunoreactivity was also observed in other cell types within the neuroepithelium.

Conclusions

Our electrophysiological recordings suggest inwardly rectifying currents with pharmacological properties consistent with Kir4.1 are present in vestibular hair cells, but not calyx terminals. Kir4.1 channels may play an important role in controlling potassium levels in the vestibular synaptic cleft.

Funding

Supported by NIH/NIDCD T32 DC012280 and the Hearing Health Foundation

PS 911

Kv4.3 is a Candidate Ion Channel for an A-current Recorded in Vestibular Calyces

Anna Lysakowski¹; Jay Goldberg²; Steven D. Price¹

¹*Department of Anatomy and Cell Biology, University of Illinois at Chicago, Chicago, IL, USA;* ²*University of Chicago*

Regularly and irregularly discharging vestibular afferents can be distinguished by their epithelial location and by the prominence of their after-hyperpolarizations (AHPs) (Goldberg, 2000). AHPs are of interest as they may determine discharge regularity and afferent gain (Smith and Goldberg 1986; Goldberg 2001; Goldberg and Holt 2015). Deeper and slower AHPs are associated with the regular discharge and low gain of dimorphic units located in the peripheral/extrastriolar zones of vestibular endorgans, in contrast to the smaller, more rapid AHPs leading to the irregular discharge and high gain of both pure calyx and dimorphic units in the central/striolar zones. Here, we studied ion channels that can mediate AHPs, including an A current (KV4.3), an SK channel (SK2) and an HCN channel (HCN2), using confocal immunohistochemistry and/or EM immunogold.

Using a KV4.3 antibody, we found virtually no KV4.3 labeling in the central/striolar zones of cristae and macular organs. The inner faces of calyx endings in the peripheral/extrastriolar zones were lightly labeled, while boutons on calretinin-positive type II hair cells were intensely labeled. These boutons in the peripheral zone were likely to be afferent boutons, presumably arising from dimorphic afferents, rather than efferent, endings because of their differing sizes and large numbers on each hair cell (cf. Lysakowski and Goldberg, 1997). In the calyx endings, labeling of KV4.3 overlapped with that of Caspr1 at the edge of Domain 1 (Lysakowski et al., 2011). Since Caspr1 is confined to the inner faces of calyx endings (Sousa et al., 2009; Lysakowski et al., 2011), the overlap indicates that KV4.3 is similarly confined. We further confirmed that the immuno-labeled boutons were afferent, rather than efferent, by labeling the efferent boutons with ChAT and synapsin antibodies. There was no overlap between the ChAT/synapsin and the Kv4.3 immuno-labels.

SK2 antibodies also labeled the unmyelinated portion of parent axons more intensely in the peripheral/extrastriolar zones, than in the central/striolar zones. HCN2 was present in calyx endings throughout the epithelium with the labeling being heavier peripherally, compared to the central zones.

In conclusion, we studied several ion channels that can mediate AHPs, including an A current (KV4.3), an SK

channel (SK2) and an HCN channel (HCN2). These were mostly localized to a greater extent in the peripheral zones of vestibular endorgans, which is where deeper and slower AHPs are associated with the regular discharge and low gain of dimorphic units.

Supported by NIH R01 DC-002058.

PS 912

Effects of KCNQ Blockade on Peripheral Vestibular Function

Choongheon Lee¹; **Joseph C. Holt²**; **Timothy A. Jones¹**

¹*University of Nebraska-Lincoln;* ²*University of Rochester*

Introduction

In many neural systems, KCNQ channels (Kv7 family) mediate an M-like current consisting of a low voltage-activated outward K⁺ current which is modulated by acetylcholine (ACh) and the activation of odd-numbered muscarinic acetylcholine receptors (i.e. m1, m3 or m5 mAChRs). In the peripheral vestibular system, mAChRs and KCNQ channels are expressed by calyceal endings in vestibular neuroepithelia suggesting that they may be targeted by the cholinergic efferent vestibular system (EVS). Although single unit recordings from turtle and mouse vestibular afferents during EVS stimulation and pharmacological interrogation have confirmed a role for mAChRs and KCNQ channels, we wanted to further understand how modulation of KCNQ channels might be used to modify vestibular function.

Methods

Vestibular sensory evoked potential (VsEPs) were used to evaluate macular function following blockade of KCNQ channels by XE991. VsEPs were measured in anesthetized C57BL/6J mice before and after drug administration. Effects of nine single doses of XE-991 ranging from 0.05 to 50 mg/kg were evaluated. Response threshold, onset latencies and amplitudes were used to quantify effects on vestibular function

Results

XE-991 produced profound changes in VsEP responses. At doses greater than 1 mg/kg a brief period of enhancement was followed by a significant dose dependent degradation of responses including prolonged latencies, reduced amplitudes and elevated thresholds. Changes reached steady values within ~20 minutes of injection and remained stable thereafter. Responses were eliminated in 2/5 animals at 50mg/kg. The ED50 for these effects ranged from 3.9 to 4.9 mg/kg. At doses

below 2.5 mg/kg, a dose dependent stable response enhancement was seen.

Conclusions

Our findings in vivo demonstrate a dose dependent degradation of the dynamic macular response to transient stimuli. Kalluri et al., 2010 showed in vitro that XE-991 transforms irregular afferents into more regular tonic afferents and this transformation would account for our findings. The present findings suggest that KCNQ channels play a critical role in vestibular function and their regulation by efferent action via mAChRs may function to adjust the dynamic response characteristics of vestibular afferents.

PS 913

Cellular Adaptations of Crista Epithelia in Egyptian Fruit Bats

Larry Hoffman¹; Ymi Ton²; Kristel Choy²; Walter Metzner²

¹Department of Head & Neck Surgery; ²Department of Integrative Biology and Physiology

A longstanding question in vestibular neuroscience concerns the adaptations of the peripheral sensory epithelia driven by different behavioral repertoires. Though these may be expected to be evident in bats by virtue of their flight and/or echolocation behaviors, previous studies failed to identify architectural differences in bat labyrinths compared to other rodents. Through the present study we tested hypotheses that the distributions of hair cell types, oncomodulin expression, and KCNQ4 expression were similar in the central zones (CZ) of cristae from Egyptian fruit bats (*Rousettus aegyptiacus*) and mouse. Immunohistochemical strategies and confocal microscopy were utilized to identify central zone calyces (using anti-calretinin, Calb2), all calyces (using anti-beta-3-tubulin, Tubb3), oncomodulin-positive hair cells (using anti-Ocm), and KCNQ4-positive calyces (using anti-KCNQ4). Bootstrap resampling analyses were utilized to test hypotheses that the empirical distributions of each tested characteristic (e.g. type I and II hair cells) from one species (e.g. *Rousettus*) could be drawn from random sampling of the other species (e.g. mouse). Probabilities < 0.05 supported rejection of a specific hypothesis, indicating that the characteristic under analysis was different in the two species. As found for utricular striolae (Choy et al., ARO Abs. 2016), the distributions of CZ type I and II hair cells were markedly different in *Rousettus* compared to mouse, where type I hair cells comprised approximately 85% of CZ hair cells in *Rousettus* compared to only 60% in mouse. Among type I hair cells, the fraction associated with Calb2-positive calyces was lower in *Rousettus* compared to mouse

(i.e. ratio of type I:II is lower in *Rousettus* compared to mouse). In both *Rousettus* and mouse, all CZ type I hair cells were positive for Ocm expression, while Ocm expression in type II hair cells was quite different in each species. Very few type II hair cells were Ocm-positive in *Rousettus* CZ, while in mouse approx. 60% of CZ type II hair cells were Ocm-positive. Additionally, Ocm expression in *Rousettus* cristae was found outside the CZ, while it was largely confined to the CZ in mouse cristae. In both *Rousettus* and mouse cristae KCNQ4 expression was found in virtually all calyces, although was markedly higher in all CZ calyces. We observed a modest expansion of high expression of KCNQ4 in calyces immediately outside the CZ in *Rousettus*, whereas it was confined to CZ calyces in mouse. Summarily, these data indicate prominent cellular adaptations that likely enhance head movement coding associated with flight and/or echolocation.

PS 914

Unifying Model of Vestibular Afferent Discharge Supports the Implementation of Sensory State-Dependent Probabilistic Inference.

Larry Hoffman¹; Michael Pauliin²; Kiri Pullar²

¹Department of Head & Neck Surgery; ²Department of Zoology; University of Otago; Dunedin, New Zealand

We are investigating models of how probabilistic inference could be implemented in spiking sensory neurons, for which the afferent vestibular system is optimally suited. These sensory data are modeled as random samples drawn from probability distributions whose parameters are kinematic head state. The first stage of investigating how the inference problem may be solved in neural circuits would be to elucidate a unifying model of discharge statistics at a given sensory (i.e. head movement) state. Fortunately, afferent vestibular neurons exhibit a rich heterogeneity of discharge among the afferent ensemble (e.g. approx. 1800 afferents projecting from each crista in the chinchilla) even when the head is at rest, representing the “null” head movement state (aka spontaneous discharge). The simplest such model of discharge at this state would be a Poisson process, and while previous studies have proposed Gamma distributions (i.e. a special case of a Poisson process) the postspike refractory period cannot be accommodated as a natural parameter of the fitted model. We have previously shown that convolution of a Gamma process to “censor” a Poisson distribution of interspike intervals provides an outstanding analytical solution that accommodated the refractory delay. In this present study we show that censoring the Poisson distribution with an inverse Gaussian process, also known as a Wald distribution (the convolution is called an exWald distribution),

provides overall better fits of the interspike interval distributions for the ensemble of >300 semicircular canal afferents recorded from anesthetized chinchillas, representing a broad range of distributions and resultant tau parameters. The inverse Gaussian process arises naturally from Brownian motion with a drift, and therefore offers a more natural theoretical application to biological processes. These data and analyses further demonstrate that stable sensory state can be represented by a unifying Poisson process, which is optimally suited for probabilistic inference. The censoring mechanism offers the advantage of limiting discharge rate, thereby saving the high energetic cost of high spike rates, though signal bandwidth is compromised. However, signal bandwidth can be recovered through the stochastic nature of the large ensemble of afferent neurons.

PS 915

Bilateral Eye Movements Evoked by Frequency Modulated Infrared Neural Stimulation of Single Vestibular Organ

Weitao Jiang¹; Suhrud M. Rajguru²; Claus-Peter Richter³

¹University of Miami Department of Otolaryngology;

²Departments of Biomedical Engineering and Otolaryngology; University of Miami; FL; ³Department of Otolaryngology-Head and Neck Surgery, Feinberg School of Medicine, Northwestern University & Resonance Medical, LLC, Chicago

Background

Bilateral vestibular dysfunction in patients leads to postural instability and chronic disequilibrium. Infrared neural stimulation (INS) has been investigated as an alternative neurostimulation modality that does not require direct contact with neural tissue and has been shown to produce significant post-synaptic afferent responses in the vestibular system. In the present study, we investigated the bilateral eye movements evoked by frequency modulated pulsed infrared stimulation of the vestibular system.

Method

All procedures were approved by the University of Miami Institutional Animal Care and Use Committee. Bilateral eye movements were recorded in Long-Evans rats anesthetized with ketamine (44 mg/kg) and xylazine (2.5 mg/kg). The animal was placed in a custom-designed modified Kopf stereotaxic frame. A head post was cemented to the skull to secure the animal's head during stimulation and recording procedures. Eye movements were recorded using a video-based eye tracking system (ISCAN inc, Woburn, MA) and a custom MATLAB program was used for analysis. Frequency modulated

infrared stimulation (1863nm, 200µs, 250pps, different radiant exposures and modulated between 0.05-1Hz) was delivered to the vestibular endorgans approached by drilling away the dorsal bony wall of the posterior ampulla. A custom designed 3-channel fiber bundle was used to deliver infrared radiation. Following the measurements, the fibers were fixed in place with dental acrylic and orientation and distance of the typical optical fiber placement relative to vestibular structures were determined using Microcomputed Tomography (Micro-CT).

Results

We observed significant clock-wise in-torsion in the right (ipsilateral) eye evoked by infrared stimulation. The frequency modulated stimuli evoked sinusoidal movements of the ipsilateral eye, whereas the contralateral eye elicited a mix horizontal and vertical movement rostrally. Depending upon the modulation frequency, amplitude of oscillating eye movement ranged from 1 to 7°. At lower modulation frequencies (0.05-0.25Hz), we observed significant eye movements phase locked to infrared stimulation. Highlighting the spatial selectivity of the infrared stimulation, we observed significantly larger eye movements for only one of the three fibers. Micro-CT reconstruction images showed the posterior canal ampullary region to be the target of infrared beam path.

Conclusions

Significant frequency-modulated eye movements continued to be evoked by the infrared stimulation even following 30+ minutes of continuous irradiation. This suggests the feasibility of INS as a potential long-term functional replacement of absent vestibular function. Future experiments will focus on optimizing the parameters of infrared neural stimulation and optimizing surgical approach to target other vestibular endorgans.

Funding

NIH/NIDCD 1R01DC013798 (SMR)

PS 916

Pulsed Infrared Modulates Endoplasmic Reticulum Calcium Cycling in Cultured Spiral and Vestibular Ganglion Neurons

Samantha Rincon¹; Julio Pasos¹; John Barrett¹; Suhrud M. Rajguru²; Suhrud Rajguru¹

¹University of Miami; ²Departments of Biomedical Engineering and Otolaryngology; University of Miami; FL

Background

Pulsed infrared radiation (IR) delivered to cells has been shown to evoke action potentials in neurons and contraction in cardiomyocytes. The mechanisms underlying the cellular responses involve a combination of a capac-

itive current that has been shown to depolarize the cell, intracellular calcium (Ca²⁺) signaling and voltage-independent mechanisms. The primary biophysical mechanism of IR response is not yet completely resolved. In the present study, we studied the intracellular calcium [Ca²⁺]_i responses that accompany the cell depolarization during IR stimulation.

Methods

Inner ear cells were cultured from p3-5 mice and loaded with Ca²⁺ binding fluorescent markers. The Ca²⁺ changes evoked by focused pulsed IR (1863nm, 200pps, 250μs, varied radiant energies) delivered using a 200 or 400 μm optical fiber were measured by tracking fluorescent intensity within cells using a confocal microscope. The images were analyzed with IMAGEJ and MATLAB. Temperature changes induced by IR were measured using Rhodamine B and a microthermistor.

Results

IR pulse trains (2-5 seconds) evoked nuclear and cytoplasmic Ca²⁺ transients (0.20 to 1.4 μM increases) in the irradiated neurons. The transient increases in [Ca²⁺]_i were maintained in extracellular medium containing zero Ca²⁺ and 1 mM BAPTA-AM. The IR pulses caused transient decreases in endoplasmic reticulum (ER) Ca²⁺ in digitonin-permeabilized cells, consistent with IR induced Ca²⁺ release from ER. Agents that block IP3 and/or ryanodine receptors (Xestopongin C and Ryanodine) blocked the IR-induced Ca²⁺ release, whereas at lower concentration of Xestopongin C, Ryanodine and caffeine, the percentage of trails with IR-induced Ca²⁺ release increased. A blocker of the ER Ca-ATPase, cyclopiazonic acid, significantly prolonged the time course of the [Ca²⁺]_i return to baseline following IR. The IR pulses produced a rapid but transient 2-11 °C increase in temperature. Preliminary results also show that INS transiently depolarized ΔΨ_p in the neurons.

Conclusions

The results suggest that ER was the primary source of observed [Ca²⁺]_i during IR neuronal excitation via rapid temperature changes. The persistence of the response in zero Ca²⁺ media indicates that the ER has an important role in Ca²⁺ buffering from the cytoplasm of these neurons. The precise photocontrol of intracellular organelles and signaling pathways altering neural activity using INS could provide high impact applications in neuroscience.

Funding

NIH/NIDCD 1R01DC013798 (SMR)

PS 917

Galvanic Vestibular Stimulation in Alert Primates: Characterizing Nonlinearity in Primary Vestibular Afferent Response to Transmastoid Stimulation

Annie Kwan¹; Diana E. Mitchell¹; Patrick A. Forbes²; Jean-Sébastien Blouin³; Kathleen E. Cullen¹

¹McGill University; ²University of British Columbia/Delft University of Technology; ³University of British Columbia

Galvanic vestibular stimulation (GVS) is a technique where current applied to surface electrodes placed on the mastoid processes behind the ears stimulates the vestibular system and consequently evokes behavioural responses in humans such as: eye movements, postural changes, and the sensation of self-motion. Because GVS is a non-invasive tool that can be used to selectively activate the vestibular system, there is a growing interest in its utility as a clinical tool for the diagnosis of vestibular disorders. In addition, the ability of GVS to drive the vestibular system has potential biomedical applications, such as immersion in virtual reality environments and prevention of motion sickness. To date, however, the physiological mechanisms mediating GVS-evoked responses remain to be fully elucidated. Thus far, the general assumption made in modelling the effects of GVS activation is that the peripheral vestibular system is activated in a linear manner. In the current study, we delivered current to surface electrodes placed behind the ears of macaque monkeys while recording primary vestibular afferent activity in order to investigate whether there are nonlinear mechanisms in early vestibular processing of GVS. Single unit recordings revealed that cathodal and anodal step GVS evoked unbalanced changes in vestibular afferent activity. Notably, response asymmetries were more substantial for irregular than regular afferents, for both the semicircular canal and otolith systems. In addition, we found discrepancies between the rate of increase in afferents' gain and phase as a function of frequency in response to stochastic GVS versus sinusoidal GVS, the latter of which is traditionally applied to study responses using linear system analyses. This finding provides further support our conclusion that the vestibular afferents respond nonlinearly to GVS, which had not previously been explored. We conclude that the effects of GVS upon vestibular afferent responses are more complex than has been generally assumed. Thus, taken together, our findings provide new insights into how GVS activates of the vestibular system, which will be vital to advancing our development of new clinical and biomedical applications.

Cardiorespiratory Responses Induced by Primary Blast to the Ear Are Mediated by the Vagus Nerve

David S. Sandlin; Alberto A. Arteaga; Yue Yu; Lan Chen; Jun Huang; Jerome Allison; Hong Zhu; Wu Zhou
University of Mississippi Medical Center

Background

Primary blast injury, i.e., that due to the pressure shock-wave of a blast, is a frequent cause of injury in both military and civilian populations. Soldiers frequently decline to use hearing protection, citing impairment of situational awareness, leaving their ears exposed during patrols. We hypothesize that the unprotected ear provides a conduit of lower resistance by which primary blast can traverse the skull and impact the brain. To test the ear's role in blast injury, we have developed a blast generator that can be specifically targeted to a small area of tissue with minimal overpressure effect on the surrounding tissues. This novel approach allows for the isolated study of the ear's role in primary blast injury by minimizing confounding factors from blast exposure to other tissues. Previously, we showed that primary blast delivered to rats' unprotected ears resulted in acute bradycardia and tachypnea similar to that seen in whole-body blast exposure, suggesting that the ear provides a vulnerable locus through which primary blast can impact the brain. We noted on ECG tracings that a heart block was induced acutely, suggestive of increased vagal output. In this study, we tested the hypothesis that the vagus nerve mediates the acute cardiorespiratory responses of the ear-only blast exposure paradigm.

Methods

Anesthetized adult male Sprague-Dawley rats were placed under continuous respiratory and cardiac monitoring. In experimental rats, the vagus nerve's cervical segment was ligated bilaterally. In rats receiving sham surgery, the neck was opened and sternocleidomastoid muscles retracted, but the carotid sheath was left intact. After baseline recording for five minutes, rats were then exposed either to primary blasts of 40psi (80% of lethal dose determined in our previous studies) or sham blasts. Cardiorespiratory monitoring continued for 5 minutes after blast exposure.

Results

Rats that underwent bilateral cervical vagus nerve ligation and were exposed to a 40psi blast were not significantly different from those rats that underwent sham blast. Rats that underwent sham surgery and 40psi blast had significantly greater responses than those who received vagal ligation and/or those that received sham blasts.

Conclusions

These data confirm that the vagus nerve mediates the cardiorespiratory responses induced by primary blast exposure isolated to the ear. Ongoing studies use this blast model to further characterize the ear's role in primary blast injury and the mechanisms by which it occurs using single unit recording and histologic examination.

Supported by R01DC014930-01 (WZ), R21EY025550-01 (WZ), R01DC012060-01 (HZ).

PS 919

Vestibular Function Change in Vasopressin-induced Hydrops Model

Minbum Kim

Department of Otorhinolaryngology, Catholic Kwandong University College of Medicine, Incheon, Korea

Objectives

To evaluate the efficacy of a new treatment for hydrops, the traditional hydrops model is not appropriate since it represents only the chronic stage of disease. Recently, a new dynamic model was introduced for acute aggravation of hydrops using the vasopressin type-2-receptor agonist, desmopressin. The purpose of this study was to evaluate vestibular function change in vasopressin-induced hydrops model.

Methods

In two to four weeks after surgical ablation of endolymphatic sacs in guinea pigs, acute aggravation of hydrops was induced by desmopressin (100ug/Kg, SC, VP). Auditory brainstem response (ABR) test and bidirectional sinusoidal harmonic acceleration (SHA) test with an animal rotator were performed before and after VP, respectively. Histologic sections parallel to the modiolar axis were made for observing changes in the Reissner's membrane and endolymphatic hydrops.

Results

In 60 to 90 min after VP, symmetry score on bidirectional SHA tests increased from 6.50 ± 7.60 to $25.23 \pm 9.84\%$ ($p=0.04$). While some animals showed larger response during rotation at the direction of hydrops ear (irritating response), the other showed smaller response (paretic response). Symmetric response was recovered in 120 to 180 min. After In all the animals, endolymphatic hydrops with the distension of Reissner's membrane were histologically observed after VP. Vestibular asymmetry was sustained over 3 h after twice VP injection with 1h interval. After 1st VP, the average symmetry score was 16.30 ± 5.82 (%), and this asymmetry was sustained to $21.38 \pm 6.43\%$ 1h after 2nd VP ($p=0.13$). The symmetry score was recovered to 5.84 ± 2.44 % in 3h after 2nd VP injection. Any animals which had showed paretic

response after 1st VP did not show irritating response after 2nd VP.

Conclusion

VP can transiently induce acute aggravation of hydrops and asymmetric vestibular dysfunction in guinea pigs. This model can be helpful to study a new treatment for the acute attack of hydrops. Furthermore, it might give some clues to explain the mechanism of bidirectional nystagmus in Meniere's disease.

PS 920

Sound-evoked Eye Movements in Awake Rats

Yue Yu; Jun Huang; David S. Sandlin; Alberto A. Artega; William Mustain; Jerome Allison; Lan Chen; Kally Xu; Hong Zhu; Wu Zhou
University of Mississippi Medical Center

Acoustic activation of the vestibular system has been well documented in humans and animal models and has been used to assess vestibular function. However, the underlying neural mechanisms remain to be elucidated. The goal of this study was to establish an awake rodent model for investigating how sound activate the vestibular system. We recorded sound-evoked movements of the left eye in 5 head restrained Long-Evans rats using a video-based eye tracker (ISCAN ETL-200), which measures horizontal and vertical eye positions at 240 frames per second with a spatial resolution of 0.1 degree. Tone bursts (125-4000Hz, 10-40 ms duration, 1 ms rise/fall, 110-130 dB peak SPL) were randomly delivered to the two ears at 5Hz. We found that tone bursts evoked well defined eye movements that were dependent on tone frequency, intensity and duration. In the horizontal direction, tone bursts evoked eye movements moving toward the nose for the ipsilateral ear stimulation, and toward the ear for the contralateral ear stimulation. In the vertical direction, tone bursts evoked upward eye movements for the ipsilateral ear stimulation and downward eye movements for the contralateral ear stimulation. All animals exhibited well-defined tuning curves with peak frequencies at 1-1500Hz. We further showed that tone-evoked eye movements were dependent on initial eye position. These results demonstrate that tone bursts can evoke well-defined eye movements that can be measured by video-based eye tracking devices and used to understand how sound activate different vestibular end organs and the vestibular-ocular reflex pathways. This information will be essential for developing discriminative tests for assessing vestibular function in animal models and humans. (Supported by R01DC014930-01 (WZ), R21EY025550-01 (WZ), R01DC012060-01 (HZ))

PS 921

Noise-induced Peripheral Vestibular Injury Is Associated with Decreased Head Postural Control in Freely Locomoting Rodents

Courtney E. Stewart¹; Ariane Kanicki²; Tarana Joshi³; Catherine A. Martin²; Guo-Peng Wang⁴; Yehoash Raphael⁵; Gabriel Corfas⁴; Richard Altschuler⁶; W. Michael King⁷

¹*University of Michigan, Kresge Hearing Research Institute;* ²*University of Michigan Medical School;* ³*Kresge Hearing Research Institute, University of Michigan;*

⁴*Kresge Hearing Research Institute, The University of Michigan;* ⁵*Department of Otolaryngology-Head and Neck Surgery, Kresge Hearing Research Institute, University of Michigan, Ann Arbor, Michigan, USA;* ⁶*University of Michigan;* ⁷*Department of Otolaryngology - Head and Neck Surgery, University of Michigan*

Introduction

The vestibular system, which plays a critical role in precise detection of head movements and orientation with respect to gravity, is essential for normal postural control and balance. Although clinical reports suggest a link between noise-induced hearing loss and balance problems, the physiology underlying this linkage is not well understood. Since the otolith organs are more susceptible to noise-induced damage than the semicircular canal cristae it is critical to develop effective tools for the evaluation of these structures, in the clinic and in research studies. The goal of the current study is to further our understanding of the effect of low frequency noise, in particular, on the peripheral vestibular system by correlating changes in head postural control during normal locomotion and vestibular stimulation with pathological changes to vestibular hair cells following noise exposure.

Methods

Adult male Sprague-Dawley rats (400-450 g) were exposed to either 120 dB pSPL (0.5-4 kHz) noise or sham conditions for six hours on a single day. Auditory function was evaluated by measuring auditory brainstem response (ABR) before and after noise exposure. Immediately following and for an additional 21 days after noise exposure, control of head posture was re-evaluated with an inertial measurement unit (IMU). Head posture was assessed during five consecutive one minute test intervals: baseline, ~3 Hz shaking, post-shake, ~5 Hz shaking, and a final post-shake interval in light and dark conditions. After completing the final measurements, animals were transcardially perfused and inner ears were collected for dissection, staining, and whole mount confocal microscopy.

Results

Preliminary analysis suggests that intense noise exposure may not only damage otolith organ sensory epithelia, but also persistently decrease locomotor activity and increase head pitch.

Conclusion

The use of an IMU to assess head postural control for evaluation of vestibular loss may be an effective tool for vestibular evaluation in awake and freely moving animals that experience vestibular trauma (Godin et al., 2015; Lee et al., 2015). Future studies will further evaluate IMU measures of head postural control in alert animals, with other established methods for evaluation of vestibular function such as VEMP or VsEP which require general anesthesia.

PS 922

Development of a Behavioral Evaluation to Analyze Sequence and Evolution of Excitotoxically-induced Vestibular Disorders

Raphaëlle Cassel¹; Pierrick Bordiga²; Chtistian Chabert³

¹Laboratoire Neurosciences Intégrative et Adaptative;

²Sensorion - CNRS; ³CNRS- Aix Marseille University

Vestibular pathologies are characterized by unpredictable episodes of vertigo accompanied by postural imbalances and loss of gaze fixation during movement. The prevalence of these pathologies is pretty high (3% of people reaching emergency department of hospitals). Current therapeutic solutions proposed to patients lack both specificity and efficiency. This unsatisfactory situation can be attributed to a deficit of knowledge of the pathogenesis mechanisms underlying vestibular disorders. During the last decade, number of pathophysiological studies carried out on cochlea suggested that glutamate excess could be common cause for many diseases. Why not the same in the vestibule? In fact, at the cellular level, excitotoxicity may be a common consequence of several vestibular pathogenic conditions (ischemia, traumatism, infection, overstimulation, ototoxic compounds) leading to synaptic damages and eventually hair cells death.

The present work is based on the development of a new animal model of excitotoxic vestibular injury and on the full exploration of behavioral alterations occurring during the subsequent three weeks. We performed a unilateral transtympanic infusion of a glutamate-receptor agonist to model an inner ear excitotoxic insult. Behavioral consequences of such interference, i.e. a vestibular syndrome, were assessed by quantification of a set of parameters relative to posture and balance. This en-

abled us to monitor objectively the evolution of vestibular dysfunction over time. We report that there are at least two distinct phases following an excitotoxic injury: an acute phase, lasting few hours and characterized by an almost complete loss of voluntary movements, and a chronic phase, lasting up to two weeks in our experimental conditions. During both phases, we observed specific balance alteration signs similar to those found in human clinical studies (head tilt, muscle dystonia inter alia). Finally, 3 weeks after the injury, no more disorder was measurable.

Thanks to previous histological studies reporting synapses alterations in similar rodent models, we postulate that the acute phase may result from significant synaptic disconnection (as a consequence of the glutamate aggression on the postsynaptic glutamate receptors), while synaptic reconnection and plasticity mechanisms may support spontaneous recovery observed during the second phase.

In the near future, these specific behavioral signs and biomarkers attached to the different stages of vestibular synaptic modifications observed in mice should lead to a transposition of this new knowledge to humans, with the final aim of assisting the medical community to efficiently diagnose the different stages of vestibular impairments and provide help for the prescription of appropriate medication.

Auditory Protheses

PD 128

Modulation Interference in Forward and Contralateral Masking In Cochlear Implants

Monita Chatterjee; Aditya Kulkarni
Boys Town National Research Hospital

Modulation Detection/Discrimination Interference (MDI) has been reported in both normal hearing and in hearing through cochlear implants (CIs). MDI in normal hearing has been more deeply investigated, and describes phenomena in which envelope-detection or discrimination processes are limited by the presence of competing modulations in the input. MDI has been shown to occur both within and across-channels, within and across ears, and impacts both modulation detection and discrimination tasks. In electrical stimulation, current spreads widely across the cochlea, making it difficult to separate peripheral from more central (retro-cochlear) interactions contributing to MDI-type phenomena. Here, we report on MDI in cochlear implant listeners in two novel conditions minimizing peripheral interactions: 1) Forward masking (forward MDI) and 2) Contralateral masking (Contralateral MDI).

Methods

In forward MDI, loudness-balanced pulse trains presented on five different electrodes served as maskers. The maskers were either sinusoidally amplitude modulated (SAM) at 50 Hz or unmodulated at the peak of their modulation versions (SSpeak). The target was presented on the middle electrode, and the task was to detect a 50-Hz AM, in a three-alternative forced-choice adaptive task. The target was presented at different delays following the masker. In contralateral MDI (with bilateral CI patients) masker pulse trains were concurrently presented with the target on the contralateral side, either on the same electrode or on a distant electrode. Maskers were either SAM (at different rates) or unmodulated (SSpeak). The listeners' task was to detect target AM at a fixed rate (50 Hz) in the presence of the different maskers, in a 3-alternative, forced choice task using the method of constant stimuli.

Results

In forward MDI, preliminary findings with four subjects show MDI effects in three of the four subjects, but no consistent effects of target delay. In concurrent MDI, preliminary findings with one subject show strong MDI effects, and broad tuning to the interferer AM rate. Contralateral MDI was observed even when the masker was presented six electrodes away on the contralateral side relative to the target electrode.

Conclusions

These results indicate that substantial MDI occurs in CI listeners even when the interferer and the target are not presented concurrently (Forward MDI) or even in the same ear (Contralateral MDI). Given that CI patients depend critically on envelope information to hear speech, such modulation-domain interference is likely to have substantial negative impact on their speech recognition capabilities in competing, fluctuating backgrounds.

PD 129

Temporal Pitch Perception by Cochlear-implant Listeners Measured at Switch-on and After 2 Months

Robert P. Carlyon¹; Francois Guerit²; Alexander J. Bilig³; Yu Chuen Tam⁴; Frances Harris⁴; John M. Deeks¹
¹MRC Cognition and Brain Sciences Unit; ²MRC Cognition & Brain Sciences Unit; ³Brain and Mind Institute, The University of Western Ontario; ⁴Addenbrookes NHS Trust

Presenting a pulse train to one cochlear-implant (CI) electrode produces a pitch that usually increases with pulse rate only up to an "upper limit" that is about 300 pps and varies markedly across subjects and electrodes. Animal experiments suggest that the limitation

arises at or prior to the inferior colliculus (IC), where neurons entrain to pulse trains up to a certain rate, above which they show only an onset response. This physiological upper limit is sensitive to auditory deprivation, and can be restored (increased) by periods of chronic stimulation. We investigated whether the psychophysical upper limit increased in adult-deafened human CI patients following activation of their implant. We therefore tested 9 users of the Cochlear device on the day of activation and two months later, using 400-pps pulse trains presented in monopolar mode to electrode 16. We used an optimally-efficient pitch-ranking procedure and eight pulse rates logarithmically spaced between 120-981 pps to measure the upper limit of pitch. Two measures controlled for potential practice effects: (i) we included a task – rate discrimination measured using an adaptive procedure and with standard and signal rates centred on 120 pps – that we did not expect to improve, (ii) each task was tested twice during each session; the reasoning was that practice effects would be at least as large within than between sessions. At the start of each session the levels of each pulse train were set to the listener's Most Comfortable Level (MCL), and these levels were used for the rate discrimination and pitch-ranking tasks. Performance on the low-rate discrimination task did not change significantly, either between or across sessions. The upper limit increased significantly between but not within sessions. Both of these findings are as predicted by an effect of neural plasticity. However, subjects set the pulse trains to a higher MCL in the second session, which might explain the increase in upper limit. If so, then because MCLs increased equally at all rates but only the upper limit changed, then that limit but not low-rate DLs must be level-dependent. Two findings providing tentative against the level-difference explanation are (i) the increase in upper limit did not correlate, across subjects, with the change in MCL between sessions, and (ii) a subset of listeners re-tested after 6 months showed further increases in MCL from 2-6 months that were not consistently accompanied by changes in the upper limit.

PD 130

Selective Attention Ability Explains Variance of Speech-in-noise Understanding Performance in Cochlear Implant Users

Inyong Choi¹; Caroline Emory¹; Subong Kim¹; Phillip E. Gander²

¹Department of Communication Sciences and Disorders, University of Iowa; ²Human Brain Research Laboratory, The University of Iowa

Selective attention is a fundamental process for our communication in noisy everyday environments. Previous

electrophysiologic studies have shown that selective attention modulates the neural representation of the auditory scene, enhancing responses to a target sound while suppressing the background. Given that most cochlear implant (CI) users complain about difficulty understanding speech within background noise, we investigated whether CI users' selective attention performance and underlying neural processes are 1) degraded compared to normal-hearing (NH) listeners and 2) correlated with their speech-in-noise understanding performance. Using speech stimuli recorded from two competing speakers (male and female), we measured fifteen CI and seventeen NH listeners' selective attention performance while their cortical neural processes were simultaneously recorded with high-density electroencephalography. We also measured the same listeners' speech recognition ability in multi-talker babble background noise. While both groups showed above-chance level performance and significantly larger evoked responses to attended stimuli in auditory cortex, the CI group's selective attention performance and neural gain control were poorer than those of NH listeners. Furthermore, a positive correlation was found between the selective attention and the speech-in-noise recognition performance in the CI group. This result suggests that degraded selective attention processes contribute to an explanation of CI users' difficulty in real-world communication.

PD 131

Acoustic Hearing Interferes with Cochlear-Implant Speech Perception for Single-Sided Deaf Listeners

Joshua G.W. Bernstein¹; Olga A. Stakhovskaya²;
Matthew J. Goupell³

¹Walter Reed National Military Medical Center, Bethesda, MD; ²Walter Reed National Military Medical Center, Bethesda, MD; Department of Hearing and Speech Sciences, University of Maryland, College Park, MD;

³Department of Hearing and Speech Sciences, University of Maryland, College Park

Background

Cochlear implants (CIs) restore some spatial-hearing abilities to individuals with single-sided deafness (SSD). In addition to providing a head-shadow advantage when the CI ear has a better signal-to-noise ratio, a CI can also provide binaural squelch in certain situations, enabling the perceptual separation of concurrent voices that originate from different spatial locations. Most SSD-CI speech-perception studies have evaluated how a CI improves performance relative to monaural (acoustic) listening. Little is known about how SSD-CI listeners perform speech-perception tasks when relying primarily on their CI ear. This study tested the hypothesis that in a multiple-talker situation, the dominant acoustic ear

would interfere with CI speech perception instead of providing a squelch benefit.

Methods

SSD-CI listeners completed a speech-identification task requiring them to perceptually separate a target talker from one same-gender interfering talker in the CI ear. The acoustic ear was presented with silence or with a copy of the interfering speech. This paradigm tested whether listeners could integrate the interfering speech in the two ears to better hear the monaural target, or conversely, whether the acoustic ear would interfere with CI speech perception. A control condition was also tested whereby SSD-CI listeners previously demonstrated a binaural-squelch advantage: the target and interfering speech were presented to the acoustic ear, and silence or just a copy of the interferer were presented to the CI ear.

Results

Presenting a copy of the interfering speech to the acoustic ear dramatically interfered with CI speech-identification performance, especially at high signal-to-noise ratios (10-20 dB) where performance decreased by as much as 40-50 percentage points. This was in sharp contrast to the control condition (target presented to the acoustic ear), where presenting the interferer to both ears significantly improved performance.

Conclusions

SSD-CI listeners experienced interference and were unable to ignore the copy of the interfering speech presented to the acoustic ear when identifying target speech in the presence of an interfering talker in the CI ear. Although a CI can provide a head-shadow benefit to improve speech perception in noise, and can improve speech perception in multitalker environments when the target speech originates on the acoustic-hearing side of the head, SSD-CI listeners may be disadvantaged in multitalker situations when relying on their CI ear to understand speech. [The views expressed in this article are those of the authors and do not reflect the official policy of the Department of Army/Navy/Air Force, Department of Defense, or U.S. Government.]

PD 132

The Role of Oxidative Stress in Electrical Stimulation-Induced Loss of Auditory Nerve Fibers in Cultured Cochlear Structures

Shufeng Li¹; Qiong Liang¹; Na Shen²; Zhengmin Wang¹

¹EYE & ENT Hospital of Fudan University; NHFPC Key Laboratory of Hearing Medicine; ²Zhongshan Hospital of Fudan University

Background

Electroacoustic stimulation (EAS) recipients often experienced delayed loss of residual low-frequency hearing. To study the role of oxidative stress in EAS hearing loss, we use an in vitro model to investigate the change of oxidative stress level, JNK/SAPK signaling pathway and cochlear structures, as well as their correction in cochlear tissues with charge-balanced biphasic electrical stimulation (ES).

Methods

Cultured cochlear tissue was stimulated with 100µA, 200µA and 400µA charge-balanced biphasic pulses for 48 hours. The ROS/RNS level in cochlear tissue was measured; the morphological changes of hair cells and auditory nerve fibers were evaluated after immunofluorescence staining; the key protein phosphorylation level in JNK/SAPK signaling pathways were evaluated by western blot; the expression of the key protein and oxidative stress-related gene were measured by real-time PCR, respectively. Ebselen was added into cochlear tissue cultures to inhibit oxidative stress. The model for cochlear oxidative damage was established by the application of proper H₂O₂ concentration in the culture. The measurements mentioned above were also performed in the model.

Results

The ratios of Fiber/IHCs in ES groups were significantly lower than that in non-ES group ($p < 0.05$). The ratio decreased with the current intensity. There was no significant difference among the ratios of OHCs/IHCs in different groups. Compared to non-ES group, the ROS/RNS levels in ES groups were significant increased ($p < 0.05$). Electrical stimulation activated the JNK/SAPK signal pathway and increased C-JUN phosphorylation but not the mRNA expression level of JNK1, JNK2, JNK3 and C-JUN. The expression levels of Gpx family were comprehensively decreased after electrical stimulation. In ES groups with 40µM Ebselen, the ratios of OHCs/IHCs and Fiber/IHCs, C-JUN phosphorylation level were comparable to those in non-ES group ($P > 0.05$) while JNK/SAPK signaling pathways were not activat

ed. These results were identically observed in oxidative stress model.

Conclusion

Electrical stimulation could cause the loss of auditory nerve fibers in cultured cochlear tissues through increasing oxidative stress level, decreasing the expression level of Gpx family and the activation of JNK/SAPK signaling pathway. Ebselen, as a mimic of Gpx, could protect cochlear tissues from ES-induced oxidative stress damage. The oxidative stress model caused similar changes observed in ES groups. Our study suggested that oxidative stress play an important role in ES-induced changes of cochlear structures.

PD 133

Lateralization of Interaural Time Differences Using Multi-electrode, Mixed-rates of Stimulation in Bilateral Cochlear Implant Listeners

Tanvi Thakkar¹; Alan Kan¹; Heath G. Jones²; Ruth Y. Litovsky³

¹University of Wisconsin-Madison; ²U.S. Army Aero-medical Research Laboratory; ³Waisman Center, University of Wisconsin, 1500 Highland Avenue, Madison, Wisconsin 53705, USA

Bilateral cochlear implant (BiCI) listeners are able to hear and understand speech in quiet, but they experience difficulties in noisy environments. Interaural time and level differences (ITDs and ILDs, respectively) allow normal-hearing listeners to navigate in noisy environments. However, for BiCI listeners, ITD sensitivity is limited and they rely mostly on ILDs. Binaural benefits are hypothesized to be limited for BiCI listeners because clinical processors have high stimulation rates which render ITD cues unusable. Encoding ITDs is challenging because high stimulation rates are needed for achieving good speech understanding, but low stimulation rates are needed for ITD sensitivity. A potential solution to this problem is to use a combination of high and low stimulation rates at different electrodes. In this study, we measured perceived lateralization of sounds comprised of various mixed-rate stimulation configurations. Lateralization is akin to sound localization in azimuth, which provides crucial information about the functional utility of binaural cues, rather than sensitivity measures obtained from left-vs-right discrimination.

Six post-lingually deafened adults participated in this experiment. Stimuli were five pitch-matched pairs of electrodes delivered using research processors (Cochlear Laura34s), with ITDs ranging from 100-1000 µs. In two baseline configurations, stimuli were either high-rate-only (1000 pulses per second, pps), or low-rate-only (100

pps). Five mixed-rate configurations were also tested, where low pulse rate electrodes were systematically introduced among high-rate electrodes, and varied either in place of stimulation or number of low-rate electrode pairs. Listeners indicated the number and location of perceived intracranial positions of the stimulus. Range of perceived lateral locations in the head was calculated from listeners' responses. Poorer ability to map ITDs to lateralized positions was indicated by a narrower range.

Broader lateralization ranges were obtained with mixed-rates, rather than high-rate-only, configurations. However, the range of lateralization observed when at least three electrodes had low-rates, was comparable to performance when low rates-only were presented. Furthermore, all but one listener reported perceiving a single coherent auditory object. These results suggest that mixed rates have the potential to convey ITDs that are mapped to coherently-perceived azimuthal locations. It suggests that the binaural system of BiCI listeners can extract pertinent cues to achieve perceived lateralization even when high-rate ITD information is presented at some cochlear locations. This result lends to the possibility of implementing ITD information in current processing strategies.

Work supported by NIH-NIDCD (R01DC003083 to RYL; R03DC015321 to AK) and NIH-NICHD (P30HD03352 to Waisman Center).

PD 134

Investigating Vowel Confusions in Cochlear Implant Listeners with Dynamic Tripolar Current Focusing

Gabrielle O'Brien¹; Wendy Parkinson¹; Heather Kreft²; Andrew J. Oxenham²; Julie A. Bierer¹

¹University of Washington; ²University of Minnesota

Current focusing strategies for cochlear implants (CIs) reduce the unwanted spread of current across the cochlea, which may prevent channel interaction between neighboring electrodes and therefore improve speech perception. One such strategy is the tripolar (TP) electrode configuration, in which the current from an active electrode is focused by two flanking electrodes stimulating with opposing polarity. Recently, we introduced a strategy called dynamic tripolar (DT) in which current is highly focused for threshold level inputs and less focused for higher stimulus intensities. In theory, DT may mimic the spread of excitation along the basilar membrane that occurs in normal hearing listeners presented with loud sounds. Another benefit of dynamic focusing is that it likely reduces the unwanted activation of side lobes with TP stimulation. In the present study, performance and error patterns were assessed on a vowel identification

task with CI listeners using DT and conventional TP and monopolar (MP) strategies.

Twenty ears, in nineteen adult CI listeners (one bilateral) participated in the study. Listeners were asked to identify ten vowels presented in the \hVd\ context. Each token was presented 6 or 9 times at 60 dB SPL. Subjects who scored 70% correct or higher were also assessed in 4-talker babble noise at a signal-to-noise ratio where the listeners scored between 40 and 60% correct with the monopolar strategy. Subjects performed the task with three stimulation paradigms: MP, TP (σ , the fraction of central electrode current output shared by the flanking electrodes, is 0.8), and DT, where $\sigma = 0.8$ at threshold and 0.5 at most comfortable level.

Of the 20 ears tested, 14 scored best with DT, 4 with TP, and 2 with MP. Regardless of overall performance, vowel error patterns often differed across electrode configurations, and were not consistent across subjects. Furthermore, errors made in DT mode did not appear to result in confusions that were more "natural"—closer in vowel space to the target sounds—than in the other conditions. Listener-specific electrograms will be examined to identify other candidate mechanisms for the improvement in vowel identification. Taken as a whole, our results suggest that improved formant frequency representation alone cannot explain the improvement in vowel identification observed for some subjects.

PD 135

Effects of Stimulating Electrode Site and Pulse Rate on Adaptation Recovery Function of the Auditory Nerve

Bahar S. Shahsavarani¹; Seth Bashford²; Shuman He³

¹Department of Communication Disorders, University of Nebraska-Lincoln; Boys Town National Research Hospital; ²Department of Electrical Engineering, University of Nebraska-Lincoln; ³Boys Town National Research Hospital

Background

Fast recovery from neural adaptation induced by prior stimulation is suggested to be important for producing peaks in the discharge rate of the auditory nerve (AN) that serve to enhance acoustic onsets in the speech waveform. This study aims to investigate potential effects of stimulating electrode site and pulse rate on adaptation recovery of the AN in cochlear implant (CI) users.

Methods

For experiment one that evaluated effects of stimulating electrode site, study participants included nine adult Cochlear Nucleus CI users ranging in age between 32 and 75 years. The stimulus was a train of biphasic, charge-balanced electrical pulses with a pulse rate of 900 pulses per second (pps). The stimulus was directly presented to seven stimulating electrodes across the electrode array.

To date, three adult Cochlear Nucleus CI users have been recruited for experiment two that evaluated effects of pulse rate on adaptation recovery function of the AN. The stimulus was trains of biphasic, charge-balanced electrical pulses with pulse rates of 500, 900, 1800, and 2400 pps. The stimulus was directly presented to three stimulating electrodes across the electrode array.

For both experiments, the stimulus was presented in a monopolar-coupled stimulation mode at the maximum comfortable level measured for each stimulating electrode and each subject. Recovery from adaptation of the AN was evaluated by measuring amplitude of the electrically-evoked compound action potential (ECAP) in response to the last pulse of the pulse train (i.e. probe pulse). All pulses occurring earlier than the probe pulse served as the masker. The masker-probe-interval (MPI) between the probe pulse and the masker pulse train increased from 1 to 256 ms in steps increasing by a factor of 2. Results: Our preliminary results showed that the ANs stimulated by the middle/apical electrodes had faster adaptation recovery than those stimulated by the basal electrodes. In addition, the ANs demonstrated faster adaptation recovery at 500 pps than other pulse rates tested in this study.

Conclusions

Effects of stimulating electrode site and pulse rate need to be considered in studies evaluating adaptation recovery of the AN.

Auditory Cortex: Human Studies

PD 136

Direct Electrical Recordings of Neural Activity Related to Auditory Figure-ground Segregation in the Human Auditory Cortex

Phillip E. Gander¹; Sukhbinder Kumar²; Kirill V. Nourski¹; Hiroyuki Oya³; Hiroto Kawasaki⁴; Matthew A. Howard¹; Timothy D. Griffiths⁵

¹Human Brain Research Laboratory, The University of Iowa; ²Institute of Neuroscience; ³University of Iowa;

⁴The University of Iowa; ⁵Newcastle University

The ability to detect a relevant sound by filtering out irrelevant sounds in the environment is crucial in day-to-day listening. This ability requires that the features of the relevant sound be grouped together as a single source (figure) and segregated from the features (background) of other competing sounds in the environment. How the auditory system performs this task is not completely understood. In the current experiment we recorded local field potentials (LFPs) from human subjects undergoing invasive ECoG monitoring for pre-surgical localization of their epileptic foci while they were listening to a stimulus in which the salience of the figure was varied systematically against a background. The subjects were implanted with depth electrodes in auditory cortex along the axis of Heschl's Gyrus (HG) and subdural grids covering the superior temporal gyrus (STG).

The subjects listened to a stimulus in which the salience of the figure was varied systematically against a background. We used a stochastic-figure-ground (SFG) stimulus developed in our lab that has been previously characterized using psychophysics and modelling. The SFG consisted of a sequence of simultaneously presented tones that were randomly distributed in log frequency space and varied from one 25 ms time frame to the next. During one time segment, a certain proportion of the tones remained the same over several consecutive time frames. This causes a figure to emerge from the background in which the salience is determined by number of tones kept fixed (the coherence) and the number of time frames over which this occurred (duration). In the current experiment, the first part (700ms) of the stimulus consisted of only the background with no figure, and in the second part the coherence of the figure was varied across trials (between 0, 2, 4 and 8). The overall duration of the figure was 28 individual 25ms time frames (700ms).

We measured event-related potentials (ERPs) and carried out single-trial time-frequency analysis using a wavelet transform. In HG responses to the figure when

compared to the acoustically matched background were minimal or non-existent. In contrast, we observed a power change in the high gamma band (60-120 Hz) on STG that peaked 200-300 ms and varied with the coherence of the stimulus for all tested subjects. We also explored the effective connectivity between HG and STG.

The data demonstrate a neural correlate of auditory figure-ground segregation in the form of high-frequency local oscillations in human non-primary auditory cortex.

PD 137

High-resolution Intracranial Recordings Provide Direct Electrophysiological Evidence for Music and Speech-selective Neural Populations in Human Auditory Cortex

Sam V. Norman-Haignere¹; Jenelle Feather²; Peter Brunner³; Anthony Ritaccio³; Josh H. McDermott¹; Nancy Kanwisher⁴; Gerwin Schalk³; Samuel V. Norman-Haignere⁵

¹MIT; ²MIT, Department of Brain and Cognitive Sciences, Cambridge, MA; ³National Center for Adaptive Neurotechnologies, Wadsworth Center, Albany, NY; Department of Neurology, Albany Medical College, Albany, NY; ⁴MIT, Department of Brain and Cognitive Sciences, McGovern Institute for Brain Research, Cambridge, MA; ⁵Howard Hughes Medical Institute Fellow of the Life Sciences Research Foundation; MIT; Boston Children's Hospital

The functional organization of human auditory cortex remains unresolved. Previously, we used 'voxel decomposition' to infer canonical components of the human cortical response to natural sounds, measured with fMRI. This analysis inferred distinct components selective for music and speech, which were localized to different non-primary regions of human auditory cortex. These components plausibly correspond to distinct underlying neural populations; but there is no direct electrophysiological evidence for such organization, and little is known about the temporal response properties of these putative neural populations. To address these questions, we recorded intracranial responses from a patient implanted with one of the highest resolution electrocorticographic (ECoG) arrays used to study auditory cortex to date (1 mm diameter electrodes, spaced 3 mm apart). We measured broadband gamma (70-140 Hz) responses to a diverse collection of 165 sounds. These sounds included many of the sounds people commonly hear, and have previously been used to characterize auditory cortex with fMRI. We then applied a decomposition method to infer canonical response time courses, whose weighted combination explained the ECoG response across all

sound-responsive electrodes (N = 52, $p < 0.001$). This analysis revealed 5 reliable components, two of which exhibited clear selectivity for music and speech, respectively, despite the lack of any functional constraints used to infer them. Notably, we also observed clear evidence for music and speech selectivity in the response of individual electrodes. The degree of this selectivity substantially exceeded that typically observed in fMRI voxels. Responses in three other patients with lower-density grids (2.3-mm diameter, 4-mm spacing) were qualitatively similar, but the degree of category selectivity was reduced. Collectively, these findings provide some of the first direct electrophysiological evidence for distinct neural populations selective for music and speech, and demonstrate the utility of high-density electrode recordings in revealing cortical tuning in humans. Ongoing work is investigating the temporal properties of the different components revealed by our analysis and their relationship to acoustic and semantic properties of music and speech.

PD 138

Electrocorticographic Delineation of Human Auditory Cortical Fields Based on Effects of Propofol Anesthesia

Kirill V. Nourski¹; Matthew Banks²; Mitchell Stein-schneider³; Ariane E. Rhone¹; Rashmi Mueller⁴; Hiroto Kawasaki⁴; Michael Todd⁴; Matthew A. Howard¹

¹Human Brain Research Laboratory, The University of Iowa; ²University of Wisconsin – Madison; ³Albert Einstein College of Medicine; ⁴The University of Iowa

Functional organization of human auditory cortex remains incompletely characterized. While posteromedial two thirds of Heschl's gyrus (HG) is generally considered part of core auditory cortex, anterolateral HG has been considered either as core or surrounding belt. Propofol, a sedative agent used for induction of general anesthesia, affects auditory cortical activity (e.g. Plourde et al., *Anesthesiology* 2006, 104:448-57; Davis et al., *PNAS* 2007, 104:16032-7). Here, we hypothesized that auditory fields defined by anatomical and physiological criteria could be further refined by their differential sensitivity to propofol.

Subjects were neurosurgical patients undergoing removal of intracranial electrodes placed to identify locations of epileptic foci. Research was approved by the University of Iowa IRB, and each subject gave informed consent for this study. Stimuli were 50 Hz click trains (0.5 s duration, 1.5 s interstimulus interval), presented continuously during a baseline period and induction of anesthesia with stepwise increases in propofol infusion rate. Electrocorticographic recordings were made simul-

taneously from depth electrodes implanted in HG and subdural grid electrodes implanted over superior temporal gyrus (STG). Depth of anesthesia was monitored using spectral entropy (Viertio-Oja et al., *Acta Anaesthesiologica Scand* 2004, 48:154-61). Averaged evoked potentials (AEPs), frequency-following responses (FFRs) and high gamma (70-150 Hz) event-related band power (ERBP) were used to characterize auditory cortical activity.

Posteromedial HG could be divided into two subdivisions based on changes in AEP and FFR during induction. In the most posteromedial aspect of the gyrus, the earliest AEP deflections were preserved, and FFRs increased during induction. In contrast, the remainder of the posteromedial HG exhibited attenuation of both the AEP and the FFR. Anterolateral HG exhibited weaker activation characterized by broad, low-voltage AEPs and no FFRs. Lateral STG exhibited limited activation by the click trains, and FFRs there dissipated during induction.

Differential patterns of auditory cortical activity during propofol induction are useful physiological markers for field delineation. Posteromedial HG is not uniform in its basic response properties and can be parcellated into at least two subdivisions. Preservation of the earliest AEP deflections and FFR likely reflect persistent synaptic activity initiated by the ventral division of the medial geniculate nucleus. Absence of the FFR in anterolateral HG and its presence on the lateral STG is not consistent with synaptic flow from lateral HG to more lateral auditory cortex on the lateral convexity. Instead, it suggests that portions of the lateral STG reflect a relatively early stage in the auditory cortical hierarchy.

PD 139

Microstructural Development of Human Primary and Nonprimary Auditory Cortex During the Perinatal Period

Brian Monson¹; Einat Liebenthal¹; Simon K. Warfield²; Jeffrey Neil²

¹Harvard Medical School, Brigham & Women's; ²Harvard Medical School, Boston Children's Hospital

Background

Variation in metrics of water diffusion, obtained from diffusion-weighted magnetic resonance imaging (MRI), has proven useful for tracking microstructural maturation of cortical gray and subcortical subplate/white matter tissue during early human brain development in vivo. In general, primary sensory cortex matures in advance of nonprimary sensory cortex, but the timing differences between primary and nonprimary auditory cortex maturation in humans is unclear. Here we used diffusion MRI to characterize the maturational timeline of primary and

nonprimary auditory cortex microstructure for preterm infants.

Methods

We analyzed longitudinal data from 90 infants born very preterm (< 30 weeks gestation) who each underwent diffusion MRI up to four times between 26 and 40 weeks postmenstrual age for a total of 173 images. Values for diffusion metrics of fractional anisotropy, mean diffusivity, axial diffusivity, and radial diffusivity were obtained from regions of interest (ROIs) placed in gray matter and adjacent subplate/white matter tissue located in left hemisphere Heschl's gyrus. We examined the variation in maturational timeline along the length of Heschl's gyrus.

Results

Our analysis reveals differing rates of maturation along the axis of Heschl's gyrus as cortex transitions from primary to nonprimary auditory regions. While primary auditory cortex was further advanced along the developmental timeline at each timepoint (as measured by diffusion parameters), nonprimary auditory cortex showed much larger changes from 26 to 40 weeks postmenstrual age than did primary auditory cortex in all diffusion metrics we examined. Diffusion MRI results indicate auditory cortex matures relatively early in brain development, consistent with histologic studies.

Conclusion

Our results indicate nonprimary auditory cortex makes more rapid changes during the perinatal period than does primary auditory cortex. This difference may be due to primary auditory cortex being further developed and nearing the tail-end of its maturational timeline. This approach may prove useful for optimizing the auditory experience for neonates during this early period.

PD 140

The Effect of Language Familiarity on the Cortical Analysis of Speech-specific Temporal Structure

Tobias Overath; Joon Paik
Duke University

Human speech is structured over multiple timescales. Phonemes, syllables and words carry information at scales ranging from a few tens of milliseconds to seconds, respectively (Rosen, 1999). Recently, we investigated the processing of such temporal structure in human auditory cortex by measuring BOLD signal changes to speech shuffled at different timescales in a foreign language (German); we showed that superior temporal sulcus (STS) is sensitive to temporal structure that is specific to speech but independent of linguistic lexical analysis (Overath et al., 2015). In the current study

we addressed the role of temporal information in the transformation from speech-specific acoustic analysis to speech-specific linguistic analysis. We directly compared responses to English and Korean speech quilts to investigate the extent to which the previous findings are influenced by linguistic analysis.

We recorded four bilingual English-Korean speakers (all female) reading from a book. 4 s long speech quilts were then created with 30, 120, 480, and 960 ms segment lengths in English and Korean; we also included 4 s long original (unaltered) speech stimuli in either language. Imaging data was acquired on a GE MR 750 3T system using a high-resolution (2x2x2 mm) EPI sequence. Participants listened to the speech stimuli and identified which of the four speakers they heard via a button box.

We applied the bilateral group functional ROI in STS from Overath et al. (2015) to probe the responses to the English and Korean speech quilts as a function of segment length. Korean speech quilts showed a parametric increase similar to the one observed before (Overath et al., 2015), while the effect was significantly stronger and more left-lateralized for English speech. In addition, activity in inferior frontal gyrus (IFG) showed an increase as a function of segment length only for English speech quilts.

The results suggest a transition from speech-specific acoustic analysis to speech-specific linguistic analysis that arises in left STS and is mediated by frontal cortex (IFG).

References

Rosen (1992) *Phil Trans Royal Soc B* 336: 367-373.
Overath, McDermott, Zarate, Poeppel (2015) *Nat Neurosci* 18: 903-911.

PD 141

Processing of Auditory and Audio-visual Stimuli in Individuals with Auditory Implants: Insights from Cochlear, Auditory Brainstem and Auditory Midbrain Implant Patients

Irina Schierholz¹; Mareike Finke¹; Andrej Kral¹;
Andreas Büchner¹; Rach Stefan²; Thomas Lenarz³;
Reinhard Dengler¹; Pascale Sandmann⁴

¹Hannover Medical School, DFG Cluster of Excellence Hearing4all; ²Leibniz Institute of Prevention Research and Epidemiology – BIPS, Bremen, Germany; ³Department of Otolaryngology, Hannover Medical School and DFG Cluster of Excellence Hearing4all; ⁴Hannover Medical School, DFG Cluster of Excellence Hearing4all; and University Hospital Cologne

Cochlear implants (CIs) are the most successful neural prostheses. Hundreds of thousands of people with severe to profound hearing loss have been able to regain access to the auditory world by the use of a CI. However, limits in application are reached in cases where essential structures beyond the cochlea are damaged. Research and development is promoted in order to obtain comparable outcomes with central auditory implants, that is, auditory brainstem implants (ABIs) and auditory midbrain implants (AMIs). However, speech recognition abilities are not only highly variable between, but also within groups of patients with CIs, ABIs and AMIs. In order to better understand how the observed variability relates to central processing differences, the current electroencephalography (EEG) study systematically compared patients with electrical stimulation at different sites of the auditory pathway with regard to their hearing abilities and auditory-cortex activation. The study, thereby, allowed a comparison across groups, covering the whole spectrum of today's available auditory neural prostheses. Patients of the Hannover Medical School (ABI: n=6; CI: n=6; AMI: n=2) and a control group of normal hearing individuals (n=6) were included in the present study. Participants performed a speeded response task, as well as a speech recognition test with auditory, visual and audio-visual stimuli. Reaction times, speech recognition scores and cortical processing of auditory and audio-visual stimuli were compared between groups. ABI and AMI patients revealed prolonged response times in auditory and audio-visual conditions compared to NH listeners and CI patients. These results were confirmed by prolonged N1 latencies and reduced N1 amplitudes of auditory event-related potentials (AEPs) in ABI and AMI patients. Interestingly, patients with central auditory implants showed a remarkable gain in performance for combined audio-visual information, in both speech and non-speech conditions. The benefit in audio-visual conditions was significantly larger when compared to CI patients and NH listeners, and it was reflected by a strong visual modulation of the auditory-cortex response in patients with central auditory implants. In sum, our results suggest that the audio-visual gain in central auditory implant patients is based on enhanced audio-visual interactions in the auditory cortex. The cortical alterations in implant patients most likely reflect a compensatory mechanism used to counteract the limited auditory input. Our observation of a strong audio-visual coupling in patients with central auditory implants may provide important implications for the optimization of rehabilitation strategies used in patients with auditory prostheses.

Supported by Deutsche Forschungsgemeinschaft (Cluster of Excellence Hearing4all)

PD 142

Influence of Task-irrelevant Feature Continuity on Attentional Modulation of Auditory-evoked Cortical Responses

Golbarg Mehraei¹; Barbara Shinn-Cunningham²; Torsten Dau³

¹*Technical University of Denmark*; ²*Boston University*;

³*Hearing Systems group, Department of Electrical Engineering, Technical University of Denmark, 2800 Kgs. Lyngby, Denmark*

In an everyday environment, listeners face the challenge of parsing the sound mixture reaching their ears into individual sources, and maintaining attention on a source of interest long enough to extract meaning. Perceptual continuity of acoustic features, such as pitch or location, has an obligatory effect on selective auditory attention. Even when a feature is not task relevant, listeners have trouble remaining focused on a sound stream if the task-irrelevant feature switches. Attention leads to modulation of auditory cortical responses evoked by attended and distractor sources. Here, we tested the hypothesis that discontinuities in a task-irrelevant feature disrupt the attentional modulation of cortical responses. We further hypothesized that individual differences in the ability to maintain focus correlate with this disruption.

Evoked response potentials (i.e. specifically, auditory N100) were recorded using electroencephalography while listeners performed an auditory attention task. On each trial, listeners were presented with two auditory streams of a sequence of five consonant vowel (CV) syllables (i.e. \ba\, \da\, \ga\), one from the left, and one from the right. Speakers of the left and right auditory stream alternated from male to female randomly from trial to trial. At the start of each trial, a visual cue was presented, instructing the listener to covertly attend to either the left, right, male, or female auditory stream. A noise burst was presented shortly after the cue, followed by the auditory streams. Listeners were instructed to count and report the number of \ga\ syllables heard in the target stream. On half the trials, a discontinuity was introduced in the task-irrelevant acoustic feature: in the attend space trials, where the talker is task-irrelevant, the talker in the attended location switched. Similarly, in the attend talker conditions, the location of the attended talker switched during the stream.

Results showed that the discontinuity of the task-irrelevant feature reduces the strength of the auditory N100 responses evoked by target CVs following the switch. This reduction of cortical attentional modulation seems to be related to behavioral performance: listeners who are hurt more, perceptually, by this discontinuity also

show a larger attenuation of the auditory N100 following the irrelevant cue switch.

These findings are consistent with a breakdown of selective auditory attention following a discontinuity in an unattended acoustic feature. The changes in the cortical responses observed here demonstrate that feature continuity has an obligatory influence on selective auditory attention and affects communication at the cocktail party.

PD 143

Adaptive Representation of Noise and Speech in Human Auditory Cortex

Bahar Khalighinejad¹; Ashesh D. Mehta²; Nima Mesgarani¹

¹*Columbia University*; ²*Hofstra Northwell School of Medicine and Feinstein Institute for Medical Research*

Humans are experts at perceiving speech, even in the presence of interfering sound sources. Recent studies suggest that this perceptual ability may arise from a noise-invariant representation of speech in the auditory brain, resulting in several computational models to explain the robust encoding of stimulus. However, little is known about the dynamic properties of neural networks as the auditory system adapts to new noisy conditions.

To understand the adaptation of auditory system during varying additive distortions, we recorded intracranial signals from four human subject who were implanted with high-density electrodes as a part of their clinical procedure. Subjects listened to continuous speech corrupted by additive background noise which changed randomly every three seconds to one of the four conditions of clean, bar, jet, and city noise.

Analysis of the neural responses to the speech signal revealed an adaptation phase which lasted between 100 to 800 ms after the onset of noise change. This was also true for transitions from noisy to clean conditions. We investigated the encoding and representation of noise at each time point with respect to the transition time, and found that the representation of noise gradually degraded as subjects adapt to the new condition. Moreover, we examined the differences in spatial and correlation patterns between the adopted and non-adapted conditions, and found that the correlation between activities of different brain regions increased during the adaptation phase.

In addition, we show that current models of stimulus-response mapping fail to replicate the dynamic adaptation property of neural responses. To explore possible computations that could predict this dynamic response

property, we implemented a cascade of Linear-Nonlinear models using a feed forward neural network. Incorporated a top-down adaptive mechanism that used the statistical structure of neural activation patterns allowed the model to replicate the temporal dynamic properties observed in the neural response at noise transitions. The proposed model thus offers insight into the biologically plausible computational mechanisms that can explain the robust speech perception observed in real-world hearing conditions.

Inner Ear: Damage and Protection II

PD 144

CMV in the Developing Mouse Cochlea and Contributions of Infection and the Immune Response to Hearing Loss

Keiko Hirose¹; Wayne Yokoyama¹; Yea Won Sung²; William Britt²

¹Washington University; ²University of Alabama, Birmingham

Background

Congenital CMV occurs in 1/200 newborns in the United States, and 10% of infants born with CMV develop hearing loss. The mechanism of hearing loss induced by CMV infection in utero is unknown. We have developed a murine model of congenital CMV infection using peripheral viral inoculation in newborn mice that results in hearing loss in up to 60% of infected mice depending on the size of the viral inoculum. This model will provide access to study the effects of cochlear viral infection during otic development.

Methods

Mouse cytomegalovirus (MCMV, Smith strain) was injected IP in P1 newborn Balb/c mouse pups. The mice were sacrificed, and the cochleas examined using MCMV IE1 (CROMA1), CD45 (common leukocyte antigen), CD3, and CD68 antibodies at P12 and P78. Serial sections were performed of plastic embedded cochleas from these two time points, and ABR was performed at P78. Whole mounts were prepared from neonatal mice and from mice with documented hearing loss to estimate the integrity of the sensory epithelium. Gene expression studies were performed to determine the pattern of activated inflammatory pathways in the inner ear associated with CMV infection.

Results

Threshold shift of 15-20 dB across all frequencies was found in mice that experienced hearing loss after CMV infection. Virus was detected in the cochlea at 4 and 11 days after infection in the lateral wall and in the ganglion.

Inflammatory cells were rampant in the inner ear at P12 and included lymphocytes, macrophages and monocytes, but not neutrophils. The hair cells and organ of Corti were uniformly preserved after CMV infection, even in mice that suffered hearing loss. Numerous genes that initiate inflammation, viral response elements such as interferons, and cell death pathways were activated in the cochlea 4, 8 and 16 days after CMV inoculation

Conclusions

When developing mouse cochleas were exposed to CMV on the first day of life, CMV entered the cochlea and infected cells in the ligament and the ganglion. Threshold shift was observed in the majority of mice, but did not appear to be accompanied by hair cell loss. Further studies will be necessary to identify the specific mechanism of hearing loss caused by congenital CMV. The mouse model of peripheral inoculation at P1 is an excellent one in which to perform these studies.

PD 146

Structure Activity Relationships Between Novel Non-ototoxic Aminoglycosides and the Bacterial Ribosome

Mary E. O'Sullivan¹; Hasan DeMirici²; Markus Huth³; Andrew A. Vu¹; Adela C. Perez¹; Thomas Effertz¹; Bob Greenhouse¹; Alan Cheng¹; Anthony J. Ricci¹

¹Stanford University, School of Medicine, Department of Otolaryngology; ²Stanford University; ³Inselspital, Universitätsspital Bern Bern, Switzerland

Background

Aminoglycosides are important antimicrobials used to treat a wide range of infections. A major drawback of usage is hearing loss caused by irreversible damage to cochlear hair cells. We have previously shown that by chemically modifying sites on the aminoglycoside backbone we can render aminoglycosides impermeant to the mechanotransduction (MET) channel and preserve hearing, whilst retaining antimicrobial activity. However, lead compounds show decreased activity against a subset of bacterial species. In bacteria, aminoglycosides disrupt protein synthesis by binding to an internal loop in helix 44 (h44) of the bacterial 16S ribosomal RNA (rRNA). Drug-rRNA interaction displaces bacterial 16S nucleotides A1492 and A1493, impairing ribosomal proofreading during transfer RNA selection. Errors in protein synthesis form the basis of antimicrobial activity. The current study is undertaken to elucidate the fundamental structure-activity relationships between aminoglycosides and their bacterial 16S target to facilitate the

development of the next-generation non-ototoxic aminoglycosides.

Methods

Eight modified sisomicin compounds were examined. Three moieties (methylsulfonyl, phenylsulfonyl, and benzoyl groups) were used to modify two specific amine sites of sisomicin (1" and 3" amine groups). Ribosome complexes isolated from *Thermus thermophilus* were crystallized in complex with aminoglycoside derivatives. Data was collected at cryogenic temperatures at the Stanford Synchrotron Radiation Lightsource and at near physiological temperatures at the Stanford Linac Coherent Light Source. Data-sets were correlated with in vivo and in vitro cochlear toxicity data, as well as antimicrobial data from 40 bacterial strains.

Results

All 1"-modified aminoglycosides were found to bind to the bacterial 16S rRNA. All modifications also reduced ototoxicity. However, only the methyl sulfonyl derivative showed antimicrobial activity, while the other substitutions lost antimicrobial activity. In contrast, no aminoglycoside-ribosome binding was detected for any 3"-modified aminoglycosides. Compounds modified at the 3" amine site showed reduced ototoxic profiles but had abolished antimicrobial activities.

Conclusions

Together, data indicate that the structure activity relationship between 1" and 3"-modified compounds and the bacterial ribosome accounts for the altered antibacterial specificities. Evidence also suggests that ribosome binding does not account for the altered antibacterial specificities detected within the 1"-modified aminoglycoside group. Since all of the 1"-modified aminoglycoside antibiotics displaced bacterial 16S nucleotides A1492 and A1493, indicating impaired ribosomal proofreading, we hypothesize that perturbed bacterial uptake is likely to dictate differences in antibacterial activities. Thus it is important to further differentiate between 1"-modified aminoglycoside antimicrobial activities so we may restore efficacy against a wide spectrum of bacteria.

Background

Noise is the most common occupational and environmental hazard, thus it is not surprising that noise-induced hearing loss (NIHL) is the second most common form of sensorineural hearing deficit, second only to age-related hearing loss (presbycusis). Development of an efficacious treatment has been hampered by the complex array of cellular and molecular pathways involved in NIHL. Our recent studies have demonstrated that calcium channel blockers and anti-inflammatory drugs can also prevent NIHL. Tetrandrine (TET), a bis-benzylisoquinoline alkaloid originally purified from a Chinese medicinal herb, shows strong antioxidant and anti-inflammatory properties, and can block calcium channels. Here, we tested whether TET could effectively protect against NIHL in mice.

Methods

Two-month old CBA/CaJ mice were used in this study. Mice were exposed to noise (110 dB SPL, 4 to 20 kHz) for 30 min., and were randomly assigned to either treated or untreated groups. The treatment drugs were injected (i.p.) with TET at different dosages either two hours before or immediately after the noise exposure. The control groups were injected with the same solution without TET. Both auditory brainstem response (ABR) and distortion product otoacoustic emission (DPOAE) assays were performed before, 12 hours and two weeks after the noise exposure. In addition, after the final ABR and DPOAE measurement, the cochlea was micro-dissected and incubated with primary antibodies to the following: (1) C-terminal binding protein 2 (mouse anti-CtBP2), and (2) myosin-VIIa (rabbit anti-myosin-VIIa) for quantifications of ribbon synapses and hair cells.

Results

To detect prophylactic and therapeutic effects of TET against NIHL, we administered TET in a single dose either two hours before or immediately after the noise exposure. One-way ANOVAs at each day revealed significant main effects of group at Day 1 [$F(2,109) = 9.017, p < 0.001$] and Day 15 [$F(2,109) = 8.883, p < 0.001$]. Thus, prophylactic and therapeutic functions of TET against NIHL were observed in mice. The prevention effect was achieved by protecting both outer hair cells, and ribbon synapses between inner hair cells and spiral ganglion neurons. Most importantly, this protection could last to one year after the initial noise exposure.

Conclusion

The present study demonstrated that TET significantly attenuated NIHL, and its prophylactic effects were achieved mainly by preventing outer hair cell loss and cochlear nerve degeneration. Most importantly, this TET protection can sustain during aging. Thus, TET can be a promising drug candidate for NIHL intervention.

PD 149

Using Mouse Cochlear Cultures as a Model System to Identify Compounds that Prevent Cisplatin-Induced Hair-Cell Loss

Sian R. Kitcher¹; Richard Goodyear²; Corné J. Kros²; Guy P. Richardson²

¹University of Sussex England; ²University of Sussex

Background

Cisplatin is a cytotoxic agent used in the treatment of various forms of cancer, but a dose-limiting side effect of permanent hearing loss caused by selective damage to cochlear hair cells has been reported in a majority of treated patients. Efforts to identify compounds that may offer protection from the damage caused by cisplatin have largely centered around high-throughput screening methods utilising the zebrafish lateral line. Less attention, however, has been paid to mammalian models which may translate more readily to clinical settings.

Methods

To investigate the protective properties of a range of compounds against the damaging effects of cisplatin we prepared organotypic cochlear cultures from P2 wild type (CD-1) mice and, after 24h, co-incubated them for a further 48h with 5 μ M cisplatin together with 50 μ M of potential protectants. Cultures were then fixed and dual stained to allow the visualisation of both the hair bundles and the cell bodies in order to determine the protective abilities of various compounds.

Results

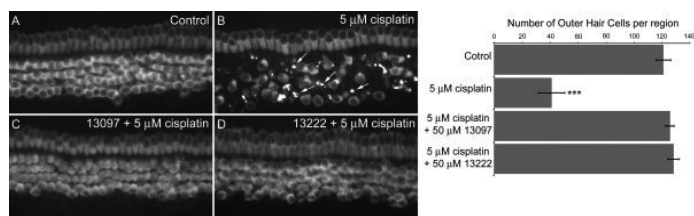
The use of a long-term (48h) low-dose (5 μM) regime with cisplatin obviates the general cytotoxic effects that are observed with most cell types in mouse cochlear cultures when using higher concentrations of the drug for the same or shorter periods. Selective loss of basal-coil outer hair cells is observed after 48h, and changes in the structure of the apical membrane and hair bundles are seen in many of the surviving hair cells. Using this system several compounds previously shown to prevent aminoglycoside-induced hair-cell death in cochlear cultures, including MET- and Kv-channel blockers, have been identified that provide effective protection against cisplatin (see Fig. 1).

Conclusions

The assay described in this study shows reliable damage of mouse cochlear hair cells that can be prevented by co-incubation with selected compounds, providing an in vitro mammalian screening protocol that could be used to pre-select compounds for testing in an in vivo model of cisplatin induced hearing loss.

Fig. 1 MET and Kv channel blockers protect mouse cochlear outer hair cells from cisplatin toxicity. Anti-myosin VI labelled hair cells in cochlear cultures following 48h incubation in medium alone (A), medium containing 5 μM cisplatin (B), and medium containing 5 μM cisplatin in the presence of 50 μM of either the Kv channel blocker UoS 13097 (C) or the MET channel blocker UoS 13222 (D). Arrows in B indicate apoptotic hair cells.

Supported by Action on Hearing Loss and the MRC



PD 150

Exosome-Mediated Protection Against Aminoglycoside-Induced Hair Cell Death

Andrew Breglio¹; Lindsey May²; Nora Welsh²; Samir El Andaloussi³; Matthew J.A. Wood⁴; Lisa Cunningham²

¹National Institute on Deafness and Other Communication Disorders; ²National Institute on Deafness and Other Communication Disorders, NIH; ³Department of Laboratory Medicine, Karolinska Institutet; ⁴Department of Physiology, Anatomy and Genetics, Oxford University

Background

Clinical treatment with aminoglycoside antibiotics often causes permanent hearing loss and/or balance dysfunction. These drugs are toxic to inner ear sensory hair cells. Our previous work has shown that heat shock of utricles in culture induces the release of HSP70 which can protect against aminoglycoside-induced hair cell death in a paracrine manner. Exosomes are a type of extracellular vesicles (EVs) that are known to be ubiquitous carriers of HSPs, especially HSP70. We therefore hypothesized that exosomes promote the survival of hair cells exposed to aminoglycosides.

Methods

The release of exosomes from heat-shocked utricles was visualized by electron microscopy and quantified by nanoparticle tracking analysis of the culture media surrounding utricles. The uptake of exosomes into recipient utricles was visualized by superresolution microscopy of fluorescently labeled exosomes. We tested the ability of exogenous exosomes to protect hair cells from aminoglycoside-induced death in vitro. Exosome protein content was analyzed by tandem mass spectrometry.

Results

Utricles cultured under control conditions showed a basal secretion of exosome-sized EVs into the culture media. Heat shocked utricles showed significantly increased release of EVs, an effect that could be abolished by treatment with the exosome secretion inhibitor GW4869. Electron microscopy of heat shocked utricles revealed multivesicular bodies containing exosomes within the sensory epithelium, including some fused with the plasma membrane.

Exosomes derived from SW480 human colon cancer cells or CT26 mouse colon cancer cells significantly improved hair cell survival in the presence of neomycin. However, exosomes derived from huMSC, HEI-OC1, C8-B4, or C8-D1A cells did not. Tandem mass spectrometry analysis of CT26 exosomes identified nearly one thousand unique mouse proteins, with HSP70 and several other members of the heat shock family present in high abundance.

Conclusions

Our results suggest that heat shock treatment, which protects against aminoglycoside-induced hair cell death, induces the release of exosomes from utricles in culture. Further, we see that exosomes purified from cell lines can protect against hair cell death in a cell type-specific manner, and that such purified exosomes can be internalized by utricles in culture. Ongoing studies are revealing the content of protective and non-protective exosomes and the details of their interactions with recipient utricles. Taken together our data suggest that exosomes

may constitute an important mechanism of intercellular signaling in the inner ear.

Funding

This work was supported by the NIDCD Division of Intramural Research.

PD 151

Combined Actions of Immune System Modulation and Antioxidant Therapy Enhance Recovery from Noise-Induced Hearing Loss

Edward J. Walsh; Timothy M. Sveeggen; Longina Dawson; Alexandra C. Bohn; JoAnn McGee
Boys Town National Research Hospital

In a previous study, the immunomodulator, glatiramer acetate (GA), was shown to protect inbred CBA/J mice from noise-induced inner ear trauma when administered prior to, and immediately following, exposure to traumatizing noise (McGee et al., 2014). In this investigation, the capacity of GA to rescue NMRI outbred mice from existing noise-induced hearing loss (NIHL) was assessed by tracking functional recovery using auditory brainstem responses (ABRs) and distortion product otoacoustic emissions (DPOAEs). When exposed to an octave-wide band of noise centered on 11.3 kHz and delivered at 97 dB SPL for one hour, recovery dynamics observed in outbred NMRI mice were similar to statistically positive recovery outcomes observed in CBA/J inbred mice following GA administration. When GA administration was combined with administration of the antioxidant, N-acetylcysteine (NAC), recovery was notably enhanced relative to recovery observed in animals receiving GA alone. In an effort to determine the enhancement potential of the combined effect, recovery was tracked following administration of NAC alone, and NAC-induced recovery approximated the action of administering GA alone. This outcome is consistent with the tentative, preliminary conclusion that GA and NAC actions are additive under the experimental conditions implemented in this investigation. In addition, we assessed the morphological consequences associated with treatment protocols in noise-traumatized animals. To achieve this goal, whole mount sections of the organ of Corti were prepared and stained with antibodies to myosin-VIIa, CtBP2 and GluA2 to assess the number of synapses between inner hair cells (IHCs) and primary auditory nerve fibers (ANFs); myosin-VIIa labeling was used to identify sensory cell bodies, CtBP2 labeling to identify presynaptic elements of ribbon synapses and GluA2 labeling was used to identify subunit 2 of AMPA glutamate receptors localized on afferent terminals, and the number of synapses/IHC was assessed using established confocal microscopy protocols. The outcome of preliminary studies indicate that the number of IHC-ANF synapses

is reduced dramatically following noise exposure in cochlear regions corresponding to frequencies approximately one-half octave above the center frequency of the noise band and higher. When animals were treated with combined GA and NAC following noise exposure, the number of IHC-ANF synapses was restored to numbers resembling that observed in control mice in preliminary estimates. Based on these findings, we conclude that immunomodulation is an effective NIHL treatment strategy, the recovery enhancement power of which is notably increased when combined with antioxidant therapy. Supported by ONR grant N000141410562.

Mechanics of the Middle Ear

PD 152

Characterization of Acoustically Induced Transient Response of Tympanic Membrane Under Normal and Pathological Conditions

Payam Razavi¹; Jeffrey Tao Cheng²; Nima Maftoon²; Michael E. Ravicz³; John J. Rosowski⁴; Cosme Furlong¹

¹Worcester Polytechnic Institute; ²Massachusetts Eye and Ear Infirmary, Harvard Medical School; ³Eaton-Peabody Laboratory, Mass. Eye & Ear Infirmary; Dept. of Otolaryngology, Harvard Medical School; ⁴Eaton-Peabody Laboratory, Mass. Eye & Ear Infirmary; Department of Otolaryngology, Harvard Medical School; Speech and Hearing Bioscience and Technology program, Harvard and M.I.T.

Background

Despite decades of research, there are still many uncertainties about how the tympanic membrane (TM) transforms sound energy into mechanical vibrations of the ossicles over a wide frequency range. Our work concentrates on studying the mechanics of live and post-mortem TMs of different mammalian species subjected to various acoustic stimuli by holographic methods. In this study, we expanded our work into characterizing TM mechanics in pathological ear conditions.

Method

We measured responses of the TM to acoustic transients in normal and pathological middle-ear conditions using the newly developed High-speed Digital Holography (HDH) that measures the TM transient motion with high spatiotemporal resolutions (i.e., >147,000 points at >42 kHz). The use of broadband acoustic impulses temporally separates the stimulus and longer-term response, and allows us to characterize the motion of the TM in response to many frequencies with a single measurement. We used human temporal bones with controlled

manipulations to mimic four middle ear pathologies including: 1- Fluid in contact with half of the TM, 2- Fluid in contact with the entire TM, 3- IncudoStapedial (IS) joint interruption, 4- stapes fixation.

Results

The TM transient motions in response to impulses in normal ears show details of initiation and superposition of different modal responses from different parts of the TM, followed by waves traveling from the umbo and manubrium towards the annulus, and subsequent reflections leading to standing waves forming between the manubrium and annulus. Quantification of wave speed across the TM surface enables determination of mechanical properties and damping of the TM. Preliminary fluid results show there is a significant reduction of the motion amplitudes and speeds in areas submerged under fluid, along with somewhat slightly higher amplitudes of motion in other areas. The amplitudes and wave speeds in cases of IS joint interruption and stapes fixation are forthcoming.

Conclusion

Our methods describe the motion of the TM in response to impulses and can assess modal patterns of TM motion, the generation, and speed of local traveling waves, local variations in material properties of the TM, and the effect of pathology on TM motion. Our preliminary results show changes in TM motions caused by various middle ear pathologies that may have clinical impacts on differential diagnosis of middle ear diseases.

Funding

We thank the NIH-NIDCD, the Massachusetts Eye and Ear Infirmary, the Worcester Polytechnic Institute, and the L. Mittal Fund.

PD 153

The Path of a Click Stimulus from Ear Canal to Umbo

Mario Milazzo¹; Elika Fallah²; Elizabeth Olson²; Michael Carapezza²

¹*The BioRobotics Institute, Scuola Superiore Sant'Anna, Pontedera (PI), Italy;* ²*Columbia University*

The tympanic membrane (TM) has a key role in transmitting sounds to the inner ear, but a concise description of how the TM performs this function remains elusive. This study probed TM operation by applying a free field click stimulus to the gerbil ear and exploring the consequent motions of the TM and umbo. Motions of the TM were measured both on radial tracks starting close to the umbo and on a grid distal and adjacent

to the umbo. The experimental results confirmed the high fidelity of sound transmission from the ear canal to the umbo. A delay of 5 - 15 μ s was seen in the onset of motion at TM points close to the umbo compared to mid-radial locations. The TM responded with a ringing motion, with different locations possessing different primary ringing frequencies. A simple analytic model from the literature, treating the TM as a string, was used to explore the experimental results. The click-based experiments and analysis led to the following description of TM operation: A transient sound pressure on the TM causes a transient initial TM motion that is \sim largest at the TM's radial midpoints. Mechanical forces generated by this initial prominent TM distortion then pull the umbo inward, leading to a delayed umbo response. The initial TM distortion also gives rise to prolonged mechanical ringing on the TM that does not result in umbo motion, likely due to deconstructive interference from the range of ringing frequencies. Thus, the umbo's response is a high-fidelity representation of the transient stimulus. Because any sound can be considered as a consecutive series of clicks, this description is applicable to any sound stimulus.

PD 154

Effect of Fibroblast Remodeling on Sound-Induced Surface Motion Patterns of 3D Printed Biodegradable Elastomeric Tympanic Membrane Grafts

Nicole L. Black¹; Jeffrey Tao Cheng²; Sabrina M. Liu¹; Elliott Kozin³; John J. Rosowski⁴; Aaron Remenschneider⁵; Jennifer A. Lewis¹

¹*Harvard John A. Paulson School of Engineering and Applied Sciences;* ²*Massachusetts Eye and Ear Infirmary, Harvard Medical School;* ³*Massachusetts Eye and Ear Infirmary;* ⁴*Eaton-Peabody Laboratory, Mass. Eye & Ear Infirmary; Department of Otology and Laryngology, Harvard Medical School; Speech and Hearing Bioscience and Technology program, Harvard and M.I.T.;* ⁵*University of Massachusetts / Massachusetts Eye and Ear Infirmary*

Background

The tympanic membrane (TM) contains radial and circular collagen fibers that aid sound conduction. Current tympanoplasty and myringoplasty graft materials, including fascia and cartilage, lack this microarchitecture, resulting in isotropic remodeled tissues and variable hearing outcomes. Additionally, autologous graft materials have unpredictable stiffness: 'too-soft' results in retraction of grafts and 'too-hard' results in poor sound conduction. Three-dimensional (3D) filamentary extrusion printing can mimic the fiber arrangement of the native TM. A biodegradable polyurethane elasto-

mer is 3D printed with micron-scale features. As the polyurethane degrades, it promotes regeneration by native cells during remodeling, creating mechanically anisotropic tissue grafts. Various arrangements of 3D-printed polyurethane fibers tune the sound induced motions of these remodeled grafts.

Methods

A novel biodegradable polyurethane is synthesized and dissolved in acetone for printing. Filamentary extrusion printing with a 100 μm nozzle produces TM grafts with various circular, radial, and parallel fiber arrangements. Cast polyurethane sheets and collagen sheets with random fiber arrangements serve as controls. The TM grafts are seeded with 250,000 green fluorescent protein-expressing human neonatal dermal fibroblasts and maintained in standard tissue culture conditions. Cellular ingrowth and collagen deposition is determined by immunofluorescence staining and confocal laser microscopy. Laser holography and Doppler vibrometry (LDV) determine the acoustic responses of the grafts before and after 7 days in culture.

Results

The Young's modulus of the biodegradable elastomer was determined to be 31.29 ± 0.66 MPa ($n=4$). Degradation studies on cast disks show a mass loss of $13.6 \pm 2.1\%$ after 5 days in PBS ($n=8$). 3D printed and control materials support fibroblast confluence and collagen deposition after 7 days. LDV demonstrates that the 30 circular / 30 radial grafts have a higher first resonant frequency than cast sheets and 30 circular only polyurethane grafts. The peak velocity of polyurethane grafts is higher than that of the collagen. Holography demonstrates frequency dependent surface motion patterns ranging from simple to complex that were more uniform in the polyurethane grafts with organized fiber arrangements. Fibroblast remodeling tends to influence acoustic response of the grafts, observed by increased first resonant frequency and complexity of the surface motion patterns, suggesting increased anisotropy in the grafts with cellularization.

Conclusions

3D printing with a novel biodegradable elastomer produces TM grafts with micron-scale fiber arrangements that are remodeled by cellular ingrowth into anisotropic tissues. The anisotropy mimics the circular and radial fiber arrangements seen in native TMs and improves sound conduction in remodeled grafts.

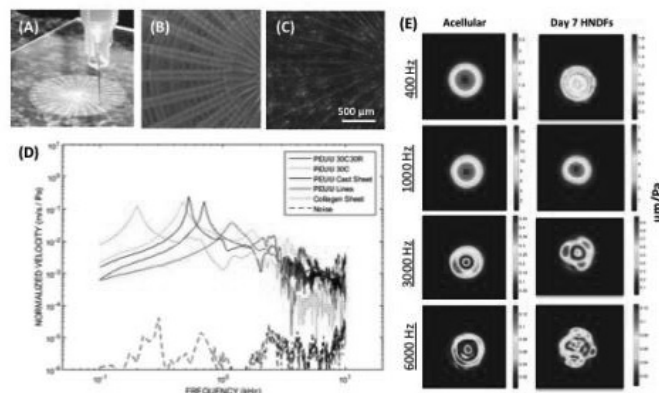


Figure 1: Filamentary extrusion 3D printing with 100 μm nozzles is used to fabricate tympanic membrane grafts from a novel biodegradable polyurethane elastomer into various fiber arrangements (A). The resultant acellular grafts (B) can be remodeled by green fluorescent protein-expressing human neonatal dermal fibroblasts (HNDFs) as the material degrades (C). Prior to cell remodeling, the 3D printed polyurethane fiber arrangements, polyurethane cast sheet, and collagen sheet have distinct sound-induced velocities at the center of circumferentially clamped grafts as determined by LDV (D). After 7 days of remodeling by fibroblasts, holography results show altered surface motion patterns on 3D printed 30C grafts (E).

PD 155

Modal Holography Detects Middle-ear Fluid

Nima Maftoon¹; **Payam Razavi**²; **Jeffrey Tao Cheng**¹; **Michael E. Ravicz**³; **Cosme Furlong**²; **John J. Rosowski**⁴

¹Massachusetts Eye and Ear Infirmary, Harvard Medical School; ²Worcester Polytechnic Institute; ³Eaton-Peabody Laboratory, Mass. Eye & Ear Infirmary; Dept. of Otolaryngology, Harvard Medical School; ⁴Eaton-Peabody Laboratory, Mass. Eye & Ear Infirmary; Department of Otolaryngology, Harvard Medical School; Speech and Hearing Bioscience and Technology program, Harvard and M.I.T.

Otitis media with effusion is the most common cause of conductive hearing loss in Children. More than 700 million otitis media cases occur annually worldwide (Monasta et al., PLOS ONE 2012). This study demonstrates the utility of experimental modal analysis of tympanic-membrane (TM) transient response for detecting liquid inside the middle-ear cavity. Our new high-speed digital holography system with a temporal resolution of less than 24 μs (Dobrev et al., J. Biomed. Opt. 2014; 19(9): 096001) enables us to measure responses of the tympanic membrane to transient stimuli with high spatial resolution (Razavi et al., Hearing Research 2016). We recorded TM transient vibration data in response to impulse stimuli in cadaveric human temporal-bone preparations, with the middle-ear cavity dry and with saline injected via the Eustachian tube, to one of two fluid levels: (1) saline was in contact with half of the TM surface (cavity was about half filled), or (2) saline was in contact

with the entire TM surface (cavity was about completely filled). Structural system identification was performed to determine the natural frequencies, damping and mode shapes of the TM using experimental modal analysis of the transient responses. First, the transient displacement of the TM in response to an acoustic click and the simultaneously-recorded sound pressure measured near the superior tympanic membrane rim were transformed to the frequency domain. Secondly, displacement-to-sound-pressure transfer functions were calculated for more than 100,000 points on the TM surface. The identification of poles and mode shapes was performed with varying over-specified modal orders. Natural frequencies and modal damping were derived from the identified poles. We calculated the pole-weighted complex variant of the modal assurance criterion (Vayssettes et al., *Int. J. Control*, 2014; 87(7): 1352–1372) to compare TM modes in different middle-ear fluid conditions. The results show that modes are altered by the saline in the middle-ear cavity. The alterations depend on saline level, with higher frequency modes (above 5 kHz) being the most affected with both saline levels. Modal motions with nodes within the region of the TM surface covered by saline were most affected. When the cavity is completely filled, all modes are significantly changed.

This work was supported by a funding from NIH/NIDCD (R01-DC008642) and a donation from L. Mittal.

PD 156

Modelling the Effects of Middle Ear Muscle Contraction on Tympanic Membrane Motion

Nathaniel T. Greene; Heath G. Jones; Sean A. Hollonbecck; William A. Ahroon
U.S. Army Aeromedical Research Laboratory

Middle ear muscle contractions (MEMCs) activate reflexively in response to loud sounds. In humans, this 'acoustic reflex' involves contraction of the stapedius muscle but not the tensor tympani muscle. Contraction of the stapedius muscle stiffens the ossicular chain and decreases the admittance of the middle ear, thus it is generally assumed that MEMCs play a role in protecting hearing from damage resulting from high-level sound stimulation. Indeed, one model developed to predict hearing loss risk for a noise exposure (the Auditory Hazard Assessment Algorithm for Humans) assumes a protective effect (i.e., a 20 dB attenuation) from MEMC. The reports of MEMC on sound transmission available in the literature, however, are more variable. In particular, the effects of MEMC on acoustic admittance and ossicular chain motion vary substantially with stimulus frequency and intensity. In particular, both measures are reduced for low frequency sounds, and not changed for higher frequencies, thus MEMCs generally produce a high-pass

effect on sound transmission into the inner ear; however, responses appear to increase in both measures during MEMC for intermediate frequencies (~1.5 kHz). In order to probe this effect, we have developed a simple 1-D acoustic model of sound transmission through the middle ear using the finite difference method. The model consists of three segments roughly approximating the external, middle, and inner ear, differing from one another via characteristic acoustic impedance. Tones of varying frequency are presented from the start of the external ear segment. MEMC was simulated by increasing the impedance of the inner ear segment representing the stapedius muscle impeding movement of the stapes. The effect of the MEMC was assessed at the boundary between the external and middle ear segments (i.e., the tympanic membrane), as well as within the external and inner ear segments in order to simulate measurements of TM velocity and sound transmission and reflection. Impedance boundaries between segments generated reflections that interacted with the incoming waves, altering both the energy transmitted into the cochlea as well as velocity measured at the TM. MEMC activation increased the impedance in the inner ear segment, increasing the impedance mismatch, and increasing the reflectance of the boundary. This impedance change resulted in frequency-dependent increases and decreases in both TM velocity and ear canal sound pressure, consistent with the pattern of responses reported previously. These results suggest that the assumption that the MEMC is protective at all frequencies must be re-considered.

PD 157

Ossicular Joint Flexibility Protects the Cochlea by Reducing the Peak Amplitude of Damaging Impulsive Stimuli

Peter Gottlieb¹; Yona Vaisbuch¹; Sunil Puria²

¹*Stanford University*; ²*Massachusetts Eye and Ear, Harvard Medical School*

Background

The presence of three distinct middle-ear ossicles is a uniquely mammalian trait whose functional benefits are still debated. We test the hypothesis that the flexibility afforded by the two synovial joints connecting the ossicles provides a protective advantage by dispersing and reducing the peak amplitudes of impulsive stimuli before they reach sensitive cochlear structures.

Methods

The 3D velocity of 9-15 points along the ossicular chain in unaltered cadaveric human temporal bones (N=9), stimulated with positive and negative acoustic impulses (amplitude = 20 Pa, width = 0.1 ms), was measured in

the time domain using a Polytec CLV-3D laser Doppler vibrometer. The measurements were then repeated after fusing one or both of the ossicular joints with dental cement. Sound transmission was characterized by measuring the amplitude, width, and delay of the impulsive velocity profile as it traveled from the eardrum to the cochlea. In particular, to be consistent between specimens, the velocity profile was examined at the umbo, malleus head, incus body, incus lenticular process, and stapes posterior crus. Additionally, the 3D motion of the ossicles in each state was calculated using a least-squares fit to rigid body motion.

Results

Motion in the stapes-normal direction was by far the largest component, and results are reported for that direction. Responses were symmetric for positive and negative stimuli. A clear delay was noted across the incus-malleus joint (IMJ) in most specimens, but a noticeable delay across the incus-stapes joint (ISJ) was evident in only half. On average, fusing both ossicular joints caused the stapes velocity profile amplitude and width to change by a factor of 1.77 ($p = 0.0057$) and 0.78 ($p = 0.011$), respectively. Fusing just the IMJ had a larger effect on amplitude (factor of 2.37), while fusing just the ISJ decreased the stapes velocity on average. The 3D motion pattern of the ossicles was also altered by fusing the joints.

Conclusion

Removing the flexibility of the ossicular joints both increases the amplitude and decreases the width of the stapes impulse velocity profile. This implies that the joints behave as a dispersive passive filter that protects the cochlea against these potentially harmful impulsive stimuli. In addition to its scientific interest, this has clinical implications in the behavior of middle-ear prostheses, which typically bypass the ossicular joints and may therefore remove this protective mechanism.

This work is supported in part by NIH grants R01 DC 05960 and F31 DC 013943A.

PD 158

3D Computational Modeling of Blast Wave Transmission through the Ear

Rong Gan; Kegan Leckness; Don U. Nakmali
University of Oklahoma

Introduction

The ear, as a sensitive air-containing organ, is extremely susceptible to damage from blast waves. Blast-induced ear injuries include the tympanic membrane (TM) rupture, ossicular chain disruption, and inner ear damage. To understand how blast waves are transmitted from the

ear canal to the TM, middle ear, and cochlea, we have conducted a series of experiments in cadaver ears or temporal bones to measure blast overpressure through the ear. However, the transfer functions of the ear canal and middle ear in response to blast overpressure and the protection mechanisms of hearing protection devices (HPDs) are still unclear. This paper reports the applications of a 3D finite element (FE) model of the human ear to predict blast pressure wave transduction. We seek to improve the design and function evaluation of HPDs for military personnel involved in the battlefield.

Methods

A 3D FE model of the human ear previously developed by our group (Fig. 1) was used for this study, which includes the ear canal, TM, middle ear ossicles connected by joints and suspended by ligaments and muscle/tendons, and the middle ear cavity. The model was transferred into Fluent/ANSYS Workbench to establish the fluid-structure interactions (FSIs) for transfer of forces and displacements between the fluid and solid domains. P0 waveform recorded at the entrance of the ear canal from the blast tests in the "head block" attached with human temporal bone was applied in FE model as the input waveform P0. The P1 waveform near the TM and P2 inside the middle ear cavity were calculated from the model and compared with the waveforms from blast experiments. The FE model was further used to simulate earplugs (Combat Arms) placed in the ear canal.

Results and Discussion

The model was first validated by comparison of P1 waveform, the pressure causing TM injury, between the FE model and experiment results. Then, the model was used to predict the blast-induced maximum stress distribution in the TM and calculate the stress change w.r.t. P1 pressure level, which determines the TM damage. Finally, different earplugs with various settings were simulated in FE model and showed the variation of protection level. This study demonstrated that the 3D FE model of the human ear was implemented and proved to accurately predict blast overpressure transmission through the ear and the function evaluations for HPDs. (Supported by DOD W81XWH-14-1-0228)

Development 2

PD 159

A Link Between Planar Polarity and Staircase-like Bundle Architecture in Hair Cells

Basile Tarchini¹; Basile Tadenev¹; Nicholas Tarchini¹; Michel Cayouette²

¹*The Jackson Laboratory*; ²*Institut de recherches cliniques de Montreal*

Sensory perception in the inner ear relies on the hair bundle, the highly polarized brush of movement detectors crowning hair cells. We previously showed that, in the mouse cochlea, the edge of the forming bundle is defined by the 'bare zone', a microvilli-free sub-region of apical membrane specified by the mInsc-LGN-Gai protein complex. We now report that LGN and Gai also occupy the very tip of stereocilia that directly abut the bare zone. We demonstrate that LGN and Gai are both essential to promote the elongation and differential identity of stereocilia across rows. Interestingly, we also uncover that total LGN-Gai protein amounts are actively balanced between the bare zone and stereocilia tips, suggesting that early planar asymmetry of protein enrichment at the bare zone confers adjacent stereocilia their tallest identity. We propose that LGN and Gai participate in a long-inferred signal originating outside of the bundle to model its staircase-like architecture, a property essential for direction-sensitivity to mechanical deflection and hearing.

PD 160

Disruption of the Wnt Secretory Pathway via Wls Ablation in the Developing Murine Cochlea

Elvis Huarcaya Najarro¹; Jennifer Huang¹; Nicolas Grillet¹; Alan Cheng²

¹*Stanford University*; ²*Stanford University, School of Medicine, Department of Otolaryngology*

Background

The Wnt pathway plays multiple roles during development, such as controlling cell fate, proliferation, polarization, and migration. In short, a Wnt-producing cell secretes the Wnt lipoprotein, which binds to its receptor(s) on Wnt-responsive cells, leading to a cellular response. Prior to secretion, Wnt proteins undergo lipid modification by the endoplasmic reticulum protein Porcupine, and then are transported for secretion by Wntless (Wls) located in the Golgi apparatus. In mice, there are 19 Wnt ligands and genetic redundancy has been reported during development of the cochlea. Therefore, to characterize the role of secreted Wnts during cochlea development, genetic ablation of Wls can be used as a

strategy to circumvent redundancy of Wnt proteins. In this study, we are characterizing the role of Wls during embryonic hair cell (HC) development, with an emphasis on planar cell polarity (PCP).

Methods

Wls expression analysis was carried out by immunostaining, qPCR and in situ hybridization. The Emx2-Cre mouse line was crossed with animals carrying the Wls floxed allele to generate Wls conditional knockout (CKO) animals, thereby ablating Wls from the embryonic mouse cochlear duct starting at E13.5. We immunostained for hair cell and supporting cell markers to assess cell types and organization of the cochlea in CKO and control animals. Phalloidin staining and scanning electron microscopy were used to visualize stereocilia bundles. Lastly, Fzd6, Dvl2, Vang1 and Vang2 staining was performed to assay the PCP pathway.

Results

Wls was expressed in the cochlear duct from E12.5 to E18.5. The Wls-ablated cochlea was shorter and wider compared to littermate controls, suggesting a defect in convergent extension. Immunostaining or in situ hybridization for Myo7a, Prox1, Atoh1, and Jag1 indicated that a full complement of hair cells and supporting cells was present in the CKO cochlea, although hair cells appeared disorganized and an intermittent fourth row of outer HC was observed. In the basal turn, stereocilia bundle orientation defects were observed. Moreover, we detected a loss of polarization of Fzd6 and Dvl2, but not Vangl2 and Vangl1, in CKO cochlea.

Conclusion

Manipulation of the Wnt secretory pathway via Wls deletion in the embryonic cochlea leads to the formation of a shorter and wider organ of Corti. These defects were accompanied by stereocilia bundle misorientation and aberrant localization of a subset of PCP core proteins. Overall, our data suggest that Wls is required for convergent extension and HC orientation.

PD 161**The Developmental Abnormality of Phalangeal Process in GJB2 Knockdown Mouse Model**

Sen Chen¹; Le Xie¹; Xia Wu¹; Jin-Tao Yu¹; Yu Sun¹; Weijia Kong²

¹Department of Otorhinolaryngology, Union Hospital, Tongji Medical College, Huazhong University of Science and Technology, Jiefang Avenue 1277, Wuhan 430022, China; ²Department of Otolaryngology, Union Hospital of Tongji Medical College, Tongji Medical College

GJB2 (coding Connexin26, Cx26) mutations are the most common causes of hereditary hearing loss. Recently, the postnatal development disorder of organ of Corti has been explored in different Cx26 null mouse models. To explore the pathological changes and the mechanism for cochlear developmental arrest, we have established transgenic mouse models by conditional knockdown of cochlear Cx26 at postnatal day 0 (P0) and 8 (P8). The auditory threshold was tested by ABR and the geometric changes were analysed by semi-thin sections. The pathological changes were visualized by scanning and transmission electron microscope (SEM and TEM). The mice in P0 knockdown group suffered severe hearing loss while the mice in P8 knockdown group have normal hearing. The organ of Corti (OC) of mice in P8 knockdown group displayed normal architecture, however, the height of OC and the distance between outer and inner Pillar cells were significantly reduced in P0 knockdown group. Additionally, phalangeal processes of both Pillar and Deiter's cells remained in juvenile stage that contacted with adjacent cells and could not mature into finger-like structure in P0 knockdown group. The microtubule in the phalangeal processes of Pillar and Deiter's cells was significantly reduced in P0 knockdown group, however it was nearly not affected in P8 knockdown group. These data indicated that the GJB2 participated in the postnatal cytoskeleton development of both Pillar and Deiter's cells. The malformed phalangeal processes may affect the supporting frame of the organ of Corti, which would be a new mechanism of GJB2-related hearing loss.

PD 162**Activin A Signaling Instructs Hair Cell Differentiation in the Mammalian Cochlea**

Angelika Doetzlhofer¹; Ana Benito-Gonzalez²; Erin J. Golden³; Meenakshi Prajapati⁴

¹Johns Hopkins School of Medicine; ²Johns Hopkins University, School of Medicine; ³University of Colorado Denver Anschutz Medical Campus; ⁴Johns Hopkins University

The mammalian auditory end organ is a highly specialized sensory organ tuned to detect and encode sound. To ensure the highly stereotyped pattern of mechano-sensory hair cell arrangement, cell cycle withdrawal and differentiation within the auditory sensory epithelium occurs in a spatial and temporally highly coordinated manner. Sensory progenitors exit the cell cycle in an apical-to-basal gradient, which is followed by a reverse gradient of differentiation. Previous studies revealed that an apical-to-basal Sonic Hedgehog signaling gradient maintains auditory sensory progenitor cells in an undifferentiated state. However, the signals that trigger their differentiation into hair cells are currently unknown.

Here, we provide evidence suggesting that activin A signaling instructs hair cell differentiation in the murine cochlea. Activins are secreted proteins that belong to the large family of TGF- β ligands. Activins signal through binding and activating type I and type II transmembrane serine/threonine kinase receptor complex. The biological activity of activins is limited by follistatin, a secreted protein that binds activins at high affinity. Confirming previous reports, we show that the activin A and its antagonist follistatin are expressed in opposing gradients within the differentiating sensory epithelium, with activin A being expressed in the cochlear base and follistatin being expressed in the cochlear apex. Moreover, we show that the emergence of activin A coincides with the onset of cochlear hair cell differentiation. Using organotypic cultures, we show that exogenous activin A induces premature differentiation of cochlear hair cells. Conversely, overexpression of follistatin, using a previously established transgenic mouse line, delays the differentiation of cochlear hair cells *in vivo* and *in vitro*. Furthermore, we find that exogenous activin A is able to rescue the inhibitory effect of follistatin on hair cell differentiation, suggesting that follistatin inhibits hair cell differentiation through antagonizing activin A activity. Finally, we provide evidence that follistatin positively regulates sensory progenitor cell proliferation. We find that higher than normal expression of follistatin severely delays sensory progenitor cell cycle withdrawal, causing an overproduction of inner hair cells. How follistatin interferes with sensory progenitor cell cycle exit is currently under investigation.

PD 163

Hepatocyte Growth Factor-c-MET Signaling Mediates the Development of Non-sensory Structures of the Mammalian Cochlea and Hearing

Takahiro Ohyama¹; Shumei Shibata²; Toru Miwa³; Hsiao-Huei Wu⁴; Pat Levitt⁴

¹USC Tina and Rick Caruso Department of Otolaryngology – Head and Neck Surgery and Zilkha Neurogenetic Institute, Keck Medicine of USC, University of Southern California; ²Department of Otorhinolaryngology – Head and Neck Surgery, Graduate School of Medical Sciences, Kyushu University; ³Department of Otolaryngology and Head and Neck Surgery, Kumamoto University; ⁴Program in Developmental Neurogenetics, Institute for the Developing Mind, The Saban Research Institute, Children's Hospital of Los Angeles, and Department of Pediatrics, Keck School of Medicine of USC

The stria vascularis is a non-sensory structure that is essential for auditory hair cell function by maintaining potassium concentration of the scala media. During mouse embryonic development, a subpopulation of neural crest cell (NCC)-derived melanocytes migrates and incorporates into a subregion of the cochlear epithelium, forming the intermediate cell layer of the stria vascularis. The relation of this developmental process to stria vascularis function is currently unknown. Recently, Schultz and colleagues have shown that an autosomal-recessive, nonsyndromic hearing loss, DFNB39, is caused by non-coding mutations of HGF (Schultz et al., 2009). Also, Mujtaba and colleagues have identified missense mutations in the c-MET locus from the DFNB97 family (Mujtaba et al., 2015). In characterizing the molecular differentiation of developing peripheral auditory structures, we discovered that Hepatocyte Growth Factor (Hgf) is expressed in the future stria vascularis of the cochlear epithelium. Its receptor tyrosine kinase, c-Met, is expressed in the cochlear epithelium and melanocyte-derived intermediate cells in the stria vascularis. We generated a series of conditional knockout mice in which HGF-c-MET signaling is inactivated specifically in the cochlear epithelium or in the migrating neural crest cells. In both cases, we observed that the migrating NCC-derived melanocytes correctly approach the ventral side of the cochlear duct at E13.5 and adhere the basal side of cochlear epithelium where the prospective stria vascularis forms by E15.5. However, these melanocytes fail to incorporate into the cochlear epithelium, causing the absence of the intermediate cell layer of the stria vascularis. The auditory hair cells formed normally at birth, but are malformed and degenerated in the adult mutant cochlea in the absence of HGF-c-Met signaling. These mutant mice present profound deafness phenotype at 4-6 week of age

with a threshold shift of 40-70 dB (SPL) across all tested frequencies. Our finding indicates that the disruption of the formation of the intermediate cells in the absence of HGF-c-MET signaling and thus results in deafness, which likely is relevant to syndromic human deafness caused by rare mutations in the HGF or c-MET genes.

PD 164

Mechanical Force Restricts the Growth of the Inner Ear Sensory Epithelia

Ksenia Gnedeva¹; Adrian Jacobo²; Joshua Salvi²; Aleksandra Petelski³; A J Hudspeth²

¹The Rockefeller University and Keck School of Medicine of USC; ²The Rockefeller University; ³Stevens Institute of Technology

Background

Unlike non-mammalian vertebrates, adult mammals cannot replenish lost hair cells, which often results in permanent deafness and balance disorders. This deficiency stems from the inability of the inner ear's sensory epithelia either to proliferate or to produce new hair cells after a certain developmental stage. Understanding what arrests growth during development is therefore critical in efforts to restore hearing and balance.

Methods

We utilized a vestibular organ, the utricle, as a model system to investigate the developmental dynamics of inner-ear sensory epithelia. By monitoring changes in the organ's size, architecture, and cell numbers during the utricle's growth we were able to create a comprehensive theoretical model that captures key features of the organ's morphogenesis. We also developed a novel, three-dimensional culture system that allowed us to test model's predictions by conducting long-term time-lapse imaging of the organ's growth.

Results

Our experimental data and model for the first time demonstrate that mechanical force that opposes the utricle's growth during development, confines cellular proliferation to the organ's periphery, and eventually arrests growth altogether. We found that activation of the Hippo signaling pathway underlies this process and that a reduction in mechanical constraint restores the utricle's growth through nuclear translocation of Yap, a transcriptional cofactor in the Hippo pathway.

Conclusions

Our results suggest that the Hippo signaling pathway plays an important role during the development of the sensory organs of the inner ear and that its activation is able to repress supporting cell proliferation. Further

characterization of the roles of Yap and Hippo signaling in the developing ear might therefore suggest ways to overcome hearing and balance impairment.

PD 165

A Human iPS Cell Model of Alström Syndrome Reveals New Molecular Mechanisms

Brigitte Malgrange¹; Amandine Czajkowski¹; Benjamin Grobarczyk²; Bénédicte Franco³; Kevin Hanon¹; Gabriella Milan⁴; Philippe P. Lefebvre⁵; Laurent Nguyen¹
¹GIGA-Neurosciences; ²University of Liege; ³UNiversité de liege; ⁴UNiversity of Padua; ⁵CHU de liege

Alström Syndrome (AS) is a human, autosomal recessive, genetic disorder characterized by numerous clinical symptoms including deafness. AS is caused by mutations in the ALMS1 gene encoding the ALMS1 protein localized in centrosomes and basal bodies of primary cilia. ALMS1 has been implicated in ciliogenesis, intracellular trafficking, cell cycle control and cellular differentiation, among others. However, the molecular mechanisms that give rise to deafness are still unknown. Here, we used human induced pluripotent stem (hiPS) cells generated from fibroblasts of healthy and AS patients to decipher the pathophysiological role of mutated ALMS1 in deafness.

We established hiPS cells from patient fibroblasts using non-integrative Sendai viral vectors. These cell lines were validated in vitro and in vivo. Using a stepwise protocol, we demonstrate that healthy hiPSCs can generate a population of otic progenitor cells (OSCs) that are then able to differentiate into hair cells (HCs) when co-cultured with mouse feeder cells. We then applied this differentiation protocol to AS hiPSCs generated from AS patients. We showed that, AS hiPS cells are able to generate OSCs and HCs similarly to wild type hiPS cells. While differentiation capabilities seem normal in AS hiPS cells, we found numerous abnormal features in AS-OSCs. In particular, AS-OSCs present cell proliferation defects and abnormal primary cilium development.

PD 166

Restoring Hearing and Balance: Introducing a New Approach

Bernd Fritzsch; Karen Elliott-Thompson; Clayton Gordy
University of Iowa, Dept of Biology.

Background

Most vertebrates have continued proliferation of hair cells, allowing for hair cell restoration, whereas mammals have no ongoing proliferation and lack hair cell

restoration, causing age and damage related decline in hearing and balance. Ruben et al (1988) suggested that better understanding of this process in non-mammals could help restore human hearing. We review this approach and suggest alternative strategies. Initial data on manipulating proliferation regulators p27kip, n-Myc, or RB showed altering cell cycle progression can increase the number of hair cells in embryos. Follow up investigation revealed these manipulations are limited to juvenile mice equivalent to late human fetuses. Elderly mice and humans do not benefit yet and a molecular understanding of this block is needed.

In vitro hair cell generation produces limited numbers of hair cells precluding implantations to cure diseases. Moreover, viability of hair cells immersed into endolymph and insertion of hair cells into the remaining organ of Corti in the right orientation remain unresolved obstacles.

In vivo hair cell restoration through molecular conversion of existing cells provided proof of principle through Atoh1-induced transdifferentiation of supporting cells after induced hair cell loss. This approach has yielded very few functional hair cells mostly in juvenile animals and is associated with acute hair cell destruction. Hopes that even partial restoration of the organ of Corti might lead to improvements of hearing are dampened by developmental data showing complete deafness after near normal development of an organ of Corti.

We propose a novel approach: instead of aiming to jump start restorative capacity in the aging ear, we propose to implant a developing otocyst to replace the defect ear. Toward this end we have begun a series of experiments to show that otocyst implantation and differentiation is possible in xenoplastic grafting of different vertebrates (Xenopus, chicken, mouse) and is possible with heterochronic transplantation (younger ears on older animals). We envision that this approach could be used to restore ears after surgical removal or in severely deaf and balance-challenged human ears using humanized pig otocyst transplantations. If further refined, this approach could help restore the lost sensory organs by making use of the natural proliferative and differentiation abilities inherent to the developing mammalian otocyst, possibly directed by the insights gained in the above outlined attempts to restore hearing or balance.

Vestibular II: Clinical Indicators of Dysfunction

PD 167

Epidemiology of Balance and Dizziness Problems in United States Adults: Results from the 2014 National Health Interview Survey

Howard J. Hoffman¹; Christa L. Themann²; Robert A. Dobie³; Anne E. Hogan⁴; Helen Cohen⁵; Gregory A. Flamme⁶; Katalin G. Losonczy⁷; Chuan-Ming Li¹; Charles C. Della Santina⁸

¹National Institute on Deafness and Other Communication Disorders, NIH; ²National Institute for Occupational Safety and Health (NIOSH), CDC; ³University of Texas Health Science Center at San Antonio; ⁴Pacific University; ⁵Dept of Otolaryngology, Baylor College of Medicine; ⁶Western Michigan University; ⁷National Institute on Deafness and Other Communication Disorders (NIDCD), NIH; ⁸Johns Hopkins University School of Medicine

Objective

Estimate prevalence and risk factors for balance and dizziness problems (BDP).

Methods

We analyzed data from the 2014 National Health Interview Survey (NHIS), a nationally-representative health interview survey of 36,697 adults, aged 18+ years. Co-variables were NHIS questions on hearing (self-reported difficulty, Gallaudet hearing scale, noise exposures, and tinnitus), health (arthritis, asthma, cancer, severe headaches/migraine, sinusitis, stroke), and limitations (cannot stand 2 hours). BDP was classified based on: "During the past 12 months, have you had a problem with dizziness, light-headedness, feeling as if you are going to pass out or faint, unsteadiness or imbalance?" We examined associations between BDP and socio-demographic, hearing, health, and functional status variables using multivariable logistic models.

Results

BDP prevalence was 14.8% (35.4 million), increasing from 11.7%, 15.8%, 19.7%, to 25.8% for adults 18-44, 45-64, 65-84, and 85+ years, respectively. Factors associated with BDP: female sex (odds ratio [OR]=1.57, 95% confidence interval [CI]:1.42-1.73), poverty-level income (OR=1.42;CI:1.20-1.68), any hearing difficulty (OR=1.34;CI:1.17-1.55), firearms noise (OR=1.29;-CI:1.15-1.43), sinusitis (OR=1.36;CI:1.19-1.55), cancer diagnosis (OR=1.54;CI:1.32-1.81), joint pain/aches (OR=1.76;CI:1.59-1.95), cannot stand 2 hours (OR=1.96;CI:1.70-2.27); ever had stroke (OR=1.96;-CI:1.54-2.49), tinnitus problem (OR=2.92;CI:2.42-3.53),

and severe headaches/migraine (OR=2.97;-CI:2.61-3.37). Specific hearing loss etiologies (due to medications/drugs, sudden onset, Meniere's, otosclerosis, ear injury-head/neck trauma) were associated with BDP. There was no association between duration of hearing loss and BDP.

Conclusion

BDP prevalence ranged from substantial for young adults to very common for the oldest. The strongest associations were with severe headaches/migraine and tinnitus, while other hearing and health conditions were also important.

PD 168

Immunocytochemical Changes in the Blood Labyrinthine Barrier of Vestibular Endorgans Obtained from Patients Diagnosed with in Meniere's Disease

Gail Ishiyama; Ivan Lopez; Akira Ishiyama
UCLA School of Medicine

Background

The keys to understand the pathophysiology of Meniere's disease are the cell-to-cell interactions and molecular mechanisms that regulate blood labyrinth barrier (BLB) integrity. We recently detected by transmission electron microscopy increased transcellular vesicular transport across vascular endothelial cells (VECs), detachment of pericyte processes, and disruption of the perivascular basement membrane in the stroma of vestibular endorgans obtained by ablative surgery from patients diagnosed with Meniere's disease. We hypothesize that Meniere's disease is associated with cellular and molecular changes in the vascular architecture of the human inner ear.

Methods

To investigate the degenerative changes in endothelial cells, pericytes, perivascular macrophages-like melanocytes, and the surrounding basement membrane, we used specific antibodies and immunofluorescence to identify changes in the protein expression of the BLB of vestibular endorgans obtained by ablative surgery from patients diagnosed with Meniere's disease. Isolectin (IB-4) to identify VECs, alpha-smooth muscle actin (α -SMA), ZO-1 and occludin to identify tight junctions of VECs was used. Laminin-beta-2, and collagen IV to identify the perivascular basement membrane was used. We compared these results with those obtained from normative vestibular endorgans microdissected from temporal bones obtained at autopsy.

Results

We detected the following changes in the microvasculature of the macula and cristae stroma from Meniere's

patients when compared with normative specimens: VECs showed decreased staining expression of the isolectin IB4, pericytes showed normal expression of α -SMA. ZO-1 and occludin immunoreactivity expression were decreased. There was also a decrease in laminin and collagen IV expression in the perivascular basement membrane.

Conclusions

The decrease of expression of several key proteins in the microvasculature of the BLB suggest that the blood labyrinthine barrier microvasculature of the vestibular endorgans from patients diagnosed with Meniere's disease may be compromised and consequentially contributed to the pathophysiology.

Support

Hearing Health Foundation emerging grant (20164266)
GI

PD 169

High Throughput Gene Expression Analysis of Delayed Endolymphatic Hydrops by RNA-seq

Dong-Dong Ren¹; Xiao-Yu Yang²; Xin-Wei Wang²;
Xiao-Qing Qian²; Fanglu Chi¹; Dongdong Ren²

¹Department of Otolaryngology and Skull Base Surgery, Eye, Ear, Nose and Throat Hospital; Fudan University, Shanghai, China; ²EYE & ENT Hospital of Fudan University

Background

Delayed endolymphatic hydrops (DEH) is characterized by endolymphatic hydrops in patients suffering from longstanding hearing loss. DEH mostly occurs in the ipsilateral ear and causes recurrent vertigo similar to the symptoms in Meniere's disease suggesting that the two disease share pathophysiological features. Recent study showed that abnormal expression of HLA, AQP and COCH genes could lead to Meniere's disease. Nevertheless, the causation of DEH is not fully established.

Object

To discover genes related to DEH in patients by RNA-seq sequencing.

Methods

To study pathogenesis in patients with DEH, we collected the whole vestibular system from three patients who undergone the labyrinthectomy, and three samples from patients with acoustic neuroma or facial neuroma who undergone translabyrinthine approach as control. We performed a high throughout RNA-Seq study of gene expression.

Results

Our bioinformatics analysis identified 13 unreported genes remarkably upregulated in patients with DEH compared with the control group, including ARRDC2, CLDN19, DCT, DDIT4, GAS7, HLA-DRB1, MME, MPZ, PLEKHA4, PMP2, PRB4, PRX, SLC9A3R2 and XIST. The results were inconsistent with abnormal genes in Meniere's disease. We found that DEH likely have a close relationship with neuropathy and autoimmune disease. Besides, cell adhesion pathway may be significant related to delayed endolymphatic hydrops.

Conclusion

RNA-Seq and bioinformatics techniques can be used as a powerful tool for discover gene-transcription in patients with DEH. DEH and Meniere's disease are probably the same disease with the different forms. Some key genes screened in this study may become candidate genes or operating targets in the future research.

Keywords

endolymphatic hydrops; RNA-Seq; transcriptome; hearing loss

PD 170

Translational Predictivity of Preclinical Model Studies of the Anti-Vertigo Drug SENS-111 for Clinical PK/PD Relationships

Jonas Dyhrfeld-Johnsen; Eric Wersinger; Mathieu Petremann; Veronique Briec; Désiré Challuau; Cindy Gueguen; Stéphanie Bressieux; Christophe Tran Van Ba; Pierre Attali
Sensorion

A major challenge in the development of targeted drug treatments for vestibular disease is the lack of validated and predictive preclinical models for selection of clinical drug candidates, in large part due to the lack of understanding of the etiology and pathophysiology of vestibular diseases. We have developed a mechanism based model of vestibular injury based on excitotoxic peripheral insult which generates a number of established, vertigo associated symptoms such as spontaneous nystagmus, postural deviations and gastric paresis. Using a combination of preclinical and clinical pharmacodynamics and pharmacokinetic approaches, we here present a clear correspondence between preclinical prediction of effective drug concentrations and clinical outcomes for the H4R receptor antagonist SENS-111 analyzed using PK/PD modeling.

Preclinical experiments using intravenous SENS-111 administration (10/20/40 mg/kg) 1h after induction of peripheral vestibular lesions in female Long-Evans rats using transtympanic injections of kainic acid (40-50 mM)

during the acute vertigo phase demonstrated a bell-shaped dose/efficacy relationship with an optimal dose of 10 mg/kg for reduction of spontaneous nystagmus frequency. This dose consistently lead to symptom reduction in the range of 20-30% already 1h after administration, while doses of 20-40 mg/kg resulted in a loss of efficacy. Systemic and local drug exposure studies determined an equilibrium between blood plasma, CSF and perilymph drug levels 1h after administration, while tissue exposures in respectively brain and inner ear tissue exceeded the drug levels in the fluid compartments. For the optimal dose of 10 mg/kg SENS-111, blood plasma concentrations did not exceed 500 ng/mL during the functional testing period while the non-effective dose of 20 mg/kg reached levels as high as 1000 ng/mL.

In a clinical phase 1b study, the effect of SENS-111 on duration of vertigo, latency of vertigo appearance, and latency of vertigo disappearance following caloric irrigation was determined in healthy volunteers in parallel with a pharmacokinetic characterization of multiple ascending doses up to 250 mg/day for 4-7 days. Using PK/PD modeling of the relationship between drug exposure levels and pharmacodynamic effects on vertigo measures, a bell-shaped exposure/efficacy relationship was determined with positive treatment effects in the 20-30% range at exposures ≤ 500 ng/mL while exposures > 500 ng/mL worsened vertigo outcome measures.

The clear clinical and preclinical correspondence of effective drug exposure levels and treatment effect size validates the predictive value of the preclinical model for clinical development of anti-vertigo drugs and strengthens the rationale for dose selection and clinical trial design in upcoming phase 2/3 trials.

PD 171

Is There a Relationship Between Vestibular Loss and Cognitive Function in Children?

Kristen Janky; Megan Thomas

Boys Town National Research Hospital

Background

Adults with vestibular loss have deficits in visuospatial working memory, spatial memory, and short-term working memory (Bigelow et al., 2015; Brandt et al., 2005; Hanes et al., 2006). Working memory deficits have been reported in children with cochlear implants (CI; Pisoni & Cleary, 2003; Cleary et al, 2001; Nitttrouer et al., 2014); however, cognitive outcomes have not been investigated specifically in children with vestibular loss. Approximately 50% of children with a CI have some degree of vestibular loss. Therefore, the purpose of this study was to determine if children with CIs and vestibular loss ev

idence greater cognitive deficits compared to children with CIs and normal vestibular function.

Subjects

<34 children with normal hearing (8 – 18 years), 19 children with CI (8 – 18 years).

Methods: Vestibular function was assessed via cervical and ocular vestibular evoked myogenic potentials, the video head impulse test, and rotary chair. Children were further subdivided into 3 groups: Children with normal hearing and vestibular function (n = 34), children with CI and normal vestibular function (n = 13), and children with CI and bilateral vestibular loss (n = 6).

Working memory was assessed by the Automated Working Memory Assessment (AWMA). To control for differences in language, executive function, and speech recognition, the following outcomes were also assessed: Behavior Rating Inventory of Executive Function (BRIEF), Clinical Evaluation of Language Fundamentals (CELF-5), Peabody Picture Vocabulary Test (PPVT-4), and Speech Recognition with AZ Bios Sentence List.

Results

There were no significant differences between the children with normal hearing and children with CI regardless of vestibular loss status for performance on the BRIEF and CELF-5. The children with CI scored significantly more poorly than the children with normal hearing on speech recognition and PPVT-4 testing; however, in the children with CI, there was no significant difference between the normal vestibular function and vestibular loss groups. These findings suggest the children with CI were matched for language, executive function, and speech recognition ability.

For the AWMA, children with CI and vestibular loss performed significantly more poorly than the children with normal hearing on all subtests of visuospatial working memory. The children with CI and vestibular loss performed significantly more poorly than the children with CI and normal vestibular function on one subtest of visuospatial working memory.

Conclusions

Our preliminary results suggest that children with cochlear implants and vestibular loss have visuospatial working memory deficits. Recruitment is ongoing.

Time Course of Caloric Nystagmus in Cases with Spinocerebellar Degeneration

Takeshi Tsutsumi¹; Ayane Makabe¹; Chiaki Hirai²;
Yukiko Yamamoto²; Takamori Takeda²; Yoshiyuki
Kawashima²

¹Tokyo Medical and Dental University; ²Department of
Otolaryngology, Tokyo Medical and Dental University

Background

The caloric test used to be one of the gold standards in the battery of tests used to evaluate vestibular function. The conventional method for caloric stimulation entails irrigation of the external ear canal while the subject lies on his/her back. However, this procedure does not induce acute onset of thermos-convection of endolymphatic fluid within the lateral semicircular canal. Caloric step stimulus technique, which loads head movement during continuous caloric irrigation of the external ear canal to abruptly enhance the increasing thermos-convection, gives an examiner the opportunity to evaluate the time course characteristics of the VOR using the caloric test. In the present study, we adopted the stimulus technique to subjects with spinocerebellar degeneration (SCD) to examine the time course characteristics and mechanisms of the changes in VOR caused by central vestibular impairment.

Methods

Caloric test combined with step stimulation were adapted to healthy subjects and patients with spinocerebellar degeneration. The onset of thermal gradient stimulation was induced acutely through continuous caloric irrigation and rapid movement of head and torso from an upright to a supine position. Responses were recorded using an electro-oculograph, and the velocity of the recorded horizontal eye movements was calculated. Slow phase eye velocity was extracted above the time axis and fitted using the method of least squares to the regression curve, which was determined as the summation of the activation and adaptation components using the following equation:

$$S(t) = A[1 - e^{-((t)/T_1)}] - A[1 - e^{-((t)/T_2)}]$$

where coefficient A (deg/s) is the strength and T1 and T2 (s) are time constants for the activation and adaptation components, respectively (Fig.1). The first half of the formula (activation response) represents the rapid rise and endurance of the VOR induced from beginning of the caloric step stimulation. The latter half (adaptation response) represents the gradual decline in the VOR.

Results

The amplitude of the curve-fitted VOR (A) were about the same between healthy and SCD subjects. In SCD patients, the time constant of the activation response (T1) was shortened (Fig.2), though that of adaptation response (T2) didn't demonstrate any difference with that of healthy subjects.

Conclusions

SCD diminished the rise of caloric VOR, though demonstrating similar decline, compared to healthy subjects. Insufficient velocity storage integration might cause this characteristic. Further investigation considering detailed focus and stage of the disease would be required.

PD 173

The c-Jun N-Terminal Kinase Inhibitor, AS602801 (bentamapimod), Decreases Schwannoma Tumor Volume and Cell Proliferation

Franklin Canady¹; Jason Clark¹; Jennifer Kersigo²;
Bernd Fritsch³; Waylan Bessler⁴; Wade Clapp⁴;
Charles Yates⁴; Marlan R. Hansen⁵

¹University of Iowa; ²University of Iowa, Department of
Biology; ³University of Iowa, Dept of Biology.; ⁴Indiana
University; ⁵University of Iowa Hospitals and Clinics,
Department of Otolaryngology- Head & Neck Surgery

Background

Vestibular schwannomas (VSs) are benign nerve sheath tumors arising from the vestibular nerve and lead to hearing loss. Most VSs are sporadic, but bilateral VSs are seen in neurofibromatosis type 2 (NF2). Currently, the main treatment options are surgical removal or radiation therapy, which in most cases results in deafness and other cranial neuropathies. Identification of pharmacological compounds that effectively limit or reduce VS growth would provide significant benefit to NF2 patients compared to current therapies. Recent in vitro studies demonstrate that c-Jun N-terminal kinase (JNK) activity is upregulated in VSs and this persistent JNK activity leads to increased cell proliferation and cell survival. Thus, JNK inhibitors reduce proliferation and induce apoptosis in human VS cells in culture. Here we employ two animal models to test the ability of the JNK inhibitor, AS602801, to reduce schwannoma growth in vivo.

Methods

Subcutaneous VS xenografts derived from acutely resected human tumors were established in 40 nude mice. Pretreatment MRI scans were taken one month after tumor implantation. Mice were randomly assigned into two groups: 60 mg/kg/day of AS602801 divided into 2 daily doses for 65 days or a control group (water). Post treatment MRI scans were taken and tumor volumes were

calculated. In a parallel study, PostnCre;Nf2f/f mice, which develop schwannomas in dorsal root ganglia (DRG) and cranial nerve sensory ganglia, were likewise randomly treated with AS602801 (n=10) or water (n=13). In these mice, serial ABR click thresholds were also measured. All mice were injected with EdU prior to sacrifice. Schwannoma tissue was sectioned and stained for DAPI (cell nuclei), anti-S100 (schwannoma cell marker), and either EdU (cell proliferation) or TUNEL (apoptosis) and the percent of EdU- and TUNEL-positive schwannoma cell nuclei were scored.

Results

Mice tolerated treatment with AS602801 without significant problems. Mice treated with AS602801 displayed a significant decrease in human VS xenograft tumor volume (-29.16%±7.71) compared to control mice (19.01%±10.37, $p < 0.001$). Further treatment with AS602801 reduced DRG volume and delayed elevation of ABR thresholds in PostnCre;Nf2f/f mice compared to control treatment. Finally, AS602801 decreased schwannoma cell proliferation in both the xenograft ($p=0.004$) and PostnCre;Nf2f/f mice ($p < 0.001$). However, AS602801 did not increase the percent of apoptotic schwannoma cell nuclei in either model ($p>0.05$).

Conclusion

Treatment with AS602801 leads to decreased schwannoma tumor volume and cell proliferation in two different animal models, suggesting that JNK inhibitors could potentially be used to help treat patients with VSs.

PD 174

Two Legs of the Vergence Triad in mTBI

Carey D. Balaban¹; Mikhaylo Szczupak²; James K. Buskirk²; Hillary Snapp³; Constanza Pelusso²; Robin C. Ashmore⁴; Alexander Kiderman⁴; Michael E. Hoffer⁵

¹University of Pittsburgh; ²Department of Otolaryngology University of Miami; ³University of Miami; ⁴Neuro Kinetics, Inc.; ⁵Department of Otolaryngology and Neurological Surgery, University of Miami

Mild traumatic brain injury (mTBI or concussion) is a public health issue that has recently received a significant amount of scientific as well as lay attention. One of the most important controversies surrounding mTBI concerns objective methods for diagnosing the condition and for judging when it is appropriate for individuals diagnosed with mTBI to return to work or play. Many groups have reported that neurosensory symptoms are common sequelae of mTBI with dizziness (vestibular issues) as well as optokinetic eye motion issues being among the most common. We have reported the use of a portable optokinetic, vestibular, and reaction time

(OVRT) device to provide point of injury diagnosis of mTBI. This device also assesses vergence eye movements and dynamic changes in pupillary diameter, which are two components of the vergence triad. Seventeen subjects with a diagnosis of mild traumatic brain injury were tested acutely (within 3 days of injury), 1 week later and 2 weeks later. Fifty age matched controls were also tested. The 0.1 Hz sinusoidal vergence pursuit stimulus was presented with a head mounted display (i-PAS, Neuro Kinetics, Pittsburgh, PA) by manipulating retinal disparity of a spot to produce vergence movements centered between the pupils. Pupil size and eye movement were measured by video-oculography at 100 Hz. The control subjects showed robust and coherent vergence eye movements and pupil size changes, with the pupil constricting as the eyes converged; they were assessed quantitatively by cross-spectral, cross-correlation and complex demodulation analyses to generate norms. The coordination between vergence eye movements and dynamic changes in pupil diameter were deranged acutely in the mTBI subjects, and improved over the two week follow-up period. We speculate that this relationship can be used as one important diagnostic feature of mTBI at or near the point of injury. The implications for these findings for optimal mTBI treatment and rehabilitation are important as well. Correcting abnormalities in this relationship may be an objective metric of patient recovery.

Author Index

Name	Abstract No.	Page No.
Aaltonen, Alina	PS 469	326
Abbas, Leila	PS 496	341
Abbas, Paul	PS 122	76
Abbas, Paul	PS 139	86
Abdala, Carolina	PS 82	54
Abdala, Carolina	SYMP 67	463
Abdala, Carolina	PS 84	55
Abdelfatah, Nelly	PS 116	72
Abdelrehim, Lamiaa	PS 14	17
Abdulhadi, Khalid	PS 121	75
Abitbol, Julia	PS 325	221
Abrams, Mikayla	PS 666	435
Abrams, Kristina	PS 362	241
Abrams, Mikayla	PS 665	435
Abrams, Daniel	PD 9	138
Aburto, María R.	PS 755	515
Acharya, Anushree	PS 130	81
Acuna, Dora	PD 99	455
Adams, Joe	PS 226	133
Adams, Brittany	PS 827	556
Adamsky, Svetlana	PS 888	590
Adamson, Robert	PS 184	110
Adenis, Victor	PS 28	25
Adler, Henry	PS 551	372
Adunka, Oliver	PS 361	240
Adunka, Oliver	PS 6006	403
Adunka, Oliver	PS 786	532
Agnew, Thomas	PS 686	477
Agrawal, Sumit	PS 307	212
Agrawal, Sumit	PS 616	408
Agrawal, Yuri	SYMP 42	303
Aguilar, Carlos	PS 686	477
Aguirre Davila, Lukas	PS 577	386
Ahlstrom, Jayne	PS 394	258
Ahlstrom, Jayne	PS 427	276
Ahmad, Aisha	PS 558	376
Ahmad, Aisha	PS 687	477
Ahmad, Aisha	PS 342	230
Ahmed, Zubair	PS 908	604
Ahmed, Zubair	PS 155	95
Ahmed, Zubair	PS 768	522
Ahmed, Zubair	PS 133	83
Ahmed, Zubair	PD 98	454
Ahmed, Zubair	PD 96	453
Ahrens, Misha	PS 436	281
Ahroon, William	PS 834	560
Ahroon, William	PD 156	629
Ahsan, Syed	PS 898	598
Aiken, Steven	PS 489	336
Aiken, Steven	PD 114	468
Akil, Omar	PS 161	98
Akiyama, Naotaro	PS 846	567
Akiyama, Naotaro	PS 835	560
Aksentijevich, Ivona	PD 94	452
Al-aameri, Raheem	PS 583	390
Al-aameri, Raheem	PS 597	398
Alagramam, Kumar	PD 58	293
Alagramam, Kumar	PS 135	84

Name	Abstract No.	Page No.
Alain, Claude	PS 43	34
Albertus, Faywell	PD 58	293
Alexander, Andrew	PS 773	525
Alfadhel, Ahmed	PS 819	551
Alhussaini, Mohamed	PS 42	33
Alhussaini, Mohamed	PS 624	413
Alhussaini, Mohamed	PS 839	563
Ali, Hussnain	PS 12	16
Alibert, Eric	PS 904	601
Alkowari, Moza	PS 121	75
Allen, Paul	PD 120	472
Allen, Jont	PS 426	275
Allen, Paul	PS 56	40
Allison, Jerome	PS 918	610
Allison, Jerome	PS 920	611
Allman, Brian	PS 325	221
Allman, Brian	PS 610	405
Allon-Shalev, Stavit	PD 82	311
Almishaal, Ali	PS 570	383
Almishaal, Ali	PS 143	88
Almishaal, Ali	PS 141	87
Alshamani, Mansour	PS 60	43
Alshawaf, Abdullah	PS 894	594
Altioe', Alessandro	PS 1	9
Altschuler, Richard	PS 608	404
Altschuler, Richard	PS 921	611
Ambrosetti, Umberto	PS 124	77
Ambrosetti, Umberto	PS 121	75
Ambrosetti, Umberto	PS 120	74
Amemiya, Yutaka	PS 892	593
Ananthakrishnan, Saradha	PS 743	508
Anbuhl, Kelsey	PS 649	426
Anbuhl, Kelsey	PS 407	265
Andeol, Guillaume	PS 399	261
Andeol, Guillaume	PS 418	271
Andeol, Guillaume	PS 420	272
Andersen, Ture	PD 118	470
Anderson, Lucy	PS 434	280
Anderson, Samira	PS 421	273
Anderson, Samira	PS 236	172
Anderson, James	PS 619	410
Anderson, Daniel	SYMP 17	168
Anderson, Sean R.	PS 654	429
Anderson, Charles	PS 257	183
Anderson, Samira	PS 239	174
Andre, Daniel	PS 895	595
Angara, Prashant	PS 414	269
Anson, Eric	PS 448	288
Anttonen, Tommi	PS 593	395
Aoustin, Jean-Marie	PS 652	427
Apawu, Aaron	PS 802	541
Apawu, Aaron	PD 15	141
Apawu, Aaron	PS 827	556
Applegate, Brian	PS 571	383
Applegate, Brian	PS 168	102
Applegate, Brian	PS 621	411
Aqtashi, Baktash	PS 838	562
Aralla, Roberta	PS 67	46

Author Index

Name	Abstract No.	Page No.
Aranke, Mayank	PS 809	545
Archer-Boyd, Alan	PS 33	28
Archer-Boyd, Alan	PS 274	192
Arduini, Stefania	PS 74	50
Arias, Kevin	PS 544	368
Arnoldner, Christoph	PD 6	6
Aronoff, Justin	PS 21	21
Aronoff, Justin	PS 657	430
Arrojo Martins, Fábio Tadeu	PD 82	311
Art, Jonathan	PS 537	364
Arteaga, Alberto	PS 918	610
Arteaga, Alberto	PS 59	42
Arteaga, Alberto	PS 920	611
Arun, Peethambaran	PS 600	400
Arya, Dev	PS 153	94
Asai, Yukako	SYMP 27	171
Ashida, Go	PD 85	447
Ashida, Go	PS 66	46
Ashman, Peter	PS 351	235
Ashmore, Robin	PD 174	639
Ashush, Hagit	PS 888	590
Askew, Charles	PS 803	541
Asokan, Meenakshi	PS 631	417
Asp, Filip	PS 648	425
Asp, Filip	PS 400	261
Asp, Filip	PS 650	426
Atai, Nadia	PS 149	91
Atcherson, Samuel	PS 304	210
Atencio, Craig	PS 439	283
Atkinson, Patrick	PD 64	296
Atkinson, Patrick	PS 210	124
Attali, Pierre	PS 235	137
Attali, Pierre	PD 170	636
Attias, Joseph	PS 613	407
Attigodu Chandrashekara, Ganesh	PS 489	336
Auerbach, Benjamin	PS 860	575
Auerbach, Benjamin	PS 629	416
Auerbach, Benjamin	PD 23	145
Auerbach, Benjamin	PS 633	418
Avan, Paul	PD 72	306
Avci, Ersin	PS 577	386
Averbeck, Bruno	PD 28	148
Avkin-Nachum, Sharon	PS 888	590
Avraham, Karen	PD 82	311
Avraham, Karen	PRES SYMP 6	2
Axe, David	PS 7	13
Ayoob, Andrew	PS 821	552
Ayoob, Andrew	PS 823	553
Azadpour, Mahan	SYMP 58	459
Azimzadeh, Julien	PS 769	523
Babola, Travis	PD 5	6
Babu, Vidya	PS 544	368
Bach, Eva	PS 735	504
Backous, Douglas	SYMP 68	463
Badii, Ramin	PS 121	75
Bae, Eun-bit	PS 677	441
Bafti, Sepand	PS 891	592
Bafti, Sepand	PS 930	596

Name	Abstract No.	Page No.
Bahloul, Amel	PD 72	306
Bai, Jun-Ping	PS 345	494
Bai, Jun ping	PS 337	227
Bai, Xiaohui	PS 494	340
Bajo, Victoria	PD 26	147
Bajo, Victoria	PS 469	326
Bajo, Victoria	PS 435	280
Bakay, Warren	PS 150	92
Bakhos, David	PS 652	427
Balaban, Carey	PS 224	131
Balaban, Carey	PS 225	132
Balaban, Carey	PS 681	443
Balaban, Carey	PD 174	639
Balaram, Pooja	PS 626	414
Ball, Greg	PS 320	218
Balmer, Timothy	PS 679	442
Baltzell, Lucas	PS 658	431
Bamberger, Morgan	PD 122	473
Banai, Karen	PD 123	474
Banakis Hartl, Renee	PS 42	33
Banakis Hartl, Renee	PS 624	413
Banakis Hartl, Renee	PS 839	563
Bance, Manohar	PS 184	110
Banks, Matthew	PD 138	618
Banks, Matthew	PS 458	320
Banks, Samantha	PS 115	72
Bankstahl, Jens	PS 310	213
Bao, Jianxin	PD 148	624
Barajas, Raquel	PS 755	515
Barbarite, Eric	PS 224	131
Barbarite, Eric	PS 225	132
Barber, Samuel	PS 226	133
Barber, Samuel	PS 305	211
Barber, Samuel	PS 808	544
Barbour, Dennis	PS 312	214
Barr, Kevin	PS 325	221
Barrett, John	PS 916	608
Barr-Gillespie, Peter	PD 71	305
Barth, Jeremy	PS 264	187
Barth, Jeremy	PS 492	338
Barth, Jeremy	PS 491	338
Barth, Jeremy	PS 321	218
Barzik, Melanie	PS 779	528
Barzik, Melanie	PS 142	88
Bas, Esperanza	PS 820	551
Bas, Esperanza	PS 351	235
Bas, Esperanza	PS 888	590
Bas, Esperanza	PS 354	237
Basch, Martin	PS 756	516
Basch, Martin	PS 105	66
Bashford, Seth	PD 135	616
Basinou, Vasiliki	PS 557	557
Basinou, Vasiliki	PD 101	456
Baskent, Deniz	SYMP 61	461
Baskent, Deniz	PS 859	575
Basta, Dietmar	PS 138	86
Basta, Dietmar	PS 498	342
Basta, Dietmar	PS 728	500

Author Index

Name	Abstract No.	Page No.
Basura, Gregory	PS 711	490
Basura, Gregory	PS 900	599
Basura, Gregory	PS 625	414
Bates, Daniel	PS 481	332
Battmer, Rolf-Dieter	PS 728	500
Batts, Shelley	PD 100	456
Batuecas-Caletrio, Angel	PD 95	452
Baudo, Robert	PS 853	571
Baudoux, Veronique	PS 904	601
Baumgärtel, Regina	PS 280	196
Baumgärtel, Regina	SYMP 51	315
Baumgartner, Robert	PS 401	262
Baumhoff, Peter	PS 259	184
Baumhoff, Peter	PS 500	343
Baumhoff, Peter	PS 732	502
Bausch, Alexander	PS 160	98
Bausch, Alexander	PS 797	537
Bausch, Alexander	PS 791	534
Bayer, Max	PS 48	36
Bazard, Parveen	PS 601	400
Bazard, Parveen	PS 27	24
Beach, Sara	PS 852	571
Bebee, Thomas	PS 110	69
Becker, Lars	PS 536	364
Becker, Lars	PS 331	224
Becker, Jonathan	PS 165	100
Becker, Lars	PS 533	362
Beckert, Michael	PS 67	46
Bedard, Noah	PS 833	559
Bedny, Marina	SYMP 4	2
Bee, Mark	PS 72	49
Bee, Mark	PS 369	245
Beebe, Nichole	PS 831	558
Beebe, Nichole	PS 746	510
Behra, Martine	PS 222	130
Behra, Martine	PS 219	129
Behrens, Peter	PD 8	7
Behrooz, Roxana	PS 376	248
Beirl, Alisha	PS 112	70
Beisel, Kirk	PS 132	82
Beitel, Ralph E.	PS 503	345
Bellier, Ludovic	PD 124	475
Belyantseva, Inna	PD 98	454
Belyantseva, Inna	PS 778	527
Belyantseva, Inna	PS 770	523
Bengel, Frank	PS 310	213
Bengtson, Jason	PS 552	373
Benichoux, Victor	PS 42	33
Benichoux, Victor	PS 649	426
Benichoux, Victor	PS 624	413
Benichoux, Victor	PS 407	265
Benichoux, Victor	PS 839	563
Benito-Gonzalez, Ana	PD 162	632
Benkafadar, Nesrine	PS 356	238
Bensimon, Jean-Loup	PS 41	32
Benteau, Tammy	PS 116	72
Berding, Georg	PS 310	213
Bergal, Jake	PS 13	16

Name	Abstract No.	Page No.
Berger, François	PS 799	539
Berger, Michael	PS 224	131
Berger, Michael	PS 225	132
Berger, Joel	PS 454	318
Berger, Claudia	PS 791	534
Bergkvist, Magnus	PS 897	597
Bergkvist, Magnus	PD 15	141
Bergles, Dwight	PD 5	6
Beri, Andrea	PS 61	43
Berkowitz, Bruce	PS 802	541
Berninger, Erik	PS 648	425
Berninger, Erik	PS 400	261
Berninger, Erik	PS 650	426
Bernstein, Leslie	PS 406	264
Bernstein, Joshua	PD 131	614
Bernstein, Joshua	PS 18	19
Bernstein, Joshua	PS 278	195
Bernstein, Joshua	PS 653	428
Bernstein, Joshua	PS 282	197
Bernstein, Joshua	PS 367	243
Berrettini, Stefano	PS 841	564
Bessler, Waylan	PD 173	638
Best, Virginia	PS 865	579
Best, Virginia	PS 401	262
Best, Virginia	PS 863	578
Beurg, Maryline	PD 73	306
Beutelmann, Rainer	PS 70	48
Beyer, Lisa A.	PS 350	235
Beyer, Lisa A.	PS 483	333
Beyer, Lisa A.	PS 158	97
Beynac, Laurianne	PS 792	535
Beynon, Andy	PS 731	501
Bhadola, Shivkumar	PS 848	568
Bhagat, Shaum	PS 81	53
Bhagat, Shaum	PS 76	51
Bhagat, Shruti	PS 121	75
Bharadwaj, Hari	PS 409	266
Bharadwaj, Hari	PS 263	186
Bhethanabotla, Venkat	PS 601	400
Bhethanabotla, Venkat	PS 27	24
Bhutta, Mahmood	PS 320	218
Bianchi, Federica	PS 388	255
Bibas, Thanos	PS 810	545
Bibas, Thanos	PS 185	111
Bibas, Thanos	PS 522	356
Bidelman, Gavin	PS 43	34
Bidelman, Gavin	PS 867	580
Bidelman, Gavin	PS 76	51
Bidelman, Gavin	PS 715	492
Bidelman, Gavin	PS 719	495
Bidelman, Gavin	PS 288	201
Bielefeld, Eric	PS 559	376
Bielski, Lynn	PD 11	139
Bierer, Julie	PS 729	500
Bierer, Amanda	PS 122	76
Bierer, Julie	PD 134	616
Bierer, Julie	PS 19	20
Bierer, Julie	PS 33	28

Author Index

Name	Abstract No.	Page No.
Bieszczad, Kasia	SYMP 37	302
Bigland, Mark	PD 41	158
Billig, Alexander	PS 476	330
Billig, Alexander	PD 129	613
Bing, Dan	PD 20	144
BinKhamis, Ghada	PS 297	206
Binnamangalam, Harshavardhan	PS 833	559
Bird, Jonathan	PS 779	528
Bird, Jonathan	PS 142	88
Birkan, Maria	PD 82	311
Bisconti, Silvia	PS 711	490
Biswas, Amitava	PS 639	421
Bizley, Jennifer	PS 254	182
Black, Nicole	PD 154	627
Black, Nicole	PS 837	562
Blackshaw, Helen	PS 810	545
Blanke, Olaf	SYMP 40	303
Blankenship, Chelsea	PD 122	473
Blanton, Susan	PS 127	79
Blevins, Nikolas	PS 716	493
Blits, Bas	PS 161	98
Bloomberg, Jacob	PS 234	137
Blough, Bruce	PS 353	236
Blouin, Jean-Sébastien	PS 917	609
Boatman-Reich, Dana	PS 702	485
Bobian, Michael	PS 530	360
Bodmer, Daniel	PS 797	537
Bodmer, Daniel	PS 791	534
Boebinger, Dana	PS 480	332
Boebinger, Dana	PS 852	571
Boerlin, Viktor	PS 791	534
Boerner, Ryan	PS 264	187
Boger, Erich	PS 347	233
Boger, Erich	PS 349	234
Bohn, Alexandra	PD 151	626
Bohorquez, Jorge	PS 605	403
Bologna, William	PS 427	276
Bonaiuto, Gregory	PS 794	536
Bondy, Brian	PS 739	506
Boney, Robert	PS 353	236
Boney, Robert	PS 885	589
Bonga, Justine D.	PD 55	291
Bonnet-Brilhault, Frederique	PS 652	427
Booth, Kevin	PS 122	76
Boothalingam, Sriram	PS 718	494
Bordiga, Pierrick	PS 922	612
Borenstein, Jeffrey	PS 618	409
Borenstein, Jeffrey	SYMP 44	304
Borenstein, Jeffrey	PS 821	552
Borenstein, Jeffrey	PS 823	553
Borkholder, David	PS 819	551
Borkholder, David	PS 822	553
Borse, Vikrant	PS 583	390
Borse, Vikrant	PS 597	398
Borse, Vikrant	PS 603	402
Böscke, Robert	PS 89	57
Bosen, Adam	PS 277	194
Bosen, Adam	SYMP 47	313

Name	Abstract No.	Page No.
Bostic, Katlyn	PS 236	172
BOUAMRANI, Ali	PS 799	539
Boulet, Jason	PS 720	495
Bourdages, George	PS 681	443
Bourien, Jérôme	PS 697	483
Bourien, Jérôme	PS 485	334
Bourien, Jerome	PS 271	191
Bourien, Jérôme	PS 356	238
Bouy, Jean Christophe	PS 399	261
Boven, Christopher	PS 426	275
Boven, Christopher	PS 31	26
Bowen, Zac	PS 252	181
Bowen, Zac	PS 461	322
Bowers, Peter	PS 190	114
Bowers, Peter	PS 194	116
Bowl, Michael	PS 768	522
Bowl, Michael	PS 686	477
Bowl, Michael	PD 72	306
Bowler, Rachael	PS 204	121
Bowling, Thomas	PS 171	103
Boyer, Eric	PS 799	539
Boyle, Patrick	PS 726	498
Boyle, Patrick	PS 138	86
Boyle, Patrick	PS 498	342
Boyle, Patrick	PS 728	500
Bozorg Grayeli, Alexis	PS 842	565
Bozorg Grayeli, Alexis	PS 232	136
Bozovic, Dolores	PS 767	522
Bozovic, Dolores	PS 780	529
Bozovic, Dolores	PS 781	529
Bradley, Allison	PS 855	572
Bradley, Allison	PS 856	573
Bradley, Allison	PD 122	473
Brainard, Michael	PD 24	146
Brake, Lee	PS 573	384
Bramhall, Naomi	PS 579	387
Brandebura, Ashley	PS 759	517
Braun, Susanne	PS 813	547
Breakefield, Xandra	PS 149	91
Breglio, Andrew	PD 150	625
Breglio, Andrew	SYMP 45	304
Breglio, Andrew	PS 806	543
Brenner, Michael	PS 789	533
Bressieux, Stéphanie	PS 441	284
Bressieux, Stéphanie	PD 170	636
Brewer, Carmen	PS 56	40
Brewer, Carmen	PS 61	43
Brewer, Carmen	PD 94	452
Brezun, Jean Michel	PS 602	401
Brichta, Alan	PD 41	158
Bridges, Mary	PS 264	187
Bridges, Mary	PS 492	338
Bridges, Mary	PS 491	338
Bridges, Mary	PS 321	218
Briec, Veronique	PD 170	636
Brigande, John	PD 2	639
Brint, Emma	PS 668	436
Brister, Eileen	PS 181	109

Author Index

Name	Abstract No.	Page No.
Britt, William	PD 144	622
Broderick, Lori	PD 94	452
Broussard, Sierra	PS 876	584
Broussard, Sierra	PS 667	436
Brown, Kevin	PS 175	105
Brown, Daniel	PS 907	603
Brown, Edward	PS 145	89
Brown, Chris	PS 502	344
Brown, Steve	PS 768	522
Brown, Chris	PS 305	211
Brown, David	PS 511	350
Brown, Andrew	PS 649	426
Brown, Carolyn	PS 122	76
Brown, Andrew	PS 403	263
Brown, Spencer	PS 253	181
Brown, Daniel	PS 575	385
Brown, Andrew	PS 624	413
Brown, Kevin	PS 786	532
Brown, LaShardai	PS 492	338
Brown, Andrew	PS 407	265
Brown, Andrew	PS 839	563
Brown, Steve	PS 686	477
Brown, Anna Leigh	PD 28	148
Brown, Chris	PS 727	499
Brown, Steve	PS 320	218
Brown, Alec	SYMP 46	304
Brown, Steve	PD 72	306
Brown, LaShardai	PS 321	218
Brown II, Rogers	PS 105	66
Brownell, William	PS 623	412
Brownstein, Zippora	PD 82	311
Bruce, Ian	PS 2	10
Bruce, Ian	PS 47	36
Bruce, Ian	PS 720	495
Brughera, Andrew	PS 64	45
Brumat, Marco	PS 124	77
Brumat, Marco	PS 120	74
Brungart, Douglas	PS 666	435
Brungart, Douglas	PS 368	244
Brungart, Douglas	PS 665	435
Brungart, Douglas	PS 417	270
Brungart, Douglas	PD 11	466
Brunner, Peter	PD 137	618
Bruschini, Luca	PS 841	564
Buchman, Craig	PS 786	532
Büchner, Andreas	PD 141	620
Buckey, Jay	PS 858	574
Budinger, Eike	SYMP 1	1
Budzevich, Mikalai	PS 822	553
Budzillo, Agata	PS 829	557
Buechel, Brian	SYMP 52	316
Buechner, Andreas	PS 287	200
Buechner, Andreas	PS 26	23
Buijink, Renate	PD 101	456
Buniello, Annalisa	PD 97	454
Burger, R. Michael	PS 520	355
Burger, R. Michael	PS 509	348
Burgess, Shawn	PD 93	451

Name	Abstract No.	Page No.
Burgess, Shawn	PS 927	595
Burgess, Shawn	PS 880	586
Burgess, Shawn	PS 219	129
Burghard, Alice	PS 290	202
Burgess, Shawn	PS 222	130
Burke, Amanda	PS 311	214
Bürli, Roland	PD 58	293
Burns, Joseph	PD 32	152
Burns, Joseph	PD 31	152
Burns, Joseph	PS 747	511
Burns, Joseph	PS 749	512
Burns, Joseph	PS 748	511
Burns, Joseph	PS 349	234
Burton, Jane	PS 588	392
Burton, Jane	PS 591	394
Burton, Martin	PS 320	218
Busch, Susan	PS 34	229
Busch, Susan	PS 188	113
Buskirk, James	PS 224	131
Buskirk, James	PS 225	132
Buskirk, James	PD 174	639
Buss, Emily	PS 763	519
Buss, Emily	PS 762	519
Buss, Emily	PS 389	256
Buss, Emily	PS 765	520
Buswinka, Christopher	PS 725	498
Butler, Blake	PD 126	476
Butler, Blake	PS 637	420
Butman, John	PD 94	452
Butts, Daniel	PS 63	44
Buzo, Byanka	PS 241	175
C. Lee, Byung	PD 98	454
Cabrera, Laurianne	PS 765	520
Cabrera, Geraldine	PS 609	405
Cacace, Anthony	PS 897	597
Cacace, Anthony	PD 15	141
Cacciabue-Rivolta, Daniela	PS 496	341
Caclin, Anne	PD 124	475
Cadge, Barbara	PS 131	81
Cadmus, Matthew	PS 275	193
Cahill, Nathan	PS 822	553
Cai, Qunfeng	PS 10	15
Cai, Qunfeng	PS 218	129
Cai, Cuiyun	PS 323	220
Cai, Cuiyun	PS 326	221
Calcus, Axelle	PS 630	417
Calcus, Axelle	PS 745	510
Caldwell, Meredith	PS 36	29
Callister, Robert	PD 41	158
Camalier, Corrie	PD 28	148
Camera, Sarah	PS 51	38
Camino, Alexandria	PS 353	236
Campbell, Dean	PS 104	65
Camuset, Jean-Paul	PS 842	565
Canady, Franklin	PD 173	638
Canlon, Barbara	PS 557	375
Canlon, Barbara	PD 101	456
Cantu, Homero	SYMP 26	171

Author Index

Name	Abstract No.	Page No.
Cao, Xiao-Jie	PS 508	348
Cao, Shuangfeng	PS 903	601
Caprara, Giusy	PS 335	226
Carapezza, Michael	PS 576	386
Carapezza, Michael	PD 153	627
Caras, Melissa	PD 27	148
Cardoso, Maïda	PS 904	601
Carey, John	PS 448	288
Carey, John	PS 58	41
Carlyon, Robert	PD 107	464
Carlyon, Stefano	PS 723	497
Carlyon, John	PS 723	497
Carlyon, Robert	PS 723	497
Carlyon, Robert	PD 129	613
Carlyon, Robert	PS 33	28
Carlyon, Robert	PS 281	196
Carlyon, Robert	PS 274	192
Carney, Laurel	PS 380	250
Carr, Catherine	PS 63	417
Carr, Catherine	PD 85	447
Carr, Catherine	PS 733	503
Carr, Catherine	PS 65	45
Carrell, Thomas	PD 13	140
Carrington, Blake	PD 93	451
Carstens, Russ	PS 110	69
Cartagena-Rivera, Alexander	PS 619	410
Carter, Robert	PS 819	551
Carvalho, Alyssa	PS 411	267
Casadei, Silvia	PD 82	311
Casey, Justin	PS 839	563
Caspary, Donald	PS 695	481
Caspary, Donald	PS 433	279
Cassel, Raphaelle	PS 922	612
Cassoulet, Anne	PS 232	136
Castells-Nobau, Anna	PS 117	73
Castracane, James	PS 897	597
Castracane, James	PD 15	141
Catamo, Eulalia	PS 120	74
Cavuscens, Samuel	PS 446	287
Cayouette, Michel	PD 159	631
Cazals, Yves	PS 602	401
Cazals, Yves	PS 904	601
Cederroth, Christopher	PS 557	375
Cederroth, Christopher	PD 101	456
Cejas, Ivette	PS 22	200
Celaya, Adelaida M	PD 147	623
Ceriani, Federico	PS 134	83
Ceriani, Federico	PS 333	225
Cervantes, Blanca	PS 147	90
Cervantes Constantino, Francisco	PS 703	486
Chabbert, Chtistian	PS 922	612
Chacko, Lejo	PS 758	516
Chadwick, Richard	PS 925	413
Chadwick, Richard	PS 619	410
Chae, Sung Won	PS 340	229
Chae, Jae Jin	PD 94	452
Chai, Renjie	PS 215	127
Chai, Renjie	PS 586	391

Name	Abstract No.	Page No.
Chai, Renjie	PS 585	391
Chait, Maria	PS 481	332
Chait, Maria	PS 705	487
Chait, Maria	SYMP 10	151
Chait, Rosy	SYMP 10	151
Chait, Maria	PS 873	583
Chait, Maria	SYMP 7	3
Chait, Maria	PS 878	585
Chait, Maria	PS 700	484
Chait, Maria	PS 704	486
Chait, Maria	PS 874	583
Chait, Maria	PS 699	484
Chakrabarti, Rituparna	PS 545	369
Challuau, Désiré	PS 441	284
Challuau, Désiré	PD 170	636
Chamseddin, Bahir	PD 92	451
Chandrasekaran, Bharath	PD 121	473
Chandrasekaran, Bharath	PS 659	431
Chang, Ki-Hong	PS 844	566
Chang, Mun Young	PS 902	600
Chang, Mun Young	PS 677	441
Chang, Hui Ho Vanessa	PS 680	443
Changquan, Wang	PS 584	390
Chapagain, Prem	PS 126	78
Charaziak, Karolina	PS 86	575
Chattaraj, Parna	PD 94	452
Chatterjee, Monita	SYMP 59	460
Chatterjee, Monita	PS 277	194
Chatterjee, Monita	SYMP 47	313
Chatterjee, Monita	PD 128	612
Chatterjee, Monita	PS 273	192
Chatzimichalis, Michail	PS 60	400
Cheatham, Mary Ann	PS 558	376
Cheatham, Mary Ann	PS 687	477
Cheatham, Mary Ann	PS 598	399
Cheatham, Mary Ann	PS 342	230
Cheek, Diane	PS 471	327
Cheeseman, Michael	PS 320	218
Chen, Jessica	PS 906	603
Chen, Taosheng	PD 55	291
Chen, Bing	PS 123	76
Chen, Daniel	PD 58	293
Chen, Zelin	PS 927	595
Chen, Jessica	PS 394	258
Chen, Zheng-Yi	SYMP 21	169
Chen, Lin	PD 18	143
Chen, Lan	PS 918	610
Chen, Yan	PS 215	127
Chen, Hongsai	PS 443	285
Chen, Jin	PD 104	457
Chen, Yen-Jung Angel	PS 811	546
Chen, Lan	PS 59	42
Chen, Chen	PS 16	98
Chen, Minghui	PS 541	366
Chen, Keguang	PS 612	406
Chen, Guang-Di	PD 21	145
Chen, Zheng-Yi	PS 205	122
Chen, Chi	PS 202	120

Author Index

Name	Abstract No.	Page No.
Chen, Shaorui	PS 678	442
Chen, Guang-Di	PS 629	416
Chen, Lei	PS 132	82
Chen, Dongye	PS 108	68
Chen, Zhuo	PS 730	501
Chen, Guang-Di	PS 825	554
Chen, Rong	PD 80	310
Chen, Guang-Di	PD 23	145
Chen, Yingying	PD 148	624
Chen, Maxin	PS 383	252
Chen, Chengfang	PS 632	418
Chen, Guang-Di	PS 633	418
Chen, Guang-Di	PD 59	293
Chen, Zongwei	PS 542	367
Chen, Qian	PS 141	87
Chen, Lan	PS 920	611
Chen, Xi	PS 772	524
Chen, Hengchao	PD 114	468
Chen, Sen	PD 161	632
Chen, Yan	PD 119	471
Chen, Jin	PS 62	44
Chen, Guang-Di	PS 903	601
Chen, Tao	PS 193	115
Chen, Tao	PS 187	112
Cheng, Elise	PS 504	345
Cheng, Cheng	PD 55	291
Cheng, Alan	PS 103	65
Cheng, Jeffrey Tao	PD 152	626
Cheng, Cheng	PS 215	127
Cheng, Weihua	PS 218	129
Cheng, Alan	PD 160	631
Cheng, Jeffrey Tao	PD 154	627
Cheng, Song	PS 620	410
Cheng, Alan	PD 70	299
Cheng, Jeffrey Tao	PD 155	628
Cheng, Alan	PD 64	296
Cheng, Alan	PS 210	124
Cheng, Cheng	PS 585	391
Cheng, Alan	PD 146	622
Cheng, Weihua	PS 896	596
Chennuri, Bhaskar	PS 176	106
Chertoff, Mark	PS 80	53
Chertoff, Mark	PS 5	11
Chew, Teng-Leong	PS 301	209
Chi, Fanglu	PS 840	563
Chi, Fanglu	PD 169	636
Chi, Fanglu	PS 136	84
Chia, Chester	PS 315	216
Chien, Wade W.	PS 804	542
Chien, Wade W.	PS 806	543
Chien, Wade W.	PS 216	128
Chintanpalli, Ananthakrishna	PS 269	190
Chiong, Charlotte	PS 130	81
Chisolm, Theresa	PS 242	176
Chittam, Harish	PS 601	400
Cho, Hyong-Ho	PS 111	70
Cho, Catherine	PS 229	134
Cho, Jung-A	PS 814	548

Name	Abstract No.	Page No.
Cho, Soyoun	PS 538	365
Cho, Hyong-Ho	PS 339	228
Cho, Catherine	PS 230	135
Choi, Moonyoung	PS 111	70
Choi, Inyong	PS 875	584
Choi, Inyong	SYMP 7	3
Choi, Inyong	PS 662	433
Choi, Mi Jin	PS 836	561
Choi, Jae Young	PS 562	378
Choi, Jun Jae	PS 677	441
Choi, Inyong	PS 477	330
Choi, Inyong	PS 284	198
Choi, Inyong	PD 130	613
Choi, Moonyoung	PS 339	228
Choo, Oak-sung	PS 360	240
Choo, Oak-sung	PS 836	561
Chou, Shih-Wei	PS 542	367
Choukir, Sahar	PS 183	110
Choung, Yun-Hoon	PS 360	240
Choung, Yun-Hoon	PS 836	561
Choy, Kristel	PS 913	607
Christensen, Douglas	PS 906	603
Christensen Andersen, Lou-Ann	PD 118	470
Christensen- Dalsgaard, Jakob	PS 63	417
Christensen- Dalsgaard, Jakob	PS 72	495
Christensen- Dalsgaard, Jakob	PS 369	245
Chrysostomou, Elena	PS 104	65
Chu, Kengyeh	PD 100	456
Chung, Jae Ho	PS 845	567
Chung, Jong Hoon	PS 836	561
Chung, Christopher	PS 790	534
Chung, Jong Woo	PS 790	534
Chung, Yoojin	SYMP 52	316
Chung, Phil-Sang	PS 4	11
Chung, Phil-Sang	PS 587	392
Chung, Chris	PD 17	142
Churchill, Tyler	PS 71	490
Ciganovic, Nikola	PS 163	99
Clapp, Wade	PD 173	638
Clark, Jason	PD 173	638
Classen, Simone	PS 501	343
Claussen, Alexander	PS 504	345
Claussen, Alexander	PS 505	346
Clavier, Odile	PS 858	574
Cleary, Miranda	PS 17	19
Coate, Thomas	SYMP 26	171
Cobo-Cuan, Ariadna	PS 73	50
Cocca, Massimiliano	PS 120	74
Coco, Laura	PS 304	210
Coffin, Allison B.	PS 353	236
Coffin, Allison B.	PD 61	294
Coffin, Allison B.	PS 885	589
Coffin, Allison B.	PS 352	589
Cohen, Julie	PS 666	435
Cohen, Helen	PD 167	635
Cohen, Bernard	PS 229	134
Cohen, Julie	PS 665	435
Cohen, Bernard	PS 230	135

Author Index

Name	Abstract No.	Page No.
Cohen, Helen	PS 234	137
Coillot, Christophe	PS 904	601
Colburn, H. Steven	PS 865	579
Colburn, H. Steven	PS 366	243
Colburn, H. Steven	PS 401	262
Colesa, Deborah	PS 725	498
Colesa, Deborah	SYMP 14	167
Colina, Sonia	PS 304	210
Colón-Cruz, Luis	PS 219	129
Cone, Barbara	PS 77	52
Cone, Barbara	PS 471	327
Cong, Tao	PS 507	347
Cong, Ning	PS 136	84
Contini, Donatella	PS 537	364
Contreras, Julio	PD 147	623
Cook, Rebecca	PS 908	604
Coomber, Ben	PS 454	318
Cooper, Nigel	PS 169	102
Cooper, Nigel	PD 52	164
Corbo, Joseph	PRES SYMP 2	1
Corey, David	PD 83	312
Corey, David	PS 774	525
Corfas, Gabriel	PD 56	292
Corfas, Gabriel	PS 921	611
Corfas, Gabriel	PD 38	156
Corfas, Gabriel	PD 40	157
Cormier, Denis	PS 819	551
Corns, Laura	PS 332	225
Corns, Laura	PS 334	226
Cortese, Matteo	PD 72	306
Corwin, Jeffrey	PD 68	298
Cosentino, Stefano	PS 723	497
Cosnier-Pucheu, Sylvie	PS 904	601
Counter, Allen	PS 800	539
COURT, Magali	PS 799	539
Cox, Brandon	PS 695	481
Cox, Brandon	PS 207	123
Cox, Brandon	PS 206	122
Cox, Roger	PS 686	477
Cox, Brandon	PS 322	219
Crair, Michael	PD 5	6
Crane, Benjamin	PD 45	160
Crane, Benjamin	PS 684	445
Crenshaw, E Bryan	PS 314	215
Crenshaw, E Bryan	PS 309	213
Crespi, Erica	PS 352	236
Crish, Samuel	PS 832	559
Crispino, Giulia	PS 134	83
Croghan, Naomi	PS 286	199
Crompton, Michael	PS 320	218
Crumling, Mark	PS 789	533
Crumling, Mark	PS 599	399
Crunden, Julia	PS 330	223
Cruzatto da Silva, Guilherme	PS 475	329
Cullen, Kathleen	PS 917	609
Cullen, Kathleen	PS 442	284
Cullen, Kathleen	PS 672	438
Cullen, Kathleen	PS 680	443

Name	Abstract No.	Page No.
Cunnane, Mary	PS 305	211
Cunningham, Lisa	PS 347	233
Cunningham, Lisa	PS 56	377
Cunningham, Lisa	PD 150	625
Cunningham, Lisa	SYMP 45	304
Cunningham, Lisa	PS 346	232
Cunningham, Lisa	PS 806	543
Cunningham, Lisa	PS 349	234
Cureoglu, Sebahattin	SYMP 46	304
Curley, Stephanie	PS 897	597
Curley, Stephanie	PD 15	625
Curry, Rebecca	PS 518	354
Curthoys, Ian	PS 907	603
Curthoys, Ian	PS 905	602
Curthoys, Ian	PS 575	385
Curthoys, Ian	PS 682	444
Curthoys, Ian	PS 449	289
Curtin, Hugh	PS 226	133
Cusimano, Maddie	PS 868	580
Cutiongco-de la Paz, Eva Maria	PS 130	81
Czajkowski, amandine	PD 165	634
D'Eustacchio, Angela	PS 124	77
Da Costa, Sandra	PS 714	492
Dabdoub, Alain	PD 35	154
Dabdoub, Alain	PS 95	61
Dabdoub, Alain	PS 211	125
Dabdoub, Alain	PS 892	593
Dahmen, Johannes	PS 460	321
Dai, Pu	SYMP 21	169
Dai, Peidong	PS 612	406
Dai, Mingjia	PS 229	134
Dai, Chunfu	PS 817	549
Dai, Peidong	PD 119	471
Dai, Peidong	PS 193	115
Dai, Peidong	PS 187	112
Dai, Mingjia	PS 230	135
Dalbert, Adrian	PS 721	496
Dalbert, Adrian	PS 192	115
Damberg, Peter	PS 800	539
Dang, Bao	PS 604	402
Danial-Faran, Nada	PD 82	311
Daniel, Sam	PS 182	109
Danti, Serena	PS 841	564
Darcy, Yuanzhao	PS 322	219
Daszynski, Damian	PD 59	293
Dau, Torsten	PS 388	255
Dau, Torsten	SYMP 53	316
Dau, Torsten	PS 8	13
Dau, Torsten	PD 142	621
Dau, Torsten	PS 429	277
Dau, Torsten	PS 472	328
Dau, Torsten	PS 413	269
Dau, Torsten	PS 386	254
Daunert, Sylvia	PS 820	551
David, Stephen	PS 384	253
David, Stephen	PS 248	179
David, Stephen	PS 456	319
Davidov, Bella	PD 82	311

Author Index

Name	Abstract No.	Page No.
Davis, William	PS 756	516
Dawes, Ryan	PS 145	89
Dawson, Longina	PD 151	626
Dawson, Sally	PS 131	81
de Cheveigné, Alain	PS 479	331
de Hoz, Livia	PS 202	120
de Hoz, Livia	PS 261	185
de Kerangal, Mathilde	PS 874	583
de Pellegars, Pauline	PS 904	601
De Seta, Daniele	PS 41	268
De Seta, Daniele	PS 348	233
De Vel, Eddy	PS 731	501
De Vito, Andrea	PS 841	564
de Vrieze, Erik	PS 117	73
de Waele, Catherine	PS 682	444
de Waele, Catherine	PS 449	289
Dean, Charlotte	PS 320	218
Deans, Michael	PS 93	60
Dearie, Alejandro	PS 609	405
Debes, Amélie	PD 124	475
Decraemer, Willem F.	PS 189	113
Deeks, John	PD 129	613
Deeks, John	PS 281	196
Deeks, John	PS 274	192
Deerinck, Thomas	PS 761	518
Deerinck, Thomas	PS 301	209
Dehais, Frédéric	PS 418	271
Deighton, Michael	PS 709	489
Dejournett, Danielle	PS 608	404
Delgutte, Bertrand	PS 378	249
Delgutte, Bertrand	PD 87	448
Delgutte, Bertrand	SYMP 52	316
Della Santina, Charles	PD 167	635
Della Santina, Charles	PS 672	438
DeMarco, Andrew	PS 710	490
DeMayo, William	PS 681	443
DeMirci, Hasan	PD 146	622
Deng, Yuqi	PS 875	584
Deng, Xiaohong	PS 133	83
Dengler, Reinhard	PD 141	620
Denny, Henry	PS 741	507
Dent, Micheal	PS 201	120
Dent, Micheal	PS 200	119
Dent, Micheal	PS 203	121
Deo, Sapna	PS 820	551
Depireux, Didier	PD 60	294
Depreux, Frederic	PS 807	543
Deroche, Mickael	PS 857	574
Deroche, Mickael	SYMP 59	460
Desai, Bimal	PS 106	66
Deshmukh, Aditi	PS 135	84
Desmadryl, Gilles	PS 485	334
Desmond, Tim	PS 625	414
DeTorres, Alvin	PS 216	128
Deussing, Jan	PS 48	332
DeVries, Lindsay	PS 729	500
Dewey, James	PS 168	102
Dewey, Rebecca	PS 298	207

Name	Abstract No.	Page No.
Dhar, Sumitrajit	PS 718	494
Dheerendra, Pradeep	SYMP 7	3
Dhooge, Ingeborg	PS 731	501
Dhukhwa, Asmita	PS 583	390
Dhukhwa, Asmita	PS 597	398
Dhukhwa, Asmita	PS 603	402
Di Pino, Antonella	PS 933	395
Di Stazio, Mariateresa	PS 121	75
Diao, Shiyong	PD 55	291
Diaz, Francisco	PS 5	11
Dick, Fred	PS 700	484
Diedesch, Anna	PS 405	264
Dietl, W	PS 758	516
Dietz, Mathias	SYMP 51	315
Dikici, Emre	PS 820	551
Dillingham, Christopher	PS 376	248
Dilwali, Sonam	PS 149	91
Dimitrijevic, Andrew	PS 855	572
Dimitrijevic, Andrew	PS 856	573
Dimitrijevic, Andrew	PS 660	432
Dimitrov, Alexander	PS 381	251
Ding, Bo	PS 594	396
Ding, Bo	PS 601	400
Ding, Bo	PS 819	551
Ding, Dalian	PD 57	292
Ding, Dalian	PS 825	554
Ding, Dalian	PS 592	395
Ding, Dalian	PD 59	293
Ding, Dalian	PS 581	388
Ding, Dalian	PS 152	93
Ding, Dalian	PS 888	590
Ding, Yue	PS 869	581
Dinh, Christine	PS 354	237
DiNino, Mishaela	PS 19	20
Divakar, Annika	PD 42	158
Divincenzo, Alexis	PS 113	71
Dixon, Angela	PS 802	541
Dixon, Angela	PS 897	597
Dixon, Angela	PD 15	625
Długaiczak, Julia	PS 682	444
Dobie, Robert	PD 167	635
Dobrev, Ivo	PS 60	638
Dobrev, Ivo	PS 192	115
Dobrev, Ivo	PS 75	512
Dobrev, Ivo	PS 838	562
Dodson, Edward	PS 361	241
Dodson, Edward	PS 6006	403
Doetzlhofer, Angelika	PD 162	632
Doetzlhofer, Angelika	PS 101	64
Doetzlhofer, Angelika	PS 104	65
Doi, Katsumi	PS 228	134
Dolan, David	PS 789	533
Dolan, David	PS 608	404
Domingo, Ysabel	PD 12	139
Domingo, Ysabel	PS 422	273
Donaldson, Gail	SYMP 60	460
Dong, Lingsheng	PD 83	312
Dong, Deana	PS 153	94

Author Index

Name	Abstract No.	Page No.
Dong, Liu	PS 584	390
Dong, Liu	PS 220	130
Dong, Yue	PS 255	182
Dong, Wei	PS 178	107
Dong, Yunpeng	PS 883	588
Dong, Yaodong	PD 64	296
Dong, Wei	PS 177	107
Dong, Youyi	PS 751	513
Dong, Lixue	PS 275	193
Dong, Lixue	PS 276	193
Dore', Chantale	PS 161	98
Dottori, Mirella	PS 894	594
Drake, Virginia	PD 60	294
Drescher, Marian	PS 543	367
Drescher, Dennis	PS 543	367
Dreyfus, Matthieu	PS 799	539
Driver, Elizabeth	PS 600	400
Driver, Elizabeth	PS 754	515
Dror, Amiel	PD 81	311
Drouillard, Mylene	PS 41	32
Drouillard, Mylène	PS 348	233
Druckenbrod, Noah	SYMP 23	170
Du, Xiaoping	PS 10	15
Du, Xiaoping	PS 218	129
Du, Tingting	PS 771	524
Du, Tingting	PS 97	62
Du, Xiaoping	PS 896	596
du Lac, Sascha	PS 299	208
Duarte, Maria	PS 727	499
Dubno, Judy	PS 394	258
Dubno, Judy	PS 264	187
Dubno, Judy	PS 486	335
Dubno, Judy	PS 131	81
Dubno, Judy	PS 427	276
Duda, Joseph	PS 770	523
Dudas, J	PS 758	516
Dueck, Wolfram	PS 505	346
Duffy, Valerie	PS 57	41
Dugas, Calli	PS 288	201
Dugué, Guillaume	PS 441	284
Dulik, Matthew	PS 110	69
Dulon, Didier	PS 546	369
Dumont, Rachel	PD 71	305
Duncan, Jeremy	PS 93	395
Duncan, Keith	PS 789	533
Duncan, Keith	PS 884	588
Duncan, Keith	PS 599	399
Dunn, Camille	PS 122	76
Dupont, Guillaume	PS 904	601
Dupont, Typhaine	PD 72	306
Duque, Daniel	PS 244	177
Duque-Afonso, Carlos	PS 550	372
Duquesne, Ulla	PS 232	136
Durham, Dianne	PS 901	599
Durin, Virginie	PD 124	475
Durisin, Martin	PD 4	5
Dyhrfeld-Johnsen, Jonas	PS 441	284
Dyhrfeld-Johnsen, Jonas	PD 170	636

Name	Abstract No.	Page No.
Dyhrfeld-Johnsen, Jonas	PS 792	535
Dziennis, Suzan	PS 358	239
Dziennis, Suzan	PS 788	533
Earl, Brian	PD 116	469
Earl, Brian	PS 490	337
Easter, James	PS 42	33
Easwar, Vijayalakshmi	PS 709	489
Eatock, Ruth Anne	PS 214	126
Eatock, Ruth Anne	PS 208	123
Eatock, Ruth Anne	PS 564	379
Ebeid, Michael	PS 114	71
Ebeid, Michael	PS 115	72
Eckhard, Andreas	PS 226	133
Eckhard, Andreas	PS 808	544
Eckrich, Tobias	PS 569	382
Eddington, Donald	PS 24	22
Edeline, Jean-Marc	PS 697	483
Edeline, Jean-Marc	PS 28	25
Edeline, Jean-Marc	PS 708	488
Edge, Albert	PS 618	409
Edge, Albert	SYMP 44	304
Edge, Albert	PD 3	5
Edge, Albert	PS 211	125
Edge, Albert	PS 808	544
Edge, Albert	PS 890	592
Edge, Albert	PS 355	237
Edwards, Mary	PS 46	35
Edwards, Brent	SYMP 32	301
Effertz, Thomas	PS 331	224
Effertz, Thomas	PD 146	622
Ehlert, Nina	PD 8	7
Eichert, Nicole	PS 582	389
Eisenberg, Laurie	SYMP 67	463
Eisenberg, Daniel	PS 367	243
Ekker, Stephen	PS 793	535
Eklöf, Martin	PS 400	261
El Andaloussi, Samir	PD 150	625
El-Amraoui, Aziz	PD 72	306
Elde, Cameron	PS 382	252
Elfarnawany, Mai	PS 307	212
Elfarnawany, Mai	PS 616	408
Elgoyhen, Ana Belén	PS 532	361
Elgoyhen, Ana Belén	PS 547	370
Elgoyhen, Ana Belén	PS 540	366
Elhilali, Mounya	PD 29	148
Elhilali, Mounya	SYMP 9	151
Elhilali, Mounya	PS 644	423
Elhilali, Mounya	PS 707	488
Eliades, Steven	PS 245	177
Eliades, Steven	PS 247	178
Elkon, Rani	PS 112	70
Elkon, Rani	PS 754	515
Elkon, Rani	PD 81	311
Ellinas, Nikos	PS 185	111
Elliott, Stephen	PD 49	163
Elliott-Thompson, Karen	PD 33	153
Elliott-Thompson, Karen	PS 924	521
Elliott-Thompson, Karen	PD 166	634

Author Index

Name	Abstract No.	Page No.
Ellis, Kathryn	PD 32	152
Ellis, Kathryn	PS 102	64
Ellisman, Mark	PS 761	518
Ellisman, Mark	PS 544	368
Ellisman, Mark	PS 301	209
Elyas, Eli	PS 623	412
Emory, Caroline	PD 130	613
Emptoz, Alice	PD 72	306
Encina-Llamas, Gerard	PS 8	13
Encina-Llamas, Gerard	PS 9	14
Engel, Jutta	PS 553	373
Engel, Jutta	PS 569	382
Enke, Ya Lang	PS 811	546
Epp, Bastian	SYMP 53	316
Epp, Bastian	PS 8	13
Epp, Bastian	PS 698	483
Epstein, Douglas	PS 110	69
Eramo, Sara M.L	PS 933	395
Erfani, Yousof	PS 2	10
Erfurt, Peter	PS 577	386
Erfurt, Peter	PS 732	502
Ernst, Arne	PS 138	86
Ernst, Arne	PS 498	342
Ernst, Arne	PS 728	500
Ernst, Arne	PS 791	534
Escera, Carles	PD 108	465
Escera, Carles	PS 440	283
Esfahani, Ehsan	PS 629	416
Eshraghi, Adrien	PS 605	403
Eshraghi, Adrien	PS 351	235
Eshraghi, Adrien	PS 809	545
Esmieu, William	PD 58	293
Espinosa-Sanchez, Juan Manuel	PS 109	68
Esquivel, Carlos	PS 580	388
Esterberg, Robert	PS 140	87
Etard, Octave	PS 292	203
Eustaquio-Martín, Almudena	PS 79	52
Eustaquio-Martín, Almudena	PS 395	259
Evertz, Florian	PS 259	184
Evsen, Lale	PS 101	64
Ewert, Donald	PS 10	15
Ewert, Stephan	PS 393	258
Ewert, Donald	PS 896	596
Fabella, Brian	PS 769	523
Falik-Zaccai, Tzippora	PD 82	311
Fallah, Elika	PD 153	627
Fallon, James	PS 501	343
Fallon, James	PS 928	576
Fallon, James	PS 720	495
Fallon, Andrew	PD 11	139
Fan, Chunxin	PS 927	495
Fan, Fan	PS 59	42
Fan, Langchen	PS 380	250
Fan, Zhaomin	PS 494	340
Fang, Jie	PD 55	291
Fang, Jie	PS 317	217
Fang, Qiaojun	PS 586	391
Fang, Cong	PS 903	601

Name	Abstract No.	Page No.
Fangyi, Chen	PS 584	390
Farrell, Brenda	PS 552	373
Farrell, Josh	PS 184	110
Farris, Hamilton	PD 1	3
Farris, Hamilton	PS 807	543
Faure, Paul	PS 379	250
Fawole, Opeoluwa	PS 127	79
Feather, Jenelle	PD 137	618
Febles, Nicole	PS 594	396
Fehrenbach, Amy	PS 715	492
Fehrenbach, Amy	PS 288	201
Feil, Robert	PS 582	389
Feinstein, Elena	PS 888	590
Fekete, Donna	PS 98	62
Felix II, Richard	PS 381	251
Fellows, Abigail	PS 858	574
Felmy, Felix	PS 734	504
Feng, Yong	PS 126	78
Feng, Yong	PS 125	78
Ferber, Alexander	PS 649	426
Ferber, Alexander	PS 407	265
Fereck, Micah	PS 906	603
Fereck, Micah	PD 77	308
Ferger, Roland	PS 68	47
Fernandez, Katharine	PS 56	40
Fernandez, Katharine	PS 271	191
Ferrary, Evelyne	PS 41	32
Ferrary, Evelyne	PS 348	233
Fetoni, Anna Rita	PS 160	98
Fetoni, Anna Rita	PS 933	395
Fettiplace, Robert	PS 568	381
Fettiplace, Robert	PS 777	527
Fettiplace, Robert	PD 73	306
Fields, Taylor	PS 656	430
Filia, Anastasia	PS 209	124
Finkbeiner, Connor	PS 214	126
Finke, Mareike	PD 141	620
Fiorillo, Benjamin	PS 808	544
Fischer, David	PD 58	293
Fischer, Christian	PS 545	369
Fischl, Matthew	PS 519	354
Fischl, Matthew	PS 48	36
Fishman, Yonatan	PS 467	325
Fitzgerald, Matthew	PS 311	214
Fitzgerald, Tracy	PS 600	400
Fitzgerald, Tracy	PS 754	515
Fitzgerald, Matthew	PS 716	493
Fitzgerald, Matthew	PS 850	569
Fitzgerald, Tracy	PS 770	523
Fitzgibbons, Peter	PS 237	173
Fitzpatrick, Douglas	PS 175	105
Fitzpatrick, Douglas	PS 432	279
Fitzpatrick, Denis	PS 452	290
Fitzpatrick, Douglas	PS 786	532
Fitzpatrick, Douglas	PS 377	249
Flaherty, Mary	PS 763	519
Flaherty, Kathleen	PS 92	521
Flamme, Gregory A.	PD 167	635

Author Index

Name	Abstract No.	Page No.
Fleming, Justin	PS 852	571
Florian, Wilke	PS 310	213
Fodor, Calli	PS 666	435
Fodor, Calli	PS 665	435
Folkerts, Monica	PD 86	447
Folmer, Robert	PD 90	449
Fong, Stephen	PS 404	263
Fontaine, Bertrand	PS 482	332
Fontbonne, Arnaud	PS 602	401
Fontenot, Tatyana	PS 175	105
Fontenot, Tatyana	PS 786	532
Forbes, Patrick	PS 917	609
Forest, Taylor	PS 625	414
Forge, Andrew	PS 133	83
Forge, Andrew	PS 803	541
Forouzandeh, Farzad	PS 819	541
Forte, Antonio	PS 292	203
Foster, Sarah	PS 358	239
Foster, Sarah	PS 787	532
Foster, Sarah	PS 788	533
Foth, Hans-Jochen	PS 40	31
Fotiadis, Dimitris	PS 185	111
Fowler, Jennifer	PS 283	198
Franaszczuk, Piotr	PS 702	485
Francis, Nikolas	PS 252	181
Francis, Shimon	SYMP 45	304
Francis, Shimon	PS 771	524
Francis, Shimon	PS 346	232
Francis, Susan	PS 298	207
Francis, Shimon	PS 97	62
Franco, Bénédicte	PD 165	634
Franco, Santos	PS 775	526
François, Florence	PS 356	238
Frank, Thomas	PD 76	308
Frankel-Segal, Aliza	PS 850	569
Franzen, Louise Delwen	PS 734	504
Frater, Attila	PS 497	341
Frear, Darcy	PS 615	408
Freeman, Burgess	PD 55	291
Freeman, Mary	PS 767	522
Freeman, Mary	PS 155	95
Freeman, Mary	PS 768	522
Freeman, Dennis	PD 47	161
Freemyer, Andrea	PS 901	599
Frejo, Lidia	PD 95	452
Frejo, Lidia	PS 109	68
Fridberger, Anders	PS 776	526
Fridberger, Anders	PS 623	412
Fridberger, Anders	PD 48	162
Friebe, Andreas	PS 582	389
Friedman, Thomas	PS 779	528
Friedman, Thomas	PS 133	83
Friedman, Thomas	PD 98	454
Friedman, Thomas	PS 142	88
Friedman, Thomas	PD 96	453
Friedman, Thomas	PS 778	527
Friedman, Thomas	PS 770	523
Friesen, Lendra M	PS 240	175

Name	Abstract No.	Page No.
Frisina, Robert	PS 594	396
Frisina, Robert	PS 601	400
Frisina, Robert	PS 819	551
Frisina, Robert	PS 242	176
Frisina, Robert	PS 822	553
Frisina, Robert	PS 27	24
Fritz, Jonathan	PS 466	324
Fritz, Jonathan	PS 244	177
Fritz, Jonathan	PS 250	180
Fritzs, Bernd	PS 39	31
Fritzs, Bernd	PD 33	153
Fritzs, Bernd	PS 924	521
Fritzs, Bernd	PD 166	634
Fritzs, Bernd	SYMP 24	170
Fritzs, Bernd	PD 173	638
Froemke, Robert	SYMP 13	166
Froemke, Robert	SYMP 34	301
Frolenkov, Gregory	PS 767	522
Frolenkov, Gregory	PS 155	95
Frolenkov, Gregory	PS 768	522
Frolenkov, Gregory	PS 607	404
Frolenkov, Gregory	PS 773	525
Frolenkov, Gregory	PD 74	50
Frolenkov, Gregory	PS 96	61
Froriep, Ulrich	PS 259	184
Frydman, Moshe	PD 82	311
Frye, Mitchell	PS 590	394
Frye, Mitchell	PS 693	480
Fu, Qian-jie	PS 15	17
Fu, Qian-jie	PS 35	29
Fuchs, Paul	PS 532	361
Fuchs, Paul	PS 554	374
Fuchs, Paul	PS 176	106
Fuchs, Paul	PS 555	374
Fuchs, Paul	PS 535	363
Fuglsang, Søren Asp	PS 479	331
Fuglsang, Søren Asp	PS 472	328
Führ, Hartmut	PS 402	262
Fuji, Hironori	PS 685	446
Fujioka, Masato	PS 90	599
Fujisaka, Yoh-ichi	PS 295	205
Fujita, Takeshi	PS 149	91
Fujita, Takeshi	PS 228	134
Fultz, Sara E.	PS 394	258
Funnell, W. Robert J.	PS 184	110
Funnell, W. Robert J.	PS 183	110
Funnell, W. Robert J.	PS 182	109
Funnell, W. Robert J.	PS 189	113
Furlong, Cosme	PD 152	626
Furlong, Cosme	PD 155	628
Furmanek, Mariusz	PS 129	80
Furness, David	PS 777	527
Furukawa, Shigeto	PS 294	205
Furukawa, Shigeto	PS 872	582
Furukawa, Shigeto	PS 873	583
Furukawa, Shigeto	PS 878	585
Fyk-Kolodziej, Bozena	PS 827	556
G Parras, Gloria	PS 440	283

Author Index

Name	Abstract No.	Page No.
Gabor, Franz	PD 6	6
Gabriele, Mark	PS 376	248
Gaese, Bernhard	PS 396	259
Gai, Yan	PS 255	182
Galaiya, Deepa	PS 620	410
Galazyuk, Alexander	PS 412	268
Galazyuk, Alexander	PS 877	585
Galazyuk, Alexander	PS 529	360
Gale, Jonathan	PS 932	347
Gale, Richard	PS 320	218
Gallant, Nathan D.	PS 594	396
Gallego-Martinez, Alvaro	PS 109	68
Galloza, Hector	PD 11	139
Gallun, Frederick	PD 90	449
Galvin, John	PS 15	92
Galvin, John	PS 35	235
Galvin, John	PS 652	427
Galvin, Alice	PS 803	541
Gamble, Darik	PS 934	185
Gamble, Marissa	PS 706	487
Gan, Rong	PD 158	630
Gan, Rong	PS 179	108
Gan, Rong	PS 180	108
Gander, Phillip	PD 136	617
Gander, Phillip	SYMP 7	3
Gander, Phillip	PS 476	330
Gander, Phillip	PS 477	330
Gander, Phillip	PD 130	613
Gandour, Jackson	PS 478	331
Gandour, Jackson	PS 717	493
Gans, Jonathan	PS 224	131
Gans, Jonathan	PS 225	132
Gansemer, Benjamin	PS 265	187
Gantz, Bruce	PS 122	76
Gao, Xue	SYMP 21	169
Gao, Xia	PS 215	127
Gao, Tingting	PS 824	554
Gao, Xia	PS 586	391
Garcia-Anoveros, Jaime	PS 39	31
Garcia-Anoveros, Jaime	PS 687	477
Garcia-Hernandez, Sofia	PS 11	15
Garcia-Hernandez, Sofia	PD 111	466
Garcia-Lazaro, Jose	PS 826	555
Garcia-Lazaro, Jose	PS 385	253
Garnham, Carolyn	PS 605	403
Garnham, Carolyn	PS 351	235
Garnham, Carolyn	PS 809	545
Garrett, Markus	PS 50	37
Gartside, Sasha	PS 744	509
Gaskins, Casey	PS 239	174
Gasparini, Paolo	PS 124	77
Gasparini, Paolo	PS 121	75
Gasparini, Paolo	PS 686	477
Gasparini, Paolo	PS 120	74
Gaucher, Quentin	PS 460	321
Gaudreault, Jacques	PS 791	534
Gaudreault, Jacques	PS 791	534
Gausterer, Julia Clara	PD 6	6

Name	Abstract No.	Page No.
Gay, Seam	PS 376	248
Gay, Jennifer	PS 634	419
Gay, Jen	PS 628	415
Geisler, Hyun-Soon	PS 632	418
Geleoc, Gwenaelle	SYMP 27	171
Geleoc, Gwenaelle	PD 1	3
Gener, Maricel Pabustan	PS 898	598
Geng, Ruishuang	PD 58	293
Geng, Ruishuang	PD 18	143
George, Alexander	PS 375	248
Gerhard, Maike	PS 402	262
Germiller, John	PS 110	69
Germiller, John	PS 314	215
Geven, Leontien Ingeborg	PS 419	271
Geworski, Lili	PS 310	213
Ghanad, Iman	PS 837	562
Ghasemahmad, Zahra	PS 463	323
Ghatalah, Laila	PS 544	368
Gholami, Honey	PS 311	214
Ghosh, Sumana	PS 583	390
Ghosh, Sumana	PS 603	402
Giardina, Christopher	PS 175	105
Giardina, Christopher	PS 786	532
Gibaja, Alejandro	PS 755	515
Giersch, Anne	PS 690	479
Giese, Arnaud	PS 908	604
Giese, Arnaud	PS 155	95
Giese, Arnaud	PS 768	522
Gilels, Felicia	PS 604	402
Gillet, Charlène	PD 112	466
Gimmon, Yoav	PS 447	287
Gimmon, Yoav	PD 46	161
Giroto, Giorgia	PS 124	77
Giroto, Giorgia	PS 121	75
Giroto, Giorgia	PS 120	74
Gist, Irene	PS 600	400
Glatzer, Jenna	PS 91	59
Gleiss, Sarah	PS 734	504
Glickman, Bess	PS 283	198
Glowatzki, Elisabeth	PS 554	374
Glowatzki, Elisabeth	PS 560	377
Glowatzki, Elisabeth	PS 555	374
Gluck, Sarah	PS 803	541
Glueckert, Rudolf	PS 758	516
Glueckert, Rudolf	PS 493	339
Gnansia, Dan	PS 28	25
Gnedeva, Ksenia	PD 164	633
Gobadi, Mostafa	PS 629	416
Gockel, Hedwig	PD 107	464
Goepfert, Martin	PS 117	73
Goktug, Asli N.	PD 55	291
Goldbach- Manky, Raphaela	PD 94	452
Goldberg, Jay	PS 911	606
Golden, Erin	PD 162	632
Golding, Nace	PS 740	507
Golding, Nace	PS 373	247
Golding, Nace	PS 739	506
Goldring, Adam	PS 568	381

Author Index

Name	Abstract No.	Page No.
Goldwyn, Joshua	PS 470	327
Goldwyn, Joshua	PS 289	202
Golob, Edward	PD 91	450
Gomeni, Roberto	PS 235	137
Gomes, Tamar	PS 314	215
Gomez, Lex	PS 284	198
Gomot, Marie	PS 652	477
Goncalves, Stefania	PS 820	551
Gong, Qin	PS 243	176
Gong, Qin	PD 109	465
Gonzalez, Nancy	PD 105	457
Gonzalez, Sergio	PS 904	601
Gonzalez, Ray	PS 641	422
Gonzalez-Garrido, Antonia	PS 214	126
Gonzalez-Garrido, Antonia	PS 208	123
Goodman, Dan	PS 378	249
Goodrich, Lisa	SYMP 23	170
Goodrich, Lisa	PS 315	216
Goodwin, Alexander	PS 805	542
Goodwin, Alexander	PS 139	86
Goodwin, Alexander	PS 113	71
Goodyear, Richard	PD 149	624
Gopal, Suhasini	PD 58	293
Gopal, Suhasini	PS 135	84
Gorbunov, Dmitry	PS 343	231
Gordon, Karen	PS 851	570
Gordon, Karen	PS 709	489
Gordon, Karen	SYMP 12	166
Gordon-Salant, Sandra	PS 237	173
Gordon-Salant, Sandra	PS 666	435
Gordon-Salant, Sandra	PS 665	435
Gordon-Salant, Sandra	PS 239	174
Gordy, Clayton	PS 924	521
Gordy, Clayton	PD 166	634
Gorga, Michael	PS 267	188
Gorina-Careta, Natàlia	PD 108	465
Gottlieb, Peter	PD 157	629
Goupell, Matthew	PD 131	614
Goupell, Matthew	PS 424	274
Goupell, Matthew	PS 18	19
Goupell, Matthew	PS 279	195
Goupell, Matthew	PS 404	263
Goupell, Matthew	PS 278	195
Goupell, Matthew	PS 653	428
Goupell, Matthew	PS 17	19
Goupell, Matthew	PS 280	196
Goupell, Matthew	PS 239	174
Goupell, Matthew	PS 367	243
Goupell, Matthew	PS 423	274
Gourévitch, Boris	PS 697	483
Goutman, Juan	PS 532	361
Goyer, David	PD 112	466
Goze-Bac, Christophe	PS 904	601
Graña, Gilberto	PS 432	279
Graña, Gilberto	PS 377	249
Grant, Wally	PS 905	602
Grant, Kenneth	PD 11	139
Grati, M'hamed	PS 126	78

Name	Abstract No.	Page No.
Grati, M'hamed	PS 567	381
Grati, M'hamed	PS 566	380
Grati, M'hamed	PS 883	588
Grati, M'hamed	PS 128	80
Gray, Sterling	PS 352	236
Green, Steven H.	PS 891	592
Green, Steven H.	PS 930	596
Green, Steven H.	PS 6	12
Green, Steven H.	PS 265	187
Green, Steven H.	PS 157	96
Green, David	PS 628	415
Greene, Nathaniel	PS 649	426
Greene, Nathaniel	PS 624	413
Greene, Nathaniel	PS 834	560
Greene, Nathaniel	PD 156	629
Greene, Nathaniel	PS 839	563
Greenhouse, Bob	PD 146	622
Greenstein, Joseph	PS 176	106
Gribizis, Alexandra	PD 5	6
Griebel, Hannah	PD 112	466
Grierson, Kiera	PS 510	349
Griest, Susan	PS 579	387
Griffin, Anne	PS 116	72
Griffith, Andrew	PD 94	452
Griffith, Andrew	PS 336	227
Griffiths, Timothy	PD 136	617
Griffiths, Timothy	SYMP 7	3
Griffiths, Timothy	PS 477	330
Grillet, Nicolas	PD 160	631
Grillone, Gregory	PS 848	568
Grimm, Giso	PS 862	577
Grimsley, Calum	PS 462	322
Grimsley, Jasmine	PS 411	267
Grimsley, Jasmine	PS 412	268
Grimsley, Jasmine	PS 415	270
Grinstead, Laura	PS 743	508
Grobarczyk, Benjamin	PD 165	634
Grolman, Wilko	PS 724	497
Grolman, Wilko	PS 474	329
Gröschel, Moritz	PS 138	86
Gröschel, Moritz	PS 498	342
Gröschel, Moritz	PS 728	500
Grose, John	PS 389	256
Grosh, Karl	PD 54	165
Grosh, Karl	PS 174	105
Gross, Kenneth	PS 592	395
Grossheim, Mike	PS 767	522
Grossheim, Mike	PS 607	404
Grossheim, Mike	PD 74	307
Grossöhmichen, Martin	PS 188	113
Groves, Andy	PS 692	480
Groves, Andy	PS 105	66
Groves, Andy	PS 217	128
Gu, Shuping	PD 64	296
Guan, Xiyang	PS 620	410
Guan, Ming	PS 586	391
Guan, Xiyang	PS 615	408
Guardia, Yeini	PS 82	54

Author Index

Name	Abstract No.	Page No.
Guardia, Yeini	PS 84	55
Gueguen, Cindy	PS 441	284
Gueguen, Cindy	PD 170	636
Guerit, Francois	PD 129	613
Guérit, François	PS 698	483
Guérit, François	PS 281	196
Guest, Hannah	PS 268	189
Guest, Hannah	PS 525	358
Gux, Amelie	PS 502	344
Guidi, Luiz	PD 106	464
Guigou, Caroline	PS 842	565
Guinan, John	PS 164	100
Guinan, John	PD 53	165
Guinan, John	PS 450	289
Guinan, John	PS 451	290
Guinand, Nils	PS 446	287
Guinand, Nils	PS 444	285
Guinand, Nils	PS 493	339
Guitart, Joan	PS 804	542
Gulsuner, Suleyman	PD 82	311
Gunewardene, Niliksha	PS 355	237
Guo, Hong	PS 220	130
Guo, Luo	PS 215	127
Guo, Weiwei	PS 507	347
Guo, Wei	PS 455	319
Guo, Min	PS 903	601
Gupta, Nilay	PS 772	524
Gurumurthy, C. B. (Guru)	SYMP 19	168
Guy, Kip	PD 55	291
Guyot, Jean-Philippe	PS 446	287
Guyot, Jean-Philippe	PS 444	285
Guyot, Jean-Philippe	PS 493	339
Hackelberg, Sandra	PS 884	588
Hackett, Troy	PS 438	282
Hackett, Troy	PS 591	394
Hackett, Troy	PS 246	178
Hadi, Shadan	PS 773	525
Hadi, Shadan	PS 96	61
Hagan, Suzannah	PS 15	17
Hagan, Suzannah	PS 35	29
Haggerty, Stephanie	PS 674	439
Hali, Mirabela	PS 802	541
Hali, Mirabela	PD 15	141
Hali, Mirabela	PS 827	556
Hall, Deborah	PS 646	424
Hall, Deborah	PS 298	207
Hall, Kate	PS 223	131
Halliday, Lorna	PS 630	417
Hallworth, Richard	PS 344	231
Hallworth, Richard	PS 132	82
Halmagyi AO, Michael	PS 682	444
Hamadani, Christine	PD 3	5
Hamel, Laura	PS 212	126
Hammer, Theresa	PS 14	17
Hammill, Tanisha	PS 580	388
Hammond-Kenny, Amy	PD 26	147
Han, Hyunju	PS 55	39
Han, Chul	PD 57	292

Name	Abstract No.	Page No.
Han, Jae Joon	PS 902	600
Han, Jae Joon	PS 54	39
Han, Chul	PS 581	388
Han, Chul	PS 152	93
Hancock, Kenneth	PS 849	569
Hancock, Kenneth	PS 293	204
Handschuh, Stephan	PS 493	339
Hankeln, Thomas	PS 895	595
Hanon, Kevin	PD 165	634
Hansen, Marlan	PS 504	345
Hansen, Marlan	PS 505	346
Hansen, Marlan	PS 122	76
Hansen, John	PS 12	16
Hansen, Marlan	PS 23	22
Hansen, Marlan	PD 173	638
Hara, Akira	PS 159	97
Harding, Joseph	PD 61	294
Hardisty-Hughes, Rachel	PS 320	218
Hardy, Katherine	PS 549	371
Hare, Christine	PS 51	38
Harley, Randall	PS 779	528
Harris, Kelly	PS 486	335
Harris, Michael	PS 361	240
Harris, Michael	PS 606	403
Harris, Suzan	PS 775	526
Harris, Frances	PD 129	613
Harrison, Ryan	PS 559	376
Harte, William	PD 58	293
Harte, James	PS 8	13
Harte, James	PS 241	175
Hartling, Curtis	PS 283	198
Hartman, Byron	PS 89	57
Hartman, Jasenia	PS 13	16
Hartman, Byron	PS 318	217
Hartmann, Julia	PS 343	231
Hartsock, Jared	PS 812	546
Hartsock, Jared	PS 817	549
Hashimoto, Makoto	PS 359	239
Hashimoto, Makoto	PS 685	446
Hashimoto, Makoto	PS 156	96
Hashimoto, Makoto	PS 357	238
Hashino, Eri	PS 87	56
Hashino, Eri	PS 88	57
Hasselmann, Florian	PS 697	483
Hastings, Michelle	PD 1	3
Hastings, Michelle	PD 2	4
Hastings, Michelle	PS 807	543
Hauser, Samantha	PS 588	392
Hauser, Samantha	PS 591	394
Hautefort, Charlotte	PS 232	136
Havenith, Sarah	PS 595	397
Hayes, John	PS 57	41
Hayward, Tamasen	PS 352	236
Haywood, Nicholas	PS 398	260
Hazlett, Emily	PS 412	268
Hazlett, Emily	PS 415	270
He, David	PS 114	71
He, Shuman	PD 135	616

Author Index

Name	Abstract No.	Page No.
He, Wenxuan	PS 499	342
He, Jenny	PD 78	309
He, Zuhong	PS 586	391
He, David	PS 132	82
He, Zuhong	PS 585	391
He, David	PS 113	71
He, Wenxuan	PD 50	163
Headley, Drew	SYMP 36	302
Hecker, Dietmar	PS 40	31
Heddleston, John	PS 301	209
Heddon, Chris	PS 31	26
Heeringa, Amarins	PD 19	144
Heeringa, Amarins	PS 515	352
Heeringa, Amarins	PD 17	142
Heffer, Leon	PS 720	495
Hegland, Erica	PS 170	103
Heil, Peter	PS 638	421
Heinz, Michael	PS 646	424
Heinz, Michael	PS 7	13
Heinz, Michael	PS 198	118
Heinz, Michael	PS 170	103
Heinz, Michael	PS 488	336
Heitzmann, Victoria	PS 76	51
Hell, Stefan	PD 76	308
Heller, Stefan	PS 266	188
Heller, Stefan	PS 89	57
Heller, Stefan	PS 318	217
Heller, Stefan	PRES SYMP 7	3
Helmstaedter, Victor	PS 732	502
Hemachandran, Sriram	PS 157	96
Hendrikse, Maartje	PS 862	577
Hendriksen, Ferry	PS 487	335
Hendry, Aenea	PS 333	225
Henry, Kenneth	PD 120	472
Henry, Kenneth	PS 362	241
Herisanu, Ioana Tereza	PS 227	133
Hermansky, Hynek	SYMP 30	300
Hernández-Perez, Heivet	PS 718	494
Herranen, Anni	PS 593	395
Herrero, Carmen	PD 147	623
Herrero, Jose	PS 365	242
Herrmann, Björn	SYMP 11	151
Herrmann, Barbara	PS 24	22
Herrmann, Barbara	PS 450	289
Herrmann, Barbara	PS 451	290
Hertzano, Ronna	PRES SYMP 4	2
Hertzano, Ronna	PS 112	70
Hertzano, Ronna	PS 328	222
Hertzano, Ronna	PS 347	233
Hertzano, Ronna	PS 754	515
Hertzano, Ronna	PS 96	61
Hertzano, Ronna	PD 79	310
Hertzano, Ronna	PD 81	311
Hertzano, Ronna	PD 60	294
Hertzano, Ronna	PS 349	234
Hetrick, Alisa	PS 154	94
Heuschen, Sylvie	PS 232	136
Hickok, Gregory	PS 876	584

Name	Abstract No.	Page No.
Hickok, Gregory	PS 667	436
Higgins, Nathan	PS 714	492
Hight, Ariel	PS 502	344
Hight, Ariel	PS 727	499
Hill, Kayla	PS 589	393
Hill, Kayla	PS 151	93
Hinsberger, Marius	PS 40	31
Hinton, Ashley	PS 750	512
Hirai, Chiaki	PD 172	638
Hirose, Yoshinobu	PS 359	239
Hirose, Keiko	PD 144	622
Hirose, Yoshinobu	PS 685	446
Hirose, Yoshinobu	PS 156	96
Hirose, Yoshinobu	PS 357	238
Hirose, Keiko	PD 62	295
Hirst, Jonathan	PS 581	388
Hjortkjær, Jens	PS 479	331
Hjortkjær, Jens	PS 472	328
Hoa, Michael	PS 766	67
Hoa, Michael	PD 94	452
Hoa, Michael	PS 216	128
Hobbs, Diana	PS 253	181
Hoch, Gerhard	PS 550	372
Hochberg, Fred	PS 149	91
Hoesli, Marco	PS 721	496
Hoetzer, Benjamin	PS 40	31
Hoffer, Michael	PS 664	434
Hoffer, Michael	PS 798	538
Hoffer, Michael	PS 224	131
Hoffer, Michael	PS 225	132
Hoffer, Michael	PD 174	639
Hoffman, Larry	PS 913	607
Hoffman, Howard	PS 57	41
Hoffman, Michael	PS 22	200
Hoffman, Howard	PD 167	635
Hoffman, Larry	PD 39	156
Hoffman, Hal	PD 94	452
Hoffman, Larry	PS 914	607
Hoffmann, Thomas	PS 119	74
Hofstetter, Au.D, Philip	PS 833	559
Hogan, Anne	PD 167	635
Hohmann, Volker	PS 862	577
Hohmann, Volker	PS 370	245
Hojjati, Ronus	PD 38	156
Holcomb, Paul	PS 761	518
Holcomb, Paul	PS 301	209
Holfoth, David	PS 204	121
Holley, Matthew	PS 688	478
Hollingsworth, Kamren	PS 600	400
Hollonbeck, Sean	PS 834	560
Hollonbeck, Sean	PD 156	629
Holman, Holly	PS 906	603
Holman, Holly	PS 143	88
Holman, Holly	PD 77	308
Holmes, Emma	PD 107	464
Holmes, Emma	PD 12	139
Holmes, Emma	PS 422	273
Holstein, Gay R.	PS 675	440

Author Index

Name	Abstract No.	Page No.
Holstein, Gay R.	PS 676	441
Holt, Jeffrey	SYMP 27	171
Holt, Jeffrey	SYMP 21	169
Holt, Joseph	PS 909	604
Holt, Joseph	PD 41	158
Holt, Avril Genene	PS 802	541
Holt, Avril Genene	PS 897	597
Holt, Joseph	PS 912	606
Holt, Lori	PS 661	432
Holt, Avril Genene	PD 15	141
Holt, Joseph	PS 362	241
Holt, Avril Genene	PS 827	556
Holt, Lori	SYMP 6	2
Holt, Jeffrey	PS 139	86
Holt, Jeffrey	PS 803	541
Homma, Kazuaki	PS 324	220
Homma, Kazuaki	PS 598	399
Honeder, Clemens	PD 6	6
Hong, Hui	PS 511	350
Hong, Seong Ah	PS 233	136
Hong, Hui	PD 113	467
Hong, Hui	PS 517	353
Hong, Juan	PD 119	471
Hood, Linda	PS 46	35
Hood, Linda	PS 314	215
Hood, Linda	PS 74	50
Horeczko, Hannah	PS 397	260
Hori, Takeshi	PS 156	96
Hörmann, Karl	PS 231	135
Horn, David	PS 272	191
Horstmann, Heinz	PS 741	507
Horvat, LeeAnn	PD 11	139
Hosoya, Makoto	PS 90	599
Hossain, Muhammad	PS 463	323
Houston, Lisa	PS 722	496
Houston, Lisa	PS 14	17
Houston, Oliver	PS 134	83
Howard, Matthew	PD 136	617
Howard, Matthew	PD 138	618
Howard, Matthew	PS 713	491
Howard, Matthew	PS 476	330
Howe, Simon	PS 525	358
Hoyt, Jeffrey	PS 830	557
Hozan, Mohsen	PS 273	192
Hsu, Meng-Chun	PS 819	551
Hsu, Chuan-Jen	PS 565	380
Hu, Xiaosu	PS 711	490
Hu, Yujuan	SYMP 21	169
Hu, Zhengqing	PS 889	591
Hu, Bo Hua	PS 590	394
Hu, Ning	PS 6	12
Hu, Hongmei	SYMP 51	315
Hu, Bo Hua	PS 693	480
Hu, Bohua	PS 751	513
Huang, Mingqian	SYMP 21	169
Huang, Jun	PS 918	610
Huang, Jun	PS 59	42
Huang, Jennifer	PD 160	631

Name	Abstract No.	Page No.
Huang, Charles	PS 798	538
Huang, Nicholas	PS 707	488
Huang, Jun	PS 920	611
Huang, Juan	PS 869	581
Huang, Yi	PS 903	601
Huarcaya Najarro, Elvis	PD 160	631
Hubbard, April	PS 662	433
Huber, Alexander	PS 226	133
Huber, Alexander	PS 721	496
Huber, Alexander	PS 60	43
Huber, Alexander	PS 192	115
Huber, Alexander	PS 75	51
Huber, Alexander	PS 838	562
Hudspeth, A J	PS 785	531
Hudspeth, A J	PD 164	633
Hudspeth, A J	PS 769	523
Hudspeth, A J	PD 51	164
Huet, Antoine	PS 485	334
Huetz, Chloe	PS 708	488
Hughes, Aaron	PS 725	498
Hughes, Aaron	SYMP 14	167
Huh, Sung-Ho	PS 103	65
Huh, Sung-Ho	PS 100	63
Huh, Dan Dongeun	SYMP 43	303
Huhnke, Jessica	PS 165	100
Hullar, Timothy	PD 92	451
Hülse, Roland	PS 231	135
Hunter, Lisa	PS 855	572
Hunter, Lisa	PS 856	573
Hunter, Lisa	PD 122	473
Huntsman, Molly	PS 738	506
Husain, Fatima	PS 426	275
Husain, Fatima	PS 524	357
Husain, Fatima	PS 627	415
Husereau, Marisa	PS 51	38
Hutchison, John	PS 242	176
Huth, Markus	PD 146	622
Hutson, Kendall	PS 432	279
Hutson, Kendall	PS 377	249
Huyck, Julia	PS 663	433
Hwang, Yujung	PS 814	548
Ibayashi, Kenji	PS 453	318
Ichiba, Kayla	PS 77	52
Iconaru, Luigi	PD 55	291
Ihlefeld, Antje	PS 20	20
Ikeda, Kazuhisa	PS 694	481
Ikeda, Takuo	PS 685	446
Ikeya, Makoto	PS 778	527
Ila, Kadri	PS 605	403
Ila, Kadri	PS 351	235
Ila, Kadri	PS 809	545
Im, Gi Jung	PS 340	229
Imanishi, Yoshikazu	PD 58	293
Imayoshi, Itaru	PS 94	60
Imtiaz, Ayesha	PS 770	523
Indzhukulian, Artur	PS 767	522
Indzhukulian, Artur	PS 774	525
Ingham, Neil J.	PD 97	454

Author Index

Name	Abstract No.	Page No.
Ingham, Neil J.	PS 330	223
Inglese, Francesco	PS 841	564
Inserra, Christopher	PS 107	67
Irvine, Dexter	SYMP 33	301
Isakov, Ofer	PD 82	311
Isenberg, Brett	SYMP 44	304
Isgrig, Kevin	PS 804	542
Isgrig, Kevin	PS 806	543
Isgrig, Kevin	PS 216	128
Ishai, Reuven	PS 837	562
Ishai, Reuven	PS 24	22
Ishidate, Fumiyoshi	PS 94	60
Ishikawa, Masaaki	PS 931	503
Ishiyama, Gail	PD 168	635
Ishiyama, Akira	PD 168	635
Ishiyama, Gail	PD 99	455
Ishiyama, Akira	PD 99	455
Ishizu, Kotato	PS 196	117
Ishizu, Kotato	PS 437	281
Issa, Mohamad	PS 711	490
Issa, John	PD 5	6
Itatani, Naoya	PS 465	324
Ito, Juichi	PS 506	347
Ito, Juichi	PS 796	537
Ito, Juichi	PS 753	514
Ito, Juichi	PS 778	527
Ivanchenko, Maryna	PS 774	525
Ivanova, Alla	PS 689	478
Iversen, Marta	PS 906	603
Iversen, Marta	PS 622	412
Iverson, Paul	PS 668	436
Iverson, Paul	PS 764	520
Iwasa, Kuni	PS 341	229
Iyaniwura, John	PS 307	212
Iyer, Nandini	PS 879	586
Iyer, Janani	PD 100	456
Iyer, Nandini	PS 368	244
Jabeen, Talat	PS 166	101
Jackson, Dakota	PS 301	209
Jacobo, Adrian	PD 164	633
Jacobs, Jessica	PD 28	148
Jacoby, Nori	PS 864	578
Jadali, Azadeh	PD 69	299
Jadali, Azadeh	PS 887	590
Jaekel, Brittany	PS 424	274
Jagadeesh, Anoop	PS 50	37
Jahan, Israt	PS 39	31
Jahan, Israt	SYMP 24	170
Jakobsson, Anne-Marie	PS 650	426
Jamesdaniel, Samson	PS 801	540
Jang, Jeong Hun	PS 360	240
Jang, Kyoung-Je	PS 836	561
Jang, Miae	PS 302	209
Janky, Kristen	PS 452	290
Janky, Kristen	PD 171	637
Jansen, Sebastian	PS 498	342
Jansson, Lina	PS 103	65
Jareño, Tania	PD 147	623

Name	Abstract No.	Page No.
Jayabal, Sriram	PS 680	443
Jayakumar, Ashik	PS 544	368
Jedrzejczak, Wiktor	PS 78	52
Jeka, John	PS 448	288
Jen, Hsin-I	PS 692	480
Jen, Hsin-I	PS 217	128
Jeng, Jing-Yi	PS 688	478
Jenkins, Herman	PS 42	33
Jenkins, Herman	PS 624	413
Jenkins, Herman	PS 839	563
Jennings, Skyler G.	PS 394	258
Jennings, Todd	PS 865	579
Jeon, EunHae	PS 673	439
Jeon, EunHae	PS 929	446
Ji, Lingchao	PD 40	157
Jiam, Nicole	PS 857	574
Jiang, Dan	PS 138	86
Jiang, Weitao	PS 915	608
Jiang, Qingqing	PS 572	384
Jiang, Peng	PS 789	533
Jiang, Han	PD 2	4
Jiang, meiyan	PD 61	294
Jiang, Weitao	PS 675	440
Jiang, Shangyuan	PS 179	108
Jiang, Haiyan	PS 592	395
Jiang, Haiyan	PD 59	293
Jiang, Weitao	PS 676	441
Jiang, Tao	PD 36	155
Jiang, meiyan	PS 551	372
Jimenez, Erin	PS 927	595
Jin, In/ki	PS 410	267
Jin, Gang	PD 80	310
Jing, Zhizi	PS 550	372
Jiradejvong, Patpong	PS 857	574
Jiradejvong, Patpong	PS 36	29
Jocewicz, Rachael	PS 866	579
Jodelka, Francine	PD 1	3
Jodelka, Francine	PD 2	4
Johannesen, Peter	PS 79	52
Johannesen, Peter	PS 241	175
Johansen, Jacob	PS 338	228
Johansson, Marlin	PS 648	425
John, Kimball	PS 224	131
John, Kimball	PS 225	132
Johnson, Erik C.	PS 21	21
Johnson, Stuart L.	PS 134	83
Johnson, Lejo-Chacko	PS 493	339
Johnson, Stuart L.	PS 538	365
Johnsrude, Ingrid	PD 107	464
Johnsrude, Ingrid	PD 12	139
Johnsrude, Ingrid	PS 476	330
Johnsrude, Ingrid	PS 422	273
Jomaa, Mohamed	PS 932	347
Jones, Douglas L.	PS 21	21
Jones, Simon	PS 470	327
Jones, Timothy	PS 912	606
Jones, Sherri	PD 70	299
Jones, Lashaka	PS 509	348

Author Index

Name	Abstract No.	Page No.
Jones, Heath	PD 133	615
Jones, Heath	PS 834	560
Jones, Heath	PD 156	629
Jones, Sherri	PD 71	305
Jones, Timothy	PD 63	296
Joo, Seol-hee	PS 117	73
Jordan, Paivi	PS 909	604
Jordan, Paivi	PD 41	158
Joris, Philip	PS 289	202
Joris, Philip	PS 742	508
Joris, Philip	PS 482	332
Joris, Philip	PS 643	423
Joshi, Suyash	SYMP 53	316
Joshi, Tarana	PS 921	611
Josuweit, Angela	PS 370	245
Joung, J.	SYMP 16	167
Jovanovic, Sasa	PS 516	352
Ju, Hyun Mi	PS 574	385
Jung, Jae Yun	PS 55	39
Jung, David	PD 3	5
Jung, Hak Hyun	PS 340	229
Jung, Sangyong	PS 550	372
Jung, Jinsei	PS 562	378
Jung, Jae Yun	PS 4	11
Jung, Lorenz	PS 419	271
Jung, Jae Yun	PS 587	392
Jürgens, Tim	SYMP 51	315
Jürgens, Tim	PS 419	271
Justal, Thomas	PS 485	334
Kabahuma, Rosemary	PS 118	73
Kabara, Lisa	PS 789	533
Kabara, Lisa	PS 608	404
Kachar, Bechara	PS 536	364
Kachar, Bechara	PD 71	305
Kachar, Bechara	PS 533	362
Kaderbay, Akil	PS 799	539
Kador, Peter	PD 59	293
Kageyama, Ryoichiro	PS 94	60
Kaier-Green, Zoe	PS 204	121
Kajikawa, Yoshinao	PS 246	178
Kalappa, Bopanna	PS 300	208
Kale, Sushrut	PS 576	386
Kalinec, Fererico	PS 811	546
Kalinski, Hagar	PS 888	590
Kalluri, Radha	PS 3	10
Kalluri, Raymond	PS 3	10
Kalluri, Radha	PD 43	159
Kamakura, Takefumi	PS 306	211
Kamal, Lara	PD 82	311
Kambalyal, Anuj	PS 544	368
Kamerer, Aryn	PS 5	11
Kameswaran, Mohan	PS 128	80
Kamiya, Kazusaku	PS 694	481
Kammerer, Bernd	PS 813	547
Kan, Alan	PS 651	427
Kan, Alan	SYMP 50	315
Kan, Alan	PS 656	430
Kan, Alan	PD 133	615

Name	Abstract No.	Page No.
Kan, Alan	PS 654	429
Kan, Alan	PS 13	16
Kanaan, Moien	PD 82	311
Kandler, Karl	PS 735	504
Kane, Catherine	PS 265	187
Kaneshiro, Blair	PS 716	493
Kang, Hijee	PS 861	577
Kanicki, Ariane	PS 608	404
Kanicki, Ariane	PS 921	611
Kannan-Sundhari, Abhiraami	PS 126	78
Kannan-Sundhari, Abhiraami	PS 567	381
Kannan-Sundhari, Abhiraami	PS 128	80
Kanold, Patrick	PS 252	181
Kanold, Patrick	PS 461	322
Kanold, Patrick	PS 636	420
Kanold, Patrick	SYMP 3	1
Kanold, Patrick	PS 635	419
Kanthaiah, Koka	PS 613	407
Kanumuri, Vivek	PS 502	344
Kanumuri, Vivek	PS 305	211
Kanumuri, Vivek	PS 727	499
Kanwisher, Nancy	PD 137	311
Kanzaki, Ryohei	PS 196	117
Kanzaki, Ryohei	PS 437	281
Karch, Stephanie	PS 834	560
Karten, Harvey	PS 431	278
Kashemirov, Boris	PD 3	5
Kashino, Makio	PS 873	583
Kashino, Makio	PS 878	585
Kassem, Sarah	PS 425	275
Kastner, Daniel	PD 94	452
Katrakazas, Panagiotis	PS 185	111
Katsuno, Tatsuya	PS 753	514
Katsuno, Tatsuya	PS 778	527
Katsuno, Tatsuya	PS 770	523
Katz, Eleonora	PS 547	370
Katz, Eleonora	PS 540	366
Kaufmann, Christopher	PS 504	345
Kaufmann, Christopher	PS 23	22
Kaur, Tejbeer	PS 583	390
Kaur, Maninder	PS 110	69
Kaur, Tejbeer	PD 117	470
Kaur, Tejbeer	PS 750	512
Kawas, Leen	PD 61	294
Kawasaki, Hiroto	PD 136	617
Kawasaki, Hiroto	PD 138	618
Kawashima, Yoshiyuki	PD 94	452
Kawashima, Yoshiyuki	PS 336	227
Kawashima, Yoshiyuki	PD 172	638
Kawauchi, Satoko	PS 526	358
Kaya, Emine Merve	PD 29	148
Kayyali, Mohammad	PS 573	384
Kazmierczak, Piotr	PS 775	526
Kazmierczak, Marcin	PS 775	526
Kazmitcheff, Guillaume	PS 41	32
Kearney, Graciela	PS 547	370
Kell, Alexander	PS 260	184
Kell, Alexander	PD 30	149

Author Index

Name	Abstract No.	Page No.
Kelley, Matthew	PD 32	152
Kelley, Matthew	PD 31	152
Kelley, Matthew	PS 600	400
Kelley, Matthew	PS 754	515
Kelley, Matthew	PS 747	511
Kelley, Matthew	PS 102	64
Kelley, Matthew	PS 749	512
Kelley, Matthew	PS 748	511
Kelley, Matthew	PS 349	234
Kelley, Matthew	PS 216	128
Kelllard, Zoe	PS 213	126
Kellner, Christian	PS 734	504
Kelly, Michael	PD 32	152
Kelly, Michael	PD 31	152
Kelly, Michael	PS 747	511
Kelly, John	PS 325	221
Kelly, Michael	PS 749	512
Kelly, Michael	PS 748	511
Kelly, Michael	PD 81	311
Kelly, John	PS 610	405
Kelly, Michael	PS 349	234
Kempfle, Judith	PS 226	133
Kempfle, Judith	PD 3	5
Kempfle, Judith	PS 808	544
Kempfle, Judith	PS 890	592
Kempton, Beth	PD 2	4
Kempton, Beth	PS 358	239
Kenna, Margaret	PS 314	215
Kersigo, Jennifer	SYMP 24	170
Kersigo, Jennifer	PD 173	638
Ketten, Darlene	PS 173	104
Kettler, Lutz	PS 733	503
Keymeulen, Sawa	PS 89	592
Khaleghi, Morteza	PS 186	111
Khalighinejad, Bahar	PD 143	621
Khalighinejad, Bahar	PS 475	329
Kheradmand, Amir	SYMP 41	303
Kidan, Amanuel Wolde	PS 163	99
Kidd, Gerald	PS 865	579
Kidd, Gerald	PS 401	262
Kidd, Gerald	PS 863	578
Kiderman, Alexander	PS 224	131
Kiderman, Alexander	PS 225	132
Kiderman, Alexander	PD 174	639
Kiefer, Lenneke	PS 895	595
Kielley, Bernadine	PS 116	72
Kiemel, Tim	PS 448	288
Kiernan, Amy	PD 37	155
Kiernan, Amy	PS 91	605
Klim, Sung Huhn	PS 562	378
Kikidis, Dimitris	PS 810	545
Kileny, Paul	PS 711	490
Kim, Yeon Ju	PS 360	240
Kim, Young Sun	PS 360	240
Kim, Dami	PS 111	70
Kim, Min-Jung	PS 528	359
Kim, Dong-Kyu	PS 570	383
Kim, Jinkyung	PS 571	383

Name	Abstract No.	Page No.
Kim, Jinsook	PS 410	267
Kim, Jeff	PS 61	43
Kim, Woo Jin	PS 844	566
Kim, Mi-Jung	PD 57	292
Kim, Eric	PS 898	598
Kim, Min-Jung	PS 696	482
Kim, Ji Hyung	PS 233	136
Kim, Sun Geum	PS 233	136
Kim, So Young	PS 902	600
Kim, Young Ho	PS 902	600
Kim, Subong	PS 662	433
Kim, Yeon Ju	PS 836	561
Kim, Young Sun	PS 836	561
Kim, Yeong Cheol	PS 836	561
Kim, Jin Young	PS 562	378
Kim, Bo Gyung	PS 562	378
Kim, Young Ho	PS 677	441
Kim, Jun Hee	PS 302	209
Kim, Sangmin	PS 621	411
Kim, Subong	PS 477	330
Kim, H. Jeffrey	PD 94	452
Kim, Young Ho	PS 54	366
Kim, Mi-Jung	PS 581	388
Kim, Mi-Jung	PS 152	93
Kim, Subong	PD 130	613
Kim, Jong-Duk	PS 818	550
Kim, Dong-Kee	PS 818	550
Kim, Gyutae	PS 673	439
Kim, Gyutae	PS 929	446
Kim, Hyun Ji	PS 929	446
Kim, Hyun Ji	PS 673	439
Kim, Kyu-Sung	PS 673	439
Kim, Kyu-Sung	PS 929	446
Kim, Kyunghee	PD 62	295
Kim, Moon Suk	PS 814	548
Kim, Dami	PS 339	228
Kim, Minbum	PS 919	610
Kindt, Katie	PS 112	70
Kindt, Katie	PD 78	309
Kindt, Katie	PS 760	518
King, Andrew	PS 460	321
King, Kelly	PS 61	405
King, Susan	PS 442	284
King, Mary-Claire	PD 82	311
King, W. Michael	PS 674	439
King, Andrew	PD 26	147
King, W. Michael	PS 921	611
King, Julia	SYMP 13	166
King, Andrew	PS 469	326
King, W. Michael	PD 38	156
King, Andrew	PS 435	280
Kingma, Herman	PS 446	287
Kingma, Herman	PS 444	285
Kingma, Herman	PS 493	339
Kinoshita, Makoto	PS 753	514
Kirchner, Rory	PD 83	312
Kirk, Jonathon	PS 505	346
Kirk, Jonathon	PS 811	546

Author Index

Name	Abstract No.	Page No.
Kirk, Jonathon	PS 812	546
Kishimoto, Ippei	PS 752	513
Kitahara, Tadashi	PS 148	91
Kitajiri, Shin-ichiro	PD 84	313
Kitajiri, Shin-ichiro	PS 778	527
Kitajiri, Shin-ichiro	PS 770	523
Kitcher, Sian	PD 149	624
Klawitter, Silke	PS 26	23
Kleindienst, AuD, PhD, CCC-A, Samantha	PS 833	559
Kliesch, Sven	PS 419	271
Klinge-Strahl, Astrid	PS 614	407
Klis, Sjaak	PS 262	186
Klis, Sjaak	PS 595	397
Klis, Sjaak	PS 487	335
Klug, Achim	PS 738	506
Klug, Julian	PS 305	211
Kluk, Karolina	PS 646	424
Kluk, Karolina	PS 268	189
Kluk, Karolina	PS 297	206
Klump, Georg	PS 199	119
Klump, Georg	PS 465	324
Klump, Georg	PS 70	48
Klyn, Niall	PS 559	376
Knipper, Marlies	PD 20	144
Knipper, Marlies	PS 632	418
Knipper, Marlies	PS 582	389
Knowles, Jeffrey	PD 24	146
Kobayashi, Yasushi	PS 526	358
Kobrina, Anastasiya	PS 201	120
Kobrina, Anastasiya	PS 200	119
Koch, Robert	PS 616	408
Kochanek, Krzysztof	PS 78	52
Kochanek, Krzysztof	PS 129	80
Kodama, Takashi	PS 299	208
Koen, Nicholas	PD 3	5
Koenecke, Nina	PS 223	131
Koesling, Doris	PS 582	389
Koh, Jin-Young	PS 113	71
Kohrman, David	PS 608	404
Kojima, Hiromi	PS 846	567
Kojima, Hiromi	PS 835	560
Kokesh, MD, John	PS 833	559
Kokkinakis, Kostas	PS 655	429
Kokx-Ryan, Melissa	PD 11	139
Kolbe, Diana	PS 113	71
Koleilat, Alaa	PS 793	535
Kolia, Nadeem	PD 45	160
Kolson, Douglas	PS 759	517
Konerding, Wiebke	PS 259	184
Kong, Weijia	SYMP 21	169
Kong, Ying-Yee	SYMP 60	460
Kong, Weijia	PS 678	442
Kong, Weijia	PD 161	632
Konrad-Martin, Dawn	PS 579	387
Kopke, Richard	PS 10	15
Kopke, Richard	PS 218	129
Kopke, Richard	PS 896	596
Köppl, Christine	PS 484	334

Name	Abstract No.	Page No.
Köppl, Christine	PD 85	447
Köppl, Christine	PS 67	46
Kopp-Scheinpflug, Conny	PS 519	354
Kopp-Scheinpflug, Conny	PS 521	355
Kopp-Scheinpflug, Conny	PS 48	36
Kopun, Judy	PS 267	188
Korrapati, Soumya	PS 766	67
Kose, Orhun	PS 182	109
Kössl, Manfred	PS 73	50
Kotak, Vibhakar	SYMP 5	9
Koullich, Elena	PD 105	457
Koumura, Takuya	PS 872	582
Koutsouris, Dimitris	PS 185	111
Kovelman, Ioulia	PS 711	490
Kozin, Elliott	PS 502	344
Kozin, Elliott	PS 305	211
Kozin, Elliott	PD 154	627
Kozin, Elliott	PS 808	544
Kozin, Elliott	PS 837	562
Kozin, Elliott	PS 727	499
Krackau, Geneviève	PD 11	139
Kraemer, Anna	PD 85	447
Kraemer, Anna	PS 65	45
Kral, Andrej	PD 7	7
Kral, Andrej	PS 577	386
Kral, Andrej	PD 127	476
Kral, Andrej	PS 464	323
Kral, Andrej	PD 141	620
Kral, Andrej	PS 259	184
Kral, Andrej	PS 500	343
Kral, Andrej	PS 732	502
Kramer, Kenneth	PS 107	67
Krantz, Ian	PS 110	69
Krantz, Ian	PS 314	215
Krass, Daniel	PS 311	214
Kraus, Nina	PS 428	277
Kraus, Nina	PD 9	138
Kravitz, Adam	PS 224	131
Kravitz, Adam	PS 225	132
Kreeger, Lauren	PS 373	247
Kreft, Heather	PD 134	616
Kreiskoether, Kim	PD 8	7
Kremer, Hannie	PS 117	73
Kretzberg, Jutta	PS 66	46
Krey, Jocelyn	PD 71	305
Krishnan, Ananthanarayan	PS 478	478
Krishnan, Ananthanarayan	PS 296	206
Krishnan, Ananthanarayan	PS 717	493
Kristaponyte, Inga	PS 529	360
Kriwacki, Richard	PD 55	291
Krizman, Jennifer	PS 428	277
Kros, Corné	PS 332	225
Kros, Corné	PS 334	226
Kros, Corné	PD 149	624
Krueger, Benjamin	PS 287	200
Krug, Edward	PS 321	218
Krystofiak, Evan	PD 71	305
Kübler, Angelika	PS 632	418

Author Index

Name	Abstract No.	Page No.
Kubli, Lina	PD 11	139
Kuchinsky, Stefanie	PS 421	273
Kuenzel, Thomas	PS 374	247
Kuenzel, Thomas	PD 112	466
Kuhl, Andre	PS 802	541
Kuhl, Andre	PD 15	141
Kujawa, Sharon	PS 8	13
Kujawa, Sharon	PS 271	191
Kujawa, Sharon	PS 823	553
Kujawa, Sharon	PS 9	14
Kujawa, Sharon	PS 238	173
Kulkarni, Mandar	PS 106	66
Kulkarni, Aditya	PD 128	612
Kumar, Sukhbinder	PD 136	617
Kumar, Sukhbinder	SYMP 7	3
Kumar, Manoj	PS 258	183
Kunal, Patel	PS 224	131
Kunal, Patel	PS 225	132
Kuner, Thomas	PS 741	507
Kuo, Bryan	PS 317	217
Kurabi, Arwa	PS 816	549
Kurabi, Arwa	PS 843	565
Kurima, Kiyoto	PD 94	452
Kurima, Kiyoto	PS 336	227
Kurioka, Takaomi	PS 483	333
Kurioka, Takaomi	PS 526	358
Kurioka, Takaomi	PS 158	97
Kurt, Simone	PS 310	213
Kurt, Simone	PS 824	554
Kurth, Stefanie	PD 112	466
Kuwada, Shigeyuki	PS 290	202
Kwan, Kelvin	PD 69	299
Kwan, Kelvin	PS 92	59
Kwan, Annie	PS 917	609
Kwan, Kelvin	PS 887	590
Kwiatkowska, Monika	PS 931	503
Kysar, Jeffrey	PS 611	406
La Bianca, Martina	PS 124	77
La Bianca, Martina	PS 121	75
Labban, Kyle	PS 397	260
Laboulais, Amandine	PS 904	601
Lacour, Stephanie	PS 502	344
Ladak, Hanif	PS 307	212
Ladak, Hanif	PS 616	408
LaFaire, Petrina	PS 383	252
Lahlou, Hanae	PS 602	401
Lai, Ke	PS 669	437
Lai, Ke	PS 670	437
Laird, Dale	PS 325	221
Lalande, Alain	PS 842	565
Lalwani, Anil	PS 25	23
Lalwani, Anil	PS 611	406
Lamas, Veronica	SYMP 21	169
Lamas, Georges	PS 449	289
Lambert, Aaron	PS 793	535
Lammers, Marc	PS 724	497
Lammers, Marc	PS 474	329
Lancelin, Denis	PS 861	577

Name	Abstract No.	Page No.
Land, Rüdiger	PD 127	476
Landau, Andrew	PS 455	319
Landegger, Lukas	PS 308	212
Landegger, Lukas	PS 149	91
Landegger, Lukas	PS 803	541
Landin-Malt, Andre	PS 106	66
Landsberger, David M.	PS 29	25
Landsberger, David M.	PS 926	201
Landsberger, David M.	PS 26	23
Landsberger, David M.	PS 30	26
Landsberger, David	SYMP 48	314
Landsberger, David M.	PS 657	430
Landsberger, David M.	PS 37	30
Lang, Hainan	PS 264	187
Lang, Steven	PS 128	80
Lang, Hainan	PS 492	338
Lang, Hainan	PS 491	338
Lang, Hainan	PS 321	218
Langenbucher, Achim	PS 40	261
Langer, Robert	PS 823	553
Large, Charles	PS 242	176
Larky, Jannine	PS 311	214
Larroze-Chicot, Philippe	PS 904	601
Lau, Bonnie K.	PS 392	257
Lauer, Amanda	PS 299	208
Laureano, Alejandra	PS 92	59
Laurell, Göran	PS 800	539
Lavedrine, Angela	PS 842	565
Lavie, Limor	PD 123	474
Lavie, Nilli	PS 705	487
Layman, Wanda	PS 317	217
Lazniewski, Michal	PS 129	80
Le, Quang	PS 159	97
LE CLEC'H, Céline	PS 799	539
Le Prell, Colleen	PS 197	118
Leake, Patricia	PS 161	98
Leake, Patricia	PS 503	345
Leal, Suzanne	PS 130	81
Lechowicz, Urszula	PS 129	80
Leckness, Kegan	PD 158	630
Lee, Yun Yeong	PS 360	240
Lee, Sungsu	PS 111	70
Lee, Daniel	PS 21	21
Lee, Min Young	PS 55	39
Lee, Adrian	PS 291	203
Lee, Daniel	PS 502	344
Lee, Brian	PD 5	6
Lee, Sun Gyeong Rose	PS 44	34
Lee, Seung Hwan	PS 845	567
Lee, Dong Wook	PS 845	567
Lee, Seungwan	PS 410	267
Lee, Hey-Kyoung	PS 636	420
Lee, Sung Ho	PS 340	229
Lee, Se Hee	PS 340	229
Lee, Daniel	PS 305	211
Lee, Norman	PS 72	49
Lee, Choongheon	PS 912	606
Lee, Yun Yeong	PS 836	561

Author Index

Name	Abstract No.	Page No.
Lee, Jaewook	PS 12	16
Lee, Min Young	PS 483	333
Lee, Norman	PS 369	245
Lee, Daniel	PS 808	544
Lee, Sungmin	PS 719	495
Lee, General	PD 11	139
Lee, Jae-Hun	PS 4	11
Lee, Min Young	PS 4	11
Lee, Daniel	PS 727	499
Lee, Jae-Hun	PS 587	392
Lee, Min Young	PS 587	392
Lee, Sangmin	PS 673	439
Lee, Sangmin	PS 929	446
Lee, Sungsu	PS 339	446
Lee, Sun Hee	PS 574	385
Lee, Daniel	PS 657	430
Lee, Min Young	PS 158	97
Lefebvre, Philippe	PD 165	634
Léger, Agnès	PS 646	424
Léger, Agnès	PS 297	206
Legrís, Elsa	PS 652	427
Leibold, Lori	PS 763	519
Leibold, Lori	PS 762	519
Leibold, Lori	PS 389	256
Lelli, Andrea	PD 72	306
Lemons, Charlsie	PD 47	161
Lemons, Charlsie	PS 171	103
Lenarz, Thomas	PD 7	7
Lenarz, Thomas	PS 577	386
Lenarz, Thomas	PD 4	5
Lenarz, Thomas	PS 34	28
Lenarz, Thomas	PD 8	7
Lenarz, Thomas	PD 141	620
Lenarz, Thomas	PS 188	113
Lenoir, Marc	PS 775	526
Lentz, Jennifer	PD 1	3
Lentz, Jennifer	PD 2	4
Lentz, Jennifer	PS 807	543
Lenz, Danielle	PS 618	409
Lenz, Danielle	SYMP 44	304
Lenz, Danielle R.	PS 211	125
Leprince, Inka	PS 520	355
Lesus, Joseph	PS 544	368
Leung, Hui Min	PD 100	456
Levine, Robert	PD 22	472
Levitt, Pat	PD 163	633
Levron, Rivka	PS 888	590
Levy, Sarah	PS 311	214
Lewis, Peter	PS 618	409
Lewis, Jennifer	PD 154	627
Lewis, Morag	PS 131	81
Lewis, Richard	PS 442	284
Lewis, Morag	PS 330	223
Leyzac, Kara	PS 900	599
Li, Quan	PS 116	72
Li, Tao	PS 126	78
Li, Huawei	PS 123	76
Li, Guoping	PS 726	498

Name	Abstract No.	Page No.
Li, Xiaoyang	PS 889	591
Li, Xiaoyi	PS 766	67
Li, Huawei	PS 215	127
Li, Chuan-Ming	PS 56	40
Li, Wei	PS 218	129
Li, Chuan-Ming	PS 57	41
Li, Chuan-Ming	PD 167	635
Li, Lingchao	PD 56	292
Li, Wenyan	PS 205	122
Li, Huawei	PS 205	122
Li, Yong	PS 586	391
Li, Jin	PS 316	216
Li, Daqing	PS 573	384
Li, Qinghui	PD 80	310
Li, Hongzhe	PS 154	94
Li, Yongqi	PS 592	395
Li, Wei	PS 817	549
Li, Xiaolin	PS 243	176
Li, Daqing	PS 815	548
Li, Huawei	PS 585	391
Li, Ji	PS 693	480
Li, Shengwei	PS 903	601
Li, Song-Zhe	PD 62	295
Li, Hui	PS 491	338
Li, Shufeng	PD 132	615
Li, Jia	PS 193	115
Li, Jianfeng	PS 494	340
Li, Jia	PS 187	112
Li, Xiaoyi	PS 216	128
Li, Qi	PS 326	221
Liang, Chun	PS 722	496
Liang, Chun	PS 14	17
Liang, Xiuyuan	PD 18	143
Liang, Chun	PD 104	457
Liang, Chun	PD 116	469
Liang, Qiong	PD 132	615
Liao, Shixiu	PS 126	78
Liao, James	PS 338	228
Liao, Hsin-I	PS 878	585
Liaud, Pierre	PS 441	284
Liaud, Pierre	PS 792	535
Liberman, M. Charles	PS 591	394
Liberman, M. Charles	PS 144	89
Liebau, Arne	PS 813	547
Liebenthal, Einat	PD 139	619
Lilian, Sigmund	PS 671	438
Lim, Rebecca	PD 41	158
Lim, Jeonghee	PS 790	534
Lim, Hubert H.	PS 40	31
Limb, Charles	PS 857	574
Limb, Charles	SYMP 59	460
Limb, Charles	PS 36	29
Lin, Yung-Song	SYMP 59	460
Lin, Frank	SYMP 63	462
Lin, Xi	PS 323	220
Lin, Shu-Wha	PS 565	380
Lin, Mei	PS 815	548
Lin, Xi	PS 326	221

Author Index

Name	Abstract No.	Page No.
Linbo, Tor	PS 140	87
Linden, Jennifer	PD 106	464
Linden, Jennifer	PS 436	281
Linden, Jennifer	PS 826	555
Linder, Thomas	PS 838	562
Lindner, Julia	PS 204	121
Lindsay, Nicola	PD 58	293
Ling, Lynne	PS 695	481
Ling, Leo	PS 445	286
Linser, Paul	PS 581	388
Linthicum, Fred	PD 99	455
Linthicum, Fred	PS 216	128
Litovsky, Ruth	PS 651	427
Litovsky, Ruth	PS 866	579
Litovsky, Ruth	PS 656	430
Litovsky, Ruth	PD 133	615
Litovsky, Ruth	PS 654	429
Litovsky, Ruth	PS 20	20
Litovsky, Ruth	PS 13	16
Litvak, Leonid	PS 16	18
Litvak, Leonid	PS 613	407
Liu, Xuezhong	PS 126	78
Liu, Xue	PS 118	73
Liu, Zhiqi	PS 153	94
Liu, David	SYMP 21	169
Liu, Zhenjie	PS 889	591
Liu, Xue	PS 664	434
Liu, Bin	PD 18	143
Liu, Dong	PS 220	130
Liu, George	PS 571	383
Liu, Xue	PS 127	79
Liu, Sabrina	PD 154	627
Liu, Andrew	PS 662	433
Liu, Wei	PS 800	539
Liu, Xuezhong	PS 567	381
Liu, Xuezhong	PS 566	380
Liu, Xue	PS 883	588
Liu, Xue	PS 128	80
Liu, Dingding	PS 586	391
Liu, Zhiqi	PS 578	387
Liu, Huizhan	PS 132	82
Liu, Ji	PS 635	419
Liu, Hong	PS 592	395
Liu, Liqian	PS 884	588
Liu, Xiaopeng	PS 633	418
Liu, Huizhan	PS 113	71
Liu, Xiao	PS 932	347
Liu, Yanju	PS 613	407
Liu, Lijie	PS 903	601
Liu, Wenwen	PS 494	340
Liu, Elizabeth	PD 46	161
Liu, Xue	PS 125	78
Llano, Daniel	PS 457	320
Llinas, Rodolfo	PS 25	23
Llorach, Gerard	PS 862	577
Lobarinas, Edward	PS 197	118
Lock, Christopher	PD 58	293
Logiadis, Miltos	PS 522	356

Name	Abstract No.	Page No.
LoGrasso, Philip	PS 354	237
Lohse, Michael	PS 435	280
Lomber, Stephen	SYMP 2	1
Lomber, Stephen	PD 126	476
Lomber, Stephen	PS 637	420
Lombroso, Adam	PD 5	6
Long, Joseph	PS 600	400
Long, Haishan	PS 589	393
Long, Haishan	PS 151	93
Long, Laura	PS 365	242
Longenecker, Ryan	PS 412	2658
Longenecker, Ryan	PS 877	585
Longenecker, Ryan	PS 529	360
Longworth-Mills, Emma	PS 87	56
Loomis, Benjamin	PS 884	588
LOPEZ, Alejandra	PS 602	401
Lopez, Ivan	PD 39	156
Lopez, Ivan	PD 168	635
Lopez, Ivan	PD 99	455
Lopez, Ivan	PS 216	128
Lopez Ramirez, Omar	PS 564	379
López-Bascuas, Luís	PS 395	259
Lopez-Escamez, Jose Antonio	PD 95	452
Lopez-escamez, Jose	PS 109	68
Lopez-Poveda, Enrique	PS 287	200
Lopez-Poveda, Enrique	PS 79	52
Lopez-Poveda, Enrique	PS 395	259
Lopez-Poveda, Enrique	PS 241	175
Lorenzi, Christian	PS 393	258
Lorenzi, Christian	PS 389	256
Lorenzi, Christian	PS 765	520
Lorenzi, Christian	PS 708	488
Lorenzi, Christian	PS 387	255
Lorrain, Daniel	PS 609	405
Losonczy, Katalin G.	PD 167	635
Losorelli, Steven	PS 311	214
Losorelli, Steven	PS 716	493
Losorelli, Steven	PS 850	569
Lovett, Michael	PS 209	124
Lovett, Michael	PD 65	297
Löwenheim, Hubert	PS 931	503
Lowther, Jill	PS 43	34
Lowy, Michelle	PS 583	390
Lowy, Michelle	PS 597	398
Lu, Kai	PS 466	324
Lu, Jianzhong	PS 10	15
Lu, Jianzhong	PS 218	129
Lu, Hui-Ping	SYMP 59	460
Lu, Xiaowei	PS 106	66
Lu, Ling	PS 586	391
Lu, Ying-Chang	PS 565	380
Lu, Yong	PS 518	354
Lu, Ting	PS 517	353
Lu, Jianzhong	PS 896	596
Lundqvist, Gabriella	PD 101	456
Luo, Hao	PS 530	360
Luo, Hao	PD 18	143
Luo, Xin	SYMP 57	459

Author Index

Name	Abstract No.	Page No.
Luo, Jinhong	PS 923	266
Luo, Hao	PS 898	598
Luo, Xin	PS 285	199
Luo, Wenwei	PS 136	84
Luo, Ping	PS 84	563
Lupo, Eric	PS 15	17
Lupo, Eric	PS 35	29
Lush, Mark	PD 67	298
Lustig, Lawrence	PS 119	74
Lustig, Lawrence R.	PS 161	98
Lutz, Brendan	PS 432	279
Luu, Ngoc-Nhi	PS 226	133
Luu, Ngoc-Nhi	PS 890	592
Lynskey, Michelle	PS 106	66
Lyon, Richard	SYMP 31	300
Lysakowski, Anna	PD 95	452
Lysakowski, Anna	PS 911	606
Lysakowski, Anna	PS 544	368
Lyu, Ah-Ra	PS 691	479
Lyu, Ah-Ra	PS 757	516
Lyzwa, Dominika	PS 744	509
M. Richard, Elodie	PD 98	454
Ma, Qi	PS 567	381
Ma, Qi	PS 566	380
Macarov, Michal	PD 82	311
MacCoss, Michael	PS 737	505
MacDonald, Ewen	PS 664	434
MacDougall, Dan	PS 184	110
MacDougall, Hamish	PS 682	444
MacLeod, Angus	PD 58	293
MacLeod, Katrina	PS 44	34
Maddox, Ross	PS 291	203
Madsen, Sara M. K.	PS 386	254
Maftoon, Nima	PD 152	626
Maftoon, Nima	PD 155	628
Maftoon, Nima	PD 53	165
Magarinos, Marta	PS 755	515
Magnani, Christophe	PS 449	289
Mahajan, Chaitanya	PS 819	551
Mahendrasingam, Shanthini	PS 777	527
Mahrt, Elena	PS 201	120
Mahrt, Elena	PS 200	119
Mahrt, Elena	PS 382	252
Mahurkar, Anup	PD 79	310
Mahurkar, Anup	PD 81	311
Maier, Hannes	PS 34	28
Maier, Hannes	PS 188	113
Mair, Katharine	PS 764	520
Majdak, Piotr	PS 401	262
Makabe, Ayane	PS 336	227
Makabe, Ayane	PD 172	628
Makashay, Matthew J.	PS 417	270
Makishima, Tomoko	PS 908	604
Malagu, Karine	PD 58	293
Malgrange, Brigitte	PD 165	634
Malinowska, Urszula	PS 702	485
Malinowski, Sebastian	PS 374	247
Malinski, Peter	PS 375	248

Name	Abstract No.	Page No.
Mallon, Ann-Marie	PS 320	218
Mamach, Martin	PS 310	213
Mamelle, Elisabeth	PS 28	25
Mamelle, Elisabeth	PS 348	233
Mammano, Fabio	PS 134	83
Mancini, Martina	PD 92	451
Manganella, Juliana	PS 314	215
Manheim, Maayan	PD 123	474
Manohar, Senthilvelan	PS 860	575
Manohar, Senthilvelan	PS 548	371
Manohar, Senthilvelan	PD 57	292
Manohar, Senthilvelan	PD 21	145
Manta, Bruno	PD 98	454
Manzari, Leonardo	PS 682	444
Manzini, Chiara	PRES SYMP 3	1
Marchán, Sandra	PD 147	623
Marcotti, Walter	PS 688	478
Marcotti, Walter	PS 549	371
Marcotti, Walter	PS 134	83
Marcotti, Walter	PS 333	225
Marcotti, Walter	PS 332	225
Marcotti, Walter	PS 334	226
Marcotti, Walter	PS 538	365
Margulies, Zachary	PD 60	294
Margulies, Zachary	PS 96	61
Marie, Aurore	PS 904	601
Mariotti Roggia, Simone	PS 490	337
Markatos, Nikolaos	PS 522	356
Marks, Kendra	PS 900	599
Marozeau, Jeremy	PS 698	483
Marquardt, Torsten	PS 497	341
Marrone, Nicole	PS 304	210
Marroquin Cortez, Roberto Enrique	PS 842	565
Marrufo-Pérez, Miriam	PS 79	52
Marrufo-Pérez, Miriam	PS 395	259
Martel, David	PS 900	599
Martel, David	PS 899	598
Martel, David	PD 19	144
Martel, David	PD 17	142
Martelletti, Elisa	PD 97	454
Martin, Donna	PD 69	299
Martin, Catherine	PS 608	404
Martin, Catherine	PS 921	611
Martin, Donna	PD 38	156
Martinelli, Giorgio P.	PS 675	440
Martinelli, Giorgio P.	PS 676	441
Martinez, Gary	PS 822	553
Martin-Sierra, Carmen	PD 95	452
Martz, Ashlee	PS 5	11
Maruyama, Ayako	PS 336	227
Marx, Mahieu	PS 652	427
Masi, Ryan	PS 51	38
Masino, Mark	PS 793	535
Masino, Aaron	PS 314	215
Masmoudi, Saber	PS 128	80
Mason, Christine	PS 865	579
Mason, Christine	PS 863	578
Mast, Fred	SYMP 39	303

Author Index

Name	Abstract No.	Page No.
Masud, Salwa	PS 617	409
Masud, Salwa F	PS 191	114
Matern, Maggie	PS 112	70
Matern, Maggie	PS 328	222
Mathers, Peter	PS 759	517
Mathew, Rajeev	PS 726	498
Mathew, Rajeev	SYMP 54	317
Mathur, Pranave	PS 141	87
Matsui, Toshiyasu	PS 526	358
Matsunobu, Takeshi	PS 526	358
Matthews, Jamie	PS 63	417
Matthews, Lois	PS 131	81
Mattingly, Jameson	PS 839	563
Mattingly, Michelle	PS 628	415
Mattison, Scott	PS 621	411
Mattley, Jane	PD 106	464
Matysiak, Artur	PS 638	421
Maulden, Amanda	PS 198	118
Maurits, Natasha	SYMP 61	461
Maxeiner, Stephan	PS 533	362
May, Patrick	PS 256	182
May, Lindsey	PS 347	233
May, Lindsey	PD 150	625
May, Lindsey	SYMP 45	304
May, Tobias	PS 413	269
May, Lindsey	PS 349	234
Mays, Joseph	PD 32	152
Mays, Joseph	PS 747	511
Mays, Joseph	PS 748	511
Mc Laughlin, Myles	PS 289	202
McAlpine, David	PS 470	327
McAlpine, David	SYMP 54	317
McAlpine, David	PS 64	421
McAlpine, David	PS 270	190
McAlpine, David	PS 398	260
McAlpine, David	PS 826	555
McAlpine, David	PS 385	253
McAndrew, Rachele	PS 397	260
McCall, Andrew	PS 681	443
McCarthy, Kathleen	PS 764	520
McCreery, Ryan	PS 762	519
McCullagh, Elizabeth McCullagh	PS 738	506
McDermott, Josh	PS 870	581
McDermott, Josh	PS 871	582
McDermott, Josh	PS 480	332
McDermott, Josh	PS 391	257
McDermott, Josh	PS 260	184
McDermott, Josh	PD 137	618
McDermott, Brian	PS 135	84
McDermott, Josh	PS 468	325
McDermott, Josh	PS 642	422
McDermott, Josh	PS 864	578
McDermott, Josh	PS 641	422
McDermott, Josh	SYMP 8	150
McDermott, Brian	PS 542	367
McDermott, Josh	PD 30	149
McDermott, Josh	PS 868	580
McDermott, Brian	PS 772	524

Name	Abstract No.	Page No.
McDowell, Malerie	PS 317	217
McGarvie, Leigh	PS 682	444
McGee, JoAnn	PD 151	626
McGovern, Melissa	PS 206	122
McInturff, Stephen	PS 600	400
McInturff, Stephen	PS 754	515
McIntyre, Kaitlin	PS 224	131
McIntyre, Kaitlin	PS 225	132
McKenna, Charles	PD 3	149
McKenna, Michael	PS 823	553
McKenna Benoit, Margo	PD 120	472
McKhann, Guy	PS 730	501
McKhann, Guy	PS 365	242
McLaughlin, Kylie	PS 598	399
McMahon, Catherine	PS 718	494
McMillan, Garnett	PS 579	387
McMurray, Mark	PS 96	61
McPherson, Malinda	PS 391	257
McWalter, Richard	PS 870	581
Meas, Steven	PS 892	593
Meaud, Julien	PD 47	161
Meaud, Julien	PS 171	103
Meenderink, Sebastiaan	PS 767	522
Meenderink, Sebastiaan	PS 780	529
Meenderink, Sebastiaan	PS 195	117
Meenderink, Sebastiaan	PS 781	529
Mehraei, Golbarg	PD 142	621
Mehta, Ashesh	PD 143	621
Mehta, Anahita	SYMP 49	314
Mehta, Preeti	PS 373	247
Mehta, Ashesh	PS 730	501
Mehta, Ashesh	PS 365	242
Mei, Ling	PD 104	457
Mei, Ling	PD 115	468
Mellon, Nancy	SYMP 69	463
Mellott, Jeffrey	PS 831	558
Mellott, Jeffrey	PS 832	559
Menardo, Julien	PS 356	238
Meneses, Zaimary	PS 581	388
Meng, Xiangying	PS 636	420
Meng, Xiangying	PS 635	419
Mercer, Evan	PS 588	392
Meredith, Frances	PS 910	605
Meredith, Frances	PD 42	158
Meredith, M Alex	SYMP 2	168
Meredith, Andrea	PS 547	370
Meredith, Meg	PS 272	191
Mergia, Evanthia	PS 582	389
Mertens, Griet	PS 926	201
Mescher, Mark	PS 821	552
Mesgarani, Nima	PD 143	621
Mesgarani, Nima	PS 730	501
Mesgarani, Nima	PS 475	329
Mesgarani, Nima	PS 365	242
Metherate, Raju	SYMP 35	302
Metzner, Walter	PS 913	607
Meyer, Arne	PS 436	281
Meyer, Lauren	PD 116	469

Author Index

Name	Abstract No.	Page No.
Mezzogori, Daniele	PS 933	395
Mi, Xiaoxiao	PS 220	130
Mi, Jing	PS 366	243
Michanski, Susann	PS 545	369
Michel, Vincent	PD 72	306
Michel, Stephen	PD 101	456
Middelink, Leonie	PS 810	545
Middleton, Jason	PS 253	181
Milan, Gabriella	PD 165	634
Milazzo, Mario	PS 841	564
Milazzo, Mario	PD 153	627
Milenkovic, Ivan	PS 513	94
Milenkovic, Ivan	PS 516	96
Milewski, Andrew	PS 785	531
Milinkeviciute, Giedre	PS 510	349
Millar, Jennifer	PS 447	287
Millar, Jennifer	PD 46	161
Miller, Christopher	PS 811	546
Miller, Derek	PS 681	443
Miller, Jeff	PS 314	215
Mills, Dawna	PS 15	17
Mills, Dawna	PS 35	29
Mills, Jason	PS 110	69
Milner, Rafal	PS 78	52
Milon, Beatrice	PS 112	70
Milon, Beatrice	PS 328	222
Milon, Beatrice	PS 347	233
Milon, Beatrice	PS 96	61
Milon, Beatrice	PD 79	310
Milon, Beatrice	PD 81	311
Milon, Beatrice	PD 60	294
Min, Jaeki	PD 55	291
Minoda, Ryosei	PS 90	58
Minowa, Osamu	PS 694	481
Mirghorbani, S.M	PS 891	592
Mirghorbani, S.M	PS 930	596
Mirkin, Michael	PS 25	23
Mishkin, Mortimer	PD 28	148
Misurelli, Sara	PS 866	579
Misurelli, Sara	PS 13	16
MITARIU, Philipp	PS 799	539
Mitchell, Diana	PS 917	609
Mitchell, Diana	PS 672	438
Mitra, Sunayana	PS 96	61
Mitra, Sunayana	PD 60	294
Mittal, Rahul	PS 126	78
Mittal, Rahul	PS 127	79
Mittal, Rahul	PS 567	381
Mittal, Rahul	PS 566	380
Mittal, Rahul	PS 883	588
Mittal, Rahul	PS 128	80
Mittal, Jeenu	PS 605	403
Mittal, Jeenu	PS 351	235
Mittal, Jeenu	PS 809	545
Mittal, Rahul	PS 125	78
Miwa, Toru	PD 163	633
Miwa, Toru	PS 90	58
Miyagi, Masaru	PD 58	293

Name	Abstract No.	Page No.
Miyoshi, Takushi	PD 84	313
Mizutari, Kunio	PS 526	358
Mjaatvedt, Corey	PS 491	338
Mller, Chris	PS 234	137
Mlynarski, Wiktor	PS 468	325
Mlynarski, Wiktor	PS 642	422
Moberly, Aaron	PS 361	240
Moberly, Aaron	PS 6006	403
Möbius, Wiebke	PS 261	185
Mock, Jeffrey	PD 91	450
Moglie, Marcelo	PS 532	361
Möhrle, Dorit	PD 20	144
Möhrle, Dorit	PS 582	389
Moleti, Arturo	PS 83	54
Molloy, Katharine	PS 705	487
Molnar, Zoltan	PD 106	464
Mombrun, Adrien	PS 799	539
Monaco, Anthony	PD 106	464
Monaghan, Jessica	PS 718	494
Monaghan, Jessica	PS 64	45
Monaghan, Jessica	PS 385	253
Monge Naldi, Arianne	PS 226	133
Monroe, Jerry D.	PS 596	397
Monson, Brian	PD 139	619
Montagne, Christopher	PD 89	449
Montagne, Christopher	PS 397	260
Montejo, Noelia	PS 904	601
Montgomery, Johanna	SYMP 25	171
Monzack, Elyssa	SYMP 45	304
Moody, Sally	PRES SYMP 3	1
Moore, David	PS 855	572
Moore, David	PS 856	573
Moore, Brian C.J.	PS 393	258
Moore, Travis	PD 86	447
Moore, David	PD 122	473
Moore, Brian C.J.	PS 386	254
Moore, Sharlen	PS 261	185
Mora, Emanuel C.	PS 73	50
Moran, Nicholas	PS 458	320
Morehead, Michael	PS 301	209
Morell, Robert	PD 32	152
Morell, Robert	PS 347	233
Morell, Robert	PS 749	512
Morell, Robert	PS 349	234
Morell, Robert	PS 216	128
Morfouace, Marie	PD 55	291
Morgan, Anna	PS 124	77
Morgan, Anna	PS 121	75
Morgan, Anna	PS 686	477
Morgan, Anna	PS 120	74
Morimoto, Takashi	PS 295	205
Morozko, Eva L.	PS 770	523
Morril, Samantha	PS 197	118
Morton, Cynthia	PS 690	479
Moser, Tobias	PS 614	407
Moser, Tobias	PS 550	372
Moser, Tobias	PD 76	308
Moser, Tobias	PS 545	369

Author Index

Name	Abstract No.	Page No.
Moss, Cynthia	PS 923	266
Moss, Cynthia	PS 364	242
Mostaert, Brian	PS 504	345
Mostaert, Brian	PS 505	346
Motallebzadeh, Hamid	PS 172	104
Moteki, Hideaki	PS 139	86
Moua, Keng	PS 651	427
Moudgalya, Sanketh S	PS 822	553
Moulin, Annie	PS 420	272
Mowery, Todd	SYMP 5	2
Mrozek, Janna Henrike	PS 70	48
Muca, Antonela	PS 802	541
Muca, Antonela	PD 15	141
Mueller, Rashmi	PD 138	618
Mugridge, Kenneth	PS 813	547
Mujeeb, Mosaheb	PS 909	604
Mukherjea, Debashree	PS 583	390
Mukherjea, Debashree	PS 597	398
Mukherjea, Debashree	PS 603	402
Mulavara, Ajitkumar	PS 234	137
Mulford, Debora	PS 56	40
Mulhern, Tj	PS 618	409
Mulhern, Tj	SYMP 44	304
Müller, Marcus	PS 810	545
Müller, Maria Katharina	PS 516	352
Müller, Marcus	PS 931	503
Mulvaney, Joanna	PD 35	154
Mulvany, Jessica	PD 148	624
Muniak, Michael	PS 510	349
Munnamalai, Vidhya	PS 98	62
Munneke, Allyson	PS 692	480
Munro, Kevin	PS 646	424
Munro, Kevin	PS 525	358
Murillo-Cuesta, Silvia	PD 147	623
Musacchia, Gabriella	PS 716	493
Musiek, Frank	PS 710	490
Muskett, Julie	PD 94	452
Mustain, William	PS 59	42
Mustain, William	PS 920	611
Mustapha, Mirna	PS 266	188
N. Gladishev, Vadim	PD 98	454
N. Khan, Shaheen	PD 96	453
Nadol, Joseph	PS 308	212
Nadol, Joseph	PS 306	211
Nadol, Joseph	PS 24	22
Nakagawa, Takayuki	PS 506	347
Nakagawa, Takayuki	PS 796	537
Nakagawa, Takayuki	PS 753	514
Nakajima, Hideko	PS 620	410
Nakajima, Hideko	PS 615	408
Nakajima, Hideko	PS 617	409
Nakajima, Hideko	PS 191	114
Nakanishi, Hiroshi	PD 94	452
Nakmali, Don	PD 158	630
Nakmali, Don	PS 179	108
Nakmali, Don	PS 180	108
Nam, Hui	PS 164	100
Nam, Jong-Hoon	PS 166	101

Name	Abstract No.	Page No.
Nam, Jong-Hoon	PS 165	100
Nance, Grace	PS 311	214
Nankali, Amir	PD 54	165
Nankali, Amir	PS 174	105
Naples, James	PS 794	536
Narasimhan, Shreya	PS 502	344
Narasimhan, Shreya	PS 727	499
Narins, Peter	PS 195	499
Narui, Yoshie	PS 784	531
Navaratnam, Dhasakumar	PS 345	232
Navaratnam, Dhasakumar	PS 689	478
Navaratnam, Dhasakumar	PS 337	227
Nave, Klaus-Armin	PS 261	228
Nayagam, Bryony	PS 894	594
Nayak, Neil	PS 820	551
Neal, Christopher	PS 901	599
Neef, Jakob	PD 76	308
Neely, Stephen	PS 85	569
Neely, Stephen	PS 617	409
Neely, Stephen	PS 267	188
Neil, Jeffrey	PD 139	619
Nelson, Lacey	PD 39	156
Nelson, Greg	PS 529	360
Nelson, Rick	PS 795	536
Nelson, Megan	PS 158	97
Nelson-Brantley, Jennifer	PS 901	599
Nemes, Peter	PRES SYMP 3	1
Nemet, Ina	PD 58	293
Nerlich, Jana	PS 513	351
Neubauer, Heinrich	PS 638	421
Neumann, William	PS 801	540
Nevue, Alexander	PS 828	556
Newlands, Shawn	PS 56	40
Newman, Rochelle	PS 424	274
Newman, Tracey	PS 434	280
Nguyen, Laurent	PD 165	634
Nguyen, Yann	PS 41	32
Nguyen, Kim	PD 3	5
Nguyen, Yann	PS 28	25
Nguyen, Yann	PS 348	233
Nguyen, Matthew	PS 748	511
Ni, Kun	PD 20	144
Ni, Wenli	PS 205	122
Ni, Guangjian	PD 49	163
Nicol, Trent	PS 428	277
Nicol, Trent	PD 9	138
Nie, Kaibao	PS 445	286
Nie, Jing	PS 87	56
Nie, Jing	PS 88	57
Niemczura, Alexandra	PS 411	267
Niemczura, Alexandra	PS 412	268
Nieratschker, Michael	PD 6	6
Nies, Florian	PS 129	80
Nieto-Diego, Javier	PS 440	283
Nikkhou Aski, Sahar	PS 800	539
Ning, Ruijing	PS 854	572
Ninoyu, Yuzuru	PD 84	313
Nishimura, Koji	PS 95	61

Author Index

Name	Abstract No.	Page No.
Nishimura, Masataka	PS 459	321
Nishimura, Tadashi	PS 148	91
Nishimura, Koji	PS 892	593
Niu, Zhijie	PS 125	78
Niwa, Mamiko	PS 536	364
Niwa, Katsuki	PS 526	358
Niwa, Mamiko	PS 533	362
Noble, William	PS 737	505
Noble, Kenyaria	PS 491	338
Noble, Kenyaria	PS 321	218
Noda, Tetsuo	PS 694	481
Noda, Teppei	PS 95	61
Noda, Teppei	PS 892	593
Nodal, Fernando	PD 26	147
Nodal, Fernando	PS 469	326
Noftz, William	PS 831	558
Nogueira, Waldo	PS 287	200
Nogueira, Waldo	PS 26	23
Noh, Tae-Soo	PS 814	548
Noij, Kimberley	PS 450	289
Noij, Kimberley	PS 451	290
Nolan, Lisa	PS 131	81
Noon, Sarah	PS 110	69
Nordmark, Jonatan	PS 254	182
Norena, Arnaud	PS 904	601
Norman-Haignere, Samuel	PS 480	332
Norman-Haignere, Samuel	PS 260	184
Norman-Haignere, Samuel	PD 137	618
Northrop, Amy	PS 600	400
Norton, Susan	PS 272	191
Nourski, Kirill	PD 136	617
Nourski, Kirill	PD 138	618
Nourski, Kirill	PS 713	491
Nourski, Kirill	PS 476	330
Nouvian, Régis	PS 485	331
Nouvian, Régis	PS 356	238
Nowack, Amy	PS 445	286
Nowotny, Manuela	PS 576	386
Nowotny, Manuela	PS 895	595
Nuttall, Alfred L	PS 358	239
Nuttall, Alfred L	PS 787	532
Nuttall, Alfred L	PS 788	533
O Maoileidigh, Daibhid	PS 785	531
O Maoileidigh, Daibhid	PS 713	491
O'Brien, Gabrielle	PD 134	616
O'brien, Daniel	PS 32	27
O'Brien, Gabrielle	PD 88	448
O'Connor, Dara	PD 35	154
O'Driscoll, Martin	PS 297	206
O'Rielly, Darren	PS 116	72
O'Sullivan, James	PS 730	501
O'Sullivan, Mary	PD 146	622
O'toole, Christopher	PS 605	403
O'toole, Christopher	PS 351	235
O'toole, Christopher	PS 809	545
Ocelli, Florian	PS 697	483
Oertel, Donata	PS 508	348
Oetjen, Henning	PS 199	119

Name	Abstract No.	Page No.
Ogawa, Yoko	PS 112	70
Ogawa, Kaoru	PS 90	599
Oghalai, John	PS 571	383
Oghalai, John	PS 168	102
Oghalai, John	PS 621	411
Oghalai, John	PS 177	107
Oghalai, John	PS 162	99
Oh, Yonghee	PS 283	198
Oh, Jeong-Hoon	PS 844	566
Oh, Yonghee	PS 371	246
Oh, Soohee	SYMP 60	460
Ohlemiller, Kevin	PD 117	470
Ohlemiller, Kevin	PS 80	53
Ohlemiller, Kevin	PD 62	295
Ohn, Tzu-Lun	PS 550	372
Ohn, Tzu-Lun	PD 76	308
Ohyama, Takahiro	PD 163	633
Oikonomou, Katerina	PD 39	156
Oizumi, Masafumi	PS 437	281
Okabe, Masataka	PS 846	567
Okamoto, Yasuhide	PS 295	205
Okano, Takayuki	PS 752	513
Okano, Takayuki	PS 102	64
Okano, Hideyuki	PS 90	58
Okayasu, Tadao	PS 148	91
Okland, Tyler	PS 839	563
Oldak, Monika	PS 129	80
Oline, Stephan	PS 509	348
Oliveira, Carlos	PS 149	91
Oliver, Douglas	PS 290	202
Oliver, Dominik	PS 343	231
Olley, Dustin	PD 81	311
Olson, Elizabeth	PS 576	286
Olson, Elizabeth	PD 153	627
Olaszewski, Rafal	PS 766	67
Olaszewski, Rafal	PS 216	128
Olt, Jennifer	PS 538	365
Olthof-Bakker, Bas	PS 744	509
Omori, Koichi	PS 752	513
Omori, Koichi	PS 796	537
Omori, Koichi	PS 753	514
Ono, Kazuya	PS 99	63
Ono, Kazuya	PS 778	527
Oostrik, Jaap	PS 117	73
Orlando, Mark	PD 120	472
Orlando, Mark	PS 56	40
Ornitz, David	PS 100	63
Ortmann, Amanda	PS 82	54
Orvis, Joshua	PD 81	311
Otero-Millan, Jorge	PS 683	444
Otsuka, Sho	PS 294	205
Ott, Sandra	PD 79	310
Ouwehand, Krista	PD 58	293
Ouyang, Jing	PS 819	551
Overath, Tobias	PD 140	619
Owens, Andrew	PD 58	293
Oxenham, Andrew	SYMP 49	314
Oxenham, Andrew	PD 134	616

Author Index

Name	Abstract No.	Page No.
Oya, Hiroyuki	PD 136	617
Ozdamar, Ozcan	PS 664	434
Ozieblo, Dominika	PS 129	80
Pace, Edward	PS 530	360
Pace, Edward	PD 18	143
Paciello, Fabiola	PS 160	98
Paciello, Fabiola	PS 933	395
Padilla, Monica	PS 15	17
Padilla, Monica	PS 35	29
Padilla, Monica	PS 30	26
Padilla, Monica	PS 37	30
Paik, Joon	PD 140	619
Pak, Natalie	PS 655	429
Pak, Jhang Ho	PS 790	534
Pak, Kwang	PS 843	565
Pak, Rebecca	PD 46	161
Palczewski, Krzysztof	PD 58	293
Palermo, Adam	PD 32	152
Palermo, Adam	PD 31	152
Palermo, Adam	PS 748	511
Palmer, Joanne	PS 810	545
Palmer, Alan	PS 454	318
Paludetti, Gaetano	PS 160	98
Paludetti, Gaetano	PS 933	395
Palumbo, Devon	PS 311	214
Pan, Bifeng	SYMP 21	169
Pan, Bifeng	PD 1	3
Pan, Huilin	PS 678	442
Pan, Bifeng	PS 139	86
Pan, Bifeng	PS 803	541
Panackal, Anil	PS 61	43
Panekkad, Ajay	PS 530	360
Panganiban, Clarisse	PS 492	338
Panganiban, Clarisse	PS 491	338
Panniello, Mariangela	PS 460	321
Papadelis, George	PS 522	356
Papathanasiou, Ilias	PS 522	356
Papesh, Melissa	PD 90	449
Pappa, Andrew	PS 175	105
Papsin, Blake	PS 851	570
Papsin, Blake	PS 709	489
Paquette, Stephen	PD 66	297
Paquette, Stephen	PS 145	89
Paquette, Stephen	PS 604	402
Paradiso, Kenneth	PS 372	246
Paraouty, Nihaad	PS 387	255
Pararas, Erin	PS 618	409
Pararas, Erin	SYMP 42	303
Pararas, Erin	PS 821	552
Pararas, Erin	PS 823	553
Parham, Kourosh	PS 794	536
Parida, Satyabrata	PS 488	336
Paris, Francesca	PS 192	115
Park, Shi-Nae	PS 528	359
Park, Sungjin	PS 570	383
Park, Yong-Ho	PS 691	479
Park, Chul Won	PS 845	567
Park, Hyo-Jin	PD 57	292

Name	Abstract No.	Page No.
Park, Shi-Nae	PS 696	482
Park, Sohyeon	PS 677	441
Park, Moo Kyun	PS 677	441
Park, Jung-sub	PS 557	375
Park, Hyo-Jin	PS 581	388
Park, Hyo-Jin	PS 152	93
Park, Jungeun	PS 223	131
Park, Shi-Nae	PS 818	550
Park, Yong-Ho	PS 757	516
Park, Ji Hun	PS 814	548
Park, Yoon Ah	PS 574	385
Parker, Dennis	PS 906	603
Parker, Andrew	PS 768	522
Parker, Andrew	PS 320	218
Parkinson, Wendy	PD 134	616
Parkinson, Wendy	PS 33	28
Parthasarathy, Aravindakshan	PS 8	13
Parthasarathy, Aravindakshan	PS 293	204
Parthasarathy, Aravindakshan	PS 9	14
Parthasarathy, Aravindakshan	PS 238	173
Pasos, Julio	PS 916	608
Pasquet, Matthieu	PS 441	284
Pastras, Christopher	PS 907	603
Pastras, Christopher	PS 575	385
Patel, Sally	PS 604	402
Patel, Meet	PS 544	368
Patel, Aashutos	PS 544	368
Patel, Seema	PD 94	452
Patel, Prachi	PS 365	242
Pater, Justin	PS 116	72
Paublete, Rocio	PS 557	375
Paul, Brandon	PS 47	36
Pauliin, Michael	PS 914	607
Pavlopoulos, Vasilios	PS 522	356
Pawley, Devon	PS 820	551
Pawlowski, Karen	PD 105	457
Payne, Shelby	PD 62	295
Peak, Allison	PS 223	131
Pearson, Selina	PS 330	223
Pechriggl, Elisabeth	PS 758	516
Pecka, Michael	PS 520	355
Pedersen, Ellen Raben	PD 118	470
Peguero, Braulio	PS 316	216
Pei, Wuhong	PS 927	595
Pei, Wuhong	PS 880	586
Pelusso, Constanza	PS 224	131
Pelusso, Constanza	PS 225	132
Pelusso, Constanza	PD 174	639
Pena, Jose Luis	PS 67	46
Peng, Sun	PS 584	390
Peng, Shu-Chen	SYMP 59	460
Peng, Tao	PS 883	588
Peng, Bo	PS 265	187
Peng, Anthony	PS 775	526
Peng, Anthony	PS 783	530
Peng, Anthony	PS 335	226
Penney, Cindy	PS 116	72
Pennington, Jeff	PS 314	215

Author Index

Name	Abstract No.	Page No.
Peppi, Marcello	PS 821	552
Peppi, Marcello	PS 823	553
Perdew, Audrey	PS 855	572
Perdew, Audrey	PS 856	573
Perdew, Audrey	PD 122	473
Pereira, Fred	PS 692	480
Perera, Anoja	PS 223	131
Perez, Adela	PD 146	622
Perez Fornos, Angelica	PS 446	287
Perez Fornos, Angelica	PS 444	285
Perez Fornos, Angelica	PS 493	339
Perez-Pinera, Pablo	SYMP 18	168
Perkel, David	PS 828	556
Perkel, David	PS 829	557
Perkel, David	PS 830	557
Perkins, Guy	PS 544	368
Perrin, Benjamin	PS 782	530
Petelski, Aleksandra	PD 164	633
Peters, Brian	PS 234	137
Petersen, Bjørn	PD 118	470
Peterson, Stephanie	PS 891	592
Peterson, Stephanie	PS 930	596
Peterson, Diana	PD 16	142
Peterson, Joy	PS 314	215
Petit, Christine	PD 72	306
Petkovic, Vesna	PS 797	537
Petralia, Ronald	PS 770	523
Petremann, Mathieu	PS 441	284
Petremann, Mathieu	PD 170	636
Petremann, Mathieu	PS 792	535
Petrillo, Marco	PS 890	592
Péus, Dominik	PS 192	115
Peusner, Kenna	PS 671	438
Pfannenschmidt, Sarah	PS 692	480
Pfiffner, Flurin	PS 721	496
Pfiffner, Flurin	PS 192	115
Pfingst, Bryan	PS 725	498
Pfingst, Bryan E.	SYMP 14	167
Phatak, Sandeep	PD 11	139
Phillips, James	PS 445	286
Phillips, Christopher	PS 445	286
Picher, Magdalena	PS 550	372
Pickett, Sarah	PS 140	87
Pidhorskyi, Stansilav	PS 301	209
Piehl, Warren	PS 445	286
Pienkowski, Martin	PS 527	359
Pierce, Marsha	PS 114	71
Pierce, Marsha	PS 115	72
Pierstorff, Erik	PS 811	546
Pietrus-Rajman, Alexander	PS 531	361
Pietsch, Markus	PS 577	386
Pillsbury, Harold	PS 175	105
Pillsbury, Harold	PS 786	532
Pineros, Jennifer	PS 798	538
Pinto-Patarroyo, Gineth	PD 94	452
Piotrowski, Tatjana	PS 223	131
Piotrowski, Tatjana	PD 67	298
Piotrowski, Tatjana	PS 223	131

Name	Abstract No.	Page No.
Pirvola, Ulla	PS 593	395
Plack, Christopher	PS 646	424
Plack, Christopher	PS 150	92
Plack, Christopher	PS 268	189
Plack, Christopher	PS 525	358
Plenz, Dietmar	PS 461	322
Plewczynski, Dariusz	PS 129	80
Plontke, Stefan	PS 813	547
Ploski, Rafal	PS 129	80
Plummer, Melissa		
Poeppel, David	PS 718	494
Polishchuk, Roman	PS 134	83
Pollak, Agnieszka	PS 129	80
Polley, Daniel	PS 849	569
Polley, Daniel	PS 631	417
Polley, Daniel	PD 125	475
Polley, Daniel	PD 25	146
Polley, Daniel	PS 293	204
Polley, Daniel	PS 455	319
Polley, Daniel	PS 852	571
Polley, Daniel	PS 626	414
Pollock, Lana	PS 772	524
Polonenko, Melissa	PS 851	570
Pomper, Ulrich	PS 699	484
Ponnath, Abhilash	PD 1	3
Ponnath, Abhilash	PS 807	543
Pontoppidan, Niels	PS 241	175
Poon, Michael	PS 609	405
Poppi, Lauren	PD 41	158
Portfors, Christine	PS 201	120
Portfors, Christine	PS 200	119
Portfors, Christine	PS 828	556
Portfors, Christine	PS 829	557
Portfors, Christine	PS 830	557
Portfors, Christine	PS 381	251
Portfors, Christine	PS 382	251
Pousson, Monique	PS 288	201
Prajapati, Meenakshi	PD 162	632
Pramanik, Gopal	PS 266	188
Prasad, Sonal	PS 776	526
Prasit, Peppi	PS 609	405
Predham, Sarah	PS 116	72
Prendergast, Garreth	PS 646	424
Prendergast, Garreth	PS 268	189
Prendergast, Garreth	PS 525	358
Prentiss, Sandra	PS 414	269
Presacco, Alessandro	PS 421	273
Presacco, Alessandro	PS 236	172
Pressnitzer, Daniel	PS 861	577
Price, Steven	PD 95	452
Price, Steven	PS 537	364
Price, Steven	PS 911	606
Prieskorn, Diane	PS 158	97
Prieve, Beth	PS 46	35
Prieve, Beth	PS 74	50
Probst, Rudolf	PS 75	51
Prochazka, Lukas	PS 192	115
Pross, Seth	PS 58	41

Author Index

Name	Abstract No.	Page No.
Prosser, Haydn	PS 114	71
Prosser, Haydn	PS 115	72
Puel, Jean-Luc	PS 697	483
Puel, Jean-Luc	PS 485	334
Puel, Jean-Luc	PS 271	191
Puel, Jean-Luc	PS 775	526
Puel, Jean-Luc	PS 356	238
Pujol, Remy	PS 214	126
Pulkki, Ville	PS 1	9
Pullar, Kiri	PS 914	607
Purcell, David	PD 107	464
Puria, Sunil	PS 167	101
Puria, Sunil	PD 75	307
Puria, Sunil	PS 186	111
Puria, Sunil	PS 177	107
Puria, Sunil	PD 157	96
Puria, Sunil	PD 53	165
Puria, Sunil	PS 172	104
Purnell, Tom	PS 320	218
Puvvada, Krishna	PS 473	328
Pyakurel, Umesh	PS 886	589
Pyakurel, Umesh	PD 63	296
Pyott, Sonja J.	PS 547	370
Pyott, Sonja J.	PS 531	361
Qamar, Raheel	PS 117	73
Qi, Jieyu	PS 586	391
Qi, Tangkai	PS 858	574
Qian, Jiang	PS 759	517
Qian, Xiao-Qing	PD 169	636
Qian, Fuping	PS 586	391
Qian, Xiaoyun	PS 586	391
Qian, Fuping	PS 585	391
Qin, Litao	PS 126	78
Qiu, Wanzhi	PS 894	594
Quesnel, Alicia M	PS 24	22
Quiñones, Patricia	PS 767	522
Quiñones, Patricia	PS 780	529
Quiñones, Patricia	PS 195	117
Quiñones, Patricia	PS 781	529
Quittner, Alexandra	SYMP 62	461
Quittner, Alexandra	PS 22	200
Quraishe, Shmma	PS 434	280
Rabbitt, Richard	PS 906	603
Rabbitt, Richard	PS 622	412
Rabbitt, Richard	PS 143	88
Rabbitt, Richard	PD 77	308
Radecke, Jan-Ole	PD 127	476
Radziwon, Kelly	PS 204	121
Radziwon, Kelly	PS 860	575
Radziwon, Kelly	PS 629	416
Radziwon, Kelly	PD 23	145
Raghu, Vishal	PS 548	371
Rahman, Irfan	PS 145	89
Rahman, Muhammad	PS 265	187
Raible, David	PD 103	65
Raible, David	PS 140	87
Raif, Kaan	PS 255	182
Rajaram, Ezhilarasan	PS 521	355

Name	Abstract No.	Page No.
Rajguru, Suhrud M.	PS 664	434
Rajguru, Suhrud M.	PS 915	608
Rajguru, Suhrud M.	PS 798	538
Rajguru, Suhrud M.	PS 675	440
Rajguru, Suhrud M.	PS 916	608
Rajguru, Suhrud M.	PS 676	441
Ramachandran, Ramnarayan	PS 588	392
Ramachandran, Ramnarayan	PS 591	394
Ramakers, Geerte	PS 724	497
Ramakrishna, Yugandhar	PS 548	371
Ramakrishna, Yugandhar	PS 539	365
Ramakrishnan, Neeliyath	PS 543	367
Ramekers, Dyan	PS 262	186
Ramekers, Dyan	PS 595	397
Ramekers, Dyan	PS 487	335
Ramkumar, Vickram	PS 583	390
Ramkumar, Vickram	PS 597	398
Ramkumar, Vickram	PS 603	402
Ranatunga, Kishani	PS 332	225
Randle, Michelle	PS 207	123
Ranieri, Maurizio	PS 446	287
Ranum, Paul	PS 122	76
Ranum, Paul	PS 805	542
Ranum, Paul	PS 139	86
Ranum, Paul	PS 113	71
Raphael, Yehoash	PS 350	235
Raphael, Yehoash	PS 483	333
Raphael, Patrick	PS 621	411
Raphael, Yehoash	PS 921	611
Raphael, Yehoash	PD 38	156
Raphael, Yehoash	SYMP 14	167
Raphael, Yehoash	PS 158	97
Rasetshwane, Daniel	PS 267	188
Rask-Andersen, Helge	SYMP 46	304
Ratay, Jessica	PD 94	452
Rathinam, Rajamani	PS 801	540
Ratnam, Rama	PS 21	21
Rauch, Steven	PS 226	133
Rauch, Steven	PS 450	289
Rauch, Steven	PS 451	290
Raufer, Stefan	PS 617	409
Raufer, Stefan	PS 191	114
Ravicz, Michael	PD 152	93
Ravicz, Michael	PD 155	95
Ravicz, Michael	PS 190	114
Ravicz, Michael	PS 194	116
Rawal, Shristi	PS 57	41
Ray, Shilajeet	PS 301	209
Razavi, Payam	PD 152	626
Razavi, Payam	PD 155	628
Rebscher, Stephen J.	PS 161	98
Recanzone, Gregg	PS 591	394
Recio-Spinoso, Alberto	PS 162	99
Recugnat, Matthieu	PS 270	190
Reed, Darrin	PS 401	262
Reed, Darrin	PS 701	485
Reeg, Hannah	PS 490	337
Rees, Adrian	PS 744	509

Author Index

Name	Abstract No.	Page No.
Reetzke, Rachel	PD 121	473
Rehman, Atteeq	PS 779	528
Rehman, Atteeq	PS 770	523
Reichenbach, Tobias	PS 292	203
Reichenbach, Tobias	PS 163	99
Reid, Kevin	PS 290	202
Reijntjes, Daniël O. J.	PS 547	370
Reijntjes, Daniel O. J.	PS 531	361
Reimann, Katrin	PS 582	389
Reiss, Lina	PS 283	198
Reiss, Lina	PS 371	246
Reiss, Lina	PS 499	342
Rekhi, Sohinder	PS 330	223
Relaño-Iborra, Helia	PS 413	269
Remenschneider, Aaron	PS 305	211
Remenschneider, Aaron	PD 154	627
Remenschneider, Aaron	PS 808	544
Remenschneider, Aaron	PS 837	562
Remis, Natalie	PS 687	477
Ren, Dong-Dong	PS 840	563
Ren, Tianying	PS 499	342
Ren, Dong-Dong	PD 169	636
Ren, Dong-Dong	PS 136	84
Ren, Liujie	PS 193	115
Ren, Liujie	PS 187	112
Ren, Tianying	PD 50	163
Renden, Robert	PS 741	507
Rennie, Katherine	PS 910	605
Rennie, Katherine	PD 42	158
Repa, Joyce	PD 105	457
Requena, Teresa	PD 95	452
Requena, Teresa	PS 109	68
Resnik, Jennifer	PD 125	475
Reuss, Stefan	PS 895	595
Reyes-Quintos, Ma. Rina	PS 130	81
Reyzer, Michelle	PS 321	218
Rhone, Ariane	PD 138	618
Rhone, Ariane	PS 713	491
Rhone, Ariane	PS 476	330
Riazuddin, Saima	PS 908	604
Riazuddin, Saima	PS 768	522
Riazuddin, Saima	PS 133	83
Riazuddin, Saima	PD 98	454
Riazuddin, Sheikh	PD 96	453
Ribas, Teresa	PD 108	465
Ricci, Anthony	PS 536	364
Ricci, Anthony	PD 75	307
Ricci, Anthony	PS 331	224
Ricci, Anthony	PD 74	307
Ricci, Anthony	PS 783	530
Ricci, Anthony	PD 146	622
Ricci, Anthony	PS 533	362
Rice, Darrian	PS 675	440
Rice, Darrian	PS 676	441
Richards, Virginia	PS 658	431
Richardson, Jason	PS 463	323
Richardson, Matthew	PS 523	356
Richardson, Matthew	PS 645	424

Name	Abstract No.	Page No.
Richardson, Guy	PD 149	624
Richter, Claus-Peter	PS 181	109
Richter, Claus-Peter	PS 39	31
Richter, Claus-Peter	PS 915	608
Richter, Claus-Peter	PS 38	30
Richter, Claus-Peter	PS 31	26
Richter, Claus-Peter	PS 146	90
Richter, Claus-Peter	PS 383	252
Richter, Claus-Peter	PS 32	27
Ridley, Courtney	PS 267	188
Riegel-Betz, Ann-Kathrin	PS 396	259
Riffel, Celia	PS 242	176
Riggle, Mark	PS 408	265
Riggle, Mark	PS 363	241
Riggs, W. Jason	PS 361	240
Riggs, W. Jason	PS 6006	403
Rigo, Frank	PD 1	3
Rigo, Frank	PD 2	4
Rigo, Frank	PS 807	543
Rincon, Samantha	PS 916	608
Rinzel, John	PS 289	202
Riordan, Gavin P.	PS 770	523
Risch, Neil	PS 119	74
Rissone, Alberto	PS 927	595
Ritaccio, Anthony	PD 137	618
Ritzl, Eva	PS 58	41
Rivero, Francisco	PD 71	305
Rivolta, Marcelo	PS 496	341
Riyahi-Alam, Sadegh	PS 307	212
Robbins, Carol	PS 316	216
Roberts, Michael	PS 375	248
Roberts, Larry	PS 900	599
Roberts, Reagan	PS 31	26
Roberts, Larry	PS 47	36
Roberts, Terri	PS 332	225
Roberts, Dale	PS 683	444
Robertson, Nahid	PS 690	479
Robinson, Linda	PS 316	216
Rocha-Sanchez, Sonia	PS 886	589
Rocha-Sanchez, Sonia	PD 63	296
Rodriguez, Roberto	PS 222	130
Rodriguez, Amanda	PS 452	290
Rodriguez, Kenny	PS 910	605
Rodriguez, Kenny	PS 910	605
Rodriguez-de la Rosa, Lourdes	PS 147	90
Roemer, Ariane	PD 7	7
Roemer, Ariane	PD 4	5
Roh, Kyoung Jin	PS 233	136
Rohacek, Alex	PS 110	69
Rolesi, Rolando	PS 160	98
Rolesi, Rolando	PS 933	395
Romain, Tiffany	PS 833	559
Roman, Richard	PS 59	42
Rønne, Filip	PS 241	175
Roosli, Christof	PS 721	496
Roosli, Christof	PS 60	43
Roosli, Christof	PS 192	115
Roosli, Christof	PS 75	51

Author Index

Name	Abstract No.	Page No.
Roosli, Christof	PS 838	562
Rosati, Rita	PS 801	540
Rosen, Merri	PS 663	433
Rosen, Stuart	PS 630	417
Rosen, Stuart	PS 765	520
Rosen, Merri	PS 634	419
Rosen, Merri	PS 628	415
Rosen, Stuart	PS 430	277
Rosenberg, Samuel	PS 327	222
Rosenberg, Samuel	PS 324	220
Rosowski, John	PD 152	626
Rosowski, John	PD 154	627
Rosowski, John	PS 620	410
Rosowski, John	PD 155	628
Rosowski, John	PS 190	114
Rosowski, John	PS 194	116
Ross, Astin	PD 94	452
Ross, Deborah	PS 246	178
Roth-Abramson, Carole	PD 11	466
Roussel, Martine F.	PD 55	291
Roux, Sylvie	PS 652	427
Roverud, Elin	PS 865	579
Roverud, Elin	PS 863	578
Roy, Pallabi	PS 782	530
Rubel, Edwin	PS 737	505
Rubel, Edwin	PS 736	505
Ruben, Robert	PS 303	210
Rubinato, Elisa	PS 121	75
Rubinstein, Jay	PS 445	286
Rubinstein, Jay	PS 272	191
Rubio, Maria	PS 11	15
Rübsamen, Rudolf	PS 513	351
Rübsamen, Rudolf	PS 516	352
Rudman, Jason	PS 118	73
Rudolf, Mark	PD 68	298
Rusheen, Aaron	PS 56	40
Ruth, Byron	PS 314	215
Rutherford, Mark	PS 556	375
Rutherford, Mark	PS 550	372
Rutherford, Mark	PD 62	295
Rutherford, Mark	PS 533	362
Rüttiger, Lukas	PD 20	144
Rüttiger, Lukas	PS 632	418
Rüttiger, Lukas	PS 582	389
Ryals, Matthew	PS 347	233
Ryals, Matthew	PS 349	234
Ryan, Allen F	PS 816	549
Ryan, Allen F	PS 843	565
Rybak, Leonard	PS 583	390
Rybak, Leonard	PS 597	398
Rybak, Leonard	PS 603	402
Ryugo, David	SYMP 64	462
Ryugo, David	PS 510	349
S Malmierca, Manuel	PS 440	283
Sabaawy, Hatem	PS 92	59
Saberi, Kourosh	PS 876	584
Saberi, Kourosh	PS 667	436
Sabin, Andrew	PS 854	572

Name	Abstract No.	Page No.
Sadeghi, Soroush	PS 548	371
Sadeghi, Soroush	PS 539	365
Sadzewicz, Lisa	PD 79	310
Saeed, Shakeel	PS 810	545
Sagers, Jessica E.	PS 308	212
Sagi, Michal	PD 82	311
Sahani, Maneesh	PS 436	281
Sahin, Mehmet	PS 313	215
Sahin, Mehmet	PD 100	456
Saidov, Nodir	PD 6	6
Saito, Naoaki	PD 84	313
Sakaguchi, Hirofumi	PD 84	313
Sakamoto, Susumu	PS 94	452
Sakano, Hitomi	PS 737	505
Sakano, Hitomi	PS 736	505
Sakellarios, Antonis	PS 185	111
Sakumura, Joey	PS 5	11
Salehi, Mansoor	PS 128	80
Salt, Alec	PS 812	546
Salt, Alec	PS 817	549
Salvi, Richard	PS 204	121
Salvi, Richard	PS 860	575
Salvi, Richard	PS 548	371
Salvi, Richard	PD 57	292
Salvi, Joshua	PS 785	531
Salvi, Richard	PD 21	145
Salvi, Richard	PS 629	416
Salvi, Joshua	PD 164	633
Salvi, Richard	PS 825	554
Salvi, Richard	PD 23	145
Salvi, Richard	PS 592	395
Salvi, Richard	PS 633	418
Salvi, Richard	PD 59	293
Salvi, Richard	PS 581	388
Salvi, Richard	PS 152	93
Salvi, Richard	PS 888	590
Samal, Ashok	PD 13	140
Samarajeewa, Anshula	PD 35	154
Samson, Nathalie	PS 697	483
Samy, Ravi	PS 722	496
Samy, Ravi	PS 14	17
San Juan, Juan	PS 711	490
Sanagustin, Javier	PD 147	623
Sanchez, Victoria	PS 242	176
Sanchez, Jason	PS 511	350
Sanchez, Jason	PD 113	467
Sanchez, Jason	PS 517	353
Sanchez-Perez, Isabel	PS 147	90
Sanders, Tessa	PS 749	512
Sandlin, David	PS 918	610
Sandlin, David	PS 59	42
Sandlin, David	PS 920	611
Sandmann, Pascale	PD 141	620
Sanes, Dan	PD 27	148
Sanes, Dan	PS 251	180
Sanes, Dan	SYMP 5	2
Sangi-Haghpeykar, Haleh	PS 234	137
Santi, Peter	SYMP 46	304

Author Index

Name	Abstract No.	Page No.
Santos Cruz de Andrade, José	PS 732	502
Santos-Cortez, Regie Lyn	PS 130	81
Santos-Perez, Sofia	PD 95	452
Santos-Sacchi, Joseph	PS 345	232
Santos-Sacchi, Joseph	PS 689	478
Santos-Sacchi, Joseph	PS 337	227
Santurette, Sébastien	PS 388	228
Sarangdhar, Gowri	PS 133	83
Sarangdhar, Gowri	PD 98	454
Saromo, Selena	PS 523	356
Sasmal, Aritra	PD 54	165
Sasmal, Aritra	PS 174	105
Sato, Mika	PD 7	7
Sato, Shunichi	PS 526	358
Sato, Mika	PS 500	343
Satoh, Yasushi	PS 526	358
Sayles, Mark	PS 198	118
Sayles, Mark	PS 742	508
Sayles, Mark	PS 482	332
Sayyid, Zahra	PD 70	299
Scannella, Sebastien	PS 418	271
Scarnati, Matthew	PS 372	246
Scarnati, Matthew	PS 372	246
Schaake, Wouter	PS 474	329
Schacht, Jochen	PS 153	94
Schacht, Jochen	PD 56	292
Schad, Maggie	PD 116	469
Schade-Mann, Thore	PS 569	382
Schaette, Roland	PS 425	275
Schaette, Roland	PS 826	555
Schaette, Roland	PS 385	253
Schafer, William	PS 768	522
Schafer, Dorothy	SYMP 22	169
Schalk, Gerwin	PD 137	618
Scharinger, Anja	PS 550	372
Schecterson, Leslayann	PS 736	505
Scheidiger, Christoph	PS 429	277
Scheidiger, Christoph	PS 413	269
Schenck, Annette	PS 117	73
Scheperle, Rachel	PS 729	500
Schey, Kevin	PS 321	218
Schick, Bernhard	PS 40	31
Schierholz, Irina	PD 141	620
Schilder, Anne GM	PS 810	545
Schillberg, Patrick	PS 402	262
Schillberg, Patrick	PS 69	479
Schilp, Sören	PS 813	547
Schimmenti, Lisa	PS 793	535
Schlobohm, Lindsay	PS 214	126
SCHMERBER, Sébastien	PS 799	539
Schmidt, Sara	PS 627	415
Schmidt, Jesper Hvass	PD 118	470
Schnee, Michael	PS 536	364
Schnee, Michael	PS 533	362
Schneider, Amy	PS 76	51
Schoen, Nathan	PS 224	131
Schoen, Nathan	PS 225	132
Schoenmaker, Esther	PS 370	245

Name	Abstract No.	Page No.
Schofield, Brett	PS 831	558
Schofield, Brett	PS 746	510
Schofield, Brett	PS 832	559
Schön, Ilona	PS 813	547
Schöpfer, Hanna	PD 6	6
Schör, Merlin	PS 60	43
Schrader, Angela	PD 117	470
Schraders, Margit	PS 117	73
Schreiner, Christoph	PS 439	283
Schreiter, Cathleen	PS 40	31
Schrepfer, Thomas	PD 56	292
Schrepfer, Thomas	PD 40	157
Schrode, Katrina	PS 299	208
Schroeder, Charles	PS 246	178
Schrott-Fischer, Anneliese	PS 758	516
Schrott-Fischer, Anneliese	PS 493	339
Schubert, Nick M. A.	PS 531	361
Schubert, Michael	PD 44	159
Schubert, Michael	PS 447	287
Schubert, Michael	PD 46	161
Schubert, Michael	PS 683	444
Schuchman, Gerald	PS 278	195
Schuermann, Michaela	PS 40	31
Schulte, Bradley	PS 131	81
Schulten, Lisanne	PS 68	47
Schulze, Jennifer	PD 4	5
Schulze, Jennifer	PD 8	7
Schwartz-Leyzac, Kara	PS 725	498
Schwartz-Leyzac, Kara	SYMP 14	167
Schwalje, Adam	PS 284	198
Schwander, Martin	PS 775	526
Schwartz, Zachary	PS 456	319
Schwarz, Hans-Christoph	PD 8	7
Schweinzger, Ivy	PD 116	469
Schweinzger, Ivy	PS 490	337
Schweizer, Felix	PD 39	156
Scott, William	PS 175	105
Scott, Peter	PS 625	414
Screven, Laurel	PS 201	120
Screven, Laurel	PS 203	121
Sebe, Joy	PD 103	87
Sebe, Joy	PS 140	87
See, Jermyn	PS 439	283
Segawa, Kohei	PS 778	527
Segil, Neil	PRES SYMP 5	2
Sekulic Jablanovic, Marijana	PS 797	537
Sellon, Jonathan	PD 47	161
Selvakumar, Dakshnamurthy	PS 543	367
Senn, Pascal	PS 931	503
Seo, Toru	PS 228	134
Seo, Young Joon	PS 574	385
Seonwoo, Hoon	PS 836	561
Serrador, Jorge	PD 44	159
Serrador, Jorge	PS 447	287
Seshadri, Saurav	PS 461	322
Settibhaktini, Harshavardhan	PS 269	190
Sewell, William	PS 821	552
Sewell, William	PS 823	553

Author Index

Name	Abstract No.	Page No.
Seymour, Michelle	PS 692	480
Sha, Su-Hua	PS 153	94
Sha, Zijie	PS 909	604
Sha, Su-Hua	PS 589	393
Sha, Su-Hua	PS 151	93
Sha, Su-Hua	PS 578	387
Sha, Su-Hua	PS 599	399
Sha, Jun	PS 903	601
Shader, Maureen	PS 279	195
Shah, Prahar	PS 775	526
Shaheen, Luke	PS 248	179
Shahsavarani, Bahar	PD 135	616
Shahsavarani, Bahar	PD 13	140
Shaikh, Noah	PS 351	235
Shamma, Shihab	PS 466	324
Shamma, Shihab	PS 244	177
Shamma, Shihab	PS 250	180
Shang, Haiqiong	PS 127	79
Shannon, Robert	PS 29	25
Shannon, Jeffrey	PS 849	569
Shannon, Robert	PS 15	17
Shannon, Robert	PS 35	29
Shannon, Robert	SYMP 55	458
Sharony, Reuven	PD 82	311
Shawn, Goodman	PS 139	86
Shayman, Corey	PD 92	451
Shearer, Eliot	PS 122	76
Sheehan, Kelly	PS 583	390
Sheehan, Kelly	PS 597	398
Sheehan, Kelly	PS 603	402
Sheets, Lavinia	PS 893	593
Sheffield, Sterling	PS 653	428
Sheffield, Abraham	PS 113	71
Shehu, Ina	SYMP 13	166
Sheikh, Aminah	PS 635	419
Sheikh, Aminah	PS 635	419
Shen, Jun	PS 123	76
Shen, Jun	PD 83	312
Shen, Jessica	PS 103	65
Shen, Yi	PS 390	256
Shen, Jun	PD 80	310
Shen, Jun	PS 690	479
Shen, Qiwen	PS 449	289
Shen, Na	PD 132	615
Shen, Yi	PS 640	421
Shepard, Robert	PS 426	275
Sheppard, Adam	PS 825	554
Shera, Christopher	PS 86	56
Shera, Christopher	PS 84	55
Sherrill, Hanna	PS 749	512
Sherrill, Hanna	PS 748	511
Sheth, Sandeep	PS 583	390
Sheth, Sameer	PS 730	501
Sheth, Sameer	PS 365	242
Sheth, Sandeep	PS 597	398
Sheth, Sandeep	PS 603	402
Shi, Haibo	PS 137	85
Shi, Hai	PS 137	85

Name	Abstract No.	Page No.
Shi, Haibo	PS 669	437
Shi, Haosong	PS 669	437
Shi, Hai	PS 669	437
Shi, Hai	PS 670	437
Shi, Haosong	PS 670	437
Shi, Haibo	PS 670	437
Shi, Xiaorui	PS 881	587
Shi, Haibo	PS 215	127
Shi, Xiudong	PS 858	574
Shi, Yuxin	PS 858	574
Shi, Xiaorui	PS 882	587
Shi, Xiaorui	PS 882	587
Shibata, Shumei	PD 163	633
Shibata, Seiji	PS 805	542
Shibata, Seiji	PS 139	86
Shibata, Seiji	PS 139	86
Shimizu, Naoki	PS 908	604
Shin, Beomyong	PS 360	240
Shin, Beomyong	PS 836	561
Shin, Jung-Bum	PS 771	524
Shin, Jung-Bum	PS 97	62
Shinn-Cunningham, Barbara	PS 875	584
Shinn-Cunningham, Barbara	PS 855	572
Shinn-Cunningham, Barbara	PS 706	487
Shinn-Cunningham, Barbara	PS 8	13
Shinn-Cunningham, Barbara	PS 409	266
Shinn-Cunningham, Barbara	PS 263	186
Shinn-Cunningham, Barbara	PD 142	621
Shinn-Cunningham, Barbara	PS 401	262
Shinn-Cunningham, Barbara	PS 745	510
Shinn-Cunningham, Barbara	PS 9	14
Shinn-Cunningham, Barbara	PS 701	485
Shiotani, Akihiro	PS 526	358
Shiramatsu, Tomoyo	PS 196	117
Shiramatsu, Tomoyo	PS 437	281
Shiramatsu, Tomoyo	PS 453	318
Shomron, Noam	PD 82	311
Shore, Susan	PS 900	599
Shore, Susan	PS 899	598
Shore, Susan	PS 53	38
Shore, Susan	PD 19	144
Shore, Susan	PS 515	352
Shore, Susan	PD 17	142
Shrestha, Brikha	PS 315	216
Shu, Yilai	PS 123	76
Shub, Daniel E.	PS 417	270
Siddiqi, Saima	PS 117	73
Siegel, Jonathan	PS 85	55
Sim, Jae Hoon	PS 60	43
Sim, Jae Hoon	PS 192	115
Sim, Jae Hoon	PS 75	51
Sim, Jae Hoon	PS 838	562
Sima, Richard	PS 299	208
Simmons, Dwayne	PS 333	225
Simon, Jonathan	PS 421	273
Simon, Jonathan	PS 236	172
Simon, Jonathan	PS 473	328
Simon, Michelle	PS 686	477

Author Index

Name	Abstract No.	Page No.
Simon, Michelle	PS 320	218
Simon, Jonathan	PS 703	486
Simones, Trevor	PS 527	359
Simpson, Brian	PS 879	586
Simpson, Brian	PS 368	244
Sinclair, Jason	PS 927	595
Sinclair, James	PS 519	354
Sinclair, Jason	PS 880	586
Sinclair, James	PS 48	36
Singer, Wibke	PS 632	418
Singh, Priya	PS 425	275
Singh, Mahendra	PS 741	507
Sinha, Ghanshyam	PS 768	522
Sinha, Sumi	PS 727	499
Sisto, Renata	PS 83	54
Sivaramakannan, Sudhamaheswari	PS 128	80
Sivaraman, Sarada	PS 149	91
Skafidas, Stan	PS 894	594
Skarzynski, Henryk	PS 78	52
Skarzynski, Henryk	PS 129	80
Skerritt-Davis, Ben	SYMP 9	151
Skerritt-Davis, Ben	PS 644	423
Skidmore, Jennifer	PD 69	299
Skoe, Erika	PS 45	35
Skoe, Erika	PS 51	38
Skoruppa, Katrin	PS 764	520
Slade, Martin	PS 580	388
Slaney, Malcolm	SYMP 31	300
Slattery, William	PS 811	546
Slee, Sean	PS 384	253
Smith, Kyle	PS 819	551
Smith, Nicholette	PS 855	572
Smith, Nicholette	PS 856	573
Smith, Douglas	PD 41	158
Smith, Spencer	PS 77	52
Smith, Michael	PS 596	397
Smith, Nicholette	PD 122	473
Smith, Richard	PS 122	76
Smith, Paul	SYMP 38	302
Smith, Richard	PS 805	542
Smith, Philip	PS 742	508
Smith, Zachary	PS 286	199
Smith, Philip	PS 482	332
Smith, Matthew	PS 832	559
Smith, Richard	PS 139	86
Smith, Richard	PS 113	71
Smith, Eve	PS 238	173
Smyth, Daniel	PS 496	341
Smyth, Daniel	PS 812	546
Smythe, Nancy	PS 492	338
Snapp, Hillary	PS 664	434
Snapp, Hillary	PS 414	269
Snapp, Hillary	PD 174	639
So, Nina	PS 249	179
So, Kathy	PS 748	511
Soares, Vitor	PS 149	91
Sobkiv, Sofia	PS 544	368
Sohal, Vikaas	PS 439	283

Name	Abstract No.	Page No.
Soleimani, Majid	PS 189	113
Soleymani, Roozbeh	SYMP 56	458
Soli, Sigfrid	PS 858	574
Someya, Shinichi	PD 57	292
Someya, Shinichi	PS 581	388
Someya, Shinichi	PS 152	93
Sommers, Thomas	PS 534	363
Son, Eun Jin	PS 233	136
Song, Yang	PS 112	70
Song, Jieun	PS 668	436
Song, Hongjun	PRES SYMP 1	1
Song, Pamela	PS 608	404
Song, Wen-jie	PS 459	321
Song, Lei	PS 345	232
Song, Lei	PS 689	478
Song, Zhichao	PS 887	590
Song, Yang	PD 79	310
Song, Yang	PD 79	310
Song, Wenhui	PS 932	347
Song, Xinyu	PS 312	214
Song, Yang	PD 81	311
Song, Yang	PD 60	294
Song, Kuhn Hee	PS 98	62
Sood, Raman	PD 93	451
Sorg, Katharina	PS 40	31
Soriano, Carmen	PS 181	109
Sotomayor, Marcos	PS 784	531
Soto-Varela, Andres	PD 95	452
Sottile, Sarah	PS 433	279
Souffi, Samira	PS 708	488
Soukup, Garrett	PS 114	71
Soukup, Garrett	PS 115	72
Southwell, Rosy	PS 704	486
Southwell, Rosy	PS 274	192
Spankovich, Christopher	PS 197	118
Spencer, Abigail	PS 618	409
Spencer, Abigail	SYMP 44	304
Spencer, Nathaniel	PS 653	428
Spencer, Nathaniel	PS 368	244
Sperry, Ethan	PD 38	156
Spielbauer, Katie	PS 349	234
Spirou, George	PS 761	518
Spirou, George	PS 759	517
Spirou, George	PS 301	209
Spita, Nathalie	SYMP 26	171
Spoth, Jaclyn	PS 860	575
Squires, Jessica	PS 116	72
Srinivasan, Arthi	PS 29	25
Srinivasan, Ramesh	PS 658	431
Srinivasan, Arthi	PS 273	192
St. George, Barrett	PS 710	490
Staecker, Hinrich	PS 901	599
Stahl, Pierre	PS 28	25
Stahn, Patricia	PS 40	31
Staisloff, Hannah	PS 657	430
Stakhovskaya, Olga	PD 131	614
Stakhovskaya, Olga	PS 18	19
Stakhovskaya, Olga	PS 18	19

Author Index

Name	Abstract No.	Page No.
Stakhovskaya, Olga	PS 404	263
Stakhovskaya, Olga	PS 653	428
Stakhovskaya, Olga	PD 11	139
Stakhovskaya, Olga	PS 367	243
Stankovic, Konstantina	PS 308	212
Stankovic, Konstantina	PS 149	91
Stankovic, Konstantina	PS 313	215
Stankovic, Konstantina	PD 100	456
Stankovic, Konstantina	PS 803	541
Stanton, Susan	PS 116	72
Stark, Gemaine	PS 283	198
Stark, Gemaine	PS 499	342
Starost, Matthew	PS 133	83
Stebbins, Karin	PS 609	405
Stecker, G. Christopher	PS 714	492
Stecker, Julie	PD 86	447
Stecker, G. Christopher	PD 86	447
Stecker, G. Christopher	PS 405	264
Steel, Karen P.	PD 97	454
Steel, Karen	PS 131	81
Steel, Karen P.	PS 131	81
Steel, Karen P.	PS 330	223
Steele, Charles	PS 167	101
Steele, Charles	PD 75	307
Steenken, Friederike	PS 484	334
Steevens, Aleta	PD 37	155
Stefan, Rach	PD 141	620
Stefanini, Cesare	PS 841	564
Stein, Amy	PS 16	18
Steinschneider, Mitchell	PS 467	325
Steinschneider, Mitchell	PD 138	618
Steinschneider, Mitchell	PS 713	491
Stepanyan, Ruben	PS 135	84
Stepanyan, Ruben	PD 74	307
Stephani, Friederike	PS 553	373
Stephen, Kegan	PD 114	468
Stephens, Laura	PS 361	240
Stephens, Laura	PS 6006	403
Stepniak, Iwona	PS 129	80
Sterkers, Olivier	PS 41	32
Sterkers, Olivier	PS 449	289
Sterkers, Olivier	PS 348	233
Stevens, Shawn	PS 14	17
Stewart, William	PS 338	228
Stewart, Courtney	PS 921	611
Steyger, Peter	PD 61	294
Steyger, Peter	PS 603	402
Steyger, Peter	PS 551	372
Stiles, Derek	PS 314	215
Stitz, Jasmine	PS 234	137
Stokroos, Robert	PS 444	285
Stolle, Michael	PD 4	5
Stolzberg, Daniel	PS 637	420
Stomackin, Glenna	PS 178	107
Stone, Jennifer	PS 214	126
Stone, Jennifer S	PS 208	123
Stone, Michael	PS 150	90
Stone, Jennifer	PD 65	297

Name	Abstract No.	Page No.
Strahl, Stefan	PS 614	407
Strand, Lisa	PS 200	119
Strenzke, Nicola	PS 550	372
Strickland, Elizabeth	PS 170	103
Strickland, Elizabeth	PS 643	423
Strimbu, Clark Elliott	PD 48	162
Strübing, Ira	PS 138	86
Stuck, Boris A	PS 231	135
Stump, Reto	PS 75	51
Stupak, Natalia	PS 926	201
Stupak, Natalia	PS 30	26
Stupak, Natalia	PS 37	30
Su, Yan	PS 600	400
Su, Yaqing	PS 378	249
Su, Yaqing	PS 378	249
Suematsu, Naofumi	PS 32	27
Sugahara, Kazuma	PS 359	239
Sugahara, Kazuma	PS 685	446
Sugahara, Kazuma	PS 156	96
Sugahara, Kazuma	PS 357	238
Suh, Myung-Whan	PS 814	548
Suh, Myung-Whan	PS 814	548
Suied, Clara	PS 399	261
Suied, Clara	PS 418	271
Suied, Clara	PS 420	272
Sulser, Patrizia	PS 192	115
Sumner, Christian	PS 454	318
Sumner, Christian	PS 454	318
Sun, Wei	PS 572	384
Sun, Willy	PS 536	364
Sun, Wei	PD 21	145
Sun, Wei	PS 495	340
Sun, Wei	PS 507	347
Sun, Hong	PS 592	395
Sun, Shan	PS 585	391
Sun, Wei	PS 693	480
Sun, Yu	PD 161	632
Sun, Gaoying	PS 494	340
Sun, Willy	PS 533	362
Sun, Jie	PS 125	78
Sundar, Isaac	PS 145	89
Sung, Yea Won	PD 144	622
Sunstrum, Julia	PD 126	476
Sunwoo, Woongsang	PS 902	600
Sunwoo, Woongsang	PS 54	39
Suresh, Chandan	PS 478	331
Suresh, Chandan	PS 296	206
Suresh, Chandan	PS 717	493
Suzuki, Hiroshi	PS 694	481
Sveeggen, Timothy	PD 151	626
Svirsky, Mario	SYMP 13	166
Swaminathan, Jayaganesh	PS 865	579
Swaminathan, Jayaganesh	PS 429	277
Swan, Dean	PS 16	18
Swanson, Austin	PS 311	214
Swiderski, Donald	PS 350	235
Swiderski, Donald	PS 483	333
Swiderski, Donald	PD 38	156

Author Index

Name	Abstract No.	Page No.
Swiderski, Donald L.	SYMP 14	167
Swiderski, Donald	PS 158	97
Szczupak, Mikhaylo	PS 224	131
Szczupak, Mikhaylo	PS 225	132
Szczupak, Mikhaylo	PD 174	639
Tabuchi, Keiji	PS 159	97
Tachos, Nikolaos	PS 185	111
Tacikowska, Grazyna	PS 129	80
Tadenev, Basile	PD 159	631
Tai, Yihsin	PS 524	357
Tai, Yihsin	PS 627	415
Tak, Sunghee	PS 43	34
Takada, Yohei	PS 158	97
Takahashi, Satoe	PS 558	376
Takahashi, Satoe	PS 327	222
Takahashi, Satoe	PS 324	220
Takahashi, Masahiro	PS 846	567
Takahashi, Haruo	PS 835	560
Takahashi, Satoe	PS 342	230
Takahashi, Hirokazu	PS 196	117
Takahashi, Hirokazu	PS 437	281
Takahashi, Hirokazu	PS 453	318
Takeda, Hiroki	PS 90	58
Takeda, Takamori	PD 172	638
Takemoto, Yosuke	PS 359	239
Takemoto, Yousuke	PS 357	238
Talaei, Sara	PS 536	364
Talaei, Sara	PS 533	362
Tam, Yu Chuen	PD 129	613
Tamames, Ilmar	PS 798	538
Tan, Xiaodong	PS 181	109
Tan, Xiaodong	PS 39	31
Tan, Winston	PS 689	478
Tan, Xiaodong	PS 383	252
Tanaka, Satomi	PS 294	205
Tandon, Vishal	PS 821	552
Tandon, Vishal	PS 823	553
Tang, Mingliang	PS 215	127
Tang, Yi-Quan	PS 768	522
Tang, Mingliang	PS 586	391
Tang, Mingliang	PS 585	391
Tang, Pei-Ciao	PS 795	536
Tao, Yong	SYMP 21	169
Tarabichi, Osama	PS 502	344
Tarang, Shikha	PS 886	589
Tarang, Shikha	PD 63	296
Tarchini, Nicholas	PD 159	631
Tarchini, Basile	PD 159	631
Tateossian, Hilda	PS 320	218
Tateya, Tomoko	PS 94	60
Tatsumi, Norifumi	PS 846	567
Taylor, Michael R.	PD 55	291
Taylor, Ruth	PS 803	541
Tearney, Guillermo	PD 100	456
Teitz, Tal	PD 55	291
Teki, Sundeeep	SYMP 7	487
Telischi, Fred	PS 820	551
Telischi, Fred	PS 798	538

Name	Abstract No.	Page No.
Telischi, Fred	PS 809	545
Telukuntla, Goutham	PS 311	214
Tempel, Bruce	PS 316	216
Terasaki, Mark	PD 39	156
Terlecky, Stanley	PS 610	405
Thai-Van, Hung	PD 124	475
Thakkar, Tanvi	PD 133	615
Thasma, Sornaraja	PS 242	176
Themann, Christa L.	PD 167	635
Thomas, Megan	PS 452	290
Thomas, Megan	PD 171	637
Tian, Guilian	PD 58	293
Tian, Cong	PS 141	87
Tichko, Parker	PS 45	35
Tierney, Adam	PS 428	277
Tillinger, Joshua	PS 809	545
Tilton, Richard	PS 110	69
Tobias, Ross	PS 310	213
Tobias-Grasso, Celina Ann	PS 130	81
Todd, N Wendell	PS 847	568
Todd, Michael	PD 138	618
Todd, Ann	PS 926	201
Todd, Ann	SYMP 48	314
Todd, Ann	PS 657	430
Toki, Hideaki	PS 694	481
Tollin, Daniel	PS 42	33
Tollin, Daniel	PS 649	426
Tollin, Daniel	PS 403	263
Tollin, Daniel	PS 624	413
Tollin, Daniel	PS 407	265
Tollin, Daniel	PS 66	46
Tollin, Daniel	PS 839	563
Tolnai, Sandra	PS 70	48
Ton, Ymi	PS 913	607
Toneto, Alain	PS 602	401
Torii, Hiroko	PS 753	514
Torrado, Aranza	PS 219	129
Torrado, Marta	PS 147	90
Torres, Renato	PS 41	32
Torres, Renato	PS 348	233
Tosic, Ivana	PS 833	559
Tóth, Brigitta	PS 401	262
Tóth, Brigitta	PS 701	485
Toupet, Michel	PS 232	136
Town, Stephen	PS 254	182
Traer, James	PS 871	582
Trahiotis, Constantine	PS 406	264
Tran, Christopher M.	PD 1	3
Tran Van Ba, Christophe	PS 441	284
Tran Van Ba, Christophe	PD 170	636
Trapani, Josef	PS 534	363
Traver, Estefania	PD 147	623
Troiani, Diana	PS 933	395
Trosman, Samuel	PS 854	572
Trussell, Laurence	PS 679	442
Tsao, Anthony	PS 524	357
Tseng, Jerry	PS 633	418
Tseng, Jerry	PD 59	293

Author Index

Name	Abstract No.	Page No.
Tsuchiya, Naotsugu	PS 437	281
Tsuda, Junko	PS 156	96
Tsunada, Joji	PS 245	177
Tsunada, Joji	PS 247	178
Tsutsumi, Takeshi	PS 336	227
Tsutsumi, Takeshi	PD 172	638
Tsuzaki, Minoru	PS 294	205
Tu, Wenhe	PS 268	189
Tubelli, Andrew	PS 173	104
Tufts, Jennifer	PS 51	38
Tuomainen, Outi	PS 630	417
Tupal, Srinivasan	PS 583	390
Turner, Katie	PS 523	356
Turner, Richard	PS 723	497
Turner, Katie	PS 645	424
Turner, Richard	PS 274	192
Tyker, Anna	PS 610	405
Tyrer, Hayley	PS 320	218
Tzounopoulos, Thanos	PS 514	351
Tzounopoulos, Thanos	PS 258	183
Tzounopoulos, Thanos	PS 300	208
Tzounopoulos, Thanos	PS 257	183
Tzvetanova, Iva	PS 261	185
Udagawa, Tomokatsu	PS 210	124
Ueyama, Takehiko	PD 84	313
Umans, Robyn A.	PD 55	291
Umugire, Alphonse	PS 111	70
Umugire, Alphonse	PS 339	228
Undurraga, Jaime	PS 726	498
Undurraga, Jaime	SYMP 54	317
Undurraga, Jaime	PS 270	190
Undurraga, Jaime	PS 398	260
Undurraga, Jaime	PS 826	555
Urban, Maxwell	PS 204	121
Urban, Nicolai	PD 76	308
Uribe, Phillip M.	PD 61	294
Uribe, Phillip M.	PS 885	589
Urioste, Rodrigo	PS 600	400
Usami, Shin-ichi	PD 84	313
Usami, Shin-ichi	PS 805	542
V Carbajal, Guillermo	PS 440	283
Vadakkan, Tegya	PS 692	480
Vaden, Kenneth	PS 427	276
Vaisbuch, Yona	PD 157	629
Vaisbuch, Yona	PS 613	407
Valdizon-Rodriguez, Roberto	PS 379	250
Valero, Michelle	PS 591	394
Valero, Michelle	PS 144	89
Van Albert, Stephen	PS 600	400
Van de Berg, Raymond	PS 446	287
Van de Berg, Raymond	PS 444	285
Van de Berg, Raymond	PS 493	339
Van de Heyning, Paul	PS 926	201
van de Warrenburg, Bart	PS 117	73
Van De Water, Thomas R	PS 888	590
Van De Water, Thomas R	PS 354	237
van den Boogert, Thomas	PS 493	339
van der Heijden, Marcel	PS 169	102

Name	Abstract No.	Page No.
van der Heijden, Marcel	PD 52	164
van der Voet, Monique	PS 117	73
van Dijk, Pim	PS 531	361
Van Es, Helmuth	PS 810	545
van Hoof, Marc	PS 493	339
Van Itallie, Christina	PS 619	410
Van Nechel, Christian	PS 232	136
Van Roon, Lieke	PS 575	385
van Tilburg, Mark	PS 450	289
Van Tongeren, Joost	PS 444	285
van Wieringen, Astrid	SYMP 54	317
Van Yper, Lindsey	PS 731	501
van Zanten, Gijsbert	PS 724	497
van Zanten, Gijsbert	PS 474	329
Vandenbergh, Luk	PS 803	541
Vandiver, Beau	PS 908	604
Varakina, Ksenya	PD 20	144
Vardonikolaki, Aikaterini	PS 522	356
Varela-Nieto, Isabel	PD 147	623
Varela-Nieto, Isabel	PS 755	515
Varghese, Leonard	PS 855	572
Varghese, Leonard	PS 745	510
Varghese, Leonard	PS 852	571
Vargo, Jonathon	PS 135	84
Varshney, Gaurav	PD 93	451
Varshney, Gaurav	PS 927	595
Varshney, Gaurav	PS 222	130
Varshney, Gaurav	PS 219	129
Vasilkov, Viacheslav	PS 49	37
Vattino, Lucas	PS 547	370
Vattino, Lucas	PS 540	366
Vedula, Else	PS 618	409
Vedula, Else	SYMP 44	304
Veile, Rose	PS 209	124
Velayos-Baeza, Antonio	PD 106	464
Velenovsky, David	PS 77	52
Velez-Ortega, A. Catalina	PS 767	522
Velez-Ortega, A. Catalina	PS 155	95
Velez-Ortega, A. Catalina	PS 773	503
Venail, Frederic	PS 235	137
Venkatasivasaisujith, Sajja	PS 600	400
Venskytis, Emily	PD 89	449
Ventura, Christopher	PD 43	159
Verhoeven, Kristien	PS 505	346
Verhoeven, Kristien	PS 812	546
Verhulst, Sarah	PS 1	9
Verhulst, Sarah	PS 49	37
Verhulst, Sarah	PS 50	37
Vermeire, Katrien	PS 731	501
Verschooten, Eric	PS 289	202
Verschooten, Eric	PS 643	423
Versnel, Huib	PS 262	186
Versnel, Huib	PS 724	497
Versnel, Huib	PS 595	397
Versnel, Huib	PS 474	329
Versnel, Huib	PS 487	335
Vesson, Jean-François	PD 124	475
Vetter, Douglas	PS 512	350

Author Index

Name	Abstract No.	Page No.
Vetter, Douglas	PS 59	42
Vetter, Douglas	PS 563	378
Vetter, Douglas	PS 561	377
Veuillet, Evelyne	PD 124	475
Vickers, Deborah	PS 726	498
Vickers, Deborah	SYMP 54	317
Videhult Pierre, Pernilla	PS 800	539
Vielman, Rene	PS 504	345
Vielman, Rene	PS 505	346
Vijayakumar, Sarath	PD 71	305
Vijayakumar, Sarath	PD 63	296
Vincent, Philippe	PS 546	369
Vogl, Christian	PS 545	369
Vogler, Nathan	PS 514	351
Voigt, Mathias	PS 464	323
Vollmer, Maike	PS 503	345
von Gersdorff, Henrique	PS 541	366
von Gersdorff, Henrique	PS 546	369
von Gersdorff, Henrique	PS 538	365
Vonck, Bernard	PS 724	497
Vonck, Bernard	PS 474	329
Vong, Angela	PS 543	367
Voysey, Graham	PD 25	146
Vozzi, Diego	PS 124	77
Vozzi, Diego	PS 121	75
Vu, Andrew	PD 146	622
Vuckovic, Dragana	PS 124	77
Vuckovic, Dragana	PS 120	74
Vuust, Peter	PD 118	470
Vyas, Pankhuri	PS 554	374
Vyas, Pankhuri	PS 555	374
Wagner, Hermann	PS 402	262
Wagner, Hermann	PS 68	47
Wagner, Anita	SYMP 61	461
Wagner, Hermann	PD 85	447
Wagner, Anita	PS 859	575
Wagner, Elizabeth	PS 771	524
Wagner, Hermann	PS 69	47
Waheed, Sajal	PS 47	36
Wake, Naoki	PS 196	117
Waked, Arifi	PS 423	274
Waldhaus, Joerg	PS 266	188
Waldmann, Bernd	PS 188	113
Walker, Kerry	PS 460	321
Walker, Steven	PS 135	84
Wallace, Mark	PS 454	318
Wallaert, Nicolas	PS 393	258
Walls, Michael	PS 198	118
Walraevens, Joris	PS 192	115
Walsh, Edward	PD 151	626
Walsh, Tom	PD 82	311
Walter, Erin	PS 239	174
Walton, Joseph	PS 601	400
Walton, Joseph	PS 819	551
Walton, Joseph	PS 822	553
Walton, Joseph	PS 27	24
Walton, Paul	PS 610	405
Wan, Jun	PS 759	517

Name	Abstract No.	Page No.
Wan, Guoqiang	PD 38	156
Wan, Guoqiang	PD 40	157
Wan, Liang Cai	PD 65	297
Wang, Xiaoqin	PS 934	185
Wang, Li	PS 126	78
Wang, Lijuan	PS 123	76
Wang, Zhengmin	PS 123	76
Wang, Jian	PS 137	85
Wang, Jiping	PS 137	85
Wang, Xin-Wei	PS 840	563
Wang, Ying	PS 600	400
Wang, Xiaoyu	PS 737	505
Wang, Yuan	PS 737	505
Wang, Hong Jun	PS 804	542
Wang, Zhaoyan	PS 443	285
Wang, Derek	PD 27	148
Wang, Shaoxun	PS 59	42
Wang, Xiaoyu	PS 511	350
Wang, Yuan	PS 511	350
Wang, Hui	PS 712	491
Wang, Jian	PS 489	336
Wang, Xiaowen	PS 630	417
Wang, Tiffany	PD 85	447
Wang, Lingyan	PD 2	4
Wang, Xuan	PS 184	110
Wang, Yuan	PS 736	505
Wang, Xiaoyu	PS 736	505
Wang, Tian	PD 70	299
Wang, Jin-Fu	SYMP 20	168
Wang, Guo-Peng	PS 350	235
Wang, Wenwen	PS 323	220
Wang, Jianjun	PS 323	220
Wang, Xin-Wei	PD 169	636
Wang, Le	PS 409	266
Wang, Xianren	PS 151	93
Wang, Yanli	PD 75	307
Wang, Yuan	PD 113	467
Wang, Xiaoyu	PD 113	467
Wang, Xuelin	PS 179	108
Wang, Nae-Yuh	SYMP 65	462
Wang, Guo-Peng	PS 921	611
Wang, Yuan	PS 431	278
Wang, Yongming	PS 585	391
Wang, Jing	PS 356	238
Wang, Xiaoqin	SYMP 15	167
Wang, Xiaohan	PS 882	587
Wang, Xiaoqin	PS 869	581
Wang, Jian	PD 114	468
Wang, Guo-Peng	PD 40	157
Wang, Jian	PS 903	601
Wang, Yongfang	PS 903	601
Wang, Zhengmin	PD 132	615
Wang, Haibo	PS 494	340
Wang, Jianjun	PS 326	221
Wang, Wenwen	PS 326	221
Wang, Li	PS 125	78
Warabi, Eiji	PS 159	97
Warchol, Mark	PS 209	124

Author Index

Name	Abstract No.	Page No.
Warchol, Mark	PD 117	470
Warchol, Mark	PD 65	297
Warchol, Mark	PS 750	512
Ward, Bryan	PS 58	41
Ward, Bryan	PS 683	444
Warfield, Simon	PD 139	619
Warnecke, Athanasia	PD 7	7
Warnecke, Athanasia	PD 4	157
Warnecke, Athanasia	PD 8	7
Warrier, Catherine	PD 9	138
Warwas, Dawid	PD 8	310
Wassmer, Sarah	PS 803	541
Watabe, Takahisa	PS 355	237
Watanabe, Hirobumi	PS 25	23
Watanabe, Naoki	PD 84	313
Watanabe, Hirobumi	PS 611	406
Watt, Alanna	PS 680	443
Wedemeyer, Carolina	PS 547	370
Wei, Yanling	PS 600	400
Weigele, Jochen	PS 133	83
Weise, Chang	PS 600	400
Wells, Sara	PS 686	477
Wells, Sara	PS 320	218
Welsh, Nora	PD 150	625
Wenstrup, Jeffrey	PS 462	322
Wenstrup, Jeffrey	PS 463	323
Wenstrup, Jeffrey	PS 415	270
Wenzel, Gentiana I.	PS 40	31
Wenzel, Angela	PS 231	135
Werner, Lynne	PS 392	257
Werner, Lynne	PS 272	191
Wersinger, Eric	PS 235	137
Wersinger, Eric	PD 170	636
Wesarg, Thomas	PS 419	271
Wess, Jessica	PS 282	197
West, Matthew	PS 218	129
West, James	SYMP 29	300
West, Matthew	PS 896	596
Westhofen, Martin	PS 227	133
Weston, Michael	PS 886	589
White, Jacqueline K.	PD 97	454
White, Patricia	PD 66	297
White, Patricia	PS 145	89
White, Karessa	PD 57	292
White, Jacqueline	PS 330	223
White, Patricia	PS 604	402
White, Mark	PS 720	495
White, Karessa	PS 581	388
White, Karessa	PS 152	93
White-Schwoch, Travis	PD 9	138
Whitlon, Donna	PS 146	90
Whitton, Jonathon	PS 849	569
Whitton, Jonathon	PS 293	204
Whitton, Jonathon	PS 852	571
Wichmann, Carolin	PS 545	369
Wickesberg, Robert	PS 426	275
Wiggin, Tim	PS 793	535
Wild, Conor	PS 476	330

Name	Abstract No.	Page No.
Wilder, Donna	PS 600	400
Wilkinson, Eric	PS 15	17
Wilkinson, Eric	PS 35	29
Wilkinson, Tracy	PS 17	19
Williams, Dan	PS 317	217
Williams, Charles	PS 829	557
Williams, Kevin M.	PS 596	397
Williams, Debbie	PS 320	218
Williams, Susan	PS 234	137
Williamson, Ross	PS 631	417
Williamson, Peter	PS 61	405
Williamson, Ross	PS 436	281
Williamson, Ross	PD 25	146
Willig, Katrin	PD 76	308
Williges, Ben	SYMP 51	315
Williges, Ben	PS 419	271
Wilson, Teresa	PS 358	239
Wilson, Teresa	PS 787	532
Wilson, Lauren	PS 17	19
Wilson, Kevin	PS 822	553
Wilson, Teresa	PS 788	533
Wilson, Elizabeth	PS 770	523
Windle, Richard	PS 826	555
Winkowski, Daniel	PS 252	181
Winkowski, Daniel	PS 461	322
Winn, Matthew	PD 10	138
Winn, Matthew	PD 88	448
Winslow, Raimond	PS 176	106
Winston, Jenna	PD 91	450
Winters, Bradley D.	PS 740	507
Wise, Andrew	PS 501	343
Wise, Andrew	PS 928	576
Wisniewski, Matthew	PS 879	586
Wiszniewski, Bernadette	PS 697	483
Withnell, Robert	PS 181	109
Withnell, Robert	PS 80	53
Witt, Adelia	PS 280	196
Wiwatpanit, Teerawat	PS 687	477
Wolak, Tomasz	PS 129	80
Wolf, Jana	PS 374	247
Wolfowitz, Amit	PS 351	235
Wolpert, Stephan	PS 810	545
Wolter, Steffen	PS 582	389
Wolters, Markus	PS 582	389
Won, JongHo	PS 272	191
Wong, Kevin	PS 848	568
Wong, Daniel	PS 479	331
Wong, Candy	PD 78	309
Wong, Hiu Tung	PS 350	235
Wong, Lok Sum	PD 34	153
Wong, Candy	PS 760	518
Wood, Matthew	PD 150	625
Wood, Scott	PD 44	159
Woods, Kevin	SYMP 8	150
Woolley, Sarah	PS 249	179
Woolman, Theodor	PD 59	293
Woolnough, Oscar	PS 454	318
Wooltorton, Julian	PS 815	548

Author Index

Name	Abstract No.	Page No.
Wright, Beverly	PS 853	571
Wright, Beverly	PS 854	572
Wright, Matthew	PS 160	98
Wright, Alexander	PS 573	384
Wright, Matthew	PS 797	537
Wu, Xudong	PD 83	312
Wu, Yaqin	PS 137	85
Wu, Mengfan	PS 668	436
Wu, Yaqin	PS 669	437
Wu, Yaqin	PS 670	437
Wu, Calvin	PS 899	598
Wu, Yuting	PS 220	130
Wu, Hao	PS 443	285
Wu, Yunan	PS 661	432
Wu, Hsiao-Huei	PD 163	633
Wu, Doris	PD 34	153
Wu, Chen-Chi	PS 565	380
Wu, Calvin	PS 53	38
Wu, Hao	PS 108	68
Wu, Jingjing	PS 554	374
Wu, Xuewen	PS 592	395
Wu, Xudong	PS 774	525
Wu, Doris	PD 36	155
Wu, Doris	PS 99	63
Wu, Jingjing Sherry	PS 560	377
Wu, Xia	PD 161	632
Wu, Calvin	PD 17	142
Wu, Jingjing Sherry	PS 555	374
Xavier, Brian	PS 848	568
Xia, Hongyi	PS 167	101
Xia, Anping	PS 177	107
Xiang, Jing	PS 722	496
Xie, Lihong	PD 35	154
Xie, Zilong	PD 121	473
Xie, Dinghua	PS 883	588
Xie, Zilong	PS 659	431
Xie, Le	PD 161	632
Xie, Ruili	PD 110	466
Xing, Yazhi	PS 264	187
Xing, Yazhi	PS 492	338
Xing, Yazhi	PS 491	338
Xing, Yazhi	PS 321	218
Xiong, Binbin	PS 590	394
Xiong, Binbin	PD 21	145
Xiong, Hao	PS 589	393
Xiong, Binbin	PS 693	480
Xiong, Shanshan	PS 257	183
Xu, Lisha	PS 927	595
Xu, Yingyue	PS 39	31
Xu, Yong	PS 898	598
Xu, Jie	PS 302	209
Xu, Zhenlin	PS 822	553
Xu, Yingyue	PS 383	252
Xu, Kally	PS 920	611
Yabushita, Gaku	PS 295	205
Yakushin, Sergei	PS 229	134
Yakushin, Sergei	PS 230	135
Yamahara, Kohei	PS 796	537

Name	Abstract No.	Page No.
Yamamoto, Norio	PS 796	537
Yamamoto, Norio	PS 753	514
Yamamoto, Yukiko	PD 172	638
Yamamoto-fukuda, Tomomi	PS 846	567
Yamamoto-fukuda, Tomomi	PS 835	560
Yamashita, Hiroshi	PS 359	239
Yamashita, Hiroshi	PS 685	446
Yamashita, Hiroshi	PS 156	96
Yamashita, Tetsuji	PS 213	126
Yamashita, Akinori	PS 148	91
Yamashita, Hiroshi	PS 357	238
Yamazaki, Hiroshi	PS 709	489
Yamins, Daniel	PS 260	184
Yan, Denise	PS 126	78
Yan, Denise	PS 118	73
Yan, Zheng	PS 137	85
Yan, Denise	PS 127	79
Yan, Denise	PS 567	381
Yan, Denise	PS 566	380
Yan, Denise	PS 128	80
Yan, Wenqing	PS 494	340
Yan, Denise	PS 125	78
Yang, Chao-Hui	PS 153	94
Yang, Xiao-Yu	PS 840	563
Yang, Shiming	SYMP 21	169
Yang, Shi-ming	PS 572	384
Yang, Wan-Wan	PS 811	546
Yang, Weiping	PS 590	394
Yang, Lin	PS 612	406
Yang, Xiao-Yu	PD 169	636
Yang, Chan Ju	PS 790	534
Yang, Shi-ming	PS 495	340
Yang, Shi-ming	PS 507	347
Yang, Xiaoyu	PS 136	84
Yang, Juanmei	PS 136	84
Yang, Jun	PS 141	87
Yang, Weiping	PS 751	513
Yang, Keum-Jin	PS 818	550
Yang, Lin	PS 193	115
Yang, Lin	PS 187	112
Yang-Hood, Aizhen	PD 62	295
Yao, Justin	PS 251	180
Yarza, Talitha Karisse	PS 130	81
Yates, Bill	PS 681	443
Yates, Charles	PD 173	638
Ye, Yi	PS 628	415
Yee, Kathleen	PS 512	350
Yee, Kathleen	PS 59	42
Yee, Kathleen	PS 563	378
Yee, Kathleen	PS 561	377
Yeh, Ariel	SYMP 21	169
Yellamsetty, Anusha	PS 81	53
Yellamsetty, Anusha	PS 715	492
Yeoh, Brandon	PS 154	94
Yi, Eunyoung	PS 340	229
Yi, Han Gyol	PD 121	473
Yi, Hongliang	PS 712	491
Yin, Shankai	PS 137	85

Author Index

Name	Abstract No.	Page No.
Yin, Shankai	PS 669	437
Yin, Shankai	PS 670	437
Yin, Shankai	PS 712	491
Yin, Pingbo	PS 250	180
Yin, Dongming	PS 193	115
Yin, Dongming	PS 187	112
Yingla, Zhang	PS 584	390
Yokell, Zachary	PS 180	108
Yokoyama, Wayne	PD 144	622
Yoneya, Makoto	PS 873	583
Yoneya, Makoto	PS 873	583
Yoon, Ji young	PS 818	550
Yoshimura, Hidekane	PS 805	542
Yosihda, Atsuhiko	PS 753	514
Youm, Ibrahima	PS 218	129
Young, Terry-Lynn	PS 116	72
Young, Hunter	PS 146	90
Young, Samuel	PS 301	209
Young, Hunter	PS 32	27
Young, Alex	PS 352	236
Young, Jesse	PS 529	360
Yousaf, Rizwan	PD 96	453
Yu, Jing	PS 840	563
Yu, Yue	PS 918	610
Yu, Yue	PS 59	42
Yu, Ning	PS 329	223
Yu, Chao	PS 364	242
Yu, Qing	PS 787	532
Yu, I-Shing	PS 565	380
Yu, Yolanda	PD 148	624
Yu, Gongqiang	PS 240	175
Yu, Yue	PS 920	611
Yu, Jin-Tao	PD 161	632
Yudintsev, Georgiy	PS 457	320
Yurjevich, Danielle	PS 743	508
Zaar, Johannes	PS 429	277
Zaar, Johannes	PS 413	269
Zabalawi, Hassan	PS 932	347
Zachary, Stephen	PS 535	363
Zakrzewski, Alexandria	PS 879	586
Zalewski, Christopher	PS 61	43
Zampino, Anthony	PS 463	323
Zazo Seco, Celia	PS 117	73
Zee, David	PS 683	444
Zemelman, Boris	PS 373	247
Zeng, Fan-Gang	PS 523	356
Zeng, Shan	PS 205	122
Zeng, Fan-Gang	PS 645	424
Zha, Mingming	PS 903	601
Zhan, Yi	PS 858	574
Zhang, Huiming	PS 530	360
Zhang, Xueguo	PS 530	360
Zhang, Jinsheng	PS 530	360
Zhang, Fawen	PS 722	496
Zhang, Jingyuan	PD 66	297
Zhang, Xiaoyu	PS 328	222
Zhang, Fawen	PS 14	17
Zhang, Jinsheng	PD 18	143

Name	Abstract No.	Page No.
Zhang, Qian	PS 114	71
Zhang, Xiaoli	PS 215	127
Zhang, Shasha	PS 215	127
Zhang, Chao	PS 520	355
Zhang, Lichun	PS 484	334
Zhang, Celia	PS 590	394
Zhang, Jinsheng	PS 898	598
Zhang, Qiuxiang	PD 78	309
Zhang, Carol	PS 442	284
Zhang, Tianyu	PS 612	406
Zhang, Shasha	PS 586	391
Zhang, Xiaoli	PS 586	391
Zhang, Haichao	PS 379	250
Zhang, Mingshu	PS 585	391
Zhang, Shasha	PS 585	391
Zhang, Xiaoli	PS 585	391
Zhang, Celia	PS 693	480
Zhang, Qian	PS 115	72
Zhang, Yang	PS 869	581
Zhang, Yue	PD 14	141
Zhang, Yue	PS 430	277
Zhang, Yanping	PD 119	471
Zhang, Jianning	PS 491	338
Zhang, Tianyu	PS 193	115
Zhang, Tianyu	PS 187	112
Zhang, Xiaochen	PD 109	465
Zhang, Yuan	PS 551	372
Zhang, Celia	PS 640	421
Zhang-Hooks, YingXin	SYMP 28	172
Zhao, Meng	PS 840	563
Zhao, Hong-Bo	PD 104	457
Zhao, Hong-Bo	PS 329	223
Zhao, Sijia	PS 873	583
Zhao, Sijia	PS 878	585
Zhao, Hong-Bo	PD 115	468
Zhao, Hong-Bo	PD 115	468
Zhao, Xuechu	PD 79	310
Zhao, Sijia	PS 700	484
Zhao, Hong-Bo	PS 62	44
Zhao, Hong-Bo	PS 62	44
Zheng, Jing	PS 558	376
Zheng, Jing	PS 327	222
Zheng, Fei	PS 213	126
Zheng, Jing	PS 342	230
Zheng, Tihua	PS 141	87
Zheng, Qing Y.	PS 141	87
Zhou, Jiayi	PS 116	72
Zhou, Yinmei	PD 55	291
Zhou, Wu	PS 918	610
Zhou, Yingjie	PS 327	222
Zhou, Yi	PD 89	449
Zhou, Wenxiao	PS 166	101
Zhou, Wu	PS 59	42
Zhou, Wu	PS 563	378
Zhou, Yingjie	PS 687	477
Zhou, Yingjie	PS 598	399
Zhou, Yinuo	PS 700	484
Zhou, Wu	PS 920	611

Author Index

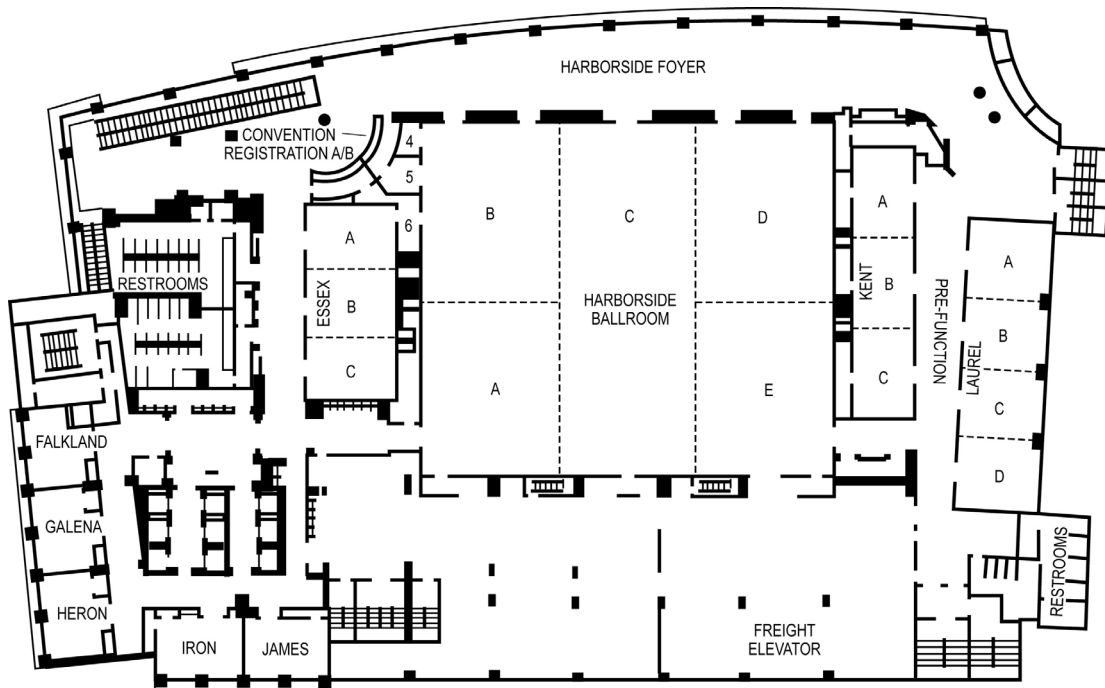
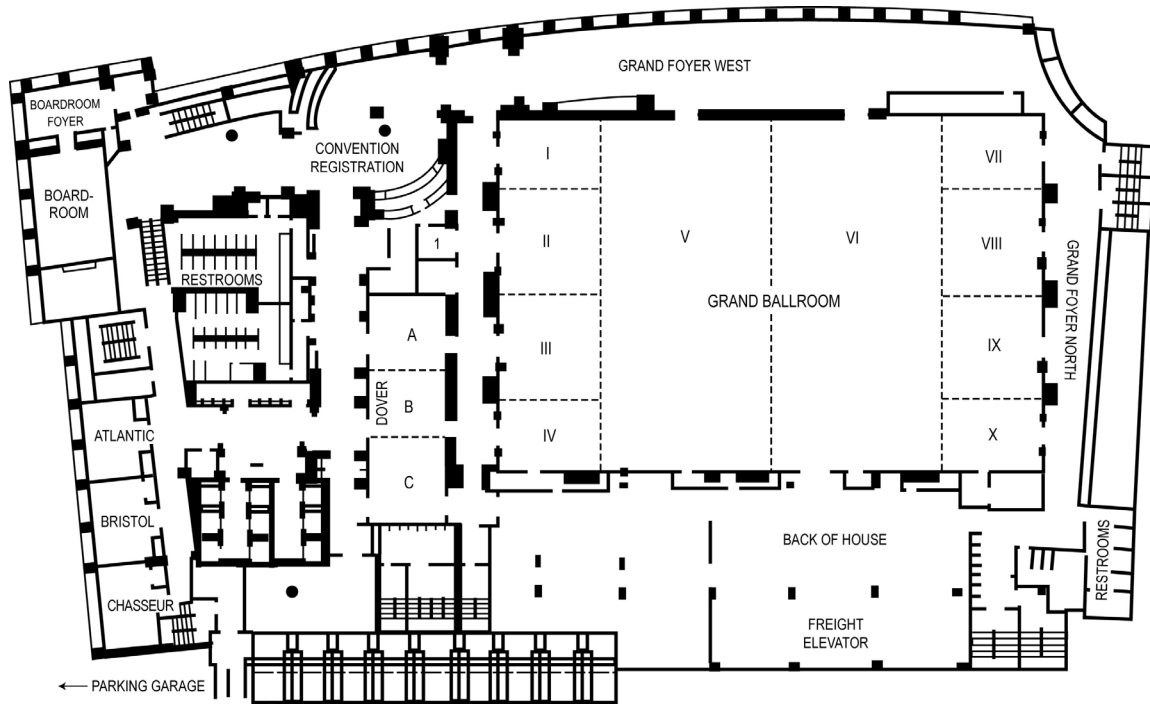
Name	Abstract No.	Page No.
Zhou, Ning	SYMP 14	167
Zhou, Ning	PS 275	193
Zhou, Ning	PS 276	193
Zhou, Yi	PS 397	260
Zhu, Xiaoxia	PS 819	551
Zhu, Hong	PS 918	610
Zhu, Chengwen	PS 215	127
Zhu, Yan	PD 104	457
Zhu, Hong	PS 59	42
Zhu, Hong	PS 59	42
Zhu, Yan	PS 329	223
Zhu, Chengjing	PD 6	6
Zhu, Ning	PS 616	408
Zhu, Yuanping	PS 589	393
Zhu, Hong	PS 563	378
Zhu, Yun	PS 678	442
Zhu, Yuanping	PS 578	387
Zhu, Xiaoxia	PS 822	553
Zhu, Yan	PD 115	468
Zhu, Yan	PD 115	468
Zhu, Bovey	PS 806	543
Zhu, Hong	PS 920	611
Zhu, Yan	PS 62	44
Zieleniewska, Magdalena	PS 702	485
Zilany, Muhammad	PS 2	10
Zimmerman, Amanda	PS 554	374
Zimmerman, Amanda	PS 555	374
Zimmermann, Ulrike	PD 20	144
Zine, Azel	PS 602	401
Zobeiri, Omid	PS 442	284
Zong, Liang	PD 104	457
Zorio, Diego	PS 736	505
Zorio, Diego	PS 431	278
Zorzi, Veronica	PS 134	83
Zosuls, Aleks	PS 173	104
Zou, Weiguo	PS 123	76
Zou, Bing	PS 118	73
Zou, Bing	PS 883	588
Zou, Bing	PS 128	80
Zou, Junhuang	PS 141	87
Zuk, Nathaniel	PD 87	448
Zuo, Jian	PD 55	291
Zuo, Jian	PS 317	217
Zuo, Jian	PS 212	126
Zuo, Jian	PS 213	126
Zwolan, Teresa	SYMP 66	462
Zwolan, Teresa A.	SYMP 14	167

BALTIMORE MARRIOTT WATERFRONT

700 Aliceanna Street, Baltimore, MD 21202

BaltimoreMarriottWaterfront.com

T 410.385.3000 | F 410.385.0330



SAVE THE DATES

FEBRUARY 10-14, 2018

41st Annual MidWinter Meeting
Manchester Grand Hyatt
San Diego, California, USA

FEBRUARY 9-13, 2019

42nd Annual MidWinter Meeting
Baltimore Marriot Waterfront
Baltimore, Maryland, USA

JANUARY 24-29, 2020

43rd Annual MidWinter Meeting
San Jose, California

FEBRUARY 20-24, 2021

44th Annual MidWinter Meeting
Renaissance SeaWorld
Orlando, Florida, USA

Association for Research in Otolaryngology

19 Mantua Road
Mt. Royal, NJ 08061

www.aro.org